Agricultural Research Institute
PUSA

LONDON
HARRISON AND SONS, LTD., PRINTERS IN ORDINARY TO HIS MAJESTY
ST MARTIN'S LANE

CONTENTS.

SERIES A VOL CXVII

No 776 December 1, 1927

PAGE

A Theory of Electric and Magnetic Birefringence in Liquids By C V Raman, F R.S, and K S Krishnan 1

Density of the Vapour in the Mercury Arc and the Relative Intensities of the Radiated Spectral Lines, with Special Reference to the Forbidden Line λ 2270 By B Venkatesachar Communicated by Lord Rayleigh, F R S (Plates 1–3) 11

On the Input Limit of an X Ray Tube with Circular Focus By A Muller Communicated by Sir William Bragg, F.R S 30

The Dielectric Constants of Ammonia, Phosphine, and Arsine By H E Watson Communicated by F G Donnan, F R S 43

An X Ray Study of the Heat Motions of the Atoms in a k Salt Crystal By R W James and E M Firth Communicated by W F R S 62

Shifts and Reversals in Fuse Spectra By A C M mmunicated by R Whiddington, F R S (Plate 4) 88

A Study of the Catalysis by Nickel of the Union of Hyd xygen by a New Method By D R Hughes and R C Bevan Comm y D L Chapman, F.R.S 101

The Average Energy of Disintegration of Radium E By C D Ellis and W A Wooster Communicated by Sir Ernest Rutherford, P R S 109

The Elasticity of the Collisions of Alpha Particles with Hydrogen Nuclei By P M S Blackett and E P Hudson Communicated by Sir Ernest Rutherford, P R S (Plate 5) 124

The Relative Stability of Nitrous Oxide and Ammonia in the Electric Discharge By W K Hutchison and C N Hinshelwood Communicated by H Hartley, F R S 131

Application of Quantum Mechanics to the Stark Effect in Helium By J S Foster Communicated by N Bohr, For Mem R S (Plates 6–13) 137

The Spectrum of Carbon Arcs in Air at High Current Densities By J W Ryde Communicated by A Fowler, F R S (Plates 14–16) 164

PAGE

Studies of Gas-Solid Equilibria. Part I.—Pressure-Temperature Equilibria between Benzene and (a) Ferric Oxide Gel, (b) Silica Gel in Sealed Systems of Known and Unalterable Total Composition By B Lambert and A. M. Clark. Communicated by F Soddy, F.R.S . . 183

Adjoint Differential Equations By F B Pidduck. Communicated by A. E H. Love, F.R S 201

The Refractive Index of Quartz By W R C Coode-Adams Communicated by T M Lowry, F R S 209

On the Temperature Factors of X-Ray Reflexion for Sodium and Chlorine in the Rock Salt Crystal By I Waller and R W James Communicated by W L. Bragg, F R S 214

On the Excitation of Polarised Light by Electron Impact II.—Mercury By H W B Skinner and E T S Appleyard Communicated by Sir Ernest Rutherford, P R S 224

On the Effect of Temperature on the Viscosity of Air By R S Edwards. Foreword by A O Rankine Communicated by H. L. Callendar, F.R.S 245

Free Motion in the Wave Mechanics By C G Darwin, F.R S . . 258

The Line Spectrum of Mercury in Absorption Occurrence of the Forbidden Line λ 2270 By Lord Rayleigh, F R S (Plate 17) 294

Minutes of Meetings of November 3, 10, 17, 1927

No 777—January 2, 1928

Address of the Pro[illegible]nest Rutherford, O M., at the Anniversary Meeting, November 30, 19[illegible] 300

The Spectrum of Do[illegible]ygen (O III) By A. Fowler, F.R.S. 317

A Vector Loci Method [illegible]ng Coupled Circuits By E Mallett Communicated by T Math[illegible] 331

The Ultra-Violet Band System of Carbon Monosulphide and its Relation to those of Carbon Monoxide (the "4th Positive" Bands) and Silicon Monoxide. By W Jevons Communicated by Prof A Fowler, F R.S 351

Spectrophotometric Observations on the Growth of Oxide Films on Iron, Nickel, and Copper By F H Constable Communicated by T M. Lowry, F.R.S 376

An Experimental Study of the Motion of a Viscous Liquid contained between Two Coaxial Cylinders By J W Lewis Communicated by Prof H M. Plummer, F.R.S (Plate 18) 388

The Spectrum of Fluorine (F I). Part II By H Dingle. Communicated by Prof. A. Fowler, F R.S 407

Resistance to a Barrier in the Shape of an Arc of a Circle. By L. Rosenhead. With Note by S Brodetsky Communicated by L. Bairstow, F.R.S. 417

PAGE

A Magnetometer for the Measurement of the Earth's Vertical Magnetic Intensity in C.G.S. Measure. By D. W. Dye. Communicated by Sir Arthur Schuster, F R.S. 434

The Thermal Conductivities of Certain Liquids. By G W. C Kaye, O B E, and W. F Higgins. Communicated by Sir Joseph Petavel, F.R.S. . 459

The Magnetic Properties of Single Crystals of Nickel By W Sucksmith, H H Potter and L. Broadway. Communicated by A P Chattock, F.R.S. 471

The Continuous Absorption of Light in Potassium Vapour By R. W. Ditchburn. Communicated by Sir J J Thomson, F.R.S 486

On a Photoelectric Theory of Sparking Potentials By J Taylor Communicated by O W. Richardson, F.R.S 508

The Crystal Structure of the Chondrodite Series By W H Taylor and J West. Communicated by W L. Bragg, F R.S 517

The Structure of Surface Films Part X.—Phenols and Monoglycerides By N K. Adam, W A Berry and H A Turner Communicated by Sir William Hardy, F.R.S 532

Minutes of Meetings of November 30, and December 8, 1927

No 778—February 1, 1928

On a New Effect in the Electric Discharge By T R Merton, F R.S 542

The Restored Electron Theory of Metals and Thermionic Formulæ By R. H. Fowler, F.R.S 549

Gaseous Combustion at High Pressures Part IX.—The In[illegible]ressure upon the "*Explosion Limits*" of *Inflammable Gas-Air, et*[illegible] By W A. Bone, F.R.S, D M Newitt, and C M. Smith 553

On a Method of Determining the State of Polarisation of Dow[illegible]ireless Waves By E V Appleton, F R.S, and J A. Ratcliffe 576

A Theory of the Optical and Electrical Properties of Li[illegible]y C V Raman, F R.S, and K. S Krishnan . 589

Experiments on the Diffraction of Cathode Rays By G P Thomson. Communicated by Sir Joseph Thomson, F R S (Plate 19) 600

The Quantum Theory of the Electron By P A M. Dirac Communicated by R H. Fowler, F R.S , 610

The Fundamental Equation of Wave Mechanics and the Metrics of Space. , By H. T Flint and J W Fisher. Communicated by O W Richardson, F.R.S . 625

Relativity and the Quantum Theory By H T Flint Communicated by O. W Richardson, F.R.S. 630

On a Minimum Proper Time and its Applications (1) to the Number of the Chemical Elements (2) to some Uncertainty Relations. By H. T. Flint and O W Richardson, F.R.S . 637

PAGE

Critical Potentials for Soft X-Ray Excitation. By U Andrewes, A. C. Davies, and F. Horton, F.R.S. 649

The Solubility of Hydrogen in Silver. By E. W R Steacie and F M. G. Johnson. Communicated by Prof A. S Eve, F.R.S 662

The Specific Heats of Ferromagnetic Substances By L. F Bates. Communicated by A W Porter, F.R.S . . 680

The Tides in Oceans on a Rotating Globe—Part I By G R. Goldsbrough. Communicated by Prof T H. Havelock, F.R.S 692

On the Extraction of Electrons from Cold Conductors in Intense Electric Fields By O W Richardson, F.R.S . 719

Minutes of Meeting of January 19, 1928

OBITUARY NOTICES

Sir William Augustus Tilden (with portrait)

Arthur William Crossley (with portrait) vi

William Burnside (with portrait) xi

Willem Einthoven (with portrait) xxvi

Henry Martyn Taylor (with portrait) xxix

Index . xxxiii

PROCEEDINGS OF
THE ROYAL SOCIETY.

Section A.—Mathematical and Physical Sciences.

A Theory of Electric and Magnetic Birefringence in Liquids.

By Prof. C. V. Raman, F.R.S., and K. S. Krishnan.

(Received July 25, 1927.)

1. *Introduction.*

The double refraction exhibited by liquids when placed in an electrostatic field is ascribed in the theory of Langevin* to an orientation of the molecules produced by the field, the orientative couple arising from an assumed electrical anisotropy of the molecule. If an optical anisotropy of the molecule is postulated in addition, the birefringence of the liquid follows as a necessary consequence. Born† modified the Langevin theory by including also the orientative effect of the field on the molecule due to the permanent electric moment, if any, possessed by it. The optical anisotropy and electrical polarity of the molecule postulated in these theories can be independently determined from observations of light-scattering and dielectric constant in the vapours of the substances. In two recent papers‡ we have attempted to discuss how far the available data for the Kerr effect can be re[illegible] with the theories of Langevin and Born. The main result emerging is [illegible] fail to give the magnitude of the Kerr constant in *liquids* [illegible] terms of the constants of the molecule as determined in the gaseo[illegible] This failure is illustrated in Table I for a number of liquids hav[illegible] ar molecules for which the optical anisotropy is known from obser[illegible] light-scattering in the vapour.

It appears hardly likely that the failure of the Langevin theory indicated by the figures in Table I can be ascribed to a real change in the optical anisotropy of the molecule when it passes from the condition of vapour to that of liquid. It seems rather that the explanation must lie in the inadequacy of the theory itself. We accordingly propose in this paper to put forward a theory of electric and magnetic double refraction, in which the fundamental premises of Langevin and Born are revised.

---

* 'Le Radium,' vol. 9, p. 249 (1910).

† 'Ann. der Physik,' vol. 55, p. 177 (1918).

‡ 'Phil. Mag.,' vol. 3, pp. 713 and 724 (1927).

Table I

Liquid.	Depolarisation of the light scattered by the corresponding vapour	Kerr constant × 10^9	
		Calculated according to Langevin's theory	' Observed
	Per cent		
Pentane	1 28	17 9	5 0
Isopentane	1 2	16 2	5 0
Hexane	1·41	19 7	4 5 5 6
Heptane	1 40	30	7 1 10 5
Octane	1 66	43	7 7 13 6
Carbon tetrachloride	0 6	14 4	7 4
Carbon bisulphide	10 7	390	322 6
Benzene	4 40	122	59·3
Cyclohexane	1 26	26	7 4

2 *The Polarisation Field in Liquids*

Both Langevin and Born assume that, while the molecule individually is anisotropic, the polarisable matter present round it is so distributed that the local polarisation field acting on the molecule is independent of its orientation in the field There is reason to believe that this assumption cannot be correct in a dense fluid, and that, in addition to considering the anisotropy of the molecule itself, we have also to postulate an anisotropic distribution of polarisable matter in its immediate neighbourhood For the purpose of a purely formal mathematical theory it is unnecessary to discuss in detail how such anisotropic distribution of matter [illegible] We assume only that the orientation of the molecule determines [illegible] of matter around it, and therefore also the local polarisation [illegible] it That the polarisation field acting on a molecule may vary w[illegible]entation in the liquid has been previously suggested by other wr[illegible] Havelock* and Lundblad † But while these writers have put for[illegible]hesis as an independent theory of electric double refraction, we, on the other hand, consider it only as modifying the premises of the Langevin-Born theory, and find that its effect, in general, is actually to diminish the magnitude of the Kerr effect to be expected Independent evidence in support of the hypothesis is furnished by studies of X-ray diffraction, by the deviations from the Lorentz refraction formula, and by observations of light-scattering, in liquids In order, however, not unduly to lengthen this paper, we refrain from presenting this evidence here, and will merely assume the existence of the " anisotropic " polarisation field.

---

* 'Roy Soc Proc,' A, vol 84, p 492 (1911)

† 'Optik der dispergierenden Medien,' p 57 (Upsala, 1920)

The total polarisation field in a liquid is usually put equal to $\frac{4}{3}\pi\chi E$, where E is the acting external field, static or optic, as the case may be, and χ is the corresponding susceptibility of the fluid per unit volume (In what follows the susceptibility in the electrostatic and optical cases will be denoted by χ_e and χ_0 respectively) We modify the foregoing assumption and consider the local polarisation field acting on a molecule to be dependent on its orientation with respect to the external field Let us assume that, when an external electrostatic field E is incident in succession along the three principal electrostatic axes of the molecule, the polarisation field acting on it, due to the surrounding molecules, is also in the same direction, being equal to $p_1\chi_e E$, $p_2\chi_e E$, and $p_3\chi_e E$, respectively Similarly, when an optical field E is incident in succession along the three optic axes of the molecule, let the optical polarisation field acting on it lie in the same direction and be equal to $q_1\chi_0 E$, $q_2\chi_0 E$, and $q_3\chi_0 E$, respectively It is possible to discuss the general case when the electrical and the optic axes of the molecule have different directions. However, the expressions come out simpler when the two sets of axes are taken to be coincident, and since we have reason to believe from independent considerations that this assumption cannot be far from the truth, we confine ourselves to this simple case

3 *Molecular Orientation in the Field*

We proceed to derive an expression for the potential energy of the molecules when placed in an electro- or magneto-[illegible]ld. Since the discussion will be exactly similar for the two cases, we s[illegible]llows, treat specifically only the electrical case

Let a_1, a_2, a_3 be the moments induced in a [illegible] unit electrostatic field *actually* acting on it, respectively along its t[illegible]nd let b_1, b_2, b_3 be the corresponding moments induced by unit field [illegible]e, μ_1, μ_2, μ_3 are the components along these axes of the perman[illegible]ment of the molecule

Suppose now an electrostatic field E is incident along the z-axis of a system of co-ordinates fixed in space Then the actual fields acting along the axes of any molecule are $E\alpha_1(1 + p_1\chi_e)$, $E\alpha_2(1 + p_2\chi_e)$, and $E\alpha_3(1 + p_3\chi_e)$, respectively, where α_1, α_2, α_3 are the direction-cosines of these axes with respect to the direction of E Denoting the orientation of the axes of the molecule with respect to the co-ordinate axes fixed in space by the usual Eulerian angles θ, ϕ, ψ, we have

$$\left.\begin{aligned} \alpha_1 &= -\sin\theta\cos\psi \\ \alpha_2 &= \sin\theta\sin\psi \\ \alpha_3 &= \cos\theta \end{aligned}\right\}. \tag{1}$$

The potential energy of the molecule in the field is given by

$$u = -[\mu_1(1+p_1\chi_e)\alpha_1 + \mu_2(1+p_2\chi_e)\alpha_2 + \mu_3(1+p_3\chi_e)\alpha_3]\,E$$
$$-\tfrac{1}{2}[a_1(1+p_1\chi_e)^2\alpha_1^2 + a_2(1+p_2\chi_e)^2\alpha_2^2 + a_3(1+p_3\chi_e)^2\alpha_3^2]\,E^2, \quad (2)$$

which may, for brevity, be denoted by

$$-(M_1\alpha_1 + M_2\alpha_2 + M_3\alpha_3)\,E - \tfrac{1}{2}(A_1\alpha_1^2 + A_2\alpha_2^2 + A_3\alpha_3^2)\,E^2, \quad (3)$$

where

$$\left.\begin{aligned} M_1 &= \mu_1(1+p_1\chi_e) \\ M_2 &= \mu_2(1+p_2\chi_e) \\ M_3 &= \mu_3(1+p_3\chi_e) \end{aligned}\right\} \quad (4)$$

and

$$\left.\begin{aligned} A_1 &= a_1(1+p_1\chi_e)^2 \\ A_2 &= a_2(1+p_2\chi_e)^2 \\ A_3 &= a_3(1+p_3\chi_e)^2 \end{aligned}\right\} \quad (5)$$

Since u is a function of the direction cosines of the axes of the molecule, there will be a tendency for the molecules in the medium to orientate, thermal agitation, of course, acting against it When equilibrium is established, from Boltzmann's theorem, the number of molecules per unit volume, the directions of whose axes are determined by the range $\sin\theta\,d\theta\,d\phi\,d\psi$, is equal to

$$Ce^{-\frac{u}{kT}}\sin\theta\,d\theta\,d\phi\,d\psi, \quad (6)$$

where C is a constant given by the relation

$\nu =$ [illegible] molecules per unit volume

$= C$ [illegible] $d\theta\,d\phi\,d\psi$ (7)

[illegible]ation of Birefringence

We have now to [illegible] of this orientation on the refractive index of the medium for light-vibrations parallel and perpendicular to the electrostatic field

Case I —Let the electric vector of the incident light-wave ($= Z$, say) be assumed to lie along the z-axis, i e , along the electrostatic field The actual optical moments induced in a molecule along its axes are $b_1(1+q_1\chi_{0z})\alpha_1 Z$, $b_2(1+q_2\chi_{0z})\alpha_2 Z$, $b_3(1+q_3\chi_{0z})\alpha_3 Z$, χ_{0z} being the optical susceptibility along the z-axis of the medium per unit volume For brevity we may denote these expressions by $B_{1z}\alpha_1 Z$, $B_{2z}\alpha_2 Z$, and $B_{3z}\alpha_3 Z$, respectively

These moments, when resolved along the z-axis, are together equal to

$$(B_{1z}\alpha_1^2 + B_{2z}\alpha_2^2 + B_{3z}\alpha_3^2)\,Z \quad (8)$$

$= m_z Z$, say

The average value of m_z taken over all the molecules is given by

$$\overline{m_z} = \frac{\int e^{-\frac{u}{kT}} m_z \sin\theta \, d\theta \, d\phi \, d\psi}{\int e^{-\frac{u}{kT}} \sin\theta \, d\theta \, d\phi \, d\psi}, \tag{9}$$

which, after a long calculation, reduces to

$$\overline{m_z} = \frac{B_{1z} + B_{2z} + B_{3z}}{3} + 2\,(\Theta_{1z} + \Theta_{2z})\,\frac{E^2}{2}, \tag{10}$$

where

$$\Theta_{1z} = \frac{1}{45kT}\,[(A_1 - A_2)(B_{1z} - B_{2z}) + (A_2 - A_3)(B_{2z} - B_{3z}) + (A_3 - A_1)(B_{3z} - B_{1z})] \tag{11}$$

$$\Theta_{2z} = \frac{1}{45k^2T^2}\,[(M_1^2 - M_2^2)(B_{1z} - B_{2z}) + (M_2^2 - M_3^2)(B_{2z} - B_{3z}) + (M_3^2 - M_1^2)(B_{3z} - B_{1z})] \tag{12}$$

Also

$$\chi_{0z} = \nu\overline{m_z} \tag{13}$$

Case II —The light-vector is perpendicular to the electrostatic field, say, along the x-axis

We can show, just as in Case I, that the average contribution from a molecule to the optical moment along the x-axis is given by

$$\overline{m_x} = \frac{B_{1x} + B_{2x} + B_{3x}}{3} \text{[illegible]} (\Theta_{1x} \text{[illegible]})\,\frac{E^2}{2}, \tag{14}$$

where

$$\left.\begin{aligned} B_{1x} &= b_1\,(1 + q_1\chi_{0x}) \\ B_{2x} &= b_2\,(1 + q_2\chi_{0x}) \\ B_{3x} &= b_3\,(1 + q_3\chi_{0x}) \end{aligned}\right\} \tag{15}$$

χ_{0x} being the optical susceptibility of the medium along the x-axis

$$\chi_{0x} = \nu\overline{m_x} \tag{16}$$

$$\Theta_{1x} = \frac{1}{45kT}\,[(A_1 - A_2)(B_{1x} - B_{2x}) + (A_2 - A_3)(B_{2x} - B_{3x}) + (A_3 - A_1)(B_{3x} - B_{1x})] \tag{17}$$

$$\Theta_{2x} = \frac{1}{45k^2T^2}\,[(M_1^2 - M_2^2)(B_{1x} - B_{2x}) + (M_2^2 - M_3^2)(B_{2x} - B_{3x}) + (M_3^2 - M_1^2)(B_{3x} - B_{1x})] \tag{18}$$

From equations (10) and (14)

$$\overline{m_z} - \overline{m_x} = \tfrac{1}{3}(b_1q_1 + b_2q_2 + b_3q_3)(\chi_{0z} - \chi_{0x}) + [2(\Theta_{1z} + \Theta_{2z}) + (\Theta_{1x} + \Theta_{2x})]\frac{E^2}{2}. \tag{19}$$

If n_p and n_s are the refractive indices of the medium for vibrations along and perpendicular to the field,

$$\overline{m_z} = \frac{n_p^2 - 1}{4\pi\nu}, \quad \overline{m_x} = \frac{n_s^2 - 1}{4\pi\nu},$$

$$\overline{m_z} - \overline{m_x} = \frac{n_p^2 - n_s^2}{4\pi\nu} = \frac{n_0(n_p - n_s)}{2\pi\nu}, \tag{20}$$

n_0 being the mean refractive index of the medium

Also

$$\chi_{0z} - \chi_{0x} = \nu(\overline{m_z} - \overline{m_x}) \tag{21}$$

From (20), (21) and (19) we have

$$n_p - n_s = \frac{2\pi\nu}{n_0}\,\frac{2(\Theta_{1z} + \Theta_{2z}) + (\Theta_{1x} + \Theta_{2x})}{1 - \frac{\nu}{3}(b_1q_1 + b_2q_2 + b_3q_3)}\,\frac{E^2}{2} \tag{22}$$

Since the values of the optical susceptibility of the medium along and perpendicular to the field are nearly equal, we may write in equation (22)

$$\Theta_{1z} = \Theta_{1x} = \Theta_1$$

and

$$\Theta_{2z} = \Theta_{2x} = \Theta_2,$$

where

$$\Theta_1 = \frac{1}{45kT}[(A_1 - A_2)(B_1 - B_2) + (A_2 - A_3)(B_2 - B_3) + (A_3 - A_1)(B_3 - B_1)], \tag{23}$$

$$\Theta_2 = \frac{1}{45k^2T^2}[(M_1^2 - M_2^2)(B_1 - B_2) + (M_2^2 - M_3^2)(B_2 - B_3) + (M_3^2 - M_1^2)(B_3 - B_1)], \tag{24}$$

$$\left.\begin{aligned} B_1 &= b_1(1 + q_1\chi_0) \\ B_2 &= b_2(1 + q_2\chi_0) \\ B_3 &= b_3(1 + q_3\chi_0) \end{aligned}\right\}, \tag{25}$$

χ_0 being the mean value of the optical susceptibility of the medium.

Also

$$\chi_0 = \nu \frac{b_1(1 + q_1\chi_0) + b_2(1 + q_2\chi_0) + b_3(1 + q_3\chi_0)}{3},$$

$$= \frac{\nu\gamma_0}{1 - \frac{\nu}{3}(b_1q_1 + b_2q_2 + b_3q_3)}, \tag{26}$$

where

$$\gamma_0 = \frac{b_1 + b_2 + b_3}{3}$$

Substituting in (22), we finally obtain for the Kerr constant

$$\mathrm{K} = \frac{n_p - n_s}{\lambda \mathrm{E}^2} = \frac{n_0^2 - 1}{4n_0\lambda} \quad \frac{3(\Theta_1 + \Theta_2)}{\gamma_0} \tag{27}$$

When the polarisation field acting on the molecules is isotropic,

$$p_1 = p_2 = p_3 = \frac{4\pi}{3},$$

and also

$$q_1 = q_2 = q_3 = \frac{4\pi}{3},$$

$$\Theta_1 = \frac{1}{45k\mathrm{T}}[(a_1 - a_2)(b_1 - b_2) + (a_2 - a_3)(b_2 - b_3) + (a_3 - a_1)(b_3 - b_1)]\left(\frac{\delta + 2}{3}\right)^2 \quad \frac{n_0^2 + 2}{3} \tag{28}$$

and

$$\Theta_2 = \frac{1}{45k^2\mathrm{T}^2}[(\mu_1^2 - \mu_2^2)(b_1 - b_2) + \text{[illegible]} - b_3) + (\mu_3^2 - \mu_1^2)(\text{[illegible]} + 2}{3}\Big)^2 \quad \frac{n^2 + 2}{3}, \tag{29}$$

where δ is the dielectric constant of the mediu [illegible] pression (27) naturally reduces to that given by the Langevin-Born [illegible]

In the above discussion we have entirely neglected the effect of electrostriction, since it will not affect the value of the *difference* in refractive indices for vibrations along and perpendicular to the incident field

5 *Comparison of Theory and Observation*

In order to apply the foregoing modified formula to any actual liquid, we have to make some assumptions regarding the origin of the anisotropy of the polarisation field. The anisotropy might arise in the following way We replace for simplicity the molecules in the medium by the equivalent doublets placed at their respective centres The finite size of the molecules imposes naturally a limit to the closeness of approach of the doublets towards each other Round any particular molecule as centre we can describe a closed surface, entry into which by other molecules is excluded by reason of their finite size The form of the surface will naturally be determined by the shape of the molecule and will therefore, in general, be non-spherical, *i e*, the distribution of polarisable matter around the molecule under consideration will have no spherical symmetry with respect to it, and hence arises an anisotropy in the polarisation field

---

* See Debye, Marx's 'Handbuch der Radiologie,' vol 6, p. 768

We may provisionally represent this surface by an ellipsoid having the molecule at its centre, and consider, as an approximation, the distribution as well as the orientation of the molecules outside to be entirely fortuitous Then the polarisation field at the centre of the ellipsoid will be equivalent to that due to a surface charge $-\chi E \cos\theta$ per unit area at any point of the surface of the ellipsoid the normal to which makes an angle θ with the direction of E

Let us consider two simple cases

Case I —The ellipsoid is a prolate spheroid of revolution ,

$$b = c = \sqrt{1 - e^2}\ a,$$

say, where a, b, c are the semi-axes of the ellipsoid The polarisation constants along the axes are*

$$p_1 = \text{[illegible]} \left(\frac{1}{e^2} - 1\right)\left(\frac{1}{2e}\log\frac{1+e}{1-e} - 1\right) \tag{30}$$

$$p_2 \text{[illegible]} \left(\frac{1}{e^2} - \frac{1-e^2}{2e^3}\log\frac{1+e}{1-e}\right) \tag{31}$$

As an example we [illegible] pentane, which is a fairly elongated molecule. From X-ray measurements, the cross-sectional diameter of the molecule is equal to 4 90 Å U and its length is about 8 7 Å U Hence, as an approximation, we may take for the semi-axes of the ellipsoid

$$a = \left(\frac{8\ 7}{2} + \frac{4\ 9}{2}\right) \text{Å U} = 6\ 8\ \text{Å.U},$$

$$b = c = 4\ 9\ \text{Å U}$$

On calculation from these dimensions

$$p_1 = q_1 = 3\ 15,$$

$$p_2 = p_3 = q_2 = q_3 = 4\ 71.$$

---

* See Maxwell, 'Treatise on Electricity and Magnetism,' 3rd edn., vol. 2, p 69

We may also reasonably take the optical ellipsoid of the molecule to be a prolate spheroid of revolution about the geometrical axis of the molecule Using for the depolarisation factor of the light scattered by the vapour the value $r = 0{\cdot}0128$ and for the refractivity at 0°C, $n - 1 = 1\ 711 \times 10^{-3}$ per atm,

$$b_1 = 12\ 15 \times 10^{-24},$$

$$b_2 = b_3 = 9\ 01 \times 10^{-24}$$

Hence

$$A_1 = 17\ 88 \times 10^{-24},$$

$$A_2 = A_3 = 15\ 66 \times 10^{-24}$$

Also

$$B_1 = 14\ 74 \times 10^{-24},$$

$$B_2 = B_3 = 11\ 88 \times 10^{-24}$$

Therefore

$$K = 5\ 5 \times 10^{-9},$$

as against $17\ 9 \times 10^{-9}$ calculated according to the Langevin theory

The observed value $= 5\ 0 \times 10^{-9}$

Case II —The ellipsoid surrounding the molecule is an oblate spheroid of revolution

$$a = b = \frac{c}{\sqrt{1 - e^2}}$$

Then

$$p_1 = p_2 = 2\pi\left(\frac{\sqrt{1 - e^2}}{e^3}\sin\ \text{[illegible]} - \frac{1 - e^2}{\text{[illegible]}}\right), \tag{32}$$

$$p_3 = 4\pi\left(\frac{1}{e^2} - \frac{\sqrt{1 -}}{e^3}\ \text{[illegible]}\right) \tag{33}$$

As an example for this case we may take b[illegible]ene The X-ray diffraction pattern of the liquid has been critically stu[illegible] Prof Sogani* and shows two rings corresponding to mean molecular distances of 4 90 Å U and about 3 42 Å U respectively Solid benzene also gives very intense lines, corresponding to a spacing approximately equal to the above distances † We may reasonably take these distances for the semi-axes of the ellipsoid

$$a = b = 4\ 90\ \text{Å U},$$

$$c = 3\ 42\ \text{Å U}$$

We then obtain

$$p_1 = p_2 = q_1 = q_2 = 3{\cdot}56,$$

$$p_3 = q_3 = 5\ 44$$

---

[*] 'Indian Journal of Physics,' vol 1, p 357 (1927)

[†] Broomé, 'Phys Z,' vol 24, p, 124 (1923)

From $r = 0{\cdot}0440$ for the vapour and from the refractivity, assuming the optical ellipsoid of the molecule to be an oblate spheroid of revolution about the geometric axis, we get

$$b_1 = b_2 = 12{\cdot}33 \times 10^{-24},$$

$$b_3 = 6{\cdot}26 \times 10^{-24},$$

$$A_1 = A_2 = 22{\cdot}36 \times 10^{-24},$$

$$A_3 = 14{\cdot}63 \times 10^{-24}$$

Also

$$B_1 = B_2 = 16{\cdot}61 \times 10^{-24},$$

$$B_3 = 9{\cdot}57 \times 10^{-24}$$

Hence

$$K = 6{\cdot}2 \times 10^{-8},$$

as against the value $12{\cdot}2 \times 10^{-8}$ calculated according to Langevin's theory.

The observed value $= 5{\cdot}93 \times 10^{-8}$

It is necessary to remark that, considering the nature of the assumptions made, the numerical agreement in these cases should not be unduly emphasised It should be considered only as indicating that the effect of the anisotropy of the polarisation field is of the order of magnitude necessary to explain the deviation of Langevin's theory from observation

An examination of Table I shows that in all cases the influence of the anisotropy of the polarisation field is to diminish the magnitude of the Kerr effect to be expected On [illegible] umption of an ellipsoidal cavity this result finds a ready explana[illegible] fact that the longer geometrical dimension of the molecule—and th[illegible] f the ellipsoid—almost always goes hand-in-hand with the direct[illegible] er electrical or optical polarisability of the molecule

6 *Summary*

In this paper a new theory of electric and magnetic double refraction in liquids is put forward, which can in essence be regarded as a modification of the Langevin-Born theory It is assumed in the latter theory that, while the molecules themselves are anisotropic, their distribution round any particular molecule in the medium can be considered as being spherically symmetrical with respect to it. This assumption can hardly be correct in any actual liquid, so that the local polarisation field acting on any molecule must depend on its orientation The Langevin-Born theory is accordingly modified so as to take this "anisotropy" of the polarisation field also into account

The modified expression for birefringence is in better accord with facts than the Langevin-Born expression. As a rule the effect of the "anisotropy" of the polarisation field is to diminish the magnitude of the birefringence to be expected This is explicable as due to the fact that, in general, the longer linear dimension of a molecule tends to be also the direction of maximum electrical and optical susceptibility The distribution of the molecules in a dense fluid therefore tends to be such that their mutual influence is equivalent to an apparent diminution in the anisotropy of the molecules

Density of the Vapour in the Mercury Arc and the Relative Intensities of the Radiated Spectral Lines, with Special Reference to the Forbidden Line 2270.

By Prof. B VENKATESACHAR, M A , Department of Physics, University of Mysore

(Communicated by Lord Rayleigh, F R S —Received July 7, 1927)

[PLATES 1–3]

Introduction

The mercury arc line $(1\,^1S_0 - 2\,^3P_2)$* is ruled out [illegible] the selection principle as the transition $2\,^3P_2 \rightarrow 1\,^1S_0$ involves a change of [illegible] inner quantum number by 2 Takamine and Fukuda,† however, have [illegible] this line in the end-on radiation from a mercury vapour lamp of "the branched arc" type devised by Dr Metcalfe and the author‡ for the study of selective absorption in luminous mercury vapour Foote, Takamine and Chenault§ have obtained the same result using an arc discharge in mercury vapour with a hot cathode Takamine‖ has recently studied the intensity variations of this line with change of current

---

[*] *Notation*.—The number to the upper left of each term symbol represents the multiplicity, and the subscript to the right the inner quantum number The lowest term number for each class of terms is that adopted by Paschen and Götze

[†] 'Phys Rev.,' vol. 25, p. 23 (1925)

[‡] 'Roy Soc. Proc.,' A, vol 100, p. 152 (1922)

[§] 'Phys. Rev ,' vol. 26, p. 165 (1925)

[‖] 'Z f Physik,' vol. 37, p. 72 (1926)

density, using a modified form of "the branched arc" The interesting fact brought out by the above investigations is that the intensity of the line increases rapidly with current density up to about 0·25 amps cm $^{-2}$, and then falls off rapidly In addition, Takamine apparently finds that the intensity variations of the line in question run parallel to those of the band at 2345 attributed to HgH

An increase in the current density in a mercury arc is usually accompanied by an increase in the density of the vapour through which the discharge passes, and one is led to expect a modification in the character of the spectrum by an increase in the concentration of normal atoms resulting from an increase of the density of the vapour, analogous to the effect of a foreign gas like helium or argon on fluorescence in mercury vapour The present investigation was undertaken with the object of studying (1) the intensity variation of the line $1\,^1S_0 - 2\,^3P_2$ as compared with the intensities of neighbouring lines when, keeping the length of the arc, the current density in it and the voltage drop between the electrodes unaltered, the density of the vapour is varied, (2) the change in its absolute intensity when the current density is altered, the density of the vapour remaining unchanged, and (3) the influence of lowering the density of the vapour on the relative and absolute intensities of the lines belonging to a series in the arc spectrum, other conditions of excitation remaining unaltered

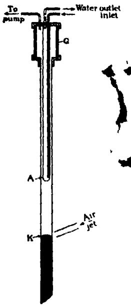

FIG 1

Apparatus

The arc discharge (fig 1) which formed the source was produced between an iron tube 36 cm long, closed at one end, and thickly electro-nickelled on the outside, and a surface of pure distilled mercury, which formed the top of a barometer column in a transparent fused quartz tube of 1 centimetre inside diameter The nickelled iron anode A and the quartz tube were joined together by two suitable iron caps and a piece of intermediary glass tube G, the cement used being shellac The anode was cooled by a current of water as shown in the figure After evacuating the apparatus by a mercury diffusion pump backed by a Hyvac pump, the arc was started by raising the mercury reservoir till the mercury surface K and the anode came in contact, and then lowering it till the arc was of the desired length. There was no condensation of mercury inside the tube above 2 to 3 cm from A. The photographs of the spectra were taken mostly with a Hilger Quartz Spectrograph (type E 2), to get the lines between 2100 and 1900 a small quartz spectrograph was improvised The plates were sensitized for the ultra-violet with Nujol The temperature of the outside surface of the quartz tube corresponding to the middle portion of the arc, which was focussed on the slit of the spectrograph, was registered by a calibrated nickel-iron thermo-couple in contact with the surface (not shown in the figure) and a millivoltmeter A large inductance was included in the circuit to steady the arc The discharge, when examined in a revolving mirror, did not exhibit the flickering often observed in mercury arcs

In describing some of the more noteworthy results the lines in the region 2258 87 ($2\,^3P_0 - 7\,^3D_1$) and 2302 09 ($2\,^3P_0 - 6\,^3D_1$) will be referred to for purposes of comparison of intensity Under suitable conditions 15 lines could be recognised in this region whose relative intensities greatly change when the density of the vapour is diminished The following wave-lengths of the lines have been measured on one of the plates with reference to the lines $2\,^3P_0 - 7\,^3D_1$, $2\,^3P_0 - 6\,^3D_1$ and $2\,^3P_0 - 5\,^3S_1$, whose wave-lengths are taken from Fowler's tables The current in the arc was 1 5 amps cm $^{-2}$ and the cathode was not cooled The relative intensities recorded in the list are from visual estimates on the plate

λ in I A	Intensity	Series Notation
2302 09	8	$2\,^3P_0 - 6\,^3D_1$
2297 94	4	$2\,^3P_1 - 9\,^3S_1$
2289 50	6	$2\,^3P_1 - 10\,^3D_2$
2285 54	3	$2\,^3P_1 - 10\,^3S_1$
2283 80	5	$2\,^3P_0 - 6\,^3S_1$
2279 39	5	$2\,^3P_1 - 11\,^3D_2$
2276 48	3	$2\,^3P_1 - 11\,^3S_1$
2271 92	5	$2\,^3P_1 - 12\,^3D_2$
2269 81	2	$1\,^1S_0 - 2\,^3P_2$ and $2\,^3P_1 - 12\,^3S_1$
2266 02	4	$2\,^3P_1 - 13\,^3D_2$
2264 36	2	$2\,^3P_1 - 13\,^3S_1$
2262 34	3	Spark line
2261 27	2	$2\,^3P_1 - 14\,^3D_2$
2260 40	1	$2\,^3P_1 - 14\,^3S_1$
2258 87	7	$2\,^3P_0 - 7\,^3D_1$

It will be seen that almost exactly in the position of the line $1\,^1S_0 - 2\,^3P_2$ (2269·79) there is also the line $2\,^3P_1 - 12\,^3S_1$ (2269 60) Allowance must be made for this coincidence in intensity measurements of the line $1\,^1S_0 - 2\,^3P_2$.

Experimental Part

In the first experiment a photograph of the spectrum was taken with an arc 6 cm long, the anode alone being cooled. The thermo-couple indicated a steady temperature of 147° C when the current density was 2 5 amps per cm $^{-2}$ On the same plate another photograph was taken in juxtaposition with the first, with the same current density, but with the cathode cooled by a jet of air, the thermo-couple indicating a steady temperature of 80° C In every case in which a jet of air was directed on the cathode for reducing the temperature of the arc particular care was taken to completely shield the part of the arc tube near the thermo-couple from the direct action of the air jet. The arc was continuous and uniform for a length of 4 cms. If the cathode is cooled beyond a certain limit the potential drop between the electrodes begins to rise rapidly and the arc eventually goes out, but it is possible so to regulate the air jet as to prevent this limit being passed The time of exposure was the same in the two cases The two photographs are shown in juxtaposition at I, II and III (Plates 1, 2) (*a*) represents the spectrum of the radiation at the lower vapour density and (*b*) that at the higher It will be seen that in I (*b*) between the lines $2\,{}^3P_1 - 13\,{}^3D_2$ and $2\,{}^3P_1 - 12\,{}^3D_2$ is a line exactly in the position of $1\,{}^1S_0 - 2\,{}^3P_2$ and $2\,{}^3P_1 - 12\,{}^3S_1$ $2\,{}^3P_1 - 13\,{}^3S_1$ is not seen in the reproduction, but is distinctly visible in the negative Therefore we have to conclude that the line between $2\,{}^3P_1 - 12\,{}^3D_2$ and $2\,{}^3P_1 - 13\,{}^3D_2$ is really $2\,{}^3P_1 - 12\,{}^3S_1$, and the forbidden line, if present at all, does not appreciably add to the brightness [illegible] ${}^3P_1 - 12\,{}^3S_1$ In I (*a*) the lines $2\,{}^3P_1 - 12\,{}^3D_2$ and $2\,{}^3P_1 - 13\,{}^3D_2$ a[illegible] The absence of the line $2\,{}^3P_1 - 11\,{}^3S_1$ makes it certain that the line [illegible]aring in the position of $2\,{}^3P_1 - 12\,{}^3S_1$ must be $1\,{}^1S_0 - 2\,{}^3P_2$, the forbidden [illegible] This line is now brighter than $2\,{}^3P_1 - 11\,{}^3D_2$ Equally marked is the incre[illegible] the brightness of the spark line 2262, relative to the line 2259 ($2\,{}^3P_0 - 7\,{}^3D_1$) This experiment shows conclusively that a lowering of the vapour density, the current density and the potential drop between the electrodes remaining unaltered, has the effect of considerably enhancing the brightness of the line $1\,{}^1S_0 - 2\,{}^3P_2$ relative to the neighbouring series lines In this respect the spark line 2262 resembles the forbidden line $1\,{}^1S_0 - 2\,{}^3P_2$. There is, however, this difference in the behaviour of the two lines In the spectrum of the radiation from the region near the cathode the spark line 2262 was found to be enhanced, whereas the forbidden line remained unaffected In the second set of experiments two photographs were taken on the same plate, the current density in one case being 2·5 amps cm.$^{-2}$ and in the other 4 amps cm.$^{-2}$. In both the temperature indicated by the thermo-couple was adjusted to 80° C by regulating the air jet The line 2270 ($1\,^1S_0 - 2\,^3P_2$) did not vary in brightness by an increase in the current density from 2 5 to 4 amps per sq cm The spark line 2262 increased in intensity when the current was raised It was more intense than the line $2\,^3P_0 - 7\,^3D_1$ It must be remarked, however, that a lowering of the surface temperature of the tube as indicated by the thermo-couple must be taken only to mean that the density of the vapour inside has fallen, no exact estimate of the change of density inside being possible in this arrangement The saturation pressure of mercury vapour at 80° C is 0 09 mm and that at 147° C about 2 mm

Series Lines.

The effect of lowering the density of the vapour is equally marked on other series lines As is well known, the spectrum of the arc in air shows only the first few lines of a series For instance not more than five lines have been recorded by Kayser and Runge in the series $2\,^3P_1 - m\,^3S_1$ The same remark applies, if anything, with greater force, to the lines of the $^1P_1{}^1D_2$ and $^1P_1{}^1S_0$ series The continuous background which is conspicuous in the radiation from an arc in air is no doubt responsible to some extent for hiding the higher members in the spectrum When the arc is formed in vacuum the higher members gain in relative intensity Nevertheless, it does not appear to have been noticed* that, for a given current density, there is an optimum density of the vapour through which the arc discharge passes for which the largest number of lines of any particular series are observed With the [illegible] described in this paper (fig 1) lines up to $2\,^1P_1 - 12\,^1S_0$ (340[illegible]) [illegible] $^1P_1 - 14\,^1D_2$ (3383·5) are distinctly observable in the spectrogram of [illegible]sion from the arc when taking a current of 2 amperes, the exposure [illegible]ng 7 minutes The cathode was not cooled and the arc was 6 cm long [illegible] and Gotz record eight lines in the $^1P_1{}^1D_2$ and four lines in the $^1P_1{}^1S_0$ series Under the same conditions of excitation lines up to the eighteenth member are clearly seen on the negative in the series $2\,^3P_1 - m\,^3D_2$ and $2\,^3P_0 - m\,^3D_1$. Now, if by directing a jet of air on the cathode the density of the vapour inside the arc tube is considerably diminished, the earlier members of all the series not only gain in intensity relative to the higher members, but under the conditions of the experiment may gain *in absolute brightness* The current density was 2·8 amps.

---

* Lord Rayleigh, in a recent interesting paper, attributes the failure of the higher members of the diffuse series to appear in the arc to Stark-effect arising from inter-atomic fields, 'Roy Soc. Proc.,' A, vol. 112, p 16 (1926)

cm $^{-2}$, the thermo-couple indicated a surface temperature of 150° C before the cathode was cooled and 80° C afterwards; other conditions of excitation were kept unaltered. In the former case no definite conclusion can be drawn regarding the vapour density inside (temp 150°), in the latter case, however, the upward stream of vapour was considerably diminished, as could be inferred from the marked fall in the amount of mercury condensed on the anode and in its vicinity a few minutes after the air jet was directed on the cathode, and the saturation vapour pressure of mercury at 80° C, about 0 1 mm of Hg, might be taken as an approximate measure of the pressure of the vapour inside. Very striking is the effect of cooling the cathode on the lines of all the series In the ${}^1P_1{}^1S_0$ and ${}^1P_1{}^1D_2$ series, lines beyond $m = 6$ rapidly fall in intensity It will be seen that in II (*a*) and III (*a*), Plates 1, 2 (low density spectrum. temperature 80° C) the lines $m = 8$ and $m = 9$ are only just visible, but that the lines $m = 3, 4, 5$ are brighter than in (*b*) (high density spectrogram temperature 150°), the enhancement of intensity being most marked in the case of the line 4916 ($2\,{}^1P_1 - 3\,{}^1S_0$) What has been said regarding lines of the ${}^1P_1{}^1D_2$ and ${}^1P_1{}^1S_0$ series applies equally to those of the ${}^3P\,{}^3D$, ${}^3P\,{}^3S$, and intercombination series, as is apparent from an inspection of I and III (Plates 1, 2) To mention only one striking instance, the line $2\,{}^3P_1 - 10\,{}^3D_2$ is stronger than $2\,{}^3P_0 - 6\,{}^3S_1$ in I (*b*), whereas in I (*a*), low density spectrogram, their relative intensities are reversed, showing that, beyond $m = 5$, the higher members of a series fall more rapidly in intensity than the lower ones when the density of the vapour through which the arc discharge passes is lowered below a certain limit An exposure of 10 minutes, which was necessary [illegible] the higher members of a series, was found to be far too long for b[illegible] such as 2536 To render an estimate of the intensity changes of these [illegible] in passing from stage (*b*) to stage (*a*) possible the exposure was reduced t[illegible] seconds The three photographs (*a*), (*b*), (*a*) (IV, Plate 2) were tak[illegible] on the same plate in juxtaposition, the two (*a*) photographs represent the low density spectrum and (*b*) represents the high density spectrum The exposure in each case was 5 seconds The statement already made that lines below $m = 5$ become brighter and that lines beyond $m = 6$ become weaker when the density of the vapour is diminished, other conditions remaining the same, is borne out by these photographs. In (*b*) the line $2\,{}^3P_2 - 7\,{}^3D_3$ is of about the same brightness as the combination line $2\,{}^3P_1 - 3\,{}^1S_0$, whereas in (*a*) (low density) the same combination line ($m = 3$) has increased in brightness, and the line $2\,{}^3P_2 - 7\,{}^3D_3$ is reduced in intensity Incidentally, it may be mentioned that the unclassified line 6123·7 remains unchanged in intensity as the arc passes to the low density stage.

Photometric Measurements

With the object of getting a quantitative idea of the intensity variation caused by a lowering of the density of the vapour, photometric measurements were made on the most prominent lines in the visible part of the spectrum An arrangement consisting of a "Lummer-Brodhun" element and two 60° flint glass prisms mounted on the table of a spectrometer provided with two collimators was used for producing in the field of view of the telescope two broad images of the slit side by side, one image being produced by the source under examination and the other by a comparison mercury vapour lamp working under steady conditions The light from the comparison lamp was polarised by a Nicol prism before falling on the corresponding collimator slit, and the adjustment to equality of brightness between the two images was effected by the rotation of another Nicol attached to the eyepiece of the telescope, whose orientation could be read off correct to a minute on a graduated circle The current in the arc was 3 amps cm $^{-2}$ The thermo-couple indicated a temperature of 150° before and 100° after the blower was directed on the cathode I_2/I_1 represents the ratio of the intensity of a line at 100° to its intensity at 150° The three lines 4916, 5790 and 5769 exhibited the largest variation —

λ	I_2/I_1
4916 $(2\,{}^1P_1 - 3\,{}^1S_0)$	1 40
5790 $(2\,{}^1P_1 - 3\,{}^1D_2)$	1 30
5769 $(2\,{}^1P_1 - 3\,{}^3D_2)$	1 30

Under the same conditions the lines [illegible] and 4047 $(2\,{}^3P - 2\,{}^3S_1)$ behaved similarly, I_2/I_1 being about 1 15

Theoretical Considerations

The spectral variation in regard to intensity in passing from stage (*b*) to stage (*a*), which has been described above, can be accounted for by taking into consideration inelastic impacts of excited and normal atoms Each second-class impact of the radiators of the lower members of a series with normal atoms gives rise to two atoms possessing abnormal kinetic energy, the excited atom, in the process, returning to the normal state or a state of lower excitation energy An atom possessing this kinetic energy—about half the excitation energy lost by the excited atom taking part in the impact—cannot by an impact with a normal atom reproduce an excited atom, yet the translational energy may be sufficient to raise an atom already excited to a higher degree of excitation. For instance, as a result of impact with an unexcited atom a mercury atom in the $2\,^3P_1$ state, in passing to the normal state, gives rise to two atoms, each possessing about the same translational energy, equal to that of a 2 4-volt electron Energetic atoms produced in this manner part with their abnormal energy to other atoms by the process of collision and thus increase the thermal energy of the vapour It may, however, sometimes happen that such an atom collides with another atom in the $2\,^3P_1$ state and produces one in the $2\,^3P_2$ state, or it may collide with an atom in the $2\,^3P_2$ state and raise it to the $2\,^1P_1$ state, the energy required to produce the latter transition being a little over that of a 1 2-volt electron What has been said for excited $2\,^3P_1$ atoms applies equally to the radiators of 5461, 4358, and of other lines The existence of such radiationless transitions is indicated by the diminution of fluorescence in mercury vapour excited by the resonance radiation, λ 2536, when nitrogen or oxygen is mixed with the vapour * That this diminution is not due to any chemical action follows from the fact that the admixture of inert monatomic gases such as helium or argon produces the same effect † It is now suggested that, in the case of the mercury arc, unexcited mercury atoms may play a similar *rôle* to that of the molecules of the foreign gas in the quenching of fluorescence The rate of loss of excited atoms of any class by impacts with normal atoms naturally increases with the density of the vapour The length of the arc, the current density in it, and the potential drop between the electrodes remaining unaltered, the increase in the intensity of the earlier members of a series when the concentration of normal atoms is diminished indicates that the increase in the rate of [illegible] of the corresponding radiators by radiationless inelastic impacts result[illegible] increase of density (stage *b*) more than compensates for any increase [illegible] of production due to the higher density

It is remarkable that in all [illegible]ries examined (including inter-combination lines) the change in the inten[illegible]ho takes place, under the conditions of the experiment, between the lines $m = 5$ and $m = 6$ On reducing the temperatures of the arc by cooling the cathode, the intensities of all lines below $m = 6$ increase and those of lines above $m = 5$ fall If the initial excited states corresponding to the transitions resulting in the emission of the higher members of a series are produced in the same manner as the initial excited states in the case of the lower members, it is difficult to account for the great reduction in the intensity of a line like $2\,^3P_1 - 8\,^3S_1$ relative to the line $2\,^3P_1 - 5\,^3S_1$ ($5\,^3S_1 - 8\,^3S_1 = 2323$) on diminishing the density of the vapour On the other hand, one should expect the reverse effect for a lowering of the concentration of normal atoms would have more marked effect in reducing the loss of excited atoms by second-class impacts with normal atoms in the case of higher excited states in which the valence electron describes larger orbits The chief source of excited atoms in the arc (beyond $m = 6$) with large valence electron orbits would appear, therefore, to be different from that of excited atoms with term numbers below five In the case of atoms in the higher states of excitation (above $m = 6$, say) the energy required to raise one to a still higher level or even to ionise it completely may be of the same order of magnitude as the kinetic energy of the available normal atoms which constitute by far the major part of the molecules in the luminous region, and impacts with such atoms can produce higher excited states The wave-number corresponding to a quantum equal to the mean kinetic energy of the gas at temperature θ may be shown to take the form

---

* Wood, 'Phys. Z.,' vol 13, p 353 (1912).

† Cario, 'Z f Physik,' vol. 10, p 185 (1922)

$$\nu = \tfrac{3}{2}\frac{R\theta}{Nhc} = 1\ 048\ \theta, \tag{1}$$

where R is the gas constant θ, the absolute temperature N, the Avogadro number h, Planck's constant, and c the velocity of light Representing the wave-number difference corresponding to the transition from a state of excitation α to a state of higher excitation β by $\nu_{\alpha\beta}$ we have

$$\frac{\text{Energy required to produce the transition}}{\text{Mean kinetic energy}} = \frac{\nu_{\alpha\beta}}{\nu} = r \text{ (say)}$$

Again representing by n_r the number of molecules in unit volume whose kinetic energies lie beyond r times the mea[illegible]gy and by n the total number of molecules per unit volume, we have

$$\frac{n_r}{n} = 1 + \sqrt{\frac{6r}{\pi}}\, e^{-\frac{3r}{2}} - \frac{2}{\sqrt{\pi}} \int_0^{\sqrt{\frac{3r}{2}}} e^{-x^2}\, dx \tag{2}$$

Let us take a particular case, the transition from the $6\,^3S_1$ to the $7\,^3S_1$ state here $\nu_{\alpha\beta} = 2765\ 0 - 2057{\cdot}5 = 707\ 5$ Taking the temperature to be 400° absolute we get from (1) 416 for ν and (2) gives for n_r/n, 0 165 Thus in a hundred neutral molecules 16 possess energies greater than $hc\nu$, and a similar calculation shows that 17 molecules in a thousand possess energies greater than $2hc\nu$ The corresponding numbers for the transition $2\,^3S_1$ to $3\,^3S_1$ are negligibly small. The increase in the temperature of the arc produced by removing the air jet from playing on the cathode has the effect not only of increasing the total molecular concentration, but also of enhancing the relative abundance of molecules, each of which possesses an amount of kinetic energy greater than the energy required to produce the transition, both effects tending to augment the intensities of the higher members of a series. The addition by this process to the atoms, say, in the $10\,^3S_1$ state results from impacts of normal atoms with excited atoms in lower energy levels, the concentration of normal atoms possessing the relative energy necessary to produce the transition diminishing with the term number of the struck excited atom For instance, about 30 per cent of normal atoms possess a translational energy above the value $hc\nu$ corresponding to the transition $8\,^3S_1 \rightarrow 9\,^3S_1$ and about 6 per cent an energy above $2hc\nu$ Except in the case of very close levels such as $3\,^1D_2$ and $3\,^3D_j$, where intertransitions to higher levels are possible by the collision of thermally energetic normal atoms, the supply to the radiators of the lower members of a series (say, of 5461) from this source may be taken to be negligible, as the concentration of molecules possessing the required energy is vanishingly small It is, however, quite otherwise with the radiators of the higher members, as has just been shown These considerations indicate that, in order to draw conclusions of a useful character, measurements of the intensity variations of spectral lines with current density must be made under conditions in which the density of the excited vapour and its temperatures are taken into account

The Forbidden Line 2270 ($1\,^1S_0 - 2\,^3P_2$)

This line behaves, in passing from stage (*b*) to stage (*a*) (low density) like the earlier members of the series lines discussed above, for as in the case of 4916 ($2\,^1P_1 - 3\,^1S_0$) and 5790 ($2\,^1P_1 - 3\,^1D_2$) its intensity is increased by lowering the concentration of normal atoms. The fact that the forbidden line grows in brightness on lowering the [illegible] of the vapour (other conditions remaining unaltered) suggests that the [illegible] of the radiation at high current densities and, therefore, generally at high vapour density, is to be ascribed to impacts of the second kind between excited atoms in the metastable state $2\,^3P_2$ and normal atoms, the struck normal atom thereby passing on to the $2\,^3P_1$ or $2\,^3P_0$ state or merely acquiring an energy of translation As the line is not enhanced near the cathode an electric field does not appear to be the cause of its emission, neither is it probable that impacts of atoms in the $2\,^3P_2$ state with normal atoms is the cause of the emission, for an increase in the concentration of normal atoms reduces the intensity of the line The existence of a strong magnetic field which might favour the emission is obviously ruled out under the conditions of the experiment These considerations would appear to indicate that the metastable state $2\,^3P_2$ is not one in which, left to itself, the excited atom remains for ever in that state, but one whose average free life is large compared with the average life of other excited atoms The chance of an atom in the metastable state losing its energy of excitation wholly or partly by radiationless impacts with normal atoms increases with increase of vapour density An approximate idea of the effect of the concentration of normal atoms on the radiation of the forbidden line may be gained by treating the problem in the manner Cario (*loc cit*) treats the case of fluorescence of mercury vapour in the presence of a foreign gas like helium or argon. If τ is the average life of the excited atom and T the average interval between two collisions of an excited atom with a normal atom the ratio of the number z_1 of excited atoms that radiate to the number $z_1 + z_2$ produced in time T is given by

$$\frac{z_1}{z_1 + z_2} = 1 - \frac{\tau}{T}\left(1 - e^{-T/\tau}\right), \tag{3}$$

z_2 is the number lost by collisions in the same time The ratio reduces to zero in the extreme case when τ is infinite, *i e*, in the case of a truly metastable atom If in any actual case τ is taken to be finite the above ratio increases with increase of T, *i e*, with diminution of density Taking 10^{-6} sec as the average free life of a mercury atom in the 2 $^3P_2$ state and the radius of the excited atom to be four times the radius of a normal atom, we get from (3), 0 015 for $z_1/(z_1 + z_2)$ at 150° C and a pressure of 1 mm of Hg, whereas at 80° C and a pressure 0 1 mm of Hg the ratio is 0 14 It must be noted that here other processes such as electronic impacts and absorption of radiation (say, of λ 5461) resulting in the loss of excited atoms in the 2 $^3P_2$ state are not considered, and it is assumed that every impact of an excited atom with a normal atom results in a radiationless transition.

Takamine (*loc cit*) thinks it probable that when the current density is increased, collisions of atoms in the metastable state and electrons resulting in radiationless transitions increase, and the intensity of the forbidden line consequently falls Though the possibility of such collisions may be admitted the enhancement of the forbidden line on lowering the density of the vapour even with current densities of the order of 3 amps per cm $^{-2}$ makes it necessary to attribute the absence of the line at high current densities in ordinary arcs (in which the concentration of normal atoms is not artificially diminished by cooling) to impacts of the second class with normal atoms As has been pointed out the life of an excited atom in the metastable state is so long that in an arc under a pressure of the order of a couple of millimetres of Hg the probability of such an atom suffering during its life an inelastic impact resulting in a radiationless transition approaches certainty.

In addition to the density of the vapour, the dimensions of the orbit of the valence electron in the excited state and the average life of the excited state affect the rate of loss of the radiators by radiationless inelastic collision with normal atoms If we assume that the average life of atoms in the excited states $2\,^3S_1$, $3\,^1D_2$, $3\,^3D_2$ and $3\,^1S_0$ to be the same photometric measurements of the intensity change of the lines $2\,^3P_{012} - 2\,^3S_1$, $2\,^1P_1 - 3\,^1D_2$, $2\,^1P_1 - 3\,^3D_2$ and $2\,^1P_1 - 3\,^1S_0$ on lowering the density of the vapour in the arc already recorded lead consistently with present ideas of spectral radiation, to the result that the dimensions of the orbits of the valence electron increase as we pass from the state $2\,^3S_1$ to the state $3\,^1S_0$ Separate measurements made on the two lines 5790 ($2\,^1P_1 - 3\,^1D_2$) and 5770 ($2\,^1P_1 - 3\,^3D_2$) give the same result ($I_2/I_1 = 1\ 30$) As the excitation energies in the higher energy levels corresponding to these two radiations do not appreciably differ, it may be taken that the rate of production of the radiators of the two lines is the same under given conditions of excitation That these two lines behave similarly when the density of the vapour is reduced therefore leads to the result that the dimensions of the orbits of the valence electron in the two initial excited states are practically the same In the case of the line 4916 ($2\,^1P_1 - 3\,^1S_0$) ($3\,^1S_0 = 9776\ 9$) the change in the intensity under the same conditions ($I_2/I_1 = 1\ 40$) is more marked than in the case of the two yellow lines, this may be taken to indicate that the size of the orbit is larger in this case For the lines 5461, 4358 and 4047 with the same initial excited state $2\,^3S_1$ ($2\,^3S_1 = 21830\ 8$) $I_2/I_1 = 1\ 15$ From this we may infer that the $2\,^3S_1$ orbit is smaller than the $3\,^1D_2$ or $3\,^3D_2$ orbit It [illegible], however, be remarked that this reasoning applies only to lines whose current term number is not more than 4, *i e*, to cases in which the excited atoms are not produced by collisions of thermally energetic normal atoms with excited atoms in lower energy levels Also the problem of the quantitative treatment of the effect of radiationless impacts of excited and normal mercury atoms in a mercury arc on the relative and absolute intensities of the radiated lines is much more complicated than the corresponding problem of the quenching of fluorescence by a foreign gas in mercury vapour In the latter case, so long as the concentration of the mercury atoms and the intensity of the external stimulus (whether a beam of resonance radiation or a stream of 4 9-volt electrons) are kept constant, a change in the molecular concentration of the foreign gas may be taken not to affect the rate of production of atoms in the $2\,^3P_1$ state, but the change alters the rate at which these excited atoms are put out of action so far as the radiation of the resonance line is concerned. This is not so in the case of the arc, where a change in the concentration of normal mercury atoms affects both the rate at which the excited atoms of any class are produced and the rate at which they are lost by radiationless impacts with normal atoms

Lord Rayleigh* has examined the spectrum of the luminous vapour issuing from a mercury vapour lamp in two stages, (I) at a short distance, about 2 cms from the anode (" out of the region of the electric current "), (II) at a much greater distance from it   He finds that the intensities of the lower members of a series relative to the higher ones are very much greater in (II) than in (I) According to the considerations put forward above, this change is to be attributed to the lower temperature and far lower density of the vapour in the region far removed from the hot anode, and the consequent paucity of normal atoms which by impacts with excited atoms could increase the excitation energy of the struck excited atoms at the expense of their own kinetic energy and thus add to the radiators of the higher members   It has been shown above that the two stages can be reproduced in the arc itself by artificially lowering the temperature and density in it

A variation in the apparatus was made to test, firstly, whether in an arc with a large dead space the intensity variations that have been already described can be observed , and, secondly, whether a foreign gas such as nitrogen introduced into the arc can take the place of an excess of mercury vapour in bringing out the higher series members   The arc discharge tube employed is shown in fig 2   A bent copper tube thickly electro-nickelled on the outside and kept

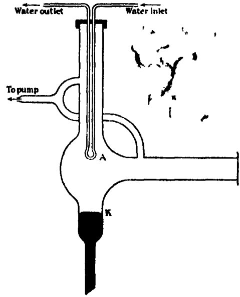

FIG 2.

---

* 'Roy Soc. Proc ,' A, vol 108, pp 267-270 (1925)

cool by a current of water formed the anode and the top of a barometer column of mercury formed the cathode in a pyrex glass tube of internal diameter 2 6 cm (fig. 2). The light to the spectrograph passed from the arc through a side tube closed by a crystalline quartz plate The evacuation was effected, as in the previous case, by a mercury diffusion pump backed by a Hyvac pump The arc was started by first heating the top of the mercury column and then passing through the vapour the discharge from a small induction coil

The study of a large number of spectrograms taken with this apparatus under different known conditions lead to the following results —

1 When the pressure is kept very low by the continuous action of the evacuating system and maintaining a free flow of water through the hollow anode, the higher members of the series lines beyond the current term number 11 are absent in the spectrogram, and lines $m = 7$, 8 and 9 are very faint and $m = 10$ is hardly visible The potential drop between the electrodes was 11 5 volts In one case a number of photographs was taken on the same plate with exposures varying from 5 minutes to 2 hours with a current of 4 amps flowing in the arc, to see if the absence of the higher members was due to the lack of right exposure But not a trace of any line beyond $m = 11$ could be seen in any case V (*a*) and VI (*a*) (Plate 3), not even in cases in which the exposure was so prolonged that the strong series lines showed photographic reversal The forbidden line 2270 under these circumstances comes out quite distinctly and stands comparison in intensity with the line $2\,^3P_0 - 6\,^3S_1$ Here, again, the spark line 2262 behaves like the forbidden line and shows up prominently in the spectrogram (VI (*a*)[illegible]

2 After shutting off t[illegible]on with the pump and admitting air into the apparatus through a leak [illegible]he pressure rose so high that the potential drop between the electrodes increased from 11 5 to 17 volts, the spectrogram, taken with an exposure of 15 minutes, revealed lines up to $m = 20$ in the series $2\,^3P_2 - m\,^3D_3$ (V (*b*), Plate 3), and till $m = 18$ in the series $2\,^3P_1 - m\,^3D_2$ (VI (*b*), Plate 3) and $2\,^3P_0 - m\,^3D_1$ On increasing the pressure still further till the voltage drop was 20 volts, it was found that the same number of lines could be again noticed, but they were fainter *and sharper* From this it seems probable that the molecules of a foreign gas can take the place of normal mercury atoms and generate radiators of higher members of series lines by impacts of the first kind with excited atoms in lower energy levels It must be mentioned that the admission of air brought out the band spectrum of nitrogen so prominently that between λ 5000 and λ 2800 it overshadowed the mercury lines to the extent of hiding all but the most prominent of them The existence

of excited nitrogen molecules after admitting air renders it somewhat doubtful whether the addition to the radiators of higher members is due to impacts of excited nitrogen molecules and excited mercury atoms in lower levels or whether it is due to impacts of thermally energetic normal molecules of nitrogen and excited mercury atoms. It is, however, not easy on the former hypothesis to account for the enhancement of the intensity of the higher members of a series *relative* to the lower ones Experiments using helium in place of air are in progress

Spark Lines

If the density of the vapour is reduced by cooling the arc, other conditions of excitation remaining unaltered, many of the spark lines which usually occur in the spectrum of the radiation from a mercury arc are greatly reduced in intensity, while others either remain unchanged or gain in intensity A classified list of the lines under the two heads is given below —

I

	Intensity in stage (*b*)	Intensity in stage (*a*), low density	Remarks
4959 7	5	0	K*
3984 1	8	4	K
3860 4	6	0	K
3820 6	8	0	K
3790 4	8	0	K
3770 7	4	0	K
3755 0	2	0	
3751 8	5	0	K
3616 0	2	0	
3579 9	2	0	
3561 5	5	[illegible]	K
3543 7	7	1	K
3430 2	3	0	Stark records a line at 3431 7
3390 5	7	2	K
3367 0	2	0	
3351 5	4	0	
2820 0	4	1	K
2774 7	2	0	K
2686 6	2	0	
2002 9 (vac)	3	0	
1974 0 (vac)	3	0	

---

* K indicates that the line was found enhanced in the spectrum of the radiation from near the cathode, K (fig 1).

II.

	Intensity in stage (*b*)	Intensity in stage (*a*), low density	Remarks
2847 8	4	4	K
2814 9*	2	2	
2262 4†	3	5	K
2260 4	0	2	K
2053 7 (vac)	1	2	
2028 3 (vac)	0	1	
1942 5 (vac)	10	>10	This line, according to Carroll, belongs to the first pair of the principal series of the spectrum of Hg^+

* The line 2814 9 has not been recorded by others as far as I can make out from the available literature My plate shows two other lines, 2813 0 and 2810 5 The latter is nebulous Paschen and Götz suggest that 2810 5 may be $2\,^3P_2 - 5\,^3P_2$ (2813 4 calc) It appears more probable that 2813 0 appearing in the plate is $2\,^3P_2 - 5\,^3P_2$

† Takamine finds that the intensity variations of this line are somewhat different from those of the neighbouring arc lines when the current density is varied (*loc cit*)

If we consider the behaviour of the spark lines to be similar to the behaviour of the arc lines we have to conclude that, in the case of those lines which, like the lower members of the series lines in the arc spectrum, either remain unaltered or increase in intensity on lowering the density of the vapour, the initial energy levels of atoms of Hg^+, which are responsible for the radiation, are low, whereas the corresponding levels in the case of the lines, which, like the higher members of the arc series, have their intensities greatly reduced under the same circumstances, are high One is therefore led to expect to find in group II of the classified list given above the earlier members of the principal and subordinate series of the spectrum of H[illegible] According to J A Carroll the lines 1942 5 and 1649 8 form the first pa[illegible] the principal series This view is supported by the absorption experiments of Compton and Turner* on the line 1942 5 It follows as a consequence that the radiators of 1942 5 are in the energy level next higher to the ground level, and accordingly we find that the line distinctly increases in intensity when the arc passes to the low density stage (VII, Plate 3) The line 1649 8 is outside the range of the spectrographs used Of the remaining lines in group II the difference between the wave-numbers of the lines 2847 8 and 2260·4 is 9122, and differs from the wave-number difference of 1942 5 and 1649·8, viz , 9133, by a quantity which is within the limits of the errors involved in the wave-length determinations of the latter pair of lines The "Rydberg doublet," 2847·8 and 2224 8, does not appear to form the first pair of a subordinate series, as the corresponding wave-number difference, viz, 9829, is far removed from 9131 Moreover, the line 2224 8 is absent in both spectrograms, though it can be produced as an enhanced line if the radiation from the cathode is focussed on the slit This line falls close to the arc line $2\,^3P_0 - 8\,^3S_1$ But it is clear from an examination of the spectrograms that the line, if present at all in stage (*b*), is absent in stage (*a*) (low density) The line 2260 2, on the other hand, increases in intensity when the density is lowered This line (2260 4) again falls almost exactly on the line $2\,^3P_1 - 14\,^3S_1$, but the absence of the lines $2\,^3P_1 - 12\,^3S_1$ and $2\,^3P_1 - 13\,^3S_1$ makes it certain that the line occupying the position of $2\,^3P_1 - 14\,^3S_1$ in I (*a*) (Plate 1), is not $2\,^3P_1 - 14\,^3S_1$, but the spark line 2260 4

---

* 'Phys. Rev ,' vol. 25, p 613 (1925) In this paper the authors refer to Carroll's classification of Hg^+ spectrum.

It is of interest to consider the manner in which the radiators of the spark lines are generated in the arc Starting from the singly ionised atom of mercury we find that the excitation energy required to produce a radiator of 1942·5 is that of a 6·4-volt electron, and the chance of an Hg^+ atom encountering an electron possessing an energy not less than this amount in the positive column is small We therefore have to look for other sources of production A likely method is by the encounter of Hg^+ atoms with neutral excited atoms in the $2\,^1P_1$ state, the excitation energy of the $2\,^1P_1$ state being that of a 6·67-volt electron Further higher energy levels may be produced by encounters of excited Hg^+ atoms produced in this manner with electrons or neutral atoms in the $2\,^3P_1$ states. This view receives support from the observation of Lord Rayleigh* that the line $1\,^1S_0 - 2\,^1P_1$ is much reduced in intensity relative to the prominent lines of the triplet series, and that at the same time the spark lines are very faint in the spectrum of the luminous vapour issuing from a mercury arc

Takamine states that in his experiments the band at 2345 ascribed to HgH always appeared with the forbidden line 2270, and that its intensity variations ran parallel to those of the latter In the experiments described in the present paper this parallelism has not been observed In the spectrograms taken with the first type of arc (fig 1) no traces of this band could be detected whether the forbidden line is present when the density of the vapour inside is artificially diminished or whether it is absent when the density of the vapour is not so diminished (I, Plate 1) With the second type of arc (fig 2) this band, together with three others on the shorter wave-length side, which have been observed by Lord Rayleigh (*loc. cit.*) in the vapour issuing from a mercury arc are prominent in the spectrogram taken with air as impurity inside the tube

---

* 'Roy Soc. Proc.,' A, vol. 108, p. 266 (1925), and vol. 112, p. 18 (1926).

(VI (*b*), Plate 3), the forbidden line being absent or very faint. In the spectrogram of the low density arc, where the forbidden line is prominent, the band is absent (VI (*a*) Plate 3)

Summary

1 The effect of altering the density of the vapour in a mercury arc (other conditions of excitation being kept unaltered) on the relative and absolute intensities of the radiated lines has been studied within the approximate pressure range of 2 mm to 0 1 mm of Hg The current density employed ranged between 1 5 amps cm $^{-2}$ and 4 amps cm $^{-2}$ The effect of lowering the density of the vapour on the series lines in the arc spectrum (including inter combination lines) is to increase the absolute intensities of all lines below $m = 5$ and diminish those of all lines above $m = 6$ It is pointed out that this result can be explained on the hypothesis that inelastic collisions between excited atoms in lower energy levels and thermally energetic normal atoms form the chief source of the radiators of the higher members of series lines To the radiators of the lower members the contribution from this source is negligible This accounts for the intensity diminution of the higher members when the vapour density is diminished On increasing the vapour density collisions between the radiators of the lower members and normal atoms resulting in radiationless transitions increase and the intensities of these lines fall The forbidden line 2270 ($1\,^1S_0 - 2\,^3P_2$), like the lower members of other series lines, increases in intensity when the arc passes to the low density stage This happens even when the current density is as high as 3 amps cm $^{-2}$

2 In one set of photometric measurements the line 4916 ($2\,^1P_1 - 3\,^1S_0$) showed the largest percentage increase of intensity on lowering the density of the vapour ($I_2/I_1 = 1\ 40$) Next came the lines 5769 ($2\,^1P_1 - 3\,^3D_2$) and 5790 ($2\,^1P_1 - 3\,^1D_2$) ($I_2/I_1 = 1\ 30$) The lines 5461, 4358 and 4047 ($2\,^3P_{012} - 2\,^3S_1$) showed the smallest increase ($I_2/I_1 = 1\ 15$) These figures suggest that the dimensions of the orbits of the valence electron in the excited states $2\,^3S_1$, $3\,^1D_2$ ($3\,^3D_2$) and $3\,^1S_0$ are in increasing order of magnitude

3 The spark lines that are excited in a mercury arc may be classified under two heads (i) those whose intensities are greatly diminished and (ii) those whose intensities remain unaltered or increase on lowering the density of the vapour To the second class belong lines whose radiators are excited Hg^+ atoms in lower energy levels, these lines are 2847 8, 2262 4, 2260 4, 2053 2, 2028 8 and 1942 5 in the wave-length range accessible to the spectrographs used. It is suggested that the lines 2847 8 and 2260 4 form the first pair of a

II

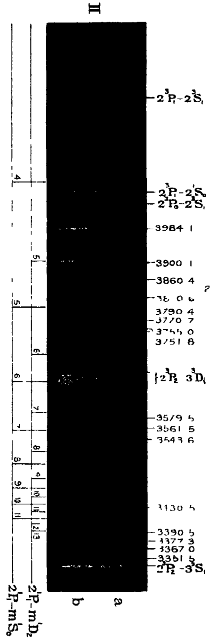
2³P₁-2³S₁
2³P₁-2¹S₀
2³P₀-2³S₁
3984 1
3900 1
3860 4
3810 6
3790 4
3770 7
3755 0
3751 8
2³P₂ 3³D₁
3579 5
3561 5
3543 6
3430 5
3390 5
3377 3
3367 0
3351 5
2³P₂-3³S₁
4
5
5
6
6
7
7
8
8
9
9
10
10
11
11
12
13
b
a
2¹P₁-m¹D₂
2¹P₁-m¹S₀

I

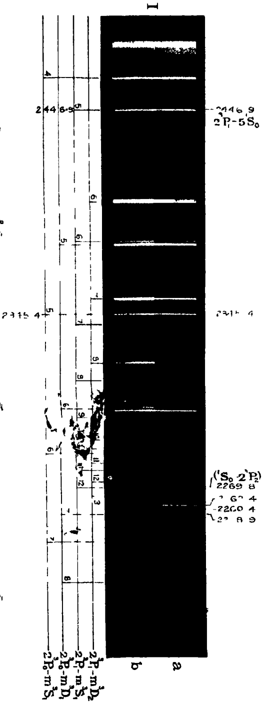
2446 9
2³P₁-5¹S₀
2446·9
2335 4
2335 4
(¹S₀ 2³P₂)
2269 8
2264 4
2260 4
2258 9
4
5
5
5
6
6
6
6
7
7
8
8
9
9
10
11
12
12
13
b
a
2³P₀-m³S₁
2³P₀-m³D₁
2³P₁-m³S₁
2³P₁-m³D₂

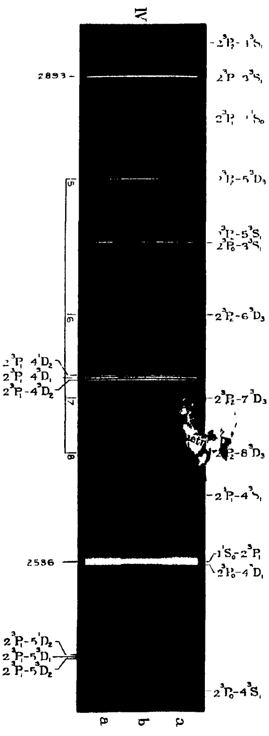
IV
2893
2536
5
6
7
8
2³P₂-1³S₁
2³P 3³S₁
2³P₁ ¹S₀
2³P₂-5³D₃
2³P₂-5³S₁
2³P₀-3³S₁
2³P₂-6³D₃
2³P₁ 4¹D₂
2³P₁ 4³D₁
2³P₁-4³D₂
2³P₂-7³D₃
2³P₂-8³D₃
2³P₁-4³S₁
1¹S₀-2³P₁
2³P₀-4³D₁
2³P₁-5¹D₂
2³P₁-5³D₁
2³P₁-5³D₂
2³P₀-4³S₁
a
b
a

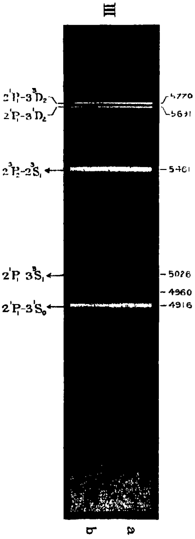
III
2¹P₁-3³D₂
2¹P₁-3¹D₂
5770
5691
2³P₂-2³S₁
5461
2¹P₁ 3³S₁
5026
4960
2¹P₁-3¹S₀
4916
b
a

VI

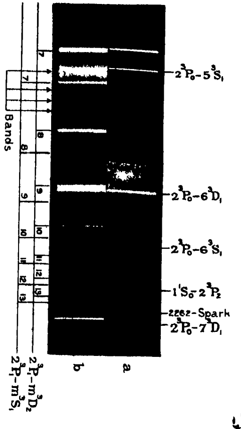
7
7
8
8
9
9
10
10
11
11
12
12
13
13
Bands
$2^3P_0-5^3S_1$
$2^3P_0-6^3D_1$
$2^3P_0-6^3S_1$
$1^1S_0-2^3P_2$
2262-Spark
$2^3P_0-7^3D_1$
$2^3P_1-m^3D_2$
$2^3P_1-m^3S_1$
b
a

V

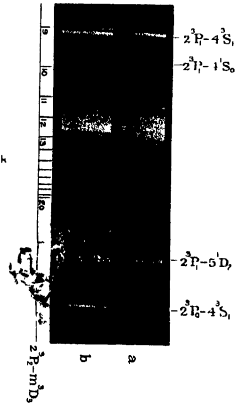
9
10
11
12
13
20
$2^3P_1-4^3S_1$
$2^3P_1-4^1S_0$
$2^3P_1-5^1D_2$
$2^3P_0-4^3S_1$
$2^3P_2-m^3D_3$
b
a

VII

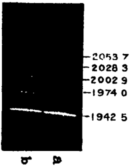
2053 7
2028 3
2002 9
1974 0
1942 5
b
a

subordinate series in the spectrum of Hg^+, 1942·5 and 1642·5, according to Carroll, forming the first pair of the principal series.

4. In a mercury vapour lamp with a large dead space it was found that higher members of series lines were developed on raising the pressure made by the introduction of air. On pumping out the air higher members beyond $m = 11$ disappeared completely, while the forbidden line 2270 and the spark line 2262 became conspicuous

DESCRIPTION OF PLATES 1–3.

In every case (*a*) represents the low density spectrum and (*b*) the high density spectrum (pressure about 2 mm. of Hg)

I, II and III are enlargements of different parts of two spectra, (*a*) and (*b*), taken on the same plate in juxtaposition and with equal exposure, the source being the arc represented in fig. 1; the cathode was cooled in the case of (*a*) IV represents corresponding portions of three photographs, (*a*), (*b*) and (*a*), taken in juxtaposition on another plate with an exposure of 5 seconds in each case. It will be seen that in all the four, series lines below $m = 6$ are brighter in (*a*) than in (*b*), and that lines beyond $m = 5$ are stronger in (*b*) than in (*a*). The forbidden line 2270 ($1\,^1S_0 - 2\,^3P_2$) and the spark lines 2262 and 2260 are enhanced in passing from (*b*) to (*a*) in I In III note that lines $2\,^3P_1 - 2\,^3S_1$ (4358) and $2\,^3P_0 - 2\,^3S_1$ (4047) are solarised in the centre by over-exposure

V and VI are parts of photographs taken with the arc represented in fig 2, as source (*a*) and (*b*) were taken on different plates, in the case of (*b*) the pressure in the tube was raised by leaking air into it Higher members of series lines absent in (*a*) are brought out in (*b*). The forbidden line 2270 and the spark line 2262 are prominent in (*a*)

VII (*a*) and VII (*b*) are reproductions from photographs taken on the same plate with the same exposure, but not in juxtaposition Of the five spark lines, two, viz., 1974 and 2003, prominent in (*b*), have almost disappeared in (*a*) 2028, though faint in both, is brighter in (*a*).

For details see paper

Correction.—In Plate 1, *read* $1\,^1S_0 - 2\,^3P_2$ *for* [illegible] $2\,^3P_2$ *and* $2\,^3P_2 - 3\,^3D_3$ *for* $2\,^3P_2 - 3\,^3D_1$.

On the Input Limit of an X-Ray Tube with Circular Focus.

By ALEX MÜLLER

(Communicated by Sir William Bragg, F R S —Received July 15, 1927)

Introduction

The input limit of an X-ray tube depends upon various factors, one of which is the heat produced on the anticathode by the impinging cathode rays

The present paper attempts a calculation of the input limit for an X-ray tube with circular focus

Statement of the Problem (First Section)

The anticathode is assumed to be a straight cylinder of circular cross section The following system of co-ordinates is chosen The X axis is the axis of the cylinder whose length is l and whose diameter a The origin O coincides with the centre of one of the boundary planes, the centre of the focus lies in the middle of the other face Both limiting planes are perpendicular to the X axis and have therefore both circular boundaries

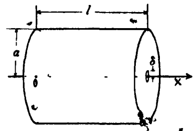

Firstly, the case will be considered where (*a*) The inflow of heat (cathode ray stream) is concentrated upon a small area round the focus centre, and (*b*) the curved surface of the cylinder and the flat end containing the origin are both kept at a constant temperature T This surface condition can be obtained by cooling with a rapid stream of water

Solution of the Problem

If T be the temperature and κ the thermal conductivity of the material, we then have for the stationary flow of heat the well-known equation

$$\operatorname{div} \kappa \operatorname{grad} T = 0$$

which holds for the inside of the cylinder

κ is, generally speaking, a function of the temperature The variation of κ with T being relatively small, κ will be treated as a constant in the present calculations The above equations written in cylindrical co-ordinates reduces therefore to

$$(1) \qquad \frac{\partial^2 T}{\partial r^2} + \frac{1}{r}\frac{\partial T}{\partial r} + \frac{\partial^2 T}{\partial X^2} = 0$$

A solution of (1) has now to be found which fulfils the boundary conditions The problem can be solved in the usual way A short analysis will be useful in the final discussion We put

$$(2) \qquad T - T_0 = \sum_1^{\infty} a_n \ \mathfrak{C}_0\left(\lambda_n \frac{r}{a}\right) \ \sinh\left(\lambda_n \frac{X}{a}\right)$$

where λ_n is the n^{th} root of $\mathfrak{C}_0(\rho) = 0$ $\mathfrak{C}_0$ is the Bessel function of zero-order (2) is a solution of (1) and vanishes for $x = 0$ and $r = a$ in agreement with the boundary conditions given so far

The next step will be to define the function describing the heat inflow in the focus This requires the knowledge of the energy distribution in the cathode ray stream in the immediate neighbourhood of the anticathode It is not intended here to discuss this distribution in detail Two important facts are known about the function $f(r)$ representing the energy inflow in the focus $f(r)$ reaches its maximum for $r = 0$ and drops very rapidly when r increases

$$(3) \qquad f(r) = A \ \ e^{-Br^2}$$

is likely to represent the actual conditions fairly well, and will be used in the present calculations A and B are two constants which can be expressed in terms of measurable quantities One of these quantities is the total amount of energy W which flows in unit time into the anticathode, and which can be calculated from the voltage and the current [illegible] the X-ray tube (The small fraction of energy which is actually converted into X-rays can be neglected here) The other quantity is the radius δ of the focus spot δ will be defined as follows —

It is the length which, when introduced into (3), will make $f(r)$ drop to half of its maximum value We therefore have

$$W = 2\pi A \int_0^a r e^{-Br^2} dr = \pi \frac{A}{B}(1 - e^{-Ba^2})$$

and

$$\tfrac{1}{2} = e^{-B\delta^2}$$

In all practical applications e^{-Ba^2} is very small compared with l and can be neglected Taking this into account, it follows that

$$(4) \qquad f(r) = W \ \ \frac{ln 2}{\pi\delta^2} e^{-\frac{ln 2}{\delta^2} r^2}$$

The coefficients a_n are now calculated in the usual way by making use of the well-known properties of the Bessel functions

$$\int_0^a \mathfrak{C}_0\left(\frac{\lambda_m}{a} r\right) \mathfrak{C}_0\left(\frac{\lambda_s}{a} r\right) r \quad dr = 0 \quad \text{if } m \neq s,\ m \text{ and } s \text{ being integers,}$$

and

$$\int_0^a \mathfrak{C}_0^2\left(\frac{\lambda_n}{a} r\right) r \; dr = \frac{a^2}{2} \mathfrak{C}_0'(\lambda_n)$$

Remembering that

$$\mathfrak{C}_0(\lambda_n) = 0, \quad n = 1, 2, 3$$

Differentiating (2) gives

$$\frac{\partial T}{\partial x} = \sum_1^\infty a_n \frac{\lambda_n}{a} \; \mathfrak{C}_0\left(\frac{\lambda_n}{a} r\right) \; \cosh\left(\frac{\lambda_n}{a} x\right)$$

and for $x = l$

$$f(r) = \kappa \sum_1^\infty a_n \frac{\lambda_n}{a} \mathfrak{C}_0\left(\frac{\lambda_n}{a} r\right) \; \cosh\left(\frac{\lambda_n}{a} l\right) \tag{5}$$

Multiplying both sides of (5) by $r \; \mathfrak{C}_0\left(\frac{\lambda_n}{a} r\right)$ and integrating between the limit $r = 0$ and $r = a$, we finally have

$$a_n = \frac{W}{a\kappa} \; \frac{2 ln 2}{\pi\delta^2} \; \frac{1}{\cos\left(\frac{\lambda_n}{a} l\right)} \; \frac{1}{\lambda_n \mathfrak{C}_0'^2(\lambda_n)} \int_0^a r \; e^{-\frac{ln 2}{\delta^2} r^2} \; \mathfrak{C}_0\left(\frac{\lambda_n}{a} r\right) \; dr \tag{6}$$

(6) combined with (2) is the complete solution of the problem stated at the beginning

The expression for a_n can be written in a much more compact form We first remember that δ is small compared with a Without introducing an appreciable error into numerical calculations, we can write

$$\int_0^a r \; e^{\frac{ln 2}{\delta^2} r^2} \mathfrak{C}_0\left(\frac{\lambda_n}{a} r\right) dr \approx \int_0^\infty r \; e^{-\frac{ln 2}{\delta^2} r^2} \mathfrak{C}_0\left(\frac{\lambda_n}{a} r\right) dr, \tag{7}$$

$r \; e^{-\frac{ln 2}{\delta^2} r^2}$ being extremely small when r reaches a The definite integral in (7) can be evaluated (see, for instance, Gray and Mathews 'Treatise on Bessel Functions') as follows

$$\int_0^\infty r \; e^{-\frac{ln 2}{\delta^2} r^2} \mathfrak{C}_0\left(\frac{\lambda_n}{a} r\right) dr \approx \frac{\delta^2}{2 ln 2} \quad e^{-\left(\frac{\lambda_n}{a}\right)^2 \frac{\delta^2}{4 ln 2}}. \tag{8}$$

Further using the approximate values for the Bessel functions and the roots λ_n

$$\mathfrak{C}_0'(y) \approx \sqrt{\frac{2}{\pi y}} \; \cos\left\{y - \frac{\pi}{4}\right\}$$

and

$$\lambda_n \approx (n - 1/4)\pi \quad n \text{ integer,}$$

we write

$$\lambda_n \mathfrak{C}_0'^2(\lambda_n) \approx \frac{2}{\pi} \, *$$

Therefore

$$a_n \approx \frac{W}{a\kappa} \frac{1}{2\cosh\left(\frac{\lambda_n}{a} l\right)} \cdot e^{-\left(\frac{\lambda_n}{a}\right)^2 \frac{\delta^2}{4 ln 2}}$$

and for $r = 0$ and $x = l$ (centre of the focus)

$$(9) \qquad T_f - T_0 \approx \frac{W}{a\kappa} \sum_1^\infty \tfrac{1}{2} \tanh\left(\frac{\lambda_n}{a} l\right) \quad e^{-\left(\frac{\lambda_n}{a}\right)^2 \frac{\delta^2}{4 ln 2}},$$

where T_f is the temperature in the centre of the focus

The series which is involved in (9) converges very rapidly (except in the case when δ/a is very small) and is well suited for numerical calculations When δ/a is very small the sum in (9) can be written in form of an integral as follows

$$s_n = \lambda_n \quad \frac{\delta}{a} \frac{1}{2\sqrt{ln 2}}$$

Using the approximate values for λ_n

$$\lambda_n \approx \pi(n - 1/4),$$

we write

$$s_{n+1} - s_n = \frac{\delta}{a} \frac{\pi}{2\sqrt{ln 2}} = \Delta s$$

and

$$l \frac{\lambda_n}{a} = s_n \quad \frac{2\sqrt{ln 2}}{\delta} \quad l = \beta \, s_n,$$

and obtain

$$T_f - T_0 \approx \frac{W}{\kappa\delta} \frac{\sqrt{ln 2}}{\pi} \sum_1^\infty e^{-s_n^2} \quad \tanh(\beta \quad s_n) \quad \Delta s$$

For δ/a vanishing this becomes

$$(10) \qquad T_f - T_0 \approx \frac{W}{\kappa\delta} \quad \frac{\sqrt{ln 2}}{\pi} \quad \int_0^\infty e^{-s^2} \tanh(\beta s) \quad ds, \; \beta = \frac{2\sqrt{ln 2}}{\delta} \quad l$$

It will be interesting to consider two limiting cases, *i e*, when β is very large and β very small

$\beta = \infty$ tanh (βs) reaches very soon the value 1 and it follows

$$(11) \qquad \underset{\beta=\infty}{T_f - T_0} \approx \frac{W}{\kappa\delta} \frac{\sqrt{ln 2}}{\pi} \int_0^\infty e^{-s^2} ds = \frac{W}{\kappa\delta} \cdot \frac{\sqrt{ln 2}}{\pi} \frac{\sqrt{\pi}}{2},$$

---

* Maximum deviation from true value (occurring when $n = 1$) is approximately 2 per cent.

β very small

$$\text{(12)} \qquad \underset{\beta\ \text{small}}{T_f - T_0} \approx \frac{W}{\kappa\delta}\frac{\sqrt{ln 2}}{\pi}\int_0^\infty \beta s e^{-s^2}\,ds = \frac{W}{\kappa\delta}\frac{\sqrt{ln 2}}{\pi}\,\frac{\beta}{2}$$

The dimensions of W and κ have to be considered κ is usually given in gm cal cm $^{-1}$ sec $^{-1}$ centigr $^{-1}$ It is convenient to express W in watts, in which case the W in the preceding formulæ has to be multiplied by 0 2389 δ, a and l are measured in cms

Before entering into a discussion another case with altered boundary conditions will be considered

Statement of the Problem (Second Section)

The only difference between the new problem and the previous one lies in the assumption that there is no flow of heat through the curved face of the cylinder, *i e*, this new boundary condition is introduced instead of the $T = T_0$ when $r = a$ The condition $T = T_0$ when $x = 0$ remains the same We therefore have

$$\text{(13)} \qquad \frac{\partial T}{\partial r} = 0 \quad \text{when} \quad r = a$$

Solution of the Problem (Second Section)

The following expression will satisfy the new conditions

$$\text{(14)} \qquad T - T_0 = \sum_1^\infty a_n \mathfrak{C}_0\left(\frac{\lambda_n}{a}r\right)\sinh\left(\frac{\lambda_n}{a}x\right) + \alpha\ x,$$

λ_n is now the n^{th} root of $\mathfrak{C}'_0(\rho) = 0$

Here again it will be ass[illegible]ed that the inflow of heat takes place only in the immediate neighbourhood o[illegible] the focus centre, *i e*, for $x = l$ and $r = a$ this inflow is zero

$$\underset{x = l}{\overset{r = a}{}}\ \frac{\partial T}{\partial x} = 0 = \sum_1^\infty a_n \frac{\lambda_n}{a}\mathfrak{C}_0(\lambda_n)\cosh\left(\frac{\lambda_n}{a}l\right) + \alpha$$

or

$$\text{(15)} \qquad \alpha = -\sum_1^\infty a_n \frac{\lambda_n}{a}\mathfrak{C}_0(\lambda_n)\cosh\left(\frac{\lambda_n}{a}l\right)$$

(In the corresponding calculations of the previous section α is zero) Substituting this expression for α into (18) leads to

$$\text{(16)} \quad T - T_0 = \sum_1^\infty a_n\left[\mathfrak{C}_0\left(\frac{\lambda_n}{a}r\right)\sinh\left(\frac{\lambda_n}{a}x\right) - x\frac{\lambda_n}{a}\mathfrak{C}_0(\lambda_n)\cosh\left(\frac{\lambda_n}{a}l\right)\right].$$

The coefficients a_n can now be calculated in exactly the same way as in the previous section

$$\frac{\partial T}{\partial x} = \sum_1^\infty a_n \frac{\lambda_n}{a}\left[\mathfrak{C}_0\left(\frac{\lambda_n}{a} r\right)\cosh\left(\frac{\lambda_n}{a} x\right) - \mathfrak{C}_0(\lambda_n)\cosh\left(\frac{\lambda_n}{a} l\right)\right]$$

and for $x = l$

$$\kappa\frac{\partial T}{\partial x} = f(r) = \kappa\sum_1^\infty a_n \frac{\lambda_n}{a}\cosh\left(\frac{\lambda_n}{a} l\right)\left[\mathfrak{C}_0\left(\frac{\lambda_n}{a} r\right) - \mathfrak{C}_0(\lambda_n)\right]$$

Multiplying both sides of this equation with $r\ \mathfrak{C}_0\left(\frac{\lambda_n}{a} r\right)$ and integrating between $r = 0$ and $r = a$ gives

$$\int_0^a r\ f(r)\,\mathfrak{C}_0\left(\frac{\lambda_n}{a} r\right)\ dr$$

$$= \kappa\ a_n \frac{\lambda_n}{a}\cosh\left(\frac{\lambda_n}{a} l\right)\left[\frac{a^2}{2}\mathfrak{C}_0^2(\lambda_n) - \mathfrak{C}_0(\lambda_n)\int_0^a r\mathfrak{C}_0\left(\frac{\lambda_n}{a} r\right)dr\right]$$

It is easily shown that

$$\int_0^a r\mathfrak{C}_0\left(\frac{\lambda_n}{a} r\right)dr = 0,^*$$

and it follows that

$$a_n = \frac{W}{a\kappa}\ \frac{2 ln 2}{\pi\delta^2}\frac{1}{\cosh\left(\frac{\lambda_n}{a} l\right)}\ \frac{1}{\lambda_n\mathfrak{C}_0^2(\lambda_n)}\int_0^a r\ \mathfrak{C}_0\left(\frac{\lambda_n}{a} r\right)e^{-\frac{ln 2}{\delta^2} r^2}\,dr$$

Introducing the same restrictions with regard to the size of δ/a and extending the limit of integration from zero to infinity

$$a_n \approx \frac{W}{a\kappa}\ \frac{1}{\pi}\ \frac{1}{\cosh\left(\frac{\lambda_n}{a} l\right)}\frac{1}{\lambda_n\mathfrak{C}_0^2(\lambda_n)}\ e^{-\frac{\lambda_n^2}{4 ln 2}\frac{\delta^2}{a^2}},$$

for $x = l$ and $r = 0$ (focus centre),

---

* Introducing a new variable $y = \frac{\lambda_n}{a} r$, we write

$$\int_0^a r\,\mathfrak{C}_0\left(\frac{\lambda_n}{a} r\right)dr = \frac{a^2}{\lambda_n^2}\int_0^{\lambda_n} y\,\mathfrak{C}_0(y)\,dy,$$

and using the well known relation

$$y\,\mathfrak{C}'_1(y) = y\,\mathfrak{C}_0(y) - \mathfrak{C}_1(y),$$

$$\int_0^{\lambda_n} y\,\mathfrak{C}_0(y)\,dy = \int_0^{\lambda_n} y\,\mathfrak{C}'_1(y)\,dy + \int_0^{\lambda_n}\mathfrak{C}_1(y)\,dy = y\,\mathfrak{C}_1(y)\Big|_0^{\lambda_n} - \int_0^{\lambda_n}\mathfrak{C}_1(y)\ dy\ + \int_0^{\lambda_n}\mathfrak{C}_1(y)\,dy,$$

and since $-\mathfrak{C}_1(\lambda_n) = \mathfrak{C}'_0(\lambda_n) = 0$,

$$\int_0^{\lambda_n} y\,\mathfrak{C}_0(y)\,dy = 0$$

$$T_f - T_0 \approx \frac{W}{a\kappa}\sum_1^{\infty}\left(\frac{1}{\lambda_n \mathfrak{C}_0^2(\lambda_n)}\frac{1}{\pi} \quad \tanh\left(\frac{\lambda_n}{a}l\right) - \frac{l}{a}\frac{1}{\pi}\frac{1}{\mathfrak{C}_0(\lambda_n)}\right) e^{-\frac{\lambda_n^2}{4\ln 2}\frac{\delta^2}{a^2}}$$

The approximate values for the Bessel function and the roots are

$$(16\text{A}) \qquad \mathfrak{C}_0(y) \approx \sqrt{\frac{2}{\pi y}}\cos\left(\frac{\pi}{4} - y\right),$$

$$(16\text{B}) \qquad \lambda_n \approx \pi(n + 1/4), \qquad n = 1,\ 2,\ 3,$$

We write

$$\lambda_n \mathfrak{C}_0^2(\lambda_n) \approx \frac{2}{\pi}$$

and obtain

$$(17) \qquad T_f - T_0 \approx \frac{W}{a\kappa}\sum_1^{\infty}\left(\tfrac{1}{2}\tanh\left(\frac{\lambda_n}{a}l\right) + \frac{l}{a}\frac{-1}{\pi\mathfrak{C}_0(\lambda_n)}\right)e^{-\frac{\lambda_n^2}{4\ln 2}\frac{\delta^2}{a^2}},$$

or, putting $\sigma = /\delta a$,

$$(18) \qquad T_f - T_0 \approx \frac{W}{\kappa\delta}\sum_1^{\infty}\frac{\sigma}{2}\tanh\left(\frac{\lambda_n}{a}l\right) \ e^{-\frac{\lambda_n^2}{4\ln 2}\sigma^2} + \frac{W}{\kappa\delta}\frac{l}{a}\frac{\sigma}{\pi}\sum_1^{\infty}\frac{-e^{-\frac{\lambda_n^2}{4\ln 2}\sigma^2}}{\mathfrak{C}_0(\lambda_n)}$$

The series which are involved in (17) or (18) converge very rapidly except when σ is very small In this case the sums can again be converted into integrals The transformation of the first term has already been given in the first section An approximate value of the second sum can be obtained by using the asymptotic expressions (16A) and (16B)

$$\frac{-1}{\pi\mathfrak{C}_0(\lambda_n)} \approx \pm\sqrt{\frac{n + 1/4}{2}}$$

The + sign holds when $n = 1,\ 2,\ 5,$

The — sign holds when $n = 2,\ 4,\ 6,$

We put

$$S = \sum_1^{\infty}\frac{-\sigma}{\pi\mathfrak{C}_0(\lambda_n)}e^{-\frac{\lambda_n^2}{4\ln 2}\sigma^2}$$

The positive terms of S can therefore be written

positive

$$+\sigma\sqrt{\frac{2m + 5/4}{2}}\,e^{-\frac{\pi^2}{4\ln 2}(2m + 5/4)^2\sigma^2}$$

the negative

$$-\sigma\sqrt{\frac{2m + 9/4}{2}}\,e^{-\frac{\pi^2}{4\ln 2}(2m + 9/4)^2\sigma^2}$$

where m is now 0, 1, 2, 3, . . therefore

$$S = \sum_0^{\infty}\sigma\left(\sqrt{m + 5/8}\quad e^{-\frac{\pi^2}{4\ln 2}(m + 5/8)^2\sigma^2} - \sqrt{m + 9\ 8}\quad e^{-\frac{\pi^2}{\ln 2}(m + 9/8)^2\sigma^2}\right).$$

Introducing new variables

$$y_m = \sigma(m + 5/8) \tag{19}$$

$$\bar{y}_m = \sigma(m + 9/8)$$

and

$$\left.\begin{aligned}\Delta y_m &= \sigma\Delta m\\ \Delta\bar{y}_m &= \sigma\Delta m\end{aligned}\right\} \text{ where } \Delta m = 1$$

and multiplying both sides with $\sqrt{\sigma}$

$$\sqrt{\sigma}S \approx \sum_0^\infty \left(\sqrt{y_m}\, e^{-\frac{\pi^2}{\ln 2} y^2_m}\ \Delta y_m - \sqrt{\bar{y}_m}\, e^{-\frac{\pi^2}{\ln 2}\bar{y}^2_m}\ \Delta\bar{y}_m\right)$$

or for very small σ

$$\sqrt{\sigma}S \approx \int_{5/8\sigma}^\infty \sqrt{y}\ \ e^{-\frac{\pi^2}{\ln 2}y^2} dy - \int_{9/8\sigma}^\infty \sqrt{y}\, e^{-\frac{\pi^2}{\ln 2}y^2} dy$$

The limits of these integrals are obtained from (19) by putting $m = 0$ and $m = \infty$ The last equation can be written as follows

$$\sqrt{\sigma}\ \ S \approx \int_{5/8\sigma}^{9/8\sigma} \sqrt{y}\, e^{-\frac{\pi^2}{\ln 2}y^2}\ dy$$

Neglecting higher terms of σ we can write

$$e^{-\frac{\pi^2}{\ln 2}y^2} \doteq 1$$

(σ varying between $5/8\,\sigma$ and $9/8\,\sigma$ and σ very small)

$$\sqrt{\sigma}S \approx \int_{5/8\sigma}^{9/8\sigma} \sqrt{y}\, dy = \frac{2}{3}\left\{\frac{9\sqrt{9} - 5\sqrt{5}}{8\ 2\sqrt{2}}\right\}\sigma\sqrt{\sigma}$$

$$S \approx 0{\cdot}466 \times \sigma, \tag{20}$$

We write* the first sum in (18) in form of an integral, substitute (20) in (18) and express W in watt

$$T_f - T_0 \approx \frac{0{\cdot}2389\,W}{\kappa\delta}\,\frac{\sqrt{\ln 2}}{\pi}\int_0^\infty e^{-x^2} \tan\beta x\, dx + \frac{0{\cdot}2389\,W}{\kappa\delta}\ \ \frac{l}{a} \times 0{\cdot}466\sigma$$

or

$$T_f - T_0 \approx \frac{W}{\kappa\delta} \times 0{\cdot}0633 \int_0^\infty e^{-x^2} \tan(\beta x)\, dx + 0{\cdot}1115\ .\ \frac{W}{\kappa}\ \ \frac{l}{a^2} \tag{21}$$

$$\beta = \frac{2\sqrt{\ln 2}}{\delta}\ \ l\ (\sigma \text{ very small})$$

---

* The variable x in this and following integrals is used with the same meaning as s in the first section.

General Discussion.

It is interesting to compare the results of the first and the second section. Dimensions, conductivity, size of the focus and input being the same, we expect to find a higher temperature in the focus centre in the case where there is no flow of heat through the curved boundary of the cylinder Comparing (9) with (17) or (10) with (21), it is seen that there is indeed an additional term in (17) or (21) which expresses this fact It is further obvious that for a very thin anticathode and small σ the two temperatures should be very nearly equal It is easily seen that the second term in (21) becomes small compared with the first when l approaches zero The first term in (21) is equal to the one in (10), *i e*, the temperatures are nearly the same The second term in (17) or (21) can, in general, assume any value between zero and infinity Its size depends upon the factor l/a^2

The Integral $\theta = \int_0^\infty e^{-x^2} \tanh(\beta x)\, dx$

A few words may be said about the method by which the integral θ can be computed This integral is a function of β There are two cases to be considered

β small —

tanh (βx) is developed in a series of increasing powers of (βx) and "e^{-x^2} series" integrated term* by term This gives —

$$\theta = \frac{1}{2}\beta - \frac{1}{6}\beta^3 + \frac{4}{15}\beta^5 - \frac{34}{105}\beta^7 \quad ,$$

β large —

A very convenient asymptotic series for θ can be found † Tanh (βx) is first developed into a series of increasing powers of $e^{-2n\beta x}$. This gives —

$$\theta = \int_0^\infty e^{-x^2} dx + 2\sum_1^\infty (-1)^n \int_0^\infty e^{-x^2-n\beta x} \; dx$$

---

* The series for tanh (βx) is convergent for $(\beta x)^2 < \left(\frac{\pi}{2}\right)^2$ The "term by term" integration between the limits zero to infinity is therefore not legitimate The upper limit of integration is $|x| < \left|\frac{\pi}{2\beta}\right|$ Owing to the fact that $e^{-\left(\frac{\pi}{2\beta}\right)^2}$ is very small when x reaches the limit, the integration can be stopped there without introducing an appreciable error into numerical calculations (always provided that β is sufficiently small)

† See, *e g*, Bromwich, "An Introduction to the Theory of Infinite Series," chapter on summation of asymptotic series.

Further

$$2\int_0^\infty e^{-x^2-2n\beta x}\,dx = 2e^{(n\beta)^2}\int_0^\infty e^{-(x+n\beta)^2}\,dx,$$

and putting $(x+n\beta)^2 = y$

$$= e^{(n\beta)^2}\int_{(n\beta)^2}^\infty \frac{1}{\sqrt{y}}\,e^{-y}\,dy$$

An integration by parts of this integral gives the following expression —

$$e^{(n\beta)^2}\int_{(n\beta)^2}^\infty \frac{1}{\sqrt{y}}\,e^{-y}\,dy = \frac{1}{n\beta}\left\{1-\frac{1}{2\,(n\beta)^2}+\frac{1\cdot 3}{2^2\,(n\beta)^4}-\frac{1\cdot 3\cdot 5}{2^3\,(n\beta)^6}+\cdots\right\}$$

and

$$\theta = \frac{\sqrt{\pi}}{2}-\frac{1}{\beta}\,ln\,2+\frac{1}{2\beta^3}\sum_1^\infty\frac{1}{\kappa^3}-\frac{1\cdot 3}{2^2\,\beta^5}\sum_1^\infty\frac{1}{\kappa^5}+\frac{1\cdot 3\cdot 5}{2^3\,\beta^7}\sum_1^\infty\frac{1}{\kappa^7},$$

$$\kappa = 1,\,2,\,3,\,4,\,\ldots\infty,$$

or

$$\theta = 0\cdot 8862-\frac{1}{\beta}\times 0\cdot 6931+\frac{1}{\beta^3}\times 0\cdot 4512-\frac{1}{\beta^5}$$
$$\times\, 0\cdot 7295+\frac{1}{\beta^7}\times 1\cdot 869-$$

Limits of Input.

The limiting input can now be calculated very easily The highest temperature in the focus which can practically be allowed is the melting temperature of the anticathode material Take first the case where the anticathode radius is very large compared with the radius of the focus spot, and where the temperature at the two boundaries is kept constant From (10) we obtain for the maximum input $W_{max.}$

$$(22)\qquad W_{max} = 15\cdot 8\times\frac{(T_m-T_0)\ \delta\ \kappa}{\theta},\quad \theta=\int_0^\infty e^{-x^2}\tanh\,(\beta x)\,dx$$

$$\beta = 2\sqrt{ln\,2}\ \frac{l}{\delta}$$

T_m = melting point (centigr)

W_{max} in watt

κ in gm cal sec $^{-1}$ cm $^{-1}$ centigr $^{-1}$

δ in cm (radius of focus spot)

The following table shows how θ varies with β —

Table I

$\beta = 2\sqrt{ln}\,2\,\frac{l}{\delta}$	$\theta = \int_0^\infty e^{-x^2} \tanh(\beta x)\,dx$
0	0
0 10	0 0498
0 50	0 235
2 50	0 632
5 00	0 751_5
10 00	0 817_2
∞	0 886_2

Let δ, a, κ, T_m be fixed and l be the variable Table I then shows that the maximum input reaches its smallest value for an infinitely long anticathode and increases very slowly when l becomes smaller An appreciable rise in W_{max} takes place only when l becomes very small, i e, when l is a small fraction of δ In other words, a considerable increase of the maximum input cannot be obtained unless the thickness of the anticathode is small compared with the focus radius In all practical work this is barred by the fact that the cooling cannot be kept up when the anticathode is very thin

A few numerical examples will finally be given, the data being taken from practical work

First Example—Kaye and Laby's tables gives the following data for the thermal conductivity of copper, $\kappa_{18} = 918$, $\kappa_{100} = 908$ (The relatively small change of κ with the temperature justifies the assumption which has been made at the beginning, namely, that κ is constant) Extrapolated to the melting point, $\kappa \approx 79_{,}$ Introducing this value in (26), we calculate a W_{max} which is too small and leave therefore a certain safety margin We assume that 1,080° centigr is the m p of copper, and that the temperature of the cooling water is in the neighbourhood of 20° The following table gives W_{max} for various thicknesses of the anticathode —

Table II

Copper anticathode, $\delta = 05$ cms, δ/a very small $\kappa \approx 79$ gm cal cm $^{-1}$ sec $^{-1}$ centigr $^{-1}$

l cms	W_{max} (watt.)
0	∞
0 003	$13\ 2 \times 10^3$
0 015	$2\ 82 \times 10^3$
0 075	$1\ 04 \times 10^3$
0 150	$0\ 880 \times 10^3$
0 300	$0\ 809 \times 10^3$
∞	$0\ 747 \times 10^3$

The table shows clearly that a substantial rise of W_{max} over its smallest value occurs only when the anticathode is very thin A strict experimental test of (22) has not been carried out yet A rough test has shown that the present deductions give at least the right order of magnitude for W_{max}

Second Example—In this example it will be assumed that the radius δ is no longer very small compared with a We put

$$\delta = 0{\cdot}05 \text{ cms} \ , \ a = 0 \ 25 \ (\sigma = 0 \ 20), \ \kappa \simeq 0 \ 79, \ T_m - T_0 = 1060$$

$$W_{max} = \frac{\kappa \ \delta \ (T_m - T_0)}{0{\cdot}2389 \times \frac{\sigma}{2} \times \sum_1^\infty e^{-\frac{\lambda_n^2}{\ln 2}\left(\frac{\sigma}{a}\right)^2} \ \tanh \frac{\lambda_n}{a} l}$$

(λ_n roots of the Bessel function of zero order)

The integral in the formula now being replaced by the sum The following table gives the result of the calculations —

Table III

l cms	W_{max} watt
0 003	13 2 × 10^3
0 015	2 82 × 10^3
0 030	1 65 × 10^3
0 075	1 04 × 10^3
0 150	0 880 × 10^3
0 300	0 841 × 10^3
∞	0 838 × 10^3

A comparison of the two examples shows that the W_{max} are the same so long as l is small For large l they begin to differ from each other, the final ratio being about 1 12

Third Example—It is well known that the cathode in a gas-filled X-ray tube becomes pitted in the centre when a discharge has been running for some time There is no doubt that this is not due to heating alone Under certain circumstances, however, a heating produced by reverse currents does take place It is interesting to find out how high the temperature is likely to rise under such conditions

A cylindrical cathode rod (aluminium) showed a circular pit of about 1 5 mms diameter, the diameter of the rod was approximately 1 5 cms The cathode was, when under working conditions, inserted into a water jacket at one end 20 cms of its length were surrounded by a gas of low pressure, the flow of heat through the curved surface of the rod being therefore practically zero. The temperature in the focus of the reverse cathode stream can be estimated with the use of formula (18). The calculation gives

$$T_f - T_0 \approx \frac{0.2389 \times W}{\kappa\delta} \left\{0.198_0 + \frac{l}{a} \times 0.0500_5\right\},$$

$$\delta = 0.075 \text{ cms}, \quad a = 0.75 \text{ cms}, \quad l = 20 \text{ cms}$$

$$T_f - T_0 \approx \frac{W}{\kappa} \times 4.88$$

The thermal conductivity of Al is 500° centigr. is approximately 0.44 gm. cal. cm $^{-1}$ sec $^{-1}$ centigr $^{-1}$ (extrapolated from data in Kaye and Laby's tables). The X-ray tube was run at about 40 kilo-volts, the reverse current being not more than one-fifth of the current recorded by the milliammeter, *i.e.*, about five milliamps. Therefore W $\approx$ 40 watt. The temperature of the cooled end of the cathode was not more than 50°–80°. The resulting temperature of the focus is therefore

$$T_f = 4.88 \ \frac{40}{0.44} + 80 = 525 \text{ centigr.},$$

which is considerably below the m.p. of aluminium (660°). This seems to support the view that the pitting was not due to melting.

In conclusion, the author wishes to express sincerest thanks to Sir William Bragg for the very encouraging interest which he has taken in this work.

The Dielectric Constants of Ammonia, Phosphine and Arsine

By H E Watson, D Sc

(Communicated by F G Donnan, F R S —Received July 21, 1927)

The dielectric constant of ammonia at various temperatures between 19° and 175° has been measured by Jona,* Bädeker† has also determined its value from 18° to 108°, and K Wolf‡ has recently measured the rate of change of dielectric constant with pressure

Jona showed that the change in dielectric constant with temperature could be represented by Debye's equation $\epsilon - 1 = N(A + B/T)$, and Zahn§ has shown that this relation also holds for the series of gases HCl, HBr, HI It was considered of interest, therefore, to make similar measurements for the gases PH_3 and AsH_3, and to repeat the determinations for NH_3, in order to provide data for another series of gases in the periodic table It has not been possible so far to examine SbH_3, as the rapid decomposition of this gas with the formation of a mirror would readily break down the insulation of a condenser of the ordinary type

A brief perusal of the literature of dielectric constants is sufficient to show that, in spite of the extreme sensitiveness of methods depending upon the use of the thermionic valve, the results do not agree as closely as might be expected. In the present research special attention has been devoted to exploring sources of constant error and to obtaining absolute values for the dielectric constants.

EXPERIMENTAL

Determinations of the dielectric constants were made at high frequency, the change in capacity with pressure of a condenser containing gas being compensated by a variable condenser in series so as to maintain the frequency of the system constant An exact setting was obtained by the method of beats with a second oscillating system

The general arrangement of the apparatus is shown in fig 1, the actual position of the component parts being a matter of some importance The main oscillating circuit consisted of a valve V, a low loss inductance C, reaction coil

---

* 'Physikal Z.,' vol 20, p 14 (1919)

† 'Z physikal Chem ,' vol 36, p 305 (1901)

‡ 'Physikal Z ,' vol. 27, p 588 (1926)

§ 'Physical Rev ,' vol 24, p 400 (1924)

R, a variable condenser K, the gas condenser G, and a switch S The whole system rested upon an earthed zinc sheet, from which it was very carefully insulated where necessary, the batteries being supported on blocks of paraffin wax. The valve V was a cosmos S P 18 red spot, very much under-run (1 18 v. on the filament, as compared with the normal 1 8), and with only

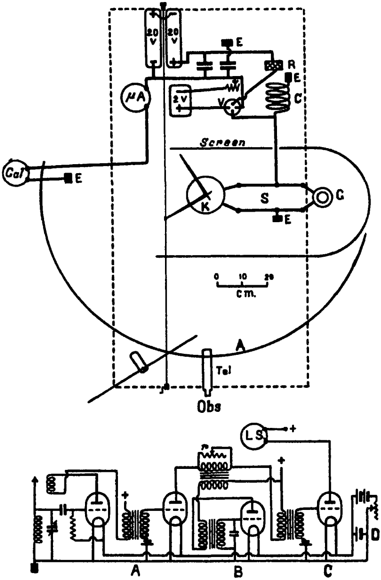

FIG 1

40 volts on the plate A microammeter (for rough settings) and a galvanometer were placed in series between the negative side of the filament and earth and measured the small grid current which was allowed to flow In this way it was possible to adjust the voltage across the condensers and also to make calibration measurements, which did not require the extreme accuracy of setting given by the beat method, in the manner described by P A Cooper * This author utilises the very sharp dip in grid current when the circuit is brought into resonance with an absorption wave meter The frequency may be measured by this means, and small energy losses, such as those due to poor insulation, are readily detected Owing to the special characteristic of the valve used, no grid bias battery was necessary, one possible source of error being thus eliminated The method had, by numerous previous trials, been found very convenient and accurate provided the condensers were screened from the inductances

All measurements were made when the grid current was 10μ A, corresponding with 2 85 volts r m s as measured by means of a Moullin voltmeter In the case of the series connection, the voltage across the gas condenser was about 8 per cent lower than this The valve characteristic under operating conditions was very straight, except just at the ends, and the harmonics could not be detected in the receiver used for the beat measurements In any case, the presence of harmonics of small amplitude can have little effect upon the results, as the dielectric constants measured were found not to change through the range of frequency studied

Three coils, which were readily interchangeable, were used in position C, they were wound over frames of pyrex tube and had inductances of 55, 160 and 1875 microhenries The switch S consisted of six copper mercury cups mounted on quartz rods 15 cm high The condenser system was surrounded by a screen 20 cm high, not closer than 15 cm to any of the wiring except where a rigid lead to the grid passed through a hole in it It was open at the top and underneath the gas condenser G, which was suspended from a wooden arm

The condenser K, upon which all the measurements were made, was of the usual semicircular rotary vane type, with five fixed plates of radius 45 mm and four moving plates, the gap being just under 1 mm, and the total capacity 250 $\mu\mu$F The fixed plates were soldered to brass strips and supported by three quartz rods platinised at the ends and soldered into sockets Before assembly, these rods were heated to redness for some time and then dropped into paraffin wax. The spindle carrying the moving plates had carefully ground long conical

---

* 'J Sci. Instrum,' vol 2, p 342 (1925)

bearings and carried two light wooden arms and two mirrors at right angles at its upper end The vanes could be rotated through about 100° by two threads, one passing over a free pulley and supporting a weight, the other similarly arranged, but passing round a friction pulley controlled by the operator By changing the threads to the other arm the condenser could be rotated through 180° The position of the plates could be read by means of the telescope T and a semicircular scale A two metres in length The whole condenser was silvered and covered with a brass cover, through a mica window in which the lead to the fixed plates passed

The gas condenser G was somewhat similar to the one described by Zahn,* and is shown in fig 2, *a* The inner cylinder had tightly fitting ends

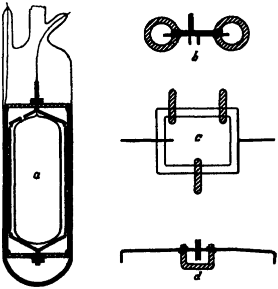

FIG 2

and contained a durosil glass bulb to reduce the volume of gas The outer cylinder had a cap over the end as a shield Two quartz discs held the inner cylinder in position These were platinised at three points at the edges and secured to the outer cylinder with small fragments of solder The inner cylinder was soldered to the top plate, but was kept in position at the bottom with a nut and spring washer to avoid strains The metal used was brass, well gilt before assembly The clearance between the cylinders was 0 5 mm and the capacity 133 $\mu\mu F$ Gilt platinum leads were used, and the whole was sealed into a durosil tube

---

* *Loc cit.*

The circuit for the production of beats is also shown in fig 1 This portion of the apparatus was situated about 2·5 metres from the oscillating circuit, and an aerial 1 metre long was used for the two lower frequencies The portion A consists of an oscillating detector and note amplifier, B is an audio-oscillator which modulates the output at a frequency of about 600, the intensity being controlled by the variable shunt *r* C is another note magnifier connected with a loud speaker S P 18 red and green spot valves were used in this receiver, and the total plate current was only 2 milliamperes The double system of low-tension batteries employed by several other observers was used, and, by regulating the discharge from the battery D, the effects of changing filament and anode voltage in the whole system could be largely compensated A screen was originally placed between the observer and the receiver, but it was found to be unnecessary, as the taking of readings through a telescope involved the observer's remaining in the same position. Small movements had no effect

When making measurements, the beat note between the two high-frequency circuits was adjusted to the exact frequency of the audio note by observation of the beats between the two.

Calibration

As has been pointed out by Zahn,[*] the accurate determination of dielectric constants is largely a problem in calibration Great attention has been paid by other observers, notably E C Fritts,[†] who used a photographic method for recording beats, to the constancy of the oscillation generators and the exact coincidence of the beats, but it is evident from their results that the main errors are constant ones arising probably from incorrect calibration.

In the present experiments the simple oscillation generators already described were found to be quite satisfactory, although possibly not altogether suitable for gases with a very low dielectric constant or for observations extending over considerable periods, but any errors arising from this source were certainly small when compared with those due to other causes

The accuracy aimed at for the final results was 1 per cent , and to attain this it was considered desirable to attempt to make all calibrations with an accuracy of 1 part in 1000 and to measure pressures and temperatures to 0 5 mm. and 0 2° respectively

All the condensers used were specially constructed or selected so as to have a very low power factor. Any defect could at once be detected by the grid current readings The insulation throughout the oscillating system was very high, and, consequently, energy losses in the condensers were assumed to be zero

---

[*] *Loc. cit*

[†] 'Physical Rev ,' vol 23, p 345 (1924)

In setting up apparatus in which connections have to be made to condensers, if the leads are short and the condensers close together, stray capacities of uncertain magnitude may be introduced, while if the leads are long, it is necessary to correct for their inductance In the present experiments the latter alternative has been adopted, as it was possible to determine the corrections with sufficient accuracy, while the location of the gas condenser a little distance (40 cm) from the variable condenser was convenient for its immersion in the constant temperature baths

If l, the inductance of the leads to a condenser of capacity C, is small enough to make $l\omega^2C$ a small quantity compared to unity, as it was in the present experiments, the apparent capacity may be written $C(1 + l\omega^2C)$ When two condensers C_1C_2 are in parallel, the inductance of the leads to C_1 being l_1 and between C_1 and C_2, l_2, the correction becomes approximately $l_1\omega^2(C_1 + C_2)^2 + l_2\omega^2C_2^2$

These formulæ were verified experimentally during the calibrations, and, on applying the corrections, the values found for the capacity of every condenser under different conditions were the same to less than 1 part in 1000, except in certain cases which are mentioned later

The condenser, which was used as a standard of capacity, consisted of a quartz tube platinised and heavily silvered inside and out and fitted with terminals This, together with its leads, was standardised at the National Physical Laboratory and found to be of constant capacity at frequencies from 300 to 1500 k c , although increasing in apparent capacity at somewhat higher frequencies The actual capacity was 156 0 $\mu\mu$ F The absolute value does not, however, affect the results

By means of this condenser Q, the setting of the variable condenser K at which it had the same capacity as Q was determined, and also several pairs of settings between which the difference in capacity was equal to that of Q A step-by-step calibration, using the small fixed condenser C shown in fig 2, *b* and *c*, was then made, and a table of values drawn up giving the capacity at all settings In making this calibration the frequency varied, but the coil inductance L was constant The inductance of the leads to C was negligible, and thus, if l is the inductance of the leads to K, the lead correction is $l\omega^2K^2 = Kl/L$ with sufficient accuracy The actual value of l/L with the three coils used was 0 0065, 0 0022 and 0 0002, and was thus not negligible in the first two cases The inductance l was determined by measuring the apparent value of the standard Q at different frequencies It is evident from these figures that considerable errors may arise when the coil inductances are very small unless allowance is made for lead inductance

The behaviour of the variable condenser K was remarkably satisfactory The absolute value over certain ranges was checked against Q at frequent intervals, and no change greater than 1 scale division in 2500 was ever observed The portion which was used for the majority of the readings was uniform within the limit of experimental error, and two careful step-by-step calibrations at the beginning and end of the experiments, using different inductances, gave, when corrected for lead inductance, identical calibration values to 0 1 μμF

The next stage was to determine the capacity of a condenser of approximately 1500 μμF capacity for use in parallel with K It was desirable that this should be as small in dimensions as possible to avoid stray capacities One or two commercial mica condensers were tried and found to stop oscillations in the circuit owing to their bad power factor A series of condensers was then constructed by platinising and silvering thin sheets of mica These had a satisfactory power factor, but were rather fragile Subsequently Dubilier-type 610 mica condensers were found to be almost as good, and these were employed throughout the experiments A series with nominal capacities 200, 300, 500, 1000, 1500 and 2000 μμF were used for the calibration in conjunction with K, the useful capacity of which was about 200 μμF Permanent leads were attached, which fitted into the mercury cups and suspended the condensers clear of surrounding objects Each condenser was calibrated in three different positions, and this afforded a means of calculating the inductance of the leads and allowing for stray capacities, which, however, were very small When the smallest inductance was used, corrections for these factors did not yield quite concordant results, owing, no doubt, to the somewhat complex nature of the circuits For example, in order to determine the value of D_{1000}, as the 1000μμF condenser was designated, it was placed in parallel with K and then replaced by D_{500} and D_{300} in different pairs of mercury cups, and the change in K necessary to bring the frequency to its previous value determined. The circuit contained several loops, and the simple lead correction appears to be insufficient for the smaller values of L If no corrections at all are applied, the difference is quite marked, for example, D_{1500} was found to have the values 1528·5 and 1533 6 when using the medium and small inductances respectively On the other hand, two distinct calibrations, with an interval of two months between them, using the large and medium inductances, after applying corrections, both gave the figure 1526 0 at 17 6° It was found that this condenser had an appreciable temperature coefficient (− 0 00033 per 1°), which was allowed for Owing to the slight uncertainty of the calibration with the small inductance, it was assumed that the true value of the capacity of this condenser at the higher frequencies was the same as the one determined with the other inductances

As already mentioned, when measurements of dielectric constant were made, the gas condenser was placed in series with the large mica condenser, and this introduced complications in the form of stray capacities Two systems of connections were used, which are shown diagrammatically in fig 3, *a* and *b*,

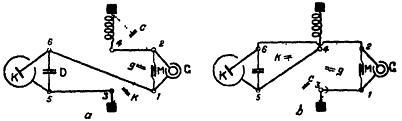

Fig 3

the numbers 1–6 denoting the mercury cups in the switch Each lead may be regarded as having two capacities, one to earth and one to adjacent leads If C is the self-capacity of the inductance coil and K and G are the capacities of the variable and gas condensers respectively, the stray capacities *c*, *k* and *g* may be represented as being in parallel with them, as indicated in the diagrams D is the large mica condenser and M a very small condenser, which will be referred to later

If, now, G increases by an amount *d*G and K is decreased by *d*K in such a way as to keep the capacity of the whole system constant, it is easy to show that

$$dG = \frac{(G+g+M)^2}{(D+K+k)^2/dK - (D+K+k+G+g+M)} \quad \text{or} \quad \frac{G'^2}{(D+K')^2/dK - (K'+G'+D)}, \qquad (1)$$

where G′K′ indicate the sum of all the apparent capacities in parallel at the points 1, 2 and 5, 6 respectively The quantities C, *c* do not enter into the equation, although in case (*b*), where *c* has a considerable value, the resonant frequency of the whole system is appreciably lower than in case (*a*) The inductance of the leads connecting the points 1–6 or 2–6 does not affect the calculation It will be observed that the quantities G′ and D occur in the equation as squares, so that any calibration errors are doubled in the result

In order to determine g and k two small platinised mica condensers M_{137} M_1 were constructed as similar in physical dimensions as possible, except that in M_1 two pieces of mica were platinised and separated by spacers, so that the capacity was only 1 45 $\mu\mu$F, that of M_{137} being 137 45 $\mu\mu$F, approximately equal to that of G M_1 was placed in the position 1-2 and a reading of K taken M_{137} was substituted for M_1 and the frequency restored to its original value by adjusting K It might reasonably be assumed that this substitution did not alter the stray capacities, and that the change in capacity was equal to the difference in the capacities, of the two condensers Consequently, two readings for different settings of K were sufficient to determine g and k Actually several were taken, one with the condenser D_{1500} in parallel with K This was repeated with G immersed in the various baths used when measuring dielectric constants the value of G being determined immediately afterwards by placing it in parallel with K With connections (*a*), g was small and varied very slightly, while k changed appreciably (6 6 to 13 4 $\mu\mu$F) according to the bath used, but this had no great effect, as it was always in parallel with a capacity of about 1600 $\mu\mu$F With connections (*b*), k was almost negligible, but g, though constant, was of considerable magnitude, the values for G′ under the same conditions being 136 6 for (*a*) and 140 6 for (*b*) Other observers do not appear to have allowed for these stray capacities In the present case the effect is perhaps exaggerated owing to the length of the leads, but with shorter leads more closely screened the error might well amount to several parts per 100

Measurements similar to the above were made for each inductance, but as they were somewhat tedious and the frequency corrections not altogether certain when using the small coil, an alternative method was adopted Two small brass condensers (fig 2, *d*), very similar to each other but with different spacing between the plates, were constructed Bent quartz rods, to which the leads were soldered, served both as spacers and insulators The difference in capacity was approximately 0 8 $\mu\mu$F, of the same order as the change in capacity of G when filled with gas One of these condensers was placed in position 1–2 and the connections arranged as if for a determination of dielectric constant by admitting gas to G Instead of this, the other condenser was substituted and the change in K necessary for restoration of the original frequency observed It was found that, with care, the condensers could be removed and replaced without producing any measurable alteration in frequency The mean of a number of observations with each coil was taken, with the following results, the figures being scale divisions change measured from a fixed point –

Coil	Small.	Medium	Large
Connections (*a*)	2036	2027	2023
,, (*b*)	1884	1883	1884

The observed changes obtained when measuring the gas can consequently be corrected for frequency, for, making the reasonable assumption that the difference in capacity of the small condensers does not change with frequency, since they have air as dielectric and very high insulation, it is evident that a change in capacity corresponding with 2036 scale divisions when the small coil is used will give rise to a change of 2027 with the medium one

This method is of no value for checking the values of G′ obtained in the way previously described, because with these very small condensers the capacity of the leads is of the same order as that of the condenser itself Mere reversal of the apparently symmetrical condenser required a change in K of 50 scale divisions for compensation It was evident, therefore, that to make a measurement of this nature it was essential not to move any metallic conductors To fulfil this condition, the capacity of the larger condenser was changed by the insertion of a small piece of mica Removal and replacement of the mica in such a way as to obtain quite consistent readings was a matter of considerable difficulty, but it was eventually accomplished with the help of small paraffin wax guides on the mica The capacity change on inserting the mica was then calculated, using two corresponding values for G′ for connections (*a*) and (*b*) previously determined, viz , 136 6 and 140 6 The results were identical, 0 960 $\mu\mu$F

There is one further correction The above figures suffice to show that a small change in the capacity of a condenser directly between the mercury cups 1-2 can be measured with some accuracy, but the gas condenser is not in this position, being connected by leads some 15 cm in length The inductance of these leads was measured by constructing two similar dummy leads and determining the apparent change in capacity of a 1000 $\mu\mu$F condenser on moving it from the end of these leads to the position 1–2 The value was 0 28 μH

If G_a is the apparent capacity of G at the points 1–2, by a slight modification of formula (1), $dK = K^2 \; dG/G_a^2$ very approximately, and, therefore, if the value of G_a were reduced to G, the change dK would become $dK \; G_a^2/G^2$ for a given value of dG That is to say, if the gas condenser could be made coincident with the small testing condensers, the changes in K would be increased to the expression just given, which may be written $dK\,(1 + 2l\omega^2G)$ It may thus be calculated that, if the two condensers were coincident and the change in K corresponding with a given change in G were 2027 scale divisions with the medium inductance, it would not be 2036 for the small one, as found experimentally, but $2036\,(1 + 2lG\,(\omega_1^2 - \omega_2^2))$ or 2049 for the frequencies actually employed By using this correction, the necessity of a separate calibration for each inductance was avoided

Effective Value of the Gas Condenser

The gross value of G was frequently determined by inserting the condenser in parallel with K It changed slowly during the experiments from 2252 scale divisions, measured from a fixed point on K, to 2264 The theoretical temperature coefficient was zero, and this was found in practice, although heating the condenser rapidly occasionally produced a small permanent change due to a shift in the position of the cylinders

The capacity due to the leads was found by constructing two dummy leads mounted on a quartz ring The total capacity introduced by these leads was measured, and then the capacity between them by removing the earthed one This was repeated with the leads shortened to the length which was not in the gas In this way it was found that the stray capacity due to the leads (excluding the capacity between the portions of the leads in the gas) was 1 45 $\mu\mu$F To this had to be added the capacity of the link 2–4, which was 1 25 $\mu\mu$F The capacity due to the quartz discs was determined by constructing a dummy condenser with a wire of correct size instead of an inner cylinder, and observing the change in capacity when a glass disc of measured dielectric constant and the same size as the quartz discs was slipped over the wire inside the cylinder The value found for two discs together was 0 20 $\mu\mu$F Thus, when the measured value of G was 136 2, the effective value or capacity which was altered by admission of gas was only 133 3 $\mu\mu$F

Preparation of Gases

Ammonia was prepared from specially purified ammonium chloride solution and potassium hydroxide Most of the moisture was removed with solid potassium hydroxide and the gas was then liquefied and the middle fraction used for the experiments

Phosphine and ***arsine*** were kindly lent by Sir Robert Robertson The former was prepared from phosphonium iodide and the latter from zinc arsenide

Both were liquefied and carefully fractionated from a considerable quantity of the gas, and were thus in a high state of purity

The whole apparatus used for manipulating the gases was made of durosil glass, and a drying tube containing calcium oxide was attached to the pump to absorb initial traces of moisture

Temperature

For simplicity, measurements were made at three temperatures only, these being approximately − 47°, 16° and 99° The presence of stray conductors anywhere near the gas condenser was early recognised as undesirable, and this was the main reason why Zahn's method of measuring temperature by means of a platinum wire wrapped round the condenser was not adopted, another reason being the fear that the platinum might accelerate the decomposition of arsine Steadiness of temperature was of more importance than its absolute value since a slight difference in temperature between the walls of the condenser produced a relatively large error Thus, in the case of arsine, a difference in temperature between the walls of 0 1° had the same effect on the dielectric constant as an error of 7° in the absolute temperature

For the lower temperature a bath of chlorobenzene partially frozen in a vacuum vessel by the addition of solid carbon dioxide was used and proved satisfactory, although as the material was not quite pure the temperature was somewhat below the normal freezing point, − 45 5° The temperature was measured by two copper-eureka thermojunctions standardised at the freezing point of mercury and the boiling point of carbon dioxide A check was afforded by measuring the vapour pressure of ammonia in the condenser The thermocouples were removed during an experiment The temperatures found are probably correct to 0 5°

For the higher temperature a similar vacuum vessel containing oil was used A glass spiral through which steam could be passed at a constant rate enclosed the condenser at the sides and bottom Temperatures were measured with a standardised thermometer and were probably accurate to at least 0 2° Both baths were stirred occasionally, but not during or for some time preceding an actual measurement At room temperature either bath was used

Method of Measurement

The oscillators were started and the condenser brought to the required temperature at least an hour before making any measurements When conditions were steady, as determined by the constancy of the beat note, the setting of K for zero beats was observed, and a small side tube connected with the apparatus was then immersed in liquid air This reduced the pressure to a negligible amount and the new reading of K for zero beats was taken The side tube was then warmed and another reading taken with the condenser full The condenser could be filled or evacuated and a reading taken in 1 5 minutes, thus reducing any effect of creep A number of such double readings were taken in each experiment

The rate of reduction of pressure on cooling was a very effective method of checking the purity of the gas for any impurities not condensible in liquid air accumulated in the side tube and diffusion through them was very slow For example, when measuring arsine at 99°, the pressure sank only to 19 mm in 1 5 minutes, and then remained fairly steady indicating decomposition, but when the residual gas was pumped off and again admitted, most of it was condensed, and, on repeating the process several times, very little hydrogen was obtained In this way it was found that the percentage decomposition in the time mentioned was of the order of 0 08 instead of the far larger figure suggested by the pressure measurements

Certain small irregularities were observed in the individual readings, particularly at the highest temperature The first reading of a series after a long wait was frequently somewhat high, and the apparent rate of change of capacity of the condenser (due to creep) was different, according as the condenser was full or empty, pointing to some temperature effect The phenomenon was most marked in the case of phosphine, but as the variations were of the same order as the experimental error it was difficult to assign a cause to them Numerous observations with ammonia were made, and the effect appeared to be caused to some extent by admitting cold gas into the condenser, as it became less marked on passing the gas through a U-tube containing quartz granules immersed in the bath No evidence of a change due to adsorption, as recorded by Bädeker,* was obtained, the slow changes after admitting or removing gas being in the opposite sense to those which would occur owing to the formation or removal of an adsorbed layer Bädeker's gas was only dried over soda-lime and was probably not as dry as the samples used in the present experiments In the present case also most of the adsorbed water was removed from the condenser by heating to 150° in a high vacuum before admitting gas

In addition to readings for the full range of pressure, several series were made by the reduction of the pressure in stages by letting the gas into the pump

---

* *Loc cit*

Readings were taken immediately before and immediately after reducing the pressure, the time required being 0 5 minute

At the end of each series of experiments the readings of K were tested by comparison with Q and the value of G was measured On several occasions G′ was also determined by inserting the condenser M_{137} in the manner already described M_1 was retained in position throughout the experiments

Results

The results obtained are shown in Table I Each value recorded is the mean of at least four concordant determinations The actual temperature and pressure at which the measurements were made is given in each case, but the final results are calculated for 760 mm and — 47°, 16° or 100° The pressure calculations at constant temperature have been made by means of formula (3) on p 58, and the temperature corrections have been deduced from the final results In both cases the corrections are small, as most of the measurements were made at a pressure near to 1 atm, while the temperatures varied very slightly from those given The only exception is ammonia, which had to be measured at reduced pressure at the lowest temperature to avoid condensation The letters *a*, *b* in the first column indicate the connections used

Table I —Dielectric Constants of Ammonia, Phosphine and Arsine

Experiment No	Pressure, mm	Temperature, °C	Frequency, *kc*	$(\epsilon - 1) \times 10^5$
		Ammonia		
1	563	15 2	1065	658
2	771	15 0	1070	656
5	670	14 0	1070	656
11*a*	735	97 1	1070	406
12*a*	780	97 5	1070	405
13*b*	779 5	97 6	1020	406
14*b*	779 5	97 8	290	406 5
15*a*	779 5	97 7	303	406
16*a*	777 5	97 2	1820	406
17*b*	776 5	97 2	1745	406 5
18*a*	782	13 9	1070	659
19*b*	776	14 6	1013	658
20*a*	775 5	16 2	1810	662
20*b*	776	16 2	1735	661
21*a*	776	15 7	303	659 5
21*b*	776	15 7	209	656 5
22*a*	775 5	16 2	1070	661
23*a*	341	—46 5	1070	1098
24*b*	341 5	—46 0	1015	1100
26*a*	775	98 0	1070	405
27*b*	775 5	98 0	1015	406
28*a*	751	98 0	1070	407
28*b*	751	98 0	1015	406 5

Table I—(continued)

Experiment No	Pressure, mm	Temperature, °C	Frequency, *kc*	$(\epsilon - 1) \times 10^6$
		Phosphine		
1*a*	755	16 0	1070	239 1
1*b*	756	16 0	1015	238 0
2*a*	791	16 3	303	237 6
2*b*	790 5	16 3	290	237 8
3*a*	790 5	16 3	1820	238 0
3*b*	790 5	16 3	1735	238 2
5*a*	769	99 6	1070	169 0
5*b*	768	99 6	1015	168 3
6*a*	789 5	99 4	1070	169 3
7*b*	750	−46 7	1015	337 4
7*a*	745	−47 0	1070	337 2
		Arsine		
1*a*	723	16 0	1070	190 2
1*b*	723	16 0	1015	188 7
2*b*	723	16 0	1735	192 3
2*a*	723	16 0	1810	192 0
3*b*	764	16 2	1015	193 0
3*a*	762	16 3	1070	192 3
4*a*	764	16 3	303	191 8
4′*a*	763 5	16 3	1810	192 0
6*a*	671 5	−46 8	1070	251 0
6*b*	670	−47 5	1015	251 0
8*a*	770	99 2	1070	145 5

The first three experiments with ammonia were of a preliminary nature under conditions somewhat differing from those already described They have not been included in calculating the mean The experiments up to No 17 were made before the measurements with phosphine and arsine, and the rest afterwards The last value for arsine is the mean of five readings, agreeing within 2 per cent, but it is not very reliable, as the gas was decomposing slightly Further experiments were not performed at this temperature owing to the risk of spoiling the condenser insulation

For the sake of comparison with the results of other observers, a few determinations were made of the dielectric constants of dry CO_2-free air and carbon dioxide, but the results are not intended to be at all comprehensive The value for a sample of benzene was also measured with the idea of checking the corrected capacity of the gas condenser, but the result differed so widely from the most recent determinations that it was useless for this purpose This matter is under investigation and will form the subject of a separate communication

In the case of air, the condenser was filled with the gas and then evacuated rapidly to 16 mm The result is the mean of five readings with an extreme variation of less than 1 per cent The carbon dioxide was condensed in liquid air in the same way as the other gases The two results are each the mean of nine agreeing among themselves to 0 6 per cent Table II shows the values for 16° and 760 mm , the actual measurements being made within 1° of this temperature at a pressure of 770 mm for air and 789 mm for carbon dioxide A few of the results obtained by other observers calculated to the same temperature and pressure are also given

Table II —Dielectric Constants of Air, Carbon Dioxide and Benzene 16°

	Frequency, kc	ϵ	Other observers	
Air	1070	1 000568	1 000557* 516‡ 540‖	1 000554† 510§ 561¶
Carbon dioxide, 1	1820	1 000950	1 000894* 1045‡	1 000930† 896§
,, 2	1070	1 000944	937**	
Benzene	656	2 290	2 2897†† 2 2654§§	2 2583‡‡
,,	1150	2 283		

* L Boltzmann, 'Sitz Akad Wiss Wien, vol 69, p 795 (1874)
† J Klemenčič, 'Sitz Akad Wiss Wien,' vol 91, p 712 (1885)
‡ M Jona, *loc cit*
§ F C Fritts 'Physical Rev ,' vol 23, p 345 (1924)
‖ C T Zahn, *loc cit*
¶ A P Carman and K H Hubbard, 'Physical Rev ,' vol 29, p 299 (1927)
** H Rohmann 'Diss Strassbourg' (1910)
†† M Grützmacher, 'Z Physik,' vol 28, p 342 (1924)
‡‡ L A Sayce and H V A Briscoe, 'J Chem Soc ,' vol 127, p 315 (1927)
§§ H Harris, *ibid* , vol 127, p 1049 (1927)

In order to determine the densities of the gases at the temperatures employed and the magnitude of the pressure corrections, use has been made of the formula

$$pv = \mathrm{RT}\left(1 - \frac{\mathrm{B}}{v}\right), \tag{2}$$

which is simplified from the general expression given by G Holst * From this, assuming that $\varepsilon - 1$ is proportional to the density or inversely proportional to v the expression

$$\frac{(\varepsilon - 1)_{p_1}}{(\varepsilon - 1)_{p_2}} = \frac{p_1}{p_2}\left(1 + (p_1 - p_2)\,\frac{\mathrm{B}}{\mathrm{RT}}\right) \tag{3}$$

may be deduced, connecting the dielectric constants at pressures p_1, p_2, but at the same temperature, where B is a small quantity In this formula $\mathrm{R} = 1/273$ and p is measured in atmospheres

---

* Leiden Comm , No 144 (1913)

The values assumed for B were as follows —

	− 47°	16°	100°
NH_3	0 029	0 0085	0 0048
PH_3	0 016	0 0065	0 002
AsH_3	0 021	0 008	0 004

The figures for ammonia are taken from the determinations of Holst * Those for phosphine were calculated from the critical constants and the values for ammonia by means of the theory of corresponding states, but the results were reduced by 20 per cent in order to make the value at 16° agree with the one deduced from Ter Gazarian's density determination † In the case of arsine there are no data, and so the value at the lowest temperature was calculated from the rate of change of dielectric constant with pressure over two different pressure ranges A similar calculation at room temperature led to the value 0 012, but the experimental error was very large, and it seemed more satisfactory to adopt the figure given, which is obtained merely by analogy with the other two gases, as is also the value for 100°

Table III gives the results of three experiments upon the variation of dielectric constant with pressure at − 47°, $\epsilon - 1$ was actually measured by determining the change in capacity as the pressure was reduced from one pressure given to the next The value in the table is the sum of all these changes from 0 to the given pressure The units are arbitrary, being scale divisions with a small correction to make the figures proportional to the change in capacity The calculated values are obtained by means of formula (3), taking the figures in brackets as the basis

Table III —Variation of Dielectric Constant with Pressure

Ammonia			Phosphine			Arsine		
p	$(\epsilon - 1)_{calc}$	$(\epsilon - 1)_{obs}$	p	$(\epsilon - 1)_{calc}$	$(\epsilon - 1)_{obs}$	p	$(\epsilon - 1)_{calc}$	$(\epsilon - 1)_{obs}$
342 5	(1378)	1378	745	(1050)	1050	669 5	(701)	701
200 2	801	804	601 5	844	844	606	633	633
108 5	432	434	402 5	562	562	405	420	420
90 0	358	362	201	279	278	205 5	212	212
61 6	245	249	102	141	141	103 5	106	106
42 0	167	168	53 5	74	73	81	84	82
22 1	88	89				62	64	61
						42	43	40
						23	24	21

---

* *Loc cit*

† 'Compt Rend,' vol 148, p 1397 (1909)

In the case of ammonia the correction for departure from the perfect gas law appears to be too large, as there is an appreciable difference between the observed and calculated values. The former are actually closer to the figures obtained on the assumption that $\varepsilon - 1$ is proportional to the pressure. With arsine at low pressures there is some discrepancy between the two sets of values. This may be analogous to the effect observed by K. Wolf* in the case of ammonia. On the whole, the differences are very small and only just beyond the limit of experimental error, so that the assumption that $\varepsilon - 1$ is proportional to the density may be said to be justified at least to a first approximation.

Reverting to Table I, an examination of the results indicates that, although there is perhaps a slight tendency for the values at the higher frequencies to be greater than the others, the variation is probably within the limit of experimental error, so that all the figures for one temperature may be taken together in calculating the mean. The agreement between individual values is considerably closer than was anticipated when the experiments were started, but this does not reduce the possibility of constant error, one of the main sources of which was in the determination of G′, the apparent capacity of the gas condenser. The experimental values varied by as much as 0.3 μμF, corresponding with an error of 0.2 per cent. from the mean. The internal temperature of the condenser when in the cold bath could not be relied upon to less than 0.5, while the small fluctuations at the higher temperature mentioned above form another source of error.

The final mean values are given in Table IV. The fourth column is derived by multiplying these values by $(1 - B/RT)$, and shows what the figures would be if the gases were perfect. The next column gives the values for a density equal to that of the perfect gas at 0° and 1 atm., that is to say, for equal numbers of molecules. From these, the value of BN in Debye's equation, $\varepsilon - 1 = N(A + B/T)$, may be calculated for any two temperatures, the figures in the table being derived from the two lower and the two higher temperatures. Since B (not the B of the gas equation) is equal to $4\pi\mu^2/9k$, k being Boltzmann's constant, 1.35×10^{-16}, and N the number of molecules $= 2.705 \times 10^{19}$ in the present case, μ the electric moment may be calculated.

From these figures it appears that ammonia and phosphine conform approximately with the Debye formula, while in the case of arsine the value of B is substantially zero, so that this gas is similar to the permanent gases as far as its dielectric constant is concerned. The two values of B for ammonia are by no means coincident, although the difference corresponds with an error of only 1 5 per cent on the lower value This is, however, probably beyond the limit of experimental error as far as relative values are concerned

---

* *Loc. cit.*

Table IV —Mean Values of Dielectric Constants at 1 Atm Pressure

Gas	t	$(\epsilon - 1)$ 10^6 obs	$(\epsilon - 1)$ 10^6 perfect	$(\epsilon - 1)$ 10^6 eq dens	BN	$\mu \times 10^{18}$
NH_3	−47	1099	1061	879	1 92	1 51
	16	659	654	692	1 79	1 46
	100	406	404 5	552 5		
PH_3	−47	337 3	330 8	273 8	0 24	0 54
	16	238 1	236 6	250 4	0 26	0 56
	100	168 7	168 5	230 2		
AsH_3	−47	251 0	245 0	202 8	0 01	0 13
	16	191 6	190 2	201 4	0 03	0 18
	100	146	146	199		

The absolute values for ammonia at 16° and 100° differ considerably from the figures 737 and 451 for the same temperatures calculated from Jona's results This author, however, states that he does not consider his absolute values accurate The ratio between corresponding results is the same within 1 per cent, so that in this respect the agreement is satisfactory It follows that Jona's value for $\mu \times 10^{18}$, viz, 1 53, is approximately the same as those found in the present experiments

Owing to the uncertainty as to the compressibilities of phosphine and arsine, the values of B for these gases are subject to revision

In conclusion, I wish to tender my best thanks to Prof F G Donnan for all the facilities he has placed at my disposal for undertaking this research, and to Sir Robert Robertson for the loan of the phosphine and arsine

Summary

1 The dielectric constants of ammonia, phosphine and arsine have each been measured at three temperatures and three frequencies, particular attention having been paid to determining the absolute values The variation of dielectric constant with pressure has also been examined

2 The absolute values found for ammonia are considerably higher than those determined by Jona, but the value of the electric moment calculated by Debye's equation is approximately the same in both cases

3 Ammonia and phosphine approximately satisfy Debye's equation for the change in dielectric constant with temperature, but there appears to be a slight deviation in the case of the former gas at the lowest temperature examined

4 The value of the electric moment is much smaller for phosphine than for ammonia, while for arsine it is still smaller

---

An X-Ray Study of the Heat Motions of the Atoms in a Rock-Salt Crystal

By R W James, M A, Senior Lecturer in Physics, and Elsie M Firth, B Sc, Samuel Bright Scholar, in the University of Manchester

(Communicated by W L Bragg, F R S — Received July 26, 1927)

1 The present paper may be divided into two parts In the first, some experiments on the intensity of reflexion of X-rays by rock-salt crystals at low temperatures are described The results of these experiments, when combined with data obtained previously at high temperatures, are compared with the theoretical formulæ of Debye and Waller for the temperature factor of X-ray reflexion.

In the second part of the paper we have attempted to get some idea of the actual amplitude of the heat-motions of the atoms in the rock-salt lattice, by analysing the F curves, or curves showing the variation of the atomic scattering power with angle of scattering, using the method of Fourier analysis introduced by Duane and Havighurst, so as to obtain the distribution of electrons in the crystal unit at different temperatures In connection with this work a new set of absolute determinations of intensity of reflexion has been made, and, from these, the F factors at different temperatures have been calculated, using the results of the experiments described in the first part of the paper

Part 1

2 The thermal agitation of the atoms in a crystal lattice causes small and irregular displacements of the atoms from the lattice planes The contributions of the atoms to the spectra formed by reflexion at any face will therefore

differ in phase from those for atoms lying exactly in an ideal set of equally spaced planes, and the intensities of the spectra will be less than they would have been had all the atoms been at rest with their centres exactly in such a set of planes. It is evident that the higher the temperature the smaller will be the intensity of the given spectrum, and also that the diminution will be much more important for the higher orders of reflexion, since the phase difference introduced by any displacement from the plane is proportional to the order.

The theory of the effect was first investigated by Debye* in a series of papers. In the earlier papers the atoms were supposed to oscillate about fixed positions of rest, to which they were bound by a quasi-elastic force, and the Maxwell-Boltzmann distribution law was used to obtain the probability of a given configuration of all the atoms of the lattice. The intensity of the spectrum of a given order for a known configuration can be calculated. If this calculated intensity is now multiplied by the probability of the configuration, and the resulting product summed over all possible configurations, the average intensity of the spectrum, which is what is observed, is obtained.

It is, of course, evident that the atoms are not bound to fixed positions of equilibrium, but to one another, and that the procedure outlined above is not justifiable, but in a later paper Debye† amended his calculation, basing his work on the ideas of Born and Kármán, in which the heat-motions are considered as a series of elastic waves in the crystal. He found that the intensities of the interference maxima should be multiplied by a factor‡ e^{-M}, where

$$M = \frac{6h^2}{\mu k\Theta} \cdot \frac{\phi(x)}{x} \cdot \frac{\sin^2\theta}{\lambda^2} \tag{2.1}$$

In this formula, which refers only to a simple cubic lattice composed of atoms of one kind, μ is the mass of an atom, h is Planck's constant, k is the gas constant per molecule, Θ is the "characteristic temperature" of the crystal, which occurs in the theory of specific-heats, $x = \Theta/T$, where T is the absolute temperature, and $\phi(x)$ is a certain function of x which Debye evaluates. θ and λ are the glancing angles of reflexion and the wave-length of the radiation respectively. The expression for M given here supposes that there is no zero-point energy. If such energy be assumed, $\phi(x)/x$ must be replaced by $\phi(x)/x + \frac{1}{4}$.

---

* 'Verh. deutsch. Phys. Ges.,' vol. 15, pp. 678, 738 and 867 (1913).

† 'Ann. d. Physik,' vol. 43, p. 49 (1914).

‡ In Debye's paper, the simple Laue theory of diffraction at a crystal grating was used, the intensity of the maxima according to this theory being proportional to the square of the structure amplitude. The same is true for the ideal "mosaic" crystal. The crystals used in this work were very nearly of the "mosaic" type, and so the temperature factors are applicable in the form in which they are discussed in this paragraph.

Later work by Waller,* whose treatment differs from that of Debye in the method of obtaining the "normal co-ordinates" in terms of which the energy of the lattice is expressed, indicates that for a simple lattice the factor should be e^{-2M} instead of e^{-M}. It is evident, therefore, that accurate measurements of the temperature factor are needed in order to test the theoretical formulæ.

3. The crystal of rock-salt is on the whole a very suitable one for this purpose. It has not, of course, a simple cubic lattice, and from this point of view sylvine, KCl, in which the two kinds of atom have nearly the same mass, would be much better. But many measurements of intensities of reflexion have been made using rock-salt, and it is known that the primary and secondary extinctions are small, so that the crystal may be treated very nearly as an ideal mosaic,† to which the formulæ for the intensity of reflexion of X-rays may be applied with some confidence. To a first approximation, we may treat the crystal as simple cubic, composed of atoms whose mass is the mean of those of sodium and chlorine.

The first measurements of the temperature factor for rock-salt were made by W. H. Bragg‡ who obtained results not inconsistent with Debye's formula. Work by Backhurst§ and by Collins‖ on other crystals seemed to show, however, that Debye's formula was at variance with facts.

A series of measurements by one of us,¶ on rock-salt, where the temperature range extended from 290° abs. to 900° abs., showed quite clearly that the rate of decrease of intensity with temperature was much more rapid than that indicated by Debye's formula. Up to about 500° abs. the results were of the order to be expected from Waller's formula, but at higher temperatures the fall was more rapid than even this would predict.

On both formulæ, the exponent M should be nearly proportional to the absolute temperature T. Within the errors of experiment, over the range of temperatures investigated, the exponent was found to be proportional to T^2. This appeared to be a very improbable law physically, but since the exponent was found to be accurately proportional to $\sin^2\theta/\lambda^2$ for the 30 reflexions investigated, as it must be if the effects are due to diffraction at the lattice at all, it appeared probable that the measurements were fairly reliable, and that in all probability the theory was no longer valid at high temperatures The elastic properties of the crystal probably change greatly at higher temperatures, and, in fact, the existence of a coefficient of expansion shows that it is not sufficient merely to take terms involving the squares of the displacements in the expression for the energy of the lattice, and the terms of higher order may well become important at high temperatures when the displacements are large It therefore appeared desirable to extend the measurements to very low temperatures, so as to include more of the range over which the theoretical formulæ were likely to be valid

---

* 'Theoretische Studien zur Interferenz- u. Dispersions theorie der Röntgen strahlen,' Upsala dissertation, 1925.

† W. L. Bragg, Darwin and James, 'Phil. Mag.,' vol. 1, p. 897 (1926).

‡ 'Phil. Mag.,' vol. 27, p. 881 (1914).

§ 'Roy. Soc. Proc.,' A, vol. 102, p. 340 (1922).

‖ 'Phys. Rev.,' vol. 24, p. 152 (1924).

¶ James, 'Phil. Mag.,' vol. 49, p. 585 (1925).

A series of observations has therefore been made with the crystal at the temperature of liquid air* Some preliminary results at low temperatures have been described in a paper communicated to the Manchester Literary and Philosophical Society,† but many more measurements have now been made

4 The crystal was held in a stout brass holder which was suspended, by means of an ebonite rod, just above the surface of liquid air contained in a Dewar flask The flask was mounted on a stand provided with the necessary adjustments for centring, and for altering the height of the crystal, the stand could be placed on the table of an X-ray ionisation-spectrometer and readily removed and replaced by a standard crystal

The Dewar flask was made of boro silicate glass and was blown with specially thin walls This was essential, as the X-rays had to pass through four thicknesses of glass, two for the incident beam and two for the reflected The flasks were made by Mr O Baumbach, who finally succeeded in producing one which was strong enough not to collapse on evacuation, and which was yet thin enough to transmit nearly 70 per cent of the molybdenum K_α radiation ($\lambda = 0\ 710$)

---

* Some measurements of the temperature factor for calcite at liquid air temperatures have been published by Nies ('Annalen der Physik,' vol 79, p 673 (1926)) He finds a greater temperature effect than either Debye's or Waller's formula would indicate He has, however, only used a single spectrum (200) for which the temperature factor is in any case small Moreover, the crystal is not even approximately simple cubic, and the oxygen atoms are not fixed by symmetry, so that the parameters expressing the structure may well be a function of the temperature. The influence of a change of parameter with temperature upon the intensity may be considerable, as has been shown by Gibbs ('Roy Soc Proc,' vol. 107, A, p 561 (1925)) in the case of quartz, and it would not appear possible to draw any definite theoretical conclusions from these results.

† 'Manchester Memoirs,' vol 71, No 2 (1926)

The brass crystal-holder was prolonged to a distance of about half a centimetre below the crystal, and was allowed to dip into the liquid air In this way the crystal was surrounded by a mass of metal which remained very nearly at the temperature of the liquid air so long as any of it was immersed The temperature was measured by a copper-constantan couple, which passed down a hole bored in the ebonite rod supporting the crystal The couple could be raised and lowered to determine the temperature gradient, and it was found that the temperature remained sensibly constant over the crystal face so long as the brass holder dipped well into the liquid air By means of a paper funnel, liquid air could be added from time to time to keep the level constant. It was desirable to pass the liquid air through filter paper to remove traces of ice which it often contained, as these were apt to form a deposit on the inside of the flask as the air evaporated To prevent moisture from the air of the room condensing on the outside of the flask, which was unsilvered, a loose spiral of manganin wire, through which a current of about 1 ampère was passed, was wound round the outside This produced an up-current of warm air which kept the flask free from any trace of moisture or frost Without this precaution, a deposit formed at once With this arrangement it is no more difficult to measure intensities at liquid-air temperature than at room temperature With spectra of high order it is, as a matter of fact, much easier owing to the greatly increased intensity

In making the measurements, each spectrum was compared with the standard (400) reflexion from rock-salt, the method being exactly that described in previous papers * The comparison was first made at room temperature with the flask in position Liquid air was then poured into the flask and the comparison was repeated The effect of the absorption in the glass was the same in both cases, apart from a possible difference due to lack of uniformity of the flask, since the angle of reflexion is not quite the same at the two temperatures owing to the thermal expansion of the crystal Experiments made turning the flask through a small angle showed, however, that this effect was negligible The ratio of the intensity at liquid-air temperature to that at room temperature could therefore be obtained

The thermo-couple was connected to a shunted unipivot galvanometer, and was calibrated, using carbon-dioxide-snow in alcohol, and liquid oxygen

5 The results of the experiments are summarised in Table I (*a*) and (*b*) In I (*a*) the spectra all have structure-amplitudes of the type Cl + Na, while those in I (*b*) are of the type Cl — Na The indices refer to the true face-centred

---

* *Cf* 'Phil Mag,' vol 49, p 590 (1925)

unit of the rock-salt structure, $a = 5\ 628$ Å, so that (200) is the first order which actually occurs when the cube face is used We have not included measurements for (200), owing to the uncertainty of the extinction correction for this spectrum

Table I —Molybdenum K_α Radiation ($\lambda = 0\ 710$)

(*a*) Spectra of type (Cl + Na)

Spectrum	θ_1	T_{abs}	ρ_T/ρ_{290}	$\left(\frac{\lambda}{\sin\theta_1}\right)^2 \log_{10}\frac{\rho_T}{\rho_{290}}$
	° ′			
(400)	14 37	84 7	1 23	0 706
(600)	22 15	85 6	1 61	0 723
(444)	25 55	84 6	1 89	0 730
(800)	30 18	83 8	2 36	0 739
(10,00)	39 7	88 1	3 39	0 671
(666)	40 59	88 0	4 13	0 723
(10,22)	40 59	88 1	4 01	0 708
				Mean 0 714

(*b*) Spectra of type (Cl — Na)

Spectrum	θ_1	T_{abs}	ρ_T/ρ_{290}	$\left(\frac{\lambda}{\sin\theta_1}\right)^2 \log_{10}\frac{\rho_T}{\rho_{290}}$
	° ′			
(331)	15 58	88 0	1 20	0 528
(333)	19 9	87 1	1 31	0 543
(511)	19 9	87 6	1 37	0 741
(555)	33 8	86 8	1 93	0 480
				Mean 0 548

Column (2) gives the glancing angle of reflexion θ_1 at 290° abs Column (4) gives ρ_T/ρ_{290} the ratio of the intensity, here measured as the integrated reflexion, at absolute temperature T to that at the standard room temperature 290° abs It will be noticed that, at the temperature of liquid air, the intensity of the (666) spectrum is more than four times as great as it is at room temperature Spectra such as (12,00), which are too weak to measure accurately at room temperature, become quite easy to measure at the low temperature

6 The temperature factor is of the form

$$\exp\left\{-bf(T)\frac{\sin^2\theta_T}{\lambda^2}\right\},$$

where $f(T)$ is some function of the absolute temperature The constant b will in general differ for atoms of different kinds For the moment suppose that the lattice is a simple one, composed of atoms of one kind only The intensity of a spectrum at temperature T can then be obtained from that at absolute zero simply by multiplying by the temperature factor θ_T is the glancing angle of reflexion at temperature T, and will vary with the temperature owing to the expansion of the crystal If ρ_T and ρ_{290} are the integrated reflexions at temperature T and at a standard temperature respectively, we shall have

$$\left(\frac{\lambda}{\sin\theta_1}\right)^2 \log\frac{\rho_T}{\rho_{290}} = -bf(\mathrm{T})\left(\frac{\sin\theta_T}{\sin\theta_1}\right)^2 + \text{const} \qquad (6\ 1)$$

Neglecting the small change in glancing angle with temperature, we should therefore have $(\lambda/\sin\theta_1)^2 \log(\rho_T/\rho_{290})$ constant, for a given pair of temperatures, for all spectra and for all wave-lengths The figures in the last column of Table I (*a*) show that for the change in temperature between 290° and 86° absolute this is the case within the errors of experiment for the spectra of type Cl + Na For the difference spectra in Table I (*b*) the corresponding figures are again roughly constant, although the agreement is not so good, and it will be noticed that they are all considerably lower We shall return to this point later, but for the moment we shall deal only with the summation spectra

Let us now consider the way in which $(\lambda/\sin\theta_1)^2 \log(\rho_T/\rho_{290})$ varies as the temperature changes If this quantity is plotted against $f(\mathrm{T})\,(\sin\theta_T/\sin\theta_1)^2$, a straight line should be obtained In the work at high temperatures, if $f(\mathrm{T})$ was put equal to T^2, the line was straight within the errors of experiment An empirical value of the exponent equal to $-1\ 162 \times 10^{-5}\,\mathrm{T}^2 \sin^2\theta/\lambda^2$ was obtained Extrapolation from this formula to liquid-air temperature gives values of the ratio ρ_T/ρ_{290} much smaller than those measured experimentally For example, the calculated ratio at 85° abs for (800) is 1 57, whereas the observed ratio is 2 36 As was expected, the empirical law breaks down at low temperatures

7 The graph in fig 1, in which all the data for the summation spectra obtained both at high and low temperatures are included, was plotted putting $f(\mathrm{T})$ equal to T It will be seen that the points lie on a straight line within the errors of experiment from about 85° abs up to about 500° abs Above this temperature, although again the points from the different spectra all lie on the same curve, the slope of the curve increases, showing that a more rapid rate of decrease of intensity with temperature has set in

The two dotted curves marked D and W were calculated from the theories of Debye and Waller respectively, using the values of $\phi(x)$ given in Debye's

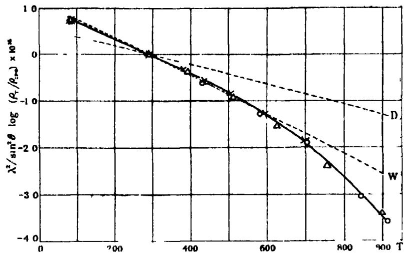

Fig 1

paper For the part of the curve between 85° abs and 500° abs , which can be treated as straight, our figures give for the summation spectra

$$2M = 2\ 449 \frac{\phi(x)}{x}\frac{\sin^2\theta}{\lambda^2}, \qquad (7\ 1)$$

or if a is the spacing of the unit cube of the crystal, and (h, k, l) are the indices of a spectrum,

$$2M = 2\ 449 \frac{\phi(x)}{x} \frac{h^2+k^2+l^2}{4a^2} \qquad (7\ 2)$$

In these formulæ, the wave-lengths and spacings are in Ångström units Taking the characteristic temperature of rock-salt as 281°, we get from Debye's formula

$$M = 1\ 38 \frac{\phi(x)}{x}\frac{\sin^2\theta}{\lambda^2}, \qquad (7\ 3)$$

so that according to Waller the exponent should be

$$2M = 2\ 76 \frac{\phi(x)}{x}\frac{\sin^2\theta}{\lambda^2} \qquad (7\ 4)$$

On the whole, the experiments support the theory of Waller The agreement is by no means perfect, but it must be remembered that the theory is calculated for a simple cubic lattice, whereas the rock-salt lattice contains atoms of two kinds In comparing theory and experiment we have treated the lattice as simple cubic having atoms whose mass is the mean of those of sodium and chlorine situated at its points This can only give an approximation to the truth At high temperatures, in particular, the experimental curve deviates widely from the theoretical. At such temperatures the excursions of the atom are a considerable fraction of an Ångström unit, and the assumptions on which the theory is based must need modification *

The curves intersect at T = 290°, because the intensity at that temperature was taken as the standard in all cases There is a little doubt as to whether the method used to allow for the general and scattered radiation in measuring the intensities is quite satisfactory Theory indicates that there should be diffuse maxima to the scattered radiation in the region of the interference maxima, which will be almost impossible to allow for in determining the intensity of the latter, with which we are concerned The effect of this error, if it exists, will in all cases be to decrease the observed ratio ρ_T/ρ_{290} at low temperatures, and it is possible, therefore, that allowance for it would improve the agreement with the results of Waller, but from the fact that the measured intensity of a spectrum appears to be independent of the width of the ionisation-chamber slit, so long as this is wide enough to receive the whole reflexion, it does not seem probable that the error due to this cause can be large

8 The difference between the temperature factors for spectra of the type Cl + Na and those of the type Cl − Na calls for comment The latter spectra are all small, and the ratio of general radiation to peak is much greater than for the summation spectra Consequently, any systematic error due to incorrect allowance for general radiation will be much more important in this case Taking into account the probability of such errors, we feel, however, that there is no doubt that the difference between the results for the two sets of spectra is a real one The variations in the individual values of $(\lambda/\sin\theta_1)^2 \log(\rho_T/\rho_{290})$ for the difference spectra are much greater than for the summation spectra This, no doubt, is due partly to experimental error There remains, however, some possibility that the differences are real, and that the temperature factor may be a function of the direction of the rays relative to the crystal axes

It is not really correct to speak of a single temperature factor for a given spectrum Each kind of atom should have its own factor, and the structure-amplitude should be taken as proportional to $F_1e^{-M_1} + F_2e^{-M_2}$, where F_1 and F_2 are the atomic scattering factors for the two kinds of atom and M_1 and M_2 are the appropriate values of M

---

* During the progress of this work a paper by Dr Waller has appeared ('Ann d Physik,' vol 83, p 154 (1927)) in which he has modified the theory, taking into account terms of higher order in the expression for the energy The results indicate that a better agreement with experiment at high temperatures can be obtained in this way

In comparing the experimental results with theory we have made the simplifying assumption that $M_1 = M_2$, or, rather, that $F_1e^{-M_1} + F_2e^{-M_2}$ can be written $(F_1 + F_2)e^{-M}$, where e^{-M} is an average temperature factor

Similarly for the difference spectra we should write for the structure amplitude $F_1e^{-M_1} - F_2e^{-M_2}$, and could again represent this approximately by $(F_1 - F_2)\,e^{-M}$ But unless M_1 and M_2 are equal, we shall not expect M and M′ to be equal To take an extreme case, if F_1 and F_2 were not very different, while M_2 were much greater than M_1, it might be possible for the structure-amplitude for the difference spectra actually to increase with increasing temperature, which of course could never be the case for the summation spectra In fluorspar the scattering power of the single calcium atom is very nearly equal to that of the two fluorine atoms, while we might perhaps expect the amplitudes of vibration of the two kinds of atom, and hence the values of M for them, to differ considerably It was to be expected, therefore, that the difference between the temperature factors for spectra of type Ca + 2F and those of type Ca − 2F would be even more marked than for the corresponding spectra in rock-salt Experiment shows that this is the case For example, for the spectra (600) and (800), the ratios ρ_T/ρ_{290} for the change from room temperature to liquid-air temperature were 1 09 and 1 29 respectively We thus find the value of $(\lambda/\sin\theta)^2 \log(\rho_T/\rho_{290})$ to be 0 124 for (600), a spectrum of the type Ca − 2F, and 0 207 for (800), which is of the type Ca + 2F, whereas the two values should have been equal had M been the same for both types of spectra at corresponding angles

If absolute measurements of the intensities of the sum and difference spectra could be made with sufficient accuracy at a number of temperatures, it would be possible to determine $F_1e^{-M_1}$ and $F_2e^{-M_2}$ for the individual atoms Up to the present, however, reliable measurements of the difference spectra at high temperatures have not been obtained

PART II

9 Absolute measurements of the intensity of reflexion of X-rays from crystals allow the atomic scattering factor F to be determined F is a dimensionless number, and may be defined as the ratio of the amplitude scattered in a given direction by the electrons in the unit of the crystal structure to that scattered in the same direction by a single electron In some cases, as in the crystal of rock-salt, F can be determined for the separate atoms A knowledge of F for the different atoms is of great importance, for on it depends, to a large

extent, our power of analysing the more complex crystal structures Moreover, from it we can determine in a direct way the distribution of electrons within the atom, or between the planes of the crystal In the second part of this paper we propose to give an account of some redeterminations of F for the rock-salt crystal, and, combining these results with those obtained for the temperature factor, to determine the distribution of electrons in the crystal at different temperatures, and so to obtain a direct estimate of the amplitude of vibration of the atoms

Most of the attempts hitherto made to determine electron distributions from the F factors have been based on the experimental results of Bragg, James and Bosanquet* for rock-salt Recently Bearden† has published a new set of absolute determinations for the same crystal, using molybdenum radiation He states that his results are in substantial agreement with those of the former authors, but unfortunately he gives no actual numbers in his paper

The figures given by Bragg, James and Bosanquet refer to rhodium radiation, while we have used molybdenum radiation in our work The only measurements of the absolute intensity of reflexion for molybdenum K_α which are available are those of Compton‡ and of Wasastjerna,§ each of whom only gives the value for (200), which may vary greatly from crystal to crystal owing to extinction We have thought it better, therefore, to redetermine the absolute value, using the actual crystal face employed as a standard in our experiments, which was also the standard used by Bragg, James and Bosanquet We have measured the absolute value of the integrated reflexion both for molybdenum and rhodium radiations, so that the work serves as a check on the earlier values

In addition, we have made an entirely new set of comparisons of the integrated reflexions for the different faces of rock-salt, which repeat the earlier work, and also extend it to considerably greater angles of reflexion All the reflexions are ultimately compared with that for (200), for which the absolute value is known, and we therefore have the absolute values for a large range of spectra

Spectra such as (12,00) and (12,44) are practically impossible to measure accurately at room temperature They were measured at the temperature of liquid air, where they are quite strong, and corrected to room temperature, using the known temperature factor The points so determined lie on the natural extension of the room-temperature intensity curve, and give confidence

---

[*] 'Phil Mag,' vol 41, p 309 (1921), vol 42, p 1 (1921), vol 44, p 433 (1922)

[†] 'Phys Rev,' vol 29, p 20 (1927)

[‡] 'Phys. Rev,' vol 10, p 95 (1917)

[§] 'Soc Sci Fenn,' II, No 15

that the curve is not seriously wrong owing to any systematic errors in applying the correction for general radiation The results of the measurements at room temperature are given in column 2 of Table II.

Table II —Integrated Reflexion and F Factors at 290° Abs for λ = 0 710

Spectrum	$\rho \times 10^6$	$F_{Cl} + F_{Na}$		
		Uncorrected	Corrected for extinction	Bosanquet's values for rhodium
200	492	17 16	20 65	
220	239	14 39	15 62	
222	143	12 59	13 18	13 20
400	98 4	11 23	11 60	11 19
440	27 6	7 40	7 46	7 55
600	21 7	6 84	6 89	7 20
444	10 53	5 27	5 28	5 55
800	5 02	4 04	4 04	4 14
660	3 16	3 34	3 34	—
10, 00	1 13	2 22	2 22	2 42
880	0 52	1 55	1 55	—
*12, 00	0 28	1 12	1 12	1 49
*12, 44	0 13	0 70	0 70	—
14, 22	—	—	—	0 7
		$F_{Cl} - F_{Na}$		
111	39 2	4 49	4 54	—
311	5 76	2 44	2 44	—
*333	2 93	2 28	2 28	—
511	3 02	2 32	2 32	—
711	1 50	2 03	2 03	2 05
555	0 64	1 53	1 53	1 58
*933	0 29	1 12	1 12	1 17
*777	0 07	0 56	0 56	—

* These intensities were measured at liquid air temperatures and corrected to 290° abs using the temperature factor

The integrated reflexion ρ is given by $E\omega/I$, where E is the total ionisation entering the chamber when the crystal rotates with uniform angular velocity ω through the reflecting position, and I is the total energy in the incident beam falling per second on the crystal face, the latter being supposed large enough to receive the whole of the incident radiation

10 As the mean of a number of observations,* we find for the (200) spectrum

---

* A difficulty mentioned by Bearden (*loc cit*) was encountered, although apparently in a lesser degree. For the absolute determinations, it was important to use an ionisation chamber of diameter so great that the beam of X-rays entering the chamber should not come near the inner electrode, which is connected with the electrometer Unless this precaution was taken, values of ρ considerably in excess of those given above were obtained.

from our standard crystal the following values of ρ, the integrated reflexion:—

$$\text{Molybdenum } K_\alpha, \qquad \rho = 0{\cdot}000492$$
$$\text{Rhodium } K_\alpha, \qquad \rho = 0{\cdot}000544$$

For rhodium, Bragg, James and Bosanquet obtained 0·000541. For molybdenum Compton gives 0·00044 and Wasastjerna 0·00046, but they, of course, used different crystals, and the discrepancies between these results and ours may well be due to extinction.

The theoretical expression for the integrated reflexion is

$$\rho = \frac{N^2\lambda^3}{2\mu}\,\frac{e^4}{m^2c^4}\cdot F^2 \operatorname{cosec} 2\theta\,\frac{1+\cos^2 2\theta}{2} = \frac{Q}{2\mu}, \tag{10·1}$$

N is the number of crystal units per unit volume, e and m are the electronic charge and mass, θ the glancing angle of reflexion, and μ the linear absorption coefficient. F is the scattering factor for the crystal unit, and includes the temperature factor, being of the form F_0e^{-M}, where F_0 is the value at absolute zero.

This expression is derived on the assumption that the crystal can be treated as a "mosaic," no single homogeneous fragment being large enough to absorb an appreciable amount of the radiation. Owing to the fact that this is not strictly true, even for a very imperfect crystal such as rock-salt, the intense spectra are somewhat weaker than they would be according to the formula. This is the phenomenon known as "extinction."* In rock-salt the fragments are small enough for primary extinction, due to the screening of the lower parts of a homogeneous fragment by its upper parts, to be negligible, but the effect of secondary extinction is quite marked.

Darwin has shown that we may allow for secondary extinction by writing, instead of μ, $\mu + gQ$, where g is a constant of the crystal, so that the formula for the integrated reflexion for the mosaic crystal, corrected for secondary extinction becomes

$$\rho = \frac{Q}{2(\mu + gQ)} \tag{10·2}$$

The term gQ, by which the ordinary absorption coefficient must be increased, is known as the "extinction" and has been denoted by ϵ. It differs, of course, for different spectra, and, for the same spectrum, for different specimens of the same crystal. For the material used in these experiments the secondary

---

* Darwin, 'Phil. Mag.,' vol. 43, p. 800 (1922); Bragg, Darwin and James, *loc. cit.*; Bragg, James and Bosanquet, 'Phil. Mag.,' vol. 42, p. 1 (1921); Wasastjerna, *loc. cit.*

extinction for rhodium radiation had already been measured.* It was found that the ordinary absorption coefficient, 10·7, was increased to 16·3 for (200), so that the extinction ϵ was 5·6. Now g does not depend on the wave-length, so that the extinction for molybdenum can be calculated at once from the ratio Q_{Mo}/Q_{Rh}. In this way we get $\epsilon = 7·45$ for (200). The ordinary linear absorption coefficient for MoK_α is 16·53,† so that the effective absorption coefficient for (200) may be taken as 24·0. Using the values of Q, it is now easy to calculate ϵ for the other spectra.

Theoretically, a knowledge of the integrated reflexions and the ordinary absorption coefficients for two wave-lengths is enough to determine the extinction for both wave-lengths, for a crystal for which primary extinction can be neglected; for if the suffixes 1 and 2 refer to the two wave-lengths, we have

$$\frac{\rho_1}{\rho_2} = \frac{Q_1}{Q_2}\,\frac{\mu_2 + gQ_2}{\mu_1 + gQ_1} \qquad (10·3)$$

The ratio Q_1/Q_2 is known, since F is the same for all wave-lengths for a given spectrum; hence, if ρ_1 and ρ_2 are measured, the extinction can be calculated. Unfortunately, the equation obtained is somewhat ill-conditioned, and the determination of ϵ depends on an accurate knowledge of μ_1 and μ_2. The values of ϵ for Mo and Rh found from the equation (10·3), using the known values of ρ_1 and ρ_2, are 7·7 and 5·8 respectively, which are in fair agreement with 7·45 and 5·6 obtained in quite another way. The agreement, however, may be partly accidental, and too much importance must not be attached to it.

11. The values of F in Table II were calculated using formula (10·1). The table gives the scattering factors for the different spectra for a single molecule of NaCl at the temperature of the laboratory, 290° abs. The value of $F_{Cl} + F_{Na}$ for an angle of scattering 0° should thus be 28. At the smallest angle at which a spectrum of this type can be measured, corresponding to an angle of scattering of 14° 31′, the waves scattered from different parts of the atom are already so far out of phase that the value of F has fallen to 20·65. For a spherically symmetrical atom F is a function of $\sin\theta/\lambda$, and thus should be independent of the wave-length for a given order. For NaCl, if F is plotted against $\sin\theta/\lambda$, the points for spectra of structure-amplitude Cl + Na all lie on one smooth curve and those of type Cl − Na all lie on another. By taking

---

* Bragg, James and Bosanquet, *loc. cit.*

† This value was the mean of a number of determinations made using slips of different thickness. It is lower than the value given by Havighurst ('Proc. Nat. Acad. Sci.,' vol. 12, p. 477 (1926)), but agrees with the measurements of Wasastjerna.

half the sum and half the difference of corresponding ordinates of the two curves, the values of F_{Cl} and F_{Na} can be calculated.

The values of F obtained in this work, although on the whole in agreement with the results of Bragg, James and Bosanquet for spectra of low order, are considerably greater for the high orders We believe that the new measurements should be more accurate, since the general steadiness of the experimental conditions was far greater than in the earlier work This view is confirmed by some measurements made by Mr Bosanquet some years ago for rhodium radiation, using substantially the same apparatus that we have employed These were intended to be a confirmation and extension of the earlier work, but were never published We are indebted to Mr Bosanquet for permission to publish some of his figures here In the last column of Table II the values of F calculated from these results are given It will be seen that they confirm the greater values of F for high-order spectra, and also illustrate the fact that F is independent of the wave-length. The high orders such as (14,22) can only be taken as giving the general magnitude of the effect, as the intensities to be measured in this case were minute

12 We may correct the curves for F_{Cl+Na} and F_{Cl-Na} for temperature, using the measured temperature factors, and so obtain F_{Cl} and F_{Na} for a variety of temperatures These values of F are given in Table III for 0°, 86°, 290° and 900° abs In figs 2 and 3 the values of F_{Cl} and F_{Na} are plotted, for these four temperatures, against sin θ/λ

Table III

$\sqrt{h^2+k^2+l^2}$	0°			86°			290°			900°		
	$\frac{\sin\theta}{\lambda}\times10^{-8}$	F_{Cl}	F_{Na}	$\frac{\sin\theta}{\lambda}\times10^{-8}$	F_{Cl}	F_{Na}	$\frac{\sin\theta}{\lambda}\times10^{-8}$	F_{Cl}	$F_{Na.}$	$\frac{\sin\theta}{\lambda}\times10^{-8}$	F_{Cl}	F_{N}
2	0 180	12 64	8 65	0 179	12 58	8 60	0 178	12 27	8 37	0 174	10 74	7 33
3	0 270	9 44	6 64	0 268	9 33	6 56	0 266	8 82	6 17	0 260	6 53	4 57
4	0 359	7 84	5 25	0 358	7 70	5 16	0 355	6 97	4 62	0 347	4 09	2 71
5	0 449	6 75	4 06	0 447	6 55	3 96	0 444	5 63	3 32	0 434	2 44	1 44
6	0 539	5 88	3 11	0 537	5 67	3 03	0 533	4 55	2 34	0 520	1 37	0 71
7	0 629	5 21	2 44	0 626	4 86	2 23	0 622	3 61	1 55	0 607	0 71	0 31
8	0 719	4 55	1 96	0 716	4 18	1 76	0 711	2 85	1 09	0 694	0 34	0 13
9	0 808	3 96	1 64	0 805	3 57	1 45	0 799	2 19	0 77	0 780	0 15	0 05
10	0 898	3 46	1 45	0 895	3 05	1 23	0 888	1 67	0 57	0 867	0 06	0 02
11	0 989	3 06	1 30	0 984	2 62	1 07	0 977	1 27	0 42	0 954	0 02	0 01
12	1 078	2 51	1 08	1 074	2 09	0 86	1 066	0 88	0 28			
13	1 168	2 04	0 91	1 162	1 65	0 70	1 154	0 57	0 22			
14	1 257	*1 61	*0 79	1 252	*1 23	*0 57	1 243	*0 33	*0 12			
15	1 348	*1 17	*0 65	1 342	*0 88	*0 46						

* Points on the curve obtained by extrapolation

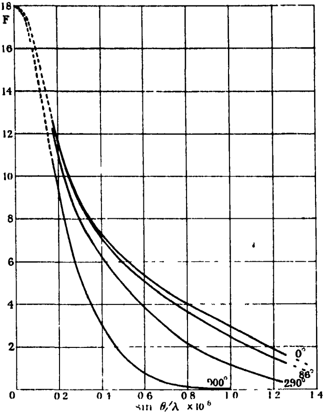

FIG 2 —Values of F for Chlorine at Different Temperatures

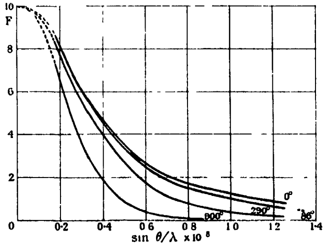

FIG 3 —Values of F for Sodium at Different Temperatures

The curves for 290° abs and for 86° abs, the mean temperatures of the liquid-air experiments, were obtained directly from the experimental results already described Those for absolute zero were obtained by extrapolation from the results at liquid-air temperature, using the value

$$2M = 2\ 449 \frac{\phi(x)}{x} \frac{\sin^2 \theta}{\lambda^2}$$

for the summation spectra and

$$2M = 1\ 880 \frac{\phi(x)}{x} \frac{\sin^2 \theta}{\lambda^2}$$

for the difference spectra, the wave-lengths, as before, being expressed in Ångstrom units The values of $\phi(x)/x$ were taken from the table given in Debye's paper. For 900° the results obtained for high temperatures* were used directly No measurements for difference spectra having been made at high temperatures, it was thought better to use the same temperature factor for both kinds of spectra This is probably nearly correct at temperatures as high as 900° abs, and in any case it is not justifiable to extrapolate from values obtained at 86° abs In fact, if one does so, one finds that, for high orders, the difference spectra at 900° abs are stronger than the summation spectra We have therefore multiplied all the intensities obtained at 290° abs by e^{-2M}, where

$$2M = 8\ 435 \frac{\sin^2 \theta}{\lambda^2},$$

a value obtained directly from the numbers given in the earlier paper

13 We may now proceed to calculate from the values of F the distribution of electrons between the planes of the crystal, and for this purpose we shall employ a method of Fourier analysis The use of Fourier series in this connection was suggested by Sir William Bragg† in his Bakerian lecture of 1915, but a method capable of yielding quantitative results was first published by Duane,‡ and has been employed with great success by Havighurst § Duane's treatment is based on the quantum theory, a full discussion of the method from the point of view taken in this paper is given by A H Compton in his recent book, 'X-Rays and Electrons'

Consider a set of crystal planes whose spacing is a, and suppose that the crystal possesses a plane of symmetry parallel to these planes Consider a thin layer, of thickness dx, parallel to the crystal planes and distant x from the origin, which lies in a symmetry plane Let there be Z electrons in the unit of crystal structure, and suppose that $Zf(x)\,dx$ denotes the number of these electrons which lie between the planes x and $x + dx$ Then it is easy to show that

---

* 'Phil Mag,' *loc cit*

† 'Phil Trans,' A, vol 215, p 253 (1915)

‡ 'Proc Nat Acad Sci,' vol 11, p 489 (1925)

§ 'Proc Nat Acad. Sci.,' vol 11, pp 502, 507 (1925), 'J Amer Chem Soc.,' vol 48, p 2113 (1926), 'Phys Rev,' vol 29, p 1 (1927)

$$Zf(x) = \frac{Z}{a} + \frac{2F_1}{a}\cos\frac{2\pi x}{a} + \frac{2F_2}{a}\cos\frac{4\pi x}{a} + \quad + \frac{2F_n}{a}\cos\frac{2\pi n x}{a} + \tag{13 1}$$

In this formula, F_n is the absolute value of F for the nth order spectrum produced by reflexion from the planes under consideration The series must be prolonged until the values of F_n become negligible For high temperatures F_n decreases very rapidly with increasing order, and the series is convergent, but for low temperatures F_n is still appreciable at the larger angles at which observations can be made Accordingly, the F curves must be extrapolated beyond the point where observation ceases, and, since there is a certain freedom of choice in the extrapolation, the fine details of the analysis at low temperatures are a little untrustworthy We have found that the main features of the curve are unaltered by changing the extrapolation slightly, although, of course, the heights of the peaks, which depend directly on the sum of the F factors, are affected by the rate at which the latter are assumed to die away

The analysis has been made for the (111) planes of rock-salt, which contain alternately chlorine and sodium atoms, for the four temperatures at which the values of F have been deduced In Table IV we give the values of F used in calculating the curves Three of these, for 86° abs, 290° abs and 900° abs. respectively, are plotted in fig 4 The curve for 0° is omitted as, on the

Table IV

Spectrum	F			
	T = 0° abs	T = 86° abs	T = 290° abs	T = 900° abs
111	4 62	4 61	4 54	4 11
222	14 63	14 45	13 18	8 98
333	2 71	2 60	2 30	0 93
444	7 73	7 18	5 28	1 09
555	2 42	2 22	1 53	0 12
666	4 61	4 12	2 00	0 05
777	1 40	1 19	0 56	0 004
888	*2 48	*1 90	*0 50	—
999	*0 36	*0 30	*0 01	—
10,10,10	*0 55	*0 32	—	—

* Values obtained by extrapolation

scale of the diagram, it would not be easy to distinguish it from that for 86° except in the immediate neighbourhood of the peaks The ordinates give the

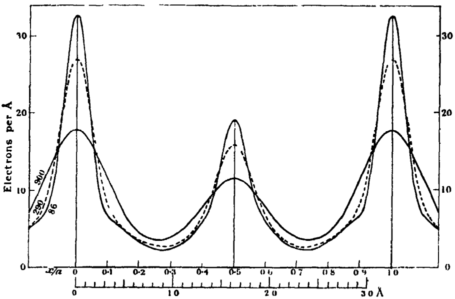

FIG 4—Distribution of Electrons in Sodium Chloride at 86°, 290° and 900° Abs

values of $Zf(x)$ in electrons per Ångstrom unit, the abscissæ give x/a, the fraction of the spacing of the crystal planes The spacing depends, of course, on the temperature it is 3 249 Å at 290° abs and about 2 4 per cent greater at 900° A scale of Ångström units, which is correct for 290°, is given below the diagram Similar analyses, made using the figures of Bragg, James and Bosanquet, are given by Compton in his book The values of F which he used had been corrected to absolute zero, using a value of the temperature factor now known to be considerably too small, but the general resemblance of Compton's curves to that for the temperature of liquid air in fig 4 is evident

If the abscissæ are expressed in Ångstrom units, the area of the curves lying between two identical planes corresponds to 28 electrons The large peaks represent the chlorine atoms, the smaller ones sodium atoms As in the curves given by Compton, the atoms are not separated for these planes, and to determine the number of electrons in each it is necessary to estimate a limit for the atoms The way in which this is done is to some extent a matter of choice, but if we assume the radius of the chlorine atom to be 1 7 Å and that of the sodium atom 1 1 Å, and taper the peaks off to these points in such a way that their sum gives the observed curve, we find the areas to be very nearly in the ratio 18 10, which is consistent with ionisation of the two atoms We do not feel, however, that the ratio of the number of electrons in the two atoms can be determined definitely in this way A somewhat different interpretation of the results might be made to give the ratio 17 11, and while our results are quite consistent with ionisation of the atoms, they cannot be taken as proving it conclusively

Assuming now that the sodium ion contains 10, and the chlorine ion 18 electrons, we can extrapolate the F curves backwards to $\sin \theta = 0$ We have used the F curves for chlorine to obtain the sheet distributions of electrons in the chlorine atom at 0° and 900° To do this we have assumed a spacing 5 628 Å for the planes, since the values of F for the spectra corresponding to this spacing can be read off very easily from the curves An exactly similar analysis is given by Compton in his book The distributions at the two temperatures are plotted in fig 5, in which the full line refers to 0° and the dotted one to 900° The irregularities on the outer part of the curve for the lower temperature are probably largely accidental, and due to the particular method of extrapolation employed The curve is smoothed off to some extent if the values of F are made to die away more slowly. But the main features of the distribution are unaltered by any reasonable change in the extrapolated portion of the F curve In particular, we believe the sudden change in slope at about 0 28 Å and the less marked one at about 0 7 Å represent some real feature in the electron distribution in the atom Similar changes of slope occur in the analyses given by Compton

14 The curves of figs 4 and 5 represent time-averages of the electron distribution over a period immensely long compared either with the periods of the electrons or with those of the atomic vibrations The differences between the distributions at the different temperatures is very marked As the temperature rises, the heights of the peaks fall, and at the same time their breadths increase, the areas remaining constant

The broadening of the peaks is, of course, due to the oscillations of the atoms about the mean position of the crystal planes, which alters the time-average of the electron distribution, and from it, it should be possible to make an estimate of the mean amplitude of the atomic vibrations We shall assume that each atom vibrates with the same amplitude about a mean position, and that all directions of vibration are equally probable By supposing the distribution of electrons determined for the absolute zero to vibrate in this way and by finding the new time-average of distribution produced by such vibration, we may estimate the mean amplitude at a given temperature, by comparing the time-averages for different amplitudes with the distribution curve actually determined for that temperature. Such a process can, of course, only give a rough idea of the atomic excursions. The atoms do not all perform simple harmonic vibrations of the same amplitude about fixed positions. There must be something in the nature of a Maxwellian distribution of amplitudes, and we cannot be sure that each atomic nucleus with all its attendant electrons vibrates as a whole. But, in spite of the obvious limitations of the assumptions made, it is possible to get interesting information concerning the order of magnitude of the atomic excursions.

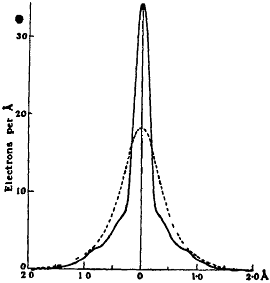

Fig. 5.—Distribution of Electrons in Chlorine at 0° and 900° Abs.

The method employed to obtain the averages is, in principle, as follows:— The average distribution in space, corresponding to a very small element of charge of density ρ, supposed at rest at absolute zero, when vibrating with an amplitude b, is a spherically symmetrical distribution throughout a sphere of radius b. The density in any spherical shell between radii r and $r + dr$ is proportional to ρ and to the time spent on the average by the vibrating charge between the distances r and $r + dr$ from its position of rest, that is to say, to the fraction of the whole period spent by a point executing simple harmonic motion between the distances r and $r + dr$ from its mean position. It is also inversely proportional to the square of the radius of the shell. The ordinates in the distribution curves of fig. 4 are proportional to P, where Pdx is the amount of charge between planes parallel to the crystal planes and distant dx apart If, therefore, the distribution of charge over the spherical shell is plotted on a curve of the same type as those shown in fig 4, it will be represented by a uniform distribution spread over a breadth $2r$, where r is the radius of the shell, the sheet density at any point within this region being uniform, and, for a given density of the original element of charge, proportional to $1/2r$ We shall get a similar distribution for any spherical shell, and the final average is obtained by adding together a large number of such distributions, each corresponding to a different shell, and each being given a weight proportional to the average time spent by the vibrating charge between the two surfaces of the shell, or, by what is more convenient in practice, taking the average for a number of shells whose radii vary harmonically between 0 and b Coming now to a distribution of charge extending, when at rest, over a considerable volume, we suppose each portion of the charge to execute vibrations of the same amplitude and period The vibrations of the different parts will not be in the same phase , but in taking the average distribution of charge over a long period we may suppose the distribution to vibrate as a whole, and apply the process of averaging described above to the whole distribution curve

The averaging was carried out by a graphical method The problem is to find the average density, at a point distant x from the origin plane, which is produced when the distribution curve for absolute zero vibrates with an amplitude b As before, suppose first of all that every particle lies at a distance r from its position at absolute zero, all directions of displacement being equally probable This is the analogue of the case of the single spherical shell discussed above, and, from consideration of that case, it may be seen that the ordinate of the average curve corresponding to this state of affairs is the mean ordinate of that part of the zero distribution curve lying between $x + r$ and $x - r$ We find this mean ordinate for a series of values of r from zero up to b, the amplitude of vibration of the charge, and plot a curve giving its values against the values of r as abscissæ To get the mean corresponding to the case when the charge is vibrating with amplitude b, we must take the average of a number $2n + 1$ of the ordinates of this curve spaced so that the abscissæ are given by $b \cos (m\pi/2n)$, where m has all integral values from 0 to $2n$ In practice, $n = 6$ gives a sufficient number of ordinates in most cases By carrying out this process for a series of values of x we can plot out the average curve for the amplitude b

15 The results are summarised in figs 6 and 7, which refer to 290° abs and 900° abs respectively In fig 6, the observed curve for 290° is shown, together

with sets of points obtained by supposing the absolute-zero distribution to vibrate with amplitudes 0 06 and 0 07 of the atomic spacings, or 0 195 Å and

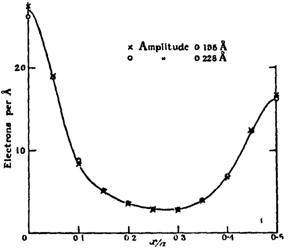

Fig 6 —Distribution Curve at 290° compared with Average Curve for amplitudes of 0 195 Å and 0 228 Å

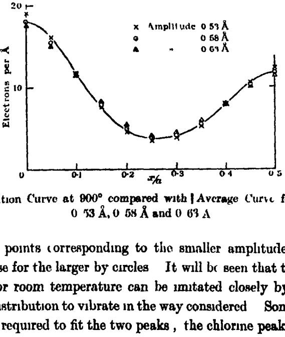

Fig 7 —Distribution Curve at 900° compared with Average Curve for amplitudes of 0 53 Å, 0 58 Å and 0 63 Å

0 228 Å The points corresponding to the smaller amplitudes are indicated by crosses, those for the larger by circles It will be seen that the general form of the curve for room temperature can be imitated closely by supposing the absolute zero distribution to vibrate in the way considered Somewhat different amplitudes are required to fit the two peaks, the chlorine peak is fitted closely by an amplitude of 0 2 Å, sodium by one of 0 23 Å It would be rash to conclude, however, that this proves the amplitudes of vibrations of the sodium

atoms to be greater than those of chlorine. This is indeed probably the case, but the actual heights of the peaks depend on the extrapolation used, and the method of averaging is only approximate, so that the results must be interpreted with caution.

For the 900° curve, amplitudes of 0·16, 0·175 and 0·19 of the crystal spacing, or 0·53 Å, 0·58 Å and 0·63 Å have been chosen. The points corresponding to these amplitudes are indicated in fig. 7 by crosses, circles and triangles respectively. In this case the amplitude 0·58 Å fits both peaks and the whole run of the curve quite closely. 0·53 Å appears to be definitely too small and 0·63 Å too large. The very close fit is somewhat surprising, considering the nature of the assumptions made, but rough as the method is, it probably gives quite a good estimate of the order of magnitude of the atomic excursions.

16. We may make a rough calculation of the atomic amplitudes in the following way:—In a vibrating lattice we cannot, of course, really speak of the amplitude of vibration of an atom about a mean position; it is only the relative amplitudes which are of significance. But for the purposes of this calculation we shall suppose that each atom is bound to a position of equilibrium by a quasi-elastic force f per unit displacement. In this case, the average energy of vibration of an atom is $\frac{1}{2}f\overline{a^2}$, where $\overline{a^2}$ is the mean-square amplitude. At a temperature as high as 900°, we can assume the average energy per atom to be $3k\mathrm{T}$, so that, equating these two quantities, we have

$$a^2 = \frac{6k\mathrm{T}}{f} \qquad (16{\cdot}1)$$

If we knew the value of the force f we could calculate $\overline{a^2}$. Now on the original simple theory of Debye, where each atom was supposed bound, by an elastic force f, to a mean position, the value of the exponent in the temperature factor is found to be

$$-\frac{16\pi^2 k}{f}\frac{\sin^2\theta}{\lambda^2}\,\mathrm{T}$$

In the more accurate elastic-wave theory, using Waller's modification, we find, for the case where $\Theta/\mathrm{T} \leqslant 1$, for the same exponent

$$-\frac{12h^2}{\mu k\Theta^2}\frac{\sin^2\theta}{\lambda^2}\,\mathrm{T},$$

where μ is the mass of an atom of the lattice, which is supposed simple-cubic. Following Debye,* we may compare these two expressions, and obtain an estimate of f, the force with which atoms must be supposed bound to their mean positions in order that their excursions in this ideal lattice should be of the same order of magnitude as those in the actual lattice From this comparison we obtain

---

* 'Ann. d. Physik,' *loc. cit.*

$$f = \tfrac{4}{3}\pi^2 \frac{k^2\Theta^2}{h^2} \quad \mu, \tag{16 2}$$

whence, from (16 1)

$$\overline{a^2} = \frac{9h^2T}{2\pi^2\mu k\Theta^2} \tag{16 3}$$

Taking μ as the mean mass of the sodium and chlorine atoms, 4 85 × 10^{-23} gm and Θ the characteristic temperature of rock salt as 281° we find

$$\sqrt{\overline{a^2}} = 0\ 58\ \text{A}$$

This is exactly the same amplitude as that found to give the best fit for 900° when the distribution curve for 0° was supposed to vibrate The exact agreement is, of course, purely accidental In fact since the observed values of the temperature factor at high temperatures are much higher than the calculated ones, we should have expected the amplitude calculated in this way to be considerably lower than that determined directly from the distribution curve but it is satisfactory to find that the values obtained in two distinct ways are at least quite consistent with one another

17 It is necessary to be clear as to what is actually determined in the analysis of the results given above The whole calculation is carried out on the assumption that the classical laws of scattering hold good, and that all the radiation scattered is coherent The distribution curves obtained are those of that hypothetical distribution of electrons which would produce the observed intensities, supposing that the atoms did consist of electrons which could be treated as free, and as scattering according to classical laws While the hypothetical "atom" so obtained may bear but little resemblance to the true state of affairs, it is nevertheless a physical constant for the atom concerned, and, as such, of empirical value for crystal analysis Further theoretical developments may modify greatly the interpretation of the results, but any such interpretation must be based on accurate quantitative measurements of the kind discussed in this paper This paper is concerned mainly with problems connected with the heat motions of the atoms, and we cannot here discuss our results in the light of the different atomic models which have been proposed We hope, however, to do this and to give fuller analyses of the F curves in a further paper

Summary

1 The ratio of the intensity of reflexion of X-rays by rock-salt at the temperature of liquid air, to that at room temperature, has been measured for a number of spectra The results show that the temperature factor is of the form exp $\{-bf(\mathrm{T}) \sin^2 \theta/\lambda^2\}$, the exponent being proportional to $\sin^2 \theta/\lambda^2$, or to the square of the order of the spectrum, within the errors of experiment For corresponding angles of reflexion, the temperature factor is considerably larger for spectra of the type Cl + Na than for those of the type Cl − Na

2 The results of these experiments, combined with those made at higher temperatures, and described in an earlier paper, are compared with the theoretical expressions for the temperature factor deduced by Debye and Waller The results, up to about 500° abs , agree fairly well with the theory of Waller At high temperatures the decrease in intensity is more rapid than theory indicates This is to be expected, since the validity of Waller's original assumptions ceases at really high temperatures Later work by Waller shows a more rapid decrease of the kind observed

3 The absolute value of the integrated reflexion for the (200) spectrum from a rock-salt crystal has been redetermined, both for molybdenum and rhodium K_α An estimate of the "extinction" for this crystal for molybdenum radiation has been made The reflexions from a number of faces of the rock-salt crystal have been compared with the (200) spectrum and thus determined in absolute measure From the values obtained, the F factors, or atomic scattering factors, of the atoms of Na and Cl have been deduced at 0°, 86°, 290° and 900° abs

4 The method of Fourier analysis has been used to calculate the distribution of electrons between the (111) planes of the crystal at different temperatures, and from the broadening of the peaks in the distribution curves the mean amplitudes of the atomic vibrations have been estimated Mean amplitudes of about 0 20 Å at 290° abs and of 0 58 Å at 900° abs , explain the observed changes in the distribution curves

5 This estimate of the amplitudes of the atomic vibrations is checked by means of an approximate calculation, which leads to results of the same order

In conclusion, we wish to express our thanks to Prof W L Bragg, F R S , for many helpful suggestions throughout the course of the work We are indebted to Dr Ivar Waller and to Mr C H Bosanquet for valuable criticisms, and to Mr W Kay and Mr W Reynolds for much help and advice in constructing the apparatus

Shifts and Reversals in Fuse-Spectra

By A C Menzies, M A, Head of the Physics Department, University College, Leicester

(Communicated by R Whiddington, F R S—Received July 29, 1927)

[Plate 4]

The present paper gives an account of the spectra obtained when wires are suddenly short-circuited so as to carry currents of upwards of 100 amperes The material of the wire is consequently vaporised, and the light from the momentary arc is photographed by the spectrograph through the metallic vapour At the same time there is a high pressure and temperature produced, so that the spectrum differs from that of the normal low-current arc in respect of absorptions, self-reversals, broadenings and shifts A study of the absorptions and self-reversals, using copper and iron wires, has led to some interesting results

The method was suggested by the work of Anderson* on electrically exploded wires, when it was particularly observed that very many of the lines were reversed It was evident that by using a lower potential or by making the discharge less sudden, fewer lines would be reversed, and so an order of reversal might be established and conclusions drawn as to depths of levels Lack of resources precluded this research, and it has been done successfully by Hori,† Déchêne,‡ and others

However, experiments with an accumulator battery showed that much could be done with potential differences of the order of 100 volts Certain lines are then absorbed, and the method possesses advantages

The importance of high-current arc spectra has been emphasised by A S King,§ who has published work on iron and other metals in the visible region, using a 500-kw generator to get currents of the order of 1000 amperes Judged by the shift produced in certain copper lines, conditions in the present experiments must have approached those obtained by King, unless the amount of the shift is greatly independent of the conditions

The simplicity of the method here described and the low power required should recommend it as a convenient source

---

* 'Astrophys J,' vol 51, p 37 (1920)

† 'Inst. Phys and Chem Res, Tokyo, Sci. Papers,' No 53 (1926)

‡ 'J de Phys et le Rad,' vol 7, p 59 (1926)

§ 'Astrophys J,' vol 62, p 238 (1925)

Procedure

A wire is lined-up in front of the slit of the spectrograph by moving it until it eclipses the light from a fixed straight-filament lamp In most of the experiments a pair of crossed cylindrical lenses (one twice the power of the other) was used to concentrate the light upon the slit, in others a spherical lens was used in order to distinguish between long and short lines At first there was uncertainty as to the place where the wire would fuse, this was overcome by cutting the wire when in place and then butting the two ends together When the current was then sent through, the fuse took place at the cut It was found convenient to mount the wire in a special holder attached to an ebonite sheet in such a way that the burst could be made to take place inside a tank with a quartz window, thus enabling the medium to be changed from air to water In another series of experiments a holder made of brass tubing was used, the wire was mounted axially in one tube, and the light was observed through a cross-tube carrying quartz windows With this, fuses *in vacuo* were investigated

The wire was short-circuited to the battery (ordinarily 110 volts, 144 ampere-hours) by a heavy, double-bladed spring-switch, controlled from a distance This was found advisable, because when the wire explodes, tiny fragments are shot out with considerable violence (see photograph showing a typical burst, with the parabolas due to glowing beads shooting out from the arc)

Photographs were taken with a Littrow-type instrument made in the departmental workshop, it employs two optical trains made by Adam Hilger, Ltd one consists of two glass 60° prisms of 3-inch side, and a plane mirror silvered on the front surface The other train is a quartz lens and a small quartz 30° prism having tin-amalgam on the back surface For observations below λ 2100 a small quartz spectrograph by Hilger (E 37) was found useful With it photographs could be taken down to λ 1,840 The dispersions used were of the order of 7 Å U per mm at λ 5000, 6 Å U per mm at λ 2500, and 12 Å U per mm at λ 2000, respectively

Currents Used

The transient nature of the current makes measurement difficult, and, indeed, it is doubtful what to understand by the " current " In the present experiments attempts were made to ascertain the order of the maximum current attained during the discharge A suitable oscillograph was not accessible, so the following two devices were used —

(*a*) A straight wire, having a resistance of one-third of an ohm, was included in series with the fusing circuit, and potential leads from the ends of this wire were included in another circuit, consisting of a high-tension battery and an Osglim lamp (see figure) The voltage of the high-tension battery was insufficient to light the Osglim lamp, but enough to maintain it lit once the discharge through the lamp had commenced (The particular lamp employed lit at 136 volts, and was maintained by voltages above 104)

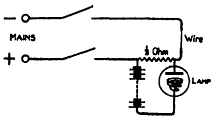

The high-tension voltage was adjusted by trial until the lamp just lit on causing a burst, showing that the total voltage was 136 As far as the writer is aware, this method is original

(*b*) The potential leads mentioned in the preceding paragraph were connected to the deflecting plates of a Braun tube, having a Wehnelt cathode The transient deflection of the electron beam was observed in a dark room, and this was subsequently compared with the deflections produced by steady voltages

With a 110-volt, 144-ampere-hour accumulator-battery and copper wire electrodes, 26 gauge, the current was about 90 amperes as measured by each method This was necessarily with a resistance of one-third ohm in series, so that when this was absent the currents must have been greater, certainly, judging by the increase in the noise and the flash, this was true One may say at a conservative estimate that the currents were of the order of 100 amperes.

Effect of the Discharge on Bands

Owing, perhaps, to the high temperature and pressure, and to the relatively large ionisation compared with that obtaining in low-current arcs, many lines broaden out, and in particular bands disappear For example, the third positive Nitrogen bands disappear This may be because the conditions are adverse to the existence of molecules, or because the bands are really there, but the band-lines are so broadened that they merge into one another and into the general background Some evidence has been found that the second cause is operating as well as the first, in many photographs the background deepens and lightens in step with the edges of bands appearing in the low-current arcs In any case, the non-appearance of these bands is helpful when the lines engage one's attention, in that they are rendered more conspicuous

Certain bands however, stretching from λ 1947 down to λ 1840, approximately, are visible in absorption in the fuse-spectra, in the ultra-violet, these appear faintly in all the photographs taken, but particularly strongly in the case of cadmium, which gives a good continuous background in the ultraviolet

The bands appear to be those attributed by Steubing* to neutral oxygen molecules, in the above-mentioned cadmium photographs extra bands are visible beyond those already recorded, these will form the subject of a future communication They appear to be due to absorption by oxygen, or some other similar carrier, in the air, between the source and the spectrograph plate

Advantages of the Method

In addition to that just described this method has the advantage that it entails no unusual apparatus Compared with the bursting of wires by condenser discharges, it has the advantage of giving a photograph with only one exposure, it does not give as many reversals but this is an advantage if the lowest levels are being sought Compared with absorption-tube or under-water spark methods the present methods allow observations to be made in low wave-length regions inaccessible to the former An attempt is to be made to carry observations into the vacuum-grating region

Copper

The results here recorded make no attempt at any completeness, but are given to record rather the type of observation possible

In the visible region many lines were found to be shifted to the red, and many broadened Reversals were not common Shifts were measured for some lines, and are shown in the following table The shifts are not necessarily comparable with one another, since they may have been taken on different plates if the lines are far apart, but it will serve to give an idea of the magnitude of the shifts

Table I

—	λ	Terms	Å U	Remarks
First plate	4509 39	$^4F_2 - {}^4D_1$	0 38	Burst using 200-volt A C
	4378 2	$^4P_2 - {}^4D_3$	0 39	
	4275 13	$^4P_3 - {}^4D_4$	0 48	
Second plate	4275 13	$^4P_3 - {}^4D_4$	0 36	Burst using 110 volt D C
	4248 97	$^4P_1 - {}^4D_1$	0 29	
	4242 26	$^4\bar{D}_2 - {}^2D'_2$	0 30	
	4177 76	$^4P_3 - {}^4D_3$	0 30	

* 'Ann d Physik,' vol 33, p 553 (1910)

In addition to the above, the following lines can be said with certainty to be shifted to the red —

λ	Terms	λ	Terms
5292 54	${}^4\bar{D}_4 - {}^4D_4$	4866 4	${}^2\bar{D}_3 - {}^2D''_3$
5144 12	${}^4\bar{D}_4 - {}^4D_3$	4697 49	${}^4F_2 - {}^4D_2$
5111 94	${}^4\bar{D}_1 - {}^4D_1$	4586 97	${}^4F_4 - {}^4D_3$
5034 33	${}^2F_3 - {}^4D_2$	4397 0	${}^4\bar{D}_3 - {}^2D''_3$
5016 63	${}^4\bar{D}_2 - {}^4D_1$	4104 23	${}^4P_2 - {}^4D_1$

$\lambda\lambda$ 4530 84, 4480 38, $(2^2P_{2,1} - 3^2S_1)$ were broadened to the red

And the following to the violet —

λ	Terms	λ	Terms
3925 27	${}^2\bar{D}_3 \quad {}^4D'_3$	3290 55	${}^4F_4 - {}^4G_5$
3921 27	${}^2D_3 - {}^4F_4$	3282 72	${}^4F_3 - {}^4G_4$
3759 50	${}^4D_2 - {}^2\bar{F}_3$	3208 24	${}^4D_2 - {}^4\bar{D}_3$
3741 25	${}^4\bar{D}_3 - {}^2G_4$	3140 32	${}^4P_3 - {}^2D''_2$
3734 23	${}^4D_2 - {}^2F_4$	3126 11	${}^4P_2 - {}^4F_3$
3354 48	${}^4F_2 - {}^4\bar{F}_2$	3116 35	${}^4P_3 - {}^2D''_3$
3349 29	${}^4F_2 - {}^4D'_2$	3099 92	${}^4P_3 - {}^4D'_4$

$\lambda\lambda$ 3861 76, 3825 05, $(2^2P_{2,1} - 4^2S_1)$ were broadened to the violet

It is noticeable that the shifted lines having high level initial terms which are moved to the red come from initial states belonging to (core + *s*) configurations, while those obviously shifted to the violet have initial terms belonging to (core + *d*) configurations (The allocation of configurations has been taken from Sommer *) Assuming the truth of this, the allocation of the following lines, which are displaced, has been greatly facilitated —

---

* 'Z. f Physik,' vol 39, p 711 (1926)

Table II – Copper Lines Classified according to Shift

(This list consists of lines not previously classified The calculated values have been obtained by the difference of terms as given by Sommer (*loc cit*), while X_2, A, B, and ${}^4G_6$ are suggested new terms, and are discussed below)

λ	ν obs	ν calc	Shift	Allocated Terms
5143 16	19437 9	19439 2	*r*	${}^2P_1 - X_2$
5070 2	19694 3	19695 0	*r*	${}^2F_4 - {}^2D'_3$
4794 0	20853 6	20853 6	*r*	${}^4\overline{D}_3 - X_2$
4642 6	21533 6	21533 7	*r*	${}^2F_3 - X_2$
4354 6	22957 8	22957 3	*r*	${}^4F_2 - X_2$
4267 40	23426 5	23427 9	ft *r* ?	${}^4\overline{D}_2 - {}^2D'_2$
4073 27	24543 2	24543 8	*r*	${}^4P_2 - {}^2D'_3$
3656 70	27338 6	27338 8	*r*	${}^4\overline{D}_2 - B$
3599 14	27776 6	27776 5	*v*	${}^4\overline{D}_4 - {}^4G_5$
3520 03	28400 7	28400 7	*r*	${}^4\overline{D}_1 - A$
3483 76	28696 1	28695 5	*v*	${}^4F_2 - {}^2F_2$
3474 57	28772 2	28772 3	*v*	${}^4\overline{D}_2 - A$
3454 70	28937 8	28936 7	*r*	${}^2\overline{D}_2 - {}^4\overline{P}_1$
3379 69	29580 0	29580 4	*r*	${}^4F_2 - B$
3365 35	29706 1	29705 3	*v*	${}^4F_3 - {}^4D'_4$
3307 95	30221 5	—	*v*	${}^4F_4 - {}^4G_6$
3231 17	30939 6	30939 2	*v*	${}^4P_1 - B$
3223 42	31014 0	31014 0	*v*	${}^4F_2 - A$
3146 82	31768 9	31768 9	*v*	${}^4P_2 - B$
3088 12	32372 8	32372 8	*v*	${}^4P_1 - A$

In consequence of the correction of λ 3599 from $2\,{}^2P_2 - 5\,{}^2S_1$ it is possible to allocate the four following lines —

λ	ν obs	ν calc	Allocated Terms
3598 01	27785 1	27785 1	$2\,{}^2P_2 - 5\,{}^2S_1$
3566 14	28033 6	28033 5	$2\,{}^2P_1 - 5\,{}^2S_1$
3463 5	28864 3	28864 2	$2\,{}^2P_2 - 6\,{}^2S_1$
3433 98	29112 4	29112 6	$2\,{}^2P_1 - 6\,{}^2S_1$

λ 3599 14 is ascribed by Sommer and others to $2\,{}^2P_2 - 5\,{}^2S_1$ It is too strong for this the intensity of successive pairs would run 6,6, 3,3, 10, —, while with the present allocation it becomes 6,6, 3,3, 2,1, 1,1 Again, this line is shifted considerably to the violet the shift has been measured, and amounts to 0 6 A U in one photograph From what has been said it will be realised that this indicates probably an initial orbit of diffuse character, $5\,{}^2S_1$ would not agree so well This line was regarded at first as an "exception," but now, regarding the initial orbit as ${}^4G_5$, it agrees well with the theory

In addition to the above, the following lines can be said with certainty to be shifted to the red —

λ	Terms	λ	Terms
5202 54	$^4\bar{D}_4 - {}^4D_4$	4866 4	$^2\bar{D}_3 - {}^2D^2_3$
5144 12	$^4\bar{D}_4 - {}^4D_3$	4697 49	$^4F_2 - {}^4D_2$
5111 94	$^4\bar{D}_1 - {}^4D_1$	4586 97	$^4F_4 - {}^4D_3$
5034 33	$^2F_3 - {}^4D_2$	4397 0	$^4\bar{D}_3 - {}^2D^2_3$
5016 63	$^4\bar{D}_2 - {}^4D_1$	4104 23	$^4P_2 - {}^4D_1$

$\lambda\lambda$ 4530 84, 4480 38, ($2^2P_{2,1} - 3^2S_1$) were broadened to the red

And the following to the violet —

λ	Terms	λ	Terms
3925 27	$^2\bar{D}_3 - {}^4D^1_3$	3290 55	$^4F_5 - {}^4G_5$
3921 27	$^2\bar{D}_3 - {}^4F_4$	3282 72	$^4F_3 - {}^4G_4$
3759 50	$^4\bar{D}_2 - {}^2F_3$	3208 24	$^2D_2 - {}^4\bar{D}_3$
3741 25	$^4\bar{D}_3 - {}^2G_4$	3140 32	$^4P_3 - {}^2D^2_2$
3734 23	$^4\bar{D}_3 - {}^2F_4$	3126 11	$^4P_3 - {}^2F_3$
3354 48	$^4F_2 - {}^4\bar{F}_2$	3116 35	$^4P_3 - {}^2D^2_3$
3349 29	$^4F_2 - {}^4D^1_2$	3099 92	$^4P_3 - {}^4D^1_4$

$\lambda\lambda$ 3861 76, 3825 05, ($2^2P_{2,1} - 4^2S_1$) were broadened to the violet

It is noticeable that the shifted lines having high level initial terms which are moved to the red come from initial states belonging to (core + *s*) configurations, while those obviously shifted to the violet have initial terms belonging to (core + *d*) configurations (The allocation of configurations has been taken from Sommer *) Assuming the truth of this, the allocation of the following lines, which are displaced, has been greatly facilitated —

---

* 'Z. f Physik,' vol 39, p 711 (1926)

Table II —Copper Lines Classified according to Shift

(This list consists of lines not previously classified The calculated values have been obtained by the difference of terms as given by Sommer (*loc cit*), while X_2, A, B, and $^4G_6$ are suggested new terms, and are discussed below)

λ	ν obs	ν calc	Shift	Allocated Terms
5143 16	19437 9	19439 2	*r*	$^2P_1 - X_2$
5076 2	19694 3	19695 0	*r*	$^2F_4 - {}^2D'_3$
4794 0	20853 6	20853 6	*r*	$^4\bar{D}_3 \quad X_2$
4642 6	21533 6	21533 7	*r*	$^2F_3 - X_2$
4354 6	22957 8	22957 3	*r*	$^4F_3 - X_2$
4267 49	23426 5	23427 0	ft *r* ?	$^4\bar{D}_2 - {}^2D'_2$
4073 27	24543 2	24543 8	*r*	$^4P_2 - {}^2D'_3$
3656 70	27338 6	27338 8	*v*	$^4\bar{D}_3 - B$
3599 14	27776 6	27776 5	*v*	$^4\bar{D}_4 \quad {}^4G_3$
3520 03	28400 7	28400 7	*i*	$^4\bar{D}_1 - A$
3483 76	28696 4	28695 5	*v*	$^4F_2 - {}^2\bar{F}_2$
3474 57	28772 2	28772 3	*r*	$^4\bar{D}_2 \quad A$
3454 70	28937 8	28936 7	*i*	$^2\bar{D}_2 - {}^2\bar{P}_1$
3379 69	29580 0	29580 4	*r*	$^4F_2 - B$
3365 35	29706 1	29705 3	*i*	$^4F_3 - {}^4D'_4$
3307 95	30221 5	—	*v*	$^4F_5 - {}^4G_6$
3231 17	30939 6	30939 2	*v*	$^4P_1 - B$
3223 42	31014 0	31014 0	*v*	$^4F_3 - A$
3146 82	31768 9	31768 9	*i*	$^4P_2 - B$
3088 12	32372 8	32372 8	*r*	$^4P_1 - A$

In consequence of the correction of λ 3599 from 2 $^2P_2$ — 5 $^2S_1$, it is possible to allocate the four following lines —

λ	ν obs	ν calc	Allocated Terms
3598 01	27785 1	27785 1	$2\ {}^2P_2 - 5\ {}^2S_1$
3566 14	28033 6	28033 5	$2\ {}^2P_1 - 5\ {}^2S_1$
3463 5	28864 3	28864 2	$2\ {}^2P_2 - 6\ {}^2S_1$
3433 98	29112 4	29112 6	$2\ {}^2P_1 - 6\ {}^2S_1$

λ 3599 14 is ascribed by Sommer and others to 2 $^2P_2$ — 5 $^2S_1$ It is too strong for this the intensity of successive pairs would run 6,6 , 3,3 , 10, — , while with the present allocation it becomes 6,6 , 3,3 , 2,1 , 1,1 Again, this line is shifted considerably to the violet the shift has been measured, and amounts to 0 6 A U in one photograph From what has been said it will be realised that this indicates probably an initial orbit of diffuse character , 5 $^2S_1$ would not agree so well This line was regarded at first as an "exception," but now, regarding the initial orbit as $^4G_5$, it agrees well with the theory

λ 3307 95 behaves in the bursts exactly in the same way as λ 3290 55, ${}^4F_5 - {}^4G_6$, and also it is stronger It would consequently fit well with ${}^4F_5 - {}^4G_6$ Unfortunately it is impossible to check this, as so far ${}^4F_5$ is the only term allocated, having $j = 5$, to combine with ${}^4G_6$

The term X_2 has $j = 2$, probably, on account of intensities, also, since it is connected with lines which shift red, it will be of structure (core + s) It can, therefore, only be the term ${}^2D^2_2$ missing from Sommer's scheme, and must go with ${}^2D^2_3$, so having a difference of wave-number of 1882 6

The term $A = -11008$ 5 is connected with lines which shift violet, and therefore will probably be a (core + d) term It could be one of the missing ${}^2S_1$, or ${}^2\bar{P}_1$, or ${}^2\bar{P}_2$

B is $-$ 9574 9 It gives lines which move to the violet, and is therefore also a (core + d) term It combines with much the same terms as A does It is suggested that A and B are the missing ${}^2\bar{P}_1$ and ${}^2\bar{P}_2$, with difference of wave-number 1433 6 If this is so, an interesting coincidence arises the sums of the wave-number differences of similar terms, belonging to the same configuration, are, approximately, in arithmetical progression ${}^2\bar{P}$, ${}^2D$, ${}^2\bar{F}$, with series limit ${}^3D$, and ${}^2\bar{P}$, ${}^2D$, ${}^2\bar{F}$ with series limit ${}^1D$, are such similar terms, while ${}^2P$, ${}^2\bar{D}$, ${}^2F$ with series limit ${}^3D$ and ${}^2P$, ${}^2\bar{D}$, ${}^2F$ with series limit ${}^1D$ are another set of similar terms The sum of the wave-number difference between ${}^2\bar{P}_1$ and ${}^2\bar{P}_2$, and between ${}^2\bar{P}^1{}_1$ and ${}^2\bar{P}^1{}_2$, is 2066 Similarly the ${}^2D$ differences give 1877, and the ${}^2\bar{F}$ differences 1675, and these three numbers are nearly in arithmetical progression

Dealing similarly with the other set, the sums of differences are 1133, 2139, 3327, which again are approximately in arithmetical progression While this seeming regularity is quite probably spurious, at least it suggests that the three terms ${}^2D^2_2$, ${}^2\bar{P}_1$, and ${}^2\bar{P}_2$, newly allocated, involve wave-number differences of the right order

Reversals

All those lines, which are reversed, have final orbits 1 ${}^2S_1$, ${}^2D_2$ or ${}^2D_3$, as was also found by Stücklen using the under-water spark * The reversals are more prominent with the 200-volt A C mains than with the 110-volt battery Also they are intensified by the use of finer wire (26 gauge was normally used, 40 gauge gave rise to more prominent reversals, but several exposures were required) *λ 2024 reversed very clearly A reproduction of a photograph* obtained with the small spectrograph is given in Plate 4 Some lines were self-reversed, others were completely reversed on the general continuous background The following lines were reversed —

---

* 'Z f Physik,' vol 34, p 562 (1925)

λ	Terms	λ	Terms
3273 97	$1\,{}^2S_1 - 2\,{}^2P_1$*	2225 67	$1\,{}^2S_1 - {}^4\overline{D}_1$*
3247 55	$1\,{}^2S_1 - 2\,{}^2P_2$*	2215 65	${}^2D_2 - {}^2\overline{D}^1_2$*
2768 80	${}^2D_2 - 3\,{}^2P_1$	2214 56	${}^2D_2 - {}^2P^1_2$*
2766 39	${}^2D_2 - 3\,{}^2P_2$	2205 6	—*
2618 38	${}^2D_3 - 3\,{}^2P_2$	2199 73	${}^2D_2 - 3616\ 7$*
2492 14	$1\,{}^2S_1 - {}^4P_2$	2199 57	${}^2D_3 - {}^2\overline{D}^1_3$*
2441 63	$1\,{}^2S_1 - {}^4P_1$	2181 68	$1\,{}^2S_1 - {}^2P_1$*
2406 66	${}^2D_2 - a_3$	2179 37	spk ?
2392 63	${}^2D_2 - b_2$	2178 91	$1\,{}^2S_1 - {}^2P_2$*
2303 11	${}^2D_2 - {}^2\overline{D}^1_3$	2176 27	—*
2294 35	—	2171 75	${}^2D_2 - c_2$*
2293 83	${}^2D_3 - a_2$*	2169 49	—*
2263 09	${}^2D_2 - {}^2P^1_1$*	2165 06	$1\,{}^2S_1 - {}^2\overline{D}_2$*
2260 49	${}^2D_2 - 4\,{}^2F_{3,4}$*	2138 44	${}^2D_3 - 4357$*
2244 24	$1\,{}^2S_1 - {}^4\overline{D}_2$*	2136 9	—*
2238 43	${}^2D_2 - 5\,{}^2F_3$*	2130 70	${}^2D_2 - {}^2F^1_3$
2236 22	${}^2D_2 - 4357$*	2124 1	${}^2D_3 - f_3$
2230 07	${}^2D_3 - {}^2F^1_4$*	2047 7	—
2227 74	${}^2D_2 - {}^2F^1_3$*	2024 3	$1\,{}^2S_1 - 3\,{}^2P_2$*

Those marked with an asterisk were strongly absorbed

In addition, the following were self-reversed —

λ	Terms	λ	Terms *
5218 17	$2\,{}^2P_2 - 3\,{}^2D_3$	2210 24	— spk
5153 23	$2\,{}^2P_1 - 3\,{}^2D_2$	2192 24	— spk
5105 55	${}^2D_3 - 2\,{}^2P_2$	2189 60	— spk
4275 13	${}^4P_3 - {}^4D_4$	2125 98	— spk
2281 0	${}^2D_3 - b_2$	2122 92	— spk
2246 98	— spk	2112 02	${}^2D_3 - c_2$
2242 60	— spk	2104 72	— spk
2218 08	— spk	—	—

---

* [*Note added September* 20, 1927 —I have been able to refer in the meantime to a paper by A. G Shenstone, 'Phys Rev,' vol 29, p 380 (1927), on the "Spark Spectrum of Copper" It is interesting to note that all the reversed lines not allocated above and marked "spk" belong to the low levels a^3D or a^1D in the copper spark]

The following lines, strong in the ordinary arc, were very much weakened in the bursts They are probably broadened out, with a violet absorption-edge They may be regarded as incipient reversals —

λ	Terms	λ	Terms
3530 39	${}^2D_2 - {}^4F_3$	3036 11	${}^2D_2 - {}^2\bar{D}_2$
3457 86	${}^2D_3 - {}^4P_2$	3010 84	${}^2D_3 - {}^4\bar{D}_3$
3337 85	${}^2D_3 - {}^4F_4$	2997 36	${}^2D_2 - {}^2\bar{D}_3$
3279 82	${}^2D_2 - {}^21_3$	2961 18	${}^2D_3 - {}^2F_4$
3156 62	${}^2D_2 - {}^4\bar{D}_1$	2882 94	${}^2D_2 - {}^2P_2$
3093 99	${}^2D_2 - {}^4\bar{D}_4$	2858 74	${}^2D_3 - {}^2\bar{D}_2$
3073 80	${}^2D_3 - {}^2F_3$	2824 38	${}^2D_2 - {}^2\bar{D}_3$
3063 42	${}^2D_2 - {}^2P_2$	–	—

It will be observed that in the table of reversed lines two new terms, 4357 and 3616 7, have been introduced

The term 4357 combines also with 1 ${}^2S_1$, 2 ${}^2S_1$ and $\zeta_{2,3}$, giving λ 1725 9, λ 6749 29, λ 3635 923, respectively It is therefore possible that it could be 5 ${}^2P_{2,1}$, in which case 3031, called by Sommer “ e ”$_2$, would fit in as 6 ${}^2P_{2,1}$

A possible term is 3616 7, combining with ${}^2D_2$, 1 ${}^2S_1$, and 2 ${}^2S_1$ to give λ 2199 73, λ 1703 7, and λ 6427 564, respectively

It is interesting to notice how the lines involving ${}^2D_{2,3}$ terms behave in the bursts It will be seen from the foregoing tables that those involving switches from initial doublet terms converging to ${}^3D$ are absorbed, and are in the first list, while those whose initial doublet terms converge to ${}^1D$ are in the third list of lines, being simply greatly weakened

Zinc

Fukuda* examined the spectra of zinc, cadmium and mercury, obtained from a spark, with the voltage regulated by means of a series gap which was set at 1 mm , 2 mm , and so on up to 5 mm , successively Shifts were then found of much the same order as are met with here in the spectra of burst wires His tables show that for these metals some spark lines showed red shifts, and some diffuse lines violet shifts, while some singlet diffuse lines shifted red

Zinc was consequently used to see if similar results could be found in the case of fuses Zinc rod (commercial) containing much lead and cadmium was used for the low current arc comparison, and some of the same rod was melted down and made into sheet (by pouring the molten metal on an inclined plane of cold brass sheet), and then cut into narrow strips, like magnesium ribbon This method is found useful for making “ wires ” of easily fusible metals

Some zinc lines were absorbed, and certain spark doublets appeared , the lines of the sharp triplet series are greatly shifted red, while λ 4630, 2 ${}^1P_1$ — 4 ${}^1D_2$, certainly shifts red The diffuse triplet λ 3346, λ 3303, λ 3282 are reversed, the emission being slightly stronger on the violet side

---

* ‘Inst Phys Chem Res , Tokyo, Sci Papers,’ No 37, p 183 (1925)

The combination line 1 $^1S_0$ — 2 $^3P_1$, λ 3076, does not shift, while the neighbouring 2 $^3P_2$ — 3 $^3S_1$, λ 3072 2, shifts red This enabled the shift of the latter to be measured with certainty, it was found to be 0 9 Å U on a particular photograph, the wire being burst on 110 volts from cells It was also found that the shift was greater in the light from the cathode

The observations agreed with those made for copper, except that the diffuse singlet line shifted red, while it was expected to shift violet (*Cf* also the behaviour of 2 $^2P_{2,1}$ — 4 $^2S_1$ for copper) This matter will be further investigated A tentative explanation of such "exceptions" is put forward in the discussion below

Fig *h*, Plate 4, shows the redward shift of the sharp triplet line 2 $^3P_2$ — 3 $^3S_1$ (λ 3072 2), the diffuse triplet being self-reversed, thus helping to show freedom from mechanical shift

Iron

Iron wires, 26 gauge, were burst with the 110-volt battery, and also by short-circuiting the 200-volt A C mains

Similar results were found as for copper, lines shifted, and reversals were common in the ultra-violet

Since the iron spectrum is not yet completely worked out, it was felt to be unprofitable to study the shifts in great detail

In the regions of the spectrum investigated, which overlapped, the observations with the bursts are in agreement with the valuable detailed observations of King,* except that in the case of one line, λ 5110, no shift could be detected, while according to King it is shifted violet The dispersion of his instrument was much greater than that of any instrument available to the writer, so that his observation is very probably justified

In consequence of the agreement found, it is felt justifiable to generalise from King's results

Shifts to the red are large for lines having as initial terms $b\ ^3F$, d^2, and δ, with $\bar{f}^2$ just slightly less Next come $\bar{d}^3$ and p^2, and then $\bar{G}^1$ and $\bar{g}^1$, p^1, $\bar{D}^2$ and f^1 (The notation and allocation of terms is due to Laporte †)

It will be observed that shift depends on two factors for its magnitude —

(1) The greatness of the term

(2) The electron configuration to which the term belongs

---

* *Loc. cit.*

† 'Nat Acad Sci Proc,' vol 12, p. 496 (1926)

(1) has already been pointed out by King , the nearer the orbit is to the confines of the atom—we might say the more " suburban " it is—the greater is its tendency to shift This is plausible, since outside influences, such as ionisation and pressure, can there have more effect

(2) is clearly present in the case of iron, as well as in that of copper For example, $\bar{f}^2$ is more " suburban " than d^2 and δ, and we should therefore expect it to be more susceptible to shift if (1) alone operated But it belongs to a different electronic configuration, and consequently is not directly comparable with d^2 and δ (according to Laporte, $\bar{f}^2$ is sd^7, while d^2 and δ are ssd^6)

It is possible to summarise the results for iron in this way Lines whose initial terms have structure (core + s), i e , d^6s, s or d^7, s, will suffer a large redward shift in the high current arc Only one exception to this rule can be found this is a new ^{3}D term at 54000 (Laporte*), and some of the lines to which it gives rise broaden to the red

Many lines are shifted to the violet, and, arguing from what happens in the case of copper, it seems safe to predict that the initial terms involved will have structures (core + d), i e , (d^6 s, d) and (d^7, d), although up to now these terms have not been allocated This should help considerably in sorting out the remaining terms of the iron arc spectrum

Reversals

The lines, whose terms are known, and which were reversed, all had as final orbits d^1 terms or $\bar{f}^1$ terms (the two lowest terms in Laporte's scheme)

The unassigned lines which reversed were principally below λ 2200 , in particular, a group from λ 1930 to λ 1964 were strongly absorbed Regularities have been sought among these reversed lines, and, as might be expected, d^1 or $\bar{f}^1$ terms are frequent A detailed account of the iron reversals is left over until the observations are complete

Discussion of the Shifts

Broadenings and shifts of spectral lines from an arc can be caused in a variety of ways they may be due to high pressure, high temperature, pole-effect (still unexplained), or to high electric fields In the present experiments it is believed that they are due to the pressure effect, and to high electric fields The shifts are more obvious for the longer wave-lengths, which suggests that pressure is at work , also it is obvious from the noise, and from the shooting-out of glowing beads of metal, that the pressure must be considerable Also King compares the high-current arc in iron with the pressure-arc of Gale and Adams,[†] and finds that the two sources give similar results

---

* *Loc cit*

High electric fields causing an incipient Stark effect are thought to be present for the present observations agree with those of Kimura and Nakamura [‡] Compare also Lowery's work with the interrupted arc [§] Kimura and Nakamura worked with an arc carrying 40 amperes, and found that the broadenings agreed with the Stark effect (they dealt with low-level term-lines only) They note, however, that in many cases, when a broadening took place to the red, a faint wing to the violet also appeared, not to be expected from the point of view of the Stark effect It is significant that this happened for lines with initial terms of diffuse character They say "This minor deviation, *i e*, a slight broadening in the direction opposite to that indicated by the Stark effect, may be due to some other causes"

It is now tentatively suggested that in the high current bursts two main causes are at work producing asymmetrical broadenings —

(*a*) The Stark effect, prominent in lines having low-level initial terms, and

(*b*) The pressure effect, which modifies the high-level terms

Our generalisation as to direction of shift being controlled by the d or s electron added, thus applies only to (*b*) So a careful discrimination between low-level and high-level terms will be necessary in order successfully to apply this criterion for diffuse and sharp types

Note added 20th September, 1927

An alternative explanation of the shifts to the red and to the violet arose in conversation with Mr D R Hartree, of St John's College, Cambridge, to whom I am indebted

Let terms s, p, d, etc, decrease in the high current arc to $s - \Delta s$, $p - \Delta p$, etc Then a line p-s will become p-$s - (\Delta p - \Delta s)$, while a line p-d will become p-$d - (\Delta p - \Delta d)$ Now if $\Delta s < \Delta p < \Delta d$, then $(\Delta p - \Delta s)$ is positive and $(\Delta p - \Delta d)$ negative This would mean a red shift for sharp lines and a violet shift for diffuse ones

This symbolic "explanation" thus requires two postulates —

(1) That the high-current arc conditions cause a decrease in all term-values

(2) That the amount of the decrease is progressively greater in the order s, p, d, etc

---

[*] *Loc cit.*

[†] 'Astrophys J,' vol 35, p 10 (1912)

[‡] 'Japanese J Phys,' vol 2 p 61 (1923)

[§] 'Phil Mag,' vol 49, p 1176 (1925)

In the present case the orbits concerned are $5s$, $4p$ and $4d$, here (2) will probably be satisfied, since the greater penetration of the $5s$ orbit will make it less subject to perturbations than the $4p$, and again the $4p$ less than the $4d$.

In keeping with this is the notorious tendency of $(p\text{-}f)$ lines to be shifted to the violet by electric fields (see *e g*, Hick's "Analysis of Spectra," p 264)

Summary.

An account is given of a simple means whereby a high-current arc is struck momentarily between wires The spectrum of copper so obtained has been compared with the low-current arc spectrum, and regularities have been sought on the bases of shifts and reversals

Five, and possibly six, new terms have been deduced, leading to the allocation of 32 new lines Some of these are identified with terms missing from Sommer's scheme

The lines which were reversed have final terms which belong to low levels, for copper they are $1\,{}^2S_1$ or ${}^2D_2$ or ${}^2D_3$ terms

Lines have a tendency to shift as the current increases, and this is due to mixed causes For high-level initial terms having structure (core + s), the lines shift to the red, for high-level initial terms having structure (core + d), the lines shift to the violet, for low-level initial terms, the lines shift in accordance with the Stark effect mainly

For iron it can be said that the magnitude of the shift depends on the magnitude of the term, and on its structure (judging from King's results) The iron spectrum is still insufficiently well-known to decide on the structure of the orbits shifted violet, but in view of the results here obtained with copper, it is predicted that these will belong to terms having structure d^7, d and $d^6\,s, d$

Further work is being done to see if this dependence of shift on electronic configuration is general, if it should prove to be so, a valuable guide will have been found for unravelling the high-level terms in spectra which at present are proving so complicated

DESCRIPTION OF PLATE 4

a, *c*, *g* are arcs between copper electrodes carrying 4 amperes
h is an arc between zinc electrodes carrying 3½ amperes
b, *d*, *e*, *f* were obtained by fusing copper wires, and *i* similarly with zinc
cd, *ce* were taken on the same plate, in *d* the wires were fused with the 200-volt A.C mains, in *e* they were fused using the 110 volt accumulator battery
ab, *hi* were taken on Iso-Wellington plates, and the other three on Hilger Schumann plates.
The first photograph is of a typical burst with copper wires, to show the white-hot particles shot out

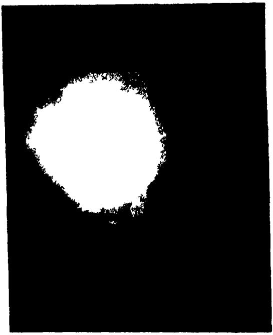

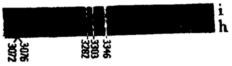
i
h
3072
3076
3282
3303
3346

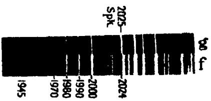
2025
Spk
g
f
1945
1970
1980
1990
2000
2024

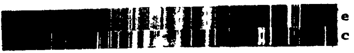
e
c

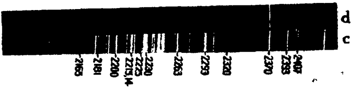
d
c
2165
2181
2200
2215,14
2225
2230
2263
2299
2320
2370
2393
2407

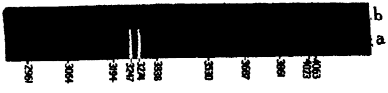
b
a
2961
3064
3194
3247
3274
3338
3530
3667
3861
4023
4063

A Study of the Catalysis by Nickel of the Union of Hydrogen and Oxygen by a New Method.

By D R HUGHES, B A., and R C BEVAN, B.A.

(Communicated by D L Chapman, F R S —Received August 3, 1927)

D L Chapman, J E Ramsbottom and C G Trotman* have shown that silver which has been heated to dull redness in oxygen is distinctly inferior as a catalyst for the reaction between hydrogen and oxygen to silver from which all the dissolved oxygen has been removed To explain this fact they advanced the working hypothesis that silver which contains more than a given concentration of dissolved oxygen is covered on its surface with an oxide which is not reduced under the conditions which obtain during the process of catalysis

In order to test the theory the catalytic activity of a comparatively easily oxidized metal, namely nickel, has been investigated The investigation has led us to the discovery of a simple and delicate method of testing whether a metallic surface is covered with a layer of oxide This method depends on the fact that a hot metal imparts less energy to a gas molecule (especially a hydrogen molecule) reflected from its surface than that communicated to the molecule under corresponding conditions by the oxide of the metal It is our intention to apply the test to a silver surface in the oxidized and in the reduced state

We shall show in this communication that when a polished surface of nickel is brought into contact with a mixture of oxygen and hydrogen at the lowest temperature at which the combination of the gases can be detected it becomes completely covered with a film of oxide (so thin that no alteration in the appearance of the surface can be detected) in a few seconds. The properties of these films formed under varying conditions have been examined, and their thickness measured The ease with which the films are formed renders the hypothesis that the mechanism of the process is the combination of oxygen with hydrogen condensed on the surface of the metal untenable

So far as they cover the same ground, the results obtained by us with nickel in a compact form are in satisfactory agreement both with those published in 1906 by W A. Bone and R V. Wheeler,† and with those furnished by several recent investigations conducted under very different conditions with nickel oxide and powdered nickel *

---

* 'Roy. Soc. Proc.,' A, vol. 107, p. 92 (1925).

† 'Phil. Trans.,' A, vol. 206, p. 1 (1906).

Experimental.

The apparatus was very similar to that used by Chapman, Ramsbottom and Trotman (*loc cit*), the chief difference being in the arrangement and dimensions of the reaction vessel and the wire The vessel was a horizontal glass tube of 2 5 cms internal diameter and 20 cms long The nickel wire which it contained was 30 25 cms long and 0 0258 cms in diameter The ratio of the volume of the oxygen container to the volume of the reaction chamber, the McLeod gauge, the condensers and the connecting tubes was 0 1702

When the wire is heated to dull redness in a vacuum or in hydrogen the metal volatilizes on to the inner surface of the reaction chamber When mercury vapour is excluded from the chamber, as it was in our experiments, this film is very reactive, and steps must be taken to avoid errors due to its presence Fortunately the film does not catalyse the union of hydrogen and oxygen at the temperature of the laboratory, although it will do so at a temperature of about 30° C It will, however, combine with oxygen, and therefore the deposited metal must be thoroughly oxidized before an experiment is performed These splashed films have been found to be exceedingly troublesome One of platinum, so thin that it cannot be seen, will bring about the rapid union of hydrogen and oxygen at the temperature of the laboratory For this reason experiments with platinum wire must be conducted in the presence of mercury vapour which " poisons " the film

The precautions taken to ensure the purity of the gases were the same as those employed by Chapman, Ramsbottom and Trotman

The selection of experiments taken from the laboratory note-book, and quoted below, contain only one example of each type

The observations made in the first two experiments suggested the method of investigation subsequently adopted

Experiments 1 *and* 2 —In Experiment 1 the wire, after it had been reduced, was heated in hydrogen at a pressure of 47960×10^{-6} mm with currents of varying magnitude, and the corresponding fall of potential determined Experiment 2 was conducted in the same manner as Experiment 1, except that the gas in which the wire was heated was a mixture of oxygen and hydrogen in the ratio of 0 1702 1 at the same total pressure, namely, 47960 × 10^{-6} mm The results are recorded below

---

* Pease and Taylor, 'J Amer Chem Soc,' vol 43, p 2179 (1921), and vol 44, p. 1637 (1922), Benton and Emmett, *ibid*, vol 46, p 2728 (1924), and vol 48, p 632 (1926), Larson and Smith, *ibid*, vol 47, p 346 (1926)

Current in amperes	0 56	0 58	0 60	0 62	0 64	0 66	0 68	0 70
Resistance in ohms of wire in hydrogen	0 830	0 885	0 990	1 105	1 230	1 390	1 540	1 665
Resistance in ohms of wire in mixture	-	—	0 735	0 765	0 795	0 835	0 890	0 970

It is obvious from the above readings that the same current raises the temperature of the wire much more when it is in hydrogen than when it is in the mixture Since the thermal conductivity of hydrogen is greater than that of oxygen, it was probable that the surface of the wire was in a very different condition in the two experiments, although we could perceive no difference in its appearance It was concluded that in the mixture the surface of the wire was oxidized To determine whether this conclusion was correct, and, if so, whether the wire which was being heated in the mixture was completely covered with oxide, the following comparisons were made

Experiments 3, 4 *and* 5 – In Experiment 3 the wire was previously heated in hydrogen

In Experiment 4 the wire was previously heated in a mixture of oxygen and hydrogen at a temperature well below that of combination

In Experiment 5 the wire was previously heated in oxygen until it had become visibly oxidized

In each case the wire was subsequently heated in hydrogen at a pressure of 12910 × 10^{-6} mm , and the resistance determined The results are recorded below

Current in amperes	0 30	0 32	0 34	0 36	0 38	0 40	0 42	0 44
Resistance in ohms, Experiment 3	0 680	0 710	0 775	0 840	0 905	1 000	1 105	1 245
Resistance, Experiment 4	0 605	0 625	0 655	0 690	0 725	0 765	0 810	0 885
Resistance, Experiment 5	0 605	0 625	0 650	0 680	0 710	0 750	0 805	0 875

It is clear that for a given current the temperature of the visibly oxidized wire is the same as that of the wire which had merely been heated in the mixture of hydrogen and oxygen, whereas the nickel which had not come into contact with oxygen was, in the same circumstances, at a much higher temperature The obvious conclusion to be drawn from the measurements is that when nickel is gently heated in the mixture of gases it becomes completely covered with a layer of oxide, and that on the average a hydrogen molecule which comes into contact with the oxide surface and then escapes removes more energy than a hydrogen molecule escaping from the metal surface at the same temperature

A surface which has been coated with oxide by gently heating it in oxygen or in a mixture of oxygen and hydrogen at a temperature not above that at which the synthesis of water can just be effected in its presence will be referred to below as a thinly oxidized wire

The differences between the coefficients of radiation of nickel, thinly oxidized nickel, and visibly oxidized nickel is not so pronounced as the differences between the amounts of heat removed from the respective surfaces by hydrogen at a low pressure This is shown by the results of Experiments 6, 7 and 8, in which the wire was heated *in vacuo*

Experiments 6, 7 *and* 8 —In Experiment 6 the wire was reduced in hydrogen and the absorbed hydrogen removed in a vacuum

In Experiment 7 a thinly oxidized wire was used, and in Experiment 8 the wire was visibly oxidized

The results obtained when the wire in the different states was heated in a vacuum are tabulated below

Current in amperes	0 30	0 32	0 34	0 36	0 38	0 40	0 42	0 44
Resistance, Experiment 6	0 965	1 040	1 140	1 250	1 360	1 490	1 600	1 095
Resistance Experiment 7	0 905	0 990	1 080	1 160	1 270	1 375	1 515	1 620
Resistance, Experiment 8	0 885	0 945	1 030	1 080	1 215	1 340	1 485	1 585

It will be seen that the heat radiated from the visibly oxidized wire is not the same as that radiated from the thinly oxidized wire This shows that the coefficient of radiation depends on the thickness of the oxidized sheath This is in contrast with the average heat removed from the surface by an escaping molecule of hydrogen which depends, as the previous experiment shows, solely on the nature of the actual surface The result is not surprising, since radiant energy can probably penetrate thin layers of an oxide

At this stage the resistance of a wire of the same length and diameter was determined at temperatures ranging between 18° and 320° The wire was wound into a coil round the bulb of a thermometer which was heated in a bath of paraffin At temperatures above 214° the thermometer and coil were enclosed in a narrow glass tube, which was immersed in a molten mixture of potassium and sodium nitrates The values obtained for the resistances agreed quite well with those calculated from the resistivity of nickel determined by Schofield.*

---

* 'Roy Soc Proc,' A, vol 107, p 206 (1925)

The values of the resistance thus found, together with the results of Experiments 3 to 8, were used to calculate the so-called accommodation coefficient[*] of hydrogen in contact with the respective surfaces At a temperature of 164° (the room temperature being 14°) the accommodation coefficient of hydrogen was found to be—

In contact with nickel	0 25
In contact with oxidized nickel	0 48

From a separate series of experiments the accommodation coefficient of oxygen in contact with oxidized nickel was found to be 0 95 The value found for hydrogen in the presence of nickel is of the same order of magnitude as that determined by other observers for the same gas in contact with most other metals, except platinum In contact with platinum the value is somewhat lower[†] It will be seen that as the value of the accommodation coefficient of hydrogen at the surface of the oxidized metal is almost twice as great as its value at the surface of the metal, the determination of the constant provides a delicate test for the presence of an oxide film on the metal If, as the above experiments indicate, nickel which has been used as a catalyst for the union of hydrogen and oxygen is completely covered with a coating of nickel oxide, the rate of formation of water in contact with such a surface ought not to differ appreciably from the rate in contact with the visibly oxidized metal under the same conditions Experiments were performed in order to see if this is the case

Experiments 9 *and* 10 —In Experiment 9 the wire was thinly oxidized and in Experiment 10 visibly oxidized The pressure and composition of the gases used in both experiments was the same In both experiments the temperature of the wire was kept as nearly as possible at 232° C In Experiment 9 the initial rate of fall of pressure was 131×10^{-6} mm per minute, and in Experiment 10, 134×10^{-6} mm per minute In other experiments the agreement was not so good, but we could obtain no evidence that the observed differences were due to a difference in the thickness of the films

Some experiments were next performed on the rate at which a reduced wire is oxidized when it comes into contact with the standard mixture of oxygen and hydrogen at the temperature at which the gases will combine at a measurable rate

Experiment 11 —The oxygen reservoir was filled with oxygen at a pressure of 44900×10^{-6} mm., and the reaction chamber was filled with hydrogen at the same pressure. The temperature of the wire was raised to 232°, and the oxygen enclosed in the reservoir was then admitted to the reaction chamber, the heating current being maintained constant at 0.55 amperes. The temperature of the wire fell in less than one minute to 102°, showing that its surface was very rapidly oxidized. At the end of the minute the heating of the wire was discontinued and the apparatus exhausted. The following experiment shows that the wire was completely oxidized.

---

[*] The ratio of the heat removed from the surface by an escaping hydrogen molecule to that which should be removed if the molecule had acquired the temperature of the surface

[†] Soddy and Berry 'Roy Soc Proc,' A, vol 84, p 576 (1911)

Experiment 12.—The reaction chamber was filled with hydrogen at a pressure of 48200×10^{-6} mm., and the temperatures of the wire determined when it was being heated with currents of different magnitudes. The oxide on the wire was then reduced, and determinations of the temperature made under corresponding conditions. Two readings obtained with a well-oxidized wire are given for comparison.

Current in amperes	0.56	0.58	0.60	0.62	0.64
Temperature of oxidized wire	100	108°	115°	127°	137°
Temperature of well oxidized wire	–	—	119°		152°
Temperature of reduced wire	233	253°	286°	317°	335°

A wire which had been in contact with oxygen at the temperature of the laboratory for a short time only was next examined.

Experiment 13.—The reduced wire was heated to redness in a vacuum with the pumps running to remove occluded hydrogen. The wire was allowed to cool, and oxygen admitted to the reaction chamber until the pressure was 109500×10^{-6} mm., and the apparatus was then rapidly exhausted. The total time during which the wire was exposed to oxygen was less than four minutes. A comparison of the following measurements with those made above shows that the surface of the wire was almost as completely oxidized as it was after the treatment to which it was subjected in the last experiment.

Current in amperes	0.56	0.58	0.60	0.62	0.64
Temperature	115	122°	129°	140°	157°

When the oxidized surface is reduced in hydrogen at a moderate temperature, the surface exhibits the properties of an oxide during most of the time the reduction is proceeding. In the last stages of the process the surface changes rapidly from oxide to metal. A comparison of the results of the two following experiments, performed at widely different temperatures, will show that this is the case.

Experiment 14 —A wire oxidized by heating it for 30 minutes in the standard mixture of oxygen and hydrogen at a temperature of 170° was reduced in hydrogen at the usual pressure of 48200×10^{-6} mm with a current of 0 60 amperes The results are tabulated below

Time in hours	0 25	2 25	5 40	16	17	17 75	18 50	20	23	25
Temperature of wire	115°	117°	117°	117°	120°	124°	129°	132°	275°	277°

The continuous fall in pressure during the first 17 hours was 1100×10^{-6} mm, and the total fall of pressure 3900×10^{-6} mm, showing that considerable reduction of the oxide occurred before even a small portion of the surface was metallic The fall in pressure would not account for an appreciable fraction of the rise in temperature

Experiment 15 was performed in the same manner as Experiment 14, except that the current employed to heat the wire was 0 68 amperes

Time in hours	0 25	1	2	3	3 50	4	4 50	4 55	4 60
Temperature of wire	160°	162°	162°	166°	169°	173°	220°	263°	335°

The last two experiments show quite clearly that the reduction does not start all over the outer surface of the oxide film Either the hydrogen penetrates the oxide film and the reduction takes place at the inter-face of the metal and the oxide, or the reduction starts at nuclei and the tiny specks of metal grow in size, at the same time penetrating the oxide film and expanding over its surface Of the two alternatives, the former seems the more probable when the film is thin *

The thickness of the coating of oxide formed on the wire in various ways was determined The measurements were made by two methods In the first method the oxidized wire was heated in hydrogen, and the fall in pressure measured In the second method a known amount of oxygen was admitted to the reaction chamber, which contained a reduced wire from which all the occluded hydrogen had been removed, and the disappearance of oxygen determined In order to make these determinations, measurements of difference of level of mercury in the balance tube of the McLeod gauge, varying between 6 mm and 18 mm in a total column of 200 mm, had to be read The errors made may therefore amount to as much as 10 per cent The film formed by bringing reduced nickel into contact with oxygen at the temperature of the laboratory, assuming it to be uniform, was found to be 3×10^{-7} cm † in thickness That formed by causing oxygen and hydrogen to combine in contact with the metal was of about three times the thickness The thickness of visible films is much greater, being of the order of a wave-length of visible light *

---

* *Vide* Pease and Taylor (*loc cit*) and Palmer, 'Roy Soc Proc,' A, vol 103, p 452 (1923)

† One film having a thickness of only 1 2 × 10^{-7} cm was prepared

Pease and Taylor have shown that water is formed much more rapidly by the interaction of copper oxide and hydrogen than by the interaction of copper oxide, hydrogen and oxygen at the same temperature, and Benton and Emmett and Larson and Smith have demonstrated that the same phenomenon is exhibited by nickel oxide We have confirmed the latter observation. When a wire which is visibly oxidized is heated to a temperature of 260° in hydrogen at the standard pressure used throughout this research the rate of fall of pressure is ten times as fast as that observed under the same conditions of temperature and pressure when the gas used is hydrogen mixed with one-seventh of its volume of oxygen Furthermore, the reduction of the oxide film by hydrogen can be detected at a much lower temperature than the catalysis of the union of hydrogen and oxygen by the same surface

Our best thanks are due to Mr D L Chapman, F R S, at whose suggestion the work was undertaken, for the help we received from him, and to Mr W H R Bird, who carried out some of the preliminary experiments

[*] These thick coloured films (especially those formed on copper) have been the subject of numerous investigations Some of the most recent of these are —W G Palmer, 'Roy Soc Proc,' A, vol 101, p 175 (1922), and vol 103 p 444 (1923), C N Hinshelwood, *ibid*, vol 102, p 318 (1923), J S Dunn, *ibid*, vol 111, p 210 (1926), F H Constable 'J Chem Soc,' p 1578 (1927) There is considerable difference of opinion concerning the structure and mode of formation of the films *vide* J S Dunn (*loc cit*)

The Average Energy of Disintegration of Radium E

By C D Ellis, Ph D, Lecturer in the University of Cambridge, and W A Wooster, B A, Charles Abercrombie Smith Student of Peterhouse, Cambridge

(Communicated by Sir Ernest Rutherford, O M, P R S —Received August 3, 1927)

The problem of the velocity of the particles emitted from the nuclei of disintegrating radioactive atoms has always attracted considerable attention It was early established that in the case of the α-rays all the particles from one substance were emitted with the same velocity, and the latest experiments of Briggs* have emphasised the high degree of homogeneity attained This result, showing that each disintegration involves exactly the same emission of energy, is easily reconcilable with our general ideas of the radioactive processes, and, as is well known, there is undoubtedly some connection between this characteristic energy and the mean life of the body

The behaviour of the β-ray bodies is in sharp contrast to this In place of the α-particles all emitted with the same energy, we find that the disintegration electrons coming from the nucleus have energies distributed over a wide range For example, in the case of radium E this continuous energy spectrum formed by the disintegration electrons has an upper limit at 1,050,000 volts, rises to a maximum at 300,000 volts, and continues certainly as low as 40,000 volts, and similar results have been obtained for other β-ray bodies If this result is interpreted as showing that different disintegrating nuclei of the same substance emit their disintegration electron with different energies, we must deduce that in this case the energy of disintegration is not a characteristic constant of the body, but can vary between wide limits Many workers have considered this to be so contrary both to the ideas of the quantum theory and the definiteness shown by radioactive disintegration that they have asserted the inhomogeneity must be a result of some secondary process, such as collision with the extra-nuclear electrons or emission of general γ-radiation, and that although we cannot observe them before they become inhomogeneous, the disintegration electrons are actually emitted from the nucleus with a definite characteristic energy as in the case of the α-particles

Such views are plausible and deserve careful consideration, but they meet with the great difficulty that it has up till now proved impossible to discover any evidence of the secondary effects which are presumed to produce the observed inhomogeneity On a previous occasion* we have discussed the secondary effects that might reasonably be expected to occur, and we showed that were these effects to be present with sufficient intensity to account for the inhomogeneity, then simple experiments would already have given direct evidence of their occurrence It was on these grounds that we concluded that the disintegration electrons must be emitted from the nucleus with varying energies, however contrary at first sight this might appear to be to the general principles of the quantum theory

---

* 'Roy. Soc Proc,' A, vol 114, p 313 (1927).

This conclusion is so fundamental for the whole subject of β-ray disintegration, and has been the occasion of so much controversy, that it is highly important to have more direct proof As will be described in the next section, it is possible to subject the two alternatives to a direct experimental test, and it may be stated at once that the result is such as to confirm our previous opinion and to show that the energy liberated at different disintegrations of atoms of the same kind varies within wide limits

General Principle of the Experiment

For the purpose of testing whether in a β-ray body every atom gives out the same energy on disintegration, it is desirable to employ a radioactive body emitting β-rays alone Such an example is found in radium E, and the following work was therefore performed on this element

The β-ray emission from radium E can be analysed by means of a magnetic field and the intensity of the rays of various energies determined by means of an ionisation chamber The result of such measurements is shown by the curve in fig 1 There are no groups of discrete energy as in the ordinary magnetic spectra owing to the absence of γ-rays, and it will be seen that the electrons may be said to form a continuous energy spectrum extending from an upper limit of 1,050,000 volts to values as low as 40,000 volts It has been established by Emeléus† that the number of electrons in this spectrum corresponds closely with the number of atoms disintegrating, and since at each disintegration one electron must be emitted from the nucleus, we can interpret this curve as showing the distribution of energy among the disintegration electrons when they have escaped from the parent atoms Up to the present time no other process by which radium E emits energy has been detected, so that there are *a priori* grounds to believe this represents the total energy of disintegration Since we must assume each disintegration to be independent

* 'Proc Camb Phil Soc,' vol. 22, p 849 (1925)

† 'Proc. Camb Phil Soc,' vol 22, p 400 (1924)

of the other atoms present, we conclude that the energy of disintegration is not a fixed characteristic quantity To take the extreme cases, there are a few

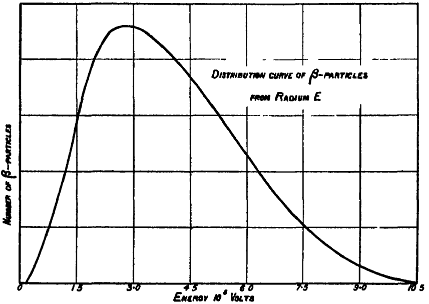

Fig 1

atoms emitting as much as 1,000,000 volts, whereas at the other end of the spectrum there are a few emitting only 4 per cent of this From this curve we can, following out this hypothesis, deduce the average energy of disintegration, and we obtain a figure about 390,000 volts Now the average energy of disintegration can be measured by another method entirely free from any hypothesis, namely, the heating effect of the β-rays This is most simply done by enclosing a source of radium E in a calorimeter whose walls are sufficiently thick to absorb completely the β-radiation If the heating effect is now measured and divided by the number of atoms disintegrating per unit time, we obtain the average energy given out on disintegration If this figure agrees with the value estimated from the distribution curve, 390,000 volts, then it is clear that the observed β-radiation accounts for the entire energy emission, and we deduce the corollary that the energy of disintegration varies from atom to atom

There is a sharp distinction between this result and that to be anticipated on the view that the energy of disintegration is a characteristic constant of the atom On this latter view, since electrons are emitted with energies as high as 1,000,000 volts, the characteristic energy cannot be less than this figure, and atoms which emit the slower electrons must get rid of their surplus energy in some other form It is well known that no large amount of penetrating radiation is emitted by radium E, so that if this hypothetical surplus energy really does exist, it must be absorbed inside the calorimeter and will contribute to the heating effect In this case the heating effect would be 2 6 times as great and would correspond to 1,000,000 volts per atom

It will be seen that a measurement of the heating effect provides a unique distinction between the two hypotheses, since one predicts a value of 390,000 and the other 1,000,000 volts per atom

The experiment is difficult to carry out because large sources of radium E are not available and the heating effect is small, but owing to the great differences predicted by the rival hypotheses, it is possible to obtain a definite result A further difficulty lies in determining the number of atoms disintegrating per second, and we obviated the necessity of knowing it by observing how the combined heat emission of the radium E and polonium varied with time From this we deduced the ratio of the mean energies liberated by the radium E and polonium and calculated the polonium energy from the energy of the α-rays We were never able to prepare a source entirely free from polonium, but this method could still be employed provided the amount of polonium initially present was found This was done by an ordinary α-ray ionisation measurement Although the polonium was separated in the preparation of the radium E, yet we can consider it to have been grown from a pure radium E source provided we antedate the moment of preparation by an appropriate number of days If the α-ray activities of the source initially and about 20 to 25 days later be found, it is clear that since the growth curve of the α-ray activity depends only on the decay constants of radium E and polonium, we can calculate the time at which the source would have been pure radium E It is not necessary to know the absolute number of α-rays emitted, as only a ratio of α-activities is involved

There are thus two types of measurement in this experiment, one of a small heating effect and the other of a fairly large α-ray activity The details of the apparatus used are described in the next two sections

Experimental Details

Heating Measurement.—The problem of measuring the heating due to the complete absorption of the β-ray of radium E presents difficulties. The rate of evolution is very small, and it is necessary to have a considerable thickness of material round the source In these experiments a thickness of approximately 1 mm of lead was used and the heat capacity of the calorimeter was large compared to the rate of heat evolution If the thermal insulation had been made very good, a considerable rise in temperature might have been obtained, but only after a long time It was felt that the accuracy depended more on being able to repeat experiments quickly than on any other feature, and as will be seen no special precaution was taken to reduce the heat loss but only to define the conditions so as to make it constant That it did remain constant was verified by repeated calibrations with a small glass tube containing a known amount of radium emanation The heat evolution in any experiment was then determined by measuring the steady temperature reached when the heat loss equalled the heat supply This steady temperature was reached in about 3 minutes, and the small rise of temperature (of the order of 1/1000° C) was measured by a system of thermocouples attached to a low-resistance sensitive Paschen galvanometer

After several trials the calorimeter which was finally used consisted of two lead tubes, 13 mm long and 3 5 mm diameter, each with a central hole of rather more than 1 mm diameter Each calorimeter fitted exactly into a thin outer sheath of silver, and were supported as shown in fig 2 (*a*) by two discs of mica A and B, which in turn were carried by the brass screw C fitting into an ebonite base DE The thermocouples were insulated by the thinnest mica possible, a sheet of the latter being attached to the calorimeter tubes by a very small quantity of soft wax The thermocouples were laid on this sheet of mica with a little wax at the junctions, and then another piece of mica laid on top and the whole pressed together with a hot iron * The two lead calorimeters were made as nearly alike as possible so as to minimise the effect of external variations of temperature on the difference of temperature between them In order still further to reduce these externally induced temperature differences, the whole calorimeter system was placed in a small cavity in a copper block, as

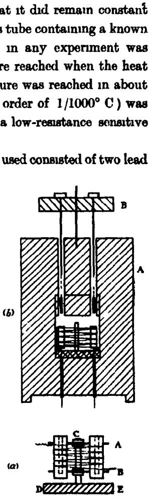

Fig 2.

---

* The temperature of the thermocouples may have been different to that of the lead tubes, but this is of no importance, since we do not require the absolute temperature rise but only to have a reproducible deflection of some instrument which registers a deflection when the calorimeters are heated, proportional to the temperature rise. That this was the case was shown by following the decay of radium emanation enclosed in a small tube

shown in fig 2 (*b*) The top portion A of this block had two small holes of diameter just greater than the internal diameter of the lead tubes and at such a distance apart that two small brass tubes of nearly the same diameter could slide smoothly from the holes in the copper block into the lead tubes One of these brass tubes contained the source of radium E and the other an inactive wire of the same thermal capacity These brass tubes were attached by means of two short lengths of thin glass rod to threads attached to brass rods fixed into the ebonite block B By this means the brass tubes could be removed from the calorimeters and kept in the upper copper block without introducing thermal disturbances The function of the small glass rods was to eliminate any possible variation in the conduction down the threads owing to their touching the sides of the copper block at different points in different experiments The composite copper block, which was half an inch thick at its thinnest part, was housed in a wooden box lined with felt, and the system afforded good protections against external variations in temperature

Whilst the α-rays of polonium are completely absorbed in the brass tube, the β-rays escape through it and are chiefly absorbed in the lead tube If this fact were to make the heating of the α- and β-rays not truly comparable, it would make the β-rays appear to have a greater heating effect relative to the α-rays than they actually have We have looked into this point carefully and it seems very unlikely that any error is caused, since each part, including the sources, were made to fit very closely one in another, and the brass tubes were so thin as to give up their heat almost instantly to the lead tubes

To avoid thermoelectric effects elsewhere in the circuit, a reversing key of special construction was placed immediately behind the calorimeter and the deflection measured was the difference in the galvanometer readings with the key in the two positions It was necessary to use a Paschen galvanometer of 12 ohms resistance, working at a sensitivity as high as 30,000 divisions per microampere, and the sensitivity was measured several times in the course of each experiment by incorporating in the reversing key an arrangement for switching in a known small standardising current *

α-Ray Measurement – It has been mentioned that only a ratio of α-ray activities was required, and we used a simple ionisation chamber connected to a high-resistance leak The wire source was mounted with its length parallel to the plane of two gauzes forming a shallow ionisation chamber, the latter being screened by an earthed gauze The source was capable of rotation about its axis, and measurements were always made for four orientations at 90° to one another, and the mean taken, in this way correcting for unevenness of distribution of the active material on the wire The source was placed farther from the ionisation chamber than the range in air at atmospheric pressure of the α-rays, and to measure the activity the pressure was reduced, and a series of deflections of the electrometer at different pressures were observed, and a measure of the activity was obtained by taking the deflections corresponding to a fixed stopping power To be independent of the sensitivity of the electrometer and the value of the high-resistance leak, this activity was expressed as a ratio to a standard polonium source This process was repeated after the radium E had nearly all decayed, and the ratio of the two activities enabled the time to be calculated at which the source consisted entirely of radium E With this arrangement, saturation of the ionisation was not attained, however, small changes of the applied voltage did not alter the ratio, and in any case any error due to this cause would tend to give finally too large a value for the heating effect of radium E

---

* A greatly enhanced accuracy was obtained both in the galvanometer readings and in the electrometer readings of the α ray activity by use of a Cambridge Instrument Company curve tracer bought with a grant from the Government Grant Committee of the Royal Society

Experimental Procedure

The source of radium E was prepared by electrolysis on to platinum or nickel wires 1 mm in diameter and 9 mm long, and immediately afterwards the α-ray activity of the polonium separated with it was measured It was then put into one of the small brass tubes of the heating apparatus and a similar inactive wire in the other These small brass tubes were then placed in the heating apparatus and held up in the waiting position in the copper block After 3 hours the disturbances due to manipulation had died away and the first heating measurement could be taken On any one day four measurements were taken, each in the following manner —First, the sensitivity of the galvanometer was determined, and then, with the brass tubes still lifted, the thermocouples were connected to the galvanometer and the residual difference of temperature determined The tubes were then lowered and the temperature difference, which after 3 minutes became steady, was measured On raising the brass tubes into the copper block the calorimeters cooled down, and in 3 minutes another measurement of the residual effect could be made The sensitivity of the galvanometer was then checked, and this whole procedure repeated for each of the four measurements made on any one day For a period of about 20 days the source was left in the brass tubes in the calorimeter and not touched in any way, and, during this time, a suitable number of heating determinations were made

After these were finished, the source was removed and the α-ray activity again measured to find the growth of polonium

Experimental Results

The heating measurements obtained in our best experiment are shown plotted against the time in fig 3A The radium E was in this case deposited on platinum.

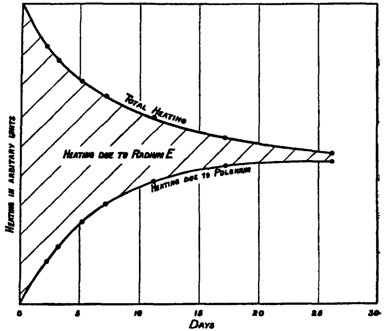

FIG 3A.

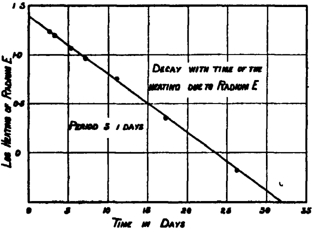

FIG. 3B.

The time is measured from the moment when the source would have consisted of pure radium E, which, by the α-ray measurements, was found to be 2 days before the first α-ray measurement was made The heating effects[*] are expressed in terms of the galvanometer deflection at a standard sensitivity of 10,000 mm per microampere, the actual deflections were about three times as great From the graph (fig 3A) it can be seen that the measurements extend over 26 days, by which time the radium E will have fallen to 0 027 of its initial value It is easy to estimate the initial value to be about 25 mm, and so it can have been at the end only 0 67 mm (see Table I *infra*) If we subtract this small quantity from the measured heating of 12 85 mm, we obtain the heating due to the polonium formed Extrapolating this backwards, using periods of 5 0 days and 139 days[†] respectively for radium E and polonium, we obtain the lower curve, showing the heating due to the polonium The difference between the two curves must show the heating effect due to radium E, and it is a most important confirmation of the accuracy of our experiments that this difference shows an exponential decay with a period of about 5 1 days This result is shown in fig 3B

To deduce the heating effect of radium E we proceed as follows —

If at zero time there are N_E radium E atoms and no polonium, then after time t there will be $N_E\lambda_E e^{-\lambda_E t}$ radium E disintegrations, per second and $N_E\lambda_E\lambda_P(e^{-\lambda_P t} - e^{-\lambda_E t})/(\lambda_E - \lambda_P)$ polonium disintegrations per second

If x denotes the ratio of the energy given out at a polonium disintegration to the average energy given out at a radium E disintegration, then at time t the ratio of the heating effect of radium E to that of polonium is

$$e^{-\lambda_E t}/(\lambda_E - \lambda_P)/x\lambda_P(e^{-\lambda_P t} - e^{-\lambda_E t})$$

The curves in fig 3A enable x to be calculated by this expression, and then division of this quantity into $5\ 22 \times 10^6$ volts, the energy of disintegration of polonium, gives the heating effect of radium E The results of analysing this experiment in this way are shown in the next table

---

[*] The figures from which the curves of fig 3A have been drawn are given in Table I.

[†] There is some doubt about the value of the period of polonium, but this is of no importance in this experiment, owing to the short duration and the final accuracy which is claimed

Table I.—Heating Effect of Radium E deduced from Curves of fig. 3.

True age	Total heating	Portion due to Po	Portion due to Radium E	x	Disintegration energy of Radium E in volts
days	mm				
2.25	22.0	3.68	18.3	15.4	339000
3.20	20.8	4.91	15.9	15.5	337000
5.20	19.0	6.99	12.0	15.5	337000
7.20	17.8	8.64	9.2	15.6	335000
11.20	16.1	10.53	5.6	14.5	360000
17.20	14.2	11.83	2.4	14.7	355000
26.20	12.85	12.18	0.67	15.1	346000

Considering the nature of the experiment, the agreement is excellent and shows that the energy of disintegration of radium E cannot be much different from 344,000 volts.

Table II summarises our results with four different sources of radium E, the experiment already quoted in detail appearing as the fourth entry. The object of columns I, II and III is to provide a basis for comparing the different experiments. Column I expresses the amount of radium E present in "equivalent milligrammes," by which is meant the amount of radium E which gives 3.72×10^7 disintegrations per second. It will be seen from the amount of material and the amount of polonium initially present that the accuracy in experiments 1, 2 and 3 was not as high as in experiment 4. We estimate the accuracy of the first three experiments to be about 15 per cent. and of the fourth about 5 per cent. We think it best to take the value from experiment 4 as the final result, with an overall accuracy of at least 10 per cent.

Table II.—Mean Energy of Disintegration of Radium E.

Source	I Amount of Radium E	II Age of source	III Ratio of Radium E heating to Po heating	IV Mean disintegration energy of Radium E
	at time of first heating measurement			
	mg	days		
1	0.13	11.3	0.50	320000
2	0.17	3.3	3.15	420000
3	0.22	12	0.43	320000
4	1.02	2.25	5.1	344000

The decay of the radium E sources were followed with an ordinary β-ray electroscope, and in each case it was found to be correct within 1 per cent, and it was not possible to obtain greater accuracy owing to the necessity of keeping the source in the calorimeter However, a short consideration will show that this accuracy, while showing the purity of the source to a per cent or so, might still leave room for serious errors in the heating measurements If there is any radium D present, then we may imagine the equilibrium amount of radium E and polonium as separated from the rest of the material* and constant both in heating and α-ray activity, and these constant amounts will have to be subtracted from all measurements Now supposing 1 per cent of the radium E is kept constant in amount by growth from this radium D, the equivalent heating correction will be only 1 per cent, since the energy of the radium D disintegration is virtually negligible but the heating correction for the corresponding amount of polonium will be about 15 per cent, as will be seen from the value of the factor x in Table I

We determined the amount of radium D present by measuring the residual β-ray activity after all the free radium E had decayed For example, in the case of the last experiment which has been quoted in detail, the source, measured 65 and 96 days after its preparation, showed a residual activity of about 1/400 The corresponding constant correction to the heating turns out to be about 4 per cent and to the age of the source of a little more than half a day These corrections have been applied to the results given

The heating effect we have measured is that due to the radiations stopped by an equivalent of 1 2 mm of lead This is sufficient to absorb completely all the β-rays, but it is well known that radium E, in addition, emits a small amount of γ-radiation To complete the measurement of the total energy given out at a disintegration, it is necessary to know the energy escaping from the calorimeters This was carried out for us by Mr Aston, and his results will be published in full very soon His method was as follows —From our heating measurements we calibrated an ordinary β ray electroscope in terms of "milligrams" of radium E (3 72 × 10^7 atoms disintegrating per second), so that he was able to compare directly the ionisation penetrating 1 2 mm of lead from the same number of disintegrating atoms of radium E, and of radium B and radium C respectively Since the penetrating power of the radium E γ-rays is intermediate between that of radium B and radium C, the ratio of the ionisation to radium B will give a lower limit and to radium C an upper limit of the ratio of energies emitted Approximate figures for the γ-ray energies of radium B and radium C are known, and in this way Mr Aston obtained a figure of 5,000 volts per atom for radium E for the energy penetrating 1 2 mm lead As was to be expected, this amount of energy is virtually negligible in this connection, and no further discussion of the accuracy of this experiment is necessary, although it has, of course, a very important bearing on our view of the β-ray disintegration

---

* This clearly depends on the presence of a sufficient quantity of polonium when the source was prepared, a condition which was always fulfilled

Discussion

The experiments described in this paper show that the average energy of disintegration of radium E is about 350,000 volts, and this energy is liberated in such a form that the major portion, 344,000 volts, is stopped by 1 2 mm lead and the remainder has an absorption coefficient in lead of 5 9 cm $^{-1}$ The interpretation of this result is simple The main energy is due to the disintegration electrons, and the small extra radiation is probably continuous γ-radiation of a relatively hard type, emitted by a few of the disintegration electrons which suffer close collisions with the planetary electrons in their escape from the atom

It is not necessary to repeat in detail the argument given in the introduction to show that this means that the same amount of energy cannot be given out at each disintegration, it is only necessary to refer again to fig 1, which shows the energy distribution among the electrons emitted by radium E The curve extends from 1,000,000 volts downwards, and if the same energy were emitted at each disintegration, then we must have found by the heating experiment a value close to 1,000,000 volts, that is, 2 8 times the experimental figure The final accuracy has been estimated as being about 10 per cent owing to inherent difficulties in the experiment, but this is quite sufficient to decide the point and, in fact, it justifies a closer comparison between the heating result and the distribution curve, which we shall now proceed to describe

The curve shown in fig 1 is taken from some experiments of Mr Madgwick carried out in the Cavendish Laboratory, and while there can be no doubt about the substantial correctness of the curve, leading as it does to the accepted absorption coefficient of the total β-rays from radium E, there is yet room for criticism in some details In the first place, the curve was obtained by the ionisation method, and to deduce the number of electrons emitted within a given range of energy it was necessary to make a correction for the variation of ionisation with energy This was carried out by multiplication of the results by β^2, where β is the velocity in terms of the velocity of light This correction is rough, but is in the right direction No account has been taken of reflection of the β-particles inside the ionisation chamber, an effect which would tend to over-emphasise the faster particles Again, owing to the necessity of covering the opening of the ionisation chamber with mica, slow electrons, if present, will not have been measured The final conclusion is that the curve of fig 1, leading to an average energy of 395,000 volts, is likely to be in error by giving too high a value for the average energy But there is another effect not concerned with the measurement which will work in the opposite direction We have assumed so far that only one electron comes from each disintegrating atom, but it is possible that the number may be slightly greater owing to occasional close collisions with a planetary electron, leading also to the ejection of the latter with a considerable energy This effect will not be large, although possibly of the order of 10 per cent, since a direct count of the number of electrons by Emeléus* gave a number 1 1 ± 0 1 electrons from each disintegrating atom, and again, the weak γ-radiation which could be assigned to this cause is small in amount but yet penetrating, indicating a very small number of close collisions

While an effect of this kind has no influence at all on the heating method of finding the mean disintegration energy, it will affect the deduction of this quantity from the distribution curve If this curve really contains $1 + \delta$ electrons on the average from each disintegrating atom, then the true average energy of the electrons emitted from the nucleus will be the average energy from the curve multiplied by $1 + \delta$ We see that there is here a possibility of a correction of about 10 per cent However, even if the counting measurements were carried out with great care, it would still be a doubtful procedure to apply this correction directly owing to the uncertainty, both in the counting and ionisation methods, of determining the number of slow electrons

The above considerations clearly indicate that the electrical methods show that the average energy per disintegration of the emitted particles is 400,000 volts to within 15 per cent, and this is in good agreement with the average total energy of disintegration found by the heating method of 350,000 volts ± 40,000 volts

We may safely generalise this result obtained for radium E to all β-ray bodies, and the long controversy about the origin of the continuous spectrum of β-rays appears to be settled

We must conclude that in a β-ray disintegration the nucleus can break up with emission of an amount of energy that varies within wide limits This is a curious conclusion and one which has frequently been questioned when it was put forward on less secure evidence on the grounds that the law of radioactive disintegration, the homogeneity of the α-rays and of the γ-rays showed a definiteness in the nucleus quite at variance with this indefiniteness of the energy of the emitted β-particles There is, however, a simple hypothesis by which these facts can be reconciled

---

* *Loc cit*

The structure of the nucleus has been discussed by Rutherford on several occasions, and recently* he suggested that there was "a concentrated inner nucleus carrying a positive charge surrounded at a distance by a number of electrons and then at a distance a number of neutral satellites circulating round the system" The neutral satellites are considered to consist of an α-particle with two electrons bound very closely and are held in equilibrium by the attractive forces either due to the polarisation of the neutral particle by the electric field from the charged central nucleus, or due to magnetic forces arising from the nucleus, or to a combination of both types of force To a first approximation we may consider these three regions as distinct, and there is no reason why the outer satellite region should not be quantised, and so give the possibility of ejection of α-particles of definite energy, but yet the electronic region unquantised in the sense that the electrons have energies varying continuously over a wide range We must, however, conclude that the γ-rays cannot be emitted from this unquantised electron region The varying energy of the disintegration electrons and the high degree of homogeneity of the γ-rays appear to make it quite impossible for the same system to be responsible for both emissions, whatever picture be made of the structure of the nucleus This is one of the most important results of this work, because although previously wherever it was necessary we have for simplicity spoken of the γ-rays being emitted by electrons, yet on several occasions we have pointed out that there was no evidence to decide this point It appears now that what we have called the electronic region of the nucleus cannot emit the γ-rays, so that by exclusion they must be emitted by what have been termed the positive regions of the nucleus There is good reason to believe the neutralised α-particles are in quantised states, so that homogeneous γ-rays could be emitted by them There are, of course, other possibilities, but at this stage it would be premature to discuss them †

It is interesting to enquire whether this picture of the free electrons in the nucleus existing in unquantised states is contrary to modern views At first sight it would certainly appear to be so, but this is not necessarily the case. For example, if we employed the orbit picture we might say that for a particle to be quantised it must be able to describe many complete orbits without disturbance, and in the confined region of the nucleus this is scarcely to be expected. The heavier positive particles will be little affected by the proximity of the electrons, but the converse will not be true. If the outer neutral α-particle shell were distributed continuously, we might perhaps still expect the inner electrons to be quantised, but with discrete particles, even if they move in regular paths, we can scarcely expect undisturbed electronic orbits close to them. This view of the unquantised electronic region is not contrary to the definiteness of the law of radioactive decay. When we measure the decay of a substance we are concerned with time intervals immensely long compared to those involved in the frequencies of rotation or movement of the component parts of the nucleus, and the final statistical result can well follow regular laws, whether the real life of the nucleus is entirely ordered or not. We would go farther and suggest that in the region of β-ray disintegration there seems to be now more hope of understanding why disintegration should ever occur. The energy resident in the electronic part will fluctuate among the electrons, and occasionally at intervals, long compared with the ordinary time scale, the energy may heap up in one electron and lead to an explosion.

---

* Rutherford, Guthrie Lecture, 'Phys Soc Proc,' vol 39, p 371 (1927)

† Rutherford ('Phil Mag,' vol 4, p 580, 1927) has pointed out that some recent theoretical work of Kuhn ('Zeit f Physik,' xliii, p 56, 1927, xliv, p 32, 1927) indicates that the homogeneity of the γ rays is incompatible with their being emitted by electrons.

We wish to express our thanks to Prof. Sir Ernest Rutherford for continual encouragement and help, and to Mr. Aston for helping us in the troublesome preparation of the radium E sources and for investigating the γ-radiation of radium E. We also acknowledge gratefully a grant (to C. D. E.) from the Government Grant Committee of the Royal Society, which defrayed part of the cost of apparatus used in this work, and also a grant (to W. A. W.) from the Board of Scientific and Industrial Research.

The Elasticity of the Collisions of Alpha Particles with Hydrogen Nuclei

By P M S Blackett and E P Hudson

(Communicated by Prof Sir E Rutherford, O M, P R S —Received August 3 1927)

[Plate 5]

Introduction

The normal collisions between alpha particles and atomic nuclei are known from scattering experiments to be approximately elastic The only cases in which inelastic nuclear collisions have been established with certainty are those in which a proton is ejected from a light nucleus In the case of nitrogen this is known to be associated with the capture of the alpha particle It is, however possible that inelastic nuclear collisions do occur, in which a nucleus is deformed but not disintegrated Smekal* has suggested the occurrence of inelastic collisions of this type Again, it is possible that an appreciable amount of energy might be radiated by the two rapidly accelerated nuclei during a close collision For although calculation shows that if the inverse square law is obeyed at all distances, the energy radiated classically by the accelerated particles will be extremely small (of the order of 10^{-4} of the total kinetic energy), it might conceivably reach a detectable amount if the forces near the nucleus vary as a very high power of the distance The existence of such forces is required by the rigid ellipsoidal model of the alpha particle proposed by Chadwick and Bieler † There is some experimental evidence of the excitation of radiation by the impact of alpha particles on matter ‡

These various possibilities make the detailed study of the elasticity of nuclear collisions of considerable interest The use of the Wilson method for the purpose has been described by Blackett § The method will be discussed here in greater detail and some new results will be given

---

* 'Phys Z,' vol 27, p 383 (1926)

† 'Phil Mag,' vol 42, p 923 (1921)

‡ Chadwick, 'Phil Mag,' vol 25, p 193 (1913), Chadwick and Russell, 'Roy Soc Proc,' A, vol 88, p 217 (1913), Slater, 'Phil Mag,' vol 42, p. 904 (1921)

§ 'Roy Soc Proc,' A, vol 103, p 65 (1923)

Theory of Method

Recently we have photographed a large number of alpha-ray tracks in hydrogen Among the many forked tracks due to the collision of fast alpha particles with protons, several were found in which the proton is projected at a small angle with the initial direction of the alpha particle, and therefore with a very high velocity Not only can these particular photographs be measured with especial accuracy, owing to the tracks being very fine and straight, but the actual angles of the fork can be calculated from the measured angles with less than the usual error A track is fine if the ionisation per unit length of track is small, and it is straight if the number of nuclear deflections per unit length of path is small Both these conditions are best fulfilled when fast particles of small charge pass through light gases The errors involved in the calculations are small because these errors, which arise from the residual lack of adjustment of the camera, decrease as the angles between the arms of the fork and the axis of the camera decrease Since in these nearly head-on collisions, making forks of narrow angle, all these angles are comparatively small, the errors in the final angles are likely also to be small These collisions, in which the alpha particle and proton approach extremely close to each other, are therefore very suitable for accurate study Of the tracks of this type photographed, only two possessed sufficient technical merit for measurements of the highest accuracy to be carried out One of these forks is reproduced in Plate 5

In this work, as well as in that already described,* no inelastic collisions between alpha particles and protons have been observed Certainly among any group of collisions photographed, some are always found which are not apparently exactly elastic, but in no case has it been possible to establish that these discrepancies are not due to an instrumental effect A collision will appear to be inelastic if, for instance, the track of one of the particles is deflected, even very slightly, by a second nuclear collision, close to the main one Then neighbouring tracks may cause a mutual distortion during track formation, as is shown in a very striking way by some photographs taken by C T R Wilson † Again, the errors involved in the calculations may take large values under certain circumstances. Tracks distorted by these instrumental errors can, however, in general be excluded from consideration, since they will fail, except by accident, to satisfy the test for coplanarity of the three parts of the fork A fork can only depart from real coplanarity if there is a transference of momentum to a third body or to radiation In the former case the track of the third body must be observed In the latter, owing to the small momentum of radiation associated with given energy, it can be shown that as much as 50 per cent of the total energy must be lost by radiation before the angle ψ between the stem and the plane through the other two arms of the fork reaches a value of 1° No fork, representing an approximately elastic collision, can therefore be considered as technically good unless it is coplanar

---

* Blackett, *loc. cit*, and 'Roy Soc Proc,' A, vol 107, p 349 (1925)

† 'Proc. Camb. Phil Soc,' vol 21, p 405 (1922)

In view of this argument we will assume that the total momentum of the two particles is the same before and after the collision If M, V and v are the mass, initial and final velocity of the alpha particle, if m and u are the mass and final velocity of the nucleus, and if ϕ and θ are the deflection of the alpha particle and angle of projection of the nucleus, we have

$$\mathrm{MV} = \mathrm{M}v \cos\phi + mu \cos\theta,$$
$$0 = \mathrm{M}v \sin\phi - mu \sin\theta$$

If we assume that the kinetic energy after the collision is only a fraction e of its value before we have

$$e\mathrm{MV}^2 = \mathrm{M}v^2 + mu^2$$

The energy lost during the collision will be $(1 - e)\mathrm{E}$, where $\mathrm{E} = \frac{1}{2}\mathrm{MV}^2$ From these equations we find, by eliminating the velocities,

$$e = (\sin^2\theta + (\mathrm{M}/m)\sin^2\phi)/\sin^2(\phi + \theta) \tag{1}$$

When $e = 1$, this reduces to

$$m/\mathrm{M} = \sin\phi/\sin(2\theta + \phi) \tag{1'}$$

For any collision for which, by the measurement of the Wilson photographs, ϕ and θ are known, the fraction e can be evaluated, since the ratio of the masses of the colliding particles is in general known exactly If, to anticipate the experimental results, the values of e so obtained differ from unity by less than the experimental error, we conclude that the energy lost, if any, is too small to be detected by this method If Δe is the average error in a single determination of e, and if we assume that we can detect an energy loss corresponding to twice the experimental error, then we will be able to detect an energy loss of $2\mathrm{E}\Delta e$ The problem of determining the least loss of energy that could be detected reduces, therefore, to the estimation of Δe

If the average random errors $\delta\phi$, $\delta\theta$, in ϕ and θ can be estimated, the average error in e can be found from the relation

$$(\Delta e)^2 = \left(\frac{\partial e}{\partial\phi}\right)^2 \delta\phi^2 + \left(\frac{\partial e}{\partial\theta}\right)^2 \delta\theta^2, \tag{2}$$

which with (1), when $e = 1$, gives

$$(\Delta e)^2 = \frac{1}{\sin^4(\phi + \theta)}[\{M/m \sin 2\phi - \sin 2(\phi + \theta)\}^2 \delta\phi^2 + \{\sin 2\theta - \sin 2(\phi + \theta^2)\}^2 \delta\theta^2] \qquad (3)$$

If, however, a considerable number n of photographs of *similar* collisions are available, we can dispense with independent knowledge of the errors of ϕ and θ, and can take Δe to be equal to the mean deviation of all the values of e from their arithmetic mean Since the average error of the arithmetic mean is $\Delta e/\sqrt{n}$, we can as before take the least detectable energy loss as twice this, that is,

$$2\Delta e/\sqrt{n}$$

From a physical point of view it is more significant perhaps to express the least detectable energy loss as a fraction, not of the initial energy of the alpha particle, but as a fraction of the energy E′, transferred during the collision to the nucleus Since

$$\frac{E'}{E} = \frac{4mM}{(M + m)^2}\cos^2\theta = 0\;64 \cos^2\theta, \qquad (4)$$

the fraction $2\Delta e \;\; E/E'$, which expresses the least detectable energy loss, can from (3) and (4) be expressed as a function of θ, since ϕ is given as a function of θ by (1′) *It is found that the reciprocal of the fraction has a flat maximum at about* $\theta = 30°$, and becomes zero for $\theta = 0°$ and $90°$ The two forks under consideration are therefore both of a favourable type for determination of an energy loss The second, for which $\theta = 31°$, is of the most favourable type obtainable

Results

The results for the two forks are given in the Table In columns 1 and 2 are given the values of ϕ and θ, calculated from three independent sets of measurements of each photograph Column 3 gives the angle ψ between the stem of the fork and the plane through the two arms (See note below) It will be seen that for the second track ψ has a value comparable with the experimental error of an angle measurement This fork is therefore coplanar within the limits of experimental error This angle is not given for the first collision, as one of the two photographic images showed the fork almost exactly " edge on " The fork could be seen by inspection to be approximately coplanar The angle ψ could not, however, usefully be calculated, since the arms of the fork in this image were too close together to be accurately measured This does not, however, affect the accuracy of ϕ and θ, since when one image gives an " edge on " view, these angles depend essentially only on the measurements of

Table

Track	1	2	3	4		5	6	7
	ϕ	θ	ψ	ϵ		$\Delta\epsilon$	$2\Delta\epsilon . E$	$2\Delta\epsilon . \frac{E}{E'}$.
	° ′	° ′					volts Å U	
I	10 13	16 57	—	1 0065	1 0047) (0 0047)	0 0052	85,000 0 15	$\frac{1}{56}$
	10 11	17 4	—	1 0020				
	10 13	17 0	—	1 0055				
			° ′					
II	14 16	31 4	0 9	1 0029	1 0002 (0 0024)	0 0031	51,000 0 24	$\frac{1}{76}$
	14 4	31 4	0 7	0 9968				
	14 12	31 2	0 10	1 0010				

Note on the Test for Coplanarity

If (a, b), (a', b'), and (a'', b'') are the angles between the axis and the rectangular projection on the two planes of the stem of the fork, and of the two arms of the fork, respectively, then the co-ordinates of the points of intersection of the three lines with the plane $z = 1$ are ($\tan a$, $\tan b$), etc (Blackett, 'Roy Soc Proc,' A, vol 103, fig 8, p 71 (1923)) The three parts of the fork will be coplanar if the three points are collinear, that is, writing a for $\tan a$, etc., for simplicity, if

$$(a - a')/(a'' - a') = (b - b')/(b'' - b')$$

If they are not collinear, the perpendicular distance P of the one point (a, b) from the line through the other two points is

$$\mathrm{P} = \frac{(a - a')(b'' - b') - (b - b')(a'' - a')}{\sqrt{\{(b'' - b')^2 + (a'' - a')^2\}}}$$

If the angles of the stem are small, as in practice they are, P equals the angle ψ in radians between the stem and the plane through the two arms

the other image Column 4 gives the values ϵ calculated from (1), for each determination of ϕ and θ. The mean value of the three determinations for each track is also given, and in brackets the mean value of $(1 - \epsilon)$

Since previous tests of the camera* with an artificial track gave a mean error in ϕ and θ of about 10′ of arc, and since, for the reasons mentioned, these two tracks are especially suitable for accurate measurement and reduction, we judge that the errors here are less than this, to be, in fact, about 6′ of arc. We estimate the error of measurement of the photographs to be about 3′ of arc, the remaining error being due to lack of adjustment of the camera. If we assume, then, that $\delta\phi = \delta\theta = 6'$, we find from (3) the values of $\Delta\epsilon$ given

---

* Blackett, *loc. cit.*

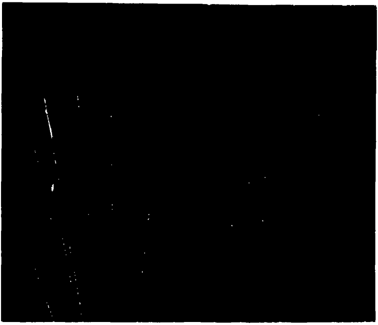

The Collision of an Alpha Particle with a Proton $\phi = 14$ $\theta = 31$ (× 3 5)

in column 5 A comparison of columns 4 and 5 shows that the collisions are elastic within the limits of experimental error A rough check on these estimated errors can be obtained by taking all six determinations of e as independent The mean value of $| e - e_m |$ is found to be 0·0025, that is, somewhat smaller than the error estimated above This is what would be expected, since actually the three determinations in a set are only partially independent, the errors of measurement are independent, but the camera errors are not

In column 6 is given the values of the quantity $2\Delta e$ E, which represents the energy loss that would have been detected if it had occurred This is expressed both in electron volts and as the wave-length of a quantum of radiation of the same energy The energy of the alpha particle is taken as $1\ 3\ 10^{-5}$ ergs, i e, 8 million electron volts This is the energy of an alpha particle of velocity $2\ 10^{9}$ cm sec^{-1} and of range 7 9 cm in air The source of alpha particles consisted of Th B and C, this source gives a mixed beam of 65 per cent 8·6 cm. particles and 35 per cent 4 9 cm particles The gas in the chamber consisted of 90 per cent hydrogen and 10 per cent oxygen, and the respective mean ranges in the chamber were 7 9 and 4 4 cm The probability that both forks were due to the fast and not to the slow alpha particles is very high, since Chadwick and Bieler* have found that the probability of the occurrence of this type of collision is very much greater for the 8 6 cm particles than for the 4 9 cm particles

In column 7 is given the least detectable loss of energy expressed as a fraction of the final energy of the proton

Conclusions

The study of the two best photographs obtained of the close collisions of alpha particles with protons has shown that the collisions are elastic within the limits of experimental error It remains possible that inelastic collisions between alpha particles and protons also occur, but that merely none such have yet been photographed

A consideration of the errors of measurement have shown that if, in the first of these two tracks, any kinetic energy is lost, it must be less than 85,000 electron volts, or, in the second, less than 51,000 electron volts If a quantum of radiation is emitted during the collisions, the wave-lengths cannot be less than 0·15 and 0 24 Å U respectively.

The least detectable loss of energy expressed as a fraction of the final energy of the proton is found for the second and most favourable track to be as low as 1½ per cent This corresponds to a 4 per cent alteration in range

---

* *Loc cit*

The probable error in an angle determination is estimated at about 6′ of arc We consider that it should not be impossible to halve this figure, by using special care to eliminate the camera errors, leaving only the error due to the lack of perfect straightness of the tracks This error appears to be of the order of 3′ of arc An accuracy of about double that given above must therefore be considered as about the limit of which the method is capable, when applied to a single fork If, however, a number n of similar forks were available, the least detectable loss of energy might be reduced again by the factor $\sqrt{n}$, in accordance with the theory of the error of the arithmetic mean

Equivalent accuracy should be obtained for the collisions of alpha particles with helium atoms, but only a much smaller accuracy is to be expected for collisions with heavier atoms such as nitrogen, owing to the lack of straightness of the tracks of the heavy atoms due to their low velocity and large charge This is unfortunate, as it is with such nuclei rather than with the exceedingly stable helium nuclei that inelastic collisions of the type discussed by Smekal might be expected

Part of the expense of this work has been borne by a grant from the Caird Fund of the British Association for the Advancement of Science

We wish to express our gratitude to Sir Ernest Rutherford for his encouragement throughout the work

The Relative Stability of Nitrous Oxide and Ammonia in the Electric Discharge

By W K Hutchison and C N Hinshelwood

(Communicated by H Hartley, F R S —Received August 4, 1927)

Reactions in gases can be brought about thermally, photochemically and electrically, as well as by the passage of α-particles, which may be regarded as a special case of the electrical method There is a good deal to be said for the view that in certain simple kinds of thermal reaction the molecules are activated by impacts of sufficient kinetic energy No connection, however, appears to exist between the mechanism of thermal activation and that of photochemical activation Energy imparted to electrons by light quanta is uneconomically employed as far as chemical effect is concerned, and the quanta of photochemically active light are usually much larger than the thermal energy of activation * It seemed interesting to inquire whether any connection could be found between the electrical and thermal mechanisms A certain general parallelism might perhaps be expected in some cases, since it is quite plausible to assume that, in an electric discharge, reactions may take place by collision of fast ions with other molecules This is not altogether unlike the collision of two molecules with large kinetic energies in a thermal reaction

The present investigation was carried out to compare the rates at which two reactions take place in a discharge tube—allowing, as far as possible, for differences in the conductivity of the gases involved—and to see whether the results agreed in a general way with what might be expected from the known thermal reactions Nitrous oxide and ammonia were chosen for experiment, the thermal decomposition of nitrous oxide being known to occur much more readily than that of ammonia

The apparatus used for comparing the stability of the two gases under electrical excitation consisted of a discharge tube, connected by a two-way tap to a McLeod gauge and to a series of pipettes whereby it could be filled with gas at any desired pressure The whole system could be evacuated by a two-stage mercury pump The current was supplied by a simple induction coil The course of the reaction was followed by reading the change in pressure on the McLeod gauge The gases to be used were stored over mercury, as shown in the figure The gas contained between A and B was allowed to expand into the larger pipette BC, then a small quantity of this rarefied gas could be enclosed between C and D, and finally shared with the discharge tube This

---

* *Cf* Bowen, 'Trans Faraday Soc,' "Photochemical Reactions in Liquids and Gases," vol 21, p 546 (1925)

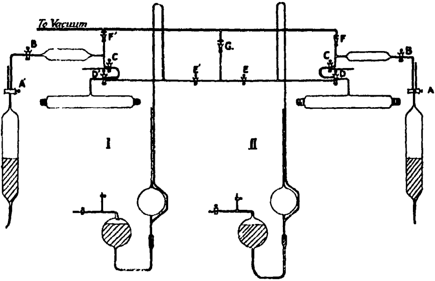

procedure, combined with evacuation of any desired part of the apparatus, allowed the introduction of gas at any required small concentration The whole apparatus was constructed in duplicate, the one half being the mirror-image of the other, as in the figure, and was sealed to the same vacuum main By this means measurements could be made on the effect of the same discharge passed simultaneously through nitrous oxide and ammonia, or through two tubes of either gas The two gauges were set to give exactly equal readings for equal pressures The actual pressures are given by the relation

100 mm gauge reading = 0 75 mm Hg

Nitrous oxide was obtained from a cylinder and dried with phosphoric oxide, ammonia from pure ammonium chloride and lime, and dried by storage over freshly burnt lime The nitrous oxide contained 5 per cent of air, which was regarded as harmless

The method of conducting an experiment was as follows —The whole apparatus was first evacuated for a long time, and baked out, the discharge passing meanwhile It was tested to make sure that it would hold a high vacuum The discharge tube was filled with the appropriate gas, the pressure measured by the gauge, and tap D closed completely The discharge was then passed for a definite time Both reactions are accompanied by an increase of pressure, which is shared with the gauge when the tap D is again opened Knowledge of the ratio of the volume of the gauge to that of the discharge tube—determined by separate experiments—allows the change in pressure in the discharge tube due to the decomposition to be calculated Owing to the passage of partially decomposed gas into the gauge when the tap is opened, one reading only can be made for each filling of the apparatus

Experiments were made with different initial pressures, and with different times and strengths of discharge

Both nitrous oxide and ammonia are completely decomposed at pressures in the region 0 7 to 2 5 mm , within a few minutes, by the discharge from a coil capable of giving a 1-inch spark in air

The observed increase of pressure, corrected for sharing with the gauge, after the discharge had passed for a long time is given below, expressed as a percentage of that to be expected theoretically

	Pt-electrodes	Al-electrodes	External electrodes
	Per cent	Per cent	Per cent
N_2O	96, 102	98, 97, 98	100, 100
NH_3	101	105, 100	99, 99

These figures show that occlusion or release of gas by the electrodes does not appreciably vitiate the results

In order to see whether the relative stability which was being measured represented anything more than a comparison of the conductivity of the two gases, and also how far it was purely a function of the electrode material, experiments were made —

(*a*) With platinum, aluminium and glass electrodes

(*b*) With the discharge passing through the two gases in series, in parallel, and independently through each alone

Under all these conditions the ammonia appeared to be about 5 to 7 times as hard to decompose as the nitrous oxide

It was first established by a large number of experiments that the absolute amount of decomposition tended to be independent of the initial pressure of the gas when the discharge was feeble, but with increasing intensity of discharge the amount of decomposition became proportional to the initial pressure, *i e* , the percentage amount was now independent of the initial pressure This, for obvious reasons, is the condition for a satisfactory comparison, and consequently all measurements were made with discharges sufficiently intense to bring the reaction into this "unimolecular" region Values of the "unimolecular velocity constant" are used for purposes of tabulation, but it must be emphasised that this implies nothing about the actual mechanism of what takes place in the discharge

The complete results of one series of experiments will now be given, and the others summarised

The first table contains the results of experiments in which the same discharge was passed through two tubes in series, containing nitrous oxide at different pressures The figures show that the percentage change is independent of the initial pressure with the discharge used Strictly, the comparison should only be made between the figures in a given line, because from one experiment to another the discharge may vary to some extent, but rough comparisons may also be made between the different experiments

Table I — Nitrous Oxide Two tubes in series External electrodes

Tube I			Tube II		
Initial pressure (gauge reading)	Corrected change	Percentage of total change	Initial pressure	Corrected change	Percentage of total change
		30 seconds discharge			
158	25 5	*34*	248	37 5	*32*
129	16	*26*	347	42 5	*26*
		60 seconds discharge			
131	35	*56*	190	54	*57*
124	35	*60*	245	72	*62*
117	19 5	*36*	397	87	*46*
376	82 5	*46*	174	43 5	*53*
345	95	*58*	103	29 5	*60*
176 5	46 5	*55*	102	22 5	*46*
		90 seconds discharge			
333	96 5	*61*	135	43 5	*68*
267	101	*80*	141	51	*76*

The second table contains similar results for ammonia

Table II—Ammonia Two tubes in series External electrodes

Tube I			Tube II		
Initial pressure	Increase	Percentage of total change	Initial pressure	Increase	Percentage of total change
		90 seconds discharge			
146	36	*25*	331	67 5	*20*
363	70	*22*	177 5	41 3	*23*
		180 seconds discharge			
129 5	57	*44*	192	85 5	*45*
129	57	*44*	266	111	*42*
129 5	47 5	*37*	368	123	*34*
215	83	*39*	145	60	*41*
329	122	*37*	169	66	*39*
		300 seconds discharge			
134	82	*61*	324	168	*52*
266	155 5	*59*	149 5	90	*60*

The third table contains the results of experiments in which one tube contained ammonia and the other nitrous oxide

Table III—Two tubes in series External electrodes

Tube I—Nitrous oxide			Tube II—Ammonia			
Initial pressure	Percentage of total change	k_{N_2O}	Initial pressure	Per centage	k_{NH_3}	k_{N_2O}/k_{NH_3}
			40 seconds discharge			
346	42 5	13 8 × 10^{-3}	347	7 8	2 02 × 10^{-3}	*6 9*
236	53	18 9	236 5	9 2	2 42 × 10^{-3}	*7 8*
			60 seconds discharge			
363	56 5	13 9 × 10^{-3}	370	11 3	2 00 × 10^{-3}	*7 0*
226	71 5	20 9	228	14 5	2 61	*8 0*
206 5	71	20 6	204	15 8	2 88	*7 2*
177	71	20 6	164	15 5	2 80	*7 4*
			80 seconds discharge			
261 5	79	19 5 × 10^{-3}	256	18 2	2 50 × 10^{-3}	*7 8*
236	70 5	19 5	232	18 1	2 50	*7 9*
			100 seconds discharge			
271	84	18 3 × 10^{-3}	256	20	2 33	*8 2*
258	86	19 7	233	22 5	2 56	*7 7*
					Average	*7 6*

Most of the nitrous oxide ultimately decomposes to $2N_2 + O_2$, the argument is unaffected by any that decomposes to $2NO + N_2$,* since the volume change is the same, and, in the low pressures employed, combination of nitric oxide and oxygen is very slow In any case we are using the velocity constants in a purely empirical way

It now remains to tabulate the results of the various series of experiments made in the way just described

		k_{N_2O}/k_{NH_3}
Single tubes	Platinum electrodes	6 4
Two tubes in series	Aluminium electrodes	4 8
Two tubes in series	External electrodes	7 6
Two tubes in parallel	External electrodes	6 5

Each comparison was made only under those conditions of discharge where previous observation had shown the reaction of each separate gas to be "unimolecular" Considering the wide range of conditions under which the four sets of experiments were carried out, it is probably fair to conclude that the ionic impacts required to decompose ammonia really are considerably more violent than those required to decompose nitrous oxide It is not easy to obtain information about the distribution of ions of different energies in a discharge of the kind employed, but, qualitatively, at any rate, the correlation between the greater stability of ammonia in the discharge and its higher thermal energy of activation is suggestive In the absence, however, of more detailed information about the mechanism of what takes place in the discharge, it is premature to proceed much beyond the statement of the experimental facts

---

* Joshi, 'Trans Faraday Soc,' vol 23, p 227 (1927)

Application of Quantum Mechanics to the Stark Effect in Helium

By J STUART FOSTER, Ph D , Assistant Professor of Physics, McGill University ,
Fellow of the International Education Board (in Copenhagen)

(Communicated by N Bohr, For Mem R S —Received August 8, 1927)

[PLATES 6-13]

Introduction —Many interesting features of the Stark-effect may be seen with unusual clearness in the arc spectra of helium, and these we shall mention very briefly before referring to the theory

The fact that an electric field applied to the source will bring out the combination lines $2p - mp$ was discovered by Koch* in 1915 Since that time many investigators have shown by Lo Surdo's method that a moderate external field is sufficient to remove all restrictions with regard to changes in the azimuthal quantum number

In contrast with the effect he observed in hydrogen, Stark† noted that the displacements of some helium components were not proportional to the applied field, and that their intensities increased rapidly with the field Recent experiments‡ reveal great variety in the relations between displacements and field strengths These will be considered in later paragraphs The intensities of components do not increase with the field in all cases, Nyquist§ being the first to report one of the many vanishing components The reappearance of one of these in higher fields has been observed by the writer ||

A second order Stark-effect in helium as well as in hydrogen was discovered by Takamine and Kokubu¶ in 1919 Observations on this slight shift towards the red have since been confirmed and extended **

The patterns of the Stark-effect in helium were found recently by the writer †† The members of a single spectral series have the same pattern

Doubtless these are rather general characteristics of the Stark-effect, which—notwithstanding the fundamental difference for weak fields from the observed

---

* 'Ann. Physik,' vol 48, p 98 (1915)

† 'Monograph,' pp 37 and 39 (1914)

‡ Foster, *ibid* , vol 114, p 47

§ 'Phys Rev ,' vol 10, p 226 (1917)

|| 'Phys Rev ,' vol 23, p 667 (1924)

¶ 'Mem Coll Sci., Kyoto,' vol 3, p 271 (1919)

** Foster, 'Astrophys Journ.,' vol 63, p 191 (1926)

†† *Ibid* , *loc cit*

Stark-effect on the hydrogen lines—for all spectra must be expected with increasing fields to show a more and more pronounced resemblance to the effect in hydrogen This gradual transformation of the Stark-effect, however, is not observed with the same clarity in other spectra, since the necessary fields are not so readily established and controlled

Before entering on a detailed theoretical discussion of the experimental results based on the new formulation of quantum mechanics, we shall briefly recall certain points of the earlier theory

On the Bohr correspondence principle, the observed selection rule with regard to changes of the azimuthal quantum number in the normal helium spectrum must be interpreted to mean that an inner perturbing central force is responsible for the difference between the helium terms and the corresponding hydrogen terms with the same principal quantum number When an external electric field is applied, the time mean position of the electrical centre of the orbit, which normally lies in the nucleus, is displaced by an amount proportional to the field , so that the resulting change in potential energy of the atom, and, therefore, the displacement of the spectral lines, is proportional to the square of the field When the electric field increases and becomes stronger than the inner perturbing field, the electrical centre of the orbit will tend to move in a plane perpendicular to the direction of the electric field, the distance of this plane from the nucleus being of the same order of magnitude as the orbital dimensions The resulting change in the potential energy of the atom is then proportional to the field and gives rise to a hydrogen-like Stark-effect The transition from weak to strong fields was treated in detail by Kramers* in the case of the relativistic hydrogen atom As pointed out by the writer in earlier papers, this theory gives an entirely satisfactory qualitative interpretation of the Stark-effect of all groups in the helium spectrum

A quantitative explanation of the " quadratic " Stark-effect, *i e*, the Stark-effect for theoretically small fields in complex spectra, has been developed by Pauli† on the basis of the dispersion theory of Kramers and Heisenberg ‡ The frequency of the external radiation incident upon the dispersing atoms is allowed to vanish, leaving the uniform electrostatic field commonly employed in Stark experiments This field is assumed to be so low that the splitting of the affected lines is small compared with the deviations of the terms from the hydrogen terms The dispersion theory then gives the intensities and positions of the new lines which appear in the field

---

* 'Z f Physik,' vol 3, p 199 (1920)

† 'K Danske Videns Selsk Medd ,' vol 7, p 3 (1925)

‡ 'Z f Physik,' vol 31, p 681 (1925)

The details of the application to helium, as well as the quantitative measurement of intensities with which the theoretical estimates are compared, were initiated by Takamine and Werner* and greatly extended by Dewey † Judging from his own experiments, the writer feels that a close application of this theory to helium is limited by the fact that a field sufficient to resolve the new combination lines is rather "high" for the theory, since it usually causes a splitting of the members of the diffuse series (used as standards of intensity) The same limitation appeared in some preliminary calculations made at the beginning of the present work It was found that the theoretical displacements of the lines near the centre of each helium group were not in satisfactory agreement with the observations

On the basis of the new quantum mechanics the Stark-effect in hydrogen has been treated by Pauli and Schrödinger who as regards the frequencies of the components have obtained the same results as Epstein and Schwarzschild on the earlier method The question of the intensity of the components has been fully treated by Schrodinger,‡ whose results form a quantitative extension§ of the qualitative estimate given earlier by Kramers|| on the basis of the correspondence principle

In his quantum mechanical discussion of the origin of the helium spectrum, Heisenberg¶ has shown that the difference between corresponding parhelium and orthohelium terms can be attributed to a resonance effect This theory shows, at the same time, that the two spectra of helium can be treated separately in such a way that the idea of a central force acting on the outer electron of an excited helium atom can be retained Therefore our treatment of the Stark-effect problem will be quite analogous to that carried out by Kramers on the basis of the earlier formulation of the quantum theory The calculations, however, are now in important respects simpler than in the older theory Indeed, the quantum mechanics allows us to calculate the displacements and intensities of the lines emitted by the perturbed system without requiring any further information regarding the nature of the inner field, apart from the term values of the unperturbed atom The present contact with experimental evidence

---

* 'Naturwiss,' vol 14, p 348 (1925)

† 'Phys Rev,' vol 28, p 1108 (1926)

‡ 'Ann d. Physik,' vol 80, p 437 (1926)

§ Foster and Chalk, 'Nature,' vol 118, p 592 (1926)

|| *Loc cit*

¶ 'Z f Physik,' vol 39, p 499 (1926)

permits, therefore, a rigid test of the theory Notwithstanding the great variety of detail revealed in the writer's fine analysis of the Stark-effect in helium, it will be shown that the theory gives a remarkably good quantitative explanation of the observed displacements and intensities

Principles of the theoretical treatment—In building up the actual atomic system to be considered, we shall start with the classical consideration of an electron revolving about a hydrogen nucleus in a central Coulomb field This system is degenerate with respect to k The Hamiltonian function is

$$\begin{aligned} H_0 &= \frac{1}{2m}(p_x^2 + p_y^2 + p_z^2) - \frac{e^2}{r} \\ &= W_0 = -\frac{Rch}{n^2}, \end{aligned} \tag{1}$$

where n is the principal quantum number

The atomic energy relative to the perturbing forces will be considered in two parts,

$$H_1 = H_1' + H_1'' \tag{2}$$

where H'_1 is due to variations in the *inner* central field of force which occur when the simple hydrogen nucleus is replaced by the helium nucleus and the inner electron of the helium atom In a classical treatment the time mean of H'_1 is the variation from H_0 corresponding to the various values of k which characterise the different parhelium or orthohelium spectral terms having the same principal quantum number Thus

$$\overline{H}_1'(k) = hc\nu_k,$$

where ν_k is the difference in cm^{-1} between the hydrogen and helium terms A relatively few values of $\overline{H}_1'$ are conveniently obtained directly from the normal spectrum, more may be found from Lo Surdo photographs, and a still greater number are given with sufficient accuracy only by the recent theory of Waller* and Heisenberg † We are here considering the electron as a point charge, neglecting the spin and the consequent fine structure of the orthohelium lines H_1'' is due to the external electric field, and its time mean is

$$\overline{H}_1'' = -eFz, \tag{3}$$

where F is the applied field taken in the direction of the z-axis, and z is the z-component of the vector drawn to the electrical centre of the orbit From a geometrical consideration it is seen that in the classical theory (compare Kramers)*

---

* 'Z f Physik,' vol 38, p 635 (1926)

† 'Z f Physik,' vol 38, p 411 (1926)

$$z = \frac{3}{2} a\varepsilon \sin \omega_k t \sin \vartheta, \tag{4}$$

where $\omega_k t$ is the angle between the major axis and the line of intersection of the plane of the orbit and a plane through the nucleus perpendicular to the field ϑ is the angle which the vector k makes with the external field, ε is the excentricity, a the major axis of the orbit

Before proceeding with the construction of the matrices of quantum mechanics which are to correspond to these Hamiltonian functions, we note that the spectral terms may be characterised by the quantum numbers n k and m ($k \leqslant n - 1$ and $m \leqslant k$) The vector k represents the angular momentum of the electron about the nucleus in zero external field, while m is the component of k in the direction of an applied field The vector m remains constant throughout varying fields, but k does not, and is retained simply as an index On the correspondence principle, transitions wherein $\Delta m = 0$ or ± 1 give rise to Stark components with electric vector respectively parallel or perpendicular to the external field This classification of the spectral terms is seen to lead directly to the patterns discovered by the writer So far as electric fields are concerned, these patterns are the principal experimental support of the classification

We now wish to form the matrix $\bar{H}_1$ corresponding to the time mean of H_1 taken over the unperturbed system This matrix has as indices n, m and k The region within which n is constant is subdivided into regions where m is constant Within each subdivision the individual terms are arranged according to the index k The matrix $\bar{H}_1$ contains terms of the type

$$\begin{aligned} \bar{H}_1{}' (n, m, k \rightarrow n, m, k) &= hc\nu (n, m, k \rightarrow n\ m, k) \\ &= hc\nu_k, \end{aligned} \tag{5}$$

which are constant or *diagonal* terms,† since they arise from a *central* field It contains, in addition, terms due to the external field The classical expression for $H_1{}''$ shows that these must appear as "first harmonic" terms of the type

$$\bar{H}_1{}'' (n, m, k \rightarrow n, m, k - 1) = -eF\ \frac{3}{2} a_0 n \frac{(n^2 - k^2)(k^2 - m^2)}{4k^2 - 1}$$

and

$$\bar{H}_1{}'' (n, m, k - 1, \rightarrow n, m, k) = -eF\ \frac{3}{2} a_0 n \frac{(n^2 - k^2)(k^2 - m^2)}{4k^2 - 1} \tag{6}$$

---

* *Loc. cit*

† As suggested to the writer by Dr Heisenberg

where the form of the terms is that given by Pauli,* a_0 being the radius of the normal hydrogen atom Observing that $n-1 \geq k \geq m$, we may write a typical subdivision of $\bar{\mathrm{H}}_1$ in the form

$$\left|\begin{array}{llll} \bar{\mathrm{H}}_1(k, k) & \bar{\mathrm{H}}_1(k, k+1) & \bar{\mathrm{H}}_1(k, k+2) & \bar{\mathrm{H}}_1(k, n-1) \\ \bar{\mathrm{H}}_1(k+1, k) & & & \\ & & & \\ \bar{\mathrm{H}}_1(n-1, k) & & & \bar{\mathrm{H}}_1(n-1, n-1) \end{array}\right| \tag{7}$$

Substituting the above values for the terms of $\bar{\mathrm{H}}_1$, dividing all terms by hc, and expressing the external field in 10 kv /cm , we have

$$\left|\begin{array}{cccc} \nu_k & -n\kappa\mathrm{F}\sqrt{f(n, m, k+1)} & 0 & 0 \\ -n\kappa\mathrm{F}\sqrt{f(n,m,k+1)} & \nu_{k+1} & -n\kappa\mathrm{F}\sqrt{f(n,m,k+2)} & 0 \\ 0 & -n\kappa\mathrm{F}\sqrt{f(n, m, k+2)} & \nu_{k+2} & \\ & & & \end{array}\right| \tag{8}$$

where $\kappa = 0\ 646$ and $f(n, m, k) = (n^2-k^2)(k^2-m^2)/(4k^2-1)$

The matrix H_0 of the unperturbed system is a diagonal matrix, the terms corresponding to $n =$ const , being of the same value,

$$\mathrm{W}_k = \mathrm{W}_k' = \qquad = -\mathrm{R}ch/n^2$$

The matrix H of the perturbed system is not a diagonal matrix Our immediate aim is to transform it into one that is, and so determine the energy of the perturbed states The method of making this transformation has been given by Born, Heisenberg and Jordan †

It is assumed that H is given as a power series in a parameter λ

$$\mathrm{H} = \mathrm{H}_0 + \lambda\mathrm{H}_1 + \lambda^2\mathrm{H}_2 + \tag{9}$$

In the present application we shall neglect terms containing the square and higher powers of λ This means the neglect of the second order Stark-effect We know the solution of

$$\mathrm{H}_0(p_0q_0) = \mathrm{W}_0, \tag{10}$$

and now wish to find an appropriate canonical transformation

$$\left.\begin{array}{l} p_k = \mathrm{S}p_0(k)\,\mathrm{S}^{-1} \\ q_k = \mathrm{S}q_0(k)\,\mathrm{S}^{-1} \end{array}\right\} \tag{11}$$

---

* 'Z f Physik,' vol 36, p 336 (1926)

† 'Z f Physik,' vol 35, p 557 (1926) See also Heisenberg, 'Math Ann,' vol 95, p 683 (1926)

made by means of a matrix S so chosen that

$$H(pq) = SH(p_0q_0)S^{-1} = W \tag{12}$$

is a diagonal matrix

Let

$$S = S_0(1 + \lambda S_1 + \quad),$$

then

$$S^{-1} = (1 - \lambda S_1 + \quad)S_0^{-1},$$

where S_0 is subject to the condition

$$S_0\tilde{S}^*{}_0 = 1,$$

and let $W = W_0 + \lambda W_1 +$

Then to first approximation

$$S_0(1 + \lambda S_1)(H_0 + \lambda H_1)(1 - \lambda S_1)S_0^{-1} = W_0 + \lambda W_1,$$

giving

$$W_0 = S_0H_0S_0^{-1} \tag{13}$$

and

$$W_1 = S_0(S_1H_0 - H_0S_1)S_0^{-1} + S_0H_1S_0^{-1} \tag{14}$$

Now from (13), since $H_0 = W_0$

$$W_0S_0 - S_0W_0 = \frac{h}{2\pi i}\dot{S}_0 = 0,$$

and

$$\dot{H}_0 = 0,$$

hence the time mean of equation (14) taken over the unperturbed system gives

$$\overline{W}_1 = S_0\overline{H}_1S_0 \tag{15}$$

or

$$W_1S_0 = S_0\overline{H}_1,$$

where W_1 is to be a diagonal matrix, and $\overline{H}_1$ has the form already found for it Let n and m be fixed The expansion of equation (15) then gives a set of linear equations for the determination of the corresponding terms in the matrix S_0 This will be a consistent set of equations, provided W_1 satisfies the equation

$$\begin{vmatrix} W_1-\overline{H}_1(k,k) & -\overline{H}_1(k,k+1) & 0 & \\ -\overline{H}_1(k+1,k) & W_1-\overline{H}_1(k+1,k+1) & -\overline{H}_1(k+1,k+2) & 0 \\ & & & \\ 0 & 0 & -\overline{H}_1(n-1,n-2) & W_1-\overline{H}_1(n-1,n-1) \end{vmatrix} = 0 \tag{16}$$

The roots of this equation of the $(n-m)$th degree are the total deviations from the original hydrogen term W_n, which the $n-m$ helium terms experience in the presence of the external field

Calculation of Displacements —We shall now calculate the displacements of some Stark components in helium, and return later to determine the matrix S_0, and the intensities of the same components by equation (11) In order to make a detailed comparison with experiments, we shall deal with the following eight-line groups —

Parhelium	Orthohelium
2P — 4Q	$2p - 4q$
2P — 5Q	$2p - 5q$
2S — 4Q	$2s - 4q$
2S — 5Q	$2s - 5q$

We need to know the effects of the perturbing forces on the terms characterised by $n = 2, 4, 5$ only As will be shown in a later paragraph, the disturbances due to the outer field in the states with $n = 2$ are almost negligible compared with the influence of the central field The observed Stark-effects, therefore, may be attributed to disturbances in the initial states only

The method of carrying out the computations* may be illustrated by an examination of the parhelium Stark components identified by the initial states with $n = 4$, $m = 1$ The displacements are measured most conveniently from the normal position of the diffuse series line, and are represented by $x = W_1 - \nu_2$, where ν_2 is the difference between the normal helium term 4D ($k = 2$) and the corresponding hydrogen term with $n = 4$ Here ν_2 expresses negative energy in cm $^{-1}$ Recalling the form of the terms in the matrix $\overline{H}_1$, as given in (8), we obtain the following form of equation (16) in the present application—

$$\begin{vmatrix} x + \lambda_1 & -4\kappa F\sqrt{\frac{12}{5}} & 0 \\ -4\kappa F\sqrt{\frac{12}{5}} & x & -4\kappa F\sqrt{\frac{8}{5}} \\ 0 & -4\kappa F\sqrt{\frac{8}{5}} & x + \lambda_3 \end{vmatrix} = 0 \qquad (17)$$

where $\lambda_k = \nu_2 - \nu_k$ Expanded, this becomes

$$x^3 + x^2(\lambda_1 + \lambda_3) + x(\lambda_1\lambda_3 - (4\kappa F)^2\ 4) - (4\kappa F)^2\left(\frac{8}{5}\lambda_1 + \frac{12}{5}\lambda_3\right) = 0 \qquad (18)$$

In the case of parhelium, $\lambda_1 = 46\ 4$ cm $^{-1}$ according to Fowler's tables, while the writer's Lo Surdo photographs give $\lambda_3 = 5\ 6$ cm $^{-1}$ F is given the values

---

* The writer is indebted to Mr W Rowles, of McGill University, for generous assistance in the calculations of the effect on the terms 5Q and $5q$

1 (i e , 10,000 v/cm), 2, 3, 4, 6, 8 and 10 In each case the roots give the displacements (from the D line) of the Stark components of 2P — 4D, 2P — 4F, and 2P — 4P (or 2S — 4Q), which are characterised by $m = 1$ The sum of the displacements in any field is $-(\lambda_1 + \lambda_3)$, i e , the algebraic sum of the shifts due to the external field alone is always zero This null effect is obviously to be expected, in any group of spectral terms with the same n and m values * The displacements of the above components, as well as all others which have been calculated in a similar way, are recorded in Table I, and plotted in figs 4 to 10

Table I —Calculated Displacements of Stark Components of Helium Line Groups

The displacements are measured from the original D (or d) line, and are expressed in cm.$^{-1}$ Each displacement really represents the excess of a perturbed initial spectral term over the normal D (or d) term with the same principal quantum number The fine structure of orthohelium as well as the very small effect of the external field on the final state is neglected

(*a*) Groups 2P — 4Q and 2S — 4Q (λλ 4922 and 3965)

	S	D			F			P	
m value of initial state	0	0	1	2	0	1	2	0	1
Polarisation in 4922 group	*ps*	*ps*	*ps*	*s*	*ps*	*ps*	*s*	*ps*	*ps*
Polarisation in 3965 group	*p*	*p*	*s*	—	*p*	*s*	—	*p*	*s*
Field in kv /cm —									
0	+506 2	—	0	—	—	— 5 6	—	−46 4	
10	6 3	+2 0	+1 75	+1 0	— 7 2	— 7 05	— 6 6	−46 9	−46 7
20	6 4	5 8	5 2	3 1	9 6	9 3	8 7	48 4	47 9
30	6 6	10 2	9 1	5 4	11 9	11 7	11 04	50 7	49 4
40	7 0	14 9	13 3	7 9	13 7	13 6	13 5	54 0	51 7
60	7 9	25 0	22 2	12 9	16 4	16 4	18 5	62 3	57 8
80	9 4	35 3	31 5	18 0	18 2	18 1	23 6	72 3	65 4
100	12 2	45 3	41 1	23 2	19 8	19 25	28 8	83 5	73 9

(*b*) Groups $2p - 4q$ and $2s - 4q$ (λλ 4471 and 3188)

	S*s*	*p*		*d*			*f*		
m value of initial state	0	0	1	0	11	2	0	1	2
Polarisation in 4471 group	*ps*	*ps*	*ps*	*ps*	*ps*	*s*	*ps*	*ps*	*s*
Polarisation in 3188 group	*p*	*p*	*s*	*p*	*s*	—	*p*	*s*	—
Field in kv /cm —									
0	+1146 4	−227 4		—	0	—	—	−7 8	—
10	+ 46 44	+227 46	+227 48	+1 23	+1 12	+0 78	— 9 13	−9 0	−8 58
20	46 54	27 63	27 7	3 75	3 5	2 7	11 95	11 0	10 4
30	46 73	27 9	28 0	6 62	6 2	4 8	15 24	14 6	12 6
40	47 0	28 3	28 53	0 5	9 0	7 2	18 8	17 93	15 0
60	47 7	29 5	30 0	15 2	14 5	12 7	26 4	24 9	20 2
80	48 6	31 1	31 9	20 5	19 8	17 1	34 2	32 1	24 0
100	50 0	33 2	34 3	25 4	24 8	22 8	42 6	39 5	30 1

---

* Compare Pauli, 'Handbuch d Physik,' von Geiger and Scheel, vol 23, "Quantum-theorie," p 146.

Table I—(continued)

(*c*) Groups 2P — 5Q and 2S — 5Q (λλ 4388 and 3614)

	S	D			F			G			P	
m value of initial state	0	0	1	2	0	1	2	1	1	2	0	1
Polarisation in 4026 group	*ps*	*ps*	*ps*	*s*	*ps*	*ps*	*s*	*ps*	*ps*	*s*	*ps*	*ps*
Polarisation in 2945 group	*p*	*p*	*s*	—	*p*	*s*	—	*p*	*s*	—	*p*	*s*
Field in kv /cm —												
0	+255 46	—	0	—	—	−2 75	—	—	−3 25	—	−24 31	−24 31
10	55 68	+7 32	+6 7	+4 65	−1 39	−1 47	−1 91	9 63	9 45	8 72	26 87	26 2
20	56 80	16 95	15 61	10 95	+0 67	+0 28	1 87	15 25	14 95	15 1	33 95	31 25
30	58 22	26 85	25 85	17 4	3 17	2 65	1 86	19 84	19 05	21 5	43 25	38 75
40	60 13	36 8	34 3	23 8	5 82	5 35	1 86	24 2	22 5	27 95	53 5	47 45
60	66 1	56 5	53 08	36 7	10 95	11 27	1 859	32 9	29 15	40 85	75 5	65 50
80	74 52	75 2	72 43	49 6	15 7	17 37	1 857	42 12	35 57	53 75	98 14	84 6
100	84 3	94 1	91 6	62 5	19 9	23 7	1 855	51 75	42 0	66 6	121 4	103 6

(*d*) Groups 2*p* — 5*q* and 2*s* — 5*q* (λλ 4026 and 2945)

	s	*p*		*d*			*f*			*g*		
m value of initial state	0	0	1	0	1	2	0	1	2	0	1	2
Polarisation in 4388 group	*ps*	*ps*	*ps*	*ps*	*ps*	*s*	*ps*	*ps*	*s*	*ps*	*ps*	*s*
Polarisation in 3614 group	*p*	*p*	*s*	*p*	*s*	—	*p*	*s*	—	*p*	*s*	—
Field in kv /cm —												
0	+570	+116	—	—	0	—	—	−3 6	—	—	− 4 1	—
10	+570 37	+116 81	+116 87	+5 72	+5 37	+4 11	−2 84	−2 77	−2 59	−11 06	−10 67	− 9 62
20	570 96	117 73	118 0	13 12	12 51	10 35	3 346	3 13	2 49	19 46	18 58	15 95
30	572 18	119 27	119 8	20 22	19 5	16 72	4 207	3 79	2 47	28 46	26 75	22 30
40	573 25	121 43	122 55	26 95	26 06	23 1	5 42	4 76	2 47	37 21	35 05	28 7
60	577 0	127 59	129 71	38 97	38 60	36 0	8 81	7 26	2 47	55 74	52 25	41 6
80	582 18	136 21	139 7	49 10	49 53	48 9	13 31	10 63	2 46	75 18	69 82	54 54
100	588 42	147 31	151 72	57 34	59 43	61 8	18 83	14 58	2 46	95 24	88 77	67 4

In order to show that the displacements so calculated give the entire observed Stark-effects, while the effects of the external field on the final states may be neglected, we have only to make a brief calculation There is but one state with $n = 1$, $m = 1$, and equation (16) states that it will not be disturbed by the field The two states with $n = 2$, $m = 0$ will be equally affected The calculated shift is only 0 04 cm $^{-1}$ in a field of 100,000 v /cm

The experiments show directly that this splitting has not been detected The way in which such elementary separations may be found, if observable, is made clear in fig 1 This figure is drawn roughly to scale (except that the splitting of the 2P level is exaggerated), and shows the theoretical effect of fields up to 100 kv /cm on the terms 4Q and 2Q The transitions leading to p and s components are indicated by full and dotted lines respectively There are two groups of transitions, in which the final states are 2P and 2S The adjoining sketch of 2P — 4P and 2S — 4P illustrates the manner in which the splitting of the original spectral terms may make their appearance in the photographs If Δ_{4P} represents the separation of the two levels of 4P at a given field strength and Δ_{2P} is the corresponding separation for 2P, then Δ_{4P} must appear as the difference between the displacements of the p and s components of 2S — 4P at the same field, while Δ_{2P} is one-half the difference between the separations of the two p and two s components respectively of 2P — 4P The separation Δ_{4P} is very easily observed in this way (see fig 5), but there is no convincing evidence of the experimental detection of Δ_{2P} *

The general equations of type (18) apply to orthohelium (considered as a singlet system) as well as parhelium As we have just seen, they give the first order displacements The remaining general equations used in the computations are shown in (19), p 164

The λ_0's and λ_1's, being the relatively large separations between the diffuse and sharp terms and the diffuse and principal terms respectively, are obtained with sufficient accuracy from Fowler's or Paschen's tables It has been found best to read the λ_3's directly from the Lo Surdo photographs, where these separations of the diffuse and P — F (or $p - f$) combination lines are clear at almost zero field We are prevented from doing this in the case of the λ_4's, owing to the fact that the P — G (and $p - g$) lines with which we are concerned are more affected by low fields, and vanish before reaching what could be accepted as zero field position The required information can be supplied, however, by the Heisenberg theory of the helium spectrum Using the formula

---

* See Plate 6 (E), 'Roy Soc Proc,' A, vol 114 (1927)

$$\left.\begin{aligned}
&\qquad\qquad n = 4\,,\ m = 2\\
&x^2 + \lambda_3 x - (4\kappa\mathrm{F})^2 = 0\\[1ex]
&\qquad\qquad n = 4\,,\ m = 0\\
&x^4 + x^3(\lambda_0 + \lambda_1 + \lambda_3) + x^2(\lambda_0\lambda_1 + \lambda_1\lambda_3 + \lambda_3\lambda_0 - (4\kappa\mathrm{F})^2\ 10)\\
&\qquad + x\Big[\lambda_0\lambda_1\lambda_3 - (4\kappa\mathrm{F})^2\Big(5\lambda_0 + \frac{9}{5}\lambda_1 + \frac{41}{5}\lambda_3\Big)\Big]\\
&\qquad - (4\kappa\mathrm{F})^2\Big(\frac{9}{5}\lambda_1 + \frac{16}{5}\lambda_3\Big)\lambda_0 + (4\kappa\mathrm{F})^4\ 9 = 0\\[1ex]
&\qquad\qquad n = 5\,,\ m = 2\\
&x^3 + x^2(\lambda_3 + \lambda_4) + x(\lambda_3\lambda_4 - (5\kappa\mathrm{F})^2\ 4) - (5\kappa\mathrm{F})^2\frac{16}{7}\lambda_4 = 0\\[1ex]
&\qquad\qquad n = 5\,,\ m = 1\\
&x^4 + x^3(\lambda_1 + \lambda_3 + \lambda_4) + x^2[(\lambda_1\lambda_3 + \lambda_3\lambda_4 + \lambda_4\lambda_1) - (5\kappa\mathrm{F})^2\ 10]\\
&\qquad + x\Big[\lambda_1\lambda_3\lambda_4 - (5\kappa\mathrm{F})^2\Big\{\frac{15}{7}\lambda_1 + \frac{128}{35}(\lambda_1 + \lambda_4) + \frac{21}{5}(\lambda_3 + \lambda_4)\Big\}\Big]\\
&\qquad - (5\kappa\mathrm{F})^2\Big(\frac{128}{35}\lambda_1\lambda_4 + \frac{21}{5}\lambda_3\lambda_4\Big) + (5\kappa\mathrm{F})^4\ 9 = 0\\[1ex]
&\qquad\qquad n = 5\,,\ m = 0\\
&x^5 + x^4(\lambda_0 + \lambda_1 + \lambda_3 + \lambda_4) + x^3(\lambda_0\lambda_1 + \lambda_1\lambda_3 + \lambda_3\lambda_4 + \lambda_4\lambda_0\\
&\quad - (5\kappa\mathrm{F})^2\ 20) + x^2\Big[\lambda_0\lambda_1\lambda_3 + \lambda_1\lambda_3\lambda_4 + \lambda_3\lambda_4\lambda_0 + \lambda_4\lambda_0\lambda_1\\
&\qquad - (5\kappa\mathrm{F})^2\Big\{\frac{16}{7}(\lambda_0 + \lambda_1) + \frac{144}{35}(\lambda_0 + \lambda_1 + \lambda_4)\\
&\qquad\qquad + \frac{28}{5}(\lambda_0 + \lambda_3 + \lambda_4) + 8(\lambda_3 + \lambda_4)\Big\}\Big]\\
&\quad + x\Big[\lambda_0\lambda_1\lambda_3\lambda_4 - (5\kappa\mathrm{F})^2\Big\{\frac{16}{7}\lambda_0\lambda_1 + \frac{144}{35}(\lambda_0\lambda_1 + \lambda_1\lambda_4 + \lambda_4\lambda_0)\\
&\qquad + \frac{28}{5}(\lambda_0\lambda_3 + \lambda_3\lambda_4 + \lambda_4\lambda_0) + 8\lambda_3\lambda_4\Big\} - (5\kappa\mathrm{F})^4\ 64\Big]\\
&\quad - (5\kappa\mathrm{F})^2\Big(\frac{144}{35}\lambda_0\lambda_1\lambda_4 + \frac{28}{5}\lambda_0\lambda_3\lambda_4\Big) + (5\kappa\mathrm{F})^4\Big(\frac{64}{5}\lambda_0 + \frac{1152}{35}\lambda_4\Big) = 0
\end{aligned}\right\}\qquad(19)$$

for δ the Rydberg correction, given by Waller,* we obtain the separation between the normal 5F and 5G terms This amounts to 0 5 cm $^{-1}$, and it is assumed to be the same in orthohelium (considered as a singlet system) This is added to the λ_3's to give the λ_4's The direct theoretical determination of λ_3 gives a value 20 per cent too low This is taken as evidence that the present approximate form for δ is not sufficiently accurate when applied to the determination of the diffuse terms There happens to be an excellent test of the correctness of the λ's in the case of the 4388 group The component of 2P — 5F having $m = 1$ crosses the normal position of the D line at 18 2 kv /cm Placing $x_2 = 0$ in the equation (19) and using the accepted λ's, we get a satisfactory theoretical value F = 18 8 kv /cm Incidentally, it is obvious that the process may be reversed, and new spectral terms determined with fair accuracy from observed Stark displacements of single lines in known fields The accepted λ's are numerically equal to the displacements at zero field, with sign opposite to that recorded in the tables

---

* *Loc cit*

Arrangements of Components in Very High Fields –Before making a detailed comparison of the theoretical displacements with the observations, let us consider the ultimate disposition of the components at extremely high fields Such a consideration leads, in fact, to a clearer understanding of certain difficulties encountered in the experimental analyses of the line groups considered in this paper

When the effects of the external field become large compared with those due to the internal field, we may assume that the displacement of a Stark component is given by

$$\Delta\nu_F = AF + B,$$

and substitute this for x in the general equations (19) Upon doing this, and equating to zero the coefficients of the two highest powers of F, we obtain as first and second approximations the following values for A and B (see equation (20), p 166)

From this data figs 2 and 3 have been constructed A suitable scale for each figure is determined from the separation of the diffuse and sharp series lines in the groups represented, viz , $\lambda\lambda$ 4922, 4472 , 4388 and 4026 The approximate theoretical positions of the components at very high fields have been connected with the positions of the lines at zero field by curves which are not intended to represent the displacements accurately The connections in lower fields (still high compared with the range covered by the actual calculations) is more clearly indicated by the large-scale insert

In very high fields the group patterns for parhelium and orthohelium are nearly identical Pairs of components characterised by m values 2 and 0

$$\left.\begin{array}{llll}
n=4, & m=2, & A=\pm 4\kappa, & B=-\frac{1}{2}\lambda_3 \\
 & m=1, & A=\pm 8\kappa, & B=-\frac{1}{10}(3\lambda_1+2\lambda_3) \\
 & & A=0, & B=-\frac{1}{5}(2\lambda_1+3\lambda_3) \\
 & m=0, & A=\pm 12\kappa, & B=-\frac{1}{20}(5\lambda_0+9\lambda_1+\lambda_3) \\
 & & A=\pm 4\kappa, & B=-\frac{1}{20}(5\lambda_0+\lambda_1+9\lambda_3) \\
n=5, & m=2, & A=\pm 10\kappa, & B=-\frac{1}{14}(7\lambda_3+3\lambda_4) \\
 & & A=0, & B=-\frac{4}{7}\lambda_4 \\
 & m=1, & A=\pm 15\kappa, & B=-\frac{1}{70}(14\lambda_1+5\lambda_4+21\lambda_3) \\
 & & A=\pm 5\kappa, & B=-\frac{1}{70}(21\lambda_1+30\lambda_4+14\lambda_3) \\
 & m=0, & A=\pm 20\kappa, & B=-\frac{1}{70}(14\lambda_0+28\lambda_1+7\lambda_3+\lambda_4) \\
 & & A=\pm 10\kappa, & B=-\frac{1}{70}(14\lambda_0+7\lambda_1+28\lambda_3+16\lambda_4) \\
 & & A=0, & B=-\frac{1}{35}(7\lambda_0+18\lambda_4)
\end{array}\right\} \quad (20)$$

coincide or run parallel in both spectra In parhelium these are components of the same original line, while in orthohelium they are components of adjacent lines

This variation is due to the inverted P terms of parhelium, and leads to wider differences in the two spectra at theoretically low fields These differences are too varied to be described in great detail here , but they have in all cases the general character needed to account for the partial or complete fine analysis observed by the writer for the various lines In view of this general agreement it seems highly probable that these diagrams give a true indication as to whether or not conditions for a better analysis of a certain line can be secured by increasing the field strength

Calculations of Intensities —The terms of a matrix S such that

$$H\,(pq) = SH\,(p_0q_0)\,S^{-1} = W$$

is a diagonal matrix are given by linear equations arising from the expansion of (15) The co-efficients of the terms in a typical set of equations are contained in the determinant on the left-hand side of equation (16) Of the two indices which identify the terms S_{il}, i is the azimuthal quantum number, i *e* , the k index of the co-efficients in (16), and l indicates the x value of some perturbed state from which transitions under consideration are to take place The indices refer to unperturbed and perturbed states respectively

After the values of S_{kx} have been calculated, the amplitudes in the perturbed system are given by

$$q = Sq_0 S^{-1}$$

where q_0 is the matrix containing the amplitudes of the unperturbed system Expansion of this gives the individual amplitudes

$$q_{ru} = \sum_s \sum_t S_{rs} \, q_{st} \, S_{tu}^{-1} \tag{21}$$

summed over all unperturbed states st permitted by the rule $\Delta k = \pm 1$ The intensity itself is given by the square of q_{ru}

This means that we are to consider first the normal transitions resulting in the sharp, principal, and diffuse lines which are emitted by the initial system perturbed slightly to remove the degeneracy with respect to k and m In conformity with the usual restrictions $\Delta k = \pm 1$ and $\Delta m = 0$ or ± 1, the lines which are unpolarised on the whole are thought to be built up from polarised components corresponding to all possible transitions The relative values of the amplitudes q_{st} of the polarised components of each normal line are found from the Kronig* intensity factors commonly employed in the Zeeman effect In the next place, we know that the perturbed system yields polarised components also, with amplitudes q_{ru} which may depend upon the disturbance due to the external (not inner central) field in both initial and final states Equation (21) shows the manner in which the terms S_{rs} and S_{tu} are used to measure this dependence

To find the intensity of a Stark component, we must first determine the terms S_{rs} where r is the fixed index of the initial perturbed state, and s is any unperturbed state (of the same principal quantum number) from which a transition may take place in the original system Similarly we need the terms S_{tu}, where t is any of the possible final states in the unperturbed system, and u is the final perturbed state with which we are concerned

In our case the calculations are much simplified by the fact that the effect of the electric field is negligible in the final state On this assumption (see calculation of this effect) we find

---

* 'Z f Physik,' vol 31, p 685 (1925)

$$\begin{aligned} S_{tu} &= 1 \text{ if } t = u \\ &= 0 \text{ if } t \neq u \end{aligned}$$

Hence the final state has nothing to do with changes in intensities which may occur with increasing external field The sum over s will consist of two members in those cases where two normal transitions $k \rightarrow k \pm 1$ can be considered We shall find that one member is negligible in all cases in the present calculation

To a close approximation the intensity of each polarised Stark component in helium is very simply given, therefore, as a fraction of the intensity of a line (sharp, principal or diffuse) in the normal helium spectrum This fraction is

$$(q_{ru})^2 = (S_{rs}\, q_{su})^2$$

where q_{su} is the amplitude of a polarised component of the normal line as given by the Kronig formulæ, and S_{rs} is the appropriate term of the S matrix so normalised that

$$\Sigma_t \, (S_{tl})^2 = 1$$

This normalisation expresses the theoretical view that the sum of the intensities of all Stark components ($n \rightarrow n'$) at any field strength will be equal to the sum of the intensities of the normal lines ($n \rightarrow n'$) of the initial system It is here assumed that (1) the number of atoms in each state nQ is the same, and (2) that the total number of atoms per unit volume emitting light remains constant throughout the various external fields It is highly improbable that the second assumption can be correctly applied to a Lo Surdo source in which the light usually appears much brighter in the stronger fields On assumption (1) it is correct to compare theoretical relative intensities with observations at a fixed field, but Lo Surdo photographs may be expected to show a general increase in intensities of components at higher fields over those given through the simplifying assumption (2) in the present calculations

We shall now write down the Kronig formulæ which we are to employ Let A represent the whole intensity of the line $k \rightarrow k - 1$ observed with *either* parallel or perpendicular polarisation Since the displacements of the levels in electric fields are the same for $+m$ and $-m$, we shall take only positive values and write down double intensities (except in the case where $m = 0$) Putting $j = k$ (for unperturbed singlet system) in Kronig's formulæ we obtain the following intensities

$$\left.\begin{array}{l}
p \text{ components} \quad (m > 0) \\
\qquad (q^0_{k,m \longleftrightarrow k-1\, m})^2 = \dfrac{6\,(k^2 - m^2)}{k\,(4k^2 - 1)}\ A \\
\text{and} \\
\qquad (q^0_{k\, 0 \longleftrightarrow k-1, 0})^2 = \dfrac{3k}{4k^2 - 1}\ A \\
s \text{ components} \\
\qquad (q^0_{k,m \longleftrightarrow k-1\ m-1})^2 = \dfrac{3}{2}\ \dfrac{(k+m)(k+m-1)}{k\,(4k^2 - 1)}\ A \\
\text{and} \\
\qquad (q^0_{k\ m \longleftrightarrow k-1\ m+1})^2 = \dfrac{3}{2}\,\dfrac{(k-m)(k-m-1)}{k\,(4k^2 - 1)}\ A
\end{array}\right\} \qquad (22)$$

In the perturbed system let x replace k as the index of the initial state, and neglect the effect of the external field on final states Then equation (21) gives the intensities of p components

$$(q_{k\ m \longleftrightarrow x, m})^2 = (q^0_{k\ m \longleftrightarrow k-1\ m}\ S_{k-1\ x} + q^0_{k\ m \longleftrightarrow k+1\ m}\ S_{k+1\ x})^2 \qquad (23)$$

and s components

$$(q_{k\ m \longleftrightarrow x, m-1})^2 = (q^0_{k, m \longleftrightarrow k-1\ m-1}\ S_{k-1, x} + q^0_{k, m \longleftrightarrow k+1\ m-1}\ S_{k+1\ x})^2$$

$$(q_{k, m \longleftrightarrow x, m+1})^2 = (q^0_{k\ m \longleftrightarrow k-1\ m+1}\ S_{k-1\ x} + q^0_{k\ m \longleftrightarrow k+1\ m+1}\ S_{k+1\ x})^2 \quad (24)$$

As an example, consider the transitions from the states 4 Q ($m = 1$) to 2P There will be p components when $\Delta m = 0$, and s components when $\Delta m = -1$ We need to determine from (17) the values of S_{kx} For convenience take the sub-determinants with the second line left out

$$S_{1x}\ \ S_{2x}\ \ S_{3x} = -4\kappa F\ \sqrt{\frac{12}{5}}\,(x_1 + \lambda_3)\ \ (x_1 + \lambda_1)\,(x_1 + \lambda_3)\ \ -4\kappa F\ \sqrt{\frac{8}{5}}\,(x_1 + \lambda_1)$$

Normalising these terms so that $\Sigma_k\, (S_{kx})^2 = 1$, we have

$$S_{2x} = \frac{(x_1 + \lambda_1)\,(x_1 + \lambda_3)}{\sqrt{\{(x_1 + \lambda_1)\,(x_1 + \lambda_3)\}^2 + 16\kappa^2 F^2 \left\{\frac{12}{5}\,(x_1 + \lambda_3)^2 + \frac{8}{5}\,(x_1 + \lambda_1)^2\right\}}}, \quad (24)$$

and similar forms for S_{1x} and S_{3x} Hence in the perturbed system the p components will have intensities given by

$$\begin{aligned}
(q_{1\ 1 \longleftrightarrow x\ 1})^2 &= (q_{1\ 1 \longleftrightarrow 2\ 1})^2\ \ S_{2x}^2 \\
&= \frac{3}{5}\ S_{2x}^2\ \ A \qquad (25)
\end{aligned}$$

from (22) S_{2x} has the value given in (24)

The *s* components will have intensities

$$(q_{1,0 \longleftrightarrow x\,1})^2 = (q^0_{1\,0 \longleftrightarrow 2,1})^2 \mathrm{S}_{2,x}{}^2$$
$$= \frac{3}{10}\ \mathrm{S}_{2\,x}{}^2\ \mathrm{A} \qquad (26)$$

The intensity of a Stark component in the group under consideration is obviously obtained by substituting its displacement x (measured from the diffuse line) in (25) or (26), hence each *s* component of this group will have one-half the intensity of the *p* component of equal displacement

As the external field approaches zero, the components of the P and F lines assume displacements $\varepsilon - \lambda_1$ and $\eta - \lambda_3$, where ε and η are small quantities which according to the equation (18) are proportional to the square of the field From (24) it follows that $\mathrm{S}_{2,\mathrm{P}}$ and $\mathrm{S}_{2,\mathrm{F}} \rightarrow 0$, while $\mathrm{S}_{2,\mathrm{D}} \rightarrow 1$ at zero field. Thus the components of the combination lines gradually weaken and vanish while each of the components of the diffuse line at the same time increases to its full intensity

The intensities of the *s* components 4Q $(m = 2) \rightarrow$ 2F are equal to

$$(\mathrm{S}_{2,x})^2{}_{m=2}\ \ q_{1,1 \longleftrightarrow 2,2} = x^2/(x^2 + 16\kappa^2\mathrm{F}^2)\ \ \frac{3}{5}\mathrm{A}$$

The intensities of the *p* (say) components 4Q $(m = 0) \rightarrow$ 2P, on the other hand, are clearly dependent upon the probabilities of two transitions in the unperturbed system, and two corresponding sets of S terms, as illustrated in fig 11

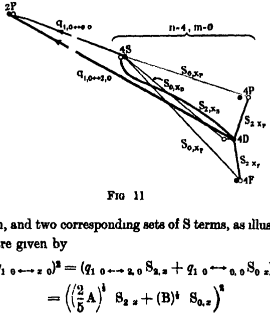

FIG 11

The intensities are given by

$$(q_{1\,0 \longleftrightarrow x\,0})^2 = (q_{1\,0 \longleftrightarrow 2,0}\,\mathrm{S}_{2,x} + q_{1\,0 \longleftrightarrow 0,0}\,\mathrm{S}_{0\,x})^2$$
$$= \left(\left(\frac{2}{5}\mathrm{A}\right)^{\frac{1}{2}}\ \mathrm{S}_{2\,x} + (\mathrm{B})^{\frac{1}{2}}\ \ \mathrm{S}_{0,x}\right)^2$$

where B is the intensity of the normal sharp series line observed with *either* polarisation Since B is much smaller than A,* and the S_{0m} terms in the present application are very small compared with the S_{2m} terms, we are justified in neglecting these quantities With this approximation, each *p* component in the group 4Q ($m = 0$) → 2P has four times the intensity of the perpendicular component

The intensities of the Stark components in the groups we are considering have been calculated at 10, 40 and 100 kv /cm , and are given in Table II

Table II —Calculated Intensities of Stark Components of Helium Line Groups

In the subdivisions (*a*) to (*d*) inclusive, the theoretical intensities are recorded as fractions of the intensity of the diffuse line at zero external field In the remaining subdivisions the intensities are fractions of the principal series line

The ratio of the intensity of sharp and diffuse lines at zero external field is taken from Sugiura's paper (*loc cit*)

(*a*) The Group 2P — 4Q (λ 4922)

Field in kv /cm	Change in *m*	Parallel Components				Perpendicular Components			
		S	D	F	P	S	D	F	P
10	2 → 1	—	—	—	—	—	0 52	0 079	—
	1 → 1, 1 → 0	—	0 50	0 098	0 0034	—	0 25	0 049	0 0017
	0 → 0, 0 → 1	0 025	0 33	0 069	0 0038	0 025	0 082	0 017	0 0009
40	2 → 1	—	—	—	—	—	0 38	0 22	—
	1 → 1, 1 → 0	--	0 39	0 15	0 059	—	0 19	0 077	0 029
	0 → 0, 0 → 1	0 025	0 26	0 094	0 047	0 025	0 065	0 024	0 012
100	2 → 1	—	—	—	—	—	0 33	0 27	—
	1 → 1, 1 → 0	—	0 35	0 068	0 18	—	0 18	0 034	0 09
	0 → 0, 0 → 1	0 025	0 24	0 045	0 12	0 025	0 059	0 011	0 029

---

* The values of A and B are given in a paper by Suguira, 'Journal de Physique,' vol 8, p 113 (1927) See especially equation (5)

Table II (continued)

(*b*) The Group $2p - 4q$ (λ 4471)

Field in kv /cm	Change in m	Parallel Components				Perpendicular Components			
		s	p	d	f	s	p	d	f
10	2 → 1	—	—	—	—	—	—	0 55	0 050
	1 → 1, 1 → 0	—	0 0002	0 53	0 071	—	0 0001	0 26	0 036
	0 → 0, 0 → 1	0 025	0 0002	0 35	0 051	0 025	0 0000	0 087	0 013
40	2 → 1	—	—	—	—	—	—	0 41	0 19
	1 → 1, 1 → 0	—	0 0030	0 37	0 22	—	0 0015	0 19	0 11
	0 → 0, 0 → 1	0 025	0 0027	0 24	0 15	0 025	0 0007	0 061	0 039
100	2 → 1	—	—	—	—	—	—	0 345	0 255
	1 → 1, 1 → 0	—	0 017	0 29	0 29	—	0 0084	0 15	0 14
	0 → 0, 0 → 1	0 025	0 015	0 19	0 20	0 025	0 0038	0 047	0 049

(*c*) The Group 2P — 5Q (λ 4388)

Field in kv /cm	Change in m	Parallel Components					Perpendicular Components				
		S	D	F	G	P	S	D	F	G	P
10	2 → 1	—	—	—	—	—	—	0 28	0 22	0 099	—
	1 → 1, 1 → 0	—	0 31	0 17	0 079	0 042	—	0 157	0 086	0 040	0 021
	0 → 0, 0 → 1	0 027	0 21	0 11	0 049	0 034	0 027	0 052	0 027	0 012	0 009
40	2 → 1	—	—	—	—	—	—	0 20	0 25	0 15	—
	1 → 1, 1 → 0	—	0 27	0 12	0 0008	0 21	—	0 13	0 060	0 0004	0 10
	0 → 0, 0 → 1	0 027	0 185	0 077	0 0025	0 135	0 027	0 046	0 019	0 0006	0 034
100	2 → 1	—	—	—	—	—	—	0 18	0 25	0 16	—
	1 → 1, 1 → 0	—	0 26	0 080	0 014	0 25	—	0 13	0 039	0 0070	0 12
	0 → 0, 0 → 1	0 025	0 17	0 070	0 0000	0 15	0 025	0 043	0 017	0 0000	0 038

(*d*) The Group $2p - 5q$ (λ 4026)

Field in kv /cm	Change in m	Parallel Components					Perpendicular Components				
		s	p	d	f	g	s	p	d	f	g
10	2 → 1	—	—	—	—	—	—	—	0 32	0 20	0 08
	1 → 1, 1 → 0	—	0 0017	0 29	0 20	0 11	—	0 0008	0 14	0 099	0 057
	0 → , 0 → 1	0 027	0 0017	0 19	0 13	0 081	0 027	0 0004	0 047	0 032	0 020
40	2 → 1	—	—	—	—	—	—	—	0 20	0 25	0 14
	1 → 1, 1 → 0	—	0 030	0 16	0 22	0 19	—	0 015	0 082	0 11	0 10
	0 → 0, 0 → 1	0 027	0 026	0 10	0 14	0 13	0 027	0 0064	0 025	0 034	0 033
100	2 → 1	—	—	—	—	—	—	—	0 18	0 26	0 16
	1 → 1, 1 → 0	—	0 13	0 060	0 18	0 23	—	0 063	0 030	0 093	0 12
	0 → 0, 0 → 1	0 027	0 11	0 02	0 10	0 16	0 026	0 027	0 0054	0 026	0 41

Table II—(continued)

(*e*) The Group 2S — 4Q (λ 3965)

Field in kv /cm	Change *m*	Parallel Components				Perpendicular Components			
		S	D	F	P	S	D	F	P
10	0 → 0, 1 → 0	0 0001	0 0068	0 0007	0 99	-	0 0057	0 0017	0 99
40	0 → 0, 1 → 0	0 0018	0 059	0 072	0 87	—	0 047	0 059	0 89
100	0 → 0, 1 → 0	0 010	0 13	0 220	0 64	—	0 12	0 24	0 63

(*f*) The Group 2*s* — 4*q* (λ 3188)

Field in kv /cm	Change in *m*	Parallel Components				Perpendicular Components			
		s	*p*	*d*	*f*	*s*	*p*	*d*	*f*
10	0 → 0, 1 → 0	0 000	0 999	0 0004	0 00013	-	0 997	0 0027	0 00034
40	0 → 0, 1 → 0	0 0004	0 99	0 0046	0 0021	—	0 995	0 0033	0 0016
100	0 → 0, 1 → 0	0 0005	0 96	0 025	0 015	—	0 970	0 019	0 011

(*g*) The Group 2S — 5Q (λ 3614)

Field in kv /cm	Change in *m*	Parallel Components					Perpendicular Components				
		S	D	F	G	P	S	D	F	G	P
10	0 → 0, 1 → 0	0 013	0 030	0 031	0 034	0 90	—	0 024	0 024	0 026	0 93
40	0 → 0, 1 → 0	0 017	0 096	0 14	0 23	0 51	—	0 091	0 16	0 29	0 45
100	0 → 0, 1 → 0	0 091	0 090	0 16	0 26	0 40	—	0 14	0 24	0 33	0 28

(*h*) The Group 2*s* — 5*q* (λ 2945)

Field in kv /cm	Change in *m*	Parallel Components					Perpendicular Components				
		s	*p*	*d*	*f*	*g*	*s*	*p*	*d*	*f*	*g*
10	0 → 0, 1 → 0	0 0004	0 99	0 0020	0 0011	0 0005	—	0 997	0 0018	0 0011	0 0005
40	0 → 0, 1 → 0	0 0066	0 92	0 031	0 023	0 013	—	0 94	0 023	0 017	0 010
100	0 → 0, 1 → 0	0 038	0 62	0 17	0 10	0 062	—	0 74	0 14	0 08	0 040

Intensities in Very High Fields – For very high fields we have found the approximate displacements of components 4Q $(m = 1) \rightarrow 2\mathrm{P}$ (see equations (20))

$$x_{\mathrm{D}} = 8\kappa\mathrm{F} - \frac{1}{10}(3\lambda_1 + 2\lambda_3)$$

$$x_{\mathrm{F}} = \quad - \frac{1}{5}(2\lambda_1 + 3\lambda_3)$$

$$x_{\mathrm{P}} = 8\kappa\mathrm{F} - \frac{1}{10}(3\lambda_1 + 2\lambda_3)$$

Since the terms containing the λ's are small compared with $8\kappa\mathrm{F}$, there is marked symmetry with regard to displacements in high fields From (25), (26) it then follows that the components with equal and opposite displacements have nearly the same intensities Even at moderate field strengths Lo Surdo photographs of most helium groups show well-developed symmetry

Comparison of Calculated Displacements and Intensities with Observations — To begin with, figs 4 to 10, inclusive (Plates 7 to 13), are purely theoretical diagrams, based on the calculated displacements and intensities For purposes of comparison, however, the writer's observations are represented by the centres of the dots Most of the observations have been taken from earlier papers, but there are a few new ones at higher fields The latter are included in Table III The fields are expressed in kv /cm, the displacements in cm^{-1}, and the intensities are indicated by the vertical lines on an arbitrary scale which varies from one figure to another The range of field strengths represented in the Lo Surdo photographs does not in any case exactly match that investigated in the theory The maximum field is marked on each plate The photographs of the groups λ 4922, λ 4026, and λ 3965 are new

We shall first examine the photographs to see if there is evidence of the full number of components expected in the scheme of patterns described in the earlier paper, and in the present theory In order to recognise the complete patterns for all lines in the groups under consideration, it is necessary to detect experimentally the initial energy levels characterised by $m = 0, 1, 2$ When the patterns appear to be incomplete, the full quota of initial levels may usually be detected in a less direct manner As an example, consider the line 2P — 5G (fig 6), which ought to yield a pattern $\frac{2}{3}$ (two *p* and three *s* components), and is found instead with the pattern $\frac{1}{1}$ Its components $m = 0, 1$ vanish before being separated from each other or from the *s* component $m = 2$ Transitions from

Table III—New Measurements of Displacements at 100,000 v /cm The components of a line are identified by the *m* value of the initial state In many cases observations have been made on two or more unresolved components

Line	Component	Displacements from normal D (or *d*) line in cm $^{-1}$	
		Parallel	Perpendicular
2 P − 4 D	0, 1	−42 0	—
− 4 D	1	—	−38 0
− 4 D	2	—	−21 0
− 4 F	0, 1	+19 5	—
− 4 F	2	—	+28 5
− 4 P	0	+83 5	—
− 4 P	1	+73 5	+73 5
2 *p* − 4 *d*	0, 1	−27 0	−25 0*
− 4 *f*	0, 1	+41 0	+41 0
− 4 *f*	2	—	+31 0
2 *p* 5 *p*	0, 1	−152	−152
− 5 *d*	0, 1	−61 0	−67 0*
− 5 *f*	0	+18 8	—
− 5 *f*	1	+15 5	—
− 5 *g*	0, 1	+94 0	+94 0
− 5 *g*	2	—	+68 0
2 S − 4 D	0	−47 0	—
− 4 D	1	—	−44 8
− 4 F	0	+20 0	—
− 4 F	1	—	+19 5
− 4 P	0	+86 0	—
− 4 P	1	—	+77 0

And at 83,000 v /cm

2 S − 5 S	0	—	—
2 S − 5 D	0	−81 0	—
− 5 D	1	—	−77 0
− 5 F	0	+19 0	—
− 5 F	1	—	+21 0
− 5 G	0	+101 5	—
− 5 G	1	—	+87 0

* Observation on unresolved components 0, 1, 2

the same initial levels, however, give the *p* and *s* components respectively of 2S − 5G These lines do not vanish (the intensities depend upon other terms of the S matrix) and are found in high fields (fig 7) with different displacements Each displacement is distinctly less than that observed for the component

$m = 2$ at (say) 40 kv /cm , hence the three levels have been resolved. The experimental pattern $\frac{2}{3}$ may now be claimed for this line, provided we accept the usual selection rule for m A complete examination of the photographs shows that all initial levels $m = 0, 1, 2$ have been found for the parhelium groups, and only a few are uncertain in orthohelium

In general, the components are displaced proportional to the square of the field as given by the earlier Bohr theory, provided the Stark-effect is small in comparison with the disturbance due to the inner field ($\Delta\nu_F < \Delta\nu_k$) Since this effect is rather common and easily observed, it has become customary to define a low field as one for which the above condition is met In a high field the displacement is a linear function of the field and $\Delta\nu_F > \Delta\nu_k$. Being dependent upon $\Delta\nu_k$, however, the range of field strengths (expressed in v /cm) through which this gradual transition takes place differs from line to line even within a single group The wide range of $\Delta\nu_k$ represented in the groups under consideration, therefore, introduces an exceptional variety into the displacements, which is further augmented by the fact that not all components in low experimental fields can be classified in either of the two theoretical groups just cited

Group 2P — 4Q (λ4922) —In the published displacements of the 4922 group the field strengths were found by applying the Epstein theory to nearby displacements of H_β components in the same fields The observations fall accurately on the theoretical curves in fig 4.

The theoretical intensities also seem entirely satisfactory, though the comparison here is qualitative, whereas it is quantitative with the displacements There is especially good agreement in the D and P lines, where the fine analysis components are clearly resolved In fields above 100 kv /cm the components F (0, 1)* are observed with very low intensity, while F (2) remains strong

Group 2S — 4Q (λ 3965) —Comparatively few observations have been made on these lines Since the displacements are due to shifts in the initial levels, they have been thoroughly tested in the 4922 group, and are here only roughly checked at 100,000 v /cm

The theoretical intensities are qualitatively right The F line is possibly a

---

* The numbers in parenthesis are the m values of the perturbed terms arising from the original term, 4F Written in full the components in question are 2P (0, 1) — 4F (0, 1) (two unresolved) and 2P (1) — 4F (2) There is no ambiguity in the present connection if we write only F (0, 1) and F (2) for these components.

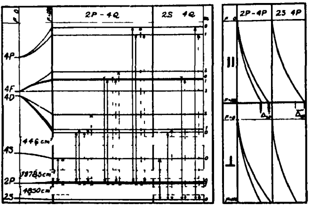

FIG 1

(For description, see p 145)

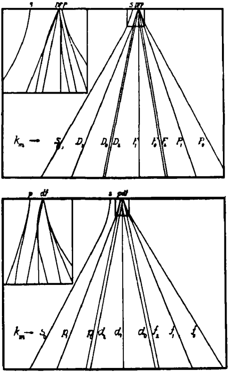

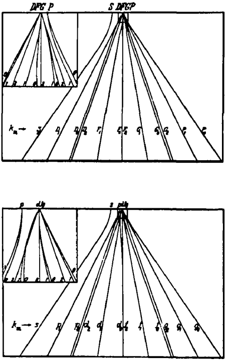

FIG 2 —Components of the Helium Groups $2P-4Q$ and $2p-4q$ in very high Electric Fields

FIG 3 —Components of the Helium Groups $2P-5Q$ and $2p-5q$ in very high Electric Fields

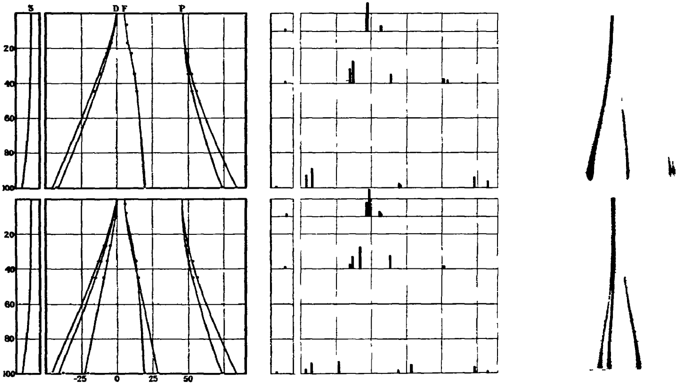

Theoretical Displacements (with observations plotted)

Theoretical Intensities

Max Field 137 kv cm

Fig 4 —The 2P — 4Q Group (λ 4922)

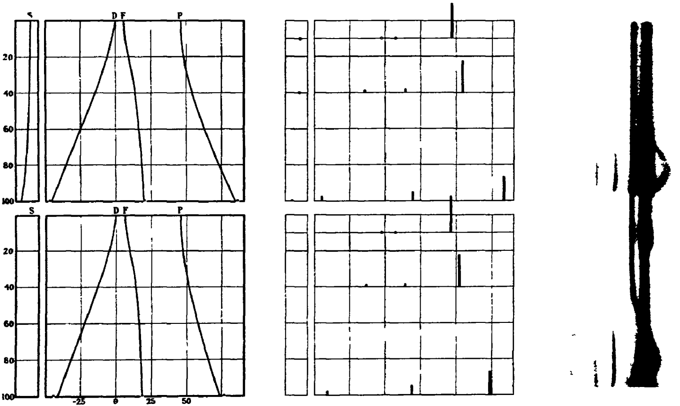

Theoretical Displacements (with observations plotted)

Theoretical Intensities

Max Field, 137 kv/cm

Fig. 5.—The 2S − 4Q Group (λ 3965)

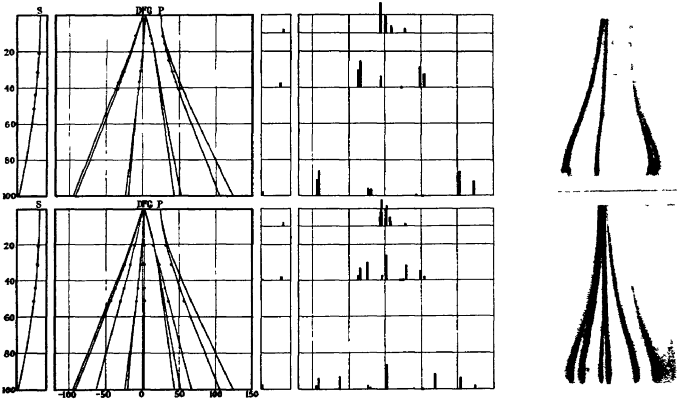

Theoretical Displacements (with observations plotted)

Theoretical Intensities.

Max Field, 40 4 kv /cm.

FIG 6 —The 2P — 5Q Group (λ 4388)

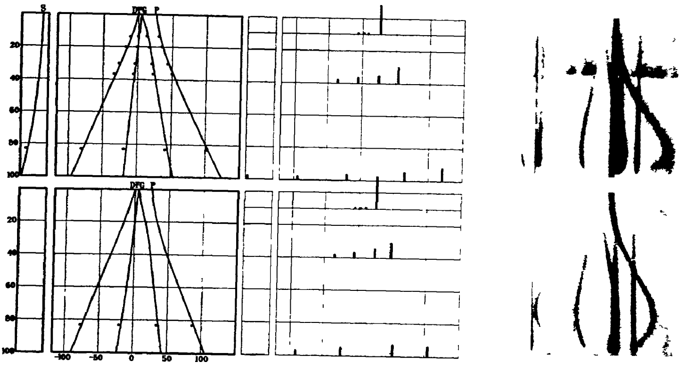

Theoretical Displacements (with observations plotted)

Theoretical Intensities

Max Field 83 kv/cm

Fig 7—The 2S – 5Q Group (λ 3614)

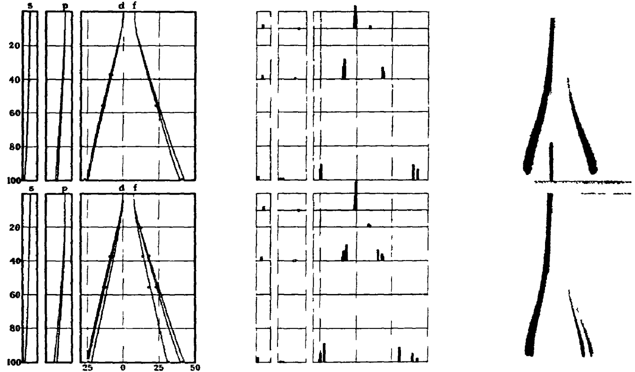

Theoretical Displacements (with observations plotted)

Theoretical Intensities

Max Field 51 2 kv cm

Fig 8 —The $2p - 4q$ Group (λ 4471)

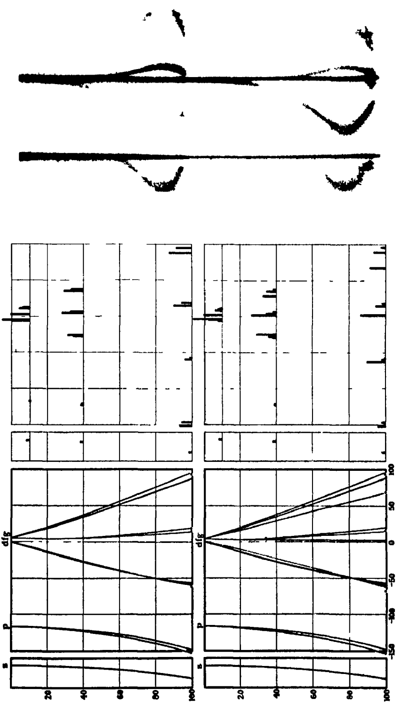

Max Field 137 kv/cm

Theoretical Intensities

Theoretical Displacements (with observations plotted

Fig 9—The $2p - 5q$ Group (λ 4026)

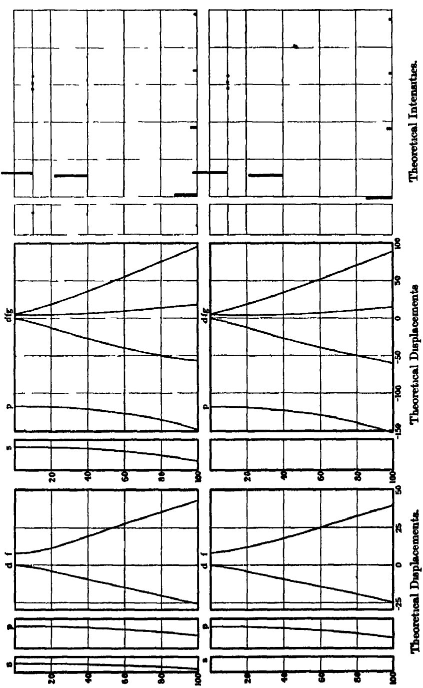

Fig. 10.—The $2s - 4q$ and $2s - 5q$ Groups (λ 3188 and λ 2945)

little stronger, relatively, than the theory claims In reality this effect is partly the result of a weakening of the D and P lines by field variations Aside from relatively slow changes in the field, which may be detected and sometimes corrected, there may be purely local changes quite beyond complete experimental control Any change of field tends to weaken the photographic impression of a component with large displacement

Group 2P — 5Q (λ 4388) — The field strengths in the original observations on the *p* components of this group were determined from the separations of components of H_γ, and Stark's experimental fields They were all too low, according to the present calculations, and have been corrected, therefore, to agree with Epstein The factor is 1 09 This correction has been applied to the old observations on the 2S — 5Q group (λ 3614) as well The fields were found in a more indirect way in the case of the S components of 2P — 5Q. An attempt was made to measure *p* and *s* components at points equidistant from the maximum field, and then determine the field strengths from the old curve for the *p* components (via H_γ and Stark) There appear to have been more serious errors here Since the *p* component D $(m = 1)$ agrees well with the theory, the corresponding *s* component of presumably the same displacement has been used to re-determine the field strengths The fact that the observations on the remaining six components now agree accurately with the theory is a sufficiently thorough test The new fields are 20 4, 30·6, 43 7, and 51 2 kv /cm

Vanishing Components —The most interesting feature in the intensities is the vanishing *p* component of the G line There is a general law about vanishing components in these groups We see from the determinant (17) that $S_{2\,s}\,(m = 1)$ must be zero when $x_1 + \lambda_1 = 0$, *i e*, a component 2P — *n*Q (1) must always entirely vanish when it assumes the frequency of the P — P combination line at zero field From similar determinants in which $m = 0$ and 2 respectively, it may be seen that the components 2 P — *n*Q (0) will be especially weak at this position, while the strong *s* components 2P — *n*Q (2) are not in the least affected [In the violet groups 2*s* — *n*Q components would theoretically entirely disappear if they ever reached the zero field position of the S — S combination line]

The components Q (0, 1) are usually unresolved In the 2P — 4Q group the components F (0, 1) become very weak in fields above 100 kv./cm , though the displacement is still much more than $-\lambda_1$ In the 2P — 5Q group the G (0, 1) line (nearest the P line) vanishes completely, as we have seen, and theoretically is expected to reappear at 100 kv /cm or a little higher field. An even better example of this effect is found in the 2P — 6Q group, where the H (0, 1) line vanishes in very low field as it passes under the P — P line, and immediately returns and continues as a rather strong line

Conditions are slightly different in orthohelium, where the *d* line is always nearest the *p* line, and the separations within the groups are somewhat greater than in parhelium For these reasons the effect in question first appears in the photographs of $2p - 6q$, where the *d* (0, 1) line has a very low intensity at high fields In the next group, however, the *d* (0, 1) line vanishes completely at very low fields

Group 2S — 5Q (λ 3614) —The slight shift toward the red of all observations at moderate fields is probably an experimental error The plate from which the measurements were taken did not show an undisplaced line except at zero field In higher fields the shifts toward the red in this and other groups indicates a small second order effect The symmetry of the displacements is rather noticeable here, since the components with constant *m* values are already sorted The symmetry is really quite pronounced in all groups, if one fixes the attention on components with constant *m*

Group $2p - 4q$ (λ 4471) —This photograph, taken with six prisms, was accompanied by H_β, poorly focussed The published fields were obtained from the experimental values given by Stark for 4471 and H_β * To make them agree with Epstein we need to multiply by a factor 1 12 This has been done in fig 8

The only apparent disagreement with regard to displacements arises in this and the following orthohelium group In these groups the two *p* components of the *d* line have been observed The theoretical separations, however, are so small that resolution is not expected under the experimental conditions

The theoretical intensities seem to be correct

Group $2p - 5q$ (λ 4026) —The present photograph roughly checks the theoretical displacements and intensities in high fields For a detailed analysis of $2p$ — *5f as a doublet* see the earlier paper, Plate 6 (C)

On the whole, the theoretical intensities in helium are in very good agreement with the present qualitative observations The agreement is possibly even better than in the case of hydrogen as presented in a recent paper by Schrodinger † Lo Surdo photographs of the Balmer lines published by the writer‡ show slight qualitative variations from Prof Stark's experimental results, and agree better with the new theory It seems most probable to the writer that the principal cause of variations in the experimental values is a small change in the field strength during the very long exposures Many workers on the Stark-effect have noticed that such fluctuations are not uncommon, and unfortunately they are rather abrupt when the field and light intensity are unusually high This suggestion is made, since it offers a possible explanation (for example) of the relative strength of the *p* components of H_β with $\Delta = \pm 10$ as well as the presence of doubtful components $\Delta = \pm 12$

---

* 'Monograph,' pp 35, 37

† *Loc. cit*

‡ H_β, 'Astrophys J,' vol 62, p 229 (1925), H_β (quantitative), Foster and Chalk, 'Nature,' vol 118, p 592 (1926), H_γ, 'Phys Rev,' *loc cit*, H_δ, *ibid*, *loc cit*

Summary

The perturbation theory of quantum mechanics has been applied to the Stark-effect in the arc spectra of helium

New measurements of displacements of helium components in fields of 100,000 v /cm and 83,000 v /cm have been recorded, together with three new photographs of helium groups in high fields

The first order displacements have been calculated at several field strengths for components of the line groups 2P — (4Q, 5Q), 2S — (4Q, 5Q) and for the corresponding orthohelium lines, considered as singlets These displacements are in good agreement with the observations at all field strengths The approximate positions of the components at extremely high fields have been calculated, and the manner in which certain components are expected to cross each other in moderate to high fields has been described In the case of two lines, at least, (2P — 4F, 2P — 5G), there is conclusive experimental evidence of such a crossing

The theoretical intensities of the components have been found for fields of 10, 40 and 100 kv /cm These agree with the qualitative observations shown in the accompanying photographs In particular, the theory accounts satisfactorily for the observed disappearance of numerous components when the displacement is equal to that of the 2P — *n*P line at zero field

In conclusion, the writer wishes to express his best thanks to Prof Bohr for his interest in this work, the major part of which was done in Copenhagen His thanks are also extended to Dr. Heisenberg for many helpful and friendly discussions

The Spectrum of Carbon Arcs in Air at High Current Densities

By J W Ryde

(Research Laboratories of the General Electric Company, Wembley)

(Communicated by A Fowler, F R S —Received August 29, 1927)

[Plates 14–16]

(1) *Introduction*

Although the spectrum of the ordinary carbon arc has been studied in great detail during the last 70 years, there seems to have been no similar study of the "High Current Density" arc which was introduced by Beck in 1914 Spectrophotometrical measurements have been made in connection with the development of this type of arc for searchlights, and photographs of the spectra obtained from the total radiation from the arc have been published The only account, however, of the spectrum from individual parts of the arc appears in a short note by Bell and Bassett *

They examined an image of the arc on a ground glass screen with a direct vision spectroscope and reported that in the arc stream 15 lines appeared when the current exceeded 100 amperes They attributed 7 of these to helium and 2 to hydrogen

The present investigation shows, on the contrary as was first suggested to the author by Prof Fowler that the spectrum of this part of the arc consists mainly of the spectra of neutral carbon, nitrogen, oxygen and hydrogen No lines were observed which could be attributed to helium even when the arc was run at 250 amperes

It is only comparatively recently that the spectra of C I and N I have been observed and up to the present they have only been produced under special conditions The ordinary carbon arc in air, for example, only excites the well-known carbon line at λ 2478 and shows no nitrogen lines at all,† while the greater excitation of the spark produces the spectrum of the ionised atoms C II and N II

---

* Louis Bell and P R Bassett, 'Science,' vol 56 p 512 (1922)

† Prof Fowler, however, has informed the author that he has recently obtained the chief lines of C I and N I in a carbon arc fed with a current not greater than 12 amperes

Merton and Johnson*, however, found that discharge tubes having carbon electrodes and containing a trace of an oxide of carbon in 20 mm to 30 mm of helium showed, when excited by mild condensed discharges, a number of new lines which were attributed to the missing C I spectrum

Again, Hardtke† showed that several new lines occurred in the spectrum of nitrogen excited by positive rays in special discharge tubes Later, Merton and Pilley‡ found that helium at about 30 mm pressure, containing a trace of pure nitrogen, when excited by a moderate condensed discharge, shows a number of lines which have been shown to be due to the neutral nitrogen atom

It is shown in what follows that cored carbon arcs at high current densities provide just the degree of excitation, intermediate between the ordinary arc and spark, which is necessary for the production of these spectra Several marked differences in the relative intensities of the lines are found compared with those obtained by the discharge tube methods Also a number of new lines, probably belonging to O I, N I or C I, have been found to appear

(2) *The High Current Arc*

An account of the development of the high current arc for searchlight purposes has been given by Lieut Commander C S Gillette§ and by Gehlhoff and Thilo ||

This arc in the form originally invented by Beck consisted of a positive carbon 16 mm in diameter cored with a mixture of rare earth fluorides and carbon, the negative was of ordinary construction and about 11 mm in diameter The arc burnt at 150 amperes, 75 volts Both carbons were slowly rotated, but it now appears that it is only necessary to rotate the positive, the object being to maintain a uniform crater The dimensions of these carbons are very much smaller than those necessary if plain carbons are used in arcs of the ordinary type carrying the same current

The intrinsic brilliancy of the ordinary carbon arc is determined by the temperature of the crater alone, and this is limited by the boiling point of carbon The Beck arc, however, has a much higher intrinsic brilliancy owing to the intense radiation from the vaporised core material

There is no need to give a description of the various mechanisms developed

---

* Merton and Johnson, 'Roy Soc Proc,' A, vol 103, p 384 (1923), Johnson, Roy Soc Proc,' A, vol 108, p 343 (1925)

† 'Ann d Physik,' vol 56, p 363 (1918)

‡ 'Roy Soc Proc,' A, vol 107, p 411 (1925)

§ 'J Amer Soc Naval Eng,' vol 34, p 527 (1922)

|| 'Helios,' 'Fach und Export Z f Electrotechnik, Nos 42, 43, 46 and 47' '1920)

to ensure regular feeding and burning These are only essential if the arc is to be used for projection purposes The spectra to be described can easily be obtained with the simplest arrangements for holding the carbons, provided sufficient electrical power, about 15 kw at 100 volts, is available It is not absolutely necessary to rotate the positive carbon unless relatively long exposures are to be given

The essential feature of the Beck type of arc is the cored positive carbon At high current densities this core, consisting of a mixture of metallic salts and carbon, produces a highly conducting flame which streams vertically upwards from the crater In ordinary arcs the arc stream plays directly on to the positive carbon and, as is well known, there is a limiting current density beyond which the arc hisses and becomes hopelessly unsteady If, however, the positive carbon is cored with a suitable material, the arc stream plays on the highly conducting flame from the crater instead of on the carbon itself Under these conditions, provided sufficient metallic vapour is continuously supplied by volatilisation of the core, a steady arc may be maintained at current densities much greater than would be possible with plain carbon electrodes

If the current through a cored carbon arc, such as described, is slowly increased from a comparatively low value, it will be found that soon after the limiting current density for ordinary arcs is exceeded, the centre of the arc stream changes colour and a bright central core is developed This may be seen in Plate 14 When this part of the arc was observed spectroscopically it was found that the development of the central core corresponded with the emission of a number of lines which were found to belong to the spectra of C I, N I, etc

Some of the strongest of these lines were observed in an arc between ordinary carbon electrodes, provided the current density was increased sufficiently, but of course at this stage the arc became very unsteady It appears, therefore, that a cored positive carbon is only needed in order to enable a steady arc to be maintained at the high current densities which are necessary to excite the carbon and nitrogen lines The composition of the core of the positive carbons used for projection work is about 50 per cent of carbon and 50 per cent of rare earth fluorides The mixture of rare earths is used to obtain maximum light emission, but they are unsuitable for investigating the spectra of the arc stream as their extremely complicated line spectra tend to confuse those to be studied For although most of the vapour from the core material streams upward in a flame from the positive carbon, nevertheless, a certain amount diffuses into the arc stream

It is best, therefore, to select a core material which gives a comparatively simple line spectrum and at the same time vaporises at a rate suitable for the maintenance of a steady arc After a number of trials calcium fluoride was selected as one of the most suitable in these respects

The cores may be made from the following batch mixture —

50 per cent CaF_2
10 per cent petroleum coke
20 per cent lamp black
20 per cent tar

These ingredients after well mixing are pressed or squirted into rods about 8 mm diameter The rods are then packed in carbon dust and baked by raising the temperature in stages of 200° C every 2 hours up to a final temperature of 800° C After 2 hours at this temperature they are then allowed to cool slowly, and when cold are inserted in carbon sheaths having an external diameter of 16 mm The negative electrodes may be ordinary plain carbons about 10 mm in diameter

(3) *The Spectrum of the High Current Arc cored with* CaF_2

The appearance of the high current arc having a positive carbon cored with calcium fluoride as described in the last section is shown in Plate 14 The photographs were taken through colour filters in order to show the structure of the flames Figs A and B were taken through filters transmitting from λ 5000 to λ 7000 and from λ 4200 to λ 5100 respectively The first filter thus transmits all the bands due to calcium compounds, while the second transmits almost all the low temperature lines (King's Class I) but no calcium bands The two photographs, therefore, show the regions of the flame which emit the calcium band and line spectra respectively

The large outer flame which only appears in Plate 14, A, is comparatively non-conducting and emits the easily excited band spectra of CaF_2 and CaO The inner flame seen in Plate 14, B, which emits the calcium arc spectrum is highly conducting and is that referred to in the previous section. The manner in which the arc stream plays upon it is well shown in the photograph

Plate 14, C, was taken through a green filter transmitting from λ 4680 to λ 5190 This cuts out the CaF_2 bands and most of the calcium line spectrum, with the exception of a few Class III lines, but transmits the most intense Swan bands The photograph shows the presence of a small intense flame filling the crater and streaming upwards for about 3 mm. (approximately one-fifth of the crater-diameter) above it The spectrum shows that this flame is due to the excitation of the Swan bands, which have recently been attributed by Johnson to a

HC–CH molecule * The fact that they appear so localised at the positive carbon is remarkable The CH bands at λ 4315 were not observed The Swan bands do not appear at all in the arc stream under normal conditions, but if a gentle stream of coal gas is directed upon it, they appear brilliantly With hydrogen the effect is not nearly so marked, but where the gas meets the arc stream the bands may be seen faintly

The arc stream will be seen from the photographs to be composed of two concentric shells surrounding a bright central core The outer shell does not appear in Plate 14, B, as it is due to the excitation of the band spectrum of CaF_2 showing that some of the calcium fluoride vapour diffuses into this region The second shell, which is barely seen in Plate 14, A, but appears strongly in Plate 14, B, is due to the CN bands, the first negative bands of nitrogen and, to a certain extent, the line spectrum of calcium The bright central core, seen best in Plate 14, A, is considered in detail later It is here that the spectra of C I, N I, O I, etc , are excited

The excitation in this part increases rapidly as the axis of the core is approached as is shown by the broadening and wave-length displacements of many of the lines, both effects being much greater at the axis than at the surface of the central core Also the lengths of the lines due to ionised carbon, C II, are shorter than those due to C I, while lines due to more easily excited atoms extend for some way beyond the core itself

(4) *Procedure*

Most of the spectrum photographs were taken with a large Hilger Quartz Littrow spectrograph E 1 having a glass prism for the visible region An image of the arc stream was thrown on the slit by means of a quartz lens Usually the axis of the central core was inclined to the slit at about 45°

The intensity of the arc stream is so great that only a few seconds' exposure is needed for the visible and ultra-violet regions The infra-red oxygen triplet at λ 8447 could be recorded on ordinary Ilford panchromatic plates with an exposure of about 10 minutes When photographing the extreme red or infra-red, the visible region of the spectrum was cut off by suitable Wratten filters to eliminate the general fogging which otherwise occurred The ultra-violet regions were photographed down to λ 2200 on the large instrument and to λ 1900 by means of a small quartz Hilger spectrograph E 27

Most of the work was done with positive carbons cored with calcium fluoride, as described above, but several plates were taken with other core materials in order to measure lines which were masked by the calcium spectrum

---

* Johnson, 'Phil Trans,' A, vol 226, p 157 (1927)

Many of the lines showed considerable broadening and also large shifts to the red Some nitrogen multiplets showed shifts of the order of 2 A The width of the lines and the magnitude of the shifts depend on the part of the arc stream being observed In general the lines are sharper and the shifts are less at the end of the arc stream nearer the positive carbon

Measurements were in all cases taken from several plates and usually the current was 160 to 200 amperes, the potential drop across the arc being about 60 to 80 volts Some photographs and visual observations were taken with currents as high as 250 amperes, but the arc was then somewhat unsteady and could not be run for long on account of overheating

(5) *The Spectrum of the Arc Stream*

The spectrum of the arc stream when the arc is burnt in air was found to consist of —

(*a*) The spectra of neutral carbon, nitrogen, oxygen, hydrogen, and a few of the strongest lines belonging to the red spectrum of argon No lines due to the ionised atoms of these elements were found, with the exception of two or possibly four C II lines Over 50 new lines were found and are attributed to C I, N I, and O I, but a distinction between the three has not yet been made except in the case of a few N I lines

(*b*) The first negative nitrogen band spectrum together with the usual CN bands As mentioned previously, the Swan bands do not appear in this part of the arc

(*c*) A moderately strong continuous spectrum extending from the infra-red beyond λ 8200 down to the ultra-violet at least as far as λ 1930

(*d*) The line spectra of the elements in the core material, and impurities such as Fe, Ti, Mn, in the carbons themselves

The spectra in (*a*) and (*b*) will be considered in the following sections The presence of the continuous spectrum prevented some of the faintest lines being seen

No lines which could be attributed to helium were found, contrary to the report by Bell and Bassett * There is no doubt that the seven lines they attributed to helium are really some of the stronger C I, N I and O I lines together with the unidentified pair at λλ 4392 and 4385 (see Table VIII)

---

* *Loc cit*

From the following tables it will be seen that in many cases there are differences between the relative intensities of the lines compared with those previously observed in discharge tubes This is particularly evident in the case of nitrogen Considering each spectrum as a whole, however, it was generally easy to estimate whether the intensity of any given line, which had previously been observed in discharge tubes, was such that it might be expected to appear in the photographs of the arc stream If, after examination of all the plates, no trace of it could be found, it is marked in the tables as " absent "

Lines which are notably diffuse are indicated by *d* following the intensity

(6) *Carbon*

In Table I the C I lines found in the arc stream are compared with those which were observed by Merton and Johnson in their helium tubes with carbon electrodes Most of their faintest lines of intensity (0) have been omitted as they would be too faint to be seen in the arc owing to the continuous spectrum described in the last section It will be seen that with the exception of these, most of the lines observed by them appear in the arc The absence of λ 4758 78 is interesting as at first sight it would appear to be a component of a multiplet including the five strong lines above it in the table No trace of it could be found, however, on any of the plates taken.

The only C II lines which appear with certainty are the doublet at about λ 2837, which according to Fowler's* classification corresponds to a transition between deep terms of the ionised atom

It appears from this table that the degree of excitation existing in the core of the arc stream is intermediate between the ordinary arc, in which only the C I line λ 2478 appears with any intensity, and Merton and Johnson's discharge tubes in which the two C II doublets at about λ 3920 and λ 2837 appear strongly, since in the arc stream the former doublet does not appear and the latter one is fainter relative to the C I lines

The carbon line at λ 1930 6 is of interest It appears so very strongly in the arc stream that there can be no doubt that it must belong to the C I spectrum and cannot be due to a $3d - 4f$ transition in the C III spectrum as classified by Millikan and Bowen †

Prof Fowler has informed the author that he has found that there are actually two lines of nearly the same wave-length and due to C I and C III respectively Both of these appear in strong carbon sparks in hydrogen or nitrogen

---

* ' Roy Soc Proc ,' A, vol 105, p 299 (1924)

† ' Phys Rev ,' vol 26, p 310 (1925)

Table I —Carbon Lines in the Arc Stream of the High Current Arc

Merton and Johnson		Arc stream		
λ	Int	λ	Int	Remarks
7116 1	(0)			A strong unidentified line int (6) occurs at λ 7118 See Table VIII
6828 5	(0)	6828 6	(2)*d*	3 A wide
6587 75	(4)			Doubtful
6583 02	(1)	6582 8	(0) ?	Doubtful line (C II)
6578 16	(4)	6577 3	(0) ?	,
5380 242	(8)	5380 55	(9)	
5052 122	(6)	5052 30	(15)	
5041 66	(3)	5041 61	(1)	
5039 05	(3)	5039 09	(2)*d*	
5023 79	(1)	5023 71	(1)*d*	
4932 00	(5)	4932 22	(5)	
4879 86	(0)	4880 0	(0)*dd*	
4826 73	(0)	4826 89	(1)	
4817 33	(1)	4817 32	(1)	
4805 95	(1)	Absent		
4775 87	(3)	4775 98	(4)	
4771 72	(4)	4771 72	(10)	
4770 00	(2)	4770 15	(4)	
4706 62	(2)	4766 60	(3)	
4762 41	(4)	4762 37	(8)	
4758 78	(2)	Absent		
4757 59	(1)	„		
4371 33	(4)	4371 44	(4)	
4352 1	(1)	4352 01	(0)*s*	
4348 07	(4)	4348 09	(0)*s*	
4312 4	(3)			Probably not present unless quite weak
4303 8	(1)	Masked		
4268 99	(2)	Confused with nitrogen negative band Probably absent		
4267 1	(2)	Confused with nitrogen band C II		
4236 0	(2)*d*	„	„	
4231 35	(1)	4231 40	(0)	
4228 28	(1)	Masked		
4213 71	(1)	Confused with cyanogen band		
4212 90	(1)	„	„	
4212 36	(1)	„	„	
4160 4	(1)*d*	„	„	
4065 1	(2)	Absent		Confused with CN band structure
4064 2	(1)	Absent ?		„ „
3920 77	(9)	Absent		C II line
3919 06	(8)	„		„
3830 2	(2)	Confused by cyanogen band structure		Not found on all plates by M and J
3804 4	(2)*d*	„	„	„
3757 1	(3)	„	„	
3753 5	(1)*d*	„	„	„ „
3729 6	(2)	Absent		
3607 0	(1)*d*	„		„ „
3604 1	(1)*d*	„		
3592 6	(1)	„		„ „
3491 45	(3)	3491 86 ?	(2)	Confused with band structure
3489 3	(3)			„ „

Table I—(continued)

Merton and Johnson		Arc stream		
λ	Int	λ	Int	Remarks
3370 5	(4)	Absent		Not found on all plates by M and J
3158 6	(2)	Masked by Ca		,, ,,
2992 6	(2)	2992 61	(0)*s*	
2947 4	(1)	Masked by Fe		
2837 60	(9)	2837 61	(3)	C II line
2836 71	(10)	2836 72	(4)	,,
2747 31	(3)	Absent		
2746 50	(2)	Masked by Fe		
2660 3	(1)	Masked by Al		
2582 9	(2)	2582 94	(3)*s*	Not found on all plates by M and J
2515 15	(1)	Absent		
2512 00	(5)	2512 03	(2)*s*	
2509 05	(2)*d*	2509 05	(2)*s*	
2478 525	(20)	2478 50	(100)	
		1930 6	(30)	

(7) *Nitrogen*

In addition to the measurements by Merton and Pilley of the N I spectrum in discharge tubes, Merrill* and Kiess† have given a number of lines in the infra-red A number of the N I lines have also been classified in quartet and doublet systems by Kiess ‡

Table II gives the infra-red lines measured by Kiess together with those found in the arc stream Only rough measurements were possible in this region

The first two columns of Table IV give the N I lines measured by Merton and Pilley and by Hardtke The corresponding lines which were found in the arc are given in column 5 A few very faint lines which were recorded by Merton and Pilley but which were not found to appear in the arc have been omitted from the table Lines marked with an asterisk were found by them on one plate only Several of these appeared in the arc Of the lines recorded by both observers, only one at λ 4114 was not found in the arc

It will be seen from the table that many of the N I lines show considerable broadening and large displacements to the red, amounting in some cases to over 2 A Fowler§ has recorded multiplets in the N II spectrum which show displacements of 0 7 A in vacuum tubes at relatively high pressures Table III

* 'Astrophys J,' vol 51, p 236 (1920), and vol 54, p 76 (1921).

† 'Science,' vol 60, p 249 (1924)

‡ 'J Opt Soc Am,' vol 11, p 1 (1925)

§ 'Roy Soc Proc,' A, vol 107, p 31 (1925)

Table II —N I Infra-Red Lines in the Arc Stream.

λ Kiess	Int	λ Arc stream	Int	Remarks
8729 07	(0)	8730	(0)	
8718 99	(1)			
8711 87	(1)	8713	(1)	
8703 42	(1)			
8686 38	(1)	8682	(2)*d*	About 10 A wide
8683 61	(2)			
8680 33	(3)			
8656 32	(1)			
8629 61	(3)	8629	(1)	
8594 34	(2)	8594	(1)	
8568 04	(1)	8569	(0)	
8242 47	(3)	8243	(3)	
8223 28	(3)	8223	(3)	
8216 16	(5)	8216	(6)	
8210 94	(2)	8211	(1)	
8200 39	(1)	8200	(1)	
8188 16	(4)	8188	(4)	
8185 05	(3)	8185	(4)	

gives average values of the displacements and widths of the lines in the multiplets classified by Kiess These values are, however, very rough and are only given to show the magnitude of the effects in the various multiplets

Table III —Displacements of N I Multiplets

Multiplet	Approximate average displacement to red	Average width of the lines in the multiplet at centre of core of arc stream
n^4D 4^4P	+1 1 A	5 A
n^4D 5^4P	+2 4	4
$n^4D - {}^4D$	+1 7	4
$4^4P - P'$	+1 6	2
$5^4P - P'$	+1 5 ?	5
$n^4D - {}^4F$	?	Confused into band 25 A wide
$2^4P - {}^4S$	0	Fairly sharp
${}^2P - {}^2D$	−0 5	2
${}^2P - {}^2S$	0	Sharp

Merton and Pilley observed three lines λλ 4099 96 (9), 4109 94 (10) and 4113 92 (5), which Kiess has classified as a doublet system P — D multiplet The two first lines appear in the arc stream as two very strong lines of intensities (10) and (15) respectively, but λ 4113 92 was not seen, although it should have been found if its intensity was greater than 1 Hardtke found the line, but it was relatively much weaker than that recorded by Merton and Pilley

It will be seen that both the quartet and doublet system multiplets P — S show no appreciable displacement and are both fairly sharp With the exception of some lines between λλ 6076 and 5545, almost all the remaining unclassified lines are neither very broad nor much displaced

Seven new lines which appeared in the arc are included in Table IV Five of these, together with the two at λλ 6945 18 and 6926 70 previously observed by Merton and Pilley, were found to constitute the complete quartet system multiplet 4P — P′ The measurements were made on the ends of the lines which corresponded to the outer parts of the core of the arc stream There the lines were fairly sharp, although they were about 2 A. wide at the centre of the core The wave-length displacement was found to be 1 6 A Deducting this amount from each of the seven lines, the 4P — P′ multiplet appears as follows —

P'_1	18 38	P'_2	38 36	P'_3	
		14432 7 (2)	37 6	14394 9 (3)	$4P_3$
		70 0		70 3	70 12
14380 8 (2)	18 1	14362 7 (1)	38 1	14324 6 (2)	$4P_2$
44 5		44 1			44 34
14336 3 (0)	17 7	14318 6 (2)			$4P_1$

The other two lines at λλ 5837 and 5820 appear to belong, together with Merton and Pilley's line at λ 5829 5, to the 5^4P — P′ multiplet The new lines are very diffuse so that accurate measurements were impossible, but the displacement to the red in the arc appears to be roughly 1 5 A The three lines are, however, among the strongest which would be expected in this multiplet, so there is little doubt of the correctness of the identification

In addition to the N I line spectrum the first negative nitrogen bands appear in the arc stream. They extend for some distance outside the central core but not quite as far as the CN bands The following heads were identified —

Group II —λλ 4708, 4651, 4599, 4554
Group III —λλ 4278, 4236

Table IV — N I Lines in the Visible and Ultra-Violet

λ Morton and Pilkey	Int	λ Hardtke	Int	λ Arc stream	Int	Remarks
7468 4	(9)			7468 7	(6)	(Kiess) 7468 74
7442 4	(9)			7442 7	(5)	,, 42 56
7423 5	(7)			7424 1	(4)	,, 23 88
				6983 6	(2)*d*	New lines completing the $P' - 4P$ multiplet These with the next two below are about 2 A wide and the whole multiplet is displaced 1 6 A to the red
				6980 7	(2)*d*	
				6975 0	(0)*d*	
				6062 2	(1)*d*	
				6953 4	(2)*d*	
6945 18	(3)			6946 6	(3)*d*	
6926 70	(2)			6928 4	(2)*d*	
6874 27	(1)			Absent		
6733 33	(3)					Confused with broadened line below
6722 60	(5)			6724	(10)*dd*	18 A wide
6713 19	(1)*					
6708 81	(2)*?			6710	(3)*dd*	About 8 A wide
6706 21	(2)*?					
6656 53	(0)					
6653 46	(4)			6654 6	(8)*d*	$n^4D - 4^4P$ multiplet Lines about 5 A wide Average shift to red about 1 1 A
6646 52	(2)					
6644 97	(7)			6646 1	(8)*d*	
6636 94	(0)			6638 2	(3)*d*	
6626 98	(0)*			6628 0	(0)*d*	
6622 55	(00)			6623 5	(3)*d*	
6499 51	(1)			6485	(30)*dd*	All the lines composing the $n^4D - {}^4F$ multiplet confused into a diffuse band 25 A wide
6491 24	(1)					
6484 88	(8)					
6483 77	(4)					
6482 74	(9)					
6481 73	(3)					
6471 02	(0)			6472 5	(1)*d*	Remainder of $n^4D - {}^4D'$ multiplet omitted Average shift to red 1 7 A
6441 70	(5)			6443 7	(4)*d*	
6420 63	(2)			6422	(2)*d*	5 A wide Shift about 1 4 A
6285 79	(0)			6280	(1)*d*	15 A wide
6279 42	(1)*					
6275 43	(0)					
6272 93	(2)					
6075 79	(3)			6076 1	(0)*d*	4 A wide
6017 74	(1)			6020 8	(4)*d*	Shift 3 A
6008 49	(9)			6010 7	(10)*d*	5 A wide Shift 2 2 A
5909 46	(5)			6002 3	(4)*d*	5 A wide Shift 2 8 A
				5837	(2)*d*	4 A wide
5829 52	(2)	5832 0	(2)	5831 0	(2)*d*	4 A wide Shift 1 5 A
				5820	(2)*d*	6 A wide
5752 65	(2)			5754	(3)*dd*	Extends over about 40 A
5623 22	(3)	5623 5	(3)	5625 9	(4)*d*	Remainder of $n^4D - 5^4P$ multiplet omitted Only these two lines seen by Hardtke and in arc
5616 57	(4)	5617 0	(3)	5618 6	(4)*d*	
5564 38	(4)	5564 0	(6)	5566 7	(4)*d*	Shift 2 3 A
5563 84	(3)*d*.*			Absent		The two lines above and below this are often broadened into one diffuse band
5560 45	(4)	5559 5	(6)	5561 9	(4)*d*	Shift 1 4 A
5545 11	(0)	5544 0	(2)	5547 0	(0)*d*	Shift 1 9 A

Table IV—(continued)

λ Morton and Pilley	Int	λ Hardtke	Int	λ Arc stream	Int	Remarks
5378 45	(00)			5378 36	(2)	
5372 66	(1)*d*	5372 5	(3)	5372 61	(2)	
5367 28	(00)*	5366 5	(1)	5366 79	(2)	
5356 75	(3)	5357 0	(3)	5356 58	(3)	
5328 67	(5)	5330 0	(4)	5328 57	(4)	
5310 60	(00)*			5310 53	(1)	
5309 48	(00)	5309 0	(2)	5309 37	(2)	
5292 74	(00)	5292 5	(2)	5292 70	(3)	
5281 17	(1)	5282 0	(3)	5281 15	(3)	
		5182	(1)	5181 80	(2)	
		5170	(1)	5169 80	(2)	
4935 03	(9)	4935 5	(3)	4935 17	(6)*s*	
4914 92	(4)	4915 5	(2)	4914 80	(4)*s*	
4881 67	(2)			4881	(0)*d* ?	Doubtful line in arc
4753 17	(2)			4753 37	(1)	
4750 26	(2)			4750 37	(1)	
4742 87	(0)			4742 84	(1)	
4735 77	(1)			4735 50	(1)	
		4670 0	(5)	4669 99	(15)	
		4660 3	(3)	4660 61	(10)	
4494 68	(5)			4494 57	(1)	Confused with N band structure
4492 45	(5)*	4492 5	(2)	Absent?		,, ,,
		4485 5	(4)	4485 36	(3)	,, ,,
		4466 5	(5)	4466 31	(1)	
4358 29	(7)			4358 04	(2)	
4336 51	(4)	4337 0	(4)	4336 55	(3)*d*	
		4324 3	(2)	4324 17	(2)	
4317 72	(4)	4317 7	(4)	4317 77	(3)	
4313 11	(3)	4313 3	(1)	4313 09	(2)	
4305 46	(6)	4305 5	(5)	4305 67	(4)	
4284 91	(2)			Absent		
4282 20	(1)			,,		
4281 35	(2)			4281 04	(0)*s*	
4253 31	(3)			4253 36	(4)	
4230 36	(4)			4230 50	(4)	
4224 90	(2)*			4224 88	(5)	
4223 09	(5)	4223 0	(3)	4223 12	(10)	
		4215	(4)	4214 80	(1)*s*	
		4213	(3)	Absent		
		4193	(3)			
		4187	(2)			
		4180	(3)			
		4166	(8)			
4151 44	(9)	4151	(10)	4151 57	(5)*s*	
		4145	(7)	4143 65	(6)	
4137 58	(4)	4137	(6)	4137 78	(4)	
4113 92	(5)	4114	(1)	Absent		In CN band, but it should have been seen if it was of intensity > 1
		4112	(1)	,,		
4109 94	(10)	4110	(10)	4109 44	(15)*d*	Both lines appear displaced towards the violet
4099 96	(9)	4100	(7)	4099 55	(10)*d*	
4037 35	(3)			Absent		
4011 07	(4)	4012	(2)	4010 5	(2)*d*	
3999 98	(3)			4000 0	(2)*d*	
3957 19	(3)			Absent		
3952 18	(3)			,,		

Table IV—(continued)

λ Merton and Pilley	Int	λ Hardtke	Int	λ Arc stream	Int	Remarks
3868 95	(2)	Masked by CN band structure				
3834 20	(4)					
3830 39	(9)					
3822 00	(5)					
3818 19	(1)					
3681 14	(3)			Absent		
3650 13	(5)			,,		
3545 60	(2)	Masked by CN band structure				
3532 63	(2)					
3437 14	(2)			Absent		

(8) *Oxygen*

Tables V and VI give the O I lines which have been identified in the arc stream The first gives the series lines, the comparison wave-lengths and series designation being taken from Fowler's report It will be seen that the intensities of the lines fall off very rapidly throughout each series, so that, in general, only the first two members appear, although the first line may be very strong

Considerable broadening and displacements to the red occur in some series, as was found in the case of N I It will be seen that the lines belonging to the four series 1P — *m*S, 1P — *m*D, 1*p* — *ms*, and 1*p* — *md* are all very diffuse, their widths being between 4 and 10 A These also show displacements to the red of the order of 2 A The magnitude of the shift in the case of the 1P — *m*D series is, however, uncertain as only one very diffuse line was seen so that no accurate measurement could be made The two series 1S — 1P and 1*s* — 1*p*, on the other hand, are comparatively sharp, particularly 1*s* — 1*p* The unclassified line at λ 7157 36 recorded by Runge and Paschen* and others† is also sharp and always appears strongly in the arc stream

Several otherwise unidentified lines agree with some of the fainter lines given by Fowler‡ in a paper on the series classification of the O II spectrum These lines are given in Table VI Fowler states that in preparing his table care was taken to exclude lines due to stages of ionisation higher than the first, so that the possibility of some of them being due to O I is not excluded Now with the exception of λ 4705, which is a doubtful line in the arc stream, none of the strong lines in Fowler's table appear, nor do any of those belonging to his

---

* 'Ann d. Physik,' vol 61, p 641 (1897), and vol 27, p 562 (1908)

† Merrill Hopper and Keith, 'Astrophys J,' vol. 54, p 26 (1921)

‡ 'Roy Soc Proc,' A, vol 110, p 476 (1926)

Table V —O I Lines in the Arc Stream

λ Fowler's report	Int	Series designation (Fowler)	λ Arc stream	Int	Remarks
8446 38		1S – 1P	8447	(2)	
4368 30	(10)	1S – 2P	4368 32	(20)	
3692 44	(7)	1S – 3P	Absent		
7254 05	(2)	1P – 3S	7257	(1)*d*	6 A wide
6046 34	(7)*d*	1P – 4S	6048 2	(1)*d*	3 A wide
5554 94	(6)*d*	1P – 5S	Absent		
7002 22	(4)	1P – 3D	7003	(2)*dd*	8 A wide Wave length only approximate
5958 53	(6)*d*	1P – 4D	Absent		
7771 97	(10)	1*s* – 1*p*	7772	(5)	
7774 01	(8)				
7775 68	(6)		7775	(5)	
3947 33	(10)				
3947 51	(7)	1*s* – 2*p*	3947 18	(5)*s*	
3947 61	(4)				
6456 07	(9)				
6454 55	(7)	1*p* – 3*s*	6457	(15)*d*	6 A wide
6453 69	(6)				
5436 83	(8)				
5435 78	(6)	1*p* – 4*s*	5438 4	(3)*d*	4 A wide
5435 16	(5)				
6158 20	(10)				
6156 78	(8)	1*p* – 3*d*	6159	(20)*d*	4 A wide
6155 99	(7)				
5330 66	(10)				
5329 59	(7)	1*p* – 4*d*	5332	(3)*dd*	10 A wide Wave length only approximate
5328 98	(6)				
7952 22	(0)		7952	(3)	
7950 84	(1)				
7947 58	(2)		7948	(3)	
7481 27	(0)				
7479 23	(0)		7480	(1)	
7476 58	(1)		7477	(1)	
7157 36			7157 4	(4)*s*	Runge and Paschen

Table VI —Additional O I lines in the Arc Stream

λ Fowler	Int	λ Arc stream	Int	Remarks
4744 85	(0)	4744 68	(0)*s*	
4705 36	(8)	4705 42 ?	(0)	Doubtful
4443 05	(5)	4443 05	(1)	
4378 40	(3)*n*	4378 1	(1)*d*	2 A wide
4371 65	(2)*n*	4372 0	(2)*d*	”
4024 04	(1)*n*	4023 7	(2)*d*	4 A wide
3893 53	(2)	3893 2	(3)*d*	3 A wide
2883 78	(3)	2883 83	(3)	O I (Paschen)
2878 95	(2)	2878 98	(3)	
2190 66	(2)	2190 64	(2)	
2189 51	(1)	2189 52	(2)	
2148 50	(0)	2148 33	(2)	

O II series classification. Hence, since O II lines would not be expected to occur in the arc, it is probable that the lines given in Table VI are really due to O I It will be seen that the three lines marked *n* by Fowler all appear diffuse in the arc

(9) *Argon*

Several lines which appeared in the red were found to correspond to strong lines in the red spectrum of argon In order to confirm this, arrangements were made to direct a gentle stream of argon on to the arc stream Viewing the spectrum visually it was found that immediately the gas was turned on very gently the lines in question brightened up considerably On increasing the supply of gas practically the whole of the red spectrum appeared

Table VII gives the argon lines which normally appear when the arc is burnt in air All the lines are quite sharp

Table VII —Argon Lines in the Arc Stream

λ Arc stream	Int	λ Arc stream	Int
8115	(0)	7504 0	(1)
7725	(0)	7384 2	(0)
7635 2	(1)	7067 2	(2)
7514 8	(1)	6965 6	(2)

(10) *Hydrogen*

The first three lines of the Balmer series are always seen in the arc when burning normally in air Their breadth is considerable For example, with a current density of the order of 10 amperes per square millimetre of the negative stream, H_α appears roughly 25 A wide and H_β about 30 A. wide The width increases with the current density H_β appears reversed over a width of about 3 A

If a stream of hydrogen or coal gas is allowed to play gently on the negative stream, the widths of H_α, H_β and H_γ increase to roughly 65, 80 and 85 A. respectively

(11) *Unidentified Lines*

Table VIII gives 53 new lines found in the arc It is probable that they belong to either oxygen, nitrogen or carbon * They have all been found on more than one plate and, with one exception, noted in the table, none of these lines extends beyond the core of the arc stream Metallic lines and those belonging to band structures extend beyond the central core and so are easily distinguished, these have been eliminated from the table

---

* Work on the identification of these lines is now in progress. Seven of them, noted in the table, may correspond with some known N and O lines, but further work is needed to confirm this.

Some of the lines are very diffuse and have a similar appearance to the broadened O I and N I lines recorded above These may, therefore, be affected with similar displacements In the case of all those marked *d*, the possibility of a wave-length shift to the red of as much as 2 A must be allowed for

Table VIII —Unidentified Lines in Arc Stream

λ Arc stream	Int	Remarks
8338	(1)	Very approximate wave length
8018	(1)*d*	Very diffuse line which may include argon line 8014 8
7908	(1)*d*	Approximate wave length
7850	(1)*d*	Very diffuse Approximate wave length
7592	(1)	
7552	(2)	May be double ?
7118 5	(6)*d*	About 8 A wide (see Table 1)
6915 6	(2)	May be double ?
6794	(2)*d*	Several A wide
6760	(1)*d*.	,,
6672	(1)*d*	,,
6111	(0)*d*	About 10 A wide
6041 9	(0)	
5805 76	(1)	
5801 17	(2)	
5793 51	(3)	
5412 02	(2)*s*	
5401 41	(1)*s*	
5343 72	(1)	
5340 56	(0)	
5314 59	(0)	N ?
5304 9	(1)	
5204	(1)*d*	4 A wide
5187 10	(1)	
4812 84	(1)	
4738 73	(1)	
4705 42	(0)	See Table VI N ?
4678 70	(3)*s*	
4671 0	(5)	Difficult to see owing to strong N line at λ 4670 N ?
4663 37	(2)	
4652 04	(6)	
4476 4	(2)	
4474 16	(4)	
4459 2	(2)	
4452 4	(1)	Confused with N band O ?
4442 00	(1)	
4437 8	(1)	”
4426 9	(2)*d*	2 A wide
4392 42	(3)	N ?
4385 53	(2)	N ?
4356 3	(4)*d*	2 A wide N ?
4343 9	(2)	
4254 75	(4)	

Table VIII—(continued)

λ Arc stream	Int	Remarks
4107 9	(7)	Confused with CN band
3954 16	(0)	
3889 1	(2)	Confused with N band
3641 0	(2)	Band structure ? Extends outside core of arc stream
2993 35	(0)s	
2904 95	(3)	
2903 26	(3)	
2902 30	(1)	
2354 12	(1)	Confused with band lines
2353 22	(1)	,,

Summary

(1) A study of the spectra excited in high current carbon arcs in air has been made The positive carbons were cored with metallic salts which, under suitable conditions, allows the limiting current density of ordinary arcs to be exceeded

(2) As the current through such arcs is increased a bright central core develops in the arc stream In this core the spectra of C I, N I, O I, together with the Balmer series and the strongest lines of the red spectrum of argon, are excited The relative intensities of the C I and N I lines, which have previously only been found in special discharge tubes, are compared with those found in the arc stream Many differences occur The first negative nitrogen bands were also observed in the arc stream

(3) Over 50 new lines were found and are ascribed to either N I, O I or C I Five of these complete the N I quartet system multiplet 4P — P′ and two others belong to the 5P — P′ multiplet

(4) Certain N I and O I lines are found to be displaced by amounts in some cases exceeding 2 A. and at the same time to be very much broadened These effects are correlated with the series classifications when known

(5) The Swan bands are strongly excited close to and inside the positive crater but do not normally occur in the arc stream They show up faintly when a jet of hydrogen is directed on the arc and very brightly when the hydrogen is replaced by coal gas

(6) No lines which could be attributed to helium were found, contrary to the report by Bell and Bassett It is shown that the lines they observed were really prominent lines belonging to the C I, N I and O I spectra

In conclusion I should like to express my appreciation of the valuable advice given by Prof A Fowler and of his interest throughout the work. Also to acknowledge the very able assistance of Miss D E Yates in measuring the plates and of Mr J H Goodchild who operated the arc

DESCRIPTION OF PLATES 14, 15 AND 16

PLATE 14 —This shows three photographs of the arc with a CaF_2 core taken through different colour filters In A the filter mainly transmitted the band spectra due to calcium compounds It thus shows the large outer flame extending upwards from the crater The bright central core of the arc stream extending from the negative carbon is well seen In B the filter mainly transmitted the low temperature calcium lines but no bands It therefore shows the inner highly conducting flame The manner in which the arc stream plays upon it instead of directly on the positive carbon may be seen.

The third photograph, C, was taken through a dense filter which transmitted the Swan bands It shows the presence of a very intense small flame just above the crater This flame is due to the Swan spectrum alone

PLATES 15 AND 16.—These show the whole of the visible and parts of the ultra violet spectrum of the arc stream. The image of the arc was projected on the slit so that the bright core of the arc stream appears in the middle of the spectrum. It is only in this part that the C I, N I and O I lines appear The strongest of these, together with the new lines, are marked All those extending beyond the central part are either metallic lines of Ca, Fe, Mn, Ti, etc , or belong to bands

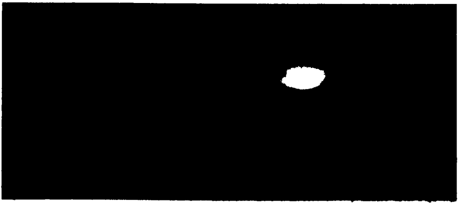

FIG C

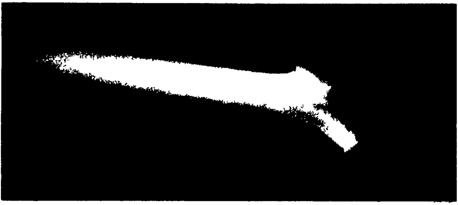

FIG B

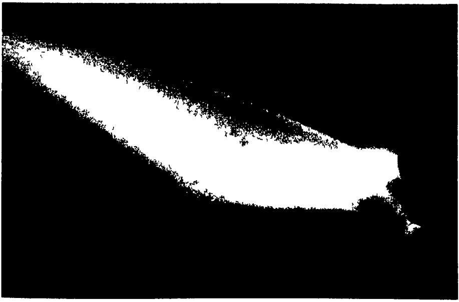

FIG A

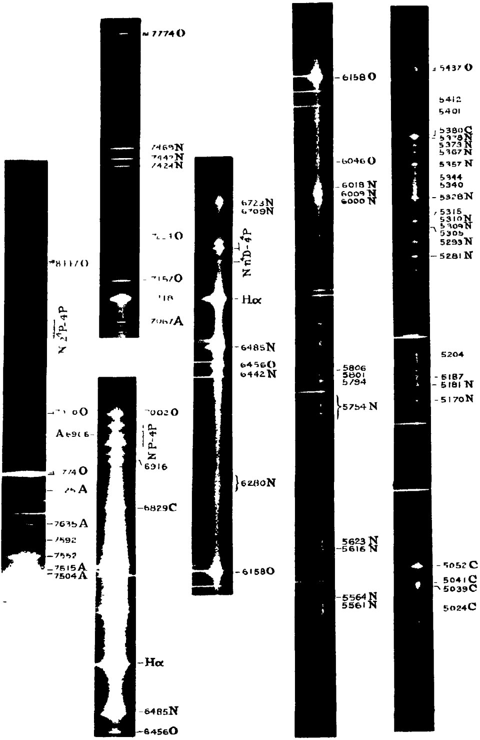

7774 O
7469 N
7442 N
7424 N
8117 O
O
7157 O
7067 A
N 2^4P-4P
O
A 6966
774 O
A
7635 A
7592
7552
7515 A
7504 A
7002 O
N P-4P
6916
6829 C
Hα
6485 N
6456 O
6723 N
6709 N
N n^4D-4P
Hα
6485 N
6456 O
6442 N
6280 N
6158 O
6158 O
6046 O
6018 N
6009 N
6000 N
5806
5801
5794
5754 N
5623 N
5616 N
5564 N
5561 N
5437 O
5412
5401
5380 C
5378 N
5373 N
5367 N
5357 N
5344
5340
5328 N
5315
5310 N
5309 N
5305
5293 N
5281 N
5204
5187
5181 N
5170 N
5052 C
5041 C
5039 C
5024 C

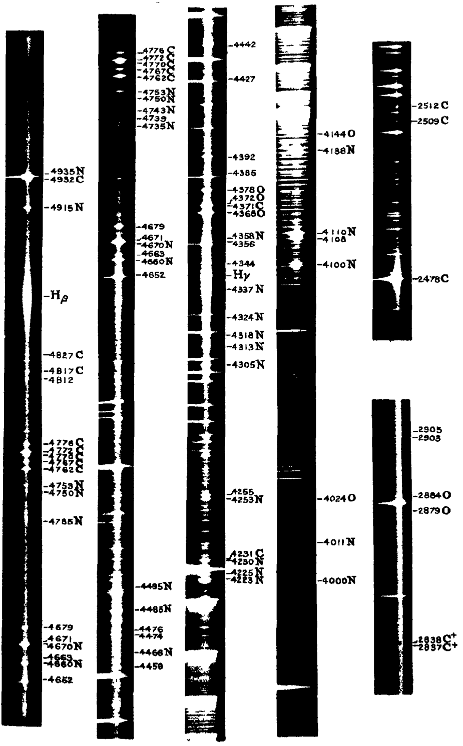

NOTE —The line λ 4144 above is due to N not O as quoted on block.

Studies of Gas-Solid Equilibria. Part I—Pressure-Temperature Equilibria between Benzene and (a) *Ferric Oxide Gel,* (b) *Silica Gel in Sealed Systems of Known and Unalterable Total Composition.*

By Bertram Lambert, M A, Fellow of Merton College, Oxford, and
Arthur M. Clark, B.A, Merton College, Oxford

(Communicated by F Soddy, F R S—Received August 11, 1927)

This work has been undertaken in order to provide more accurate and reliable data than are at present available for the examination of the theoretical aspects of gas-solid equilibria

The principles of experiment underlying the section of the investigation dealt with in Part I may be summarized as follows —

(i) An accurately known weight (*in vacuo*) of the "activated" gel, in the form of small granules, is introduced into an all-glass apparatus part of which consists of an evacuated mercury manometer

(ii) After very thorough evacuation of the system, an accurately known weight (*in vacuo*) of pure benzene is distilled into the apparatus and the system sealed.

(iii) The whole sealed system is then heated in a vapour bath to definite temperatures, within a range 30° to 130° C, and the equilibrium pressure for each temperature read off on the manometer, these pressures are corrected to express the absolute equilibrium pressures in centimetres of mercury at 0° C

(iv) A number of such sealed systems is prepared containing gradually increasing weights of benzene per gram of gel used. The equilibrium pressures of each system are investigated within the same temperature range and so, by plotting pressures against temperatures, a series of pressure-temperature curves is obtained for systems of different total composition

The conditions are the simplest possible—each system containing only a known weight of solid adsorbent, a known weight of pure benzene, and an evacuated manometer

The total composition of each sealed system is unalterable during the whole course of investigation, although there must be some alteration of the benzene-content of the solid phase as the temperature is raised or lowered, this point is dealt with later

(a) The Benzene-Ferric Oxide Gel Systems

Preparation of Adsorbent Ferric Oxide Gel

The ferric oxide gel was prepared and "activated" as follows —

An aqueous solution of caustic soda containing 8 per cent by weight of NaOH was slowly added to a well-stirred aqueous solution of ferric chloride containing 30 per cent by weight of $FeCl_3$ The precipitated ferric hydroxide hydrogel, after being left to stand for 12 hours, was washed free from soluble salts and filtered The filtered precipitate was extruded through a circular die of 6 mm diameter and the vermiform product dried in a current of air, at the ordinary room temperature, until no further shrinkage took place At this stage the product was hard and brittle, freshly fractured surfaces showed a brilliant lustre and the material was transparent when examined in thin flakes under the microscope Subsequent drying at 100° C, in a rapid current of air caused further shrinkage with loss of more water, and the product was then broken up into granules and sieved so as to obtain approximately uniform pieces The granules which were passed by a "20-mesh" sieve and retained by a "24-mesh" sieve were finally "activated" by heating in a current of dry air, at 170° C, until there was no further loss of weight The process of activation caused no alteration in the appearance of the material, which remained bright and lustrous

This method of preparation and "activation" produced a hard solid with strongly adsorptive properties, the adsorptive power for condensible vapours was of the same order as that of a good "active" cocoanut charcoal

Although prolonged subjection of the gel to a current of dry air at 170° C caused no further detectable loss of water, the material (considered as Fe_2O_3) still contained about 4 per cent of water which could, however, only be removed by heating to much higher temperatures, this resulted in a profound alteration in the gel and a complete destruction of its adsorptive power.

Weighing of Portions of Gel in vacuo

The apparatus used for this operation is shown in fig 1 It consisted of a glass bulb A of about 120 c c capacity closed by a long, accurately ground cap B to which was sealed a stopcock C A second ground joint D enabled connection to be made to a large drying tube containing phosphorus pentoxide, a large bulb containing active cocoanut charcoal and an automatic mercury pump

About 100 grams of the activated gel were placed in the bulb A which was then closed by the ground joint B, rubber grease being put only at the lower part of this ground joint Connection was now made to the mercury pump and the drying tube and charcoal bulb beyond the lubricated ground joint D All connections other than the lubricated ground joints were sealed glass connections

The apparatus was thoroughly evacuated while the bulb A was maintained at a temperature of 150° C by means of an air bath The heating and evacuation were continued until, after closing the stopcock C, detaching at D, washing the grease from D with ether, and weighing, a weight was obtained which remained unaltered after reassembling the apparatus and giving it a further spell of heating and evacuation This operation was carried out with the utmost care, from 70 to 100 hours' heating and evacuation being necessary before it was complete, and the gel underwent no further loss in weight In the last stages of the operation the evacuated tube, sealed into the system and containing 50 grams of active cocoanut charcoal, was cooled for several hours in liquid air so as to " freeze out " any residual gases

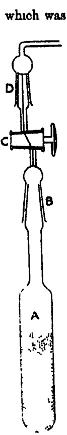

FIG 1

After the apparatus had reached a constant weight, the stopcock C was cautiously opened and dry air allowed to enter the bulb A The lubricated joint B was then carefully " unmade " and a quantity of the gel poured out into the tube in which it was to be used The joint B was now "remade" and the bulb A heated and evacuated as before until its weight was constant The difference in weight of the evacuated apparatus before and after the removal of the gel gave the exact weight (*in vacuo*) of the gel removed

These operations were repeated until ten accurately known weights of gel had been obtained and transferred to their respective reaction tubes

Very careful tests showed that the " unmaking " and " remaking " of the lubricated joint B could be carried out without the introduction of any appreciable error if the rubber grease was put only on the lower part of the joint

Construction of Evacuated Mercury Manometers

Each reaction tube containing an accurately known weight of gel was now to be sealed to an evacuated mercury manometer

Much difficulty was experienced in the production of absolutely reliable mercury manometers which could be submitted to temperatures ranging from 30° to 130° C, for long periods, without developing inaccuracies It was necessary to ensure the complete removal of air-films from the glass surfaces and dissolved air from the mercury, or tiny bubbles gradually formed in the closed limb of the manometer and the readings became unreliable

The design of the manometers is seen in fig 2, in which a manometer is shown attached to the reaction tube, etc The two limbs of the manometer were made of tubing of 5 mm bore, a capillary portion being sealed in at the U-bend so as to prevent the too-rapid movement of the mercury The closed limb was 80 cms in length, and it was fused to the open limb by means of a solid piece of glass rod This method of construction gave great stability, without any further support, and allowed of readings being taken along the whole length of the manometer limbs

The closed limb had to be cut for the purpose of cleaning and steaming the glass surfaces After re-sealing this limb, the open limb of the manometer was sealed to a bulb containing mercury and to a rapidly acting mercury vapour pump The whole apparatus was thoroughly evacuated and strongly heated for an hour, with a large flame, so as to remove adsorbed air from the glass surfaces and dissolved air from the mercury The mercury was then distilled into the manometer and, after cooling, air was allowed slowly to enter the open limb

This procedure resulted in the production of a most satisfactory and reliable manometer which gave readings identical with those of a standard barometer before and after use in these experiments

Ten such manometers were made for attachment to the ten gel tubes used

Introduction of accurately known Weights of Benzene into the Reaction Systems.

The experimental procedure in this important operation was evolved after many trials and may be summarized thus —

A weighed sealed tube, with a capillary point on which a scratch was made, and containing an approximately known quantity of benzene *in vacuo*, was opened by breaking off its capillary point in an evacuated tube sealed to the evacuated system containing manometer and known weight of gel The benzene was then distilled on to the gel by cooling the gel tube in a freezing mixture of solid carbon dioxide and ether, the reaction system being sealed off while the gel tube remained in the freezing mixture The empty benzene tube, with the broken-off capillary point and any glass splinters, was then carefully removed and weighed From the known weights of the full and empty tube, after making the necessary corrections for the displacement of air, the weight (*in vacuo*) of benzene introduced into the adsorption system could be determined with great accuracy

Fig 2 shows the apparatus used in this operation The known weight of gel was contained in the tube A sealed to the evacuated manometer B This system was sealed to the wide tube E as shown, constrictions being made at C and D for sealing-off purposes The wide tube E contained (resting in the side-branch F, with its capillary point projecting into E) a sealed tube, of accurately

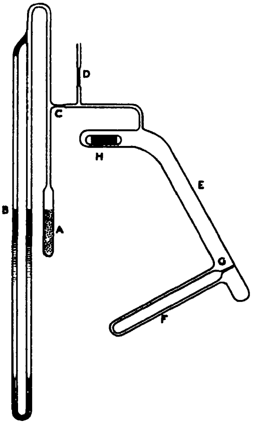

FIG 2

known weight, containing benzene *in vacuo*, this tube had a fine scratch made on the capillary at G Resting, as shown, in a horizontal extension of the wide tube E, was a "bullet" H made by sealing up a soft iron cylinder inside a silica tube Sealed connections were made beyond D to a large drying tube containing phosphorus pentoxide, a bulb containing 50 grams of active cocoanut charcoal and an automatic mercury pump

The whole sealed apparatus was thoroughly evacuated, while the tube A was surrounded by an air-bath heated to 150° C and the rest of the glass parts heated (from time to time) by a large flame After 60 to 70 hours' continuous evacuation, traces of residual gases were "frozen out" by immersing the bulb containing active charcoal in liquid air for several hours, the pump connections being then sealed off at D

The capillary point of the benzene tube was now broken off at G by causing the "bullet" (by means of an electromagnet) to fall on it Even before the gel tube was cooled the benzene vapour was so rapidly adsorbed by the gel that the benzene in F solidified, it then distilled on to the gel quite rapidly, and it was only necessary to cool the gel tube at the end of the operation, when the last traces of benzene vapour had to be made to enter the gel system At this stage the gel tube A was surrounded by a freezing mixture of solid carbon dioxide and ether, and after some hours—while A was still immersed in the freezing mixture—the gel system was sealed off at the constriction C

The wide tube E was opened and the empty benzene tube, with its broken-off point and any glass splinters, carefully removed and weighed The difference between the full and empty benzene tube (after making the necessary corrections for air displacement) gave the exact weight of benzene distilled on to the gel

A sealed glass system was thus obtained containing an accurately known weight of ferric oxide gel, an accurately known weight of benzene and an evacuated manometer

NOTE —In order to maintain the simplicity of the system, the benzene used was purified with great care Sulphur compounds were removed by the usual well-known methods and, after drying, the purified benzene was partially frozen and the solid removed from the liquid as completely as possible, this operation was repeated three times The product was then distilled in a sealed all-glass apparatus, the middle third only of the distillate being collected in a flask containing clean metallic sodium This flask was sealed into a system containing the tubes in which the final product was to be collected The system was thoroughly evacuated and the benzene was then distilled into the tubes, which were sealed off and weighed The tubes were calibrated so that the quantities of benzene contained in them was approximately known The exact weights of the contained benzene were determined as described above

The fact that the vapour-pressure curve of system X (see p 209) is identical with that of pure benzene, drawn from the results of Regnault and of Young, is evidence of the purity of the benzene used in these experiments as well as of the accuracy of the experimental methods used

Ten benzene-ferric oxide gel systems were prepared by the methods described above, the total composition of each of these systems is given in Table I below —

Table I

Number of system	Weight of gel in grams	Weight of benzene in grams	Grams of benzene per gram of gel
I	8 7780	0 2083	0 0237
II	7 4115	0 2821	0 0380
III	7 7292	0 5723	0 0740
IV	7 9587	0 7006	0 0922
V	7 0243	0 7942	0 1131
VI	7 1459	0 8507	0 1191
VII	5 3996	0 6747	0 1249
VIII	6 0441	0 8647	0 1431
IX	6 4154	1 1791	0 1839
X	7 2558	1 6473	0 2270

The equilibrium pressures of benzene vapour in these systems were determined at various known temperatures within a range of 30° to 130° C

Determination of Equilibrium Pressures at Known and Controlled Temperatures between 30° *and* 130° *C*

Each of the sealed systems was, in turn, placed in a vapour bath the temperature of which could be varied within a definite range and could be kept controlled —for long periods and throughout its whole length—to within ± 0 05° C of any desired temperature within its range After sufficient time had elapsed for a system to come to definite equilibrium at any one chosen temperature, the pressure of the benzene vapour was read off directly on the attached manometer by means of a cathetometer This pressure was then corrected and expressed as an actual pressure in centimetres of mercury at 0° C Each system was examined in this way and the equilibrium pressures determined for several known temperatures within the range 30° to 130° C

The construction of the constant temperature vapour bath is shown in fig 3 It consisted essentially of a glass tube A of length 120 cms and internal diameter 5 5 cms The lower end was closed and blown out into a bulb B to contain the liquid which was to be boiled The bulb was heated electrically by passing the "main" current through a nichrome resistance wire CC′ wound on a coating of asbestos fibre which was moulded round the bulb, a controlling rheostat was used in series with the heating wire A further thick coating of asbestos fibre was moulded on over the heating wire and the whole heating system lagged by packing with slag wool in a metal container

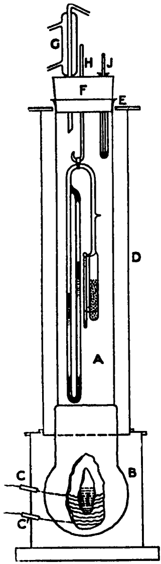

Fig 3.

The exposed outer glass surface of the vapour bath was protected by a cylindrical sleeve D of polished sheet aluminium which was provided, at back and front, with slits for illuminating and reading the manometer and thermometer The top of this sleeve was covered with a sheet of asbestos board E to minimise the effect of convection currents around the vapour bath

The open end of the tube A was closed by a bung F carrying a glass rod H, with hook, as shown, to support the sealed system under investigation The bung also carried an efficient condenser G and a closed glass tube in which was an accurate thermometer J with its bulb immersed in mercury, a second thermometer was attached to the gel tube as shown in the figure The thermometers were standardized instruments and could be read to 0 05° C

Constancy of temperature throughout the interior of the vapour bath was obtained by the steady boiling of a pure liquid at an accurately controlled pressure The pressure was controlled most successfully (with fluctuations of less than 0 01 mm of mercury, even over long periods) by means of a manostat made and used in the manner described by Wade and Merriman (' Jour Chem Soc Trans ,' vol 99, p 984 (1911)) The manostat was worked by means of a good water-pump, and the inevitable fluctuations in the latter were successfully overcome by the use of large air " buffers " and chokes of capillary tubing

Two separate vapour baths were used, one containing pure alcohol (for the range 30° to 70° C) and the other containing pure chlorbenzene (for the range 70° to 130° C) Steadiness of ebullition was obtained in the former by the addition of mercury, and in the latter by the addition of platinum tetrahedra

The equilibrium pressures determined for the ten systems are given, with the corresponding temperatures, in Table II below, and the results are plotted in Graph I Each curve in the graph is marked with the number of the system which it represents (Table I)

Table II

Number of system	Temperatures	Pressures in cms Hg at 0°
	°	
I	29 5	0 024
	48 8	0 077
	57 7	0 119
	68 35	0 237
	74 4	0 378
	80 4	0 527
	93 0	0 956
	102 8	1 487
	110 4	2 048
	115 0	2 425
	120 7	3 012
	131 9	4 421
II	27 35	0 093
	46 6	0 317
	55 25	0 463
	60 3	0 611
	81 7	1 731
	95 2	3 013
	106 7	4 724
	115 3	6 339
	132 25	10 951
III	25 15	0 722
	38 0	1 528
	47 7	2 489
	55 4	3 514
	61 2	4 551
	64 9	5 362
	70 7	6 795
	80 2	9 828
	86 75	12 552
	94 0	15 928
	°	
III (contd)	103 6	21 531
	109 7	25 705
	114 7	29 463
	121 5	34 925
	131 6	44 365
IV	29 4	1 630
	41 4	3 069
	54 7	5 500
	60 1	6 993
	65 85	8 836
	78 3	14 235
	91 25	22 485
	98 8	28 451
	107 7	37 325
	114 0	44 050
	122 70	54 950
	132 2	67 282
V	33 6	3 106
	40 2	4 298
	44 85	5 335
	52 6	7 509
	65 25	12 693
	73 0	17 221
	84 1	25 498
	91 5	32 371
	101 5	43 158
	105 8	49 607
	110 8	56 726
	115 8	64 387
	119 6	70 500

Table II—(continued)

Number of system	Temperatures	Pressures in cms Hg at 0°
	°	
VI	31 8	3 057
	47 1	6 410
	57 4	9 949
	63 4	12 618
	68 4	15 328
	81 5	24 875
	92 6	35 936
	100 0	44 803
	107 6	56 233
	113 5	64 718
VII	31 9	3 273
	43 9	5 917
	50 3	7 931
	56 2	10 099
	60 7	12 137
	65 0	14 407
	70 65	17 873
	78 0	23 928
	89 9	34 366
	98 6	44 550
	106 7	56 129
	112 5	64 927
	117 7	73 459
VIII	34 0	4 386
	46 1	7 792
	53 0	10 380
	58 4	12 993
	65 65	17 405
	73 4	23 926
	83 6	33 486
	92 3	44 491
	99 8	55 924
	107 3	67 939
IX	33 5	5 496
	45 7	9 742
	53 0	13 340
	58 2	16 546
	63 8	20 497
IX (contd)	71 25	27 203
	78 3	34 646
	90 5	53 502
	100 8	72 913
IX	(Repeated in reverse order)	
	95 3	64 390
	78 35	35 197
	57 75	16 108
	46 0	9 575
	39 3	7 149
X	31 6	12 781
	43 75	21 442
	50 2	27 433
	57 45	35 521
	64 65	45 856
	78 6	71 203

VAPOUR PRESSURES OF PURE BENZENE

Temperatures	Pressures (cms mercury at 0° C)	
	Young	Regnault
°		
20	7 466	7 565
30	11 824	12 024
40	18 108	18 362
50	26 897	27 137
60	38 858	39 010
70	54 740	54 742
80	75 362	75 186

In systems I to VIII the equilibrium pressures obtained for any one temperature were definitely repeatable to within ± 0 005 cm The same equilibrium pressure could be obtained for a particular temperature whether the system was brought to that temperature from a lower or from a higher temperature A system which had been left to stand at the ordinary room temperature for a period of several weeks showed, on re-investigation, exactly the same pressure-temperature relationships, the pressure-temperature curves I to VIII may therefore be said to be completely reversible

In system IX, where the quantity of benzene present approaches saturation value for the gel, the pressure-temperature curve was not quite reversible over

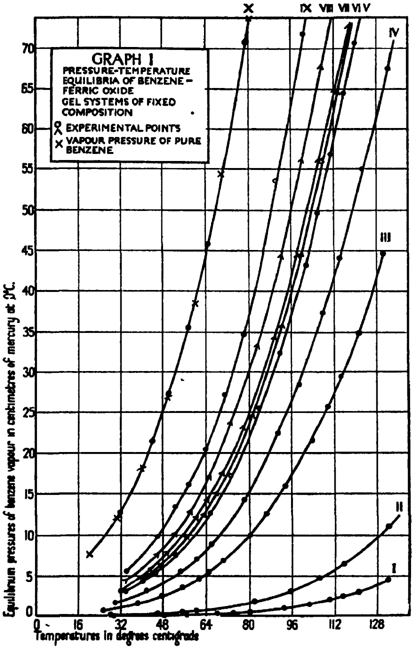

the upper temperature range In Table II above are given the equilibrium pressures obtained by approaching the particular equilibrium temperature from lower and from higher temperatures If curves be drawn from these points on a large-scale graph, the curves do not coincide over the upper temperature range, the departure from coincidence never reaches a value of 2 per cent, but it is real and certainly outside the limits of our experimental error although it cannot be shown on the small-scale Graph I

In system X the quantity of benzene present was more than sufficient to saturate the gel and the equilibrium pressures obtained with this system afford a very satisfactory proof of the accuracy of the experimental technique and of the purity of the gaseous phase In Table II above the values obtained for this system are given alongside the vapour pressures given for pure benzene by Young and by Regnault In Graph I these latter values (marked +) are plotted on the curve X along with our experimental values (marked 0)

(b) THE BENZENE-SILICA GEL SYSTEMS

A similar series of experiments was carried out using silica gel, as the solid adsorbent, in place of ferric-oxide gel The silica gel used was a commercial product—part of a sample obtained from The Silica Gel Corporation of America It was treated throughout in precisely the same way as the ferric oxide gel, and the experiments with the two gel adsorbents are definitely comparable

Eight benzene-silica gel systems were prepared by the methods described above, the total composition of each of these systems is given in Table III below --

Table III

Number of system	Composition Grams of benzene per gram of gel
I	0 0329
II	0 0487
III	0 0747
IV	0 1123
V	0 1312
VI	0 1367
VII	0 1494
VIII	0 1502

The equilibrium pressures determined for the eight systems are given, with the corresponding temperatures, in Table IV below, and the results are plotted in Graph II Each curve in the graph is marked with the number of the system which it represents (Table III)

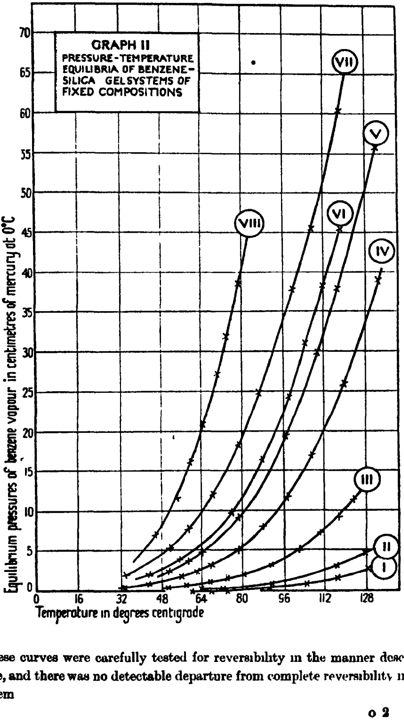

These curves were carefully tested for reversibility in the manner described above, and there was no detectable departure from complete reversibility in any of them

Table IV

Number of system	Temperatures	Pressures in cms Hg at 0°
I	61 4	0 139
	66 0	0 160
	73 8	0 204
	89 4	0 470
	105 1	0 901
	116 6	1 517
	128 6	2 479
II	47 1	0 119
	63 5	0 241
	70 4	0 318
	91 0	0 798
	116 5	2 961
	127 2	4 618
III	50 4	0 431
	57 9	0 658
	67 5	1 054
	73 8	1 490
	80 5	1 979
	91 0	3 095
	101 7	5 051
	110 5	7 104
	117 1	9 164
	122 9	11 348
IV	33 9	0 469
	43 45	0 847
	55 8	1 675
	62 1	2 338
	67 45	3 083
	78 35	5 096
	87 85	7 934
	97 7	11 765
	106 85	16 972
	119 2	25 941
	132 45	39 051
	°	
V	42 2	1 480
	51 05	2 406
	58 9	3 592
	64 15	4 722
	78 35	9 156
	96 9	19 352
	100 3	29 750
	117 2	37 858
	132 1	56 055
VI	31 6	0 980
	43 6	1 933
	55 1	3 888
	76 0	9 785
	87 5	16 407
	98 0	24 200
	104 9	30 919
	111 6	38 124
	118 7	45 654
VII	34 2	1 908
	51 65	5 240
	59 1	7 656
	68 6	11 909
	78 6	18 298
	86 55	24 685
	99 6	37 700
	107 3	45 508
	118 25	60 351
VIII	46 1	7 004
	54 35	11 677
	60 1	16 111
	64 95	20 871
	70 35	27 148
	73 85	31 915
	78 35	38 516

Pressure-Concentration Relationships "derived" from the Pressure-Temperature Curves

Graph III shows four pressure-concentration isothermals "derived" directly from the pressure-temperature curves of the ten benzene-ferric-oxide gel systems The isothermals are marked A, B, C, D, and they represent the pressure-concentration relationships between benzene and ferric-oxide gel at 40°, 60°, 80° and 100° C, respectively

The concentration of benzene per gram of gel, in each of the systems, has been taken as constant throughout the temperature range investigated, in conse-

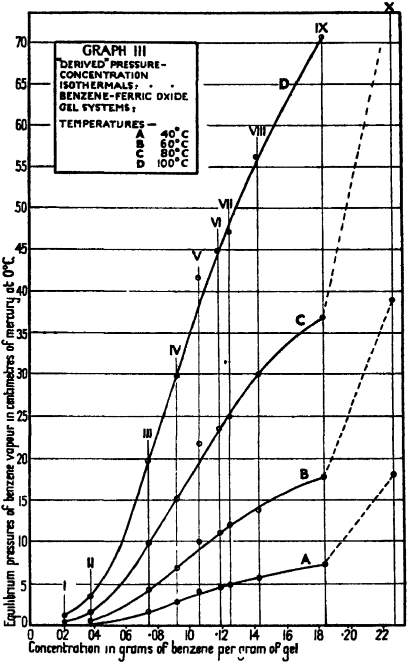

quence, the points on the isothermals "derived" from the ten systems lie on ten straight lines perpendicular to the concentration axis and cutting this axis at the total known benzene concentration for the different systems

These straight lines are marked, in the graph, with Roman numerals to correspond with the systems as designated in Tables I and II and in Graph I

In system X the pressure values are identical with those of pure benzene (*vide supra*)

Graph IV shows three pressure concentration isothermals "derived," in a precisely similar manner, from the pressure-temperature curves of the eight benzene-silica gel systems The isothermals are marked A, B, C, and they represent the pressure-concentration relationships between benzene and silica gel at 40°, 60°, and 80° C respectively

The numbering corresponds with the designation of the systems in Tables III and IV and in Graph II

Under IX are marked the pressure values for pure benzene

Isothermals "derived" in this way do not express the *exact* pressure-concentration relationships for the particular temperatures involved In our experimental investigation of the pressure-temperature relationships in a sealed system we are not dealing with a solid phase of absolutely constant composition When the temperature (and pressure) of such a system is raised, the solid phase must get progressively poorer in benzene by the passage of benzene from the solid to vapour phase In each system therefore the benzene vapour pressure registered at any point in the investigated temperature range must be in equilibrium with a solid phase poorer in benzene than a pressure registered at a lower temperature

Since the free internal volumes of the systems were small, and since there were no sudden changes in the compositions of the solid phases investigated, it was considered unlikely that the *shape* of the isothermals "derived" by this method would be appreciably affected by this error

On account of the very striking difference in shape between the isothermals "derived" for the two closely analogous systems it seemed desirable, however, to determine what the effect of this error was on the shape of the "derived" isothermals

The free internal volumes of two of the systems were therefore measured

NOTE —This was a lengthy and laborious operation Each system was opened at the point where it originally had been sealed up A fine-bore stopcock was sealed on at this opening and the system was thoroughly evacuated until all traces of benzene vapour had been removed This involved heating the gel tube to 150° C continuously for several days and nights and "freezing out" the benzene vapour on to active charcoal

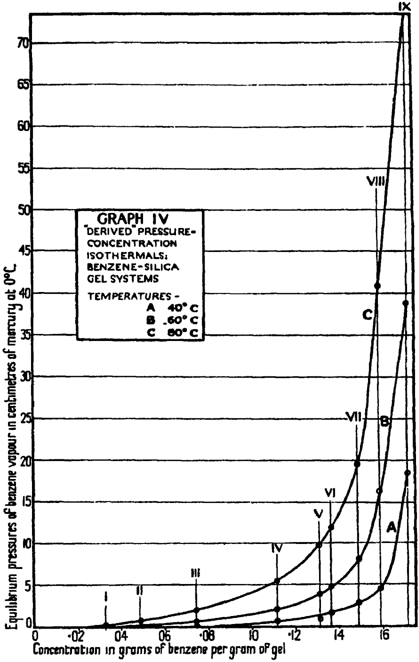

contained in bulbs immersed in liquid air When this lengthy process was complete, the stopcock was closed and the evacuated system sealed on to an accurate gas burette Pure, dry hydrogen was measured in

> the burette and then allowed to enter the evacuated system until this was filled to atmospheric pressure, when the volume of hydrogen required was read off Independent experiments had shown that the amount of hydrogen adsorbed by the gel, at the ordinary temperature, could be neglected without appreciable error The volume of the two systems could thus be determined with reasonable accuracy

The free internal volumes of the two systems were found to be 39 0 c c and 39 5 c c at atmospheric pressure The free internal volumes at other pressures were calculated from a knowledge of the internal diameter of the manometer limb Since the dimensions of all the systems were closely alike and an approximate measure of the free internal volumes was all that was required, the free internal volumes of all of them were taken to be the same

From this knowledge of the approximate free internal volumes of the systems, at all pressures, it was possible to calculate the weight of benzene in the vapour phase at any temperature and pressure, by deducting this weight from the known total weight of benzene in each of the systems, the concentration of benzene in the solid phase could be obtained for all temperatures and pressures investigated

Corrected isothermals could thus be constructed This was done, and it was found that the shapes of the corrected isothermals were not appreciably different from those " derived " as shown above and plotted in Graphs III and IV

> NOTE —It is interesting that the plotting of the logarithms of the uncorrected benzene pressures against the reciprocals of the absolute temperatures gave curves which lay closely on straight lines at low pressures, but showed deviations at high pressures—the curves tending to slope more steeply towards the log-pressure axis, when plotted from values obtained from corrected vapour-pressure curves, the logarithmic curves showed very little deviation from straight lines throughout their whole length

It would seem to be most probable, then, that the shapes of the adsorption isothermals for the benzene-ferric-oxide gel systems are markedly different from those of the closely analogous benzene-silica gel systems The adequacy of Zsigmondy's Capillary Theory to explain the adsorptive processes of inelastic gels would therefore seem to be very doubtful

It was felt, however, that a careful investigation of the relationships between these same gels and a condensible vapour should be carried out isothermally, and at several temperatures, if this striking difference between the two analogous adsorbents was to be settled beyond all doubt

Part II of this work deals with the direct isothermal investigation of the relationships between benzene and the same two gels, several temperatures have been studied and highly accurate conditions of experiment have been worked out The investigation is almost complete, and the results fully confirm the striking difference between the adsorptive processes of the two gels

The theoretical significance of the work will be discussed in Part II

Adjoint Differential Equations

By F B Pidduck

(Communicated by A E H Love, F R S —Received August 31, 1927)

1 That adjoint differential equations have an analogue in the theory of linear difference equations seems to have been first observed by Bortolotti [*] The relation is essentially that of a matrix $\|a_{rs}\|$ to its transposed matrix $\|a_{sr}\|$ It seems desirable, from this point of view, to carry out the transition from difference to differential equations, and thus prove that the analogy is a real one This is done in Art 2 There are further consequences of general interest A set of linear equations corresponds to a differential equation *and* its boundary conditions, and thus we can find an interpretation of the adjoint boundary conditions introduced by Birkhoff[†] into the theory of linear differential equations (Arts 3–6) The relation between the two Green's functions, implicit in Birkhoff's work, then becomes evident (Art 7)

2 We first prove that if the equations

$$a_{r1}y_1 + a_{r2}y_2 + \quad + a_{rn}y_n = f_r \quad (r = 1 \text{ to } n) \tag{1}$$

are so constituted that they merge into the differential equation

$$\mathrm{L}(y) \equiv a_m \frac{d^m y}{dx^m} + \quad + a_1 \frac{dy}{dx} + a_0 y = f \tag{2}$$

by passing to an infinite number of infinitesimally spaced unknowns, the transposed equations

$$a_{1r}z_1 + a_{2r}z_2 + \quad + a_{nr}z_n = g_r \tag{3}$$

merge into the adjoint equation

$$\mathrm{M}(z) \equiv (-)^m \frac{d^m}{dx^m}(a_m z) + \quad - \frac{d}{dx}(a_1 z) + a_0 z = g \tag{4}$$

---

[*] 'Acc Linc Rend,' vol 5, Sem 1, p 349 (1896)

[†] 'Trans Amer Math Soc,' vol 9, p 373 (1908)

The domain of x can be considered to extend from $x = 0$ to $x = 1$ without loss of generality Let y_r be the value of y when $x = x_r = r/n$, and let f_r, g_r be the values of f and g It will be convenient to work so that the differential coefficients which appear in the limit of equations (1) are backward coefficients, and those which appear in the limit of (3) forward coefficients Then the first m of equations (1) correspond to boundary conditions and the remaining $n - m$ to the differential equation Confining our attention to the latter, let us replace equation (2) by a set of linear equations connecting $y_{r-m}, \ldots, y_{r-1}, y_r$ Write E for the operator which moves a suffix back by one unit, D for the difference operator which merges into a backward differential operator d/dx Then, since $\mathrm{E} = 1 - \mathrm{D}/n$, we have the usual formulæ

$$y_{r-p} = \sum_{s=0}^{p} (-)^s \, {}_p\mathrm{C}_s \frac{y^{(s)}}{n^s} \quad (p = 0 \text{ to } m), \tag{5}$$

where $y^{(s)}$ stands in the first instance for $\mathrm{D}^s y_r$, and

$$\frac{y^{(q)}}{n^q} = \sum_{p=0}^{q} (-)^p \, {}_q\mathrm{C}_p \, y_{r-p} \quad (q = 0 \text{ to } m) \tag{6}$$

The typical equation corresponding to (2) is now

$$\sum_{p=0}^{m} \sum_{q=0}^{m} (-)^p \, n^q \, {}_q\mathrm{C}_p \, y_{r-p} \, (a_q)_r = f_r,$$

where $(a_q)_r$ is the value of $a_q(x)$ when $x = x_r$ and ${}_q\mathrm{C}_p$ is taken as zero when $p > q$ Thus

$$a_{r\ r-p} = \sum_{q=0}^{m} (-)^p \, n^q \, {}_q\mathrm{C}_p \, (a_q)_r \tag{7}$$

Let D_1 stand for the difference operator which merges into a forward differential operator acting only on the a's, D_2 for a similar operator acting only on z, the variable in the transposed equations Changing r into $r + p$ in (7), we have

$$a_{r+p\ r} = \sum_{q=0}^{m} (-)^p \, n^q \, {}_q\mathrm{C}_p \left(1 + \frac{\mathrm{D}_1}{n}\right)^p a_q$$

The linear form on the left-hand side of (3) is now

$$\sum_{p=0}^{m} a_{r+p\ r} \, z_{r+p} = \sum_{p=0}^{m} \sum_{q=0}^{m} (-)^p \, n^q \, {}_q\mathrm{C}_p \left(1 + \frac{\mathrm{D}_1}{n}\right)^p a_q \left(1 + \frac{\mathrm{D}_2}{n}\right)^p z$$

$$= \sum_{p=0}^{m} \sum_{q=0}^{m} (-)^p \, n^q \, {}_q\mathrm{C}_p \left(1 + \frac{\mathrm{D}_1 + \mathrm{D}_2}{n} + \frac{\mathrm{D}_1 \mathrm{D}_2}{n^2}\right)^p (a_q z)$$

Writing ξ for $\mathrm{D}_1 + \mathrm{D}_2 + \mathrm{D}_1 \mathrm{D}_2 / n$, the linear form is

$$\sum_{q=0}^{m} n^q \sum_{p=0}^{m} (-)^p \, {}_q\mathrm{C}_p \left(1 + \frac{\xi}{n}\right)^p (a_q z) = \sum_{q=0}^{m} (-)^q \, \xi^q \, (a_q z),$$

and ξ merges into the total differential operator d/dx when n becomes infinite Hence the transposed form becomes simply

$$\sum_{q=0}^{m} (-)^{q} \frac{d^{q}}{dx^{q}}(a_{q}z),$$

as it should

3 The theory of the boundary conditions will be explained first for the case $m = 3$, of which the matrix is laid out below, taking $n = 8$ for simplicity

$$\begin{array}{cccccccc|}
a_{11} & & & & & a_{16} & a_{17} & a_{18} \\
a_{21} & a_{22} & & & & a_{26} & a_{27} & a_{28} \\
a_{31} & a_{32} & a_{33} & & & a_{36} & a_{37} & a_{38} \\
a_{41} & a_{42} & a_{43} & a_{44} & & & & \\
 & a_{52} & a_{53} & a_{54} & a_{55} & & & \\
 & & a_{63} & a_{64} & a_{65} & a_{66} & & \\
 & & & a_{74} & a_{75} & a_{76} & a_{77} & \\
 & & & & a_{85} & a_{86} & a_{87} & a_{88}
\end{array} \qquad (8)$$

The method consists essentially in reducing the first three untransposed equations, which correspond to boundary conditions, to the special form shown above, in which the first square contains no elements to the right of its main diagonal Suppose, for simplicity, that the differential and adjoint equations, and the given boundary conditions, are homogeneous The latter are, in the first instance, three linear equations connecting $y(0)$, $y^{(1)}(0)$, $y^{(2)}(0)$, $y(1)$, $y^{(1)}(1)$, $y^{(2)}(1)$, which are transformed by difference formulæ into

$$c_{r1}y_1 + c_{r2}y_2 + c_{r3}y_3 + d_{r1}y_6 + d_{r2}y_7 + d_{r3}y_8 = 0,$$

where $r = 1, 2, 3$ The nine elements c_{rs} can be replaced, by linear combination of the equations, by nine arbitrary elements Let three of them be put zero as above, the others remaining arbitrary for the moment

Consider the transposed equations, represented by the columns of the matrix (8) We proved in Art 2 that the middle set of $n - 2m$ equations, represented here merely by columns 4 and 5, merge into the adjoint differential equation when n becomes infinite We now adjust the six surviving elements in the first square of the matrix until the equations represented by columns 1, 2 and 3 also merge into the adjoint equation When this has been done, the *last three columns* yield three linear equations having an obvious analogy with those derived from the *first three rows* A glance at the matrix shows the nature of the symmetry at which we have been aiming the first three untransposed equations are boundary conditions and the last five differential equations, while the first five transposed equations are differential equations and the last three boundary conditions These latter equations are combined linearly in a way which is explained in Art 4, the terms of highest order of magnitude are extracted, and the equations merge into three "adjoint" boundary conditions, or linear equations connecting $z\,(0)$, $z^{(1)}\,(0)$, $z^{(2)}\,(0)$, $z\,(1)$, $z^{(1)}\,(1)$, $z^{(2)}\,(1)$, for the adjoint differential equation

4 To carry out the process in detail, let the given boundary conditions be

$$\sum_{s=1}^{m} \alpha_{rs}\, y^{(s-1)}\,(0) + \sum_{s=1}^{m} \alpha_{rs}'\, y^{(s-1)}\,(1) = 0,$$

or in matrix notation

$$\alpha u + \alpha' u' = 0, \tag{9}$$

where α and α' are the matrices of coefficients just written down, u is an m-dimensional vector whose rth component is $y^{(r-1)}\,(0)$ and u' an m-dimensional vector whose rth component is $y^{(r-1)}\,(1)$ Let y be an m-dimensional vector whose rth component is y_r, and y' one whose rth component is y_{n-m+r} Then the conversion formulæ

$$y_r = \sum_{s=1}^{m} {}_{r-1}\mathrm{C}_{s-1} \frac{y^{(s-1)}\,(0)}{n^{s-1}}, \qquad y_r' = \sum_{s=1}^{m} (-)^{s-1}\, {}_{m-r}\mathrm{C}_{s-1} \frac{y^{(s-1)}\,(1)}{n^{s-1}}$$

can be written $y = \mathrm{A}u$, $y' = \mathrm{A}'u'$, where A and A′ are matrices of order m defined by the equations

$$\mathrm{A} = \left\| {}_{r-1}\mathrm{C}_{s-1} \frac{1}{n^{s-1}} \right\|, \qquad \mathrm{A}' = \left\| (-)^{s-1}\, {}_{m-r}\mathrm{C}_{s-1} \frac{1}{n^{s-1}} \right\| \tag{10}$$

Let a_t denote the matrix in the first square of (8), a suffix t denoting transposition of rows and columns The elements of this matrix are calculated from equation (7), and each $(a_q)_r$ is expressed in terms of $(a_q)_0$ by a difference operator, so as to be ready to pass over into $a_q\,(0)$ and its derivates Thus

$$a = \left\| \sum_{q=0}^{m} (-)^{s-r}\, {}_{q}\mathrm{C}_{s-r}\, n^{q} \left(1 + \frac{\mathrm{D}_1}{n}\right)^{s-1} a_q\,(0) \right\|. \tag{11}$$

The matrix in the last square of (8) is similarly a_t', where

$$a' = \left\| \sum_{q=0}^{m} (-)^{s-r}\, {}_{q}\mathrm{C}_{s-r}\, n^{q} \left(1 - \frac{\mathrm{D}_1}{n}\right)^{m-s} a_q\,(1) \right\| \tag{12}$$

Operating on the boundary conditions $\alpha A^{-1} y + \alpha' A'^{-1} y' = 0$ with $a_t A \alpha^{-1}$, we have $a_t y + a_t A \alpha^{-1} \alpha' A'^{-1} y' = 0$. This is the process of adjustment referred to in Art. 3, whereby the first m transposed equations are made ready to merge into the adjoint equation. The matrix in the second square of (8) (i.e. the square which is filled up completely) has in consequence become $a_t A \alpha^{-1} \alpha' A'^{-1}$, and its transposed matrix is $A_t'^{-1} \alpha_t' \alpha_t^{-1} A_t a$. The last m transposed equations are therefore summarised in the vector equation $A_t'^{-1} \alpha_t' \alpha_t^{-1} A_t a z + a' z' = 0$. Let v be an m-dimensional vector whose rth component is $z^{(r-1)}(0)$, and v' one whose rth component is $z^{(r-1)}(1)$. Then $z = Av$, $z' = A'v'$. Substituting we have the last m transposed equations in the form

$$\alpha_t^{-1} A_t a A v + \alpha_t'^{-1} A_t' a' A' v' = 0, \tag{13}$$

in which we have so far taken no step towards passing to the limit. The rth component of the vector aAv is

$$(aAv)_r = \sum_{s=1}^{m} \sum_{k=1}^{m} a_{rk} A_{ks} v_s = \sum_{s=1}^{m} \sum_{k=1}^{m} a_{rk} A_{ks} D_k^{s-1} z(0)$$

Substituting for a_{rk} and A_{ks} from (11) and (10) and summing with respect to s, we have

$$(aAv)_r = \sum_{q=0}^{m} \sum_{k=1}^{m} (-)^{k-r} {}_qC_{k-r} n^q \left(1 + \frac{\xi}{n}\right)^{k-1} [a_q(0) z(0)] \tag{14}$$

where $\xi \equiv D_1 + D_2 + D_1 D_2/n$ as before. The rth component of the vector $a'A'v'$ is similarly

$$(a'A'v')_r = \sum_{q=0}^{m} \sum_{k=1}^{m} (-)^{k-r} {}_qC_{k-r} n^q \left(1 - \frac{\eta}{n}\right)^{m-k} [a_q(1) z(1)] \tag{15}$$

where $\eta \equiv D_1 + D_2 - D_1 D_2/n$.

5. The problem of finding the limit of the vectors $A_t a A v$ and $A_t' a' A' v'$ being difficult in general, we consider only the case $m = 2$, that is, the differential equation

$$a_2(x) \frac{d^2 y}{dx^2} + a_1(x) \frac{dy}{dx} + a_0(x) y = 0 \tag{16}$$

with boundary conditions

$$\left.\begin{aligned} \alpha_{11} y(0) + \alpha_{12} y^{(1)}(0) + \alpha_{11}' y(1) + \alpha_{12}' y^{(1)}(1) = 0 \\ \alpha_{21} y(0) + \alpha_{22} y^{(1)}(0) + \alpha_{21}' y(1) + \alpha_{22}' y^{(1)}(1) = 0 \end{aligned}\right\} \tag{17}$$

Keeping only terms of order n^2 and n, we find from (14) and (15)

$$(aAv)_1 = -n^2 a_2(0) z(0) - 2n a_2(0) z^{(1)}(0) - 2n a_2^{(1)}(0) z(0),$$

$$(aAv)_2 = n^2 a_2(0) z(0) + n a_2(0) z^{(1)}(0) + n a_2^{(1)}(0) z(0) + n a_1(0) z(0),$$

$$(a'A'v')_1 = -n^2 a_2(1) z(1) - n a_2(1) z^{(1)}(1) - n a_2^{(1)}(1) z(1),$$

$$(a'A'v')_2 = n^2 a_2(1) z(1) + n a_1(1) z(1)$$

Since

$$A_t = \begin{Vmatrix} 1 & 1 \\ 0 & 1/n \end{Vmatrix}, \qquad A_t' = \begin{Vmatrix} 1 & 1 \\ -1/n & 0 \end{Vmatrix},$$

we have to terms of order n

$$(A_t a A v)_1 = -n a_2(0)\, z^{(1)}(0) - n\,(a_2^{(1)}(0) - a_1(0))\, z(0),$$
$$(A_t a A v)_2 = n a_2(0)\, z(0),$$
$$(A_t' a' A' v')_1 = -n a_2(1)\, z^{(1)}(1) - n\,(a_2^{(1)}(1) - a_1(1))\, z(1),$$
$$(A_t' a' A' v')_2 = n a_2(1)\, z(1)$$

Thus in the limit the components of $A_t a A v$ can be taken to be

$$a_2(0)\, z^{(1)}(0) + (a_2^{(1)}(0) - a_1(0))\, z(0), \qquad -a_2(0)\, z(0),$$

and the components of $A_t' a' A' v'$ to be

$$a_2(1)\, z^{(1)}(1) + (a_2^{(1)}(1) - a_1(1))\, z(1), \qquad -a_2(1)\, z(1)$$

It follows from (13) that the boundary conditions adjoint to (17) are

$$\left.\begin{aligned} &(\alpha_{11}\alpha_{22} - \alpha_{12}\alpha_{21})^{-1}\,[\alpha_{22}\{a_2(0)\, z^{(1)}(0) + (a_2^{(1)}(0) - a_1(0))\, z(0)\} \\ &\qquad\qquad + \alpha_{21} a_2(0)\, z(0)] \\ &+ (\alpha_{11}'\alpha_{22}' - \alpha_{12}'\alpha_{21}')^{-1}\,[\alpha_{22}'\{a_2(1)\, z^{(1)}(1) + (a_2^{(1)}(1) - a_1(1))\, z(1)\} \\ &\qquad\qquad + \alpha_{21}' a_2(1)\, z(1)] = 0, \\ &(\alpha_{11}\alpha_{22} - \alpha_{12}\alpha_{21})^{-1}\,[\alpha_{12}\{a_2(0)\, z^{(1)}(0) + (a_2^{(1)}(0) - a_1(0))\, z(0)\} \\ &\qquad\qquad + \alpha_{11} a_2(0)\, z(0)] \\ &+ (\alpha_{11}'\alpha_{22}' - \alpha_{12}'\alpha_{21}')^{-1}\,[\alpha_{12}'\{a_2(1)\, z^{(1)}(1) + (a_2^{(1)}(1) - a_1(1))\, z(1)\} \\ &\qquad\qquad + \alpha_{11}' a_2(1)\, z(1)] = 0 \end{aligned}\right\} \quad (18)$$

Making

$$\alpha_{21}, \alpha_{22} \to 0, \quad \alpha_{11} = -h_0, \quad \alpha_{12} = 1,$$
$$\alpha_{11}', \alpha_{12}' \to 0, \quad \alpha_{21}' = h_1, \quad \alpha_{22}' = 1,$$

we have, corresponding to the boundary conditions

$$\frac{dy}{dx} = h_0 y \text{ at } x = 0, \quad \frac{dy}{dx} + h_1 y = 0 \text{ at } x = 1$$

of equation (16), the adjoint boundary conditions

$$\frac{dz}{dx} = k_0 z \quad \text{at} \quad x = 0, \ \frac{dz}{dx} + k_1 z = 0 \quad \text{at} \quad x = 1,$$

where

$$k_0 = h_0 - \frac{a_2^{(1)}(0) - a_1(0)}{a_2(0)}, \qquad k_1 = h_1 + \frac{a_2^{(1)}(1) - a_1(1)}{a_2(1)}$$

6 That the foregoing boundary conditions are identical with Birkhoff's is probable in advance, since Birkhoff's conditions are constructed to make

$$\int_0^1 \{z\mathrm{L}(y) - y\mathrm{M}(z)\}\,dx \equiv [\mathrm{P}(y, z)]_0^1 = 0,$$

the analogue of the simple identity $\zeta\Phi\eta - \eta\Phi_t\zeta = 0$, where η, ζ are any two vectors and Φ is any matrix The notation is one that we shall use later, $\zeta\Phi\eta$ standing for the scalar product of ζ and $\Phi\eta$, which is the same as the scalar product of $\zeta\Phi$ (or $\Phi_t\zeta$) and η in Gibbs' dyadic notation Birkhoff's rule is as follows Let $[\mathrm{P}(y, z)]_0^1$ be expressed in the form $\sum_{r=1}^{2m} \mathrm{V}_r(y)\,\mathrm{W}_{2m+1-r}(z)$, where $\mathrm{V}_1(y) = 0 \quad \mathrm{V}_m(y) = 0$ are the given boundary conditions and $\mathrm{V}_{m+1}(y), \quad \mathrm{V}_{2m}(y)$ are m other linearly independent forms of the same type The adjoint boundary conditions are then $\mathrm{W}_1(z) = 0, \quad \mathrm{W}_m(z) = 0$ Towards carrying out this rule, we observe that

$$[\mathrm{P}(y, z)]_0^1 = u'\Theta v' - u\Theta v, \tag{19}$$

where the vectors u, v, u', v' are defined in Art 4, and Θ is a known matrix Let the functions $\mathrm{V}_1(y), \quad \mathrm{V}_m(y)$ be regarded as before as the components of a vector $\alpha u + \alpha' u'$, the functions $\mathrm{V}_{m+1}(y), \quad \mathrm{V}_{2m}(y)$ as components of $\beta u + \beta' u'$, the functions $\mathrm{W}_{2m}(z), \quad \mathrm{W}_{m+1}(z)$ as components of $\gamma v + \gamma' v'$ and the functions $\mathrm{W}_m(z), \quad \mathrm{W}_1(z)$ as components of $\delta v + \delta' v'$ We have to determine the matrices δ, δ' so as to make

$$[\mathrm{P}(y, z)]_0^1 = (\alpha u + \alpha' u')(\gamma v + \gamma' v') + (\beta u + \beta' u')(\delta v + \delta' v'),$$

where the products are scalar products In dyadic notation

$$[\mathrm{P}(y, z)]_0^1 = (u\alpha_t + u'\alpha_t')(\gamma v + \gamma' v') + (u\beta_t + u'\beta_t')(\delta v + \delta' v')$$

Hence from (19), since the products are associative,

$$\alpha_t\gamma + \beta_t\delta = -\Theta, \qquad \alpha_t\gamma' + \beta_t\delta' = 0,$$
$$\alpha_t'\gamma + \beta_t'\delta = 0, \qquad \alpha_t'\gamma' + \beta_t'\delta' = \Theta$$

Eliminating γ and γ', we have

$$(\alpha_t^{-1}\beta_t - \alpha_t'^{-1}\beta_t')\,\delta = -\alpha_t^{-1}\Theta, \qquad (\alpha_t^{-1}\beta_t - \alpha_t'^{-1}\beta_t')\,\delta' = -\alpha_t'^{-1}\Theta$$

The adjoint boundary conditions given by Birkhoff's rule are therefore

$$\alpha_t^{-1}\Theta v + \alpha_t'^{-1}\Theta v' = 0 \tag{20}$$

In the case $m = 2$ we find at once that Θv has components

$$a_2(0)\, z^{(1)}(0) + (a_2^{(1)}(0) - a_1(0))\, z(0), \qquad -a_2(0)\, z(0),$$

and $\Theta v'$ has components

$$a_2(1)\, z^{(1)}(1) + (a_2^{(1)}(1) - a_1(1))\, z(1), \quad -a_2(1)\, z(1)$$

These are the expressions already found for the limits of the vectors $A_t a A v$ and $A_t' a' A' v'$ Hence the two methods agree I refrained from working out Birkhoff's rule before completing the theory of Arts 3-5, from curiosity as to whether the limiting process would prove sufficiently powerful to dispense with hints from other sources

7 The relation between the two Green's functions is now almost intuitive Returning to equations (1), let $\|k_{rs}\|$ be $-n$ times the matrix reciprocal to $\|a_{rs}\|$ Then the solution of equations (1) is

$$y_r = -\frac{1}{n}(k_{r1} f_1 + k_{r2} f_2 + \qquad + k_{rn} f_n)$$

As $n \to \infty$, r/n and s/n tending to the argument x and parameter ξ respectively, $\|k_{rs}\|$ tends to Green's function $K(x, \xi)$, and the equation just written down becomes

$$y = -\int_0^1 K(x, \xi) f(\xi)\, d\xi$$

Since the transposed matrix of $\|k_{rs}\|$ is $\|k_{sr}\|$, Green's function of the adjoint equation, with adjoint boundary conditions, is $K(\xi, x)$

The Refractive Index of Quartz

By Dr W R C Coode-Adams

(Communicated by Prof T M Lowry, F R S —Received September 26, 1927)

The recent publication of a new series of values for the optical rotatory power of quartz, and of a new formula for its rotatory dispersion (Lowry and Coode-Adams, 'Phil Trans,' A, vol 226, pp 391–466 (1927)), has provided an opportunity for reconsidering the formula for the refractive dispersion of the crystal Prior to the appearance of this paper, the characteristic frequencies which provide the dispersion-constants in Drude's equation for optical rotatory power had always been deduced by indirect methods Thus, the characteristic infra-red frequencies were taken (Lowry, 'Phil, Trans,' A, vol 212, pp 261–297 (1912)) from the observations of Rubens and Nichols,* who determined the wave-lengths (at 8 5 μ, 9 02 μ and 20 75 μ) at which the crystal behaves as a metallic reflector and gives rise to strongly marked "Reststrahlen" The ultra-violet frequencies in Drude's formula (which were also used in the 1912 paper cited above) were deduced, on the other hand, from the data for the refractive dispersion of the crystal, but although it was clear that *two* characteristic frequencies in the distant ultra-violet region must be taken into account, their magnitudes were so ill-defined that it was only possible to give a numerical value to one of them, the other being provisionally located at infinity, since a zero value was assigned to λ_q^2 In the 1927 paper, however, in order to express the numerical data with sufficient accuracy, it was found necessary to abandon finally the frequencies deduced by Drude from the other optical properties of quartz, and to work out new and independent values from the rotations themselves Moreover, with the help of these new data it was possible not only to correct the "known" constant of Drude's equation from $\lambda^2 =$ 0 010627 to 0 01275, but also to assign a finite value to his "unknown" ultra-violet constant, the value of which was changed from $\lambda^2 = 0$ to 0 00097 The infra-red frequency, on the other hand, although its influence could not be entirely neglected, was of such small importance that its magnitude remained wholly indeterminate, even with the help of a new series of measurements of the rotatory power of the crystal in the infra-red to $\lambda = 2\ 5\ \mu$.

The object of the present paper is to show how, reversing the process used by Drude, a new formula for the refractive index of quartz can be arrived at

---

[*] 'Ann d Physik,' vol. 60, p 418 (1897), and 'Phil. Mag.,' vol. 20, p 886 (1910)

by making use of the ultra-violet frequencies calculated from the optical rotations The degree of accuracy of these constants is still uncertain, and it is impossible to say to what extent they may be modified by further observations at shorter wave-lengths , but they are at least of a much higher order of accuracy than any of the numbers available previously, since the more accessible of the two constants, which has been increased by about 20 per cent from its former value, is now correct within a limit which may perhaps be estimated at about 1 per cent , whereas the other, which was formerly quite unknown, is now perhaps correct within about 5 per cent

On the experimental side, the measurements in the visible and ultra-violet regions, made by Gifford in 1902 (' Roy Soc Proc ,' vol 70, p 329 (1902)) to six places of decimals, provide a most valuable series of data for checking the formula, but the full exploitation of these data has only recently been rendered possible by the introduction of trustworthy wave-lengths, based upon measurements with the interferometer

Apart from Cauchy's formula

$$n = \mathrm{A} + \frac{\mathrm{B}}{\lambda^2} + \frac{\mathrm{C}}{\lambda^4} +, \text{ etc} \tag{1}$$

(which has no theoretical basis or interest, except the use of the *square* of the wave-lengths instead of the wave-lengths themselves), the only equations that come into consideration are Sellmeier's equation

$$n^2 = 1 + \Sigma \frac{\mathrm{D}^2}{\lambda^2 - \lambda_m{}^2}, \tag{2}$$

which represents the excess of n^2 above unity as a hyperbolic function of λ^2 (just like a simple rotatory dispersion), and the Ketteler-Helmholtz equation

$$n^2 = n_\infty^2 + \Sigma \frac{\mathrm{M}_m}{\lambda^2 - \lambda_m{}^2}, \tag{3}$$

which represents the excess of n^2 above its value at infinite wave-length, as the sum of a number of terms of similar type In the latter equation λ_m is the wave-length corresponding to the natural frequency of an electron and M_m is a refraction-constant that goes with it, whilst n_∞^2 should be equal to the specific inductive capacity of the medium

The most accurate evolution of the constants for quartz in a formula of this type is due to Rubens (R Wood, ' Physical Optics,' p 391), who expressed his own measurements of n by the equation

$$n^2 = 2{\cdot}35681 + 0\ 010654/(\lambda^2 - 0\ 010627) - 0\ 01113\ \lambda^2 - 0\ 0001023\ \lambda^4$$

We can, however, now make further progress by introducing into the formula

$$n^2 = n_\infty^2 + \frac{M_1}{\lambda^2 - \lambda_1^2} + \frac{M_2}{\lambda^2 - \lambda_2^2},$$

the dispersion constants of the equation for the optical rotatory power of quartz

$$\lambda_1^2 = 0\ 0127493\ \mu^2 \text{ or } \lambda_1 = 1130 \text{ Å U}$$
$$\lambda_1^2 = 0\ 000974\ \mu^2 \text{ or } \lambda_2 = 310 \text{ Å U}$$

The values of λ_1^2 and λ_2^2 are here quoted in the precise form in which they were left by the final adjustment of the equation to fit the optical rotations, but the values of λ_1 and λ_2 have been rounded off to 10 Å U as a rough guess at their approximate accuracy The resulting equation contains three arbitrary constants, namely, M_1, M_2 and n^2 These can be evaluated by inserting three of the experimental values for n, and solving the three resulting simultaneous equations They thus lead to the equation

$$n^2 = 2\ 347696 + \frac{0\ 004207}{\lambda^2 - 0\ 012749} + \frac{0\ 00810}{\lambda^2 - 0\ 000974}$$

A series of eight values of n, calculated from this equation, are shown in comparison with the corresponding experimental values in Table I It will be seen that ± differences are given at three points, corresponding with the number of arbitrary constants in the equation, but that the curve follows a sinuous course, with regular + and − differences between the ± values It is therefore clear that one more arbitrary constant must be used to make the equation fit the data, and this can be supplied, just as in the case of optical rotations, by introducing an infra-red term with a known dispersion-constant, $\lambda_3 = 10\ 4$, $\lambda_3^2 = 108$ (taken from R W Wood's 'Physical Optics,' p 391, where it is used as a weighted mean of the three frequencies cited above), and an arbitrary refraction-constant, the value of which was found, by solving

Table I —Refractive Index of Quartz, First Formula

Wave length	Observed	Calculated	Difference
7685 23	1 53906	1 53906	—
6563 04	1 54193	1 54162	+0 00031
5892 948	1 54426	1 54388	+0 00038
4340 66	1 55398	1 55398	—
3302 80	1 56974	1 57044	−0 00070
2748 71	1 58753	1 58848	−0 00095
2312 98	1 61403	1 61403	—
2265 11	1 61820	1 61793	+0 00027

the equation, to be $M_3 = 127\ 2$ Table II shows a series of 18 values of n calculated from the equation --

$$n^2 = 3\ 53445 + \frac{0\ 008067}{\lambda^2 - 0\ 0127493} + \frac{0\ 002682}{\lambda^2 - 0\ 000974} + \frac{127\ 2}{\lambda^2 - 108}$$

Table II – Refractive Index of Quartz, Second Formula

Wave length	Observed	Calculated	Difference
7950 46 Rb	1 53851	1 53851	—
7685 23 K	1 53906	1 53906	–
7065 20 He	1 54050	1 54051	–0 00001
6563 04 H	1 54193	1 53193	—
5892 948 Na	1 54426	1 54426	—
5270 36 Fe	1 54718	1 54718	—
4861 49 H	1 54970	1 54967	+0 00003
4340 66 H	1 55398	1 55398	—
3961 68 Al	1 55824	1 55824	—
3610 66 Cd	1 56347	1 56350	–0 00003
3302 80 Zn	1 56974	1 56974	—
3034 21 Sn	1 57699	1 57697	+0 00002
2748 71 Cd	1 58753	1 58754	–0 00001
2573 10 Cd	1 59625	1 59624	+0 00001
2312 98 Cd	1 61404	1 61403	+0 00001
2265 11 Cd	1 61820	1 61820	
2194 60 Cd	1 62499	1 62505	–0 00006
2144 35 Cd	1 63047	1 63050	–0 00003

in comparison with the experimental values of Gifford for the ordinary ray in dextro-quartz The wave-lengths cited by Gifford have been altered where later measurements have introduced appreciable corrections, and the last readings in the ultra-violet have been omitted on account of the doubt which still exists as to the correct wave-lengths in a region where a change of 0 1 Å U already introduces an error in the fifth decimal of the refractive index Reference to the table shows that the calculated and observed readings agree absolutely to the fifth decimal place in 9 cases out of 18, and that the average error of all the values is only 0 00001, moreover, there is no indication of anything systematic in the distribution of the positive and negative differences

The validity of the equation in the near infra red can be tested by using the data of Cavallo ('Comptes Rendus,' vol 126, p 728 (1898)), which are set out in Table III to five decimals, and the data of Rubens and Nichols ('Ann d Physik,' vol 60, p 418 (1897)) for longer infra red wave-lengths, which are set out in Table IV to four decimals The differences in Table II are all negative, and amount on the average to — 0·00008, but since Gifford's value for the rubidium line Rb 7950 46 shows a ± difference at a wave-length which differs only by 57 Å U. from the first reading of Cavallo's table, it is not unlikely that a systematic error of this magnitude is present in his refractions (or a corre-

Table III —Refractive Index of Quartz in the Infra-Red (Cavallo's Values)

Wave length	Observed	Calculated	Difference
8007	1 53834	1 53840	−0 00006
8325	1 53773	1 53779	−0 00006
8671	1 53712	1 53717	−0 00005
9047	1 53649	1 53655	−0 00006
9460	1 53583	1 53590	−0 00007
9914	1 53514	1 53522	−0 00008
10973	1 53366	1 53375	−0 00009
12288	1 53192	1 53204	−0 00012
13070	1 53090	1 53104	−0 00014

Table IV - Refractive Index of Quartz in the Infra-Red (Rubens and Nichols' Values)

Wave length	Observed	Calculated	Difference
μ			
1 617	1 5271	1 52695	+0 0001
1 969	1 5216	1 52171	−0 0001
2 32	1 5156	1 51555	±
2 60	1 5090	1 50981	+0 0001
2 86	1 5039	1 50382	+0 0001
3 06	1 4985	1 49866	−0 0002
3 21	1 4942	1 49452	−0 0003
3 42	1 4877	1 48812	−0 0004
3 67	1 4790	1 47985	0 0008
3 84	1 4739	1 47347	+0 0004
4 01	1 4678	1 46674	+0 0011
4 15	1 4619	1 46079	+0 0011
4 26	1 4567	1 45585	+0 0008

sponding error in the wave lengths) used by him This conclusion is confirmed by the fact that the differences in Table IV, which covers a much larger range of wave-lengths, are irregular in sign, although considerably larger in magnitude (0 0004 on the average), as might perhaps be expected in a region where the wave-lengths themselves are only recorded to three significant figures We therefore conclude that the new formula, which fits Gifford's data for the visible and ultra-violet regions with a degree of accuracy that has never been attained hitherto, also provides an adequate representation of the most trustworthy data for the infra-red This satisfactory agreement is also a valuable confirmation of the trustworthiness of the dispersion-constants of the equation used to express the rotatory dispersion of quartz

The constant term 3 53445 in the new formula should be equal to the specific inductive capacity of quartz This is given by Thornton as 3 78 and by Schulze as 3 20 for $\lambda = 75$ cm

On the Temperature Factors of X-Ray Reflexion for Sodium and Chlorine in the Rock-Salt Crystal

By IVAR WALLER, Ph D , and R W JAMES, M A

(Communicated by W L Bragg, F R S —Received October 4, 1927)

1 The influence of temperature on the intensity of reflexion of X-rays by crystals was first dealt with theoretically by Debye,[*] and later by Waller,[†] each of whom based their work on the dynamical theory of crystal lattices due to Born and Kármán Measurements of the temperature coefficient for rock-salt at high temperatures have been made by James,[‡] and at the temperature of liquid air by James and Miss Firth [§] In their paper, the latter compare the observed intensities, both at high and low temperatures, with those predicted by Waller's theoretical treatment, and find, for temperatures up to about 500° Abs , a substantial agreement, although throughout that range the diminution of intensity with temperature is rather less rapid than theory indicates Above 500° Abs , the observed rate of decrease of intensity is much greater than the theoretical rate

In making the comparison with theory several simplifying assumptions were made which were equivalent to assuming the lattice to consist of only one kind of atom Now the work of Waller on crystals containing more than one kind of atom shows that it is necessary to consider a separate temperature coefficient for each type

Suppose that F_1 and F_2 are the average atomic scattering factors, at a given angle, for chlorine and sodium respectively at absolute zero, then the amplitude factor at a temperature T, for spectra where the waves scattered by the chlorine and sodium atoms are in phase will be $F_1e^{-M_1} + F_2e^{-M_2}$, and for spectra where they are out of phase $F_1e^{-M_1} - F_2e^{-M_2}$, M_1 and M_2 being functions of T, and θ the angle of scattering, which will in general differ for the two atoms In comparing experiment with theory, it was assumed that the structure-amplitude for the summation spectra could be written $(F_1 + F_2)e^{-M}$, which experiment showed to be very nearly true, and the value of M was evaluated from the Debye-Waller theory, treating the rock-salt lattice as a simple cubic lattice composed of atoms of one kind, whose mass was the mean of those of chlorine and sodium. It was pointed out that the assumption of a single value of M was evidently not permissible, since this would lead to the same temperature factor for both sum and difference spectra The observed factor is, however, always smaller for the difference spectra, which might well be the case if M_1 were not equal to M_2 Moreover, in the calculation of M, the characteristic temperature of the crystal was used, which for crystals containing more than one kind of atom is hardly justifiable, and it would be better to use a formula depending on the elastic constants It therefore appears to be desirable to consider the whole matter in greater detail

---

[*] 'Ann d Physik,' vol 43, p 29 (1914)

[†] 'Z f Physik,' vol 17, p 398 (1923) Uppsala Univ Årsskrift, 1925 , 'Ann d Physik vol 83, p 153 (1927)

[‡] 'Phil Mag ,' vol. 49, p 585 (1925)

[§] 'Roy Soc Proc ,' A. *supra*, p 64

2 Although the formula for the general case of a crystal with many kinds of atom has been worked out, it is not possible, owing to our lack of knowledge of the nature of the interatomic forces, to calculate the values of M with any certainty It is, however, possible to calculate a certain mean value of the temperature coefficient which can be compared with experiment, and also to obtain some information about the individual values of M

For a lattice having cubic symmetry of the NaCl type we have

$$M_\kappa = 8\pi^2 \sin^2\theta \quad \overline{u^2_{\kappa x}}/\lambda^2, \tag{1}$$

where $\overline{u^2_{\kappa x}}$ is the mean of the squares of the displacements in any arbitrary direction x, of atoms of the type κ, from their mean positions For values of the temperature sufficiently high (approximately $T > \Theta/2\pi$, where Θ is the characteristic temperature) we may write*

$$\overline{u^2_{\kappa x}} = \alpha_\kappa + \beta_\kappa T + \gamma_\kappa/T + \delta_\kappa/T^3 + \tag{2}$$

In this expression

$$\gamma_\kappa = \frac{1}{12 m_\kappa}\left(\frac{h}{2\pi}\right)^2 \frac{1}{k},$$

where m_κ is the mass of the atom, h is Planck's constant and k is the Boltzmann gas constant γ_κ therefore does not depend on the atomic forces, and can be calculated directly δ_κ depends on the atomic forces, but can be estimated with sufficient accuracy, since the term containing it is very small. If zero-point energy having Planck's value be assumed, α_κ is equal to zero

β_κ cannot be calculated directly, but the following "weighted mean,"

$$\bar{\beta} = \frac{\Sigma m_\kappa \beta_\kappa}{\Sigma m_\kappa},$$

can be determined with some degree of accuracy from the elastic constants

---

* This result follows directly from the formulæ on p 21 *et seq* in the Uppsala Universitets Årsskrift (Waller)

We shall now proceed to calculate β for sodium and chlorine from the experimental results, in order to compare the weighted mean of the values so obtained with that calculated from the values of the elastic constants of rock-salt

3 At a given temperature, say T_a, we can determine from the intensity measurements $(F_1e^{-M_1} + F_2e^{-M_2})_a$ and $(F_1e^{-M_1} - F_2e^{-M_2})_a$, as functions of the glancing angle of reflexion θ By plotting these quantities against $\sin\theta$ and taking half the sum and half the difference of corresponding ordinates of the two curves, we can obtain $(F_1e^{-M_1})_a$ and $(F_2e^{-M_2})_a$ These are the quantities usually referred to as the values of F for chlorine and sodium at the temperatures concerned If the measurements are repeated for a second temperature, T_b, we can obtain in the same way $(F_1e^{-M_1})_b$ and $(F_2e^{-M_2})_b$ From the ratio of the corresponding quantities at the two temperatures, and at corresponding glancing angles, $(M_1)_a - (M_1)_b$ and $(M_2)_a - (M_2)_b$ follow at once

From equations (1) and (2), we have

$$\frac{\lambda^2}{8\pi^2 \sin^2\theta}\{(M_\kappa)_a - (M_\kappa)_b\} = \beta_\kappa (T_a - T_b) + \gamma_\kappa\left(\frac{1}{T_a} - \frac{1}{T_b}\right) + \delta_\kappa\left(\frac{1}{T_a^3} - \frac{1}{T_b^3}\right) + \qquad (4)$$

For a given pair of temperatures, T_a and T_b, $\{(M_\kappa)_a - (M_\kappa)_b\}\,\lambda^2/\sin^2\theta$ should be a constant for all values of θ for each kind of atom If this quantity is determined from experiments at two known temperatures, β_κ can be calculated from equation (4), since all the other quantities which occur in the equation are known

In the experiments of James and Miss Firth, measurements were made at room temperature and at the temperature of liquid air Only four difference spectra were measured at both temperatures, (331), (333), (511) and (555), corresponding to only three separate glancing angles The values of $(M_\kappa)_a - (M_\kappa)_b$ can therefore only be determined for these three angles Table I gives the values of Fe^{-M} for 290° Abs and 86° Abs

In column (5) are tabulated the differences in M divided by the sum of the squares of the indices of the spectra These quantities should be constant, since $\sin^2\theta/\lambda^2 = (h^2 + k^2 + l^2)/4a^2$, where a is the spacing of the unit cell It will be seen that the variation is not large considering the data on which the numbers are based, and we can take the figures as showing that the value of M is different for the two atoms and that it varies as $(\sin\theta/\lambda)^2$ for each

5 Using the mean values of $\{(M_\kappa)_{290} - (M_\kappa)_{86}\}/(h^2 + k^2 + l^2)$, we may now calculate the value of β_κ for each atom from equation (4) For chlorine, we

Table I

$h^2 + k^2 + l^2$	$(F_1 e^{-M_1})_{86}$	$(F_1 e^{-M_1})_{290}$	$(M_1)_{290} - (M_1)_{86}$	$\frac{(M_1)_{290} - (M_1)_{86}}{h^2 + k^2 + l^2}$
		I(*a*)—Chlorine		
19	7 26	6 44	0 119	0 00628
27	6 45	5 39	0 180	0 00667
75	3 71	2 40	0 436	0 00581
				Mean 0 00625
		I(*b*)—Sodium		
19	4 69	4 09	0 137	0 00721
27	3 79	3 09	0 204	0 00757
75	1 58	0 87	0 597	0 00795
				Mean 0 00758

have $m_1 = 5\ 85\ \ 10^{-23}$ gm, and for sodium $m_2 = 3\ 80\ \ 10^{-23}$ gm From (3), therefore, $\gamma_1 = 1\ 130\ \ 10^{-17}$, $\gamma_2 = 1\ 744\ \ 10^{-17}$ An estimate of δ gives with sufficient accuracy a value $-1\ 1\ \ 10^{-14}$ Substituting these values in equation (4), putting $T_a = 290°$, $T_b = 86°$ and $(\lambda/\sin\theta)^2 = 4a^2/(h^2 + k^2 + l^2)$, where $a = 5\ 628\ \ 10^{-8}$ cm, we obtain, for chlorine $\beta_1 = 5\ 31\ \ 10^{-21}$, and for sodium $\beta_2 = 6\ 56\ \ 10^{-21}$

6 We may now compare these results with theory For a crystal of the rock-salt type, it can be shown* that the following formula is approximately true —

$$\bar{\beta} = \frac{m_1\beta_1 + m_2\beta_2}{m_1 + m_2}$$

$$= \frac{k}{12(m_1 + m_2)}\left\{\frac{\sqrt[3]{3\pi^2}}{\pi^2}\,\rho a^2\,\frac{c_{44}(2c_{11} + c_{44}) + \frac{1}{5}b_1(c_{11} + c_{12})}{c_{11}c_{44}^2 + \frac{1}{5}b_1(c_{11} + c_{12})c_{44} + \frac{1}{125}b_1^2 b_2} + \frac{3}{\pi\nu_0^2}\right\} \tag{5}$$

Here $b_1 = c_{11} - c_{12} - 2c_{44}$, $b_2 = c_{11} + 2c_{12} + c_{44}$, and c_{11}, c_{12}, c_{44} are the elastic constants of the crystal in the notation of Voigt From Voigt's values for rock-salt we put $c_{11} = 4\ 650\ \ 10^{11}$, $c_{12} = 1\ 294\ \ 10^{11}$, $c_{44} = 1\ 270 . 10^{11}$ $\nu_0 = c/\lambda_0$, the proper frequency corresponding to the residual rays Using the dispersion formula of Maclaurin,† Havelock‡ has calculated the value 61 9 μ

---

* The deduction of this formula will be given shortly in another paper

† 'Roy Soc Proc,' A, vol 81, p 367 (1908)

‡ 'Roy Soc Proc,' A, vol 105, p 488 (1924)

for λ_0 Taking ρ, the density of rock-salt as 2 17, and a the length of the cube edge of the lattice unit as 5 628 Å we find,

$$\bar{\beta} = (m_1\beta_1 + m_2\beta_2)/(m_1 + m_2) = \underline{5\ 7\ \ 10^{-21}}\ \text{(calculated from the elastic constants)}$$

The values of β_1 and β_2 calculated from the experimental results are 5 31 10^{-21} and 6 56 10^{-21} respectively This gives

$$\bar{\beta} = \frac{(5\ 85 \times 5\ 31 + 3\ 80 \times 6\ 56)\ \ 10^{-21}}{5\ 85 + 3\ 80} = \underline{5\ 8\ \ 10^{-21}}\ \text{(calculated from X-ray results)}$$

The agreement between theory and experiment is thus very close, indeed closer than could reasonably have been expected from the method of calculation, and may well be partly accidental

7 From the values of β for the two atoms we can calculate the values of M for any temperature, assuming Planck's value of the zero-point energy, so that $\alpha = 0$ For a temperature T we get, neglecting the term involving δ, which is very small even at the temperature of liquid air, and which becomes rapidly smaller as the temperature increases,

$$M_{Cl}/(h^2 + k^2 + l^2) = \frac{2\pi^2}{a^2}\left\{5\ 31\ \ 10^{-5}\,T + \frac{1\ 131\ \ 10^{-3}}{T}\right\}, \tag{6}$$

$$M_{Na}/(h^2 + k^2 + l^2) = \frac{2\pi^2}{a^2}\left\{6\ 56\ \ 10^{-5}\,T + \frac{1\ 744\ \ 10^{-3}}{T}\right\}, \tag{6A}$$

where a is the length of the unit cube edge in Angstrom units *

Substituting these values in equation (1) we may now calculate the value of $\overline{u^2_{\kappa x}}$ for either atom at any temperature at which the expansion (2) is valid. This gives for chlorine at 290° Abs, $\overline{u^2_{1x}} = 0\ 0158\ \ 10^{-16}$ cm^2 and for sodium $\overline{u^2_{2x}} = 0\ 0196\ \ 10^{-16}$ cm^2

If $\overline{u_\kappa^2}$ is the mean of the square of the total displacement of an atom, we have for a crystal of the rock-salt type

$$\overline{u^2_\kappa} = 3\overline{u^2_{\kappa x}}.$$

Hence we obtain $\sqrt{\overline{u^2_{Cl}}} = 0\ 217$ Å and $\sqrt{\overline{u^2_{Na}}} = 0\ 242$ Å James and Miss Firth, from the change in electron distribution in the crystal with temperature, calculated in a direct way from their experimental results using the method of Fourier analysis introduced by Duane, find for the mean amplitude of vibration

---

* In making these calculations, the small change in a due to thermal expansion is neglected throughout

at 290° Abs, 0 20 Å for chlorine, and 0 23 Å for sodium The agreement is satisfactory, but is rather closer than would have been expected, for their method is equivalent to supposing absence of zero-point energy The difference is, however, in the right direction

The results show quite definitely that the mean amplitude of the sodium atoms is greater than that of the chlorine atoms This is due mainly to the difference in the coefficient β for the two atoms It should be pointed out that this difference is not due to the different masses of the two atoms, since it may be proved* that if the same forces act on both, β should be the same for each We may, therefore, draw the conclusion that the forces acting on the two kinds of atom are not equal, and that the chlorine atoms are, to speak somewhat vaguely, more firmly bound than the sodium atoms

8 Assuming as before the existence of zero-point energy, we can calculate the values of F_{Cl} and F_{Na} corresponding to absence of all vibrational energy To do this, we calculate M for sodium and chlorine at 86° and 290° and multiply the figures given in Table III of the experimental paper for F_{Na} and F_{Cl} at those temperatures, by the appropriate values of e^M This gives two curves for F_{Cl} and two for F_{Na} for the atoms at rest The pairs of curves should, of course, coincide if the figures are consistent In fig 1 the points indicated by circles were calculated from the values at 290°, and those by crosses from the values at 86° It is satisfactory to find that the two sets of curves agree, for no difference spectra of order higher than (555) could be measured at room temperature, and the values of these spectra for high orders at 290° were calculated from those measured at 86°, using a value of the temperature factor estimated from the lower orders From the fact that the curves agree over the whole range, we may assume that no great error was introduced in this way

The dotted curves in fig 1 were plotted from the values of F at absolute zero given by James and Miss Firth The method used by them to reduce the experimental results to absolute zero, although not entirely satisfactory, since the separate M's were not calculated, is very nearly equivalent to assuming absence of zero-point energy The figure thus gives some idea of the difference between the F curves calculated assuming presence or absence of such energy In Table II the values of F from which the curves were constructed are given

---

* Waller, *loc cit*, p 30

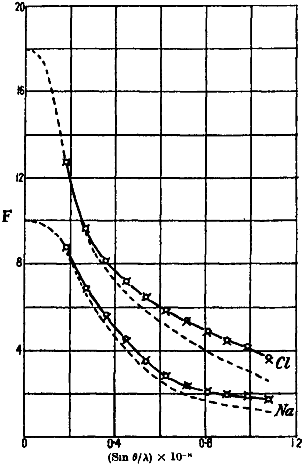

Fig 1

Table II -Values of F for Na and Cl for Absence of Vibrational Energy of the Atoms

sin $\theta/\lambda \times 10^{8}$	Assuming Planck's zero point energy		Approximate values assuming absence of zero point energy (James and Miss Firth)	
	F_{Cl}	F_{Na}	F_{Cl}	F_{Na}
0 180	12 75	8 78	12 64	8 65
0 270	9 63	6 88	9 44	6 64
0 359	8 16	5 63	7 84	5 25
0 449	7 20	4 50	6 75	4 06
0 539	6 48	3 50	5 88	3 11
0 629	5 84	2 82	5 21	2 44
0 719	5 36	2 38	4 55	1 96
0 808	4 86	2 08	3 96	1 64
0 898	4 46	1 93	3 46	1 45
0 989	4 17	1 88	3 06	1 30
1 078	3 63	1 63	2 51	1 08

9 Finally, we shall calculate from the values of M, the intensities of reflexion to be expected at high temperatures, and compare them with the observed results, in order to see whether it is possible, from measurements made at room temperature and at the temperature of liquid air, to predict the results of observations at high temperatures From equations (6) and (6A) the values of M_1 and M_2 for a given spectrum at a series of temperatures are calculated, and the ratio $(F_1e^{-M_1} + F_2e^{-M_2})^2_T \quad (F_1e^{-M_1} + F_2e^{-M_2})^2_{290}$ determined for each This gives the ratio of the intensity at temperature T to that at 290° Values obtained in this way for the spectra (400), (600) and (800)[*] are plotted in fig 2 The curves show the calculated values and the crosses the observed

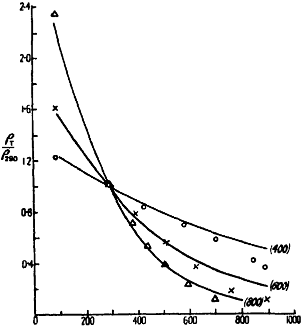

Fig 2

values of the ratio for these spectra at different temperatures The agreement is as close as can be expected up to about 500° Abs , for higher temperatures the decrease in intensity is much more rapid than the theory on which these calculations are based predicts This agrees with the results given in the earlier paper [†] Such a departure is to be expected at high temperatures, since it will probably no longer be possible to neglect cubes and higher powers of the displacements in the expression for the energy of the lattice

---

[*] These spectra are called (200), (300) and (400) in the paper on high temperatures (' Phil Mag ,' *loc cit*), being referred to the small cube of 2 814 Å edge

[†] Waller, ' Ann. d Physik,' vol 83, p 153 (1927)

On the whole, the values both at high and low temperatures are seen to be quite consistent among themselves, and, up to about 500° Abs, to be in quantitative agreement with theory

It should, however, be pointed out that we have neglected the excess of the general radiation which is concentrated in the interference maxima It is impossible to calculate this without detailed knowledge of the mosaic structure of the crystal, but between the temperature of liquid air and room temperature it may introduce an error of a few per cent We hope to be able to investigate this point later

Summary

In a crystal such as rock-salt the contributions of the two kinds of atom to the structure amplitude for a given spectrum are proportional to $F_1 e^{-M_1}$ and $F_2 e^{-M_2}$ respectively, where F_1 and F_2 are the atomic scattering powers of the chlorine and sodium atoms, supposed reduced to a state of rest, and M_1 and M_2 are functions of the temperature which may differ for the two atoms

It can be shown that, over a considerable range of temperatures, the following expansion is valid —

$$M_\kappa = 8\pi^2 \frac{\sin^2\theta}{\lambda^2}\{\alpha_\kappa + \beta_\kappa T + \gamma_\kappa/T + \delta_\kappa/T^3 + \ldots\}, \tag{7}$$

where T is the absolute temperature The term α_κ is zero if Planck's value of the zero-point energy be assumed, and γ_κ and δ_κ may be calculated with sufficient accuracy from the atomic constants The coefficient β_κ depends on the interatomic forces and cannot be determined directly, although a weighted mean $\beta = (m_1\beta_1 + m_2\beta_2)/(m_1 + m_2)$, where m_1 and m_2 are the masses of the atoms, can be calculated in terms of the elastic constants

In the present paper the values of the coefficients β for the two kinds of atom in rock-salt are determined, using formula (7), from the experimental results of James and Miss Firth on the intensity of reflexion of X rays from rock-salt crystals at low temperatures The values of β determined in this way give $\bar{\beta} = 5{\cdot}8 \cdot 10^{-21}$, whereas from Voigt's values of the elastic constants of rock-salt we obtain $\bar{\beta} = 5{\cdot}7 \cdot 10^{-21}$

Assuming the existence of zero-point energy, the values of M for each atom can be evaluated It is found that at corresponding temperatures and glancing angles M is greater for sodium than for chlorine The difference in M for the

two atoms implies that equal forces do not act on each, the chlorine atoms being more firmly bound

From the values of M for the two atoms, the root-mean-square amplitude of vibration at 290° Abs for sodium and chlorine are calculated to be 0 242 Å and 0 217 Å respectively

Using the separate values of M, the values of F for chlorine and sodium, corresponding to absence of all vibrational energy, are calculated from the observations of James and Miss Firth, and the curves so obtained are compared with those given in their paper, in which absence of zero-point energy was assumed

From the values of M for the two atoms, curves showing the variation of the intensity of reflexion of X-rays with temperature are drawn for the (400), (600) and (800) spectra of rock-salt, and these are compared with the measurements of James at high temperatures It is found that the observed and calculated results agree up to about 500° Abs

The results of this paper show that Waller's theoretical formula for the temperature coefficient agrees with experiment in the case of rock-salt from 86° Abs up to about 500° Abs , if allowance is made for the different values of M for the two atoms

On the Excitation of Polarised Light by Electron Impact
II —*Mercury*

By H W B Skinner and E T S Appleyard

(Communicated by Sir Ernest Rutherford, P R S —Received September 26, 1927 —Revised October 26, 1927)

§ 1 *Introduction*

In a number of recent papers* descriptions have been given of how the light from atoms excited by a directed stream of electrons is polarised, in the absence of any external field of force In particular we may refer to the paper by one of the present writers (Paper I), where some of the characteristics of the effect in mercury were discussed It was found that the different lines of the spectrum were differently polarised, both in magnitude and direction The behaviour of the polarisation when a magnetic field is applied to the mercury atoms was found to be identical with the effect produced by a similar field on the polarisation when the light is excited by the absorption of plane polarised light, the electric vector of which is parallel to the direction of the stream of electrons In this way, the polarisation of the light excited by electron impact was shown to be closely related to the polarisation of resonance radiation, which had been investigated by Wood and Ellett† and others In the paper referred to, the measurement of the polarisation of the spectral lines was, except in an individual instance, only qualitative Since its appearance two papers have appeared in which polarisation measurements of the mercury lines excited by electron impact have appeared Eldridge and Olsen‡ gave qualitative results, and these confirmed those which we had given Quarder§ gives quantitative measurements which are also for the most part in general accord The aim of the present paper is to describe quantitative results, and, as will be seen, these are not in all cases in detailed agreement with those given by Quarder The second aim is to determine the variation of the polarisation with the velocity of the electron stream, a point which has not been previously attempted.

In Paper I it was shown that the magnitude of the polarisation is intimately connected with the dynamics of the collision process By the electron impact, the atom is raised from its normal state into an upper quantum state, and by its return into the normal state, or into another state, light is emitted The magnitude of the polarisation depends on both of these processes, but the second process, the actual emission of the light, is well understood Polarisation measurements therefore give a powerful means of investigating the collision of an electron with an atom in the case when excitation of the atom takes place, and it is in this that their main interest lies

---

* Kossel and Gerthsen, 'Ann. d Physik,' vol 77, p 273 (1925), Ellett, Foote and Mohler, 'Phys Rev,' vol 27, p 31 (1926), Skinner, 'Roy Soc Proc,' A, vol 112, p 642 (1926)

† 'Phys. Rev,' vol 24, p 243 (1924), Hanle, 'Z f Physik,' vol 30, p 93 (1924)

‡ 'Phys Rev,' vol. 28, p. 1150 (1926)

§ 'Z f Physik,' vol 41, p 674 (1927)

§ 2 *The Electron Tube*

The tube used to provide a powerful, directed stream of electrons was the same as that described in Paper I, to which we refer for details A stream of electrons from an oxide-coated filament is defined in the usual way by slits and passes vertically into a field-free box with a hole cut in the side for observation A light trap is provided so that no polarisation errors can come from the reflexion of the light inside the tube The only difference from the previous tube is that the window in the present experiments was of clear fused quartz, fixed on with hard enamel The ground-glass joint by which the filament could be removed was used dry, being sealed round the outside with wax With these alterations it was possible to bake out the tube to some extent Since the tube runs at a fairly high current, the charging up of surface films on the electrodes was found to be troublesome, as it prevented precise definition of the speed of the electron stream It was found, however, that these films are easily and rapidly removed completely by running the tube at a potential of about 2,000 volts The vanishing of the films is easily tested In mercury the green line starts to be excited at 7 7 volts, and the yellow at 8 8 The visual effect of these lines together is a bluish white, while if the yellow lines are absent the colour is green It was possible to obtain streams of pure green colour passing throughout the length of the observation chamber without apparent diminution of intensity, thus showing that the velocity of the electrons was sufficiently constant along the length of the stream

The definition of the stream can be controlled by choice of the potentials applied to the various electrodes of the tube (see Paper I) It was possible to obtain a stream which traversed the field-free observation box practically without spreading

For the exact determination of the velocity of the beam, it is necessary to take into account the existence of contact potentials The magnitude of these was found in several ways, *e g*, (1) determination of the ionisation potential of mercury, (2) determination of the first critical potential from the intensity of the line λ 2537, (3) determination of the critical potential corresponding to the green line λ 5161 from the rise of its intensity These methods agreed fairly well, the third method proved the most convenient, and by using it the contact potential could be eliminated to within about 0 2 volt

The filament was of platinum strip and had a voltage-fall across its effective portion of about 0 7 volt The breadth of the electron stream was usually about 1 or 2 mm, and at the lower electron velocities there was very little light emitted from points outside the stream with the current used With the higher velocities (100–200 volts) the stray light was more considerable, and on this account it is probable that the polarisations measured in these cases may be a little too small Even with these velocities the stream was sharply defined, and the intensity of the light emitted from within the stream was very much greater than that emitted from outside it

§ 3 *Polarisation Measurements*

The measurement of the percentage polarisations of individual spectral lines has proved to be of considerable difficulty if consistent results are to be obtained In our case the problem is simplified by the fact that we know, from symmetry considerations, that the plane of polarisation must be either parallel or perpendicular to the electron stream, *i e*, horizontal or vertical In this case the principle of the method is very simple With some form of double-image prism we split up the light into the horizontal and vertical polarised components which, after passing through the spectrograph, give two spots on the plate corresponding to each spectral line The intensity ratio I_1/I_2 of the light which has produced the spots is found by the methods of photographic photometry The percentage polarisation Π is then given as

$$\Pi = 100 \frac{I_1 - I_2}{I_1 + I_2}$$

We take a polarisation with the electric vector parallel to the electron stream as positive

The spectrograph used is a large Hilger quartz instrument (E_1), of the Littrow type, the focal length of the collimating lens is about 1½ metres A high dispersion instrument is a great advantage in polarisation measurements since then the lines can be separated using a fairly wide slit (in our case 0 08 mm) An image of the vertical electron stream was projected on to the slit

For the double-image prism we used at first a Wollaston prism of calcite placed between the slit and the collimating lens of the spectrograph But there is a serious disadvantage in this arrangement The difficulty is that the two beams of light, polarised respectively horizontally and vertically, suffer different reflexion losses at the surface of the refracting prism of the spectrograph Further, they suffer a different loss at the surface of the photographic plate which is inclined at about 60° to the beam

These differences may give an apparent polarisation of as much as 25 per cent, which is very unsatisfactory in itself for the measurement of weak polarisations Also small uncompensated rotation effects in the quartz units of the spectrograph make this correction vary in an extremely complicated way with the wave-length The difference due to reflexion at the photographic plate makes the constancy of this correction dependent on the uniformity of the gelatine surface of the plate Owing to these causes it was found difficult to obtain very satisfactory measurements using the Wollaston prism

We really need a prism to replace the Wollaston prism which first splits up the light into the two polarised components, and then depolarises it [*] With the Littrow type of spectrograph, this is easily obtained We have only to replace the internally reflecting prism (of quartz, with the optic axis parallel to the slit) by one with the optic axis parallel to the body of the spectrograph The light travels in the prism, first perpendicular to the optic axis [†] In this part of the path there are introduced no rotation effects Secondly, the light is split up by double-reflexion at the oblique face (the angular separation is about 1/3°), and it emerges along the optic axis of the quartz In this last part of the path large rotation effects are introduced, and since the aperture of the prism used is finite, these rotations are different for different parts of the beam Hence we have effectively a depolarisation

The arrangement has the further advantage that by the elimination of four reflecting surfaces much light is saved

With this prism, the correction was always less than 5 per cent It has the disadvantage that it doubles the spectra horizontally, and hence one has to be careful to avoid the overlapping of lines Also on account of the tilted plate, one has to sacrifice the sharp focus of the spectroscope to some extent in order to get the two images equally in focus But for the problem of determining the polarisation, this does not affect the accuracy of the results in the case of the mercury lines In any case, the disadvantages are easily outweighed by the great advantage of the small correction

---

[*] We may here note that Quarder (*loc cit*) seems to have relied on his quartz collimating lens (of about 30 cm focal length and 4 cm diameter) to depolarise the light As numerical calculation shows, this would be quite inadequate He does not state that he has applied any correction at all, and it seems probable that some, at any rate, of the discrepancies between his measurements and ours are due to this cause.

[†] It was possible to verify that the fact that the spectrograph takes a cone of light of finite angle, and that therefore the light is not strictly perpendicular to the optic axis of the quartz, did not introduce any error by photographing the spectrum of a source of light completely polarised by an air-separated Nicol prism. Only one spectrum image appeared

The correction was determined for every set of exposures by photographing the spectrum of an unpolarised source of light We used the photometric mercury lamp which is mentioned below This proved to give very nearly unpolarised light, and in obtaining the correction it was only necessary to reverse the direction of the lamp (from horizontal to vertical) half-way through the exposure

There remains in this method a trouble which is due to the position of the double-image prism The ideal place for this is close to the collimating lens of the spectroscope But this position would be difficult to arrange with the type of double-image prism described above, and in our case was anyhow impracticable owing to the large size of the collimating lens Actually the prism was about 10 cm from the slit This has the consequence that the two beams of light which go to form the two polarised images do not traverse exactly the same path between the source and the slit This would not matter if the source were sharply focussed on the slit But without an achromatic projecting lens, this condition cannot be exactly fulfilled for all wave-lengths It is necesary, therefore, to keep the focal length of the projecting lens as short as possible so that the length of the " spectrum " of images formed by it may be as short as possible We used a fused quartz projecting lens 17 cm in focal length, and photographed the spectrum in two halves (1) 2400–3200 A U , (2) 3200–4400 A U , focussing carefully for a mean wave-length of the stronger lines in each case With this arrangement small errors might arise if the image of the electron beam were not *symmetrically* placed about the slit It was necessary, therefore, to take extreme care with regard to this setting of the image on the slit It is important also that the electron beam itself shall give a symmetrical distribution of light, and care was taken to ensure this With the projecting lens mentioned, it was found that if this care were taken, it was possible to obtain consistent results to within about 3 per cent of polarisation

In the case of the line λ 2537 one must work differently It is necessary to use the mercury at a pressure corresponding to a temperature of — 15° to — 20° C This would entail a very long exposure if a spectroscope were used, but by taking advantage of the fact that with an electron speed between 4 9 and 7·7 volts no other line which can get through the fused quartz window of the tube is excited, we can dispense with the use of the spectrograph altogether We therefore used simply a camera with a quartz lens and placed a Wollaston double-image prism just in front of the camera lens The photographs showed that the electron stream remained well defined In this way the problem becomes very much simplified

We now come to the photometric determinations, and here our practice was a usual one For the purpose of determining the intensity corresponding to a given density on the photographic plate, we have used as standard an 8-step optical wedge of platinum on quartz * In our case it was prepared by sputtering It was calibrated for several wave-lengths, using a steady source of light (a filament-maintained low-pressure mercury arc lamp†) and a rotating sector of variable aperture‡ an image of which was projected on to the aperture of the collimating lens of the spectrograph, the absorption of the wedge is then obtained by photographic photometry It was found to be nearly, but not exactly, independent of the wave-length The error in the wedge calibration is responsible for an uncertainty of about 2 per cent of polarisation in the absolute values, for the more strongly polarised lines For

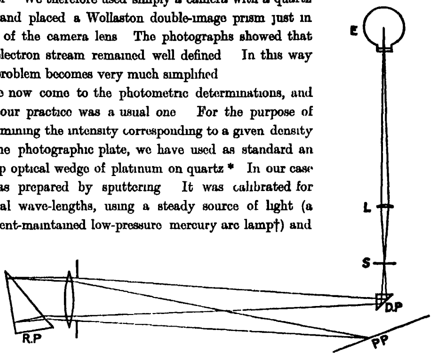

Fig 1 —Optical System

E = Electron tube
L = Fused quartz lens
S = Spectroscopic slit
D P = Double image prism
R P = Refracting prism
P P = Photographic plate

---

* Dorgelo, 'Phys Zeit,' vol 26, p 757 (1925), Merton, 'Roy Soc Proc,' A, vol 106, p. 378 (1924)

† It may be useful to note that the light emitted from a lamp of this type can be enormously increased by applying the magnetic field of a small suitably placed electro-magnet The filament type of lamp is much preferable to the ordinary mercury lamp for photometric work on account of its steadiness

‡ Kindly lent by Mr R W Ditchburn.

the violet region of spectrum it was possible to obtain the calibration more directly by comparing the quartz-platinum wedge against a standard wedge by means of a microphotometer

For use, the wedge was mounted in contact with a fixed slit of suitable width and was fixed in place of the usual spectrograph slit Using the mercury lamp to give a patch of light on the slit as nearly as possible uniform, a spectrum was photographed with the wedge in place Any lack of uniformity of the light spot was corrected by photographing the spectrum a second time with the wedge removed

A series of exposures thus consisted of the following parts —

(1) Exposures of the light from the electron tube (working at various voltages) using the double-image prism
(2) Exposure of the mercury lamp using the double-image prism to obtain the "spectrograph correction"
(3) Wedge exposure with mercury lamp
(4) Further exposure with the same setting of the optical system as (3) but without wedge

All the exposures of a set were given the same time (either ½ hour or 1 hour) It was found by trial to be unnecessary to perform the plate calibration (exposures 3 and 4) for each set of plates developed, for plates from the same box, the calibration could be obtained with sufficient accuracy once for all Subsequent exposures were developed under standard conditions (in a tank in which the developer could be violently and uniformly agitated)

The density of the various photographic images was measured by means of a photoelectric microphotometer In this way the percentage polarisation of any line could be obtained

§ 4 *Experimental Results*

Before describing the results, it is necessary to consider the type of excitation produced in the electron tube One type of excitation, that by collisions of the second kind with atoms, cannot play any part in our case on account of the comparatively low gas pressure A line may therefore be excited in two ways, (*a*) directly, and (*b*) by a "cascade" effect By this is meant that the line may be emitted as one of a group during the passage of the atom from the excited state to the normal state For example, λ 2537 ($1\ ^1S_0 - 2\ ^3P_1$) might be emitted after direct excitation into the $2\ ^3P_1$ level Or it might be emitted along with λ 4358 ($2\ ^3P_1 - 2\ ^3S_1$), after excitation into the $2\ ^3S_1$ state Since λ 4358 is intense, it seems probable that the cascade type of excitation must occur for λ 2537 For the other lines we have investigated, the cascade excitation may also play a part, for high velocities We shall return to this point later But for the more important case of velocities only a few volts above the critical potentials for the lines, it cannot play any appreciable part on account of the small probability of electrons of these velocities exciting the atoms into the higher states Hence we must conclude that, for sufficiently low electron velocities at any rate, the excitation is practically entirely direct

On account of its considerably smaller critical voltage, the line λ 2537 is somewhat exceptional in this respect, and this fact is one cause of the necessity of investigating the line separately We are practically limited to the region in which no other lines except λ 1849 ($1\,{}^1S_0 - 2\,{}^1P_1$) are excited at all (namely, 4 9 to 7 7 volts) Another probable disturbing factor is the strong absorption of λ 2537 by the normal mercury atom We found that when λ 2537 is excited along with the other lines at a relatively high gas pressure, it is nearly unpolarised

We therefore investigated λ 2537 in the restricted region of voltages, using a mercury pressure corresponding to −15° to −20° C The current in the electron stream was in this case about 1/30th ma The remaining lines were investigated, using a mercury pressure corresponding to room temperature (about 1/1000th mm) The current was about 1/3 ma The earth's magnetic field was balanced by means of a pair of Helmholtz coils to within less than 1/50th gauss A field of the order of the earth's horizontal component did not affect the polarisation in individual cases tested, but we have not verified this for all the lines As other investigators have found, the polarisation appeared to be independent of the current in the tube unless this reached a considerably higher value than that actually used The various disturbing effects connected with arcing may begin to come in

The lines λ 5461 and λλ 5770, 5791 (together) were treated visually, using a Babinet compensator, and appropriate light filters, on account of the slow speed of panchromatic plates All the remaining measurements are photometric

The polarisation of various lines is plotted against the *square root* of the voltage of the electron stream in figs 2 to 12 The dotted lines marked by the letter E indicate the corresponding critical voltages The points plotted are direct measurements and no averaging has been used It was found possible to obtain more consistent values for voltages on the high velocity side of the polarisation maxima than for voltages on the low velocity side We think this is due to the

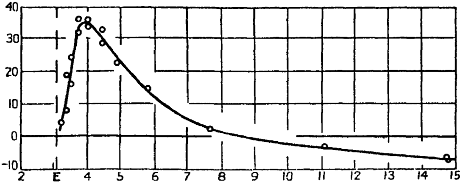

Fig 2 —λ 4347 ($2\,^1P_1 - 4\,^1D_2$)

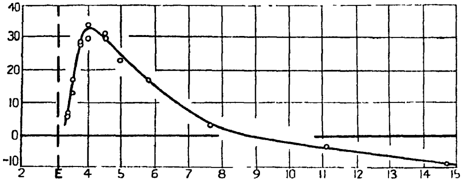

Fig 3 —λ 3906 ($2\,^1P_1 - 5\,^1D_2$)

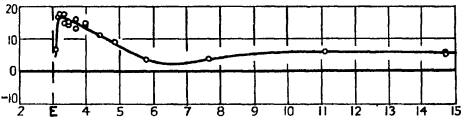

Fig 4 —λ 3650 ($2\,^3P_2 - 3\,^3D_3$)

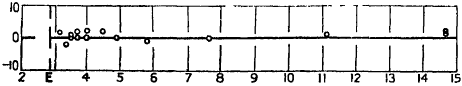

Fig 5 —λ 4078 ($2\,^3P_1 - 2\,^1S_0$)

Ordinates represent Percentage Polarisation Abscissæ represent $\sqrt{\text{volts}}$

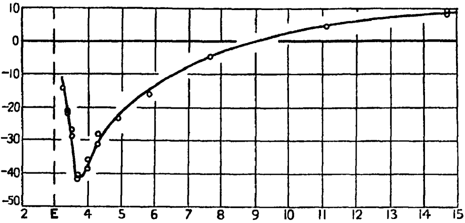

FIG 6 —λ 3663 ($2\,^3P_2 - 3\,^1D_2$)

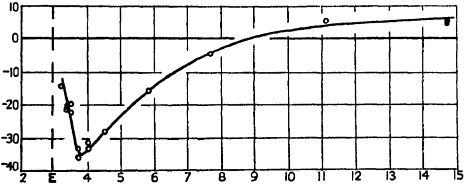

FIG 7 —λ 3655 ($2\,^3P_2 - 3\,^3D_2$)

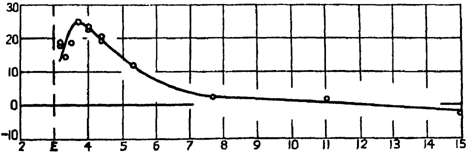

FIG 8 —λ 2967 ($2\,^3P_0 - 3\,^3D_1$)

Ordinates represent Percentage Polarisation Abscissæ represent $\sqrt{\text{volts}}$

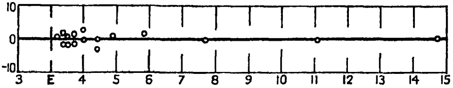

FIG 9 —λ 3341 ($2\,^3P_2 - 3\,^3S_1$)

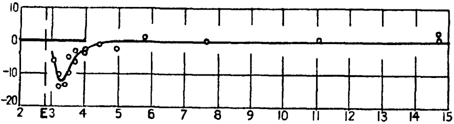

FIG 10 —λ 4358 ($2\,^3P_1 - 2\,^3S_1$)

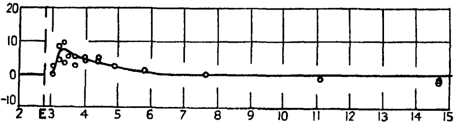

FIG 11 —λ 4047 ($2\,^3P_0 - 2\,^3S_1$)

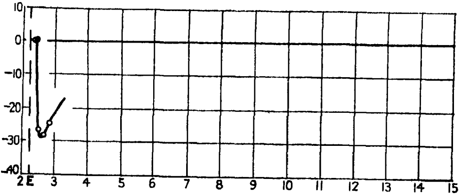

FIG 12 —λ 2537 ($1\,^1S_0 - 2\,^3P_1$)

Ordinates represent Percentage Polarisation Abscissae represent $\sqrt{\text{volts}}$.

extreme rapidity in many cases of the variation of the polarisation with the voltage for low voltages, it may be that the velocity of the electron stream was not sufficiently well defined with the actual apparatus used (*i e*, with a voltage fall across the filament) to ensure exact consistency In some cases (*e g*, λ 2537) a variation of the voltage by less than half a volt appears to cause a considerable change in the polarisation

The lines are polarised in various ways We have established the absence of any appreciable polarisation for the lines λ 4078 ($2\,{}^3P_1 - 2\,{}^1S_0$) and λ 4108 ($2\,{}^1P_1 - 4\,{}^1S_0$) This is an important point for the theory Some of the lines are polarised positively (*i e*, with the electric vector parallel to the electron stream) and some negatively For high velocities there is in most cases a definite reversal of the sign of the polarisation But the line λ 3650 ($2\,{}^3P_2 - 3\,{}^3D_3$) is as seen in fig 4 exceptional, and the line λ 3021 ($2\,{}^3P_2 - 4\,{}^3D_3$) shows precisely similar characteristics

The most striking features of the curves are the steep increase in the polarisation with increasing voltage for low velocities and the subsequent maximum which are found for all the most strongly polarised lines The steepness of the rise seems to vary, it is greatest in the cases of λ 2537 ($1\,{}^1S_0 - 2\,{}^3P_1$) and the series beginning with λ 3650 ($2\,{}^3P_2 - 3\,{}^3D_3$) The position of the maximum is also appreciably different for different lines For λ 2537 we obtained zero values of the polarisation for a voltage slightly exceeding the excitation potential, in some other cases one has only to make a small extrapolation in order to be able to say that, at the critical voltage, the polarisation is zero It seems likely that the existence of the maximum is a general property of all polarised lines It was proved in the case of λλ 5770, 5791 that the maximum is still obtained when a magnetic field of 12 gauss is applied parallel to the electron stream

In general, lines of a given spectral series are polarised to the same extent within the limits of error of measurement, and the polarisation curves are similar There is, in some favourable cases, an indication that the maximum on the polarisation curve is shifted slightly to correspond to the variation in the critical exciting voltage, but the shift is small (about a volt) and we cannot be sure of it The curves for λ 4347 ($2\,{}^1P_1 - 4\,{}^1D_2$) and λ 3906 ($2\,{}^1P_1 - 5\,{}^1D_2$) illustrate well the general similarity

The lines whose curves are given in figs 2 to 12 are only a part of those measured The remainder show similar features In Table I we give the maximum polarisation $\Pi_{\max}$ and the approximate voltages $V_{\max}$ at which the maxima occur We have divided the lines into two classes, (*a*) the most accurately measurable for which $\Pi_{\max}$ should be correct to within 4 per cent

Table I

Line			Volts		Per cent polarisation		
Excited state	Series	λ	V_e	$V_{max.}$	Π_{18} Quarder	$\Pi_{max.}$	P
Singlet	$2\,^1P_1-3\,^1D_2$	5791	8 8	14	40	28*	60
	$2\,^1P_1-3\,^3D_2$	5770					
	$2\,^1P_1-4\,^1D_2$	4347	9 5	15	45	35	60
	$2\,^1P_1-5\,^1D_2$	3906	9 8	16	50	33	60
	$2\,^1P_1-6\,^1D_2$	3704	10 0	(16)	50	(31)	60
	$2\,^3P_2-3\,^1D_2$	3663	8 8	14	−45	−41†	−100
	$2\,^3P_2-4\,^1D_2$	3027	9 5	(16)	−45	(−33)	−100
	$2\,^3P_1-3\,^1D_2$	3132	8 8	14	40	28‡	60
	$2\,^3P_1-4\,^1D_2$	2655	9 5	15	50	27	60
	$2\,^3P_1-2\,^1S_0$	4078	7 9	—	10	0	0
	$2\,^1P_1-4\,^1S_0$	4108	9 5	—	10	0	0
Triplet	$2\,^3P_2-3\,^3D_3$	3650	8 8	11	15	18	50
	$2\,^3P_2-4\,^3D_3$	3021	9 5	12	15	20	50
	$2\,^3P_2-5\,^3D_3$	2803	9 8	(16)	15	(19)	50
	$2\,^3P_2-3\,^3D_2$	3655	8 8	14	—	−35§	−100
	$2\,^3P_2-4\,^3D_2$	3023	9 5	(17)	—	(−26)§	−100
	$2\,^3P_1-3\,^3D_2$	3126	8 8	14	20	28	60
	$2\,^3P_1-4\,^3D_2$	2652	9 5	16	33	23	60
	$2\,^3P_1-4\,^3D_1$	2654	9 5	—	—	(−17)‖	−100
	$2\,^3P_0-3\,^3D_1$	2967	8 8	14	33	25	100
	$2\,^3P_0-4\,^3D_1$	2535	9 5	(14)	—	(18)	100
	$2\,^3P_2-2\,^3S_1$	5461	7 7	—	7	0	14
	$2\,^3P_2-3\,^3S_1$	3341	9 1	—	7	0	14
	$2\,^3P_2-4\,^3S_1$	2925	9 6	—	7	(0)	14
	$2\,^3P_1-2\,^3S_1$	4358	7 7	11	15	−12	−100
	$2\,^3P_1-3\,^3S_1$	2894	9 1	12	15	− 6	−100
	$2\,^3P_0-2\,^3S_1$	4047	7 7	11	33	8	100
	$1\,^1S_0-2\,^3P_1$	2537	4 9	6 7	−30¶	−30	100

Remarks

* A faint line $2\,^1P_1-3\,^3D_1$ is inseparable from λ 5791, but is probably of small effect It is likely by analogy with other cases that λ 5770 is slightly less polarised than λ 5791

† A faint line $2\,^3P_2-3\,^3D_1$ is inseparable from λ 3063, and the value given may be a little too small for this reason

‡ The line $2\,^3P_1-3\,^3D_1$ is inseparable from λ 3132 Estimating from the intensities of the next members of the series, it is probable that the value given is too small by about 5 per cent of polarisation

§ These lines are very near to much stronger lines, and the polarisation given is probably rather too small.

‖ Value for 15 volts

¶ Value of Ellett, Foote and Mohler for 7 volts of polarisation, and (*b*) the fainter, less accurately measurable, for which it should be correct only to within about 8 per cent The values for lines of the second class are indicated by brackets, *e g* (19) The column V_0 gives the corresponding critical voltages for the excitation of the lines The polarisations Π_{16} measured by Quarder (*loc cit*) for an exciting voltage of 16 volts are added for comparison The two sets of values agree in a general way, but there are many cases of detailed disagreement A possible cause of the discrepancy has been suggested The remaining column P is theoretical and will be discussed later

§ 5 *Theoretical Discussion*

In Paper I, it was definitely proved that the polarisation effects we are considering are determined simply by the directed character of the electron stream A further important property, established experimentally there, is that as far as the effects of an applied magnetic field are concerned,* the behaviour of the polarisation of the light excited by electron impact is identical with the behaviour of the polarisation of the light excited by resonance when the electric vector of the absorbed radiation is taken parallel to the direction of the electron stream In particular, in both cases, the polarisation is unaffected by a field parallel to the electron stream (or electric vector) Now it was known that in the case of resonance, correct values for the amount of the polarisation were only obtained on the classical quantum theory in the case when there is a magnetic field applied For the case when there is no field, one had merely to assume the effect independent of the presence of a field applied parallel to the electric vector

It was therefore clear that to obtain a corresponding theory of the excitation of polarised light by electron impact, the case when the magnetic field is applied parallel to the electron stream must be treated, and that the independence of the effect on a field applied parallel to the electron stream must be assumed This assumption may be called the assumption of spectroscopic stability

The theory of Paper I is based on the principle of the conservation of angular momentum for the collision Consider first the limiting case when the velocity of the electron after impact is zero—*i e*, the electron has just the minimum energy necessary for excitation Following Ellett, Foote and Mohler (*loc cit*), we make the assumption that, in this case, the vector change of angular momentum of the atom is in a direction at right angles to the initial direction of motion of the electron, or, in other words, the electron cannot carry away from the collision any angular momentum This assumption may be extended to the general case by supposing that if v_0 is the initial velocity of the electron and Δv the change in velocity it suffers during the collision, then *the angular momentum change of the atom is at right angles to* Δv (assumption A)

---

* A slight mistake in Part I of this paper, which deals with the magnetic effects, may here be corrected. On pp 652, 653, $\omega/2\pi\beta$ should be $2\pi\omega/\beta$ The values given for τ are correct.

This assumption implies a restriction of the type of orbit which the electron can describe during the excitation process, as is easily seen by considering particular examples But in the case of large electron velocities, when the energy of excitation is not sufficient to diminish appreciably the energy of the electron, assumption A would appear to follow necessarily from symmetry considerations In the limiting case of small final velocities, it follows from the classical mechanics *

Applied in the limiting case when the electron has only the minimum energy necessary for excitation, assumption A leads immediately to the following relation for the change in the magnetic quantum number m of the atom, caused by the impact -

$$\Delta m = 0 \tag{1}$$

Using this, one obtains the polarisation directly from a knowledge of the intensities of the Zeeman components of the line in question For a detailed account of the theory, we refer to Paper I

It is important to note that *the relation* (1) *also follows, for the "ideal" case when the velocity of the electron after collision is parallel to the velocity before the collision* This result is independent of the magnitude of v_0, and even of the general assumption A For it seems impossible to doubt, on any theory, that, in this particular case, the angular momentum transferred must be at right angles to v_0 We thus see that there is a *correlation between the magnitude of the observed polarisation and the degree to which the electrons are scattered when the excitation takes place*

When the energy of the exciting electron is greater than the critical energy, a scattering of the electrons must be expected to take place Thus, Δv is not necessarily parallel to v_0, and the relation (1) is not necessarily true One anticipated that the most probable direction for Δv would change from a direction parallel to v_0 for small velocities, to one perpendicular to v_0 for large velocities Thus one was led to expect that the percentage polarisation of a given spectrum line would decrease progressively with increasing electron velocities A quantitative prediction was not possible, since we do not know how the electrons of a given velocity are scattered on collision.

---

* We are indebted to Mr P M S Blackett for pointing out that assumption A is only true classically if the law of force between the electron and the atom varies more rapidly than the inverse third power of the distance between them But since the atom is neutral, we must expect this condition to be satisfied

In a recent paper Oppenheimer* has considered the polarisation effects from the standpoint of the new quantum theory He has concluded —

(*a*) That the polarisation of the light excited by a single collision is independent of a magnetic field parallel to Δv When the polarisation is large the most probable direction for Δv is nearly parallel to v_0, and thus the independence of the observed effect on a field parallel to v_0 is interpreted In this way Oppenheimer has established the assumption of spectroscopic stability The effect of a field in a direction inclined to the electron stream is also correctly calculated

(*b*) That the method of calculation by means of the angular momentum principle, and in particular assumption A, are correct

Thus Oppenheimer has shown that the theory of Paper I is right within the limits of his method of calculation

Actually the experiments have shown that the polarisation *decreases to zero* from a maximum value as the velocity of the electrons is diminished to the critical value Thus the theory fails definitely in the one case where it can be applied quantitatively But Oppenheimer's method of approximation leaves open the possibility of the failure of his conclusions, *in the case of very small final electron velocities* It is probable, therefore, that this effect may receive an interpretation on the quantum mechanics,† though it is inconsistent with the classical

For excitation by electrons whose velocity is not too small, we are undoubtedly justified in applying the theory of Paper I The large value of the polarisation at the maximum therefore shows definitely that, at the corresponding velocity, a large fraction of the electrons are scattered nearly straight forward With this conclusion we may compare the observation of Dymond,‡ who showed directly that in helium, with moderate electron velocities, a large fraction is scattered nearly straight forward when excitation takes place

For excitation by electrons of small velocity, we are on uncertain ground, as the experiments have shown that the theory of Paper I is untenable in this region. But it seems reasonable to assume, even in this case, a correlation between the value of the polarisation and the degree of scattering of the electrons If this is granted, we may conclude that, as the velocity of the electrons is diminished from a value corresponding to the maximum of the polarisation curves, the electrons are scattered more and more violently, until in the limiting case, corresponding to the zero value of the polarisation, the angular distribution of the electrons must be more or less uniform

---

* 'Z f Physik,' vol. 43, p. 27 (1927)

† Dr J R Oppenheimer has very kindly informed us of this fact

‡ 'Phys Rev,' vol 29, p 433 (1927)

We are thus led to postulate a probable anomalous scattering of the electrons of velocity slightly in excess of the minimum excitation velocity * It is interesting to note that the final velocity of these electrons is of the same order of magnitude as the velocity of the electrons for which the Ramsauer effect is observed Further, that the method of approximation used by Oppenheimer does not suffice for a theory of the Ramsauer effect

We now come to the consideration of the relative magnitudes of the polarisation for the various lines, and we shall be dealing with the case where the velocity of the exciting electron is sufficiently great for the theory of Paper I to be valid If we take the "*ideal*" case when the electron is not deflected during the collision, we have stated that the polarisation may be calculated from equation 1 In this way, we obtain a standard value P for the polarisation The actually observed polarisation will be less than P owing to the scattering of the electrons, and we cannot calculate how much less it will be On the other hand, it seems reasonable to suppose that the scattering will not be very different in the case of the various spectrum lines Thus we may compare with the *relative* values of P the *relative* values of the polarisation observed, for example, at the maxima of the polarisation curves

In Paper I, a qualitative comparison of this sort (but using the values of the polarisation corresponding to a definite electron velocity instead of the maximum values) was made, and it was found that, up to a point, there was good agreement The results are amplified by those of the present paper In Table I the values of P are inserted, and it is seen that, in most cases, and especially for the lines for which the excited state is a singlet state, the maximum polarisation $\Pi_{\max}$ is roughly expressed by the relation

$$\Pi_{\max} = \tfrac{1}{2} P$$

In particular we may note the absence of polarisation in the cases of the lines λ 4078 ($2\,{}^3P_1 - 2\,{}^1S_0$) and λ 4108 ($2\,{}^1P_1 - 4\,{}^1S_0$) Further, if we extrapolate the curves back to the excitation points in the manner of fig 13, we obtain, in most cases, values not far removed from P

But as was noted in Paper I, there are several flagrant exceptions to this rule

---

* An experiment for the direct verification of this effect will be undertaken shortly

The lines λ 2537 ($1\ ^1S_0 - 2\ ^3P_1$), λ 4047 ($2\ ^3P_0 - 2\ ^3S_1$), and λ 4358 ($2\ ^3P_1 - 2\ ^3S_1$) and a higher member of the same series are seen to violate it completely

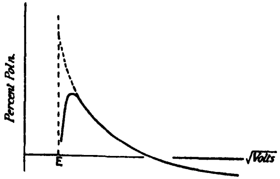

Fig 13

The first of these lines is polarised in the wrong direction, as was first observed by Ellett, Foote, and Mohler (*loc cit*) The others are polarised in the right direction but much more weakly than would be expected The line λ 2967 ($2\ ^3P_0 - 3\ ^3D_1$) and the next member of its series and the line λ 2654 ($2\ ^3P_1 - 4\ ^3D_1$) are polarised distinctly more weakly than would be expected, and it seems probable that the lines of the series beginning with λ 5461 ($2\ ^3P_2 - 3\ ^1S_1$) can also be included among the exceptional lines in spite of the low value of P

In Paper I, it was suggested that the reason for this breakdown of the classical theory of the effect is that we have neglected to take into account the *spin* of the exciting electron If the direction of the spin axis of the electron is not the same before and after the collision, angular momentum must have been transferred to the atom by a process not considered in the theory Thus the assumption allows the modification of equation 1 and so provides a possibility of the interpretation of the anomalous results Oppenheimer's calculations have strongly supported this point of view He has pointed out that the anomalous lines in question all correspond to *intercombination switches* from the normal singlet state of mercury on excitation (*i e*, the lines are those which correspond to the excitation of the atom into a triplet state) He has suggested that the spin comes in as a "*resonance effect*" in Heisenberg's* sense This leads to the assumption that the orbital angular momentum of the exciting electron must be *separately* coupled with the orbital angular momentum of the atom, its spin angular momentum with the spin angular momentum of the atom In other words, in the "ideal" calculation, the change in the orbital angular momentum Δl of the atom on excitation (instead of the vector Δj in the calculation when spin is neglected) must be at right angles to the electron stream Since the angle between l and j is known, the direction of j corresponding to the excited state is fixed

---

* 'Z f Physik,' vol 41, p 239 (1927)

In this way, it is possible to estimate the order of the correction which has to be applied to the values P for the intercombination lines And in fact the calculation shows that the correction will be greatest for λ 2537, as is observed The angle between j and l which determines the correction is only considerable in the case of the lines for which j is equal to 1 in the excited state, and these in fact are the exceptional lines In the case of lines for which j is 2 in the excited state the correction will be small, but it is interesting to note that, in an especially favourable case, it is detectable The lines λ 2652 ($2\,{}^3P_1 - 4\,{}^3D_2$) and λ 2655 ($2\,{}^3P_1 - 4\,{}^1D_2$) are a close pair, for one of which the excited state is a triplet state and for the other a singlet state Any errors in measurement (but the purely photographic) must be the same for both these lines Their polarisation curves are shown in fig 14, and it is seen that λ 2655 is definitely about 4 per cent more strongly polarised than λ 2652 Thus it seems that qualitatively the theory of the separate coupling of the "orbital" and "spin" angular momenta describes the facts very satisfactorily But it should be pointed out that there seems to be a difficulty in applying the theory to a non-degenerate system, and hence an exact calculation of the effect of the spin on the values P has not yet been made It would seem that in spite of this, the case for the necessity of the consideration of the spin of the exciting electron in the excitation process is established

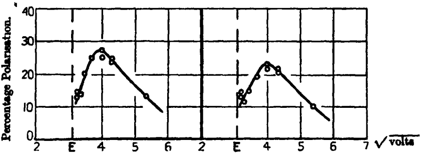

FIG 14 —λ 2655 ($2\,{}^3P_1 - 4\,{}^1D_2$) λ 2652 ($2\,{}^3P_1 - 4\,{}^3D_2$)

There remains for consideration the polarisation effects for very high velocities of excitation Quarder (*loc cit*), measuring the polarisation of the total light emitted from an electron tube, working with mercury, has shown that for small velocities the light is polarised with the electric vector parallel to the stream (*i e*, positively) As the electron speed increases the polarisation sinks to zero and subsequently becomes more and more negative No spectroscopic analysis was used Our curves show the beginnings of this effect in the case of individual spectrum lines In nearly all cases where there is a large positive polarisation for small electron speeds, for a large electron speed the polarisation is negative If it is negative for small speeds, it is positive for large, and if the polarisation is zero for small speeds, it remains zero An exception, however, occurs in the case of the lines λ 3650 ($2\,{}^3P_2 - 3\,{}^3D_3$) and λ 3021 ($2\,{}^3P_2 - 4\,{}^3D_3$) These lines show a positive polarisation for small speeds which decreases with the speed For large velocities, it still remains positive

The general lines of an explanation of this effect are clear and have been pointed out by Oppenheimer For moderate velocities of the exciting electron, the most probable direction for Δv is nearly parallel to the direction of the electron stream For very large velocities, on the other hand, it is nearly perpendicular to the electron stream Hence a reversal of the direction of the polarisation for very large velocities is to be anticipated The exceptional effect in the case of λλ 3650, 3021 is not accounted for, but it is possible that even in this case, the reversal takes place for higher electron velocities

Oppenheimer has remarked in this connection that this effect would scarcely be anticipated, owing to the fact that one would expect most of the light emitted from atoms excited by fast electrons to come, not from direct excitation, but from a "cascade" effect This view is supported by the work of Dymond (*loc cit*), who showed that the probabilities of the switches in helium, corresponding to the excitation of the stronger lines, are measurable for small electron velocities, but vanish for large velocities If the "cascade" effect is large in mercury, one would not expect to find any appreciable polarisation for high velocities, since a "cascade" emission would appear to imply that the direction of the electron stream cannot appreciably affect the characteristics of the light emitted Hence it seems that we must assume that, in mercury at any rate, a considerable part of the excitation is direct, even for high excitation velocities

Summary

The paper continues the study of the polarisation of the mercury lines excited by a directed stream of electrons, which was begun in a previous paper Photometric determinations of the percentage polarisation of the individual lines are described, the velocity of the exciting electron stream being varied from 9 to 200 volts The different lines show different polarisation characteristics,

some being unpolarised, some polarised with the electric vector in a direction parallel to the electron stream, and some polarised in the perpendicular direction The polarised lines show a characteristic variation of the polarisation with the electron speed, the most salient feature being a maximum of polarisation for an electron velocity corresponding to a few volts above the excitation point A reversed polarisation for high electron velocities is found in most cases It is shown that the various polarisation effects may be interpreted to give information about the dynamics of the collision process in which an atom is excited by electron impact

It is hoped shortly to give an account of the excitation of polarised light in helium

We had the advantage of discussing the interpretation of the results with Dr J R Oppenheimer, and are much indebted to him for his contributions In conclusion, we should like to thank Mr R H Fowler, F R S, for valuable discussion, and Sir Ernest Rutherford, P R S, for providing the means for carrying out the work and for his constant interest The work was performed during the tenure by one of us of a Senior 1851 Exhibition Studentship, and he is greatly indebted to the Commissioners for their assistance

On the Effect of Temperature on the Viscosity of Air

By R S Edwards, A R C S, B Sc, with a foreword by A O Rankine, D Sc, Professor of Physics in the Imperial College of Science and Technology

(Communicated by H L Callendar, F R S—Received June 10, 1927)

Foreword

It appeared that further experiments on the viscosity of air were desirable in order to discriminate between the results of F A Williams* and those of most previous observers, and to test his conclusion respecting the validity of Sutherland's law of the variation of viscosity with temperature It happened that this could be done easily and expeditiously in the laboratories of the Imperial College Mr R S Edwards, the author of the following paper, was in the midst of preparations for determining the viscosity of neon at a number of temperatures ranging from atmospheric temperature to the normal boiling point of sulphur, and at my suggestion diverted his attention to the behaviour of air at the same temperatures It is true that this range (about 430 centigrade degrees) is not so extensive as the thousand degrees covered by Williams' experiments, but it includes all that region in which, according to Williams, the value of Sutherland's constant displays the large increase upon which I have cast doubt †

Edwards' method of temperature control and estimation involves heating by the saturated vapour of selected substances of well-established boiling points, and would appear to be more reliable than the electrical heating, and particularly the temperature measurement by a single thermocouple, as employed by Williams In the present experiments also, considerable variations of the pressure conditions have been made, with consistent results, thus proving the validity of the transpiration formula assumed No such internal evidence of accuracy was provided in Williams' experiments

It will be seen that Edwards' new data provide a very definite confirmation of the work of the observers previous to Williams quoted in my paper (*loc cit*) No evidence has been found of a breakdown of Sutherland's law between 15° C and 444 5° C , on the contrary, further proof of the validity of the law is provided, and the value of Sutherland's constant, namely 118, over this range is found to be in close agreement with the usually accepted value calculated between the limits of 0° C to 100° C The effect of Edwards' experiments is thus to render still more doubtful the reliability of Williams' data

---

* 'Roy Soc Proc,' A, vol 110, p 141 (1926)

† 'Roy Soc Proc,' A, vol 111, p 219 (1926)

1 *Introduction*

The experiments described in this paper were undertaken in view of the uncertainty introduced by the work of F A Williams* with regard to the previously accepted variation of the viscosity of air with temperature His results were criticised by A O Rankine,† mainly with respect to the methods of temperature control and measurement employed In any further investigation, therefore, it was necessary to ensure that the various temperatures at which measurements were taken should be accurately known, without at the same time unduly restricting the range

To satisfy these conditions it was decided to use vapour jackets to heat the capillary tube, using only substances which have definite and well-known boiling points under atmospheric pressure The two important advantages arising from the use of vapour jackets are that steady temperatures over a long period are ensured, and the actual boiling points do not need measuring, it being sufficient to use the present accepted values The use of an electric furnace, as in Williams' experiments, while allowing a greater range, renders both the temperature control and measurement uncertain in comparison with the method just mentioned The procedure finally adopted was to enclose the air in a fairly large bulb, and to allow it to escape through a capillary tube, both the bulb and the tube being surrounded by the vapour jacket, which was successively maintained at the various temperatures at which readings were taken

2 *Theory of the Method*

The apparatus can be represented for theoretical purposes by fig 1 Consider a bulb of volume V and a capillary maintained at a temperature Θ, and suppose that at any instant the pressure of the gas in the bulb is p Let the steady

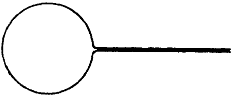

FIG 1

---

* 'Roy Soc Proc,' A, vol 110 p 141 (1926)
† 'Roy Soc Proc,' A, vol 111, p 219 (1926)

external pressure be p_0, p being greater than p_0 We then have, applying Meyer's well-known transpiration formula differentially,

$$dm R\Theta = \pi r^4 (p^2 - p_0^2)\, dt/16l\eta_\theta,$$

where,

dm = mass gas flowing through capillary in time dt,

R = gas constant,

Θ = absolute temperature, θ the corresponding centigrade temperature,

r = radius capillary, l = length capillary,

η_θ = viscosity of gas at Θ

But since $pV = mR\Theta$, where m = mass of gas in bulb at any instant, we have $Vdp = dmR\Theta$ Therefore, substituting,

$$-Vdp = \pi r^4 (p^2 - p_0^2)\, dt/16l\eta_\theta$$

(The negative sign is to allow for the fact that p decreases as t increases)

Therefore,

$$-\int_{P_1+p_0}^{P_2+p_0} \frac{dp}{p^2 - p_0^2} = \frac{\pi r^4 t}{16lV\eta_\theta},$$

where $(P_1 + p_0)$, $(P_2 + p_0)$ are the initial and final pressures in the bulb respectively, and t = time flow

Therefore,

$$\frac{1}{2p_0} \log_e \left\{ \frac{(P_2 + 2p_0)\, P_1}{(P_1 + 2p_0)\, P_2} \right\} = \frac{\pi r^4 t}{16lV\eta_\theta}$$

The value of η_θ thus determined has to be corrected for the slipping of the gas over the walls of the capillary tube If ξ_θ is the coefficient of slip at Θ, η_θ will then be given by

$$\eta_\theta = \frac{\pi r^4 t}{8lV} \frac{p_0 (1 + 4\xi_\theta/r)}{\log_e \{(P_2 + 2p_0)\, P_1/(P_1 + 2p_0)\, P_2\}}$$

The term $\pi r^4/8lV$ will be independent of the temperature if the bulb and tube are of the same material If, therefore, we write K for this constant term we have

$$\frac{\log_e \{(P_2 + 2p_0)\, P_1/(P_1 + 2p_0)\, P_2\}}{tp_0} = \frac{K(1 + 4\xi_\theta/r)}{\eta_\theta} \qquad (1)$$

Hence, if the values of $K(1 + 4\xi_\theta/r)/\eta_\theta$ are determined for two different temperatures, say Θ_1 and Θ_2, by measurements of the four quantities P_1, P_2, P_0 and t, we have at once the ratio $\eta_{\theta_2}/\eta_{\theta_1}$, provided an approximate value of the radius is known

3 *Experimental Method and Apparatus*

It will be noticed from the above theory that the accuracy of the method depends upon the measurements of the comparatively small quantities, P_1 and P_2 These were determined as follows The mercury reservoir (see fig 2, which is a diagrammatic sketch of the apparatus) was lowered until the mercury stood at some convenient level in the bulb L, the tap T_3 being closed, T_1 and T_2 open T_1 was then closed, and the reservoir raised until the mercury stood above the junction of the two limbs of the manometer M This raised the pressures in the bulb B, and the space between the mercury in the limb *b* and the tap T_1 above atmospheric T_2 was then temporarily closed, T_1 opened, and, finally, T_2 re-opened * The difference of level between the mercury in the two limbs *a* and *b* of the manometer then indicated the excess pressure above atmospheric of the gas in B The mercury in *a* was then adjusted to a convenient level, kept the same throughout the experiments, and when the pressure in the bulb had remained steady for some minutes, T_2 was closed, T_3 opened, and the stop-watch started The mercury levels in *a* and *b* were then noted with a cathetometer which read to 1/10 mm , and the difference of the two readings gave P_1 The atmospheric pressure was also noted

At the end of the run T_3 was closed, and the watch stopped simultaneously The reservoir was then lowered until the mercury level in *b* was approximately in the position which it was expected to occupy when T_2 was opened This having been done, T_2 was opened, and the level in *a* adjusted to the position it occupied at the start, and the difference between the levels in the two limbs noted This difference, subject to two corrections, gave P_2 Finally the mercury was lowered until the level was again at some convenient position in the bulb L, and the cycle of operations could then be repeated By varying the initial level in L, P_1 could be made to have any desired value

In order that a large temperature range could be employed, the apparatus was made of pyrex glass, which does not soften below 750° C The bulb B, as shown in fig 2, was made a long narrow cylinder in shape to facilitate effective jacketing The connecting tube to the tap T_2 was made of narrow-bore quill tubing in order to reduce the volume of the exposed portion. To ensure a steady temperature for the gas between T_2 and the mercury level in *a* and for the manometer M, a water jacket, as shown in fig 2, was placed round this portion of the apparatus, and a stream of water kept running through it A small opal glass lamp was placed behind the mercury levels to facilitate reading, this arrangement was very satisfactory, and the lamp being small the heat

---

* It was necessary to close T_2 temporarily, because otherwise, on opening T_1, the sudden change of pressure above the limb *b* dragged the mercury level in *a* below the junction and a violent rush of air from *a* to *b* took place.

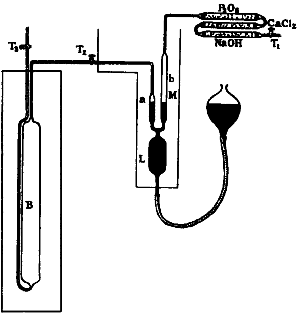

Fig 2

from it did not disturb the temperature of the bath The limbs of the manometer M were made of 1 2 cm internal diameter tubing, capillary depression effects thus being rendered negligible The apparatus was exhausted and filled with pure dry air several times initially, and the tubes containing NaOH, $CaCl_2$, P_2O_5 served to free from CO_2 and dry the air drawn into the apparatus in preparation for each reading by the process described above The whole apparatus was mounted on a rigid wooden stand, with an extended arm to act as a support for the bulb and also as carrier for the mercury reservoir, for which a device was arranged to permit of the necessary fine adjustment The capillary used was examined by a microscope, and measurement showed that the bore was circular to within 1 per cent, and of the same magnitude at both ends The following list gives the dimensions of the apparatus —

Volume bulb = 606 3 c c at 15° C

Volume portion bulb exposed = 0 80 c c = 0 13 per cent of total volume

Volume of tube from capillary to tap T_3 = 0 90 c c.

Radius capillary = 0 013 cm (measured by microscope)

Length capillary = 76·7 cms

Volume from tap T_2 to fixed level in limb *a* = 3 85 c c

5 *Corrections to Formula*

As mentioned in § 3, the difference of level measured at the end of the run does not give P_2 directly On opening the tap T_2, a volume V at pressure $(P_2 + P_0)$ and temperature Θ is mixed with a volume v at pressure $(P_1 + p_0)$ and temperature Θ', where v = volume from tap T_2 to fixed level in limb a, and Θ' is the temperature of the manometer Hence we have, by the gas laws,

$$V(P_2 + P_0)/\Theta + v(P_1 + p_0)/\Theta' = (p_0 + P)(V/\Theta + v/\Theta')$$

i e,

$$P_2 = P_1 - v\Theta(P_1 - P)/V\Theta',$$

where $(P + p_0)$ is the uniform pressure attained on mixing and P is the excess pressure actually measured Since $v\Theta/V\Theta'$ was always small, the values given in the previous paragraph for v and V were sufficiently accurate for the purposes of the correction

One further correction to the value of P_2 thus determined was necessary When the tap T_3 was closed at the end of the run, the pressure in the connecting tube from the capillary to T_3 was p_0, and a flow of gas took place until the pressure was raised to that of the bulb The resultant effect was that the pressure in the bulb was reduced by an amount dependent on the volume of the connecting tube and the excess pressure in the bulb Assuming that the temperature of the tube was the same as that of the bulb, the correction for any given excess pressure was calculated The values were as follows —

Excess pressure	Correction
2 cms	0 003 cm
3 cms	0 0045 cm
4 cms	0 006 cm
5 cms	0 0074 cm

The coefficient of slip has been shown to be equal to 0 85 λ, where λ = mean free path in the gas * If λ is expressed in terms of the viscosity, using Knudsen's expression for the viscosity, viz, $\eta = 0\ 31 v\rho\lambda$, we have $\xi = 1\ 72\eta/\sqrt{p\rho}$ Using the gas equation this can be expressed as $\xi = 2\ 913\eta\sqrt{\Theta}/p$ In this expression p is the mean pressure, which in this case varies logarithmically with time, in the capillary over a run $4\xi_0/r$ was, however, always so small that the change in p, which was about 5 per cent, caused a difference of only 1/10,000 in the factor $(I + 4\xi_0/r)$ Hence it was sufficient to take an average value for the pressure in the capillary and apply the resultant factor to the mean of the readings for K/η_0 at a given temperature

---

* Knudsen, 'Ann d Physik,' vol 28, p 75 (1909)

4 *Constant Temperature Jackets Employed*

Readings were taken at five temperatures—viz , 15°, 100°, 184 4°, 302°, 444 5° C A fast flowing water jacket was utilised at 15° C , and this temperature was used as the comparison temperature for the others

At 100° C a separate boiler was used, and the steam passed into the jacket at A and out at B, as shown in fig 3 (*a*) The tap T served to drain off excess condensed steam from time to time

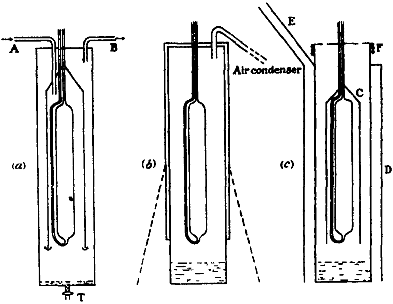

FIG 3

At 184 4° and 302° C aniline and diphenylamine were used to supply the vapour, and the apparatus used is represented in fig 3 (*b*) The substance was placed in the bottom of the vessel, the gas flame being immediately underneath An external air condenser was used to condense the vapour At 302° C it was found necessary, in order to obtain steady boiling, to place an asbestos cone round the lower half of the vessel, shown dotted in figure This device conserved the heat and reduced the rate at which the diphenylamine was boiled The upper portion of the vessel was jacketed in the usual manner At both temperatures it was important to boil rapidly at first to drive over impurities , once this had been accomplished it was found possible to adjust the gas supply so that the vapour just trickled over Under these conditions very steady temperatures were attained

The arrangement used at 444 5° C (the temperature of boiling sulphur) is shown in fig 3 (*c*) Considerable difficulty was experienced at this temperature in heating the whole vessel, but finally the arrangement shown in the figure was adopted and proved fairly satisfactory An asbestos cylinder D was placed round the vessel, and the hot gases from the burner at the base passed up through the interspace and escaped by the chimney E A coil of composition tubing F wound round the top of the jacket, through which a current of cold water was circulated, served to condense the sulphur, and the cover G protected the bulb from the condensed vapour The bulb and manometer acted as a gas thermometer sensitive to 0 05° C, and hence a check on the constancy of the various temperatures was provided by the apparatus itself A thermometer placed with its bulb just below the lid of the vessel was used to test whether the jacket was hot throughout At 15° C the temperature of the water bath was measured with a mercury thermometer graduated to 1/10° C, which had been calibrated by comparison with a standard The other temperatures were obtained from boiling-point tables, allowance being made for variation of these boiling points with pressure

6 *Calculation of Results*

In order to have a basis for comparison with the results of other observers, it was decided to take Millikan's formula for the viscosity of air at room temperatures as standard, and to express the results in terms of this standard value Millikan* gave

$$\eta_\theta = 0\ 00018240 - 0\ 000000493\,(23 - \theta)\ \text{C G S units}$$

over the range 23° C to 12° C

Therefore we have $\eta_{15} = 0\ 00017846$ C G S units

Expressed in terms of practical units, formula (1) becomes

$$\frac{\log_{10}\{(P_2 + 2p_0)\,P_1/(P_1 + 2p_0)\,P_2\}}{tp_0} = \frac{15\pi r^4 g\rho_0\,(1 + 4\xi_\theta/r)}{4\ 606 lV\eta_\theta}, \tag{2}$$

where the pressures are measured in centimetres of mercury at 0° C, and the time in minutes ρ_0 = density mercury at 0° C Hence,

$$K = 15\pi r^4 g\rho_0/4\ 606 lV \tag{3}$$

P_1 and P_2 were measured at θ', the temperature of the manometer, and were not reduced to 0° C, the slight error thus introduced, about 1/15,000 in the term $P_1\,(P_2 + 2p_0)/P_2\,(P_1 + 2p_0)$, being negligible

---

* 'Ann d Physik,' vol 41, p 759 (1913)

7 *Results*

Table I gives the series of observations at room temperature The column headed P gives the difference of level in the limbs *a* and *b* of the manometer at the end of the run The rest of the symbols have the same significance as in formula (2)

Table I

Time (mins)	Baromr (cm Hg 0° C)	θ (°C)	θ' (°C)	P_1	P	P_2	$\frac{K(I+4\xi/r)}{\eta_\theta}$ $(\times 10^4)$	$\frac{K(I+4\xi/r)}{\eta_{15}}$ $(\times 10^4)$
				(cm Hg at θ' °C)				
11 28	75 44	14 60	14 90	6 535	2 495	2 469	4 839	4 823
7 930	75 44	14 62	14 90	7 265	3 675	3 655	4 818	4 812
10 60	75 44	14 62	14 91	7 865	3 100	3 132	4 836	4 830
7 403	75 44	14 62	14 91	6 735	3 535	3 517	4 832	4 826
6 020	77 18	15 50	15 95	5 270	3 120	3 110	4 804	4 809
9 850	77 18	15 58	16 05	8 040	3 390	3 362	4 814	4 823
12 15	77 18	15 50	16 10	8 623	2 975	2 939	4 820	4 826
16 05	77 18	15 23	16 05	8 515	2 105	2 063	4 822	4 826
12 33	77 17	10 51	10 33	7 920	2 670	2 637	4 869	4 809
7 350	77 17	10 56	10 36	7 170	3 730	3 711	4 882	4 823
9 515	76 83	10 11	10 00	7 500	3 233	3 208	4 886	4 821
16 37	76 70	10 44	10 08	7 850	1 850	1 842	4 879	4 816
11 08	76 70	10 38	10 05	7 815	2 940	2 909	4 882	4 820
12 82	76 67	10 34	10 10	7 680	2 503	2 470	4 867	4 803
9 477	75 63	10 75	10 54	6 410	2 810	2 791	4 891	4 837
8 572	75 69	10 93	10 64	6 360	3 020	3 003	4 877	4 822
6 985	75 69	10 98	10 65	6 120	3 340	3 327	4 860	4 807
7 977	75 71	10 88	10 63	5 720	2 860	2 846	4 889	4 834

The last column gives the values of $K(I + 4\xi_\theta/r)/\eta_\theta$ corrected to 15° C, using Millikan's formula given above Mean value

$$K(I + 4\xi_{15}/r)/\eta_{15} = 4\ 8204 \times 10^{-4}\ \text{C G S units}$$

The value of $(I + 4\xi/r)$ at 15° C, taking $r = 0\ 013$ cm, is 1 0025, therefore,

$$K = 8\ 5819 \times 10^{-8}$$

Substituting this value for K in (3), a value for r of 0 0131 cm is obtained, which is in good agreement with that measured by the microscope

Table II gives the results of observations at the other temperatures These have been corrected for variation of boiling point with pressure, assuming the rate of change of viscosity with temperature from the results of previous observers

Table II

θ (° C)	$\frac{K(I+4\xi/r)}{\eta_\theta}$ (× 10^4)	θ (° C)	$\frac{K(I+4\xi/r)}{\eta_\theta}$ (× 10^4)	θ (° C)	$\frac{K(I+4\xi/r)}{\eta_\theta}$ (× 10^4)	θ (° C)	$\frac{K(I+4\xi/r)}{\eta_\theta}$ (× 10^4)
100 0	3 938	184 4	3 419	302 0	2 915	444 5	2 525
	3 939		3 405		2 920		2 505
	3 936		3 416		2 923		2 521
	3 937		3 398		2 919		2 532
	3 958		3 405		2 919		2 505
	3 958		3 420		2 926		2 545
	3 938		3 419		2 923		2 524
	3 951		3 400		2 914		2 532
	3 939		3 423		2 927		2 534
	3 961		3 416		2 926		2 535
	3 961		3 404		2 925		2 512
	3 959		3 402		2 927		—
	3 948		3 399		2 928		—
	—		3 404		2 916		—
Means	3 948		3 409		2 922		2 525

The values of the factor $(I + 4\xi_\theta/r)$ were

Temp (° C)	100 0	184 4	302 0	444 5
$(I + 4\xi_\theta/r)$	1 0036	1 0046	1 0060	1 0077

Substituting these factors, the following mean values were obtained for the viscosity —

Table III

Temp (° C)	15 0	100 0	184 4	302 0	444 5
η_θ (× 10^4 C G S units)	1 7846	2 181	2 529	2 954	3 425

8 *Accuracy of the Results*

As mentioned in § 3, the accuracy of the method is dependent on that attained in the measurement of the initial and final excess pressures P_1 and P_2, but since they appear in the logarithmic term in the expression for η, a given error in P_1 and P_2 does not necessarily involve a proportionate error in the value obtained for η If the ratio P_1/P_2 is denoted by x, it follows from (2) that η is proportional to $I/\log_e x$ Therefore,

$$d\eta/\eta \propto dx/x \log_e x$$

Consequently, for a given error in x, the error in η will be greater or smaller than this, according to whether x is less or greater than e Since P_1 was never less than 1 7 times as great as P_2, the error in measuring P_1 can be neglected in comparison with that of P_2 to enable the accuracy attained to be estimated P_1 and P_2 were observed by a cathetometer reading to 0 1 mm, and the smallest value of P_2 being 1 84 cms, the error in P_2 would be of the order of 0 5 per cent As can be seen from Table II, the values of x less than e always corresponded with values of P_2 of at least 3 cms (this held for all the readings taken), for which the error in measurement was naturally less than 0 5 per cent,, so that to a large extent the two factors in the expression for $d\eta/\eta$ compensated for each other Considering the two extreme cases in Table II, we have

P_1	P_2	x	$d\eta/\eta$
5 270	3 110	1 67	1 95 dx/x = 0 65 per cent
7 850	1 842	4 27	0 69 dx/x = 0 40 ,,

The values of dx/x being calculated on the basis discussed above, all the other readings taken were within the range covered by these two extreme cases, and consequently the accuracy of the individual readings may be taken to be about 0 5 per cent Since the time of flow was never less than six minutes, and was measured to an accuracy of at least one second, any error in t would not invalidate the above conclusions On the basis of an accuracy in individual readings of 0 5 per cent, it seems reasonable to suppose that the accuracy of the means of the groups of results would be about one part in one thousand

It will be noticed in Table II that the readings at room temperature were taken in two groups at about 15° C and 10 6° C respectively A comparison of the means of the two groups will therefore provide a test of the above assumptions, for the ratio of the viscosities, as determined from the results, should agree with the accepted ratio calculated from Millikan's formula For the purposes of the comparison the mean result for each group was taken to correspond with the mean temperature of the group This is justifiable over the small ranges considered The mean temperatures were 15 03° C and 10 58° C, the observed ratio $\eta_{15}/\eta_{10\ 6}$ was 1 0116 and calculated 1 0122, which agree to well within one part in a thousand This result substantiates the claim made above that a group of readings with an estimated individual accuracy of 0 5 per cent and a group variation of about 0 8 per cent, as can be seen from Tables II and III, give a mean value which is accurate to 0 1 per cent

The results at 444 5° C are not so consistent, individual readings varying as much as 1 6 per cent (Table III) These variations were due to changes in the temperature of the bath, amounting to 0 2° C, caused by unavoidable fluctuations in the large amount of heat necessary to keep the bath hot, and the formation of iron sulphide inside the vessel However, considered on the same basis as the other readings, the mean value at 444 5° C may be regarded as accurate to about 0 4 per cent

9 *Discussion of Results*

A convenient basis of comparison with the results of previous observers is afforded by the ratios η_θ/η_{15} This has been done in Table IV, in which the present results are compared with the means of earlier observers, as quoted by Rankine (*loc cit*) and with those of Williams (*loc cit*)

Table IV

η_θ/η_{15}	Mean previous observers	Williams	Present results
η_{100}/η_{15}	1 220	1 190	1 222
η_{184}/η_{15}	1 420	1 370	1 417
η_{302}/η_{15}	1 656	1 621	1 656
η_{444}/η_{15}	—	1 909	1 919

The present results are thus seen to be in agreement with the work of previous observers, with the exception of Williams, and the extended temperature range shows that his results are probably still too low at 444 5° C, though the discrepancy is smaller Sutherland's formula for the viscosity of a gas is $\eta_\theta = k\Theta^{1/2}/(1 + C/\Theta)$, or more conveniently for our purpose, $\eta_\theta = k\Theta^{3/2}/(C + \Theta)$, where C = Sutherland's constant and Θ = absolute temperature Previous to the work of Williams, Sutherland's formula had been accepted as an accurate representation of the change of viscosity of a gas with temperature, even though the theoretical basis upon which it was founded had been questioned * Consequently the formula can be used as a further basis of comparison between the results of various observers It can be seen at once that $\Theta^{3/2}/\eta_\theta$ plotted against Θ as ordinate should give a straight line, and the negatived intercept on the Θ axis will give the value of C This has been done, as shown in fig 4 The value of C as determined by the present results is 118, which agrees with the previously accepted value of 117 Williams' results and the means of the earlier observers' results expressed in terms of Millikan's value for η_{15} have also been plotted, and while these latter coincide almost exactly with the present points, those of Williams show striking variations The strict obeyance of Sutherland's formula by the present results exhibited in fig 4, where every point fits the mean straight line to within $\frac{1}{3}$ per cent, enables the conclusion to be drawn that C does not change in the neighbourhood of 300° C as put forward by Williams Further, since the investigation has been extended into the region for which Williams considers the true value is 172, and no disagreement with the formula found, it appears that Williams' results are exceptional and inaccurate, probably on account of the method of temperature measurement, which A O Rankine (*loc cit*) has criticised

---

* Chapman, 'Phil Trans,' A, vol 211, p 432 (1912), James, 'Proc Camb Soc,' vol 20, p 447 (1921), Enskog, 'Upsala Diss' (1917)

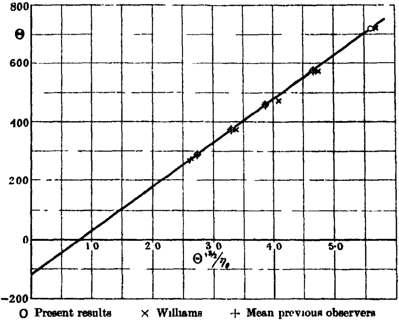

FIG 4

In conclusion, the author would like to express his appreciation to Prof A. O Rankine for the advice and encouragement he has constantly given throughout the investigation

Summary

(1) The ratios of the viscosities of air at various temperatures between 15° C and 444 5° C have been determined, using a constant volume method and vapour jackets to obtain definite temperatures

(2) The results have been compared with the work of previous observers, and Sutherland's formula shown to be strictly obeyed over the range considered, and a value of 118 obtained for his constant

Free Motion in the Wave Mechanics

By Prof C G Darwin, F R S

(Received October 25, 1927)

The present work is a discussion of a number of simple problems of the free motion of electrons and atoms from the point of view of the wave mechanics The author has had the advantage of many conversations with Prof N Bohr on the subject, and it was composed under this inspiration Bohr* has recently published his views on the foundations of the theory, and it would be out of place to enter here deeply into the matter, but some review of principles is unavoidable if the technical processes are to be understood Perhaps the chief point of the work is to show how a simple, even old-fashioned, technique is entirely adequate to deal with these very new problems

§ 1 *General Principles*

The matrix and the wave mechanics have both been already developed to great lengths as a calculus of stationary states, but they have not yet got so far in what we may call dynamics, a description of the *progress* of events More and more complicated phenomena have been fitted into the same scheme, but not much has been done in making this scheme intuitively understandable One of the most important contributions is a recent work by Heisenberg,† who develops an " uncertainty relation " by showing how each observation of a system, say an electron, always itself introduces some disturbance, so that the exact state at the beginning of each new experiment is essentially unknowable Heisenberg works from the matrix point of view, but Bohr has pointed out that the " uncertainty relation," exhibited by Heisenberg simply as an experimental result, becomes quite natural on wave principles, and is indeed nothing more than an expression of those principles

The central difficulty of the quantum theory has always been the conflict between waves and particles On the one hand, we have the theorems of conservation of matter, energy, etc , these tell us that matter keeps together, and endow a particle or a quantity of energy with individuality, so that we can trace its history On the other hand, we have the theorems of interference—of light and now of matter as well, which as definitely tell us that the things which we before regarded as particles must spread, and so must lose their individuality The recent work of Bohr explains, at any rate in outline, how the apparent contradiction is to be reconciled The two lines of thought are not contradictory, but complementary They do not come into conflict because they never meet To verify conservation we must obviously have an enclosed system, and this excludes observation of what happens in the enclosure If nothing is observable, it is only proper to say that nothing is happening, the system is settled into a spaceless and timeless stationary state outside our intuitions On the other hand, if we want to observe what happens we must make a hole in the enclosure and see what leaks out By the very act conservation is destroyed, but in exchange we get interference phenomena, and these introduce geometry and so a connection with space and time This very inadequate description shows that we are entitled, when we want to discuss happenings in space and time, to make full use of the wave theory and to pay no attention to the conservation difficulties, because in fact these do not arise

---

* Transactions of Volta Centenary Congress at Como (1927)

† 'Z f Physik,' vol. 43, p. 172 (1927)

It is almost impossible to *describe* the result of any experiment except in terms of particles—a scintillation, a deposit on a plate, etc —and this language is quite incompatible with the language of waves, which is used in the solution A necessary part of the discussion of any problem is therefore the translation of the formal mathematical solution, which is in wave form, into terms of particles We shall call this process the *interpretation*, and only use the word in this technical sense

The general treatment of a problem will then fall into three stages First there is the solution of the appropriate wave equation with the appropriate initial conditions This gives a Schrödinger function (in general complex) at every time and value of the co-ordinates Next we multiply this by its conjugate When dealing with electrons this quantity is usually called the electric density, but it seems better to have a more general name and one not possessing such definite connotations We shall call it the *intensity*, extending the meaning, already usual for light and sound, to cover material waves as well Lastly, there is the *interpretation*, when we say that the intensity of the wave is a measure of the probability that a particle will be observed This stage is to be regarded rather as a concession to our ingrained habits of thought than as an essential part of the problem

As long as they were both concerned only with stationary states, the matrix and wave methods were equivalent and only differed in mathematical convenience But when the time enters into the question an important distinction arises, for the solution of the wave equation suggests, and our type of problem requires, that we should not merely take a single solution of the equation, but that we should build up one by superposition of an infinite number of separate solutions each of which corresponds to a stationary state It is a great merit of the wave theory that it *invites* this superposition, with matrices the corresponding generalisation does not suggest itself, and has indeed hardly been used *

Now the admissibility of superposition has important consequences in changing our physical outlook In the older quantum theory we made the interpretation at the beginning of the discussion, so that a stationary state meant an orbital motion and it was therefore axiomatic that an atom could only be *in one* state at a time But *now we only make the interpretation* when some effect is actually observed, and there is no reason why the atom should not be in several states simultaneously, for a stationary state is merely a solution of the wave equation that happens to be harmonic in the time We are excluding questions of the emission of radiation (though perhaps the most important and difficult of the whole quantum theory) and shall take as our guiding principle that the interpretation is to be delayed as long as possible For example, in the Stern-Gerlach experiment we do not say that the field splits the atoms into two groups and then separates these *We say that a wave goes through* the field, and when we calculate its intensity at the terminal plate we find that it has two maxima, which we then interpret as two patches of atoms With the simple Stern-Gerlach experiment either way of regarding the matter leads to the same result, but experiments can easily be devised which would discriminate between them Consider a stream of silver atoms going along the direction of x These atoms go through a non-uniform field which polarises them along the direction $\pm y$ and a slit is arranged so that only the $+y$ ones emerge These then enter a uniform field along z *According to the* older theory this will instantaneously split them into two groups pointing along $\pm z$, and if, after emerging from this field, they enter another non-uniform field along y, they will again be split into two groups along $\pm y$, and so will produce two patches on the terminal plate But when superposition is allowed the matter is different, for (as we shall see in § 9) in the uniform field the atoms simply precess round z at the same rate as given in classical mechanics Suppose this field to be so long that the total angle of precession is 180° Then on entering the second non-uniform field they will all be pointing along $-y$, and there will be only one patch on the terminal plate On the principle of superposition it is this that we shall expect to observe

---

* Heisenberg's wave packet (*loc. cit*, p 188) makes use of it, but this is practically a wave method. It also perhaps occurs in Dirac's work, but the language is so different that the relationship is hard to trace.

We must now consider the interpretation in more detail, and shall see that rather different things are included under the same name The solution of any problem takes the following course—one degree of freedom will suffice for illustration We first solve the wave equation and find a function $\psi(q, t)$ which conforms to some initial prescribed form, say $\psi(q, o) = f(q)$ From this we construct the intensity $\rho(q, t) = |\psi(q,t)|^2$, and then we have to begin to think of particles Now when we think of a particle, we are almost forced to think of a position in space, so our most primitive principle of interpretation must be connected with co-ordinates representing something in space, say x, the position of a free electron (or the centre of gravity of an atom, but not the position of an electron in an atom) In such a case we take as our principle that the intensity $\rho(x, t)$ is interpreted as giving probability $\rho(x, t)\,dx \Big/ \int_{-\infty}^{\infty} \rho(x, t)\,dx$ that the electron will be in the range from x to $x + dx$ at the time t It is perhaps a matter of taste whether we regard this as an observed rule by which the wave theory is verified, or a definition of what we mean by a particle, or even as a definition of what we mean by space

By making use of Heisenberg's "γ-ray microscope" we may include under the conception of observable quantities the position of an electron in an atom Hence we may extend the relation of intensity with probability to such co-ordinates, saying that $\rho(q, t)\,dq \Big/ \int \rho(q, t)\,dq$ measures the probability of the particle being in the range dq at q, even though this co-ordinate is only brought into space by such a highly impracticable process as the microscope A problem of this kind is discussed in § 8

There is yet another form in which the interpretation has to be made—in fact, that which has been most used in the subject—and this is in determining the probability that the atom is in some *one* stationary state Compared to our previous interpretation this is a cross-classification, and the distinction is best appreciated by considering the analogy of light The intensity of light can be regarded in two different ways, either by measuring the density of electro-magnetic energy at a point and so giving the intensity at that point, or else by making a spectral analysis, not now at a point but in a region of space, and determining the distribution of energy in the spectrum The former process is analogous to that which we have discussed, and the latter to the analysis into stationary states In the optical case the two methods of analysis are united mathematically by equating together expressions for the whole energy in the region, one of which gives it as an integral over the volume, and the other over the frequencies of the spectrum , then the element of the volume integrand is the intensity at a point, and that in the frequency integrand is the spectral intensity The essential point is that we equate two integral expressions and then pick out terms from the integrands, and this is the method we must pursue here In a system having stationary states the wave solution takes the form

$$\psi(q, t) = \sum_n c_n \psi_n(q)\, e^{-i\frac{2\pi}{h}W_n t},$$

where the functions ψ_n are all mutually orthogonal The integrated intensity will be

$$\int \rho(q, t)\, dq = \int \sum_n \sum_m c_n c_m^* \psi_n(q)\, \psi_m^*(q)\, e^{-i\frac{2\pi}{h}(W_n - W_m)t}\, dq$$
$$= \sum_n |c_n|^2 \int |\psi_n(q)|^2\, dq$$

by virtue of the orthogonality of the ψ_n's We now pick out the term connected with the nth state and say that this is the probability of the atom being in the nth state If the ψ's are normalised to unity, we have $|c_n|^2/\sum_n |c_n|^2$ Incidentally we see why it is so convenient to use normalised functions for stationary states , when considering intensity at a point on the other hand, normalisation would merely consist in multiplying the whole solution by a constant and is quite trivial

In dealing with the interpretation we have touched on one of the great difficulties which have made it hard to gain physical insight into the wave theory This is the fact that the wave equation is not in ordinary space but in a co-ordinate space, and the question arises how this co-ordinate space is to be transcribed into ordinary space It would appear that most of the difficulty has arisen from an attempt to apply it illegitimately to enclosed systems, which are really outside the idea of space In most of the problems we shall discuss the question hardly arises, but where it does the correct procedure is so obvious that there is no need to deal with it in advance It is tempting to believe that this will be found to be always the case

The problems of the present work have been mostly chosen as being the simplest possible, and the methods are almost wholly those of the classical wave theory As to physical content, there is a very close relationship with the work of Dirac† and Heisenberg, but the language is so different that it would not be profitable to trace the connections Following these other methods Kennard* has recently solved some of the same problems, and it is hardly necessary to say has obtained the same results

---

† 'Roy. Soc Proc ,' vol. 113, p. 621 (1927), etc

§ 2 *The Description of Motions*

Our whole outlook on any problem will, of course, be very different from that to which dynamics have accustomed us, and the old habit of thought is so ingrained that it may not be amiss to examine the difference more closely Thus when we thought of a stream of electrons, we might, for example, have described it by assigning at every point a distribution of velocities, say Maxwellian, round a certain mean velocity But now all individuality is lost and we think of each electron as itself possessing the whole Maxwellian distribution It is thus indifferent whether we speak of one electron or of a stream † If we attempt to contradict this by saying that experiments have been made which prove that the distribution is real, in that some electrons are observed to have velocity higher than the average and some lower, the answer is that the observing instrument has itself created these different velocities, in just the same way as a spectroscope creates coloured light out of white

Again, consider the free motion of an electron As a particle it moves along a *line*, but the wave solution is a set of plane waves without any special line for the motion This is in conformity with the "uncertainty relation" which, when the direction of motion is accurately given, refuses to define the line of motion at all Now in all practical problems some sort of spatial limitation is imposed, and to see how this is to be done here we may profitably turn to the analogous case of optics

It is often possible to separate optical problems into two parts, which we may call the wave problem and the ray problem respectively In the wave problem an unlimited wave can be used to give the general features of the result, and the question of the limitation of the beam by slits, etc , can be introduced later in determining such things as the resolving power of the instrument This second part—sometimes called the "theory of optical instruments"—often does not arise or else is very simple and so it tends to be forgotten that it is quite as essential as the first part This neglect is due to the character of the experiments with which optics have been concerned during the last century, more importance has come to be attributed to the interference fringes seen through a half-wave plate than to the fact that things look double when seen through a crystal Now the wave aspect of *matter* is a century behind that of light, and so the class of experiments that have hitherto been done with electrons have not called into play any such complicated interference phenomena For this reason the ray problem—depending on the limitation of beams—is for electrons quite as important as the wave problem But that is not all, for electrons have the complication that the wave velocity depends very strongly on the wave-length, so that group velocity is a very important consideration, and the actual motion of rays cannot be directly seen even qualitatively from the solution of the wave problem without a proper consideration of the limitation of the beam It thus proves more convenient not to attempt to separate the problem into two parts, but to construct solutions of the wave equation which contain the limitations *ab initio* With this method all that remains of the ray problem is merely the derivation of the intensity from the amplitude by squaring its modulus

---

* 'Z f Physik,' vol. 44, p 326 (1927)

† If, regarded as particles, the electrons are so close together that they influence one another's motions, then the wave equation will not be reducible to a set of independent equations for each of them The system would not be in space, and the method of observation must be described before anything can be said about their relationship to space In the present paper such very dense streams are excluded.

The first attack on a problem of this kind is due to Schrödinger,* who constructed a "wave packet" for a harmonic oscillator This is exactly the sort of thing we require, but his packet is a very exceptional case without general application In experiments a beam of electrons is usually limited by passing through a slit, but this gives rise to rather troublesome Fresnel diffraction formulæ and so is not mathematically very convenient For the most part we shall make use of a different limitation, which was introduced by Heisenberg In the language of particles he supposes that the uncertainty of position is given by a Gaussian error function, corresponding to this we shall look for solutions in which the electron wave is located in a region of space defined by an error function The chief reason for its use is mathematical convenience, as there is no other form which yields simple mathematical functions for solutions, but in many cases it can be justified physically For example, if electrons are emitted by a hot filament, their velocities should have a Gaussian distribution, which will be represented in the wave theory by waves of which the amplitude contains an error function Again, if we determine the position of an electron by means of Heisenberg's "microscope," we shall make an error in fixing it, and may invert the probability and attribute this error to the uncertainty relation, and so adopt the error function for the limitation on the initial position of the electron

---

* 'Naturwissenschaften,' vol. 14, p. 664 (1926)

In this connection one feature of the present processes perhaps deserves mention, because of its difference from what we are accustomed to in dynamics There we think of a particle describing a trajectory and can take any point of the trajectory indifferently as starting point of the motion But in the wave theory the experimental conditions always mark out some special position, say a slit, as starting point, and at other places the waves will have spread Thus, unlike the case of dynamics, we do not expect to get a solution in which the starting point is quite indifferent

When de Broglie first developed his wave theory he based it largely on the help of relativity The consequence is that the wave velocity of an electron is much greater than the velocity of light This is ultimately correct of course, but it is an unnecessary complication always to have to consider relativity in dealing with quite slow motions We shall throughout the present work avoid doing so by taking a factor $e^{-i\frac{2\pi}{h}mc^2t}$ out of our wave functions, which is done by a simple and familiar modification of the wave equation We shall, of course, get quite a different value for the wave velocity from that of de Broglie To borrow an analogy from the practice of wireless telephony, we are observing our waves with the help of a heterodyne frequency mc^2/h, and when we speak of the phase of a wave we mean the phase of the sound heard in the telephone, not that of the æthereal vibrations

§ 3 *Methods of Solution*

There is no new principle in deriving the wave equation If the Hamiltonian of our system is $H(\quad q_s \quad p_s \quad)$ we set down as wave equation†

$$H\left(\quad q_s \quad \frac{h}{2\pi i}\frac{\partial}{\partial q_s} \quad\right)\psi = -\frac{h}{2\pi i}\frac{\partial\psi}{\partial t}$$

In doing this we need not consider the question of the order of operations in H, because it does not arise in any of our problems We suppose that ψ is given for every value of the q's at $t = 0$, and the solution of the wave problem consists in finding its value everywhere at any other time We next have the ray problem We take the conjugate complex quantity ψ^* and form

$$\psi\psi^* = \rho(\quad q_s \quad t),$$

---

† In practical work I can strongly recommend the convenience of taking $h = 2\pi$ This was used throughout the present work, saves a great deal of writing, and reduces the use of Fourier integrals to the standard form. It is easy to restore h at the end by dimensional principles.

which is the intensity, a real function of the time and co-ordinates Lastly, we have the interpretation, when we change our language and speak of particles instead of waves and probabilities instead of intensities.

To come to details, we will treat of one degree of freedom We take the system

$$H(x, p) = \tfrac{1}{2}p^2 + V(x) \tag{3 1}$$

The associated wave equation is

$$\frac{1}{2}\left(\frac{h}{2\pi i}\right)^2 \frac{\partial^2}{\partial x^2}\psi + V(x)\,\psi = -\frac{h}{2\pi i}\frac{\partial\psi}{\partial t} \tag{3 2}$$

We need as solution a function $\psi(x, t)$ which at time $t = 0$ is a given complex function $f(x)$ The best methods of solving make use of Fourier integrals in a variety of ways which we must consider Put

$$\psi(x, t) = \int e^{i\frac{2\pi}{h}Wt}\,\psi(x, W)\,\phi(W)\,dW, \tag{3 3}$$

where $\phi(W)$ is undetermined The integration goes from $-\infty$ *to* ∞ Throughout the paper we shall imply these limits without writing them in the integrals Then $\psi(x, W)$ must satisfy Schrodinger's original equation

$$H\left(x, \frac{h}{2\pi i}\frac{\partial}{\partial x}\right)\psi = W\psi \tag{3 4}$$

The functions $\psi(x, W)$ constitute a complete mutually orthogonal set of functions, either with W arbitrary or having a discrete set of proper values We shall chiefly be concerned with the case where W may be continuous and shall assume this, though the other case works just as well The function $\psi(x, W)$ need not be normalised, but is to be selected as a continuous function of W The initial condition is

$$f(x) = \int \psi(x, W)\,\phi(W)\,dW, \tag{3 5}$$

and by the orthogonal property we can determine

$$\phi(W) = \int f(x)\,\psi^*(x, W)\,dx \Big/ \iint \psi(x, W')\,\psi^*(x, W)\,dW'\,dx$$

(3 3) then gives $\psi(x, t)$ by writing in the value of $\phi(W)$ We can then at once set down the intensity and make the interpretation

The functions $\psi(x, t)$ and $\psi(x, W)$ contain as variables the dynamically conjugate quantities t and W and are related together by the Fourier integral (3 3) A similar process can be applied for any other conjugate pair and is very useful For example, set

$$\psi(x, t) = \int e^{i\frac{2\pi}{h}px}\,\psi(p, t)\,dp \tag{3 6}$$

Here p has been introduced simply as the variable of a Fourier integral, and this is all that momentum really is in the wave mechanics , but we can connect it formally with the dynamical momentum by considering that

$$\frac{h}{2\pi i}\frac{\partial}{\partial x}\psi(x, t) = \int e^{\frac{2\pi}{h}px}\,\psi(p, t) \quad p \quad dp$$

It is easy to show that $\psi(p, t)$ obeys a wave equation which is obtained by interchanging the roles of co-ordinate and momentum in the Hamiltonian

More useful than the function $\psi(p, t)$ is the function $\psi(p, \mathrm{W})$ defined by

$$\psi(x, t) = \iint e^{i\frac{2\pi}{h}(px - \mathrm{W}t)}\,\psi(p, \mathrm{W})\,dp\,d\mathrm{W}, \tag{3 7}$$

since it gives a most convenient way of solving the wave equation in many problems If we substitute (3 7) in (3 2) we get

$$\iint e^{i\frac{2\pi}{h}(px - \mathrm{W}t)}\,\psi(p, \mathrm{W})\,\{\mathrm{H}(x, p) - \mathrm{W}\}\,dp\,d\mathrm{W} = 0, \tag{3 8}$$

an integral equation that can be set down at once from the Hamiltonian without even writing out the wave equation It is often easy to solve and in many cases gives the solution in its most convenient form

Consider, for example, the case of a free electron in one dimension— $\mathrm{H} = \frac{1}{2m}p^2$ Then for each value of p in the integral choose $\mathrm{W} - \frac{1}{2m}p^2$ and (3 8) will be satisfied This means that we are to omit the W integration in (3 7) and write

$$\psi(x, t) = \int e^{i\frac{2\pi}{h}\left(px - \frac{p^2}{2m}t\right)}\,\phi(p)\,dp, \tag{3 9}$$

where $\phi(p)$ is arbitrary We shall take this as the standard form of the solution The verification that it satisfies the wave equation is immediate

A more complicated example is that of uniformly accelerated motion, say,

$$\mathrm{H} = \frac{1}{2m}p^2 - mgx \tag{3 10}$$

Pursuing the same course we take (3 7) as solution, where now

$$\iint e^{i\frac{2\pi}{h}(px - \mathrm{W}t)}\,\psi(p, \mathrm{W})\left\{\frac{1}{2m}p^2 - mgx - \mathrm{W}\right\}dp\,d\mathrm{W} = 0$$

We integrate the term in mgx by parts, so as to remove the x, and reject the integrated term by assuming that the disturbance vanishes for infinite values Then we have

$$\iint e^{i\frac{2\pi}{h}(px - \mathrm{W}t)}\left\{\left(\frac{1}{2m}p^2 - \mathrm{W}\right)\psi(p, \mathrm{W}) + \frac{h}{2\pi i}mg\frac{\partial\psi}{\partial p}\right\}dp\,d\mathrm{W} = 0$$

The factor in brackets vanishes if

$$\psi(p, W) = e^{i\frac{2\pi}{h}\left(\frac{W}{mg}p - \frac{1}{6}\frac{p^3}{m^2g}\right)}\phi(W) \qquad (3\ 11)$$

with $\phi(W)$ arbitrary So we have

$$\psi(x, t) = \iint e^{i\frac{2\pi}{h}\left(px - Wt + \frac{Wp}{mg} - \frac{1}{6}\frac{p^3}{m^2g}\right)}\phi(W)\,dp\,dW \qquad (3\ 12)$$

If we solved for $\psi(x, W)$ directly we should find it a troublesome function, of which even the asymptotic approximations are quite inconvenient We shall see that the whole problem of accelerated motion can be treated by the present method without any discussion of this function

The method is, of course, always available, but does not always lead to the simplest solution For example, in the case of a harmonic oscillator Schrodinger's direct solution for $\psi(x, W)$ is just as good, as is evident because, for $H = \frac{1}{2}p^2 + \frac{1}{2}\omega^2x^2$, the wave equation in the p-space will have the same form as in the x-space Nevertheless, similar methods are often useful For example, in Schrodinger's original solution for the hydrogen atom the substitution

$$\psi(r, \theta, \phi, t) = S_k(\theta, \phi)\, r^k \int e^{i\frac{2\pi}{h}(pr - Wt)}\phi(p, W)\,dp\,dW$$

leads immediately, by means of one integration by parts, to the Laplacian method of solution used by Schrodinger himself

§ 4 *Electrons under No Forces, One Dimension*

The free motion of an electron in one dimension has already been disposed of by Heisenberg from the point of view of matrices His process does not have much direct cognizance of phases, and so can to some extent take short cuts by not working out these unobservable quantities, but this advantage is outweighed by the much more difficult ideas involved

We take $H = \frac{1}{2m}p^2$ and have seen that the solution is in the form (3 9) Following Heisenberg, we suppose that the initial disturbance is given by a "wave packet" of the form

$$f(x) = \exp\left[-\frac{1}{2\sigma^2}(x - x_0)^2 + i\frac{2\pi}{h}mv(x - x_0)\right] \qquad (4\ 1)$$

The initial intensity thus is

$$\rho(x, 0) = e^{-\frac{1}{\sigma^2}(x - x_0)^2} \qquad (4\ 2)$$

Making the interpretation, this measures the relative probabilities for the initial position of the electron, and we may conveniently express it by saying that the electron is at $x_0 \pm \sigma$ The complex part of (4 1) has been chosen so that the velocity is nearly v, as we shall see

To determine $\phi(p)$ we have

$$\int e^{i\frac{2\pi}{h}px}\,\phi(p)\,dp = \exp\left[-\frac{1}{2\sigma^2}(x-x_0)^2 + i\frac{2\pi}{h}mv(x-x_0)\right],$$

and so inverting the Fourier integral we get

$$\phi(p) = \frac{\sigma}{h}\sqrt{2\pi}\exp\left[-\tfrac{1}{2}\left(\frac{2\pi\sigma}{h}\right)^2(p-mv)^2 - i\frac{2\pi}{h}px_0\right] \qquad (4\ 3)$$

As we shall verify, this is interpreted as meaning that the momentum is $mv \pm h/2\pi\sigma$, using the $\pm$ sign in the same sense as above Substitute in (3 9) and carry out the integration and we get

$$\psi(x,t) = \frac{\sigma}{\sqrt{\left(\sigma^2 + i\frac{ht}{2\pi m}\right)}}\exp\left[-\tfrac{1}{2}\frac{(x-x_0-vt)^2}{\sigma^2 + i\frac{ht}{2\pi m}} + i\frac{2\pi}{h}mv\left(x-x_0-\tfrac{1}{2}vt\right)\right] \qquad (4\ 4)$$

It can, of course, be verified by direct substitution that this satisfies the wave equation *

We derive the intensity by multiplying by the conjugate and have

$$\rho(x,t) = \frac{\sigma}{\sqrt{[\sigma^2 + (ht/2\pi\sigma m)^2]}}\exp - \frac{(x-x_0-vt)^2}{\sigma^2 + (ht/2\pi\sigma m)^2}, \qquad (4\ 5)$$

so that the electron at time t is interpreted as being at

$$x_0 + vt \pm \sqrt{[\sigma^2 + (ht/2\pi\sigma m)^2]}$$

We explain this by saying that the initial position was $x_0 \pm \sigma$, and the velocity is $v \pm h/2\pi\sigma m$, so that at time t the position will be $x_0 + vt \pm \sigma \pm ht/2\pi\sigma m$, and as the two uncertainties are independent they are compounded by squares. The product of the uncertainties of co-ordinate and momentum is $h/2\pi$, which is Heisenberg's uncertainty relation Observe how the limitation on the initial position of a stream of electrons of necessity leads to an uncertainty in their velocity, and so to their "straggling" along the direction of motion

---

* The term outside the exponential is necessary in order to satisfy the wave equation, but is otherwise uninteresting. It would usually be found convenient and sufficient to drop it. In the present work it has, however, been usually retained for the sake of completeness

We may write (4 4) (omitting the first factor) as

$$\exp\left[-\tfrac{1}{2}\frac{(x-x_0-vt)^2}{\sigma^2+(ht/2\pi\sigma m)^2}\left\{1-i\frac{ht}{2\pi\sigma^2 m}\right\}+i\frac{2\pi}{h}mv\left(x-x_0-\tfrac{1}{2}vt\right)\right] \quad (4\ 6)$$

The imaginary part describes the phase For a short time the quadratic term will be small and so the planes of zero phase will be given by $x = x_0 + \frac{1}{2}vt + n\dfrac{h}{mv}$ for integral values of n, that is to say, the phase velocity is half the ray velocity Later the phase becomes more confused on account of the quadratic terms, which give a contribution like a Fresnel diffraction expression, but there does not seem any point in studying the complicated geometry of these phases until experiments are devised to bring them into evidence

The error function with which we started ceases to be one in the ordinary sense on account of the imaginary quadratic term We may conveniently from the mathematical point of view include such complex values of σ under the name of error function, and may if we like regard the motion as starting from such a complex value But, as pointed out in § 2, there is one outstanding time in the motion, that when $\sigma^2 + iht/2\pi m$ becomes purely real, which it is natural to regard as the initial time, because that is where the experimental limitation occurs, and where the straggling is less than it is either before or after

The great advantage of taking the initial disturbance $f(x)$ as given by an error function (in the extended sense) is that only so is it possible to work out the integrals completely In the general case we can put down

$$\psi(x, t) = \frac{1}{h}\int e^{i\frac{2\pi}{h}\left(px-\frac{p^2}{2m}t\right)}dp\int e^{-i\frac{2\pi}{h}p\xi}f(\xi)\,d\xi, \quad (4\ 7)$$

which gives $\psi(x, 0) = f(x)$ We can then carry out one integration and have

$$\psi(x, t) = \sqrt{\frac{m}{ht}}\,e^{-i\frac{\pi}{4}}\int e^{i\frac{\pi m}{ht}(x-\xi)^2}f(\xi)\,d\xi \quad (4\ 8)$$

It is now clear that only when $f(x)$ is an error function is the other integration simple

§ 5 *Electrons under No Forces, Three Dimensions*

An exactly similar solution holds for three dimensions If p, q, r are the components of momentum in directions x, y, z, the Hamiltonian is

$$H = \frac{1}{2m}(p^2+q^2+r^2) \quad (5\ 1)$$

and the wave equation is

$$\frac{1}{2m}\left(\frac{h}{2\pi i}\right)^2 \Delta\psi = -\frac{h}{2\pi i}\frac{\partial\psi}{\partial t} \tag{5.2}$$

The form of solution that corresponds to (3.9) is

$$\psi(x, y, z, t) = \int^{(3)} e^{i\frac{2\pi}{h}\left(px+qy+rz-\frac{p^2+q^2+r^2}{2m}t\right)} \phi(p, q, r)\, dp\, dq\, dr \tag{5.3}$$

When the initial disturbance is given we can evaluate ϕ by putting $t = 0$ and using Fourier's theorem, and can then substitute back into (5.3).

Take as initial disturbance the wave packet

$$\exp\left[-\tfrac{1}{2}\left\{\frac{(x-x_0)^2}{\sigma^2}+\frac{(y-y_0)^2}{\tau^2}+\frac{(z-z_0)^2}{\upsilon^2}\right\} + i\frac{2\pi}{h}m\{u(x-x_0)+v(y-y_0)+w(z-z_0)\}\right] \tag{5.4}$$

Then

$$\phi = \frac{\sigma\tau\upsilon}{h^3}(2\pi)^{3/2}\exp\left[-\tfrac{1}{2}\left(\frac{2\pi}{h}\right)^2\left\{\sigma^2(p-mu)^2+\tau^2(q-mv)^2 + \upsilon^2(r-mw)^2\right\} - i\frac{2\pi}{h}(px_0+qy_0+rz_0)\right] \tag{5.5}$$

and

$$\psi = \frac{\sigma\tau\upsilon}{\sigma'\tau'\upsilon'}\exp\left[-\tfrac{1}{2}\left\{\frac{(x-x_0-ut)^2}{\sigma'^2}+\frac{(y-y_0-vt)^2}{\tau'^2}+\frac{(z-z_0-wt)^2}{\upsilon'^2}\right\} + i\frac{2\pi}{h}m\{u(x-x_0-\tfrac{1}{2}ut)+v(y-y_0-vt) + w(z-z_0-\tfrac{1}{2}wt)\}\right], \tag{5.6}$$

where

$$\sigma'^2 = \sigma^2 + iht/2\pi m, \quad \tau'^2 = \tau^2 + iht/2\pi m, \quad \upsilon'^2 = \upsilon^2 + iht/2\pi m$$

There is no need for us to write out the intensity, since it too is exactly like the case of one dimension. We have got the wave representing an electron initially at $x_0 \pm \sigma$, $y_0 \pm \tau$, $z_0 \pm \upsilon$, and moving with velocity $u \pm h/2\pi\sigma m$, $v \pm h/2\pi\tau m$, $w \pm h/2\pi\upsilon m$. If $v = w = 0$, we may say that we have roughly represented a stream of electrons emitted by a hot filament so as to have uncertainty $h/2\pi\sigma m$ in their velocity, then rapidly* accelerated to velocity u, and then passed through a slit of breadth 2τ and height 2υ. From the similarity of the expressions for σ' and τ', υ' we see that the lateral scattering of the stream obeys the same rule as the longitudinal straggling.

To give a more accurate account of electrons going through a slit, we must make use of the Fresnel diffraction formulæ This is quite a classical question and need be only shortly touched on The chief way in which it differs from the diffraction of light arises from the variable wave velocity, which prevents the use of "retarded" wave functions We are compelled instead to analyse by Fourier integrals

---

* Rapidly, because otherwise they would straggle during the acceleration.

We suppose that the wave function, together with its differential along the normal, is known at every time and at every point on a closed surface S, and we have to evaluate it at any point inside S It is best to make a slightly different analysis from that which we had before, by writing

$$\psi(x, y, z, t) = \int e^{-i\frac{2\pi}{h}\frac{s^2}{2m}t}\,\psi(x, y, z, s)\,ds,$$

and using $\psi(x, y, z\ s)$ Do the same for $\frac{\partial}{\partial n}\psi(x, y, z, t)$ Then $\psi(x, y, z, s)$ and $\frac{\partial}{\partial n}\psi(x\ y\ z, s)$ are known for every value of s and at every point x, y, z on S Let $x_1, y_1\ z_1$ be the point inside S at which we require ψ and let

$$r^2 = (x - x_1)^2 + (y - y_1)^2 + (z - z_1)^2$$

Then the application of Green's theorem in the usual way gives

$$\psi(x_1, y_1\ z_1, t) = \frac{1}{4\pi}\int e^{-i\frac{2\pi}{h}\frac{s^2}{2m}t}\iint\left\{\psi(x, y, z, s)\frac{\partial}{\partial n}\frac{e^{i\frac{2\pi}{h}sr}}{r}\right.$$
$$\left. - \frac{e^{i\frac{2\pi}{h}sr}}{r}\frac{\partial}{\partial n}\psi(x, y, z, s)\right\}dS$$

This formula makes it easy to work out the effect of a slit or grating by suitable choice of the surface S We shall not enter into the matter beyond noting that, just as for light, so here, when S is a plane, we get a factor i representing the quarter wave-length change necessary to give the Huyghenian wave construction, and a factor $1 + \cos\theta$ (θ being the angle of deviation of the rays) which explains why the wave construction excludes a transmission of the wave backwards

§ 6 *Electrons under Constant Electric Force*

Our purpose is partly the illustration of a variety of methods, and so we shall treat of the motion of an electron under uniform acceleration in two different ways, the first of which is the more general application of principle, but not quite so simple mathematically It will suffice to consider the motion in one dimension, as the three can be treated independently

We take (3 12) as the form of solution, and (4 1) as initial disturbance $\phi(\mathrm{W})$ is then determined from

$$\iint e^{i\frac{2\pi}{h}\left(px+\frac{\mathrm{W}p}{mg}-\frac{1}{6}\frac{p^3}{m^2g}\right)}\phi(\mathrm{W})\,dp\,d\mathrm{W}$$
$$=\exp\left[-\frac{1}{2\sigma^2}(x-x_0)^2+i\frac{2\pi}{h}mv(x-x_0)\right]$$

by two inversions (involving multiplication by $e^{-i\frac{2\pi}{h}qx}$ and integration for x, and by $e^{-i\frac{2\pi}{h}\left(\frac{\mathrm{W}}{mg}q-\frac{1}{6}\frac{q^3}{m^2g}\right)}$ and integration for q respectively) We get

$$\phi(\mathrm{W})=\frac{\sigma\sqrt{2\pi}}{h^2mg}\int\exp\left[-\tfrac{1}{2}\left(\frac{2\pi\sigma}{h}\right)^2(q-mv)^2\right.$$
$$\left.-i\frac{2\pi}{h}\left(\frac{\mathrm{W}q}{mg}-\frac{1}{6}\frac{q^3}{m^2g}+qx_0\right)\right]dq \qquad (6\ 1)$$

If this is substituted in (3 12) the integrations can be carried out in the order W, p, q The result is

$$\psi(x,t)=\frac{\sigma}{\sqrt{\sigma^2+iht/2\pi m}}\exp\left[-\tfrac{1}{2}\frac{(x-x_0-vt-\frac{1}{2}gt^2)^2}{\sigma^2+iht/2\pi m}\right.$$
$$\left.+i\frac{2\pi}{h}\{mv(x-x_0-\tfrac{1}{2}vt-\tfrac{1}{2}gt^2)+mgt(x-\tfrac{1}{6}gt^2)\}\right] \qquad (6\ 2)$$

The intensity is

$$\rho(x,t)=\frac{\sigma}{\sqrt{[\sigma^2+(ht/2\pi\sigma m)^2]}}\exp-\frac{(x-x_0-vt-\frac{1}{2}gt^2)^2}{\sigma^2+(ht/2\pi\sigma m)^2}$$

We thus see that the ray goes from $x_0\pm\sigma$ to $x_0+vt+\frac{1}{2}gt^2\pm\sigma\pm ht/2\pi\sigma m$, giving the ordinary formula for accelerated motion, and a straggling exactly the same as that of unaccelerated notion The phase obeys a rather complicated rule, and is of no direct importance, though its various terms are required in order that the wave equation may be satisfied by (6 2) If there were a grating, placed, say, at 45° to the vertical, and if we wished to know the positions of the diffraction maxima after the falling electrons had passed through it, these terms would have to be considered, but such a case is too remote to discuss at present

Though the above is the most general method of dealing with accelerated motion, it has the disadvantage that g occurs in the denominator, so that the transition to the case of no acceleration is troublesome The second method is free from this difficulty, being, loosely speaking, an approximative method which happens to give an accurate solution. We look for a solution in the form

$$\psi(x, t) = \int e^{i\frac{2\pi}{h}\left(px - \frac{p^2}{2m}t\right)} \phi(p, t)\, dp \tag{6 3}$$

Substitute in the wave equation and we have

$$\int e^{i\frac{2\pi}{h}\left(px - \frac{p^2}{2m}t\right)} \left\{ -mgx\phi + \frac{h}{2\pi i}\frac{\partial\phi}{\partial t}\right\} dp = 0$$

Integrating the term in x by parts we get

$$\int e^{i\frac{2\pi}{h}\left(px - \frac{p^2}{2m}t\right)} \left\{ \frac{h}{2\pi i}\frac{\partial\phi}{\partial t} + \frac{h}{2\pi i} mg \frac{\partial\phi}{\partial p} - gpt\phi\right\} dp = 0 ,$$

and so the equation is satisfied if we take

$$\frac{\partial\phi}{\partial p} + \frac{1}{mg}\frac{\partial\phi}{\partial t} = \frac{2\pi i}{h}\frac{pt}{m}\phi, \tag{6 4}$$

of which the solution is

$$\phi(p, t) = \chi(p - mgt)\, e^{i\frac{2\pi}{h}\left(\frac{1}{2}gpt^2 - \frac{1}{6}mg^2t^3\right)} \tag{6 5}$$

with χ arbitrary The initial value (4 1) at once determines

$$\gamma(p) = \frac{\sigma}{h}\sqrt{2\pi}\,\exp\left[-\tfrac{1}{2}\left(\frac{2\pi\sigma}{h}\right)^2 (p - mv)^2 - i\frac{2\pi}{h}px_0\right]$$

We change p into $p - mgt$ in this and substitute in (6 5) and then the integration of (6 3) immediately leads to (6 2)

If the acceleration varies slowly, either with time or place, a solution can be constructed by piecing together solutions for regions within which the acceleration is sensibly constant , but we shall not enter into this more complicated question If the variation of force is so rapid as to give perceptible differences within the region of the wave packet, the motion will differ from that predicted by classical mechanics The approximative method would then fail and it would be necessary to find a true solution of the wave equation

§ 7 *Electrons under Constant Magnetic Force*

In a uniform magnetic field we have of course to show that an electron describes a circle with angular velocity twice the Larmor rotation, and for this purpose the terms in the square of the magnetic force are essential, just as they are in the particle problem Taking p, q, r as the momenta and ω as the Larmor rotation about z (magnetic force $= 2mc\omega/e$), we have

$$\mathrm{H} = \frac{1}{2m}(p^2 + q^2 + r^2) + \omega(xq - yp) + \tfrac{1}{2}m\omega^2(x^2 + y^2), \tag{7 1}$$

so that the wave equation is

$$\frac{1}{2m}\left(\frac{h}{2\pi i}\right)^2 \Delta\psi + \omega\frac{h}{2\pi i}\left(x\frac{\partial}{\partial y} - y\frac{\partial}{\partial x}\right)\psi + \tfrac{1}{2}m\omega^2(x^2+y^2)\,\psi = -\frac{h}{2\pi i}\frac{\partial\psi}{\partial t} \qquad (7\ 2)$$

The solution is best found by transforming to rotating axes Put

$$\left.\begin{aligned} x &= x'\cos\omega t' - y'\sin\omega t' \\ y &= y'\cos\omega t' + x'\sin\omega t' \\ t &= t' \end{aligned}\right\}, \qquad (7\ 3)$$

and we get

$$\frac{\partial}{\partial t'} = \frac{\partial}{\partial t} + \omega\left(x\frac{\partial}{\partial y} - y\frac{\partial}{\partial x}\right) \quad \text{and} \quad \Delta' = \Delta,$$

so that the equation becomes

$$\frac{1}{2m}\left(\frac{h}{2\pi i}\right)^2 \Delta'\psi + \tfrac{1}{2}m\omega^2(x'^2+y'^2) + \frac{h}{2\pi i}\frac{\partial\psi}{\partial t'} = 0 \qquad (7\ 4)$$

The solution separates into products of functions of x', y', z That of z is like the motion without field and represents a gradual spreading of the wave along the direction of the magnetic field It calls for no further comment On the other hand, the motion in x' and y' differs from those we have so far considered in that the proper values are discontinuous Let

$$\mathrm{F}_u(z) = e^{\frac{z^2}{2}}\left(\frac{d}{dz}\right)^u e^{-z^2}, \qquad (7\ 5)$$

so that

$$\frac{d^2}{dz^2}\mathrm{F}_u(z) = [z^2 - (2u+1)]\,\mathrm{F}_u(z)$$

Then our solution can be written as

$$\psi = \sum_{u\ v} \mathrm{A}_{u\ v}\,\mathrm{F}_u\left(x'\ \sqrt{\frac{2\pi m\omega}{h}}\right)\mathrm{F}_v\left(y'\ \sqrt{\frac{2\pi m\omega}{h}}\right)e^{-i(u+v+1)\omega t'}, \qquad (7\ 6)$$

where $\mathrm{A}_{u\ v}$ are arbitrary

The most important feature of this expression is that ψ is unchanged if t is increased by π/ω For consider the point in space $x_0 y_0$ At time $t = \pi/\omega$ the point which overlies it has $x' = -x_0$, and since $\mathrm{F}_u(-z) = (-)^u\,\mathrm{F}_u(z)$ we shall have

$$\mathrm{F}_u\left(x'\ \sqrt{\frac{2\pi m\omega}{h}}\right) = (-)^u\,\mathrm{F}_u\left(x_0\ \sqrt{\frac{2\pi m\omega}{h}}\right)$$

Similarly for y, and the last factor in (7 6) gives another factor $(-1)^{u+v}$, so that altogether $\psi\,(t = \pi/\omega) = \psi\,(t = 0)$ for all values of x, y Thus, unlike the case of free motion without field, there is no progressive spreading of the waves, but the wave packet returns to its original form in period π/ω The process may be described in the same way as it is for particles Schrödinger has shown that for a harmonic oscillator a wave packet can be constructed which, though it spreads in the intermediate states, always returns to its original form at each end of the swing In the $x'y'$ co-ordinates we have a harmonic oscillator, for which this will be true , but these are rotating co-ordinates, and when the packet has swung across to its extreme position on the other side, the rotation will have carried this position just round to the point from which the motion started Thus the packet will describe a circle with twice the Larmor rotation, and, though there will be a change in the form of the disturbance in intermediate positions, it will exactly return to its initial form on the completion of the circle

It is perhaps possible to evaluate the $A_{u, v}$'s for a wave packet of the Gaussian type that we have been using, but the work would be an unprofitable piece of mathematics which we shall not attempt We may, however, exhibit a special case which can easily be got by adapting Schrodinger's wave packet Put $A_{u, v} = 0$ when $v \neq 0$ and $A_{u, 0} = \frac{1}{u!}\left(-\frac{a}{2}\sqrt{\frac{2\pi m\omega}{h}}\right)^u$, and we find on changing over from x', y' to x, y that

$$\psi = \exp\left[-i\omega t - \tfrac{1}{2}\frac{2\pi m\omega}{h}\{x^2 + y^2 - 2ae^{-i\omega t}(x\cos\omega t + y\sin\omega t) + \tfrac{1}{2}a^2e^{-2i\omega t}\}\right], \quad (7\ 7)$$

an expression exactly satisfying the wave equation The intensity is

$$\rho = \exp -\frac{2\pi m\omega}{h}\{(x - a\cos^2\omega t)^2 + (y - a\cos\omega t\sin\omega t)^2 - \tfrac{1}{4}a^2\}$$

Thus the locus of greatest intensity is the circle with the points, 0, 0 and a, 0 as diameter and is described with angular velocity 2ω The packet is, however, not a very concentrated one, since ω is usually rather small If we want a packet initially concentrated in a small region, it will during the motion spread over a wide region This is interpreted by the consideration that the initial concentration corresponds to great uncertainty in the velocity, and so great uncertainty in the radius and tangent of the circle that the electron will describe The return of the packet to its original size corresponds to the fact that all these circles are described in the same time

If we are prepared to give up consideration of more than a small arc of the circle, we can treat the problem approximately by neglecting ω^2 For purposes of later reference we shall include the z motion again We then have in x', y', z a problem just like that of § 5 and can take as the solution

$$\psi(x, y, z, t) = \int^{(3)} e^{i\frac{2\pi}{h}\left(px' + qy' + rz - \frac{p^2+q^2+r^2}{2m}t\right)}\phi(p, q, r)\,dp\,dq\,dr \quad (7\ 8)$$

It will make a sufficient illustration if we take a rather simpler initial disturbance than (5 4) We take

$$\psi\,(x, y, z, 0) = \exp\left[-\frac{1}{2\sigma^2}(x^2 + y^2 + z^2) + i\,\frac{2\pi}{h}\,mvx\right] \tag{7 9}$$

Then

$$\phi\,(p, q, r) = \frac{\sigma^3\,(2\pi)^{3/2}}{h^3}\exp -\tfrac{1}{2}\left(\frac{2\pi\sigma}{h}\right)^2[(p - mv)^2 + q^2 + r^2] \tag{7 10}$$

and

$$\psi\,(x, y, z, t) = \frac{\sigma^3}{(\sigma^2 + iht/2\pi m)^{3/2}}\exp\left[-\tfrac{1}{2}\,\frac{(x' - vt)^2 + y'^2 + z^2}{\sigma^2 + iht/2\pi m}\right.$$
$$\left. + i\,\frac{2\pi}{h}\,mv\,(x' - \tfrac{1}{2}\,vt)\right]$$

or neglecting ω^2

$$\psi = \frac{\sigma^3}{(\sigma^2 + iht/2\pi m)^{3/2}}\exp\left[-\tfrac{1}{2}\,\frac{(x + y\omega t - vt)^2 + (y - x\omega t)^2 + z^2}{\sigma^2 + iht/2\pi m}\right.$$
$$\left. + i\,\frac{2\pi}{h}\,mv\,(x + y\omega t - \tfrac{1}{2}vt)\right] \tag{7 11}$$

The ray depends on the first term in the exponent The greatest intensity is at

$$x + y\omega t - vt = 0, \qquad y - x\omega t = 0, \qquad z = 0,$$

which gives approximately

$$x = vt, \qquad y = v\omega t^2, \qquad z = 0,$$

representing a velocity v and radius of curvature $v/2\omega$, that is, angular velocity 2ω The spread is just what it would be without field It is of interest to observe the second term in (7 11), which gives the phase of the wave We see that just as the wave velocity is half the ray velocity, so the wave angular velocity is half the ray angular velocity In fact, the wave turns with exactly the Larmor rotation

§ 8 *A Wave Packet in an Atom*

We shall next consider a problem that falls into a rather different category, because the motion is in an atom and has no very direct concern with space Bohr has shown that Heisenberg's uncertainty relation only applies to a free electron, and requires modification for one in an atom, where the classification is by stationary states, not by positions He considers the conjugacy of energy and time in a hydrogen atom and uses an argument from an experiment conceived in optical dispersion We require to find in which of several quantum states round about the nth the atom is, and the determination will take a certain time to do.* If W_1 is the precision with which we wish to fix the energy, and t_1 the time needed to do so, then $W_1 t_1 \sim nh$, which tends to infinity for high quantum states, whereas for a free electron $W_1 t_1 \sim h$. This theorem is in the language of particles and we shall make an inverse interpretation and discuss what is the corresponding theorem for waves.

An electron is initially concentrated near a field of force in some sort of wave packet. For example, we may imagine that by means of Heisenberg's γ-ray microscope we have detected an electron near a hydrogen nucleus in the form of a packet like (5.4) with x_0, etc., so adjusted that on the older quantum theory the particle would describe the nth circular quantum orbit. The wave will propagate itself in a determinate way, and to work this out we only require to develop the initial disturbance in a series of proper functions appropriate to the atom and associate with each of these a harmonic time factor. The phases of the time factors change at different rates, and (apart from special cases like the harmonic oscillator of Schrödinger) they will gradually fall out of step, so that they will finally be completely discoordinated. When this has happened we can no longer speak of a wave packet at all, but only of an atom possessing a number of stationary states simultaneously. Now make the interpretation. There is a certain probability of the atom being in any *one* stationary state, and as the states have different energies, the energy of the atom is uncertain. We take this uncertainty for W_1. Again, it takes some time for the packet to break up, and until it does so we cannot speak of a *single* stationary state at all. So we take for t_1 the length of time that the packet takes to become completely discoordinated. We shall then show that $W_1 t_1 \sim nh$.

We shall only deal with high quantum states, and this makes it possible to apply to the wave theory the results of general dynamics. We take the case of one degree of freedom, a co-ordinate q which is describing a librating movement, a cyclic movement goes in the same way and is rather simpler Let $H(q, p)$ be the Hamiltonian and let us suppose that the whole problem is solved according to the methods of the older quantum theory We then know the solution $S(q, J)$ of the Hamilton-Jacobi equation and can use S to define a contact transformation This introduces the angle variable w, which increases by unity every time that q describes a libration H can be expressed in terms of J without w as $W(J)$, and if $\omega = \partial W/\partial J$, the motion of the system is given by $w = \omega t + \epsilon$ The quantum states are given by $J = nh$

---

* The argument is briefly this. Consider how long an experiment with a hydrogen atom must take in order to decide whether the atom is in the nth or $(n+1)$th state. A way of deciding would be to observe the dispersion of light of such a frequency that it is below the natural frequency of the line $n \rightarrow (n-1)$ and above that of $(n+1) \rightarrow n$. Thus we must use light of which the frequency is sufficiently definite only to have a "tolerance" of amount $\Delta\nu = R\left(\frac{1}{(n-1)^2} - \frac{1}{n^2}\right) - R\left(\frac{1}{n^2} - \frac{1}{(n+1)^2}\right)$ or approximately $6R/n^4$. This requires a train containing at least $\nu/\Delta\nu$ waves, and takes a time $t_1 = 1/\Delta\nu$ to pass over the atom. With such a train we can test whether the energy is Rh/n^2 or $Rh/(n+1)^2$, that is, we can measure the energy with precision $Rh\left(\frac{1}{n^2} - \frac{1}{(n+1)^2}\right)$, or approximately $2Rh/n^3$. Thus $W_1 t_1, \sim \frac{1}{3}nh$.

The solution of the wave equation of H can be expressed asymptotically in terms of S Associated with the proper value $W(J)$ we have

$$\psi(q, W) \sim e^{i\frac{2\pi}{h}S(q\ J)} f(q)$$

By substituting in the wave equation* we can determine regression formulæ for the terms of $f(q)$ The leading term is $(\partial S/\partial q)^{-\frac{1}{2}}$, and this shows the limitation on the asymptotic series, for $\partial S/\partial q$ vanishes at the turning points of the motion of the librating particle The series is available well outside this region, where the exponent is real and negative, and well inside where the exponent is pure imaginary, but it fails near the turning points We shall not investigate this failure, but shall assume that in spite of it we may use $e^{i\frac{2\pi}{h}S(q, J)}$ as solution of the wave equation The sequence of proper functions is obtained by putting $J = nh$, and we shall write the typical one as $e^{i\frac{2\pi}{h}S_n(q)}$ In order that the coefficients in the expression for intensity may represent actual probabilities, the functions must be normalised In the present form they are so normalised with sufficient accuracy, for the modulus is unity within the range of the particle's motion and small outside, and the ranges are nearly of the same extent for all the states near the nth

Consider the expression

$$\psi(q, t) \sim \sum_m \exp\left[-\tfrac{1}{2}\alpha^2(m-n)^2 + i\frac{2\pi}{h}\{S_m(q) - S_m(q_0) - W_m t\}\right], \quad (8\ 1)$$

which satisfies the wave equation approximately When $t = 0$ every term is real at $q = q_0$, and so, if α is small, the intensity will be very great there, whereas at other places the terms nearly cut out In fact (8 1) represents a wave packet starting at q_0 We must sum the series in order to exhibit the packet, and we shall thus be able to see how it spreads until it disappears On account of the first term in the exponent only values of m near n contribute to the sum, and for these we may write

---

* We may take this to be $\frac{1}{2}\left(\frac{h}{2\pi i}\right)^2\frac{\partial^2\psi}{\partial q^2} + V(q)\psi = W\psi$

$$S_m(q) = S_n(q) + h(m-n)\frac{\partial S_n(q)}{\partial J} + \tfrac{1}{2}h^2(m-n)^2\frac{\partial^2 S_n(q)}{\partial J^2}, \text{ etc.}$$

Thus, writing w_n for $\partial S_n/\partial J$, we have

$$\begin{aligned}\psi = \sum_m \exp\Big[-\tfrac{1}{2}\alpha^2(m-n)^2 + i\frac{2\pi}{h}\Big\{&S_n(q) - S_n(q_0) - W_n t \\ &+ h(m-n)(w_n(q) - w_n(q_0) - \omega_n t) \\ &+ \tfrac{1}{2}h^2(m-n)^2\Big(\frac{\partial w_n(q)}{\partial J} - \frac{\partial w_n(q_0)}{\partial J} - \frac{\partial^2 W_n}{\partial J^2}t\Big)\Big\}\Big]\end{aligned}$$

This can now be summed by a well-known theorem of Jacobi,* and gives (apart from an unimportant term outside the exponential)

$$\psi \sim \exp\left[i\frac{2\pi}{h}\{S_n(q) - S_n(q_0) - W_n t\} - \frac{1}{2}\,\frac{(2\pi)^2\{w_n(q) - w_n(q_0) - \omega_n t\}^2}{\alpha^2 - i2\pi h\left\{\dfrac{\partial w_n(q)}{\partial J} - \dfrac{\partial w_n(q_0)}{\partial J} - \dfrac{\partial^2 W_n t}{\partial J^2}\right\}}\right] \tag{8.2}$$

Here the numerator of the second term is many-valued, and the smallest value is to be taken. The intensity is

$$\rho \sim \exp - \frac{(2\pi)^2\{w_n(q) - w_n(q_0) - \omega_n t\}^2}{\alpha^2 + \left(\dfrac{2\pi h}{\alpha}\right)^2\left\{\dfrac{\partial^2 W_n}{\partial J^2}t - \dfrac{\partial w_n(q)}{\partial J} + \dfrac{\partial w_n(q_0)}{\partial J}\right\}^2} \tag{8.3}$$

We may also express this by saying that the electron is at

$$w_n(q) = w_n(q_0) + \omega_n t \pm \frac{\alpha}{2\pi} \pm \frac{h}{\alpha}\left\{\frac{\partial W_n}{\partial J^2}t - \frac{\partial w_n(q)}{\partial J} + \frac{\partial w_n(q_0)}{\partial J}\right\} \tag{8.4}$$

Here q occurs on both sides, so that we ought really to solve the equation to determine the limits of the wave packet. If, however, h/α is fairly small, we can see how the packet will behave without doing so. Imagine that we have a γ ray microscope, with which we can detect the electron at any moment (but in conformity with Heisenberg's principle the observation can only be made once, as its disturbance will spoil the atom for later use). (8.4) then expresses the range in which we shall probably find the electron. At first it will swing to and fro through the range allowed for q in the nth quantum state, but the size of the packet will fluctuate a little on account of the term

$$\frac{h}{\alpha}\left\{\frac{\partial w_n(q)}{\partial J} - \frac{\partial w_n(q_0)}{\partial J}\right\},$$

---

* See, for instance, Whittaker and Watson, 'Modern Analysis,' p. 124.

which for a librating motion vanishes twice in every cycle.* Thus we should locate the electron rather precisely twice in the cycle and not quite so precisely at other times. If we attempted to map out the motion by the study of many similar atoms—remember that each may only be used once—we should get something very like the orbit of the particle in the *n*th state, but the discrepancies in the various determinations would be just enough to leave it open which state near the *n*th was the exact orbit represented. With the lapse of time, however, the term $\frac{h}{\alpha}\frac{\partial^2 W_n}{\partial J^2} t$ grows in importance and spreads out the region in which we may find the electron. This region will finally fill the whole range of q, and then we can no longer speak of a packet at all. To fill the whole range of q, w must be uncertain by unity and this shows that

$$t_1 = \tfrac{1}{2}\frac{\alpha}{h}\bigg/\frac{\partial^2 W_n}{\partial J^2} \tag{8.5}$$

To find the uncertainty in the energy we return to (8.1). When the phases have all become discoordinated, the intensity is simply $\sum_m e^{-\alpha^2(m-n)^2}$ and the separate terms represent then the probabilities of the atom being in each state. To define the uncertainty of the energy we naturally take a mean-square formula and have

$$(W_1)^2 = \sum_m (W_m - W_n)^2 e^{-\alpha^2(m-n)^2}\bigg/\sum_m e^{-\alpha^2(m-n)^2}$$

We write $W_n + h\,(m - n)\,\frac{\partial W_n}{\partial J}$ for W_m and replace the sum by an integral. Then

$$(W_1)^2 = \frac{1}{2\alpha^2}\left(h\,\frac{\partial W_n}{\partial J}\right)^2 \tag{8.6}$$

Thus

$$W_1 t_1 = \frac{1}{2\sqrt{2}}\,\frac{\partial W_n}{\partial J}\bigg/\frac{\partial^2 W_n}{\partial J^2} \tag{8.7}$$

This applies to any system that can be quantised. In the case of a harmonic oscillator $W = \omega J$ and $\partial^2 W/\partial J^2 = 0$, so that the wave takes an infinite time to spread. For the hydrogen atom $W = -A/2J^2$ and $W_1 t_1 = \frac{J}{6\sqrt{2}} \sim nh$. A similar form holds for any case where W is proportional to a power of J other than the first.

---

* When a non periodic motion is treated by the present method, these terms do not fluctuate but increase, and this prevents the useful application of the method to such cases.

We have only treated of one degree of freedom, as other cases are trivial. If there are two non-degenerate degrees the spreading will occur independently with regard to each, and we shall merely have to take the higher quantum number of the two for our theorem If the system is degenerate, there is no spreading between the degenerate degrees

§ 9 *Atoms in a Uniform Magnetic Field*

In considering the motion of atoms we at once meet a new problem in that the wave equation is not in ordinary space, while the observations must be interpreted in space It will suffice to consider an atom composed of one electron and one proton The wave equation will then be an equation in six variables corresponding to the three co-ordinates of each particle, but a transformation can be made which replaces these co-ordinates by X, Y, Z those of the centre of gravity, and x, y, z those of the electron relative to the proton The observation of the atom must be supposed to take place by its producing a scintillation like an α-particle, or being deposited on a plate as in the experiments of Stern and Gerlach, and this makes it easy to see how the system must be related to space, for we must obviously identify X, Y, Z with space and suppose x, y, z to be not directly observable We shall avoid irrelevant complications by only allowing the atom to be in a p-state (and indeed the p-state of lowest energy), it will be clear that this sufficiently illustrates the process Such an atom would show a Stern-Gerlach pattern of three members, viz 1, 0, — 1 Bohr magnetons

If M is the total mass and $1/m$ the sum of the reciprocals of the masses of proton and electron, the Hamiltonian is

$$\frac{1}{2\mathrm{M}}\left(\mathrm{P}^2+\mathrm{Q}^2+\mathrm{R}^2\right)+\frac{1}{2m}\left(p^2+q^2+r^2\right)-\frac{e^2}{s}, \tag{9 1}$$

where s is the distance between the particles, and P r are the momenta conjugate to X z The wave equation is

$$\left\{\frac{1}{2\mathrm{M}}\left(\frac{h}{2\pi i}\right)^2\Delta_{\mathrm{X}}+\frac{1}{2m}\left(\frac{h}{2\pi i}\right)^2\Delta_x-\frac{e^2}{s}\right\}\psi=-\frac{h}{2\pi i}\frac{\partial\psi}{\partial t}, \tag{9 2}$$

where Δ_{X}, Δ_x are the usual operators Δ, referring respectively to the co-ordinates X, Y, Z and x, y, z Consider first the equation

$$\frac{1}{2m}\left(\frac{h}{2\pi i}\right)^2\Delta_x\psi-\frac{e^2}{s}\psi=\mathrm{W}\psi \tag{9 3}$$

If we limit ourselves to the lowest p-states, we have the following solutions —

$$\mathrm{W}=\mathrm{W}_1, \quad \psi=\chi_1, \chi_0, \chi_{-1},$$

where $W_1 = -2\pi^2 me^4/4h^2$,

$$\chi_1 = (x + iy) f(s), \quad \chi_0 = z f(s), \quad \chi_{-1} = (x - iy) f(s) \tag{9 4}$$

with $f(s) = e^{-s\,2\pi^2 me^2/h^2}$

As the Stern-Gerlach experiment will show in the next section, $\chi_1, \chi_0, \chi_{-1}$ correspond to atoms with 1, 0, -1 Bohr magnetons We try as solution of

$$\psi = \chi_1\phi_1(X, Y, Z, t) + \chi_0\phi_0(X, Y, Z, t) + \chi_{-1}\phi_{-1}(X, Y, Z, t) \tag{9 5}$$

and have

$$\frac{1}{2M}\left(\frac{h}{2\pi i}\right)^2 \Delta_X\psi = -\frac{h}{2\pi i}\frac{\partial\psi}{\partial t} - W_1\psi$$

This is the equation for rectilinear motion, the term in W_1 simply giving an extra factor $e^{-i\frac{2\pi}{h}W_1 t}$ There is no need to discuss it further

Consider now the case of motion in the presence of a uniform magnetic field When the square of the field is negligible, this simply adds on a term $\omega(xq - yp)$ to the Hamiltonian, where the field is along z and of strength* $\omega\ \dfrac{2mc}{e}$ The wave equation therefore has a term $\dfrac{h}{2\pi i}\,\omega\left(x\dfrac{\partial}{\partial y} - y\dfrac{\partial}{\partial x}\right)\psi$ Since

$$\left(x\frac{\partial}{\partial y} - y\frac{\partial}{\partial x}\right)\left\{\begin{matrix}\chi_1 & & i\chi_1 \\ \chi_0 & = & 0 \\ \chi_{-1} & & -i\chi_{-1}\end{matrix}\right\}, \tag{9 6}$$

we get on substituting (9 5)

$$\frac{1}{2M}\left(\frac{h}{2\pi i}\right)^2\{\chi_1\Delta_X\phi_1 + \chi_0\Delta_X\phi_0 + \chi_{-1}\Delta_X\phi_{-1}\} + \phi_1\left(W_1 + \frac{\omega h}{2\pi}\right)\chi_1$$
$$+ \phi_0 W_1\chi_0 + \phi_{-1}\left(W_1 - \frac{\omega h}{2\pi}\right)\chi_{-1} = -\frac{h}{2\pi i}\frac{\partial\psi}{\partial t}$$

Pick out the coefficients of $\chi_1, \chi_0, \chi_{-1}$ and solve for the ϕ's Then the appropriate solution is

$$\psi = \int^{(3)} \exp i\frac{2\pi}{h}\left\{PX + QY + RZ - \frac{1}{2M}(P^2 + Q^2 + R^2)t - W_1 t\right\}$$
$$\times\ \theta(P, Q, R)\{a_1 e^{-i\omega t}\chi_1 + a_0\chi_0 + a_1 e^{i\omega t}\chi_{-1}\}\, dP\, dQ\, dR \tag{9 7}$$

The last factor only contains the internal co-ordinates which are not observed, and the first shows that the motion is rectilinear, just as before

---

* Strictly speaking, there are small mixed terms in x and X which average out, and the quantity here is not really m but $\dfrac{m_1 m_2}{m_1 - m_2}$, where m_1, m_2 are the masses of the particles

This is all that we can strictly say about the motion, and it requires a Stern-Gerlach experiment to evoke the character of the last bracket in (9 7) But, by imagining that the uniform field might be followed at will by a suitably chosen non-uniform one, we may be allowed to make an interpretation of what is not actually being observed, and we then say that the atom undergoes a uniform precession at rate ω about the z axis Consider, for example, an atom of which the original state is $(x + iz) f(s)$, which means that it has one Bohr magneton along $-y$ Then this factor must become

$$\begin{aligned}[\tfrac{1}{2}(x + iy) e^{-i\omega t} + iz + \tfrac{1}{2}(x - iy) e^{i\omega t}] f(s)&\\ = (x \cos \omega t + y \sin \omega t + iz) f(s)&\end{aligned}$$

and this expresses a magneton turning from $-y$ to x, then to $+y$, etc , with angular velocity ω Thus, as stated in § 1, the atom behaves exactly as it would in classical dynamics We may note that this gives an explanation, though very incomplete, of why the Langevin formula for magnetic susceptibility is reinstated by the wave mechanics, as shown by Van Vleck *

§ 10 *The Stern-Gerlach Effect*

To exhibit the Stern-Gerlach effect we need little more than a combination of the process of the last section with that of § 6 The wave going through the non-uniform field, like light going through a crystal, is resolved into components which are propagated differently, so that, if the field is long enough and the terminal plate far enough, the components produce separate patches on the plate

We take a pencil of atoms going along the direction of X, in a field of components 0, $-\kappa$Y, H $+ \kappa$Z This is the simplest non-uniform field satisfying the electromagnetic equations We shall suppose that H is so large that near the origin, in the region passed by the pencil, the resultant magnetic force is nearly along Z, and we shall as usual take the square of the magnetic force to be negligible The wave equation now is

$$\begin{aligned}\frac{1}{2\mathrm{M}}\left(\frac{h}{2\pi i}\right)^2 \Delta_{\mathbf{X}}\psi + \frac{1}{2m}\left(\frac{h}{2\pi i}\right)^2 \Delta_x \psi - \frac{e^2}{s}\psi&\\ + \frac{e}{2mc}\frac{h}{2\pi i}\left\{(\mathrm{H} + \kappa\mathrm{Z})\left(x\frac{\partial}{\partial y} - y\frac{\partial}{\partial x}\right)\right.&\\ \left. - \kappa\mathrm{Y}\left(\frac{\partial}{\partial x} - x\frac{\partial}{\partial z}\right)\right\}\psi = -\frac{h}{2\pi i}\frac{\partial\psi}{\partial t}& \qquad (10\ 1)\end{aligned}$$

---

* 'Phys. Rev ,' vol 29, p 727 (1927)

We follow the second method of § 6 and so take as solution

$$\psi = \int^{(3)} \exp \imath \frac{2\pi}{h}\left(\mathrm{PX} + \mathrm{QY} + \mathrm{RZ} - \frac{\mathrm{P}^2 + \mathrm{Q}^2 + \mathrm{R}^2}{2\mathrm{M}} t - \mathrm{W}_1 t\right)$$

$$\times \{\theta_1 (\mathrm{P, Q, R}, t)\, \chi_1 + \theta_0 (\mathrm{P, Q, R}, t)\, \chi_0 + \theta_{-1} (\mathrm{P, Q, R}, t)\, \chi_{-1}\}\, d\mathrm{P}\, d\mathrm{Q}\, d\mathrm{R} \tag{10 2}$$

In substituting in (10 1) we have to make use of (9 6) and also of the relations

$$\left(z\frac{\partial}{\partial x} - x\frac{\partial}{\partial z}\right)\left\{\begin{array}{lll} \chi_1 & & \chi_0 \\ \chi_0 & = - & \frac{1}{2}(\chi_1 + \chi_{-1}) \\ \chi_{-1} & & \chi_0 \end{array}\right\}. \tag{10 3}$$

We thus get

$$\int^{(3)} d\mathrm{P}\, d\mathrm{Q}\, d\mathrm{R} \exp \imath \frac{2\pi}{h} \left(\mathrm{PX} + \mathrm{QY} + \mathrm{RZ} - \frac{\mathrm{P}^2 + \mathrm{Q}^2 + \mathrm{R}^2}{2\mathrm{M}} t - \mathrm{W}_1 t\right)$$

$$\times \left\{\frac{e}{2mc}\frac{h}{2\pi\imath}\Big[(\mathrm{H} + \kappa\mathrm{Z})(\imath\theta_1\chi_1 - \imath\theta_{-1}\chi_{-1})\right.$$

$$- \kappa\mathrm{Y}\left(\theta_1\chi_0 - \tfrac{1}{2}\theta_0(\chi_1 + \chi_{-1}) + \theta_{-1}\chi_0\right)\Big]$$

$$\left. + \frac{h}{2\pi\imath}\left(\frac{\partial\theta_1}{\partial t}\chi_1 + \frac{\partial\theta_0}{\partial t}\chi_0 + \frac{\partial\theta_{-1}}{\partial t}\chi_{-1}\right)\right\} = 0$$

Integrate by parts the terms in Y and Z, and equate to zero the coefficients of the χ's and we have

$$\left.\begin{aligned} \imath\frac{\partial\theta_1}{\partial t} &= \frac{e\mathrm{H}}{2mc}\theta_1 + \frac{e\kappa}{2mc}\left[-\frac{h}{2\pi\imath}\frac{\partial\theta_1}{\partial \mathrm{R}} + \frac{\mathrm{R}}{\mathrm{M}}t\theta_1 + \frac{1}{2}\frac{h}{2\pi}\frac{\partial\theta_0}{\partial \mathrm{Q}} - \frac{\imath}{2}\frac{\mathrm{Q}}{\mathrm{M}}t\theta_0\right] \\ \imath\frac{\partial\theta_0}{\partial t} &= \frac{e\kappa}{2mc}\left[-\frac{h}{2\pi}\left(\frac{\partial\theta_1}{\partial \mathrm{Q}} + \frac{\partial\theta_{-1}}{\partial \mathrm{Q}}\right) + \imath\frac{\mathrm{Q}}{\mathrm{M}}t(\theta_1 + \theta_{-1})\right] \\ \imath\frac{\partial\theta_{-1}}{\partial t} &= -\frac{e\mathrm{H}}{2mc}\theta_{-1} + \frac{e\kappa}{2mc}\left[\frac{h}{2\pi\imath}\frac{\partial\theta_{-1}}{\partial \mathrm{R}} - \frac{\mathrm{R}}{\mathrm{M}}t\theta_{-1} + \frac{1}{2}\frac{h}{2\pi}\frac{\partial\theta_0}{\partial \mathrm{Q}} - \frac{\imath}{2}\frac{\mathrm{Q}}{\mathrm{M}}t\theta_0\right] \end{aligned}\right\}, \tag{10 4}$$

These equations differ from (6 4) in the presence of the cross-terms (those involving Q) This is due to the fact that the direction of the magnetic force varies from point to point, so that the χ's do not represent exactly the proper functions suitable to each position, and with waves, unlike particles, we cannot treat of each position separately It is physically fairly obvious that this little complication will have no effect, but to demonstrate it we must use the fact that H is great compared to the variations of the field in the region traversed by the waves If κ were to vanish we should have

$$\theta_1 = \theta_1' e^{-\imath\frac{e\mathrm{H}}{2mc}t}, \quad \theta_0 = \theta_0', \quad \theta_{-1} = \theta_{-1}' e^{\imath\frac{e\mathrm{H}}{2mc}t}$$

We form the equation for θ_1'

$$\iota\,\frac{\partial\theta_1'}{\delta t} = \frac{e\kappa}{2mc}\left(-\frac{h}{2\pi\iota}\frac{\partial\theta_1'}{\partial R} + \frac{R}{M}\,t\theta_1'\right) + \tfrac{1}{2}\ \frac{e\kappa}{2mc}\,e^{\iota\frac{eH}{2mc}t}\left(\frac{h}{2\pi}\frac{\partial\theta_0'}{\partial Q} - \iota\frac{Q}{M}t\,\theta_0'\right)$$

The last expression in this undergoes rapid fluctuations on account of the exponential factor, and if we only ask for the average of θ_1' over the period of a Larmor rotation, it will be insignificant in its effect Thus, since we only want averaged results, we may drop out from (10 4) all the cross terms, and this reduces those equations to the form (6 4), which has been solved In writing down the solution we may omit the terms in κ^2, and have

$$\left.\begin{aligned}
\theta_1 &= \theta_1^0\left(P, Q, R + \frac{e\kappa}{2mc}\frac{h}{2\pi M}\,t\right)\exp\left[-\iota\frac{eH}{2mc}\,t - \iota\frac{e\kappa}{2mc}\tfrac{1}{2}\frac{R}{M}\,t^2\right]\\
\theta_0 &= \theta_0^0\,(P, Q, R)\\
\theta_{-1} &= \theta_{-1}\left(P, Q, R - \frac{e\kappa}{2mc}\frac{h}{2\pi M}\,t\right)\exp\left[\iota\frac{eH}{2mc}\,t + \iota\frac{e\kappa}{2mc}\tfrac{1}{2}\frac{R}{M}\,t^2\right]
\end{aligned}\right\}\quad(10\ 5)$$

We take as initial disturbance

$$\psi = (a_1\chi_1 + a_0\chi_0 + a_{-1}\chi_{-1})\exp\left[-\tfrac{1}{2}\left(\frac{X^2}{\sigma^2} + \frac{Y^2}{\tau^2} + \frac{Z^2}{\upsilon^2}\right) + \iota\frac{2\pi}{h}MVX\right], \quad (10\ 6)$$

which may be taken as a stream of atoms, of arbitrary orientation given by $a_1\,a_0\,a_{-1}$, with velocity $V \pm \frac{h}{2\pi\sigma M}$ along the X-direction, passing, roughly speaking, through a slit of breadth 2τ and height 2υ By the method of (5 5) we immediately have as initial values

$$\theta_1^0 = a_1\,S, \quad \theta_0^0 = a_0\,S, \quad \theta_{-1}^0 = a_{-1}\,S,$$

where

$$S = \frac{\sigma\tau\upsilon}{h^3}(2\pi)^{3/2}\exp\ -\tfrac{1}{2}\left(\frac{2\pi}{h}\right)^2[\sigma^2(P - MV)^2 + \tau^2Q^2 + \upsilon^2R^2]$$

We change the arguments of the θ's in conformity with (10 5), substitute in (10 2) and carry out the integrations The result is

$$\begin{aligned}
\psi = \frac{\sigma\tau\upsilon}{\sigma'\tau'\upsilon'}&\exp\left[-\tfrac{1}{2}\frac{(X - Vt)^2}{\sigma'^2} - \tfrac{1}{2}\frac{Y^2}{\tau'^2} + \iota\frac{2\pi}{h}MV(X - \tfrac{1}{2}Vt) - \iota\frac{2\pi}{h}W_1t\right]\\
&\times\left\{a_1\chi_1\exp\left[-\iota\frac{e}{2mc}(H + \kappa Z)\,t - \tfrac{1}{2}\left(Z + \tfrac{1}{2}\frac{e\kappa}{2mc}\frac{h}{2\pi M}\,t\right)^2\Big/\upsilon'^2\right]\right.\\
&+ a_0\chi_0\exp\ -\tfrac{1}{2}\ Z^2/\upsilon'^2\\
&\left.+ a_{-1}\chi_{-1}\exp\left[\iota\frac{e}{2mc}(H + \kappa Z)\,t - \tfrac{1}{2}\left(Z - \tfrac{1}{2}\frac{e\kappa}{2mc}\frac{h}{2\pi M}\,t\right)^2\Big/\upsilon'^2\right]\right\}, \quad (10\ 7)
\end{aligned}$$

where $\sigma'^2 = \sigma^2 + \iota ht/2\pi\sigma M$, etc From this we form the intensity by multiplying by the conjugate and integrating over the internal co-ordinates Let $J_1 = \int^{(3)} |\chi_1|^2 \, dx \, dy \, dz$, etc , and writing σ''^2 for $\sigma^2 + (ht/2\pi\sigma M)^2$, etc , we have

$$\rho(X, Y, Z, t)$$
$$= \frac{\sigma\tau\upsilon}{\sigma''\tau''\upsilon''}\exp\left[-\frac{(X-Vt)^2}{\sigma''^2}-\frac{Y^2}{\tau''^2}\right]\left\{|a_1|^2 J_1 \exp -\left(Z+\tfrac{1}{2}\frac{e\kappa}{2mc}\frac{h}{2\pi M}t^2\right)^2\Big/\upsilon''^2\right.$$
$$+ |a_0|^2 J_0 \exp - Z^2/\upsilon''^2$$
$$\left. + |a_{-1}|^2 J_{-1} \exp -\left(Z - \tfrac{1}{2}\frac{e\kappa}{2mc}\frac{h}{2\pi M}t^2\right)^2\Big/\upsilon''^2\right\}$$

There are thus three rays, one of which accelerates upwards at rate $\frac{e\kappa}{2mc}\frac{h}{2\pi M}$, one goes straight, and one downwards also at rate $\frac{e\kappa}{2mc}\frac{h}{2\pi M}$ This acceleration corresponds to a force $\frac{e\kappa}{2mc}\frac{h}{2\pi}$ acting on a particle of mass M, and as κ is the differential of the magnetic force, this force would be called into play by attributing to the particle magnetic moment $\frac{e}{2mc}\frac{h}{2\pi}$ In fact, we have exactly the three components of the Stern-Gerlach effect as it would be observed with our atomic model

§ 11 *The Spinning Electron*

Our last problem will be the motion of the spinning or polarised electron The wave theory of this was recently developed by the present writer* for motion in an atom, but the case of free motion was deferred In a recent paper Pauli† has discussed the matter, and it will be well first to consider his results, which are rather different from those we shall have here Pauli treats the following problem An assembly of electrons are all pointing along and none away from a magnetic field The field suddenly changes in direction through angle θ Then he claims that the electrons will divide into two groups, one along and one away from the new field, and their numbers will be in the ratio $\cos^2\frac{\theta}{2} \quad \sin^2\frac{\theta}{2}$.

In the first place it is very questionable whether it is legitimate to postulate a sudden change of field To produce it we should have to construct a set of rapidly changing electromagnetic forces These could be analysed into electric waves, and if the change is to be very abrupt, some of these waves will have very high frequency It can hardly be right to make the sudden change without considering the Compton effect of these waves, which would be an elaborate business, and anyhow was not contemplated But even if we admit the sudden change, on our present view it will not split the electrons into two groups, for we have seen (with atoms) that in a uniform field they will simply precess round the axis of the new field It requires a non-uniform field to separate them, and in that case Pauli's result is valid The magnetic moment is initially $\cos\theta$, and the assembly is separated into two parts of moment ± 1, and the ratio of the intensities, or the number of the electrons, must be in the ratio $(1 + \cos\theta)\ \ (1 - \cos\theta)$

---

* 'Roy Soc Proc ,' vol. 116, p 227 (1927)

† 'Z f Physik,' vol. 43, p. 601 (1927)

The polarised electron has four wave equations We shall take these from the paper cited (equations (5 2)), but make the modification that excludes relativity This means that we remove a factor $e^{-i\frac{2\pi}{h}mc^2t}$ from the wave function, and omit terms involving $1/c^2$ The interaction between the wave components was represented by means of a vector operator U involving both electric and magnetic forces, but the electric terms are of order $1/c^2$ and so fall out here The equations are only accurate to the first order in the magnetic field, so that we must only look for solutions to this degree of precision , we have no right to follow an electron round the complete circle in a uniform magnetic field

Equations (3 1) and (5 2) of the other paper are modified to conform to the present usage If the external magnetic field has components $\frac{2mc}{e}\{\omega_1, \omega_2, \omega_3\}$ and if the operator D means

$$\frac{1}{2m}\left(\frac{h}{2\pi i}\right)^2\Delta + \frac{h}{2\pi i}\left\{\frac{\partial}{\partial t} + \omega_1\left(y\frac{\partial}{\partial z} - z\frac{\partial}{\partial y}\right)\right.$$
$$\left. + \omega_2\left(z\frac{\partial}{\partial x} - x\frac{\partial}{\partial z}\right) + \omega_3\left(x\frac{\partial}{\partial y} - y\frac{\partial}{\partial x}\right)\right\},$$

the equations are

$$\left.\begin{aligned}
&\mathrm{DX}_1 - \frac{h}{2\pi i}\,\omega_1\mathrm{X}_4 - \frac{h}{2\pi i}\,\omega_2\mathrm{X}_3 + \frac{h}{2\pi i}\,\omega_3\mathrm{X}_2 = 0\\
&\mathrm{DX}_2 - \frac{h}{2\pi i}\,\omega_2\mathrm{X}_4 - \frac{h}{2\pi i}\,\omega_3\mathrm{X}_1 + \frac{h}{2\pi i}\,\omega_1\mathrm{X}_3 = 0\\
&\mathrm{DX}_3 - \frac{h}{2\pi i}\,\omega_3\mathrm{X}_4 - \frac{h}{2\pi i}\,\omega_1\mathrm{X}_2 + \frac{h}{2\pi i}\,\omega_2\mathrm{X}_1 = 0\\
&\mathrm{DX}_4 + \frac{h}{2\pi i}\,\omega_1\mathrm{X}_1 + \frac{h}{2\pi i}\,\omega_2\mathrm{X}_2 + \frac{h}{2\pi i}\,\omega_3\mathrm{X}_3 = 0
\end{aligned}\right\} \qquad (11\ 1)$$

Of the four X's, X_1, X_2, X_3 are the components of a vector and X_4 is scalar. When there are electric forces, their potential must be added to D in the usual way, but we shall have no occasion to do so here.

The wave functions which are a solution of (11.1) have the peculiarity that they are partly indeterminate, that is to say, a number of different solutions will give results that are physically indistinguishable. In fact, equations can be set down for two fully determinate quantities f, g, and then with any fixed arbitrary constants α, β (but constants that must be transformed when the axes are changed) we can take

$$X_1 = \alpha f + \beta g,\; X_2 = i\alpha f - i\beta g,\;\; X_3 = -\beta f + \alpha g,\;\; X_4 = i\beta f + i\alpha g \quad (11.2)$$

In consequence of these relations the X's must obey the relation

$$X_1^2 + X_2^2 + X_3^2 + X_4^2 = 0 \qquad (11.3)$$

(not, be it observed $|X_1|^2$, etc.), but as long as complex quantities are retained in the wave theory, it is not easy to see a physical meaning in this relation.†

The use of f and g often abbreviates the mathematics, but if we are to endow the wave with any sort of physical reality, we must suppose that some two *things* are being carried by it; f and g are then inadmissible, because they obey a rather complicated law of transformation for changes of axes, and we cannot suppose that *things* carried by the wave have a knowledge of the axes we happen to be using. Nothing in theory as it at present stands compels us to prefer any special values of α, β, as all known conditions are satisfied anyhow, but by examining a free electron we shall see that a certain special choice is appropriate.

The equations (11.1) determine the wave amplitudes. To determine the intensity we have to form the quantity

$$\rho = X_1X_1^* + X_2X_2^* + X_3X_3^* + X_4X_4^* \qquad (11.4)$$

This measures the chance of finding the electric charge at a point. We also have to consider the magnetic moment, which is composed of two parts. The first is the magnetism due to the convection of electricity, which we may disregard as being unconnected with the spin and fully explained. The second part is the intensity of intrinsic magnetic moment and its components are proportional to

$$\mu_1 = -i\,(X_2^*X_3 - X_2X_3^* - X_1^*X_4 + X_1X_4^*), \qquad (11.5)$$

etc. These quantities should bear an absolute ratio $h/4\pi mc$ to the electron intensity, but by supposing a suitable unit of magnetic moment, we need not consider this

---

† If we simply separate the X's into real and imaginary parts, (11.3) implies that the two four vectors are of equal magnitude and perpendicular. But this does not get us much farther.

The interpretation into terms of particles brings in a slightly different conception from that which we have hitherto had, for we have four intensities now, but they are all to be interpreted as belonging to the same electron. We might, for example, have wave functions such that ρ has a maximum at a point A, whereas μ has a maximum at a different point B There is no discrepancy in this, it means that the particle is most likely to be found at A, but if it is found there its axis is rather uncertain. On the other hand, the electron is less likely to be at B, but if it is found there it is very certain how it will be pointing Thus our formulæ give just the necessary flexibility in describing the uncertainty relation for the spinning electron

With these preliminaries we may now return to the solution If there is no magnetic field, each of the four equations (11 1) is independent, apart from the condition (11 3) To represent a stream of electrons all having the same polarisation, we only require to multiply the expression (5 6) by four arbitrary constants, provided these satisfy (11 3) This suggests the possibility of giving the wave components a canonical form by a special choice of α, β in (11 2) In the motion there are two directions which are of pre-eminent importance, the direction of the polarisation, and the direction of motion, the latter must be included because, as they stand, our equations do not admit of the relativity transformation If there is any canonical form for the vector, it must be related to one or both of these directions Trial shows that it is best to consider only the polarisation, and that any solution can be brought into the form

$$X_1 = il_1 P, \qquad X_2 = il_2 P, \qquad X_3 = il_3 P, \qquad X_4 = P, \tag{11 6}$$

where P is the expression (5 6), and l_1, l_2, l_3 are real and, in order that (11 3) may hold, $l_1^2 + l_2^2 + l_3^2 = 1$ If we substitute in (11 5) we immediately see that the magnetic moment is along the line of direction cosines l_1 l_2 l_3 This special solution of the wave equations we shall call the *canonical form*

We will next apply a uniform magnetic field along z The equation (11 1) become

$$\left.\begin{aligned} DX_1 + \frac{h\omega}{2\pi i} X_2 = 0, \quad DX_3 - \frac{h\omega}{2\pi i} X_4 = 0 \\ DX_2 - \frac{h\omega}{2\pi i} X_1 = 0, \quad DX_4 + \frac{h\omega}{2\pi i} X_3 = 0 \end{aligned}\right\}, \tag{11.7}$$

where D is now

$$\frac{1}{2m}\left(\frac{h}{2\pi i}\right)^2 \Delta + \frac{h}{2\pi i}\left[\frac{\partial}{\partial t} + \omega\left(x\frac{\partial}{\partial y} - y\frac{\partial}{\partial x}\right)\right]$$

the operator used, by itself, in the last part of § 7 We can form four separated equations in $X_1 \pm iX_2$, $X_3 \pm iX_4$, and then the solution is so like (7 11) that we need only give the result We take as initial disturbance the form (11 6), in which P stands for (7 9) This represents a stream of electrons polarised along the direction l_1 l_2 l_3 and projected from the origin along the x-axis with velocity v Let P′ represent (7 11), so that it satisfies $DP' = 0$ Then the solution of (11 7) is

$$\left.\begin{aligned} X_1 &= i\,(l_1 \cos \omega t - l_2 \sin \omega t)\,P' \\ X_1 &= i\,(l_2 \cos \omega t + l_1 \sin \omega t)\,P' \\ X_3 &= i\,(l_3 \cos \omega t - i \sin \omega t)\,P' \\ X_4 &= (\cos \omega t - il_3 \sin \omega t)\,P' \end{aligned}\right\} \quad (11\ 8)$$

The associated four intensities are

$$\left.\begin{aligned} \rho &= 2\,|P'|^2 \\ \mu_1 &= (l_1 \cos 2\omega t - l_2 \sin 2\omega t)\,2\,|P'|^2 \\ \mu_2 &= (l_2 \cos 2\omega t + l_1 \sin 2\omega t)\,2\,|P'|^2 \\ \mu_3 &= l_3\,2\,|P'|^2 \end{aligned}\right\} \quad (11\ 9)$$

We thus see that the magnetic moment turns at rate 2ω just as the ray itself does, so that the magnets preserve their direction relative to the direction of motion of the electrons We also see that a similar principle holds for the waves The phase turns at rate ω, as we saw in § 7, and we now see that the wave vector turns at this rate too This is exactly true for the components perpendicular to the magnetic field, but requires qualification for that along the field, since this has an interaction with the scalar part of the wave X_4 If we may disregard this complication, we may express the magnetic character of the electron very simply by saying that in a magnetic field the wave vector turns with the wave front at the rate of the Larmor precession From this statement all the properties of the spinning electron follow, the ratio of magnetic moment to angular momentum is e/mc and not $e/2mc$, and finally the anomalous Zeeman effect is not at all anomalous!

The Stern-Gerlach effect for an electron is rather more troublesome than for an atom, because of the difficulty of devising a suitable non-uniform field, for the wave packet will approximately describe a circle and so rapidly pass out of the central region of such a field as that used in § 10 It will suffice here to show that it reduces to the same process as for the atom If in (11 1) the ω's are regarded as constant, it is always possible to recombine the equations into four in separated variables For example, with the force along z the equations are to be taken in $X_1 \pm iX_2$, $X_3 \pm iX_4$, in the general case the combinations are given by simple algebra which we need not work out Apply this analysis to the non-uniform field, taking as direction for the resolution that of the field at the centre of the instantaneous position of the wave packet For simplicity, let us suppose that this is the z direction Then just as in § 10 we can see that the transverse non-uniformity does not matter, so that we can regard ω as varying with z and apply the method of § 6 This then shows that the rays split into two and we have the Stern-Gerlach effect

We have seen that an undesirable feature in the present way of treating the spinning electron is the ambiguity in the vector and invariant which together represent it This ambiguity does not affect observed results, but is unsatisfactory when we try to make a physical picture of the wave In the case of a free electron not acted on by forces, we have seen that there is a natural way of resolving it by the introduction of the canonical form, and it is much to be desired that this form should be extended to other cases I have not hitherto had any success in doing this

One way of attempting it is to take a polarised wave packet starting in free space and passing into a field of force Then if we start with the canonical form in free space, the X's are all given initially and the whole solution will therefore be definite It would then be natural to call the solution inside the field canonical (Observe that on this principle there is no reason to believe that (11 8) is the canonical solution for a constant magnetic field) But the matter is not so simple as this , for if the canonical form is to have any utility, we must suppose that when the electrons emerge into free space they will, if completely polarised, again have a wave solution in canonical form For example, imagine that we have a non-uniform field, roughly speaking along z, and that a stream of electrons pointing along x enters it On emerging there will be two streams pointing along $\pm z$, and these ought automatically to come into canonical form It seems at first sight very improbable that they would do so, but the following consideration perhaps tells the other way Take the simple electron of § 7 and send it near the field of a magnet Before it approaches the field the wave front is perpendicular to the ray We may presumably imagine the field pieced together out of parts each sensibly constant, and in each of these the wave front turns at half the rate of the ray, and yet on emergence into free space the wave front must again be perpendicular to the ray, for that is the only solution corresponding to rectilinear propagation in free space It would be interesting to see how this comes about, but a cursory examination of the present material does not help much, because the quadratic term in the phase factor (see (4 6)) enormously outweighs the linear and confuses the matter In fact, the waves become so involved that it seems impossible to follow them through in detail without much more elaborate mathematics If in this case we know, without being able to prove, that the wave front must return to a position perpendicular to the ray, it seems not impossible that in our more complicated process the vector should return to the canonical form If it should be proved to do so, we might claim to have a good line of attack on the question of finding the general canonical form But at present we must conclude that nothing can be done to remove the ambiguity in the vector wave of the electron

Summary

Whereas hitherto the wave mechanics has mostly been applied to a study of stationary states, the present paper deals with its application to cases where there is a *progress* of events After a review of principles and a description of the new way in which motion must be regarded, the following problems are discussed -

The free motion of an electron under no forces
The motions of an electron in uniform electric and magnetic fields
The motion of an electron in an atom
The motion of an atom in a uniform magnetic field
The Stern-Gerlach effect
The motion of the spinning electron

The Line Spectrum of Mercury in Absorption. Occurrence of the "Forbidden" Line λ 2270 $1\,^1S_0 - 1\,^3P_2$.

By Lord Rayleigh, F.R.S.

(Received November 11, 1927.)

[Plate 17.]

The mercury line $1\,^1S_0 - 1\,^3P_2$, which is forbidden by the selection rule for inner quantum numbers, has none the less been observed to occur in emission under certain special conditions. It has not been observed in the spectrum of the ordinary mercury lamp, but Takamine and Fukuda* have observed it in the spectrum of a "branched arc" in which a small fraction of the current of a mercury vacuum arc was taken off from a supplementary anode. The line was very faint compared with the resonance line $1\,^1S_0 - 1\,^3P_1$ or other strong lines of the mercury spectrum.

I have myself observed it in the excited vapour (afterglow) from a low-current discharge of 1/10 milliampere.†

In this case, and also less conspicuously in Takamine and Fukuda's experiment, it is associated with the band spectrum, and there has been a suspicion in the mind of others, as well as in my own, that there is something special about the conditions in which the transition from $1\,^3P_2$ to $1\,^1S_0$ occurs: something more, I mean, than the accumulation of a large number of excited atoms in the $1\,^3P_2$ state. The more atoms there are in this state, the more often will a spontaneous transition take place, if such a spontaneous transition has any finite probability of occurring in unit time. But this is precisely the question at issue. It may be that the transition is not spontaneous, but requires special extraneous conditions.

The question deserves consideration, not only in connection with the particular instance, but with reference to "forbidden" transitions in general, which appear likely to be of importance in cosmical physics.

Thus Bowen‡ has given reasons for thinking that the hitherto unidentified bright lines in the nebulæ have such an origin, and McLennan, Ruedy, and McLeod§ discuss forbidden transitions in connection with the view of Hopfield that the green auroral line, due to oxygen, results from such a transition. The following passage may be quoted from their paper in illustration of the class of ideas above referred to —

---

* 'Phys. Review,' vol. 25, p. 23 (1925).

† 'Roy. Soc. Proc.,' A, vol. 114, p. 620 (1927).

‡ 'Nature,' October 1, 1927.

§ 'Trans. Roy. Soc., Canada" (1927).

"To account for the occurrence of the forbidden frequences in the spectrum of *atomic* mercury, it is only necessary to recall that owing to loose coupling the constituent atoms are easily separable, and to suppose that on dissociation of molecules, at least one of the constituent atoms is left in one or other of the $1\,^3P$ states To account for the transitions $1\,^3P_0 - 1\,^1S_0$ and $1\,^3P_2 - 1\,^1S_0$, it is only necessary to suppose that while the two dissociated atoms are far enough apart to prevent their acting as a molecular unit, they may still be close enough together for each to be under the influence of the electromagnetic field of the other "*

It seemed that the subject would be considerably clarified if the line could be observed in absorption This problem naturally presented itself in connection with my experiment on the band-absorption of mercury †

It is true that the absorption of mercury has often been examined before by experienced observers, and that this line has not been noticed , but it is not easy to overrate the importance of knowing what to look for, and it seemed possible that after all the line might be found The most important conditions appeared to be the use of large spectroscopic resolving power, and the largest mass of mercury that could be used As regards the latter, the limit seems to arise (*loc cit*) from the apparently continuous absorption that is believed to start at the resonance line $1\,^1S_0 - {}^1P_1$ λ 1849, and which extends progressively to longer waves as the mass of mercury vapour is increased ‡

High resolving power is usually much more important for detecting a weak line absorption than a weak line emission For in the case of a narrow absorption line it is essential to avoid the encroachment of the neighbouring part of the continuous background, which masks the effect sought for In the case of an emission spectrum on a dark background nothing of the kind occurs, unless another bright line happens by ill-fortune to be very near It is hardly necessary to labour this point Every experimenter knows how conspicuous the D line appears in a Bunsen flame, with any dispersing arrangement, however crude But to see it well in absorption, in the spectrum of daylight for instance, requires a fairly efficient instrument It escaped the observation of Newton.

---

* In making this quotation I have altered the spectroscopic notation to agree with that used above.—R.

† 'Roy. Soc. Proc.,' A, vol. 116, p. 702 (1927)

‡ *It is not certain whether this is merely a question of mass, or whether density enters as well.*

The Hilger quartz Littrow spectrograph was one which I was enabled to purchase by a grant from the Royal Society The dispersion in this region is about 0 5 mm per Å, and the definition is very good

The mercury was in a column 45 cm in length, boiling at a pressure of 96 cm of mercury It was contained in a quartz tube with plane ends, the arrangements being as described in connection with the band absorption.*

As a source of light, the continuous hydrogen spectrum was used in the first experiments, but the continuous spectrum accompanying the cadmium spark was found (with the appliances at hand) to be brighter It is specially good in the spectral region near 2270 A small drift due to temperature change is fatal Hence the importance of reasonably short exposure

With these arrangements a very definite positive result was obtained† (see Plate 17, A) An iron comparison spectrum was used, and the mercury absorption line is seen to be decidedly sharper than the iron lines This is with an absorbing column 45 cm long, and mercury boiling under 96 cm pressure

The experiment was repeated with diminution of pressure At 45 cm length and 76 cm pressure the line could still be photographed, though much less clearly With 5 cm length and 76 cm pressure it was altogether invisible

In some of the experiments sharp dark lines (clear in the negative) were noticed at 2268 00, 2263 05, and 2261 82 These, however, are present in the cadmium source when the mercury column is removed ‡

In view of the presence of these other dark lines in the cadmium source, it is important to remark that the line 2270 was first found in absorption with the continuous hydrogen spectrum as source As a further check, a mercury lamp of "atmospheric" pattern was used, *i e*, with the mercury vapour under atmospheric pressure Such a lamp gives a continuous background, and, as already mentioned, the forbidden line 2270 is not present in emission. The lamp thus affords a substitute for the cadmium spark, for examining the absorption produced by an independent non-luminous mercury column used as before The forbidden line is then obtained in absorption as with other sources of continuous background

I have not attempted a critical determination of the wave-length of the absorption line 2270 In the absence of interferometer standards in this part of the spectrum, it seems premature to do so Relative to the adjacent iron lines 2270 87 and 2269 13, as given by Messrs Hilger on their photographic map from their own measures, the wave-length was determined as 2269 79 The term values in Fowler's Report lead to the wave-length 2269 96

---

* 'Roy Soc Proc,' *loc cit*

† A preliminary notice appeared in 'Nature,' August 27, 1927

‡ The nature of these lines is not relevant to the present investigation. It is evident on close scrutiny that the cadmium source is not continuous at all parts, but has structure, and these dark lines (emission absent) seem to be connected with it.

It is remarkable that the forbidden line is very sharp and narrow in spite of the fact that it is obtained in mercury vapour of somewhat more than the atmospheric density The effective resolving power was not enough to allow of any satisfactory estimate of the breadth of the line, but it cannot much exceed 0 08 Å This statement is made in a general sense only, without reference to strict definition of breadth

It was desired to compare the breadth and intensity with the resonance line, as obtained with mercury vapour saturated at room temperature but an unexpected difficulty was encountered, for it was found impossible to get rid of the resonance line even when all mercury was as far as possible removed The room was well ventilated by opening all available windows, and the inside of the spectrograph was ventilated with a fan immediately before the exposure But even then the resonance line was more conspicuous than the forbidden line had been with 45 cm of mercury at 96 cm pressure !*

However, some exposures were made with the room and the instrument ventilated as far as possible, and the 44-cm tube either *in vacuo* (Plate 17, B) or in air (Plate 17, C) In air the resonance line is broader than *in vacuo*, as is known from the work of R W Wood and others The photographs reproduced confirm this, but, owing to the presence of extraneous mercury already mentioned, the results *in vacuo* are not of very definite significance

The breadth of the resonance line in air was estimated at rather more than 0 2 Å

We may conclude, therefore, that the breadth of the resonance line in *saturated air* at atmospheric pressure is several times greater than the breadth of the forbidden line in *pure mercury vapour* at atmospheric pressure, and that the total radiation absorbed is also several times greater We may say that the forbidden line requires something like 10^7 times as much mercury to bring it into evidence as the resonance line requires

---

* I did not pursue the question of where this mercury came from. It may have been from the mercury mirror in the Littrow spectrograph. Evidently this test for mercury is very sensitive The possibility suggests itself of detecting mercury vapour in the open air of the country in this way I do not know of any experiment made hitherto which puts this question to an adequate test. If we assume, as is probable, that there are traces of mercury, as of almost all other metals, in ordinary rocks, the presence of traces of mercury vapour in the air does not seem particularly unlikely Dr Aston has recently drawn attention to the fact that there are traces of it in coal. The method would lend itself very well to a qualitative test for mercury in rocks and minerals.

The forbidden line $1\,^1S_0 - 1\,^3P_0$ 2656 was first observed in emission by Fukuda* and afterwards by myself† in the vapour removed from a low current low voltage discharge

It was now carefully looked for in absorption under conditions similar to those used for observing λ 2270 The mercury tube had in the meantime been shortened slightly (44 cm) in putting on new end windows, and good photographs were taken at pressures of 46 cm , 61 cm , and 76 cm. In none of them was there the slightest indication of the absorption line sought In the last (76 cm pressure) the limit had been nearly reached, for the general absorption starting at the resonance line 2537 expanding towards the red had now seriously weakened the continuous background

As we have seen, this quantity of mercury reveals the absorption of 2270 definitely, though not to the best advantage. In this region rather denser mercury vapour can be used before the general absorption becomes prohibitive

The attempts to observe $1\,^1S_0 - 1\,^3P_0$ 2656, though not strictly quantitative, probably justify a statement that under equal energy density of incident radiation a transition from the normal to the $1\,^3P_0$ state has a less probability than one to the $1\,^3P_2$ state

Since the line 2270 appears in absorption, it follows, according to the elementary principles of black-body radiation as developed by Balfour Stewart (1858) and Kirchoff (1860) that at high temperatures the line must also appear in emission The only way out of this conclusion appears to be by assuming that the line is no longer absorbed at high temperatures. It is not likely that this alternative will be preferred, for it would make complete havoc of nearly everything that has been recently written on the subject of quantum theory in relation to black-body radiation. Consider, for instance, Einstein's treatment of this subject According to this there is a specific probability of transition of an atom from the normal state to a given higher state in time Δt, proportional to the energy density of the incident radiation of appropriate frequency, and independent of the temperature

We must admit, then, that absorption of the forbidden line involves its temperature emission as well, and since there does not seem to be much room for postulating special external conditions of favoured atoms in the absorption

---

* 'Phys. Chem. Research Inst., Tokyo, Sc. Papers,' vol. 4, p. 171 (1926).

† 'Roy. Soc. Proc.,' *loc. cit.* I regret that in this publication I overlooked the work of Fukuda.

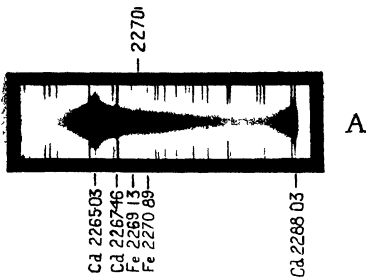

A.—The absorption line 2270. Cadmium spark as background. Iron arc comparison spectrum. 45 cm mercury at 96 cm pressure.

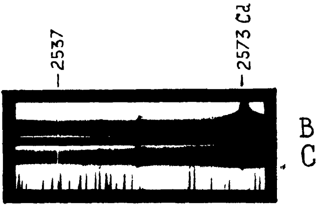

B.—Absorption line 2537. Cadmium spark as background. 44 cm mercury vapour saturated at room temperature (11° C.) *in vacuo*.

C.—Ditto. 44 cm mercury saturated at room temperature (11° C.) in air. Note that the mercury line is broader than B, and much broader than A.

The photographs are reproduced in negative.

(*Facing p.* 298.)

process, it would seem necessary to admit that the emission process too may occur without such specially favourable environment.

It would, no doubt, be desirable to examine whether mass absorption of λ 2270 remained undiminished in rare vapour. Unfortunately the experiment does not seem practicable. The absorption effect has not been established without some difficulty even for vapour of atmospheric density.

Summary

The forbidden line of mercury $1\,{}^1S_0 - 1\,{}^3P_0$ 2270 can be observed as a sharp absorption line in the unexcited vapour

The quantity of mercury required appears to be of the order 10^7 times as much as for the resonance line $1\,{}^1S_0 - 1\,{}^3P_1$, 2537

Address of the President, Sir Ernest Rutherford, O M , at the Anniversary Meeting, November 30, 1927

At this Anniversary Meeting we are naturally conscious of the losses suffered by our Society during the year These include thirteen of our Fellows and three Foreign Members We have also to record the loss of one of our Fellows under Statute 12, **Edward Cecil Guinness, Earl of Iveagh**, elected 1906

Sir **William Augustus Tilden** passed away on December 11, 1926, in his 85th year He was appointed Professor of Chemistry and Metallurgy in the Mason College, Birmingham, in 1880, and in 1894 became Professor of Chemistry in the Royal College of Science , he retained this latter position until his retirement in 1909 Much of Tilden's early work was concerned with the terpenes and he was the first to show that the hydrocarbon, isoprene, undergoes polymerisation with formation of caoutchouc His Bakerian Lecture in 1900 dealt with the relation between atomic weight and specific heat, and he was awarded the Davy Medal in 1908 A man of many accomplishments and a courtly gentleman, he gained the affection and esteem of all with whom he came in contact

J J **Lister** made his mark in the science of Zoology by his important discoveries on the life-history and morphology of the Foraminifera and by his contributions to our knowledge of Mycetozoa During his travels in the Pacific Ocean he made many valuable additions to our knowledge in several branches of the science and enriched our collections of the organisms that construct coral reefs His father and grandfather were Fellows of the Royal Society, and his uncle, Lord Lister, was formerly our President

Sir **George Greenhill**, for more than 30 years professor at the Royal Artillery College, Woolwich, was a mathematician of distinction and one of the foremost authorities on the science of ballistics He especially excelled in the application of dynamics to the practical problems of everyday life, where his interests ranged from aeroplanes and ships to spinning-tops

Arthur William Crossley was taken from us at the early age of 58 years He was successively Lecturer in Chemistry in the Medical School of St Thomas' Hospital, and Professor of Chemistry to the Pharmaceutical Society and to

King's College, London, as an accomplished organic chemist he contributed much to our knowledge of the hydro-aromatic compounds On the outbreak of war, Crossley threw himself whole-heartedly into the national effort and became the first Secretary to the Advisory Committee of the Trench Warfare Department, he was given the rank of lieutenant-colonel, R E, and undertook the organisation of the newly founded Experimental Station at Porton, a task which he performed with conspicuous success After the war he became the first Director of the Shirley Institute, Manchester, the home of the research association dealing with the cotton industry The results of Crossley's marked ability as an initiator of organised scientific effort will long remain as a memorial to a brilliant leader.

ERNEST HENRY STARLING, who died at the relatively early age of 63 years, was the first of the Royal Society's Research Professors, being appointed first Foulerton Professor in 1922 For more than 30 years Starling has been recognised as an outstanding figure in Physiology, and the investigations which he carried out with energy and enthusiasm have effected a clarification of knowledge and a new orientation of ideas concerning a succession of the most important functions of the body His earliest studies, made like so many later ones in co-operation with his great friend and scientific partner, the late Sir William Bayliss, were directed to analysis of the action of the mammalian heart

Though his activities were for many years diverted to other problems, his interest in the heart and the factors regulating its function remained with him always, and became again effective in his later years in a series of masterly researches These he carried out, with a succession of able colleagues and pupils, on the mammalian heart, isolated by a method of his own devising, from the vessels of the major circulation, and performing its function under conditions which allowed the rate at which the blood entered the heart, and the resistance encountered in its ejection, to be artificially controlled—the well-known "heart-lung preparation"

In the intervening years he had completed and published, largely with Bayliss, a series of researches in which the physical laws governing filtration, diffusion and osmosis through membranes were applied to explain the formation and absorption of lymph There followed further co-operative investigations with Bayliss on the movements of the intestinal walls, their co-ordination by the local nervous plexuses and their general control by the central nervous system, and then—most famous, probably, of all their joint researches—their work on the stimulation of pancreatic secretion following the discharge of the stomach contents into the small intestine This led to the discovery of "secretin" and the formation of general conceptions of the control of bodily functions by chemical messengers or "hormones," embodied in Bayliss and Starling's joint Croonian Lecture before this Society

During the war and the years immediately following it, Starling gave his whole energies to the service of the State, as director of investigations on defence against chemical warfare, as chemical adviser to the army at Salonica, and later as chairman of the Royal Society's Food Committee, Scientific Adviser to the Ministry of Food and British Scientific Delegate to the Interallied Food Commission

When his thoughts and activities were at last free to return to their own natural channels, he began a large and exacting series of investigations in which he combined some of his earlier methods to study the formation of urine under conditions artificially controlled and varied These researches with many which grew from them, he continued to prosecute during his tenure of the Foulerton Professorship He enjoyed the assistance and collaboration of a succession of able colleagues and of visiting workers from many countries, eager to learn his methods and to imbibe his ideas It might have been hoped that the new conditions of freedom from the responsibilities of administration and formal teaching would have enabled him to conserve his physical powers, but Starling's restless energy and burning enthusiasm forbade all thought of relaxation, till at length a physique, weakened by illness, broke under the strain

By Starling's death the Royal Society has lost not only a great investigator who has rendered one of its Chairs illustrious by his brilliant record of research as Foulerton Professor, but a Fellow who has been generous of efficient service to the Society on its Council and its Committees, who has been proud of its traditions and jealous for its fame and prosperity He was awarded a Royal Medal in 1913 In and beyond this Society he was a stalwart champion of the claims of research and of the interests of his scientific colleagues Physiology, above all, was the central interest and enthusiasm of his life In its faithful and single-minded pursuit he had always one end in view, this, to quote from his own beautiful Harveian Oration was "to attain to a comprehension of the 'wisdom of the body and the understanding of the heart,' and thereby to the mastery of disease and pain, which will enable us to relieve the burden of mankind"

By the death of GÖSTA MITTAG-LEFFLER, mathematical science lost one of its outstanding figures, one who played a notable part in the great development of the Theory of Functions which occurred in the latter half of the last century Even more memorable, perhaps, than his additions to the growth of knowledge, was his foundation of the *Acta Mathematica* in 1882, a journal which he conducted with loving care for over 40 years to the inestimable benefit of mathematical science He will be long remembered for his critical studies in the history of mathematics, for his activities at international gatherings, and for his outstanding personality

Henry Richardson Procter, who died in his 80th year, was head of the Procter International Research Laboratory of the University of Leeds His laboratory, as its name implies, was built by subscriptions from all over the world, to further by fundamental scientific research the advance of leather technology, and to commemorate Prof Procter's unique services in the leather industry

Prof W Burnside was Professor of Mathematics at the Royal Naval College for over 30 years Of much originality and power as a mathematician and distinguished as a teacher, his contributions to mathematical knowledge covered a wide variety of subjects, his earlier papers dealing mainly with hydrodynamics and waves, a large number of later papers with the Theory of Functions, and his more mature work with the Theory of Groups, a subject with which his name will always be associated His book *The Theory of Groups*, first published in 1897 and again in 1909, is a standard exposition of the subject, much of it the result of his own researches

Sir Arthur Shipley was in his early years a well-known contributor to the scientific journals on Parasitology, but when appointed to the Mastership of a Cambridge College and involved in the administrative duties of the University, he devoted his great organising powers to the wider dissemination of scientific truths and to the application of biological knowledge to the solution of problems in Agriculture and Fisheries

As a scientific adviser to several Government Departments, as Chairman of the Marine Biological Association, and in many other activities, he rendered most valuable assistance to the promotion of Science and the welfare of the community

The death of Prof A Liversidge, in his 80th year, removes one of the pioneers of scientific education in one of our great Dominions At one time Demonstrator of Chemistry in Cambridge, he was elected in 1873 to the Chair of Chemistry in the University of Sydney, and held this post for 35 years He was active in promoting scientific and technical education in Australia and was largely responsible for founding the Australasian Association for the Advancement of

Science, which has been of signal service in bringing together the widely scattered scientific workers An ardent collector of minerals and meteorites, his scientific contributions were mainly connected with experimental mineralogy On his retirement he resided in England, where he had a wide circle of friends

WILLIAM EINTHOVEN, for 42 years Professor of Physiology in the University of Leyden, Nobel Laureate in Medicine, was elected a Foreign Member of the Society in 1926 His long scientific career was devoted to the invention and perfecting of physical apparatus of the greatest delicacy and precision for the record and analysis of processes occurring in the living body or having a physiological interest His string galvanometer, originally devised for recording the fleeting electrical changes which accompany the different stages of the beat of the heart, and now in world-wide use in hospitals as well as physiological laboratories, has also found application in a wide range of purely physical investigations

The scientific world deplores the loss at the age of 67 of SVANTE ARRHENIUS, Foreign Member and Davy Medallist of our Society and Nobel Laureate Shortly after his graduation he published, in 1889, a famous paper in which he advanced the theory of ionic dissociation to explain the properties of electrolytes This theory, and the modifications of it proposed from time to time, have stimulated an enormous amount of research in all lands, and indeed Arrhenius may justly be regarded as one of the founders of modern Physical Chemistry A man of wide scientific interest and almost encyclopædic knowledge, he made valuable contributions in many branches of science As Director of the Nobel Institute in Stockholm he guided an active school of research, not only in problems of physical chemistry but in the application of physico-chemical ideas to physiological and biological problems, particularly to serum-therapy Nor must we omit an excursion into the realm of cosmical physics, where he brought his wide knowledge to bear in interesting speculations on many subjects, such as the cause of variations of the earth's climate, the origin of our solar system and the dissemination of life throughout the universe A man of forceful personality, of courageous and original mind, his early death will be mourned by a wide circle of friends throughout the scientific world

HENRY MARTYN TAYLOR was known to many generations of mathematicians as Tutor and Lecturer of Trinity College, Cambridge Failing eyesight restricted his activities in middle age, and after his sight was completely lost he devoted himself with energy to the preparation and publication of embossed books for the blind Courageous in adversity, he continued to take an active part in public affairs and was Mayor of Cambridge and for many years a Magistrate

In these notices I should like to include the name of A. A. LAWSON, at one time Lecturer in the University of Glasgow and later Professor of Botany in the University of Sydney, who was a Selected Candidate for our Fellowship, but died before the date of formal election. His tenure of the professorship in Sydney was marked by the erection of a new Botanical Institute, which was opened in 1926 shortly before his death. A botanist of distinction and a worker in many lands, he made contributions to our knowledge in cytology and the morphology of the gymnosperms, and developed in Sydney an active school of research.

Turning to other matters, I would like to say a few words on some events in the past year of special interest to the welfare of our Society. In 1925, Messrs. Brunner, Mond & Co. gave a grant of £500 for three years towards the publication fund. In substitution for this grant, Sir Alfred Mond, on behalf of Imperial Chemical Industries, Ltd., has this year given a grant of £1,000 a year, until further notice, to help meet the deficit in the publication funds. This is a very welcome gift to the Society in a direction where help is much needed. Not only has the cost of printing greatly increased since the war, but there has been a notable increase in the number of papers published by the Society. This is specially marked in the 'A Proceedings,' where, in place of one or two volumes per year before the war, three or four volumes now appear, the separate numbers being issued with promptness and regularity.

On the Biological side, where the process of differentiation into separate subjects has probably gone further, the healthy and progressive activities of the specialist societies, which the Royal Society regards with pride as its children, has prevented so large an expansion in our published Proceedings. The expansion on this side of the Society's activities is more clearly shown in 'The Philosophical Transactions,' where the Society is able to do the important service to science of issuing large and elaborately illustrated monographs, the publication of which would be beyond the scope or the resources of the specialist organisations.

Anyone who reads our 'Proceedings' cannot fail to be impressed in general by the great variety and importance of the papers appearing in them. In some respects our Society is now the most important medium of publication of papers in Experimental and Theoretical Physics and Physical Chemistry in this country. This development of the Society's activity owes much to the energy and devoted work of the Physical Secretary, Dr. Jeans. This growth has in many ways thrown a heavy burden on some of the Fellows of our Society, for it is to be remembered that in general each paper has to be reported on favourably by one or two referees before it is accepted for publication. This difficult work of adjudication has been undertaken uncomplainingly by our Fellows, and we are grateful to them for invaluable help in this important matter.

While the growth of the 'A Proceedings' and their punctual publication has led to a marked increase in the sales, there still remains a deficit, which is in part met from the residue of the Government Grant but mainly by special grants in aid from the Messel and Mond Bequest Funds In no way can our Society be more helpful to the progress of science than by prompt publication of records of important original work, and it would be a great advantage if our Society could have at its disposal ample funds specially allocated for this important purpose

During the last few years, your officers have given much thought to methods of improving the attendance of Fellows at the ordinary meetings While special lectures and discussions, and many of the ordinary meetings, are in general well attended, there are occasions when important and interesting papers are read before a very small audience Quite apart from the painful impression left on the presiding officers, the sparse attendance has inevitably a discouraging effect on the reader of the paper, particularly, as is often the case, if he has come from a distance and spent much time and trouble in order to present the subject matter of his paper in an interesting way With a view to improvement, the Secretaries in recent years have endeavoured to choose a group of related papers of special interest for reading and discussion at a particular meeting While this to some extent has been successful in its purpose, no one who has the interests of the Society at heart can feel entirely satisfied with the present state of affairs

It is only by the co-operation and goodwill of our Fellows that we can hope to remedy this defect in our meetings If only a small fraction of our Fellows who have a special knowledge of the subject matter of the group of papers to be read at a particular meeting, made a point of attending, we could be sure of an interesting meeting and discussion, profitable alike to all concerned I would, therefore, urge on our members the duty of attending as far as possible the meetings of our Society, even though it may involve some sacrifice of their time and energy, and even of their inclinations

In the early days of our Society it was customary for members and their friends to perform experiments of special interest before the Fellows, quite apart from any question of publication of the results We know from the history of our Society the importance attached to such demonstrations and their value in disseminating information in various branches of science. This custom gradually fell into abeyance, probably as a result of the ever-increasing specialisation of the sciences, and apart from the Soirées, it is only on special occasions in recent years that experimental demonstrations have been made at our meetings.

It has occurred to some of our members that it would be a definite advantage to the Society if the old custom were revived, and the members encouraged to show experiments of special interest and novelty during tea-time, before the beginning of the ordinary meeting There can be no doubt that such demonstrations would add greatly to the interest of the meetings and might indirectly help to increase the attendance during the reading of papers

In order to give this suggestion a fair trial, portable demonstration tables have been placed in the tea-room with connections for water, gas, and electric current In every branch of science, and particularly in the biological sciences, there must be many simple experiments and preparations which can readily be shown in such an extemporised laboratory—demonstrations that would prove of interest not only to the specialist but to the Society in general I trust that our Fellows will not only avail themselves of these facilities but also encourage their scientific friends to do so

In the short time at my disposal, I would like to make a few remarks on the results of investigations carried out in recent years to produce intense magnetic fields and high voltages for general scientific purposes In the past our laboratories have had to be content with the comparatively weak magnetic fields provided by the ordinary electro-magnets and the voltages supplied by simple electrostatic machines and induction coils In order to push further our investigations in many directions, much stronger magnetic fields and higher voltages are required in the laboratory Scientific men thus naturally follow with great interest advances in these directions, whether undertaken for purely scientific or for technical uses

By means of modern electrostatic machines, it is not difficult to produce weak direct currents at potentials from 200,000 to 300,000 volts, while a large well-insulated induction coil can give momentary voltages of a similar magnitude The wide use of X-rays for diagnostic and therapeutic purposes has led to a marked improvement in apparatus for exciting intense X-rays The requirement of very penetrating X-rays for deep therapy in our hospitals has led to the construction of comparatively light transformers, which will supply the requisite small currents at voltages between 300,000 and 500,000

One of the simplest ways of producing very high voltages is by the Tesla transformer, in which the oscillatory discharge of a Leyden Jar is passed through the primary of an air transformer In this way it is not difficult to produce voltages in the secondary of the order of a million volts, and I understand as much as five million volts have been obtained in the Carnegie Institute at Washington. The striking effects produced by these rapidly oscillating discharges from a Tesla coil, and the immunity with which long sparks may be taken through the body, are well known to all The rapid frequency of the oscillations and the comparatively small energy given to the secondary of a Tesla coil has, however, restricted its use for general technical purposes as a source of high voltages, although it is now finding an application for the testing of insulating materials

In order to transmit electrical power economically over long distances, there is a continuous tendency to raise the voltage in the transmission lines This increase of the operating voltage has led to the need of very high voltages to test the insulating properties of these lines and their transformers and the effect of electric surges in them In the course of the last few years a number of high-voltage plants have been installed for testing purposes in various countries, which give from one to two million volts These voltages may be obtained either by a very large well-insulated power transformer or more generally by a cascade method employing several transformers in which the secondary current of one transformer passes through the primary of a second, and so on, the cores of the successive transformers being mounted on insulating pedestals This cascade method is very advantageous for the purpose, since it allows a great reduction in weight and dimensions of the transformers Such a high-tension plant in full operation is a striking sight, giving a torrent of sparks several yards in length and resembling a rapid succession of lightning flashes on a small scale Actually the highest voltage so far obtained by these methods is very small compared with the voltage in a normal lightning flash from a cloud to the earth, where the difference of potential may be as high as a thousand million volts

There appears to be no obvious limit to the voltages obtainable by the cascade arrangement of transformers, except that of expense and the size of the building required to install them I am informed that the General Electric Company, of Schenectady, have a working plant giving 2,800,000 volts (max) and hope soon to have ready a plant to give 6 million volts

While no doubt the development of such high voltages serves a useful technical purpose, from the purely scientific point of view interest is mainly centred on the application of these high potentials to vacuum tubes in order to obtain a copious supply of high-speed electrons and high-speed atoms So far we have not yet succeeded in approaching, much less surpassing, the success of the radioactive elements, in providing us with high-speed α-particles and swift electrons The α-particle from radium C is liberated with an energy of 7 6 million electron volts, *i e*, it has the energy acquired by an electron in a vacuum which has fallen through this difference of potential The swiftest β-rays from radium have an energy of about 3 million electron volts, while a voltage of more than 2 million would be required to produce X-rays of the penetrating power of the γ-rays

The application of high voltages to vacuum tubes presents serious technical problems, but a vigorous attack on this side of the question has been recently undertaken by Dr Coolidge, whom we are glad to welcome as one of our Medallists to-day In 1894, Lenard made the discovery that high-speed cathode rays generated in a discharge tube could be transmitted into the open air through a very thin window, and made many important observations on the laws of absorption of these swift particles The voltage used to accelerate the electrons in these experiments seldom exceeded 80,000 volts and the rays were stopped in passing through a few inches of air Taking advantage of the great improvements in vacuum technique and the ease of supply of electrons from a glowing filament, Dr Coolidge has constructed an electron tube which will stand 300,000 volts, the rays passing into the air through a thin plate of chrome-nickel-iron alloy about 0 0005 inch thick

It has not so far been found practicable to apply much more than 300,000 volts to a single tube, on account of the danger of a flash over, due possibly to the pulling-out of electrons from the cathode by the intense electric field For the application of still higher voltages, a number of tubes are arranged in series and communicating with one another, the fall of potential in each being about 300,000 volts In these preliminary experiments, a large induction coil has been used to generate the voltage So far experiments have been made with three tubes in series and 900,000 volts, giving a supply of electrons corresponding to one or two milliamperes through the thin window in the last tube This gives an intense beam of high-velocity electrons, which spreads out into a hemisphere, due to the scattering of the electrons in passing through the metal window and the surrounding air, extending to a distance of about two metres from the window Marked luminous effects are produced in the air itself and in phosphorescent bodies placed in the path of the rays I am informed by Dr Coolidge that further experiments are in progress and it is hoped to extend the system for still higher voltages

While the energy acquired by the individual electrons in falling through 900,000 volts is smaller than that possessed by the swifter β-particles expelled from radium, the number emitted from the electron tube is very much greater, for example, the number of electrons per second corresponding to a current of 2 milliamperes is equivalent to the number of β-rays emitted per second from about 150,000 grammes of radium in equilibrium

While important progress has been made in artificially producing streams of swift electrons, there is still much work to be done before we can hope to produce streams of atoms and electrons of a much higher individual energy than the α or β-particle spontaneously liberated from radioactive bodies As we have seen, the α-particle from radium C is initially expelled with an energy of about 8 million electron volts So far the α-particle has the greatest individual energy of any particle known to science, and for this reason it has been invaluable in exploring the inner structure of the atom and giving us important data on the magnitude of the deflecting field in the neighbourhood of atomic nuclei and of the dimensions of the nuclei In case of some of the lighter atoms, the α-particle has sufficient energy to penetrate deeply into the nucleus and to cause its disintegration manifested by the liberation of swift protons

It would be of great scientific interest if it were possible in laboratory experiments to have a supply of electrons and atoms of matter in general, of which the individual energy of motion is greater even than that of the α-particle This would open up an extraordinarily interesting field of investigation which could not fail to give us information of great value, not only on the constitution and stability of atomic nuclei but in many other directions

It has long been my ambition to have available for study a copious supply of atoms and electrons which have an individual energy far transcending that of the α and β-particles from radioactive bodies I am hopeful that I may yet have my wish fulfilled, but it is obvious that many experimental difficulties will have to be surmounted before this can be realised, even on a laboratory scale

We shall now consider briefly the present situation with regard to the production of intense magnetic fields Electro-magnets are ordinarily employed for this purpose and the magnetic fields obtainable are in the main limited by the magnetic saturation of the iron. By the use of large electro-magnets and conical pole pieces, the magnetic induction can be concentrated to some extent For example, in the large Weiss electro-magnet, a field of 80,000 gauss can be obtained over a volume corresponding to about a pin's head, and a field of about 50,000 gauss through a volume of about 20 cubic mm. In general, however, most experiments have been restricted to fields less than 35,000 gauss.

In order to push this method of obtaining magnetic fields to the practical limit, Prof Cotton, of Paris, has designed and has under construction a very large electro-magnet The cross-section of the iron will be of the order of one square metre, and about 500 kilowatts will be required to excite it Such a large electro-magnet will not give a much stronger maximum field than existing ones, but will produce a field of given intensity through a larger volume No doubt this electro-magnet will prove very useful in experiments where steady fields of high intensity are required through a reasonable volume

In order to provide magnetic fields of the order of half a million gauss, the use of the electro-magnet must be abandoned Some years ago, Dr Kapitza suggested that intense momentary magnetic fields could be obtained by sending a very strong current through a coil for such a short interval that the heating effect in the coil is restricted to a permissible value It is well known that momentary currents of great intensity can be produced by the discharge of a large high-voltage condenser through a coil Experiments of this kind have been made by Dr Wall, in which the duration of the discharge was of the order of one-thousandth of a second It is estimated that in this way a field of about 200,000 gauss may be reached

In his experiments to obtain intense magnetic fields, Dr Kapitza at first employed a special form of accumulator to send a very strong current through a coil for about one-hundredth of a second, the current if necessary being sharply broken after this interval In this way it was shown to be practicable to carry out experiments on the Zeeman effect, and in bending α-particles in magnetic fields considerably stronger than those obtainable with ordinary methods In subsequent experiments, a generator of special design was installed, which gives a very large current, of the order of 70,000 amps at 2000 volts when short-circuited A heavy current from the generator is passed for about one-hundredth of a second through a coil and then sharply broken by means of a specially designed automatic break By this means very strong momentary currents can be produced

The main difficulty in these experiments has been to construct a coil strong enough to withstand the enormous disrupting forces which arise when a large current is passed through the coil By special attention to the design, a coil has been constructed which gives a field of 320,000 gauss over a volume of about 3 c cm. without any signs of fracture Measurements have been regularly carried out in fields of this magnitude It is anticipated that the present design of coil will give about 500,000 gauss before bursting, and that still higher fields can be obtained in coils specially constructed for the purpose An account of these experiments has recently been published in the Society's Proceedings

As the current only lasts about one-hundredth of a second, oscillograph methods have to be employed to determine the strength of the current and magnetic field There seems to be no inherent difficulty in conducting magnetic experiments in these momentary fields, for the shortness of the time available is in many cases compensated for by the magnitude of the effects which arise in such intense fields

The investigations, which have been carried out in the Cavendish Laboratory, Cambridge, have been made possible by the generous support of the Department of Scientific and Industrial Research, which has defrayed the cost of the apparatus and experiments.

The application of these new methods of producing intense fields opens up a wide region of research, where all magnetic properties can be examined in fields 10 to 20 times stronger than those hitherto available Such researches cannot fail to yield results of great interest and importance and to advance our knowledge of magnetic phenomena

While the application of external magnetic fields of the order of one-million gauss will no doubt markedly perturb the orbits of electrons in the outer structure of the atom, it is not to be anticipated that it will seriously affect the stability of atomic nuclei General evidence indicates that the magnetic fields within the nucleus are much too great for such a relatively weak external field to cause a disruption of the nucleus In this direction, the bombardment by high-speed particles is likely to be far more effective than the strongest magnetic field we can hope to generate

The advance of science depends to a large extent on the development of new technical methods and their application to scientific problems The recent work to which I have referred, on the development of methods of producing high voltages and intense magnetic fields, is not only of great interest to scientific men in itself but promises to provide us with more powerful methods of attack on a number of fundamental problems

The Copley Medal is awarded to Sir Charles Scott Sherrington, O M, my immediate predecessor in this Presidential Chair

Sherrington early chose as the special field of his investigations the physiology of the central nervous system. To this, during some thirty years, he has steadily devoted his great skill in experiment, bringing the immense complexities of its function within the range of objective analysis, and revealing fundamental plan and orderly sequence in the reflex actions by which it controls the activities of the body, and continuously adjusts them to the environment The results of this work have been embodied in a series of some two hundred original memoirs, presenting a continuous record of progressive investigation The earlier stages have been brought under review and treated synthetically by Sherrington in his now famous Silliman Lectures on " The Integrative Action of the Nervous System " In these he deals with the occurrence and significance of the muscular rigidity which appears when the higher brain is removed, with the co-ordination of muscular movements by reciprocal excitation and inhibition of antagonistic muscles, with the rhythmical, phasic activity which the conflict produces in the centres concerned with certain movements, and with the appearance of a purposeful character which the integrating action impresses on many forms of reflex response

During more recent years our own Proceedings have borne steady witness to the progress made in the finer analysis of the functions of the central nervous system by Sherrington himself and by pupils using the methods which he has created, and building on the foundations which he has laid

The influence of Sherrington's investigations has spread far beyond the limits of his own laboratory and has inaugurated a new era in neurological investigation throughout the world In this connection we may fittingly pay a tribute to the memory of one of the most eminent among those who have drawn inspiration from Sherrington's work and from personal contact with himself Rudolph Magnus, of Utrecht, whose early death in this year the whole world of science deplores, found there the impulse to his own original and far-reaching investigations, the results of which he embodied in the Croonian Lecture to this Society two years ago, on " Animal Posture " In every civilised country, in the neurological clinic as well as in the laboratory of physiology and of experimental psychology, the influence of Sherrington's work is felt, giving the clue to the understanding of many of the motor symptoms of nervous disorder, and holding out promise that even the higher functions of the central nervous system will not remain permanently beyond the reach of man's experimental enquiry

A Royal Medal is awarded to Prof John Cunningham McLennan

For more than thirty years Dr J C McLennan has been an energetic and enthusiastic experimenter, having published over one hundred papers in the principal scientific publications of England and America These are mainly concerned with radio-activity, gaseous conduction of electricity, the spectra of the elements, and the liquefaction of gases In all these subjects he has made substantial and much-used contributions to quantitative knowledge, generally of high accuracy

Among his works of outstanding merit may be mentioned the measurements he has made with his pupils on the fine structure of spectral lines, which are of much importance to modern theories of the mechanism of the atom Recently he has had a sensational success in tracing to its source the elusive auroral line λ 5577, an extremely difficult task which had baffled the skill of many previous investigators This is important not only in itself but on account of the information it yields as to the structure of the upper atmosphere

Apart from his own researches, he has built up a most efficient School of Physics in Toronto, and is largely responsible for the present strong position of physical science in Canada He has devoted much energy to the establishment of a cryogenic laboratory in Toronto, a heavy task which he has carried out with much success

During the war, he was in charge of important scientific work for the Admiralty , he developed with great energy the supply of helium from the natural sources in Canada and the States, and rendered material assistance in connection with anti-submarine warfare, especially in mining operations on a large scale and of novel character

A Royal Medal is awarded to Sir Thomas Lewis

From 1911 onwards to the present day, Sir Thomas Lewis has taken a leading part in the remarkable growth of our knowledge of the mammalian heart-beat, which has been one of the conspicuous scientific achievements of the period in question Until he began his work, nothing was known for certain of the relations of the specialised structures known to anatomists with the origin and propagation of the beat of the heart Lewis's researches enabled him to locate the point of origin of the beat, and to plot out the course of the wave of excitation over the ventricles and auricles of mammals By extending these observations to the hearts of representative vertebrates, he was able to compare the modes of spread of the wave with the special forms of the electrocardiagram, and thus to appreciate clearly the meanings of the several deflections Further extension to diseased hearts led to the interpretation of the abnormalities of the electrocardiagraphic record

In 1911 Lewis was able to show that, as Cushny had previously suggested, certain cardiac irregularities are due to fibrillation of the auricles , and his later clinical and experimental work on auricular fibrillation and flutter suggest that the irregularities are due to the formation of an endless circulating wave of contraction in the auricles

In this special field of physiology and pathology, of such great importance to medicine, Lewis's researches have replaced a mass of scattered, suggestive observations by a coherent and established theory His book on this subject, which is necessarily based, to a large extent, upon his own observations, is recognised as authoritative throughout the world.

Quite recently Lewis has published another book which embodies the results of investigations of the peripheral circulation, upon which he has been engaged during the past twelve years The response to other kinds of stimulus closely resembles that invoked by injection of histamine into a puncture, and Lewis produces strong evidence that even the response to pressure is due to the liberation in the tissue of a chemical compound, which, if not actually histamine, resembles that substance very closely in its physiological effects

In these investigations, which may be taken as models for the application of exact methods to human physiology and pathology, Lewis shows the same qualities of accurate experimentation and exact reasoning which are so conspicuous in his work upon the heart's action

The Davy Medal is awarded to Prof Arthur Amos Noyes

Prof Noyes was the torch-bearer of the modern theories of solution to the West, and under his guidance there grew up in the Massachusetts Institute of Technology a school of research in physical chemistry which held the leading place in America His researches have been chiefly concerned with the properties of solutions, in particular of electrolytic solutions Soon after the inception of the electrolytic dissociation theory of Arrhenius, it was recognised that all was not well with the strong electrolytes Whilst qualitatively their properties were accounted for by the theory, there yet existed marked quantitative discrepancies Accurate measurement of the properties of such solutions was the first requisite for the attack of the problem, and to this task Noyes applied himself His investigation of the conductance of aqueous solutions up to temperatures as high as 300° forms a classical example of exact physicochemical measurement executed under conditions of great experimental difficulty

His work on the influence exerted by one salt on the solubility of another, on transport numbers and the mobilities of the ions, on the ionisation of pure water at different temperatures, is all directed to the same end Noyes showed the importance of the classification of the strong electrolytes according to their valency type, and over twenty years ago attempted to take into account the electrostatic forces between the ions He thus foreshadowed the modern theory now so widely developed by Noyes himself amongst other workers

Outside this field Noyes made many additions to our knowledge of solutions, for example, the mass-action theory of acid indicators, velocities of reactions of different orders, and reaction-velocity in heterogeneous systems Noyes has exercised a great influence on physical chemistry, not only by the value of his experimental work, but by his careful analysis of the fundamental concepts of the science, and by his clear and logical presentation of their nature and their interrelations

The Buchanan Medal is awarded to Dr Major Greenwood

Dr Greenwood, Professor of Epidemiology and Vital Statistics, University of London (London School of Hygiene), is specially distinguished for the statistical study of medical subjects, having applied the statistical method to the elucidation of many problems of physiology, pathology, hygiene and epidemiology He has been pre-eminent in encouraging and developing the use of modern statistical methods by medical laboratory investigators and in securing the adequate planning and execution of field investigations He is almost unique in the possession of both the medical knowledge and mathematical ability which are essential in these researches Dr Greenwood is the author (with Prof E L Collis) of a book on 'The Health of the Industrial Worker,' and of numerous biometric studies dealing with the causation, prevention and treatment of disease

The Hughes Medal is awarded to William David Coolidge, a distinguished member of the scientific staff of the General Electric Company of America

Science is under a great debt to Dr Coolidge for the invention and production of a new type of X-ray tube, called by his name, of great flexibility and power, which has proved of great service not only in Medical Radiology but in numerous scientific researches In the last few years, he has applied his unrivalled technical knowledge to the generation of high-velocity cathode rays, which can be passed into the air through a thin window as in Lenard's pioneer experiments thirty years ago Such researches are of great importance to science as they promise to provide us with new methods of obtaining a copious supply of swift electrons and high-speed atoms of matter for experimental investigations

The Spectrum of Doubly Ionised Oxygen (O III)

By A. Fowler, D.Sc., F.R.S., Yarrow Research Professor of the Royal Society, Imperial College, South Kensington.

(Received November 4, 1927.)

Introductory

In continuation of previous investigations of the spectra of the lighter elements, the present paper gives an account of the spectrum of doubly ionised oxygen. The lines have been observed mainly with suitably strong discharges in vacuum tubes, and have been distinguished from those of O II by the usual method of comparing the intensities of the lines under the action of different discharges. Most of the stronger lines have been measured with considerable accuracy on plates taken with a 10-ft. concave grating, or with a large quartz spectrograph. As was expected, the spectrum is generally similar to that of N II,* and the terms so far determined are in entire accordance with Hund's theory.

Notation

It has been found that the system of numeration used for the terms of N II is not conveniently adaptable to certain other spectra, and in the present communication a modified form which seems likely to be of more general application, has been adopted. In particular, it has seemed desirable to assign the same prefix to all terms which arise from the same electron configuration. A convenient procedure, which has already been followed to some extent by others, is to use the orbital designation of the "series electron" as a prefix, with small italic letters for electron orbits, as distinct from the capital letters used for terms. Thus, $3s\,{}^3P_2$ will indicate that the ^3P term in question is due to a configuration in which the series electron occupies a 3_1 orbit. Combination possibilities are then shown by the application of the ordinary selection rule for azimuthal quantum numbers to the electron symbols, in addition to the inner quantum number rule applicable to the term symbols. For example, a $2s\,{}^1P_1$ might combine with a $3p\,{}^1P_1$, but not with a $3s\,{}^1P_1$ or $3d\,{}^1D_2$ term. In this way it becomes unnecessary to "dash" any of the term or electron symbols in connection with the simpler spectra.

For complex spectra, combination possibilities can be sufficiently indicated by assigning undashed electron symbols to the principal family of terms, and dashed symbols to other families, in accordance with the rules for electron transitions ($\Delta k = \pm 1$ for one electron and $\Delta k = 0$ or 2 for a second) When there are more than two families of terms, they may be distinguished by additional dashes to the electron symbols, an even number for what would otherwise be undashed terms, and an odd number for the remainder, in accordance with previous usage

---

* A. Fowler and L. J. Freeman, 'Roy. Soc. Proc.,' A, vol. 114, p. 662 (1927).

When different sets of terms arise from a given configuration, but with different states of the ion or " core," terms of similar type in the same group may be distinguished by arbitrary numerical superscripts applied to the *term* symbols For example, in the spectrum of O II there are three $3d\,{}^2$D terms, each based upon a different state of the O III core, which may be ^{3}P, ^{1}D, or ^{1}S, these may be distinguished by retaining $3d\,{}^2$D for the term based upon ^{3}P (the deepest term of O III), and writing $3d\,{}^2\text{D}^1$, $3d\,{}^2\text{D}^2$ for the others Such superscripts, of course, are not connected in any way with the combination properties of the terms

Rydberg sequences are naturally shown by such a succession of terms, for example, as $2s\,{}^1$P, $3s\,{}^1$P, $4s\,{}^1$P

Predicted Terms of O III

The spectrum of O III may be considered as arising from the addition of an electron to an O IV core, which has five external electrons This core is normally in the ^{2}P state (like the neutral atom of boron), and the addition of another electron generates a family of singlet and triplet terms, as shown in Table I The prefixes for these terms, as already explained, are $2p$, $3s$, and so on

Table I Predicted Terms of O III

K	L		M			N				Terms
1_1	2_1	2_2	3_1	3_2	3_3	4_1	4_2			
2	2	1						$s^2 p$		[^{2}P] O IV core
2	2	2						$s^2 p^2$	$2p$	^{3}P ^{1}D ^{1}S
2	2	1	1					$s^2 p\ s$	$3s$	^{3}P ^{1}P
2	2	1		1				$s^2 p\ p$	$3p$	^{3}D ^{3}P ^{3}S ^{1}D ^{1}P ^{1}S
2	2	1			1			$s^2 p\ d$	$3d$	^{3}F ^{3}D ^{3}P ^{1}F ^{1}D ^{1}P
2	2	1				1		$s^2 p\ s$	$4s$	^{3}P ^{1}P
2	2	1					1	$s^2 p\ p$	$4p$	^{3}D ^{3}P ^{3}S ^{1}D ^{1}P ^{1}S
2	1	2						$s\,p^2$		[^{4}P ^{2}D ^{2}P ^{2}S] O IV core
2	1	3						$s\,p^3$	$2p'$	^{5}S ^{3}D ^{3}P ^{3}S ^{1}D ^{1}P Other quintet, triplet and singlet terms

There is a second family of terms, depending upon a state of the O IV core, in which one of the 2_1 electrons has already been displaced to a 2_2 orbit This configuration (of O IV) yields the terms ^4P, ^2D, ^2P, ^2S, of which the first is the deepest, and the addition of the sixth electron gives rise to quintet, triplet, and singlet terms These may be distinguished from terms of the first family by dashing the electron symbols, and intercombinations may then occur in accordance with the usual rules for dashed terms The deepest of the terms of this second family are indicated in the last row of Table I

In Table I the electron configurations are shown in two different ways, the first of which needs no explanation The second (column 5) is a convenient way of summarising the configuration which has been used by Russell and others The two K, or 1_1, electrons being disregarded, since they do not contribute to the spectroscopic terms, the configuration of the electrons in uncompleted shells is indicated by writing s for n_1, p for n_2, and so on, the number of electrons of each type being shown by an appropriate superscript When an electron is in an excited state, the corresponding orbit symbol is separated from the others by a dot Thus $s^2 p \cdot s$, in the table, means that two of the electrons in the uncompleted L shell are in 2_1 orbits, one in 2_2, and the last in an excited n_1 orbit

Term Values

The occurrence of triplets and multiplets made it comparatively easy to trace many of the triplet terms, and approximate values were assigned to them, in the first instance, by the application of a simple Rydberg formula to the two ^3S terms which were early recognised While the present work was awaiting the identification of singlet terms, most of the triplet terms and combinations were independently discovered and published by C Mihul,* in complete agreement with the writer's results Credit is solely due to M Mihul, however, for the first identification of quintet terms

Intercombinations between singlet and triplet terms are much less conspicuous than in the corresponding spectrum of N II, and were not very readily identified A beginning was eventually made with the following pairs of lines, having separations already known in connection with triplet terms —

$$\left.\begin{array}{l} 3p\,^3D_1 - 3d\,^1P_1 = 30868\ 95\ (5) \\ 3p\,^3D_2 - 3d\,^1P_1 = 30732\ 62\ (3) \end{array}\right. \quad \Delta\nu = 136\ 32$$

$$\left.\begin{array}{l} 3d\,^1P_1 - 4p\,^3D_1 = 41752\ 5\ (5) \\ 3d\,^1P_1 - 4p\,^3D_2 = 41859\ 8\ (1) \end{array}\right. \quad \Delta\nu = 107\ 2$$

---

* 'Comptes Rendus,' vol. 183, p. 1035 (1926), vol. 184, pp. 89, 874, 1055 (1927)

With the values of the triplet terms previously determined, these gave very closely accordant values for $3d\,{}^1\mathrm{P}_1$, and there could be little doubt that the identification was correct Using the finally adopted values for the triplet terms (Table II), it results that

$$3d\,{}^1\mathrm{P}_1 = 119859{\cdot}28$$

Next, by comparison with N II, it seemed probable that $3p\,{}^1\mathrm{D}_2$ would be somewhat greater than $3p\,{}^3\mathrm{D}$, and it was accordingly estimated that a strong combination with $3d\,{}^1\mathrm{P}_1$ would be found in a position $\nu > 31000$ The line 33777·60 (6) led to a value for $3p\,{}^1\mathrm{D}_2$ which was subsequently justified by other appropriate combinations, including a very faint line representing an intercombination. Thus —

$$\begin{array}{rl}
3d\,{}^1\mathrm{P}_1 = & 119859\ 28 \\
 & \underline{\ \ 33777\ 60\ (6)} \\
3p\,{}^1\mathrm{D}_2 = & \underline{153636\ 88}
\end{array}
\qquad\qquad
\begin{array}{rl}
3s\,{}^3\mathrm{P}_1 = & 177217\ 85 \\
3p\,{}^1\mathrm{D}_2 = & \underline{153636\ 88} \\
 & \ \ 23580\ 97 \\
\text{Observed} & \underline{\ \ 23581\ 1\ (00)}
\end{array}$$

The term $3p\,{}^1\mathrm{D}_2$ should combine with $3s\,{}^1\mathrm{P}_1$, giving a strong line of wave-number less than $3s\,{}^3\mathrm{P} - 3p\,{}^1\mathrm{D}_2$, i e < 23300 The only suitable line appears to be 17876 55 (6), and, adopting this, the value of $3s\,{}^1\mathrm{P}_1$ is found as follows —

$$\begin{array}{rl}
3p\,{}^1\mathrm{D}_2 = & 153636\ 88 \\
 & \underline{\ \ 17876\ 55\ (6)} \\
3s\,{}^1\mathrm{P}_1 = & \underline{171513\ 43}
\end{array}$$

This in turn would be expected to combine with $3p\,{}^1\mathrm{S}_0$, and the most probable representative is 25235 34 (8), giving

$$3p\,{}^1\mathrm{S}_0 = 146278\ 09$$

Other singlet terms were provisionally identified in a similar manner by the selection of lines which led to values of appropriate magnitude for them Confirmatory combinations were found in some cases, and a general confirmation is afforded by comparison with the terms of N II

An important contribution to the investigation has been made by I S Bowen* by the classification of six singlets of O III observed by him in the extreme ultra-violet, namely,

---

* 'Phys. Rev,' vol. 29, p. 241 (1927).

Bowen		λ	ν	Δ ν
$a\mathrm{S} - b\mathrm{P}$	$2p\,{}^1\mathrm{S}_0 - 2p'\,{}^1\mathrm{P}_1$	597 82 (4)	167274	22916
$a\mathrm{D} - b\mathrm{P}$	$2p\,{}^1\mathrm{D}_2 - 2p'\,{}^1\mathrm{P}_1$	525 79 (6)	190190	
$a\mathrm{S} - 3k\mathrm{P}$	$2p\,{}^1\mathrm{S}_0 - 3s\,{}^1\mathrm{P}_1$	434 91 (2)	229933	22899
$a\mathrm{D} - 3k\mathrm{P}$	$2p\,{}^1\mathrm{D}_2 - 3s\,{}^1\mathrm{P}_1$	395 52 (2)	252832	
$a\mathrm{S} - 3n\mathrm{P}$	$2p\,{}^1\mathrm{S}_0 - 3d\,{}^1\mathrm{P}_1$	355 06 (0)	281643	22919
$a\mathrm{D} - 3n\mathrm{P}$	$2p\,{}^1\mathrm{D}_2 - 3d\,{}^1\mathrm{P}_1$	328 34 (0)	304562	

Bowen did not assign values to any of these terms, but $3s\,{}^1\mathrm{P}_1$ and $3d\,{}^1\mathrm{P}_1$ having now been identified, the values of $2p\,{}^1\mathrm{D}_2$, $2p\,{}^1\mathrm{S}_0$ and $2p'\,{}^1\mathrm{P}_1$ can be determined It thus seems probable that the most accurate term values for the whole spectrum will be yielded by the sequence of three $p\,{}^1\mathrm{D}_2$ terms These are represented with fair approximation by a simple Rydberg formula, but more accurately by the formula

$$p\,{}^1\mathrm{D}_2 = 9\mathrm{R}/[m + 0\ 545336 - 0\ 019824/m]^2, \quad \mathrm{R} = 109737, \quad m = 1, 2, 3$$

This gives

$$2p\,{}^1\mathrm{D}_2 = 424385, \quad 3p\,{}^1\mathrm{D}_2 = 153637, \quad 4p\,{}^1\mathrm{D}_2 = 78869$$

As the correcting term is so small, these values are unlikely to be much in error They agree closely with those adopted in the first instance by the application of a simple Rydberg formula to the two ${}^3\mathrm{S}$ terms

The $2p\,{}^3\mathrm{P}$ terms were derived in the first instance from the unresolved lines λ 374 3 and λ 305 7, indicated by Bowen as probably representing the combinations of these terms with $3d\,{}^3\mathrm{P}$ and $3d\,{}^3\mathrm{D}$ respectively If the unresolved lines be taken as the strongest components of the resulting multiplets, we have

	λ	ν		
$2p\,{}^3\mathrm{P}_2 - 3s\,{}^3\mathrm{P}_2 =$	374 3	267165 ,	$3s\,{}^3\mathrm{P}_2 = 176961,$	$2p\,{}^3\mathrm{P}_2 = 444126,$
$2p\,{}^3\mathrm{P}_2 - 3d\,{}^3\mathrm{D}_3 =$	305 7	327118 ,	$3d\,{}^3\mathrm{D}_3 = 117243,$	$2p\,{}^3\mathrm{P}_2 = 444361$

The value of $2p\,{}^3\mathrm{P}_2$ thus indicated is about 20,000 units greater than that of $2p\,{}^1\mathrm{D}_2$, in good agreement with the theoretical estimate of Fowler (R H) and Hartree,* and the identifications of the lines in question are probably correct

The separations $2p\,{}^3\mathrm{P}_0 - 2p\,{}^3\mathrm{P}_1 = 116$, and $2p\,{}^3\mathrm{P}_1 - 2p\,{}^3\mathrm{P}_2 = 193$, are given with considerable accuracy by combinations between these terms and those of the second family ($2p'$ terms), the values of which naturally follow in correct relation to those of the first family Further support for the above identifications is afforded by the probable combinations $2p'\,^3\mathrm{P} - 3p\,^3\mathrm{D}$ (λ 658·4) and $2p\,^3\mathrm{P} - 3d\,^3\mathrm{P}$ (λ 303·7) noted during the present investigation.

---

* 'Roy Soc Proc.,' A, vol. 111, p. 91 (1926)

Lines of O III in Gaseous Nebulæ.

A possibility of evaluating the $2p\,^3\mathrm{P}$ terms with greater accuracy is opened up by Bowen's recent important suggestion* that the two well-known green lines in the spectra of gaseous nebulæ may represent the irregular, or "forbidden," combinations $2p\,^3\mathrm{P}_2 - 2p\,^1\mathrm{D}_2$, $2p\,^3\mathrm{P}_1 - 2p\,^1\mathrm{D}_2$ of O III. This possibility is strengthened by the occurrence of a nebular line λ 4362·54, the wave-number of which (22912·5) corresponds closely with the irregular combination $2p\,^1\mathrm{D}_2 - 2p\,^1\mathrm{S}_0$. The somewhat similar assignment of other nebular lines to irregular combinations among the deeper terms of O II and N II increases the probability of Bowen's suggestion being correct. It is therefore desirable to examine the consequences of adopting the suggested O III origins of the three nebular lines in question.

If the interval 22913 indicated by λ 4362·54 be taken to represent the differences between Bowen's singlets noted above, it results that

	ν	Δν
$2p\,^1\mathrm{D}_2 =$	424385	22913
$2p\,^1\mathrm{S}_0 =$	401472	

The assignment of the green nebular lines to O III was based upon the fact that for these lines $\Delta\nu = 193$ is identical with $2p\,^3\mathrm{P}_1 - 2p\,^3\mathrm{P}_2$ of O III, and assuming this to be correct, the $2p\,^3\mathrm{P}$ terms at once follow. Thus:—

	λ	ν
Nebular line	5006·84	19967·1 $= 2p\,^3\mathrm{P}_2 - 2p\,^1\mathrm{D}_2$,
,,	4958·91	20160·1 $= 2p\,^3\mathrm{P}_1 - 2p\,^1\mathrm{D}_2$.

With $2p\,^1\mathrm{D}_2 = 424385$, already determined, and since $2p\,^3\mathrm{P}_0 - 2p\,^3\mathrm{P}_1 = 116$, it results that

$$2p\,^3\mathrm{P}_2 = 444352\,,\quad 2p\,^3\mathrm{P}_1 = 444545\,,\quad 2p\,^3\mathrm{P}_0 = 444661.$$

The value of $2p\,^3\mathrm{P}_2$ thus determined is as close as can be expected to that derived from the unresolved lines λ 374·3 and λ 305·7, and even if the nebular identifications are erroneous, it cannot be greatly in error The values of the $2p\ ^3P$ terms thus obtained with the aid of the nebular lines have accordingly been adopted in preference to those roughly indicated by unresolved multiplets in the extreme ultra-violet

---

* 'Nature,' vol. 120, p. 473 (Oct. 1, 1927); see also A. Fowler, 'Nature,' vol. 120, pp. 582 and 617 (October 22 and October 29).

If this be justified, it is of interest to note that the nebular lines may be utilised in this way for a calculation of the structures and positions, probably exact to about 0 001 A, of the unresolved multiplets λ 374 3 and λ 305 7, as shown below -

	$2p\ ^3P_2$ 444352	$2p\ ^3P_1$ 444545	$2p\ ^3P_0$ 444461
$3s\ ^3P_0$ = 177336		267209 λ 374 239	
$3s\ ^3P_1$ = 177218	267134 λ 374 344	267327 λ 374 074	267443 λ 373 911
$3s\ ^3P_2$ = 176961	267391 λ 373 984	267584 λ 373 714	Observed λ = 374 3
$3d\ ^3D_1$ = 117366	326986 λ 305 824	327179 λ 305 643	327295 λ 305 535
$3d\ ^3D_2$ = 117317	327035 λ 305 778	327228 λ 305 597	
$3d\ ^3D_3$ = 117243	327109 λ 305 708		Observed λ = 305 7

The terms which have been determined as above described are collected in Table II The notation of Bowen, and that adopted for N II in the paper to which reference has been made, are indicated in order to facilitate comparisons The quintet terms discovered by Mihul have not yet been found in combination with the triplets, and no attempt has been made to estimate their values

Most of the triplet, and all of the quintet combinations have already been set out by Mihul, and it is not considered necessary to repeat them, except in so far as they are shown in the catalogue which follows

The ionisation potential of O III as determined from the deepest ^3P term is 54 88 volts

Table II — Terms of O III

Bowen	N II		ν	$\Delta\nu$
$a\,^3P$	$1\,^3P$	$2p\,^3P_0$	444661	
		$^3P_1$	444545	*116*
		$^3P_2$	444352	*193*
$a\,^1D$	$1\,^1D_2'$	$2p\,^1D_2$	424385	
$a\,^1S$	$1\,^1S_0'$	$2p\,^1S_0$	401472	
$3k\,^3P$	$1\,^3P$	$3s\,^3P_0$	177336 21	
		$^3P_1$	177217 85	*118 36*
		$^3P_2$	176960 91	*256 94*
$3k\,^1P$	$1\,^1P_1'$	$3s\,^1P_1$	171513 43	
$3m\,^1D$	$2\,^1D_2'$	$3p\,^1D_2$	153636 88	
$3m\,^3D$	$1\,^3D'$	$3p\,^3D_1$	150728 24	
		$^3D_2$	150591 90	*136 34*
		$^3D_3$	150371 85	*220 05*
$3m\,^3S$	$1\,^3S_1'$	$3p\,^3S_1$	147036 00	
$3m\,^1S_0$	$2\,^1S_0'$	$3p\,^1S_0$	146278 09	
$3m\,^3P$	$2\,^3P$	$3p\,^3P_0$	144365 29	
		$^3P_1$	144283 19	*82 10*
		$^3P_2$	144152 65	*130 54*
$3m\,^1P$	$1\,^1P_1$	$3p\,^1P_1$	130792 43	
	$1\,^1F_3'$	$3d\,^1F_3$	120132 09	
	$1\,^3F'$	$3d\,^3F_2$	120131 04	
		$^3F_3$	119935 25	*195 79*
		$^3F_4$	119757 09	*178 16*
$3n\,^1P$	$1\,^1P_1'''$	$3d\,^1P_1$	119859 28	
$3n\,^3D$	$1\,^3D$	$3d\,^3D_1$	117365 56	
		$^3D_2$	117316 32	*49 24*
		$^3D_3$	117242 60	*73 72*
$3n\,^3P$	$1\,^3P'''$	$3d\,^3P_2$	115125 52	
		$^3P_1$	115011 52	*−114 00*
		$^3P_0$	114950 07	*−61 45*
$3n\,^1D$	$1\,^1D_2$	$3d\,^1D_2$	111816 4	
$4k\,^3P$	$2\,^3P'$	$4s\,^3P_0$	94484	
		$^3P_1$	94599	*115*
		$^3P_2$	94857	*258*
$4k\,^1P$	$2\,^1P_1'$	$4s\,^1P_1$	91712 ?	
$4m\,^1D$	$3\,^1D_2'$	$4p\,^1D_2$	78869 6	
$4m\,^3D$	$2\,^3D_1'$	$4p\,^3D_1$	78106 59	
		$^3D_2$	77999 49	*107 10*
		$^3D_3$	77792 46	*207 03*
$4m\,^3S$	$2\,^3S_1'$	$4p\,^3S_1$	76641 30	
$4m\,^1S$	$3\,^1S_0'$	$4p\,^1S_0$	74993 ?	
$4m\,^3P$	$3\,^3P$	$4p\,^3P_0$	74266 8	
		$^3P_1$	74177 8	*89 0*
		$^3P_2$	74069 3	*108 5*
$4m\,^1P$	$2\,^1P_1$	$4p\,^1P_1$	72981 ?	
$b\,^5S$	$\beta\,^5S$	$2p'\,^5S_2$	—	
$b\,^3D$	$\beta\,^3D$	$2p'\,^3D_3$	324633	
		$^3D_{12}$	324605	−28
$b\,^3P$	$\beta\,^3P'$	$2p'\,^3P_{12}$	302277	
		$^3P_0$	302261	−16
$b\,^1P$	$\beta\,^1P'$	$2p'\,^1P_1$	234197	
$b\,^1D$	$\beta\,^1D$	$2p'\,^1D_2$	—	
$b\,^3S$	$\beta\,^3S$	$2p'\,^3S_1$	247572	

Catalogue of O III Lines

The observations included in the present catalogue (Table III) extend from the red to λ 2228 in the ultra-violet Other observations, extending to about λ 820 are still under discussion in connection with the probable presence of lines representing higher stages of ionisation than O III It is possible, indeed, that some of the unclassified lines in the present list may be of this character, as the experimental evidence for the distinction is not very conclusive

The wave-lengths (in I A) and intensities are given in the first column, the wave-numbers (*in vacuo*) in the second, and the classification in the third Lines enclosed in brackets have been calculated from multiplet structures The position of the faint lines on the red side of λ 3962 have been determined only with small dispersion and should be regarded as approximate Bowen's classified lines in the extreme ultra-violet, with three additions, and Mihul's quintet identifications have been included in the catalogue for the sake of completeness

It should be noted that there is evidence of instability of the wave-lengths of certain groups of lines, especially in the $^3D\,^3F$ multiplets, and that consequently some of the tabulated wave-lengths are subject to revision by as much as 0 1 A This question of variable wave-lengths in oxygen and certain other elements is under separate investigation

Table III —Catalogue and Classification of O III Lines

λ	ν	Classification	λ	ν	Classification
5592 37 (6)	17876 55	$3s\,^1P_1-3p\,^1D_2$	*4379 55 (3*n*)	22827 0	
5508 11 (1)	18150 0		*4376 15 (1*n*)	22844 7	
5268 06 (2)	18977 0	$3p\,^1P_1-3d\,^1D_2$	4239 5 (00)	23581 1	$3s\,^3P_1-3p\,^1D_2$
4569 50 (1*n*)	21878 1		4177 8 (00)	23929 3	
4555 30 (0)	21946 3		4125 5 (00*n*)	24232 7	
4538 8 (0*n*)	22026 1		4081 10 (1)	24496 3	
4534 0 (0*n*)	22049 4		4073 90 (0)	24539 6	
4529 7 (00)	22070 3		3971 2 (00)	25774 2	
4482 78 (1*n*)	22301 3		3961 59 (8)	25235 34	$3d\,^1P_1-3p\,^1S_0$
4474 95 (1*n*)	22340 4		3951 82 (0)	25297 66	
4470 9 (00*n*)	22360 6		3935 0 (2*n*)	25405 8	
4461 56 (1)	22407 4		3869 1 (1*nn*)	25838 5	
4458 44 (1*n*)	22423 1		3816 75 (1)	26192 60	
4454 00 (1*n*)	22445 5		3810 96 (2)	26232 69	$3s\,^3P_2-3p\,^3D_1$
4440 1 (0)	22515 7		3791 26 (6)	26369 00	$3s\,^3P_2-3p\,^3D_2$
4435 4 (00*n*)	22539 6		3774 00 (6)	26489 59	$3s\,^3P_1-3p\,^3D_1$
4434 43 (2*n*)	22544 5		3759 87 (9)	26589 06	$3s\,^3P_2-3p\,^3D_3$
4430 2 (00*n*)	22566 0		3757 21 (5)	26607 96	$3s\,^3P_0-3p\,^3D_1$
4424 3 (00*n*)	22596 1		3754 67 (7)	26625 96	$3s\,^3P_1-3p\,^3D_2$
4408 14 (1*n*)	22679 0		3734 80 (1)	26767 61	$^5D_3-{}^5P_3$
4389·3 (00*n*)	22776 3		3733 20 (0)	26779 08	
4385 73 (0)	22794 8		3732 13 (1)	26786 76	$3p\,^3P_2-3d\,^3D_1$

* Erroneously entered in list of O II lines (' Roy Soc Proc ,' A, vol 110, p 481)

Table III—(continued)

λ	ν	Classification	λ	ν	Classification
3729 70 (1)	26804 21		3362 38 (4)	29732 33	$^5P_3-{}^5P_2'$
3728 70 (1)	26811 40		3355 92 (3)	29789 56	
3725 30 (3)	26835 87	$3p\ {}^3P_2-3d\ {}^3D_2$	3350 99 (4)	29833 38	$^5P_3-{}^5P_3'$
3721 95 (1)	26860 02	$^5D_1-{}^5P_2$	3350 68 (3)	29836 14	$^5P_2-{}^5P_1'$
3720 86 (3)	26867 80	$^5D_3-{}^5P_3$	3348 05 (2)	29859 58	
3719 82 (00)	26875 40		3344 26 (2)	29893 42	$^5P_2-{}^5P_2'$
3715 08 (6)	26909 69	$3p\ {}^3P_2-3d\ {}^3D_3$	3340 74 (6)	29924 91	$3s\ {}^3P_2\quad 3p\ {}^3S_1$
3714 50 (0)	26913 90		3336 78 (3)	29960 42	$^5P_1-{}^5P_1'$
3714 03 (2)	26917 30	$3p\ {}^3P_1-3d\ {}^3D_1$	3333 00 (4)	29994 40	$^5P_2-{}^5P_3'$
3712 48 (2)	26928 54	$^5D_2-{}^5P_2$	3332 49 (1)	29999 17	
3709 52 (2)	26950 13	$^5D_0-{}^5P_1$	3330 40 (4)	30017 82	$^5P_1-{}^5P_2'$
3707 24 (6)	26966 60	$3p\ {}^3P_1-3d\ {}^3D_2$	3326 16 (0)	30056 08	
3704 73 (3)	26984 88	$^5D_1-{}^5P_1$	3312 30 (5)	30181 85	$3s\ {}^3P_1-3p\ {}^3S_1$
3703 37 (5)	26994 77	$^5D_4-{}^5P_3$	3305 77 (0)	30241 33	$3p\ {}^3D_3-3d\ {}^3F_2$
3702 75 (5)	26999 30	$3p\ {}^3P_0-3d\ {}^3D_1$	3299 36 (3)	30300 21	$3s\ {}^3P_0-3p\ {}^3S_1$
3698 70 (5)	27028 86	$^5D_3-{}^5P_2$	3284 57 (4)	30436 65	$3p\ {}^3D_3-3d\ {}^3F_3$
3695 37 (4)	27053 22	$^5D_2-{}^5P_1$	3281 94 (3)	30461 04	$3p\ {}^3D_2-3d\ {}^3F_2$
3653 00 (1)	27367 0		3269 04 (0)	30581 23	
3650 70 (0)	27384 2		3267 31 (5)	30597 43	$3p\ {}^3D_1-3d\ {}^3F_2$
3649 20 (00)	27395 5		3265 46 (10)	30614 76	$3p\ {}^3D_3-3d\ {}^3F_4$
3647 70 (0)	27406 8		3260 98 (8)	30656 82	$3p\ {}^3D_2-3d\ {}^3F_3$
3646 84 (2)	27413 2		3258 77 (0)	30677 61	
3645 20 (1)	27425 6		3257 20 (1)	30692 39	
3638 70 (3)	27474 5		3254 50 (0)	30717 86	
3556 92 (1)	28106 2		3252 94 (2)	30732 63	$3p\ {}^3D_2\quad 3d\ {}^1P_1$
3531 39 (0)	28309 4		3238 57 (5)	30868 95	$3p\ {}^3D_1-3d\ {}^1P_1$
[3475 26]	[28766 6]	$^5D_4-{}^5F_3$	3207 67 (1)	31166 30	
3466 90 (0)	28835 98	$^5D_3-{}^5F_2$	3200 95 (1)	31231 73	
3466 15 (2)	28842 22	$^5D_4-{}^5F_4$	3132 86 (6)	31910 50	$3p\ {}^3S_1-3d\ {}^3P_2$
3464 20 (1*n*)	28858 5		3121 71 (5)	32024 47	$3p\ {}^3S_1-3d\ {}^3P_1$
3459 98 (2)	28893 66	$^5D_3-{}^5F_3$	3115 73 (4)	32085 93	$3p\ {}^3S_1-3d\ {}^3P_0$
3459 52 (0)	28897 50	$^5D_2-{}^5F_1$	3088 04 (2)	32373 64	
3455 12 (5)	28934 12	$^5D_4-{}^5F_5$	3084 76 (1)	32408 05	
3454 90 (2)	28936 14	$^5D_2-{}^5F_2$	3059 30 (6)	32677 74	$3s\ {}^3P_2-3p\ {}^3P_1$
3451 33 (1)	28966 07	$^5D_1-{}^5F_1$	3047 13 (8)	32808 25	$3s\ {}^3P_2-3p\ {}^3P_2$
3450 94 (4)	28969 34	$^5D_3-{}^5F_4$	3043 02 (5)	32852 56	$3s\ {}^3P_1-3p\ {}^3P_0$
†[3448 02]	[28993 7]	$^5D_2-{}^5F_3$	3035 43 (4)	32934 70	$3s\ {}^3P_1-3p\ {}^3P_1$
3447 22 (1)	29000 60	$^5D_0-{}^5F_1$	3034 32 (0)	32946 75	$3d\ {}^1D_2-4p\ {}^1D_2$
3446 73 (2)	29004 73	$^5D_1-{}^5F_2$	3024 57 (4)	33052 96	$3s\ {}^3P_0-3p\ {}^3P_1$
3444 10 (5)	29026 87	$3p\ {}^3P_2-3d\ {}^3P_2$	3024 36 (1)	33055 25	$3p\ {}^3D_2-3d\ {}^3D_3$
3440 39 (4)	29058 17		3023 45 (5)	33065 20	$3s\ {}^3P_1-3p\ {}^3P_2$
3435 42 (1)	29100 21		3017 63 (5)	33128 97	$3p\ {}^3D_3-3d\ {}^3D_3$
3430 60 (4)	29141 09	$3p\ {}^3P_2-3d\ {}^3P_1$	3008 79 (3)	33226 30	$3p\ {}^3D_1-3d\ {}^3D_2$
3428 67 (3)	29157 50	$3p\ {}^3P_1-3d\ {}^3P_2$	3004 35 (4)	33275 40	$3p\ {}^3D_2-3d\ {}^3D_2$
3427 41 (3*n*)	29168 22		2997 71 (2)	33349 10	$3p\ {}^3D_3-3d\ {}^3D_2$
3423 42 (1*n*)	29202 21		2996 51 (3)	33362 46	$3p\ {}^3D_1-3d\ {}^3D_1$
3415 29 (3)	29271 72	$3p\ {}^3P_1-3d\ {}^3P_1$	2992 11 (2)	33411 51	$3p\ {}^3D_2-3d\ {}^3D_1$
3411 74 (1)	29302 18		2983 78 (9)	33504 79	$3p\ {}^1D_2-3d\ {}^1F_3$
3408 13 (1)	29333 22	$3p\ {}^3P_1-3d\ {}^3P_0$	2983 66 (1)	33506 13	$3p\ {}^1D_2-3d\ {}^3F_3$
3405 74 (2)	29353 80	$3p\ {}^3P_0-3d\ {}^3P_1$	2959 68 (5)	33777 60	$3p\ {}^1D_2-3d\ {}^1P_1$
3403 58 (1)	29372 43		2836 34 (4)	35246 36	$3p\ {}^3D_3-3d\ {}^3P_2$
3394 26 (1)	29453 08		2818 69 (1)	35467 18	$3p\ {}^3D_2-3d\ {}^3P_2$
3384 95 (4)	29534 09		2809 63 (3)	35581 42	$3p\ {}^3D_2-3d\ {}^3P_1$
3383 85 (2)	29543 69		2798 91 (1)	35717 69	$3p\ {}^3D_1-3d\ {}^3P_1$
3382·69 (3)	29553 82		2794 09 (2)	35779 30	$3p\ {}^3D_1-3d\ {}^3P_0$
3381 27 (0)	29566 23		2756 22 (1)	36270 9	$3p\ {}^1D_2-3d\ {}^3D_1$
3369 40 (00)	29670 38	$3p\ {}^3S_1-3d\ {}^3D_1$	2752 47 (0)	36320 3	$3p\ {}^1D_2-3d\ {}^3D_2$
3363 83 (1)	29719 51	$3p\ {}^3S_1-3d\ {}^3D_2$	2739 15 (0)	36496 9	

† Masked by O II

Table III—(continued)

λ.	ν	Classification
2735 14 (1)	36550 4	
2726 95 (1)	36660 2	
2713 40 (2)	26843 2	$3d\,^3P_0-4p\,^3D_1$
2710 37 (0)	36884 4	
2708 87 (1)	36904 8	$3d\,^3P_1-4p\,^3D_1$
2701 05 (3)	37011 7	$3d\,^3P_1-4p\,^3D_2$
2696 00 (3)	37081 0	
2695 49 (6)	37088 0	
2692 74 (1)	37125 9	$3d\,^3P_2-4p\,^3D_2$
2691 54 (00)	37142 4	
2688 04 (00)	37190 8	
2687 53 (5)	37197 9	
2686 14 (10)	37217 1	$^5P_3-^5S_2$
2684 88 (1*n*)	37234 6	
2683 65 (4)	37251 6	
2681 42 (2*n*)	37282 6	
2677·81 (3*n*)	37332 9	$3d\,^3P_2-4p\,^3D_3$
2677 08 (1)	37343 0	
2674 57 (8)	37378 1	$^5P_2-^5S_2$
2669 97 (2*n*)	37442 5	
2665 69 (7)	37502 6	$^5P_1-^5S_2$
2661 57 (0)	37560 7	
*2628 31 (1*n*)	38036	
2625 7 (0*n*)	38074	
2624 69 (0)	38088 39	
*2623 0 (1*n*)	38113	
2622 32 (2)	38122 8	
2620 10 (0)	38155 1	
2618 82 (00)	38179 8	
2617 00 (1)	38200 3	
*2616 2 (00*n*)	38212	
2609 59 (4)	38308 76	$3d\,^3P_0-4p\,^3S_1$
2605 41 (6)	38370 22	$3d\,^3P_1-4p\,^3S_1$
2597 69 (8)	38484 23	$3d\,^3P_2-4p\,^3S_1$
2596 79 (00)	38497 6	
2593 72 (0)	38543 1	
2588 23 (0)	38624 9	
2582 92 (1*n*)	38701 3	
2580 70 (00)	38737 6	
2578 27 (00)	38774 1	
2577 17 (0)	38790 6	
2576 11 (1)	38806 6	
*2572 5 (0*n*)	38861	
*2569 6 (0*n*)	38905	
2569 11 (1)	38912 3	
2566 53 (00)	38951 5	
2558 06 (8)	39080 41	$3p\,^1P_1-4s\,^1P_1$?
2555 64 (0)	39117 4	
2549 62 (2)	39209 8	$3p\,^3D_2-4p\,^3D_1$
2547 45 (2)	39243 2	$3p\,^3D_3-4p\,^3D_3$
2546 43 (4)	39258 9	$3p\,^3D_1-4p\,^3D_1$
2542 68 (5)	39316·8	$3p\,^3D_2-4p\,^3D_2$
2541·80 (00*n*)	39330 4	
2540 1 (00)	39357	
2539 50 (2)	39366 0	$3p\,^3D_1-4p\,^3D_2$
2534 06 (6*n*)	39450 2	$3p\,^3D_2-4p\,^3D_3$
2532 5 (00)	39475	
2531 8 (00)	39486	
2529 36 (1)	39523 8	$3p\,^3D_3-4p\,^3D_2$
2517 36 (1)	39712 2	
2516 11 (00)	39730 5	
2512 41 (0)	39790 4	
2507 73 (1)	39864 7	
*2504 7 (00*n*)	39913	
2501 78 (00)	39959 5	
2499 22 (00)	40000 4	
2493 74 (1)	40083 3	
2493 37 (1)	40094 3	
2492 2 (00*n*)	40113	
2489 0 (00)	40165	
2488 3 (00*n*)	40176	
2485 27 (00)	40224 9	
2483 24 (0)	40257 8	
2482 60 (0)	40268 2	
2480 73 (1)	40298 7	
2475 73 (00)	40379 9	
2474 57 (0)	40398 8	
2458 1 (00)	40670	
2457 8 (00)	40674	$3d\,^3D_2-4p\,^3S_1$
2454 99 (8)	40721 0	$3s\,^1P_1-3p\,^1P_1$
2454 21 (0)	40734 0	
2453 54 (2*n*)	40745 1	$3d\,^3P_1-4p\,^3P_0$
2451 91 (2*n*)	40772 2	$3d\,^3P_0-4p\,^3P_1$
2451 09 (0*n*)	40785 8	
2450 06 (2*n*)	40803 0	
2449 38 (2*n*)	40814 3	
2448 21 (1*n*)	40833 8	$3d\,^3P_1-4p\,^3P_1$
2446 92 (00)	40855 3	
2441 72 (2*n*)	40942 3	$3d\,^3P_1-4p\,^3P_2$
2441 41 (00)	40947 5	$3d\,^3P_2-4p\,^3P_1$
2441 06 (2*n*)	40953 4	
2438 83 (5*n*)	40990 8	$3d\,^1P_1-4p\,^1D_2$
2438 05 (00)	41004 0	
2434 96 (2*n*)	41056 0	$3d\,^3P_2-4p\,^3P_2$
2431 69 (0*n*)	41112 2	
2429 65 (0*n*)	41145 7	
2429 35 (1*n*)	41150 8	
2426 94 (2*n*)	41191 6	
2426 35 (0*n*)	41201 7	
2425 93 (2*n*)	41208 8	
2422 84 (5*n*)	41261 3	$3d\,^1F_3-4p\,^1D_2$
2421 2 (00*n*)	41289	
2401 51 (0*n*)	41627 8	
2399 25 (0*n*)	41667 0	
2398 97 (00*n*)	41671 8	
2394 33 (5*n*)	41752 6	$3d\,^1P_1-4p\,^3D_1$
2390 44 (8*n*)	41820 5	$3p\,^1D_2-3d\,^1D_2$
2388 20 (1)	41859 8	$3d\,^1P_1-4p\,^3D_2$
2383 92 (6*n*)	41934 9	$3d\,^3F_3-4p\,^3D_2$
2382 32 (7*n*)	41963 1	$3d\,^3F_4-4p\,^3D_3$
2378 90 (4*n*)	42023 4	$3d\,^3F_2-4p\,^3D_1$
2372 82 (2*n*)	42131 1	$3d\,^3F_2-4p\,^3D_2$

* Very diffuse

Table III—(continued)

λ	ν	Classification	λ	ν	Classification
2372 21 (3*n*)	42142 0	$3d\ {}^3F_3-4p\ {}^3D_3$			
2345 02 (0*n*)	42630 5		Observations by Bowen		
2327 97 (1*n*)	42942 7				
2324 83 (0*n*)	43000 7	O II ?	835 288 (9)	119719 2	$2p\ {}^3P_2-2p'\ {}^3D_3$
2319 52 (2*n*)	43099 1	$3p\ {}^3D_1-4p\ {}^3P_0$	835 094 (3)	119747 0	$2p\ {}^3P_2-2p'\ {}^3D_{12}$
2317 37 (3*n*)	43139 1	$3p\ {}^3D_2-4p\ {}^3P_1$	833 741 (8)	119941 3	$2p\ {}^3P_1-2p'\ {}^3D_{12}$
2315 52 (4*n*)	43173 6	$3p\ {}^3D_3-4p\ {}^3P_2$	832 926 (7)	120058 7	$2p\ {}^3P_0-2p'\ {}^3D_1$
2314 76 (2*n*)	43187 7	$3p\ {}^3D_1-4p\ {}^3P_1$			
2311 58 (2)	43247 1	$3p\ {}^3D_2-4p\ {}^3P_2$	703 853 (7)	142075 1	$2p\ {}^3P_2-2p'\ {}^3P_{12}$
2308 70 (1*n*)	43301 1	O III ?	702 898 (6)	142268 2	$2p\ {}^3P_1-2p'\ {}^3P_{12}$
2306 04 (00)	43351 0		702 817 (6)	142284 5	$2p\ {}^3P_1-2p'\ {}^3P_0$
2295 51 (00)	43549 0		702 327 (6)	142383 8	$2p\ {}^3P_0-2p'\ {}^3P_1$
2288 36 (00)	43685 9				
2288 12 (00)	43690 5		*658 4 (0)	151883	$2p'\ {}^3P_2-3p\ {}^3D_3$
2287 21 (1*n*)	43707 9		*644 159 (6)	155241	$2p'\ {}^3P_{12}-3p\ {}^3S_1$ Also O II
2285 66 (2*n*)	43737 5		597 82 (4)	167274	$2p\ {}^1S_0-2p'\ {}^1P_1$
2285 07 (00*n*)	43749		525 79 (6)	190190	$2p\ {}^1D_2-2p'\ {}^1P_1$
2252 84 (0*n*)	44374 6		508 180 (6)	196781	$2p\ {}^3P_2-2p'\ {}^3S_1$
2228 15 (3*n*)	44866 3	$3d\ {}^1P_1-4p\ {}^1S_0$	507 684 (5)	196973	$2p\ {}^3P_1-2p'\ {}^3S_1$
2132 50 (1)	46878 5	$3d\ {}^1P_1-4p\ {}^1P_1$?	507 384 (4)	197089	$2p\ {}^3P_0-2p'\ {}^3S_1$
			434 91 (2)	229933	$2p\ {}^1S_0-3s\ {}^1P_1$
			395 52 (2)	252832	$2p\ {}^1D_2-3s\ {}^1P_1$
λ vac			374 3 (4)	267165	$2p\ {}^3P-3s\ {}^3P$
			335 06 (0)	281643	$2p\ {}^1S_0-3d\ {}^1P_1$
1916 48 (2)	52179	$3p\ {}^3S_1-4s\ {}^3P_2$	328 34 (0)	304562	$2p\ {}^1D_2-3d\ {}^1P_1$
1907 06 (1)	52437	$3p\ {}^3S_1-4s\ {}^3P_1$	305 7 (3)	327118	$2p\ {}^3P-3d\ {}^3D$
1902 89 (1)	52552	$3p\ {}^3S_1-4s\ {}^3P_0$	*303 7 (2)	329272	$2p\ {}^3P-3d\ {}^3P$

* Suggested by present author

Comparison of O III with N II

It is of interest to compare the terms of O III with those of N II, as in Table IV, where the relations between the two are shown in the form of the ratios O III N II

As regards the triplets, there is no ambiguity in the assignment of term types, and for these it will be seen that the ratios increase continuously from 1 862 in the $2p$ level to a maximum slightly in excess of 2 25 ($= 9R/4R$) in the $3d$ level The variations are similar to those found in corresponding comparisons of other spectra For example, in comparing the doublet terms of Al III with those of Mg II,* it may be deduced that the ratios for the deepest *s*, *p* and *d* levels are 1 89, 2 05 and 2 28 respectively

In consequence of the absence of extended sequences, it is difficult to assign the types of singlet terms in complex spectra with the same certainty as for triplets In the case of O III, however, there can be little doubt as to the correct assignment of the $p\ {}^1D_2$ terms, or of $3d\ {}^1P_1$, and thence of $3d\ {}^1D_2$. The

---

* A. Fowler, 'Roy Soc. Proc.,' A, vol. 103, p. 427 (1923)

Table IV —Comparison of Terms of O III and N II

N II	O III.	N II	O III	O III/N II
1 $^3P_0$	$2p\ ^3P_0$	238849	444661	1 862
1 $^1D_2'$	$2p\ ^1D_2$	223531	424385	1 899
1 $^1S_0'$	$2p\ ^1S_0$	147119	401472	2 729
1 $^3P_0'$	$3s\ ^3P_0$	89937	177336	1 972
1 $^1P_1'$	$3s\ ^1P_1$	89658	171513	1 913
2 $^1D_2'$	$3p\ ^1D_2$	74235	153637	2 069
1 $^3D_1'$	$3p\ ^3D_1$	72324	150728	2 084
1 $^3S_1'$	$3p\ ^3S_1$	69954	147036	2 102
2 $^1S_0'$	$3p\ ^1S_0$	60573	146278	2 415
2 $^3P_0$	$3p\ ^3P_0$	68273	144365	2 115
1 $^1P_1$	$3p\ ^1P_1$	64634	130792	2 023
1 $^1F_3'$	$3d\ ^1F_3$	52168	120132	2 302
1 $^3F_2'$	$3d\ ^3F_2$	52334	120131	2 296
1 $^1P_1'''$	$3d\ ^1P_1$	51755	119859	2 316
1 $^3D_1$	$3d\ ^3D_1$	51408	117365	2 285
1 $^3P_2'''$	$3d\ ^3P_2$	49909†	115126†	2 307
1 $^1D_2$	$3d\ ^1D_2$	48726	111816	2 294
2 $^3P_0'$	$4s\ ^3P_0$	42306	94484	2 234
2 $^1P_1'$	$4s\ ^1P_1$	40987	91712 ?	2 238
3 $^1D_2'$	$4p\ ^1D_2$	*37045 ?	78869	2 129
2 $^3D_1'$	$4p\ ^3D_1$	36132	78107	2 162
2 $^3S_1'$	$4p\ ^3S_1$	35314	76641	2 170
3 $^1S_0'$	$4p\ ^1S_0$		74993 ?	
3 $^3P_0$	$4p\ ^3P_0$	*33035	74267	2 249
3 $^1P_1$	$4p\ ^1P_1$		72981 ?	

* Added to N II in the course of the present investigation
† Inverted terms

$3p\ ^1S_0$ and $3p\ ^1P_1$ terms might possibly be considered as interchangeable, but the apparent occurrence of $3p\ ^1P_1 - 3d\ ^1D_2$ (18977) is substantial support for the assignments adopted The magnitudes of these terms are also in favour of the arrangement shown in the table, since $3p\ ^1S_0$ (146278) unites with $2p\ ^1S_0$ (401472) in a formula with a small correcting term, whereas the substitution of $3p\ ^1P_1$ (130792) for $3p\ ^1S_0$ would require a large correcting term

There is greater difficulty with regard to the singlets of N II, and the comparison with O III suggests some modification of the original allocations Thus, consideration of magnitudes suggests that 1 $^1D_2$ and 1 $^1P'''$ of N II should be interchanged, and since this is in no way inconsistent with the observed combinations, these terms have been interchanged in Table IV With this modification, the ratios for the singlets are in reasonable agreement with those for triplets, except for $2p\ ^1S_0$ and $3p\ ^1S_0$, which are notably discordant An interchange of $3p\ ^1S_0$ (60573) and $3p\ ^1P_1$ (64634) would not entirely remove the discordance, and would lead to an irregular combination $^1S_0 - {}^1D_2$ for the line 15908 28 (3) These terms have accordingly been left in their original form The terms $2p\,^1S_0$ and $3p\,^1S_0$ of N II thus remain much smaller than would be expected from the comparison with O III, but they involve strong lines and no alternative term values have yet been found

Summary

The paper includes a catalogue of more than 300 lines attributed to O III, of which about one-half have been classified by the author and others As was expected, the spectrum is generally similar to that of N II, and the terms so far determined are in complete agreement with Hund's theory

The assigned term values are based upon a sequence of three singlet D terms The deepest term is of the type $^3P_0$, and for this the value 444661 has been determined by adopting Bowen's suggestion that the well-known green lines λ 5006 8, λ 4958 9 in the spectra of gaseous nebulæ are due to irregular combinations of deep terms of O III The corresponding ionisation potential of O III is 54 88 volts

The author desires to express his thanks to Mr E W H Selwyn, B Sc, who, with the aid of a grant from the Department of Scientific and Industrial Research, has been able to give valuable assistance in the experimental work involved in the preparation of the foregoing paper

A Vector Loci Method of Treating Coupled Circuits

By E Mallett, D Sc

(Communicated by T Mather, F R.S —Received November 25, 1925, Revised October 4, 1927)

Introduction

If in the first of two coupled circuits an electromotive force of constant amplitude and variable frequency is introduced, the currents in the primary and secondary respectively may be written $i_1 = e/Z'$ and $i_2 = e/Z''$ where Z' and Z'' are complex impedance operators. The loci of these impedances as ω is varied have definite geometrical forms Z'' is a parabola and Z' a cissoid family If a parabola $y^2 = (-x)\,p$ where p depends only on the inductances and resistances of the two circuits is drawn, and a pole O is taken a certain distance to the left of the vertex a, then OP represents the impedance Z'' to a certain scale The greater the coupling between the two circuits the longer is Oa ' As ω increases from a small value, P, starting on the lower arm of the parabola far to the left, moves counter clockwise round the parabola If O is near a there will be a single minimum value of OP, and a single maximum value of the current i_2 But if the coupling and therefore Oa is larger, there will be two minimum values separated by a maximum value, corresponding to the well-known double hump i_2/ω curve

The locus of Z' is the cissoid family of curves The straight line of zero coupling bulges at the axis as the coupling is increased, and develops a loop as the coupling is still further increased Here again a double minimum impedance appears, corresponding to the double hump resonance curves.

The current loci are the inverse of these impedance loci, and these are drawn to scale for a particular case

When the circuit condensers are varied instead of ω the loci degenerate into straight lines and circles

Many properties of coupled circuits are explained and derived from the geometry of the curves, and it is shown that with certain circuit conditions fulfilled, the curves are of the same form for any type of coupling

I *Magnetic Coupling*

When an e m f is introduced in the first circuit of capacity C_1, inductance L_1 and total resistance R_1, coupled by a mutual inductance M with a second circuit, $L_2C_2R_2$, the primary and secondary currents can be written respectively $i_1 = e/Z'$ and $i_2 = e/Z''$ where $Z' = Z_1 + \omega^2M^2/Z_2$, $Z'' = j(\omega^2M^2 + Z_1Z_2)/\omega M$ and $Z_1 = R_1 + j(\omega L_1 - 1/\omega C_1)$, $Z_2 = R_2 + j(\omega L_2 - 1/\omega C_2)$

(*A*) *Circuits tuned*, so that $L_1C_1 = L_2C_2 = 1/\omega_0^2$ *Z'' and i_2.*

To find the locus of Z'', we first find the locus of

$$Z_1Z_2 = R_1R_2 - X_1X_2 + j(X_1R_2 + X_2R_1),$$

which in cartesian co-ordinates gives

$$\left.\begin{aligned} &x = R_1R_2 - L_1L_2(\omega - \omega_0^2/\omega), \quad y = (L_1R_2 + L_2R_1)(\omega - \omega_0/\omega) \\ &\text{whence} \\ &y^2 = \{(L_1R_2 + L_2R_1)^2/L_1L_2\}\{R_1R_2 - x\} = p(R_1R_2 - x) \end{aligned}\right\} \quad (1)$$

This curve is a parabola (fig 1) with the intercept on the x axis $Oa = R_1R_2$ In the special case where the two circuits are identical, that is where the locus is that of Z^2, $Oa = R^2$ and $Ob = Oc = 2R^2$ That is, O is at the focus of the parabola

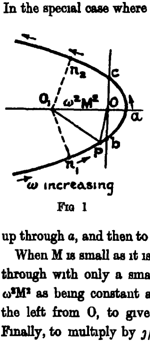

FIG 1

It is to be noted that the locus of Z_1Z_2 depends only on the inductance and resistance values of the circuits, the condenser values are only used in fixing the values of ω round the parabola

As ω increases from a small to a large value through ω_0 the extremity, P, of the vector OP representing Z_1Z_2 moves in the direction shown by the arrows starting from the extreme left on the lower half of the parabola, moving to the right and up through a, and then to the left along the upper half

When M is small as it is in most wireless circuits and the resonance is passed through with only a small change of ω, we may as an approximation take ω^2M^2 as being constant and simply measure off $OO_1 = \omega^2M^2$ horizontally to the left from O, to give the new pole O_1, such that $O_1P = \omega^2M^2 + Z_1Z_2$ Finally, to multiply by $j/\omega M$ we turn the whole diagram counter-clockwise through 90° (or take Ob as the new reference axis) and alter the scale

The magnitude of the secondary current is inversely proportional to the length O_1P As P travels round the parabola O_1P at first decreases in size, reaches a minimum at n_1, increases again to a maximum at a, decreases to a minimum at n_2, and finally increases indefinitely If, therefore, i_2 is plotted against ω, the well-known double hump curve is produced. If, however, the coupling is sufficiently loose, *i e*, OO_1 small enough, O_1P does not reach a maximum until P lies on a, the double hump disappears giving a single peak resonance curve

We can find the coupling at which the double hump just begins to appear as that which makes $O_1n_1 = O_1a$ where O_1n_1 is the length of the normal from O_1 to the parabola

This occurs when $O_1a = p/2$, *i e*,

$$\omega^2M^2 = (L_1R_2 + L_2R_1)^2/2L_1L_2 = \tfrac{1}{2}R_1R_2\,(\Delta_2/\Delta_1 + \Delta_1/\Delta_2) \qquad (2)$$

where Δ_1 and Δ_2 are the decay factors of the two circuits

When the decay factors are the same this critical coupling is given by $\omega^2M^2 = R_1R_2$

To be exact, the ω at O_1a is not quite the same as that at O_1n Thus at the normal $(R_1R_2 - x) = \omega^2M^2 + R_1R_2 - p/2$, but from equation (1)

$$(R_1R_2 - x) = L_1L_2\,(\omega - \omega_0^2/\omega)^2$$

Equating the right-hand sides gives

$$\omega\,(1 - \tau^2) + 2\omega^2\,(\Delta_1^2 + \Delta_2^2) + \Delta_0^4 = 0$$

where $\tau^2 = M^2/L_1L_2$

If the terms containing R are neglected this yields the well-known expression $\omega = \omega_0/\sqrt{1 \pm \tau}$ for the frequencies of the humps, but a closer solution is obtained as

$$\omega = \frac{\omega_0}{\sqrt{1 \pm \tau}}\left(1 \pm \frac{\Delta_1^2 + \Delta_2^2}{2\omega_0^2\tau}\right) \qquad (3)$$

The magnitude of the secondary current at the humps is ${}_{m}i_2 = (\omega M/O_1n)\,e$ and since $\overline{O_1n}^2 = p\,(O_1a - p/4)$,

$${}_{m}i_2^2 = \omega^2M^2e^2/[4L_1L_2\,(\Delta_1 + \Delta_2)^2\,\{\omega^2M^2 - L_1L_2\,(\Delta_2 - \Delta_1)^2\}] \qquad (4)$$

If the circuits have the same or nearly the same decay factors, so that $\Delta_2 - \Delta_1$ is O or its square times L_1L_2 negligible in comparison with ω^2M^2, then

$${}_{m}i_2 = e/2\sqrt{L_1L_2}\,(\Delta_1 + \Delta_2) \qquad (5)$$

This then proves the well-known fact that an increase of coupling beyond the critical value produces no alteration in the secondary current maximum It appears, however, to be subject to modification when the decay factors of the two circuits are appreciably different

At critical coupling given by (2), equation (4) becomes

$${}_{m}i_2^2 = (\Delta_1^2 + \Delta_2^2)\,e^2/2L_1L_2\,(\Delta_1 + \Delta_2)^4, \qquad (6)$$

and this gives the maximum value of the secondary current with the two circuits with "sufficient" coupling An increase of coupling beyond the critical value will result in a decrease in the maximum amplitude, while a decrease of coupling will result at first in an increase of secondary current. When the coupling is below the critical value maximum secondary current occurs along O_1a, and its magnitude is $mi_2 = \omega Me/(\omega^2M^2 + R_1R_2)$ This is a maximum when $\omega^2M^2 = R_1R_2$, and is then $e/2\sqrt{R_1R_2}$ which is the value given by equations (5) and (6) when $\Delta_1 = \Delta_2$ This is then the maximum possible value of the secondary current

As an example, the parabola of fig 2 is plotted for the case of two circuits tuned to a value of $\omega_0 = 0\ 5 \times 10^6$ with $L_1 = 4000$ μH, $C_1 = 1000$ μμF,

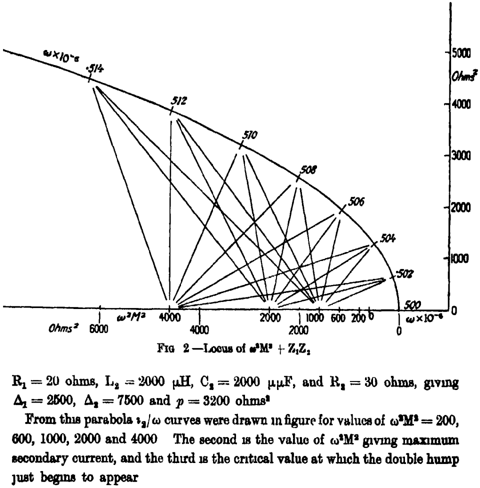

FIG 2—Locus of $\omega^2M^2 + Z_1Z_2$

$R_1 = 20$ ohms, $L_2 = 2000$ μH, $C_2 = 2000$ μμF, and $R_2 = 30$ ohms, giving $\Delta_1 = 2500$, $\Delta_2 = 7500$ and $p = 3200$ ohms²

From this parabola i_2/ω curves were drawn in figure for values of $\omega^2M^2 = 200$, 600, 1000, 2000 and 4000 The second is the value of ω^2M^2 giving maximum secondary current, and the third is the critical value at which the double hump just begins to appear

In fig 3 the vector loci of i_2 is plotted by inverting the parabola of fig 2 with various poles O_1 and multiplying by ωM. The reference vector e is drawn vertically upwards. At ω_0 the secondary current lags 90° behind the primary

Key

Fig	ω
1	$0{\cdot}500 \times 10^6$
2	0·502
3	0·504
4	0·506
5	0·508
6	0·510
7	0·512
8	0·514

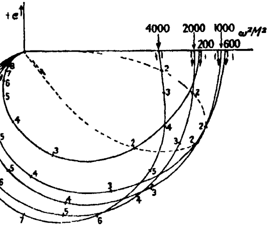

Fig. 3.—Loci of i_2. Unequal Decay Factors (Scale, 1″ = 10mA/volt.)

e.m.f. As the frequency is increased from a low value, the phase angle of the secondary current varies through 360°, from 90° in front of the primary e.m.f. to 270° behind it. The phase angle at any particular frequency depends upon the coupling, and curves are readily drawn showing the loci of secondary current with frequency held constant and coupling varied. Thus the dotted curve is drawn for an angular frequency of $0{\cdot}502 \times 10^6$, with direction counterclockwise as the coupling is increased.

With very loose coupling the locus of i_2 with varying ω tends to become a cardioid, while with very tight coupling it approaches a pair of circles. These extremes correspond in fig. 2 to the pole O_1 approaching the focus of the parabola, and to the pole O_1 being so far to the left along the axis that the locus of P is very nearly straight while the current changes are most marked.

In the case where the coupling is greater than critical, so that two humps appear, we shall have no difficulty in drawing the Z'' parabola from an experimentally determined i_2/ω curve. This parabola is $1/\omega M$ times the size of the Z_1Z_2 parabola, but is otherwise unaltered on the assumption of very small changes of ω. If any ray is drawn through the vertex a to meet the parabola in a point P, since O_1P is the value of Z'' for this frequency, the value of the angular frequency for the point P can be read off from the Z''/ω curve. If now we call the angle PaY β we have

$$\tan\beta = L_1L_2(\omega - \omega_0^2/\omega)/(L_1R_2 + L_2R_1)$$

whence

$$d\omega/d\tan\beta = \Delta_1 + \Delta_2$$

since ω_0^2/ω^2 is very nearly one.

Evidently, therefore, a construction similar to that of the circle construction in the simple resonance curve* will give the sum of the decay factors of the two circuits

This is applied in fig 4 to the i_2/ω curve from fig 3 with $\omega^2M^2 = 4000$ We suppose that the curve i_2 per volt applied to the primary has been obtained experimentally The values of i_2 are entered against the corresponding angular frequencies, and at each the value of Z'' is calculated as $1000/i_2$ where i_2 is in milliamps per volt

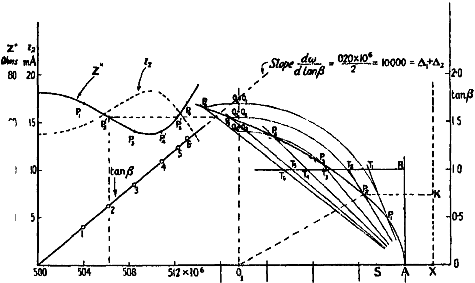

FIG 4

The values of Z'' are plotted against ω on the left-hand side of fig 4

For insertion in the formula $O_1n = \sqrt{p'(O_1a - p'/4)}$ to find p' of the Z'' parabola we have $O_1n = 55 \cdot 1$ and $O_1a = 72 \cdot 8$, and obtain $p' = 50 \cdot 6$ ohms

A parabola with $p' = 50 \cdot 6$ ohms is drawn on the right-hand side of fig 4 The pole for Z'' is found by marking off $AO_1 = 72 \cdot 8$ ohms. The angular frequencies for the various points P are found by drawing arcs with O_1 as centre and O_1P as radii to meet the vertical through O_1 in points Q and projecting horizontally from Q to meet the Z''/ω curve in the corresponding points P'

Here it must be remembered that as the Z''/ω curve is drawn from left to right so the parabola is described from A to the left (Only one-half each of the curve and parabola is drawn. The other half if symmetrical) A vertical

---

* 'J Inst Elect Engrs,' vol 62, p 517

AR equal to unity to some suitable scale is drawn through A and a horizontal through R The rays AP meet this horizontal in the points T Then RT is the tan β corresponding to the ω found for P, and the length RT erected at this ω on the left of the diagram gives a point on the tan β/ω curve The slope of this is found to be 10,000, in agreement with the known value of $\Delta_1 + \Delta_2$

Coupling Tight —When the coupling is considerably greater than critical the pole O_1 of the $Z''/j\omega M$ parabola is situated far to the left along the axis The current locus approximates to a pair of circles, while the current resonance curve is composed of two humps becoming more and more like separate simple resonance curves further and further apart

In order to obtain an expression for the effective decay factors Δ' of these humps, we notice that as P moves to the right on the lower half of the parabola (or to the left on the upper half) with increase of ω_1 O_1 also moves to the left, owing to the now appreciable change of ω^2M^2 Thus as α is the angle the ray O_1P makes the normal drawn from O_1 to the parabola, the movement of O_1 causes an increase (or decrease) of tan α for a given change of ω The movement of O_1 is small and the locus of P nearly horizontal, so that no great error will be caused by assuming that $\delta\omega$ is measured along x and that the normal is measured by y Tan α therefore is given by $\delta x/y$ where δx is the difference from the peak value, and is in part due to the movement of P and in part due to the movement of O_1

For the first part we have from (1) $d(-x)\ d\omega = 2L_1L_2\omega\ (1 - \omega_0^4/\omega^4)$ and for the second part $d(-x)/d\omega = 2\omega M^2$, so that the whole change is given by $d(-x)/d\omega = 2L_1L_2\omega\ (1 - \omega_0^4/\omega^4) - 2\omega M^2$

The expression is to be evaluated at the frequencies of the peaks, which are given with sufficient accuracy by $\omega = \omega_0/\sqrt{1 \pm \tau}$ Since $\Delta' = d\omega/d \tan\alpha$ we obtain

$$\Delta' = \tfrac{1}{2}(\Delta_1 + \Delta_2)/(1 \pm \tau) \tag{7}$$

(*b*) *Z′ and i_1* —In cartesian co-ordinates the locus of Z′ is given by

$$\left.\begin{aligned} x &= R_1 + \omega^2M^2R_2/(R_2^2 + X_2^2) \\ y &= X_1 - (\omega^2M^2X_2)/(R_2^2 + X_2^2) \end{aligned}\right\} \tag{8}$$

Moving the y axis so that $x' = x - R_1 - L_1R_2/L_2$ and eliminating X_1 and X_2 gives

$$y^2 = (x')^2\,\frac{\omega^2M^2/R_2 - L_1R_2/L_2 - x'}{L_1R_2/L_2 + x'} \tag{9}$$

the equation to a family of curves (with various values of M) such as those shown in fig. 5, which is drawn for the example considered previously When

$\omega^2M^2/R_2 - L_1R_2/L_2 = 0$, ($\omega^2M^2 = 1800$), the loop shrinks into a cusp and the curve is a cissoid For smaller values of M the cusp is rounded off With larger and larger values of M the loop becomes larger and larger, but the curves will be distorted as the alterations of ω in ω^2M^2 will become significant

The original axis of y was situated a distance $R_1 + L_1R_2/L_2$ to the left of the final axis, which passes through the cusp.

The line $x = R_1$ or $x' = - L_1R_2/L_2$ is an asymptote to the curves, and is the locus of Z′ when $M = 0$, i e, it is simply the locus of Z_1.

It will be noticed that all the points for a given frequency lie on a straight line passing through the cusp One such line is drawn dotted through the points for $\omega = 0·504 \times 10^6$

That this should be so can be seen by eliminating ω^2M^2 from equation (8) giving

$$xX_2 + yR_2 = R_1X_2 + R_2X_1$$

The line passes through the cusp and its slope is $- \delta\omega/\Delta_2$

The loci of i_1 are obtained from those of Z′ by inversion, and are drawn in fig 6 The curves all lie within the i_1 circle obtained with $\omega^2M^2 = 0$ As ω^2M^2 is increased the circle flattens, then develops a re-entrant part which in turn becomes a re-entrant cusp and a re-entrant loop

The labour of drawing a separate ray on figs 5 and 6 to find each ω point on fig 6 was avoided by making use of the fact that the ω lines of fig 5 invert to circles in fig 6 Since all the lines pass through the cusp C, all the circles must pass through the inverted cusp C, and also through the origin O of fig 6 Their centres must therefore lie on the vertical drawn midway between O and C, and the distance of the centre from the horizontal is given by $- \frac{1}{4}\overline{OC}\,\Delta_2/\delta\omega$

Frequencies of Maximum Current —In order to find an expression for the hump frequencies of the primary current, we must find the frequency at which the ray OP is normal to the curves of fig 5 The equation of ON the normal with the origin at the cusp is

$$R_1 + L_1R_2/L_2 + x = y \tan\theta$$

where θ is the angle between ON and the line drawn vertically downwards through N, and is also the angle made with the horizontal by the tangent to the curve at N The solution for the normals is therefore given by the equation

$$x = - y\left(\frac{dy}{dx}\right)_{\text{curve}} - (R_1 + L_1R_2/L_2)$$

which yields

$$\frac{\omega^2M^2}{R_2^2 + L_2^2(\omega - \omega_0^2/\omega)^2} = \frac{L_1}{L_2}\Big/\sqrt{1 + \frac{2R_1R_2}{\omega^2M^2} + 2\frac{L_1}{L_2}\frac{R_2^2}{\omega^2M^2}} \qquad (10)$$

If the resistance terms are neglected the solutions become $\omega = \omega_0/\sqrt{1 \pm \tau}$ as with the same approximation with the secondary current

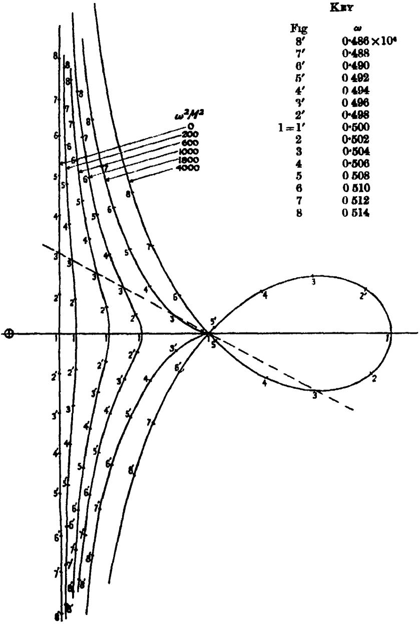

Key

Fig	ω
8′	$0·486 \times 10^4$
7′	0·488
6′	0·490
5′	0·492
4′	0·494
3′	0·496
2′	0·498
1 = 1′	0·500
2	0·502
3	0·504
4	0·506
5	0·508
6	0·510
7	0·512
8	0·514

FIG 5.—Loci of Z′ (Scale 1″ = 40 ohms.)

With tight coupling, or with very small damping, the denominator of the right-hand side may be expanded by the Binomial Theorem, leading to the

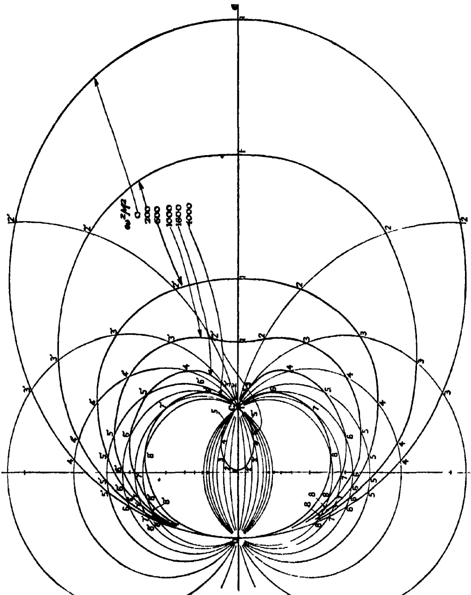

Fig. 6.—Loci of i_1 (Scale 1″ = 10mA.) Key as in Fig. 5.

useful approximation $\omega^2 M^2 + R_1 R_2 = L_1 L_2(\omega^2 - 2\omega_0^2 + \omega_0^4/\omega^2)$ and a solution

$$\omega = \frac{\omega_0}{\sqrt{1 \mp \tau}}\left(1 \pm \frac{\Delta_1 \Delta_2}{\omega_0^2 \tau}\right), \tag{11}$$

very nearly.

Comparing this with formula (3) for the secondary humps, it is seen that the correction factor on the resistanceless circuit frequencies is in the opposite direction to that in the secondary current case, and $\Delta_1 \Delta_2$ occurs in the factor instead of $\frac{1}{2}(\Delta_1^2 + \Delta_2^2)$ If the decay factors of the two circuits are the same the correction is the same in magnitude, but it is still oppositely directed Fig 7 shows the relative positions of the humps with regard to frequency

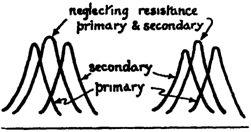

Fig 7.

Care must, however, be exercised in using formula (11) In cases where the coupling is small we may arrive at a very close approximation by assuming that the denominator of the R H.S of (10) is constant and writing

$$\sqrt{1 + \frac{2R_1R_2}{\omega^2M^2} + 2\,\frac{L_1}{L_2}\,\frac{R_2^2}{\omega^2M^2}} = 1 + \frac{L_1}{L_2}\,\frac{R_2^2}{\omega^2M^2} + \frac{4L_1L_2}{\omega^2M^2}\,\kappa \qquad (12)$$

Using for ω the value given by the resistanceless theory, a value of κ can always be found When the coupling is tight and the L H S can be expanded in two terms, we have $\kappa = \Delta_1 \Delta_2$, and it is easily seen that the values of ω required will be very nearly given by replacing $\Delta_1 \Delta_2$ in formula (11) by the value of κ found from (12) κ may be negative It may also be zero for one value of the coupling, in which case the current peak occurs at the actual value given by the ideal (resistanceless) circuits

Coupling Tight —As the coupling becomes closer and closer, the loop of fig 5 becomes larger and larger and more and more nearly a circle, while the curve at the cusp becomes more and more nearly a pair of straight lines, whose slopes are given by

$$\frac{dy}{dx} = \sqrt{\frac{\omega^2M^2}{R_2^2}\,\frac{L_2}{L_1} - 1}$$

From these slopes we can find the current values at the peaks of the two humps For the value of $Z'_{\min.} = (R_1 + L_1R_2/L_2)\cos\beta$, where β is the angle between the line and the vertical and is also the angle between the normal to the line and the horizontal Thus tan $(90 - \beta) = dy/dx$ and

$$Z'_{\min} = 2L_1 (\Delta_1 + \Delta_2) \left(1 - \frac{2(1 \pm \tau)}{\omega^2 \tau^2} \Delta_2^2\right) \tag{13}$$

The slopes of the lines are also of value in finding the values of the effective decay factors of the two current humps which are readily found to be given by the same expression as that for the effective decay factors at the peaks of the secondary current humps (equation (7))

Comparing the primary current humps with the secondary current humps it will be seen that the amplitude of the latter is greater than that of the former, and the small difference of frequency at the maximum will be noted

A more striking difference is in the phase angles, which is made clear by reference to the vector current loci of figs 3 and 6 The phase of the primary current, starting with small values of 90° in front of the primary e m f changes through 0 to nearly 90° behind as the first hump is described and from nearly 90° behind through 0 to nearly 90° in front in going through the trough, and finally from 90° in front through 0 to 90° behind in describing the second hump The phase angle thus passes through 180° (nearly) twice, from 90° leading to 90° lagging In the case of the secondary current, however, the phase of the current with regard to the primary e m f changes through 360° The current starts with small ω values by being 90° ahead, it then decreases through 0 to 90° lagging while the first hump is described, and decreases again from 90° lagging through 180° lagging to 270° lagging while the second hump is described.

The trough between the humps may be of interest especially when the damping of the secondary circuit is considerably less than that of the primary, when the definition of the two humps will be pronounced even though the coupling is not very tight An example of this is the quartz crystal oscillator

The right-hand region of the impedance locus in this case approximates to a circle, with pole distant $R_1 + L_1R_2/L_2$ from the circle In some cases this may be very small compared with $\omega^2M^2/R_2 - L_1R_2/L_2$, in which case the pole is very nearly on the circle, and the current trough is nearly a straight line

B Two Circuits Nearly Tuned —When the two circuits are a little out of tune, and when the coupling is not too tight, so that the frequency over the resonance is not very different from the natural frequency of either circuit alone, we can obtain some useful approximations, and show that the form of the locus is the same, but that the pole is moved away from the axis of symmetry

Let ω_1 and ω_2 be the values of $1/\sqrt{L_1C_1}$ and $1/\sqrt{L_2C_2}$ respectively

Then we have, since under the conditions contemplated, ω_1/ω will not be very different from (1),

$$X_1 = 2L_1(\omega - \omega_1)$$

$$X_2 = 2L_2(\omega - \omega_2)$$

Hence the locus of Z_1Z_2 is given in cartesian co-ordinates by

$$\left.\begin{aligned} x &= R_1R_2 - 4L_1L_2(\omega - \omega_1)(\omega - \omega_2) \\ y &= 2L_1R_2(\omega - \omega_1) + 2L_2R_1(\omega - \omega_2) \end{aligned}\right\} \qquad (14)$$

Now the maximum value of x will be obtained when $\omega = \frac{1}{2}(\omega_1 + \omega_2)$, and then

$$\left.\begin{aligned} x_m &= R_1R_2 + L_1L_2(\omega_1 - \omega_2)^2 \\ y_m &= (L_2R_1 - L_1R_2)(\omega_1 - \omega_2) \end{aligned}\right\} \qquad (15)$$

Transferring to new axes $x' = x - x_m$, $y' = y - y_m$, we obtain

$$x' = -L_1L_2\{(\omega_1 + \omega_2) - 2\omega\}^2$$

$$y' = (L_1R_2 + L_2R_1)(\omega_1 + \omega_2 - 2\omega)$$

and

$$y'^2 = \frac{(L_1R_2 + L_2R_1)^2}{L_1L_2}(-x')$$

Hence the locus of Z_1Z_2 in this case is the same parabola as in the tuned circuits case, but the distribution of ω round the parabola is different and the position of the pole is different The parabola is determined only by the R and L values, the ω positions and the position of the pole depend upon ω_1 and ω_2, that is on the condenser values

The ω points may be put in by either of the equations (14), and the pole by equations (15) In general the pole will be off the axis of the parabola, but in the special case of $y_m = 0$ or $\Delta_1 = \Delta_2$ as well as, of course, in the case of $\omega_1 = \omega_2$, the pole lies on the axis If ω_1 and ω_2 are looked upon as variables, *i e*, if the condenser values are altered but all else remains constant, we obtain from (15)

$$y_m^2 = \{(L_2R_1 - L_1R_2)^2/L_1L_2\}\{-x_m + R_1R_2\}$$

Thus the locus of the pole is also a parabola, having the same axis as the Z_1Z_2 parabola, and with its vertex distance R_1R_2 to the left of the vertex of the Z_1Z_2 parabola When the decay factors of the two circuits are the same, the parabola of the pole of Z_1Z_2 degenerates to a straight line coinciding with the axis

Having now obtained the locus Z_1Z_2 and its pole, we measure off ω^2M^2 horizontally to the left to obtain a new pole O_1 such that the rays O_1P to the parabola when multiplied by $j/\omega M$ give Z'', which on inversion gives i_2

This construction is indicated in fig 8 This diagram brings out clearly the fact that generally the current humps are of different height As to which hump, the lower frequency or the higher, is the larger is determined by the sign of y_m in equation (15) If such a current curve is obtained experimentally, we have the problem of finding the corresponding parabola If AB and EF are the lengths of the current hump maxima, and CD is the length of the current trough, and we draw concentric circles of radii $r_1 = 1/\mathrm{AB}$, $r_2 = 1/\mathrm{CD}$, $r_3 = 1/\mathrm{EF}$, we have to find a parabola with axis horizontal to touch the three circles Probably the simplest manner of doing this is to draw out a family of parabolas on tracing paper and so find the one that most nearly fits the circles Having found the parabola, we can apply the construction of fig 4 to find the value of $\Delta_1 + \Delta_2$

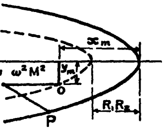

Fig 8

In a similar manner it is readily shown that the locus of Z' for the untuned case is identical with that of the tuned case, but has its pole depressed below the horizontal axis through the cusp by an amount $2L_1(\omega_2 - \omega_1)$ The impedance minima and therefore the current maxima will always be different, even in the case when the decay factors of the circuits are the same

C Condensers Varied, Constant —When ω is constant and the circuit condensers are varied, the loci become straight lines and circles

II *Direct Coupling by Common Impedance*

When the coupling between the two circuits is by a common impedance Z_e, we have for finding the primary and secondary currents

$$Z' = Z_1 - Z_e^2/Z_2,$$
$$Z'' = (Z_1 Z_2 - Z_e^2)/Z_e,$$

where Z_1 is the series impedance of L_1 R_1 C_1 and Z_e and Z_2 that of R_2 L_2 C_2 and Z_c.

These expressions are of exactly the same form as those for mutual inductance coupling, and give the same form of loci When the common impedance is a condenser C_c, ωM in the mutual case is replaced by $1/\omega C_c$. With couplings below the critical value the maximum secondary current is obtained when $X_1 = X_2 = 0$ or $\omega = \sqrt{(C_1 + C_e)/L_1 C_1 C_e} = \sqrt{(C_2 + C_e)/L_2 C_2 C_e}$. The coupling for maximum secondary current is that which makes $1/\omega^2 C_c^2 = R_1 R_2$

The critical coupling condenser value is found from

$$1/\omega^2 C_c^2 = R_1 R_2 \quad \tfrac{1}{2}(\Delta_2/\Delta_1 + \Delta_1/\Delta_2)$$

If the coupling impedance is a pure resistance R_c each circuit will be further damped by this resistance

The pole of $Z_1 Z_2$ will be $(R_1 + R_c)(R_2 + R_c)$ from the vertex of the parabola, and the pole of $Z''R_c$ will be $(R_1 + R_c)(R_2 + R_c) - R_c^2 = R_1 R_2 + (R_1 + R_2) R_c$ from the vertex So that the condition for a double hump to appear becomes

$$R_1 R_2 + (R_1 + R_2) R_c \geqslant \{(L_1 (R_2 + R_c) + L_2 (R_1 + R_c))\}/2 L_1 L_2,$$

a condition which cannot be fulfilled It appears therefore that a double hump resonance curve for the secondary current cannot be obtained with resistance coupling

III *Direct Coupling by Impedance not Common*

In the case where the coupling is by an impedance Z_c not common to the two circuits, we obtain

$$Z'' = -\omega^2 C_1 C_2 Z_c (L_1 Z_2/C_1 Z_c + L_2 Z_1/C_2 Z_c + Z_1 Z_2)$$
$$Z' = Z_1 + 1/\omega^2 C_1^2 (L_2/C_2 Z_2 + Z_c)$$

When the coupling impedance Z_c is a condenser C_c and the primary and secondary circuits are tuned Z'' is given by

$$\frac{Z''}{j\omega C_1 C_2/C_c} = R_1 R_2 - L_1 L_2 (\omega - \omega_0^2/\omega)^2 - \omega C_c (L_1 L_2/C_1 + L_1 L_2/C_2)(\omega - \omega_0^2/\omega)^2$$
$$+ j\{(L_1 R_2 + L_2 R_1)(\omega - \omega_0^2/\omega) + \omega C_c (L_1 R_2/C_1 + L_2 R_1/C_2)\}$$

An examination of this expression shows that the locus of $Z''/j\omega C_1 C_2/C_c$ is a parabola $y^2 = p(-x)$, that the value of p is the same as in the case of magnetic coupling, but that the position of the pole is determined by the expressions

$$-x_p = R_1 R_2 + \tfrac{1}{4}\omega^2 C_c^2 L_1 L_2 (1/C_1 + 1/C_2)^2$$
$$y_p = -\omega C_c \{L_1 L_2 (\Delta_2 - \Delta_1)(1/C_1 - 1/C_2)\}$$

In the magnetic coupling case we had for the distance of the pole from the vertex $-x_p = R_1 R_2 + \omega^2 M^2$ Comparing this with the above, we see that M is replaced by $\tfrac{1}{2} C_c \sqrt{L_1 L_2}(1/C_1 + 1/C_2)$ In the magnetic case the parabola is to be multiplied by $j/\omega M$ to obtain Z'', whereas with the capacity coupling it is to be multiplied by $j\omega C_1 C_2/C_c$. M therefore in this case corresponds to $C_c/\omega^2 C_1 C_2$, and it is only when $C_1 = C_2$ and therefore $L_1 = L_2$ that these two quantities which replace M in different parts of the expression are equal, and that a real parallel can be drawn between the two cases This appears also from the expression for y_p, which is 0 when $C_1 = C_2$ In the magnetic case y_p is always 0 when the circuits are tuned

It appears that y_p is also zero when $\Delta_1 = \Delta_2$, and we conclude therefore that in the case of capacity coupling, when the circuits are tuned and the coupling condenser is large enough for two humps to appear, that these humps will only be of equal size if the decay factors of the circuit are the same, or if the condenser's values are the same In all other cases the pole is displaced from the axis of the parabola, and the current humps will be of unequal height

The distribution of ω round the parabola is most conveniently done from the expression

$$y = (L_1R_2 + L_2R_1)\{\omega - \omega_0^2/\omega + \tfrac{1}{2}\omega C_c(1/C_1 + 1/C_2)\} \tag{16}$$

It is seen that at the vertex of the parabola, i e, at or near the trough of the current curve, when $y = 0$

$$\omega^2 = \omega_0^2/\{1 + \tfrac{1}{2}C_c(1/C_1 + 1/C_2)\},$$

and that unlike the magnetic coupling case, the ω distribution is altered when the coupling is altered

Making our usual approximations and writing

$$\tfrac{1}{4}\omega C_c(1/C_1 + 1/C_2) = \omega_a,$$

so that ω_a is the difference of the frequency at the vertex of the parabola from ω_0, we have

$$y = 2(L_1R_2 + L_2R_1)(\omega - \omega_0 - \omega_a)$$

So that to find the frequencies in the case of capacity coupling we simply substract ω_a from each of the values found for the Z_1Z_2 parabola

The frequencies of the current hump maxima and of the trough minimum can be determined by using exercise 11, p 214, of Salmon's Conic Sections — "The co-ordinates of the points on the curve ($y^2 = px$), the normals at which pass through a given point $x'y'$ are given by the solutions of

$$2y^3 + (p^2 - 2px')\,y = p^2y' \text{''} \tag{17}$$

Substituting the values of x_p and y_p for x' and y', y from (16) and p, and solving we obtain the three solutions (on neglecting the effect of the resistances)

$$\omega = \omega_0/\sqrt{1 + C_c(1/C_1 + 1/C_2)},$$

$$\omega = \omega_0/\sqrt{1 + \tfrac{1}{2}C_c(1/C_1 + 1/C_2)}$$

and

$$\omega = \omega_0,$$

which determine the frequencies of the lower hump, the trough and the higher hump

If the effect of resistance is to be taken into account the best way is to draw out the parabola and find the points graphically

IV *Combined Capacity and Mutual Coupling*

A case of considerable interest in all high-frequency circuits is that of combined capacity and mutual coupling, owing to the general impossibility of avoiding capacity coupling when only mutual is intended

In addition to a coupling condenser C_e not common to the circuits the inductances are imagined to be coupled with a mutual M, and we obtain

$$Z'' = -\frac{\left\{\left(1+\frac{C_e}{C_1}+\frac{C_e}{C_2}\right)\omega^2M^2+2M\frac{C_e}{C_1C_2}\right\}+\left\{\left(\frac{L_1}{C_1}Z_2+\frac{L_2}{C_2}Z_1\right)j\omega C_e+Z_1Z_2\right\}}{j\omega M\left(1+\frac{C_e}{C_1}+\frac{C_e}{C_2}\right)+j\frac{C_e}{\omega C_1C_2}}$$

We note that the whole of the variables are contained in the last term of the numerator, which is the parabola $Z''/j\omega C_1C_2/C_e$ of the case of capacity coupling only

So we may write

$$Z''\left\{-j\omega M\left(1+\frac{C_e}{C_1}+\frac{C_e}{C_2}\right)-j\,\frac{C_e}{\omega C_1C_2}\right\} = \left\{\left(1+\frac{C_e}{C_1}+\frac{C_e}{C_2}\right)\omega^2M^2 + 2M\,\frac{C_e}{C_1C_2} + \begin{pmatrix}\text{the capacity}\\ \text{parabola}\end{pmatrix}\right\},$$

from which by constructing the capacity parabola, and finding a new pole $(1 + C_e/C_1 + C_e/C_2)\,\omega^2M^2 + 2MC_e/C_1C_2$ to the left of the original, the left-hand side can be found for any frequency, and finally Z'' by multiplication by

$$1/\{-j\omega M\,(1 + C_e/C_1 + C_e/C_2) - jC_e/\omega C_1C_2\}$$

For the frequencies of the humps and troughs we have for substitution in equation (17) y from equation (16), p as before, and

$$x' = x_p = R_1R_2 + \tfrac{1}{4}\omega^2C_e^2L_1L_2\,(1/C_1 + 1/C_2)^2$$
$$+ (C_e/C_1 + C_e/C_2 + 1)\,\omega M^2 + 2MC_e/C_1C_2,$$
$$y' = y_p = -\,\omega C_e\,\{\tfrac{1}{2}\,(L_1R_2 - L_2R_1)\,(1/C_1 - 1/C_2)\},$$

giving as solution for the trough (on neglecting terms with R)

$$\omega = \omega_0/\sqrt{1 + \tfrac{1}{2}C_e\,(1/C_1 + 1/C_2)}$$

as before

The two remaining solutions (for the humps) are to be obtained from

$$L_1^2L_2^2\{(\omega - \omega_0^2/\omega)^2 + \tfrac{1}{2}\omega C_c(1/C_1 + 1/C_2)\}^2$$
$$= \{\tfrac{1}{4}\omega^2C_c^2L_1^2L_2^2(1/C_1 + 1/C_2)^2 + L_1L_2\omega^2M^2(1 + C_c/C_1 + C_c/C_2)$$
$$+ 2ML_1L_2C_c/C_1C_2\}$$

This affords in general no neat solution, but when the capacity coupling is small, as in the case of stray capacities, so that $C_c(1/C_1 + 1/C_2)$ may be neglected in comparison with 1, and when also C_1 and C_2 are nearly equal so that $\frac{1}{2}(C_1 + C_2) = \sqrt{C_1C_2}$, then the equation becomes

$$(\omega - \omega_0^2/\omega) + \tfrac{1}{2}\omega C_c(1/C_1 + 1/C_2) = \pm\{\tfrac{1}{2}\omega C_c(1/C_1 + 1/C_2) + \omega M/\sqrt{L_1L_2}\}$$

Taking the positive sign gives $\omega = \omega_0/\sqrt{1 - \tau}$ for the higher frequency, *i e*, the higher hump coincides with the hump for mutual alone, provided M positive

If M is negative, $\omega = \omega_0/\sqrt{1 + \tau}$ and the lower hump with mutual alone is not moved by the presence of the capacity coupling

Taking the negative sign we have

$$\omega = \omega_0/\sqrt{1 + C_c(1/C_1 + 1/C_2) + \tau}$$

If M is positive the frequency of the lower frequency hump is still further lowered by the capacity coupling If M is negative the frequency of the higher frequency hump is lowered by the presence of the capacity These effects are indicated in fig 9 The effect of the capacity coupling in the ω distribution is to make

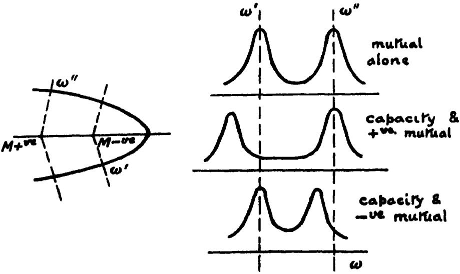

FIG 9

ω' and $\omega'' = \omega_0/\sqrt{1 \mp \tau}$ unsymmetrically placed on a parabola The poles for M positive and M negative are as indicated, with the resulting resonance curves

V *Summary and Conclusions*

Z'' can be obtained from a parabola $y^2 = p\,(-x)$ by drawing rays to the parabola from a pole $x_p\, y_p$ and dividing each ray by a vector A. The distribution of ω round the parabola is found from

$$y = 4L_1L_2\,(\Delta_1 + \Delta_2)\,(\omega - \omega_0 + \omega_a)$$

and in all cases

$$p = 4L_1L_2\,(\Delta_1 + \Delta_2)^2$$

When the circuits are tuned the values of $x_p\; y_p$ A and ω_a for various types of coupling are as follows —

(i) Magnetic coupling—

$$\begin{aligned} -x_p &= R_1R_2 + \omega^2M^2 \\ y_p &= 0 \\ A &= -j\omega M \\ \omega_a &= 0 \end{aligned}$$

(This is coupling my mutual inductance If the coupling is by a common inductance l, l replaces M in the above expressions and Z_1 and Z_2 refer to whole circuits composed of $L_1\; C_1\; l$ and $L_2\; C_2\; l$ with their total resistances)

(ii) Coupling by a common condenser—

$$\begin{aligned} -x_p &= R_1R_2 + 1/\omega^2C_c^2 \\ y_p &= 0 \\ A &= -j/\omega C_c \\ \omega_a &= 0 \end{aligned}$$

(Here again Z_1 and Z_2 must comprise the whole circuits L_1C_1 and C_c, and $L_2\; C_2$ and C_c)

(iii) Coupling by series condenser C_c between circuits- -

$$\begin{aligned} -x_p &= R_1R_2 + \tfrac{1}{4}\omega^2C_c^2L_1L_2\,(1/C_1 + 1/C_2)^2 \\ -\;y_p &= \omega C_c\,\{\tfrac{1}{2}\,(L_1R_2 - L_2R_1)\,(1/C_1 - 1/C_2)\} \\ A &= -jC_c/\omega C_1C_2 \\ \omega_a &= \tfrac{1}{2}\omega C_c\,(1/C_1 + 1/C_2) \end{aligned}$$

(iv) Combined magnetic and electrostatic ((i) and (iii)—

$$-x_p = R_1R_2 + \omega^2M^2(1 + C_e/C_1 + C_e/C_2) + 2MC_e/C_1C_2$$
$$+ \tfrac{1}{4}\omega^2C_e^2L_1L_2(1/C_1 + 1/C_2)^2$$

$$-y_p = \omega C_e \tfrac{1}{2}(L_1R_2 - L_2R_1)(1/C_1 - 1/C_2)$$

$$A = -j\omega M - jC_e/\omega C_1C_2$$

$$\omega_a = \tfrac{1}{4}\omega C_e(1/C_1 + 1/C_2)$$

It is seen that in the first case, that of magnetic coupling,

$$-x_p - R_1R_2 = -A^2,$$

and that this condition is also fulfilled in the second case This, in fact, may be taken as one criterion for an exact parallel existing between any type of coupling and magnetic coupling Another essential is that $y_p = 0$ These conditions are seen to be not fulfilled in general in cases (iii) and (iv), but in case (iii) if C_1 is not very different from C_2 and/or the decay factors are nearly the same,

$$y_p = 0 \text{ and } -x_p - R_1R_2 = C_e^2/\omega^2C_1^2C_2^2 = -A^2,$$

and the conditions are fulfilled

And if in case (iv), in addition to C_1 and C_2 and Δ_1 and Δ_2 being not very different, $C_e(1/C_1 + 1/C_2)$ can be neglected compared with unity

$$-x_p - R_1R_2 = \{\omega M + C_e/\omega C_1C_2\}^2 = -A^2$$

With these circuit conditions understood therefore, and they are conditions very often fulfilled in wireless circuits, we may say that all types of coupling are exactly similar in their effects to coupling by mutual inductance, and that all expressions for the case of mutual inductance can be converted to expressions for other types by replacing ωM by $1/\omega C_e$ in case (ii), $C_e/\omega C_1C_2$ in case (iii), and $(\omega M + C_e/\omega C_1C_2)$ in case (iv), with the additional provision in the last two cases, that the ω distribution must be altered by ω_a

It seems reasonable to assume, therefore, that all of the work in Section I, including the effect of slight distuning of the circuits, and the drawing of Z' loci, can readily be adapted to any type of coupling

The Ultra-Violet Band-System of Carbon Monosulphide and its Relation to those of Carbon Monoxide (the "4th Positive" Bands) and Silicon Monoxide

By W Jevons, D Sc, F Inst P, Lecturer in Physics in the Military College of Science, Woolwich

(Communicated by Prof A Fowler, F R S—Received October 8, 1927)

1 *Introductory Previous Observations*

In 1913 L C Martin[*] discovered an ultra-violet band-system in the tube discharge through carbon disulphide vapour and in the carbon arc fed with sulphur, and ascribed it, on experimental evidence, to the CS molecule The bands are degraded towards the red, and the majority of them are double headed Martin arranged all but seven of the observed bands into seven groups (A, B, G) each formed by closely neighbouring bands The present communication records the quantum analysis of the band-heads, and the substantial similarity of structure between this CS system, the ultra-violet system of SiO and the "4th Positive" system of CO

A brief examination of the photographs reproduced by Martin and of the wave-numbers derived from his tabulated wave-lengths leads to a Deslandres scheme for the band-heads and to a plausible assignment of the initial and final vibrational quantum numbers, n', n'' In this scheme each of Martin's seven groups is a sequence[†] of bands corresponding to a constant change of vibrational quantum number, $n'' - n'$, except that groups B and C together with one band of group A form only one sequence, $n'' - n' = -2$ It further appears that of the pair of heads (bracketed in Martin's table of data) of each double-headed band, the less refrangible head is formed by a Q branch, the corresponding P branch having, of course, no head, and therefore remaining undetected with the dispersion employed by Martin (about 7 8 A/mm at λ 2420 to 12 7 A/mm at λ 2850)

Though there seemed little doubt as to the correctness of the above conclusions from Martin's data, there were certain difficulties, two of which may be mentioned here Firstly, it was necessary in some cases to discard Martin's pairing of the heads in order to secure regularity in the Deslandres schemes of R and Q heads, *e g* , the head at λ2819 29, though the *less* refrangible head of a bracketed pair, is the R head of the 4,6 band, and the *more* refrangible head λ 2818 37 in the same bracket does not, apparently, belong to the same band, nor indeed to the same system Secondly, the 0,0 band, which should be one of the most strongly developed bands of the system, does not appear in Martin's table Near its expected position (about λ 2575) Martin records a strong head λ 2579, which, however, does not belong to the same band-system, as is clear from Martin's observation that its appearance varies greatly under different conditions , thus, it is the strongest of all the bands in this region in the sulphur-fed carbon arc where the whole CS system is weak, but it is relatively weaker in the CS_2 tube discharge where the CS system is strong Martin further states that in the latter source the head in question "is evidently superposed on another group with a fairly strong band near 2573 " The group and band here mentioned are evidently the $n'' - n' = 0$ sequence and the 0,0 band respectively

---

[*] L. C Martin, 'Roy Soc Proc,' A, vol 89, p 127 (1913)

[†] The term "sequence" is now widely used for what Prof A Fowler and several former workers in his laboratory have called a "group" See, for example, 'Roy Soc Proc,' A, vol 79, p 509, 1907 (TiO), vol 86, p 112, 1912 (CN), vol. 89, p 127, 1913 (CS), vol 110, p 356, 1926 (SnCl), and vol 112, p 407, 1926 (CN) In Tables II–VI of the present paper the data for a sequence of bands appear along a diagonal downwards from left to right.

2 *New Data Assignment of Vibrational Quantum Numbers*

These and other considerations showed the necessity of new observations As the quartz spectrograph accessible to me at the time of writing has too small a dispersion for the purpose, Prof A Fowler kindly lent me the excellent spectrograms of the CS_2 discharge taken by Dr. Martin, who readily concurred in my re-examining them in the light of knowledge gained since he discovered this band-system

In the best spectrogram (the one from which strips 1 and 2 of Dr Martin's Plate 6 were reproduced) the bands are much more distinctly recorded a few millimetres away from the edge of the Fe arc comparison spectrum than they are where the two spectra overlap In the new observations, therefore, the plan adopted has been first to measure against Fe wave-lengths the best defined heads in the overlap, and then to measure all the heads detectable away from the Fe spectrum, using the previously determined wave-lengths of some of the heads as standards In this way more heads have been measured and greater relative accuracy obtained (at the expense, no doubt, of absolute accuracy) than would have been possible by measuring directly against overlapping Fe lines The difference in the methods of measurement is responsible for the fact that the discrepancy between Martin's wave-length and the writer's for the same head is sometimes rather large (*e g* , 0 3 A for the R head of the 2,2 band)

Table I gives the positions, intensities and classification of the heads as given by Martin, and the corresponding data resulting from the re-examination. The data for the R heads are shown in romans and those for the Q heads in italics, and Martin's brackets for his pairs are retained. The substantial agreement of Martin's empirical classification with that resulting from the present investigation and the few modifications and additions made in the course of the latter are at once obvious.

The wave-numbers *in vacuo* (from the newer measurements) and their first differences are arranged in Deslandres schemes of vertical (n') and horizontal (n'') progressions in Table II, (*a*) $\nu_{\text{R head}}$ and (*b*) $\nu_{\text{Q head}}$. The observed separations of the two heads ($\nu_{\text{R head}} - \nu_{\text{Q head}}$) are similarly arranged in Table III.

On brief inspection of Tables II and III, considerable irregularities, far exceeding the smaller irregularities resulting from observational errors are easily seen in connection with the four bands of the horizontal progression $n' = 1$. Thus in Table II (*b*) it is clear from a consideration of the horizontal rows of first differences that their Q heads are displaced to the red, relatively to the other n'' progressions, and, further, from Table II (*a*) their R heads are relatively displaced to the further ultra-violet. Correspondingly, the separations of the R and Q heads in Table III are much larger for these four bands than for the rest of the system. All these four bands are particularly difficult to measure on account of lack of sharpness of their heads. This is especially true of the 1,0 band, in the neighbourhood of which the spectrograms show some half-dozen features which may be heads, the selection of two of these as the R and Q heads is rather uncertain. In Table I six measurements made in this region are tentatively given, together with identifications of the R and Q heads which were suggested by comparison with the 1,1, 1,2 and 1,3 bands of the same progression. We shall refer again to the $n' = 1$ progression in sections 4, 5 and 6, but for the immediate present we will omit them from our discussion of the structure of the system.

Table I —Heads of CS Bands (Degraded towards the red) R heads in romans Q heads in italics

Martin					Jevons						
Group	Int	λ_{air} (I A)	ν_{vac} (cm $^{-1}$)	$\Delta\nu$	n', n''	Branch	Int	λ_{air} (I A)	ν_{vac} (cm $^{-1}$)	$\Delta\nu$ (R—Q)	Notes (see p 360)
					5,2	R	000	2418 40	41337 1		
A	0 5	2436 00	41038 4		6,3	R	1	36 01	038 3	6 8	
						Q	*0*	*36 41*	*031 5*		
					10,6	R	000	40 14	40968 8		
B	2	44 56	40894 8	8 9	2,0	R	3	44 80	890 7	10 5	
		45 09	*885 9*			Q	*2*	*45 43*	*880 2*		
A	1	53 45	746 6	11 8							1 (*a*)
		54 16	734 8		7,4	R	1	54 27	733 0		
B	2	60 02	637 8	11 3	3,1	R	5	60 17	635 3	10 2	
		60 70	*626 5*			Q	*3*	*60 79*	*625 1*		n
A	1	73 21	421 1		8,5	R	3	73 44	417 3		
B	2	76 89	361 0		4,2	R	4	76 99	359 4	7 7	
						Q	*3*	*77 46*	*351 7*		
					9,6	R	0	93 19	097 2		
A	4	93 41	093 6		5,3	R	6	93 66	089 6	7 2	
						Q	*4*	*94 11*	*082 4*		
							3	2506 01	39892 1		1 (*b*)
							'3	06 69	881 2		1 (*b*)
						R	'*4l*	07 32	871 2		
?	5ı	2508 14	39858 2	19 9	1 0		'*3l*	08 22	856 9	33 2'	1 (*c*)
							'*3l*	08 84	847 1		1 (*b*)
		09 39	*838 3*			Q	*5*	*09 41*	*838 0*		

C	6	2511 29	39808 2		6,4	R	3n	2511 23	39809 1		
D	6	22 97 *23 79*	623 9 *611 0*	12 9	2,1	R Q	7 *5*	23 23 *23 99*	619 8 *607 9*	11 9	
C	2	29 90	515 4		7,5	R	3	29 97	514 3		
„	2	35 54	427 5	11 4			12*l*	35 50	428 1		1 (*c*)
		36 27	416 1				12*l*	36 06	419 4		1 (*c*), ui
D	6	38 55 *39 29*	380 7 *369 3*	11 4	3,2	R Q	8 *6*	38 69 *39 51*	378 6 *365 9*	12 7	
C	2	49 44	212 5		8 6	R	3	49 47	212 1		
D	6	55 74 *56 10*	115 9 *110 4*	5 5	4,3	R Q	5 *4*	55 78 *56 30*	115 3 *107 3*	8 0	
C	1	69 61	38904 8		9 7	R	1n	69 51	38906 3		
D	2	72 64	858 9		5,4	R Q	5 *5*	72 67 *73 30*	858 5 *849 0*	9 5	
					0,0	R Q	10*l* *7*	75 64 *76 70*	813 7 *797 7*	16 0	
E	8	79 12	761 3								1 (*a*)
„	4	87 26	639 4				5	87 36	637 9		1 (*c*)
? E	6 10	90 22 *91 93*	595 2 *569 8*		1,1	R Q	6n *8*	89 66 *92 06*	603 6 *567 8*	33 8	1 (*a*)
E	8	2605 59 *06 94*	367 6 *347 7*	19 9	2,2	R Q	10 *8*	2605 88 *06 93*	363 3 *347 9*	15 4	
E	6	21 52 *22 53*	134 4 *119 8*	14 6	3 3	R Q	7 *5*	21 63 *22 58*	132 8 *119 5*	13 3	

Table I —(continued)

Martin					Jevons						
Group	Int	λ_{air} (I A)	ν_{vac} (cm $^{-1}$)	$\Delta\nu$	n' n''	Branch	Int	λ_{air} (I A)	ν_{vac} (cm $^{-1}$)	$\Delta\nu$ (R – Q)	Notes (see p 360)
?	4	2629 59	38017 4		8,7	R	1	2629 51	38018 6		1 (*a*)
		30 70	001 4								
E	4	38 85	37884 0	14 6	4,4	R	2	38 96	37882 4	13 3	
		39 87	*869 4*			Q	*2*	*39 89*	*869 1*		
					7 5	R	00	56 17	637 0		
?	2	60 34	578 0				4	60 35	577 9		1 (*c*), IV
F	10*nn*	61 85	556 7	30 6			4	61 91	555 9		1 (*c*)
					0,1	R	10	62 56	546 7	20 6	
		64 02	*526 1*			Q	*8*	*64 02*	*526 1*		
?	2	74 66	376 8				4	74 56	378 2		1 (*c*), V
F	8*nn*	77 44	338 0	29 0	1,2	R	6*n*	77 01	344 0	33 4	
		79 52	*309 0*			Q	*5*	*79 41*	*310 6*		
F	8*nn*	92 66	127 0	25 5	2,3	R	8*n*	93 22	119 3	18 4	
		94 51	*101 5*			Q	*7*	*94 55*	*100 9*		
							1	2708 07	36915 7		1 (*b*)
F	6	2709 01	36902 9	19 0	3,4	R	7	08 94	903 9	18 5	
		10 41	*883 9*			Q	*4*	*10 30*	*885 4*		
F	4	26 62	664 2		4,5	P	4	26 68	663 8		
							0	34 64	557 1		1 (*b*)

F	2	44 49	425 9		5,6	R	3	43 91	433 6		11
							11	53 74	303 5		1 (*b*)
G	6	54 73	290 5	28 6	0,2	R	*7l*	54 73	290 5	23 2	1 (*b*)
						'R	6	55 16	284 8		
		56 90	*261 9*			Q	*5*	*56 49*	*267 3*		
					6,7	R	1	62 69	185 9		
G	6ı	69 46	097 5	31 8	1,3	R	*3nn*	69 17	101 3	36 3	
		71 90	*965 7*			Q	*4n*	*71 96*	*065 0*		
G	5	85 16	35894 0	31 3	2,4	1R	'4	85 01	35895 9	18 9	1 (*c*)
						R	5	85 68	887 3		
		87 59	*862 7*			Q	*5*	*87 15*	*868 4*		
G	4	2801 58	683 6	25 4	3,5	R	5	2801 46	685 2	23 8	
		03 58	*658 2*			Q	*3*	*03 33*	*661 4*		
G	4	18 37	471 1				'1n	18 19	473 3		1 (*c*)
		19 29	459 5		4,6	R	3	19 51	456 7		
G	4	37 21	235 6		5,7	R	2	36 79	240 8		
					0,3	R	2	52 35	048 5	25 3	
						Q	*2*	*54 41*	*023 2*		

Table II.—Wave-numbers of CS Band-heads arranged in n' and n'' Progressions

(*a*) $\nu_{R \text{ head}}$

n' \ n''	0		1		2		3		4		5		6		7	
0	38813 7	1267 0	37546 7	1256 2	36290 5	1242 0	35048 5									
	1057 5		1056 9		1053 5		1052 8									
1	39871 2	1267 6	38603 6	1259 6	37344 0	1242 7	36101 3		(vi)							
	1019 5		1016 2		1019 3		1018 0									
2	40890 7	1270 9	39619 8	1256 5	38363 3	1244 0	37119 3	1232 0	35887 3		(vii)					
			1015 5		1015 3		1013 5		1016 6							
3			40635 3	1256 7	39378 6	1245 8	38132 8	1228 9	36903 9	1218 7	35685 2		(vii)			
					980 8		982 5		978 5		978 6					
4			(xii)		40359 4	1244 1	39115 3	1232 9	37882 4	1218 6	36663 8	1207 1	35456 7			
					977 7		974 3		976 1		973 2		976 9			
5					41337 1	1247 5	40089 6	1231 1	38858 5	1221 5	37637 0	1203 4	36433 6	1192 8	35240 8	
							948 7		950 6						945 1	
6							41038 3	1229 2	39809 1		(x)		(iv)		36185 9	(viii)
									923 9							
7									40733 0	1218 7	39514 3		(xi)		(ix)	
											903 0					
8											40417 3	1205 2	39212 1	1193 5	38018 6	
													885 1		887 7	
9											(xii)		40097 2	1190 9	38906 3	
													871 6			
10													40968 8			

(b) $\nu_{Q\ \mathrm{head}}$

n'' \ n'	0		1		2		3		4		5	6	7
0	38797 7	1271 6	37526 1	1258 8	36267 3	1244 1	35023 2						
	1040 3		1041 7		1043 3		1041 8						
1	39838 0	1270 2	38567 8	1257 2	37310 6	1245 6	36065 0						
	1042 2		1040 1		1037 3		1035 9						
2	40880 2	1272 3	39607 9	1260 0	38347 9	1247 0	37100 9	1232 5	35868 4				
			1017 2		1018 0		1018 6		1017 0				
3			40625 1	1259 2	39365 9	1246 4	38119 5	1234 1	36885 4	1224 0	35661 4		
					935 8		987 8		983 7				
4					40351 7	1244 4	39107 3	1238 2	37869 1				
							975 1		979 9				
5							40082 4	1233 4	38849 0			(vi)	
							949 1						
6							41031 5						

NOTES TO TABLES

s = indistinct (in Martin's data)
n = nebulous
? = doubtful head
l — line like
} in intensity columns

i —Head not included in CS system given in Table II

(*a*) Measured by Martin only
(*b*) Measured by the writer only
(*c*) Measured by Martin and the writer

ii —Wave length given in Martin's table as λ2460 07, but was probably intended to be λ2460 70 which is a more likely value

iii —May be the edge of Hg line λ 2536 52

iv —The wave length given in Martin's table is λ2659 34, which is clearly 1 A too low

v —From the very low intensity of the 5,5 band it is expected that the 6,6 band ($\nu_{\text{R head}}$ 37380) would be far too weak to be detectable The band shown in Table I near this position is of much too high intensity, as well as of slightly too low wave number, to be the 6,6 band, and is therefore excluded from Tables II (*a*), IV and V This is in agreement with Martin's non allocation of the band to his group F

vi —A probable head (int 2) was measured at λ 2744 91, ν 36420 3, which is near the Q head of the 5,6 band It was not considered certain enough for inclusion in the tables, but may account for the large discrepancy between Martin's and the writer's measures of the R head

vii —From a consideration of the intensities (section 5) the 1,4, 2 5 and 3,6 bands of sequence + 3 *may* be *expected to be present*, *their observation* would probably be hindered by the occurrence of the sulphur bands in this region

viii —The 6,8 band ($\nu_{\text{R head}}$ 35006) may be present, but hidden by the sulphur bands A doubtful band was roughly measured at λ2855 4 ν 35011, but was too uncertain to include in the tables

ix —The 7,5 band ($\nu_{\text{R head}}$ 37113), if present, would be masked by the 2,3 band In any case it should be too weak to be detectable (see section 5)

x The 6,5 band ($\nu_{\text{R head}}$ 38587) is probably present but hidden by overlying 1,1 band

xi —The 7,6 band ($\nu_{\text{R head}}$ 38307) may be present but hidden by the overlying 2,2 band

xii – Though theory (see section 5) indicates a diminution of intensity in these parts of the system, it should be noted that the sensitivity of an ordinary photographic plate is also diminished in this region The 9,5 band ($\nu_{\text{R head}}$ 41306) and still earlier bands of sequence 4, and the 4,1 band ($\nu_{\text{R head}}$ 41618) of sequence − 3 might perhaps be recorded in a long exposure with an oiled or a Schumann plate

Table III —Intervals between R and Q Heads

($\nu_{R\,head} - \nu_{Q\,head}$)

n' \ n''	0	1	2	3	4	5	6	7
0	16 0	20 6	23 2	25 9				
1	33 2	35 8	33 4	36 1				
2	10 5	11 9	15 4	18 4	18 0			
3		10 2	12 7	13 3	18 5	23 8		
4			7 7	8 0	13 3			
5				7 2	9 5			
6				6 8				

3 *Intervals between R and Q Heads Representation by Formulæ*

Even though none of the bands is adequately resolved for measurements of line structure, there is considerable justification for ascribing the two heads of each band to its R and Q branches, it is mainly to be found in a comparison of the observed variation of the interval between the two heads with n' and n'' with the variation of the interval $\nu_{R\,head} - \nu_{Q\,head}$ indicated by the quantum theory of band structure

Considering the $n'n''$ band and using as far as possible the notation of the recent report of the National Research Council,* we have for the Q head –

$$\nu_{Q\,head} = \nu_e + \omega_0\, n'(1 - x'n') - \omega_0\, n''(1 - x''n''), \tag{1}$$

and for any line of the R branch -

$$\nu_R - \nu_{Q\,head} = B_n + 2B_{n'}\,m + (B_{n'} - B_n\ \ )m^2$$

---

* 'Nat Res Council Bulletin, "Molecular Spectra in Gases" (Washington, 1926) *Notation* —For convenience, the significance of the symbols used is quoted here —

′ and ″ represent the more and the less excited states (upper and lower energy levels)

n = vibrational quantum number

m = effective rotational quantum number = (nuclear angular momentum *for* less excited state) $2\pi/h$

ω_0 = frequency of vibration of infinitesimal amplitude for rotationless molecule

$B_n = h/8\pi^2 I_n$ where I_n = moment of inertia of vibrating molecule and

B_0 and I_0 similarly apply to the vibrationless molecule

$$x = \left(\frac{3}{2} + \frac{15}{2}b + \frac{3}{2}c + \frac{15}{4}b^2\right)u$$

$$\alpha = \frac{3}{2}(1 + 2b + \quad)\,\omega_0 u^2$$

where $u = h/4\pi^2 I_0\omega_0$, and b and c are constants of the law of force assumed

For the R head

$$\left(\frac{d\nu_{\mathrm{R}}}{dm} = 0\right), \qquad m_{\mathrm{R\ head}} = -\frac{\mathrm{B}_{n''}}{\mathrm{B}_{n'} - \mathrm{B}_{n''}},$$

hence

$$\nu_{\mathrm{R\ head}} - \nu_{\mathrm{Q\ head}} = -\frac{\mathrm{B}_{n'}\ \mathrm{B}_{n''}}{\mathrm{B}_{n'} - \mathrm{B}_{n''}}$$
$$= \mathrm{B}_{n'}(1 - z)^{-1}$$

where $z = \mathrm{B}_{n'}/\mathrm{B}_{n''}$ which is less, though often not much less, than unity for bands which are degraded towards the red ($\mathrm{I}_{n'} > \mathrm{I}_{n''}$) as these are, hence

$$\nu_{\mathrm{R\ head}} - \nu_{\mathrm{Q\ head}} = \mathrm{B}_{n'}\ (1 + z + z^2 + z^3 + \quad),$$

a slowly convergent series

Putting $\mathrm{B}_{n'} = \mathrm{B}_0 - \alpha' n'$, $\mathrm{B}_{n''} = \mathrm{B}_{0''} - \alpha'' n''$, and $\mathrm{B}_{0'}/\mathrm{B}_{0''} = z_0$, expanding, and omitting small terms in n'^3, n''^3, $n'^2 n''$, $n' n''^2$, and higher powers, we arrive at the form —

$$\nu_{\mathrm{R\ head}} - \nu_{\mathrm{Q\ head}} = \kappa + \zeta' n' + \eta' n'^2 + \zeta'' n'' + \eta'' n''^2 + \theta n' n'' \tag{2}$$

where

$$\begin{aligned}
\kappa &= \quad (1 + z_0 + z_0^2 + z_0^3 + \quad)\ \mathrm{B}_0 \\
\zeta' &= -\alpha'\ (1 + 2z_0 + 3z_0^2 \quad) \\
\zeta'' &= \alpha''\ (z_0^2 + 2z_0^3 + 3z_0^4 \quad) \\
\eta' &= \alpha'^2\ (z_0 + 3z_0^2 + \quad)/\mathrm{B}_0 \\
\eta'' &= \alpha''^2\ (z_0^3 + 3z_0^4 + \quad)/\mathrm{B}_{0'} \\
\theta &= -2\alpha'\alpha''\ (z_0^2 + 3z_0^3 + \quad)/\mathrm{B}_0
\end{aligned}$$

Hence, adding (1) and (2),

$$\nu_{\mathrm{R\ head}} = (\nu_e + \kappa) + (\omega_{0'} + \zeta')n' - (\omega_0 x' - \eta')n'^2 - (\omega_0 - \zeta'')n'' + (\omega_{0''} x'' + \eta'')n''^2 + \theta n' n'' \tag{3}$$

Now Birge* and Mecke† have pointed out that for all systems so far analysed α' and α'' are positive ‡ Since also B_0', B_0'' and therefore z_0 are positive, we

---

* R T Birge, 'Phys Rev,' vol 25, p 240, abs 23 (1925)

† R Mecke, 'Z f Physik,' vol 32, p 823 (1925)

‡ This observation is equivalent to the Birge–Mecke rule that, without known exception, the frequency of vibration of a molecule increases as its moment of inertia decreases, and *vice versa* For, from

$$\mathrm{B}_n = \mathrm{B}_0 - \alpha n$$

we have

$$h/8\pi^2\mathrm{I}_n = h/8\pi^2\mathrm{I}_0 - \alpha n$$

or

$$1/\mathrm{I}_n = 1/\mathrm{I}_0 - 8\pi^2\alpha n/h$$

Thus if α is positive, I_n decreases as n increases and therefore as ω_n increases This corresponds with the general rule that in any given sequence n' and n'' increase in the direction in which the bands are degraded, *i e*, in the present case towards the smaller wave-numbers, *as is clear from* Table II have, for bands degraded to the red, positive values for κ, ζ'', η' and η'' and negative values for ζ' and θ Further, since α' and α'' are small compared with B_0, these coefficients are clearly of three different orders of magnitude, κ being relatively large, ζ' and ζ'' smaller, and η', θ and η'' still smaller The implication of equation (2) is, then, that the interval $\nu_{\text{R head}} - \nu_{\text{Q head}}$ of the n', n'' band (i) decreases from band to band in an n' progression as n' increases, and (ii) increases in an n'' progression as n'' increases

Table III shows that, apart from the anomalous bands of the progression $n' = 1$, the observed separations of the heads vary exactly in this way The observations, therefore, show at least qualitative agreement with the theory if the assignment of n', n'' values and the attribution of the heads to R and Q branches be as shown in Tables I, II and III

The evaluation of the coefficients in equations (1) and (3) from the observed wave-numbers is somewhat uncertain on account of the displacements (noted on p 353) of the bands of the progression $n' = 1$ (and, as will appear presently, of other n'' progressions) Omitting the $n' = 1$ bands, the following expressions have been derived --

$$\nu_{\text{R head}} = 38921.1 + 1070.2\,(n' + \tfrac{1}{2}) - 10.11\,(n' + \tfrac{1}{2})^2 - 1282.0\,(n'' + \tfrac{1}{2}) + 6.42\,(n'' + \tfrac{1}{2})^2 - 0.24\,(n' + \tfrac{1}{2})\,(n'' + \tfrac{1}{2}) \quad (4)$$

$$\nu_{\text{Q head}} = 38902.5 + 1072.2\,(n' + \tfrac{1}{2}) - 10.05\,(n' + \tfrac{1}{2})^2 - 1282.5\,(n'' + \tfrac{1}{2}) + 6.00\,(n'' + \tfrac{1}{2})^2 \quad (5)$$

and therefore

$$\nu_{\text{R head}} - \nu_{\text{Q head}} = 18.6 - 2.0\,(n' + \tfrac{1}{2}) - 0.06\,(n' + \tfrac{1}{2})^2 + 0.5\,(n'' + \tfrac{1}{2}) + 0.42\,(n'' + \tfrac{1}{2})^2 - 0.24\,(n' + \tfrac{1}{2})\,(n'' + \tfrac{1}{2}) \quad (6)$$

The addition of $\frac{1}{2}$ to the integral values of the vibrational quantum numbers is indicated by the new quantum mechanics and is adopted here*, otherwise equations (4), (5) and (6) are of the same forms as (3) (1) and (2) respectively The accuracy of the present observations is not such as to demand this use of half-quanta for the vibrational energies.* The R head data definitely show the need for a factor in $n'n''$, or $(n' + \frac{1}{2})(n'' + \frac{1}{2})$, in equation (4) but do not satisfactorily settle the value of its coefficient θ; the estimated value $\theta = -0.24$ is judged to be about the best obtainable from the data.

---

* Alternatively we may leave equations (1), (2) (3) unaltered and give half integral values to n' and n'', as was done earlier by Mulliken in the case of BO (‘Phys Rev’ vol 25, pp 119 and 259 (1925)) For descriptive purposes it seems more convenient to retain the integral values of n' and n'' (as shown in all the tables of the present paper), and add $\frac{1}{2}$ in deriving the energies, as has recently been done by Ferguson (‘Nature,’ vol 120 p 298 (1927)) in the case of AuCl, thus we may still speak of the 0 0 band, the 9 7 band etc, instead of re designating them the $\frac{1}{2}$,$\frac{1}{2}$ band, the 9$\frac{1}{2}$,7$\frac{1}{2}$ band, etc

Formulæ (4), (5) and (6) are readily convertible into:—

$$\nu_{\text{R head}} = 38814.2 + 1060.0n' - 10.11n'^2 - 1275.7n'' + 6.42n''^2 - 0.24n'n'', \tag{7}$$

$$\nu_{\text{Q head}} = 38796.3 + 1062.2n' - 10.05n'^2 - 1276.5n'' + 6.00n''^2, \tag{8}$$

$$\nu_{\text{R head}} - \nu_{\text{Q head}} = 17.9 - 2.2n' - 0.06n'^2 + 0.8n'' + 0.42n''^2 - 0.24n'n'', \tag{9}$$

which involve whole quanta of vibrational energy, and are identical in form with (3), (1) and (2) respectively. It may be noted here that while equation (8) in n', n'' gives for the system-origin, $\nu_e = 38796.3$ cm^{-1} (the origin of the 0,0 band), equation (5) in $n' + \frac{1}{2}$, $n'' + \frac{1}{2}$ locates it at 38902.5 cm^{-1}, which is very near the origin of the 9,7 band. Further, the frequencies of very small vibration of the non-rotating molecule in its initial and final states are

$\omega_0 = 1062.2$ cm^{-1}, $\omega_0 = 1276.5$ cm^{-1} according to (5), and
$\omega_0 = 1072.2$ cm^{-1}, $\omega_0 = 1282.5$ cm^{-1} according to (8),

the proportional increase $(\omega_0 - \omega_0)/\omega_{0\,\text{mean}}$ is 18.3 per cent. from (5) and 17.9 per cent. from (8).

Comparing equations (2) and (6) we find that the signs obtained for the coefficients κ, ζ', ζ'', η'' and θ are those required by the theory, and that, in further accord with the theory, κ $(= 18.6$ cm$^{-1})$ is much greater than the other coefficients, whose values, however, are less trustworthy, as may be seen by comparing the order of their magnitudes with that of the expressions given under equation (2). Only η' is wrong in sign. The discrepancies are not surprising in view of the facts next to be considered.

4. *Perturbations of Vibrational Energy Levels in the Initial State.*

The differences between the observed and calculated values of $\nu_{\text{R head}}$, $\nu_{\text{Q head}}$ and $\nu_{\text{R head}} - \nu_{\text{Q head}}$ which are shown in Table IV are in many cases

---

[*] Mulliken (*loc. cit.*) has pointed out that accurate measurement of an isotope effect is the only practical means yet known of deciding with certainty between whole and half-quanta of vibrational energy. The present spectrograms show no indication of the sulphur isotope effect, as might be expected from the great preponderance of S^{32} over S^{33} and S^{34} found by F. W. Aston ('Nature,' vol. 117, p. 893 (1926), and 'Roy. Soc. Proc.,' A, vol. 115, p. 504 (1927)), viz., $S^{32}/(S^{33} + S^{34}) =$ about 97/3. It was, in fact, Dr. Aston's announcement of the S isotopes that directed the writer's attention to the CS band system.

well outside the limits of observational errors A study of this table of residuals brings out certain anomalies in the distribution of vibrational energy levels for the initial state

(1) In Table IV, (*a*) and (*b*), there is a distinct tendency for the residuals in an n'' progression (*i e*, a horizontal row) to be of the same sign and often of very roughly the same order of magnitude, while in an n' progression (*i e*, a vertical column) they show no such tendency Thus the means of the residuals in most of the n'' progressions are large compared with the means in all the n' progressions, omitting the anomalous bands having $n' = 1$ (see p 353) The inference is that the distribution of some of the lower vibrational energy levels in the initial state (particularly $n' = 1$, but also $n' = 4, 2, 3, 5$) differs appreciably from the regular distribution given by a smooth formula of the type (1) which generally applies in other bands-ystems, in the initial state we evidently have "perturbed" vibrational levels, while in the final state no such irregularities are appreciable

Table IV —Residuals

(*a*) *R Head*, $\nu_{obs} - \nu_{calc}$ (Table II (*a*)– formula (4))

n' \ n''	0	1	2	3	4	5	6	7	
0	−0 5	1 8	2 0	3 6					1 8
1	7 1	9 0	6 1	7 3					7 4
2	−3 0	−4 1	−3 7	−3 6	−4 4				−3 8
3		2 2	2 6	1 1	3 7	3 7			2 7
4			−5 3	−4 8	−6 0	−5 7	−6 8		−5 7
5			3 9	1 2	2 1	−0 3	2 6	3 2	2 1
6				1 9	4 9			1 2	2 7
7					1 1	2 0			1 5
8						−2 0	−0 2	0 4	−0 6
9							−1 8	1 7	0 0
10							3 4		3 4
	−1 7	0 0	0 0	−0 1	0 2	−0 5	−0 6	1 6	Means

Table IV—(continued)

(b) *Q Head*, $\nu_{obs} - \nu_{calc}$ (Table II (*b*)—formula (5))

n' \ n''	0	1	2	3	4	5	5	7	
0	1 4	0 2	0 0	2 4					1 0
1	−10 4	−10 1	−8 8	−7 9					−9 3
2	−0 2	−2 0	−3 5	−4 0	−2 0				−2 3
3		3 3	2 6	2 7	3 1	1 6			2 7
4			−3 4	−1 3	−5 0				−3 2
5				2 1	3 2				2 6
6				−0 4					−0 4
	0 6	0 5	−1 1	0 2	−0 2	1 6			Means

Note — In taking the mean residuals shown at the foot of (*a*) and (*b*), for the n progressions, the $n' = 1$ bands have been omitted

(*c*) *R - Q Interval*, $\Delta\nu_{obs} - \Delta\nu_{calc}$ (Table III —formula (6))

n \ n''	0	1	2	3	4	5	6	7
0	−1 9	1 5	2 0	1 2				
1	17 6	10 2	15 0	15 2				
2	−2 8	2 1	0 2	0 4	−2 4			
3		−1 1	0 1	−1 5	0 7	2 1		
4			−1 9	3 5	−1 0			
5				−0 9	−1 1			
6				2 3				

(ii) Taking any one n'' progression for which there are sufficient Q head data and comparing the means of the residuals for the R heads in Table IV (*a*) with those for the Q heads in Table IV (*b*), it is noticed that in general they are of the same sign and of very roughly the same magnitude, that is to say, in general each band as a whole shows roughly the same displacement as its origin This is in accordance with the fact that the differences, shown in Tabe IV (*c*) between the observed and calculated values of the interval $\nu_{R\ head} - \nu_{Q\ head}$ are not much greater than the errors of observation This is true of the progressions

$n' = 0, 2, 3, 4$ and 5, but does not apply to the progression $n' = 6$ (which can be disregarded since it involves only one measured Q head) nor to the progression of anomalous bands, $n' = 1$ It is not true of the n' progressions

The inference is that for the initial state of the molecule the rotational energy levels tend to show the same perturbation as the vibrational energy level with which they are associated, but the vibrational level $n' = 1$ is abnormal in this respect It has already been noted (p 353) that the heads of some of the $n' = 1$ bands are difficult to identify, if the identifications shown in Tables I and II are correct, it would appear from the opposite sign of the residuals for the R and Q heads that the rotational levels are perturbed in the opposite sense to the vibrational energy level $n' = 1$, with which they are associated From the remarks at the end of section 2 it appears that the abnormally big intervals between the heads of the $n' = 1$ bands may alternatively be interpreted by supposing each of these bands have an R branch in addition to the three branches (P, Q and R) occurring in the other bands of the system, and that the measured R head is formed by the additional branch

5 *Intensities*

On account of the rapid variation of the plate sensitivity from one end of the system to the other, the estimates of photographic blackening permit of only a rough discussion of the distribution of intensity amongst the bands In Table V the intensities of the R heads, which we may take as indications of

Table V - Intensities of R Heads of CS Bands

n' \ n''	0	1	2	3	4	5	6	7
0	10	10	7	2				
1	4?	6n	6n	3nn				
2	3	7	10	8n	5			
3		5	8	7	7	5		
4			4	5	2	4	3	
5			000	6	5	00	3	2
6				1	3n			1
7					1	3		
8						3	8	1
9							0	1n
10							000	

the intensities of the bands themselves (apart from the $n'=1$ bands), are arranged in the same way as to the wave-numbers, intervals and residuals in Tables II, III and IV The table shows that the distribution of intensity is of the commonest type,* which is now known to be characteristic of a small change in the moment of inertia and in the vibration frequency of the emitting molecule. Thus, (i), in sequence 0 there is a maximum at the 0,0 band (one of the strongest three bands of the system) a somewhat smaller intensity at the 1,1 band, a regain of intensity at the 2,2 band (which is as strong as the 0,0 band), followed by a rapid fall (ii) In some, at least, of the other sequences there is a maximum not at the first (i e, lowest n',n'') band, but at a band of higher n',n'' values further along the sequence, e g at the 3,2 band in sequence − 1, at the 5,3 band in sequence − 2, and at the 8,5 band in sequence − 3†, similarly, sequences + 1 and + 2 have maxima at or near the 2,3 and the 3,5 bands, but also at their first bands 0,1 and 0,2 respectively (iii) In progressions with relatively high values of n' or n'' there are two intensity maxima, one on either side of the band of sequence 0, which is weak or missing, e g, in the n' progressions having $n'' = 4$, 5, 6 and 7, and the n'' progressions having $n' = 4$, 5 and 6 As n' and n'' diminish to zero the two maxima converge towards the greater maximum at the 0,0 band

These observations are in qualitative agreement with Condon's theory,‡ according to which the intensity maxima are distributed along a parabola-like curve having sequence 0 as its axis, and the 0,0 band as its vertex, provided that the change in moment of inertia is small, with increasing change in moment of inertia both the width of the parabola and the interval between its vertex and the 0,0 band increase The locus of the maxima for CS, roughly indicated in Table V, is much wider than that given by Condon for the $^2S \rightarrow {}^2S$ system of SiN (proportional decrease $(I_0 - I_0)/I_{0\,\mathrm{mean}} =$ only 1 6 per cent), about as wide as that for the $^2S \rightarrow {}^2S$ system of AlO (decrease of $I_0 = 5$ 9 per cent), and distinctly narrower than that for the "4th positive" bands of CO (decrease of $I_0 = 14$ 8 per cent) We may conclude that the proportional decrease of moment of inertia for the emission of the CS system is of the same order as for the emission of the AlO system

We arrive at roughly the same conclusion from a consideration of the vibration frequencies of these molecules, thus, for the CS system the proportional increase $(\omega_0 - \omega_0)/\omega_{0\,\mathrm{mean}} = 18\ 3$ per cent from (5), which is between that for the AlO system (11 5 per cent) and that for the CO "4th positive" system (35 2 per cent from (11)), but very much nearer to the former From Mecke's correlation of the proportional changes in moment of inertia and vibration frequency,[*] we should therefore expect the decrease $(I_{0'} - I_0)/I_{0\,\mathrm{mean}}$ for the CS system to be slightly greater than that for the AlO system but much less than that for the CO "4th positive" system

---

* The features of this "normal" distribution have been described by Mulliken ('Phys Rev,' vol 26, pp 19 and 333 (1925)) and Birge (Report, pp 129, 134–138, 140 and 248

† But see note (xii) to tables, p 360

‡ E. Condon, 'Phys Rev,' vol 28, p 1182 (1926)

This qualitative agreement of the observed intensity distribution with theory leaves no room for reasonable doubt as to the correctness of the *n′*,*n″* assignments shown in the tables

Having ascertained that the moment of inertia changes by an ordinary amount, we turn to the relative intensities of the two heads of each band, and can say at once that they are in accordance with the view that the heads belong to the R and Q branches—a view which has already received strong support in section 3 from the study of the variation of the interval between the two heads In general the less refrangible (Q) head is the less intense, as would be expected from the fact that the Q head is a confluence of the earliest (*i e*, lowest *j*-value) lines of the branch, which are very weak except at very low temperatures, while the lines forming the head of the R branch have higher *j*-values and are probably not far from the maximum intensity of the branch at ordinary discharge-tube temperatures In the next section we shall see that the bands are probably of a type ($^1P \rightarrow {}^1S$) in which the Q *branch* as a whole has twice the intensity of the R *branch* as a whole [†] This is, of course, quite compatible with the observation that the Q *head* is weaker than the R *head*

The bands of the progression $n' = 1$ are abnormal in this respect, their R heads being less, instead of more, intense than their Q heads This may be in accordance with the abnormally big interval between the two heads of each of these bands, for the R head will be formed of lines of abnormally high *j*-values, perhaps some distance from the maximum intensity of the branch On this view the R head would not only be relatively weak, but also rather ill-defined, which is actually found to be the case

---

[*] See Birge, Report, p 233, for a discussion of Mecke's correlation ('Z f Physik,' vol. 32, p 823, 1925), and pp 230–232 for the I_0 and ω_0 data for the SiN, AlO and CO systems

[†] R S Mulliken, 'Phys Rev,' vol 29, p 391 (1927)

6. *The Ultra Violet Band Systems of CS and SiO in Relation to the "Fourth Positive" ($1\,^1P \rightarrow 1\,^1S$) System of CO*

In sections 3 and 5 the presence of a well-defined Q branch has been established entirely from a study of the data for the CS heads. In Martin's spectrograms the heads appear to be single but none of the bands is sufficiently resolved to permit of observations on the band-lines which would indicate whether each branch is really single. CS being an even molecule, it seems likely that these bands, with a strong and apparently single Q branch, correspond to an electronic transition $^1S \rightarrow {^1P}$ or *vice versa* and that they may be the CS analogue of either the Deslandres Lyman "4th positive" bands or the Ångstrom-Thalén bands of CO (an even molecule with eight less extra-nuclear electrons than CS).

Birge* has ascribed the former of these CO systems to the electronic transition $1\,^1P \rightarrow 1\,^1S$ and the latter to the transition $2\,^1S \rightarrow 1\,^1P$, where $1\,^1S$, $1\,^1P$ and $2\,^1S$ designate the normal, second excited and third excited electronic states respectively of the neutral CO molecule, the first excited level being the triple $1\,^3P$. These transitions have received support in Mulliken's† detailed discussions of band structure and electronic states of molecules. Mulliken and Birge have given electronic energy level diagrams showing the remarkably close parallel between the relative positions and multiplicities of the known electronic levels of CO (and CO^+) and those of the comparable atom Mg (and Mg^+). This parallel has, of course, been used as a guide in the designation of the CO levels.‡ By analogy with the "resonance line," $1\,^1P \rightarrow 1\,^1S$, of Mg in the ultra-violet at λ 2852·11, ν 35051·4, we may speak of the ultra-violet ("4th positive") system as the "resonance system" of CO, while the visible (Ångstrom) system is the CO counterpart of the Mg line $2\,^1S \rightarrow 1\,^1P$ in the infra-red at λ 11828·8, ν 8451·7.

Now the atom comparable with CS (22 electrons) is Ca (20 electrons of which two are valence electrons, and singlet and triplet spectroscopic terms). The Ca "resonance line" $1\,^1P \rightarrow 1\,^1S$ is the well-known "flame line" in the violet, λ 4226 73, ν 23652 4, while the $2\,^1S \rightarrow 1\,^1P$ transition gives the infra red line λ 10345 0, ν 9664 2 It seems natural to suppose that the ultra-violet CS system corresponds to the former Ca line rather than to the latter, that is to say, it is probably the CS "resonance," or $1\,^1P \rightarrow 1\,^1S$, system analogous to the CO "4th positive' system, rather than the CS counterpart of the CO Ångström system There seem to be three arguments in favour of this interpretation

---

* R. T. Birge, 'Nature,' vol. 117, pp. 229 and 300 (1925); 'Phys. Rev.,' vol. 28, p. 1157 (1926).

† R. S. Mulliken, 'Phys. Rev.,' vol. 28, pp. 481 and 1202 (1926).

‡ The numerals preceding the term type letter and multiplicity prefix are those in common usage in investigations of atomic spectra, and are less by x than the total quantum number for the term in the spectrum of the corresponding atom, where $x = 2$ for S and P terms of Mg (in the case of CO) and $x = 3$ for S and P terms of Ca (in the cases of CS and SiO). The numerals do not necessarily carry any implication as to the total quantum number of the electronic terms of the molecular spectrum.

Firstly, the "4th positive" CO bands, like the CS bands are degraded to the red, *i e*, have ω_0 less than ω_0 , while the Ångstrom bands are degraded to the violet ($\omega_0 > \omega_0$) Birge (Report, p 241) points out that while it is no longer held that, as he once supposed, the relative values of ω_0 are a criterion for the identification of electronic states of all molecules, it still appears to be true that in a molecule like CO the S states have higher values of ω_0 than the P states For the CS bands ($\omega_0 < \omega_0$), the initial state should, therefore, be a P, and the final an S state, rather than *vice versa*

Secondly, Birge* has given for the R heads of the '4th positive" CO system the (revised) formula†

$$\nu_{\text{R head}} = 64737 + 1497\ 28n' - 17\ 24n'^2 - 2149\ 71n'' + 12\ 703n''^2 \qquad (10)$$

which in conformity with the new mechanics may be converted to

$$\begin{aligned}\nu_{\text{R head}} = 65062 + 1514\ 52\,(n' + \tfrac{1}{2}) - 17\ 24\,(n' + \tfrac{1}{2})^2 \\ - 2162\ 44\,(n'' + \tfrac{1}{2}) + 12\ 703\,(n'' + \tfrac{1}{2})^2 \qquad (11)\end{aligned}$$

From (11), $\nu_e + \kappa = 65062\ \text{cm}^{-1}$ (see equation (3)) For the present purpose $\nu_e + \kappa$ will suffice instead of the system origin, ν_e, which is a few units less than 65062 cm $^{-1}$, but cannot be located as there are no data for the Q heads The ratio of corresponding transitions $1\,^1P \rightarrow 1\,^1S$ in CO and Mg is very nearly given by

$$(\nu_e + \kappa)_{\text{CO}}/\nu_{\text{Mg}} = 65062/35051\ 4 = 1\ 856$$

To compare with this we have the ratio of the constant term in equation (4) for the R heads of the CS system to the $1\,^1P \rightarrow 1\,^1S$ line of Ca, namely

$$(\nu_e + \kappa)_{\text{CS}}/\nu_{\text{Ca}} = 38921\ 1/23652\ 4 = 1\ 646$$

The proximity of these two ratios suggests that the CS system is the analogue of the $1\,^1P \rightarrow 1\,^1S$ ("resonance") system of CO

---

* 'Phys Rev,' vol 28, p 1167 (1926)

† Strictly, equations (10) and (12) should have a term in $n'n''$, and (11) and (13) a corresponding term in $(n' + \frac{1}{2})(n'' + \frac{1}{2})$, as in equations (3), (7) and (4) For the available data such terms can be neglected

Thirdly, we have seen in section 4 that the initial state of the molecule is characterised by appreciable perturbations of some of the lower vibrational energy levels, especially the $n' = 1$ level (for which the abnormal interval $\nu_{R\ head} - \nu_{Q\ head}$ may indicate either the presence of additional R branches or perturbations of rotational energy levels) When these vibrational perturbations were found, it was thought that they were without parallel in other spectra, the writer having overlooked Birge's description of a similar displacement of the vibrational levels $n'' = 1, 2, 3$ relatively to $n'' = 0$ in the final ($1\,^1P$) state for the CO Ångström system * The evidence for the perturbation is found in the following results of measurements by Jassé† on the 0,0 and 1,0 Ångstrom bands

(i) The R heads of the 0,0 and 1,0 bands are displaced towards the violet by 6 2 and 6 4 cm $^{-1}$ from the positions calculated by Birge using other R heads of the same two n'' progressions ($n' = 0$ and 1)

(ii) The interval between head and origin (written as $\nu_{R\ head} - \nu_{Q\ head}$ in this paper) is about 2 cm $^{-1}$ greater for the 0,0 band than for the 0,1, 0,2 and 0,3 bands as measured by Hulthén ‡

(iii) The 0,0 band has not only the singlet P, Q and R branches similar to those in the other bands (analysed by Hulthén), but also what appear to be additional branches P′ and R′, which give the same band-origin as P, Q and R Since the vibrational levels $n'' = 0, 1, 2$ of the final ($1\,^1P$) state for the emission of the Ångstrom system are $n' = 0, 1, 2$ of the initial ($1\,^1P$) state for the emission of the "4th positive" system, sufficiently precise measurements of the $n' = 0$ bands of the latter system should reveal anomalies like those quoted above for the $n'' = 0$ Ångström bands There is a considerable similarity between the anomalies here indicated for the "4th positive" bands and those described in section 4 for the CS bands In both cases it is the initial states which have the perturbed lower vibrational energy levels In both cases the separation of the R heads of the $n' = 0$ bands and the $n' = 1$ bands is abnormally big (compare (i) above with Table II (*a*)) In the CO progression $n' = 0$, and in the CS progression $n' = 1$ the interval between the R and Q heads is abnormally big and additional branches are suspected (compare (ii) and (iii) above with the latter part of section 4)

---

* Prof R S Mulliken kindly drew the writer's attention to this ('Phys. Rev,' vol 28, pp 1170-1172, 1926), in the course of a very helpful discussion of sections 5 and 6 of this paper

† O Jassé, 'C R, vol 182, p 692 (1926)

‡ E Hulthén, 'Ann der Phys,' vol 71, p 41 (1923)

To sum up, then, three properties in common to the two systems suggest a common electronic transition ($1\,^1P \rightarrow 1\,^1S$) (*a*) degradation to the red (*i.e.*, $\omega_{0'} < \omega_{0''}$), (*b*) roughly the same ratio of wave-numbers of system-origin and resonance line of comparable atom, and (*c*) perturbations of low vibrational energy levels in the initial state.

We will now consider the molecule SiO which, like CS,* has 22 extra-nuclear electrons and gives the ultra-violet system of bands (degraded to the red) discovered by de Gramont and de Watteville and investigated later by del Campo,† by Porlezza,‡ and by the writer.§ This system has property (*a*) and, as will now be shown, property (*b*) in common with the $1\,^1P \rightarrow 1\,^1S$ systems of CO and CS, and probably corresponds to the same transition, as Cameron‖ has already conjectured. The available data do not reveal property (*c*), but suffice for the demonstration of (*b*). -

From the writer's classification and empirical parameters n and p Kratzer,¶ Mecke** and Birge†† have each assigned n', n'' values ($n' = 77 - n$, $n'' = 103 - p$) and given an approximate formula for the R heads. Kratzer's, for example, is—

$$\nu_{\text{R head}} = 42644 + 842{\cdot}65n' - 5{\cdot}45n'^2 - 1234{\cdot}54n'' + 5{\cdot}95n''^2, \quad (12)$$

which when converted into the form of (4) and (11) becomes‡‡ —

$$\nu_{\text{R head}} = 42840 + 848{\cdot}1\,(n' + \tfrac{1}{2}) - 5{\cdot}45\,(n' + \tfrac{1}{2})^2 - 1240{\cdot}5\,(n'' + \tfrac{1}{2}) + 5{\cdot}95\,(n'' + \tfrac{1}{2})^2 \quad (13)$$

As in the case of the CO "4th positive" bands, data for the Q heads are lacking, and $\nu_e + \kappa$ from (13) must be used instead of ν_e to get the approximate value of the ratio of the SiO system-origin to the $1\,^1P \rightarrow 1\,^1S$ line of the comparable atom Ca Hence, to compare with the values 1·856 and 1 646 for the CO/Mg and CS/Ca ratios already given (p 371), we have

---

* The fact that CS and SiO happen to have exactly the same molecular weight, namely, 44·06 (CS = 12·00 + 32·06, SiO = 28·06 + 16·00) has no bearing on the relations discussed in this section, which are a matter of extra-nuclear electrons (22 in CS and SiO and 14 in CO, 2 being less firmly bound than the rest in each molecule, like the 2 valence electrons in the atoms Ca and Mg), and of the relative strengths of binding.

† A. del Campo, 'An. Soc. Esp. de Fis. y Quim.,' vol. 13, p. 98 (1913); A. del Campo and J. Estalella, *ibid.*, vol. 20, p. 586 (1922).

‡ C. Porlezza, 'Atti accad. Lincei,' vol. 31 (ii), p. 513 (1923).

§ W. Jevons, 'Roy. Soc. Proc.,' A, vol. 106, p. 174 (1924).

‖ W. H. B. Cameron, 'Phil. Mag.' (7), vol. 3, p. 110 (1925).

¶ A. Kratzer, 'Phys. Berichte,' vol. 6, p. 1398 (1925).

** R. Mecke, 'Phys. Zs.,' vol. 26, pp. 231 and 235 (1925).

†† Report, pp. 130 and 232.

‡‡ See footnote † on p. 371.

$$(\nu_e + \kappa)_{SiO}/\nu_{Ca} = 42840/23652\ 4 = 1\ 811$$

This implies an even closer resemblance between the CO and SiO than between CO and CS, a result which is amply supported by the intensity distribution and the vibration frequencies for SiO

The intensities of the SiO heads, as shown in one of the writer's small dispersion spectrograms of the uncondensed discharge through a mixture of $SiCl_4$ vapour and oxygen are set out in Table VI * The distribution is of the "normal" type as in the case of CS described in section 5, but the width of the parabola along which the intensity maxima lie in Table VI is greater than that for CS (Table V) and of the same order as that given by Condon for the CO "4th positive" system

Table VI —Intensities of R Heads of SiO Bands

n′ \ n″	0	1	2	3	4	5	6	7	8	9	10
0	5n	7	6	5	4	2	000				
1	6	6	3	4	5	9	8	2			
2	4	*	5	3		4	9	7	4		
3	2	1	1		2?			4	8	3	
4	1	2	*							1	2
5		0									

* Hidden by 1,0 band

Again, the proportional increase of vibrational frequency $(\omega_0 - \omega_0)/\omega_{0\,\mathrm{mean}}$, of SiO from equation (13) is 37 6 per cent which is very near that for CO (35 2 per cent) but greater than that for CS (18 3 per cent) Both the intensity distribution and the vibration frequencies, then, point to a proportional decrease of moment of inertia of SiO in the transition $1\,{}^1P \rightarrow 1\,{}^1S$ of the same order as that in the case of CO, but greater than that in the case of CS

With a view to further confirmation of the assignment of the transition $1\,{}^1P \rightarrow 1\,{}^1S$ to the ultra-violet systems of CS and SiO, the writer hopes to investigate the structure of one or more of their bands by means of a large Littrow quartz spectrograph now being constructed through the aid of a recent grant by the Government Grant Committee of the Royal Society In the course of such work it is also intended to search for further CS and SiO systems analogous to the Ångström and other CO systems A consideration of CO/Mg, CS/Ca and SiO/Ca ratios, such as those given on pp 371 and 374, should serve as rough guides in the location of predicted systems Some of the bands recorded by Cameron may indeed belong to one or more of such SiO systems

---

* These intensities are listed in Table I of the writer's 1924 paper They are now arranged in exactly the same way as the wave numbers of the R heads of SiO in Table II of that paper

7 *Summary*

Martin (1913) discovered a band-system in the region λ 2837 — λ 2436 in the CS_2 tube discharge and in the sulphur-fed carbon arc On experimental evidence he ascribed it to CS The author has made rather more extensive measurements of the heads in Martin's spectrograms and assigned vibrational quantum numbers n', n''

A study of the variations of the interval between the two heads of each double-headed band with n' and n'' shows that the two heads belong to the R and Q branches respectively The bands are probably of the simplest type, with single R, Q and P branches

Observed anomalies in the bands having $n' = 1$ show that the vibrational level $n' = 1$ of the initial state is displaced from its normal position, its distance from the $n' = 0$ level is abnormally large compared with that indicated by the spacing of the other n' levels Similar anomalies have previously been described by Birge for the final state of the CO Angstrom ($2\,^1S \rightarrow 1\,^1P$) system, which is also the initial state of the CO ' 4th positive " ($1\,^1P \rightarrow 1\,^1S$) system

This is one of several points of similarity between the latter and the CS system In certain other respects the ultra-violet systems of SiO and CS (each of which molecules has 22 electrons, and has Ca as its comparable atom) both resemble the ' 4th positive" system of CO (14 electrons, comparable atom Mg), thus the bands of all three systems degrade to the red, and each of the three system-origins (ν_e) has roughly the same ratio to the $1\,^1P \rightarrow 1\,^1S$ line of the comparable atom The SiO and CS systems are therefore attributed to the electronic transition $1\,^1P \rightarrow 1\,^1S$, where $1\,^1S$ is the normal state and $1\,^1P$ the second excited state of the molecule

The CO and SiO systems are more nearly alike than the CO and CS systems as regards (*a*) the ratio of system-origin to comparable atomic line, (*b*) the proportional increase in vibrational frequency, and (*c*) the intensity distribution, and, therefore, the proportional decrease in moment of inertia

The writer has much pleasure in thanking Prof A Fowler and Dr L C. Martin for the use of the CS spectrograms, and the Government Grant Committee of the Royal Society for the Hilger micrometer used in the measurements

Spectrophotometric Observations on the Growth of Oxide Films on Iron, Nickel, and Copper

By F Hurn Constable, M A, Ph D (London, Cambridge), Fellow of St John's College, Cambridge

(Communicated by T M Lowry, F R S —Received October 8, 1927)

A detailed study of the colours shown during the oxidation of activated copper films supported on china clay* has shown that the primary cause of the colour sequence produced is the interference of the incident light in a thin layer of the highly refracting oxide covering the individual grains composing the film There are, however, a number of secondary factors which produce modification in the colour sequences These are the dispersion of the metallic oxides, their specific absorption, and the variation in the intensity of the light absorbed by the metallic reflector at the back of the film with the wave-length of the incident light The growth of the oxide films was studied on thin films of iron, nickel, and copper supported on china clay rods, and also on massive rods of these metals, in order to throw light on the part played by these secondary factors Comparative spectrophotometric observations were made of the character of the reflected light at frequent intervals during the oxidation. The apparatus used has already been described (*loc cit*, pp 575-576)

The Production of Thin Activated Films of Nickel and Iron on China Clay

Cupric oxide films may be strongly ignited yet continue to adhere to their supports Strong ignition of an iron or nickel film results in its destruction, since the oxide forms large and rather hard crystals, which brush off the rods very easily

Pure green oxide of nickel was very finely ground in an agate mortar, and made into a stiff paste with partially oxidised oleic acid The paste was gently rubbed into the china clay rod, which was warmed to drive off the oleic acid When the deposit had become quite hard, it was rubbed with an oxide coated china clay rod to remove the larger crystals from the film, and to make the deposit uniform in colour Two similar coatings of nickel were given to the rod, till the whole presented a uniform dull grey colour

Iron films were produced similarly, but using both ferrous oxalate, and ferric oxide mixed with the oleic acid These iron films were also of a grey colour The copper films were prepared as previously described (*loc cit* , p 573)

---

* 'Roy Soc Proc,' A, vol 115, p 570 (1927)

Reduction and Activation of the Films

Pure hydrogen was used for the reduction, but owing to the varying speeds of reduction with the nature of the oxide, different temperatures were used in each case It was always found possible to activate the films by alternate oxidation and reduction, and in each case a terminal condition was attained very rapidly, which state was characterised by a much brighter surface

The rate of oxidation increased in each case after the first few oxidations and reductions, but not afterwards In the same way the catalytic activity of the films approached a maximum at the third or fourth reduction, after which a slight decrease was noticeable

The spectrophotometric observations of the light reflected from the surface of films of iron, nickel, and copper during activation by alternate oxidation and reduction are shown in fig 1 The temperatures at which the alternate oxidations and reductions took place are shown on the figure Curve A shows the intensity* of the reflected light after the first reduction, and the succeeding curves show that the reflecting power of these metallic films increases to a maximum

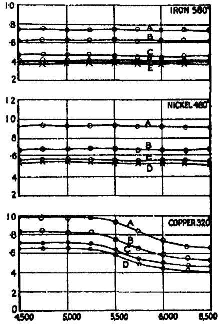

Fig 1—Increase in Reflecting Power of Metallic Films on Activation (China Clay Standard) Ordinates represent $\log_{10} \phi_1/\phi_2$ and abscissæ wave-lengths in Å U

It was noticed (except in the case of iron which oxidised too fast) that the colour sequence shown during the oxidation of the reduced metals brightened very considerably during the activation. Slight variations were observed to occur in the colour sequence as judged by the eye, but very little difference could be traced in the curves obtained by means of the spectrophotometer

---

* *Loc cit*, p 578 It is most convenient to measure and plot the logarithm of the reciprocal of the intensity of the reflected light against the wave length The higher the curve on the figure the duller the colour

The increase in the brilliancy of the colours occurs as the metal increases in reflecting power The coarse structure of the surface is preserved in the film of oxide covering it, and the reflecting power of the film of oxide formed on the surface never increases much beyond that of the original metallic surface Thus if the original surface is dull, the whole colour sequence shown during oxidation is dull, while if bright, the whole sequence is bright We have thus obtained the explanation of the brightening of the colour sequence that follows on activation, the increasing brightness being the result of the greater reflecting power of the activated metal underlying the film of oxide for all wave-lengths

Observations with a metallurgical microscope showed that the original structure consisted of very coarse grains, which were progressively broken down during the first three oxidations and reductions, finally attaining an approximately uniform size considerably smaller than the original The removal of the coarser inequalities in the surface causes a considerable improvement in the reflecting capacity, the nature of the reflected light being unaltered

Experiments conducted on the oxidation of a metallic copper rod, which was composed of surfaces of burnished, sand-papered, and electrolytically deposited metal, showed that the composite nature of the reflected light was approximately independent of the irregular nature of the surface, only its intensity being altered The results are shown in fig 2 A sand-papered rod of steel was used as the standard of comparison

The suffix 1 indicates the curves obtained from burnished copper, 2 from sand-papered metal, 3 and 4 from two different surfaces of electrolytic copper Both specimens of electrolytic copper were deposited from copper sulphate solution, with a current density of 0 058 amp per square centimetre for 2 and 15 minutes respectively The curves lettered A are the intensity curves for the metal surfaces, B is for a red-brown oxide film, C for a dark blue, D for a silvery greenish grey, and E for a yellow oxide film The colours shown on the burnished copper were the brightest, while those formed during the oxidation of the electrolytic copper were very dull indeed The brightness of the colour sequence in these cases is directly caused by the increased power of reflection of the metallic surface on which the oxide layer is formed, the intensity curves for each colour sequence being the same in type as the wave-length changes, the series of curves being shifted upwards the duller the metal surface on which they are formed.

The oxide films of thickness corresponding to silver grey and yellow have the same order of reflecting power for light as the original metal surface

It is very suggestive that the maxima of absorption become equally feeble in these three cases as the wave-length increases towards the red, this being

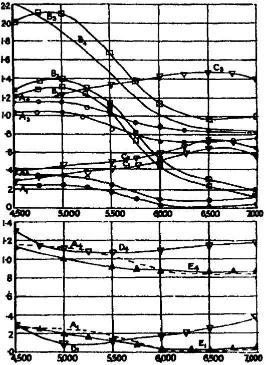

FIG 2 —Spectrophotometric Analysis of the Light from Oxidised Surfaces of Burnished, Sand papered, and Electrolytic Copper (Metallic Iron Standard) Ordinates represent $\log_{10} \phi_1/\phi_2$, and abscissae wave lengths in Å U

evidence that the enhanced intensity of the reddish colours of the sequence on metallic copper is assisted by the strong reflection of red light by the copper backing of the films The absorption in the cupric oxide film itself is fairly general and does not extinguish any one wave-length any more than any other When the light from the thin film of cupric oxide is compared with that from a similar rod of metallic copper, the light absorption at the maximum is approximately the same for red and blue films, suggesting that the slight departure from Newton's series of colours is in this case wholly caused by the selective reflection of red light from the back of the oxide film The same behaviour was observed with the films formed by a mixture of hydrogen sulphide and air on metallic copper Owing to the black colour of copper sulphide uniform absorption would be expected, and hence the probability is strengthened that the oxide film on activated copper is cupric and not cuprous oxide, which would show strong specific absorption The experimental results are shown in fig 3

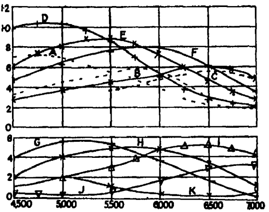

FIG 3—Cupric Oxide Films on Activated Copper, Cuprous Oxide, and Sulphide Films, on Metallic Copper (Metallic Copper Standard) Ordinates represent $\log_{10} \phi_1/\phi_2$, and abscissæ wave lengths in Å.U

Curves A, B, and C are for an activated film, showing red-brown, violet, and blue colours respectively on oxidation The curves are very similar to those obtained at room temperature by the action of a wet mixture of hydrogen sulphide and air on metallic copper, G, H, I, J, and K The oxidation of massive copper at 285° C, however, gave the curves D, E, and F in which there is a more marked absorption in the violet, and in this case the film must be almost completely cuprous oxide

This observation explains why the intensity of the deep blue colour of the sequence on metallic copper is variable with the conditions of oxidation We have, therefore, obtained a practically complete explanation of the deviations of the colour sequence shown during the oxidation of copper from that shown by thin air films

The Colours shown during the Oxidation of Activated Thin Films of Nickel and Iron on China Clay

The experimental method used has been previously described A china clay standard was used for the nickel film, and a reduced iron standard which had been fully activated for the study of the colour sequence shown by the activated reduced iron

Table I—The Colours shown by Activated Reduced Nickel (fig 4) and Activated Reduced Iron (fig 5)

A—Grey nickel (fig 4)	A—Metallic iron (fig 5)
B—Faint brown	B—Light straw
C—Light brown	C—Brownish yellow
D—Very dark brown	D—Red brown
E—Violet	E—Violet
F—Very dark blue	F Intense blue
G—Lighter blue	G—Steely blue green
H—Green grey	H—Yellow
I—Yellow	I—Yellow
J—Full brown	J—Yellowish brown
K—Violet	K—Dirty orange
L—Blue	L—Orange
M—Greenish final colour of nickelous oxide	M—Red brown
	N—Grey
	O—Final steel grey colour

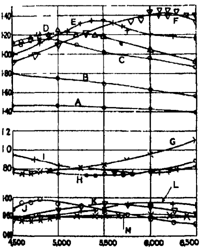

Fig 4—Oxidation Colours of Nickel Films on China Clay, 550° C (China Clay Standard)

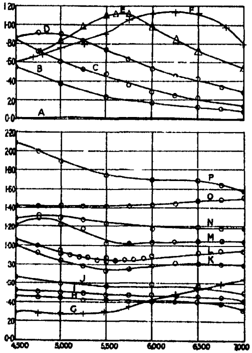

Fig 5—Oxidation Colours of Iron Films on China Clay, 380° C (Reduced Iron Standard)

Ordinates represent $\log_{10} \phi_1/\phi_2$, and abscissæ wave-lengths in Å U

The oxidation of the iron rod was allowed to proceed for 22 hours at 380° C The surface was covered with an easily removable layer of ferric oxide, which was the cause of the curve P. On wiping off the oxide by means of a clean linen rag the surface appeared a steely grey colour and showed the spectrum illustrated by curve O. It is evident that the colour sequence after the first blue is completely distorted by the strong specific absorption of the ferrous ferric oxide mixture, the dispersion of the oxide, and the tendency of the oxide to form a detached coating over the surface.

The Study of the Oxidation Colours of the Massive Metals, Nickel, Iron, and Copper

A burnished iron rod was substituted for the china clay rod at F (*loc cit*, p 376, *fig* 1) as the standard of comparison for the coloured films on the massive metal. The diameter of the iron, nickel, and copper rods used was 0·29 cm in each case burnishing the metallic steel standard, and the rods before oxidation produced a very great increase in the amount of light travelling through the photometer to the Hilger spectrometer, making the experimental adjust-

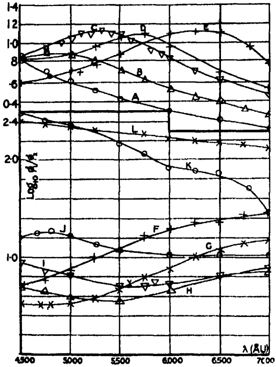

FIG 6 —The Oxidation Colours on a Metallic Steel Rod at 550° C. A, yellowish brown. B, red brown. C, purple. D, violet. E, blue. F, lighter blue. G, still lighter blue green. H, silvery green. I, yellowish. J, brown. K, rusty brown caused by all-night exposure to 550° C. L, steely blue-grey colour left on wiping off the ferric oxide from the surface.

ment of the triply divided eye-piece very much easier In addition, the longest wave-length that could be studied was increased from 6500 to 7000 Å U

The results for metallic copper have already been given (fig 2), the results for iron are shown in fig 6, and the results for nickel were very similar to those for activated reduced nickel (fig 4) The progressive movement of the absorption band is marked in each case, and is followed by the appearance of a reflection band, and followed again by another absorption band Thus the interference mechanism of production of the colours is established for the three metals

The Comparison of the Colour Sequences shown by Oxide Films on Iron Nickel, and Copper

While the red colours predominate in the films produced on copper, and the deep blue colours hardly appear at all, on nickel no reds were observed, their place being taken by browns The blue colours were very strongly accentuated The interference maximum was far less marked in the red region of the spectrum than in the blue, while on nickel the intensity of the absorption slowly increased as the wave-lengths lengthened When the reflection maximum shows up on the curves for copper it is feeble at the blue end of the spectrum, but rapidly increases in intensity towards the red end The same is true for the activated reduced metal (*loc cit*, p 578), but this metal seems to oxidise to cupric oxide making the blues more intense than is the case on massive copper when cuprous oxide is formed The specific reflection at the back of the oxide film enhances the red colours

Metallic nickel and iron reflect the visible waves nearly equally and hence modifications in the colour sequences are produced by the increasing specific absorption of the continually thickening oxide films In the cases of both nickel and iron the absorption increases in intensity as the film thickens, and the wave-length of the absorption band increases from violet to red Thus the blue colours are very intense The absorption shown by the iron film was very strong indeed The behaviour corresponds roughly with the known absorption of the oxides The final colour of the nickel film was green, while that of the iron was steely blue-grey

Evidence of Dispersion

The second order colours in the case of nickel show the presence of only a single absorption or reflection band, confirming that the dispersion of nickel oxide (NiO) is comparatively small Spectrophotometric observations of the films on copper and iron, on the other hand, show very distinctly that a considerable dispersion exists in the oxide film. Kundt's values for blue and red light have been used to evaluate the constants in Cauchy's formula, giving the following results for the variation in refractive index with wave-length, λ being expressed in Å.U.

(1) For copper oxide ($n\,Cu_2O + m\,CuO$)

$$\mu = 2.21 + 17.9 \times 10^6/\lambda^2,$$

(2) For nickel oxide (NiO)

$$\mu = 2.02 + 6.83 \times 10^6/\lambda^2,$$

(3) For iron oxide ($n\,Fe_2O_3 + m\,FeO$)

$$\mu = 1.35 + 18.8 \times 10^6/\lambda^2,$$

from which the curves in fig. 7 are drawn.

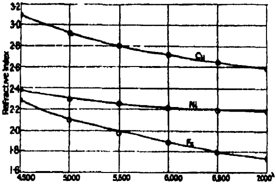

Fig. 7.—The Dispersion of Iron, Nickel, and Copper Oxides.

The nature of the oxides obtained by Kundt is not stated in his paper, but since they were obtained by ignition of the metal in air it seems probable that these values may be reasonably used to calculate the thickness of the oxide film corresponding to the various colours. The use of these values of the refractive index for the more complicated second order colours found with copper and iron confirm that a considerable dispersion exists and causes further modification in Newton's series of colours.

Table III.—Dispersion in Copper Oxide Films showing Second Order Colours

Wave-length of reflection Maximum = λ_r.	μ	Wave length of absorption Maximum λ_a	μ	Thickness of film $3\lambda_a/4\mu$	 $\lambda_r/2\mu$
6280 Å U.	2·67	4700 Å U	3·02	1·16 × 10^{-5}	1·17 × 10^{-5}
6500	2·64	5250	2·86	1·26 × 10^{-5}	1·38 × 10^{-5}

Dispersion in Iron Oxide Films showing Second Order Colours

6000	1·98	4700	2·20	1·60 × 10^{-5}	1·52 × 10^{-5}

The thicknesses of homogeneous films of a given colour have been worked out from the graphical data given in this paper. It is necessary to remember in applying these results that in practice the film may crack considerably and thus is composed of overlying portions of different colours and thicknesses.

Table IV.—The Colour and Corresponding Thicknesses of Copper Oxide Films

Order of colour	Colour of film by reflected light	Thickness of homogeneous film of same colour
I	Dark brown	0·38 × 10^{-5} cms
	Red brown	0·42
	Very dark purple	0·45
	Very dark violet	0·48
	Dark blue	0·50
	Pale blue green	0·83
II	Pale silvery green	0·88
	Yellowish green	0·97
	Full yellow	0·98
	Old gold	1·11
	Orange	1·20
	Red	1·26

Table V.—The Colours and Corresponding Thicknesses of Nickel Oxide Films

Order	Colour	Thickness
I	Pale brown	0·49 × 10^{-5} cms
	Dark brown	0·54
	Purple	0·57
	Very dark violet	0·60
	Very dark blue	0·76
II	Silvery green	1·12
	Yellowish green	1·20
	Yellow	1·26
	Straw	1·35
	Yellowish brown	1·62
	Dark brown	1·72

Table VI.—The Colour and Corresponding Thicknesses of Iron Oxide Films on Steel (up to blue)

Order	Colour	Thickness
I	Straw	0·46 × 10^{-5} cms
	Reddish yellow	0·52
	Brownish red	0·58
	Purple	0·63
	Violet	0·68
	Blue	0·72

The sequence beyond blue is very dull because of the great absorption of the oxide, and the great dispersion, so that the correlation of the apparent colour with the thickness would be of little practical value on account of the difficulty of recognising the colour in any particular case.

The chemical composition of the film in the case of nickel is practically that of nickelous oxide, but in the case of copper and iron, mixed oxide films are formed. The effect of this mixture is not very marked upon the refractive index, but is very serious, if it is desired to estimate the quantity of oxygen contained in a film of given thickness. The error produced in an estimation of the mass of oxidised metal in the film is smaller. These tables were applied to the study of the rate of oxidation of the three metals at such temperatures that a rapid colour sequence, that was easily timed, was produced. Slow oxidation rates were avoided for they gave anomalous results, due to the fact that the oxide attained a terminal thickness, corresponding to a definite colour, which increased very much more slowly than would be expected from the parabolic law of oxidation.

If a be the thickness of the oxide film at time t and S be the surface area of the oxide and ρ be the density of the oxide. Then the parabolic law becomes

$$\rho^2 S^2 a^2 = kt \quad \text{or} \quad k = \rho^2 S^2 a^2/t$$

where k is a constant, characteristic of the rate of oxidation of the metal, and variable with the temperature. In each case the first red colour was observed and the time required noted. When, owing to the rapidity of the growth of the oxide film, this time was too short to be conveniently measurable, a second order red was taken, but these results would not fit in with the first owing to the marked departure from the parabolic law.

The results show that iron oxidises at a rate intermediate between that of copper and nickel, and thus the order found by Pilling and Bedworth and by Dunn is changed at still lower temperatures.

My thanks are again due to Prof T M Lowry, F R S, for the continued loan of his spectrophotometer

Summary

A spectrophotometric study has been made of the light reflected from thin films of oxide of successively increasing thickness formed upon cylinders of metallic iron, nickel, and copper The same observations have been made for thin films of these metals supported on china clay rods

It was found that the reflecting power of the metallic films increased considerably on activation, and that this increased power of reflection at the back of the thin film was sufficient to explain the brightening of the oxidation colours consequent upon the activation of the metal Colours whose brightness varied over a wide range were simultaneously produced upon a cylinder of copper, the surface of which was divided into four equal portions The first was burnished, the second sand-papered, and the third and fourth were electrolytically deposited under different conditions The brightness of the respective colour sequences varied in the same way as the brightness of the metal surface on which they were produced

The colour sequence on copper showed the red colours very strongly, while the blues were variable in intensity, but always much more feeble This was due in part to the strong specific reflection of red light by the metallic copper

The sequence on nickel was remarkable for the absence of red colour, only browns being visible The dark blues were of remarkable intensity This effect was attributed to the strong specific absorption of nickelous oxide

The colours on iron were normal, but after the blue colour had been reached the colours became rapidly duller owing to the strong absorption of the oxide film, complicated by considerable dispersion Using Kundt's values for the refractive indices, and Cauchy's formula, tables of the absolute thicknesses of the oxide films corresponding to various colours were calculated

The tables were used, with observations of the rate of formation of the colours, to show that between 300 to 500° C the order of the velocity of oxidation decreases from copper to iron to nickel

The curves obtained from the spectrophotometric observations were in all cases sufficient to establish interference as the main cause of the colour sequences shown by these metals on oxidation

An Experimental Study of the Motion of a Viscous Liquid contained between Two Coaxial Cylinders.

By J W Lewis, M Sc, Lecturer in Physics, Military College of Science, Woolwich.

(Communicated by Prof H C Plummer, F R S —Received October 11, 1927)

[Plate 18]

The stability of a viscous liquid contained between two coaxial cylinders which are capable of independent rotation has been investigated by G I Taylor * At low speeds of rotation the motion of the liquid is two-dimensional, each particle of liquid rotating in a circle concentric with the cylinders This type of motion is possible whether the cylinders rotate in the same or in opposite directions, and is stable for velocities of the inner cylinder not exceeding a certain critical value At the critical speed the laminar motion is succeeded by a three-dimensional motion, such that the circulation of the liquid is confined to a series of annular compartments, one above the other When both cylinders rotate in the same direction, the height of each compartment equals the distance between the cylinders, and the motion in an axial plane appears to consist of a series of vortices in square compartments, adjacent vortices rotating in opposite directions For cylinders rotating in opposite directions there are, at a given horizontal level, two annular compartments side by side and concentric with the cylinders In this case, the circulation in an axial plane appears to consist of two series of vortices, adjacent vortices both vertically and horizontally rotating in opposite directions

By using coloured liquid filaments to follow the motion, Taylor verified experimentally, within a limited range, the expression for the critical velocity at which the stream-line motion becomes unstable and certain other points The apparatus used was large and robust, the length of the cylinders being 90 cm , and it was unsuitable for investigating the motion under varying conditions, such as with inner cylinders of different diameters and with liquids giving a wide range in viscosity

The object of the present work has been to investigate the motion under a much greater variety of conditions, especially with a view to seeing when the theoretical equations break down The apparatus is small, the length of the outer cylinder being only 17 cm, and the motion of the liquid is followed by means of suspended particles. This method offers several advantages over the use of coloured liquids, which, owing to diffusion, gives a transitory effect only. With suspended particles the motion can be studied for any length of time, and any changes in the motion easily observed. It is possible, for instance, to compare the speeds at which the vortices come in and go out. By suitable illumination the motion in any particular plane may be examined and photographed. Moreover, by making the apparatus small, a device can be introduced to minimise the distortion due to refraction. It is also an easy matter to make experiments with a large number of inner cylinders, and to use liquids giving a wide range of viscosities.

---

* 'Phil Trans ,' A, vol 223, p 289 (1923), where references to previous work are given

The chief points to which attention has been given are:—

(*a*) The photography of the motion.

(*b*) The application of Taylor's criterion for the critical speed for inner cylinders of different diameters, using liquids of different viscosities, especially with a view to ascertaining the range for which the criterion is valid.

(*c*) The spacing of the vortices.

(*d*) A comparison of the speeds of the inner cylinder at which the vortices come in and go out.

(*e*) Observation of the different types of motion after laminar motion becomes unstable.

Apparatus

A description of the apparatus as first used has already been given,* but further experience has suggested several modifications, and a diagram of the apparatus in its present form is given in fig. 1.

AA is the inner cylinder, which is a rod of silver steel. BB is the outer cylinder of lead glass, of length 17 cm, inner diameter 0.900 cm, and outer diameter approximately 1.085 cm. Both cylinders were specially prepared, as described later, to be perfectly straight and of uniform circular cross-section. They are capable of independent rotation, and the housings for the bearings which hold them are carried by a massive upright of mild steel NN, which is screwed to a mild steel base MM.

The lower end of the steel cylinder is pivoted into E, while the upper end has an adapter J, which makes a good friction fit into the wheel G. The wheel itself is fitted with a ball bearing, the housing of which (K) is screwed to the top of the steel pillar The position of this housing can be altered to adjust the inner cylinder to lie centrally in the outer glass cylinder

---

* Andrade and Lewis, 'J. Sci. Instr.,' vol. 1, p. 373 (1924).

The glass cylinder passes through the wheel F, and fits loosely over the projection on E, being held in position at each end by two screws and a spring plunger, which are fixed in rings on F and E, and bear on brass tubes cemented over the ends of the glass tube The tube is sealed at the bottom by many applications of a dilute solution of shellac The middle of the tube passes

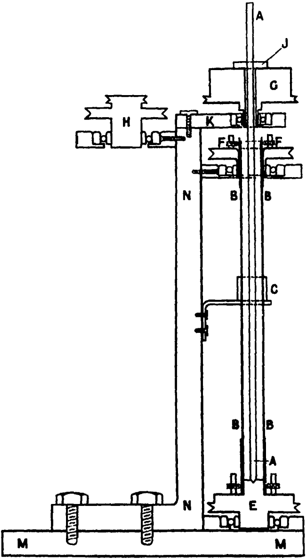

Fig 1

through a cubical block of glass C, bored parallel to an edge to admit the tube Observation of the fluid motion is made through the cube, its object being to diminish the distortion due to refraction The space between the tube and cube is lubricated with a mixture of xylene and monobromonaphthalene adjusted to have the same refractive index as the glass

Great care was taken to ensure that the two cylinders revolved concentrically The bearings for the wheels F and E were first aligned by fitting into them a brass rod, and then adjusting the attachment of their housings to NN until the rod could turn freely The glass cylinder was roughly adjusted to be concentric with the bearings by the aid of a microscope focussed on the outside edge, and then cemented down with shellac to the wheel E While the shellac was still plastic, liquid was introduced into the tube and an inner cylinder placed in position Then, by observing the movement of the meniscus as the cylinders were rotated in turn, it was an easy matter to adjust them both to revolve concentrically Once the cylinders have been centred, the wheel G can be removed, and an inner cylinder and its adapter quickly replaced by another without the necessity of recentring Since, during the experiments, inner cylinders of different diameters were used, this method of mounting them was found very satisfactory

H is a pulley wheel which transmits the drive from a small motor with a reduction of speed A similar pulley is mounted on the base for transmitting motion to the outside cylinder The inner and outer cylinders are both geared to the same motor through a system of pulleys, by means of which the speed ratio is fixed The drive is transmitted to the cylinders by cotton threads, which do not set up the vibration always experienced when rubber bands or spring belting were used.

The optical system is mounted on an optical bench, which is pivoted at the end remote from the apparatus, and controlled at the other end by a lever which enables the observer to displace the beam at will from the front to the middle of the annular space between the cylinders Light from a slit illuminated by an arc is converged on to a sphero-cylindrical lens, which produces a flat beam of small convergence A water cell is inserted in the path of the beam, minimising heating effects and consequent convection currents in the liquid under investigation The flat beam is arranged to illuminate, and so effectively to isolate, any section which it is desired to study

The Preparation of the Cylinders

To avoid any possible disturbance due to irregularity of the cylinders, great care was taken to make them straight and of circular and uniform cross-section to a high degree of accuracy Silver steel rods, guaranteed of uniform cross-section to an accuracy of 0 001 cm, proved to be satisfactory as regards uniformity of cross-section, but not as regards straightness, which latter was improved by careful grinding on a lathe The straightness was then tested by supporting a rod on two V's and rotating it slowly, observation of an intermediate part being made with a reading microscope No measurable deviation from straightness was detected, although an error of less than 0 001 cm could have been easily detected In this way four rods were prepared with radii of 0 2631, 0 3143, 0 3435 and 0 3842 cm, respectively It was found necessary to measure the radii of these rods to a high degree of accuracy, an error of 1 per cent in the measurement of the largest of them gives an error of 7 per cent in the calculated value of the critical speed

In preparing the glass cylinder, a preliminary selection was made from a large number of glass tubes Lead-glass tubes were found to be more uniform in diameter and optically more homogeneous than soda-glass tubes, which are in general full of striæ Those tubes which were found to be fairly straight when tested on a surface plate were examined for uniformity of bore by the method developed by Anderson and Barr * The tubes were immersed vertically in a liquid of about the same refractive index† as the glass, and their diameters measured in several azimuths at different heights by a travelling microscope The selected tube was then ground true and polished The preliminary grinding was carried out by Messrs E R Watts and Son, Ltd, Camberwell The final grinding and polishing was carried out in the laboratory on a rod coated with pitch, sira rouge being used as the polishing medium The diameter was then found to be uniform to 0 001 cm, as measured in different azimuths throughout the length of the tube Its value was measured by equalising the refractive indices of liquid and glass for a particular wave-length, and equals 0 900 cm In order to test its straightness, the tube was supported horizontally at the ends on two circular steel rods whose top surfaces were collinear The whole was immersed in a glass trough containing a liquid of about the same refractive index, and deviation from straightness was looked for as the tube was rotated No measurable deviation was found.

---

* 'J Sci Instr,' vol 1, p 9 (1923)

† A suitable mixture of aniline and xylene

Measurement of Speed

For the measurement of the speed of the cylinders a stroboscopic method was employed Fitting round the wheels G and E, which rotate with the cylinders, are white strips marked with equidistant vertical lines As the cylinders rotate these lines are observed through a disc pierced with equidistant radial slits, and driven through a variable gear by a phonic motor The speed of the disc is adjusted until the vertical lines on a cylinder give a stationary figure, when the speed of the cylinder can be deduced from the reading of the variable gear

A diagram of the strobometer, the design of which was suggested by Prof Andrade, is given in fig 2 A cardboard disc A, having a circle of radial slits, is mounted on the back of an ebonite disc B, which is carried on a horizontal spindle mounted in ball bearings A thin sheet of rubber is fixed to the front face of B C is a small disc of red fibre, which is bevelled at the outside to give a smooth rim It is mounted on a straight aluminium spindle supported in ball bearings at F and F, and presses against the rubber-covered face of B The pressure between the discs is adjusted until, as C rotates, the friction between them is just sufficient to cause a rotation of B without any slipping

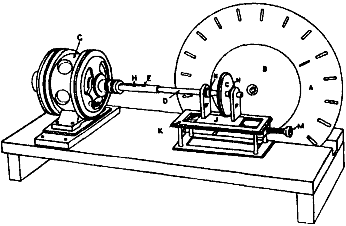

Fig 2

The spindle D is coupled to the phonic motor by the tube F, which is attached to the motor by a flexible coupling (a piece of pressure tubing proved very effective) The spindle can slide freely along the tube, but a stud H, fixed in the spindle and passing through a longitudinal slot in the tube, prevents any relative rotation

The speed of the phonic motor is controlled by an electrically maintained tuning-fork (50 D V per sec) in the usual way C therefore rotates at a constant speed, but the speed of B depends on the distance of C from B's axis of rotation By giving C a motion across the face of B, a continual variation in the speed of the latter can be obtained For this purpose, the housings F, F for the bearings of D are rigidly fixed to the slide J, moving in grooves on a framework K by the motion of the screw M acting against a spring as in a travelling microscope J and K are provided with a scale and vernier which indicate the position of C to 0 001 inch, an accuracy well above that required

For the purpose of calibrating the scale reading in terms of the speed of the disc A, the photographic and time-marking apparatus of a sound-ranging set were fortunately available A lamp was placed behind a single narrow radial slit cut in the face of the disc A, and an image of this slit focussed on the photographic strip Then, as the wheel rotated, each revolution was recorded simultaneously with a time scale on the photographic strip In this way it was possible to measure the actual speed of the disc corresponding to a particular setting of the scale and vernier At the same time, the absence of slip was verified by measuring the speed over different intervals of time Furthermore, it was found that the observed speeds of revolution for different settings of the same scale reading were satisfactorily consistent

The range of the instrument for single figures is for speeds from 7 to 3 5 revs per sec , but by using multiple figures the range can be widened from 21 to 1 7 revs per sec

Observation of the Motion

The liquid used for general observation of the motion was xylene Its refractive index (1 497) being lower than that of glass (1 571), distortion is not entirely avoided, but its kinematic viscosity is such that the change in the type of motion occurs at a reasonable speed for all the cylinders even when the speed ratio is high After experimenting with several different types of particles, fine aluminium powder was found to be the most suitable A small quantity of the powder is shaken with the liquid, and allowed to settle down for about two hours, when the suspension is decanted off and diluted down with more xylene

The liquid is introduced between the cylinders, and illuminated through one of the faces of the cube by a flat beam Its motion, due to rotation of the cylinders, is observed through a low-power microscope set horizontally at right-angles to the beam Photographs showing the type of motion observed under different conditions are given in Plate 18, figs 3–10

When convection currents due to heating are absent and the cylinders are at rest, the particles appear as stationary points of light On rotating the cylinders, the particles move with the liquid and indicate its motion For speeds of the inner cylinder less than a critical value, the appearance of the motion in a radial plane is shown in fig 3 The particles are describing circular paths concentric with the cylinders The photographs show no difference between the cases when μ, the ratio of the speed of the outer cylinder to that of the inner, is zero, positive or negative, though in the latter case the liquid is divided into two portions, an inner portion rotating in one direction and an outer rotating in the opposite direction This difference in the direction of motion is easily detected by visual observation Fig 8 shows the appearance in a vertical plane passing through a point between the two cylinders Here again, when μ is negative, visual observation shows that the liquid at the edge of the tube is moving in an opposite direction to the liquid near the inner cylinder

When the speed of the inner cylinder exceeds a critical value, the type of motion is entirely different the particles move in the complicated manner previously described Fig 4 shows the appearance in a radial plane when μ is zero The vortices are in approximately square compartments extending across the interspace between the cylinders, and adjacent vortices are rotating in opposite directions For negative values of μ the appearance is as shown in figs 5 and 6 There are really two systems of vortices side by side, though, owing to distortion and also to the less vigorous nature of the outer system, these latter cannot be distinguished

A comparison of figs 4 and 5 shows that in fig 5 the vortices (which are the inner system) are smaller and also their centres are displaced towards the inner cylinder In fig 6, for which $-\mu$ is greater than in fig 5, the difference is still more pronounced Fig 7 shows the vortex system for positive values of μ, it is the same as when μ is zero (fig 4) When μ is zero or positive, the appearance of the vortex motion in a vertical plane passing through a point between the two cylinders is shown in fig 9, and when μ is negative, in fig 10 In the latter case, the dividing line between the two systems of vortices can be discerned near the edges of the tube

The photographs were obtained on Ilford Press plates, using a Beck apochromatic objective of 40-mm focal length and the sun as source of light The time of exposure is governed by the speed of rotation of the cylinders and the thickness of the beam, and is obviously not the same for each particle By exposing the plate for about $\frac{1}{2}$ sec the paths of many different particles are recorded on the same plate It is to be observed that much larger particles were used for the photography than for the measurement of the critical speeds

Determination of the Critical Speed

Assuming that when instability occurs the subsequent motion of the liquid is three-dimensional and symmetrical (about the axis), Taylor obtains a mathematical expression for the critical speed of the inner cylinder in terms of the coefficient of kinematic viscosity of the liquid, the radii of the cylinders, and the ratio of their velocities When the cylinders are rotating in the same direction, the critical velocity Ω_1 of the inner cylinder, at which the stream-line motion becomes unstable, is given by

$$\Omega_1^2 = \pi^4\nu^2(R_1+R_2)\Big/\Big[2d^3R_1^2\Big(1-\frac{R_2^2\mu}{R_1^2}\Big)(1-\mu) \times\Big\{0.0571\Big(\frac{1+\mu}{1-\mu}-0.652\,d/R_1\Big)+0.00056\Big(\frac{1+\mu}{1-\mu}-0.652\,d/R_1\Big)^{-1}\Big\}\Big], \quad (1)$$

where

Ω_1 = angular velocity of the inner cylinder,
Ω_2 = angular velocity of the outer cylinder,
R_1 = radius of the inner cylinder,
R_2 = radius of the outer cylinder,
$d = R_2 - R_1$,
$\mu = \Omega_2/\Omega_1$,
ν = the kinematic viscosity of the liquid

In this expression the term $0.652d/R_1$, which is subtracted from the factor $(1+\mu)/(1-\mu)$, is a correction due to the fact that d, the distance between the cylinders, is not negligible compared with R_1 This correction neglects second order terms of the ratio d/R_1 and may be expected to hold until d/R_1 exceeds one-third

There is not a simple expression similar to (1) for negative values of μ—i e, when the cylinders rotate in opposite directions—but the same expression applies until the term $0.00056\{(1+\mu)/(1-\mu)-0.652d/R_1\}^{-1}$ is comparable with $0.0571\{(1+\mu)/(1-\mu)-0.652d/R_1\}$

The verification of the expression predicting the critical speed of the inner cylinder at which the type of motion changes requires a knowledge of μ, the ratio of the speed of the outer cylinder to that of the inner, and of ν, the kinematic viscosity of the liquid

The speed ratio of the cylinders was determined by running the motor at a constant speed, and measuring the speed of each cylinder in turn with the strobometer

The viscosity of the liquid was measured at a series of temperatures with a U tube viscometer, which gives the kinematic viscosity directly, and requires only a small quantity of liquid A consideration of Einstein's* formula for the viscosity of a suspension of small spheres shows that the effect of a few fine particles on the viscosity is inappreciable, and measurements of the viscosity of xylene both with and without particles showed that a much more concentrated suspension than that used in the experiments did not appreciably alter the viscosity

The critical speed of the inner cylinder at which the type of motion changes was first roughly determined by observing the motion in a radial plane through the microscope as the speed was slowly increased The strobometer was then adjusted until the vertical lines on the inner cylinder gave a stationary figure when observed through the rotating disc The operation was then repeated, but this time, as the critical speed was approached, the change in the speed was made more slowly Another observer meanwhile observed the vertical lines, and, at a given signal, he made any necessary adjustments to the strobometer When several consistent settings for the critical speed had been made in this way, its value was obtained by reference to the calibration curve The inner cylinder was then removed, and the temperature of the liquid taken with a thermometer the viscosity could then be obtained from a viscosity temperature curve

The first series of measurements was made with the outer cylinder fixed (*i e*, μ equals zero) for three liquids—xylene, a mixture of nitrobenzene and xylene, and nitrobenzene—giving a variation of the coefficient of kinematic viscosity over the range 0 008 to 0 018 C G S The nitrobenzene was not used with the largest inner cylinder because the critical speed is too high to be accurately determined The values of the critical speeds obtained with the different liquids are compared with one another and with the value calculated from the theoretical expression by dividing the critical speed by the coefficient of kinematic viscosity The constancy of this ratio is the condition that two geometrically similar motions are also dynamically similar The experimental results are given in Table I Though the ratio d/R_1 varies from 0·17 to 0 71, the ratio of the critical speed to the kinematic viscosity obtained experimentally agrees with the calculated value equally well for each of the inner cylinders used, and for all the liquids † It thus appears that when μ equals

---

* Einstein, 'Ann d. Physik,' vol 19, p 289 (1906)

† The inner cylinder of radius 0 3435 cm was not used for these experiments, as, at the time, it did not run centrally

Table I

Dimensions of cylinders	Liquid	Temperature °C	Kinematic viscosity ν	Critical speed, revs per sec	$\frac{\text{revs per sec}}{\nu}$ observed	$\frac{\text{revs per sec}}{\nu}$ calculated.	Percentage difference
R_1 = 0 2631 cm	Xylene	13 2	0 00859	2 13	247 9	247 8	+ 0 04
		12 3	0 00869	2 16	248 6		+ 0 32
R_2 = 0 45 cm		11 8	0 00875	2 18	249 2		+ 0 56
d/R_1 = 0 71	Nitrobenzene and xylene	17 0	0 01150	2 87	249 6		+ 0 72
		18 8	0 01127	2 79	247 6		+ 0 08
		18 8	0 01127	2 77	245 8		− 0 81
	Nitrobenzene	15 0	0 01830	4 48	244 7		− 1 25
		15 4	0 01818	4 47	245 9		− 0 77
R_1 = 0 3143 cm	Xylene	18 7	0 00794	2 43	306 1	302 7	+ 1 12
		12 4	0 00868	2 63	303 1		+ 0 13
R_2 = 0 45 cm		17 6	0 00805	2 46	305 6		+ 0 95
d/R_1 = 0 43	Nitrobenzene and xylene	17 7	0 01140	3 46	303 5		+ 0 26
		18 1	0 01137	3 47	305 2		+ 0 82
		14 7	0 01196	3 63	303 5		+ 0 26
	Nitrobenzene	14 2	0 01856	5 65	304 4		+ 0 56
		15 7	0 01809	5 48	303 0		+ 0 10
R_1 = 0 3842 cm	Xylene	12 5	0 00866	6 02	695 2	690 1	+ 0 65
		11 0	0 00883	6 14	694 3		+ 0 52
R_2 = 0 45 cm		9 6	0 00900	6 29	699 0		+ 1 20
d/R_1 = 0 17	Nitrobenzene and xylene	14 9	0 01193	8 30	695 8		+ 0 74
		17 9	0 01139	7 92	695 2		+ 0 65
		17 6	0 01142	8 00	698 8		+ 1 17

zero, the theoretical expression is applicable even though the ratio d/R_1 is as high as 0 71

It is possible, then, to use this type of apparatus for the measurement of viscosities, and in certain circumstances it might offer advantages over other methods Since the outer cylinder is kept fixed, the construction of the apparatus would be much simplified, and it could be calibrated by measuring the critical speed for a liquid of known viscosity As with other types of viscometers, it would be necessary to choose the dimensions of the cylinders according to the range of viscosities to be measured

Since the critical speed for air is too high to be obtained with the apparatus, a rough apparatus of different dimensions was constructed to find out if the same expression also holds for gases The motion of air was followed by means of the smoke from a cigarette The change in the type of motion at a certain speed is the same as that for liquids On the assumption that the smoke particles did not alter the viscosity of the air, the observed value of the critical speed was 8 6 revs per sec , as compared with the calculated value of 7 96 revs. per sec It is certain, however, that the above assumption is not allowable, for while a given concentration of smoke gave consistent results, the values obtained for different kinds of smoke did not agree

For the experiments with both cylinders rotating, xylene was the only liquid

Table II

Dimensions of cylinders (1)	μ (2)	Experimental value of revs per sec ν at which laminar motion becomes unstable (3)	Calculated value of revs per sec ν at which laminar motion becomes unstable (4)	Experimental value of revs per sec ν at which the vortex motion reverts to laminar motion (5)
R_1 = 0 2631 cm R_2 = 0 450 cm d/R_1 = 0 71	+0 294	531	499 9	488
	+0 248	431	370 0	398
	+0 237	402	353 3	377
	+0 229	350	342 9	322
	+0 175	312	297 1	276
	0 0	248	247 8	230
	−0 182	246	263 1	227
	−0 238	259	280 3	235
	−0 337	288	—	261
	−0 433 P	322	—	301
	−0 555 P	380	—	354
R_1 = 0 3143 cm R_2 = 0 450 cm d/R_1 = 0 43	+0 435	711	695 5	675
	+0 417	650	606 4	614
	+0 294	406	391 7	385
	+0 180	345	333 0	321
	0 0	303	302 7	289
	−0 292	333	327 1	309
	−0 426 P	381	352 5	350
	−0 692 P	518	—	472
	−0 975 P	682	—	650
R_1 = 0 3435 cm R_2 = 0 450 cm d/R_1 = 0 31	+0 498	780	779 8	750
	+0 412	570	571 5	550
	+0 293	465	464 0	442
	+0 161	410	408 1	397
	0 0	386	386 3	374
	−0 161	397	388 2	379
	−0 295	424	450 0	402
	−0 410 P	460	463 5	428
	−0 492 P	483	—	466
	−0 610 P	555	—	526
	−0 705 P	601	—	580
R_1 = 0 3842 cm R_2 = 0 450 cm d/R_1 = 0 17	+0 412	852	855 3	846
	+0 293	770	769 0	760
	+0 161	722	716 1	706
	0 0	695	690 1	680
	−0 161	702	695 0	684
	−0 293	729	719 0	702
	−0 412	772	752 3	—

used, since, by virtue of its low viscosity, the critical speed is low enough to be easily observed for all the inner cylinders Consequent on a slight movement of the cube due to lack of uniformity in the thickness of the glass tube, observation with both cylinders rotating becomes difficult when the speed of the inner cylinder exceeds about 6 revs per sec The experimental values of the ratio of the critical speed to the kinematic viscosity are compared with the calculated values in columns 3 and 4 of Table II Reference to column 5 will be made later It is observed that the experimental and the calculated values are in good agreement for positive values of μ when the ratio of d/R_1 is 0 17 and 0 31, but not for the larger ratios, except as already pointed out, when $\mu = 0$ When μ is negative, the agreement between the observed and the calculated values can only be called good for the value of $\mu = -0\ 16$, using the largest of the inner cylinders

Spacing of the Vortices

When d, the thickness of the liquid layer, is small compared with R_1, the radius of the inner cylinder, Taylor's theory predicts that for positive values of μ the vortices occupy square compartments—*i e*, their spacing equals the thickness of the liquid layer When μ is negative, the spacing varies with μ, it is less than the spacing when μ is positive and decreases as $-\mu$ increases

Many measurements of the spacing were made by means of a travelling microscope for $\mu = 0$, using inner cylinders of different sizes and liquids of different viscosities A typical selection from the values obtained are given in Table III Each value is the mean spacing of a series of vortices, the inner cylinder being started from rest in each case

For each value of d/R_1, the spacing of the vortices may vary within certain limits The actual value obtained appeared to be independent of the acceleration of the inner cylinder through the critical speed and the viscosity of the liquid The spacing may be greater or less than the theoretical value, though it is generally less The maximum variation occurs for the largest value of d/R_1 when it is as much as 14 per cent When d/R_1 is 0 17—*i e*, of the order assumed in arriving at the theoretical value—the variation from this value is not greater than 4 5 per cent, which is about the experimental error of measurement for this small spacing

Certain observations showed that the motion is not necessarily periodic at the moment instability sets in, but the vortices move up or down and readjust themselves until they are regularly spaced

Measurements for both positive and negative values of μ showed a similar variation in the spacing of the vortices, and as $-\mu$ was increased the spacing

Table III

Dimensions of cylinders	Theoretical spacing (cm) $d = R_2 - R_1$	Observed spacings (cm)			Maximum per cent variation from the theoretical spacing
		Carbon tetrachloride $\nu = 0\ 0065$	Xylene $\nu = 0\ 0084$	Nitrobenzene $\nu = 0\ 0183$	
R_1 = 0 2631 cm R_2 = 0 45 cm d/R_1 = 0 71	0 187	0 201, 0 193 0 192, 0 190 0 187, 0 185 0 182, 0 167 0 161	0 186, 0 183 0 180, 0 178 0 176, 0 174 0 172, 0 168 0 164	0 183, 0 181 0 180, 0 179 0 176, 0 172 0 166	14
R_1 = 0 3143 cm R_2 = 0 45 cm d/R_1 = 0 43	0 136	0 135, 0 133 0 132, 0 131	0 142, 0 139 0 135, 0 128 0 125	0 136, 0 133 0 132, 0 129 0 124, 0 122	10
R_1 = 0 3435 cm R_2 = 0 45 cm d/R_1 = 0 31	0 106	0 104, 0 103 0 101, 0 100 0 099	0 100, 0 099 0 098	0 102, 0 101 0 099, 0 098	7 5
R_1 = 0 3842 cm R_2 = 0 45 cm d/R_1 = 0 17	0 066	0 067, 0 066 0 065	0 066, 0 065 0 064, 0 063	— —	4 5

decreased in a manner similar to that observed by Taylor The decrease in the size of the vortices is seen by comparing figs 5 and 6, Plate 18

The nature of the motion at the open end of the liquid column was also observed by arranging that the liquid only reached to the level of the cube The uppermost vortex is always much longer than those beneath it, and may exceed the theoretical value by as much as 12 per cent The effect of adding a small drop of liquid is generally to cause a readjustment of the vortices It is impossible for a small vortex to exist at the free end of the liquid column One did form occasionally by the addition of a suitable quantity of liquid, but it was unstable, and a readjustment took place until the end vortex became long again

It is to be observed that though the spacing of the vortices may vary within fairly wide limits, the critical speed at which the vortices set in shows no such variation

Subsequent Motion of the Liquid

It has already been pointed out that by using suspended particles any changes in the type of motion can be easily followed. The following observations of the motion were made with xylene ($\nu = 0\ 008$ approximately) —

Considering first the case when μ equals zero or is positive, if, when the vortices have set in, the speed is maintained constant, then they persist indefinitely, though sometimes there is a gradual vertical displacement of the whole system When the speed is gradually reduced, the vortices persist until the speed of the inner cylinder is below that at which they set in. The speed of the inner cylinder at which the reversion of the motion occurs is quite as definite as the speed at which the laminar motion becomes unstable, though the exact speed of rotation at which the change takes place is more difficult to observe Measurements of the ratio of the revs per sec to the kinematic viscosity when the reversion to laminar motion occurs are given in column 5 of Table II The turbulence occurring at a critical velocity in the flow of a liquid in a straight circular tube shows a similar persistence as the flow is reduced to a lower critical velocity It was observed that if the speed of the inner cylinder was slowly increased from rest to a value between what may be called the upper and lower critical speeds, the vortex motion could be initiated by setting up a disturbance such as that caused by jolting the bench At speeds below the "lower" critical speed such a disturbance produced no effect In the rough experiments with air, variation of the speed produced similar changes in the type of motion As the interspace between the cylinders is decreased—*i e*, d/R_1 is made smaller—the two critical speeds become closer together In fig 11 the values of the ratio of the difference in the two critical speeds to the upper critical speed, obtained from several determinations, have been plotted as dots against the corresponding values of d/R_1 The points so obtained lie about a straight line passing through the origin The points obtained from measurements of the critical speeds for air are plotted on the same diagram as circles

If, after the vortices had formed, the speed was further increased, then for values of d/R_1 equal to 0 71, 0 43 and 0 31, the vortex type of motion remained unchanged up to the highest speed obtained with the apparatus, *i e*, about 19 revs per sec for the inner cylinder For $d/R_1 = 0\ 17$ the vortex motion broke down when the speed of the inner cylinder was about 14 revs per sec, the motion then becoming irregularly turbulent

When μ is negative, there is a similar difference between the speeds at which the laminar motion becomes unstable and at which the vortex motion reverts to laminar motion These are compared in the columns 3 and 5 of Table II On increasing the speed after the vortices have formed, then when $-\mu$ exceeds a certain value depending on the size of the inner cylinder, the steady vortex motion is succeeded by a new type of motion The vortices appear to pulsate up and down, their direction of rotation changing with each pulsation. The period of this pulsation appears to bear no simple relation to the periods of revolution of the cylinders. The pulsating type of motion was observed by Taylor, who describes the appearance as seen by using a coloured liquid as follows " Shortly after the symmetrical vortex system had formed itself, it was seen that every alternate vortex began to expand on one side and to contract on the opposite side of the cylinder On the other hand, the intermediate vortices began to expand to fill the spaces from which the first had contracted, and to contract in the parts where the first set had expanded As seen in side elevation, it looked as though each vortex was pulsating so that its cross-section varied periodically, though with an oscillation of increasing amplitude " Though it is difficult to judge what is happening to the annulus of liquid as a whole, the observations with suspended particles, which are unaffected by diffusion, supplement the observations described above It is found that, provided the speed is kept constant, the pulsating motion persists indefinitely and with fixed amplitude There appears to be no consistency in the speeds at which the pulsating type of motion sets in , sometimes the motion changed straightway at the critical speed to the pulsating type In

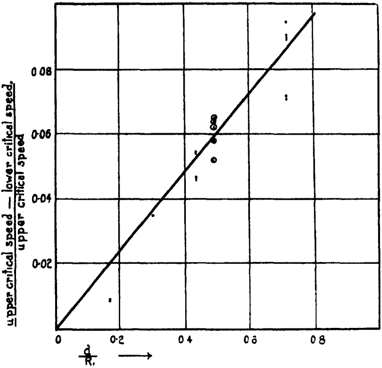

Fig 11 —The values obtained with liquids are represented by dots and the values with air by circles

Table II the values of μ marked with a P are those at which the pulsating type of motion occurred At still greater speeds the motion becomes irregularly turbulent When the symmetrical vortex motion is succeeded by the pulsating motion, then, as the speed is gradually reduced, the pulsations die out and the vortices become steady again, and finally change to laminar motion

The spiral form of instability observed by Taylor was only seen on a few occasions, it sometimes occurred when the pulsating type was expected Taylor observed that if there was a circulation in the axial plane during the steady motion before instability, then, on the formation of the vortices, they were wrapped as a spiral round the inner cylinder, and were alternately large and small When this type of motion did occur, the appearance of the particles in a radial plane was that of a series of vortices travelling up the tube and separated by spaces in which it was difficult to detect the type of motion This spiral form of instability was only observed when μ was negative

Stability diagrams similar to those given by Taylor* are shown in figs 12–15. The ratios of revs per sec to ν for the inner cylinder, at which the motion becomes unstable as the speed is gradually increased from rest, are plotted against the corresponding ratios of the outer cylinder The full line connects the observed points, which are represented by dots the centres of the small circles represent calculated points The dotted lines on each of these diagrams are drawn through points (represented by crosses) corresponding to the speeds at which the vortex motion reverts to laminar motion For all points on the diagram above the full line, the motion is unstable, for points below the dotted line it is stable, while in the region between the two lines the motion is evidently stable for small disturbances, but, as found experimentally, not for large disturbances

The conditions for the stability of an inviscid liquid in similar circumstances have been given by the late Lord Rayleigh † For cylinders rotating in opposite directions, laminar motion is unstable at all speeds, if they rotate in the same direction, the motion is stable or unstable according as $\Omega_2 R_2^2$ is greater or less than $\Omega_1 R_1^2$ The straight lines in figs 12–15, which are given by $\Omega_1/\Omega_2 = R_2^2/R_1^2$, may be called the stability curves for an inviscid liquid A viscous liquid is also stable if $\Omega_2 R_2^2$ is greater than $\Omega_1 R_1^2$, and when $\Omega_2 R_2^2$ is less than $\Omega_1 R_1^2$ the motion is stable until Ω_1 exceeds the critical value given by the expression (1)

---

* *Loc. cit.*, p. 339

† 'Roy Soc. Proc,' A, vol. 93, p 148 (1916)

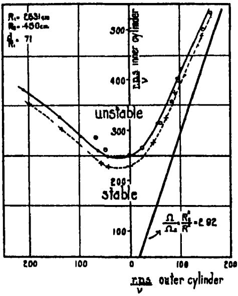

FIG 12

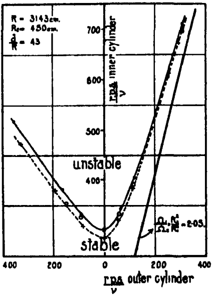

FIG 13

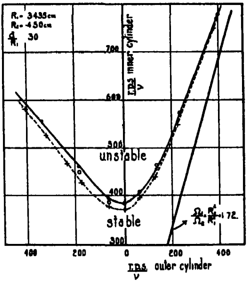

FIG 14

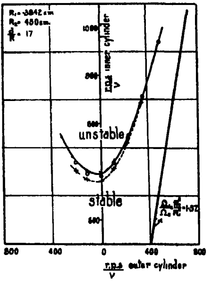

FIG 15

In figs. 12, 13, 14, 15 the experimental values of revs. per sec /ν at which laminar motion becomes unstable are represented by dots and the calculated values by circles the experimental values of revs. per sec /ν at which the vortex motion reverts to laminar motion are represented by crosses.

The author desires to express his warmest thanks to Prof E N da C Andrade, who suggested the experiments, and to whom he is indebted for suggestions and advice, and for facilities for carrying out the work

Summary

1 A description is given of the apparatus in which suspended particles are used to follow the motion of a viscous liquid between two cylinders, either or both of which can be rotated, and of a stroboscopic device for measuring the speeds of the cylinders

2 The mathematical laws deduced by G I Taylor for the case when the ratio of the interspace (d) to the radius (R_1) of the inner cylinder is small have been confirmed, using xylene as liquid and inner cylinders of different radii

3 When the outer cylinder is fixed, the expression for the critical velocity at which the laminar motion gives place to vortex motion is found to hold for values of the ratio d/R_1 as high as 0·71, and for liquids whose coefficient of kinematic viscosity varies from 0 006 to 0 018 C G S

4 When the outer cylinder is fixed, the determination of the critical speed can be used for the measurement of kinematic viscosities The dimensions of the cylinders should be such that the critical speed is low, when observation of the change in the type of motion is easy When $R_1 = 0\ 26$ cm , and $R_2 = 0\ 45$ cm , kinematic viscosities from 0·008 to 0 012 C G S can be measured with certainty to within 1 per cent

5 If, when the vortex motion has set in, the speed of the cylinders is reduced, then the motion reverts to the laminar state at a critical speed, which is fixed for given dimensions and liquid This critical speed is definitely lower than the critical speed given by Taylor's formula, at which the vortex motion sets in

6 The upper and lower critical speeds tend to become equal as the ratio d/R_1 is decreased

7 When d/R_1 is large, the spacing of the vortices may vary within fairly wide limits, though there is no such large variation in the speed at which the vortices set in

8 Photographs are given of the motion observed in a radial plane and in a plane passing through a point between the cylinders, both for the laminar and the vortex motion when μ, the ratio of the outer cylinder to that of the inner, is positive, negative and zero respectively

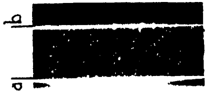

FIG 3

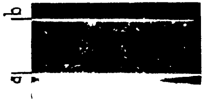

FIG 4

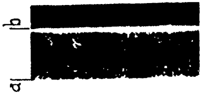

FIG 5

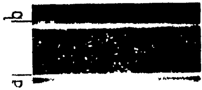

FIG 6

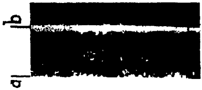

FIG 7

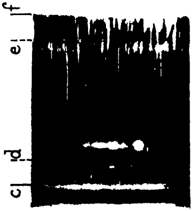

FIG 8

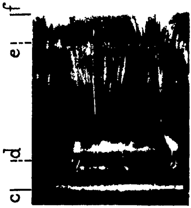

FIG 9

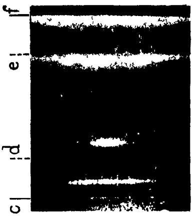

FIG 10

DESCRIPTION OF PLATE 18.

$R_1 = 0·263$ cm., $R_2 = 0·450$ cm

Figs. 3, 4, 5, 6, 7 show the motion observed in the plane *ab*, and figs. 8, 9, 10 the motion in the plane *cdef*.

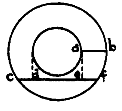

Fig 3.—Laminar motion when μ is positive, negative or zero

Fig 4.—Vortices when μ is zero

Fig 5.—Vortices when μ is $-0·29$

Fig 6.—Vortices when μ is $-0·43$

Fig 7.—Vortices when μ is positive

Fig 8.—Laminar motion when μ is positive, negative or zero.

Fig 9.—Vortices when μ is positive or zero

Fig 10.—Vortices when μ is $-0·43$

The Spectrum of Fluorine (FI). Part II.

By Herbert Dingle, B.Sc., Assistant Professor of Physics, Imperial College of Science and Technology.

(Communicated by A. Fowler, F.R.S.—Received November 4, 1927.)

Introductory.

In a former paper* an account was given of an investigation of the spectrum of neutral fluorine obtained by passing discharges through vacuum tubes containing silicon tetrafluoride. The observations have now been extended farther into the infra-red, and a number of new lines observed. The additional data have enabled the spectrum to be analysed more thoroughly than was previously possible, and a more complete correlation with the scheme of terms predicted by the Heisenberg-Hund theory has been established. The observations of Bowen† in the extreme ultra-violet have been of great assistance in the analysis, and have led to a slight modification of the term-assignments tentatively suggested in the former paper.

Experimental Arrangements.

The spectrum was produced in the same manner as before, and photographed on neocyanine plates. Exposures of nine to ten hours, using a rapid glass spectrograph with an average dispersion of 61 A per millimetre for the range λ 7800–λ 8500, yielded a spectrum of moderate strength. (This spectrograph, formerly the property of the late Mr W Willis, was presented to the Imperial College by his brother, Mr J Willis) Both strong and weak discharges were used, in order to distinguish any enhanced lines that might be produced The elimination of impurity lines was conducted on the principles described in the earlier paper, and a spectrum of the silicon spark in hydrogen was photographed with a more rapid instrument of lower dispersion for the purpose of separating, as far as possible, the lines of silicon from those of fluorine This showed, however, in the region concerned, only a weak, very nebulous line at the position of a pair, λλ 8231 0 (2), 8214 6 (0), appearing on the vacuum tube plates This pair behaved differently from the lines of FI under varying stimulus, and may accordingly be attributed to silicon—probably to Si III The lines which varied in intensity from plate to plate in the same manner as the already established lines of FI are given in Table I They are probably due to fluorine, but, as in the earlier observations, the complete absence of silicon lines cannot be regarded as certain

---

* 'Roy. Soc. Proc.,' A, vol. 113, p. 323 (1926).

† 'Phys. Rev.,' vol. 29, p. 231 (1927).

Table I —Lines probably due to Neutral Fluorine

λ (Int)	ν	Combinations (based on ^{1}D state of core)
8299 5 (1)	12045 6	
73 6 (1)	083 3	
61 9 (0)	100 4	$3s\,^2D_2^1 - 3p\,^2P_2^1$
8194 6 (4)	199 8	$3s\,^2D_2^1 - 3p\,^2P_1^1$
83 5 (2)	216 4	$3s\,^2D_3^1 - 3p\,^2P_2^1$
59 9 (00)	251 7	
28 2 (0)	299 5	
02 9 (1+)	337 9	
8093 2 (0+)	352 7	
76 0 (0+)	379 0	
64 1 (00)	397 2	
39 8 (0)	434 7	
7849 2 (0)	736 7	
7698 9 (½)	985 3	
65 0 (½)	13042 7	
54 7 (00)	060 3	

Analysis of the Spectrum

In the former paper a number of quartet and doublet terms were deduced and correlated with terms to be expected on the Heisenberg-Hund theory from the addition of an electron to an ion, F$^+$, in a state corresponding to its deepest term, ^{3}P Among these terms was a ^{2}P term (designated aP_{21}) having a separation of 533, the reality of which was stated to be questionable owing to violations of the intensity rules, both in the components of a multiplet in which the term took part and also in the Zeeman pattern of one of the lines of the multiplet De Bruin[*] shortly afterwards proposed an alternative arrangement, according to which the ^{2}P term referred to is rejected, and a new doublet term introduced, of similar type, having a separation of 250 This required the existence of a line at λ 7956, beyond the range of wave-lengths then investigated, and led de Bruin to suggest a slightly extended analysis involving intercombinations between doublet and quartet terms

There are several objections to de Bruin's scheme In the first place, the predicted line at λ 7956 does not appear on the plates in the region concerned which have now been obtained In view of the strength of the observed lines of the suggested multiplet to which it would belong, it is therefore probable that it does not exist Secondly, de Bruin's classification of the extreme ultra-violet lines is inconsistent with the more recent classification by Bowen,[†] and, further, would imply improbably high excitation potentials for FI [‡] Thirdly, the suggested intercombination between ^{4}P and ^{2}P terms is an "irregular" or "forbidden" combination between terms arising from the same n_k electron configuration Fourthly, the same interval, 325, is attributed to two different ^{2}P terms, referred to respectively as a^2P and b^2P

It appears, therefore, that de Bruin's analysis cannot be accepted On the other hand, the detection by Bowen of the ground-term, $^2P_{21}$, of FI, with a separation of about 407, makes it improbable that the separation of 533 in a less deep ^{2}P term is real A slightly modified analysis (see Table III) is therefore here proposed, in which this separation is rejected and the interval 250, proposed by de Bruin for a ^{2}P term, is adopted as a ^{2}D interval A ^{2}D term, giving lines in the region concerned, is predicted by theory, but was previously unidentified, and the arrangement has the further merit of revealing two intercombination multiplets (including a group previously described as "unidentified combination or intercombination") which act as a check on the relative term values in the doublet and quartet systems It should be remarked that the line $3s\,^4P_1 - 3p\,^2S_1$ is exceptionally faint compared with its companion, $3s\,^2P_2 - 3p\,^2S_1$, but evidence in favour of the proposed classification of these lines is found in the fact that the Zeeman effect for the latter, as observed by Carragan,[§] agrees with calculation

---

[*] 'Verslagen K. Acad. Amsterdam, Afd Natuurkunde,' vol 35, No 10 (1926)

[†] *Loc cit.*

[‡] See 'Nature,' vol. 119, p 86 (1927).

[§] 'Astroph. J,' vol. 63, p. 145 (1926).

Table II.—Theoretical Scheme of more Prominent Terms of Spectrum FI.
(Terms which have been detected are printed in italics.)

F^+		F		
Electrons in uncompleted shell.	Terms	Orbit of added electron	Terms	
			Prefix	Term symbol.
$2_1 2_1 \quad 2_2 2_2 2_2 2_2$	$^3\mathrm{P}$, $^1\mathrm{D}$, $^1\mathrm{S}$	2_2	$2p$	^2P
	$^3\mathrm{P}$	3_1	$3s$	$^4P \qquad ^2P$
		3_2	$3p$	$^4D \ ^4P \ ^4S \qquad ^2D \ ^2P \ ^2S$
		3_3	$3d$	$^4\mathrm{F} \ ^4\mathrm{D} \ ^4\mathrm{P} \qquad ^2\mathrm{F} \ ^2\mathrm{D} \ ^2\mathrm{P}$
		4_1	$4s$	$^4\mathrm{P} \qquad ^2\mathrm{P}$

Table III, which is to be considered in conjunction with the theoretical term scheme of Table II, contains a notation which is explained elsewhere[*] by Prof. Fowler. Each term symbol is prefixed by a symbol representing the orbit of the "travelling electron" corresponding to that term as given in Table II; thus, $3p\,^2\mathrm{S}_1$ denotes the $^2\mathrm{S}_1$ term corresponding to the orbit 3_2 of the added electron. In this system of notation the combination possibilities, so far as they are determined by the azimuthal quantum numbers, are indicated by the ordinary rules applied to the prefixes, and dashes after the term symbols proper are unnecessary.

The new term values are derived from a Rydberg formula calculated from the terms $2p\,^2\mathrm{P}$ and $3p\,^2\mathrm{P}$, viz.:—

$$(m + 1)p\,^2\mathrm{P} = \frac{\mathrm{R}}{(m - 0{\cdot}14705)^2}$$

In obtaining this formula the mean values of the components of the $^2\mathrm{P}$ terms were taken. The corresponding ionisation potential is 18·6 volts, which is probably rather high. It should be noted that, owing to the detection of intercombinations between the doublet and quartet systems, all the new term values in Table III are relatively accurate, whereas in the older list there is no relation between the doublet and quartet terms.

The term denoted by Y was detected by Bowen from a combination with the ground-term, $2p\,^2\mathrm{P}_{21}$, viz.:—

$$\left.\begin{matrix}809{\cdot}60\ (3)\\ 806{\cdot}92\ (4)\end{matrix}\right\}\Delta\nu = 410$$

---

[*] *V. supra*, p. 317.

Table III —Values of more Prominent Terms of FI

Data of former paper				Data now proposed		
Designation	Term values		Theoretical equivalent	Designation and theoretical equivalent	Term values	
	$\Delta\nu$	ν			ν	$\Delta\nu$
				$2p\,{}^2P_2{}^*$	150959	407
				$2p\,{}^2P_1{}^*$	552	
${}^4P_3$	47022 00	274 69	$3s\,{}^4P_3$	$3s\,{}^4P_3$	48547 00	274 69
${}^4P_2$	46747 31	159 95	$3s\,{}^4P_2$	$3s\,{}^4P_2$	272 31	159 95
${}^4P_1$	587 36		$3s\,{}^4P_1$	$3s\,{}^4P_1$	112 36	
${}^2P_2{}'*$	30651 0	325 8	$3p\,{}^2P_2$	$3s\,{}^2P_2$	46221 4	325 3
$P_1{}'$	325 7		$3p\,{}^2P_1$	$3s\,{}^2P_1$	45896 1	
${}^4P_3{}'$	33500 8	122 9	$3p\,{}^4P_3$	$3p\,{}^4P_3$	35034 8	122 9
${}^4P_2{}'$	386 9	102 7	$3p\,{}^4P_2$	$3p\,{}^4P_2$	34911 9	102 7
${}^4P_1{}'$	284 2		$3p\,{}^4P_1$	$3p\,{}^4P_1$	809 2	
${}^4D_4$	32440 44	176 61	$3p\,{}^4D_4$	$3p\,{}^4D_4$	33965 44	176 61
${}^4D_3$	263 83	144 51	$3p\,{}^4D_3$	$3p\,{}^4D_3$	788 83	144 51
${}^4D_2$	119 32	83 38	$3p\,{}^4D_2$	$3p\,{}^4D_2$	644 32	83 38
${}^4D_1$	035 94		$3p\,{}^4D_1$	$3p\,{}^4D_1$	560 94	
				$3p\,{}^2D_3$	33329 9	250 0
				$3p\,{}^2D_2$	079 9	
				$3p\,{}^2S_1$	32547 2	
${}^4S_2$	31000 00		$3p\,{}^4S_2$	$3p\,{}^4S_2$	32525 00	
X	30491 0		—	$3p\,{}^2P_2$	32015 8	145 0
bP_2	16445 4	145 0	$3d\,{}^2P_2$ or $4s\,{}^2P_2$			
bP_1	300 4		$3d\,{}^2P_1$ or $4s\,{}^2P_1$	$3p\,{}^2P_1$	31870 8	
				Y*	27033	
aP_2	44000 0	532 7	$3s\,{}^2P_2$			
aP_1	43467 3		$3s\,{}^2P_1$			

* Detected by Bowen

It was regarded by him as one of the terms corresponding to the orbit $3d$ of the travelling electron This identification is doubtful, however, since such terms should give one, three, and four lines respectively, in combination with $2p\,^2P_{21}$ The intensity of the observed pair makes it probable that other lines of the group, if existing, would have been detected, and it is unlikely that they are blended with the observed lines owing to the exactness with which the separation agrees with the $2p\,^2P_{21}$ interval Possibly the Y term may arise from the configuration, " one 2_1, six 2_2," of the external electrons, which has been found by Bowen to yield strong lines in FII, FIII, FIV and similar spectra Such a configuration would correspond to a $2p'\,^2S$ term, which would have the same combining properties as those shown by Y

The multiplets from which the new terms in Table III have been derived are set out in Table IV With the addition of the quartet combinations and the group $^2P_{21}' - b\,^2P_{21}$, given in the earlier paper as well as Bowen's multiplets,

Table IV

(a) Doublet Combinations

Term values	$3s\,^2P_2$ 46221 4	325 3	$3s\,^2P_1$ 45896 1	Combinations
$3p\,^2S_1$ − 32547 2	13674 0* (4)	324 8	13349 2* (0)	$3s\,^2P_{21}$ $3p\,^2S_1$
$3p\,^2D_3$ − 33329 9	12891 5* (5)			$3s\,^2P_{21}$ − $3p\,^2D_{32}$
250 0	250 3			
$3p\,^2D_2$ − 33079 9	13141 8* (2)	325 8	12816 0* (4)	

(b) Doublet-Quartet Intercombinations

Term values	$3s\,^4P_3$ 48547 00	274 69	$3s\,^4P_2$ 48272 31	159 95	$3s\,^4P_1$ 48112 36	Combinations
$3p\,^2P_2$ − 32015 8	16531 1† (4)	274 8	16256 3† (2)	159 9	16096 4† (3)	$3s\,^4P_{321}$ $3p\,^2P_{21}$
145 0						
$3p\,^2P_1$ = 31870 8			[16401 5]§		[16241 6]§	
$3p\,^2D_3$ = 33329 9	15217 0* (0)	274 6	14942 4* (1½)		‡	$3s\,^4P_{321}$ − $3p\,^2D_{32}$
250 0			250 2			
$3p\,^2D_2$ = 33079 9	[15467 1]§		15192 6† (4)	160 4	15032 2* (0)	

* Recorded in former paper

† Recorded by Gale and Monk, intensity scale higher than that for other lines

‡ de Bruin, in connection with a different interpretation of some of the lines of this multiplet, includes the line λ 6763 (ν 14782), the wave number of which is equal to the difference $3s\,^4P_1 - 3p\,^2D_3$ As was indicated in the former paper, this line is quite different in character from the other lines of the spectrum, and the relationship is probably accidental

§ Calculated values only

they form the whole of the combinations which have been detected among the terms of Table III It will be noticed that all the terms in Table II corresponding to the $2p$, $3s$, and $3p$ orbits of the travelling electron have now been identified

Terms based on Metastable States of the Core

The normal configuration of the F^+ ion corresponds to the three terms, ^3P, ^1D, ^1S The spectrum FI may contain terms based on any of these states, the most prominent being those based on the ^3P term, which have already been considered The theoretical terms corresponding to the ^1D and ^1S states of the ion, or "core," are given in Table V Their numerical values should be lower than those for corresponding electron configurations based on the ^3P state, but the term differences (*i e*, the wave-numbers of the spectrum lines) should be of the same order of magnitude, and should therefore represent lines in the same region of the spectrum We might, therefore, expect to find terms corresponding to the $3s$ and $3p$ orbits of the travelling electron for each of the states ^1D and ^1S of the core

Table V —Theoretical Scheme of Terms of FI based on Metastable States of the Core

(Terms which have been detected are printed in italics)

Orbit of added electron	Prefix	Term symbol	
		Core in ^1D state	Core in ^1S state
3_1	$3s$	$^2D^1$	$^2S^2$
3_2	$3p$	$^2\mathrm{F}^1$ $^2D^1$ $^2P^1$	$^2P^2$
3_3	$3d$	$^2\mathrm{G}^1$ $^2\mathrm{F}^1$ $^2\mathrm{D}^1$ $^2\mathrm{P}^1$ $^2\mathrm{S}^1$	$^2\mathrm{D}^2$
4_1	$4s$	$^2\mathrm{D}^1$	$^2\mathrm{S}^2$

Multiplets possibly involving such terms have been detected among the newly observed lines and the unclassified lines contained in the former paper They are given in Table VI, and the relative term values are collected in Table VII Terms based on the ^1D and ^1S states of the core have the indices 1 and 2, respectively, at the top right-hand corner of the term symbols, to distinguish them from the terms arising from the same electron configurations but based on the ^3P state of the core No intercombinations have been found between the terms corresponding to the three states of the core, so that arbitrary values have been adopted for the $3s\,^2D^1$ and $3s\,^2S^2$ terms It might be remarked that the whole of the lines given in the main table of the earlier paper, with the exception of the peculiar line λ 6763, have now been classified, as well as seven of the lines recorded as possibly due to fluorine

Table VI

(*a*) Combinations between Terms based on ^{1}D state of Core

Term values	$3s\,^3D_3{}^1$ 35000 0	116 2	$3s\,^3D_2{}^1$ 34883 8	Combinations
$3p\,^3D_3{}^1$ = 20077 2	14922 8† (1)	116 3	14806 5† (0)	$3s\,^3D_{32}{}^1 - 3p\,^3D_{32}{}^1$
77 1	77 0		77 2	
$3p\,^3D_2{}^1$ — 20000 1	14999 8†‡ (1)	116 1	14883 7† (1)	
$3p\,^3P_2{}^1$ = 22783 5	12216 4 (2)	116 0	12100 4 (0)	$3s\,^3D_{32}{}^1 - 3p\,^3P_{21}{}^1$
99 4			99 4	
$3p\,^3P_1{}^1$ = 22684 1			12199 8 (4)	
	Z_3 37417 5	43 0	Z_2 37374 5	
$3p\,^3P_2{}^1$ = 22783 5	14634 0† (0)	43 0	14591 0† (1)	$Z_{32} - 3p\,^3P_{21}{}^1$
99 4			99 3	
$3p\,^3P_1{}^1$ = 22684 1			14690 3† (½)	

(*b*) Combinations between Terms based on ^{1}S state of Core

Term values	$3p\,^3P_2{}^3$ 11332 0	9 8	$3p\,^3P_1{}^3$ 11322 2	Combinations
$3s\,^3S_1{}^3$ = 25000 0	13668 0* (2)	9 8	13677 8* (3)	$3s\,^3S_1{}^3 - 3p\,^3P_{21}{}^3$

* Recorded in former paper

† Recorded in former paper as possibly due to fluorine (FI)

‡ Owing to an error in transcription, this line was wrongly recorded in former paper as λ 6665 910 (ν 14997 57) instead of λ 6664 910 (ν 14999 82)

Table VII

Designation	Term values	
	ν	$\Delta\nu$
(*a*) Relative Values of Terms of FI based on ^1D state of Core		
$3s\,{}^2D_3^1$	35000 0*	116 2
$3s\,{}^2D_2^1$	34883 8	
$3p\,{}^2P_2^1$	22783 5	99 4
$3p\,{}^2P_1^1$	22684 1	
$3p\,{}^2D_3^1$	20077 2	77 1
$3p\,{}^2D_2^1$	20000 1	
(*b*) Relative Values of Terms of FI based on ^1S state of Core		
$3s\,{}^2S_1^2$	25000 0*	
$3p\,{}^2P_2^2$	11332 0	9 8
$3p\,{}^2P_1^2$	11322 2	
(*c*) Unidentified Term †		
Z_3	37417 5	43 0
Z_2	37374 5	

* Assumed values

† The values of this term are relative to the term values in section (*a*) of the table

The term Z_{32} cannot at present be identified The separation 43 0 does not occur with undoubted significance elsewhere, but is regarded as real on experimental grounds The three lines forming the group, $Z_{32} - 3p\,{}^2P_{21}^1$, show similar and somewhat peculiar variations of intensity on different plates, and are, therefore, probably closely associated

With regard to the lines still remaining unclassified, attention might be directed to two "triplets" occurring among the newly measured lines, viz —

12045 6 (1)	**206 1**	12251 7 (00)	**145·5**	12397 2 (00)
12299 5 (0)	**53 2**	12352 7 (0+)	**82·0**	12434 7 (0)

These have the same separations as the following lines recorded by Gale and Monk, viz —

15375 6 (1) **205 4** 15581 0 (3) **145 7** 15726 7 (1)
16618 0 (1) **53 1** 16671 1 (1) **82 3** 16753 4 (0)

If these separations are significant, they must belong to the quartet system and probably to the terms $3d\ ^4P$ and $4s\ ^4P$ Combinations of such terms with terms based on the ^3P state of the core would be expected to give lines farther in the infra-red than the region so far investigated, but combinations with terms based on the ^1D for ^1S state of the core might well be responsible for the lines

Summary

(1) The spectrum FI has been investigated in the region λ 7600–λ 8400, and the wave-lengths of 16 lines have been measured

(2) The analysis of the spectrum previously made has been slightly modified and extended, and an approximate ionisation potential of 18 6 volts calculated

(3) Relative term values of FI, based on the two metastable states of the core, have been deduced

Resistance to a Barrier in the Shape of an Arc of a Circle

By L Rosenhead, B Sc

With Note by S Brodetsky, M A , Ph D

(Communicated by L Bairstow, F R S —Received July 7, 1927)

Comparatively little progress in the solution of the problem of discontinuous fluid motion past a curved barrier was made until Levi-Civita formulated a method of transforming that part of the barrier which is in contact with the moving fluid into a semi-circle in an Argand diagram This, indeed, was the starting point of much work of interest and importance Useful accounts of the problem of motion past any barrier together with extensions, are given by Cisotti* and Brillouin † Leaving out of account such barriers as are made up of one or more planes, problems which can be solved by the older methods based on Schwartz-Christoffel transformations the only applications of Levi-Civita's method to curved barriers seem to be that made by Brillouin in the paper referred to, and those made by S Brodetsky in 1922 ‡ The work of Brillouin however, and that of other investigators§ are essentially backward processes, in which a likely expression is written down and the streaming motion implied, as well as the shape of the boundary, are investigated A more direct attack is obtained by suitably choosing the coefficients in Levi-Civita's general formula, and arriving at the solution for a given curved barrier by a series of steps in successive approximation The solution of the problem for a circular barrier placed symmetrically in the streaming fluid has been obtained in this manner by S Brodetsky ||

The object of this paper is to solve the problem of the circular barrier placed in any position in the streaming fluid subject to the condition, however, that neither of the ends of the barrier are in the "dead" fluid—i e , the radius of curvature of the free stream line is zero at each end This immediately restricts the barrier, if convex to the streaming fluid, to be of angular extent less than 110 2° ¶

---

* 'Idromeccanica Piana,' vol 2 Milano (1922)

† 'Ann Chim Phys ,' vol 23, pp 145–230 (1911)

‡ 'Roy Soc Proc ,' A vol 102, pp 361 and 542

§ See, *e g* , Greenhill's "Theory of a Stream Line past a Curved Wing" 'Advisory Committee for Aeronautics' London, 1916

|| See 'Fluid Motion Past Circular Barriers, Scripta Univ Bibl Heirosolym ,' vol 1, No xi (1923)

¶ *Ibid* , p 8

A circular barrier can be either concave to the streaming fluid or convex to it Using the ordinary conventions in the z plane of fig 1, the angle of contingence at A measured from C is positive for concave or positive camber, negative for convex or negative camber The kind and angular extent of the circular barrier will therefore be indicated by the sign and value of the angle of contingence at A, measured from C It has been proved in the last-named paper that there is an upper limit to the arithmetical value of the negative angle of contingence at A --namely, about 55 1° --for otherwise the free stream line would leave the barrier at some point between C and A

The motion is two dimensional Let the complex variable $z\,(\equiv x + \iota y)$ define position in any plane perpendicular to the generators of the barrier, the x axis being parallel to the direction of the stream at infinity We define —

$$u = \frac{\partial \phi}{\partial x} = \frac{\partial \psi}{\partial y}, \qquad v = \frac{\partial \phi}{\partial y} = -\frac{\partial \psi}{\partial x},$$

where u, v are the velocity components, and ϕ, ψ are the velocity potential and stream function, respectively Let $w \equiv \phi + \iota\psi$ and define ζ, Ω, r, θ so that

$$\zeta = re^{\iota\theta} = \frac{dz}{dw}, \quad \Omega = \log \zeta = \log r + \iota\theta$$

Fig 1 shows the z, w, ζ, Ω, τ planes for such a problem C is the point of bifurcation of the stream line IC , CA, CA′ are the stream lines in contact with the barrier , AJ, A′J′ are the free stream lines We take the standard dimensions to be unit velocity at infinity, unit value of $\frac{1}{2}(\sqrt{\text{CA}} + \sqrt{\text{CA}'})$ as measured in the w plane, and unit density *

We introduce the transformation in which the variable $\tau \equiv \rho e^{\iota\sigma}$ is given by $\sqrt{w} = \frac{1}{2\iota}\left(\tau - \frac{1}{\tau}\right) - \sin\sigma_0$, where the point C is given by $\tau = e^{\iota\sigma_0}$ It is immediately verified that the barrier ACA is the semi-circle $\rho = 1$, $-\frac{\pi}{2} \leq \sigma \leq \frac{\pi}{2}$ in the τ plane, while the free stream lines AJ, A′J′ become the two halves of the diameter along the imaginary axis, namely, $\tau = \iota\rho$, $-1 \leq \rho \leq 1$ In the general problem we write

$$\begin{aligned} \Omega &= \lambda \log\{(1 + e^{\iota\sigma_0}\tau)/(1 - e^{\iota\sigma_0}\tau)\} + A_1\tau + \tfrac{1}{2}\iota A_2\tau^2 + \tfrac{1}{3}A_3\tau^3 + \\ &\equiv a_1\tau + \tfrac{1}{2}\iota a_2\tau^2 + \tfrac{1}{3}a_3\tau^3 + \tfrac{1}{4}\iota a_4\tau^4 + \quad , \end{aligned} \tag{1}$$

where the A's, a's are all real and the expansion in (1) is convergent for $|\tau| \leq 1$ $\lambda\pi$ is the angle at C measured away from the streaming fluid

---

* See Brodetsky, 'Roy Soc Proc ,' A, vol 102, p 361 (1922)

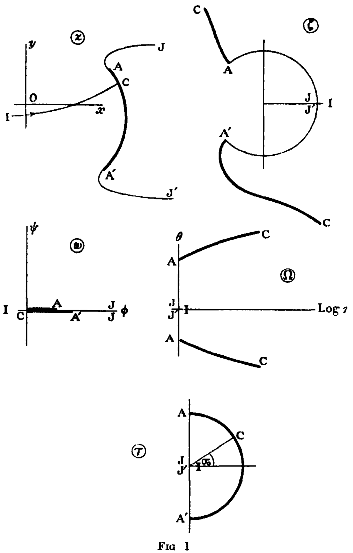

FIG 1

In the case of the circular barrier, the angle between the two tangents at any two points on the barrier is π, hence $\lambda = 1$ In addition we have

$$a_1 = A_1 + 2\cos\sigma_0, \qquad a_2 = A_2 - 2\sin 2\sigma_0,$$

$$a_3 = A_3 + 2\cos 3\sigma_0, \qquad a_4 = A_4 - 2\sin 4\sigma_0, \text{ etc}$$

On the barrier, $\tau = e^{\iota\sigma}$, therefore

$$\Omega = \log\{(1 + e^{\iota\sigma + \iota\sigma_0})/(1 - e^{\iota\sigma + \iota\sigma_0})\} + A_1 e^{\iota\sigma} + \tfrac{1}{2}\iota A_2 e^{2\iota\sigma} + \tfrac{1}{3}A_3 e^{3\iota\sigma}$$

$$\equiv \log r + \iota\theta$$

We get

$$\log r = \tfrac{1}{2}\log\left\{\frac{1+\cos(\sigma+\sigma_0)}{1-\cos(\sigma-\sigma_0)}\right\} + A_1\cos\sigma - \tfrac{1}{2}A_2\sin 2\sigma$$

$$+ \tfrac{1}{3}A_3\cos 3\sigma - \tfrac{1}{4}A_4\sin 4\sigma \quad , \quad (2)$$

$$\theta = \tan^{-1}\frac{\sin(\sigma+\sigma_0)}{1+\cos(\sigma+\sigma_0)} + \tan^{-1}\frac{\sin(\sigma-\sigma_0)}{1-\cos(\sigma-\sigma_0)}$$

$$+ A_1\sin\sigma + \tfrac{1}{2}A_2\cos 2\sigma_0 + \tfrac{1}{3}A_3\sin 3\sigma$$

$$= \pm\frac{\pi}{2} + \sigma_0 + A_1\sin\sigma + \tfrac{1}{2}A_2\cos 2\sigma + \tfrac{1}{3}A_3\sin 3\sigma \qquad (3)$$

(We use $\pm\pi/2$ according as $\sigma \gtrless \sigma_0$.) The angular extent β of the barrier

$$= (\theta_A - \theta_{A'}) - \pi$$

$$= 2(A_1 - \tfrac{1}{3}A_3 + \tfrac{1}{5}A_5 - \tfrac{1}{7}A_7 \quad) \qquad (4)$$

Now $r = |dz/dw|$. On the barrier $|dz| = ds$, and $w = \phi$. Therefore

$$r = ds/d\phi$$

Also $\sqrt{\phi} = (\sin\sigma - \sin\sigma_0)$, therefore

$$ds/d\sigma = r\,(d\phi/d\sigma) = 2r\cos\sigma\,(\sin\sigma - \sin\sigma_0)$$

If R is the radius of curvature of the barrier,

$$R = \frac{ds}{d\theta} = \frac{ds/d\sigma}{d\theta/d\sigma}$$

$$= 2\cos\sigma\,(\sin\sigma - \sin\sigma_0)\left\{\frac{1+\cos(\sigma+\sigma_0)}{1-\cos(\sigma-\sigma_0)}\right\}^{\frac{1}{2}}\frac{E\,(A_1\cos\sigma - \frac{1}{2}A_2\sin 2\sigma + \frac{1}{3}A_3\cos 3\sigma \quad)}{A_1\cos\sigma - A_2\sin 2\sigma + A_3\cos 3\sigma}$$

$$= 2\{1 + \cos(\sigma+\sigma_0)\}\frac{E\,(A_1\cos\sigma - \frac{1}{2}A_2\sin 2\sigma + \frac{1}{3}A_3\cos 3\sigma \quad)}{A_1 - A_2\dfrac{\sin 2\sigma}{\cos\sigma} + A_3\dfrac{\cos 3\sigma}{\cos\sigma}} \qquad (5)$$

The A's must now be chosen in such a way that R is constant, i.e., independent of σ between $\pm\pi/2$.

Consider the free stream lines. Along AJ we must put $\tau = i\rho$, $0 \le \rho \le 1$. Therefore

$$r = 1, \text{ and } \theta = a_1\rho - \tfrac{1}{2}a_2\rho^2 - \tfrac{1}{3}a_3\rho^3 + \tfrac{1}{4}a_4\rho^4 + \tfrac{1}{5}a_5\rho^5$$

The stream line AJ must be convex to the moving fluid—i.e., $ds/d\theta$ must be negative,

$$ds = r\,d\phi = d\phi\,, \qquad \phi = \{\tfrac{1}{2}(\rho + 1/\rho) - \sin\sigma_0\}^2 d\rho/d\theta$$

Therefore

$$\frac{ds}{d\theta} = \frac{ds}{d\rho}\,\frac{d\rho}{d\theta} = \frac{ds}{d\phi}\,\frac{d\phi}{d\rho}\,\frac{d\rho}{d\theta}$$

$$= \frac{d\phi}{d\rho}\,\frac{d\rho}{d\theta} = -\frac{(1-\rho^2)}{\rho^2}\,\{\tfrac{1}{2}(\rho+1/\rho) \quad \sin\sigma_0\}^2\,\frac{d\rho}{d\theta}$$

Therefore $d\theta/d\rho$ must be positive in the range $0 \leq \rho \leq 1$,

i e,

$$a_1 - a_2\rho - a_3\rho^2 + a_4\rho^3 + a_5\rho^4 \quad > 0, \quad 0 \leq \rho \leq 1 \tag{6}$$

Similarly along A′J′, by putting $\tau = -i\rho$ where $0 \leq \rho \leq 1$, the condition that the stream line is convex to the fluid is found to be

$$a_1 + a_2\rho - a_3\rho^2 - a_4\rho^3 + a_5\rho^4 \quad > 0, \quad 0 \leq \rho \leq 1 \tag{7}$$

The angular extent of the barrier, and the angle made by the axis of the barrier with the direction of streaming, completely specify the conditions of the problem The results will depend on these two quantities and since the quantities are entirely independent, we should expect the final result to be a function of two parameters

As a first approximation put $A_4 = A_5 = A_6 = \ldots = 0$, so that we can arrange that the radius of curvature should be the same at three points on the barrier The points chosen are $\sigma = \pi/2, 0, -\pi/2$ and so we postulate that

$$\frac{2(1-s)}{A_1-2A_2-3A_3} = 2(1+c)\frac{E(A_1+\frac{1}{3}A_3)}{A_1+A_3} = \frac{2(1+s)}{A_1+2A_2+3A_3},$$

where $s \equiv \sin\sigma_0$ and $c \equiv \cos\sigma_0$, and each fraction represents the radius R Choose as our two parameters

$$\sigma_0 \quad \text{and} \quad \xi = \frac{A_1+A_3}{2(A_1-3A_3)}$$

Hence

$$\left.\begin{aligned} A_1 &= \frac{3(6\xi+1)}{2(10\xi+1)}\log_e\left(\frac{2\xi}{1+c}\right) \\ A_2 &= \frac{6s}{2(10\xi+1)}\log_e\left(\frac{2\xi}{1+c}\right) \\ A_3 &= \frac{3(2\xi-1)}{2(10\xi+1)}\log_e\left(\frac{2\xi}{1+c}\right) \end{aligned}\right\} \tag{8}$$

We note now that ξ must be positive, for $2\xi = (1+c)\,e^{A_1+\frac{1}{3}A_3}$ which is always positive Also the angular extent is

$$\beta = 2(A_1-\tfrac{1}{3}A_3) = \frac{4(4\xi+1)}{10\xi+1}\log_e\left(\frac{2\xi}{1+c}\right) \tag{9}$$

Hence if the barrier is convex to the stream, β must be negative, i e, $2\xi < (1 + c)$, if plane, $A_1 = A_2 = A_3 = 0$, i e, $2\xi = (1 + c)$, if concave $2\xi > (1 + c)$ We note also that when β is negative, A_1 and A_2 are also negative

R can now be expressed in terms of σ, σ_0 and ξ, and if it be plotted against σ, having given definite values to σ_0 and ξ, the extent of the variation of the function R from its value at the three points $\sigma = \pi/2$, 0, $-\pi/2$, can at once be seen

It is now necessary to ascertain the possible values of ξ and σ_0, and any relations that may exist between them These are found by considering the conditions that the free stream lines are convex to the streaming fluid

The general condition that AJ is convex to the streaming fluid is

$$a_1 - a_2\rho - a_3\rho^2 + a_4\rho^3 + a_5\rho^4 \qquad > 0 ,$$

if in this we put $A_4 = A_5 = A_6 = \qquad = 0$, the condition becomes

$$A_1 - A_2\rho - A_3\rho^2 + 2c/(1 - 2\rho s + \rho^2) > 0, \quad 0 \leq \rho \leq 1 \tag{10}$$

Similarly, the condition that A′J′ is convex to the streaming fluid becomes

$$A_1 + A_2\rho - A_3\rho^2 + 2c/(1 + 2\rho s + \rho^2) > 0, \quad 0 \leq \rho \leq 1 \tag{11}$$

σ_0 is taken positive, for the relative configuration of the fluid and barrier is the same whether σ_0 is positive or negative If the barrier is convex to the streaming fluid, and if σ_0 is positive, then the axis of the barrier will make a positive angle with the direction of streaming, and the stream line will be in a more critical position at A′ than at A It is therefore condition (11) that has to be considered This can be shown mathematically as follows Let

$$X_1 \equiv A_1 - A_2\rho - A_3\rho^2 + 2c/(1 - 2\rho s + \rho^2),$$

and

$$X_2 \equiv A_1 + A_2\rho - A_3\rho^2 + 2c/(1 + 2\rho s + \rho^2)$$

It is required to show that if condition (11) is satisfied, then condition (10) is satisfied automatically, i e, $X_1 - X_2 > 0$, or

$$4sc/(1 + 2\rho^2 \cos 2\sigma_0 + \rho^4) > A_2$$

This is true, for the left-hand side of the inequality is always positive, whereas A_2 is always negative when the barrier is convex to the streaming fluid Now let

$$f(\rho) \equiv A_1 + A_2\rho - A_3\rho^2 + 2c/(1 + 2\rho s + \rho^2),$$

then

$$f(1) \equiv A_1 + A_2 - A_3 + c/(1 + s)$$

We can show that if $f(1) \geq 0$, then $f(\rho) > f(1)$ for all values of ρ The condition that $f(\rho)$ should diminish gradually as ρ increases from $0 \to 1$ is that $d\{f(\rho)\}/d\rho$ be negative for all values of ρ in the range This gives

$$A_2 - 2\rho A_3 - 4c(s+\rho)/(1+2\rho s+\rho^2)^2 < 0,$$

i e ,

$$4c\,(1+(s/\rho))/(1+2\rho s+\rho^2)^2 - A_2/\rho > -2A_3$$

The left-hand side of this inequality is positive, for A_2 is negative Also the left-hand side diminishes as ρ increases so that if the inequality is true for $\rho = 1$, it is true for all values of ρ Hence we need

$$c/(1+s) > A_2 - 2A_3$$

But we know that $f(1) \geq 0$, i e ,

$$c/(1+s) \geq A_3 - A_2 - A_1$$

Also the difference

$$(A_3 - A_2 - A_1) - (A_2 - 2A_3) = 3A_3 - 2A_2 - A_1$$
$$= -\frac{6(1+s)}{10\xi+1}\log_e\left(\frac{2\xi}{1+c}\right),$$

and this is positive, since $2\xi < (1+c)$ Thus

$$(A_3 - A_2 - A_1) > A_2 - 2A_3$$

or

$$c/(1+s) > A_2 - 2A_3,$$

which is the required condition Hence if $A_1 + A_2 - A_3 + c/(1+s) \geq 0$, condition $X_2 > 0$ is satisfied for every point on the barrier

In the limiting case—i e , when the curvature of the free stream at A_1 just becomes finite,

$$A_1 + A_2 - A_3 + c/(1+s) = 0,$$

i e ,

$$\frac{3(2\xi+s+1)}{10\xi+1}\log_e\left(\frac{2\xi}{1+c}\right) + \frac{c}{1+s} = 0 \tag{12}$$

Below are tabulated values of σ_0 and ξ which satisfy this equation

σ_0 degrees	ξ	A_1	A_2	A_3	β radians
0	0 3970	− 0 9426	0 0000	0 0574	− 1 9234
9	0 4609	− 0 7738	− 0 0643	0 0161	− 1 5584
18	0 5159	− 0 6354	− 0 0959	− 0 0049	− 1 2676
27	0 5600	− 0 5190	− 0 1081	− 0 0143	− 1 0285
36	0 5918	− 0 4182	− 0 1080	− 0 0169	− 0 8252
45	0 6106	− 0 3299	− 0 1000	− 0 0156	− 0 6494
54	0 6152	− 0 2509	− 0 0865	− 0 0123	− 0 4936
63	0 6060	− 0 1793	− 0 9689	− 0 0082	− 0 3532
72	0 5827	− 0 1148	− 0 0486	− 0 0042	− 0 2268
81	0 5471	− 0 0549	− 0 0253	− 0 0012	− 0 1090
90	0 5000	0 0000	0 0000	0 0000	0 0000

The preceding table gives ξ and σ_0 corresponding to the limiting positions in which barriers of various angular extents can be placed Thus, if we are given the general problem of a barrier of angular extent β (which must lie between 0 and $-1\ 9234$ radians), it is possible to obtain the values of ξ and σ_0, corresponding to its limiting position, by interpolating, or by solving for ξ and σ_0 the two equations

$$\beta = \frac{4(4\xi+1)}{(10\xi+1)}\log_e\left(\frac{2\xi}{1+c}\right),$$

$$\frac{3(2\xi+1+s)}{(10\xi+1)}\log_e\left(\frac{2\xi}{1+c}\right)+\frac{c}{1+s}=0$$

ξ can be eliminated from these equations giving rise to a single equation in σ_0

$$4c+\beta(1+s)(4+5s)$$
$$=4(1+s)(1+2s)\log\left[-(3\beta(1+s)^2+4c)/(1+c)\{3\beta(1+s)+8c\}\right] \quad (13)$$

In the general case, when the stream line starts with infinite curvature at the terminations of the barrier, ξ and σ_0 can have any value subject to the conditions that ξ is greater, and σ_0 less, than those values which correspond to the limiting position of the barrier under consideration An upper limit for σ_0 and a lower limit for ξ are thus determined The following diagram makes this clear

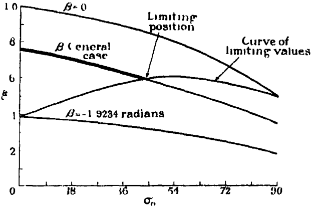

FIG 2

The upper limit for ξ corresponds to the symmetrical case—i e, $\sigma_0=0$—and its value for a barrier of given angular extent is obtained from the equation

$$\beta = \frac{4(4\xi+1)}{(10\xi+1)}\log_e\xi$$

The case of a barrier convex to the stream is thus fully discussed

We can also reasonably adopt a limiting position for a barrier concave to the

stream, namely, when the tangent at either A or A′ is parallel to the direction of streaming This immediately restricts the barrier to be of angular extent less than 180° We shall take σ_0 positive, so that the limiting case occurs at A

In the general position we must have $\pi > \theta_A$,

i e,

$$\pi > \pi/2 + \sigma_0 + \frac{4(4\xi+1) - 3s}{2(10\xi+1)} \log_e\left(\frac{2\xi}{1+c}\right),$$

or

$$\pi/2 - \sigma_0 > \frac{\beta}{2}\left\{1 - \frac{3s}{4(4\xi+1)}\right\}$$

The values of ξ and σ_0 which make the tangent at A parallel to the direction of streaming are obtained from the two equations

$$\pi/2 - \sigma_0 = \frac{\beta}{2}\left\{1 - \frac{3s}{4(4\xi+1)}\right\},$$

$$\beta = \frac{4(4\xi+1)}{10\xi+1} \log_e\left(\frac{2\xi}{1+c}\right),$$

ξ can be eliminated from these equations, leaving a single equation in σ_0 —

$$\frac{5\beta s - 4(\beta + 2\sigma_0 - \pi)}{8s} = \log_e \frac{3\beta s - 4(\beta + 2\sigma_0 - \pi)}{8(1+c)(\beta + 2\sigma_0 - \pi)} \tag{14}$$

We have tabulated the upper and lower limits to ξ and σ_0 for various barriers *i e*, the values of the parameters corresponding to the symmetrical and limiting positions The limiting values to ξ and σ_0, for convex and concave barriers, are separated by a horizontal line to indicate that they were obtained from different considerations

β in degrees	β in radians	ξ for symmetrical case $\sigma_0 = 0$	ξ for limiting position	σ_0 for limiting position Degrees
— 110 2	— 1 9234	0 3970	0 3970	0 00
— 100	— 1 7453	0 4277	0 4272	4 18
— 90	1 5708	0 4607	0 4586	8 39
— 80	1 3963	0 4978	0 4913	13 49
- 70	— 1 2217	0 5388	0 5247	19 34
— 60	- 1 0472	0 5847	0 5586	26 10
— 50	— 0 8727	0 6357	0 5853	33 46
— 40	— 0 6981	0 6928	0 6066	42 22
— 30	- 0 5236	0 7569	0 6158	52 7
— 20	— 0 3491	0 8287	0 6055	63 16
— 10	— 0 1745	0 9093	0 5683	75 58
0	0 0000	1 0000	0 5000	90 00
10	0 1745	1 1018	0 5837	86 7
20	0 3491	1 2163	0 6842	81 59
30	0 5236	1 3451	0 8041	77 36
40	0 6981	1 4899	0 9464	73 00
50	0 8727	1 6527	1 1142	68 12
60	1 0472	1 8357	1 3102	63 13

Particular cases can be considered To explain the method, one of these cases will be discussed fully

Take the case $\beta = +10^\circ$, so that the barrier has angular extent 10°, and is concave to the stream Choose $\sigma_0 = 86^\circ 7'$, say, then the parameter ξ which satisfies the equation (9) is equal to 0 5837 (As a matter of fact, these two parameters give the limiting position of the barrier) From these values of ξ and σ_0 we find A_1, A_2, and A_3 from (8) R and θ are then given for different values of σ, ranging between $\pm$ 90° by (5) Plot R, R sin θ, R cos θ, against θ The value of $\int R\, d\theta$ (*i e*, the length of the barrier) can be obtained by graphical integration Similarly the values of $\int R \sin\theta\, d\theta$ and $\int R \cos\theta\, d\theta$ can be found for various points on the curve Since $x = \int R \cos\theta\, d\theta$ and $y = \int R \sin\theta\, d\theta$, the Cartesian co-ordinates of any point on the barrier are known There is actually a big variation in R, yet on plotting, the barrier is found to be very approximately circular The effect of the big variation in R is, in fact, nullified by the very small range of θ in which it occurs The radius of the barrier so plotted is not, however, exactly equal to the calculated value of R at the three specified points A second approximation to the value of R is obtained by dividing the length $\int R\, d\theta$, obtained by graphical methods, by the angular extent of the barrier under consideration If an arc of a circle is drawn with this radius, the end points coinciding with the ends of the plotted barrier, the two curves are found to be almost identical This method gives considerable accuracy in the case of small angular extent, and it is only when the angular extent becomes large—*e g*, $\beta = 90^\circ$—that the error begins to become perceptible Even then the error in the radius is at most 1 5 per cent

In this way we can work out and tabulate pairs of values of values of ξ and σ_0, which, if substituted in the Levi-Civita formula, give circular barriers of known radii, angular extents and positions

It is more usual and convenient to describe a barrier by its camber and angle of attack We define the camber as

$$\eta = \frac{\text{Sagitta of Barrier}}{\text{Chord of Barrier}} = \tfrac{1}{2}\tan \beta/4$$

Also the line AA′ is parallel to the bisector of the exterior angle between the tangents at A and A′ Hence

$$\alpha + \tfrac{1}{2}(\theta_A + \theta_{A'}) = \pi, \quad \textit{i e.}, \alpha = \tfrac{1}{2}(\pi - 2\sigma_0 + A_2) \tag{15}$$

In our notation, the components of thrust on unit length of the barrier (measured perpendicularly to the z plane) are P_x' and P_y', given by the equations

$$P_x' = \tfrac{1}{4}\pi\, a_1^2, \quad P_y' = \tfrac{1}{4}\pi\,(a_2 + 4a_1 \sin\sigma_0)$$

(See Cisotti, p 175, and Brillouin, p 195) If P_x' and P_y' are divided by $2R \sin \beta/2$, the resulting values are the components of drag and lift on a barrier of unit chord, but of the same camber and orientation Let these quantities be P_x and P_y, and their resultant $P = \sqrt{P_x^2 + P_y^2}$

This resultant thrust passes through the centre of the circle, for the pressure is everywhere normal to the surface Its line of action will cut the chord of the barrier in the point D given by

$$\frac{AD}{DA'} = \frac{\sin \widehat{DOA}}{\sin \widehat{DOA'}} = \frac{\sin\left\{\dfrac{\beta}{2} - \left(\tan^{-1}\dfrac{P_y}{P_x} + \alpha - \dfrac{\pi}{2}\right)\right\}}{\sin\left\{\dfrac{\beta}{2} + \left(\tan^{-1}\dfrac{P_y}{P_x} + \alpha - \dfrac{\pi}{2}\right)\right\}}$$

$$= -\frac{\cos\left\{\dfrac{\beta}{2} - \alpha - \tan^{-1}\dfrac{P_y}{P_x}\right\}}{\cos\left\{\dfrac{\beta}{2} + \alpha + \tan^{-1}\dfrac{P_y}{P_x}\right\}} \qquad (16)$$

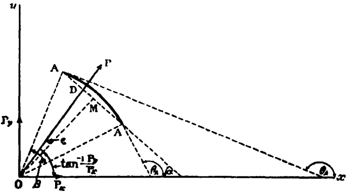

Fig 3

This is valid for barriers convex or concave to the stream

If $\beta = 0$, so that the barrier is flat, this ratio becomes $-\dfrac{\cos(-\pi/2)}{\cos(\pi/2)}$ and is therefore apparently indeterminate In the case of the plane barrier, however, $2\xi = (1 + c)$ Let us therefore put $2\xi = (1 + c)(1 + h)$ where powers of h higher than the first can be neglected It can be easily verified that

$$\operatorname*{Lt}_{h \to 0}\left(\frac{AD}{DA'}\right) = \frac{2(4 + \pi c) - 3s}{2(4 + \pi c) + 3s},$$

and the distance of D from the mid-point of the barrier is

$$\tfrac{3}{4}ls/(4+\tfrac{8}{3}c) \tag{17}$$

where l is the length of the chord The exact value of this distance is

$$\tfrac{3}{4}ls/(4+\pi c)$$

The error divided by the chord is therefore

$$\frac{\frac{3}{8}(\pi-\frac{8}{3})\sin 2\sigma_0}{(4+\pi c)(4+\frac{8}{3}c)}=\frac{1}{90}\,\frac{\sin 2\sigma_0}{1+1\cdot 452\cos\sigma_0+0\cdot 524\cos^2\sigma_0} \tag{18}$$

The maximum value of this expression is about $\frac{1}{300}$, so that we get an accuracy of about $\frac{1}{3}$ per cent by means of this approximation

In order to demonstrate clearly the effect of the camber on the resultant resistance P experienced by the barrier, we give the resistance experienced by a plane barrier of unit length, but with the same angle of attack as the circular barrier These figures are put in brackets above the figures giving the thrusts on the corresponding circular barriers As is to be expected, the thrust on a concave barrier is greater, and that on a convex barrier less, than the thrust on a corresponding plane barrier

Returning to the case of the circular barrier, it is possible to determine ξ and σ_0 so that the barrier has given camber and angle of attack They are determined from the following equations —

$$\beta=\frac{4(4\xi+1)}{(10\xi+1)}\log_e\left(\frac{2\xi}{1+c}\right),$$

$$\alpha=(\pi/2)-\sigma_0+\frac{3s}{2(10\xi+1)}\log_e\left(\frac{2\xi}{1+c}\right)$$

ξ can here be eliminated, giving rise to an equation in σ_0 —

$$2(1+c)=\left[\frac{3\beta s}{8\{\sigma_0+\alpha-\pi/2\}}-1\right]e^{-\frac{5\beta}{8}+\frac{\sigma_0+\alpha-\pi/2}{\sin\sigma_0}}. \tag{19}$$

In the table (pp 430, 431) we give the angular distance of the centre of pressure from the centre of the barrier It is

$$\epsilon=\tan^{-1}\frac{P_y}{P_x}+\alpha-\pi/2$$

We also give the exact position of the centre of pressure on the chord D by

$$\frac{MD}{AA'}=\frac{1}{2}\,\frac{1-AD/DA'}{1+AD/DA'}.$$

(MD/AA′) and P have been plotted against α, and these graphs illustrate well-known phenomena associated with cambered aerofoils

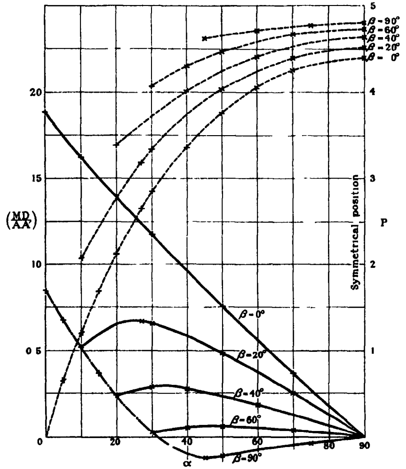

FIG 4

The —— curves are the (MD/AA′) curves
The curves are the P curves

Consider the graph of (MD/AA′) against α In a symmetrical position the centre of pressure is, of course, at the mid-point M. As α decreases we see that for certain barriers the centre of pressure moves up towards A It attains a certain position at which its distance from M is a maximum, and then, as α decreases still further, it returns towards M. This is very marked for small camber A well-known phenomenon is thus explained mathematically

For barriers of comparatively large angular extent, *e g*, β = 90°, the centre

ξ	α_0	A_1	α_1	A_2	α_2	A_3	R	β
	° ′							°
0 5683	75 58	– 0 0881	0 3969	– 0 0388	– 0 9798	– 0 0027	25 39	– 10
0 6055	63 16	– 0 1772	0 7226	– 0 0683	– 1 6753	– 0 0081	13 58	– 20
0 6158	52 7	– 0 2661	0 9621	– 0 0895	– 2 0281	– 0 0131	9 22	– 30
0 6800	37 50	– 0 2681	1 3115	– 0 0648	– 2 0026	– 0 0190	9 91	– 30
0 5837	86 7	0 0883	0 2237	0 0392	– 0 2312	0 0033	26 10	10
0 6842	81 59	0 1789	0 4579	0 0694	– 0 4830	0 0129	14 82	20
0 8637	64 31	0 1817	1 0422	0 0531	– 1 5005	0 0214	17 84	20
0 8933	61 26	0 1820	1 1384	0 0503	– 1 6296	0 0225	18 33	20
1 0649	40 56	0 1839	1 6948	0 0326	– 1 9473	0 0281	21 26	20
1 1772	20 28	0 1849	2 0587	0 0161	– 1 2943	0 0311	23 48	20
1 2163	0	0 1852	2 1852	0	0	0 0320	23 88	20
0 8041	77 36	0 2712	0 7006	0 0910	– 0 7480	0 0283	11 17	30
0 9464	73 0	0 3653	0 9501	0 1046	– 1 0138	0 0486	9 41	40
1 0761	62 31	0 3681	1 2911	0 0876	– 1 5501	0 0569	10 70	40
1 1938	52 3	0 3700	1 5990	0 0715	– 1 8627	0 0629	11 65	40
1 3787	31 11	0 3726	2 0836	0 0416	– 1 7303	0 0706	13 15	40
1 4899	0	0 3739	2 3739	0	0	0 0745	13 93	40
1 3105	63 13	0 5576	1 4588	0 1123	– 1 4968	0 1020	8 28	60
1 4599	52 37	0 5603	1 7746	0 0912	– 1 8385	0 1102	9 02	60
1 5894	42 3	0 5624	2 0475	0 0715	– 1 9179	0 1163	9 69	60
1 7721	21 0	0 5648	2 4319	0 0348	– 1 3035	0 1235	10 63	60
1 8357	0	0 5655	2 5655	0	0	0 1257	10 95	60
2 0984	47 37	0 8522	2 2004	0 0926	– 1 8001	0 2005	8 01	90
2 1854	42 18	0 8533	2 3326	0 0814	– 1 9097	0 2038	8 31	90
2 3383	31 41	0 8551	2 5570	0 0599	– 1 7279	0 2090	8 83	90
2 4810	15 50	0 8566	2 7807	0 0294	– 1 0206	0 2136	9 27	90
2 5315	0	0 8571	2 8571	0	0	0 2151	9 45	90

of pressure seems to move down towards A′ as α decreases, without any upward motion to A at all

η	α	P_x	P_y	P	$\tan^{-1}\frac{P_y}{P_x}$	ϵ	AD/DA′	MD/AA′
	° ′				° ′	° ′		
− 0 0218	12 55	0 0280	0 0995	(0 1493) 0 1034	74 18	2 47	0 2856	0 2778
− 0 0437	24 47	0 0883	0 1532	(0 2477) 0 1768	60 3	5 10	0 3220	0 2564
− 0 0658	35 19	0 1523	0 1661	(0 3123) 0 2253	47 29	7 12	0 3592	0 2357
− 0 0658	50 19	0 2633	0 1860	(0 3767) 0 3224	35 15	4 26	0 5511	0 1447
0 0218	5 0	0 0085	0 1142	(0 0641) 0 1145	85 41	0 41	0 7600	0 0682
0 0437	10 0	0 0320	0 2031	(0 1200) 0 2056	81 3	1 3	0 8119	0 0519
0 0437	27 0	0 1377	0 2869	(0 2628) 0 3182	64 21	1 21	0 7642	0 0668
0 0437	30 0	0 1599	0 2924	(0 2820) 0 3333	61 20	1 20	0 7668	0 0660
0 0437	50 0	0 3055	0 2653	(0 3756) 0 4046	40 58	0 58	0 8253	0 0479
0 0437	70 0	0 4082	0 1527	(0 4246) 0 4358	20 30	0 30	0 9057	0 0247
0 0437	90 0	0 4522	0	(0 4399) 0 4522	0	0	1 0000	0
0 0658	15 0	0 0667	0 2702	(0 1689) 0 2783	76 8	1 8	0 8626	0 0369
0 0882	20 0	0 1101	0 3197	(0 2117) 0 3381	71 0	1 0	0 9085	0 0240
0 0882	30 0	0 1789	0 3253	(0 2820) 0 3713	61 12	1 12	0 8912	0 0288
0 0882	40 0	0 2523	0 3132	(0 3355) 0 4022	51 9	1 9	0 8955	0 0276
0 0882	60 0	0 3791	0 2256	(0 4048) 0 4411	30 46	0 46	0 9291	0 0184
0 0882	90 0	0 4645	0	(0 4399) 0 4645	0	0	1 0000	0
0 1340	30 0	0 2019	0 3521	(0 2820) 0 4059	60 11	0 11	0 9890	0 0028
0 1340	40 0	0 2742	0 3310	(0 3355) 0 4298	50 22	0 22	0 9781	0 0055
0 1340	50 0	0 3398	0 2892	(0 3756) 0 4462	40 24	0 24	0 9761	0 0060
0 1340	70 0	0 4370	0 1613	(0 4246) 0 4658	20 15	0 15	0 9850	0 0038
0 1340	90 0	0 4719	0	(0 4399) 0 4719	0	0	1 0000	0
0 2071	45 0	0 3357	0 3191	(0 3571) 0 4632	43 33	− 1 27	1 0519	− 0 0126
0 2071	50 0	0 3636	0 2920	(0 3756) 0 4663	38 46	− 1 17	1 0458	− 0 0112
0 2071	60 0	0 4113	0 2292	(0 4048) 0 4708	29 8	− 0 52	1 0307	− 0 0076
0 2071	75 0	0 4632	0 1207	(0 4314) 0 4786	14 36	− 0 24	1 0141	− 0 0035
0 2071	90 0	0 4797	0	(0 4399) 0 4797	0	0	1 0000	0

The – – – curve represents the positions of the centres of pressure for the limiting positions of concave barriers It meets $\alpha = 0$ at MD/AA′ = 0 085

Consider the graph of P against α It is at once seen that the effect of camber is much more marked when the angle of attack is small than when the angle of attack is large This has been known since Lilienthal, who found that the thrust could be doubled and even trebled, at small angles of attack, by using a slightly cambered surface instead of a plane surface

The following empirical formula for small cambers demonstrates this clearly —

$$P = \frac{\pi \sin \alpha}{4 + \pi \sin \alpha} \left\{ 1 + \frac{20}{9} \frac{2 + \cos \alpha + 3 \cos^2 \alpha}{\sin \alpha \, (4 + \pi \sin \alpha)} \eta \right\}$$

General Summary

We have found the solution of the general problem of discontinuous fluid motion past circular barriers The results in the symmetrical case agree exactly with those found by Brodetsky The plane barrier is dealt with as a particular case of the preceding theory, and the results obtained in this manner agree very closely with those obtained from the well-known exact solution The approximations obtained by using the first three constants in the Levi-Civita expansion are found to be very good Barriers convex to the stream are fully discussed, while barriers concave to the stream yield interesting results which are verified by experiment, especially the effect of camber on the thrust and on the motion of the centre of pressure

In conclusion, I would like to place on record my sincere thanks and great indebtedness to Prof Brodetsky, who not only suggested this problem to me, but also gave me the benefit of his advice and criticism throughout the whole of the investigations

NOTE

The results obtained by Mr Rosenhead are interesting from several points of view In the first place they demonstrate the power of Levi-Civita's method in the problem of discontinuous fluid motion The accuracy obtained with the use of only a few coefficients A in the solution (1) above is quite remarkable Prof Levi-Civita remarked upon this circumstance when commenting on similar cases of discontinuous fluid motion at the International Congress for Applied Mechanics at Zurich, in September, 1926 We can consider any given barrier as defined by means of the radius of curvature R in terms of the direction of the tangent θ We see that it is a comparatively easy matter to obtain coefficients A_1, A_2, giving R in (5) such a relationship to θ in (3) as is very close indeed to the given relationship Thus some cases of the elliptic strut placed in a stream have been dealt with in this manner with considerable success

In the case of the concave barriers discussed by Mr Rosenhead, the remarkable effects of the camber deserve attention It was to be expected that circular barriers concave to the stream would give increased thrust, but the increases obtained for small camber are strikingly great, especially with small angles of attack A camber of 0 088 times the chord, or just over one-twelfth of the chord, is seen to produce an increase of over 60 per cent with angle of attack 20° Even a camber of one-twenty-third of the chord gives an increase of about 70 per cent at angle of attack 10°

But perhaps the most interesting point about Mr Rosenhead's results is with regard to the centre of pressure The shift of the centre of pressure of an aerofoil is one of its important characteristics The way in which the centre of pressure travels is seen to be dependent upon the camber For cambers above a certain value, round about one-sixth of the chord, the centre of pressure moves backwards as the angle of attack is diminished For smaller cambers the centre of pressure moves forwards as the angle of attack is diminished from 90°, reaches a stationary position, and then moves backwards as the angle of attack is further diminished This becomes more marked the smaller the camber, as is evident from the continuous curves in fig 4 The curve, consisting of dashes and dots, makes it clear that as the camber decreases to zero, the barrier becoming flat, the centre of pressure goes through a more and more marked forward and backward excursion For zero camber, or $\beta = 0°$, the centre of pressure goes forward until the angle of attack is zero, reaching the position $MD/AA' = 0\ 188$ But at the zero angle of attack the centre of pressure seems to jump back to $MD/AA' =$ about 0 085, if we consider the flat plate to be the limiting case of a circularly cambered barrier

It would be wrong to make extravagant claims for the method of discontinuous fluid motion, but Mr Rosenhead's work, as well as the results obtained by the present writer, show that it is perhaps more useful than is often supposed

S B

A Magnetometer for the Measurement of the Earth's Vertical Magnetic Intensity in C G S Measure

By D W Dye, D Sc (of the National Physical Laboratory)

(Communicated by Sir Arthur Schuster, F R S —Received August 18, 1927)

I *Introduction*

The measurement of the vertical component of the earth's magnetic field is a less simple operation than that of the horizontal component

The horizontal field measurements are on a satisfactory basis, whether made by the swinging magnet method, or by the more recently developed electric magnetometers, in which known magnetic fields may be provided by means of known currents flowing through coils of known dimensions

In the horizontal intensity magnetometers an indicating system is suspended or supported so that it can turn about a truly vertical axis In a vertical intensity instrument, the corresponding suspension of an indicating device about a truly horizontal axis is by no means so simple

At present, therefore, vertical intensity measurements are deduced indirectly from horizontal intensity measurements combined with measurements of the angle of dip This latter quantity cannot be measured with very great precision, and the accuracy of the finally deduced vertical intensity becomes less as the angle of dip becomes greater towards the magnetic poles

The advantages of a direct method of measuring vertical intensity need no stressing, quite recently a novel absolute vertical intensity magnetometer has been developed by D La Cour in Denmark ('Terrestrial Magnetism,' vol 31, p 153, 1926)

In this instrument a large, flat circular coil is turned about a horizontal axis from one position with its plane horizontal to the other similar position displaced 180° from the first The flux linkage so produced is balanced by the flux linkage with the secondary winding of a mutual inductance when a known current change is made in the primary winding

From the published information on the instrument, the method appears to have considerable value and the accuracy attainable will doubtless be improved by further development

The vertical intensity magnetometer forming the subject of the present paper makes use of the principle of balancing the vertical component of the earth's field by a vertical field produced by a steady current passing through a Helmholtz coil system Some possibilities in this direction have been indicated by F E Smith in his description of the horizontal force magnetometer developed at the National Physical Laboratory (F E Smith, 'Phil Trans,' A, vol 223), along the principle first described by A Schuster ('Terrestrial Magnetism,' 1914) This principle applied to the horizontal intensity measurements was to orient the Helmholtz coil about a vertical axis and to observe the angle at which $H = F \cos \alpha$, where F is the actual field produced at the centre of the coil and α is the angle which its horizontal axis makes with the magnetic meridian

This principle could have been applied to a vertical force magnetometer, but the difficulties of determining when the resultant small field is truly horizontal are great The direct annulment of the earth's vertical field appears to be a more satisfactory principle

The principle of the magnetometer is carried into effect by setting up the Helmholtz coil system with its axis truly vertical The measurement consists in adjusting and measuring the current through the coil system at that exact value necessary to produce a field equal and opposite to the earth's vertical component

One of the most important features of such a method is the means whereby the exact annulment is observed

There are a number of possibilities, for example —

(*a*) A small exploring coil may be rotated about a horizontal axis which must be directed very precisely along the magnetic meridian

The electromotive force induced in such a coil will become zero, at every instant, when the vertical component of the resultant magnetic field is zero, since it is then directed along the meridian and is parallel with the axis of rotation of the exploring coil

The condition of zero-induced electromotive force may be observed either on a direct current galvanometer, by the help of a commutator on the coil spindle, or it may be observed on a vibration galvanometer, tuned to a frequency resonant to the rate of revolution of the coil

(*b*) A small indicating magnet might be suspended about a horizontal axis with its magnetic axis horizontal as in a vertical force magnetograph The difficulties of using such a system are great, and the uncertainties regarding the conditions of balance consequent upon a gravity torque cannot easily be reduced to small quantities (*c*) A flat coil can be pivoted or suspended so that its plane is vertical and so that it can deflect about a horizontal axis If a steady current is sent through the coil, a deflection will result The deflection will become zero when the vertical field is zero

(*d*) A very light coil can be suspended so that it may vibrate about a horizontal axis in a similar manner to a coil-type vibration galvanometer If such a coil is supplied with alternating current of the same frequency as that of its free resonant vibration, it is very sensitive to a magnetic field in a suitable direction

It is probable that any of these methods could be made satisfactory from the point of view of sensitivity, convenience and accuracy, and some of them have been tried

The method actually developed finally has been that outlined under (*d*), using a vibrating coil

The reasons for choosing this method are—(1) No revolving parts are required in the apparatus in the magnetic field provided by the Helmholtz system, and (2) no delicate pivoting or suspension of the detecting device is necessary The control forces required to give the vibrating coil a convenient resonant vibration frequency are relatively large, so that its statical position is located with great certainty and constancy

II *Principle of the Magnetometer*

The principle of the magnetometer is therefore carried into effect as follows — The Helmholtz coil system is set up with its axis truly vertical At the centre of the system a small, flat and very light coil is suspended about an axis of vibration The plane of the coil is vertical, and its axis of vibration is horizontal The coil is mounted in a frame in such a manner that these two conditions may be very nearly satisfied

A relatively large alternating current at the frequency of resonant vibration is sent through the vibrating coil Under these conditions a large vibration results from the inter-action between the alternating current and the earth's vertical magnetic field This vibration is reduced to zero when the applied vertical field exactly annuls the earth's vertical component The determination of V consists in observing the current required to give an exact condition of rest or balance on the vibrating coil This current multiplied by the calculated or otherwise determined constant of the Helmholtz coil gives the value of V in C G S measure corresponding to that reading

III *Simple Theory of the Vibration Coil Detector*

The vibratory coil cannot be assumed to occupy the ideal position, in which its plane is truly vertical and its axis of vibration truly horizontal

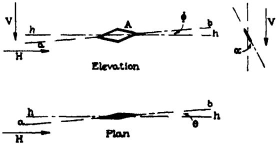

Fig 1

Let the vibrating coil A (fig 1) be suspended about an axis of vibration *ab* and assume that the trace of this axis on the horizontal plane makes an angle θ with the magnetic meridian *hh*, the trace of the axis on the vertical plane makes a small angle ϕ with the horizontal plane Finally, let the plane of the coil make a small angle α with the vertical plane containing the axis of vibration

It is convenient to consider the resolution of the vertical and horizontal components of the earth's magnetic field into components in the directions of the three principal axes of the vibrating coil These axes are

(1) perpendicular to the plane of the coil,
(2) along the axis of vibration of the coil,
(3) in the plane of the coil and perpendicular to its vibration axis

Of these three components, only (3) is effective in producing a vibratory force on the coil when carrying the alternating current

Resolving V and H into the plane of the coil and perpendicular to the axis of vibration, the resultant field which is effective in producing a vibrating force becomes

$$V \cos \phi \cos \alpha + H \sin \phi \cos \theta \cos \alpha + H \sin \theta \sin \alpha \tag{1}$$

This is the field which is reduced to zero by the field applied by current through the Helmholtz coil system

The component of the applied vertical field U parallel to the resultant given by (1) is

$$U \cos \phi \cos \alpha, \tag{2}$$

where U is the vertical field produced by the current in the Helmholtz coil

When a condition of balance is obtained, the earth's vertical component is given by equating (1) and (2), whence

$$V = U - H\left(\frac{\sin\phi\cos\theta\cos\alpha + \sin\theta\sin\alpha}{\cos\phi\cos\alpha}\right) \tag{3}$$

$$= U - H\left(\tan\phi\cos\theta + \frac{\sin\theta\tan\alpha}{\cos\phi}\right)$$

It is seen, therefore, that V cannot be determined from a single observation unless the small angles α and ϕ and the angle θ are known It cannot be presumed that these angles may be known, but, fortunately, the correction term due to H can be entirely eliminated by orientating the vibrating coil and its frame about a vertical axis, through an angle of 180° The effect is exactly equivalent to reversing the sign of H

If we observe two values U_1 and U_2 of the applied vertical field required for balance in the two respective positions θ_1 and θ_2, where $\theta_2 = \theta_1 + \pi$, the mean value will give V exactly

So that $V = \frac{1}{2}(U_1 + U_2)$, and

$$H(\tan\phi\cos\theta + \sin\theta\tan\alpha/\cos\phi) = \tfrac{1}{2}(U_1 - U_2)$$

By means of levelling screws on the frame carrying the vibrating coil, an adjustment of the small angles ϕ and α can be made By successive observations in the two positions giving U_1 and U_2 we can make $U_1 - U_2$ zero The condition satisfied will then be

$$\tan\phi\cos\theta = -\sin\theta\tan\alpha/\cos\phi \tag{5}$$

It is seen, therefore, that a single adjustment of this kind cannot ensure ϕ and α being zero or of small importance for a small change in either of them

It has been shown that the correction term exactly cancels out by orientation of the vibrating coil axis through 180°, but it is not desirable that accuracy of observation by the magnetometer should depend upon an exact orientation of the vibrating coil axis

In practice ϕ and α may be considered always small, but θ may have any value we choose An examination of the correction term due to H as given by (4) shows that, when θ is either small, or nearly equal to π, *i e*, when the axis of vibration lies nearly along the meridian, the vibratory force due to H is mainly dependent upon the angle ϕ, which is the angle of inclination of the vibration axis to the horizontal plane It is hardly dependent at all upon the angle α (between the plane of the vibrating coil and the vertical plane) Accordingly, when the vibration axis is nearly parallel to H, an adjustment of ϕ until $U_1 = U_2$ must result in causing ϕ to be very small indeed

Again, suppose two values U_3 and U_4 are observed, with the axis of the vibrating coil in the two positions at right angles to the magnetic meridian ($\theta = 1/2\,\pi$ and $3/2\,\pi$), the vibrating force due to H will be mainly on account of the small departure from verticality of the plane of the vibrating coil and hardly at all upon the inclination of its vibration axis By successive observations of U_3 and U_4 and adjustment of the angle α by means of the levelling screws on the coil mounting, the angle α can be reduced to a second order quantity One or two alternate adjustments of ϕ and α by successive observations of U_1, U_2 and U_3, U_4 will result in the reduction of ϕ and α to negligibly small angles When this adjustment has been obtained, the balance is undisturbed for all values of θ The vibration axis can be in any azimuth and the same value of U will give the balance

In the actual use of the instrument the observations are taken with the axis of the vibrating coil along the meridian (θ small) In the nature of its construction the vibrating coil is liable to small variations in the angle α, which its plane makes with the vertical, but the angle ϕ is not apt to change much, since the suspensions are under considerable tension and so define the axis of vibration with precision and constancy When θ is nearly 0 or π, small variations in α do not affect the balance

Errors of the Method —When making the observations there will be a small uncertainty in the orientation of the vibration axis, so that if θ is 0 in one position it will be $\pi + \Delta\theta$ in the second position instead of π The mean of the two readings U_1 and U_2 will then give a value for V which is in error by the amount

$$H\alpha\Delta\theta$$

The procedure in the adjustments outlined above will enable the angle α to be reduced to 1/1000 radian with certainty In order that the error $H\alpha\Delta\theta/V$ may not be greater than one part in a hundred thousand it will only be necessary to set θ to an accuracy equivalent to V/100 H Actually θ can be set to an accuracy at least as high as 1/1000 radian, so that except in regions near the magnetic equator, where V/H will be small, there will not be any appreciable error due to $\Delta\theta$

Two other sources of error arise in the adjustment of the instrument, due (*a*) to errors in setting the axis of orientation truly vertical and (*b*) in setting the axis of the Helmholtz coil parallel to this axis These errors are dealt with in a short appendix, from which it will be seen that a small angular error ψ between the axis of orientation and the vertical will introduce an error into the measurement of V, which at its maximum is equal to H ψ It is seen, therefore, that this error is in the first order of small quantities The axis of orientation must therefore be set vertical with great precision The instrument is provided with very sensitive levels, and the turntable, which virtually defines the vertical axis of orientation, revolves on a ball race of large diameter A careful test showed that the departure from verticality of the axis was certainly not greater than 1 part in 50,000 and was probably less than half this amount

IV *Description of the Magnetometer.*

(*a*) *Helmholtz Coil System* —This system comprises the same marble cylinder which forms the essential part of the horizontal force magnetometer described very fully by F E Smith in the paper previously referred to For full details of the measurements of the diameter and pitch of the windings, etc , the reader is referred to that paper The variations of the radial and axial fields of the coil over a region near its centre have also been fully investigated and need not be discussed here It will suffice to say that within a sphere of 2 cm diameter the maximum difference in axial intensity from that at the centre of the system is less than 4 parts in 10^6

The calculated constant of the coil system is

$$U_t = 3\ 59595\, i\,(1 - 7\ 9 \times 10^{-6}[t - 17]),$$

where U_t is the axial magnetic force in C G S units when the cylinder is at the temperature t° C

i is the current in absolute measure

The constant $+ 7\ 9 \times 10^{-6}$ is the measured thermal expansion coefficient of the marble in length and diameter The constant 3 59595 is believed to be accurate to 1 part in 10^5 from the measured dimensions This value refers to the dimensions measured in 1921 These may have slightly altered since then, but the present observations are on the assumption of unchanged dimensions

The original base and turntable have been used in the present magnetometer, but in order to support the cylinder with its axis vertical, a non-magnetic bronze platform has been made to fit, on its under side, the existing cradles on the turntable, and to provide on its upper surface three levelling and three centering screws for the support and adjustment to verticality of the marble cylinder

The general appearance of the magnetometer will be seen by reference to the photograph, fig 2, in which the triangular stiff platform can be seen. The turntable is provided with an accurately engraved angular scale, whereby it may be set in azimuth at any desired angle to an accuracy of a few seconds of arc

The levels on the base are very sensitive and enable the axis of the turntable to be set vertical to an accuracy of about 1 part in 100,000

Within the cylinder is supported a circular bronze table upon a tubular pillar fixed to the turntable Upon this table is mounted the vibration detector coil This can be seen in the photograph, whereby its small size may be judged The detecting coil and its mounting is shown in more detail in fig 3. It consists essentially of the very light, flat diamond-shaped coil C strained between phosphor-bronze suspensions, which are carried in a frame provided with means for adjusting the tension for tuning purposes The coil in its frame is an

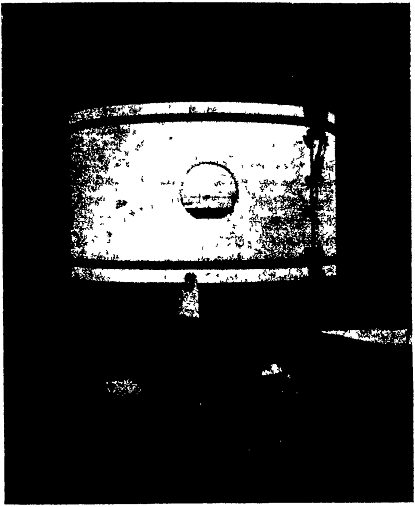

FIG 2

independent unit, so that replacenent is simple in case of accidental breakage of the suspensions The frame and coil are mounted on a three-armed base,

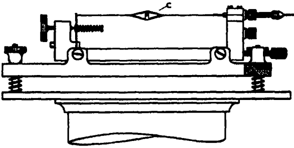

FIG 3

which registers on three bolts projecting up from the table By means of bronze springs underneath and spherical seating nuts above, the adjustments to the vibration coil are made, whereby its axis of vibration is made horizontal and its plane is made vertical The clamping arrangements also enable the coil to be adjusted so that its centre is approximately at the centre of the Helmholtz system A sheet copper cover with hole facing the small mirror on the coil serves to protect it from draughts and other disturbances, which otherwise cause the light spot to wander up and down on the scale

There is considerable latitude in the design of the vibration coil, but that used in the experiments had 100 turns of enamelled wire 0 05 mm diameter Its length was about 2 cm and its width about 1 cm The mass of the coil and mirror was about 150 mgm The vibration frequency can be chosen to have any suitable value between wide limits by using the appropriate control torque given by the suspensions Frequencies between about 100 and 5 cycles per second were tried In all sizes of vibration coil used, greater sensitivity was obtained the lower the resonant frequency chosen. But at the lowest frequencies the time taken by the vibration coil to come to rest was so long that the observations became very tedious A frequency of 15 cycles per second was found to be a good compromise The damping decrement of the vibration coil was such that with an initial vibration of the light spot of 1 cm on the scale, a time of about 20 seconds was required for the spot to come sensibly to rest

The sensitivity is such that a vibration of about 25 mm on a scale at 2 metres distance results from the application of a field of 40 γ The condition of rest of the vibrating spot corresponds to a residual vibration less than 0 1 mm, since the eye is very susceptible to a vibration at the rate of about 15 per second

The coil is small enough in size to ensure that the mean field of the Helmholtz system over the region occupied by it does not differ from that on the axis by more than 2 parts in 10^6

(*b*) ***Auxiliary Apparatus*** —The auxiliary apparatus necessary to the magnetometer, in addition to galvanometer lamps, scales and batteries, are—

(1) a small source of alternating current at a frequency of about 15 cycles per second,

(2) means of measuring and adjusting the Helmholtz coil current to a high degree of accuracy

(1) Various sources of alternating current were tried These included a self-maintained tuning fork, a valve oscillator, and an alternator Of these only the alternator proved satisfactory The reason of this was that, with the other sources, a perfect balance was unobtainable, even when the magnetic field had been exactly compensated A residual vibration of 15 or 20 mm resulted when either a tuning fork or valve oscillator was used as source This was puzzling at first, but was ultimately found to be due to heating effects of the current The vibration coil is very small in surface, and, in order to obtain sensitivity, it is necessary to send a relatively large current through it (70 milliamperes) The energy dissipated in the coil is about 0 2 watt Owing to an inevitable dissymmetry of the coil, the alternate heating and cooling of each cycle sets up a small vibratory force, which, of course, is quite independent of the magnetic field in which the coil is supported With a symmetrical wave form, however, the heating and cooling should have a frequency twice that of the source, and hence at the most should produce only a minute forced vibration at the double frequency, since the vibration coil is completely out of tune to this frequency The case is, on the other hand, otherwise if harmonics of frequency $2n$ are present An unsymmetrical wave form results so that the heating during one half-wave is not equal to that during the next half-wave A vibrative force at the resonant frequency will result and will cause a residual vibration which cannot be reduced to zero by any adjustment of the magnetic field. Various kinds of circuits were tried, but no absolutely perfect balance could be obtained with any other source than an alternator With almost any kind of alternator, however, a perfect balance can be obtained The actual alternator used was a small machine used as a rotary converter run from a 6-volt battery With the ball bearings and special brushes supplied the current taken was only 0 4 amp

It was provided with a governor of the frictional gramophone type, in order that the speed might keep sufficiently constant to remain sensibly synchronous with the frequency of the vibrating coil At the normal speed the root mean square voltage was about 4 This voltage provided 70 milliamperes in the vibrating coil The speed continually varied slightly in use, but this did not matter in practice, since the condition of a slight want of balance on the vibration coil always showed itself when the observation was continued for one minute The small alternator behaved very satisfactorily throughout the experiments In general, it was only necessary to adjust the speed once or twice during a run of about an hour and a half In some cases the whole run was made without any readjustment

(2) *Measurement of Current*—The current measurement was made in some cases by a straightforward potentiometer method using a standard resistance coil of 1 ohm resistance This method is very flexible, as it will allow measurements in any part of the world with the one set up, but requires the potentiometer and necessitates repeated adjustment of the potentiometer current during a run In the later runs the independent potentiometer was dispensed with and was replaced by a direct potentiometer method, whereby part of the potential difference on the resistance combination was balanced against a standard cell The most convenient arrangement for this is as shown in fig 6 in Appendix II, in which the corrections and calibration of the current-measuring system are discussed

In all cases where observations are made at a fixed station, the direct potentiometer method has much to recommend it It can readily be adapted to give direct readings of the change in V over a range of a few parts in a thousand

On an instrument intended to be used at places widely separated, where V might have values ranging from 0 to 0 6 C G S units, a separate potentiometer system would be much more flexible but not quite so accurate

V *General Arrangement of the Apparatus*

The general layout of the magnetometer and its auxiliaries is as shown in fig 4 The current-measuring system shown in the figure was that actually used, but the scheme suggested in Appendix II is preferable and will be used on future occasions

The Helmholtz coil system CC is set up about the vertical axis *ab* Its windings are supplied with current from a 20-volt battery V_1 Rough adjustment is provided by a three-dial rheostat P with good contacts and carrying capacity for the current of about 1 2 amp The current-measuring arrangements actually used consisted of standard resistance combination R_1 of about 0·8 ohm in series with standard resistance R_2 of 0 01 ohm R_2 was shunted by a slide wire S of about 0·76 ohm, in series with which was a diluting resistance S_1 of 1 ohm to increase the openness of the scale of S in terms of change of current.

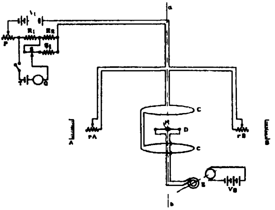

FIG 4

This combination enables a potential difference of 1·0183 volt to be obtained with potential contact at the middle of S when the appropriate current is passed through the Helmholtz coils and the resistance combination. The standard cell T, galvanometer and tapping key enabled the potential difference observed to be adjusted to exact equality and opposition to that of the standard cell.

From a knowledge of the exact values of R_1, R_2, S and S_1, the current corresponding to any reading on the slide wire was calculated. The rest of the current circuit consists of the fine adjustment resistances *r*A, *r*B, each in the form of a mercury channel and short-circuiting slider. These resistances are placed respectively near the vertical scales A and B, upon which the vibration of the light spot reflected from the vibration coil is received.

The line joining AB is approximately at right angles to the meridian, so that the axis of the vibration coil D lies approximately along the meridian when the light spot is on A or B.

The vibration coil is mounted as at D and carries a very small mirror M. The coil is connected to the slip rings of the little motor converter, shown diagrammatically at E. The direct-current motor end is connected to a 6-volt battery V_2.

In addition to the scales A, B, and the galvanometer lamps near them (not shown), there are two other lamps and scales along a line perpendicular to the plane of the diagram through the centre of the system. These latter are used at the commencement of a series of observations for the purpose of adjusting the plane of the vibration coil to its electrically vertical position The actual observations are taken only on scales A and B alternately

In the actual experiments made at the laboratory the direct current measuring apparatus and battery V_1 were, for convenience, in the main building, whilst the magnetometer itself was in a special hut removed from local magnetic disturbances arising within the laboratory

The motor converter and its battery V_2 were set up just outside the hut at a distance of about 4 metres from the magnetometer It was so arranged that the vibration of the light spot was visible through the doorway when adjusting the governor and speed of the converter to that corresponding to resonance of the vibration coil

A test was made to determine the stray field, produced by the permanent magnets of the motor converter, at the centre of the magnetometer With the position of the converter such that the stray field was vertical, it was found to be equal to about 5 γ at 4 metres distance By turning the converter so that the stray field is horizontal, therefore, the error becomes quite negligible

A vertical force magnetograph for recording continuously the changes in V during a series of observations on the magnetometer was constructed and set up

The instrument consisted of a cobalt-steel magnet 5 mm diameter and 20 mm long The magnet was mounted transversely on a brass spindle provided with adjustable gravity control weights at right angles to one another and to the spindle Thin phosphor-bronze suspensions attached one to each end of the spindle, and lightly strained in line to supports on a base, formed the horizontal axis of suspension

A damping vane between copper plates served to render the system just aperiodic The gravity control was adjusted to be nearly equal and opposite to that due to the vertical component acting on the magnet The control force was finally adjusted by means of a small magnet which provided a weak horizontal field directed along the magnetograph magnet axis

The image of a Nernst filament formed by reflection from a mirror on the magnet fell on a narrow horizontal slit, having first passed through a prism to turn the movement of the reflected ray into a horizontal plane A long band of photographic paper slowly revolving behind the slit recorded the variations in V.

The sensitivity was such that a displacement of about 1 mm was produced by a field change of 1 γ

The photographic paper moved at the rate of about 40 cm per hour

The effect of the magnetograph magnet upon the magnetometer was quite negligible at the distance of 4 metres which separated them

VI *Experimental Observations with the Magnetometer*

(*a*) *Adjustments* —Having made a few preliminary runs in order to gain experience in the use of the instrument, it was set up in the magnetic hut in the laboratory grounds

It was soon seen both by the magnetometer and by the magnetograph record that accurate observations were impossible during the daytime owing to train and tram disturbances Continuous, rapid, and very large excursions (up to 100 γ magnitude) occurred all the time The accurate runs were therefore made at night during the hours of 1 30 and 4 0 a m

The turntable was first levelled as accurately as possible, using the sensitive levels on it The resulting position of the axis of turning was vertical to a probable accuracy of 1/50,000 radian

The marble cylinder was then centred and levelled on its platform by the aid of a dial gauge which could indicate an eccentricity of 0 01 mm The gauge was held in a rigid clamp so that its foot pressed against the outer cylindrical surface of the cylinder By alternate observations at the lower end of the cylinder and adjustment of the centring screws, followed by observations at the upper end and adjustment of the levelling screws, the cylinder was brought into a truly concentric position with respect to the axis of turning

The galvanometer lamps and scales were then adjusted so that the image of the cross wires on the lamp lens formed after reflection from the small mirror on the vibration coil (at rest) fell on definite lines on the scales, thus locating the two positions of the vibration coil axis approximately along the magnetic meridian The other two lamps and scales were set up and adjusted to correspond to positions of the axis of D at right angles to the meridian The current having been switched on and having become steady, the next adjustments made were those of the vibration coil The light spot was brought to position on scale A and the mercury rheostat *r*A was adjusted until balance was obtained. The magnetometer was then oriented round until the light spot was on scale B A small vibration of the light spot resulted. By temporary adjustment of *r*B for balance, an estimate of the difference in current for balance in the A and B positions was obtained The rheostat *r*B was then placed midway between its new and old positions The vibration, now reduced to about half its original value, was reduced to zero by adjustment of the axis of vibration of the coil by means of the appropriate levelling screw on D

A similar procedure was carried through with the vibration coil axis in the two E W directions, except that adjustment to equality was now made by adjustment of the plane of the vibrating coil

After one or two repetitions of each of the above adjustments, a condition was arrived at such that for any of the four positions of orientation of the vibrating coil axis the current for balance was the same to within 2 or 3 parts in 10,000

These adjustments satisfactorily completed, the actual observations constituting a run were made as follows —

(*b*) *Observations* —(i) A calibration of the magnetograph was made by means of a known small current passed through a two-turn coil in a horizontal plane centrally disposed around the small suspended magnet constituting the essential part of the magnetograph This current was such that a change of 25 γ was made in the vertical field The sensitivity of the magnetograph was such that a deflection of its recording light spot of about 30 mm resulted The calibrating field was applied in both positive and negative directions

(ii) The magnetometer was brought into the A position and balance of the light spot obtained by adjustment of rA The light spot had crossed lines on it and was observed with a lens It was found possible to obtain a balance of great sharpness The vibration at 15 cycles per second is peculiarly susceptible to the eye, and the condition of rest, when obtained, corresponded to a vibration less than 0 1 mm amplitude Under the steady conditions appertaining to the night observations and on a magnetically quiet occasion, the balance remained sensibly perfect for a minute or more at a time

(iii) When the balance had been obtained and was seen to be real and steady, a signal by means of a tapping key and lamp was given to an observer stationed at the current-measuring apparatus He, forthwith, adjusted the slider on S until a balance on galvanometer G was obtained The reading on S was noted and the time at which the signalling flash occurred was also entered

Simultaneously with the flashing signal to the observer a locating signal was given to the recording magnetograph This signal took the simple form of lighting a lamp, at a distance of about 10 feet, in front of the narrow slit in the box containing the photographic paper, upon which the magnetograph record was in course of exposure This signal gave a fine line on the record and identified on it the instant at which the magnetometer observation was made

(iv) The magnetometer was turned to the B position and the procedure as outlined under (*b*) and (*c*) was carried out, the adjustment of current being made by means of rB

A complete series of observations alternately on A and B was thus made throughout a period of about one and a half hours. During such a period between 30 to 40 observations were made.

At a few intervals, readings of the temperature of the marble cylinder of the magnetometer were made and of the standard resistance coils R_1, R_2. The standard cell was in an oil bath in a vault and remained absolutely steady throughout a run

During the run observations were made to see that the rotary converter was remaining in tune with the vibrating coil In order to ascertain this, one of the rheostats rA or rB was offset so as to produce a change in current sufficient to give several centimetres vibration of the light spot It was then seen whether this vibration was as large as it should be If it was small, a readjustment of speed was made In general the small unavoidable variations of speed were such that the vibrating coil continually went into and out of tune, so that the vibration varied from a maximum to about one-half of this value During any period of one minute, however, the light spot nearly always reached an amplitude nearly equal to its maximum amplitude It was only occasionally, therefore, that an observation was in error owing to insensitivity resulting from the vibrating coil being out of tune

In the course of every observation a small displacement equivalent to about 1 part in 10^4 in current was made, and a reading was not accepted unless the resulting small vibration was visible

At the conclusion of a series of observations, a second calibration of the magnetograph was made

The observations when obtained were dealt with as follows —From a knowledge of R_1, R_2, S and S_1, a factor was determined for converting differences from an arbitrarily chosen reading on S into differences in γ units from the base line value corresponding to the arbitrary reading

These values of γ differences were entered opposite the corresponding S readings for the alternate A and B observations numbered in sequence 1, 2, 3, etc

The values for the mean of each pair of observations, 1 and 2, 2 and 3, 3 and 4, etc., were then taken These are the final V differences corresponding to the mean value of B at the instants 1 and 2, 2 and 3, etc

The displacements from an arbitrary base line on the magnetograph record were next read off the record at the instants 1, 2, 3, etc These, converted to γ differences, were then treated similarly to the magnetometer readings so as to give the mean values for the readings 1 and 2, 2 and 3, etc

Finally, the differences between the magnetograph and the magnetometer deduced values of "γ difference" were taken These latter should, of course, under ideal conditions, be quite constant The variations in these differences give a measure of the uncertainty in any reading resulting from all the uncertainties in the chain of observations connecting them

The final results deduced were the differences between the mean value of the differences of all the comparison readings and the individual difference readings The mean variation from the mean given at the bottom of the last column is a measure of the probable amount by which any observation is different from the mean of a number of such observations This latter figure is therefore a rough measure of the probable inaccuracy associated with the process of observation. It must not be confused, of course, with inaccuracies in the absolute measurement of the whole vertical field associated with constant errors in the current measurement and in the constants and the set-up of the magnetometer The results of a typical series of observations just as taken are given in the Table following

Columns (1) and (2) give respectively the number and instant of the observation

Colunns (3) and (4) give the slide-wire readings for the A and B positions alternatively taken from an arbitrary zero position near the centre of its scale.

Column (5) gives the means between the successive pairs, and column (6) gives the corresponding values in γ units

Column (7) gives the deduced mean values of γ differences, from an arbitrary base line, as read off from the magnetograph record

Column (8) gives the differences between corresponding readings in columns (6) and (7) in γ units

Column (9) gives the differences between the mean of all the values in column (8) and each individual reading The mean value of the differences shown in column (9) is 0 85 γ, and the maximum positive and negative values are 2 4 γ and 2 7 γ respectively

The values of the various items by which the base-line value is calculated corresponding to the zero on the slide were

$R_1 = 1\ 00036$ int ohm

$R_2 +$ leads $= 5\ 5071$ int ohm

$x = 0\ 37$ ohm

$S + S_1 = 1\ 76$ ohm

Voltage of standard cell at 15° C $= 1{\cdot}01842$ int volt

Helmholtz coil constant at 16° C $= 3{\cdot}59598$

Calculated base-line value $V_0 = 4315_2\ \gamma$ units

Table

(1) Obs.	(2) G M.T	(3) Slide Wire A	(4) Slide Wire B	(5) Means successive pairs	(6) γ units	(7) Magneto graph means, γ	(8) Differences (6) − (7)	(9) Differences from mean of (8) γ units
1	1-29-15	−0 025		−0 037	10 7	−13 8	24 5	−2 7
2	1-31-20		−0 050	−0 041	11 9	−14 2	26 1	−1 1
3	33-45	−0 032		−0 040	11 6	−14 5	26 1	−1 1
4	26-50		−0 048	−0 043	12 5	−14 7	27 2	0
5	41-15	−0 038		−0 043	12 5	−15 1	27 6	+0 4
6	42-40		−0 049	−0 042	12 2	−15 2	27 4	+0 2
7	48-20	−0 035		−0 043	12 5	−15 1	27 6	+0 4
8	50-38		−0 052	−0 046	13 3	−15 2	28 5	+1 3
9	53-32	− 0 041		−0 046	13 3	−15 2	28 5	+1 3
10	55-01		−0 051	−0 041	11 9	−15 3	27 2	0
11	57-28	−0 031		−0 043	12 5	−15 5	28 0	+0 8
12	59-43		−0 055	−0 042	12 2	−15 6	27 8	+0 6
13	2-01-35	−0 030		−0 039	11 3	−15 8	27 1	−0 1
14	05-35		−0 048	−0 041	11 9	−16 0	27 9	+0 7
15	07-43	−0 034		−0 042	12 2	−16 5	28 7	+1 5
16	09-20		−0 051	−0 042	12 2	−16 3	28 5	+1 0
17	14-08	−0 042		−0 044	12 7	−15 9	28 6	+1 4
18	15-30		−0 046	−0 039	11 3	−15 7	27 0	−0 2
19	17-35	−0 032		−0 039	11 3	−15 7	27 0	−0 2
20	19-42		−0 045	−0 039	11 3	− 15 7	27 0	−0 2
21	22-32	−0 031		−0 038	11 0	−15 9	26 9	−0 3
22	23-46		−0 045	−0 038	11 0	- 16 0	27 0	−0 2
23	26-00	−0 026		−0 036	10 4	−16 4	26 8	−0 4
24	27-15		−0 035	−0 032	9 3	−16 4	25 7	−1 5
25	29-43	−0 035		−0 035	10 1	−16 3	26 4	−0 8
26	31-05		−0 040	−0 037	10 7	−16 3	27 0	−0 2
27	32-22	−0 025		−0 033	9 6	−16 1	25 7	−1 5
28	34-13		−0 038	−0 032	9 3	−16 0	25 3	−1 9
29	36-40	−0 032		−0 035	10 1	−16 5	26 6	−0 6
30	37-53		−0 056	−0 044	12 7	−16 9	29 6	+2 4
31	39-32	−0 016		- 0 036	10 4	−17 3	27 7	+0 5
						Mean	27 2	
						Mean variation from mean 0 85 γ		

In the present investigation, however, no particular importance is to be attached to this base-line value, since the aim has been rather to prove the system than to obtain results by the magnetometer

It would seem, therefore, that, *as far as observational accuracy is concerned*, any single observation has a probable error not greater than 1 γ and the maximum probable error is about 2 5 γ From the same standpoint, the probable error in base-line value as given by the mean of 30 observations would be about 0 3 γ, or less than one part in a hundred thousand in V, in England

These conclusions are borne out by a number of runs made during a period of about three weeks On many of these occasions the temperature of the magnetograph was not constant, and it became necessary to apply an estimated correction for this drift in the magnetograph trace The mean of the various values of "mean variation from the mean" was about 0 8 γ, and the maximum value was 1 2 γ

Under steady magnetic conditions, therefore, it may be considered experimentally proved that the mean base-line value given by 30 observations taken during an hour would not be uncertain, due to observational errors, by more than 0 3 γ

The variations of temperature, and the uncertainties associated with the magnetograph from one day to another, were such that it was not possible to test the constancy of base-line values given by the magnetometer

It is hoped to transfer the instrument to the Abinger Magnetic Observatory, and after setting it up there to carry out a series of observations of V with a view to proving the accuracy of determination of a base line

VII *Probable Errors*

The errors associated with a determination of V may be classified as due to (*a*) the method, (*b*) the measurements, and (*c*) the magnetometer The errors associated with the method are as follows —

(*a*) The vibrating coil may be slightly magnetic but its mass is so small that the change in the resultant field due to hysteresis, etc, is probably quite negligible A residual vibratory torque due to heating and cooling of the coil and its suspensions may still be present even with the symmetrical wave form given by the alternator If this torque were in phase with the main torque, a balance would still be obtainable by the appropriate resultant very small vertical field which would automatically be applied to obtain it A reversal of the connections to the vibrating coil would reverse the sign of the main torque but would not reverse a torque due to heating A different current would then be needed for balance An experiment showed no measurable difference due to reversal of the vibrating coil connections It is, moreover, exceedingly unlikely that a vibrating torque due to heating and cooling would not have a component in quadrature with the main torque. In such a case a perfect balance would be unobtainable by simple adjustment of the Helmholtz coil current Actually the balance when obtained was very sharp.

A further experiment tried in order to see the effect of an asymmetrical wave form was tried This consisted in superposing a small steady current upon the alternating current flowing in the detector coil The effect of this was apparent, as no perfect balance could be obtained, thus proving that the thermally produced fundamental frequency torque had a component in quadrature with the main torque The effect was small and the setting of the Helmholtz current for approximate balance appeared to be unaffected by reversal of the connections on the vibrating coil

The errors associated with the location of the vibrating coil have been discussed, and it has been shown that such errors are proportional to H and therefore increase towards the magnetic equator By the method of observing in two positions of the vibrating coil axis 180° apart, it has been shown that the error may be reduced to less than 1 γ when $H = 0\ 5$ C G S unit

There is a possible source of small error in the inevitable lack of perfect geometrical symmetry of the vibrating coil If the suspensions are not strictly coincident with the axis of vibration, a small torque will result, since they are considerably displaced from the centre of the Helmholtz coil and are therefore not in a zero vertical magnetic field when this condition is obtained at the centre Such error must be very small, since there are about 400 cm of wire in the coil at an effective radius of about 3 mm from the axis, whereas the suspension will almost certainly be within 0 3 mm of the effective axis of vibration and has an effective length of about 3 cm only

(*b*) The errors associated with the measurements are those due to inaccuracy of observation and uncertainty in measurement of the current in the Helmholtz coil The sensitivity is such that variations in setting the current may amount to the equivalent of 2 5 γ in a single observation, with a probable variation of 1 γ The mean of a series of 20 observations would have a probable error of less than 0 5 γ, due to limitation of sensitivity on the vibration coil

The error associated with observing the current will include a small drift which may occur between the instant of the magnetometer observation and the observation of current on the potentiometer This error is likely to be less than one part in a hundred thousand The error in the finally deduced current might be as great as 1 part in 10^5, but the possible error in the unit in which the current is measured is 2 or 3 parts in 10^5, whether this unit is derived from standard resistances and a standard cell, or, as at the laboratory, from an absolute unit given by the current balance

(*c*) The errors associated with the magnetometer are those due to errors in setting up and errors in its constant

The former error has been discussed and was seen to be probably not greater than $H/10^5V$, or in γ units $H/10^5$

The error associated with the dimensions of the coil can only be estimated by a repetition of the measurements of length and diameter Previous experience has shown that slow changes in the dimensions of marble cylinders do occur in the course of a few years, and they may in the present case amount to a few parts in a hundred thousand

From these considerations it would appear that the complete magnetometer and its accessories form a means of obtaining a base-line value for vertical intensity which would be consistent to 1 or 2 γ, but that the absolute value of the field in C G S units is subject to an uncertainty of about twice this amount

In conclusion, my thanks are due to the Metrology Department for the design and construction of parts of the mounting, to Mr P Vigoureux for much careful assistance in the observations and in the method of presenting the matter in Appendix I My thanks are also due to the Director and to Dr Chree for kindly interest in the development of the magnetometer

APPENDIX I

General case in which a Helmholtz coil system is set up with its axis nearly vertical and can be oriented about another axis nearly vertical This latter is an axis of reference

The detecting coil is set up with its plane nearly vertical and its axis of vibration pointing in any direction in a nearly horizontal plane, and capable of orientation about the axis of reference

Let OX, OY and OZ be three axes of reference such that OY is coincident with the nearly vertical axis around which the Helmholtz coil and the vibrating coil can be oriented

Let U_M be the field produced by the Helmholtz coil and let its direction cosines be ξ, η and ζ, where ξ and ζ are nearly zero and η nearly unity

Let the direction cosines of the vertical be λ, μ and ν, where λ and ν are nearly zero and μ is nearly unity

Let the earth's field be F and its direction cosines be l, m and n None of these is necessarily small

Let the direction cosines of a line in the plane of the vibrating coil and perpendicular to its axis of vibration be α, β and γ, where α and γ are small and β is nearly unity

The angle between F and the line α, β, γ is $\cos^{-1}(\alpha\xi + \beta\eta + \gamma\zeta)$

The vibratory torque due to F is proportional to

$$F(\alpha l + \beta m + \gamma n).$$

Again, the angle between V_m and the line α, β, γ is

$$\cos^{-1}(\alpha\xi + \beta\eta + \gamma\zeta)$$

and the vibratory torque is proportional to

$$U_M(\alpha\xi + \beta\eta + \gamma\zeta)$$

By adjustment of U_M to the value U_{M1} we can reduce the vibratory torque to zero, so that

$$F(\alpha l + \beta m + \gamma n) = U_{M1}(\alpha\xi + \beta\eta + \gamma\zeta) \tag{1}$$

Now let the Helmholtz coil and the vibrating coil be oriented about the nearly vertical axis of reference OY through an angle π

The new direction cosines become

$$\begin{array}{ccc} -\xi & \eta & -\zeta \\ \lambda & \mu & \nu \\ l & m & n \\ -\alpha & \beta & -\gamma \end{array}$$

By adjustment of U_M to the value U_{M2}, such that the vibratory torque is again zero, we have

$$F(-\alpha l + \beta m - \gamma n) = U_{M2}(\alpha\xi + \beta\eta + \gamma\zeta) \tag{2}$$

The mean of (1) and (2) gives

$$F\beta m = \tfrac{1}{2}(U_{M1} + U_{M2})(\alpha\xi + \beta\eta + \gamma\zeta) \tag{3}$$

The vertical component of the earth's field $= V$ is given by

$$V = F(\lambda l + \mu m + \nu n) \tag{4}$$

Eliminating F from (3) and (4) gives

$$\tfrac{1}{2}(U_{M1} + U_M) = \frac{V\beta\eta}{(\lambda l + \mu m + \nu n)(\alpha\xi + \beta\eta + \gamma\zeta)}$$

Neglecting products of small quantities this gives

$$\tfrac{1}{2}(U_{M1} + U_{M2}) = V \frac{1}{\mu\eta}\left(1 - \frac{\lambda l}{\mu m} - \frac{\nu n}{\mu m} - \frac{\alpha\xi}{\beta\eta} - \frac{\nu\zeta}{\beta\eta}\right) \tag{5}$$

In practice the plane and the axis of vibration of the vibrating coil are adjusted so that α and γ are small by the process whereby U_{M1} is made nearly equal to U_{M2} Also, the Helmholtz coil is adjusted so that ξ and ζ are very small

We may therefore safely neglect the last two terms in equation (5) The simplified expression for V becomes

$$V = \mu\eta\left(\frac{U_{M1} + U_{M2}}{2}\right)\left(1 - \frac{\lambda l + \nu n}{\mu m}\right) \tag{6}$$

The angles $\cos^{-1}\lambda$ and $\cos^{-1}\eta$ can most certainly be adjusted to values smaller than 0 0001 radian. The values of μ and η will therefore differ from unity by a quite negligible amount

The correction which has to be applied to the mean of the two U readings reduces to the simple term $-(\lambda l + \nu n)$ in relation to unity

It is thus seen that the only quantity finally involved in these corrections arising from the adjustments of the magnetometer is the departure from verticality of the axis about which the Helmholtz coil and the vibrating coil are oriented

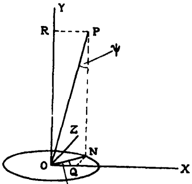

FIG 5

The physical significance of the remaining correction terms is best seen by reference to fig 5

OX, OY and OZ are the axes of reference of which OY is the axis of turning OP is the vertical whose direction cosines λ, μ and ν are given by OQ, OR and NQ respectively

The actual angle which the axis of turning makes with the vertical is ψ, and the vertical plane containing OY makes the angle A with the plane OXY

We then have

$$\frac{\nu}{\mu} = \frac{\nu}{\sqrt{\nu^2+\lambda^2}} \quad \frac{\sqrt{\nu^2+\lambda^2}}{\mu} = \tan\psi \sin A,$$

and $\lambda\mu = \tan\psi\cos A$.

Treating the earth's field F in the same manner as the vertical we have

$$\frac{n}{m} = \frac{\sqrt{n^2+l^2}}{m} \cdot \frac{n}{\sqrt{n^2+l^2}} = \frac{H}{V}\sin\beta, \quad \frac{l}{m} = \frac{H}{V} \cos\beta$$

On substitution of these terms into the expression

$$\nu n + \lambda l/\mu m,$$

the correction term becomes

$$-\frac{H}{V}\tan\psi(\cos A\cos B + \sin A\sin B) = -\frac{H}{V}\tan\psi\cos(A - B) \qquad (7)$$

The maximum value which the correction can have occurs when the vertical plane containing the axis of rotation coincides with the vertical plane containing the earth's field, i e, A = B. The correction is then $-H\psi/V$

Expressed as an error in relation to unity, it is seen that the error may be large in regions near the magnetic equator, but expressed in terms of γ units the error is simply $H\psi$ For a maximum value of H equal to 0 5 C G S unit, it is seen that ψ should be reduced to 2×10^{-5} radian for an accuracy of 1 γ to be obtained

With the present instrument such an angle of departure of the axis of turning from the vertical can just be detected

APPENDIX II

Measurement of the Current

The measuring circuit is as shown in fig 6

R_1 is a standard four-terminal resistance shunted by the higher resistance R_2 of such value that a potential difference about 6 parts in 1000 greater than that of a standard cell results when the appropriate current flows through the combination

Since R_2 is shunted across the current terminals of R_1, it is necessary to know approximately the resistance of the current leads, shown as r_1

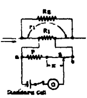

FIG 6

Across the potential terminals of R_1, is shunted a relatively high resistance P in series with a slide wire of resistance S The slide wire has a resistance of about 0 005 that of P

The standard cell of voltage E is connected through tapping key and galvanometer to the potential points a and b

If a total current I is sent through this network, then the potential difference required is that between the points a and b, where b is at any reading x on the slide wire

This potential difference is given by

$$\mathrm{PD} = \mathrm{I} \ \frac{\mathrm{P} + x}{\mathrm{P} + \mathrm{S}} \ \frac{\mathrm{R}_1\mathrm{R}_2}{\mathrm{R}_2 + \dfrac{\mathrm{R}_1(\mathrm{P}+\mathrm{S})}{\mathrm{R}_1 + \mathrm{P} + \mathrm{S}} + r_1},$$

whence

$$\mathrm{I} = \mathrm{E} \ \frac{\mathrm{P} + \mathrm{S}}{\mathrm{P} + x} \ \frac{\mathrm{R}_2 + \dfrac{\mathrm{R}_1(\mathrm{P}+\mathrm{S})}{\mathrm{R}_1 + \mathrm{P} + \mathrm{S}} + r_1}{\mathrm{R}_1\mathrm{R}_2},$$

The calibration of the scale of the slide wire S in terms of a small change in current is given by $\dfrac{d\mathrm{I}}{\mathrm{I}} = -\dfrac{dx}{\mathrm{P} + x}$

In the case of the Helmholtz coil described, and for the value of V in England, the value of I is about 1 19 amperes

It is convenient to use a slide wire of 1 ohm resistance and to choose a value of P such that the slide wire covers a range of about 5 parts in 1000 in V Under these conditions P becomes 200 ohms

If $R_1 = 1$ ohm and $R_2 = 6$ ohms, then the effect of the current leads of R_1 is small, but not quite negligible, if they have a resistance of 0 0001 ohm

For a base line corresponding to a value of x equal to 0 5 ohm the value of I becomes

$$1\ 01830 \times \frac{201}{200\ 5} \times \frac{6 + \frac{201}{202}}{6} \text{ amperes}$$

$$= 1\ 19017$$

For a change of slide wire reading of 0 001 ohm the proportionate change of current necessary to give balance is equal to

$$\frac{0\ 001}{200\ 5} = 5 \text{ parts in } 10^6$$

It is thus seen that accuracy to one part in a hundred thousand can be obtained and observed if R_1 and E are known to this accuracy

A more open scale can be obtained on the slide wire at the expense of a smaller range, by choosing a higher value of P By introducing the constant of the Helmholtz coil into the calculations, it is easy to calibrate the scale of S to read change of V directly in γ units

The Thermal Conductivities of Certain Liquids

By G W C Kaye, O B E, M A, D Sc, and W F Higgins, M Sc, Physics Department, The National Physical Laboratory

(Communicated by Sir Joseph Petavel, F R S —Received September 14, 1927)

The determination of the thermal conductivity of liquids and the variation with temperature has received the attention of a number of workers in the past, notably, Lees in 1898, R Weber in 1903, and Goldschmidt in 1911 In general, however, the temperature ranges explored were somewhat restricted, and the present work was accordingly directed to determining the conductivities of a number of the more common liquids up to the highest temperatures feasible

In measuring the thermal conductivity of a liquid it is, of course, essential that convection effects should be reduced to a minimum This may be effected by employing small temperature differences across a thin horizontal layer of the liquid, the heat flow being directed downwards

Apparatus

An apparatus was accordingly designed in which a thin horizontal layer of the liquid was sandwiched between two aluminium blocks, the upper "hot block" containing an electric heating coil and the lower "cold block" being provided with radiating fins Escape of heat from the hot block in an upward direction was prevented by mounting above the hot block, and separated from it by a thin film of air, an aluminium "guard plate" containing a subsidiary heating coil * The current through the subsidiary coil was then adjusted until there was no temperature drop across the air film, so that apart from a small loss from the sides of the hot block, the energy supplied to the main heating coil was all transmitted downwards through the test liquid The apparatus was completely enclosed in a thermostatically controlled oven which was raised to the appropriate temperature for the purpose of the test in hand By this means the unavoidable surface losses were reduced as the oven temperature was usually only some 10° C below that of the hot block

The apparatus is shown diagrammatically to scale in fig 1 The aluminium blocks were cylindrical and 5 cms in diameter, so that the area of the test layer of liquid was about 20 sq cms The temperatures at the faces of the two blocks between which the liquid was held were measured by thermocouples of which the aluminium blocks each served as one arm, the other being of con-

---

* We find that a similar device was employed by Hercus and Laby in measuring the conductivity of air 'Roy Soc Proc,' A., vol. 95, p 190 (1918)

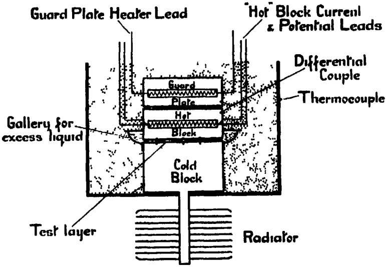

FIG 1

stantan * For the purpose, holes of small diameter were drilled from the sides of the blocks in a slanting direction until the test faces were reached at the appropriate points Constantan wires were then inserted through the holes and provided with thin glass sheaths to insulate them from the aluminium, except at the actual faces where they were held in firm contact by small aluminium pegs The faces of the blocks with the couples in position were then ground flat to a high degree of accuracy

Round the upper end of the cold block a small trough or gallery was affixed to hold the test liquid during assembly and to provide sufficient surplus to ensure that the space between the cold and hot blocks was always filled It was obviously desirable that this gallery should be of material of low thermal conductivity, and it was, of course, essential that it should not be attacked by any of the liquids to be investigated, and, further, that its junction with the aluminium should remain liquid-tight as the temperature was raised After some trials, asbestos paper was eventually chosen This was moulded into shape while damp and secured to the aluminium block by a few turns of

---

* The use of aluminium constantan couples for the measurement of temperatures has been discussed in a previous paper by the present authors, see "Thermal Conductivity of Vitreous Silica," 'Roy Soc Proc,' A, vol 113, p 335 (1926)

wire pressing the asbestos into a shallow groove in the side of the cold block After being allowed to dry it was treated with bakelite varnish and heated to the appropriate temperature, the process being repeated several times This method of construction proved fully satisfactory The gallery was finally fitted with a loose mica cover

The hot block was made up of two parts which screwed together and enclosed an electric heating grid of nichrome wire wound on mica A similar construction was adopted for the guard plate The temperature of the hot block ranged between about 20° C and 200° C (where feasible), and the power inputs were varied over a range of from 3 to 20 watts

To separate the hot and cold blocks at a known distance three short lengths of glass rod, resting on their sides and of suitable diameter, were interposed In the case of water, however, it was found more convenient to use three tiny pieces of silica plate cemented by a trace of bakelite varnish to the surface of the cold block, as it was found that the glass rods tended to float away during assembly Preliminary tests had shown that the thickness of the liquid should not exceed 0 5 mm , and accordingly the experiments were conducted with thicknesses ranging from 0 25 to 0 5 mm The operation of assembling the apparatus so that no air bubbles were trapped between the two surfaces was a matter of some practice The hot block was gradually lowered in a tilted position into the liquid and was gently brought into the horizontal position, the air being swept to one side as more and more of the hot block became wetted by the liquid The blocks were then aligned axially by means of centering screws which were withdrawn during the course of an experiment The guard plate and hot block were similarly separated by glass distance pieces and a differential couple served to indicate whether their surfaces were at the same temperature It may be added that the various test liquids were freed from air by pre-heating to as high a temperature as was feasible

The apparatus was surrounded by a metal enclosure the intervening space being packed with asbestos wool and the whole was contained in the oven already referred to The oven was heated electrically and a fan was provided to circulate the air, baffles being introduced to secure uniformity of temperature around the apparatus

Corrections to be Applied to Experimental Data

(*a*) *Lateral loss of heat* —As already mentioned, heat loss from the hot block in an upward direction was prevented by the guard plate , there was, however, a small loss of heat from the sides of the hot block which had to be allowed for The surrounding space being closely packed with asbestos wool, this side loss was due to conduction and not to radiation or convection, and should, therefore, depend directly upon the difference of temperature between the hot block and the metal enclosure The magnitude of the correction was determined experimentally by taking observations under normal conditions when the test liquid was replaced by a material of known conductivity between the hot and cold blocks Balsa wood was chosen for the purpose, as its conductivity is low and consequently the side loss becomes relatively more pronounced and so more readily measurable A series of observations were made for different power inputs and different thicknesses of balsa wood, and it was found that the lateral loss was proportional, as was anticipated, to the temperature difference between the hot block and the surrounding metal enclosure Quantitatively, the loss amounted to 0 0234 watts per °C difference in temperature This would include any loss of heat along the leads of the heating coil which, however, would be small in amount

(*b*) *Heat transferred through liquid in gallery* —By reference to fig 1, it will be noted that, apart from the heat passing directly across the test layer of liquid, it was possible for heat to be transmitted from the hot to the cold block via the surplus liquid in the gallery As in the case of the lateral loss, steps were taken to enhance the effect in order to obtain a more accurate estimate of its magnitude This was done by increasing the thermal resistance of the test layer by inserting a disc of ebonite (1 mm thick) between the test faces, and observations were then made for a series of temperature differences between the hot and cold blocks, first with the gallery full of liquid and then empty It was found that the correction to be subtracted from the power input, on this score, was proportional to the temperature difference, and to the conductivity of the liquid, and was given numerically (when the gallery was full, as under normal conditions of experiment) by the expression K × 42 0 watts per °C difference between the blocks (K being the approximate conductivity of the liquid under test) The magnitude of this correction found in no case to exceed 3 per cent

As an independent check on the above, the following experiment was carried out The apparatus was set up in the normal way with water as the liquid under test Observations were made at constant power input, first with the gallery full and afterwards from time to time as evaporation gradually lowered the level of the water, until ultimately the test layer itself began to disappear Fig 2 shows the gradual change with time in the temperature difference between the hot and cold blocks It will be noted that for a period of about seven hours the temperature difference increased steadily, corresponding to an

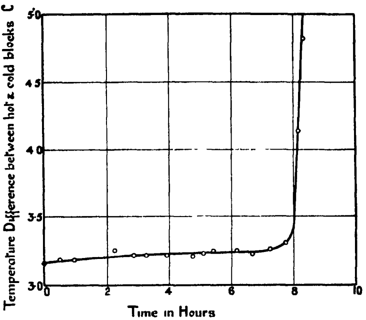

FIG 2

apparent decrease of conductivity This was followed by a rapid rise obviously due to the disappearance of the layer of water between the blocks The beginning of the curve (with the trough full) corresponded to a conductivity of 0 00161$_0$, which, when subjected to the correction factor given above, reduced to 0 00157$_7$ This was in good agreement with the value given by the curve just before the rapid rise, viz , 0 00157$_2$ where obviously no correction was required

(c) *Heat lost by evaporation* -Another possible source of heat loss was that producing evaporation from the free surface of the liquid in the gallery The case of water was studied in view of its high latent heat of evaporation and the fact that observations could be taken nearer the boiling-point than in the case of the other liquids A rough experiment showed that for water, up to 1 c c per hour was lost by evaporation at the higher temperatures which was equivalent to a correction amounting to 5 per cent of the power input In the case of the other liquids, the correction was so small that it did not need to be taken into account

As the evaporation depends upon the temperature of the water and is independent of the amount of heat passing through the test layer, the most direct way of ascertaining the correction necessary was to carry out a series of experiments at different power inputs at the same mean temperature of the water and so to deduce the power loss due to evaporation at that temperature At 60° C this amounted to 0 53 watt It was established experimentally that the rate of loss of weight of the water due to evaporation at any particular temperature was proportional to the vapour pressure, thus affording a convenient means of calculating the correction for evaporation at any temperature desired

(*d*) *Heat loss through guard plate* —Under normal working conditions it was found possible to adjust the current through the guard-plate heater so that the difference of temperature between the two sides of the air gap corresponded to less than 3 microvolts, *i e* about 0 07° C For the particular dimensions of air gap used, calculation showed that the corresponding correction on this score amounted to less than 1/10 per cent of the power input, which was negligible This conclusion was confirmed by making the temperature drop across the air gap relatively large and observing the resulting effect on the apparent conductivity of a sample liquid Even when the temperature drop across the air gap was as high as 2° C the effect on the measured conductivity of the liquid amounted to only about 4 per cent

(*e*) *Heat conducted through distance-pieces* —The possibility of error arising out of conduction of heat through the distance-pieces separating the hot and cold blocks was also considered As already stated, short glass rods were used in most instances, and the area of the contact between their sides and the aluminium blocks was so small that the effect was negligible In the case of water, the flat plates of vitreous silica used had a total area 0 05 sq cm The conductivity of vitreous silica being about twice that of water, the effect was equivalent to increasing the effective area of the test layer by 0 05 sq cm and consequently the observed conductivity was in error by about 0 2 per cent This was well within the experimental accuracy and so did not need to be taken into account

Typical Experiment

The following data were obtained in the course of a typical experiment on glycerine at a mean temperature of 50° C —

Liquid Glycerine

Dimensions —

Thickness of test layer (d)	0 0357 cm
Area of test layer (A)	20 27 sq cms

Temperature measurements —

Hot-face thermocouples (three)	2134, 2132, 2133 microvolts
Equivalent mean hot-face temperature	52·20° C
Cold-face thermocouples (three)	1945, 1943 1945 microvolts
Equivalent mean cold-face temperature	17·80° C
Temperature drop over test layer ($\delta\theta$)	4·40° C
Mean temperature of liquid	50·00° C

Power supply to hot block —

Current	1·0709 amp
Potential drop	7·072 volts
Power supplied	7·574 watts

Corrections to power supply —

(*a*) Side loss —

Temperature difference between hot block and metal enclosure	10·53° C
Correction 10·53 × 0·0234	= 0·246 watt

(*b*) Loss through excess liquid —

Temperature difference between hot and cold blocks	4·40° C
Approximate conductivity	0·00068
Correction 0·00068 × 4·40 × 42·0	= 0·126 watt

(*c*) Evaporation loss	Nil
Corrected power (W), 7·574 — 0·246 — 0·126	= 7·202 watts

Thermal conductivity of glycerine at 50·0° *C*

$$= \frac{Wd}{4\cdot18 A\delta\theta} = \frac{7\cdot202 \times 0\cdot0357}{4\cdot18 \times 20\cdot27 \times 4\cdot40}$$

$$= 0\cdot00069_0 \text{ c g s}$$

Results

Figs 3 to 5 show the variation of thermal conductivity with temperature for the various liquids The small numbers by the side of the plotted points indicate the sequence in which the observations were made If more than one thickness of liquid was experimented with, the observations are suitably identified In all cases the results can be represented by straight lines from which the bulk of the individual observations do not depart by more than 1 per cent It will be seen that water and glycerine, the two liquids with the

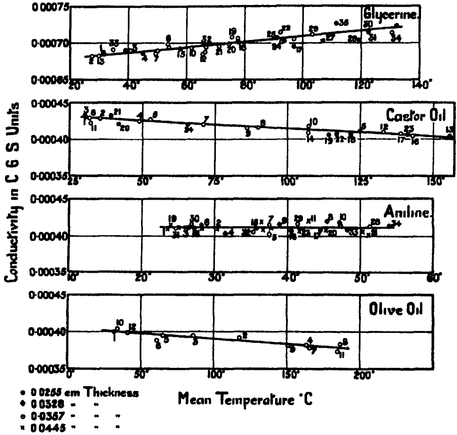

FIG 3

highest conductivities, were unique in exhibiting an increase of conductivity with temperature In the case of water (fig 5), the divergences from the mean straight line are slightly larger, as the method is not quite so well adapted for the measurement of conductivities as high as that of water which in this physical constant, as in many others, is anomalous As previously mentioned, the experiments on water involved an additional correction for evaporation which further reduced the accuracy For the sake of comparison, the results of Jakob and Bridgman are added to fig 5

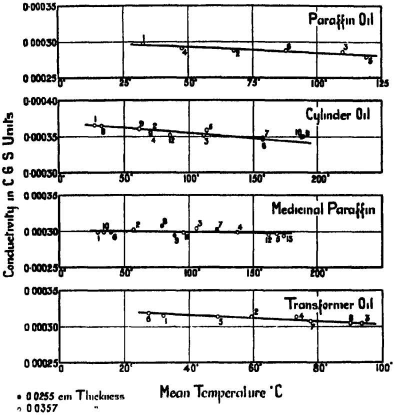
Paraffin Oil
0·00035
0 00030
0 00025
0°
25°
50°
75°
100°
125
Cylinder Oil
0·00040
0·00035
0·00030
0°
50°
100°
150°
200°
Medicinal Paraffin
0 00035
0 00030
0·00025
0°
50°
100°
150°
200°
Transformer Oil
0 00035
0 00030
0 00025
0
20°
40°
60°
80°
100°
Conductivity in C G S Units
Mean Temperature °C
• 0 0255 cm Thickness
○ 0 0357 "

FIG 4

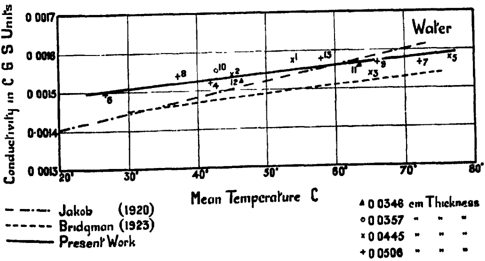
Water
0 0017
0 0016
0 0015
0·0014
0 0013
20°
30°
40°
50°
60°
70°
80°
Conductivity in C G S Units
Mean Temperature C
— —·— Jakob (1920)
- - - - - - Bridgman (1923)
———— Present Work
▲ 0 0348 cm Thickness
○ 0 0357 " " "
× 0 0445 " " "
+ 0 0506 " " "

FIG 5

Table I.—Thermal Conductivity of Liquids

Conductivity (c.g.s.) at a temperature of	Distilled water	Glycerine (Brit. Pharm.)	Castor oil	Aniline	Olive oil	Cylinder oil (medium)	Transformer oil	Medicinal paraffin (Brit. Pharm.)	Paraffin oil (Acid free)
°C									
0	0.00145	0.000673	0.000437	0.000412	0.000405	0.000370	0.000324	0.000301	0.000300
20	0.00149	0.000680	0.000432	0.000412	0.000402	0.000366	0.000320	0.000300	0.000297
40	0.00153	0.000687	0.000428	0.000412	0.000399	0.000363	0.000316	0.000300	0.000294
60	0.00156	0.000695	0.000424	—	0.000397	0.000360	0.000312	0.000300	0.000291
80	0.00160	0.000702	0.000420	—	0.000394	0.000357	0.000308	0.000299	0.000288
100	—	0.000709	0.000415	—	0.000391	0.000354	0.000304	0.000299	0.000284
120	—	0.000716	0.000411	—	0.000388	0.000351	—	0.000299	0.000281
140	—	0.000723	0.000406	—	0.000385	0.000348	—	0.000298	—
160	—	—	0.000402	—	0.000382	0.000345	—	0.000298	—
180	—	—	—	—	0.000379	0.000342	—	0.000298	—
200	—	—	—	—	0.000376	0.000339	—	—	—
Temperature coefficient α $[K_t = K_0 (1 - \alpha t)]$	$+0.001_2$	$+0.0005_3$	-0.0005_6	0.0000	-0.0003_5	-0.0004_1	-0.0006_2	−0.00007	-0.0005_5
Density at 18° C	1.000	1.25_8	0.96_4	1.02_2	0.91_3	0.89_4	0.84_1	0.88_2	0.81_2

Note.—The data in the above table are given to three significant figures, but it is not claimed that the accuracy of the determinations in general exceeds ± 1 per cent, while in the case of water the accuracy is probably slightly lower. Further, the values given at 0° C. are obtained by extrapolation of the graphs.

Table II —Comparison of Results with Published Data

Liquid		Lees[1] (1898)	Milner and Chattock[2] (1899)	R Weber[3] (1903)	Goldschmidt[4] (1911)	Jakob[5] (1920)	Bridgman[6] (1923)	Davis[7] (1924)	Present work
Water	k_{25}	0 00136	0 00144*	0 00131	0 00155*	0 00143	0 00143	0 00144	0 00150
	α	−0 0055	Positive	—	—	+0 0030	+0 0015	+0 002	+0 0012
Glycerine	k_{25}	0 0 068	—	0 00066	0 0073*	—	—	—	0 000682
	α	−0 0044	—	—	—	—	—	—	+0 00053
Aniline	k_{25}	—	—	—	0 000434*	—	—	0 00044	0 000412
	α	—	—	—	—	—	—	$-0\ 000_3$	0 0000
Olive oil	k_{25}	—	—	—	—	—	—	0 00040	0 000401
	α	—	—	—	—	—	—	$-0\ 000_5$	−0 00035
Transformer oil	k_{25}	—	—	—	—	—	—	0 00032	0 000319
	α	—	—	—	—	—	—	Negative	−0 00062
Paraffin oil	k_{25}	—	—	0 000346	—	—	—	0 00030	0 000297
	α	—	—	—	—	—	—	Negative	−0 00055

* Results reduced to 25 C using present authors temperature coefficient

[1] Lees, 'Phil. Trans,' A, vol 191 p 399 (1898)
[2] Milner & Chattock, 'Phil Mag, vol. 48, p 46 (1899)
[3] P Weber, 'Ann d Physik,' vol 11, p 1047 (1903)
[4] Goldschmidt, 'Phys Zeits,' vol 12, p 417 (1911)
[5] Jakob, Ann d Physik, vol 63, p 537 (1920)
[6] Bridgman, 'Nat Acad Sci Proc, vol 9, p 341 (1923)
[7] Davis, Phil Mag, vol 47, p 1057 (1924)

The results for the various liquids are also summarised in Table I (p 468), which gives the conductivities read off from the curves at each 20° C The values of the coefficient α in the expression $K_t = K_0 (1 + \alpha t)$ are also tabulated together with the densities at 18° C

Comparison of Results with Published Data

A comparison of some of the results of the present work with previously published data is given in Table II (p 469), where the values of the conductivity at 25° C are tabulated, together with the temperature coefficients In general, the agreement of the present results with the more recent data is good, particularly in the case of the results published by Davis which, however, are comparative and rest on Goldschmidt's value for toluol at air temperature It may be remarked that Davis used the capillary-tube and heated-wire method of Goldschmidt which differs fundamentally from that employed in the present work

Summary

The thermal conductivities of a number of common liquids, including water, glycerine, aniline and various oils, have been determined by a " plate ' method, over a range of temperatures up to 200° C (where feasible) The test layers had an area of about 20 sq cms and thicknesses up to 0 5 mm The following table summarises the chief results

Table III

Liquid	Conductivity at 20° C	Temperature coefficient α in expression $K_t = K_0 (1 + \alpha t)$
Water	$0\ 0014_9$	$+0\ 001_2$
Glycerine	$0\ 00068_0$	$+0\ 0005_2$
Castor oil	$0\ 00043_2$	$-0\ 0005_6$
Aniline	$0\ 00041_2$	$0\ 0000$
Olive oil	$0\ 00040_2$	$-0\ 0003_5$
Cylinder oil	$0\ 00036_8$	$-0\ 0004_1$
Transformer oil	$0\ 00032_1$	$-0\ 0006_2$
Medicinal paraffin	$0\ 00030_6$	$-0\ 0000_7$
Paraffin oil	$0\ 00029_8$	$-0\ 0005_5$

We are glad again to acknowledge the constructional skill and observational accuracy of Mr D E A Jones, of the Observer staff of the Laboratory

The Magnetic Properties of Single Crystals of Nickel

By W Sucksmith, B Sc , H H Potter, Ph D , Lecturers in Physics, University of Bristol, and L Broadway, B Sc

(Communicated by A P Chattock, F R S —Received August 9, 1927)

Introduction

In recent years the production of single crystals of iron* has led to investigations of their magnetic properties Following the lines of the experiments of Weiss† and his co-workers on natural crystals of pyrrhotite, etc , Beck,‡ Webster,§ and Honda and Kaya|| have examined the magnetic intensity with respect to the crystal axes Results of great interest have been obtained, but a satisfactory theoretical interpretation is still wanting

It appeared desirable for various reasons to obtain corresponding results for nickel In the first place, the structure is that of a face-centred cube, and comparison with iron, which has a body-centred cubic structure, appeared likely to yield valuable results Furthermore thermo-magnetic changes are simpler and more easily studied than in the case of iron, partly on account of the lower critical temperature

The paper divides itself naturally into two parts, the first of which is devoted to the perpendicular and parallel components of magnetisation in nickel, and the second a critical discussion of the torsion method of measuring the parallel component in single crystals of ferromagnetic materials

Part I

Preparation of Specimens

The nickel crystals¶ were prepared from Mond pellets by slow cooling from the molten liquid contained in a long cylindrical "Alundum" crucible In no case did a single crystal occupy the whole cross-section of the crucible, but the specimens obtained were quite large enough for the examination of directional magnetic properties We hope later to improve the technique of crystal pro-

---

* Edwards and Pfeil, 'J Iron and Steel Inst.,' vol. 109, p 129 (1924)

† Weiss, 'J de Phys.,' vol. 4, p 469 (1905), etc

‡ 'Dissert. Zurich,' 1918 , see also 'Bull Nat. Res Counc ,' vol. 3, p. 180 (1922)

§ 'Roy Soc Proc ,' A, vol 107, p 496 (1925)

|| 'Sci. Rep Tôhoku,' vol. 15, p. 721 (1926)

¶ Sucksmith and Potter, 'Nature,' vol 118, p 730 (1926) duction and to examine other magnetic properties of single crystals The purity of the crystals produced was about 99 6 per cent

In the early stages of the work the positions of the crystal planes were determined by X-ray examination * Later, however, we found that the etch reflections could be utilised,† and the use of this method in preference to X-rays considerably reduced the amount of labour involved

Single crystals of nickel are much softer than the ordinary polycrystalline metal, and consequently distortion is easily produced by mechanical working To minimise this, the specimens were prepared by grinding by hand on a fine oil-stone The first step was to grind the surface parallel to the required crystal plane A thin slab about 2 mm thick was then cut from the crystal with a fine jeweller's saw, and the sawn face ground parallel until the thickness was reduced to about 0 5 mm In this way the portion of crystal distorted by sawing was removed The slab was then soldered between a similar slab of brass and the end of a hard steel rod of the same diameter as the finished specimen The crystal and brass were then ground down together to the diameter of the rod, this procedure preventing the burring of the edges of the specimen

The identification of a (100) plane is easy, since these planes appear as etch planes Frequently the (100) reflections were weak compared with those from (111) planes, but the positions could be checked by reference to the (111) reflections Etch reflections do not occur from (110) planes, and these had to be located by bisecting the angle between two suitable (111) planes We estimate the accuracy of the cutting of these discs to 2 or 3 degrees

Method of Investigation

The investigation of the magnetic properties is divided into the measurement of the component of magnetisation (*a*) parallel to the applied field and (*b*) perpendicular to the field, and the variations of these two vectors as the field is rotated in the plane of the disc For the measurement of the perpendicular component we have used the method of Weiss, in which the specimen is suspended with its plane horizontal, and the couple exerted by a uniform field H on the body (volume v) is given by vI_N H, where I_N is the component of magnetisation perpendicular to the field This is determined for various orientations of the field with respect to the disc, the couple disappearing when the magnetisation and the field are parallel (For further details, see Weiss and Webster

---

* Müller, 'Roy Soc. Proc ,' A, vol. 105, p 500 (1924)

† Potter and Sucksmith, 'Nature,' vol. 119, p. 924 (1927).

loc cit) We shall show later that the method used by Weiss and Webster for the measurement of the parallel component leads to incorrect results in the case of nickel In the measurement of this component we have therefore used the ballistic method which was employed by Honda and Kaya

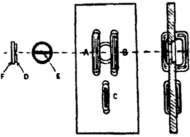

FIG 1

The arrangement of the secondary coils for the measurement of the parallel component is shown in fig 1 A piece of ebonite 1/16th inch thick was drilled suitably to carry the three secondary coils A, B, and C, and the specimen F The coils A and B surround the specimen, whilst C is used to neutralise the H lines through A and B The hole between A and B is drilled half-way through the ebonite and is of such a size that the specimen rotates smoothly in it A small hole coaxial with the specimen carrier goes through the ebonite, and a fine scratch on the specimen is viewed through this hole by means of a telemicroscope with cross-wire and circular scale, which allows the orientation of the disc with respect to the field to be determined to 1° or less An ebonite disc D of slightly smaller diameter than the specimen F was shellacced to the back of the latter For the purpose of rotating the specimen a small screw driver could be inserted in a saw-cut E in the ebonite disc A small quantity of thick grease on the edges of the specimen ensured smooth rotation and prevented displacement between measurements The ebonite former was securely fixed between the poles of the electromagnet used to produce the field There are disadvantages in using an iron-cored magnet, particularly for low values of the field, but owing to lower initial susceptibility of nickel, this difficulty is not so marked as it would be in the case of iron crystals

The total number of lines of induction threading the secondary is proportional to I_P, but the factor of proportionality is not calculable since the flux has to be corrected for demagnetising field and for uncut lines The demagnetising factors N, in the plane of the discs, have been obtained by assuming that the specimens are oblate spheroids, in which case

$$N = 2\pi\left\{\frac{\sqrt{1-e^2}}{e^3}\sin^{-1} e - \frac{1-e^2}{e^2}\right\},$$

where e is the eccentricity

Results

(100) *Plane Parallel Component* -Dimensions of crystal-thickness 0 041 cm, diameter 0 393 cm The curves showing the relationship between the parallel component of magnetisation I_P and the orientation of the disc for different values of the magnetising field are shown in fig 2 They are periodic in 90° and show maxima along the digonal and minima along the tetragonal axes The greatest fluctuations in intensity take place just below saturation The values of the field corrected for demagnetising factor are shown on the right of the figure Owing to different intensities in different directions, the demagnetising field varies according to the orientation of the crystal for a given applied field The fields in the figure refer to the digonal axes The apparent fluctuations are therefore somewhat reduced on account of the effective field along the tetragonal axis being greater than that along the digonal

Fig 6 shows the relation between H and I along the two principal axes in the (100) planes Corresponding points on the two curves were obtained for the same external field, but owing to the different demagnetising fields along the two axes, the points referring to the tetragonal are displaced towards the right The maximum fluctuation is about 10 per cent and occurs at an intensity of 360 units For this curve as for all others—except figs 3 and 5, which refer to the perpendicular component- the actual values of the intensities are calculated on the assumption that the saturation intensity is 450 units

(100) *Plane Perpendicular Component* - Fig 3 shows the fluctuations of the perpendicular component I_N in the (100) plane for four different values of the effective field Fig 3 (*a*) is the means of two curves obtained with fields rotating in opposite directions This is necessary on account of appreciable rotating hysteresis exhibited by these crystals at low fields The total hysteresis loss is of the order of a few hundred ergs per cubic centimetre, which is very small compared with the loss in polycrystalline nickel (see also Sucksmith and Potter, *loc cit*) In fig 8 (*a*) the maximum values of I_N are plotted agaınt the effective field The curves in fig 3 are periodic in 90°, the values of I_N being zero along the digonal and tetragonal axes When the field is along the digonal axis, the suspended system is stable, but with the field along the tetragonal axis the system is in unstable equilibrium For an iron crystal cut in the (100) plane the system is stable when the field is along the tetragonal and unstable when it is along the digonal axis The question of these unstable positions has been dealt with by Webster (*loc cit*, p 502), who concludes that the instability is inherent in the method rather than in the crystal It might be well to

point out that the real cause of stability or instability is the relative rates of rotation of the two vectors I and H These coincide along both digonal and tetragonal axes in both iron and nickel In the neighbourhood of the digonal axes I rotates more quickly than H in the case of iron and thus gives rise to an apparent instability In the neighbourhood of the tetragonal axes I rotates less quickly than H and thus gives an apparently stable position The reverse is true in the case of nickel

It will be seen that the curves are practically sinusoidal, but that the amplitudes vary This may be attributed to distortion, inhomogeneity, or error in cutting The fields given are, as before, the effective fields along the digonal axis

(110) *Plane Parallel Component*—Dimensions of crystal, thickness 0 041 cm, diameter 0 388 cm The variations with orientation of the field of the parallel component of magnetisation are shown in fig 4 The maxima occur along the trigonal axes with a small minimum along the digonal and a more pronounced minimum along the tetragonal axis As before, the maximum

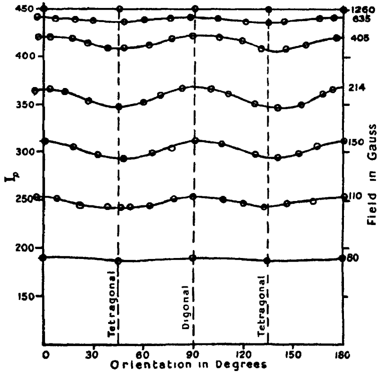

FIG 2.

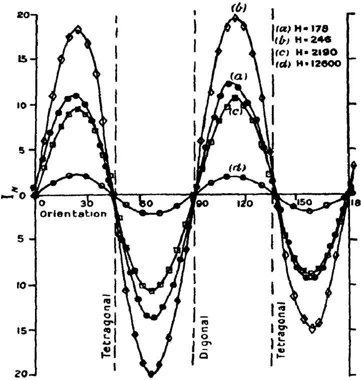
(b)
(a) H = 178
(b) H = 246
(c) H = 2190
(d) H = 12600
(a)
(c)
(d)
20
15
10
5
I_N 0
5
10
15
20
0
30
60
90
120
150
180
Orientation
Tetragonal
Digonal
Tetragonal

FIG 3.

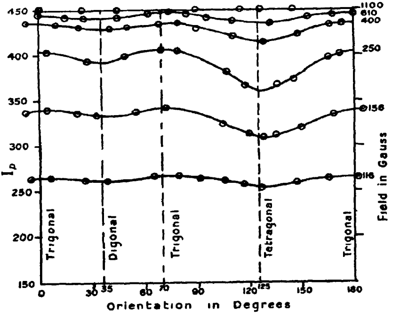
450
400
350
300
250
200
150
I_D
1100
610
400
250
156
116
Field in Gauss
Trigonal
Digonal
Trigonal
Tetragonal
Trigonal
0
30
35
60
70
90
120
125
150
180
Orientation in Degrees

FIG. 4.

variations occur in the region just below saturation. The fields given on the right-hand side of the figure are the effective fields along the trigonal axes

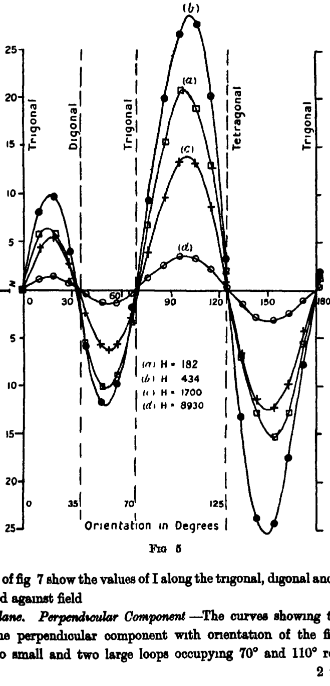

FIG 5

The curves of fig 7 show the values of I along the trigonal, digonal and tetragonal axes plotted against field

(110) *Plane. Perpendicular Component*—The curves showing the fluctuations of the perpendicular component with orientation of the field (fig 5) exhibit two small and two large loops occupying 70° and 110° respectively

The component is zero along the trigonal, digonal and tetragonal axes, and is apparently unstable along the two latter axes. The curve at 182 gauss is the mean of two curves (see above)

The variation of I_N with field is shown in fig 8 (*b*), the ordinates being the means of the maxima of the two large loops of fig 5

Fig 8 (*c*) refers to a second crystal cut in the (110) plane A complete set of measurements of I_N and I_P were made with this crystal, but the curves are not reproduced owing to close resemblance to those of figs 4 and 5 The chief differences in the two crystals are shown by comparison of fig 8 (*b*) and 8 (*c*) These differences are possibly due to slight distortion or inhomogeneity of the crystals

(111) *Plane* —We have prepared altogether six specimens cut in the (111) plane Great difficulty was experienced in getting any consistent results for this plane The maxima of the perpendicular components are all very small (= 3 units), amounting to only about 10 per cent of the values in the (100) and (110) planes. The majority of the curves showed four unequal loops in 180°, only one crystal showing six loops (as would be expected from symmetry considerations) Two of these loops which were small even at high fields, disappeared completely at low fields (*cf* certain results of Quittner on the (111) plane in magnetite, 'Ann d Phys,' vol 30, p 289 (1909)) Some of the curves obtained with the remaining five crystals showed signs of additional points of inflexion, possibly indicating the beginnings of the development of extra loops

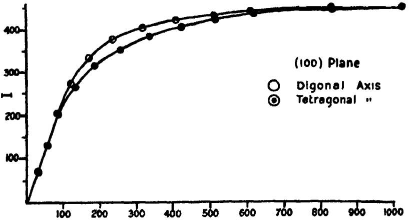

Fig 6

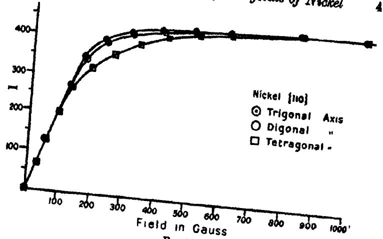

Fig 7

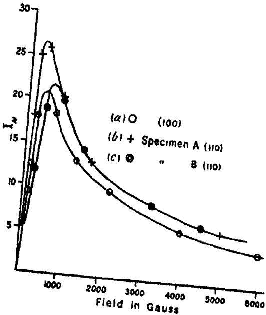

Fig. 8.

Discussion of Results

(100) *Plane*—The results in the (100) plane are similar to those obtained by other experimenters on iron, except that the maxima and quasi-stable positions of the magnetisation are along the digonal axes, and the minima and apparently unstable positions along the tetragonal This is exactly as would be expected

from the crystal structure In the (100) plane of iron the atoms are arranged at the corners of squares the sides of which are along the tetragonal axes (see fig 9 (*a*)) The same is true in the case of nickel except that the sides of the squares are along the digonal axes (see fig 9 (*b*))

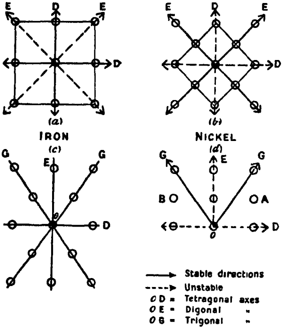

Fig 9

(110) *Plane*—The results in the (110) plane are more interesting on account of the marked difference of the atomic arrangements in the (110) planes of iron and nickel These two arrangements are shown in figs 9 (*c*) and (*d*) In iron the parallel component shows a maximum along the tetragonal, minima along the two trigonal axes, and a subsidiary maximum along the digonal On the other hand, in nickel, I_P shows maxima along the trigonal axes, a minimum along the tetragonal axis, and a subsidiary minimum along the digonal axis In both metals I_N vanishes along the digonal, trigonal and tetragonal axes

In the light of Honda's theory[*] the vanishing of I_N along the trigonal axis in nickel is, at first sight, surprising, as Honda's treatment in its simplest form would lead one to expect this component to vanish along the directions OA, OB This difficulty arises only on account of the treatment being two-dimensional When the problem is considered in three dimensions, it is apparent that owing to the symmetry about the trigonal axes the magnetisation must coincide with the field when the latter is applied along this direction, provided that all the atoms are magnetically similar

---

[*] 'Sci. Rep. Tohoku,' vol 5, p. 153 (1916)

It is noticeable that the maximum value of I_N in the (100) is $4\frac{1}{2}$ per cent, and in the (110) planes about $4\frac{1}{2}$ and 6 per cent of the saturation value of the intensity

In iron ((100) plane) the values vary considerably according to different observers, *e g*, Beck gives $I_{N\,(\max)}/I_{P\,(\max)}$ 14 per cent, Webster for discs A and B obtains 4 per cent and 6 per cent respectively, and Honda 16 per cent

Webster's suggestion that the magnitude of the perpendicular component, and hence the molecular field, is determined by the impurity (particularly by the manganese and phosphorous contents) is hardly borne out by Honda's results The analyses of Honda's specimens and Webster's disc B agree quite closely, especially in percentages of M_n and P, whereas $I_{N\,(\max)}$ is about three times as great in Honda's crystal as in Webster's

The maximum value of I_N in the (111) plane of nickel is less than 1 per cent of the saturation intensity, and this probably accounts for our failure to obtain reasonable curves in this plane Thus the result of any distortion or inhomogeneity would be to superpose an effect which might be large enough to swamp the original perpendicular component The existence of slight rotational hysteresis indicates that the crystals are not perfect

Figs 6 and 7 indicate that the initial susceptibilities are approximately constant and independent of direction in the crystal The actual magnitude is uncertain chiefly owing to the fact that the calculated demagnetising factor is assumed to be that of an oblate spheroid, whereas the specimens are in reality cylindrical discs Furthermore, at low intensities the demagnetising field is large compared with the effective field, and any error in the former has a correspondingly large effect on the latter The (I — H) curves show no sudden changes of slope, such as have been observed by Honda in iron, but this point needs closer investigation, as again error in demagnetising factor may tend to mask any such changes We hope to return to these points later, in connection with magnetostriction in nickel crystals in which the demagnetising factor will be reduced by the use of rods

PART II

This part of the paper is devoted mainly to a criticism of the method employed by Weiss and Webster for the measurement of the component of magnetisation of magnetic crystals parallel to the field The principle of the method is as follows. The crystal is suspended in a vertical plane by a torsion fibre with the magnetic field in the plane of the disc The field H is then rotated out of the plane of the disc by a small angle ϕ and a couple C applied to the suspension so as to bring the crystal back to its original position The condition for equilibrium is given by

$$C = HI_P\, v \sin\phi$$

This assumes that I_P, the parallel component of magnetisation, is in the plane of the disc, whereas it is displaced from this plane by an angle α We shall now show that the linear correction used by Webster for this displacement of I_P is insufficient

Let I_P be the true intensity and suppose it makes an angle α with the plane of the disc (fig 10) Then we have

$$C = HI_P\, v \sin(\phi - \alpha) = HI_P{}'\, v \sin\phi, \tag{1}$$

where $I_P{}'$ is the apparent value of the intensity obtained by assuming that I_P remains in the plane of the disc If ϕ and α are small, we have

$$I_P{}' = I_P\,(1 - \alpha/\phi) \tag{2}$$

We shall at first assume that the crystal is magnetically isotropic and consider the demagnetising coefficients due to shape alone

Let N_1 and N_2 be the demagnetising coefficients in and perpendicular to the plane of the specimen. The effective field perpendicular to the disc is

$$H \sin\phi - N_2 I_P \sin\alpha,$$

and that in the plane of the disc is $H \cos\phi - N_1 I_P \cos\alpha$ The resultant field must be along the direction of I and consequently we have

$$\frac{H \sin\phi - N_2 I_P \sin\alpha}{H \cos\phi - N_1 I_P \cos\alpha} = \frac{\sin\alpha}{\cos\alpha},$$

whence we have

$$H \sin(\phi - \alpha) = \tfrac{1}{2} I_P\,(N_2 - N_1) \sin 2\alpha,$$

or, if ϕ and α are small,*

$$\frac{\alpha}{\phi} = \frac{H}{H + (N_2 - N_1)\, I_P} \tag{3}$$

Substituting in (2) we have

$$I_P{}' = I_P \left\{1 - \frac{H}{H + (N_2 - N_1) I_P}\right\}, \tag{4}$$

or

$$I_P = \tfrac{1}{2} I_P{}' + \sqrt{\frac{I_P{}'^2}{4} + \frac{H\, I_P{}'}{N_2 - N_1}} \tag{5}$$

---

* The magnitude of the angle ϕ varied from 1° to 3° in these experiments.

Above saturation I_P' decreases with increasing field, and so long as H is small compared with $(N_2 - N_1) I_P$, I_P' decreases linearly with increasing H, as is evident from equation (4). For higher values of H, I_P' will fall off less rapidly In iron an approximately linear relation is obtained by Webster up to about 6000 gauss (see Webster, *loc cit*, p 501, graph 1), but in nickel the departure from the linear law is very pronounced on account of the lower value of I_P. We have repeated Webster's curve for the (100) plane in iron, and using fields up to 13,000 gauss, the curvature becomes appreciable In fact, Webster's curve for disc B can be made distinctly concave upwards if the last point (approximately 7700 gauss) is omitted Omitting this point, and redrawing this curve, the saturation value of I_P calculated by means of equation (5) is certainly higher than 1620, probably about 1650 units This is assuming that N_2 and N_1 are calculable from the dimensions of the specimen

The results for nickel are shown in fig 10 Curve (*a*) gives I_P' (along the digonal axis in the (100) plane) as calculated from equation (1), whereas curve (*b*) shows the value of I_P calculated from equation (5) The values of N_2 and N_1 are calculated from the dimensions of the specimen (given above) The values of the field given are not corrected for demagnetising factor, since in equation (5) H is the external field The correction to be applied to I_P' is greater in nickel than in iron on account of the lower saturation intensity in the former Weiss's experiments on normal pyrrhotite (saturation intensity $= 50$ units) do not appear to be seriously affected by the correction on account of the fact that this substance has a pronounced plane of easy magnetisation, from which the vector I is not easily deviated Consequently this correction, which is due to the component of magnetisation normal to the disc is small for specimens cut in this plane

We have so far considered only magnetically isotropic substances Curves (*c*) and (*e*) of fig 10 show the effect of crystalline structure Curve (*c*) gives the value of I_P' along the trigonal axis in the (110) plane plotted against H, whilst (*e*) shows the corresponding values of I_P' along the tetragonal axis Even in the region well beyond saturation, these curves show little signs of approaching one another This means that there is still an apparent variation in the parallel component with orientation of the specimen, whereas the results of the ballistic method (figs 4 and 7) show that there is practically no fluctuations above 1000 gauss

When curve (*c*) is corrected using equation (5) ($N_2 - N_1 = 8\ 6$, which is the value calculated from geometrical considerations), curve (*d*) is obtained Curve (*f*) results from curve (*e*) similarly corrected In the region above saturation

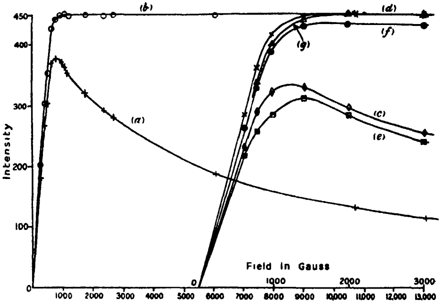

Fig 10.

the divergence between (*f*) and (*d*) can be explained if it is assumed that the crystal structure has an influence on the effective value of the demagnetising factors Thus along the trigonal axis we have

$$I_P' = I_P \{1 - H (H + N'I_P)\},$$

where $N' = N_2 - N_1$, and along the tetragonal axis

$$I_P'' = I_P \{1 - H (H + N''I_P)\}$$

If N'' is put = 7·6, the resultant curve is (*g*) This procedure is equivalent to a decrease = 1·0 in the value of N_2 $I_P' - I_P''$ is easily shown to be a maximum at about 3500 gauss, and then decreases very slowly with increasing field The correction is obviously insufficient in the region just below saturation, where curves (*d*) and (*g*) do not coincide and where the actual atomic grouping would undoubtedly have to be considered

The difference between curves (*c*) and (*e*) might be explained if the specimen were not circular, but it would be necessary to postulate an extraordinary shape The slight irregularities of our specimens were quite inadequate to explain the results Furthermore, curves corresponding to figs 2 and 4 were obtained by the torsion method for both (100) and (110) planes These were of exactly the same shape as those obtained by the ballistic method, but the fluctuations persisted even at the highest fields used, *i e*, about 13,000 gauss, though to a lesser degree in the former plane

An absolute determination of I_P along the trigonal axis of crystal B gave 443 units at saturation, but this value is somewhat unreliable on account of the doubt as to the effective values of the demagnetising coefficients We have shown that quasi-saturation is obtained along the trigonal axis if the value of N′ used is that calculated from the shape, but there appears to be no *a priori* reason why this value of the demagnetising coefficient should need modification for the tetragonal axis and not for the trigonal In all the figures except 3 and 5 a saturation value of 450 units is assumed

It seems possible that a careful investigation of the relations between H and I_P' especially if carried out for a wide range of values of ϕ, might lead to some information as to the nature of the crystal forces

Summary and Conclusions

The magnetic properties of single crystals of nickel have been examined in the principal crystal planes The component of magnetisation parallel to the field was measured by the induction method, whilst the component perpendicular to the field was measured by a torsion method The reason for the use of the induction method is given in Part II of the paper, in which it is shown that the existence of directional properties in the crystal invalidates the use of the torsion method for the measurement of the parallel component

The magnetisation and field coincide along the directions of the symmetry axes, the direction of easiest magnetisation being along the trigonal axis

Our grateful thanks are due to Mr S H Piper for valuable help with X-ray examinations of the crystals We are also indebted to the Colston Research Society of the University of Bristol for a grant towards the expenses of the investigation

The Continuous Absorption of Light in Potassium Vapour

By R W Ditchburn, B A, Trinity College, Cambridge, Isaac Newton Student

(Communicated by Sir J J Thomson —Received August 16, 1927)

1 —Introduction.

While considerable attention has been paid to the line and band absorption of the alkali metals, very little work has been done on the continuous absorption R W Wood* and Holtzmark† have observed the existence of this absorption, and Harrison‡ has made some measurements on the continuous absorption of sodium in the region 2500 Å U -2150 Å U In the present paper, results are given for potassium over a wide range of wave-length (4000 Å U -2200 Å U) and under widely different experimental conditions

The ordinary methods of spectrophotometry have usually been designed to measure the absorption of solutions, etc , and are not suitable for measuring the absorption in a vapour unless the vapour pressure can be kept absolutely constant A method of spectrophotometry has been developed by which it is possible to obtain measurements of the relative absorption coefficients for different wave-lengths correct to about 2 per cent without keeping the vapour pressure absolutely constant While the method is specially suitable for the measurement of an absorption which is not quite steady, it is really of quite general application

The main features of the results can be explained on the view that the measured absorption is the sum of the absorption due to the potassium atom and that due to the molecule

2 —Experimental

(a) *The Optical System*

With a constant source of ultra-violet light the very simple optical system shown in fig. 1 may be used The light from the source D is collimated by a lens L_1, passes as a parallel beam through the tube T and a reducing sector S, and is focussed on the slit of the quartz prism spectrograph G by a lens L_2

---

* 'Astroph. J ,' vol. 29, p 97

† 'Phys. Z.,' vol. 20, p. 88.

‡ 'Phys. Rev ,' vol. 24, p. 466.

The source of light is a hydrogen capillary discharge tube viewed end on through a quartz window The reducing sector is of a type which reduces the intensity

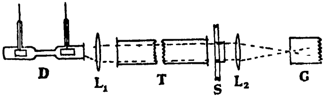

FIG 1 —Optical System

of the light and not the exposure time More details of the source of light and of the reducing sector are given in another paper *

The order of experiment is as follows The sector is opened to its maximum aperture and photographs are taken (*a*) with the absorption tube cold, (*b*) with it hot and thus filled with metallic vapour, (*c*) with it cold again A series of photographs is then taken with the intensity reduced in known ratios by altering the angle of the sector These serve to calibrate the plates and are photometrically compared with the absorption spectrum

(*b*) *The Absorption Tubes*

The alkali metal is vaporised in a steel tube whose ends are water-cooled A filling gas (nitrogen or argon) prevents the metal from distilling over too rapidly For about half of the experiments a short tube (shown in fig 2A) was

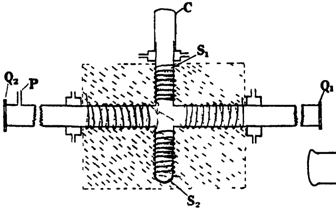

FIG 2A. Absorption Tubes.

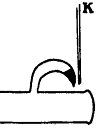

FIG 2B.

used This had two side tubes, S_1 and S_2, welded to the main tube The end of S_2 is permanently closed by a welded steel cap. The potassium is introduced through S_1 and allowed to drop into the tube S_2 from which it can be distilled into the main tube S_1 was closed by a glass cap C, which is waxed on to the water cooler Q_1 and Q_2 are quartz windows

---

* 'Proc Camb Phil Soc,' vol. 23, p. 959.

Each side tube and each branch of the main tube has separate nichrome heating coils, which are insulated from the steel tubing by thin layers of mica and heavily lagged with asbestos The side tube P is connected to the vacuum apparatus by a short piece of rubber tubing, which gives a little freedom of movement when focussing the light down the tube The tube is about 70 cms long and 2 5 cms internal diameter In order to prevent a deposit forming on the window it was found necessary to have about 20 cms of cold tube between the water coolers and the windows Thus the length of the column of vapour is only 16 cms

When it became desirable to measure the absorption for very low vapour pressures another tube was made This is over 2 metres long, giving a column of vapour of about 160 cms It has only one side tube and the potassium is introduced straight into the main tube

(c) *The Manipulation of the Metal*

When it is not necessary to have the metal very pure, it is sufficient to scrape off the outer layer of oxide and wash it two or three times in ether which contains a few per cent of alcohol This removes the oil in which the metal is stored and most of the remaining oxide The metal is then dropped into the tube through S_1, the cap is fixed on and the tube evacuated as quickly as possible

To obtain really pure potassium vapour more elaborate methods have to be used The metal is first washed, then filtered and distilled several times *in vacuo* It is finally distilled into a tube of about 5 mm diameter with a narrow neck The neck of this tube is broken under ether just before the tube is put into the main tube Thus only a minute surface has any chance of coming into contact with the air and this is partly protected by the ether

The extra purification of the metal has not been found to produce any appreciable difference in the results, and for most purposes the first crude method is good enough

(d) *The Photometer*

The microphotometer used is of the photo-electric type The density of a small slit area of the plate is compared with that of a standard wedge by allowing the light to pass alternately through the plate and the wedge to a photo-electric cell

(e) *Order of Measurements*

The plate has 10 or 11 spectra of which 4 or 5 are absorption spectra and the rest are taken for calibration purposes The order of measurement is as follows —

(1) The clear plate is measured at about half a dozen places just on the lower side of spectrum (1)

(2) Spectrum (1) is measured at intervals of about a millimetre over the range of wave-lengths being investigated If spectrum (1) is an absorption spectrum, extra readings are taken in the region of the series-limit Distances along the spectrum are measured by reference to the position of a standard line (usually Hβ or Hγ)

(3) The clear plate is measured at half a dozen places midway between spectrum (1) and spectrum (2)

(4) Spectrum (2) is measured as spectrum (1) and so on

(*f*) *Method of Calculation*

To deduce the absorption coefficient we now proceed in the following way —

(1) Curves are drawn for the density of the clear plate at points between the spectra

(2) From every density reading on a spectrum is subtracted the mean of the densities of the clear plate on the two sides of it

(3) For each spectrum the corrected density readings are plotted against the distance from the standard line A set of these are shown in fig 3 Curves (i) to (vi) are calibration curves and curves (vii) and (viii) are absorption curves In curve (vii) the line absorption is indicated by dotted lines, but to avoid confusion it is omitted from curve (viii) and also from all the absorption curves in figs 5–9

(4) Calibration curves are now plotted for different wave-lengths (fig 4) This is done by taking the ordinates at a given abscissa on fig 3 and plotting them against the logarithms of the corresponding intensities

(5) Using the ordinates of curve (vii) or (viii), fig 3, the logarithms of the percentage transmission may now be read off from fig 4

(6) In order to obtain the relative absorption coefficients we proceed in the following way.—

If T = percentage transmission

N_1 = number of atoms per cubic centimetre

d = thickness of absorbing layer

α = atomic absorption coefficient

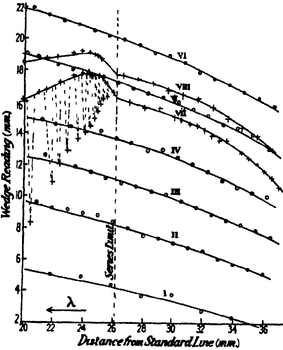

FIG 3 —Density Curves.

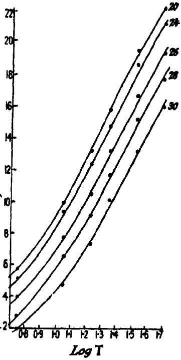

FIG 4 —Calibration Curves.

Then

$$T/100 = e^{-\alpha N_1 d}$$

$$2 - \log_{10} T = C\,\alpha = \alpha' \qquad (1)$$

where C is a quantity which does not vary with the wave-length

Thus α' ($= 2 - \log T$) is plotted against wave-length in the curves which show the variation of the absorption coefficient with wave-length (figs 5–8)

(*g*) *Experimental Errors*

An estimate of the accuracy of the method from the consistency of the measurements would be misleading, but by the methods described below it is possible to make the errors non-systematic and to estimate their magnitude

(1) *Photometric errors* —The error in individual density readings can be made less than a half per cent except when the density is very low or very high The estimation of the absorption coefficient depends on the difference of two density measurements When the absorption coefficient (on the scale plotted) is between 0 4 and 1 0 units, 60 per cent to 90 per cent of the light is being absorbed and the difference is so large that the error in the absorption coefficient

should not be much more than 1 per cent To test the size of these errors directly one plate was measured twice In the second set of measurements the slit-width and all the other adjustments of the photometer were altered considerably In order to exaggerate the error the adjustments of the photometer were altered and reset in the middle of the second series of measurements (This is never done in the ordinary measurements) The maximum separation of the absorption curves was 3 per cent , the average error being much less Thus under the usual conditions of measurement it seems reasonable to assess the photometric error at about 1 per cent When the coefficient is less than 0 3 the percentage error will increase It will also be somewhat greater for wavelengths less than λ 2350, because owing to the reduced sensitivity of the plate this region is usually of low density

(2) ***The unevenness of the plate*** —The unevenness of the plate causes three different types of errors, (*a*) small local variations with a " probability distribution," due principally to the fact that the plate is grained and not continuous , (*b*) variations due to uneven development, and (*c*) variations due to uneven thickness of the gelatine, etc Types (*b*) and (*c*) cause differences in density between points which have received equal exposure The size of the differences increases rapidly as the distance between the points to be compared increases, and is particularly great if one point happens to be near the edge of the plate

Errors of the type (*a*) are enormously reduced by using a process plate (with a fine grain) and a suitable developer The curve drawn in fig 3 effectively averages out these errors It will be seen from the curves that the departure of points from the line is really quite small and that there is never any doubt about where to draw the curve

Plate variations of the type (*b*) are much more serious than those of type (*a*), because they might introduce systematic errors into the absorption curves which would not be detected in calculation These errors are only partially compensated by subtracting the density of the neighbouring clear plate from the measured densities The variations are reduced by brushing the negative vigorously during development with a camel's-hair brush A few of the later plates were developed in a tank described by Dobson, Griffiths and Harrison* in which a plunger drives the developer across the plate at high speed Too little work was done with this type of development to see how much improvement was obtained.

Strictly speaking all the calibration spectra are compared with every absorption spectrum, because they are all used in drawing the calibration curves from which the transmission is read off In the neighbourhood of a given density, however, the configuration of a calibration curve is mainly controlled by the densities of two of the calibration spectra (i e, the one whose density is immediately above and the one whose density is immediately below the density in question) Thus in reading from the calibration curve one is really interpolating the density of the absorption spectrum between those of two of the calibration spectra, the other calibration spectra are being used only to make a more accurate interpolation than would be given by taking proportional parts For this reason it is desirable to arrange the spectra on the plate so that an absorption spectrum lies as near as possible to the two calibration spectra with which it is being most directly compared If this is done the points whose densities are being compared lie close together on the plate and errors of types (*b*) and (*c*) are very much reduced

---

* ' Photometric Photometry,' Ch. 5.

If the calibration spectra were arranged on the plate in some systematic way (*e g*, so that all those of high intensity were near the edges of the plate), a systematic error might be introduced into the curves For this reason the order is made unsystematic and no spectrum is placed very near the edge

With a view to reducing plate variations and also to increase the sensitiveness of the plate in the region 2350 Å U -2100 Å U some of the plates were subjected to a little prefogging, but no real improvement was obtained The gradient of the calibration curves for these wave-lengths is not steep over any range of densities, probably because the absorption of the gelatine is so strong that only a thin layer of silver bromide is effective Since the prefogging made the densities rather high in the 3500 Å U -4000 Å U it was not generally employed

Under the best conditions the magnitude of these two kinds of photographic errors can be made less than 1 per cent Under average conditions they are probably 2 to 3 per cent A few plates exhibited larger variation—these were rejected It does not seem to be possible to get more accurate measurements without the use of special plates

(3) *Errors due to variation of source*—If the source varied arbitrarily the calibration curves would not be smooth Some of the early experiments were spoilt by sudden variations of the source, but with the source finally used no trouble was experienced from this cause In taking the spectra of reduced intensity, large sector angles and small sector angles were used alternately. If the calibration spectra had been taken in order, from the strongest to the weakest, a systematic error might have been introduced by a continuous increase or decrease of the intensity of the course

(4) *Errors in the setting of the sector and in the timing of exposures*—These may be neglected in comparison with other experimental errors

Thus the total error is nearly all photographic and is about 2 to 3 per cent, except for absorptions of less than 0 3 or wave-lengths less than 2350 A U

(*h*) *Absorption due to Impurities*

The question of absorption due to impurities needs careful consideration. It may be seen quite simply that spurious absorption due to impurities is not likely unless there is an impurity whose vapour pressure is of the same order as that of potassium Anything which absorbs equally when the tube is hot and when it is cold does not affect the absorption curves, but merely reduces the effective intensity of the source of light Thus any impurity whose vapour pressure is much greater than that of the potassium would quickly boil over into the cold part of the tube where it would be ineffective Any impurity whose vapour pressure is much less than that of the potassium will have no effect because its molecules never get into the vapour state Direct tests have been made for absorption due to (1) the oil in which the potassium is stored, (2) a compound such as potassium nitride, (3) mercury or a mercury-potassium molecule, (4) a film deposited on the quartz windows In every case the result of the test was satisfactory

Sodium is really the only impurity which is at all likely to be causing trouble The sodium lines were seen on all absorption spectra except those corresponding to small amounts of absorption, but they were much weaker than the corresponding potassium lines If the sodium and potassium are present in proportion to their vapour pressures the proportion of the former would be about 5 per cent Attempts were made to reduce the proportion of sodium present by repeatedly distilling the potassium These were not successful probably because the percentage of sodium in the vapour would remain unaltered so long as there was any liquid sodium present in the tube, *i e*, so long as the vapour was saturated Thus the amount of sodium in the vapour would not begin to be affected till the amount present in the potassium had been reduced below 1 in 10^4 The sodium atoms should not have any absorption for wave-lengths much greater than 2413 A U (the sodium series-limit), and one would expect some change in the absorption at this point No such change is found even in those curves where the change at the potassium limit is strongest

The above considerations show that it is unlikely that much of the absorption is caused by impurities, but since it is very difficult to prove a negative proposition, the following positive argument may be regarded as more satisfactory.

The absorption at the potassium lines is certainly proportional to the number of potassium atoms present (when the pressure of the filling gas is unaltered) As will be shown below it is to be expected that when the vapour pressure is increased by slightly increasing the temperature, the number of molecules will increase more rapidly than the number of atoms Thus if the continuous absorption is due to potassium molecules and atoms, we should expect it to increase somewhat more rapidly than the line absorption (in experiments where the pressure of the filling gas is constant) and this is found to be the case

(i) *Approximate values of the atomic absorption coefficients*

The method described above gives only relative absorption coefficients since we do not know the pressure of the absorbing vapour It is possible to obtain approximate values for the mass absorption coefficients if we assume that the line absorption (*i e*, the integrated absorption over a series-line) is always proportional to the number of atoms present By heating a little potassium in an evacuated glass bulb to a known temperature the line absorption coefficient at the 4044 doublet may be determined, the vapour pressure being calculated from the temperature * A bulb of the form shown in fig 2B was heated in an electric furnace Temperatures were measured by a thermo-couple K, placed up against the part of the tube which contained the liquid potassium In order to avoid temperature differences, which might be caused by currents of cold air from outside, the holes in the furnace wall through which the light passed were closed with quartz windows

The difficulty of the method is almost all due to the rapidity with which the potassium attacks the glass Preliminary purification seemed to reduce the speed of the reaction, and it was hoped that careful distillation might overcome the trouble When, however, the potassium had been distilled several times, the bulb into which it was finally distilled having been outgassed for several hours at a very high vacuum, it was found that there was no improvement whatever The action seemed to be rather more rapid than with a bulb that had not been outgassed Under the action of the vapour the glass becomes opaque to ultra-violet light even before it ceases to transmit the visible This made it impossible to make any measurements on the 3446 doublet The rapid action of the metal on the glass made it impossible to obtain any measurements on the continuous absorption of the vapour, but the depth and width of the absorption line could be determined by taking the difference between it and the surrounding continuous spectrum The absorption of 4044 for a known number of atoms is thus obtained, and if we wish to know the effective number of atoms for one of the experiments in the iron tube it is only necessary to measure the 4044 absorption This cannot be done accurately because the 4044 line is too near to some of the lines in the source and also because in most of the iron-tube experiments the 4044 absorption is too big to measure, the plate being "clear" at the centre of the line The lowest 4044 absorptions in the iron tube are just comparable with the highest in the glass tube For this reason the value obtained is only an approximate one and is more likely to be too high than too low

---

* Using the vapour pressure measurements of Kroner 'Ann. d. Physik,' vol. 40, p. 438 (1913).

3 —RESULTS

The results are represented in figs 5–8 by curves of relative absorption coefficient α' (as defined on p 490 above) against wave-length The percentage of light transmitted at any wave-length may be obtained by taking the antilogarithm of $(2 - \alpha')$ For experiments in the short tube the vapour pressure measured in millimetres of mercury is numerically about 10 times the value of α' at the series-limit For experiments with the long tube it is about 10 times less for the same amount of absorption

Details of conditions under which the curves were obtained are inserted on the graphs

Before discussing the possibility of separating the molecular and atomic

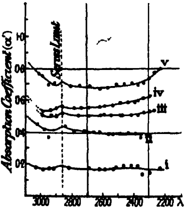

FIG 5.—Absorption Curves. Short Tube. Filling Gas: i, ii, iii, Ar, 26 cms.; iv, v, N_2, 24 cms.

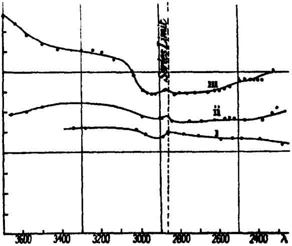

FIG 6—Absorption Curves. Short Tube. Filling Gas. N_2, 90 cms.

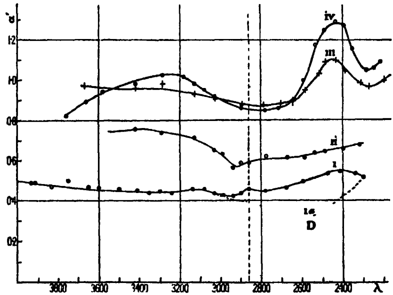

Fig 7.—Absorption Curves. Long Tube Filling Gas i, N_2, 50 cms., ii, iii, iv, N_2, 70 cms.

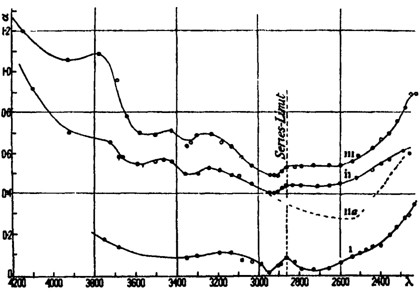

Fig. 8.—Absorption Curves. Long Tube. Filling Gas i, N_2, 1·3 cms., ii, iii, N_2, 3 cms.

absorption, it may be well to call attention to the changes in the experimental curves caused by changes of the vapour pressure of potassium, the pressure of the filling gas and the temperature

Comparing the different curves of fig. 5 we see that practically no change in absorption is caused by varying the vapour pressure by a factor of 3 (from about 2 to about 7 mms) and the curves obtained with nitrogen are essentially the same as those obtained with argon Comparing the curves of fig 6 among themselves, we see that for a high pressure of the filling gas and a high vapour pressure the absorption increases on both sides of the series-limit, but more on the long wave-length side For lower vapour pressures it is approximately constant from 3400 Å U to 2300 Å U Comparing the curves of fig 6 with those of fig 5 it may be seen that when the pressure of the filling gas is already high a further increase produces only minor differences

Turning now to the experiments with the long tube (and remembering that in all these the vapour pressure is about 10 times lower than that for the same amount of absorption in the short tube), we see from curve (i) of fig 7 that when the pressure of the filling gas is high and the vapour pressure low the absorption varies very little with wave-length Curve (ii) shows that when the vapour pressure is raised (the pressure of the filling gas being high) the absorption increases on both sides of the series-limit but more rapidly on the long wave-length side In the experiments, whose results are shown in fig 8, the pressure of the filling gas was made very low (1 3 cms for curve (i), 3 cms for curves (ii) and (iii)) With lower pressures the potassium distils over so rapidly that it is impossible to keep sufficient atoms in the path of the light to produce any measurable absorption These curves show marked differences from all the previous curves The absorption increases rapidly on both sides of the limit and now the increase on the short wave-length side is much more rapid than that on the long wave-length side A number of subsidiary maxima appear and the size of these increases very rapidly when the vapour pressure is increased, *i e*, when the temperature is raised The exact condition producing these maxima and the maxima in curves (iii) and (iv) of fig 7 is not completely understood It seems probable that at the temperatures usually employed they are too small to be detected—so that they are seen only when some part of the tube is at a high temperature (600° C or more) In the case of the experiments shown in fig 8, where the pressure of the filling gas was low, the temperature had to be raised to maintain the necessary vapour density In the case of the experiments shown in curves (iii) and (iv) of fig 7, the temperature of the ends of the tube was made high for the purpose of bringing out this effect The most remarkable thing about it is the comparatively small difference between the conditions when it can scarcely be detected and the conditions when it is strong It is as though it "appeared" at a certain temperature These maxima are possibly due to absorption by molecules which are not in the normal state * It may be that the steel wall has some catalytic effect on the action which produces these molecules, but the whole effect is exceedingly complex and does not at present seem likely to repay investigation

In all the curves there is a shallow minimum a little on the long wave-length side of the series-limit and a change of slope at the limit This feature is, however, very inconspicuous at high pressures of the filling gas and only becomes really prominent in fig 8 It is worth noting that even in curve (i), fig 8, the pressure of the foreign gas is over 100 times greater than the vapour pressure of the potassium It is undoubtedly desirable to have results for lower pressures of the filling gas, in fact for the case of potassium in vacuum These could only be obtained in a quartz bulb, and to use this some method must be found of completely preventing the potassium from attacking the quartz It would be possible to get results for higher pressures of the filling gas, but the difference between the results for pressures of 26 cms and 90 cms is so small that it does not seem likely that anything interesting would be obtained by a further increase to, say, 10-atmospheres

4 —INTERPRETATION OF RESULTS

An attempt has been made to separate the atomic and molecular absorption on the assumption that the molecular absorption is directly proportional to the molecular concentration and the atomic absorption to the atomic concentration

Let Mρ be the molecular absorption coefficient for amolec ular concentration, M and Nσ the atomic coefficient for an atomic concentration N, and consider two experiments in which the atomic concentrations are N_1, N_2 and the molecular concentrations M_1, M_2 respectively Let α_1 and α_2 be the measured absorption coefficients

[α_1, α_2, ρ, σ all refer to one and the same wave-length]

Then we have

$$\left.\begin{array}{l} N_1\sigma + M_1\rho = \alpha_1 \\ N_2\sigma + M_2\rho = \alpha_2 \end{array}\right\}. \tag{1}$$

The solution of these two simultaneous equations for ρ and σ may be written

$$= \frac{1}{N_1(1 - g/f)}[g\alpha_1 - \alpha_2] \tag{2}$$

$$= \frac{1}{M_1(1 - f/g)}[\alpha_1 - f\alpha_2] \tag{3}$$

where $f = N_1/N_2$ and $g = M_1/M_2$

---

* Smith ('Roy Soc Proc,' vol. 106, p. 400) analyses the sodium band absorption and shows that the absorbing molecules have not all the same initial moment of inertia.

Thus it is possible to obtain curves showing the variation of ρ and σ provided f and g are known and that f/g is not too nearly unity The value of f may be determined by comparing the line absorptions and that of g by comparing the continuous absorption at wave-lengths considerably on the long wave-length side of the series-limit since the absorption in that region should be nearly all molecular.

After the separation has been made it is possible to check the assumptions on which it was founded This is done by obtaining two molecular curves by subtracting the atomic absorption from the two experimental curves If the assumptions are correct the ordinates of the two molecular curves should bear a constant ratio (equal to g) for all different wave-lengths If this condition is not fulfilled the method of separation has failed and the " difference " curves are meaningless

Since both the molecular and atomic absorptions are affected by changes in the pressure of the filling gas, the method is applicable only to pairs of curves obtained with the same pressure When applied to such curves the test shows that in general the assumptions are not justified This is probably because some of the molecules are not in the normal state For a few pairs of curves, however, the test is approximately satisfied, suggesting that in these experiments the absorption due to the normal molecule is predominant

Even though a satisfactory quantitative separation is not possible, one can distinguish the main features of the molecular and atomic absorptions by considering the progressive differences between the results of experiments done under conditions favourable to the production of molecules and of those done under conditions favourable to the production of atoms In this way it is possible to get definite results from the molecular absorption, because conditions are available under which 90 per cent of the whole absorption is due to molecules The atomic absorption cannot be so definitely distinguished because the atomic absorption is never more than 50 per cent of the whole

The Atomic Absorption

Theoretically the atomic absorption has been calculated by Kramers,* Milne,† Becker‡ and Oppenheimer § Kramers' theory was worked out for the X-ray case and contains approximations which make it inapplicable to the optical case The theories of Becker and Milne are similar in that they both use statistical thermodynamics and the principle of detailed balancing to establish a relation between the series-limit absorption and the probability of capture of an electron by an ionised atom The difference in their estimates of their probability of capture leads to different absorption curves Both estimates of capture probability are invalidated by later work, and consequently the results for the series-limit absorption are also invalidated Oppenheimer's theory is based on Schrödinger's wave-mechanics and is worked out for a hydrogen-like atom It gives good agreement in the X-ray region and might be expected to be approximately true for the optical series-limits of the alkali metals It takes no account, however, of the possibility of the absorbing atom being disturbed by neighbouring atoms Thus if there are differences between experimental curves for high and low pressures it might be expected to agree better with the latter The curve predicted by this theory is shown in fig 9 (curve (i)) The continuous absorption starts on the long wave-length side of the series limit and increases to a maximum at the limit where there is a discontinuous change of gradient (but no discontinuous change of magnitude), on the short wave-length side it is approximately proportional to $\lambda^{5/2}$ The absorption value of the atomic absorption coefficient at the limit is $10^{-12}\,\lambda$, i e, 2×10^{-17}

---

* 'Phil. Mag.,' vol. 44, p. 836 (1922).

† 'Phil. Mag.,' vol 47, p. 209 (1924).

‡ 'Z f Physik,' vol. 18, p. 325 (1923).

§ 'Z. f Physik,' vol. 41, p. 268 (1927).

The experimental curve taken under the best conditions for comparison with the theory is curve (i), fig 7, where the pressure of the filling gas is very low and where the vapour pressure is also low, thus favouring the existence of a large proportion of atoms Two " atomic curves " obtained by applying the method of separation described above are shown in fig 9, curves (ii) and (iii) Curve (iii) is obtained by the separation of two curves with 60 cms and curve (ii) by the separation of two curves with 3 cms of filling gas present Comparison of these curves (and others) seems to suggest that, at low pressures, the atomic absorption starts on the long wave-length side of the limit, increases to a maximum at the limit and then decreases to about 2700 Å U where there is minimum and increases again to about 2400 Å U The effect of increasing the pressure seems to be to smooth out the maximum at the limit and the minimum at 2700 Å U, so that at high pressures the atomic absorption increases continuously from 3000 Å U to 2400 Å U

The observed curve for low pressures disagrees with the theoretical curve for wave-lengths shorter than 2700 Å U It is quite possible that the molecular and atomic curves have not been correctly separated and that the increase of absorption on the short wave-length side of 2700 Å U is all due to molecules. If this is so it is difficult to explain why the rate of increase is greatest when the vapour pressure is least That there is some essential difference between the case theoretically considered and that experimentally worked out is shown

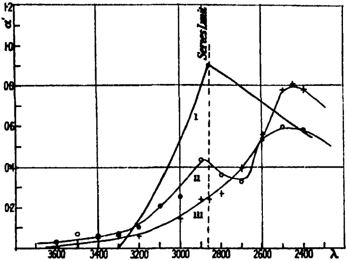

FIG 9—Atomic Absorption. Curve I, Theoretical, II, Atomic Curve (Low Pressure), III, Atomic Curve (High Pressure)

by comparison of the absolute values for the atomic absorption coefficient at the series-limit The theoretical value is of the order 10^{-17}, the experimental, 10^{-19} As has been already stated the experimental value is more likely to be too high than too low Even if the separation of molecular and atomic absorption is completely wrong and all the absorption is due to the atoms there is still a discrepancy of a factor of 40 In this connection it may be noted that Foote, Mohler and Chenault* deduce a value 10^{-18} for sodium from Harrison's† experiments, while the writer has derived the value 10^{-24} for cæsium from the photoionisation experiment of Little ‡ These results show that there is an increasing departure from the theory as the atomic weight increases This suggests that the discrepancy is really due to some fundamental distinction between the "hydrogen like" atom and the alkali metals A calculation by Sugiura§ shows large and unexpected differences between sodium and hydrogen line absorptions

On the other hand it is also possible that the difference may be due to a perturbation by other potassium atoms The work of Datta|| has shown that the

---

* 'Phys. Rev,' vol. 27, p. 37 (1926)

† 'Phys. Rev,' vol 24, p. 466 (1924)

‡ 'Phys. Rev,' vol. 28, p 848 (1926)

§ 'Phil. Mag,' vol. 4, p. 495 (1927)

|| 'Z f. Phys.,' vol. 37, p. 625 (1926)

polarisation of the resonance radiation is destroyed by other potassium atoms coming with a distance of 10^{-4} cms Under the conditions of the present experiment the mean distance apart of the atoms is only 10^{-6} cms , so that a serious perturbation is quite possible

[*Note added October* 20 —It has been suggested to the writer that the difference might be explained if the absorbed radiation were partially or wholly re-emitted The transmission of radiation through the vapour would then be analogous to Schuster's investigation of " radiation through a foggy atmosphere "* Under these conditions the radiation would be reduced by a factor $(1 + N_1\alpha d)^{-1}$ instead of $e^{-N_1\alpha d}$ in traversing a thickness d of the vapour Since in the present experiments $N_1\alpha d$ is never much greater than unity, the difference between the two factors is never greater than 50 per cent Thus, even if all the absorbed radiation were re-emitted and if Schuster's conditions obtained, only a small portion of the discrepancy would be explained But the conditions of the present experiments are much less favourable to the transmission of the re-emitted radiation than the conditions of Schuster's investigation, since in the narrow tube nearly all the re-emitted radiation must strike the walls of the tube Most of the radiation which strikes the wall of the tube is absorbed, and of the small fraction which is diffusely reflected the majority must strike the wall again and be absorbed Thus practically all the light which strikes the wall of the tube is lost from the beam The effect of re-emission in the present case may be conveniently calculated by using an investigation on the transmission of γ-rays through matter † It is there shown that if β is the absorption coefficient and h is the fraction of the absorbed radiation which is re-emitted, then the intensity of radiation after passing through a thickness d is

$$I = \frac{2\,I_0\gamma\delta}{(\beta - \tfrac{1}{2}h + \gamma)e^{\gamma d} - (\beta - \tfrac{1}{2}h - \gamma)e^{-\gamma d}}$$

where

$$\gamma = \sqrt{\beta(\beta - h)}$$

In the present case it is necessary to put $h =$ the fraction of radiation re-emitted within the solid angle subtended by the extreme end of the tube at a point in the vapour Assuming that all the radiation is re-emitted in arbitrary directions, h is then of the order 1 per cent and the above expression may be simplified so that $I = I_0\,e^{-(\beta - \frac{1}{2}h)d}$ to a good approximation. Putting in the value of h from the geometry of the apparatus it is found that the effect on the absorption coefficient is never greater than 0 3 per cent and is usually much less

---

* Schuster, 'Ap. J ,' vol. 21, p. 1 (1905)

† J J Thomson, 'Discharge through Gases,' p. 406 (1906 edn.).

It may be worth while to state that a direct test showed that the vapour is not emitting any appreciable amount of light at the temperatures used]

Molecular Absorption

For wave-lengths greater than 3100 Å U there is no continuous absorption by the atom, and the experimental curve must be regarded as a curve of molecular absorption For shorter wave-lengths the form of the curve is shown by the dotted portions of curve (i), fig 7, and curve (ii), fig 8 The absorption in this region decreases with decreasing wave-length to about 2500 Å U. where there is probably a discontinuous change of slope For shorter wave-lengths the absorption increases and probably reaches a maximum for some wave-length a little shorter than 2200 Å U The effect of increasing the pressure of the filling gas is to smooth out the curves The subsidiary maxima disappear and the general trend of the curve becomes much more nearly parallel to the axis of wave-length

The exact wave-length of the change of gradient (marked D on curve (i*a*), fig 7) is not quite certain because it depends on the separation of the molecular and atomic absorptions, but the general form of the curve is not subject to this uncertainty

The explanation of the continuous molecular absorption is suggested by some experiments on the photo-electric effect in potassium described by Lawrence [*] The results of these experiments give the relative numbers of ions produced by light of unity intensity and different wave-lengths There is a photo-electric threshold at 2600 Å U and for frequencies greater than the threshold frequency the efficiency of ionisation increases with decreasing wave-length. These photoionisation results may be explained equally well if the ionisation is due to any of the transitions

$$K_2 \rightarrow K^+ + K^- \qquad (1)$$

$$K_2 \rightarrow K_2^+ + \epsilon \qquad (2)$$

$$K_2 \rightarrow K^+ + K + \epsilon \qquad (3)$$

If the third of these is the correct explanation, as Lawrence asumes, the difference between the molecular and atomic thresholds gives the energy required to dissociate the molecule into two neutral atoms This energy according to Lawrence is about 0 4 volts [†]

---

[*] 'Phil. Mag.,' vol. 50, p. 345 (1925)

[†] Owing to the fact that Lawrence was unable to use strictly monochromatic light this value is subject to a small correction of about + 0 1 volt.

The increase of absorption at about 2500 Å U. is thus due to processes which ionise the molecule The continuous absorption on the long wave-length side of the molecular photo-electric threshold may be adequately explained as being due to processes which split the molecule into two atoms, one in the normal and one in an excited state The energy necessary for such a transition is equal to $E_n + E_d$ where E_d is the energy of dissociation and E_n is the difference of energy between the *n*th atomic state and the normal state If the quantum absorbed possesses more energy than $E_n + E_d$ the extra amount is used up as kinetic energy of the dissociated atoms and thus truly continuous absorption is possible * If this explanation is correct we shall expect to have a series of absorption thresholds at wave-lengths corresponding to E_d, $(E_d + E_2)$, $(E_d + E_3)$ $(E_d + E_i)$, where E_i is the energy necessary to ionise the atom E_d is situated at about 24,000 Å U so that no measurements are possible in this region. $(E_d + E_2)$ is about 5800 Å U and some measurements of absorption were made in this region to see whether there was any change in the gradient of the absorption curve at this point A sharp increase is found at 5820 Å U It is worth noting that there is some continuous absorption on the long wave-length side of 5820 Å U, so that dissociation by light of the molecule K_2 into two normal atoms is apparently possible Changes in absorption might be expected at 3447 Å U, 3020 Å U 2555 Å U, corresponding to $E_d + E_3$, $E_d + E_4$, $E_d + E_1$ None of these can be identified with certainty (except 2555 Å U) probably because they are weaker and a small change of gradient is not easily distinguished in the presence of the series-lines and the faint bands which accompany them The increase at 2550 Å U is clearly seen but is not so sharp as the one at 5820 Å U This is to be expected since the threshold at 2550 Å U is really the limit of a converging series of thresholds The value of the dissociation energy obtained from the difference between 5820 Å U and the first excited state of the potassium atom gives the best determination of the value of the dissociation energy The value thus obtained (0 51 volt) is used below in the calculation of the fraction of atoms associated

This explanation of the molecular absorption suggests that the molecule is ionised into one neutral atom, one ionised atom and one electron, *i e*, that the third type of transition (described above) really takes place A direct experiment to determine the form of the ion is desirable

---

* Franck, Kuhn and Rollefsen have recently published work on silver-iodide, sodium-chloride, etc., for which a similar explanation is given. ('Z. f. Phys.,' vol. 43, p. 155 and p. 164).

A Fluorescence Experiment

When the molecule has been dissociated into one normal and one excited atom the latter must return to its normal state either by collision or by radiation Thus, if the pressure is low enough, the continuous absorption of wave-lengths shorter than 5820 Å U should lead to the fluorescent emission of the first doublet of the series Some difficulty might be anticipated in making the observation, because at very low vapour pressures there is too little absorption and at higher vapour pressures the fluorescence would be quenched by collisions with other atoms and molecules Since the first potassium doublet is in the infra-red it was decided to look for the analogous effect in sodium, *i e*, D line fluorescence as a result of stimulation in the region 5000 Å U → 3500 Å U

An absorption tube similar to the one shown in fig 2A, but of a larger diameter, was adapted for the observation of the fluorescence A pointolite was used as source Direct stimulation was prevented by passing the light through a column of sodium vapour in an auxiliary tube and so removing the D lines (and the 3303 doublet) without seriously reducing its intensity in the region 5000 Å U – 3000 Å U After a few preliminary trials, the effect was quite definitely observed When the pump was kept running so that the pressure due to the occluded gas was kept down to about 0 1 mm the D lines could be clearly seen, and there was a dark patch in the spectrum between them and the green bands When the pressure was allowed to increase, however, band (or continuous) fluorescence appeared in the yellow so that the D lines could no longer be distinguished For higher pressures still, only the green bands could be seen

The above experiment shows the existence of excited atoms due to molecular absorption These may be produced either by the direct dissociation of the molecule by radiation (as we have assumed above) or by the molecule being excited by radiation and then dissociated by a collision of the second kind A calculation based on collision frequencies indicates that while the second process is possible it is probably not the effective mechanism

Proportion of Molecules in the Vapour

The value obtained for the energy of dissociation of the molecule (together with other known constants) enables us to calculate the fraction of atoms associated under different conditions of temperature and vapour pressure The method employed is the method of partitions derived in the most general way by Fowler [*] Neglecting the vibrational states of the molecule and states of the atom other than the normal state we obtain the dissociation equation :

$$\frac{C_m}{C_a^2} = \frac{4\pi^{\frac{1}{2}} h R^2}{(mkT)^{\frac{1}{2}}} e^{U_0/kT} \tag{1}$$

Where C_m and C_a are the molecular and atomic concentrations, R is the radius of gyration of the potassium molecule,[†] U_0 is the energy of dissociation in ergs per molecule and the other symbols have their usual meanings Since only a small fraction of the molecules is associated we may put

$$C_a = N\frac{273}{T} \frac{p}{760} \tag{2}$$

where p is the vapour pressure in millimetres Hg

N is the number of molecules per cubic centimetre at S T P

From (1) and (2) we have

$$\text{Fraction associated} = \gamma = \frac{4\pi^{\frac{1}{2}} h R^2}{(mkT)^{\frac{1}{2}}} \frac{N}{T} \frac{273}{760} p e^{U_0/kT} \tag{3}$$

or

$$\log_{10}\gamma = A - 1\cdot 5 \log_{10} T + \frac{U_0}{2\cdot 3\, kT} + \log_{10} p \tag{3}$$

The variation of γ with T may best be seen by using the vapour pressure equation

$$\log_{10} p = -\frac{\lambda_0}{2\cdot 3kT} + B\log_{10} T + \iota \tag{4}$$

(where λ_0 = latent heat of vaporisation as $T \rightarrow 0$ and A, ι are constants) This gives with (3) the equation

$$\log_{10}\gamma = (A + \iota) + (B - 1\cdot 5)\log_{10} T + \frac{U_0 - \lambda_0}{2\cdot 3kT} \tag{5}$$

Since B is not large the main variation of γ with T is controlled by the last term in the equation Since[‡] λ is greater than U_0 the term is negative and we see at once that the fraction associated in saturated vapour increases with the temperature This result has been assumed above in explaining the absorption curves, and Harrison and Slater[§] make the same assumption in explaining some experiments of the former[||] on line absorption It is interesting to have this quantitative verification

---

[*] 'Phil. Mag.,' vol. 45, p. 1 (1923). The writer is indebted to Mr R. H. Fowler for advice on this matter

[†] Obtained from a paper by Smith, 'Roy Soc. Proc.,' A, vol. 106, p. 400 (1926)

[‡] As deduced from the vapour pressure curves of Kroner (*loc. cit.*)

[§] 'Phys. Rev,' vol. 26, p. 276 (1925).

[||] 'Phys. Rev,' vol. 25, p. 238 (1925)

In order to calculate the fraction associated at different temperatures it is simplest to return to equation (3) and insert numerical values In this way we find

$$\log_{10} \gamma = - 3\ 0 - 1\ 5 \log_{10} \mathrm{T} + \frac{2\ 58 \times 10^3}{\mathrm{T}} + \log_{10} p \qquad (10)$$

and hence obtain the values

Temp	γ
277° C	6×10^{-4}
377° C	$1\ 4 \times 10^{-3}$
477° C	$3\ 4 \times 10^{-3}$

This gives the fraction of atoms associated in saturated vapour Under the experimental conditions the vapour is not truly saturated and the fraction associated is therefore less The presence of the filling gas will further reduce the proportion of molecules It is not likely that these effects will be large and the fraction associated for experiments in the long tube should lie between 10^{-3} and 10^{-4}, say, 3×10^{-4} This gives a value for the molecular absorption coefficient of 3×10^{-16} compared with 10^{-19} for the atomic continuous absorption and 6×10^{-14} for the most intense line absorption

The above calculation would need supplementing if there were another type of molecule with an appreciably different heat of dissociation. The existence of such a molecule is not likely, because if it had a dissociation energy of less than 1 2 volts its photo-electric threshold ought to have been detected directly by Lawrence and indirectly by the present work If its dissociation energy were greater than 1 1 volts, a very large fraction of the atoms would be associated (giving a result in conflict with vapour density measurements) and also the proportion of molecules would decrease instead of increasing with temperature

Summary

Experiments designed to measure the continuous absorption of light in the alkali-metal vapours are described The absorption found is believed to be due to a combination of molecular and atomic absorption. The possibility of separating these is discussed

The results are discussed in connection with the theory of atomic and molecular absorption The amount of atomic absorption appears to be much less than that expected

An experiment in which continuous absorption produces line fluorescence is

described and explained in connection with the molecular absorption The heat of dissociation of the potassium molecule is derived from the absorption curves and used to calculate the degree of association in potassium vapour at different temperatures

In conclusion I wish to express my thanks to Sir J J Thomson for his interest and advice throughout this work

---

On a Photoelectric Theory of Sparking Potentials

By JAMES TAYLOR, D Sc, Ph D, Physical Institute, University of Utrecht

(Communicated by O W Richardson, F R.S —Received October 13, 1927)

Introduction

In recent papers (1) a new photoelectric theory of sparking potentials was put forward, in which it was assumed that no ionisation by collision of the positive ions against the gas molecules or atoms is produced, but that the additional ionisation required for the initiation of the self-sustained electric discharge is to be found in the photoelectric effect at the cathode surface of the radiation accompanying the neutralisation of the positive ions there

According to this theory, the sparking potential v_c is a function of the photoelectric emissivity of the cathode for those radiations accompanying the neutralisation of the positive ions at the cathode

If we assume that for n_0 electrons produced originally at the cathode (by the ionising factors), $n_0\,\phi\,(\mathrm{V}, p)$ electrons are gathered to the anode, where $\phi\,(\mathrm{V}, p)$ is a function depending upon the voltage across the tube and the pressure of the gas, etc , then the number of positive ions arriving at the cathode is

$$n = n_0\,[\phi\,(\mathrm{V}, p) - 1] \qquad (1)$$

The neutralisation of these positive ions at the cathode surface is accompanied, we shall suppose, by the emission of radiation, some of which falls upon the cathode surface and produces the emission of photoelectrons Let the ratio of the number of electrons given off from the cathode by the photoelectric effect to the number of positive ions neutralised there be γ Then we have the following condition for the production of a self-sustained electrical discharge,

$$\gamma\, n_0\,[\phi\,(\mathrm{V}, p) - 1] \geqq n_0, \qquad (2)$$

and consequently the sparking potential v_c for these conditions is given by

$$\phi(v_c, p) = \frac{1+\gamma}{\gamma} \tag{3}$$

If we adopt Townsend's theory of the function $\phi(V, p)$, equation (3) resolves itself for the case of plane parallel electrodes into the following relation,

$$v_c = Xx = \frac{X}{\alpha} \log \frac{1+\gamma}{\gamma}, \tag{4}$$

where X is the electric field between the electrodes and x is the distance apart, α is the Townsend ionisation co-efficient

Now γ is usually small with respect to unity, so that we may approximate equation (4) to the following form —

$$v_c = \frac{X}{\alpha} \log \frac{1}{\gamma}, \tag{5}$$

and, further, if we take any function P, such that $P = N\gamma$, where N is some constant, we may express the equation (5) as

$$v_c = \frac{X}{\alpha}\left[\log \frac{1}{P} + \log N\right] \tag{6}$$

The problem now arises of devising a method for the concomitant measurement of v_c and γ (or of P)

Experimental Method

Discharge Tube System —Fig 1 shows diagrammatically the composite tube used in the experiments The main discharge vessel comprised electrodes A and B, of nickel, of the following dimensions diameter of electrodes, 5 cm , radius of curvature, 10 cm , distance between electrodes $\simeq$ 20 mms

A side tube T_1 contained a special four-electrode hot-wire discharge-tube device for the production of radiation It comprised a tungsten spiral filament W, surrounded by a nickel cylinder C, which was provided with two gauze windows W_1 and W_2 The cylinder C was enclosed completely in a nickel gauze cage D

A second side tube T_2 contained a nickel electrode X, opposite the window W_2, and a circular loop electrode Y, of tungsten wire

A third side tube T_3 was partly filled with coconut charcoal

The whole tube was constructed of pyrex glass, with tungsten leads-in.

The side tube T_4 was connected, via a liquid-air trap, to a high-vacuum pumping installation and a gas-supply system, but in such a way that the discharge-tube system and liquid-air trap could be completely cut off from the rest of the apparatus by pressure-operated mercury seals

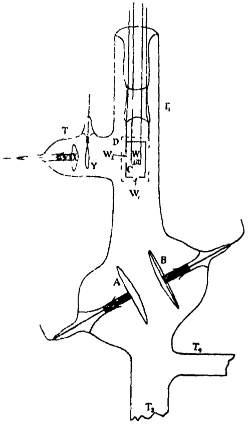

FIG 1

A photograph of the tube before it was modified by addition of the charcoal adsorption tube is given

Previous to experiment the apparatus was thoroughly " baked out " The filament and cylinder were " glowed out," and the charcoal was heated for about two days at between 400° and 500° C to activate it

Gas Purification —It was found after considerable experiment that helium was the most suitable gas to utilise—indeed, it is the only gas that can be purified rapidly and continuously by carbon at liquid-air temperature (the most efficient method of purification)

The gas utilised had been prepared from monazite sand, and was purified initially by phosphorus pentoxide, heated copper, heated calcium and a large calcium arc, until " spectroscopically pure " I am indebted to Mr Willemse, of this Institute, for the helium used

The gas was introduced into the discharge tube as required, and it could be maintained pure by keeping the side tube T_3 in liquid air

Electrical Arrangements *—The sparking potentials were determined in the manner previously described (2)

Initially, the action of the four-electrode discharge-tube device was explored thoroughly The filament carried a maximum current of 10 amps, but was usually run at about 6 5 amps It was not possible to detect any photoelectric effect of the radiation proceeding from the heated tungsten filament upon the electrode A, at least not with the sensitive galvanometer utilised in the work to be described When, however, gas was introduced into the tube and a potential of a few tens of volts maintained between the cylinder and the filament, a production of radiation occurred part of this radiation passed through the windows W_1 and W_2, and "irradiated" the electrodes A and X Thus, if A was maintained at a negative potential and suitably connected to a sensitive galvanometer, a measurable current of the order of 10^{-10} to 10^{-8} amps, according to circumstances, was obtained

---

* I am indebted to the Armstrong College Research Fund Committee for an apparatus grant for this work

The potential distributions on the various electrodes required to prevent any collection by A of negative or positive ions were examined Suitable values were found to be filament, 0 to + 12 volts, cylinder, 40 or 50, gauze cage, − 12, B and W, zero The potentials of X and A were negative, and could be adjusted to suitable values

Under these circumstances the current from A exhibited all the properties of a simple photoelectric current The potential of A was so chosen that no ionisation by collision occurred

In the initial investigations many interesting observations on the functioning and behaviour of the four-electrode discharge device were made In the actual experiments the radiation emitted by the windows as measured by the photoelectric effect was (other factors remaining constant) found to be constant over very long periods of time, and none of the effects to be described could be traced to the discharge box

The auxiliary tube T_2 was used for test purposes, and for examining the constancy of radiation, etc

The electric batteries used gave voltages constant to one part in a thousand

Experimental Verification of the Photoelectric Theory

We may assume that the radiation proceeding from the low-potential discharge device is of approximately the same character as that arising from the neutralisation of the positive ions This radiation falls upon the cathode A of the discharge tube, and produces a photoelectric effect P that is measured by the sensitive galvanometer We may assume that P will be a proportional measure of γ, so that we may write $P = N\gamma$, where N is some constant. Consequently, by concomitant measurements of the sparking potential v_s (between the electrodes A and B) and the photoelectric current P, we may examine the validity of equations (1) to (6)

Variation of v_c with Progressive Gas Purification.

On performing experiments, at different pressures, upon the variation of v_c, with progressive purification of the helium by means of the charcoal cooled in liquid air, remarkable results were obtained

In the beginning of the purifying process, when the gas impurities were relatively large, there occurred the well-known rapid decrease of the value of the sparking potential until a minimum value was obtained With continued purification v_c did not, as could be expected, remain constant, but a slow rise occurred until a value of anything from 10 to 600 volts, according to circumstances, higher than the minimum value was attained

A series of sparking potential values, beginning from the time of putting on the liquid air, is shown in Table I

Table I

—	v_c	Pressure	Time
	volts	mm	mins
No liquid air on traps	272	1 38	—
Liquid air on glass trap	274	1 28	—
Liquid air put round charcoal tube	274	—	0
	220	—	5
	210	—	6
	199	—	7
	196	1 21	8
	252	1 15	15
	262	1 14	21
	262	1 14	—
	v_c remained constant after this point		

The wall of the side tube was heated slightly to give off a minute quantity of gas, whilst all the other conditions remained the same as before v_c fell immediately to about 230 volts, and rose afterwards until it attained the value 262 once more

It might be expected that the final rise in the v_c value is brought about by decrease in the pressure of the helium due to cooling by, and adsorption in the charcoal Investigation showed that such an explanation was incorrect First of all, it was found that the rate of change of v_c with pressure of helium was not great, and, further, the greatest change occurred after the pressure had attained an almost constant value (Table II) Finally, introduction of new helium to make up for the pressure loss showed definitely that the effects did not proceed from this cause. We shall see later that other facts support this conclusion

Table II

—	v_c volts.	Pressure
		mm
Initial value before liquid air put on	200	2 8
Minimum value	171	2 8–2 7
Final maximum value	192	2 7
More helium was introduced	—	2 9
Final maximum value	187	2 9

A change of 0 2 mm produces a change of about 5 volts in the value of v_c Now the maximum pressure difference between the minimum and maximum value of v_c is not more than 0 05 mm, so that the change of v_c due to pressure diminution is negligible compared with that arising from the purifying process

Concomitant measurements of P showed a fall from a maximum at the minimum sparking potential to a minimum at the final higher sparking potential

A number of tentative explanations of the phenomena were considered Some of these attributed the final rise in v_c to change in the gas properties due to the extreme purification, but the difficulties in the way of such views are serious Finally, the following explanation was adopted as being the most probable —

(1) After the liquid air is put on the charcoal, the helium rapidly becomes pure, so that only slight traces of foreign gases remain, a fall of v_c to a minimum value occurs, and the gas properties then remain almost constant, being unaffected by the extremely small amounts of impurity

(2) The gas layer on the surface of the cathode undergoes slow change, probably by evaporation of the surface gas molecules into the helium, and the final disappearance in the adsorption tube T_3 This slow change of the cathodic surface is accompanied by a progressive decrease of the photoelectric emissivity (such as accompanies "outgassing" of metals) and increase of v_c, until the cathode modification has attained equilibrium under the existing conditions of gas-impurity pressure, etc

This explanation was supported by the observation that if, when the maximum value of v_c had been attained, a small quantity of gas was driven off the walls of one of the tubes by local heating with a small flame, a large reduction of the value of the sparking potential immediately occurred, and the higher value of v_c was only attained again after some considerable time

Variation of v_c with P

Now if we accept the foregoing explanation of the variation of the sparking potential with intensive purification, we have at once a convenient method for the concomitant measurement of v_c and P, with pure gas of constant properties

The values of v_c and P must be measured from the time-point corresponding to the minimum of v_c onwards, or vice versa Such investigations were carried out over a range of pressures The possible pressures were, of course, largely determined by the necessity of having P sufficiently great for convenient measurement

The filament current in the four-electrode device was usually of the order of 6 5 to 7 amps, the filament-cylinder voltage about 50, and the discharge current of the order of one/m a

The experimental procedure was as follows A measurement of P was carried out, v_c was determined immediately afterwards, and then P was re-determined, or, alternatively, a measurement of P was taken between two measurements of v_c Since the measurements are carried out whilst the electrode condition was gradually changing, it is not possible to get exactly corresponding values of v_c and P, and this introduces an experimental error into the determinations

The graphs of fig 2 show the relation between v_c and log 1/P for different pressures All the points obtained are shown In the graph for a pressure of

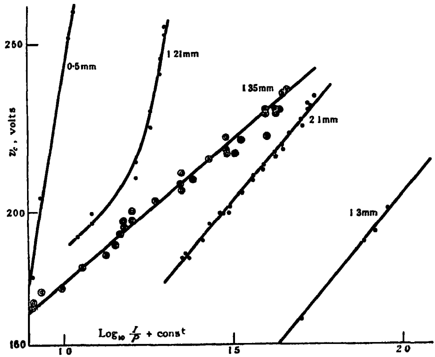

FIG 2

1 35 mm the ⊙ points correspond to measurements made with progressive purification, whilst the ◎ are for the reverse process The graphs for 1 3 mm and 1 35 mm correspond to initially different electrode conditions v_c is given on the natural scale, but in the abscissæ a suitable constant is added for each set of results, so that the curves may be brought on the same diagram

It is evident that throughout the region investigated—and, indeed, it is a region characterised by considerable changes in v_c—the graphs showing the relation between the corresponding values of v_c and P are smooth curves, and the relation between v_c and log 1/P is approximately linear (with one exception)

These results are in agreement with equations (1) to (6) Further, the values of α calculated from equation (6) agreed, within the limits of experimental error, especially for the higher pressures, with previously determined experimental values (see Table III) We may consequently conclude that the results give strong evidence in favour of the photoelectric theory of sparking potentials for the case of helium It is probable also that the other rare gases would yield similar results

Table III

Pressure	X/α from equation (6)	X volts per cm	α calculated	α/P from Gill and Pidduck	α from Gill and Pidduck
mm					
0 5	77 2	60–130	0 8–1 7	2 1–2 45	1 0–1 2
1 3	37 5	80–100	2 1–2 7	1 5–1 7	1 9–2 2
1 35	37	85–120	2 3–3 2	1 6–1 9	2 2–2 6
2 1	51 5	92 5–127	1 8–2 5	1 1–1 6	2 4–3 3
5 5	38	105	2 8	0 6	3 0

In a future paper the variations of γ under different conditions will be considered

It is a pleasure to me to express my gratitude to Prof Ornstein for his continued interest in the work, and for the great inspiration and help which he has afforded during the progress of the research, also to the International Education Board for the Fellowship which enabled the work to be carried out

Summary

The paper describes a photoelectric theory of sparking potentials, according to which the latter is a function of the photoelectric emissivity of the cathode

for the radiations accompanying the neutralisation of the positive ions at the cathode surface It is assumed that no ionisation by collision is produced by the positive ions in the gas

Adopting the Townsend theory of ionisation by collision by electrons, the following expression is arrived at for the sparking potential v_c (plane parallel electrodes) —

$$v_c = \frac{X}{\alpha} \log \frac{1+\gamma}{\gamma},$$

where X is the electric field (volts per centimetre), α is the number of electrons produced per centimetre by one electron, by collision, and γ is the number of electrons produced at the cathode by the neutralisation of one positive ion

The validity of the theory is examined for the case of helium, which can be thoroughly purified by means of charcoal in liquid air The results show definitely that the sparking potential is a continuous function of the photoelectric emissivity of the cathode for the radiation emitted by the gas The quantitative agreement with the above equation is very good

REFERENCES

(1) 'Roy Soc Proc,' A, vol 114, p 73 (1927), 'Phil. Mag,' vol 3, p 753 (1927), Dissertation, Utrecht (1927)

(2) Reference (1), also 'Phil Mag,' vol 3, p 368 (1927), *ibid.*, vol. 3, p 753 (1927)

(3) Gill and Pidduck, 'Phil Mag,' vol 23, p 844 (1912)

The Crystal Structure of the Chondrodite Series

By W H Taylor, Research Student, Manchester University, and J West, John Harling Fellow, Manchester University.

(Communicated by W L Bragg, F R S —Received October 22, 1927)

1 —*Introduction*

The chondrodite group of minerals comprises prolectite ($H_2Mg_3SiO_6$), chondrodite ($H_2Mg_5Si_2O_{10}$), humite ($H_2Mg_7Si_3O_{14}$) and clinohumite ($H_2Mg_9Si_4O_{18}$) We have so far been unable to obtain a specimen of the first—there seems, indeed, to be some doubt as to its existence—and, in consequence, the present paper is concerned with the last three members only *

Our conclusions are based on X-ray data obtained by the rotating crystal method and by the ionisation spectrometer None of the crystal specimens was suitable for absolute measurements of the intensity of reflexion, and the investigation has therefore been wholly qualitative in character This, of course, increases considerably the difficulty of the problem, especially in so far as an accurate determination of parameters is concerned , for in attacking crystal structures of even moderate complexity, the advisability of a quantitative study is being more and more realised In the present case, we are dealing with crystals possessing a very large number of parameters (*e g* , 24 in chondrodite, 36 in humite and 45 in clinohumite), and even a detailed quantitative examination might be unsuccessful without the use of some guiding principle or principles These principles will be apparent later

2 —*Interest of the Group*

The chondrodite group is interesting for several reasons

(*a*) In the first place, it supplies an excellent example of morphotropy

Penfield and Howe† were the first to draw attention to the fact that in passing through the series in the order given above, the *c*/*a* or *c*/*b* ratio changed in a simple and progressive manner with additions of the molecule Mg_2SiO_4

---

* We are deeply indebted to Dr A. Hutchinson, F R.S , of the Mineralogical Laboratory, Cambridge, for the loan of the crystals used in this investigation. The specimen of chondrodite was from the Tilly Foster mine , that of clinohumite from Vesuvius. The last-named crystal was measured by Miller and checked by Lewis.

† 'Z f Kryst.,' vol. 23, p. 78 (1894).

(olivine)* whilst the *a*/*b* ratio remained unaltered The question was later discussed in greater detail and with similar conclusions by Barlow and Pope† from the standpoint of a theory of atomic volumes in crystals, and the significance of the relationship of the series with olivine was stressed The crystallographic data from which the conclusions were drawn are given in Table I Actually the morphotropy is not quite so simple, as will be clear from Table II, which is based on X-ray data If, however, we denote the thickness of the unit cell in a direction perpendicular to the *c* face by *c*′, simple relations similar to those of Table I for the crystallographic *c* axis are found to exist for *c*′ (see last column of Table IV)

Table I (from Groth)

			a	*b*	*c*	*β*
Prolectite	$[SiO_4]Mg[Mg(F, OH)]_2$	monoclinic prism	1 0803	1	3 × 0 6287	90
Chondrodite	$[SiO_4]_2Mg_3[Mg(F, OH)]_2$	,,	1 0803	1	5 × 0 6289	90
Humite	$[SiO_4]_3Mg_5[Mg(F, OH)]_2$	rhomb bipyr	1 0802	1	7 × 0 6291	—
Clinohumite	$[SiO_4]_4Mg_7[Mg(F, OH)]_2$	monoclinic prism	1 0803	1 : 9	× 0 6288	90°
			b	2*a*	2*c*	
Olivine	$[SiO_4]Mg_2$	rhomb bipyr	1 0735	1 : 2	× 0 6295	

Table II

		No of molecules to cell	*a*	*b*	*c*	α	*c*′
			Å	Å	Å	° ′	Å.
Chondrodite	$Mg(F, OH)_2\ 2Mg_2SiO_4$	2	4 733	10 27	7 87	109 2	5 × 1 488
Humite	$Mg(F, OH)_2\ 3Mg_2SiO_4$	4	4 738	10 23	20 86	—	14 × 1 490
Clinohumite	$Mg(F, OH)_2\ 4Mg_2SiO_4$	2	4 745	10 27	13 68	100 50	9 × 1 492
Olivine	Mg_2SiO_4	4	4 755	10 21	5 98	—	4 × 1 495

Table III

	Indices (Crystallographic)	Indices (X ray)
Chondrodite	$h\ k\ l$	$k/2, h, \left(\frac{l-h}{4}\right)$
Humite	$h\ k\ l$	$k/2, h, l/2$
Clinohumite	$h\ k\ l$	$k/2, h, \left(\frac{l-h}{4}\right)$
Olivine	$h\ k\ l$	h, k, l

---

* A portion of the magnesium in the chondrodite series is isomorphously replaced by iron, we have therefore described the Mg_2SiO_4 as olivine rather than forsterite.

† Barlow and Pope, 'Trans. Chem. Soc,' vol. 89, p 1675 (1906), Pope, 'Proc. Roy. Inst.,' p. 823 (1910)

With further regard to the morphotropy of the series, it is curious that whilst the addition of one molecule of Mg_2SiO_4 to the monoclinic chondrodite *raises* the symmetry to that of orthorhombic humite, the addition of a further molecule of Mg_2SiO_4 *lowers* the symmetry to that of monoclinic clinohumite Any proposed structure must, of course, explain this change

(*b*) The series is interesting in the second place because all three crystals are found to be based on the hexagonal form of the two possible close-packed arrangements of oxygen atoms It is indeed the early realisation of this fact which has simplified and made possible an attack on the structures The important question of oxygen close-packing in certain crystals has been discussed fully, with examples, in a series of recent papers [*] We have, therefore, in a later section, only indicated the evidence for such packing in the present case

(*c*) A further point of interest lies in the fact that the Mg_2SiO_4 portion of the crystals is found to possess the olivine structure This evidence of the incorporation of a structure—itself not simple—within a further structure is of considerable importance It is hardly likely that this series constitutes a solitary example, and it is tempting to suggest that many of the complex silicates may in reality be compounds of this character, *i e*, may include within themselves structures which are known to exist alone Such a possibility is at any rate worthy of consideration when investigating crystals of complex composition and low symmetry, for apart from its interest, it facilitates enormously the general analysis of the structure

3 —*The Unit Cells*

Data relating to the unit cells are given in Table II The cell dimensions were first found approximately in the usual way from the rotation photographs, and then determined more accurately on the spectrometer In order to make the series conveniently comparable with olivine, we have taken the crystallographic *b* axis as our *a* axis, and *vice versa* This is a little unfortunate in the case of the monoclinic members, since it departs from the conventional use of β as the interaxial angle differing from 90° For purposes of reference, therefore, we give in Table III the connection between the crystallographic indices based on Table I and those adopted in the present paper from the data given in Table II Apart, however, from the question of terminology, it will be noticed that in the case of chondrodite and clinohumite, the true *c* axis is not perpendicular to the *a* and *b* axes as hitherto supposed, and in the case of all three crystals the true axial ratios c/a are not equal to, although they are simply related to, the crystallographic axial ratios. Dimensional considerations will show that it is of course possible to choose from the lattice points a cell (not the true one) which will satisfy the crystallographic data.

---

[*] Bragg and Brown, 'Roy Soc. Proc,' A, vol. 110, p 34 (1926), Bragg and West, *ibid.* vol. 114, p. 450 (1927).

Examining Table II we see that whilst the a and b axes remain unchanged throughout the series, c', the thickness of the unit cell perpendicular to the c-face varies in a simple manner as mentioned above. This relationship, as well as the similarity of the members of the series to olivine, is illustrated by fig. 1,

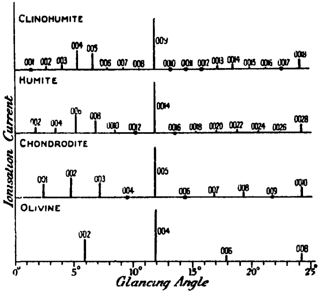

FIG 1.—Comparison of Spectra from c-Faces.

in which are collected the X-ray spectra from the c face of the four crystals concerned. Neglecting for the moment the small spectra, we notice that although the main reflexions in each case occur at the same glancing angle (about 12°, corresponding for RhK$_\alpha$ radiation to a spacing of 1.49 Å), it is the *fourth* order reflexion in olivine, the *fifth* in chondrodite, the *fourteenth* in humite and the *ninth* in clinohumite. We may remark here that the existence of this large reflexion (and of its second order at 24°) shows that in each crystal there are densely packed layers of atoms parallel to (001) spaced at intervals of 1.49 Å.

4.—*The Space Groups*

(*a*) *Humite.*—Taken in conjunction with the fact that humite belongs to the rhombic bipyramidal class of crystals, an analysis of the usual six X-ray rotation photographs taken about the three rectangular axes in turn as axes of rotation, shows the space group to be V_h^{16}

For details of this space group, reference should be made to any of the usual sources, *e g*, Niggli's 'Geometrische Kristallographie des Diskontinuums,' p 201 We shall merely note that the unit cell, which is simple orthorhombic, has two reflexion planes parallel to the *c*-face and contains two sets of symmetry centres The general position involves eight equivalent points, whilst a position on the reflexion planes or at a symmetry centre involves only four If we denote by θ_1, θ_2, θ_3 (where $\theta_1 = 2\pi x/a$, $\theta_2 = 2\pi y/b$, $\theta_3 = 2\pi z/c$), the co-ordinates of an atom in the general position, then the structure factor for the resulting eight equivalent positions when considering reflexions from a plane $(h\ k\ l)$ is proportional to

$$8 \cos [h\ \theta_1 + (h + k)\ \pi/2] \cos [k\ \theta_2 + (h + k + l)\ \pi/2] \cos [l\ \theta_3 + l\ \pi/2], \tag{1}$$

an expression which contains the criteria of the space group

(*b*) *Chondrodite and clinohumite* —These two are both members of the monoclinic prismatic class We have therefore to choose from six space groups C_{2h}^1 C_{2h}^6 An analysis of the rotation-photographs taken about the crystal axes and an axis perpendicular to the *c*-face as axes of rotation shows the space group to be either C_{2h}^4 or C_{2h}^5, the lattice being simple monoclinic The only distinction between the two groups is to be found in the spacing of the $(h00)$ planes (these would according to crystallographic convention be the $(0k0)$ planes) In the former case, C_{2h}^4, they are normal, in the latter they are halved A careful examination on the ionisation spectrometer of the *a*-faces of chondrodite and clinohumite showed all spectra to be absent except the fourth and eighth orders It seems very unlikely that the space group can be C_{2h}^4, for this would require the structure factor for the two crystals to be zero in six out of a possible eight reflexions, whilst in the case of C_{2h}^5 we require a zero factor for the (200) and (600) only Further, the strong similarity existing between corresponding rotation-photographs of olivine, humite, chondrodite and clinohumite leads us to expect that the (200) and (600) spectra, which are very weak or absent in olivine and humite, may well be absent in chondrodite and clinohumite In adopting C_{2h}^5 as the space group of chondrodite and clinohumite, we are aware that we are making an assumption , we cannot consider the space group proved On the other hand, in view of the clear evidence of structural similarity amongst all the members of the series, it is perhaps significant—as in the case of V_h^{16}, the space group common to humite and olivine—that the space group C_{2h}^5

in contradistinction to C_{2h}^4 possesses a set of screw axes parallel to the *a* axes of the crystals concerned, this is, in fact, the essential difference between these two alternative space groups

Details of the space group C_{2h}^5 are given in Niggli's book, p 158 We may note, in contrast to the case of humite, that the unit cell (which contains two molecules instead of four) has no reflexion planes, but has four sets of centres of symmetry The general position involves four equivalent points, whilst each set of centres of symmetry involves two such points Denoting by θ_1 θ_2 θ_3, as before, the co-ordinates of an atom in the general position, the structure factor for the resulting four equivalent positions is proportional to

$$4 \cos [h \theta_1 + (h + k)\pi/2] \cos [k \theta_2 + l \theta_3 + (h + k) \pi/2] \qquad (2)$$

5 — *The Structures*

Preliminary discussion – In fig 2 are collected sets of corresponding X-ray rotation-photographs for olivine and the members of the chondrodite series

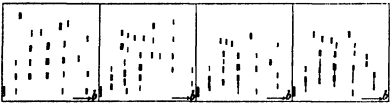

Rotated about axis perpendicular to *c* face

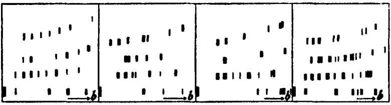

Rotated about *a*-axis

Olivine Chondrodite Humite Clinohumite.

FIG 2.—Comparison of Corresponding Rotation-photographs

The very definite similarity which is seen to exist amongst them can only be explained by supposing a basic similarity in structure Such a similarity is further supported by the dimensional and other data given below in Table IV

The structure of olivine has been determined by W L Bragg and G B Brown,* and for details reference should be made to the original paper. Briefly,

---

* Bragg and Brown, '*Z f Kryst.*,' vol. 63, p. 538 (1926).

Table IV

	a	*b*	*c′*	Volume per O atom	Refractive index
	Å	Å	A	Å³	
Olivine	4 755 = 2 × 2 38	10 21 = 4 × 2 55	4 × 1 495	18 20	1 65
Chondrodite	4 733 = 2 × 2 37	10 27 = 4 × 2 57	5 × 1 488	18 10	1 62
Humite	4 738 = 2 × 2 37	10 23 = 4 × 2 56	14 × 1 490	18 10	1 60
Clinohumite	4 745 = 2 × 2 37	10 27 = 4 × 2 57	9 × 1 492	18 18	?

the structure is based on a simple orthorhombic lattice, space group V_h^{16}, the unit cell containing four molecules The oxygen atoms are very nearly in hexagonal close packing, and the metal and silicon atoms are distributed amongst the available interstices so as to form a three-dimensional pattern consistent with the symmetry requirements of the space group

If in the case of chondrodite, humite and clinohumite we suppose that dimensionally the OH group may be treated as an oxygen atom—in this case both the oxygen atom and the OH group will be included in the term " oxygen atom "—we may reasonably infer from the above facts that such atoms are arranged at any rate in approximate hexagonal close packing, and suppose that the differences in the crystals are due to the differences in the patterns formed by the metal and silicon atoms (*e g*, it will be clear later that the minor spectra in fig 1 are almost wholly due to the silicon atoms) From the further fact that with very few exceptions all the reflexions are prominent which in hexagonal close packing should be strong, we must suppose that the distortion from such ' oxygen " arrangement is small By neglecting the distortion we simplify the problem, for the latter now reduces to that of determining the pattern formed by the Mg and Si atoms which must occupy some of the interstices amongst the " oxygen " atoms, *i e*, we have to find which " holes" these Mg and Si atoms occupy Since some distortion of a regular arrangement is possible, we must further investigate the precise position of each Mg or Si atom

6 —*The Structures in Detail*

It is convenient to deal first with chondrodite since it involves the smallest number of parameters.

(*a*) *Chondrodite* —The unit cell contains four Si, ten Mg, sixteen O atoms and four OH groups.

Positions of O *atoms and* OH *groups* —Treating the OH groups as O atoms for the moment, trial shows that the only way of fitting these hexagonally close packed atoms into the scheme of symmetry elements is that illustrated in fig 3 No symmetry centres are occupied, but the atoms are "in contact" at two of the four sets of centres present,* so that we have one set of OH groups and four sets of O atoms in the general position.

The Mg *atoms* —Now, except for the sets of symmetry centres which involve two equivalent points, all other positions have four equivalent points Since, therefore, owing to the peculiar arrangement of the "oxygen" atom only two sets of symmetry centres are available and since there are ten Mg atoms, it is clear that one only of the sets of symmetry centres is occupied by the Mg atoms, the remaining eight atoms being divided into two sets in the general position We note that these symmetry centres—and therefore two Mg atoms—are at the centres of groups of six O atoms We may reasonably suppose the remaining eight Mg atoms to be similarly placed (this supposition is indeed justified by spatial considerations as well as by analogy with olivine)

The Si *atoms* —Only one set of symmetry centres is now available, and we have only four Si atoms in the cell These must, therefore, lie in the general position Moreover they cannot lie within groups of six "oxygen" atoms as do the Mg atoms, for, unless we suppose a large and improbable departure from the close packing justified above, the resulting character of the crystal planes are found to be too simple to explain the observed reflexions The Si atoms are therefore within groups of four "oxygen" atoms

Distinction between OH *groups and* O *atoms* —It is not possible at the present stage of structure technique, even with quantitative data, to distinguish directly between an OH group and an O atom In the present case, however, we can do so indirectly if we assume that the "oxygens" surrounding the silicon atoms are wholly oxygens In this case by fixing the positions of the Si atoms we fix those of the SiO_4 groups, when the OH groups will be automatically located

Presence of the olivine structure —The number of possible arrangements of Mg and Si atoms is not great, it can be further reduced if we suppose, as is most reasonable, that the atoms will be distributed through the structure in a diffuse manner *Two of the possible arrangements are found to include the olivine structure as a unit in the pattern* This is, of course, very suggestive, it might almost be anticipated from the similarity between the X-ray data for olivine and chondrodite referred to above

In one of these possible structures—that which analysis shows to be correct

---

* We have taken one of these centres of symmetry as the origin of co-ordinates.

—the OH groups are situated immediately about centres of symmetry The arrangement is represented in fig 3

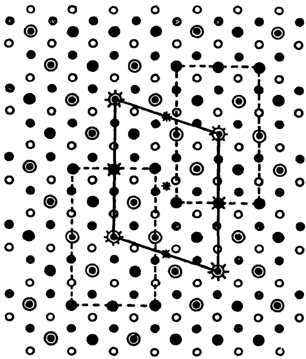

FIG 3—Chondrodite (excluding Silicon Atoms)

● ◉ Mg atoms in plane of paper and $\frac{1}{2}a$ below this plane.
○ ● O atoms or OH groups $\frac{1}{4}a$ above and $\frac{1}{4}a$ below plane.
Asterisks denote centres of symmetry in unit cell.

The olivine unit, which is of course orthorhombic, is indicated by broken lines, as also is its repetition across a centre of symmetry, the unit cell, which is monosymmetric, is represented by full lines Actually, the "olivine" extends indefinitely in directions parallel to the a and b axes But as will be clear from the diagram, in a direction perpendicular to these axes (and therefore parallel to c') there are periodic discontinuities where we find Mg atoms and OH groups. We have in effect, alternate layers of $Mg(OH)_2$ and olivine in the proportion represented by the chemical formula We have for this reason chosen to write the formula $Mg(OH)_2\ 2Mg_2SiO_4$

It would be absurd with the data at our disposal to attempt to determine accurately the values of the numerous parameters involved We find, however, that if we give to our "olivine unit" the *actual* olivine structure in which certain small displacements are given to the Mg and Si atoms from the ideal positions at the centres of their respective groups of oxygen atoms, the agreement between the structure factors and the observed intensities of reflexion is definitely better than if we use what we may term an ideal structure *

The co-ordinates of the atomic positions adopted for chondrodite are given in Table VI They have been deduced from an analysis of the intensities of reflexion from a very large number of planes of which only the *ool* series is represented in Table V In examining this table and the similar tables for humite and clinohumite, it should be remembered that the intensity of reflexion falls off rapidly as the glancing angle increases, and that the scattering power of

Table V —Results for Chondrodite

Indices	Sin θ	Approximate contribution of atoms *			Observed intensity
		O	Mg	Si	
001	0 0412	0	0	−1 2	m w
002	0 0825	0	0	−3 2	m
003	0 1237	0	0	3 2	m
004	0 1650	0	0	1 2	nil
005	0 2062	−20	−10	−4	v s
006	0 2475	0	0	1 2	nil
007	0 2887	0	0	3 2	w
008	0 3300	0	0	−3 2	w
009	0 3712	0	0	−1 2	nil
0010	0 4125	20	10	4	m w

Reflexions from sixty crystal planes were examined

* *I e*, when the figure 20 is placed in column O, it implies a contribution to the amplitude of the reflected wave which is twenty times as great as that due to a single oxygen atom

Table VI —Co-ordinates of Atoms in Chondrodite

Atom	Number	$\theta_1 = 2\pi x/a$	$\theta_2 = 2\pi y/b$	$\theta_3 = 2\pi z/c$
		°	°	°
O_A	4	−90	12	108
O_B	4	−90	84	36
O_C	4	90	60	180
O_D	4	90	−48	108
OH	4	90	24	36
Mg_1	4	0	61	108
Mg_2	2	180	0	180
Mg_3	4	180	−36	36
Si	4	36	54	−108

---

* We have allowed the "oxygen" atom to remain in the ideal position (as in olivine), although it is probable that a slight distortion will occur

an oxygen atom diminishes more rapidly as the angle of scattering increases than do those of Mg and Si

Returning to fig 2, it is clear that the structural similarity of clinohumite and humite to olivine must be of the same character as that of chondrodite Now we have seen that the structure of chondrodite includes within itself that of olivine We may assume this will be true of clinohumite and humite Further, in chondrodite, the $Mg(OH)_2$ and Mg_2SiO_4 occur as alternating layers parallel to the c-face The occurrence of these layers might be expected to confer some special property upon the crystal not possessed by olivine, and perhaps it is worthy of note that, unlike olivine, all the members of the chondrodite series exhibit lamellar twinning We may anticipate, though we do not assume, the occurrence of alternating layers of $Mg(OH)_2$ and Mg_2SiO_4 in appropriate relative thicknesses in clinohumite and humite

The assumption that the Mg_2SiO_4 in the two remaining crystals exists as olivine, facilitates enormously the analysis We have already justified the assumption of "oxygen" close packing Our problem therefore reduces to that of distributing the Mg and Si atoms amongst the available holes in such a way that whilst obtaining the olivine arrangement we satisfy the symmetry elements of the space group The problem is quite simple, and automatically reproduces the alternating layer arrangement of $Mg(OH)_2$ and olivine as found for chondrodite Our experimental results are in complete accordance with the structures so obtained We may, however, further point out that we have explored but rejected other structures which were possible geometrically

In view of the detailed treatment of chondrodite above, we give only a brief outline of the work on clinohumite and humite

(*b*) *Clinohumite*—In the unit cell we have eighteen Mg, eight Si, thirty-two O atoms and four OH groups As in the case of chondrodite, which has the same space group, only one set of symmetry centres is occupied, and that by two Mg atoms, the remaining atoms are all in the general position There were four molecules of Mg_2SiO_4 in the unit cell of chondrodite, and the "olivine block" referred to above was found to be the actual unit cell of olivine In clinohumite, we have eight molecules of Mg_2SiO_4 In view of the morphotropic relations already discussed, this suggests that if an olivine block exists in clinohumite, it can be obtained by extending that in chondrodite to twice its thickness in the c' direction Owing to its size, there are only two ways of fitting such a block into the unit cell of clinohumite In one of them the OH groups are about symmetry centres, and of those tried it is this structure which has been alone found to explain the experimental results The symmetry elements cause the repetition of this block to result in a series of layers of olivine separated by layers of $Mg(OH)_2$, the layers of olivine being twice as thick as those in chondrodite A diagram of the structure is given in fig 4 In Table VII we give a portion of the results of a comparison between the observed intensity of reflexion and the corresponding structure factors based on the co-ordinates of the atomic positions of Table VIII

Table VII —Results for Clinohumite.

Indices.	Sin θ	Approximate contribution of atoms			Observed intensity
		O	Mg	Si	
001	0 0228	0	0	−1 0	nil
002	0 0457	0	0	−1 4	v w
003	0 0685	0	0	−2 0	w
004	0 0914	0	0	−5 8	m
005	0 1142	0	0	5 8	m
006	0 1371	0	0	2 0	v w
007	0 1599	0	0	1 4	v w
008	0 1828	0	0	1 0	trace
009	0 2056	−36 0	−18 0	−8 0	v.s
0010	0 2285	0	0	1 0	nil
0011	0 2513	0	0	1 4	nil
0012	0 2742	0	0	2 0	nil
0013	0 2970	0	0	5 8	w
0014	0 3199	0	0	−5 8	w
0015	0 3427	0	0	−2 0	v w
0016	0 3656	0	0	−1 4	trace
0017	0 3884	0	0	−1 0	nil
0018	0 4113	36 0	18 0	8 0	m w

Reflexions from eighty planes were examined

Table VIII —Co-ordinates of Atomic Positions in Clinohumite

Atom	Number	$\theta_1 = 2\pi x/a$	$\theta_2 = 2\pi y/b$	$\theta_3 = 2\pi z/c$
		°	°	°
O_A	4	−90	0	60
O_B	4	−90	80	20
O_C	4	90	40	100
O_D	4	−90	100	100
O_E	4	90	120	60
O_F	4	90	140	140
O_G	4	−90	20	140
O_K	4	90	60	180
OH	4	90	20	20
Mg_1	4	0	49	60
Mg_2	4	180	−20	100
Mg_3	4	180	−40	20
Mg_4	2	180	0	180
Mg_5	4	180	91	140
Si_1	4	36	66	−60
Si_2	4	36	26	140

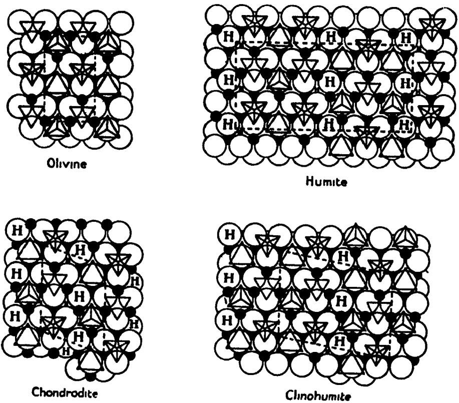

Olivine

Humite

Chondrodite

Clinohumite

FIG 4.—Structures viewed along *a* axis.

○ (H) O atoms and OH groups respectively Those fully visible are in a layer ¼*a* above, those partially visible are ¼*a* below plane of paper

● Mg atoms. Those fully visible are ½*a* above, and those partially visible are in plane of paper

The Si atoms are not always visible in such a position the tetrahedrons of O atoms which enclose them are therefore outlined instead.

indicates a group with apex upwards the corresponding Si atom is therefore *a*/8 above the oxygen plane AAA.

indicates a group with apex downwards the corresponding Si atom is *a*/8 below the oxygen plane AAA.

Humite —There are four molecules in the unit cell, so that we have to locate twenty-eight Mg, twelve Si, forty-eight O atoms and eight OH groups The space group is V_h^{16}, and trial shows that there is only one way of fitting the assumed hexagonal close packed arrangement of O atoms and OH groups into the scheme of symmetry elements. It is one in which oxygen atoms (or OH groups) lie in pairs immediately about centres of symmetry, eight lie on the reflexion planes parallel to the *c*-face and the rest are in the general position There are a number of options for the positions of the Mg and Si atoms Owing to the oxygen arrangement, no centres of symmetry are available; since therefore the general position involves eight equivalent points, at least four Mg and four Si atoms must lie on the reflexion planes, the other atoms being in the general positions A direct deduction of the structure from first principles would be very involved, but with the evidence of the structures of chondrodite and clinohumite before us, we may assume the Mg_2SiO_4 portion of humite to possess the olivine structure There are twelve molecules of Mg_2SiO_4 in the unit cell, and we find that by appropriately placing in the cell a block of olivine identical with that in chondrodite, except that its thickness is one and a half times that in chondrodite—and therefore contains six molecules—we are able to account completely for our experimental results The block is situated on the reflexion planes, the OH groups once more being about symmetry centres The structure again reduces to a set of alternate layers of $Mg(OH)_2$ and olivine, the layer of olivine in humite being one and a half times that in chondrodite A diagram of the structure is given in fig 4 Certain experimental results and the co-ordinates of the atomic positions are given in Tables IX and X respectively

Table IX —Results for Humite

Indices	Sin θ	Approximate contribution of atoms			Observed intensity
		O	Mg	Si	
002	0 0294	0	0	−2 4	w
004	0 0588	0	0	−3 2	w
006	0 0882	0	0	−8 8	m
008	0 1176	0	0	8 8	m
0010	0 1470	0	0	3 2	v w
0012	0 1764	0	0	2 4	v w
0014	0 2058	−56	−28	−12 0	v s
0016	0 2352	0	0	2 4	nil
0018	0 2646	0	0	3 2	nil
0020	0 2940	0	0	8 8	v w
0022	0 3234	0	0	8 8	v w
0024	0 3528	0	0	3 2	nil
0026	0 3822	0	0	2 4	trace
0028	0 4116	56	28	12 0	m w

Reflexions from sixty planes were examined

Table X —Co-ordinates of Atomic Positions in Humite

Atom	Number	$\theta_1 = 2\pi x/a$	$\theta_2 = 2\pi y/b$	$\theta_3 = 2\pi z/c$
		°	°	°
O_A	8	−90	75	64
O_B	8	90	15	64
O_C	8	−90	75	13
O_D	8	90	105	39
O_E	4	90	105	90
O_F	4	−90	−15	90
O_G	8	−90	−15	39
OH	8	90	15	13
Mg_1	4	180	56	90
Mg_2	8	0	34	39
Mg_3	8	180	−45	13
Mg_4	8	0	135	64
Si_1	4	36	− 9	90
Si_2	8	216	99	39

6 —*Conclusion*

In brief, the three structures discussed above consist of alternate layers—parallel to the *c*-face—of $Mg(OH)_2$ and Mg_2SiO_4 based on an arrangement of oxygen atoms and OH groups in hexagonal close packing The oxygen atoms appear to determine the dimensional relations of the unit cell whilst the Mg and Si atoms appear to control the pattern and therefore the cell symmetry Moreover the Mg_2SiO_4 portion possesses the olivine structure

From the standpoint of layers, one fundamental difference between the three structures lies in the fact that whilst the $Mg(OH)_2$ layer maintains the same thickness in all the crystals, that of the olivine layer (measured perpendicular to the *c*-face) has the ratio in chondrodite, humite and clinohumite of 2 3 4 respectively (*cf* the formulæ $Mg(OH)_2\ 2Mg_2SiO_4$, $Mg(OH)_2\ 3Mg_2SiO_4$, $Mg(OH)_2\ 4Mg_2SiO_4$) This variation in thickness affects, of course, the character of the atomic pattern and the distance within which this pattern is repeated For example, whilst the pattern is repeated within the same length in the directions of the *a* and *b* axes in all the crystals, this is not so in a direction perpendicular to the *c*-face, this results in the morphotropic relations discussed earlier

A further difference between the layers of olivine structure is that, unlike those in chondrodite and clinohumite, the layers in humite are bisected by reflexion planes parallel to the *c*-face, the difference is an inevitable consequence of the number of rows of oxygen atoms in each case This causes alternate layers of Mg $(OH)_2$ in humite to be mirror images of each other The ultimate result is an atomic pattern of higher symmetry than obtains in chondrodite or clinohumite, a result achieved by increasing the size of the unit cell (see Table II). This explains the orthorhombic symmetry of humite in contrast to the monoclinic symmetry of the two other members of the series

In conclusion, we wish to express our warmest thanks to Prof. W L Bragg, F R S, for his interest and generous advice throughout the course of the work

---

The Structure of Surface Films Part X —Phenols and Monoglycerides

By N K ADAM, W A BERRY, and H A. TURNER.

(Communicated by Sir William Hardy, F R S —Received November 3, 1927— Revised, November 28, 1927)

In Part VIII of this series,* the expanded films were shown to be of two main kinds, the liquid expanded films, which are definitely coherent films having a small surface vapour pressure, and the vapour expanded films, which had no region of constant vapour pressure but passed continuously into the gaseous state on increasing the area

The structure there suggested for the liquid expanded films was that the molecules were in contact, the chains being coiled down in helices with vertical axis, the diameter of each coil of the helix being about the same as the diameter of the cyclohexane ring The reason for this suggestion was that all the liquid expanded films known at that time had an area at no compression very close to 48 sq Å U, and there seemed no reason for the coincidence of area in so many different cases, other than that the chains, in some peculiar configuration, determined the area of the film The hypothesis however presented some considerable difficulties, notably in the manner in which the area decreased with increasing compression

Now two series of compounds have been found in which the areas of the liquid expanded state differ widely from this figure, and the hypothesis of coiled chains must be abandoned

The Phenols

Fig 1 shows the pressure-area curves of *p*-dodecyl and *p*-nonyl phenols The curve for nonyl phenol is the dotted one at the right. Dodecyl phenol gives a condensed film below 16°, the area at no compression being 24·5 ± 0·5 sq Å U, in fair agreement with the area of the condensed films of the longer chain phenols described in Part IV[*] No doubt this is the cross-section of the benzene ring vertically in the surface There appears to be a perceptible thermal expansion of the condensed film near to the expansion temperature The condensed film is solid and shows some hysteresis[†], if a compression is applied suddenly the pressure rises and then falls slowly to a point rather below the initial value, if the compression is lowered, the pressure falls and then rises slowly The hysteresis is less than that of hydrolecithin, described in Part VIII, but is quite noticeable with the improved apparatus

---

* 'Roy Soc. Proc,' A, vol. 112, p. 372 (1926).

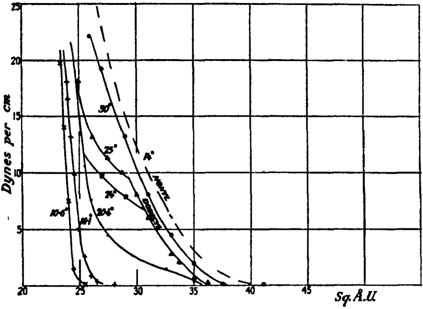

Fig 1

The hysteresis is puzzling, it is not clear why a comparatively simple group like phenol should unpack *slowly* from a close-packing on removing compression, and it is a little surprising that on compression the final packing should not be taken up at once The compressibility shows that there is probably little re-arrangement of the heads of the molecules on compression. It is of the order 1 per cent decrease in area for 5 dynes per centimetre increase of pressure, assuming that the phenol heads of length roughly 6 Å U bear the whole of this, the pressure required for 1 per cent decrease is 83 megabars, which is little below that needed to compress benzene by 1 per cent of its volume

---

[*] 'Roy Soc. Proc.,' A, vol. 103, p. 676 (1923)

[†] This delayed adjustment of strain to stress should perhaps be classified as "elastic after-working," not "hysteresis."

The expanded films are liquid expanded They show an extremely small vapour pressure, about 0 01 dyne per centimetre for dodecyl phenol and 0 03 for nonyl phenol The half expansion temperatures under 1 4 dynes are 19° ± 2 for dodecyl phenol, for nonyl phenol some 30° lower, but this has not, of course, been observed The process of expansion is of the usual nature, but since the area of the expanded film is less, and that of the condensed film greater, the distances along the abscissa are shorter than usual and the transition regions between expanded and condensed films are steeper

The methyl ether of dodecyl phenol gave almost identical curves and had the same expansion temperature within experimental error The film has a tendency to collapse, like those of the longer chain phenol methyl ethers, but it has a greater stability than the hexadecyl compound This is in accordance with the usual rule that the longer the chain the less the resistance of the film to collapse

The area of the expanded film of dodecyl phenol, at no compression, is 37 sq A U, and that of nonyl phenol 39 These *may* be identical within experimental error, but are quite different from the 48 sq A U of the majority of the previously examined compounds There is nothing unusual, except the area, about these liquid expanded films, and up to 50° there is no further expansion beyond the slight steady increase of area with temperature which the expanded films always seem to undergo

In Part VIII, hexadecyl phenol was among the compounds included in the table of areas about 48 sq A U But with this compound the measurements had to be made at about 60°, because of the high expansion temperature, and the unavoidable contamination at temperatures above 50° is so great that there is grave danger of too large areas being recorded For this paper, care was taken to select compounds with sufficiently short chains to make measurements at or about room temperature, and the areas are probably correct within two units. It seems certain that the phenols form liquid expanded films of an area close to 38 sq A U at no compression

The α-Monoglycerides

Fig 2 gives the curves for α-monomyristin and α-monopalmitin,

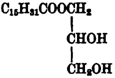

$$\begin{array}{l} C_{15}H_{31}COOCH_2 \\ \qquad\qquad\quad | \\ \qquad\qquad\quad CHOH \\ \qquad\qquad\quad | \\ \qquad\qquad\quad CH_2OH \end{array}$$

They form both condensed and expanded films The expansion is of the usual type, but the area at no compression is 70 sq Å U ± 3 The surface vapour

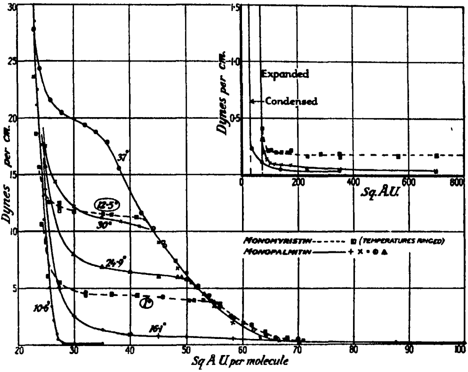

FIG 2

pressure is 0 17 for monomyristin and less than 0 04 for monopalmitin There is very little change in area of the expanded films between 0° and 40° The transition region between expanded and condensed film is longer than usual, and more nearly horizontal, because the area of the expanded film is unusually great, but the transition region is definitely not horizontal The only respect in which these liquid expanded films differ from earlier ones is that the coefficient of thermal expansion is too small to measure

The condensed films are liquid, though rather viscous at low temperatures, dust on the surface obviously does not move very easily The films do not pack to close-packed chains, but to the close-packed head variety of film in which there is no appreciable re-arrangement under compression The area at no compression is 26 3 ± 0 5 sq Å U This is probably contact of the glycerine heads of the molecules, with the three carbons nearly vertically above each other, the attached oxygen atoms could easily account for the area being some 30 per cent greater than that of close-packed chains The compressibility is about 1 per cent decrease for 2 5 dynes per centimetre compression between 15 and 25 dynes, if we suppose that the glycerine heads, which must be about 4 2 A U in length, bear the whole of this compression, the pressure for 1 per cent decrease in area amounts to 60 megabars, which is not far short of the pressure required to compress most organic compounds by 1 per cent of their volume There does not seem therefore to be much re-arrangement on compression

Note on the " close packed head " and " close packed chain " types of condensed film

Müller* has recently found the cross section of a hydrocarbon chain, by X-ray measurements on crystals, to be 18 3 sq A U In the thin films on water the area 20 5± about 0 3 sq A U has been found with a great variety of heads, the long hydrocarbon chain being present in each case It has been supposed that the type of film in which this area occurs is one with close-packed, vertical, chains, for no closer packing has yet been found with the films, and the compressibility of the films in this condition is so small as to indicate that the molecules are close-packed along a considerable length In the thin films there is often also another type of condensed film, in which the area is greater and is determined by the nature of the heads These have been supposed to have the heads closely packed, and there seems no reason against this hypothesis Probably, with the " close-packed head " type of film, the area is first determined by the packing of the heads, and then the chains, being flexible, adjust themselves so as to fill the space above the close packed heads as completely as possible This will probably involve a tilt of the chains In many cases simple compression forces the " close-packed head " structure into the " close-packed chain " one, the heads are probably tucked away into the recesses which must exist in the chains It is experimentally found that certain bulky head groups, such as the bromo-acid, and the phenol, will not pack away sufficiently for the chains to come into contact, and in some cases the heads form a practically incompressible structure, as with the mono-glycerides of this paper

The close-packed chain structure, in view of Müller's results, cannot be a vertically oriented mass of chains packed as closely as in the crystal If the chains are packed as closely as in the crystal, they must be tilted at about 27° to the vertical If, however, they are vertical they must be spaced out in some manner to about 10 per cent greater area than in the crystal There is no direct evidence to decide which alternative is correct It is possible that, by carefully re-measuring each series of compounds which has been thought to give the same close packed chain type of film, the mean area of which is 20 5, differences might be found characteristic of each series, and with the new apparatus now in use it is possible with great care to obtain results to 2 per cent accuracy in areas. If such differences are found, the films formerly called "close-packed chains" will have to be considered as having the heads only packed as closely as possible, the chains being slightly tilted Further work is required on this point

---

* 'Roy Soc Proc,' A, vol. 114, p. 559 (1927)

Structure of the Liquid Expanded Films

The coiled chain theory mentioned above becomes untenable with the wide range of areas now known

To account for the area by a tilt of the molecules, a tilt of about 75° to the vertical would give an area of 70 sq A U, and one of $67\frac{1}{2}°$ the area of 48, assuming that the very much tilted chains are packed as closely as are the vertical chains in the condensed films The assumption is so uncertain that little weight can be attached to such estimates of the degree of tilt

The puzzle is, why should the molecules find a stable state of the films at one, and only one, tilt of the chains ?

Forms of the tilted chain theory of the expanded films have been discussed recently by Langmuir* and Garner † It has been suggested that if the tilt is uniform, we should except solidity in the expanded films, whereas these films are always liquid The argument is not conclusive, because very often condensed films, with the molecules close-packed and nearly vertical, are liquid

Langmuir's theory is that there is no definite tilt but that the chains are in constant motion, similar to that of chains in a hydrocarbon liquid, except for the more or less considerable restriction imposed by the necessity of keeping the heads in the water At present we see little evidence either for or against this view, or that of a definite tilt

Langmuir also suggests that the expanded film is a kind of compromise between the condensed state and the gaseous, the heads trying to make the film gaseous and the chains to retain the molecules cohering We think the evidence available is against this view, for the heads seem to make a considerable contribution to the lateral attraction between molecules, both in the condensed and the expanded states Some idea of the magnitude of the lateral attraction between heads in the condensed films can be obtained by considering the expansion temperatures; with a constant length of chain, the greater the contribution to the adhesion made by the heads, the higher will be the expansion temperature. In the expanded films, the cohesion can be estimated roughly by the degree of departure from the gaseous condition. There are a few cases where a condensed film expands into a gaseous film with but little cohesion; others form "vapour expanded" films, which pass on diminution of pressure into gaseous films without discontinuity; others form liquid expanded films, where the cohesion is sufficient to form a separate surface phase. The following table shows that, as a general rule, those films which have the low expansion temperatures form vapour or gaseous films when expanded. Since the differences are only in the nature of the heads, the contribution of the heads to the lateral adhesion between molecules must be of the same nature in the expanded as in the condensed states, and the influence of the heads in the condensed films is very marked. Hence probably the heads contribute substantially to the cohesion in the expanded state.

---

* "3rd Colloid Symp Monog," p. 72 (1925), "Colloid Chemistry," ed. Alexander, vol. 1, p 543 (1926)

† 'Trans. Faraday Soc.,' vol. 22, p 498 (1926)

Table of expansion temperatures and states of expanded films. Chain $C_{16}H_{33}$ in each case. Temperatures of half expansion under 1.4 dynes per centimetre.

Substance	Head	Temperature	State
Margaric acid (on N/10 NaOH)	$COONa$ (ionised)	ca. 2	G
Hexadecyl acetate	$OOC\cdot CH_3$	20	V
α bromostearic acid (on HCl)	$CH_2BrCOOH$	22	L
Ethyl margarate	$COOC_2H_5$	23	V
Methyl margarate	$COOCH_3$	34	prob. V
Hexadecyl methyl ketone	$COCH_3$	34	V
Margaric acid (on HCl)	$COOH$	37.5	L
Margaric aldoxime	$CH\cdot NOH$	42	prob. L
Margaric amide	$CONH_2$	44	L
Heptadecyl alcohol	CH_2OH	54	L
Hexadecyl phenol	C_6H_4OH	55	L

G = gaseous film. V = vapour expanded—in all these cases there is much cohesion in the vapour expanded films near the expansion temperature. L = liquid expanded.

The bromo-acids are the only substances which are out of place in the table. There is a quite probable reason for this, for the bromine atoms keep the chains a little spaced out beyond their closest packing, so that though the lateral adhesion between *heads* may be large in the condensed state, the *chains* may exert less than their normal adhesion, and consequently the expansion temperature is lower than would be expected from the other members of the table.

This influence of the bromine atoms would not be so large, if present at all, in the expanded films, owing to the tilt of the molecules

The table is not final, as the observations on the state of the films are not yet very numerous, sometimes the observations have had to be made on a substance of rather different chain length from that of the table The exterpolation as regards expansion temperature is probably always correct to 3°, in the case of the state of the films, observations are available on one member of the series, and there is the rule now established on about eight series, with a moderate variation of chain length, that if one member of the series has a given state of expanded film just above the expansion temperature, all the others have the same state near their expansion temperatures

The evidence seems to warrant no more than saying there is either a definite and uniform angle of tilt at each stage of compression of the expanded films, or a motion of the molecules through various angles of tilt, which is equivalent, averaged over time and in its effect on the area, to a single angle of tilt

It is not clear, from the structure of the molecules, or the probable contour of the fields of force, why there should be just one stable position of tilt between the vertical and horizontal orientations Neither is it obvious what direction future research should take in order to discover the fine details of structure of these films, or the cause of their existence

Preparation and Identification of Material

The phenols were prepared by a slight modification of the method employed in Part IV of this series * The purified acid was converted into the acid chloride and condensed with anisole in the presence of aluminium chloride The ketone so formed was reduced with amalgamated zinc and hydrochloric acid according to Clemmensen's method This gave a derivative of anisole with one long chain in the nucleus The position of this chain in relation to the methoxyl group was not determined in the two cases of this paper, but certainly it is practically a para orientation, since Krafft has shown that the hexadecyl phenol identical with the one described in Part IV is para, that the ketone made with palmitic acid is also para, and in addition it is practically always the case that the acyl groups enter in the para position to the methoxyl groups in the Friedel Crafts reaction

Finally the long chain substituted anisole was boiled for several hours with concentrated hydriodic acid, to remove the methyl group, and the phenol remaining was distilled *in vacuo*, after washing *p*-dodecyl anisole melted at

---

* 'Roy Soc Proc,' A, vol. 103, p 676 (1923)

27–28°; *p*-dodecyl phenol at 64·5–65·5°. Analysis gave C = 82·21 per cent., H = 11·50 per cent., theory 82·37 per cent. and 11·53 per cent.

The *p*-nonyl anisole was not purified. *p*-nonyl phenol melted at 39–40°. C = 81·64, H = 10·95 per cent., theory 81·75 per cent. and 10·99 per cent.

The α-monoglycerides were prepared by the action of the acid chlorides in presence of quinoline on acetone glycerine according to Fischer's method, and subsequently hydrolysis of the acetone compound of the monoglyceride by acid.* We found α-monomyristin melting point 70–71°, C = 73·78, H = 10·55 per cent., theory 73·85 per cent. and 10·42 per cent. Hydrolysis with N/5 alcoholic soda gave the total myristic acid 75·5 per cent. (theory 75·5), titration showed an inappreciable amount of free acid (sensitivity 0·4 per cent.).

α-monopalmitin melting point 76–77°, Fischer's value 78–79°. Hydrolysis showed 77·5 per cent. total palmitic acid (theory 77·6), free acid was inappreciable (sensitivity 0·24 per cent.).

Modifications of Technique

Some slight modifications have been made in the apparatus with torsion wires for measuring surface pressure, which do not affect its working but simplify its construction and use. The silk or silica fibres connecting the float to the framework ("microbalance") mounted on the upper torsion wire, and to the mirror, have been replaced by very fine silver wires soldered on. Wires of 0·04 mm. diameter stand ordinary working conditions for a long time; wires of 0·03 mm. break rather frequently on the apparatus used for measurement of the higher pressures. They can be soldered without serious difficulty.

The gold ribbons at the ends of the float have been replaced by platinum, which is far easier to solder, as the gold dissolves, if the iron is applied a second too long.

The manipulation has been simplified by always setting the dial to zero before taking a reading. Three zero adjustments have been used, in decreasing order of coarseness; first, rider weights on the "microbalance" arm; second, turning of a torsion head on the lower wire which carries the mirror; third, raising or lowering the scale on to which the spot of light from the mirror is thrown, by rack and pinion, till the light spot is on a definite mark with the dial at zero. The last two adjustments take together only a few seconds. To eliminate unnecessary calculation the coarser instrument has been graduated to read dynes per centimetre directly; the graduation can be verified in a minute or two and remains practically constant. The solutions are usually made up so that the scale readings in centimetres are also areas per molecule in square Å U, with 20 drops from the fine pipette Leaks past the ends of the barrier and of the ribbons may occur, they are found by putting on a film under compression and dusting the suspected spot, any escape of the film is at once made visible by the movements of the dust To stop leaks, the water is led up by a fine point until the crack in the barrier system is entirely submerged, and once stopped in this way, the leaks never seem to recur, unless the apparatus is moved

---

* 'Ber. deut. Chem. Ges.,' vol. 53, p. 1605 (1920).

We are much indebted to Messrs J Crosfield & Sons, Ltd, for a gift of pure fatty acids

Summary

Two series with liquid expanded films of area (at no compression) different from 48 sq Å U have been found, the phenols of 39 and the α-monoglycerides of 70 sq Å U The hypothesis of coiled chains for the liquid expanded films cannot therefore be maintained The possibilities of tilted molecules are discussed and the evidence found inconclusive in favour of any specific form of a tilted molecule theory, although all forms appear possible

Since the heads appear to contribute to the cohesion in the expanded films, Langmuir's theory that the chains hold the films together against a disruptive force exerted by the heads appears incorrect

The monoglycerides form condensed films with close-packed heads, not appreciably re-arranged by compression, area 26 3 sq Å U at no compression. Müller's suggestion that the chains are tilted is not incompatible with the theory of close-packed heads

The condensed film of dodecyl phenol shows elastic after-working on compression and decompression.

On a New Effect in the Electric Discharge.

By T R Merton, F R S

(Received November 29, 1927)

There are a number of spectra which are seen under appropriate conditions of excitation in vacuum tubes containing helium with a small trace of some other gas, but which are difficult to isolate under other conditions In particular the arc spectrum of carbon[*] and the band spectrum known as the comet tail spectrum can be observed very favourably under these conditions This latter spectrum, which is characteristic of the tails of comets, was first observed in the laboratory by Fowler[†] in carbon monoxide at very low pressures, and recent analyses of the spectrum leave no doubt that it is to be attributed to the carbon monoxide molecule In the course of the investigation of this spectrum in vacuum tubes containing helium[‡] some very peculiar types of striated discharge were observed, and further investigation leads to the conclusion that these striæ are of a very special type and are quite different to those which are usually observed in vacuum tubes They exhibit certain peculiarities which may perhaps justify the suggestion that this type of discharge is akin to the rare phenomenon known as ball lightning The striæ usually observed in vacuum tubes may be classified as stationary and moving striæ The former have been observed since the earliest investigations of the electric discharge in gases at low pressures, and their appearance and behaviour is so well known as to need no description The moving striations, first observed by Wullner,[§] have recently been the subject of more critical investigations by Aston and Kikuchi[||] and Whiddington,[¶] who by the application of stroboscopic methods have observed in pure gases striations moving with velocities of from 10^3 to 10^6 cm per second

More recently Langmuir[**] has described a peculiar type of streamer discharge which he has observed in argon containing a small amount of tungsten vapour which was introduced by the sputtering of a tungsten filament Whilst the phenomena described by Langmuir bear a certain resemblance to those described in the present communication, inasmuch as in both cases the formation of a particulate cloud has been observed, the conditions of experiment are so different as to make it almost certain that the phenomena are different in origin. Langmuir's observations were made with a direct current discharge, using an electrically heated tungsten filament as the cathode, and the streamer discharge observed by him was very sensitive to weak magnetic fields, whilst the disc discharge which has been the subject of the present investigation can only be maintained with an alternating current discharge, and is entirely unaffected by weak magnetic fields

---

[*] Merton and Johnson, 'Roy Soc Proc,' A, vol 103, p 383 (1923)

[†] 'M N R Ast Soc,' vol 70, p 484 (1910)

[‡] Merton and Johnson, *loc cit*

[§] 'Pogg Ann,' Jubelband, p 32 (1874)

[||] 'Roy Soc Proc,' A, vol 98, p 50 (1921)

[¶] 'Proc. Roy Inst,' p 1 (1926)

[**] 'Science,' vol 60, p 392 (1924)

The discharge tubes used in the present investigation were provided with tubes of about 20 mm bore and from 20 to 40 cm in length in place of the usual capillary Electrodes of carbon were used, and side tubes blown out into small bulbs containing phosphorus pentoxide, caustic potash and potassium permanganate were attached A palladium regulator was sometimes used for the removal of any excess of hydrogen In the case of tubes filled with helium, purification was effected by means of charcoal cooled with liquid air, and tubes filled with neon and argon were freed from diatomic impurities by means of side tubes provided with magnesium electrodes When a heavy discharge was passed between these electrodes, all diatomic impurities excepting hydrogen were rapidly absorbed The phenomena can be observed over a fairly wide range of pressure, but a pressure of from 30 to 40 mm of mercury seems to be most favourable

Helium tubes when prepared in the manner described above show at first the Ångstrom carbon bands and the Swan bands with the line spectrum of helium, but after prolonged running and heating of the palladium regulator these bands are replaced by the comet tail spectrum, and at an intermediate stage the triplet system of bands* is generally seen At a certain stage there is sometimes a magnificent display of striæ which wave about in an irregular manner, sometimes rotating about the axis of the tube, and are obviously in a very unstable state It is worth recording that when condensed discharges are passed through these tubes there is a "clean-up" of diatomic gases It may be mentioned that if a tube with carbon electrodes is filled with nitrogen and excited with an uncondensed discharge, the nitrogen is rapidly absorbed and a brown film, presumably of paracyanogen, is formed on the glass round the electrodes A state is reached at which the helium tube, when excited by the uncondensed discharge from a high tension transformer fed with alternating current at 50 cycles, shows an almost uniform green glow, the spectrum of which consists of the comet tail bands, a feeble line spectrum of helium and faint Swan bands With currents of moderate intensity this state of affairs will, as a rule, persist without any apparent change for a long time, but it is possible, either by introducing a condenser and spark-gap into the circuit or sometimes by a sudden variation of the current, to start a disturbance which gives rise to an entirely different type of discharge It has been shown that a condensed discharge under these conditions gives rise to the band spectrum of helium and the arc spectrum of carbon By means of a suitably designed switch the uncondensed discharge could be rapidly changed over to the condensed discharge and back again to the uncondensed discharge After this has been done several times, the glow in the tube becomes irregular, and bright yellow patches, showing the helium spectrum brilliantly, are seen The patches form a rather irregular spiral down the length of the tube, but as a rule disappear a short time after the condenser and spark-gap have been cut out After a time a stage is reached at which, in place of the irregular spiral patches, a symmetrical disc, sometimes 10 mm in thickness, seems to gather together rather suddenly after the condenser and spark-gap are cut out, and after showing at first some tendency to wander about the tube ultimately settles down in some fixed position The disc sometimes will persist for as long as 10 minutes before breaking up and leaving the uniform green glow which was at first seen in the tube A number of these discs are frequently formed in a long discharge tube, but this state of affairs does not appear to be so stable, and the discs either break up or more often join together to form a single disc The union of two discs is a very striking phenomenon and invariably follows the same course The two discs slowly approach one another and are suddenly replaced by a group of bright longitudinal streamers, usually about 20 mm in length, which rotate about the axis of the tube for some time and are then suddenly replaced by a single disc These phenomena are of quite regular occurrence, but there is another type of stria which is occasionally seen, namely, a single narrow longitudinal band which rotates round the axis of the tube The bright groups of longitudinal striæ, which are always formed for a short time when two discs unite, can be made more persistent if the spark-gap is closed without taking the condenser out of the circuit Under these conditions, by a careful regulation of the current, either the longitudinal groups or the discs can be maintained, the latter being formed at higher current densities

---

* Merton and Johnson, *loc. cit*

The spectrum of the discs differs in two respects from that of the green glow The helium lines, which are feeble in the green glow, and the comet bands are very bright in the discs, but the Swan bands can only be seen in the green glow, being entirely absent in the discs

Prof R W Wood has suggested to me that, as in the case of Langmuir's experiments, an examination with a powerful beam of light might be of value A beam of sunlight, with the aid of a heliostat and a large aperture lens, was brought to a focus in the tube It was at once apparent that the sunlight was scattered strongly in the neighbourhood of the discs, the scattered light being almost sky blue in colour, and examination with a Nicol prism showed that it was almost completely polarised There can be very little doubt that this scattering is due to very small particles of carbon, and the discs seem to be surrounded by an envelope of these scattering particles Under favourable conditions the blue light scattered by the cloud may be visually almost as bright as the green glow, in which there is no perceptible scattering The scattered light can as a rule be seen for some time after the discharge has been cut off, and this method has revealed another interesting fact When the discharge is in the condition in which there are groups of longitudinal striæ rotating round the axis of the tube (or better still the single rotating longitudinal band), these striæ also show powerful scattering, and on switching off the discharge it is seen that the longitudinal streaks of scattered light, which persist like ghosts of the striæ, continue to rotate The same effect has occasionally been seen in the case of very small discs which do not fill the entire tube, but rotate round the axis This shows that the rotation is not simply due to a change in the path of the discharge but that the gas itself is set in motion

The structure of the discs is not uniform They have a rather bright core and the central section seems to be rather bluish in colour, the outer parts being a light salmon pink An examination of the discharge has been made by two stroboscopic methods In the first method a disc provided with narrow slots was mounted on a synchronous motor which was driven from the same source of alternating current as that which supplied the high tension transformer, thus enabling observations to be made at any desired phase It was found that the discs became narrower at maximum and widened out with a slight minimum in the centre as zero phase was approached, and there was no perceptible afterglow at zero phase This is in harmony with the observation that if the current was switched off for more than a fraction of a second, the disc did not reappear on turning it on again, but with a short interruption of the current the disc would sometimes re-form itself from a diffuse region of luminosity which rapidly contracted to the normal condition of the disc An examination with a rotating mirror has confirmed these observations and has revealed the fact that, in addition to the stationary discs, there are rapidly moving striations throughout the tube, similar to those observed by Aston (*loc cit*) and by Whiddington (*loc cit*), but these are very faint in comparison with the discs Mr A C G Egerton, F R S, has kindly allowed me to repeat some of these observations in his laboratory with a transformer operating at 500 cycles Under these conditions the discs are much thinner, in harmony with the observation that they tend to spread out towards zero phase

It is well known that the striations usually observed in tubes containing air and many other gases are very sensitive even to weak magnetic fields, and that when a permanent horseshoe magnet is brought near one end of such tubes, the striæ along the whole length of the tubes are displaced Under similar conditions the discs are unaffected, and a magnet brought right up to the tube where the disc is situated produces no noticeable change in its appearance On the other hand, if a piece of earthed metal foil is wrapped round the tube, the discs tend to settle inside it

Investigations with unidirectional discharges have thrown a good deal of light on the mechanism of the disc discharge A commutator was fitted to the synchronous motor, and by a suitable arrangement of brushes the high tension alternating current from the transformer could be made unidirectional A change-over switch was arranged so that the disc could be formed in the usual manner with the alternating discharge, and then by throwing over the switch the current could be made unidirectional This is a very striking experiment On throwing over the switch the disc breaks up and at the same time moves towards the anode so rapidly that its motion can be barely followed by eye, and in the course of 10 or 15 seconds it is seen that practically the whole of the volatile carbon compounds have migrated to the cathode end of the tube, the anode bulb and about two-thirds of the positive column, showing practically nothing but the line spectrum of helium That this localisation of the spectra is not due to the changed electrical conditions but to an actual transfer of the carbon compounds is shown by the fact that it persists for some considerable time after the discharge has again been made alternating, and, indeed, until the gases have again become mixed by diffusion It has been known for many years that migration of gases occurs under certain conditions in the electric discharge, but the extreme rapidity of the effect in these tubes, considering that the pressure is in the neighbourhood of 35 mm of mercury, is very striking The disc can be made to travel down the tube with any desired velocity by connecting a number of accumulators in series with the high tension alternating current, thus giving the current a certain bias in one or the other direction. If the accumulators are thrown in after the stationary disc has been formed in the usual way, the disc immediately wanders off in the direction of the anode, its velocity depending on the voltage applied With a bias of as little as 16 volts it moved slowly but definitely, and with 100 volts its motion was quite rapid

A large number of mixtures of gases have been investigated, but in no other case excepting that of a neon tube provided with carbon electrodes has the disc discharge been observed, and in this case it was only observed four times for a few seconds The results obtained with neon and argon tubes with carbon electrodes are of some interest The tubes were exactly similar in construction to those used in the case of helium The comet bands appear rather feebly in neon but cannot be observed at all in the argon tubes *

In neon it is very rare that the conditions necessary for the production of the disc discharge are realised, though on four occasions after passing the condensed discharge the discs formed for a few seconds when a very heavy current was used On one of these occasions it was possible to make the observation that the discs moved to the anode when the current was made unidirectional As a rule the appearance of the discharge in neon and argon is quite different, and in neither of these gases has any fog been observed The most usual type of discharge in neon after the condensed discharge has passed for some time is that of a pair of filaments, one starting at each pole and terminating in a bright ball about a centimetre from the other pole Sometimes more than two filaments are formed, and in argon there are generally two or three filaments starting from each pole These filaments seem to wander about aimlessly but avoid one another On bringing up a horsehoe magnet it is seen that the filaments starting from one pole are deflected in one direction and those starting from the other pole in the opposite direction, showing that some filaments convey one half of the cycle and the others the other half This has been confirmed by stroboscopic investigation In both neon and argon, as in the case of helium, there is a rapid migration of the carbon compounds to the cathode when the discharge is made unidirectional It may be mentioned that in helium containing a trace of nitrogen a similar migration of the nitrogen is observed With other gases the effect is not conspicuous

A theoretical treatment of all these phenomena cannot at present be given, but a discussion of certain main features may be attempted In the first place

---

* Johnson and Cameron, 'Roy Soc Proc,' A, vol 106, p 195 (1924), Cameron, 'Phil Mag,' vol 1, p 405 (1926)

the formation of the carbon fog seems to present no theoretical difficulty Direct observation shows that the discs contain a high concentration of excited helium atoms, and it may be presumed that these have the energy necessary to decompose, by collisions of the "second kind," the carbon monoxide molecules It is to be presumed that very few, if any, neon or argon atoms acquire sufficient energy to accomplish this In the second place the migration of the carbon compounds to the cathode can be accounted for by assuming that these molecules readily lose electrons, but only rarely acquire a negative charge, resulting in a general migration to the cathode The explanation of the disc discharge is not so obvious, but it is probably closely related to the migration of the carbon compounds

The spectrum of the disc shows that it is a region of much higher potential gradient than the rest of the positive column, in which the luminosity is feeble and the Swan bands are seen in addition to the comet bands and weak helium lines One of the tubes had a short piece of fine tungsten filament sealed in the wall of the tube and extending across the tube perpendicular to its axis With a rather heavy current it was seen that the filament was heated to visible redness when a well-developed disc passed over it Experiment shows that something in the nature of a cataclysm is needed to establish the disc at all, but granted that it is once formed its maintenance may perhaps be accounted for by assuming that the steep potential gradient in the disc is due to a scarcity of carbon monoxide molecules in this region, and that this scarcity is kept up by the fact that any molecule that strays into that region at once loses an electron and is shot out towards the cathode for the time being We now see why the direct current bias superposed on the alternating current causes the disc to travel towards the anode, since the removal of carbon monoxide molecules is more effective in one direction than the other The part played by the formation of the carbon fog is not quite clear, and whilst it is an experimental result that the disc discharge has only been observed regularly where a carbon fog is formed, it is not certain whether the formation of a particulate cloud is essential to the disc discharge or whether it merely makes it easier to produce it in the laboratory The discs observed are certainly regions where chemical decomposition is taking place Prof F A Lindemann, F R S, has pointed out to me that a considerable amount of energy is absorbed in the formation of a particulate carbon fog, and this may well have some effect on the ease with which the phenomenon can be produced The disc discharge is most readily obtained with rather powerful discharges, and on the few occasions that I have seen it in neon, currents of the order of 0 2 ampere were employed One might perhaps suppose that with sufficiently powerful discharges the disc discharge might be formed in other gas mixtures, and it is very tempting to speculate that the rare phenomenon known as ball lightning is an example of a single disc descending from a charged cloud to the earth. If, for example, the disc gave rise to a copious supply of nitrogen atoms, in place of the carbon fog observed in the laboratory, the damage which is said to occur when ball lightning encounters material objects would be accounted for

---

The Restored Electron Theory of Metals and Thermionic Formulæ

By R H Fowler, F R.S

(Received December 6, 1927)

In a recent paper* Sommerfeld has completely reinstated the electron theory of metallic conduction and other thermo-electric effects in good conductors by applying the Fermi-Dirac statistics to an atmosphere of free electrons in the metal, of a concentration of the order of one per atom It is the purpose of this note to call attention to an application of this theory which Sommerfeld does not discuss, namely, the calculation of the density of evaporated electrons in equilibrium with the heated metal † This calculation, of course, bears on the well-known formula for thermionic emission and gives it a form on which I wish to comment

It is for some reasons desirable to establish the vapour-pressure formula on the new basis without particularised assumptions as to the mechanism of emission and absorption of electrons To do this we have only to consider the equilibrium state of an assembly of electrons in two phases—one a volume outside the metal in which the energies of the electrons are the characteristics of the Schrödinger waves proper to such an enclosure in which the potential energy of an electron is zero, the other a similar volume inside the metal, with similar characteristics, but now, of course, all diminished by a large (constant) negative potential energy χ_0. Outside the density is low and the degeneracy is negligible, so that we have (practically) classical distributions Inside the electrons are almost tight-packed and the degeneracy is of dominant importance It follows at once by the usual statistical arguments* that if $\overline{\mathrm{N}}$ is the average number of electrons in either phase, ϵ_σ the characteristics and g_σ the weights for electrons in that phase, then

---

* Sommerfeld, 'Naturwiss,' p 825 (1927)

† I have recently learnt that this application too will be considered by Sommerfeld in a more detailed account of this theory now in course of publication.

$$\overline{\mathrm{N}} = \mu \frac{\partial}{\partial \mu} \Sigma_\sigma g_\sigma \log (1 + \mu e^{-\epsilon_\sigma/k\mathrm{T}}) \tag{1}$$

In this equation μ is a parameter equivalent to the thermodynamic *partial potential of the electrons* In all cases $g_\sigma = 2$, the number of orientations of the electron, but we shall retain the symbol g for ease of comparison with Sommerfeld, since he omits it and takes $g = 1$ In the vapour μ is small and we have, if $\overline{n_f}$ is the equilibrium concentration there,

$$\overline{n_f} = g \frac{(2\pi mk\mathrm{T})^{3/2}}{h^3} \mu \tag{2}$$

In the metal $\mu e^{\chi_0/k\mathrm{T}}$ is large [in fact $\log \mu + \chi_0/k\mathrm{T}$ is itself large] and we have, if $\bar{n}$ is the equilibrium concentration,

$$\bar{n} = g \frac{(2\pi mk\mathrm{T})^{3/2}}{h^3} \frac{2}{\sqrt{\pi}} \left[\tfrac{2}{3} \{\log (\mu e^{\chi_0/k\mathrm{T}})\}^{3/2} + \frac{\pi^2}{12} \{\log (\mu e^{\chi_0/k\mathrm{T}})\}^{-\frac{1}{2}} \right] \tag{3}$$

Terms of order $\{\log (\mu e^{\chi_0/k\mathrm{T}})\}^{-3/2}$ have been omitted in (3) The equilibrium state is characterised by the same value of μ in all phases, so that, solving (3) for μ and inserting in (2), we find

$$\log \mu = -\frac{\chi_0}{k\mathrm{T}} + \frac{h^2}{2m} \left(\frac{3\bar{n}}{4rg} \right)^{2/3} \frac{1}{k\mathrm{T}} - \frac{\pi^2}{12} \frac{2m}{h^2} \left(\frac{4\pi g}{3\bar{n}} \right)^{2/3} k\mathrm{T}, \tag{4}$$

$$\overline{n_f} = g \frac{(2\pi mk\mathrm{T})^{3/2}}{h^3} e^{-\chi/k\mathrm{T} - \tau k\mathrm{T}(\bar{n})^{2/3}}, \tag{5}$$

where

$$\chi = \chi_0 - \frac{h^2}{2m} \left(\frac{3\bar{n}}{4\pi g} \right)^{2/3},$$

$$\tau = \frac{\pi^2}{12} \frac{2m}{h^2} \left(\frac{4\pi q}{3} \right)^{2/3} \tag{6}$$

Formula (5) differs from those recently used in thermionic theory† in two ways, by the factor g (= 2) and the extra term in the exponential The latter is equivalent to taking account of "the specific heat of electricity" Sommerfeld

---

[*] For the development of these formulæ, see Dirac, 'Roy Soc Proc,' A, vol 112, p 661 (1926), Pauli, 'Zeit für Phys,' vol 41, p 80 (1927), Fermi, 'Zeit für Phys,' vol 36, p. 902 (1926), Fowler, 'Roy Soc Proc,' A, vol 113, p 432 (1926), 'M N R A.S,' vol 87, p 114 (1926)

[†] See, for example, Dushman, 'Phys Rev.,' vol. 21, p 623 (1923), Richardson, 'The Emission of Electricity from Hot Bodies' (1921)

has already discussed this, and shown that the value given by the theory is in good general agreement with the observed values It is small and need not be further analysed here, beyond recording that, as σ is an equilibrium property of the metal, and terms depending on it are perhaps most simply obtained, as here, by direct calculation of the thermodynamic functions

The occurrence of the extra factor 2 (g) in (5) is of some interest, and has not been previously noted, though its presence must have been suspected by many, ever since the spinning electron was introduced If we apply the usual argument about the equality of rates of emission and reabsorption in the equilibrium state, the thermionic saturation current derived from (5) is

$$I = gA\,(1 - r)T^2 e^{-\chi/kT}, \tag{7}$$

where A has the usual value[*]

$$A = \frac{2\pi k^2 m\varepsilon}{h^3}, \tag{8}$$

ε being the electronic charge The numerical value of A when the current is reckoned in amperes per square centimetre is sufficiently nearly 60 The fraction of electrons reflected out of those incident on the metal from the gas phase is r, and r *may* depend on the temperature

It has been found that the best determinations of the electronic emission for the metals tungsten, molybdenum, tantalum and platinum (and probably others) *in a very pure state* agree very well with this value 60, that is, with making $g\,(1 - r) = 1$ The emission observed, however, from metals affected by surface impurities, *e g* , cæsiated or thoriated tungsten filaments and many of the oxide-coated filaments used in Wehneld cathodes, do not agree with this value, but require smaller values, as small, perhaps, as 3 amperes per square centimetre I refer only to emissions which have been properly observed and analysed over a wide temperature range, so that the form of (7) with r constant is known to hold sufficiently exactly It has always been to me an unsatisfactory feature in the theory of this effect that agreement was ever reached (on the older theory) with a value of the reflection coefficient r practically zero Direct experiments to determine r, so far as these can be relied on, never suggest a zero reflection, but rather a reflection of the order of $\frac{1}{2}$[†] Moreover, admitting the extreme sensitivity of thermionic effects to the nature of the *surface* layer, it is still unreasonable to expect a variation of r over almost the full range 0 to 1 with the changing nature of the surface The present theory is far more satisfactory in suggesting that the minimum value of r is about ½, occurring for perfectly clean metallic surfaces The maximum remains as before at 1 The minimum is then in full accord with direct experiment *

---

[*] Dushman, *loc cit.*

[†] Richardson, *loc cit*, pp 55, 170

The argument of the foregoing paragraph has been presented as if the observed variations in the constant A′ of the equation for the current

$$I = A'T^2e^{-\chi/kT} \tag{9}$$

were to be interpreted directly as variations in the reflection coefficient of the surface It is assumed, of course, that the current is known to be accurately of this form I do not know if any other writers have ventured to commit themselves explicitly to this view I believe it to be certainly correct The main object of this note is to present this view and suggest that it is of some importance Changes of A′ due to surface films are almost invariably connected with changes in χ in a way which can be accounted for theoretically

To make this further progress in thermionic theory it is necessary to consider the mechanism of the reflection process, and a discussion of this mechanism on simple assumptions seems now to be possible, using quantum mechanics and the electronic theory of the metal reinstated by Sommerfeld In a paper now in course of publication Nordheim† has shown how to derive formula (7) by considering the numbers of electrons incident on the discontinuity or sharp gradient of the potential at the boundary of the metal, and their reflection coefficient there But he has gone further by actually evaluating the reflection coefficient by a study of the behaviour of the plane Schrodinger-de Broglie wave representing the electron when it falls on a plane of discontinuity or sharp gradient in the potential If the rise in the potential energy of the electrons takes place in a single clean step at the surface, as might be expected for an uncontaminated metal, then the theoretical reflection coefficient is of the order of ½ If, then, the surface is contaminated and this is represented by a thin layer in which the potential gradient is reversed so that the complete step from inside to outside is diminished, the coefficient $(1 - r)$ is also diminished, it may be in suitable cases by a large factor, just as the observations show One must not press the numerical agreement as, of course, the problem has been over simplified by abolishing the atomic structure of the metal A complete discussion will be found in Nordheim's paper

---

* In certain cases where the surface film is more electro positive than the primary metal values of A′ appear to be obtained from the form (9), which are greater than 120 Such values, if substantiated, must be accounted for somewhat differently

† Nordheim, 'Zeit für Phys' (*in the Press*)

Gaseous Combustion at High Pressures Part IX —The Influence of Pressure upon the "Explosion Limits" of Inflammable Gas-Air, etc., Mixtures

By William A Bone, D Sc, F R S, D M Newitt, Ph D, and
C M Smith, B Sc

(Received November 24, 1927)

Introduction

It has long been known that for mixtures of any particular combustible gas and air (or oxygen) there are, under given physical conditions, certain limits of composition within (but not outside of) which self-propagation of flame will occur indefinitely after ignition has once been effected These limits, usually referred to as the "lower" and "upper" limits of inflammability, respectively, at given temperature and pressure vary somewhat (i) with the position of the source of ignition, since the progress of the flame may be assisted or retarded by convection currents according as it has to pass in an upward, horizontal, or downward direction, and (ii) according to the size and material of the containing vessel

It has also been established during recent years that what may be termed the "range of inflammability" of mixtures of any particular gas and air (oxygen) is widened when the temperature is raised Thus, for example, according to H G White, the "ranges of inflammability" for downward propagation of flame at atmospheric pressure of gas-air mixtures steadily widen with increasing temperature,* e g —

Combustible gas.	Hydrogen	Carbonic oxide	Methane
Temp. ° C	Per cent	Per cent	Per cent
17	9 4 to 71 5	16 3 to 70 0	6 3 to 12 9
100	8 8 to 73 5	14 8 to 71 5	5 95 to 13 7
200	7 9 to 76 0	13 5 to 73 0	5 50 to 14 6
400	6 3 to 81 5	11 4 to 77 5	4 80 to 16 6

Comparatively little, and that less certainly, is known about the influence of pressure upon such "limits of inflammability," because until quite recently little or no work had been done at initial pressures higher than about 10 atmospheres, and even so the available data have been insufficient for a proper judgment of the matter

---

* 'Trans. Chem Soc.,' vol 127, pp 672–84 (1925)

In the year 1914 Terres and Plentz* found that the " ranges of explosibility " of mixtures of air with hydrogen or carbonic oxide, respectively, were narrowed at each end on increasing the pressure (at room temperature) from 1 to 10 atmospheres In the case of methane-air mixtures, however, an opposite effect was observed, the " range of explosibility " widening slightly with said pressure increment, in the sense of the " higher " limit being raised a little more than the " lower " Their data, which referred to downward propagation of flame at room temperature in a closed cylindrical iron vessel, 37 cm long × 8 cm diameter, were as follows —

Mixtures	Fxplosion range Per cent combustible gas at	
	1 atmosphere	10 atmospheres
Hydrogen air	9 0 to 68 5	9 5 to 67 5
CO air	15 9 to 72 9	18 4 to 62 4
Methane air	6 0 to 13 0	6 6 to 14 0

The above results for methane-air mixtures were substantially confirmed in 1918 by W Mason and R V Wheeler, whose published data for downward flame propagation at room temperature were as follows† —

Pressure	Percentage methane in mixture at	
	Lower limit	Upper limit
mm		
760	6 00	13 00
1250	6 05	13 15
2900	6 20	13 60
4650	6 40	14 05

As it seemed desirable that the matter should be investigated over a much wider range of initial pressure than had been employed by the workers referred to, some months ago experiments were instituted in the Imperial College High Pressure Research Laboratories with such object in view The present paper embodies the results of our observations upon the " explosion-ranges " at room temperature of hydrogen air, methane-air, and carbonic oxide air mixtures at varying initial pressures up to 125 atmospheres

---

* ' J Gasbel.,' vol 57, pp 995, 1016, 1025 (1914)

† ' Trans. Chem. Soc ,' vol 113, p 45 (1918)

Whilst our experiments were in progress, however, G Berl and G Wenger* published the results of some experiments recently made by them upon the influence of pressure upon the "combustion limits" of mixtures of air with various inflammable gases and vapours They showed, *inter alia*, that the "lower" limit for hydrogen air mixtures, which started at 7 0 per cent at atmospheric pressure, rose steeply with pressure up to 10 8 per cent at 21 atmospheres, after which it fell gradually to 8 4 per cent at 210 atmospheres With "weak ignition" the curve of the "upper limit" rose with pressure, smoothly concave to the pressure axis, from 60 per cent of hydrogen at 1 atmosphere to 73 5 per cent at 210 atmospheres, but with strong ignition," it fell from 71 5 per cent at 1 atmosphere to 69 per cent at 10 atmospheres, then slowly rose to 74 per cent at 210 atmospheres The "combustion range" of methane air mixtures was found at first to diminish somewhat as the initial pressure rose from 1 to 21 atmospheres, after which it rapidly increased with pressure up to 400 atmospheres, thus —

Pressure Atmospheres	Combustion range Per cent methane with air
1	6 6 to 12 7
21	7 5 to 12 0
400	5 2 to 46 0

We shall refer to these results later on in discussing our own, meanwhile, from Berl and Wenger's experiments (which, however, did not include any with CO air mixtures) it seemed that whilst generally the "combustion ranges" of the mixtures studied widened with increasing pressure, in some cases the effect of a moderate pressure increase (*e g*, up to about 20 atmospheres) might be to narrow them somewhat

In our experiments the "explosion limits" at room temperature of hydrogen-air, methane air, and CO air mixtures have been determined from initial pressures of 1, 5, 10, 30, 50, 75 and 125 atmospheres, respectively, whilst those of CO-"helium air" and CO "argon-air" (*i e*, of mixtures of carbonic oxide with an "air" composed of 20 9 per cent of oxygen and 79 1 per cent of helium, or argon, respectively) were in each case determined at initial pressures of 10 and 50 atmospheres, respectively The results showed un mistakably that, whereas the general effect of increased pressure is to widen the "explosion limits" of either hydrogen-air or methane-air mixtures, those of CO-air mixtures are steadily narrowed thereby, and particularly so when the "inert" constituent of the "air" is nitrogen

---

* 'Z angew Chemie,' vol 40, p 245 (1927).

EXPERIMENTAL

Criteria of "Explosion Limits"

Except in experiments at initial pressures of 1 and 5 atmospheres, and occasionally at 10 atmospheres also, one or other of our two spherical bombs Nos 2 or 3 (fig 1, explosion chamber in each case = 240 c c) described in Parts III and V of this series* (*q v*) was employed In such cases, although it was impossible to see the flames, the explosion could be followed both by means of pressure-time records, obtained by means of our Petavel recording manometer, and by chemical analysis of the products The criteria of "limit mixtures" finally adopted after a series of preliminary trials were —

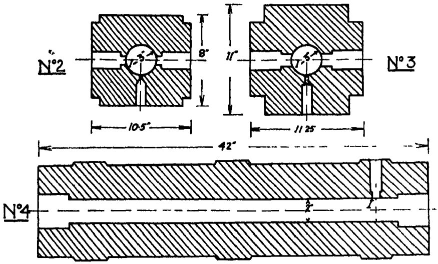

FIG 1

(i) *For* H_2*-Air and* CH_4*-Air Mixtures* —The lower and upper limits were indicated by the weakest and strongest mixtures, respectively, which when fired propagated flame with 99 to 100 per cent combustion, this being regarded as proof that the flame had completely filled the explosion chamber

(ii) *With* CO-*Air Mixtures* —Each of the two "limit-mixtures" at a particular pressure was clearly indicated by an abrupt change in the "percentage combustion" when mixtures of slightly varying CO-contents in the neighbourhood of each "limit" were fired in the bomb, as shown in each case by the point of intersection of the horizontal and vertical portions of the "percentage combustion diagrams" accompanying the text.* A careful study of these diagrams in conjunction with the corresponding tables will, we think, satisfy everyone familiar with the art that the "explosion limits" at each particular pressure may be correctly ascertained in this way.

---

* 'Roy Soc Proc,' A, vol. 103, p 205 (1923), and vol 108, p 393 (1925)

In experiments at initial pressure of 1, 5 and sometimes even 10 atmospheres we employed our cylindrical bomb No. 4 (fig. 1, explosion chamber = 75 cm. long × 5 cm. diameter, capacity = 2 litres) fitted at each end with a quartz window, so that the explosion could be judged by the eye. Here the criterion of the "lower" or "upper" explosion limit, as the case might be, at any given pressure was the weakest or strongest mixture, respectively, at that pressure through which, on ignition, there resulted propagation of flame from one end to the other of the explosion chamber. It should here be explained that, whereas as soon as the upper limit in a particular case had been passed, flame usually ceased to be propagated at all through the mixture, there were always mixtures weaker than the "lower" limit mixture which would allow of a certain limited flame propagation with all degrees of partial combustion; none of these mixtures, however, would propagate flame indefinitely. In the cases of some very weak mixtures, which on ignition gave up to about 10 per cent. complete combustion, this may have occurred merely in a halo or cap around the source of ignition, but was extinguished before it had penetrated far into the main body of the mixture.

The experimental results for the various mixtures investigated can be shown most conveniently in the following series of tables and curves, interspersed with such explanatory paragraphs as may be necessary to their interpretation. In the tables,

P_i = initial pressure in atmospheres at which the mixtures were fired.

P_m = observed maximum pressure in atmospheres attained in the explosion.

t_m = time in seconds taken for the attainment of P_m from the commencement of the pressure-rise.

It should also be noted that such expressions as "100 *per cent. combustion*" always mean that so much of the combustible gas or oxygen (whichever was present in defect) was used up in the explosion.

---

* See Part VII hereof, *ibid.*, vol. 115, p. 45 (1927).

The source of ignition used for all explosions between the "upper" and "lower" limits was always the fusion of a half-inch length of thin platinum wire (diameter = 0·005 inch, stretched between two studs in the ignition plug) by means of an electric current from a battery of secondary cells with p.d. = 12 volts. In some cases, however, after the "upper" limit had been passed we tried *fusing* the wire by means of D.C. direct from the mains (p.d. = 110 volts), in which circumstances the fusion of the wire is always of an explosive character. In no case, however, did such drastic procedure effect the ignition of a mixture outside the limits as determined by the first-named method of ignition.

We think that, in each case examined, the proportion of combustible gas in the "lower" and "upper" limit mixtures, respectively, may be deduced from our experimental results always to within 0·3 per cent. (and usually less) of the true value. In the case of the "lower" limit mixture, this is probably slightly "lower," but in the case of the "higher" limit mixture slightly higher, than that found experimentally. We have, therefore, placed "arrow" signs in the tabulated results accordingly.

It should also be noted that (i) our limit values are independent of any surface combustion effects at the source of ignition, and (ii) in all cases the gases employed in making the various experimental mixtures were very slowly passed into the bomb from cylinders (at 100 to 150 atmospheres) through an 8-inch long tube packed with freshly prepared and specially purified phosphoric anhydride, so that in each case the explosive mixtures would be fired in a uniformly extremely dry condition.

Hydrogen-Air Mixtures

(1) *With* $P_i = 1$ *Atmosphere*

The "lower-limit" mixture, as determined in the cylindrical bomb No. 4, contained 9·9 per cent. of hydrogen; owing to the very faint visibility of the flame at this pressure, however, a reliable figure for the H_2-content of the "upper-limit" mixture was unobtainable.

(2) *With* $P_i = 5$ *Atmospheres*

The visibilities of the flames at this pressure permitted the determinations of both limit mixtures in our cylindrical bomb No. 4 as follows:—

Lower-limit mixture = 9·9 H_2/90·1 Air

Upper-limit mixture = 68·4 H_2/31·6 Air

(3) *With* P_i = 10 *Atmospheres* (*Spherical Bomb No* 2)

H_2 in mixture	P_m obs	t_m	Percentage combustion
Per cent	Atmospheres	Seconds	
8 4	18 0	0 70	40 0
9 6	20 0	1 00	73 0
10 0	27 5	0 65	94 0 Lower
10 2	34 0	0 40	100 0 limit
10 7	38 0	0 30	100 0
67 4	42 0	0 10	100 0
68 4	42 0	0 13	100 0
68 5	40 5	0 15	100 0 Upper
68 9		would not fire	limit

Determinations made in the cylindrical bomb No 4 gave results closely agreeing with the above, which were thus confirmed

(4) *With* P_i = 30 *Atmospheres* (*Spherical Bomb No* 2)

H_2 in mixture	P_m obs	t_m	Percentage combustion
Per cent	Atmospheres	Seconds	
9 0	60 0	0 55	54 0
9 7	80 0	0 80	93 9
10 0	99 0	0 85	96 4 Lower
10 6	97 0	0 76	100 0 limit
71 1	116 0	0 49	100 0
71 4	113 0	0 53	100 0
71 9	111 0	0 62	100 0 Upper limit
72 0 72 8	would	not fire	

(5) *With* $P_i = 50$ *Atmospheres (Spherical Bomb No* 2)

H_2 in mixture	P_m obs	t_m	Percentage combustion
Per cent	Atmospheres	Seconds	
9 2	142 0	1 29	86 8
9 5	154 0	1 04	89 0
9 7	184 0	0 60	97 2
10 0	197 0	0 39	99 8 ← Lower limit
72 8	164 0	1 26	100 0
73 1	190 0	0 60	100 0
73 3	178 0	0 80	100 0 ← Upper limit
73 4	60 0	1 25	53 0

(6) *With* $P_i = 75$ *Atmospheres (Spherical Bomb No* 2)

H_2 in mixture	P_m obs	t_m	Percentage combustion
Per cent	Atmospheres	Seconds	
9 0	249 0	1 04	75 0
9 3	260 0	0 90	89 2
9 6	277 0	0 72	92 0
9 9	277 0 290 0	0 74 1 00	96 0 100 0 ← Lower limit
10 0	289 0	0 90	100 0
10 3	314 0	0 34	100 0
72 0	310 0	0 51	100 0
73 6	281 0	0 90	100 0
73 7	273 0	1 21	100 0
74 2	270 0	1 13	100 0 Upper
74 6	did not fire		← limit

(7) *With* P_i = 125 *Atmospheres* (*Spherical Bomb No* 4).

H_2 in mixture	P_m obs	t_m	Percentage combustion
Per cent	Atmospheres	Seconds	
9 5	440 0	1 00	92 0
9 9	—	—	100 0 ← Lower limit
11 0	480 0	0 98	100 0
72 6	510 0	0 43	100 0
73 2	495 0	0 52	100 0
74 1	470 0	0 57	100 0
74 8	465 0	0 70	100 0 ← Upper limit
75 2	did not fire		

Summary — The experiments showed unmistakably that (i) whilst at all pressures there were mixtures containing less hydrogen than our criterion for the "lower limit," which could be ignited without the flame spreading throughout the whole of the explosion chamber, (ii) the composition of the "lower-limit" mixture giving 100 per cent combustion was hardly (if at all) affected by any increase in the initial pressure between 1 and 125 atmospheres, but (iii) the hydrogen content of the "upper-limit" mixture steadily increased as the initial pressure was raised between said limits, as follows —

Initial pressure	Percentage H_2 in "upper-limit" mixture *
Atmospheres	
5	68 4
10	68 5+
30	71 9
50	73 3
75	74 2+
125	74 8+

It is thus seen that, whilst the composition of the "lower-limit" mixture (namely, about 9 9 H_2/90 1 air) giving 100 per cent combustion was, practically speaking, unaffected, the "explosion range" of hydrogen air mixture was progressively widened by successive increases in the initial pressure, at any rate at pressures above 10 atmospheres This is also shown graphically in the curves reproduced in fig 2

---

* A + or — sign in this (or similar other) column denotes that the figure in question is probably fractionally lower or higher, respectively, than the true value

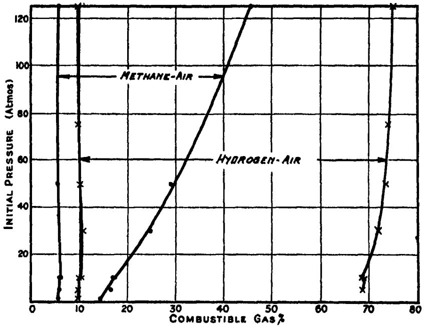

FIG 2.—Limits of Explosibility of Hydrogen-Air and Methane-Air Mixtures Influence of Initial Pressure.

B —METHANE-AIR MIXTURES

The methane used in the experiments was chemically pure, having been prepared by the action of dilute hydrochloric acid upon aluminum carbide and subsequently freed from hydrogen by liquefaction and fractional vaporisation of the liquid hydrocarbon, whose purity was finally confirmed by an explosion analysis The same criteria were adopted for the "lower" and "upper" explosion limits as in the hydrogen-air experiments

(1) *With* $P_i = 1$ *and* 5 *Atmospheres (Cylindrical Bomb No* 4)

The compositions found for the two "limit" mixtures in each case were as follows —

P_i	Percentage CH_4 in limit mixture	
	"Lower"	"Upper"
Atmospheres 1 0	5 6	14 3
5 0	5 7	16 4

(2) *With* P_i = 10 *Atmospheres* (*Spherical Bomb No* 2)

CH_4 in mixture	P_m obs	t_m	Percentage combustion
Per cent.	Atmospheres	Seconds	
5 7	28 0	0 44	17 2
5 8	26 0	0 50	15 1 Lower
6 0	44 0	0 78	100 0 limit
6 2	52 5	0 48	100 0
16 0	34 0	0 90	100 0
16 8	41 0	1 19	100 0
17 1	42 0	1 22	100 0 Upper
17 4	16 4	—	78 0 limit

In corresponding experiments with the cylindrical bomb No 4, results (namely, 5 8 per cent methane for the "lower" limit and 17 0 per cent methane for the "upper" limit mixture) almost identical with the above were obtained

(3) *With* P_i = 30 *Atmospheres* (*Spherical Bomb No.* 2)

CH_4 in mixture	P_m obs	t_m.	Percentage combustion
Per cent	Atmospheres	Seconds	
4 7	did not fire		
5 2 to 5 6	combustion started but speedily died out		7 to 8 only Lower
5 9	148 0	0 98	100 0 limit.
6 2	152 0	0 70	100 0
22 2	167 0	1 05	100 0
22 9	155 0	1 35	100 0
23 5	151 0	1 54	100 0
24 6	149 0	1 77	100·0 Upper limit
24 9	45 0	0 50	combustion started but soon died out
25 7	40 0	—	

(4) *With* P_i = 50 *Atmospheres (Spherical Bomb No.* 2)

CH_4 in mixture	P_m obs	t_m	Percentage combustion
Per cent	Atmospheres	Seconds	
4·8	78·0	—	only slight combustion which soon died out
5·3	80·0	–	
5·4	227·0	1·20	100·0 ← Lower limit
5·7	227·0	1·37	100·0
5·8	243·0	1·06	100·0
27·1	243·0	2·01	100·0
28·4	253·0	1·94	100·0
28·5	231·0	2·35	100·0
29·0	248·0	1·89	100·0 Upper ← limit
29·8	70·0	—	only slight combustion

(5) *With* P_i = 125 *Atmospheres (Spherical Bomb No.* 3)

CH_4 in mixture	P_m obs	t_m	Percentage combustion
Per cent	Atmospheres	Seconds	
5·4	160·0	—	6 to 7 soon died out
5·6	210·0	–	
5·7	655·0	1·58	100·0 ← Lower limit
5·8	748·0	1·41	100·0
5·9	810·0	0·81	100·0
41·4	625·0	1·65	100·0
45·5	550·0	2·39	100·0 Upper ← limit
46·0	180·0	—	about 5 soon died out
48·0	180·0	—	

Summary.—These results show unmistakably that, whilst the methane content of the "lower-limit" methane air mixture is but little (if any) affected, that of the "upper limit" mixture is considerably raised by progressive increases in the initial pressure between 1 and 125 atmospheres, thus, we have —

Initial pressure	Per cent methane in limit mixture	
	Lower	Upper
Atmospheres		
1 0	5 6	14 3
5 0	5 7	16 4
10 0	6 0—	17 1+
30 0	5 9—	24 6+
50 0	5 4	29 0+
125	5 7	45 5+

The above are also shown graphically in fig 2

It should however, be observed that, in the experiments with the spherical bombs (of same capacities) when pressure time records were taken it was found that as the initial pressure increased the time taken for the attainment of maximum pressure (t_m) with each 'limit mixture' also increased thus we found —

P_i	t_m for limit mixtures	
	Lower	Upper
Atmospheres	Seconds	Seconds
10	0 78	1 22
30	0 98	1 77
50	1 29	1 89
125	1 58	2 30

C.—CARBONIC OXIDE-AIR MIXTURES

In working with these mixtures it was soon found that at or near the two "explosion limits" combustion was never quite '100 per cent complete," although the flame had undoubtedly filled the explosion chamber Consequently, a rather different criterion had to be adopted for judging the actual "limit mixtures" from that used in either the hydrogen air or the methane air series After a number of preliminary experiments, the criterion explained on p 557 was adopted as being in our judgment the best. This will (we think) be evident from a study of the "percentage combustion" diagrams shown in figs 3 and 4 respectively

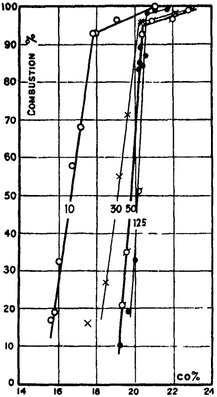

FIG 3 —Percentage Combustion of CO-Air Mixtures at and near the "Lower" Limit

The carbonic oxide used in the experiments had been prepared by warming a mixture of formic and sulphuric acids, the gas evolved being subsequently well scrubbed by passage through a tall tower packed with pumice down which a strong solution of caustic soda was dropped, and it was quite free from either hydrogen or any hydrocarbon impurity

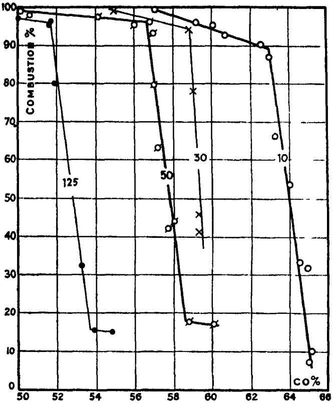

FIG 4 —Percentage Combustion of CO-Air Mixtures at and near the "Upper" Limit.

(1) *With* $P_t = 1$ *or* 5 *Atmospheres* (*Cylindrical Bomb No* 4)

The composition found for the two "limit" mixtures in each case was as follows —

P_t	Per cent CO in limit mixture	
	Lower	Upper
Atmospheres 1 0 5 0	 14 2 15 4	 71 0 67 5

Combustion was never more than between 90 8 and 94 4 per cent complete, although flame was propagated throughout the whole explosion chamber in each case

(2) *With* P_i = 10 *Atmospheres* (*Spherical Bomb No* 2)

CO in mixture	P_m obs	t_m	Percentage combustion	
Per cent	Atmospheres	Seconds		
16 0	24 5	0 61	32 2	
16 7	32 0	0 61	58 0	
17 1	38 0	0 56	68 4	
17 8	36 0	0 71	93 1	← Lower limit = 17 8 CO
17 9	42 0	0 52	92 8	
19 0	52 3	0 43	97 0	
21 0	57 1	0 28	100 0	
55 0	53 5	0 25	99 0	
57 0	49 0	0 40	90 8	
59 2	45 0	0 50	95 9	
60 7	46 0	0 50	92 7	
62 5	43 7	0 50	90 1	
62 9	41 0	0 63	87 2	← Upper limit = 62 8 CO
63 2	30 2	0 40	66 1	
64 0	28 0	0 48	53 5	
64 9	22 0	0 61	31 8	
65 1	16 0	0 60	10 0	

(3) *With* P_i = 30 *Atmospheres* (*Spherical Bomb No* 2)

CO in mixture	P_m obs	t_m	Percentage combustion	
Per cent	Atmospheres	Seconds		
19.4	60.0	0.80	26.7	
19.1	92.0	0.75	55.0	
19.5	112.0	0.73	71.5	
20.3	167.0	0.76	95.5	← Lower limit = 20.3 CO
22.1	188.0	0.54	98.2	
55.0	171.0	0.53	99.0	
57.1	170.0	0.59	99.0	
58.8	153.0	0.89	94.2	← Upper limit = 58.8 CO
59.0	119.0	1.11	78.0	
59.2	75.0	1.00	45.6	

(4) *With* P_i = 50 *Atmospheres* (*Spherical Bomb No* 2)

CO in mixture	P_m obs	t_m	Percentage combustion	
Per cent	Atmospheres	Seconds		
19.6	110.0	0.60	35.0	
20.1	92.0	0.85	51.1	
20.3	268.0	1.08	95.0	Lower
20.9	275.0	0.95	96.6	← limit = 20.6 CO
22.8	325.0	0.61	99.5	
23.5	342.0	0.49	100.0	
56.0	263.0	0.92	95.7	Upper
56.9	256.0	1.19	96.7	← limit = 56.8 CO
57.0	253.0	1.05	92.7	
57.2	163.0	1.05	63.0	
57.7	130.0	1.07	42.0	

(5) *With* $P_i = 125$ *Atmospheres* (*Spherical Bomb No* 3)

CO in mixture	P_m obs	t_m	Percentage combustion
Per cent.	Atmospheres	Seconds	
20 2	—	—	32 5
20 2	830 0	1 10	83 0
20 4	850 0	1 10	84 6
20 5	867 0	0 86	87 0
20 7	900 0	1 24	98 4 ← Lower limit = 20 7 CO
21 1	948 0	1 34	98 8
21 7	945 0	0 64	98 9
50 8	850 0	1 04	99 0
51 6	810 0	1 27	95 2 ← Upper limit = 51 6 CO
51 9	750 0	1 00	80 0
53 3	200 0	0 9	32 0

Summary The so ascertained CO-contents of the "lower" and "upper" limit CO-air mixtures, respectively—assuming the validity of the criterion adopted, which, we think, will be evident from the "percentage-combustion" diagrams shown in figs 3 and 4—are shown in fig 5 and the following table —

Initial pressure	Per cent CO in limit mixture	
	Lower	Upper
Atmospheres		
1 0	14 2	71 0
5 0	15 4	67 5
10 0	17 8	62 8
30 0	20 3	58 8
50 0	20 6	56 8
125 0	20 7	51 6

It thus appears that, contrary to what has been established for both hydrogen-air and methane-air mixtures, the "explosion range" of carbonic oxide-air mixtures narrows considerably as the initial pressure rises The composition of each of the two "limit" mixtures was shifted by increasing pressure towards that of the most explosive mixture But whilst that of the "lower" limit mixture seemed to be but little affected by further pressure-rises beyond 30

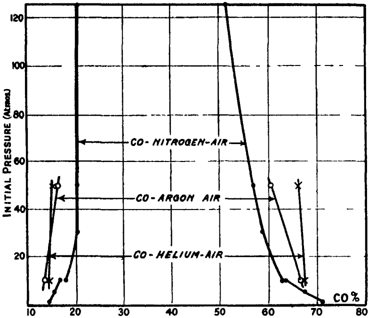

FIG 5 —Limits of Explosibility of Carbonic Oxide with Nitrogen-, Argon, and Helium-Air Influence of Initial Pressure

atmospheres (doubtless due to the fact that the "theoretical" mixture—which is nearly, if not quite, the most explosive of all—contains 28 3 per cent of carbonic oxide) that of the "upper" limit mixture was progressively altered throughout the whole pressure-range investigated Indeed, it would seem possible that at a sufficiently high pressure the two limits would meet, or, in other words, that no CO-air mixture would propagate flame at room temperature or thereabout This is a point which, however, could not be determined by means of the apparatus at our disposal, but with the new bomb apparatus (capable of withstanding pressures up to 20,000 atmospheres) which will shortly be installed in our laboratory, we hope in due course to settle it

D —Carbonic Oxide ' Helium-Air " Mixtures

It was thought advisable to pursue the matter a stage further by examining the behaviour of mixtures of carbonic oxide with an "air" containing 20 9 of oxygen and the remainder helium, so as to eliminate altogether any nitrogen-influence from the system Accordingly, two series of experiments were made in spherical bomb No 2 with mixtures of X CO with Y (20·9 O_2 + 79·1 He)—where (X + Y) = 100—at initial pressures of 10 and 50 atmospheres, respectively, using the same criterion for " limit " mixtures as had been employed throughout the CO-air series The results, details of which are plotted in the " percentage combustion diagrams " shown in figs 6 and 7, showed the following probable CO-contents for each of the two " limit " mixtures in each case —

Initial pressure	Per cent CO in limit mixture	
	Lower	Upper
Atmospheres		
10	13·9	67·3
50	15·1	66·2

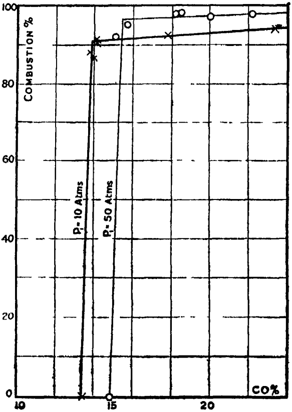

Fig. 6.—CO-Helium-Air Mixtures near Lower Limit of Explosibility

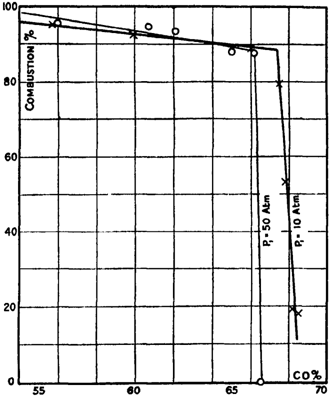

FIG 7 —CO Helium Air Mixtures near Upper Limit of Explosibility

It is thus seen that, whilst a slight narrowing of the "explosion range" resulted from increasing the initial pressure from 10 to 50 atmospheres, it was nothing like that observed in the corresponding experiments with nitrogen as the diluent (see fig 5)

E —CARBONIC OXIDE AND "ARGON-AIR" MIXTURES

Finally, the effects upon the "explosion limits" of using an "air" containing 20 9 per cent. of oxygen and 79 1 of argon as the "supporter" of combustion were studied in No 2 spherical bomb at initial pressures of 10 and 50 atmospheres, with the following summarised results for the CO-contents of each of the two "limit" mixtures at each pressure The detailed results of each of the series of experiments involved are plotted on the "percentage combustion diagram " shown in figs 8 and 9, and summarised in fig 5, from which their character may be judged

Initial pressure	Per cent CO in limit mixture	
	Lower	Upper
Atmospheres 10 50	 14 0 15 3	 66 0 60 4

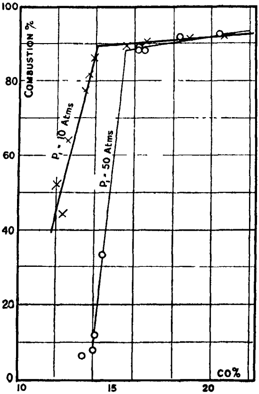

FIG 8 —CO Argon-Air Mixtures near Lower Limit of Explosibility

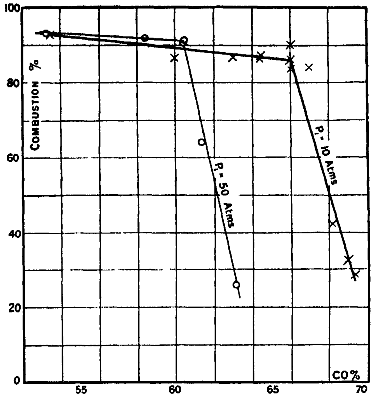

Fig 9 —CO Argon Air Mixtures near Upper Limit of Explosibility

General Summary

From the foregoing it will be seen that, in cases of hydrogen-air and methane-air mixtures, our results confirm those of Berl and Wenger so far as the general widening influence of increasing pressure upon the explosion range is concerned, although our actual figures for the two limits differ somewhat from theirs The differences, however, are perhaps not greater than might be expected considering that, whereas their figures refer to downward propagation of flame, ours refer to propagation more or less horizontally across a sphere

Another point of difference between our results and theirs is that, whereas they found distinct evidence of a narrowing of the limits between 10 and 30 atmospheres (after which increasing pressure widened them again), we found only a very slight indication of such tendency round about 10 atmospheres initial pressure Possibly in their case the observation in question was (as they themselves suggested) due to igniting conditions, for whereas they used spark-ignition, we have used the electrical fusion of a platinum wire, which we have found to be more independent of pressure than spark-ignition.

In the case of CO-" air " mixtures a progressive increase in the initial pressure progressively narrows the explosion range, a feature which is much more marked with nitrogen or argon than with helium as the diluent From our experimental results it seems probable that at some very high initial pressure carbonic oxide-" air " mixtures will become non-explosive at ordinary temperatures, but this is a point which we propose investigating as soon as our new super-pressure bomb (which is on order) has been installed in our laboratories

In conclusion we desire to thank the Department of Scientific and Industrial Research as well as the Government Grant Committee of the Royal Society for generous grants out of which the cost of the expensive apparatus used in the research has been defrayed, and to the D S I R we are also indebted for personal grants which have enabled two of us (D M N and C M S) to devote our whole time to the research

---

On a Method of Determining the State of Polarisation of Downcoming Wireless Waves.

By E V Appleton, F R S, and J A Ratcliffe, B A

(Received November 23, 1927)

1 *Introduction*

In recent papers* an account has been given of the application of certain experimental methods to the study of the characteristics of wireless waves deviated through large angles by the upper atmosphere Observations by these methods have shown that, for wave-lengths of the order of 300 to 500 metres the downcoming waves possess, in general, components of electric force both in and at right angles to the plane of propagation and that somewhat similar changes of intensity take place in both components during the dark hours, but information on the nature of the polarisation (*i e*, on the numerical values of the constants of ellipticity) has been lacking Such information would be of interest from two standpoints In the first place it has been shown that, if the electrical carriers in the upper atmosphere are of electronic mass, the influence of the earth's magnetic field would be such as to cause the reproduction of magneto-optical phenomena for wave-lengths within the wireless spectrum. In such a case we might expect to find some relation between the measured constants of ellipticity and the direction of transmission with reference to the earth's magnetic field. Secondly, a matter of practical interest, since all recent experimental work has confirmed the original suggestions of Eckersley and Bellini that the errors experienced in coil direction finding are due to the presence of a component of electric force at right angles to the plane of propagation, and, since signal variations are due to the component in the plane of propagation, we might expect some correlation between directional errors and fading, if the downcoming ray is of sensibly constant polarisation. Attempts to find such a correlation have been made by Reich[*] but with negative results.

---

* 'Roy Soc. Proc.,' A, vol. 109, p. 621 (1925); vol. 113, p. 450 (1926), vol. 115, p. 291 (1927).

2. *Theoretical Basis of Methods used.*

Let us assume that the downcoming wave possesses normally[†] polarised components of electric and magnetic force E_1 and H_1, while the corresponding magnitudes for the abnormally polarised component are E_1' and H_1'. In our particular experimental conditions (reception at a distance of 70 to 80 miles from a 400-metre transmitter) a ground wave, with electric and magnetic vectors E_0 and H_0 is present. Let the phase difference between the ground wave and the normal and abnormal components of the downcoming wave be θ and θ' respectively. Our problem is to determine the ratio of the axes E_1/E_1'[‡] (or H_1/H_1') and the phase difference $(\theta' - \theta)$ by means of measurements made on the ground. We must, therefore, consider in detail the stationary interference system produced at the receiving station by the ground waves, the downcoming waves incident on the ground and their reflected components at the ground.

Let us first consider more closely the specification of the downcoming wave. Suppose that the positive directions of the normal and abnormal components of electric force are represented by OY and OX in fig. 1. The magnitudes of these two forces are shown in the diagram, p being the angular frequency of the waves and t the time. The direction of propagation is here assumed to be at right angles to the paper and away from the reader. The direction OX is to the right for an observer looking from the sending to the receiving stations For increasing values of t, such as we are considering, the rotation is left-handed if $(\theta' - \theta)$ lies in the first or second quadrants while it is right-handed if it lies in the third or fourth quadrants We must thus know the sign and magnitude of $(\theta' - \theta)$ to be able to complete the specification of ellipticity This rather elementary point is mentioned because it happens that the first part of the experimental method to be described yields directly only the value of $\cos(\theta' - \theta)$ There is thus an ambiguity as to the sign of $\theta' - \theta$ which means that although the type of polarisation is known the sense of rotation cannot be specified From other considerations, however, we are able to deduce from the data the value of $\sin(\theta' - \theta)$ so that the value of $(\theta' - \theta)$ and thus the sense of rotation can be stated

---

[*] 'J. Franklin Inst.,' vol. 203, p. 537 (1927).

[†] As in previous papers, the normally polarised component of electric force lies in the plane of propagation, which is a vertical plane through the sending and receiving stations.

[‡] Actually we determine not E_1/E_1', but $E_1/E_1' \cos i_1$, where i_1 is the angle of incidence of the downcoming ray at the ground, but since i_1 is measurable by experiments previously described, the value of E_1/E_1' may be deduced.

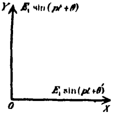

FIG 1

When the downcoming ray reaches the ground it is reflected there, and, for the 400-metre waves we have used, the reflection approximates to that from a perfect conductor We thus have a ground plan of magnetic forces* as shown in fig 2A Here both OA and OB are horizontal, OA lying in the plane of propagation, while OB points to the right for an observer looking from the sending to the receiving station. The magnitudes of OA and OB, in terms of the atmospheric and ground ray intensities, are shown in the figure The system is completed by a vertical electric force of magnitude $(E_0 \sin pt + 2\,E_1 \sin i_1 \sin(pt + \theta))$ passing through O, the positive direction of which is out of the paper

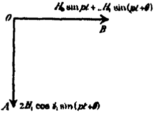
$H_0 \sin pt + 2H_1 \sin(pt+\theta)$
O
B
A
$2H_1 \cos i_1 \sin(pt+\theta)$

FIG 2A.

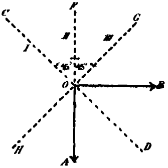

FIG 2B.

---

* *Vide* Appleton and Barnett, "Electrician," vol. 95, p. 678 (1925).

Let us suppose that we are able to measure the amplitude of these horizontal magnetic forces by observations on the signal electromotive forces produced in three differently orientated vertical loops the planes of which (see fig 2B) cut the horizontal plane of fig 2A in CD FA and GH Here one loop (No II) is in the plane of propagation while the other two are inclined at 45° to it *

The magnetic forces linked with the three loops are therefore in order

$$\left.\begin{array}{ll}\text{Loop I} & \dfrac{1}{\sqrt{2}}(\mathrm{H}_0 \sin pt + 2\mathrm{H}_1 \sin (pt + \theta) \\ & \qquad\qquad - 2\mathrm{H}_1 \cos i_1 \sin (pt + \theta)) \\ \text{Loop II} & (\mathrm{H}_0 \sin pt + 2\mathrm{H}_1 \sin (pt + \theta)) \\ \text{Loop III} & \dfrac{1}{\sqrt{2}}(\mathrm{H}_0 \sin pt + 2\mathrm{H}_1 \sin (pt + \theta) \\ & \qquad\qquad + 2\mathrm{H}_1 \cos i_1 \sin (pt + \theta))\end{array}\right\} \quad (1)$$

We note that these expressions involve six unknowns H_0 H_1 H_1 θ θ and $\cos i_1$ so that even were we able to measure the resultant magnetic forces linked with the three loops the determination of the unknown quantities is impossible From the point of view of the present investigation however we may regard $2\mathrm{H}_1 \cos i_1$ as a single variable since by other experiments we can find the value of i_1 Also since the ground wave is known to be sensibly constant we can make $2\mathrm{H}_1/\mathrm{H}_0$ and $2\mathrm{H}_1 \cos i_1/\mathrm{H}_0$ our variables (written *a* and *b* respectively) thus expressing our results in terms of H_0 the magnitude of which could if necessary be determined by a separate experiment The number of variables has therefore been reduced from six to four but the problem appears still insoluble since only three equations can be made We therefore cannot proceed by the direct method of measuring the signal amplitudes on the three loops and have to resort to the artifice of making a small wave length change at the sending station and observe the resulting signal maxima and minima at the receiving station In this way we can in effect make θ and a certain function of $(\theta - \theta)$ pass through known values and by using in our calculations only the signal magnitudes for which the known values can be assigned to these quantities so reduce the number of variables For such an artifice to succeed there must obviously be some other sacrifice in generality In this problem it is that we have to assume that the quantities H_1 H_1 and $(\theta - \theta)$ do not alter when the wave-length of the transmitter is slightly changed and also that they are not altered by natural fluctuations during the period (usually about 15 seconds) required to get a photographic record of the signal interference maxima and minima on the three loops in succession Mention is made below, in the discussion of the results, of the reasons which lead us to believe that these assumptions are justified in the examples taken for calculation

---

* The angle of 45° has been chosen for convenience in calculation. Many experiments have been made using a non symmetrical arrangement of loops. Nothing is gained thereby, so far as the principle of the experiment is concerned but such experiments were considered as being necessary to confirm the results obtained with the symmetrical arrangement

Let us now consider the effect of changing continuously the transmitter wave-length for a case such as we are considering We take the example of the signals received on No II loop The magnetic force linked with this loop may be written

$$H_0 \sin pt + 2H_1 \sin p\left(t - \frac{D}{c}\right),$$

or

$$H_0 \sin pt + 2H_1 \sin (pt + \theta),$$

where

$$\theta = -\frac{pD}{c} \qquad (2)$$

D is the path difference between ground and atmospheric waves and c the velocity of light

Thus we may say that θ increases in a positive direction when the sending station frequency is decreased, and in a negative direction when the frequency is increased

The expressions in (1), for the magnetic forces linked with the three loops may be written

$$\left.\begin{array}{ll} \text{Loop I} & \frac{H_0}{\sqrt{2}}(\sin pt + \sqrt{a^2 - 2ab\cos x + b^2}\sin(pt + \theta + \zeta_1)) \\ \text{Loop II} & H_0(\sin pt + a\sin(pt + \theta)) \\ \text{Loop III} & \frac{H_0}{\sqrt{2}}(\sin pt + \sqrt{a^2 + 2ab\cos x + b^2}\sin(pt + \theta + \zeta_2)) \end{array}\right\}, \quad (3)$$

where

$$x = \theta' - \theta,\ \tan\zeta_1 = -b\sin x/(a - b\cos x) \text{ and } \tan\zeta_2 = b\sin x/(a + b\cos x) \quad (4)$$

Now during a wave-length change θ alters gradually and the values of the electromotive forces produced in the loops, which are proportional to the expressions in (3) for the magnetic forces, pass through maximum and minimum values.

A maximum value will be denoted by M and a minimum value by m. From (3) we may therefore write

$$\left.\begin{array}{c}\left(\dfrac{\mathrm{M}-m}{\mathrm{M}+m}\right)_{\mathrm{I}}=\sqrt{a^2-2ab\cos x+b^2},\quad\left(\dfrac{\mathrm{M}-m}{\mathrm{M}+m}\right)_{\mathrm{II}}=a,\\ \left(\dfrac{\mathrm{M}-m}{\mathrm{M}+m}\right)_{\mathrm{III}}=\sqrt{a^2+2ab\cos x+b^2}\end{array}\right\},\tag{5}$$

where the subscripts refer to the particular loop concerned The quantities on the left-hand sides of (5) may be determined from measurements of the signal maxima and minima as measured separately using the three loops in rapid succession and thus the three unknowns a, b and $\cos x$ may be determined As mentioned previously these quantities specify the type of polarisation of the downcoming wave so far as the ratio of the axes and phase difference is concerned, but they do not tell us which of the component vibrations leads in time

We can, however, determine the value of $\sin x$ in the following way During an increase of the frequency of the sending station we assume, in accordance with our convention, that the angular phase difference between ground and atmospheric rays passes in order through the quadrants from the fourth to the first whereas for a decrease of frequency it passes in the reverse order For any particular frequency of the transmitter (such as that corresponding to one of the end points of the wave-length change) we can therefore read off from the photographs the quantities θ, $(\theta+\zeta_1)$ and $(\theta+\zeta_2)$ both in sign and magnitude It is convenient to take these in pairs from which we can find the values of ζ_1, ζ_2 and $(\zeta_1-\zeta_2)$ Since a, b and $\cos x$ are known we can find the value of $\sin x$ from the value of ζ_1 or ζ_2 or $\zeta_1-\zeta_2$, and when both $\cos x$ and $\sin x$ are known the value of x may be specified Further, since when $\cos x$ is known, $\sin x$ can have one of only two possible values, the substitutions in (5), (6) or (7) serve as a rough check in the values of a, b and $\cos x$ deduced from the amplitudes of the interference "fringes" obtained on the three loops

3 *Experimental Arrangements*

The experiments consisted in recording the signal variations, due to a continuous change of transmitter wave-length, as received successively on three loop aerials. The loop aerials were all similar, each consisting of a single turn of wire forming an isosceles triangle of height 14 metres and base 35 metres The loops were arranged with their vertical axes of symmetry coincident One of the loops (No II) was always directed towards the transmitting station and was thus situated in the plane of propagation The other two loops were always perpendicular to each other and, as previously mentioned, were usually symmetrically arranged with respect to No II loop On occasions they were, however, arranged to make unequal angles with the plane of propagation

By means of a switching arrangement any one of the three loops could be made to form part of a tuned circuit to which was coupled a "flatly-tuned" high frequency amplifier The arrangement of switches was such that when one of the loops was tuned and coupled to the amplifier, the other two loops were entirely disconnected Since no current flows in the idle loops it is believed that they do not sensibly distort the electromagnetic field in the vicinity of the loop in circuit, although there is, in general, an appreciable mutual inductance between two loops situated at 45° to each other To make quite sure on this point experiments were carried out using a single wire aerial in place of loop No II In this case the vertical wire aerial was situated along the axis of symmetry of loops I and III so that there was no magnetic coupling between any two of the three aerial systems Similar results were obtained in this case as in the case in which the three loops were used

The amplifier characteristic was arranged to be flat over a wave-length range of 10 metres about a mean wave-length within the 300 to 500-metre range This was accomplished by using a six valve amplifier employing transformers wound with resistance wire, or, in the case of the more powerful transmissions, a resistance-capacity coupled amplifier The amplified high frequency currents from the output end of the amplifier were passed through a transformer in the secondary circuit of which was a stable crystal detector in series with an Einthoven string galvanometer On testing the whole assembly by means of a calibrated oscillator it was found that the galvanometer deflection was, to the required degree of accuracy, proportional to the square of the high frequency electromotive force introduced into the loop circuit, and this relation has therefore been assumed in all calculations

During a set of observations the transmitter wave-length was changed alternately up and down the range of 10 metres, each change being made in 3 seconds The upper and lower limits of wave-length were maintained for 2 seconds between the changes During the pauses the amplifier was switched* from one loop to the next The loops were usually switched on in the repeated order I, II, III, so that in a record lasting a minute examples of the signal variations resulting from both an increase and a decrease of wave-length were obtained on any particular loop

---

* Telephonic communication was maintained between the transmitting and receiving stations to facilitate correct timing.

4 *Method of Interpreting the Signal Records*

The actual methods employed in calculating the values of a, b and x are best illustrated by the consideration of an example Fig 3 represents the signal current curve obtained at 4 55 a m G M T on May 28, 1927, using the Birmingham B B C transmitter The signal records were made at the Radio Research Station, Dogsthorpe, Peterborough The symmetrical arrangement of receiving loops was used

For the first wave-length change we can read off the signal maximum and minimum values and, allowing for the square law relation between signal electromotive force and current, calculate for any adjacent pair (such as y_0 and y_1), the value of M/m

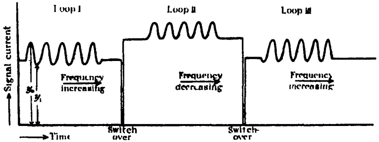

FIG 3

Using an average value of M/m the value of $(M - m)/(M + m)_I$ can be found In a similar way the corresponding quantities for the other two loops may be calculated From these values, using (5) the values of a, b and $\cos x$ may be found Now for these particular experimental conditions the value of i_1 is known to lie between 24° and 30° for which $\cos i_1$ lies between 0 91 and 0 87 Taking an average value of 0 89 we see that, knowing a, b and $\cos x$ the ratio of the axes H_1/H_1' (or 0 89 a/b) and the phase difference of the components of the downcoming ray may be stated

As will be seen from the results given below, the ratio of the axes is found to be approximately unity, while the value of $\cos x$ is approximately zero for all the cases investigated. Such results indicate that the downcoming ray is approximately circularly polarised, but do not distinguish between right-handed and left-handed rotation The method used for doing this will now be described by reference again to the example of fig 3. The first wave-length change was an increase of frequency so that, in accordance with our convention, the phase difference $(\theta + \zeta_1)$ between ground and atmospheric waves at the end of the change is seen to be about $-\frac{3}{4}\pi$ For the same conditions on the second loop the phase difference θ is approximately $+ \pi$ Thus $\tan \zeta_1$ is approximately $- 1$ and since in (5) $\cos x$ is found to be approximately zero, and a and b are, roughly, equal, the value of $\sin x$ is approximately $+ 1$ so that $(\theta' - \theta)$ is approximately $+ \frac{1}{2}\pi$ indicating anti-clock-wise rotation in the example considered

In just the same way we can find ζ_2 or $(\zeta_1 - \zeta_2)$ from appropriate pairs of adjacent end-points of the "fringe" records and thus find approximate values for $\sin x$

5 *Summary of Experimental Results*

Observations have been made for transmissions in a south to north direction using the National Physical Laboratory transmitter, and in a west to east direction using the Birmingham B B C transmitter In all, some three hundred sets of three successive records on the loops have been made, but as the results have been remarkably uniform only a few examples need be quoted in detail apart from the general result As previously mentioned, the method is only valid if the downcoming ray is not altered in polarisation during the wave-length changes By examining the constancy of the "fringe" amplitudes and also the constancy of the phase relation during the pauses it has been possible to make sure that these conditions were fulfilled in the examples taken for calculation Occasionally instances have been observed in which the nature of the polarisation has changed as the wave-length has been varied For example, in one case, there were always more interference maxima and minima in loop III than on loop II indicating that the phase angle $(\theta - \theta')$ underwent a progressive change with frequency

Date	Time G M.T	Transmitter	H_1/H_1'	Phase difference	Sense of rotation	Remarks
				°		
19.3 27	4 42 a m	National Physical Laboratory	1 2	80	Left handed	Non symmetrical loops
19 3 27	4 51 a m	,,	1 0	88	,,	
5 4 27	3 54 a m	,,	1 0	61	,,	,,
5 4 27	4 39 a m	,,	0 8	95	,,	
6 4 27	4 0 a m	,,	1 0	90	,,	,,
6 4 27	4 5 a m	,,	0 87	114	,,	
23,4 27	4 40 a m	,,	0 72	100	,,	Symmetrical loops
23 4 27	5 31 a m	,,	1 33	84	,,	
28 5 27	2 47 a m	Birmingham	0 90	120	,,	,,
28 5 27	3 25 a m	,,	1 00	70	,,	
11 6 27	2 48 a m	,,	0 75	123	,,	Non-symmetrical loops
11 6 27	4.53 a m	,,	1 24	102	,,	

The figures in the above table are chosen to give an indication of the values commonly measured The mean and most frequent values of over a hundred such sets for the National Physical Laboratory transmissions and over fifty sets for the Birmingham transmission are as shown in the table below -

Transmitter	H_1/H_1'		Phase difference	
	Mean	Most frequent	Mean	Most frequent
			°	°
National Physical Laboratory	0 97	0 92	86	90
Birmingham	0 90	0 90	100	100

The result of these experiments is therefore that the downcoming ray is approximately circularly polarised with a left-handed rotation

6 *Discussion of Results*

In attempting to explain the results obtained in this series of experiments we naturally consider first whether the left-handed circularly polarised wave, detected as a downcoming wave, was originally emitted by the sending station and has preserved this polarisation during its passage through the atmosphere A consideration of the shapes of the aerials at Teddington and Birmingham lends little support to such an explanation, for in each case any unbalanced horizontal portion of the aerial lies in the plane of propagation for the case of a receiver at Peterborough, so that in the case of both transmitters the emitted wave is approximately normally polarised We therefore conclude that the circular polarisation has been brought about by the action of the atmosphere Such a conclusion is in keeping with the deductions made from observations on directional errors

In considering the influence of the upper atmosphere in determining the nature of the polarisation of the waves returned from it, there appear to be, at first sight, three possible ways in which the abnormal polarisation could be brought about

In the first place, if the ray were laterally deviated, so that it departed from the plane of propagation, the abnormal polarisation might be brought about by reflection at a sharp boundary of ionised gas But the experiments of Smith-Rose and Barfield have shown that such lateral deviation is not very appreciable for conditions similar to those of the present series of experiments Moreover, it is difficult to see why such oblique reflection from the layer should always result in the production of a left-handed polarisation.

The two other possibilities are concerned with the action of the earth's magnetic field, and differ only in so far as we regard the waves as being reflected or gradually refracted by the ionisation in the upper atmosphere If the waves were reflected at the layer we should expect phenomena analogous to those of the Kerr effect (magnetic) to occur, and, since the earth's lines of magnetic force are more nearly vertical than horizontal, the rotation and production of ellipticity associated with polar reflection might be expected We believe, however, that for the wave-lengths we are using, the degree of transition from non-conductivity to conductivity is not sharp in terms of a wave-length and that the deviation takes place by ionic refraction We are therefore led to inquire whether any satisfactory explanation of the results of the experiments can be given, taking into account the fact that both the refractive index and the absorption coefficient of the ionised gas in the layer are influenced by the earth's magnetic field

The chief phenomena to be expected due to the influence of a magnetic field for propagation in a straight line through an ionised gas, have been previously given The main result of the presence of the field is that, in general, for any given direction, two waves of different polarisations and experiencing different attenuations are propagated with different phase velocities For example, in the case of propagation in the direction of the magnetic field, the refractive index μ and the absorption coefficient κ are given by

$$\mu^2 = 1 - \frac{4\pi \mathrm{N}e^2/m}{p\,(p \mp p_0)}, \tag{6}$$

and

$$\kappa = \frac{1}{2\tau c}\,\frac{4\pi \mathrm{N}e^2/m}{(p \mp p_0)^2}, \tag{7}$$

where N is the number of electrons (of charge e and mass m) per cubic centimetre, τ the time between two collisions of an electron with gas molecules, p the angular frequency of the waves and p_0 a characteristic frequency corresponding to a wave-length of about 200 metres The velocity of radiation in free space is denoted by c For both μ and κ there are therefore two values corresponding to the double signs The upper sign, in the case of negative electrons, corresponds to the case of a right-handed circularly polarised ray, while the lower sign corresponds to a left-handed circularly polarised ray We thus see that for propagation in this direction and for our conditions, in which p_0 is approximately equal to $2p$, the absorption coefficient of the right-handed ray is about nine times the absorption coefficient of the left-handed ray If the absorption is at all marked therefore, while the waves are travelling in this direction, the effect of the relative weakening of the right-handed ray will cause the resulting ray to become left-handed elliptically polarised In the case in which the right-handed ray is very strongly absorbed, the final polarisation will be circular and left-handed

But since we possess practically no information about the gradient of ionisation in the layer, we are unable to picture the trajectory of the ray and are thus unable to estimate the relative absorptions and polarisations of the component vibrations throughout the atmospheric path, although we can, of course, derive formulæ similar to those of (9) and (10) for any direction of propagation relative to the magnetic field The solution of the general problem therefore seems hopeless in the present state of our knowledge, but perhaps the following less general considerations have some bearing on it

We should expect that the polarisation of the downcoming ray would correspond to that which it last possessed when in the ionised layer Now for high-angle deviation in England, we know that the ray leaves the layer in a direction inclined at a small angle to the lines of magnetic force In the case of the National Physical Laboratory transmissions this angle must be approximately zero, while in the case of the Birmingham transmissions it is probably about 30° If there is appreciable absorption while the downcoming waves travel in this direction, we should expect that the differential absorption would leave the resulting polarisation at the ground predominantly left-handed According to such an interpretation we should not expect much difference between the south to north and west to east transmission, which agrees with the experimental results Most probably the greatest difference is to be expected between south to north and north to south transmissions and when facilities are available we hope to test this point But it will easily be seen that the most direct test of the above interpretation would be to carry out similar experiments at corresponding points in the Southern Hemisphere, where the resulting polarisation should be right-handed if the effect is due to the action of the earth's magnetic field

It has been mentioned in the introduction that, if the downcoming ray has a reasonably constant state of polarisation, we should expect to find a close correlation between "directional errors" and "fading" In order to detect such a correlation it is essential to make observations on the apparent bearing and signal strength as nearly as possible at the same place Reich (*loc cit*) used observing stations one or two miles apart In experiments carried out at Peterborough, using aerials at the same place, and arranged so that no mutual coupling exists between them, we have found that there is a close correlation between directional errors and fading, such as could be explained by assuming that the downcoming ray was circularly polarised

This work was carried out as part of the programme of the Radio Research Board and is communicated by permission of the Department of Scientific and Industrial Research We are much indebted to those who have co-operated in these experiments, to Dr R L Smith-Rose, Mr E L Hatcher and Mr A C Haxton, of the National Physical Laboratory, to Dr M A F Barnett and Mr W C Brown, of the Peterborough Radio Research Station, and to the Chief Engineer (Captain P P Eckersley) and Birmingham Station Staff of the British Broadcasting Corporation

Summary

1 An experimental method of determining the polarisation constants of ellipticity of downcoming wireless waves is described

2 The use of the method in a series of measurements in England with 400 metre waves has shown that the downcoming waves are in general elliptically polarised and that the polarisation is approximately circular The sense of rotation is found to be left-handed

3 It is shown that, according to the magneto-ionic theory of atmospheric deflection of wireless waves, in which the influence of the earth's magnetic field is recognised, such left-handed elliptical polarisation might be expected if the electrical carriers in the ionised layer are of electronic mass, but that similar measurements made in the Southern Hemisphere would yield evidence which would very materially confirm or disprove such an interpretation

A Theory of the Optical and Electrical Properties of Liquids.

By Prof. C V. RAMAN, F R.S, and K. S KRISHNAN.

(Received September 19, 1927)

1 *Introduction*

Theories of the optical behaviour of liquids generally base themselves on the postulate that the well-known Lorentz formula $(n^2 - 1)/(n^2 + 2)\rho =$ constant correctly expresses the relation between the refractive index and density of a liquid It has long been known, however, that this formula is at best only an approximation The quantity $(n^2 - 1)/(n^2 + 2)\ \rho$ is found experimentally to be not invariable, its deviation from constancy becoming more and more marked as the density is increased The change in the value of $(n^2 - 1)/(n^2 + 2)\rho$ in passing from the state of vapour to that of a liquid under ordinary conditions, is usually quite appreciable, as might be instanced by the case of benzene, for which Wasastjerna* found for the D-line a molecular refraction of 27 20 in the vapour state, while the corresponding value for the liquid is 26 18, that is, 3 8 per cent lower The deviations from the Lorentz formula appear most striking when we use it to compute the change in the refractive index of a liquid produced by alterations of temperature or pressure Here, again, we might instance the case of benzene, for which the observed value of $dn/dt = -6\ 4 \times 10^{-4}$ per degree Centigrade for the D-line at 20° C, and that of $dn/dp = 5\ 06 \times 10^{-5}$ per atmosphere, while the calculated values are $dn/dt = -7\ 15 \times 10^{-4}$ and $dn/dp = 5\ 66 \times 10^{-5}$ The observed values are thus numerically about 10 per cent smaller in either case, indicating that $(n^2 - 1)/(n^2 + 2)\ \rho$ diminishes more and more quickly as the density is increased An expression of the form $(n^2 - 1)/(n^2 + 2)\ \rho = a - b\rho^2$, where a and b are positive constants, has been found to represent the refraction of carbon dioxide over a wide range of density more closely than the original Lorentz formula † It has been deduced theoretically on certain suppositions regarding the magnitude of the polarisation field in liquids, which are, however, somewhat arbitrary in nature.

Considering next the electrical behaviour of liquids, we find that the formula proposed by Debye $(\epsilon - 1)/(\epsilon + 2)\ \rho = A + B/T$ is not adequate to explain the dielectric properties of many known liquids To illustrate this, we may again consider the case of benzene, whose dielectric constant has been determined over a wide range of temperatures* and pressures † Since A and B in the formula are essentially positive constants, it follows that $(\epsilon - 1)/(\epsilon + 2)\ \rho$ should remain invariable when the liquid is compressed isothermally, and that it should *diminish* with rising temperature Actually it is found with benzene that the quantity in question falls steadily with increasing pressure and *increases* with rising temperature A similar apparently anomalous behaviour is shown by many other liquids whose molecules have a negligible electrical polarity Liquids of marked electrical polarity show a diminution of $(\epsilon - 1)/(\epsilon + 2)\ \rho$ with rising temperature as demanded by the formula, but they deviate from it by showing a diminution of the same quantity when isothermally compressed, the latter effect being usually even more marked than for non-polar compounds ‡

---

* 'Soc. Sci. Fenn., Phys.-Math ,' vol. 2, No 13 (1924).

† Phillips, 'Roy Soc Proc ,' A, vol. 97, p. 225 (1920)

It will be clear from the foregoing review that the existing theories of the optical and electrical behaviour of liquids are far from being satisfactory It is proposed in this paper to put forward a new theory which appears to us competent to offer at least an insight into the whole range of facts referred to We believe that it is capable of doing more, that is, of actually giving a quantitative explanation of the behaviour of actual liquids for which the necessary data for evaluating the constants appearing in our formulæ are available In order, however, not to lengthen the paper unduly, we shall confine ourselves to a general discussion, leaving the details for fuller treatment in separate papers

2 *The Refractivity of Liquids*

We shall first consider the optical problem, which is relatively simple In any satisfactory treatment of it we have necessarily to take into account the fact which has been clearly established by recent investigations, namely, that a liquid can be regarded as an optically isotropic medium only when we do not push the analysis of its structure into regions of molecular dimensions In the first place, it is established by investigations on light-scattering that all known molecules are optically anisotropic, in other words, that they are polarisable to different extents in different directions From this circumstance it follows that the refractivity of a liquid is really an average effect determined by the contributions of molecules variously orientated relatively to one another and to the field of the incident radiation. Further, it is known from X-ray studies that many actual molecules are highly asymmetric in their geometric form. In view of this fact we would not be justified in treating the distribution of polarisable matter surrounding any given molecule in a dense fluid as completely symmetrical. It follows, therefore, that the local field acting on any molecule due to the polarisation of its immediate neighbours, cannot be regarded as independent of the orientation of the molecule in the field. The study of light-scattering in liquids furnishes striking evidence in support of this idea and indeed enables us in simple cases to actually determine how the polarisation field acting on a molecule varies with its orientation with respect to the incident beam of light. We shall in what follows proceed to develop the theory of refraction in liquids on the assumption that the molecules are optically anisotropic and that the polarisation field acting on the molecule is a function of its orientation.

---

* Isnardi, 'Z f. Physik,' vol. 9, p. 153 (1922)

† Francke, 'Ann d. Physik,' vol. 77, p. 159 (1925)

‡ Grenacher, 'Ann. d. Physik,' vol 77, p 138 (1925)

Let us choose the optic axes of any given molecule as the axes of a co-ordinate system ξ, η, ζ fixed to it, whose orientations with respect to another system of axes x, y, z fixed in space are given by the Eulerian angles θ, ϕ, ψ. Let b_1, b_2, b_3 be the moments induced in the molecule per unit field (due to a light-wave) *actually* acting on it respectively along its three axes ξ, η, ζ. When the external field is incident along any one of these axes, say along the ξ-axis, the polarisation field acting on the molecule will, in general, have components also along the η- and ζ-axes. Let p_{11}, p_{12}, p_{13} be the numerical factors which determine the polarisation fields acting along the ξ-, η-, ζ-axes when the external field is incident along the ξ-axis, and let p_{21}, p_{22}, p_{23} and p_{31}, p_{32}, p_{33} be similar factors when the external field lies along the η- and ζ-axes, $p_{ik} = p_{ki}$.

Suppose now the field of the incident light-wave, equal to E, say, lies along the z-axis. Then the moments induced in the molecule under consideration along its three axes are obviously

$$\left.\begin{aligned} &b_1\,[\alpha_1 + \chi\,(p_{11}\alpha_1 + p_{21}\alpha_2 + p_{31}\alpha_3)]\,\mathrm{E} \\ &b_2\,[\alpha_2 + \chi\,(p_{12}\alpha_1 + p_{22}\alpha_2 + p_{32}\alpha_3)]\,\mathrm{E} \\ \text{and}\qquad &b_3\,[\alpha_3 + \chi\,(p_{13}\alpha_1 + p_{23}\alpha_2 + p_{33}\alpha_3)]\,\mathrm{E} \end{aligned}\right\} \qquad (1)$$

respectively, where χ is the mean moment induced in unit volume of the fluid by unit field of the incident light-wave, α_1, α_2, α_3 are the cosines of the angles which the ξ-, η-, ζ-axes make with the direction of the field E, and are given by

$$\alpha_1 = -\sin\theta\cos\psi, \quad \alpha_2 = \sin\theta\sin\psi, \quad \alpha_3 = \cos\theta \qquad (2)$$

These moments when resolved along the direction of the incident field are together equal to

$$[b_1(1 + p_{11}\chi)\alpha_1^2 + b_2(1 + p_{22}\chi)\alpha_2^2 + b_3(1 + p_{33}\chi)\alpha_3^2$$
$$+ \chi\{p_{12}(b_1 + b_2)\alpha_1\alpha_2 + p_{23}(b_2 + b_3)\alpha_2\alpha_3 + p_{31}(b_3 + b_1)\alpha_3\alpha_1\}] \times \mathrm{E} \quad (3)$$

Now the average values of α_1^2, α_2^2 and α_3^2 taken over all orientations of the molecules with respect to the incident field are equal to $\frac{1}{3}$, while the average values of $\alpha_1\alpha_2$, $\alpha_2\alpha_3$ and $\alpha_3\alpha_1$ vanish Hence it readily follows that the average moment induced in a molecule in the medium by unit incident field is given by

$$m = \tfrac{1}{3}(b_1' + b_2' + b_3'), \quad (4)$$

where b_1', b_2', b_3' denote the coefficients of α_1^2, α_2^2, α_3^2 respectively in (3) above

Further

$$\chi = \nu m = (n^2 - 1)/4\pi, \quad (5)$$

ν being the number of molecules per unit volume and n the refractive index

Putting

$$p_{11} = \tfrac{4}{3}\pi + \sigma_1, \quad p_{22} = \tfrac{4}{3}\pi + \sigma_2, \quad p_{33} = \tfrac{4}{3}\pi + \sigma_3,$$

and using relation (5), we obtain from (4)

$$\frac{n^2 - 1}{n^2 + 2} = \frac{4\pi}{3}\nu\frac{b_1 + b_2 + b_3}{3} + \frac{n^2 - 1}{n^2 + 2}\nu\frac{b_1\sigma_1 + b_2\sigma_2 + b_3\sigma_3}{3}, \quad (6)$$

which may be written in the form

$$\frac{n^2 - 1}{n^2 + 2} = \nu\mathrm{C} + \frac{n^2 - 1}{n^2 + 2}\nu\Phi, \quad (7)$$

where

$$\Phi = \tfrac{1}{3}(b_1\sigma_1 + b_2\sigma_2 + b_3\sigma_3) \quad (8)$$

and C is a constant characteristic of the molecule. We shall now consider three special cases

Case (*a*)

$$\sigma_1 = \sigma_2 = \sigma_3 = 0,$$

and therefore

$$p_{11} = p_{22} = p_{33} = \tfrac{4}{3}\pi \quad (9)$$

We find in this case that equation (7) reduces absolutely to the Lorentz formula.

The assumption (9) is equivalent to the supposition that the local field acting on the molecule is equal to that at the centre of a spherical cavity excavated around it

Case (*b*)

$$\sigma_1 + \sigma_2 + \sigma_3 = 0,$$

and therefore

$$p_{11} + p_{22} + p_{33} = 4\pi \tag{10}$$

If, in addition, $b_1 = b_2 = b_3$, *i e* , if the molecule is optically isotropic, equation (7) again reduces to the Lorentz formula Equation (10) amounts to assuming that the local field acting on the molecule is equal to that at the centre of an ellipsoidal cavity with three unequal axes,* scooped around the molecule It may also be interpreted in the sense that the *mean* polarisation field acting on the molecule averaged over all orientations is the same as at the centre of a spherical cavity

Case (*c*)

$$\sigma_1 + \sigma_2 + \sigma_3 \neq 0$$

This is equivalent to the assumption that the mean polarisation field differs from that obtainable at the centre of a spherical cavity around the molecule

In Case (*a*) we obtain no deviation from the Lorentz formula at all In Case (*b*) we obtain a deviation provided the molecule is optically anisotropic, and in Case (*c*) we may obtain a deviation from the Lorentz formula even for optically isotropic molecules

3 *The Dielectric Constant of Liquids*

For the corresponding electrical problem we choose the principal axes of electrostatic polarisability of the molecule as its ξ-, η-, ζ-axes When an electrostatic field E is incident in the medium along the z-axis, the actual fields acting on the molecule along its axes are given by

$$\left.\begin{aligned} \mathrm{E}_1 &= [\alpha_1 + \chi_e (q_{11}\alpha_1 + q_{21}\alpha_2 + q_{31}\alpha_3)]\,\mathrm{E} \\ \mathrm{E}_2 &= [\alpha_2 + \chi_e (q_{12}\alpha_1 + q_{22}\alpha_2 + q_{32}\alpha_3)]\,\mathrm{E} \\ \text{and}\quad \mathrm{E}_3 &= [\alpha_3 + \chi_e (q_{13}\alpha_1 + q_{23}\alpha_2 + q_{33}\alpha_3)]\,\mathrm{E} \end{aligned}\right\}, \tag{11}$$

where χ_e is the mean electrostatic moment produced in unit volume of the medium per unit incident field , and the q's denote the constants of the static polarisation fields acting on the molecule, analogous to the p's in the optical problem If μ_1, μ_2, μ_3 be the components of the permanent electric moment μ of the molecule resolved along the ξ-, η-, ζ-axes and a_1, a_2, a_3 the moments induced in it by unit field acting along these axes, the contribution from the molecule under consideration to the moment along the direction of the incident field is given by

---

* See Routh, 'Analytical Statics,' vol. 2, p. 100

$$\begin{aligned} \mathrm{L} = [&a_1 (1 + q_{11}\chi_e) \alpha_1^2 + a_2 (1 + q_{22}\chi_e) \alpha_2^2 + a_3 (1 + q_{33}\chi_e) \alpha_3^2 \\ &+ \{q_{12} (a_1 + a_2) \alpha_1\alpha_2 + q_{23} (a_2 + a_3) \alpha_2\alpha_3 + q_{31} (a_3 + a_1) \alpha_3\alpha_1\}\chi_e] \times \mathrm{E} \\ &+ \mu_1\alpha_1 + \mu_2\alpha_2 + \mu_3\alpha_3. \end{aligned} \tag{12}$$

The potential energy of the molecule in the field due to the existence of the permanent moment in it, is given by

$$\begin{aligned} u &= -(\mu_1\mathrm{E}_1 + \mu_2\mathrm{E}_2 + \mu_3\mathrm{E}_3) \\ &= -(\mathrm{M}_1\alpha_1 + \mathrm{M}_2\alpha_2 + \mathrm{M}_3\alpha_3)\,\mathrm{E}, \end{aligned} \tag{13}$$

where

$$\left.\begin{aligned} \mathrm{M}_1 &= \mu_1 + \chi_e (q_{11}\mu_1 + q_{21}\mu_2 + q_{31}\mu_3) \\ \mathrm{M}_2 &= \mu_2 + \chi_e (q_{12}\mu_1 + q_{22}\mu_2 + q_{32}\mu_3) \\ \mathrm{M}_3 &= \mu_3 + \chi_e (q_{13}\mu_1 + q_{23}\mu_2 + q_{33}\mu_3) \end{aligned}\right\} \tag{14}$$

By Boltzmann's theorem the number of molecules per unit volume whose orientations in the field correspond to the range $\sin\theta\, d\theta\, d\phi\, d\psi$ is equal to

$$c\, e^{-u/kT} \sin\theta\, d\theta\, d\phi\, d\psi, \tag{15}$$

where c is a constant which can be evaluated from the obvious relation

$$c \int_{\theta=0}^{\theta=\pi} \int_{\phi=0}^{\phi=2\pi} \int_{\psi=0}^{\psi=2\pi} e^{-u/kT} \sin\theta\, d\theta\, d\phi\, d\psi = \nu, \tag{16}$$

the total number of molecules per unit volume

The average contribution from a molecule in the medium to the moment along the field

$$= \frac{\iiint e^{-u/kT}\, \mathrm{L} \sin\theta\, d\theta\, d\phi\, d\psi}{\iiint e^{-u/kT} \sin\theta\, d\theta\, d\phi\, d\psi} = m_e \mathrm{E} \text{ (say)}, \tag{17}$$

the limits of integration being the same as in (16), and neglecting terms involving E^2 and higher powers of E. On actual evaluation of the integrals in (17) we obtain

$$\begin{aligned} m_e = {} & \frac{a_1 (1 + q_{11}\chi_e) + a_2 (1 + q_{22}\chi_e) + a_3 (1 + q_{33}\chi_e)}{3} \\ & + \frac{1}{3kT} (\mathrm{M}_1\mu_1 + \mathrm{M}_2\mu_2 + \mathrm{M}_3\mu_3) \end{aligned} \tag{18}$$

Further,

$$\chi_e = \nu m_e = \frac{\varepsilon - 1}{4\pi}, \tag{19}$$

where ε is the dielectric constant.

Using this relation and putting

$$q_{11} = \tfrac{4}{3}\pi + s_1, \quad q_{22} = \tfrac{4}{3}\pi + s_2, \quad q_{33} = \tfrac{4}{3}\pi + s_3$$

we obtain from (18)

$$\begin{aligned}\frac{\varepsilon-1}{\varepsilon+2} &= \frac{4\pi}{3}\,\nu\left(\frac{a_1+a_2+a_3}{3}+\frac{\mu^2}{3kT}\right)+\frac{\varepsilon-1}{\varepsilon+2}\,\nu\left\{\frac{a_1s_1+a_2s_2+a_3s_3}{3}\right.\\ &\qquad\qquad\left.+\frac{1}{3kT}\left(\Sigma\mu_i^2 s_i+2\Sigma\mu_i\mu_k q_{ik}\right)\right\}\\ &= \frac{4\pi}{3}\,\nu\left(\frac{a_1+a_2+a_3}{3}+\frac{\mu^2}{3kT}\right)+\frac{\varepsilon-1}{\varepsilon+2}\,\nu\left(\Psi+\frac{1}{3kT}\,\Theta\right) \end{aligned}\tag{20}$$

where

$$\Psi = \tfrac{1}{3}\left(a_1s_1 + a_2s_2 + a_3s_3\right) \tag{21}$$

and

$$\Theta = \mu_1^2 s_1 + \mu_2^2 s_2 + \mu_3^2 s_3 + 2\left(\mu_1\mu_2 q_{12} + \mu_2\mu_3 q_{23} + \mu_3\mu_1 q_{31}\right) \tag{22}$$

The second term in (20) containing Ψ and Θ appears as an addition to the first term which is identical with Debye's expression. We may rewrite (20) in the form

$$\frac{\varepsilon - 1}{\varepsilon + 2} = \nu\left(\frac{4\pi}{3}\,\frac{a_1 + a_2 + a_3}{3} + \frac{\varepsilon - 1}{\varepsilon + 2}\,\Psi\right) + \frac{\nu}{3kT}\left(\frac{4\pi}{3}\,\mu^2 + \frac{\varepsilon - 1}{\varepsilon + 2}\,\Theta\right) \tag{23}$$

The first term on the right hand side of (23) has a form similar to the expression for refractivity obtained in the preceding section and does not explicitly involve the temperature. The second term, on the other hand, is inversely proportional to the absolute temperature.

4. *Discussion of the Theory*

Our formulæ offer a natural explanation why with increase of density the Lorentz refraction constant usually diminishes. Equation (7) runs

$$\frac{n^2 - 1}{n^2 + 2} = \nu C + \nu\,\frac{n^2 - 1}{n^2 + 2}\,\Phi,$$

where

$$\Phi = \tfrac{1}{3}\left(b_1\sigma_1 + b_2\sigma_2 + b_3\sigma_3\right)$$

The expression for the dielectric constant of non polar liquids is very similar see equation (23) above, and the following remarks may be regarded as applying equally well in respect of the same

The constants b_1, b_2, b_3 represent the polarisabilities of the molecule along its optic axes and are therefore essentially positive We shall, for the present at any rate, be justified in making the simplifying assumption, see equation (10) above, that $p_{11} + p_{22} + p_{33} = 4\pi$, in other words, that the polarisation field acting on the molecule *when averaged over all its orientations* is the same as at the centre of a spherical cavity We have, then, $\sigma_1 + \sigma_2 + \sigma_3 = 0$, and it follows that σ_1, σ_2, σ_3 cannot all have the same sign

If

and

$$\left.\begin{array}{l} b_1 > b_2 > b_3 \\ \sigma_1 < \sigma_2 < \sigma_3 \end{array}\right\}, \tag{24}$$

it is easily shown that the value of Φ, that is, of $\frac{1}{3}(b_1\sigma_1 + b_2\sigma_2 + b_3\sigma_3)$ is necessarily negative In other words, provided the condition stated in (24) is satisfied, the value of $(n^2 - 1)/(n^2 + 2)$ would necessarily have a smaller value than that given by the Lorentz formula

The condition stated in (24) has a physical significance, namely, that the direction in the molecule corresponding to maximum polarisability is that along which the field due to its neighbours has a minimum value, and vice versa That this condition would be satisfied in most cases seems highly probable If we can regard the chemical molecule as roughly equivalent to an ellipsoidal particle of polarisable matter, its longest axis would be the one of maximum polarisability and its shortest axis that of minimum polarisability If we consider a liquid composed of such molecules, it is obvious that the centre of a second molecule could approach that of the first most closely in the direction of the shortest axis, and least closely in the direction of its longest axis The polarisation field due to its neighbours would be the sum of the fields due to the individual molecules occupying various positions with respect to it If we consider a particular molecule in such position that the line joining the centres of the two molecules is parallel to the external field, its influence would appear as an addition to the field, while if the joining line is perpendicular to the field, its influence would be equivalent to a diminution of the external field These effects would conspire to diminish the aggregate polarisation field acting on the molecule when the external field is along its longest dimension, and to increase it when the field is along its shortest dimension, in comparison with the case of spherical molecules This is precisely the result which is required to satisfy the condition stated in (24) above.

It must, however, be remembered that the preceding argument is based on the assumption that the optical anisotropy of the molecule is determined by its geometric shape The origin of the optical anisotropy of molecules as evidenced in observations on light-scattering has been the subject of discussion in recent papers * It is found that pronounced asymmetry of geometric form does not necessarily mean pronounced optical anisotropy, the latter being determined by the chemical nature and arrangement of the atoms in the molecule Nevertheless, the order of the geometric dimensions of a molecule in different directions is usually also the order of its optical polarisabilities along those directions It must not be forgotten, however, that there may be exceptions to this rule †

Returning now to formula (7), we may, since the second term on the right is much smaller than the first, write it in the form

$$\frac{n^2-1}{n^2+2} = \nu C(1+\nu\Phi), \tag{25}$$

from which it is seen that apart from any possible variation of Φ with density or temperature, the correction to the Lorentz formula increases in importance with increasing density There is *prima facie* reason to believe that Φ must itself increase numerically with increasing density of the fluid To realise this, we recall the argument set out above regarding the relation between the geometric form of the molecule and the polarisation field acting on it In the gaseous condition, or even in a dense vapour, there would ordinarily be almost complete freedom of orientation for the molecules Further, the fraction of the time during which a molecule is in actual collision with a neighbour is a small part of the whole, and hence, in determining the polarisation field, we would not be sensibly in error in ignoring the non-spherical shape of the molecule altogether It is only when the density becomes comparable with that of a liquid that a molecule is almost continually in collision with one or other of its neighbours, and that in evaluating the polarisation field we cannot ignore the restrictions imposed by the geometric form of the molecules on their relative positions and orientations These considerations indicate a progressive change in the *character* of the polarisation field acting on a molecule as the density increases At low densities, the field acting on a molecule would be appreciably the same as if it were placed at the centre of a spherical cavity excavated around it, and would be independent of its orientation. At higher densities, the non-spherical shape of the molecule would begin to influence the results A detailed treatment of the problem on the basis of the kinetic theory would be complicated by the circumstance that the molecules are themselves optically anisotropic and that therefore the mutual influence of two molecules depends both on their relative position and their relative orientation Ignoring this difficulty, however, we may make the simplifying assumption that the surrounding molecules can be regarded as equivalent to a distribution of polarisable matter which is of uniform density and symmetrical except in a small region surrounding the given molecule With increasing density, this small region and its lack of symmetry become of greater importance, until finally, when a density as great as that of the amorphous solid is reached, we shall not be much in error in regarding the molecule as practically embedded in a cavity having its own shape, the dependence of the polarisation field on the orientation of the molecule relatively to the external field then reaching its maximum value We thus arrive at the general conclusion that the value of Φ increases numerically with increasing density, beginning with zero at low densities and reaching a limiting value at densities as high as those of the amorphous solid The correction $\nu\Phi$ appearing in our modified form of the Lorentz formula must therefore increase at a greater rate than in proportion to the density, during a greater part of its course

---

* See K. R. Ramanathan, 'Roy Soc Proc,' A, vol. 107, p. 684 (1924), vol 110, p 123 (1926) Also T H. Havelock, 'Phil. Mag,' vol. 3, pp. 158, 433 (1927).

† From some observations by Mr I. Ramakrishna Rao in the authors' laboratory, on light-scattering in formic and acetic acid vapours, it appears that these form such exceptions. The available data on refractivity appear also to indicate an *increase* of the Lorentz constant of refractivity with increasing density

A clearer view of the whole subject may be obtained in the following way In section 2, we obtained the expression (equation (4))

$$m = \tfrac{1}{3}(b_1' + b_2' + b_3'),$$

where

$$b_1' = b_1[1 + \chi(\tfrac{4}{3}\pi + \sigma_1)],$$

etc , etc , for the average moment induced in a molecule per unit external field. In a rarefied medium we have

$$m = \tfrac{1}{3}(b_1 + b_2 + b_3)$$

The ratios b_1 b_2 b_3 are a measure of the optical anisotropy of the molecule in the state of vapour In the dense fluid the ratios b_1' b_2' b_3' similarly indicate the optical anisotropy of the molecule as effectively modified by the influence of its neighbours The preceding discussion shows that the result of such influence is to diminish these ratios and make them approach more nearly to unity, in other words, to diminish the effective optical anisotropy of the molecule, and that a diminution in refractivity is a necessary consequence of the same effect

Independent evidence that the effect of increasing density is to cause an apparent diminution in the optical and electrical anisotropies of the molecule, is furnished by studies of the electrical birefringence of liquids, and by the study of the depolarisation of the light scattered by liquids at different temperatures The authors have developed a theory of electric birefringence in liquids, and a theory of light-scattering in liquids, based on ideas very similar to those underlying the present paper, and find strong support for these theories in the experimental evidence available The theory of light-scattering in liquids indicates that it is possible in simple cases to evaluate the quantities appearing in the formulæ of the present paper and thus offer a quantitative test of the proposed theory of refraction and dielectric behaviour Very encouraging results have already been obtained in this direction, but to enter into these details would be foreign to the scope of this paper

5 *Summary*

A review of the experimental evidence shows that the existing theories of the refractivity and dielectric behaviour of liquids are inadequate to explain all that is known concerning the changes of these properties with density and temperature A new theory is accordingly developed in this paper, which is based on the idea that the molecules of the fluid are optically and electrically anisotropic, and that, in addition, the polarisation field, acting on a molecule in a dense fluid, varies with its orientation relatively to the external field The theory offers an immediate explanation why in general an *increased* density causes a *diminished* molecular refractivity as calculated from the Lorentz formula It is shown that these changes in refractivity and dielectric constant are closely related to a change in the effective optical or electrical anisotropy of the molecules produced by the influence of its immediate neighbours Similar ideas have been adopted in theories of electric birefringence and of light-scattering in liquids developed by the authors, which have found strong experimental support, and with the aid of which the anisotropic constants appearing in the formulæ of the present paper can be evaluated

Experiments on the Diffraction of Cathode Rays

By G P Thomson, M A., Fellow of Corpus Christi College and Professor of
Natural Philosophy in the University of Aberdeen

(Communicated by Sir Joseph Thomson, F R S —Received November 4, 1927)

[Plate 19]

1 M L de Broglie has introduced a theory of mechanics according to which a moving particle behaves as a group of waves whose velocity and wave-length are governed by the speed and mass of the particle In fact if m_0 is the mass for slow speed and v the speed of a freely moving particle, the wave-length is given by $\lambda = h\sqrt{1 - v^2/c^2}/m_0 v$, and the wave velocity V by $V = c^2/v$, the group velocity being v, the velocity of the particle Here c is the velocity of light and it will be seen that the wave velocity is greater than c There is nothing impossible in this because the waves are regarded as purely geometrical —" phase waves "—not as carrying energy Compare, in ordinary optical theory, the case of substances, such as sodium, for which the refractive index is less than unity The above is for free space , in the presence of a field of force V varies, and the consequent bending of the waves by refraction corresponds, on the new theory, to the deviation of the path of the particle by the field of force, on the old

The consequences of this theory have been worked out by de Broglie, Schrodinger and others and applied to problems in spectroscopy where they have provided the solution of several outstanding difficulties left by the older theory of orbits In view, however, of the extremely fundamental nature of the theory it is highly desirable that it should rest on more direct evidence, and, in particular, that it should be shown capable of predicting as well as of merely explaining Dymond[*] has obtained some remarkable results on the scattering of slow electrons in helium which are of the general nature to be expected in this theory, but our knowledge of the structure of helium, together with the mathematical difficulties of the problem have so far prevented any exact comparison of the theory with experiment Davisson and Kunsman[†] and Davisson and Germer[‡] have obtained results on the reflection of slow electrons from the surfaces of crystals, especially nickel, which show good qualitative agreement with the

[*] 'Nature,' vol. 118, p. 336 (1926)

[†] 'Phys. Rev ,' vol. 22, p. 243 (1923).

[‡] 'Nature,' vol. 119, p. 558 (1927)

theory but a discrepancy of 30 per cent in certain magnitudes It is hoped that the experiments described in this paper will advance the matter a stage further They are a development of some experiments of which a preliminary account appeared recently in 'Nature'*

2. These experiments were begun last year with the idea of extending Dymond's experiments on scattering to solid films and faster electrons, where it seemed probable that the technique developed for dealing with positive ray-scattering could be applied with advantage The results now obtained, however, are best looked at from a slightly different point of view to that applicable to Dymond's work, namely, as follows

On the de Broglie theory the electron is considered as a group of waves and its motion through matter is determined by considerations of scattering and diffraction For electrons of 25,000 volts energy the wave-length λ calculated from the above formula is about 0 75 × 10^{-9} cm This is of the order of that of hard X-rays and the waves associated with electrons of this energy should behave in many respects like hard X-rays In fact on this view there is a very close analogy between the two The quantum effects of X-rays are regarded as due to centres of energy guided by waves, while in the case of the electrons the motion of the electric charge, in which the energy is centred, is regarded as taking place along the rays of the group of phase waves associated with it In particular the electrons should show diffraction effects when passed through a crystal identical with those shown by X-rays of the same wave-length It is, perhaps, hardly necessary to say that this does not mean that the two are indistinguishable Unlike X-rays the electrons are deflected by electric and magnetic fields They carry a charge, and for equal wave-lengths, have much less energy and less penetrating power

3 In essence the experiments to be described consist in sending a beam of approximately homogeneous cathode rays through a very thin film at normal incidence and receiving them on a photographic plate some distance behind If the film consists of a number of minute crystals arranged at random we should get a pattern identical with that obtained in a Hull-Debye-Scherrer apparatus with X-rays of the same wave-length If certain directions of crystal predominate the pattern will be modified in a calculable manner It will be seen below that both these cases have been found The only other necessary condition is that the film shall be so thin that the electron in its passage through it is only scattered once, otherwise the pattern will be hopelessly blurred by the superposition of the deflections and will appear on the photographic plates as a

---

* Thomson and Reid, 'Nature,' vol. 119, p. 890 (1927).

nearly uniform blackening except, perhaps, for an increased intensity near the place corresponding to the direction of the original beam

It is this requirement which gives rise to the chief experimental difficulties and accounts for the effect not having been observed before

4 The experimental arrangement used (see fig 1) is of the simplest Cathode rays generated by an induction coil in the tube A pass through the fine tube B of bore 0 23 mm and length 6 cms, and strike a film mounted at C B is shielded from magnetic effects by the iron tube shaded in fig 1 Between C and the plate at D is a distance of 32 5 cms and the plate can be lowered in two stages by a magnetic release This enables two exposures to be taken on each plate which is an advantage as it is difficult to estimate the best time of exposure to show up the pattern At E is a willemite screen which can be used to examine the rays while the plate is still in the upper part of the camera The camera was exhausted to a low vacuum, the gas coming through the fine tube from A being removed by a three-stage mercury vapour pump The voltage of the discharge was measured as carefully as possible by means of a spark gap between 4 cms aluminium spheres A preliminary experiment of deflecting the rays by a magnet on their path between C and D showed that they were very nearly homogeneous, the spot on the plate deflecting as a whole except for a very faint tail

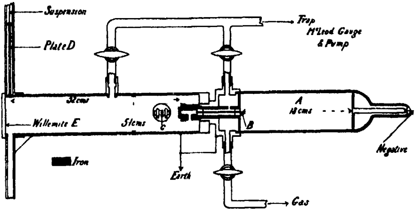

FIG 1

5 Specimens of the results obtained with films of aluminium, gold, celluloid, and a substance X (at first thought to be platinum), are shown in the plate It will be seen that in all cases the general effect is that of a series of concentric rings round the spot made by the undeflected beam In some cases these rings are uniform round the circumference, in others the intensity is more or less

concentrated in a series of spots on the circumference It should be said at once that there can be no doubt that the whole pattern is due to cathode rays which have been deflected by the film Thus in the absence of the film only the central spot is seen, and if a magnet is brought up between C and D the whole pattern is shifted together In some cases, when it is bright enough, this can be seen by following the changes in appearance of the willemite screen when a magnet is brought near In others, when the rings could not be seen on the screen, photographs were taken with a magnetic field between C and D strong enough to move the central spot, which could always be seen, through a considerable distance In all cases the pattern showed the spot at the centre of the rings, showing that spot and rings had been deflected together They thus are due to cathode rays of appreciably the same velocity

6 *Variation with the Energy of the Rays* —If the rings are in any way of the nature of a diffraction pattern their size, for a given film, must vary inversely as the wave-length of the waves concerned According to the formula of de Broglie $\lambda = h\sqrt{1 - v^2/c^2}/m_0v$ If v/c is small $\lambda = h/m_0v$ and if P is the potential difference in volts through which the rays have fallen to acquire their energy, $= v\sqrt{2eP/300m_0}$ Thus λ is proportional to $\sqrt{P}$ and if D is the diameter of any given ring $D\sqrt{P}$ should be constant If the accurate formula is used and allowance made for the variation of mass with velocity in the acceleration of the ray, it is easy to show that $\lambda = h\sqrt{150/ePm_0}/(1 + eP/1200m_0c^2)$ The correcting term never exceeds 3 per cent in these experiments The following table shows the constancy for various films of $D\sqrt{P}\,(1 + Pe/1200m_0c^2)$ About equally good agreement is shown by the simple expression $D\sqrt{P}$.

Aluminium

Plate	S G	P	D_1	$D_1\sqrt{P}\,(1+Pl/1200\,m_0c^2)$
	mms		cms	
October 7 (3)	5	17,500	3 1	415
October 10 (2)	9 5	30,500	2 45	434
October 7 (2)	10	31,800	2 32	418
October 7 (4)	13	40,000	2 12	430
October 7 (5)	14 5	44,000	2 08	445
October 7 (6)	16 5	48,600	1 90	430
October 11 (1)	16 5	48,600	1 98	446
October 12 (2)	20	56,500	1 83	446
October 12 (3)	20	56,500	1 80	438
				Mean 434

Gold

Plate	S G	P	D	$D\sqrt{P}(1+Pe/1200\,m_0c^2)$
	mms		cms	
October 13 (1)	7 5	24 600	2 50	398
October 12 (4)	10	31 800	2 15	390
October 12 (5)	12 75	39 400	2 00	404
October 12 (6)	15 25	45 600	1 86	405
October 12 (7)	19	54 300	1 63	388
October 17	22	61 200	1 61	410
				Mean 399

This close agreement is in itself strong evidence for the de Broglie theory and justifies us in considering in detail the other consequences to be expected on this view

7 Suppose that a beam of cathode rays is incident at an angle θ on a plane of indices (hkl) of a small element of crystal According to the Bragg formula it will be reflected provided that $2d \sin \theta = n \lambda$ where d is the spacing between parallel planes of the type $(h\ k\ l)$ If L is the distance of the plate this will give rise to a mark on the plate at a distance D/2 from the central spot where $D = 4\,\theta\,L = 2n\,\lambda\,L/d$ assuming θ is small

If a large number of small crystals are present arranged at random so that some are present at all angles we shall have a ring of diameter given by the above formula for every spacing d in the crystal lattice and $n = 1\ 2\ 3$ etc This is of course the well known Hull Debye Scherrer pattern for powdered crystals If the crystals have definite orientations with respect to the film some of these rings will be absent Thus consider a crystal with rectangular axes and suppose a $(1\ 0\ 0)$ face is always (approximately) parallel to the film surface we shall have reflections from $(0\ 1\ 0)$ and $(0\ 1\ 1)$ faces because the small angle θ required can be provided by the slight divergence of the cathode ray beam and by lack of flatness in the film On the other hand the reflection from $(1\ 1\ 1)$ will not appear because the rays would have to make a large angle with the plane of the film in order to be incident on $(1\ 1\ 1)$ at the small angle required by the law $2\,d \sin \theta = n\,\lambda$ remembering that λ is of the order of 1/50 that of d If further the crystals are so orientated that not merely is one axis perpendicular to the film but the

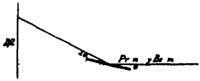

FIG 2

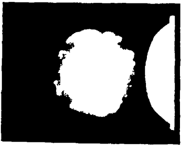

Fig 1 —Aluminium

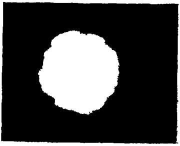

Fig 2 —Aluminium

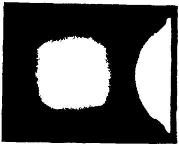

Fig 3 —Aluminium

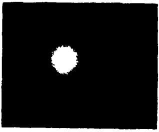

Fig 4 —Gold

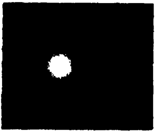

Fig 5 —Celluloid

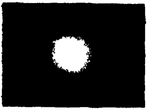

Fig 6 —Film X

axes in the film are not arranged at random, then the rings which do appear will not be of uniform intensity, each direction of the axes giving rise, in the case of cubic symmetry, to four spots on the circumference of the ring.

8. *Aluminium.*—Let us examine the results obtained with aluminium from this point of view. The films used were the thinnest foil etched down by floating in caustic potash till they were transparent. It is difficult to estimate the thickness actually used as the films so formed are not uniform, but probably to give good results they must not be more than 10^{-5} cm. Looking at figs. 1 and 2 (Plate 19), we see that the rings are non-uniform so that presumably the crystals have become orientated in the process of rolling the film. Besides the inner ring D_1, two others, D_2 and D_3, can be distinguished outside it,* and traces of a fourth between D_2 and D_3. The ratios of D_2/D, D_3/D_1 are shown below.

Plate	Oct 12 (3)	Oct 11 (1)	Oct 7 (6)	Oct. 7 (5)	Oct 7 (2)	Oct 7 (2)	Oct. 7 (1)	Mean
D_2/D_1	1.41	1.39	1.42	1.37	1.38	1.42	1.41	1.40
D_3/D_1	—	—	2.15	—	2.02	—	—	2.08

In some of the cases in which no value of D_3/D_1 is given the ring was outside the field on view, in some it was too faint to measure. It will be seen that the ratios correspond closely to $\sqrt{2} . 1$ and $2 : 1$.

Now aluminium is found from X-ray experiments to have a fore-centred cubic lattice. For such a lattice the distances "d" of the planes are given by $d = a/\sqrt{h^2 + k^2 + l^2}$ where h, k, l are the indices of the plane and "a" the side of the unit cube. If some of the quantities (h, k, l) are odd and some even, counting zero even, all are to be doubled.

Now, if one axis is perpendicular to the film, the possible planes are those for which one index is zero, and the smallest values of h, k, l are (1, 0, 0), (1, 1, 0), (1, 2, 0), etc. Now $D = 2n\lambda L \sqrt{h^2 + k^2 + l^2}/a$, hence doubling the indices when required we have in succession $Da/\lambda L = n4$, $n4\sqrt{2}$, $n4\sqrt{5}$, etc. If we put $n = 1, 2$ in the first and $n = 2$ in the second, we get $Da/\lambda L = 4, 4\sqrt{2}, 8$ or in the ratio $1 : \sqrt{2} : 2$ as found for D_1 D_2 D_3, and it is easy to see that any other ring will be outside these. The faint ring between D_2 and D_3 is, I think, probably due to a few of them not being orientated in the way assumed. As far as can be measured its diameter is to D_1 as $\sqrt{3} : 1$ and thus would correspond to the second order reflection from a (1, 1, 1) plane.

In the examples reproduced there are too many crystals, as shown by the numerous spots, for their symmetry to show up clearly Fortunately I found another specimen which was apparently, in the small region used, almost a single crystal Here the inner circle D_1 was reduced to four short arcs at the corners of a square while D_2 took the same form with the difference that the diagonals of the two squares make an angle of 45° with each other This specimen was rather thicker, and the background of general scattered rays was heavier, it is reproduced in fig 3, Plate 19 Since the (1, 1, 0) planes are at 45° to the (1, 0, 0) planes this result is in exact agreement with what would be expected on the theory

---

* D_3 is not visible in the reproductions.

Finally we can compare the calculated value of "*a*" with that found for aluminium by X-ray analysis The values for three specimens agreed with each other within the limits of experimental error, and excluding some experiments at very high voltages for which the spark gap measurements have a large probable error, I find as a mean $a = 3\ 80 \times 10^{-8}$, the value given by X-ray analysis is $a = 4\ 046 \times 10^{-8}$ There is a discrepancy of 6 per cent While this is outside the casual error of experiment, as may be seen from a consideration of the agreement of the figures on p 603, it may perhaps be due to a systematic error * The measurement of energy by spark gap is not a very satisfactory method, especially when a rapidly alternating potential like that of an induction coil is used, and there may quite possibly be a systematic error due to this On the other hand there may be some correction required in the theory The discrepancy would have been one or two per cent less if the relativity correction had been ignored.

9 *Gold*—Gold films were prepared from the thinnest leaf obtainable by reduction in aqua regia The pattern due to one is shown in fig 4, Plate 19, and the constancy of $D'\sqrt{P}$ is shown in the table above Here D' is the mean of the diameters of the two inner rings† which at the lower energy of rays were unresolved Here the rings are quite continuous, indicating the presence of many crystals and suggesting that they are probably orientated at random, as might be expected from the fact that the leaf is prepared by beating Gold also has a face-centred cubic lattice Assuming that the crystals are at random, we must take all possible values of (*h*, *k*, *l*), and resulting values of $Da/2\lambda L$ are shown below

(By treating, *e g*, (4, 0, 0) as different from (2, 0, 0) we avoid the necessity of introducing n as a separate variable) The " observed " values are ratios calculated so as to make the diameter of the first ring $\sqrt{3}$

---

* See note at the end of the paper

† Shown in the reproduction as a rather broad ring with a fine dark circle dividing it into two

(h, k, l)	$\sqrt{h^2+k^2+l^2}$		Observed	
			October 17	October 12 (7)
(2, 1, 1)	$\sqrt{3}$		$\sqrt{3}$	$\sqrt{3}$
(2, 0, 0)	$\sqrt{4}$ = 2 00		2 05	2 02
(2, 2, 0)	$\sqrt{8}$ = 2 83		2 81	2 83
(1, 1, 3)	$\sqrt{11}$ = 3 32	3 40 mean	3 40	3 33
(2, 2, 2)	$\sqrt{12}$ = 3 47			
(4, 0, 0)	$\sqrt{16}$ = 4 00		absent	absent
(3, 3, 1)	$\sqrt{19}$ = 4 36	4 41 mean	4 44	4 45
(4, 2, 0)	$\sqrt{20}$ = 4 47			

It will be seen that the agreement is very good, that all the rings can be accounted for, and that all the rings to be expected in the region covered by the plate are present, except the higher order of the (1, 0, 0) which might be expected to be very faint The rings $\sqrt{11}$ and $\sqrt{12}$, and again $\sqrt{19}$ and $\sqrt{20}$ are not resolved

As regards the absolute value of " a " I find $a = 3\ 80 \times 10^{-8}$ The X-ray result is $a = 4\ 065 \times 10^{-8}$, a discrepancy of 6½ per cent, to which the same remarks apply as in the case of aluminium

10 *Celluloid* —A few photographs were taken with a thin film of celluloid, of the order of 5×10^{-6} cm thick, similar to those used by Mr Reid in the experiments described in ' Nature ' One of these is shown in fig 5, Plate 19 There is a well-defined inner ring and a much fainter outer one of about twice the size not visible in the reproduction Mr Reid is continuing the work on these films with the apparatus originally used, which, while slightly more complicated, has the advantage that the energy of the rays can be measured with much greater accuracy It is hoped that a detailed account of this work will shortly be ready for publication

Film X —The first experiments with the apparatus described were made with a thin film believed to be platinum This was obtained by acting with aqua regia on the film formed on the inside of a bulb by cathode spluttering from platinum It was found accidentally in the course of cleaning the bulb that the film came off in the acid in flakes 2 or 3 mm. across Two of the most transparent of these were mounted and tested The thinnest showed a very well-marked inner ring* (fig 6, Plate 19) and a faint outer one (not reproducible) of about twice the size The thicker film only showed the inner ring, and that rather faintly, but the size was the same The inner ring of the thinner specimen varied in size with the voltage in the way now familiar, as shown in the following table —

Spark gap	Voltage	Diameter	$D\sqrt{V}$
mm		mm	
3 25	12,000	18 5	203
4 5	16,100	15 8	200
7 0	23,200	12 9	196
9 25	29,600	11 9	205
13 0	39,900	10 0	200
14 75	44,400	9 7	204
			Mean 201

The absolute size of the ring is, however, exactly half that to be expected from platinum taken as a face-centred cube of side $3\ 91 \times 10^{-8}$ It is almost exactly that of the celluloid ring though the latter is rather sharper It seems possible that these films were really due to some greasy substance present on the bulb (which was originally used for quite a different purpose) A film of this substance would be selected as apparently the thinnest owing to its transparency Attempts were made to obtain films of undoubted platinum by the same process, but they were unsuccessful as the films always broke while drying on the mount This increases the probability that the films in question were not platinum

It is difficult to prepare thin platinum films by the methods that has been successful with gold and aluminium as I have been unable to obtain sufficiently thin foil to start with †

Conclusions

The detailed agreement shown in these experiments with the de Broglie theory must, I think, be regarded as strong evidence in its favour These means accepting the view that ordinary Newtonian mechanics (including the relativity modifications) are only a first approximation to the truth, bearing the same relation to the complete theory that geometrical optics does to the wave theory However difficult it may seem to accept such a sweeping generalisation, it seems impossible to explain the results obtained except by the assumption of some kind of diffraction, and the numerical agreement with the wave-length given by the theory is striking It should be emphasised that there are no adjustable constants, the agreement is direct except for a 5 per cent error It is an important question whether this error is an experimental one in the measurement of the speed of the rays, as suggested above, or whether it represents some correction on the simple theory * Further experiments on this point are in progress It is also hoped to extend Dymond's results by obtaining the diffraction pattern for the molecules of a gas with these fast rays My sincere thanks are due to Mr C G Fraser and to Mr J D McKay for their valuable assistance in preparing the films and making the experiments

---

* In this case the solarisation near the undeflected beam gives the appearance of an extra inner ring. A similar effect, less marked, can be seen in figs. 3, 4 and 5. These false rings can easily be distinguished in practice by taking photographs with varying exposures.

† *Note added in Proof* —I have since been able to show that platinum films give the rings to be expected from the known crystal structure of the metal, see 'Nature,' December 3, p 802

Summary

1 Experiments are described giving the patterns formed by cathode rays scattered by thin films of aluminium, gold, celluloid, and an unknown substance

2 These patterns are closely similar to those obtained with X-rays in the "powder method"

3 The sizes of the patterns agree to 5 per cent with those predicted on the de Broglie theory of wave mechanics, regarding the phenomenon as one of diffraction of the phase waves associated with the electrons

[*Note added in Proof*—I have now traced the error to a loss of potential in the high tension leads, ammeter, etc If the spark gap is measured directly across the discharge tube instead of, as in the above experiments, near the coil, the value found for "*a*" in the case of platinum is within 1 per cent of that found by X-rays, while with the measurements taken in the old way there is a discrepancy of 6 per cent as in the case of the other metals, the results with which are therefore also explained.]

---

* It may be remarked that Davissons and Germers' results appear to show an error of about the same magnitude in the same direction.

The Quantum Theory of the Electron.

By P A. M Dirac, St John's College, Cambridge

(Communicated by R H Fowler, F R S —Received January 2, 1928)

The new quantum mechanics, when applied to the problem of the structure of the atom with point-charge electrons, does not give results in agreement with experiment The discrepancies consist of " duplexity " phenomena, the observed number of stationary states for an electron in an atom being twice the number given by the theory To meet the difficulty, Goudsmit and Uhlenbeck have introduced the idea of an electron with a spin angular momentum of half a quantum and a magnetic moment of one Bohr magneton This model for the electron has been fitted into the new mechanics by Pauli,* and Darwin,† working with an equivalent theory, has shown that it gives results in agreement with experiment for hydrogen-like spectra to the first order of accuracy

The question remains as to why Nature should have chosen this particular model for the electron instead of being satisfied with the point-charge One would like to find some incompleteness in the previous methods of applying quantum mechanics to the point-charge electron such that, when removed, the whole of the duplexity phenomena follow without arbitrary assumptions In the present paper it is shown that this is the case, the incompleteness of the previous theories lying in their disagreement with relativity, or, alternatetively, with the general transformation theory of quantum mechanics It appears that the simplest Hamiltonian for a point-charge electron satisfying the requirements of both relativity and the general transformation theory leads to an explanation of all duplexity phenomena without further assumption. All the same there is a great deal of truth in the spinning electron model, at least as a first approximation The most important failure of the model seems to be that the magnitude of the resultant orbital angular momentum of an electron moving in an orbit in a central field of force is not a constant, as the model leads one to expect

---

* Pauli, ' Z f. Physik,' vol 43, p 601 (1927)

† Darwin, ' Roy Soc Proc ,' A, vol 116, p 227 (1927)

§ 1 *Previous Relativity Treatments*

The relativity Hamiltonian according to the classical theory for a point electron moving in an arbitrary electro-magnetic field with scalar potential A_0 and vector potential $\mathbf{A}$ is

$$\mathrm{F} \equiv \left(\frac{\mathrm{W}}{c} + \frac{e}{c}\mathrm{A}_0\right)^2 + \left(\mathbf{p} + \frac{e}{c}\mathbf{A}\right)^2 + m^2c^2,$$

where $\mathbf{p}$ is the momentum vector It has been suggested by Gordon* that the operator of the wave equation of the quantum theory should be obtained from this F by the same procedure as in non-relativity theory, namely, by putting

$$\mathrm{W} = ih\frac{\partial}{\partial t},$$
$$p_r = -ih\frac{\partial}{\partial x_r}, \qquad r = 1, 2, 3,$$

in it This gives the wave equation

$$\mathrm{F}\psi \equiv \left[\left(ih\frac{\partial}{c\,\partial t} + \frac{e}{c}\mathrm{A}_0\right)^2 + \Sigma_r\left(-ih\frac{\partial}{\partial x_r} + \frac{e}{c}\mathrm{A}_r\right)^2 + m^2c^2\right]\psi = 0, \quad (1)$$

the wave function ψ being a function of x_1, x_2, x_3, t This gives rise to two difficulties

The first is in connection with the physical interpretation of ψ Gordon, and also independently Klein,† from considerations of the conservation theorems, make the assumption that if ψ_m, ψ_n are two solutions

$$\rho_{mn} = -\frac{e}{2mc^2}\left\{ih\left(\psi_m\frac{\partial\bar{\psi}_n}{\partial t} - \bar{\psi}_n\frac{\partial\psi_m}{\partial t}\right) + 2e\mathrm{A}_0\psi_m\bar{\psi}_n\right\}$$

and

$$\mathbf{I}_{mn} = -\frac{e}{2m}\left\{-ih\left(\psi_m \operatorname{grad}\bar{\psi}_n - \bar{\psi}_n \operatorname{grad}\psi_m\right) + 2\frac{e}{c}\mathbf{A}_m\psi_m\bar{\psi}_n\right\}$$

are to be interpreted as the charge and current associated with the transition $m \rightarrow n$ This appears to be satisfactory so far as emission and absorption of radiation are concerned, but is not so general as the interpretation of the non-relativity quantum mechanics, which has been developed‡ sufficiently to enable one to answer the question What is the probability of any dynamical variable at any specified time having a value lying between any specified limits, when the system is represented by a given wave function ψ_n? The Gordon-Klein interpretation can answer such questions if they refer to the position of the electron (by the use of ρ_{mn}), but not if they refer to its momentum, or angular momentum or any other dynamical variable. We should expect the interpretation of the relativity theory to be just as general as that of the non-relativity theory.

---

* Gordon, 'Z f Physik,' vol. 40, p 117 (1926)

† Klein, 'Z f Physik,' vol 41, p 407 (1927)

‡ Jordan, 'Z f Physik,' vol 40, p 809 (1927), Dirac, 'Roy Soc Proc,' A, vol 113, p 621 (1927)

The general interpretation of non-relativity quantum mechanics is based on the transformation theory, and is made possible by the wave equation being of the form

$$(\mathrm{H}-\mathrm{W})\,\psi=0, \tag{2}$$

i.e., being linear in W or $\partial/\partial t$, so that the wave function at any time determines the wave function at any later time. The wave equation of the relativity theory must also be linear in W if the general interpretation is to be possible.

The second difficulty in Gordon's interpretation arises from the fact that if one takes the conjugate imaginary of equation (1), one gets

$$\left[\left(-\frac{\mathrm{W}}{c}+\frac{e}{c}\mathrm{A}_0\right)^2+\left(-\mathbf{p}+\frac{e}{c}\mathbf{A}\right)^2+m^2c^2\right]\psi=0,$$

which is the same as one would get if one put $-e$ for e. The wave equation (1) thus refers equally well to an electron with charge e as to one with charge $-e$. If one considers for definiteness the limiting case of large quantum numbers one would find that some of the solutions of the wave equation are wave packets moving in the way a particle of charge $-e$ would move on the classical theory, while others are wave packets moving in the way a particle of charge e would move classically. For this second class of solutions W has a negative value. One gets over the difficulty on the classical theory by arbitrarily excluding those solutions that have a negative W. One cannot do this on the quantum theory, since in general a perturbation will cause transitions from states with W positive to states with W negative. Such a transition would appear experimentally as the electron suddenly changing its charge from $-e$ to e, a phenomenon which has not been observed. The true relativity wave equation should thus be such that its solutions split up into two non-combining sets, referring respectively to the charge $-e$ and the charge e.

In the present paper we shall be concerned only with the removal of the first of these two difficulties. The resulting theory is therefore still only an approximation, but it appears to be good enough to account for all the duplexity phenomena without arbitrary assumptions.

§ 2 *The Hamiltonian for No Field*

Our problem is to obtain a wave equation of the form (2) which shall be invariant under a Lorentz transformation and shall be equivalent to (1) in the limit of large quantum numbers We shall consider first the case of no field, when equation (1) reduces to

$$(-p_0^2 + \mathbf{p}^2 + m^2c^2)\,\psi = 0 \tag{3}$$

if one puts

$$p_0 = \frac{W}{c} = ih\frac{\partial}{c\,\partial t}$$

The symmetry between p_0 and p_1, p_2, p_3 required by relativity shows that, since the Hamiltonian we want is linear in p_0, it must also be linear in p_1, p_2 and p_3 Our wave equation is therefore of the form

$$(p_0 + \alpha_1 p_1 + \alpha_2 p_2 + \alpha_3 p_3 + \beta)\,\psi = 0, \tag{4}$$

where for the present all that is known about the dynamical variables or operators α_1, α_2, α_3, β is that they are independent of p_0, p_1, p_2, p_3, i e , that they commute with t, x_1, x_2, x_3 Since we are considering the case of a particle moving in empty space, so that all points in space are equivalent, we should expect the Hamiltonian not to involve t, x_1, x_2, x_3 This means that α_1, α_2, α_3, β are independent of t, x_1, x_2, x_3, i e , that they commute with p_0, p_1, p_2, p_3 We are therefore obliged to have other dynamical variables besides the co-ordinates and momenta of the electron, in order that α_1, α_2, α_3, β may be functions of them The wave function ψ must then involve more variables than merely x_1, x_2, x_3, t

Equation (4) leads to

$$\begin{aligned} 0 &= (-p_0 + \alpha_1 p_1 + \alpha_2 p_2 + \alpha_3 p_3 + \beta)(p_0 + \alpha_1 p_1 + \alpha_2 p_2 + \alpha_3 p_3 + \beta)\,\psi \\ &= [-p_0^2 + \Sigma\,\alpha_1^2 p_1^2 + \Sigma\,(\alpha_1\alpha_2 + \alpha_2\alpha_1)\,p_1 p_2 + \beta^2 + \Sigma\,(\alpha_1\beta + \beta\alpha_1)\,p_1]\,\psi, \end{aligned} \tag{5}$$

where the Σ refers to cyclic permutation of the suffixes 1, 2, 3 This agrees with (3) if

$$\left.\begin{array}{ll} \alpha_r^2 = 1, & \alpha_r\alpha_s + \alpha_s\alpha_r = 0 \quad (r \neq s) \\ \beta^2 = m^2c^2, & \alpha_r\beta + \beta\alpha_r = 0 \end{array}\right\} \quad r, s = 1, 2, 3$$

If we put $\beta = \alpha_4 mc$, these conditions become

$$\alpha_\mu^2 = 1 \qquad \alpha_\mu\alpha_\nu + \alpha_\nu\alpha_\mu = 0 \; (\mu \neq \nu) \qquad \mu, \nu = 1, 2, 3, 4 \tag{6}$$

We can suppose the α_μ's to be expressed as matrices in some matrix scheme, the matrix elements of α_μ being, say, $\alpha_\mu(\zeta'\ \zeta'')$ The wave function ψ must now be a function of ζ as well as x_1, x_2, x_3, t The result of α_μ multiplied into ψ will be a function $(\alpha_\mu\psi)$ of x_1, x_2, x_3, t, ζ defined by

$$(\alpha_\mu\psi)(x, t, \zeta) = \Sigma_{\zeta'}\, \alpha_\mu(\zeta\zeta')\, \psi(x, t, \zeta')$$

We must now find four matrices α_μ to satisfy the conditions (6) We make use of the matrices

$$\sigma_1 = \begin{pmatrix} 0 & 1 \\ 1 & 0 \end{pmatrix} \qquad \sigma_2 = \begin{pmatrix} 0 & -i \\ i & 0 \end{pmatrix} \qquad \sigma_3 = \begin{pmatrix} 1 & 0 \\ 0 & -1 \end{pmatrix}$$

which Pauli introduced* to describe the three components of spin angular momentum These matrices have just the properties

$$\sigma_r^2 = 1 \qquad \sigma_r\sigma_s + \sigma_s\sigma_r = 0, \qquad (r \neq s), \tag{7}$$

that we require for our α's We cannot, however, just take the σ's to be three of our α's, because then it would not be possible to find the fourth We must extend the σ's in a diagonal manner to bring in two more rows and columns, so that we can introduce three more matrices ρ_1, ρ_2, ρ_3 of the same form as $\sigma_1, \sigma_2, \sigma_3$, but referring to different rows and columns, thus —

$$\sigma_1 = \left\{\begin{matrix} 0 & 1 & 0 & 0 \\ 1 & 0 & 0 & 0 \\ 0 & 0 & 0 & 1 \\ 0 & 0 & 1 & 0 \end{matrix}\right\} \quad \sigma_2 = \left\{\begin{matrix} 0 & -i & 0 & 0 \\ i & 0 & 0 & 0 \\ 0 & 0 & 0 & -i \\ 0 & 0 & i & 0 \end{matrix}\right\} \quad \sigma_3 = \left\{\begin{matrix} 1 & 0 & 0 & 0 \\ 0 & -1 & 0 & 0 \\ 0 & 0 & 1 & 0 \\ 0 & 0 & 0 & -1 \end{matrix}\right\},$$

$$\rho_1 = \left\{\begin{matrix} 0 & 0 & 1 & 0 \\ 0 & 0 & 0 & 1 \\ 1 & 0 & 0 & 0 \\ 0 & 1 & 0 & 0 \end{matrix}\right\} \quad \rho_2 = \left\{\begin{matrix} 0 & 0 & -i & 0 \\ 0 & 0 & 0 & -i \\ i & 0 & 0 & 0 \\ 0 & i & 0 & 0 \end{matrix}\right\} \quad \rho_3 = \left\{\begin{matrix} 1 & 0 & 0 & 0 \\ 0 & 1 & 0 & 0 \\ 0 & 0 & -1 & 0 \\ 0 & 0 & 0 & -1 \end{matrix}\right\}$$

The ρ's are obtained from the σ's by interchanging the second and third rows, and the second and third columns We now have, in addition to equations (7)

and also
$$\left.\begin{matrix} \rho_r^2 = 1 \qquad \rho_r\rho_s + \rho_s\rho_r = 0 \qquad (r \neq s), \\ \rho_r\sigma_t = \sigma_t\rho_r. \end{matrix}\right\} \tag{7'}$$

---

* Pauli, *loc. cit.*

If we now take

$$\alpha_1 = \rho_1\sigma_1, \qquad \alpha_2 = \rho_1\sigma_2, \qquad \alpha_3 = \rho_1\sigma_3, \qquad \alpha_4 = \rho_3,$$

all the conditions (6) are satisfied, *e g* ,

$$\alpha_1^2 = \rho_1\sigma_1\rho_1\sigma_1 = \rho_1^2\sigma_1^2 = 1$$

$$\alpha_1\alpha_2 = \rho_1\sigma_1\rho_1\sigma_2 = \rho_1^2\sigma_1\sigma_2 = -\rho_1^2\sigma_2\sigma_1 = -\alpha_2\alpha_1$$

The following equations are to be noted for later reference

$$\left.\begin{aligned} \rho_1\rho_2 &= i\rho_3 = -\rho_2\rho_1 \\ \sigma_1\sigma_2 &= i\sigma_3 = -\sigma_2\sigma_1 \end{aligned}\right\}, \tag{8}$$

together with the equations obtained by cyclic permutation of the suffixes

The wave equation (4) now takes the form

$$[p_0 + \rho_1 (\boldsymbol{\sigma}, \mathbf{p}) + \rho_3 mc]\, \psi = 0, \tag{9}$$

where $\boldsymbol{\sigma}$ denotes the vector $(\sigma_1, \sigma_2, \sigma_3)$.

§ 3 *Proof of Invariance under a Lorentz Transformation.*

Multiply equation (9) by ρ_3 on the left-hand side It becomes, with the help of (8),

$$[\rho_3 p_0 + i\rho_2 (\sigma_1 p_1 + \sigma_2 p_2 + \sigma_3 p_3) + mc]\, \psi = 0$$

Putting

$$p_0 = ip_4,$$

$$\rho_3 = \gamma_4, \qquad \rho_2\sigma_r = \gamma_r, \qquad r = 1, 2, 3, \tag{10}$$

we have

$$[i\Sigma\gamma_\mu p_\mu + mc]\, \psi = 0, \qquad \mu = 1, 2, 3, 4 \tag{11}$$

The p_μ transform under a Lorentz transformation according to the law

$$p_\mu' = \Sigma_\nu a_{\mu\nu} p_\nu,$$

where the coefficients $a_{\mu\nu}$ are c-numbers satisfying

$$\Sigma_\mu a_{\mu\nu} a_{\mu\tau} = \delta_{\nu\tau}, \qquad \Sigma_\tau a_{\mu\tau} a_{\nu\tau} = \delta_{\mu\nu}$$

The wave equation therefore transforms into

$$[i\Sigma\gamma_\mu' p_\mu' + mc]\, \psi = 0, \tag{12}$$

where

$$\gamma_\mu' = \Sigma_\nu a_{\mu\nu}\gamma_\nu$$

Now the γ_μ, like the α_μ, satisfy

$$\gamma_\mu^2 = 1, \qquad \gamma_\mu\gamma_\nu + \gamma_\nu\gamma_\mu = 0, \qquad (\mu \neq \nu)$$

These relations can be summed up in the single equation

$$\gamma_\mu \gamma_\nu + \gamma_\nu \gamma_\mu = 2\delta_{\mu\nu}$$

We have

$$\begin{aligned}\gamma_\mu' \gamma_\nu' + \gamma_\nu' \gamma_\mu' &= \Sigma_{\tau\lambda} a_{\mu\tau} a_{\nu\lambda} (\gamma_\tau \gamma_\lambda + \gamma_\lambda \gamma_\tau) \\ &= 2\Sigma_{\tau\lambda} a_{\mu\tau} a_{\nu\lambda} \delta_{\tau\lambda} \\ &= 2\Sigma_\tau a_{\mu\tau} a_{\nu\tau} = 2\delta_{\mu\nu}\end{aligned}$$

Thus the γ_μ' satisfy the same relations as the γ_μ Thus we can put, analogously to (10)

$$\gamma_4' = \rho_3' \qquad \gamma_r' = \rho_2' \sigma_r'$$

where the ρ''s and σ''s are easily verified to satisfy the relations corresponding to (7), (7′) and (8), if ρ_2' and ρ_1' are defined by $\rho_2' = -i\gamma_1'\gamma_2'\gamma_3'$, $\rho_1' = -i\rho_2'\rho_3'$

We shall now show that, by a canonical transformation, the ρ''s and σ''s may be brought into the form of the ρ's and σ's From the equation $\rho_3'^2 = 1$, it follows that the only possible characteristic values for ρ_3' are ± 1 If one applies to ρ_3' a canonical transformation with the transformation function ρ_1', the result is

$$\rho_1' \rho_3' (\rho_1')^{-1} = - \rho_3' \rho_1' (\rho_1')^{-1} = - \rho_3'$$

Since characteristic values are not changed by a canonical transformation, ρ_3' must have the same characteristic values as $-\rho_3'$ Hence the characteristic values of ρ_3' are $+1$ twice and -1 twice The same argument applies to each of the other ρ''s, and to each of the σ''s

Since ρ_3' and σ_3' commute, they can be brought simultaneously to the diagonal form by a canonical transformation They will then have for their diagonal elements each $+1$ twice and -1 twice Thus, by suitably rearranging the rows and columns, they can be brought into the form ρ_3 and σ_3 respectively (The possibility $\rho_3' = \pm \sigma_3'$ is excluded by the existence of matrices that commute with one but not with the other)

Any matrix containing four rows and columns can be expressed as

$$c + \Sigma_r c_r \sigma_r + \Sigma_r c_r' \rho_r + \Sigma_{rs} c_{rs} \rho_r \sigma_s \tag{13}$$

where the sixteen coefficients c, c_r, c_r', c_{rs} are c-numbers By expressing σ_1' in this way, we see, from the fact that it commutes with $\rho_3' = \rho_3$ and anticommutes* with $\sigma_3' = \sigma_3$, that it must be of the form

$$\sigma_1' = c_1 \sigma_1 + c_2 \sigma_2 + c_{31} \rho_3 \sigma_1 + c_{32} \rho_3 \sigma_2,$$

---

* We say that a anticommutes with b when $ab = - ba$.

i e , of the form

$$\sigma_1' = \left\{\begin{matrix} 0 & a_{12} & 0 & 0 \\ a_{21} & 0 & 0 & 0 \\ 0 & 0 & 0 & a_{34} \\ 0 & 0 & a_{43} & 0 \end{matrix}\right\}$$

The condition $\sigma_1'^2 = 1$ shows that $a_{12}a_{21} = 1$, $a_{34}a_{43} = 1$ If we now apply the canonical transformation first row to be multiplied by $(a_{21}/a_{12})^{\frac{1}{2}}$ and third row to be multiplied by $(a_{43}/a_{34})^{\frac{1}{2}}$, and first and third columns to be divided by the same expressions, σ_1' will be brought into the form of σ_1, and the diagonal matrices σ_3' and ρ_3' will not be changed

If we now express ρ_1' in the form (13) and use the conditions that it commutes with $\sigma_1' = \sigma_1$ and $\sigma_3' = \sigma_3$ and anticommutes with $\rho_3' = \rho_3$, we see that it must be of the form

$$\rho_1' = c_1'\rho_1 + c_2'\rho_2$$

The condition $\rho_1'^2 = 1$ shows that $c_1'^2 + c_2'^2 = 1$, or $c_1' = \cos\theta$, $c_2' = \sin\theta$ Hence ρ_1' is of the form

$$\rho_1' = \left\{\begin{matrix} 0 & 0 & e^{-i\theta} & 0 \\ 0 & 0 & 0 & e^{-i\theta} \\ e^{i\theta} & 0 & 0 & 0 \\ 0 & e^{i\theta} & 0 & 0 \end{matrix}\right\}$$

If we now apply the canonical transformation first and second rows to be multiplied by $e^{i\theta}$ and first and second columns to be divided by the same expression, ρ_1' will be brought into the form ρ_1, and σ_1, σ_3, ρ_3 will not be altered ρ_2' and σ_2' must now be of the form ρ_2 and σ_2, on account of the relations $i\rho_2' = \rho_3'\rho_1'$, $i\sigma_2' = \sigma_3'\sigma_1'$

Thus by a succession of canonical transformations, which can be combined to form a single canonical transformation, the ρ''s and σ''s can be brought into the form of the ρ's and σ's The new wave equation (12) can in this way be brought back into the form of the original wave equation (11) or (9), so that the results that follow from this original wave equation must be independent of the frame of reference used

§ 4. *The Hamiltonian for an Arbitrary Field.*

To obtain the Hamiltonian for an electron in an electromagnetic field with scalar potential A_0 and vector potential $\mathbf{A}$, we adopt the usual procedure of substituting $p_0 + e/c \cdot A_0$ for p_0 and $\mathbf{p} + e/c \cdot \mathbf{A}$ for $\mathbf{p}$ in the Hamiltonian for no field. From equation (9) we thus obtain

$$\left[p_0 + \frac{e}{c}A_0 + \rho_1\left(\boldsymbol{\sigma}, \mathbf{p} + \frac{e}{c}\mathbf{A}\right) + \rho_3 mc\right]\psi = 0 \tag{14}$$

This wave equation appears to be sufficient to account for all the duplexity phenomena. On account of the matrices ρ and σ containing four rows and columns, it will have four times as many solutions as the non-relativity wave equation, and twice as many as the previous relativity wave equation (1). Since half the solutions must be rejected as referring to the charge $+e$ on the electron, the correct number will be left to account for duplexity phenomena. The proof given in the preceding section of invariance under a Lorentz transformation applies equally well to the more general wave equation (14).

We can obtain a rough idea of how (14) differs from the previous relativity wave equation (1) by multiplying it up analogously to (5). This gives, if we write e' for e/c

$$\begin{aligned} 0 &= \left[-(p_0 + e'A_0) + \rho_1(\boldsymbol{\sigma}, \mathbf{p} + e'\mathbf{A}) + \rho_3 mc\right] \\ &\qquad\qquad \times \left[(p_0 + e'A_0) + \rho_1(\boldsymbol{\sigma}, \mathbf{p} + e'\mathbf{A}) + \rho_3 mc\right]\psi \\ &= \left[-(p_0 + e'A_0)^2 + (\boldsymbol{\sigma}, \mathbf{p} + e'\mathbf{A})^2 + m^2c^2 \right. \\ &\qquad \left. + \rho_1\{(\boldsymbol{\sigma}, \mathbf{p} + e'\mathbf{A})(p_0 + e'A_0) - (p_0 + e'A_0)(\boldsymbol{\sigma}, \mathbf{p} + e'\mathbf{A})\}\right]\psi \end{aligned} \tag{15}$$

We now use the general formula, that if $\mathbf{B}$ and $\mathbf{C}$ are any two vectors that commute with $\boldsymbol{\sigma}$

$$\begin{aligned} (\boldsymbol{\sigma}, \mathbf{B})(\boldsymbol{\sigma}, \mathbf{C}) &= \Sigma\, \sigma_1^2 B_1 C_1 + \Sigma\,(\sigma_1\sigma_2 B_1 C_2 + \sigma_2\sigma_1 B_2 C_1) \\ &= (\mathbf{B}, \mathbf{C}) + i\,\Sigma\, \sigma_3 (B_1 C_2 - B_2 C_1) \\ &= (\mathbf{B}, \mathbf{C}) + i\,(\boldsymbol{\sigma}, \mathbf{B} \times \mathbf{C}) \end{aligned} \tag{16}$$

Taking $\mathbf{B} = \mathbf{C} = \mathbf{p} + e'\mathbf{A}$, we find

$$\begin{aligned} (\boldsymbol{\sigma}, \mathbf{p} + e'\mathbf{A})^2 &= (\mathbf{p} + e'\mathbf{A})^2 + i\,\Sigma\, \sigma_3 \\ &\qquad [(p_1 + e'A_1)(p_2 + e'A_2) - (p_2 + e'A_2)(p_1 + e'A_1)] \\ &= (\mathbf{p} + e'\mathbf{A})^2 + he'(\boldsymbol{\sigma}, \operatorname{curl} \mathbf{A}) \end{aligned}$$

Thus (15) becomes

$$0 = \Big[-(p_0 + e'A_0)^2 + (\mathbf{p} + e'\mathbf{A})^2 + m^2c^2 + e'h(\boldsymbol{\sigma}, \text{curl } \mathbf{A}) \\ - ie'h\rho_1\left(\boldsymbol{\sigma}, \text{grad } A_0 + \frac{1}{c}\frac{\partial \mathbf{A}}{\partial t}\right)\Big]\psi$$

$$= [-(p_0 + e'A_0)^2 + (\mathbf{p} + e'\mathbf{A})^2 + m^2c^2 + e'h(\boldsymbol{\sigma}, \mathbf{H}) + ie'h\rho_1(\boldsymbol{\sigma}, \mathbf{E})]\,\psi,$$

where **E** and **H** are the electric and magnetic vectors of the field

This differs from (1) by the two extra terms

$$\frac{eh}{c}(\boldsymbol{\sigma}, \mathbf{H}) + \frac{ieh}{c}\rho_1(\boldsymbol{\sigma}, \mathbf{E})$$

in F These two terms, when divided by the factor $2m$, can be regarded as the additional potential energy of the electron due to its new degree of freedom The electron will therefore behave as though it has a magnetic moment $eh/2mc$ $\boldsymbol{\sigma}$ and an electric moment $ieh/2mc$ $\rho_1\boldsymbol{\sigma}$ This magnetic moment is just that assumed in the spinning electron model The electric moment, being a pure imaginary, we should not expect to appear in the model It is doubtful whether the electric moment has any physical meaning, since the Hamiltonian in (14) that we started from is real, and the imaginary part only appeared when we multiplied it up in an artificial way in order to make it resemble the Hamiltonian of previous theories

§ 5 *The Angular Momentum Integrals for Motion in a Central Field*

We shall consider in greater detail the motion of an electron in a central field of force We put $\mathbf{A} = 0$ and $e'A_0 = V(r)$, an arbitrary function of the radius r, so that the Hamiltonian in (14) becomes

$$F \equiv p_0 + V + \rho_1(\boldsymbol{\sigma}, \mathbf{p}) + \rho_3 mc$$

We shall determine the periodic solutions of the wave equation $F\psi = 0$, which means that p_0 is to be counted as a parameter instead of an operator, it is, in fact, just $1/c$ times the energy level

We shall first find the angular momentum integrals of the motion. The orbital angular momentum **m** is defined by

$$\mathbf{m} = \mathbf{x} \times \mathbf{p},$$

and satisfies the following " Vertauschungs " relations

$$\left.\begin{array}{ll} m_1x_1 - x_1m_1 = 0, & m_1x_2 - x_2m_1 = ihx_3 \\ m_1p_1 - p_1m_1 = 0, & m_1p_2 - p_2m_1 = ihp_3 \\ \mathbf{m} \times \mathbf{m} = ih\mathbf{m}, & \mathbf{m}^2m_1 - m_1\mathbf{m}^2 = 0, \end{array}\right\}, \qquad (17)$$

together with similar relations obtained by permuting the suffixes Also **m** commutes with r, and with p_r, the momentum canonically conjugate to r

We have

$$m_1 \mathrm{F} - \mathrm{F} m_1 = \rho_1 \{ m_1 (\boldsymbol{\sigma}, \mathbf{p}) - (\boldsymbol{\sigma}, \mathbf{p}) m_1 \}$$
$$= \rho_1 (\boldsymbol{\sigma}, m_1 \mathbf{p} - \mathbf{p} m_1)$$
$$= ih\rho_1 (\sigma_2 p_3 - \sigma_3 p_2),$$

and so

$$\mathbf{m}\mathrm{F} - \mathrm{F}\mathbf{m} = ih\rho_1 \, \boldsymbol{\sigma} \times \mathbf{p} \tag{18}$$

Thus **m** is not a constant of the motion We have further

$$\sigma_1 \mathrm{F} - \mathrm{F} \sigma_1 = \rho_1 \{ \sigma_1 (\boldsymbol{\sigma}, \mathbf{p}) - (\boldsymbol{\sigma}, \mathbf{p}) \sigma_1 \}$$
$$= \rho_1 (\sigma_1 \boldsymbol{\sigma} - \boldsymbol{\sigma} \sigma_1, \mathbf{p})$$
$$= 2i\rho_1 (\sigma_3 p_2 - \sigma_2 p_3),$$

with the help of (8), and so

$$\boldsymbol{\sigma} \mathrm{F} - \mathrm{F} \boldsymbol{\sigma} = -2i\rho_1 \, \boldsymbol{\sigma} \times \mathbf{p}$$

Hence

$$(\mathbf{m} + \tfrac{1}{2} h \boldsymbol{\sigma}) \mathrm{F} - \mathrm{F} (\mathbf{m} + \tfrac{1}{2} h \boldsymbol{\sigma}) = 0$$

Thus $\mathbf{m} + \frac{1}{2} h \boldsymbol{\sigma}$ (= **M** say) is a constant of the motion We can interpret this result by saying that the electron has a spin angular momentum of $\frac{1}{2} h \boldsymbol{\sigma}$, which, added to the orbital angular momentum **m**, gives the total angular momentum **M**, which is a constant of the motion

The Vertauschungs relations (17) all hold when M's are written for the m's In particular

$$\mathbf{M} \times \mathbf{M} = ih\mathbf{M} \quad \text{and} \quad \mathbf{M}^2 \mathrm{M}_3 = \mathrm{M}_3 \mathbf{M}^2$$

M_3 will be an action variable of the system Since the characteristic values of m_3 must be integral multiples of h in order that the wave function may be single-valued, the characteristic values of M_3 must be half odd integral multiples of h If we put

$$\mathbf{M}^2 = (j^2 - \tfrac{1}{4}) h^2, \tag{19}$$

j will be another quantum number, and the characteristic values of M_3 will extend from $(j - \frac{1}{2}) h$ to $(-j + \frac{1}{2}) h$ [*] Thus j takes integral values.

One easily verifies from (18) that $\mathbf{m}^2$ does not commute with F, and is thus not a constant of the motion This makes a difference between the present theory and the previous spinning electron theory, in which $\mathbf{m}^2$ is constant, and defines the azimuthal quantum number k by a relation similar to (19). We shall find that our j plays the same part as the k of the previous theory.

---

[*] See 'Roy Soc Proc,' A, vol. 111, p 281 (1926)

§ 6 *The Energy Levels for Motion in a Central Field*

We shall now obtain the wave equation as a differential equation in r, with the variables that specify the orientation of the whole system removed We can do this by the use only of elementary non-commutative algebra in the following way

In formula (16) take $\mathbf{B} = \mathbf{C} = \mathbf{m}$ This gives

$$\begin{aligned}(\boldsymbol{\sigma}, \mathbf{m})^2 &= \mathbf{m}^2 + i\,(\boldsymbol{\sigma}, \mathbf{m} \times \mathbf{m}) \qquad (20)\\ &= (\mathbf{m} + \tfrac{1}{2}h\,\boldsymbol{\sigma})^2 - h\,(\boldsymbol{\sigma}, \mathbf{m}) - \tfrac{1}{4}h^2\,\boldsymbol{\sigma}^2 - h\,(\boldsymbol{\sigma}, \mathbf{m})\\ &= \mathbf{M}^2 - 2h\,(\boldsymbol{\sigma}, \mathbf{m}) - \tfrac{3}{4}h^2\end{aligned}$$

Hence

$$\{(\boldsymbol{\sigma}, \mathbf{m}) + h\}^2 = \mathbf{M}^2 + \tfrac{1}{4}h^2 = j^2h^2$$

Up to the present we have defined j only through j^2, so that we could now, if we liked, take jh equal to $(\boldsymbol{\sigma}, \mathbf{m}) + h$ This would not be convenient since we want j to be a constant of the motion while $(\boldsymbol{\sigma}, \mathbf{m}) + h$ is not, although its square is We have, in fact, by another application of (16),

$$(\boldsymbol{\sigma}, \mathbf{m})\,(\boldsymbol{\sigma}, \mathbf{p}) = i\,(\boldsymbol{\sigma}, \mathbf{m} \times \mathbf{p})$$

since $(\mathbf{m}, \mathbf{p}) = 0$, and similarly

$$(\boldsymbol{\sigma}, \mathbf{p})\,(\boldsymbol{\sigma}, \mathbf{m}) = i\,(\boldsymbol{\sigma}, \mathbf{p} \times \mathbf{m}),$$

so that

$$\begin{aligned}(\boldsymbol{\sigma}, \mathbf{m})\,(\boldsymbol{\sigma}, \mathbf{p}) + (\boldsymbol{\sigma}, \mathbf{p})\,(\boldsymbol{\sigma}, \mathbf{m}) &= i\Sigma\sigma_1\,(m_2p_3 - m_3p_2 + p_2m_3 - p_3m_2)\\ &= i\Sigma\sigma_1\;\; 2ihp_1 = -2h\,(\boldsymbol{\sigma}, \mathbf{p}),\end{aligned}$$

or

$$\{(\boldsymbol{\sigma}, \mathbf{m}) + h\}\,(\boldsymbol{\sigma}, \mathbf{p}) + (\boldsymbol{\sigma}, \mathbf{p})\,\{(\boldsymbol{\sigma}, \mathbf{m}) + h\} = 0$$

Thus $(\boldsymbol{\sigma}, \mathbf{m}) + h$ anticommutes with one of the terms in F, namely, $\rho_1\,(\boldsymbol{\sigma}, \mathbf{p})$ and commutes with the other three Hence $\rho_3\{(\boldsymbol{\sigma}, \mathbf{m}) + h\}$ commutes with all four, and is therefore a constant of the motion But the square of $\rho_3\{(\boldsymbol{\sigma}, \mathbf{m}) + h\}$ must also equal j^2h^2 We therefore take

$$jh = \rho_3\,\{(\boldsymbol{\sigma}, \mathbf{m}) + h\} \qquad (21)$$

We have, by a further application of (16)

$$(\boldsymbol{\sigma}, \mathbf{x})\,(\boldsymbol{\sigma}, \mathbf{p}) = (\mathbf{x}, \mathbf{p}) + i\,(\boldsymbol{\sigma}, \mathbf{m})$$

Now a permissible definition of p_r is

$$(\mathbf{x}, \mathbf{p}) = rp_r + ih,$$

and from (21)

$$(\boldsymbol{\sigma}, \mathbf{m}) = \rho_3 jh - h$$

Hence

$$(\boldsymbol{\sigma}, \mathbf{x})\,(\boldsymbol{\sigma}, \mathbf{p}) = rp_r + i\rho_3 jh \qquad (22)$$

Introduce the quantity ϵ defined by

$$r\epsilon = \rho_1 (\boldsymbol{\sigma}, \mathbf{x}) \tag{23}$$

Since r commutes with ρ_1 and with $(\boldsymbol{\sigma}, \mathbf{x})$, it must commute with ϵ We thus have

$$r^2\epsilon^2 = [\rho_1 (\boldsymbol{\sigma}, \mathbf{x})]^2 = (\boldsymbol{\sigma}, \mathbf{x})^2 = \mathbf{x}^2 = r^2$$

or

$$\epsilon^2 = 1$$

Since there is symmetry between $\mathbf{x}$ and $\mathbf{p}$ so far as angular momentum is concerned, $\rho_1 (\boldsymbol{\sigma}, \mathbf{x})$, like $\rho_1 (\boldsymbol{\sigma}, \mathbf{p})$, must commute with $\mathbf{M}$ and j Hence ϵ commutes with $\mathbf{M}$ and j Further, ϵ must commute with p_r, since we have

$$(\boldsymbol{\sigma}, \mathbf{x}) (\mathbf{x}, \mathbf{p}) - (\mathbf{x}, \mathbf{p}) (\boldsymbol{\sigma}, \mathbf{x}) = ih (\boldsymbol{\sigma}, \mathbf{x}),$$

which gives

$$r\epsilon (rp_r + ih) - (rp_r + ih) r\epsilon = ihr\epsilon,$$

which reduces to

$$\epsilon p_r - p_r \epsilon = 0.$$

From (22) and (23) we now have

$$r\epsilon\rho_1 (\boldsymbol{\sigma}, \mathbf{p}) = rp_r + i\rho_3 jh$$

or

$$\rho_1 (\boldsymbol{\sigma}, \mathbf{p}) = \epsilon p_r + i\epsilon\rho_3 jh/r$$

Thus

$$\mathrm{F} = p_0 + \mathrm{V} + \epsilon p_r + i\epsilon\rho_3 jh/r + \rho_3 mc \tag{24}$$

Equation (23) shows that ϵ anticommutes with ρ_3 We can therefore by a canonical transformation (involving perhaps the x's and p's as well as the σ's and ρ's) bring ϵ into the form of the ρ_2 of § 2 without changing ρ_3, and without changing any of the other variables occurring on the right-hand side of (24), since these other variables all commute with ϵ $i\epsilon\rho_3$ will now be of the form $i\rho_2\rho_3 = -\rho_1$, so that the wave equation takes the form

$$\mathrm{F}\psi \equiv [p_0 + \mathrm{V} + \rho_2 p_r - \rho_1 jh/r + \rho_3 mc]\, \psi = 0$$

If we write this equation out in full, calling the components of ψ referring to the first and third rows (or columns) of the matrices ψ_α and ψ_β respectively, we get

$$(\mathrm{F}\psi)_\alpha \equiv (p_0 + \mathrm{V})\, \psi_\alpha - h \frac{\partial}{\partial r} \psi_\beta - \frac{jh}{r} \psi_\beta + mc\psi_\alpha = 0,$$

$$(\mathrm{F}\psi)_\beta \equiv (p_0 + \mathrm{V})\, \psi_\beta + h \frac{\partial}{\partial r} \psi_\alpha - \frac{jh}{r} \psi_\alpha - mc\psi_\beta = 0.$$

The second and fourth components give just a repetition of these two equations. We shall now eliminate ψ_α. If we write $h\mathrm{B}$ for $p_0 + \mathrm{V} + mc$, the first equation becomes

$$\left(\frac{\partial}{\partial r} + \frac{\jmath}{r}\right)\psi_\beta = \mathrm{B}\psi_\alpha,$$

which gives on differentiating

$$\begin{aligned}\frac{\partial^2}{\partial r^2}\psi_\beta + \frac{\jmath}{r}\frac{\partial}{\partial r}\psi_\beta - \frac{\jmath}{r^2}\psi_\beta &= \mathrm{B}\frac{\partial}{\partial r}\psi_\alpha + \frac{\partial \mathrm{B}}{\partial r}\psi_\alpha \\ &= \frac{\mathrm{B}}{h}\left[-(p_0 + \mathrm{V} - mc)\psi_\beta + \frac{\jmath h}{r}\psi_\alpha\right] + \frac{1}{h}\frac{\partial \mathrm{V}}{\partial r}\psi_\alpha \\ &= -\frac{(p_0+\mathrm{V})^2 - m^2c^2}{h^2}\psi_\beta + \left(\frac{\jmath}{r} + \frac{1}{\mathrm{B}h}\frac{\partial \mathrm{V}}{\partial r}\right)\left(\frac{\partial}{\partial r} + \frac{\jmath}{r}\right)\psi_\beta\end{aligned}$$

This reduces to

$$\frac{\partial^2}{\partial r^2}\psi_\beta + \left[\frac{(p_0+\mathrm{V})^2 - m^2c^2}{h^2} - \frac{\jmath(\jmath+1)}{r^2}\right]\psi_\beta - \frac{1}{\mathrm{B}h}\frac{\partial \mathrm{V}}{\partial r}\left(\frac{\partial}{\partial r} + \frac{\jmath}{r}\right)\psi_\beta = 0 \qquad (25)$$

The values of the parameter p_0 for which this equation has a solution finite at $r = 0$ and $r = \infty$ are $1/c$ times the energy levels of the system. To compare this equation with those of previous theories, we put $\psi_\beta = r\chi$, so that

$$\frac{\partial^2}{\partial r^2}\chi + \frac{2}{r}\frac{\partial}{\partial r}\chi + \left[\frac{(p_0+\mathrm{V})^2 - m^2c^2}{h^2} - \frac{\jmath(\jmath+1)}{r^2}\right]\chi - \frac{1}{\mathrm{B}h}\frac{\partial \mathrm{V}}{\partial r}\left(\frac{\partial}{\partial r} + \frac{\jmath+1}{r}\right)\chi = 0 \qquad (26)$$

If one neglects the last term, which is small on account of B being large, this equation becomes the same as the ordinary Schroedinger equation for the system, with relativity correction included. Since $\jmath$ has, from its definition, both positive and negative integral characteristic values, our equation will give twice as many energy levels when the last term is not neglected.

We shall now compare the last term of (26), which is of the same order of magnitude as the relativity correction, with the spin correction given by Darwin and Pauli. To do this we must eliminate the $\partial\chi/\partial r$ term by a further transformation of the wave function. We put

$$\chi = \mathrm{B}^{-\frac{1}{2}}\chi_1,$$

which gives

$$\begin{aligned}\frac{\partial^2}{\partial r^2}\chi_1 + \frac{2}{r}\frac{\partial}{\partial r}\chi_1 + \left[\frac{(p_0+\mathrm{V})^2 - m^2c^2}{h^2} - \frac{\jmath(\jmath+1)}{r^2}\right]\chi_1 \\ + \left[\frac{1}{\mathrm{B}h}\frac{\jmath}{r}\frac{\partial \mathrm{V}}{\partial r} - \frac{1}{2}\frac{1}{\mathrm{B}h}\frac{\partial^2 \mathrm{V}}{\partial r^2} + \frac{3}{4}\frac{1}{\mathrm{B}^2h^2}\left(\frac{\partial \mathrm{V}}{\partial r}\right)^2\right]\chi_1 = 0 \qquad (27)\end{aligned}$$

The correction is now, to the first order of accuracy

$$\frac{1}{Bh}\left(\frac{j}{r}\frac{\partial V}{\partial r}-\frac{1}{2}\frac{\partial^2 V}{\partial r^2}\right),$$

where $Bh = 2mc$ (provided p_0 is positive) For the hydrogen atom we must put $V = e^2/cr$ The first order correction now becomes

$$-\frac{e^2}{2mc^2r^3}(j+1) \tag{28}$$

If we write $-j$ for $j + 1$ in (27), we do not alter the terms representing the unperturbed system, so

$$\frac{e^2}{2mc^2r^3}\,j \tag{28'}$$

will give a second possible correction for the same unperturbed term

In the theory of Pauli and Darwin, the corresponding correcting term is

$$\frac{e^2}{2mhc^2r^3}(\boldsymbol{\sigma}, \mathbf{m})$$

when the Thomas factor $\frac{1}{2}$ is included We must remember that in the Pauli-Darwin theory, the resultant orbital angular momentum k plays the part of our j We must define k by

$$\mathbf{m}^2 = k(k+1)h^2$$

instead of by the exact analogue of (19), in order that it may have integral characteristic values, like j We have from (20)

$$(\boldsymbol{\sigma}, \mathbf{m})^2 = k(k+1)h^2 - h(\boldsymbol{\sigma}, \mathbf{m})$$

or

$$\{(\boldsymbol{\sigma}, \mathbf{m}) + \tfrac{1}{2}h\}^2 = (k+\tfrac{1}{2})^2h^2,$$

hence

$$(\boldsymbol{\sigma}, \mathbf{m}) = kh \text{ or } -(k+1)h$$

The correction thus becomes

$$\frac{e^2}{2mc^2r^3}k \quad\text{or}\quad -\frac{e^2}{2mc^2r^3}(k+1),$$

which agrees with (28) and (28') The present theory will thus, in the first approximation, lead to the same energy levels as those obtained by Darwin, which are in agreement with experiment

The Fundamental Equation of Wave Mechanics and the Metrics of Space

By H T Flint and J W Fisher, Wheatstone Laboratory, King's College, London

(Communicated by O W Richardson, F R S —Received May 17, 1927 —Revised December 14, 1927)

The relativity theory of Weyl and Eddington is an extension of what may be described as the geometric principle of relativity to the metrics of space This extension permits the inclusion of electromagnetic phenomena into a system of geometry and metrics so that we have a consistent and fundamental scheme for the description of gravitational and electromagnetic phenomena

Recently considerable light has been thrown on the relation between classical and quantum theory by the work of de Broglie, Schroedinger and others

In a recent paper* we indicated the possibility of uniting the two views by an addition to Maxwell's equations, in the present we attempt a union by means of a law of metrics of space time The wave equation on this view would then appear as a law of metrics just as the law of gravitation is a law of geometry A law of this kind is not at all superfluous in the theory

Weyl makes a definite assumption in his law for change of length associated with parallel displacement, Eddington on the other hand dispenses with the assumption and leaves open this law The assumption of the law of metrics is an appeal to experiment to decide this point for us, and if we are right in identifying this law with the wave equation the answer will be found in the domain of quantum phenomena

In the following account we shall use the notation employed in Prof Eddington's book, "The Mathematical Theory of Relativity," and in particular in Part II, ch VII

Every point of four dimensional space is characterised by four co-ordinates (x^1, x^2, x^3, x^4) together with a metrical quantity λ We shall assume that this quantity λ is a function of the co-ordinates of the point with which it is associated Any vector with components (A^1, A^2, A^3, A^4), which will be referred to as the vector A^μ, has a "length," the square of the magnitude of which is defined to be

$$\lambda^2 g_{\mu\nu} A^\mu A^\nu$$

---

* 'Roy Soc Proc,' A, vol 115, p 208 (1927)

A vector, A'^{μ}, at the adjacent point $(x^{\nu} + \delta x^{\nu})$ is said to be parallel to A^{μ} if

$$A'^{\mu} = A^{\mu} - \Gamma^{\mu}_{\nu\alpha} A^{\nu} \delta x^{\alpha},$$

where $\Gamma^{\mu}_{\nu\alpha}$ has the usual significance and is symmetrical in ν and α The vector A'^{μ} is said to be equal to A^{μ} if in addition to being parallel to it, it has the same length, *i e*,

$$\lambda'^{2} g'_{\mu\nu} A'^{\mu} A'^{\nu} = \lambda^{2} g_{\mu\nu} A^{\mu} A^{\nu} \tag{1}$$

where λ' is the value appropriate to λ at the point $(x^{\nu} + \delta x^{\nu})$, *i e*,

$$\lambda' = \lambda + \frac{\partial \lambda}{\partial x^{\nu}} \delta x^{\nu}$$

From this by applying the usual methods it follows that

$$\left.\begin{aligned} g_{\mu\nu} \frac{\delta\lambda}{\lambda} + K_{\mu\nu,\sigma}\, \delta x^{\sigma} = 0 \\ \text{or} \qquad 4\frac{\delta\lambda}{\lambda} + g^{\mu\nu} K_{\mu\nu,\sigma}\, \delta x^{\sigma} = 0 \end{aligned}\right\} \tag{2}$$

Weyl makes the special assumption

$$K_{\mu\nu,\sigma} = g_{\mu\nu}\, \kappa_{\sigma},$$

where κ_{σ} is a component of the covariant companion of the four-vector electrodynamic potential

With this assumption

$$\text{therefore} \qquad \left.\begin{aligned} S_{\mu\nu,\sigma} &= g_{\mu\nu}\, \kappa_{\sigma} - g_{\mu\sigma}\, \kappa_{\nu} - g_{\nu\sigma}\, \kappa_{\mu} \\ S^{\sigma}_{\mu\nu} &= g_{\mu\nu}\, \kappa^{\sigma} - g^{\sigma}_{\mu}\, \kappa_{\nu} - g^{\sigma}_{\nu}\, \kappa_{\mu} \end{aligned}\right\}. \tag{3}$$

Eddington, however, does not make this assumption for $K_{\mu\nu,\sigma}$

We pass on to consider what may be regarded as the variation of a vector in this system of geometry and metrics

If the vector, A^{μ}, depends on the co-ordinates, x^{μ}, then the change in A^{μ} for a change of x^{μ} to $x^{\mu} + \delta x^{\mu}$ is

$$\frac{\partial A^{\mu}}{\partial x^{\sigma}} \delta x^{\sigma}$$

But the new vector is not

$$A^{\mu} + \frac{\partial A^{\mu}}{\partial x^{\sigma}} \delta x^{\sigma}$$

for we have seen that when x^{μ} undergoes the change to $x^{\mu} + \delta x^{\mu}$ the components of the vector A^{μ} become $A^{\mu} - \Gamma^{\mu}_{\nu\alpha} A^{\nu} \delta x^{\alpha}$ Thus we must distinguish between an actual change and an apparent change, the latter being $-\Gamma^{\mu}_{\nu s} A^{\nu} \delta x^{s}$ The actual change is thus the expression

$$
\begin{aligned}
&\frac{\partial A^{\mu}}{\partial x^{\sigma}} \delta x^{\sigma} + \Gamma^{\mu}_{\nu s} A^{\nu} \delta x^{s} \\
&\qquad = \left(\frac{\partial A^{\mu}}{\partial x^{\sigma}} + \Gamma^{\mu}_{\nu\sigma} A^{\nu} \right) \delta x^{\sigma} \\
&\qquad = \left(\frac{\partial A^{\mu}}{\partial x^{\sigma}} + \left\{ {\nu\sigma \atop \mu} \right\} A^{\nu} + S^{\mu}_{\nu\sigma} A^{\nu} \right) \delta x^{\sigma}
\end{aligned}
$$

Thus the divergence of A^{μ} in our more complicated system of geometry and metrics is obtained from the expression

$$\frac{\partial A^{\mu}}{\partial x^{\sigma}} + \left\{ {\nu\sigma \atop \mu} \right\} A^{\nu} + S^{\mu}_{\nu\sigma} A^{\nu}$$

by writing $\sigma = \mu$, whence we obtain

$$\frac{\partial A^{\mu}}{\partial x^{\mu}} + \left\{ {\nu\mu \atop \mu} \right\} A^{\nu} + S^{\mu}_{\nu\mu} A^{\nu} \tag{4}$$

The first and second terms of this expression may be reduced to

$$\frac{1}{\sqrt{g}} \frac{\partial}{\partial x^{\mu}} (\sqrt{g}\, A^{\mu})$$

It is clear from equation (2) that since $K_{\mu\nu,\sigma}$ is not determined λ also is undetermined

We propose to subject λ to a restriction This restriction or law for λ we may describe as a natural law of metrics, provided, of course, the law fits in with natural phenomena

Laws of Nature are usually expressible by mathematical expressions of surprising simplicity The expressions familiar in the region of electromagnetic phenomena are the divergence, gradient and axial of vector, scalar and tensor quantities

Now λ is a scalar quantity, and guided by the same considerations which lead to one assumption in the last paper, where we made an attempt to add to Maxwell's equations, we first form the gradient of λ, viz., $\frac{\partial \lambda}{dx^{\nu}}$, and then derive the divergence of this vector

We then write

$$\operatorname{div} \frac{\partial \lambda}{\partial x^{\nu}} = k\lambda, \tag{5}$$

where the operation of divergence is to be understood in the extended sense of (4)

Equation (5) written in full is then

$$\frac{1}{\sqrt{g}}\frac{\partial}{\partial x^{\mu}}\left(\sqrt{g}\quad g^{\mu\alpha}\frac{\partial\lambda}{\partial x^{\alpha}}\right)+S^{\mu}{}_{\nu\mu}\,g^{\nu\alpha}\frac{\partial\lambda}{\partial x^{\alpha}}=k\lambda \tag{6}$$

We must determine the value of $S^{\mu}{}_{\nu\mu}$

By definition we have

$$S_{\mu\nu\sigma}=K_{\mu\nu\sigma}-K_{\mu\sigma\nu}-K_{\nu\sigma\mu},$$

and on inner multiplication by $g^{\mu\sigma}$ this gives

$$S^{\mu}{}_{\nu\mu}=-g^{\mu\sigma}K_{\mu\sigma\nu}$$

From the equations (2) we have

$$\begin{aligned}4\frac{\partial\lambda}{\partial x^{\sigma}}\quad &-g^{\mu\nu}{}_{\mu}K_{\nu\sigma}\lambda\\ &=-g^{mn}K_{mn,\sigma}\lambda,\end{aligned}$$

replacing μ and ν by m and n to avoid confusion on substituting in (6) which leads to

$$\frac{1}{\sqrt{g}}\frac{\partial}{\partial x^{\mu}}\left(\sqrt{g}\,g^{\mu\alpha}\frac{\partial\lambda}{\partial x^{\alpha}}\right)+\tfrac{1}{4}g^{\mu\epsilon}K_{\mu\epsilon,\nu}\,g^{\nu\alpha}g^{mn}K_{mn,\alpha}\,\lambda=k\lambda,$$

or

$$\frac{1}{\sqrt{g}}\frac{\partial}{\partial x^{\mu}}\left(\sqrt{g}\,g^{\mu\alpha}\frac{\partial\lambda}{\partial x^{\alpha}}\right)+\tfrac{1}{4}\left(g^{\mu\epsilon}K_{\mu\epsilon,\nu}\right)\left(g^{mn}K^{\nu}{}_{mn}\right)\lambda=k\lambda \tag{7}$$

Equation (7) which we describe as expressing the law of metrics in four dimensional space is identical with the wave equation of quantum mechanics This equation is usually expressed in terms of a quantity ψ, the physical meaning of which has been, and still is, the subject of discussion

In equation (7) we identify ψ with the gauge factor λ and the solutions of (7) give us, of course, the same results as are obtained in quantum mechanics

In the course of the development of the new theories the fundamental equation originally adopted by Shroedinger has been more and more generalised, the generalisation being in the direction of introducing more complex expressions in the places occupied by $g^{\mu\epsilon}K_{\mu\epsilon,\nu}$ and $g^{mn}K^{\nu}{}_{mn}$ in equation (7).

It is perhaps too early to pronounce in favour of a particular form for these expressions. The point of view taken here is that the particular value which describes quantum phenomena best will determine the value of $K_{\mu\epsilon,\nu}$

We may note that $\frac{1}{2} g^{\mu\epsilon} K_{\mu\epsilon,\nu}$ is a covariant vector, which may be denoted by L_ν and that $\frac{1}{2} g^{mn} K^{\nu}_{mn} = L^\nu$ so that (9) may be written

$$\frac{1}{\sqrt{g}} \frac{\partial}{\partial x^\mu}\left(\sqrt{g}\, g^{\mu\alpha} \frac{\partial \lambda}{\partial x^\alpha}\right) + L_\nu L^\nu \lambda = k\lambda.$$

If we compare this with the real part of Schroedinger's general wave equation viz.,

$$\frac{1}{\sqrt{g}} \frac{\partial}{\partial x^\mu}\left(\sqrt{g}\, g^{\mu\alpha} \frac{\partial \psi}{\partial x^\alpha}\right) - \frac{4\pi^2}{h^2}\left\{\left(\frac{\partial W}{\partial x^i} - \frac{e}{c}\phi_i\right)\left(\frac{\partial W}{\partial x_i} - \frac{e}{c}\phi^i\right) + m^2c^2\right\}\psi = 0,$$

we have

$$k = \frac{4\pi^2 m^2 c^2}{h^2}$$

and

$$L_\nu = \frac{2\pi i}{h}\left(\frac{\partial W}{\partial x^\nu} - \frac{e}{c}\phi_\nu\right),$$

where W is the action function of Hamiltonian mechanics so that the momentum

$$p_\nu = \frac{\partial W}{\partial x^\nu},$$

and we have to identify L_ν with

$$\frac{2\pi i}{h}\left(p_\nu - \frac{e}{c}\phi_\nu\right)*$$

It is interesting to compare this with Weyl's assumption for $K_{\mu\epsilon,\nu}$ which was

$$K_{\mu\epsilon,\nu} = -g_{\mu\epsilon}\phi_\nu$$

[*Note added December* 11, 1927.—There is a serious difficulty in this interpretation of L_ν which has been pointed out to us by one of the referees. This is removed in a later paper by one of us (H. T. F.). The main point in this paper is the derivation of an equation identical in form with the wave equation from a consideration of metrics and we believe that this cannot result from a mere coincidence.]

---

* Since arriving at the conclusions described above, we note that in the current number of the 'Zeitschrift für Physik,' London considers by another method the possibility of identifying the ψ of the wave equation with the λ of Weyl's theory. He concludes that this is not possible without a radical change in that theory.

Relativity and the Quantum Theory

By H T Flint

(Communicated by O W Richardson, F R S —Received November 5, 1927)

In Einstein's theory of gravitation it is assumed that the geometry of space-time is characterised by the following equation for the measurement of displacement —

$$ds^2 = g_{mn}\, dx^m\, dx^n \qquad \left\{\begin{matrix} m \\ n \end{matrix}\right. = 1, 2, 3, 4,$$

the sign of summation being omitted for convenience

It is supposed that the coefficients, of which g_{mn} is the type, are dependent upon the content of space, and the relation existing between them is the law of gravitation

To this geometrical scheme Maxwell's equations describing electromagnetic phenomena can be readily adapted, the equations being immediately interpretable as tensor equations But these phenomena do not correspond to a geometrical property in the same way as the gravitational phenomena, and from the point of view of the whole-hearted relativist the position is unsatisfactory

Weyl's theory provides a remedy

It is assumed that when a displacement vector undergoes a parallel displacement in a purely gravitational field there is no change of length, while in the presence of an electromagnetic field a change of length occurs

This means that we pass from purely gravitational to the inclusion of electromagnetic phenomena merely by the introduction of this view of the metrics of space, just as we pass from the consideration of phenomena without a gravitational field to gravitational phenomena by a change from Euclidean to Riemannian geometry, *i e*, by a change from $ds^2 = \Sigma\, dx^2$ to $ds^2 = g_{mn}\, dx^m\, dx^n$

A displacement vector with components, A^1, A^2, A^3, A^4, which will be described as the vector A^m, has length, l, determined by

$$l^2 = g_{mn}\, A^m A^n$$

If in a displacement to a neighbouring point it becomes the vector $(A^m + \delta A^m)$ it is said to have undergone a parallel displacement provided that

$$\delta A^m = -\, \Gamma^m_{\ np}\, A^n \quad \delta x^p,$$

where δx^p is a component of the displacement and $\Gamma^m_{\ np}$ is a coefficient, the expression on the right being summed for the values of n and p If we write

$A'^m = A^m + \delta A^m$ the square of the length of the vector after displacement is

$$l^2 + \delta l^2 = g'_{mn} A'^m A'^n,$$

where g'_{mn} denotes the value of this coefficient at the neighbouring point In a purely gravitational field $\delta l^2 = 0$, but according to Weyl this is not the case in a gravitational and electromagnetic field

He assumes for this case that

$$\frac{\delta l}{l} = \kappa_s \delta x^s,$$

where κ_s is a component of the electromagnetic potential

We shall now consider this from a different point of view and develop our ideas in an attempt to show the relation existing between the quantum theory and the metrics of space

It will be assumed that the element of length $(ds)^2$ is to be measured by the expression

$$(ds)^2 = \lambda^2 g_{mn} \, dx^m \, dx^n,$$

where λ is a function of position and the g's are the ordinary gravitational components

In the same way the square of a displacement vector, A^m, will be measured by

$$A^2 = \lambda^2 g_{mn} A^m A^n$$

Two vectors, A^m and A'^m, situated at neighbouring points whose co-ordinates differ by δx^m, are said to be equal if

$$\lambda^2 g_{mn} A^m A^n = \lambda'^2 g'_{mn} A'^m A'^n, \tag{1}$$

where λ and λ', q_{mn} and g'_{mn} denote the values at the two points respectively and where A'^m is derived by parallel displacement from A^m, *i e* ,

$$A'^m = A^m - \Gamma^m_{np} A^n \, \delta x^p$$

From (1) we derive

$$\lambda^2 g_{mn} A^m A^n = \left(\lambda + \frac{\partial \lambda}{\partial x^t} \, \partial x^t\right)^2 \left(g_{mn} + \frac{\partial q_{mn}}{\partial x^n} \, \partial x^n\right)(A^m - \Gamma^m_{pq} A^p \, \delta x^q)(A^n - \Gamma^n_{rs} A^r \, \delta x^s),$$

a relation which must be true for all displacement vectors and for all displacements, δx^m It follows from this that if we write

$$\Gamma_{mn,s} = g_{st} \Gamma^t_{mn}$$

and

$$K_{mn,s} = \tfrac{1}{2}\left(\frac{\partial g_{mn}}{\partial x^s} - \Gamma_{sm,n} - \Gamma_{sn,m}\right),$$

then

$$g_{mn} \frac{\delta \lambda^2}{\lambda^2} = - 2K_{mn,s} \, \delta x^s$$

We may derive this also by noting that if l^2 is used to denote the Riemannian square of A^m, *i.e.*,

$$l^2 = g_{mn}A^mA^n,$$

then (1) is equivalent to

$$\delta(\lambda^2 l^2) = 0, \tag{2}$$

under the conditions of the displacement.

Thus

$$\frac{\delta\lambda^2}{\lambda^2} + \frac{\delta l^2}{l^2} = 0.$$

Now

$$\delta l^2 = 2K_{mn,s}A^mA^n\,\delta x^s.\text{*}$$

Hence, since

$$\delta l^2 = -\frac{\delta\lambda^2}{\lambda^2}l^2 = -\frac{\delta\lambda^2}{\lambda^2}g_{mn}A^mA^n,$$

we have

$$2K_{mn,s}A^mA^n\,\delta x^s = -\frac{\delta\lambda^2}{\lambda^2}g_{mn}A^mA^n,$$

a result which can only be true for all vectors if

$$g_{mn}\frac{\delta\lambda^2}{\lambda^2} = -2\kappa_{mn,s}\,\delta x^s. \tag{3}$$

In Weyl's theory $K_{mn,s}$ is made equal to $g_{mn}\kappa_s$, so that

$$\frac{\delta\lambda^2}{\lambda^2} = -2\kappa_s\,\delta x^s. \tag{4}$$

From the point of view we have taken, this gives rise to a difficulty. The integration of (4) leads to

$$\lambda = C\,e^{-\int\kappa_s dx^s}, \tag{5}$$

but the integral in this expression depends on the path of integration and λ is not a single valued function of position.

If a value of λ were laid down appropriate to each point in space, any subsequent movements would reduce the standards of measurement to a state of chaos.

An electron starting from a point provided with a definite value of λ would return to the point after completing a circuit with a value depending upon the path described.

A definite value could be maintained by permitting only those complete paths which left the value unchanged, as, for example, those for which $\int\kappa_s\,dx^s$ has the value $2\pi n$.

---

* Eddington, 'The Mathematical Theory of Relativity,' § 93.

We shall make the assumption that

$$\frac{\delta\lambda}{\lambda} = \mathrm{L}_s \, \delta x^s, \tag{6}$$

and later determine the meaning of L_s by reference to quantum phenomena as described by Schroedinger's equation

In (6) we have made use of the relation

$$\mathrm{K}_{mn\,s} = -\, g_{mn} \, \mathrm{L}_s$$

instead of

$$\mathrm{K}_{mn,s} = g_{mn} \, \kappa_s,$$

as in Weyl's theory, *i e*, we have avoided the identification of L_s as a component of the electromagnetic potential

The simplest example to which Schroedinger's equation can be applied is that of an electron in a purely gravitational field

The equation in this case is

$$\operatorname{div}\ (\mathrm{grad}\ \ \psi) = k\ \psi, \tag{7}$$

where k is a constant

In equation (7) the operations of divergence and gradient are to be interpreted for Riemannian space If we wish to extend this equation to take into account the case of an electron in an electromagnetic field, it should be sufficient to interpret the operators in the wider sense of the system of geometry and metrics we have been discussing We shall then see that, provided we interpret Schroedinger's ψ as our scale factor λ, the equation (7) becomes the wave equation for an electron moving in an electromagnetic field for $k = -\frac{4\pi^2 m^2}{h^2}$ We may mention here that it appears to have occurred first to F London to seek a relation between ψ and λ *

In our system the divergence of a vector, A^m, may be written

$$\operatorname{div}\ \mathrm{A}^m = \frac{\partial \mathrm{A}^m}{\partial x^m} + \Gamma^m{}_{nm}\mathrm{A}^n \tag{8}$$

This result follows readily from a consideration of the variation of a vector whose components are functions of the co-ordinates, and the details of the derivation were given in the last paper

---

* 'Z f. Physik,' vol. 42, p 375 (1927)

The value of $\Gamma^{m}{}_{nm}$ may be derived from the following relations —

$$\Gamma_{mn,s} = \begin{bmatrix} mn \\ s \end{bmatrix} + S_{mn,s}, \tag{9}$$

where

$$\begin{bmatrix} mn \\ s \end{bmatrix} = \tfrac{1}{2}\left[\frac{\partial g_{ms}}{\partial x^{n}} + \frac{\partial g_{ns}}{\partial x_{m}} - \frac{\partial g_{mn}}{\partial x_{s}}\right]$$

and

$$S_{mn,s} = K_{mn,s} - K_{ms,n} - K_{ns,m} \tag{10}$$

From this it follows that

$$\Gamma^{s}{}_{mn} = \begin{Bmatrix} mn \\ s \end{Bmatrix} + S^{s}{}_{mn},$$

where

$$S^{s}{}_{mn} = g^{sp}\, S_{mn,p} \tag{11}$$

Hence we have

$$\Gamma^{m}{}_{nm} = \begin{Bmatrix} mn \\ m \end{Bmatrix} + S^{m}{}_{nm},$$

for the expressions are symmetrical in m and n

We make use of the well-known result

$$\begin{Bmatrix} mn \\ m \end{Bmatrix} = \frac{1}{\sqrt{g}}\frac{\partial}{\partial x^{n}}\sqrt{g}$$

and we can proceed to evaluate $S^{m}{}_{nm}$ by means of (10) and (11) Since

$$K_{mn,s} = -\,g_{mn}L_{s}$$

we find

$$S^{m}{}_{mn} = 4L_{n}$$

Proceeding exactly as in the former paper we find

$$\operatorname{div}\ (\text{grad}\ \phi) = \frac{1}{\sqrt{g}}\frac{\partial}{\partial x^{m}}\left(\sqrt{g}\,g^{ms}\frac{\partial\phi}{\partial x^{s}}\right) + 4L_{m}\,g^{ms}\frac{\partial\phi}{\partial x^{s}}$$

In the particular case when $\phi = \lambda$

$$\operatorname{div}\ (\text{grad}\ \lambda) = \frac{1}{\sqrt{g}}\frac{\partial}{\partial x^{m}}\left(\sqrt{g}\,g^{ms}\frac{\partial\lambda}{\partial x^{s}}\right) + 4L_{m}L^{m}\lambda \tag{12}$$

Thus the form taken by equation (7) is

$$\frac{1}{\sqrt{g}}\frac{\partial}{\partial x^{m}}\left(\sqrt{g}\,g^{ms}\frac{\partial}{\partial x^{s}}\right) + 4\left(L_{m}L^{m} - \frac{\pi^{2}m^{2}}{h^{2}}\right)\lambda = 0, \tag{13}$$

and this is exactly Schroedinger's equation provided we make the substitution

$$L_{m} = \frac{\pi i}{h}\Pi_{m},$$

where Π_{m} is the momentum This use of the term momentum is justified, for Π_{m} has the same significance in a gravitational and electromagnetic field as the mechanical momentum, p_m, in generalised dynamics.* p_m is expressed usually as the differential coefficient, $\frac{\partial W}{\partial x^m}$, of a function W In the same way we shall suppose that Π_m can be so expressed and consequently λ will be a point function.

It has been usual to write

$$\Pi_m = p_m + e\kappa_m \tag{14}$$

for an electron in an electromagnetic field, regarding p_m as the mechanical momentum and κ_m as the electromagnetic potential

But the latter is not a complete differential We make the suggestion that Π_m is the significant quantity in the case of a gravitational and electromagnetic field and that it is strictly incorrect to regard it as made up of these two parts In the presence of an electromagnetic field, p_m in equation (14) is no longer the mechanical momentum, $\frac{\partial W}{\partial x^m}$, but is itself influenced by the field or by what generates the field through the gravitational components g_{np}, since $p_n = mg_{np}\frac{dx_p}{ds}$, where m is the mass The gravitational effect of an electron, which could excite the field, has been worked out† by Nordstrõm and G B Jeffery

If, then, we make this substitution, we obtain

$$\left(\frac{h}{2\pi i}\right)^2 \frac{1}{\sqrt{g}} \frac{\partial}{\partial x^m}\left(\sqrt{g}\, g^{ms} \frac{\partial \lambda}{\partial x^s}\right) + (\Pi_m \Pi^m + m^2)\,\lambda = 0, \tag{15}$$

the well-known equation of Schroedinger

If the electromagnetic field be removed, Π_m becomes the momentum $p_m\left(= \frac{\partial W}{\partial x^m}\right)$, since there is no contribution to Π_m either through K_m or the gravitational effect of the field

In this case we have from (6)

$$\frac{1}{\lambda}\frac{\partial \lambda}{\partial x^s} = \frac{\pi i}{h}\, p_s,$$

whence

$$\lambda = Ce^{\frac{\pi i}{h}\int p_s\, dx^s}$$

and we may make C = 1 for convenience

In the absence of any electromagnetic field the proper measure of the length of a line element is

$$(ds)^2 = g_{mn}\, dx^m\, dx^n,$$

so that in this case λ^2 is unity

---

* See W Wilson, 'Roy Soc Proc,' A, vol 102 p 478 (1923)

† See Eddington, 'The Mathematical Theory of Relativity,' p 185

This is the case if $\frac{2\pi i}{h}\int p_s\,dx^s = 2\pi n i$, since $e^{2\pi n i} = 1$ if n is an integer

Thus the condition is

$$\int p_s\,dx^s = nh, \tag{16}$$

which is similar to the integral conditions of the old quantum theory, but is less stringent, for the old quantum conditions were $\int p\,dq = nh$ for each component of momentum, p, and for each corresponding co-ordinate q, the integration being taken for a complete cycle of values, q

Here the condition is

$$\int (p_1\,dx' + p_2\,dx^2 + p_3\,dx^3 + p_4\,dx^4) = nh$$

In this case

$$p_s = mg_{sn}\frac{dx^n}{ds},$$

so that

$$\begin{aligned}\int p_s\,dx^s &= m\int g_{sn}\frac{dx^n}{ds}\;dx\\ &= m\int g_{sn}\frac{dx^n}{ds}\;\frac{dx^s}{ds}\;ds\\ &= m\int ds\\ &= ms.\end{aligned}$$

Thus (16) leads to

$$s = n\frac{h}{m},$$

indicating that the path of the electron is made up of integral multiples of a fundamental unit of length h/m

This result follows from another consideration,* and from both points of view the suggestion is that the world-line of the electron is to be considered as made up of these units of length, nothing less being observable directly or indirectly in experiment

Since length and time are fundamentally the same, it follows that time also is measured in terms of a fundamental indivisible unit

This imposes an upper limit to observed frequency, the maximum being the reciprocal of this unit, viz , m/h, which is equal to the frequency of de Broglie's "phénomène périodique "

---

* Flint and Fisher, 'Roy Soc Proc.,' A, vol 115, p 210 (1927).

The fact that the world-line is to be regarded as made up of a repetition of similar units means that a periodicity is associated with the electron, the frequency being m/h

We may conclude, assuming that the system of metrics described has any application to physics, that the wave equation gives the value of the scale factor, λ, and this means that in atomic phenomena we discover the natural scale factor

We might, of course, regard equation (11) as an equation for L_m or Π_m, which is readily derived from (6) The wave equation thus represents a "law of metrics," and is to be compared with the law of gravitation, which may be described as a geometrical law

---

On a Minimum Proper Time and its Applications (1) *to the Number of the Chemical Elements* (2) *to some Uncertainty Relations.*

By H T FLINT, D Sc , King's College, London, and O W RICHARDSON, F R S , Yarrow Research Professor of the Royal Society

(Received December 14, 1927)

§ 1. In a recent paper* by one of us the conclusion was reached that the proper time of a particle had a minimum value h/mc^2 where m is the rest mass This conclusion was based on a simple assumption about the metrics of space which was found to be in agreement with Schroedinger's wave equation. The following considerations show that the same conclusion can be reached by a method which is independent of the system of metrics referred to

The expression for the momentum of a particle of rest mass m in relativity mechanics is

$$p_\alpha = m g_{\alpha\beta} \frac{dx^\beta}{ds}, \tag{1}$$

where s denotes an arc of the world line. If $p^\alpha \left(= m\,\dfrac{dx^\alpha}{ds}\right)$ denote the contravariant vector corresponding to p_α we have

$$p_\alpha p^\alpha = m^2. \tag{2}$$

---

* 'Roy. Soc. Proc.,' vol. 117, p. 625.

Associated with the momentum is the action W since

$$p_\alpha = \frac{\partial W}{\partial x_\alpha}$$

hence

$$g^{\alpha\beta}\frac{\partial W}{\partial x^\alpha}\frac{\partial W}{\partial x^\beta} = m^2,$$

or

$$|\operatorname{grad} W|^2 = m^2$$

This is a simple case of equation (1″) of Schroedinger's second paper (' Ann. d Physik,' (4), vol 79, p 492 (1926)), that equation, however, referring to a problem in classical dynamics in a notation like that employed in the theory of relativity

$$\frac{\partial W}{dx^\alpha}\frac{dx^\alpha}{ds} = m, \tag{3}$$

from which we see that the world line with direction cosines $\frac{dx^\alpha}{ds}$ $(\alpha = 1, 2, 3, 4)$ is perpendicular to the surface W = const This is easy to illustrate in a two dimensional diagram plotting x^1 (or x) against x^4 (or u) From (3)

$$\frac{dW}{ds} = m,$$

and

$$W = ms + W_0 \tag{4}$$

If we plot surfaces of action as we plot equipotential surfaces in statics we naturally do so at intervals separated by the quantum of action h and so draw the series W_0, $W_0 + h$, $W_0 + 2h$, etc By equation (4) these cut the line OP at ints separated by intervals of magnitude m or if we change to the second as unit time and give h its C.G S value the tervals are of length h/mc

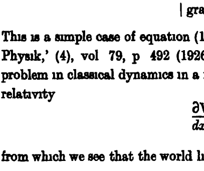

The interval h between the surfaces is e smallest quantity of action and we may erefore expect that h/mc is the smallest observable length on account of the mutual relation between the line and the surface. Associated with this length is the proper time h/mc^2 so that we are led to the principle that in four dimensions the smallest observable length is h/mc and the smallest observable proper time is h/mc^2.

In the rest of this paper m will be used for the ordinary mass, the rest mass being indicated by m_0.

§ 2 *On the Number of the Chemical Elements*

These relations involve a limit on the atomic numbers of the chemical elements The limit can be ascertained in various ways Of the known existing elements the highest atomic number N is possessed by uranium for which N = 92

Let us now consider the application to the motion of an electron round a nucleus. The orbit is assumed to be circular for simplicity The proper time τ and the ordinary time t are related by

$$\tau = (1 - v^2/c^2)^{\frac{1}{2}}\, t. \tag{1.1}$$

We should thus conclude for an electronic orbit with period

$$t = 2\pi r/v \tag{1.2}$$

that

$$\left(1-\frac{v^2}{c^2}\right)^{\frac{1}{2}} \frac{2\pi r}{v} > \frac{h}{m_0 c^2}. \tag{1.3}$$

From the usual equations

$$mrv = h/2\pi \quad \text{and} \quad mv^2/r = \mathrm{N}e^2/r^2 \tag{1.4}$$

we have

$$v = 2\pi \mathrm{N}e^2/h \quad \text{and} \quad r = h/2\pi mv \tag{1.5}$$

together with

$$m = m_0\left(1-\frac{v^2}{c^2}\right)^{-\frac{1}{2}} \tag{1.6}$$

From (1.3)

$$\left(1-\frac{v^2}{c^2}\right)^{\frac{1}{2}} \frac{h}{mv^2} > \frac{h}{m_0 c^2},$$

and (1.6)

$$1 - v^2/c^2 > v^2/c^2$$

or

$$v < c \div \sqrt{2}. \tag{1.7}$$

Hence, from (1.5)

$$2\pi \mathrm{N}e^2/h < c/\sqrt{2},$$

and

$$\mathrm{N} < \frac{1}{2\sqrt{2}} \frac{hc}{\pi e^2} \tag{1.8}$$

Using $h = 6{\cdot}55 \times 10^{-27}$, $c = 3 \times 10^{10}$, $e = 4{\cdot}77 \times 10^{-10}$ this gives $\mathrm{N} < 98$.

[The occurrence of the maximum orbital velocity $c/\sqrt{2}$ is interesting. This velocity bears the same relation to the velocity of light as the velocity of a body falling from infinity to the earth's surface bears to the velocity of a satellite which just clears the surface in its orbit.]

This particular limitation on the orbital velocity makes it possible to make an application similar to the foregoing using the lower limit h/m_0c on the ordinary length instead of on the four dimensional length. We have

$$ds^2 = dx^2 + dy^2 + dz^2 - c^2\,dt^2$$
$$= dl^2 - c^2dt^2 = dl^2\,(1 - c^2/v^2),$$

if $v = \frac{dl}{dt}$. Thus in the limiting case when $v = c/\sqrt{2}$,

$$ds^2 = -\,dl^2$$

so that the measured lengths (*i e*, neglecting the imaginary $\sqrt{-1}$) of ds and dl are the same. Naturally it leads to the same result as that obtained already, viz,

$$\mathrm{N} < \frac{1}{2\sqrt{2}}\,\frac{hc}{\pi c^2}\,(\simeq 98)$$

We shall now consider the radiation emitted in the combination of an electron with a massive nucleus. The energy of the electron in the orbit is

$$\mathrm{W} = c^2\,(m - m_0) - \mathrm{N}e^2/r, \tag{1.9}$$

$$= m_0c^2\,(1 - v^2/c^2)^{\frac{1}{2}} - m_0c^2 \tag{1.10}$$

and the frequency of the emitted radiation is

$$\nu = -\,\mathrm{W}/h = \frac{m_0c^2}{h} - \frac{m_0c^2}{h}\left(1 - \frac{v^2}{c^2}\right)^{\frac{1}{2}} \tag{1.11}$$

This is obviously less than m_0c^2/h, the maximum frequency already postulated in the previous paper. On account of the limitation $v < c/\sqrt{2}$ we also have

$$\nu < \frac{m_0c^2}{h}\left(1 - \frac{1}{\sqrt{2}}\right), \tag{1.12}$$

and this limitation implies $\mathrm{N} < \frac{1}{2\sqrt{2}}\,\frac{hc}{\pi e^2}$ as before.

If we substitute from (1.5) in (1.10) and (1.11) we get

$$\mathrm{W} = m_0c^2\left(\sqrt{1 - \frac{4\pi^2\mathrm{N}^2e^4}{c^2h^2}} - 1\right) \tag{1.10'}$$

and

$$\nu = \frac{m_0c^2}{h}\left(1 - \sqrt{1 - \frac{4\pi^2\mathrm{N}^2e^4}{c^2h^2}}\right). \tag{1.11'}$$

These equations enable another but somewhat higher limit to be placed on the number of the chemical elements. It is evident from equation (1.11′) which involves nothing beyond the assumption of Sommerfeld's relativistic theory of the motion of an electron round a nucleus, that if N were to become greater than $ch/2\pi e^2$ the frequency ν would become complex. This means that Schroedinger's ψ function for this state would contain factors $e^{\pm\kappa t}$ where t is the time and κ is real, being, in fact, equal to $-2\pi\frac{m_0c^2}{h}\sqrt{\frac{4\pi^2N^2e^4}{c^2h^2}-1}$. Such factors would make the function increase or decrease indefinitely with lapse of time and their presence means that the solution does not exist and that the state which it represents is incapable of existence

Again we see from (1 10′) which also involves nothing beyond the assumptions underlying Sommerfeld's theory, that the lost energy $-$ W becomes complex if N exceeds $ch/2\pi e^2$ At the limit where $N = ch/2\pi e^2$ we have $-W = m_0c^2$ the energy of an electron at rest according to de Broglie This means that the lost energy cannot exceed m_0c^2, which is a very natural result if the lost energy comes out of the energy of the periodic phenomenon of the electron which loses it

It thus appears that the limit $N \ngtr ch/2\pi e^2$ is required by the relativistic formulæ for the motion of an electron round a nucleus apart from the atomicity relations which lead us to the sharper limit $N \ngtr ch/2\sqrt{2}\pi e^2$ There is nothing in this which puts a limit on the atomic number of a bare nucleus The limit is on the charge of a nucleus which can build up a chemical atom So far as this restriction goes very hot stars might contain nuclei with higher values of N than those possessed by any chemical element

In some remarkable calculations on the stability of liquid stars Jeans* has found limits for N of 93 2 and 93 9 by two methods These methods are probably not sufficiently accurate to distinguish these from our value which is 4 units higher.

§ 3 *Extension to any Quantum Number and consideration of the Nucleus*

So far we have only considered circular orbits with the quantum number 1 The equation (1 3)

$$(1 - v^2/c^2)^{\frac{1}{2}}\quad 2\pi r/v \nless h/m_0c^2$$

will apply to a circular orbit of any quantum number But the equations (1 4) became

$$mrv = nh/2\pi \quad \text{and} \quad mv^2/r = Ne^2/r^2 \tag{2 1}$$

---

* 'M.N.R.A.S.,' vol. 87, p 735 (1927).

for a circular orbit of quantum number n. Hence

$$\frac{nh}{mv^2}(1 - v^2/c^2)^{\frac{1}{2}} \nless h/m_0c^2,$$

$$n(1 - v^2/c^2) \nless v^2/c^2$$

$$v^2/c^2 \ngtr n/n + 1 \qquad (2\ 2)$$

It is satisfactory to note that the limiting value of v approaches c as n approaches ∞, *i.e.*, for a free electron.

For an extra nuclear electron we have from (2 1)

$$v = \frac{2\pi}{nh}\mathrm{N}e^2 \ngtr c\sqrt{\frac{n}{n+1}}$$

$$\mathrm{N} \ngtr n\left(\frac{n}{n+1}\right)^{\frac{1}{2}}\frac{ch}{2\pi e^2}$$

$$n\left(\frac{n}{n+1}\right)^{\frac{1}{2}} \nless \frac{2\pi e^2}{ch}\mathrm{N}$$

This shows that the limit $\mathrm{N} < 98$ only applies to atoms provided with K electrons ($n = 1$) If we were to admit the existence of atoms with electrons for which the lowest quantum number was 2 or more higher values of N would be admissible However, the proper discussion of this requires the consideration of non-circular orbits when it would probably be found that some of the others would become impossible

N becomes proportional to n for large values of n so that there is nothing in this which sets any limit to the nuclear charge of a nucleus which can exist in the presence of free electrons

It is important to observe that equation (2 2) does not involve the mass, charge or any other properties of the particle It states that no particle can execute an n quantum circular orbit with a velocity greater than $\sqrt{\frac{n}{n+1}}\,c$ If the same principle is applied to a Planck oscillator it leads to $v \ngtr \sqrt{\frac{2n}{2n+1}}\,c$ and for a rigid rotator $v \ngtr \sqrt{\frac{n/2}{n/2+1}}\,c$

Let us now turn to consider the nucleus A detailed theory of its structure has recently been put forward by Rutherford* It supposes that in the heavier nuclei there are satellites which consist of uncharged helium atoms. These are polarised in the field of the nucleus and move in orbits, treated as circular, under the forces thus arising The velocity in an orbit with n quanta is given by

---

* 'Phil. Mag.,' vol. 4, p 580 (1927).

$$v^2 = \frac{n^4h^4}{2a^2M^2e^2(2\pi)^4N^2}$$

where M is the mass of the satellite (rest mass M_0) Thus

$$v^2 \bigg/ \left(1 - \frac{v^2}{c^2}\right)^{3/2} = \frac{n^4h^4}{2a^2M_0{}^2e^2(2\pi)^4N^2}.$$

Since

$$v^2/c^2 \not> n/(n+1)$$

$$\frac{v^2}{c^2}\left(1 - \frac{v^2}{c^2}\right)^{-3/2} \not> \frac{n}{n+1}(n+1)^{3/2} \not> n\,(n+1)^{1/2}$$

Therefore

$$\frac{n^4h^4}{2\,(2\pi)^4\,a^2M_0{}^2e^2c^2N^2} \not> n\,(n+1)^{1/2}$$

and

$$N^2 \not< \frac{n^3}{(n+1)^{1/2}}\,\frac{h^4}{2\,(2\pi)^4\,a^2M_0{}^2e^2c^2}$$

Taking $a = 6 \times 10^{-13}$ cm $M_0 = 6{\cdot}60 \times 10^{-24}$ gm., $e = 4\ 77 \times 10^{-10}$, $h = 6\ 55 \times 10^{-27}$, and $c = 3 \times 10^{10}$, we find

$$N \not< 6{\cdot}82 \times 10^{-3}\,\frac{n^{3/2}}{(n+1)^{1/4}}$$

This relation is interesting in that for any given N it gives an upper limit to the quantum number n This is evidently fairly large and we can write approximately

$$n^{5/4} \not> 146\ 7\ N$$

In the case of N = 92 (uranium)

$$n \not> 2000 \text{ approx}$$

The outermost orbit in this element is that for which $n = 28$ so there is according to this a large number of possible inner orbits, the quantum numbers for the orbits of the intra-nuclear satellites increasing with diminishing orbital radius $\left(r \propto \frac{1}{n}\right)$.

Rutherford also supposes that there are in the nuclei certain electrons revolving in orbits with a velocity approaching that of light This also is in agreement with the relation $v^2/c^2 \not< n/n + 1$ provided their quantum numbers n are not too low. This is all we can say about them until the nature of the field of force in which they are moving is known.

§ 4. *Uncertainty Relations.*

The uncertainty relations which have been developed in collaboration by Bohr and Heisenberg* rest on the theory of optical instruments and especially on the researches of the late Lord Rayleigh on resolving power and allied questions. It follows from the fact that the vector which specifies a monochromatic wave contains the factor exp $i2\pi\,(\gamma s - \nu t)$, where γ is the reciprocal wave length and ν the frequency, and from the principles of optical interference that there are uncertainties $\Delta\gamma$, Δs, $\Delta\nu$, Δt in these quantities which are governed by the relations

$$\left.\begin{array}{l}\Delta s\;\Delta\gamma \sim 1\\ \Delta t\;\Delta\nu \sim 1\end{array}\right\} \qquad (3\;1)$$

The sign $\sim$ is meant to indicate that the quantities on either side of it are of the same order of magnitude In view of the relations $\mathrm{E} = h\nu$† and $\mathrm{P} = h\gamma$,‡ E and P being the energy and momentum respectively of a light quantum, the relations (3 1) will also involve that

$$\left.\begin{array}{l}\Delta s\;\Delta \mathrm{P} \sim h\\ \Delta t\;\Delta \mathrm{E} \sim h\end{array}\right\} \qquad (3\;2)$$

The expressions (3 1) and (3 2) are the uncertainty relations of Bohr and Heisenberg

As an illustration we may consider the special case of a plane grating The condition§ that the minimum for λ' should coincide with the maximum for λ is

$$\lambda'/(\lambda - \lambda') = \mathrm{N}n \qquad (3\;3)$$

where n is the order of the spectrum and N the number of rulings Hence if Δ denotes the uncertainty in the measurements we have

$$\Delta\lambda \sim \lambda/(\mathrm{N}n) \text{ and } \Delta\gamma = \Delta\lambda^{-1} = \lambda^{-2}\,\Delta\lambda \sim (\mathrm{N}n\lambda)^{-1} \qquad (3\;4)$$

For the uncertainty in s we have $\Delta s = \Delta x \;\sin\theta$ where θ is the angular deviation and x is the distance from the axis We cannot distinguish by observation between values of x which lie within a distance of the order of magnitude of $x - x'$ where

$$x = rn\lambda\, d^{-1} \quad \text{and} \quad x' = rn\lambda'\, d^{-1}, \qquad (3\;5)$$

---

* *Cf.* Heisenberg, 'Zeits. für Physik,' vol 43, p. 172 (1927), Bohr, 'Nature,' 1927.

† Einstein, 'Ann. der Physik,' vol 17, p. 146 (1905), Bohr, 'Phil Mag.,' vol. 26, p. 1 (1913).

‡ Richardson, 'Phil. Mag.,' vol. 25, p. 144 (1913)

§ Schuster's 'Optics,' p. 109

if r is the distance from the grating to the image, d is the distance between the rulings and λ and λ' satisfy (3 3). Hence

$$\Delta s = \sin\theta\ \Delta x \sim \sin\theta\,(\lambda - \lambda')\, rnd^{-1} \sim r\lambda\,(\mathrm{N}d)^{-1}\sin\theta \tag{3 6}$$

and

$$\Delta s\ \Delta\gamma \sim r\,.\,\sin\theta/(\mathrm{N}n\quad \mathrm{N}d) \sim r\lambda\,(\mathrm{N}d)^{-2}. \tag{3 7}$$

The quantity $r\lambda\,(\mathrm{N}d)^{-2}$ is the product of the distance from the grating to the image and the wave-length of the light divided by the square of the linear aperture If the wave-length is such that the angular deviation is equal to half the linear aperture divided by r the value of $rd\,(\mathrm{N}d)^{-2}$ is unity, and it will be of this order of magnitude in any practical case

Similar physical justifications, such as by a consideration of the interaction of light and an electron in the Compton effect, can readily be given for the relations (3 2) This can be considered as a confirmation of their general derivation from (3 1) by using the linear relations between E, P and ν, γ

These uncertainty relations are general and their evidential basis is of an empirical character Whilst this foundation may be strong we find its mixture of wave theory and power of observational discrimination to some extent unattractive. This is not a scientific objection but a matter of taste It is, of course, necessary to bring in the wave theory in order to give a meaning to ν.

The conclusions of the former paper lead to a set of uncertainty relations which, though not the same, have a similar content and which rest on an entirely different basis, namely, on the basis of the considerations set forth in § 1 of the present paper These relations can be established in a number of ways Our first deduction was as follows —

The motion, in a space in which there is no electromagnetic field, of a charge of rest mass m_0 along a line s is discontinuous in such a way that $m_0 s$ changes by multiples of h/c If we suppose that this applies to ordinary space and time we may expect uncertainties of at least the following amounts in the various quantities γ $(= \nu/c)$, s, ν, t, P and E —

$$\Delta s = h/m_0 c, \qquad \Delta t = h/m_0 c^2, \tag{3 8}$$

$$\Delta\nu = \Delta\left(\frac{1}{t}\right) = \frac{1}{t - \Delta t} - \frac{1}{t} = \nu^2 \Delta t = h\nu^2/m_0 c^2, \tag{3 9}$$

$$\Delta\gamma = \Delta\left(\frac{1}{\lambda}\right) = h\nu^2/m_0 c,^3 \tag{3 10}$$

$$\Delta \mathrm{E} = h\Delta\nu = h^2\nu^2/m_0 c^2, \tag{3 11}$$

$$\Delta \mathrm{P} = \frac{h}{c}\ \Delta\nu = h^2\nu^2/m_0 c^3 \tag{3 12}$$

From (8), (9) and ,10)

$$\Delta s\ \Delta\gamma = \Delta\nu\ \Delta t = h^2\nu^2/m_0{}^2 c^4 \tag{3 13}$$

Since ν has a maximum value m_0c^2/h these products (3·13) always lie between 0 and 1, $h^2\nu^2/m_0{}^2c^4$ tending to zero as $\nu \rightarrow 0$ and tending to 1 as $\nu \rightarrow \nu_{\max}$. From (3·11) and (3·12)

$$\Delta P\, \Delta s = \Delta E\, \Delta t = h\,(\Delta\nu\, \Delta t) = h\,.\,h^2\nu^2/m_0{}^2c^4. \qquad (3·14)$$

These products always lie between 0 and h since $h\,.\,h^2\nu^2/m_0{}^2c$ tends to zero as $\nu \rightarrow 0$ and to h as $\nu \rightarrow \nu_{\max}$.

The products (3·13) and (3·14) are not the same as the corresponding products of Bohr and Heisenberg as the interplay between the pairs of conjugated quantities has not been taken into account. But this interplay cannot wipe out any of the essential inaccuracy in the separate quantities. It can only increase the inaccuracy, not diminish it. It follows that the present expressions for the essential inaccuracies should never be greater than those got by Bohr and Heisenberg. This is the case. And there is a further point of interest. According to (3·7) $\Delta s\, \Delta\gamma$ has its least value as λ diminishes, *i.e.*, as ν increases to its maximum value. Our product (3·13) increases to its greatest value 1 as $\nu \rightarrow \nu_{\max}$. This is essentially the same magnitude as that of (3·7), so that, for the highest frequencies the disordering effect of the interaction is obliterated or, at any rate, is reduced to a minimum. This is reasonable as the opportunity for a further disordering by the interaction will increase as the space time extension in the interaction increases.

The discontinuous changes in length to be expected are $2·44 \times 10^{-10}$ cm. for an electron $1·314 \times 10^{-13}$ cm. for a proton and $3·31 \times 10^{-14}$ cm. for an alpha particle. These different lengths may have some bearing on the question as to whether the results of the experiments on atomic scattering of electrons and α particles respectively, as ordinarily interpreted, are entirely harmonious. There seems to be some difference of opinion on this point. The maximum frequency is about 10^{20} sec $^{-1}$ and the minimum wave-length about 3×10^{-10} cm.

§ 5. It may be urged that this treatment cannot be right as the maximum frequency referred to is not an invariant under a Lorentz transformation. We have seen, however, in § 2 that there is a definite maximum frequency m_0c^2/h in connection with the motion of an electron about a nucleus so that it is possible to give a physical interpretation to such a maximum frequency. In any event we believe that this difficulty, if it be one, is avoided by the following treatment.

We start from the principle that the least "proper" time is h/m_0c^2 and the corresponding smallest length in four dimensions ih/m_0c. Now

$$\begin{aligned} ds^2 = dx^2 + dy^2 + dz^2 + du^2 &= dl^2 - c^2dt^2 \\ = (v^2 - c^2)\, dt^2 \qquad &= -(c^2 - v^2)\, dt^2 \end{aligned}$$

putting

$$\frac{dl}{dt} = v$$

Thus

$$ds = i\sqrt{c^2 - v^2}\,dt$$

Also

$$ds^2 = dl^2\,(1 - c^2/v^2) = -\,(c^2/v^2 - 1)\,dl^2$$

and

$$ds = i\sqrt{(c^2 - v^2)/v^2}\,dl$$

Thus the smallest observable interval of ordinary time is given by

$$dt = \frac{h}{m_0c}\Big/\sqrt{c^2 - v^2} = h/m_0c^2\sqrt{1 - \beta^2}, \qquad \beta = \frac{v}{c}$$

and of ordinary length by

$$dl = \frac{h}{m_0c}\Big/\sqrt{\frac{c^2 - v^2}{v^2}} = \frac{h}{m_0c}\,\frac{\beta}{\sqrt{1 - \beta^2}}$$

Both these intervals depend upon the velocity of the mass m_0 with which they are associated. For velocities approaching the velocity of light they become very large which means that it is impossible to measure intervals of time and length in association with such rapidly moving particles. But for β particles so fast that $\frac{v}{c} = 0.99$ the intervals are still very small, *e.g.*, $dl = 7.0 \times \frac{h}{m_0c}$ a quantity of the order 10^{-9} cm and the interval of time is of the order 10^{-19} sec. This result that the observational errors in length and time are very great when the velocity approaches that of light does no violence to our present views. The theory of relativity teaches that a velocity c in a particle or in anything which transmits energy is only attainable as a limiting case. Here we except a light quantum or photon which will be considered separately below. The deduction from the principle of the existence of a least proper time is that any accurate measurements on a particle moving with this velocity would be impossible.

We now turn to the consideration of the four dimensional invariant quantity which corresponds to the momentum. This is $m_0 \dfrac{ds}{d\tau}$ where ds is an element of the world line of the particle and $d\tau$ the associated proper time. The components of this quantity are p_x, p_y, p_z, p_u where the first three are the ordinary momentum components mv_x, mv_y, mv_z and $p_u = i\mathrm{E}/c$ where E the energy of the particle $= mc^2 = m_0c^2/\sqrt{1 - v^2/c^2}$. We have $p_x^2 + p_y^2 + p_z^2 + p_u^2 = m^2v^2 - m^2c^2 = \dfrac{m_0^2}{1 - v^2/c^2}\,(v^2 - c^2) = -\,m_0^2c^2$

Thus

$$\left| m_0 \frac{ds}{d\tau} \right| = i m_0 c \text{ (an invariant)}$$

According to our view in making any observation on a length s we shall record a value $n \frac{ih}{m_0c}$, and we know that we cannot be certain that this length is correct within ih/m_0c Similarly in recording the time τ we record $n\, h/m_0c^2$ with liability to an error h/m_0c^2. The value of the momentum we seek is the invariant im_0c but we determine

$$m_0 \frac{(n \pm 1)\, ih/m_0c}{(n \pm 1)\, ih/m_0c^2} = m_0c\, i \frac{n \pm 1}{n \pm 1}$$

the numerator and denominator being as small as we can make them, since $m_0 \frac{ds}{d\tau} = \lim m_0 \frac{s}{\tau}$ The worst possible error occurs when we take $m_0c \frac{n+1}{n-1}$ and the magnitude of the error is then $m_0c \quad i \quad \frac{2}{n-1}$.

If we denote the error in s by Δs and in the momentum by Δp we have

$$\Delta s \ \Delta p = \frac{2h}{n-1} \text{ numerically}$$

The worst case is for $n = 1$ but this is of no practical significance for it corresponds to an observation of one fundamental unit of length which is recorded as corresponding to zero proper time It affords another illustration of the impossibility of making accurate deductions on the limiting length If $n = 2$ $\Delta s \ \Delta p = 2h$, if $n = 3$ $\Delta s \ \Delta p = h$, and so on We conclude that the errors are at most comparable with h and that they arise from the inherent inaccuracy in the observations of a few units of length and time

Now Δs is the length of a 4-vector with components $\Delta x \ \Delta y \ \Delta z \ ic\Delta t$, and Δp is the tensor of a 4-vector with components $\Delta p_x \ \Delta p_y \ \Delta p_z \ \frac{i}{c}\Delta E$, from which we conclude that the following maximum error products exist —

$\Delta p_x \ \Delta x = \frac{2h}{n-1}$ and similarly for y and z and also $\Delta E \ \Delta t = \frac{2h}{n-1}$. Let these be written $\Delta p \ \Delta q \sim h$. Δq is an ordinary length or time and cannot be observed if $< \frac{h}{m_0c} \frac{\beta}{\sqrt{1-\beta^2}}$ This is an error of necessity Thus we have a corresponding error in Δp given by

$$\Delta p \sim m_0c \frac{\sqrt{1-\beta^2}}{\beta},$$

this approaches zero as $v \to c$, the corresponding Δq at the same time increasing beyond limit but the product remaining of the order h, at most. A similar consideration applied to $\Delta E \, \Delta t$ shows $\Delta E \sim m_0 c^2 \frac{\sqrt{1-\beta^2}}{\beta}$, and this also approaches 0 as $v \to c$ whilst $\Delta t \to \infty$, but the product $\Delta E \, \Delta t$ remains of the order h, at most.

So far we have confined this application to material particles including electrons and protons and excluding light quanta or photons. We are not sure that this exclusion is necessary. If we seek to locate a photon in space and time since it travels with the velocity c the errors are infinite. On the other hand, if we ask for its energy or momentum we get a definite answer. We also get a definite answer if we ask for the action of a photon although we are unable to locate it in space and time. Well this seems to correspond to the properties which are actually attributed to photons.

We expect these limitations to apply to electrons in atoms as well as to free electrons.

Critical Potentials for Soft X-Ray Excitation.

By Ursula Andrewes, Ph.D., Ann Catherine Davies, D.Sc., and Frank Horton, F.R.S.

(Received October 27, 1927.)

In the 'Proceedings of the Royal Society,' A, vol. 110, p. 64 (1926), the authors have described an investigation of the critical potentials corresponding to the values of the electron energy associated with some of the softer X-ray levels of the elements chromium, manganese, iron, cobalt, nickel, copper, and zinc. In this investigation a greater number of critical voltages were found for each element than had been anticipated. An attempt was made to determine which of the critical potentials corresponded to the M_I and $M_{II, III}$ levels for the element in question, by extrapolating the appropriate Moseley curves, and also to account for all the critical potentials in terms of single or multiple electron displacements from the M group. The significance of the various critical potentials obtained experimentally has also been further discussed in a subsequent paper by two of the authors.* The results recorded in the present paper have been obtained from a continuation of the experiments, in which more convenient methods of measuring the photoelectric current produced by the soft X-rays have been employed

---

* 'Phil. Mag.,' vol. 2, p. 1253 (1926).

The experimental tube in which the electron bombardment of the various metals took place, and in which the resulting radiation was detected, has been described in previous papers In the present research, the photoelectric current, which served as a measure of the radiation produced by the bombardment, was usually measured by observing the steady deflexion of an electrometer needle instead of by timing its motion This method has the advantage that it allows of a series of observations being taken more rapidly than is possible by the timing method, so that the chances of variations occurring in the conditions of the apparatus during the experiment are considerably reduced, and series of observations can be made over larger voltage ranges and at smaller voltage intervals Moreover, it was found possible to make the electrometer measurements more sensitive by this method, an advantage which was especially useful when the slowest bombarding streams were being used

The Measurement of the Photoelectric Currents

Two different devices were adopted in employing the steady deflexion method of using a quadrant electrometer to measure the small photoelectric currents dealt with in the research The first was the ordinary device of using the electrometer to indicate the potential difference between the ends of a very high resistance through which the current under observation was flowing A liquid resistance is often employed for this purpose—a mixture of alcohol and xylol, for instance, being used by some experimenters. Others have found the older device of lines ruled in Indian ink more useful The success of this latter method possibly depends on the brand of ink used We experimented with Indian ink lines ruled on sealing wax, but found that the measured values of the resistances made in this way were not constant but gradually increased with time, even when the resistance was enclosed in an air-tight container and kept under constant conditions Other materials tried as high resistances were glass very lightly covered with platinum by sputtering *in vacuo*, and certain metallic oxides in the form of thin rods. The high resistance with which success was ultimately obtained was made of ordinary soda-glass containing a little cupric oxide dissolved in it This material was prepared by grinding glass and cupric oxide together very finely in a mortar The mixture was then melted, care being taken to avoid reducing the oxide, and a bright blue lump of glass was obtained. A small piece of this was melted on to the ends of two thin copper wires (to serve as leads) and drawn out into a thread in an oxidising flame. The suitability of the resistance was tested with the electrometer When it was found to be too low, some of the blue glass was remelted with more ordinary soda-glass until a suitable composition was obtained Threads of convenient resistance—about 10^{11} to 10^{13} ohms—were sealed up in glass tubes by means of sealing-wax plugs at the ends of the tubes, through which the copper leads passed After being sealed up in this way the resistances of the threads used in the present experiments were found to remain very constant The resistance of the thread used in most of the experiments was 5×10^{11} ohms

In order to use a single resistance of this type over the whole range of voltages investigated for any one metal, a potential difference of a few tenths of a volt was applied, when necessary, between one end of the glass thread and earth, so as to bring the electrometer needle into a position where its motion could be observed When the instrument was being used to measure a positive current (caused by the loss of electrons from the detecting plate of the apparatus), the positive pole of the small potential difference was earthed The direction of this potential difference was reversed when a negative current was under observation

The second device by means of which the photoelectric currents were measured by observations of steady deflexions of the electrometer was by using a three electrode thermionic valve in the manner indicated diagrammatically in the figure. The valves used for this purpose were of the type in which the filament and the anode leads were at opposite ends of the valve, so that the possibility of leakage between these electrodes (over the glass) was reduced to a minimum

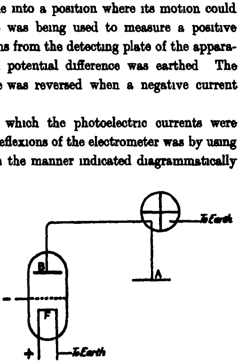

Both the anode B of the valve and the photoelectric plate A of the apparatus were connected to the insulated quadrants of the electrometer The negative end of the filament was earthed, and the grid was made slightly negative to the filament. During the course of the experiment the plate A of the apparatus loses electrons by photoelectric action of the soft X-rays. This causes the quadrants to which the plate is attached, and also the connected anode B of the valve, to gain a gradually increasing positive charge. As the potential of the anode rises, electrons from the valve filament are attracted through the grid to the plate in increasing numbers until a condition is reached when the rate of gain of electrons by the anode and the quadrants to which it is connected, just balances the rate of loss by the photoelectric plate, at which stage a constant deflexion of the electrometer needle is obtained In order to obtain a measure of the photoelectric current from the value of this steady deflexion, it is necessary to know the value of the electron current to the anode of the valve under the existing conditions of filament temperature and potential difference between the electrodes For this purpose the photoelectric current from the plate was stopped by cooling the filament of the experimental tube The anode of the valve, the plate A of the experimental tube, and the connected quadrants were then charged to a positive potential of a few tenths of a volt, so that the electrometer indicated a positive deflexion in excess of any recorded during the measurements of the photoelectric current The anode, plate, and quadrants were then insulated, and the needle at once began to move towards its zero position on account of the flow of electrons in the valve The times at which the reflected spot of light passed different points of the scale were noted, and a graph of time against deflexion was plotted By drawing tangents to the resulting curve, the rate of change of potential corresponding to any deflexion could be found, and hence the negative current corresponding to any deflexion could be calculated Measures of the currents determined in this way were plotted against the corresponding deflexions, and a calibration curve was thus obtained for the valve under the particular conditions of filament temperature and grid voltage The calibration curves were very nearly but not quite linear, the current increasing rather more rapidly than in direct proportion to the deflexion. When the photoelectric current is flowing in the experimental tube, the electrometer deflexion under any given conditions remains steady because the negative current balances the positive current Hence the photoelectric current corresponding to any value of the observed steady deflexion can be read from the calibration curve The sensitivity of the arrangement could be varied either by altering the heating current of the filament, or the voltage on the grid, or by both these adjustments The valve method of obtaining a steady electrometer deflexion was found to be satisfactory over the whole voltage range investigated in these experiments. The ratio of the photoelectric current to the corresponding value of the electron emission current was plotted against the accelerating voltage, and critical potentials were located from the resulting curves

Experimental Results and Discussion

Many of the voltage regions in which critical points had already been found for the various elements in our earlier work were examined again, using the steady deflexion method of measuring the photoelectric current, and in no case where the region of a former critical point was investigated was the critical stage not revealed by the modified method, although in one or two cases the taking of more curves caused us to modify slightly our decision as to the exact location of the critical point Not only was the existence of each of the critical stages found in our earlier work confirmed for those cases in which the appropriate voltage range was definitely examined, but certain new critical points were revealed in the present investigation The detection of these is doubtless to be attributed to the advantages of the steady deflexion method of experimenting In many cases when a new critical point had been located by using one of the steady deflexion devices, its existence was further tested by examining the appropriate voltage region with the other one, and also by the usual timing method

All the critical points given in our earlier paper were not definitely tested by the steady deflexion method because of the considerable time involved in making adequate tests of the genuineness of each of the newly revealed points Those not definitely examined further were the points for the existence of which the evidence already obtained was most convincing The numbers given in Table I summarise the results of the authors' investigations for the elements in question up to the present time Suggestions of other critical points were sometimes obtained, but where there was any considerable amount of negative evidence as well, or where the evidence was not sufficient to locate the point with certainty, it has not been included in the table

In order to give an indication of the relative amounts of evidence for the existence of each critical point, the values have been graded as shown in the table The classification has been arrived at by considering (*a*) the number of curves obtained which show evidence of the critical point in question, (*b*) the number of curves, if any, covering the appropriate voltage range, in which the point was not indicated, (*c*) the extent of the deviation of different measurements from the mean value given, (*d*) whether the evidence was obtained both by the usual timing method and by the steady deflexion method of measuring the photoelectric current In grade I*a* are included all those values for which there are a large number of curves obtained by both the steady deflexion and the timing methods, showing evidence of the point and very

Table I

Cr 24	Volts	45	*66*	*75*	88	115	141	*149*	155	*165*	*178*	186	208
	ν/R	3 32	4 87	5 54	6 50	8 49	10 41	11 01	11 45	12 19	13 14	13 74	15 37
	Grade	I*b*	I*a*	I*a*	I*b*	I*a*	III	III	I*a*	I*a*	I*a*	I*a*	III
Mn 25	Volts	49	*73*	*88*	*105*	113	117	134	*157*	*179*	*189*		
	ν/R	3 62	5 39	6 50	7 76	8 35	8 64	9 90	11 6	13 22	13 96		
	Grade	I*b*	I*a*	I*a*	I*a*	II	I*a*	I*a*	I*a*	III	III		
Fe 26	Volts	*52*	*78*	*95*	*110*	117	*171*	*186*	219				
	ν/R	3 84	5 76	7 02	8 12	8 04	12 63	13 74	16 17				
	Grade	I*a*	I*a*	I*b*	III	III	I*b*	II	III				
Co 27	Volts	63	83	*99*	*118*	155	*176*	186	*196*	208	215		
	ν/R	4 65	6 13	7 31	8 72	11 45	13 00	13 74	14 47	15 37	15 88		
	Grade	III	I*b*	I*a*	I*a*	II	I*b*	III	I*a*	III	II		
Ni 28	Volts	70	98	*108*	117	161	*184*	*200*					
	ν/R	5 17	7 24	7 98	8 64	11 90	13 59	14 77					
	Grade	II	I*a*	I*a*	III	II	I*b*	I*a*					
Cu 29	Volts	56	67	75	85	*116*	131	153	*196*	*212*			
	ν/R	4 14	4 95	5 54	6 28	8 57	9 68	11 30	14 47	15 66			
	Grade	III	I*a*	II	II	I*a*	III	III	I*a*	III			
Zn 30	Volts	96	*124*	137	145	*204*	*219*						
	ν/R	7 09	9 16	10 12	10 71	15 07	16 17						
	Grade	II	I*a*	III	II	III	III						

few, if any, which fail to show it Grade I*b* consists of those points for which the evidence previously obtained by the timing method was very convincing but for which tests by the steady deflexion method were not made, and also of a few points at the lower voltage ranges where only the steady deflexion method was employed For those points which are in grade II, either the existing evidence, though quite good, is less extensive than for the values in grade I*a* or there are more curves failing to show the point, which detract somewhat from the large number which do In grade III are placed those points for which, of the evidence available, that locating the point is rather less satisfactory than that for points in grade II, and also a few cases for which all the available evidence is positive, but for which fewer curves have been taken and these all by one method

In our earlier papers no correction was applied to the observed critical voltages to allow for the work done on the bombarding electrons when they entered the target, due to crossing the threshold and to the contact potential difference between the hot filament and the target The results recorded in the present paper have been corrected for these effects as well as for the factors the correction for which is determinable by direct experiment in the manner explained in the papers referred to. As shown by Richardson and Chalklin* the correction for work done on entering the target differs by a negligible amount from the voltage equivalent of the latent heat of evaporation of electrons from the hot cathode, and is independent of the target employed. The critical potentials in the table (which are given to the nearest volt) include a correction of 5 volts applied on this account. The values which correspond to those given in our earlier papers are printed in italics. In addition to the equivalent voltages of the critical stages, the corresponding values of ν/R are also given.

The large number of critical stages indicated makes it very difficult to suggest how they are to be accounted for in terms of single or multiple electron displacements within the atom. The possible significance of some of them may, however, be deduced by considering some recent measurements of X-ray emission lines and absorption limits. In our earlier paper it was shown that critical potentials in the voltage region under consideration were concerned with the removal of electrons from the M levels in these atoms. A recent paper by Thoræus† includes some new precision measurements by Åse of the K absorption edge, and by means of these values and the emission line K_{β_1} Thoræus has computed the values of the $[M_{II,III}]$ absorption edge‡ for ten elements from Cr (24) to Br (35). The value of the quantity $M_{III}-N_{II,III}$ can be obtained from the difference of the emission lines K_{β_2} and K_{β_1}, and this was calculated in our earlier paper, in which it was suggested that the lowest critical potential which we found for iron corresponded to this transition.

In Table II the ν/R values of $M_{III}-N_{II,III}$ are given in the second column, the ν/R values of $[M_{II,III}]$ computed by Thoræus in the third column, while the ν/R values of the 45 volts point for chromium, the 49 volts point for manganese, the 52 volts point for iron, the 63 volts point for cobalt, the 70 volts point for nickel and the 75 volts point for copper, are given in the fourth column for comparison.

It may be seen from the table that in each case the experimental value selected for inclusion lies in between those for $M_{III}-N_{II,III}$ and those for $[M_{II,III}]$. For the elements under consideration the ν/R values of the quantities $M_{II,III}-N_{II,III}$ and $M_{II,III}-N_{I}$ do not differ appreciably. The ν/R values of all transitions of a single electron from the level $M_{II,III}$ must lie between the ν/R values of $M_{II,III}-N_{I}$ and $M_{II,III}$. It therefore seems reasonable to suggest

---

[*] O. W. Richardson and F. C. Chalklin, 'Roy. Soc. Proc.,' A, vol. 110, p. 247 (1926).

[†] R. Thoræus, 'Phil. Mag.,' vol. 2, p. 1007 (1926).

[‡] In referring to levels deduced from measurements of absorption limits, the symbols for these are placed in square brackets [ ] for reasons discussed in our earlier paper.

Table II.

Element	ν/R values		
	M_{III}—$N_{II,III}$ calculated from K_{β_2}—K_{β_1}	$[M_{II\,III}]$ Thorsæus's computation	Authors' observed values
Cr 24	2 86	3 61	3 32
Mn 25	3 21	3 70	3 62
Fe 26	3 64	4 17	3 84
Co 27	4 12	4 73	4 65
Ni 28	4 76	5 40	5 17
Cu 29	5 41	5 68	5 54

that the critical potentials selected may be associated with such transitions from this level By means of the frequency relations

$$[L_{III}] = [K]—K_{\alpha_1},$$
$$[M_I] = [L_{III}]—L_l,$$

Thorsæus has calculated also the values of $[M_I]$ using his own recent measurements of the line L_l and the values of [K] due to Åse

The values of M_I—$N_{II,III}$ can also now be calculated using precision measurements of lines only, by means of the relation $M_I—N_{II,III} = K_{\beta_2}—K_{\alpha_1}—L_l$ This we have done and the values are given in the second column of Table III, the third column of which contains Thorsæus's values of $[M_I]$. In the fourth column the ν/R values of the 95 volts point for iron, the 99 volts point for cobalt, the 108 volts point for nickel and the 116 volts point for copper are given for comparison

Table III

Element	ν/R values		
	M_I—$N_{II,III}$ calculated from K_{β_2}—K_{α_1}—L_l.	$[M_I]$ Thorsæus's computation	Authors' observed values
Fe 26	6 65	7 10	7 02
Co 27	7 12	7 70	7 31
Ni 28	7 67	8 27	7 98
Cu 29	8 56	8 84	8 57

The line L_l has not been measured for chromium or for manganese so that the comparison cannot be made for these elements Before the publication of the measurements by Thoræus, the only information to be gained about the $[M_I]$ values was from extrapolation of the values of $M_I—N_I$ which could be calculated from the relation $M_I—N_I = L_{\gamma 5} - L_\eta$ from measurements of these lines extending down to the element Rb (37) From this extrapolation we suggested in our earlier paper that the critical potentials given previously at 106 volts for iron and 113 volts for cobalt, were to be associated with the removal of an electron from the M_I level, but it seems from the comparison in Table III that this was incorrect, and that if any of the measured critical potentials really correspond to encounters with atoms which result in the displacement of an electron from the M_I level it is the lower ones, mentioned above, which do so None of the values found for zinc fit in between the two computed values in either case This can only be interpreted as showing that inelastic collisions resulting in displacements of a single electron from the levels M_I and $M_{II, III}$, respectively, do not reveal themselves when a zinc target is submitted to electron bombardment under the conditions of these experiments

Our results were carefully scrutinised to see if any of the critical points we had obtained could reasonably be ascribed to the metal under test becoming covered by tungsten sputtered from the hot filament during the course of the work The targets were so arranged in the apparatus that when the upper surface became blackened by use, they could be turned over and the other surface exposed to the bombardment When both surfaces of the metals showed signs of blackening, the targets were removed from the apparatus and cleaned There is a good deal of variation in the values of the critical potentials which have been ascribed to tungsten by different experimenters who have investigated this metal, but from a careful consideration of the values most generally obtained we are satisfied that none of these were indicated in our experiments Moreover, a consideration of the number of curves taken when the targets were perfectly clean, indicates that none of the points which have been attributed to the elements under test could be due to sputtered tungsten It may be added that even when tests were made with the targets considerably blackened by sputtered deposit we did not find any consistent appearance of any new critical point

Comparison with the Results of other Experimenters

Of the elements under consideration zinc alone does not appear to have been examined by any other investigator Miss Levi* has recorded the finding of critical points at 60 8 volts for chromium, and at 67 volts for manganese These values when corrected for work done on the electron on entering the target become 65 7 volts and 71 9 volts respectively The values obtained by various experimenters for critical potentials for soft X-ray excitation from the elements iron, cobalt, nickel, and copper, are set out in Tables IV and V for the region covering that in which critical points have been found for these elements in the present research The results obtained by Petry for the critical potentials for secondary electron emission from iron, nickel, and copper, are also included for comparison All the values given in the tables are comparable in that they include a correction to allow for work done on the bombarding electron on entering the target * Thus the present position as regards the location of critical points for these elements, in the voltage region tabulated, can be judged

---

* M. Levi, 'Trans R.S Canada,' vol. 18, p. 159 (1924)

In considering the possible interpretation of the critical potentials for soft X-ray excitation, and for secondary electron emission, in terms of electron displacements within the individual atoms of the elements, it seems that one might expect to find more critical stages for soft X-ray excitation than for secondary emission in the same way that for the ordinary critical potentials of a gas there are more radiation points than ionisation points, because of the possibility of displacements to virtual orbits On the other hand one would not expect to be able to identify the potentials corresponding to displacements from a given initial level to all the successively more remote virtual orbits up to the ionisation stage, by the method employed in the soft X-ray excitation investigations One might conceivably, however, obtain indications of the first few such transitions from any given level In such cases we should expect to find those critical potentials for secondary electron emission which correspond to ionisation of the atoms by removal of electrons from successively more deeply seated levels, all somewhat higher than the critical potentials for soft X-ray excitation corresponding to the displacement of electrons from the same levels

In the eighth columns of Tables IV and V the voltages corresponding to the computed ν/R values of $[M_{II,\,III}]$ and $[M_I]$ from Tables II and III are given for comparison It is interesting to note that in the case of the elements iron, nickel, and copper, the three elements under consideration which have been examined by Petry, one of the critical points for secondary electron emission

[*] In the case of values not corrected for this factor by the investigator, 5 volts has been added when the values were given to the nearest volt by the investigator, and 4 9 volts when the values were given to the nearest tenth of a volt

Table IV —Voltages of Critical Points

Element	Authors' values	Richardson and Chalklin	Rollefson	Thomas	Chu	Petry	Calculated.	Remarks.*
Iron	52	50 6	51 7	51 3				In addition to the critical potentials given in the table, Thomas gives the following in the region under consideration 67 6, 87 0 ?, 91 2 ?, 125 7, 131 8, 140 7, 212 0, Rollefson the following 145 8, 165 0, Kurth the value 55, and Petry the value 70 4
				54 6	57	55 5	56 5 $[M_{II,III}]$	
		63 7		62 0		63 8		
	78	75 6		75 3	73			
		84 8	86 6	82 7	85	85 1		
	95	95 0		94 8		97 6	96 1 $[M_I]$	
			100 3					
	110	107 6		103 5				
	117	115 1	116 1	112 2		119 4		
		137 6	135 3	136 0				
			152 0	150 2				
			158 3	159 8		157 2		
	171			169 4		175 6		
				181 6				
	186	189 7						
				192 0		193 3		
	219	221 5		221 3				
Copper	56					56 9		In addition to the critical potentials given in the table, Compton and Thomas give the following values in the region under consideration 64 5, 82 5, 92 2, 98 8, 104 5, 108 2, 111 0, 127 1, 140 6, 148 4, 164 6, 168 3, 178 6, and Kurth the value 111
	67			66 9	67			
	75			73 5		73 5	76 9 $[M_{II,III}]$	
	85			86 7	84			
				94 5 *	95			
	116			{115 2 117 8			119 7 $[M_I]$	
	131			132 9 ?				
	153			157 1				
				188 8				
	196							
				204 8				
	212							
				216 8				

* See note, Table V

Table V —Voltages of Critical Points

Element	Authors' values.	Richardson and Chalklin.	Thomas	Chu	Levi	Petry	Calculated.	Remarks.*
Cobalt	63		62 8				64 04 $[M_{II\ III}]$	In addition to the critical potentials given in the table, Thomas gives the following in the region under consideration 70 7, 76 7, 81 0, 89 4 ?, 92 5 ?, 104 4, 131 4, 138 3, 143 8, 163 5.
	83		84 3					
	99		97 7		98 1		104 2 $[M_I]$	
			114 3					
	118							
			125 5					
	155		154 0					
	176		173 3					
	186		185 5					
	196		195 6					
	208							
	215		214					
Nickel ..	70		71 9			72 6	73 1 $[M_{II\ III}]$	In addition to the critical potentials given in the table, Thomas gives the following values in the region under consideration 91 2 ?, 94 9 ? 127 0, 133 7, 145 0, 178 2
		80	79 8	80	81 7			
						84 5		
		88 9	87 2					
	98	99 0	98 3					
				103				
	108		106 5		107 7		111 9 (M_I)	
	117		116 6			115 3		
		140 3	139 6					
			156 8					
	161							
			167 3			172		
	184		186 2					
	200		197 7					

* The values in the tables are collected from the following papers —O W Richardson and F. C Chalklin, 'Roy Soc. Proc,' A, vol. 110, p. 247 (1926), G K. Rollefson, 'Phys. Rev,' vol. 23, p. 35 (1924), C H Thomas, 'Phys. Rev,' vol. 26, p 739 (1925), K. T Compton and C H. Thomas, 'Phys. Rev.,' vol. 28, p. 601 (1926), C T Chu, 'Journ Franklin Institute,' p. 615 (1925), R L Petry, 'Phys Rev,' vol. 26, p. 346 (1925), and vol. 28, p. 362 (1926), E H Kurth, 'Phys. Rev,' vol. 18, p. 461 (1921), M Levi, 'Trans R.S Canada,' vol 18, p 159 (1924)

found by him falls near to the calculated value of $[M_{II, III}]$ for each of these elements, with which value, as already shown, there is a satisfactory relationship to one of the critical potentials for soft X-ray excitation

Farnsworth* has carried out a considerable number of investigations into the secondary electron emission from various elements as a function of the voltage accelerating the primary electron stream, and has examined iron and copper, among other elements, in this way For both these elements he found that the ratio of secondary to primary electron current as a function of the primary voltage showed definite sharp maxima and minima in the low voltage region, but that the slight changes in the curves which occurred at higher voltages varied with various uncontrollable conditions He concluded that these had no real significance Farnsworth has also examined the velocity distribution curves of the secondary electrons from these metals, and has concluded from these experiments that the changes in slope in the low voltage region of his ratio curves are not significant of genuine atomic critical potentials, but are due to the surface arrangement of atoms It seems possible that some of the critical potentials for soft X-ray excitation which have been detected for the elements used in the present research, may be accounted for in this way also The M electrons are not very deeply seated within the atoms of these elements, and it is possible that the close proximity of neighbouring atoms modifies the orbits of these electrons, so that their disturbance by the bombarding stream occurs at voltages which are different from those corresponding to the critical stages for single atoms

The Efficiency of Soft X-ray Excitation

The efficiency of different elements in regard to the production of ordinary X-rays has been found to be proportional to the atomic number of the element In the region of soft X-rays, Richardson and Chalklin were led to conclude from their experiments with carbon, tungsten, nickel and iron that the efficiency was roughly proportional to the square root of the atomic number of the element rather than to the atomic number itself More recently, Richardson and Robertson,† from experiments with a greater number of elements in an apparatus specially constructed for the purpose, have concluded that the relation is more correctly expressed by the statement that the efficiency is proportional to the "effective atomic number" of the element, this being a periodic function of the actual atomic number

---

* H E Farnsworth, 'Phys Rev.,' vol 25, p 41 (1925); vol 27, p 413 (1926); vol. 29, p. 908 (1927)

† O. W. Richardson and F. S. Robertson, 'Roy. Soc Proc.,' A, vol 115, p 280 (1927)

The question of the relative efficiencies of the different elements used, as regards soft X-ray excitation, was not a primary object of the present investigation, but the experimental records have been carefully examined to see if any conclusions on this point could be drawn, the ratio, at a given voltage, of the photoelectric current to the thermionic current being taken as a measure of the efficiency of soft X-ray emission. This ratio for any one target was found, however, to vary to some extent with the actual value of the thermionic current, and also to be not always constant for a given value of this current. In a few instances we have records of the examination at low voltages of several elements in rapid succession under the same conditions, and in these cases the efficiency appears to be nearly the same for all the targets.

The authors desire to acknowledge their indebtedness to the Government Grant Committee of the Royal Society for the means of purchasing some of the apparatus and materials used in this research.

The Solubility of Hydrogen in Silver

By E. W. R. Steacie and F. M. G. Johnson, Department of Chemistry, McGill University, Montreal.

(Communicated by Prof. A. S. Eve, F.R.S.—Received September 29, 1927.)

Introduction

In a previous paper* the authors have discussed the solubility and rate of solution of oxygen in silver.

The object of the present communication is to extend these results to the system hydrogen-silver.

A number of papers of a more or less qualitative nature have been published on the solubility of hydrogen in silver. Graham† obtained an absorption of 0.2 volume of hydrogen per volume of silver wire, and 0.9 volume for silver which had been reduced from the oxide. Chabrier‡ found that hydrogen which had been activated by the silent discharge was absorbed by silver. Neumann and Streintz[*] obtained negative results. Baxter[†] found an absorption of 0·5 to 2·8 volumes for silver which had been reduced from the oxide. Richards[‡] investigated the solubility of hydrogen in silver in order to determine if any error were introduced into atomic weight measurements from this source. He found no weighable amount of hydrogen. Le Chatelier[§] stated that silver absorbed hydrogen at temperatures above 600° C. and that the dissolved gas lowered the melting point 30° C. Berthelot[||] found that thin silver foil spattered in the presence of hydrogen at high temperatures, pointing to the formation of an unstable hydride. Heald[¶] found a slight absorption of hydrogen by thin silver films deposited on glass, but Baker[**] found no absorption under identically the same conditions.

---

* 'Roy. Soc. Proc.,' A, vol. 112, p. 542 (1926).

† 'Phil. Mag.,' vol. 32, p. 503 (1866).

‡ 'C. R.,' vol. 75, p. 484 (1872).

The first attempt at a thorough investigation of the subject was made by Sieverts,[††] who obtained evidence of an absorption of 0·13 volume of hydrogen from 600° C. to 800° C. His apparatus, however, was not sensitive enough to detect as small an amount as this with any degree of certainty. There were also several serious sources of error in his determinations. He did not allow sufficient time for the establishment of equilibrium; thus in one experiment he heated the tube containing silver from 20° C. to 800° C. and cooled it again to 300° C. in 158 minutes, taking pressure readings at various temperatures en route. The amount of time taken for the whole experiment was barely sufficient for equilibrium at one temperature only, except at the highest temperatures. Most of the hydrogen which disappeared in the course of his experiments was not recovered on heating *in vacuo*. This was undoubtedly due in part to diffusion through the quartz bulb, for which no correction was made. In addition a certain amount of hydrogen may have been used up in reducing traces of oxides.

The foregoing will serve to show that there is practically nothing in the literature on the solubility of hydrogen in silver in which much confidence may be placed.

---

[*] 'Wied. Ann.,' vol. 46, p. 431 (1892); 'Monats. Chem.,' vol. 12, p. 655 (1891).

[†] 'J. Am. Chem. Soc.,' vol. 22, p. 362 (1899).

[‡] 'Z. Anorg. Chem.,' vol. 47, p. 70 (1905).

[§] 'Z. Phys. Chem.,' vol. 8, p. 186 (1891).

[||] 'Ann. Chim. Phys.,' 7th series, vol. 22, p. 305 (1901).

[¶] 'Phys. Rev.,' vol. 24, p. 269 (1907).

[**] 'Phys. Rev.,' vol. 25, p. 422 (1908).

[††] 'Z. Phys. Chem.,' vol. 60, p. 129 (1907); *ibid.*, vol. 68, p. 115 (1910).

Description of Apparatus

The apparatus employed was essentially the same as that previously used with oxygen and silver It consisted of a manometer connected to a bulb of known volume which contained silver foil A definite volume of gas was admitted to the bulb and the pressure was read The temperature was measured by means of a constant volume nitrogen thermometer Knowing the temperature and the volume of the tube containing the silver, together with the volume of the dead space above the manometer, which was at room temperature, the pressure of the gas could be calculated If the observed pressure were lower than that calculated, then the drop in pressure was a measure of the absorption

Owing to the fact that hydrogen is absorbed by some glasses, and also diffuses through them at an appreciable rate, preliminary trials were made with various types of glass Soft glass obviously could not be used over a sufficiently wide range of temperature Pyrex glass was found to absorb hydrogen at a slow but appreciable rate Jena combustion tubing showed a similar but somewhat smaller absorption Experiments with quartz showed that while the diffusion of hydrogen through quartz was considerable, devitrification of the tube had very little effect on the rate of diffusion It was finally decided to use a quartz tube and to correct for the gas lost by diffusion by means of a blank experiment with an empty tube, made from the same piece of quartz, and having as nearly as possible the same wall thickness and area of surface Incidentally this enabled us to make a series of determinations on the rate of diffusion of hydrogen through quartz at various temperatures and pressures

The apparatus, except for the addition of the blank, was the same as that described in a previous paper (*loc cit*) The blank consisted of a complete duplicate of the absorption apparatus, except, of course, that the bulb was empty instead of being filled with silver

Two samples of silver foil were used, which were 0 40 mm and 0·12 mm thick respectively The silver was prepared by reducing purified silver chloride with sugar and sodium hydroxide, as previously described

Hydrogen was prepared by the electrolysis of dilute sulphuric acid The gas was passed through a tower containing sticks of potassium hydroxide to free it from sulphur trioxide, and then over red-hot platinised asbestos to remove traces of oxygen It was dried by bubbling through concentrated sulphuric acid, and stored in a reservoir over phosphorus pentoxide

Experimental Procedure

Before commencing an experiment, the furnace was heated to about 750° C, and both the absorption apparatus and the blank were evacuated continuously for from 6 to 10 hours Two Langmuir condensation pumps were used in series, and the pressure maintained during the evacuation was about 10^{-5} mm Measured amounts of hydrogen were then admitted to both the absorption apparatus and the blank at the same time The amount of gas let in to the blank was adjusted so as to produce the same pressure as that which existed in the absorption apparatus Readings of pressure and temperature were taken from time to time for a number of hours Owing to the absorption, the pressure fell more rapidly in the absorption apparatus than in the blank The pressures were kept the same, however, except at the moment when a reading was being taken, by lowering the level of the mercury in the manometer of the blank apparatus

At the conclusion of the experiment the gas in the two tubes was pumped out, collected, and measured

Sample Calculation

The complete data for one experiment are given in Table I

Absorption Apparatus —Part of the volume, V_1, is in the furnace at a temperature T_1, the remainder, V_2, is at room temperature, T_2 Hence

$$P\ (V_1/T_1 + V_2/T_2) = K$$

In this case $V_1 = 8\ 680$ c c, $V_2 = 3\ 671$ c c The constant, K, can be calculated from the volume of gas admitted, 0 780 c c, and is 0 2168 Hence P can be calculated for any values of T_1 and T_2 In the third column of Table I is given the observed pressure, and in the fourth column that calculated in this way In column five is given the difference between the observed and calculated pressures (for example, 0 28 cm at 20 minutes) This difference is due partly to the disappearance of gas by diffusion through the quartz, and partly to absorption by the silver The amount of gas which has disappeared, expressed in cubic centimetres at N T P, is equal to

$$0{\cdot}28 \times 273/76\ (V_1/T_1 + V_2/T_2) = 0\ 022 \text{ c c}$$

Blank Apparatus —The amount of gas which has disappeared from the blank by diffusion can be calculated in the same way For the blank $V_1 = 12\ 124$ c c, and $V_2 = 2\ 776$ c c At 20 minutes the observed pressure is lower than that calculated by 0 05 cm, which is equivalent to a loss of 0 004 c c. of gas

Table I

	Absorption Apparatus	Blank
	c c	c c
Volume of gas (N T P)	0 780	0 800
K	0 2168	0 2225

Room temperature.	Temperature	Absorption apparatus				Blank				Time	Ab-sorption, corrected	Ab-sorption, volumes.
		Observed pressure	Calculated pressure	Pressure difference	Cubic centimetres absorbed.	Observed pressure	Calculated pressure	Pressure difference	Cubic centimetres diffused			
° C	° K	cms	cms	cms		cms	cms	cms		mins	c c	
27 8	976	10 10	10 28	0 18	0 014	10 25	10 25	0 00	0 000	0 5	0 014	0 004
27 7	976	10 07	10 28	0 21	0 016	10 24	10 25	0 01	0 001	5	0 015	0 005
27 6	975	10 02	10 27	0 25	0 019	10 21	10 24	0 03	0 002	10	0 017	0 005
27 3	972	9 98	10 26	0 28	0 022	10 18	10 23	0 05	0 004	20	0 018	0 006
27 2	974	9 96	10 27	0 31	0 024	10 16	10 24	0 08	0 006	40	0 018	0 006
27 3	973	9 90	10 26	0 36	0 028	10 12	10 23	0 11	0 009	60	0 019	0 006
27 0	975	9 83	10 27	0 44	0 034	10 08	10 24	0 16	0 013	100	0 021	0 006
26 3	973	9 76	10 26	0 50	0 039	10 01	10 23	0 22	0 017	145	0 022	0 007
25 1	973	9 62	10 26	0 64	0 047	9 93	10 23	0 30	0 023	220	0 024	0 007
26 0	973	9 57	10 26	0 69	0 053	9 88	10 23	0 35	0 028	295	0 025	0 008
26 0	973	9 49	10 26	0 77	0 057	9 82	10 23	0 41	0 033	350	0 024	0 007
26 1	977	9 33	10 29	0 96	0 071	9 68	10 26	0 58	0 046	530	0 025	0 008

Absorption constant for next 12 hours

In the absorption apparatus 0·022 c c of gas has disappeared by absorption and diffusion, 0 004 c c of this is due to diffusion, hence the amount absorbed is 0 018 c c The silver weighed 34·08 grs , assuming the density to be 10 5, this is equivalent to 3 25 c c Hence the absorption expressed in volumes of hydrogen per volume of silver is 0 018/3 25 = 0 006

As may be seen from Table I, about 300 minutes were required to establish equilibrium

At the conclusion of the experiment the absorption apparatus was evacuated and the gas was collected and measured

Volume of gas at start (cubic centimetres) at N T P	= 0 780
Volume pumped out at end	= 0 701
Gas not recovered	= 0 079
Gas lost by diffusion (calculated from blank)	= 0 083
Difference	= 0 004

Hence all the gas absorbed by the silver was recovered, within the limits of experimental error

Experimental Results

Solubility of Hydrogen in Silver - No apparent change in the silver took place, except for the development of a somewhat crystalline appearance on the surface, as previously noticed with oxygen

The solubility of hydrogen in silver at various temperatures and pressures is given in Table II

Table II —Solubility of Hydrogen in Silver

Press	Temperature							
	200° C		300° C		400° C		500° C	
	Absorption volumes	$\sqrt{P}/Q$	Absorption volumes	$\sqrt{P}/Q$	Absorption volumes	$\sqrt{P}/Q$	Absorption volumes	$\sqrt{P}/Q$
cms 5	0	—	trace	—	trace	—	0 003	748
10	0	—	trace	—	0 002	—	0 004	790
20	0	—	trace	—	0 003	1490	0 006	745
40	0	—	trace	—	0 004	1585	0 008	792
80	0	—	trace	—	0 006	1492	0 012	746

Table II—(continued)

Press	Temperature							
	600° C		700° C		800° C		900° C	
	Absorption volumes	$\sqrt{P}/Q$	Absorption volumes	$\sqrt{P}/Q$	Absorption volumes	$\sqrt{P}/Q$	Absorption volumes	$\sqrt{P}/Q$
cms								
5	0 005	450	0 006	371	0 009	249	0 012	187
10	0 007	453	0 009	352	0 013	244	0 016	198
20	0 010	450	0 013	345	0 018	249	0 023	194
40	0 014	453	0 018	352	0 025	253	0 033	191
80	0 019	472	0 025	358	0 036	249	0 046	195

Diffusion of Hydrogen through Quartz —The pressure in the blank apparatus fell rapidly at first, presumably due to the solution of hydrogen in quartz, after this the rate at which the gas disappeared was constant and was apparently due simply to diffusion The results for the rate of diffusion are given in Table III

Table III —Rate of Diffusion of Hydrogen through Quartz.

Average wall thickness = 0 95 mm

Surface area = 47 5 sq cms

D = rate of diffusion in cubic centimetres (at N T P) per 1000 minutes

Press	Temperature							
	200° C		300° C		400° C		500° C	
	D	P/D	D	P/D	D	P/D	D	P/D
cms								
5	trace	—	0 003	1665	0 006	834	0 009	557
10	0 003	3340	0 006	1665	0 010	1000	0 017	588
20	0 006	3340	0 011	1820	0 021	955	0 033	607
40	0 013	3080	0 023	1740	0 041	975	0 066	607
80	0 023	3480	0 049	1640	0 079	1012	0 134	596
Mean		3310		1706		985		599

Table III—(continued)

	Temperature							
	600° C		700° C		800° C		900° C	
	D	P/D	D	P/D	D	P/D	D	P/D
cms								
5	0 014	357	0 037	135	0 071	70 5	0 137	36 5
10	0 029	345	0 071	141	0 145	69 0	0 270	37 0
20	0 058	345	0 160	125	0 294	68 1	0 550	36 4
40	0 114	351	0 325	123	0 581	68 8	1 095	36 5
80	0 230	348	0 615	130	1 160	69 0	2 226	35 9
Mean		349		131		69 1		36 5

The limit of accuracy of a single observation is about 0 002 c c Allowing an equal error for the corresponding blank experiment, the maximum possible error would be about 0 004 c c, or slightly more than 0 001 volume The values given in Table II are therefore good to about 5 per cent at the higher temperatures and pressures The absorptions at temperatures below 500° C are of the same order of magnitude as the experimental error, and are therefore to be taken as merely qualitative indications of a very small absorption at low temperatures

The rates of diffusion at higher temperatures are probably accurate to within 1 per cent as far as the effect of temperature and pressure on the rate is concerned The accuracy of the absolute values depends on the accuracy with which the thickness of the tube was measured This was somewhat uncertain in the region where the capillary was fused to the wide tube The thickness was measured at a number of places, and the averge is given in Table III This is probably uncertain to about 10 per cent

Discussion of Results

(I) *The Diffusion of Hydrogen through Quartz* —From Table III it is evident that the ratio P/D (where P is the pressure and D the rate of diffusion) is constant at constant temperature, *i e*, the rate of diffusion is directly proportional to the pressure This is in agreement with the results of Bodenstein and Kranendieck,* Wüstner,† and Williams and Ferguson ‡ Accordingly, the gas must diffuse through quartz as molecular hydrogen

---

* 'Nernst Festschrift,' p. 100 (1912)

† 'Ann. Physik,' vol. 46, p. 1095 (1915).

‡ 'J. Am. Chem. Soc.,' vol. 46, p. 2160 (1922).

In fig 1 the logarithms of the rates of diffusion are plotted against temperature The points all fall on straight lines within the limits of experimental error The same relationship has been found to hold by Wüstner, and Williams and Ferguson

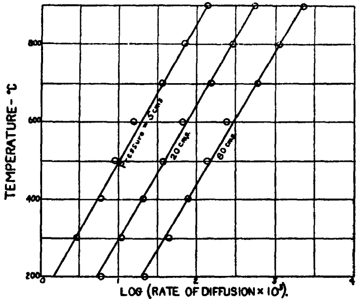

FIG 1.—Rate of Diffusion of Hydrogen through Quartz.

The actual values obtained are similar to those of Williams and Ferguson, but the temperature coefficient is somewhat greater, and hence our results are higher than theirs at high temperatures For the sake of comparison, the values are given in Table IV, in cubic centimetres of gas at 0° C and 76 cms pressure diffusing through 1 sq cm per hour, for a wall thickness of 1 mm.

Table IV —Rate of Diffusion of Hydrogen through Quartz

Temperature	Steacie and Johnson	Williams and Ferguson
°C		
440	1 2	1 6, 1 5, 1 9
610	3 5	5 1, 4 6, 6 2
727	8 1	12 0, 9 5, 8 0
881	25 0	17 7, 15 0

It is possible that the discrepancy is due to differences in the samples of quartz, although the samples used in both investigations were from the same source, the Thermal Syndicate, Ltd. The values, however, are of the same order of magnitude, and the general effect of temperature and pressure is the same.

The fact that the rate of diffusion is proportional to the pressure, and that consequently the diffusing gas is in the molecular state, leads naturally to the conclusion that the process of diffusion is of a more or less mechanical nature, and is probably due merely to the passage of the gas through interstices in the quartz This view receives support from the fact that the only gases which are known to diffuse through quartz are hydrogen and helium, the two lightest gases

If the diffusion occurs in this way, however, it would naturally be expected that hydrogen, being the lighter of the two, would have the higher rate of diffusion. Actually, however, helium diffuses about 22 times as fast as hydrogen.* A possible explanation of this lies in the fact that the helium atom is symmetrical in form, while the hydrogen molecule is presumably unsymmetrical, and, taking an extreme case, a spherical atom would be expected to diffuse much more rapidly than an elongated molecule having about the same total volume It is noteworthy that the temperature coefficients of the rates of diffusion of hydrogen and helium are almost identical, as would be the case if the process were one of capillary effusion The temperature coefficient for helium becomes slightly greater than that for hydrogen at high temperatures, but this is to be expected, as the increased rotational energy of the hydrogen molecule would decrease the rate of diffusion to a certain extent

Jacquerot and Perrot† have obtained a ratio for hydrogen and helium with porcelain which agrees with that calculated for a simple case of capillary diffusion It would appear probable that the capillary spaces through which the gas diffuses are considerably larger in the case of porcelain than with quartz Consequently, the effect of the shape of the molecules would be outweighed by their relative masses It is only when the size of the pores is just slightly larger than the size of the gas molecule that the shape would become the predominating factor in the process of diffusion

If the diffusion of hydrogen through quartz is a simple case of effusion, the temperature coefficient can be calculated from the kinetic theory The chance of a molecule hitting an opening is proportional to its velocity and hence to $\sqrt{T}$ The rate of diffusion depends on both the chance of collision with an opening and on the number of molecules present. At constant pressure the number of molecules will be proportional to $1/T$ Hence the rate of diffusion will be proportional to $1/\sqrt{T}$ The actual increase in the rate of diffusion with increasing temperature is far greater than this There is, however, another factor which might account for this, and that is the increase in the size of the pores due to the thermal expansion of the quartz

---

* Williams and Ferguson, *loc. cit.*

† 'Arch. Sci. Phys. Nat. Genève,' vol. 20, p. 128 (1905).

(II) *The Solubility of Hydrogen in Silver*.—As previously mentioned, the results in the literature are very conflicting The values obtained in this investigation are given in Table II, and are plotted in fig 2 They are much smaller than any of those obtained in previous investigations, with the exception of that of Neumann and Streintz, who obtained negative results The explanation of this lies in the fact that most of the previous workers did not exhaust their apparatus for a sufficiently long time before making observations As we have mentioned in the previous paper, the last traces of dissolved gases are only very slowly removed from metals. The same point has recently been emphasised by Bircumshaw* in connection with the solubility of hydrogen in aluminium and tin Consequently most of the excess absorption reported has been due to loss of hydrogen by combination with residual oxygen In the case of the investigation of Sieverts, this conclusion receives support from the fact that he was unable to recover the majority of the hydrogen which had disappeared. Silver which has been fused in air and rapidly cooled will contain practically the entire amount of oxygen which it dissolved at the melting point, say, from 0 3 to 0 4 volume of gas per volume of silver Hence, if it is not thoroughly pumped out, as much as 0 6 to 0 8 volume of hydrogen may be used up in the formation of water It is not surprising, therefore, that in the earlier investigations absorptions of about 0 6 to 0 8 volume of hydrogen were obtained, and that the gas was not recovered on heating *in vacuo*.

An outstanding example of this kind is the investigation of Bone and Wheeler † In connection with their work on the catalysis of the hydrogen-oxygen reaction by hot surfaces, they measured the absorption of hydrogen by silver, and obtained the very high value of 11 4 volumes at a dull red heat Of this only about 1 3 volumes were given off on heating *in vacuo* The excess hydrogen was undoubtedly used up in combining with dissolved and adsorbed oxygen, the majority of which had not been removed by exhaustion as they merely used a "moist vacuum" There still remains, however, the comparatively large absorption of 1 3 volumes to be accounted for The silver gauze had been repeatedly used as a catalyst and had developed a more or less spongy surface, as evidenced by photomicrographs given in their paper Owing to the large surface, therefore, adsorption would come into play as well as absorption, and their results are not comparable with those obtained with silver in massive form

---

* 'Phil. Mag.,' 7th series, vol. 1, p. 510 (1926).

† 'Phil. Trans.,' A, vol. 206, p. 1 (1906).

The conclusion of Richards that, for atomic weight purposes, silver melted in hydrogen is as good as that melted in a vacuum is verified by our determinations. The maximum absorption found was 0 046 volume of hydrogen per volume of silver, or about 4 1 × 10^{-7} grams of hydrogen per gram of silver

The observation of Le Chatelier, that the melting point of silver is lowered 30° by the presence of dissolved hydrogen, has not been confirmed We were unable to detect any difference in the melting point of silver in hydrogen and in a vacuum This is to be expected, as the amount of gas absorbed is so small that it could not have any appreciable effect on the melting point

Effect of Temperature —In fig 2 the absorption is plotted against temperature at various pressures Below 400° C the absorption is extremely small, above this it increases rapidly with increasing temperature The temperature coefficient is, however, much smaller than that observed with oxygen and silver That the absorption is an exponential function of the temperature is shown by Table V The values of log Absorption/Temperature are practically constant, except for the one value at 400° C, which is too low Owing to the very small absorption at this temperature, however, the value is rather uncertain. If the absorption at 400° C were increased by an amount equal to the probable experimental error, the value of log Abs /T would be brought into agreement with that at higher temperatures

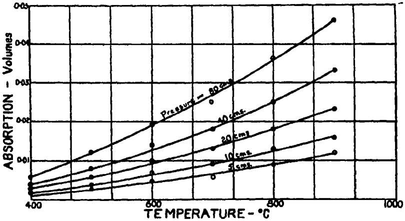

FIG. 2.—Variation of Solubility with Temperature.

Table V.—Variation of Absorption with Temperature.

Pressure = 80 cms

Temperature ° K	673	773	873	973	1073	1173
$\frac{\log_{10}\text{Abs}}{\text{T}} \times 10^4$	1 15	1 40	1 46	1 44	1 45	1 42

Effect of Pressure.—The effect of pressure on absorption is shown in Table II, and the results are plotted in fig 3 As may be seen from Table II, the ratio

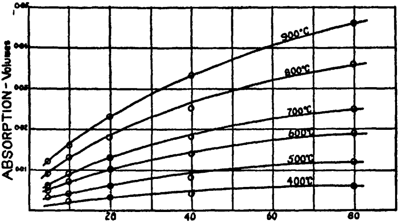

Fig 3.—Variation of Solubility with Pressure.

$\sqrt{\text{P}}/\text{Q}$, where P is the pressure and Q the absorption, is constant at constant temperature It accordingly follows from Henry's Law that the dissolved hydrogen must be dissociated into atoms, or else that it must exist in the form of a dissolved hydride containing one atom of hydrogen to the molecule This seems to be a general relationship which holds for the solubility of all gases in metals, with the exception of hydrogen in palladium,* and in some of the rare earth metals †

Effect of Surface.—Identical values for the absorption were obtained with silver foil of two different thicknesses. Hence the effect of adsorption is negligible compared with that of solution. The high values obtained by Bone and Wheeler make it possible that even at a red heat adsorption will predominate if the surface is sufficiently large On the other hand, Benton and Elgin* obtained no evidence of adsorption at 110° C with silver sponge As adsorption usually decreases with increasing temperature, it seems likely that Bone and Wheeler are in error, especially in view of the inaccuracies in their experiments which we have pointed out above

---

* Hoitsema,' 'Z. Phys. Chem.,' vol. 17, p. 1 (1895); Holt, Edgar, and Firth, *ibid.*, vol. 82, p. 513 (1913), Sieverts, *ibid.*, vol. 88, p. 105 (1914).

† Sieverts, Müller-Goldegg, and Roell, 'Z. Anorg. Chem.,' vol. 131, p. 65 (1923), vol. 146, p. 149 (1925), vol. 150, p. 261 (1926), and vol. 153, p. 289 (1926).

The Rate of Solution —Owing to the small amount of hydrogen absorbed at the lower temperatures, and to the speed with which equilibrium was established at the higher temperatures, the measurement of the rate of solution was not practicable, as comparatively small errors in the amount of gas absorbed would have a very large effect on the rate of solution. The rate of solution is, however, rather slow compared to that of oxygen. At 700° C from 50 to 100 minutes were required for equilibrium, depending on the pressure At 800° C, 10 or 15 minutes were sufficient, and at 900° C saturation was reached practically instantaneously At the lower temperatures at least 24 hours were required

Since the rate of solution is much slower than that of oxygen, the rate of diffusion of hydrogen through silver must be considerably smaller than that found for oxygen †

(III) *The Absorption of Hydrogen compared with that of Oxygen* —It is interesting to compare the results obtained with hydrogen with those for oxygen, since silver is one of the very few metals for which the absorption for more than one gas has been measured with any degree of accuracy

The effect of pressure on absorption is the same for both gases, the absorption being proportional to the square root of the pressure Hence both gases are dissociated in solution Whether the dissociated gas remains in the atomic state, is ionised, or reacts to form a hydride or oxide containing one atom of hydrogen or oxygen to the molecule, cannot be decided by pressure measurements alone The state of the dissolved gas will be discussed further later

The amount of hydrogen absorbed by silver is much less than that of oxygen This is not surprising, since silver has a much greater affinity for oxygen than for hydrogen, as shown by the fact that it forms one definite stable oxide Ag_2O, and perhaps others, such as Ag_2O_3, and Ag_2O_2, while there is no reliable evidence that a hydride of silver has ever been prepared

The effect of temperature on the absorption of hydrogen by silver is entirely different from that with oxygen With oxygen there is a clearly defined minimum at about 400° C, after which the absorption increases rapidly with increasing temperature With hydrogen there is no such minimum. In a previous paper it was concluded from a consideration of the effect of temperature on the solubility and rate of solution of oxygen in silver, that the minimum in the solubility at 400° C must be due either to a change in the manner of combination of the oxygen, or to a change in the silver from one allotropic modification to another The fact that there is no similar behaviour with hydrogen seems to render unlikely the possibility of another form of silver existing above 400° C, and the cause of the peculiar behaviour of oxygen and silver must be the state in which the oxygen exists in solution. It is noteworthy that the minimum in the solubility of oxygen in silver at 400° C corresponds exactly with the minimum in the heat of formation of silver oxide, calculated by Keyes and Hara[*] from their measurements of the dissociation pressure of oxygen in equilibrium with silver oxide

---

* 'J Am. Chem. Soc.,' vol. 48, p. 3027 (1926).

† Johnson and Larose, 'J. Am Chem Soc.,' vol. 46, p. 1377 (1924), and vol. 49, p. 312 (1927).

General Discussion.

The Diffusion of Gases through Metals.—The absorption of gases by metals and the diffusion of gases through metals are phenomena which are dependent upon each other Since a gas molecule or atom must diffuse into the metal before it can be absorbed, it is of interest to discuss the mechanism of diffusion before considering absorption The system oxygen-silver has been fairly thoroughly investigated, and it will be used as a typical system for purposes of discussion.

The fact that the rate of diffusion is proportional to the square root of the pressure points to diffusion taking place by means of atoms and not molecules, As indicated above, the absorbed gas is also in the dissociated condition. Since the diffusion of oxygen through silver is due to atomic and not to molecular oxygen, it is natural to suppose that the rate of diffusion will depend on the concentration of atomic oxygen outside the metal

If we accept Langmuir's theory of the mechanism of adsorption,[†] and assume that every oxygen molecule which strikes a silver surface condenses, while the rate at which oxygen atoms evaporate from the surface depends on the temperature, then adsorption will be a time lag between the rate of condensation and the rate of evaporation The amount of gas adsorbed will decrease as the temperature is raised because the rate of evaporation increases, while the rate of condensation remains almost constant

---

[*] 'J Am. Chem. Soc.,' vol. 44, p. 479 (1922)

[†] 'J. Am. Chem. Soc,' vol. 38, p. 2221 (1916)

Atomic oxygen will be in existence only at the moment when an adsorbed atom evaporates from the surface At low temperatures the life of an adsorbed atom is comparatively long, and consequently there will be very few leaving the surface, and hence very little free (*i e*, unadsorbed) atomic oxygen in contact with the surface At high temperatures, the life of an adsorbed atom on the surface will be extremely short The surface will thus have very little adsorbed gas. Every molecule which strikes the surface will still be condensed, but will almost immediately leave again in the form of atoms Hence as the temperature rises, although the actual amount of adsorption decreases, the concentration of atomic oxygen in the neighbourhood of the surface will increase rapidly Those atoms which leave the surface in an outward direction will recombine at once to form molecular oxygen Some, however, will leave it in an *inward* direction and will diffuse into the metal The number entering the metal, *i e*, the rate of diffusion, will depend on the concentration of free atoms at the surface, and will consequently increase very rapidly with rising temperature The rate of diffusion will thus depend simply on the rate of formation of atomic oxygen at the surface, that is, on the rate of evaporation of adsorbed atoms from the surface The effect of temperature on the rate of evaporation from the surface is given by

$$M = A\sqrt{T} \exp(-\lambda/RT),^*$$

where A is a constant and λ is the internal latent heat of evaporation It has been shown by Johnson and Larose (*loc cit*) that the rate of diffusion of oxygen through silver is expressed by Richardson's equation

$$Q = K\sqrt{T} \exp(-q/RT),$$

where Q is the rate of diffusion and q and K are constants Richardson's equation also holds for the diffusion of hydrogen through platinum,† nickel,‡ and steel § The above two equations are identical in form, and hence it seems fairly well established that the rate of diffusion depends on the rate of evaporation of adsorbed atoms from the surface

The Absorption of Gases by Metals —In the absorption of oxygen by silver, the higher the temperature the farther is the system removed from the dissociation temperature of Ag_2O It might, therefore, be expected that the absorption would decrease with increasing temperature. Actually the reverse occurs once the minimum at 400° C is passed, and in general with almost all gases and metals the absorption increases with increasing temperature It is possible to account for this on much the same basis as Langmuir has used for adsorption

---

* Langmuir, 'J Am. Chem. Soc.,' vol. 35, p. 122 (1913).

† Richardson, 'Phil. Mag,' 6th series, vol. 7, p. 266 (1904); Richardson, Nicol and Parnell, *ibid.*, vol. 8, p 1 (1904)

‡ Deming and Hendricks, 'J. Am. Chem. Soc,' vol. 45, p. 2857 (1923).

§ Ryder, 'Elect. J.,' vol. 17, p. 161 (1920)

As we have shown above, oxygen atoms diffuse through silver at a rate which is proportional to the concentration of atomic oxygen outside the metal If we assume that every oxygen atom which hits a silver atom in the *interior* of the silver reacts to form a compound, and that the oxide thus formed dissociates at a rate which depends on the temperature, the absorption will be a time lag between the rate of combination and the rate of dissociation. With adsorption the rate of condensation increases only slowly with rising temperature, while the rate of evaporation increases rapidly, hence adsorption decreases with increasing temperature With absorption, however, while the rate of dissociation increases rapidly with rise in temperature, the rate of combination depends on the number of atoms diffusing through the metal and this increases very rapidly with increasing temperature Hence in general absorption will increase as the temperature increases

From this point of view, absorption and adsorption are fundamentally similar. Adsorption takes place on the surface and depends on the number of hits registered by gas molecules Absorption takes place inside the metal and depends on the number of hits by diffusing atoms

The amount of gas absorbed is thus a balance between two opposing factors In the case of silver and oxygen, the rate of diffusion is extremely small at low temperatures It is therefore possible that the minimum in the solubility at 400° C is due to the fact that the rise in temperature above the dissociation temperature causes a greatly increased rate of dissociation of silver oxide, which is not outweighed by the increased rate of diffusion until 400° C is reached It is noteworthy that the rate of diffusion only becomes appreciable in the neighbourhood of 400° C It is probable that minima would be discovered with other gases and metals if sufficiently accurate measurements were made at low temperatures

There are very few cases in which the absorption does not increase with increasing temperature Decreases are shown with rising temperature in the absorption of hydrogen by palladium, and by some of the rare earth metals. For these, as mentioned above, the absorption is not proportional to the square root of the pressure, and hence is not due to atomic hydrogen, but either to molecular hydrogen or to compound formation. The only other cases of this sort are the absorption of hydrogen by vanadium and titanium,* and the absorption of nitrogen by iron,† where there seems to be little doubt that definite compounds are formed

It appears probable that the absorption of gases by metals is only a particular case of a much more general phenomenon If a gas and a solid possess a mutual attraction for one another, as manifested by the formation of a definite chemical compound at low temperatures, it is very unlikely that this affinity will cease altogether at some sharply defined dissociation temperature Thus with oxygen and silver, although much above the dissociation temperature of Ag_2O, the gas still possesses sufficient affinity for the silver to dissolve in it at high temperatures It seems probable that if any gas and solid unite to form a definite compound at low temperatures, then the gas will dissolve in the solid to some extent at temperatures above the dissociation temperature of the compound. Thus, for example, we would expect oxygen to dissolve in the lower oxide of a metal at temperatures above that at which the higher oxide dissociates Similarly, water would be expected to dissolve to some extent in solid salts above the dissociation temperature of hydrates A certain amount of evidence exists for the solubility of oxygen in lower oxides Thus Leblanc and Sachse‡ have obtained evidence of the absorption of oxygen by NiO at 350° C, and Leblanc§ detected the absorption of oxygen by litharge

Summary

The solubility of hydrogen in silver has been investigated from 200° to 900° C at pressures from 5 to 80 cms The solubility first becomes appreciable at 400° C The solubility increases exponentially with increasing temperature It is proportional to the square root of the pressure

A mechanism has been suggested for the absorption of gases by metals, and the connection between absorption, adsorption, and diffusion has been discussed

The diffusion of hydrogen through quartz has also been measured from 200° to 900° C It has been shown that the assumption that the diffusion of hydrogen through quartz is of a mechanical nature is in accord with the observed facts

---

* Sieverts, Huber and Kirschfeld, 'Ber d. Chem. Ges.,' vol. 59, p. 2891 (1926).

† Neumann, 'Stahl und Eisen,' vol. 34, p. 252.

‡ 'Z. Elektrochem.,' vol. 32, p. 204 (1926).

§ 'Ann. Chim. Phys.,' vol. 6, p. 480 (1846).

The Specific Heats of Ferromagnetic Substances

By L F Bates, B.Sc, Ph D

(Communicated by A W Porter, F R S —Received October 4, 1927)

Introduction.

It is well known that a close relation must exist between the thermal and the magnetic properties of a ferromagnetic substance On the basis of his theory of the internal molecular field, Weiss[*] predicted a discontinuity in the specific heat of a ferromagnetic substance in the region of its critical point His reasoning may be briefly summarised as follows The mutual potential energy, E, of a number of elementary magnets, each of moment μ and making an angle θ with the applied field H, is given by $E = -\frac{1}{2}\Sigma\,\mu\,H\cos\theta$, so that when we consider a cubic centimetre of the given substance we may write $E = -\frac{1}{2}H\,I$, where I is the intensity of magnetisation Since the substance is ferromagnetic, we must suppose, according to Weiss, the existence of a molecular field of considerable magnitude, equal to N I, where N is a constant which is obtainable from a knowledge of the Curie constant and the critical point of the substance. Thus we may further write $E = -\frac{1}{2}NI^2$, and, since E is negative, we must provide heat in order to demagnetise the substance The amount of heat necessary to demagnetise 1 gm of the substance is therefore $\frac{1}{2J}\,\frac{N}{\rho}\,.\,I^2$, where ρ is the density of the substance Now I varies with the temperature, so that the heat necessary to demagnetise a substance results in an apparent increase of its specific heat by an amount

$$\frac{\partial}{\partial T}\left(\frac{1}{2J}\;\frac{N}{\rho}\;I^2\right) = \frac{1}{2J}\;\frac{N}{\rho}\;\frac{\partial I^2}{\partial T}$$

From curves showing the variation of magnetisation with temperature, Weiss concluded that the specific heat of a ferromagnetic substance should rise to a maximum at the critical temperature, and should then decrease discontinuously, owing to the sudden disappearance of the magnetic term at that temperature Experiments on the specific heats of nickel, iron and magnetite were made by Weiss and Beck[†] by the method of mixtures, which was later refined by Weiss and his collaborators.* They heated the material under investigation to a temperature T° C, and then plunged it into a calorimeter containing water. In this way they found the mean specific heat of the substance between 16° C and T° C A curve was plotted with the value of this mean specific heat against T, and from this curve the value of the true specific heat at any given temperature was deduced. Their results were not completely in accord with theory, the best agreement being obtained in the case of nickel. We need not consider their results in detail, for it has been pointed out that these experiments were not altogether above criticism For example, Sucksmith and Potter† have drawn attention to the effect of the continual quenching of their material, and to the high degree of accuracy, namely, 1 part in 16,000, which would be necessary in these experiments if the specific heat of nickel were to be accurate to 1 per cent in the range of the temperature from 350° C to 354° C Sucksmith and Potter also emphasised the importance of determining magnetic and calorimetric data for the same specimen simultaneously, and they carried out experiments on specimens of nickel and Heusler alloy in which the specific heat was measured at different temperatures by a modification of the Nernst-Eucken method, and the magnetisation was simultaneously measured by a ballistic method Measurements were thus made at temperatures up to 410° C Their results were markedly different from what would be expected on the Weiss theory. They found that change in specific heat was not confined to a limited region around the critical point, but was spread over a considerable range of temperature In fact, they suggested that the critical point indicates a certain stage in a transition which takes place over a range of temperature of some hundred degrees and which is not complete at the critical temperature

---

[*] See Weiss and Foex, "Le Magnétisme," p. 145, or Weiss and Beck, 'J. de Physique,' vol. 7, p. 249 (1908)

[†] 'J de Physique,' vol. 7, p. 249 (1908)

The publication of an article on magnetism by P Debye‡ drew the writer's attention to the existence of a group of compounds of manganese discovered by Hilpert and Dieckmann§, namely, manganese phosphide, manganese arsenide, manganese antimonide, manganese bismuthide These substances have critical temperatures at 26°, 45°, 330° and 380° C respectively It will be observed that two of these substances have critical points which are conveniently low so that the writer considered that they would form excellent materials for an examination of the variation of the specific heat in the neighbourhood of the critical point, and it was decided to make first measurements with manganese arsenide

---

* Dumas, 'Arch. Sci. Phys. Nat.,' vol. 27, pp. 352, 453 (1909), Weiss, Piccard and Carrard, *ibid.*, vol. 42, p. 378 (1916), and vol. 43, pp. 22, 113 and 199 (1917); Piccard and Carrard, *ibid*, p. 451 (1915).

† 'Roy. Soc. Proc.,' A, vol. 112, p. 157 (1926).

‡ 'Handbuch der Radiologie,' VI, p. 668 (1926).

§ 'Jahr. der Rad. und Electrok.,' vol. 10, p. 91 (1913).

Preparation of Material.—The manganese arsenide used in these experiments was made in the manner described by Hilpert and Dieckmann* who state that this method gives rise to a single compound of the form MnAs. An amalgam of mercury and manganese was formed by electrolysis of a concentrated solution of manganese chloride A piece of so-called pure metallic manganese, made by the thermal process was placed inside an extraction thimble and used as anode, and a pool of mercury as cathode The resulting amalgam was quickly washed with distilled water, pressed through a linen cloth and placed in a pyrex distillation flask which was quickly evacuated. The mercury was then driven off by heating, so that finally pure manganese in the form of a black pyrophoric powder remained in the flask The powder was rendered non-pyrophoric by allowing a little coal gas to enter the flask before air was admitted The manganese was then placed in a clear silica tube together with metallic arsenic in the proportions of about 2 7 gm and 5 6 gm respectively, *i e*, with excess arsenic The tube was evacuated, sealed and heated to 750° C for 10 to 12 hours in a muffle furnace On cooling, the excess arsenic condensed at the end of the tube which cooled first, and was removed The compound, which probably contained some free arsenic, appeared as a hard compact mass This was finely powdered and digested in concentrated hydrochloric acid for some days It was then washed in water and alcohol and dried Mr H Terrey, B Sc, Lecturer in Chemistry, kindly analysed a sample of the final product and found that it consisted almost exactly of one part of manganese combined with one part of arsenic This, of course, does not tell us whether we are dealing with a simple compound or with a solid solution of manganese and arsenic

Preliminary Experiments.—In a footnote to their paper,† Hilpert and Dieckmann stated that these compounds of manganese showed a temperature hysteresis The temperature hysteresis was examined in a series of preliminary experiments in which the magnetic induction of a specimen, placed in a constant field, was measured at various temperatures The way in which the magnetic induction varies is shown in fig 1 The substance ceases to be ferromagnetic in the neighbourhood of 45° C If, however, the temperature is reduced after the specimen has been rendered paramagnetic, it is seen that the induction changes but slightly until a temperature between 33·5° and 34° is reached, when the substance rapidly regains its ferromagnetic properties If the temperature is raised to some point below 45° C , *e g* , to 42° C , then on reducing

---

* 'Ber d. Chem. Ges.,' vol. 44 (2), p. 2380 (1911)

† 'Ber. d. Chem. Ges.,' vol. 44, p. 1615 (1911).

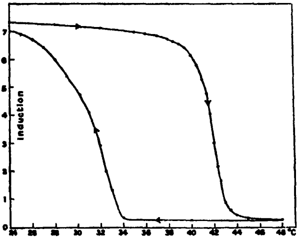

FIG 1.

the temperature, the induction changes very little until in the neighbourhood of 34° C when the substance again begins to regain its initial ferromagnetic properties very rapidly

Apparatus for Thermal Measurements —For an accurate examination of its thermal properties it was obvious that heat had to be supplied to the substance very slowly, and the following modification of the Nernst-Eucken method was used The substance was placed in a copper calorimeter A, fig 2, made of tubing 5 cm long, 1·85 cm internal diameter and 0 97 mm thick It was closed at one end by a thin copper plate and at the other end by a copper cover which fitted over the tubing and which could be soldered in position. Inside A was placed a light frame of copper wire, of the shape shown in E, fig 2, which served as a former on which were wound a heating wire and a thin wire for the measurement of temperature The heating wire was of No 42 double silk covered manganin, and was wound round the straight wire of the frame and passed between the portions *xx* of the arms of the frame The temperature filament was of No 44 double silk covered platinum wire and was wound on the portions *yy* of the frame The wires were held in position by touches of shellac In this way the heating and temperature filaments were distributed as efficiently as possible throughout the interior of the containing vessel. As the rate of supply of heat was always low, there was little doubt that the substance changed uniformly throughout its mass and that the temperature as recorded by the platinum wire was trustworthy. The heating and temperature filaments were provided with leads of No 32 double silk covered copper wire. In filling the calorimeter A, a layer of the substance was first placed at the bottom of the vessel, the copper wire frame was placed inside, and the remainder of the substance added slowly In all, 42 15 gm. were used. During the filling the vessel was repeatedly tapped by a large bar magnet and the substance was thus closely packed. When the vessel was full, the copper leads were threaded through two small holes in the copper cover, and the latter was soldered in position. The small holes through which the leads emerged were filled with molten shellac, so that the calorimeter should have been airtight, although this provision could not be tested and was probably not necessary Three small copper hooks soldered to the outside of the calorimeter permitted it to be suspended by threads from the cover of the thin walled brass vessel B. The cover of B could be cemented in position with hard wax. It was provided with a brass tube inside which was cemented a glass tube C which permitted the outer vessel to be connected to a two-stage Hyvac pump. The thin copper leads to the calorimeter passed along the glass tube and emerged at D where a glass stopper was cemented in position. Just outside D the thin leads to the temperature filament were soldered to heavy copper leads and connected to a very excellent form of Callendar and Griffith's bridge, for the loan of which I am greatly indebted to Mr N. Eumorfopoulos A pair of compensating leads were provided, and for convenience the thin ends of these leads were not placed inside the brass vessel, but were placed in contact with the brass tube, and the slight departure from the usual practice in this case could not have introduced any perceptible error The brass vessel was mounted in a tank of water which was kept in violent agitation. The heating filament was connected in series with a battery, rheostat and milliammeter

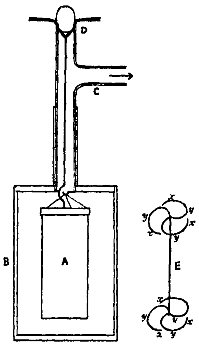

FIG. 2.

Procedure.—The temperature filament was first calibrated by noting its resistance when the brass vessel contained air, and the water was kept at constant temperatures for long periods by means of an electrical heater. In each experiment the brass vessel was thoroughly evacuated and surrounded with melting ice until the resistance of the filament corresponded to a temperature of 2° to 3° C. This was done in order to ensure that the initial state of the substance was the same in each experiment, and to be able to heat the substance in a perfectly definite manner. A definite value of the heating current was chosen, and since the resistance was of manganin, it was only necessary to maintain this current constant in order to ensure a constant rate of supply of heat. The heating current was switched on and the times at which the temperature filament attained consecutive values differing by 0·1 ohm (or 0·05 or 0·025 ohm when necessary) were noted. An increase of resistance of 0·1 ohm corresponded to an increase of temperature of about 1° C. Hence the amounts of heat necessary to cause definite rises of temperature of the calorimeter system were known. The specific heat of the copper of which the calorimeter was made was found by the method of mixtures, so that the thermal capacity of the copper case and wires was known. To ensure that the radiation correction was negligible, the temperature of the water surrounding the brass vessel was raised at the same rate as the temperature of the calorimeter. Thus, at the moment when the filament acquired a temperature corresponding to a resistance of R ohms, the temperature of the bath was raised to correspond to a resistance of R + 0·05 ohm, and this temperature was maintained until a resistance of R + 0·1 ohm was attained by the filament, whereupon the temperature of the water was again adjusted.

Results.—The specific heat of the compound could thus be found over a series of small temperature intervals. To be free from accidental errors the mean values of the times were taken for 10 such experiments, in which heat was supplied at the constant rate of 0·03243 calorie per second. To give an idea of the accuracy attained, it may be mentioned that the times for which heat was supplied in the separate experiments to raise the temperature of the system from 25·5° to 53·8° were respectively 8917, 9124, 8924, 8819, 8958, 8864, 9044, 8815, 8656 and 8998 seconds. The mean value was 8912 seconds, corresponding to the supply of 289·0 calories. All these experiments gave graphs which showed the same variation of specific heat with temperature. The values for the complete set of experiments are shown in fig. 3, where it will be seen that the specific heat rises slowly from a value of 0·122 at 28° C. to a value of 0·14 at 36° C., then rises with increasing rapidity to a value of about 0·8 in the neighbourhood of 42° C., then falls rapidly to a value of 0·13 at 45° C., and thence to a slightly defined minimum value of 0 10 at 46·5° C, after which it slowly rises with increase in temperature This minimum was presumably due to the sudden change in the rate at which the temperature of the calorimeter system rose

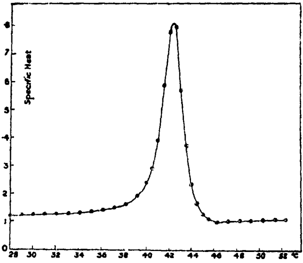

Fig 3

Now, the above results were obtained with a value of the heating current such that the temperature of the calorimeter and its contents rose from 25° C. to 52 8° C in approximately 2¼ hours The chief errors likely to arise were those due to non-uniform heating of the specimen and to radiation It was possible to ascertain the order of magnitude of these errors by repeating the experiments with different rates of supply of heat Accordingly, six experiments were made with a heating current of 54 0 milliamperes, corresponding to a rate of supply of heat of 0 04929 calorie per second, so that the time taken to raise the temperature of the system through the above range was now 1 hour 40 minutes instead of 2¼ hours The times for which heat was supplied to produce this rise in temperature in the several experiments were 5892, 5863, 5872, 5956, 5984 and 6009 seconds respectively. The mean value is 5929 seconds, which corresponds to the supply of 292 3 calories, which is in satisfactory agreement with the value 289·0 obtained in the first experiments. The specific heat curve in this case was very similar to fig 3, but the initial specific heat was somewhat larger than in fig 3 Thus at 28° C. the specific heat in the first case was 0·122, whilst in the second case it was 0 129, and the rate of increase of specific heat between 28° and 36° was greater in the second case. The maximum value of the specific heat was somewhat less, and the minimum was more pronounced, but the position of the maximum was the same in both curves, and the values of the specific heat above 46° C were practically identical in both. These features show that the radiation effects in these two sets of experiments must have been very small. The results indicated that in the second case heat was being supplied to the system rather too quickly, so that in the region below the critical point the material did not change its state as uniformly as in Curve I.

Some experiments, which were tedious, were also made with extremely slow rates of supply of heat to the system. For example, in one experiment the heating current was 32·74 milliamperes, and the time required to raise the temperature of the system from 25° to 53·8° was nearly 5 hours. Naturally, a high order of accuracy would not be expected with such a slow rate of heating. The results of this experiment are given in fig. 4.

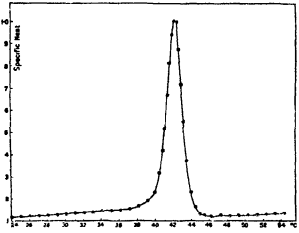

FIG. 4.

It will be seen that the value of the specific heat from 28° C. to 38° C. is in good agreement with the value obtained in the first case, but the rise of specific heat between 38° and 42° is much more rapid, and the final value of the specific heat above 46° C. is higher. The minimum is, however, much less pronounced. The position of the maximum value of the specific heat, found by producing the ascending and descending arms until they meet, was the same in all experiments within the limits of experimental error. In the three cases the maximum occurred at 42·16, 42·21 and 42·26° C. respectively, the mean value of which may be taken as 42·2° C.

The real difference between these three cases lies in the shape of the peak. There is no doubt that the slower the heat is supplied to the system, the more pronounced does the peak become, although it is difficult to believe that the peak could become much more pronounced than in fig 4, if the rate of supply of heat were still further decreased.

A few experiments were made in which the calorimeter and its contents were first heated to about 55° C and were then allowed to cool, whilst the temperature of the surroundings was constantly adjusted to be 15° C less than that of the temperature filament The results showed that the specific heat of the compound rose slowly with fall in temperature between 45° and 35°, probably due to non-uniform cooling of the material A rapid increase in specific heat then occurred, and a maximum was reached This maximum was poorly defined because of the limitations of the cooling method. Between 28° and 25° the specific heat fell rapidly, and finally approached a value which was nearly constant Experiments were also made in which the calorimeter system was heated to 54° C and then allowed to cool slowly to 35°, when it was again heated The specific heat over the range 35° to 54° was found to be nearly constant under these conditions

Magnetic Properties —We now have to examine the magnetic properties of the substance more fully It was felt that the best mode of attack was to examine the magnetic induction of the substance when placed in a strong magnetic field Some of the substance was therefore packed tightly in a copper tube 6 cm long and 0 55 cm in internal diameter Of this tube a solenoid of No 32 double silk covered copper wire was wound The tube was mounted at right angles to a brass rod and placed between the poles of an electromagnet. An exactly similar solenoid, wound on an empty tube, was mounted side by side with the first The tubes were placed in a bath of paraffin oil which was heated electrically and vigorously stirred The solenoids were connected in series with a ballistic galvanometer of long period The tubes were placed with their axes parallel to the lines of force of the electromagnet. The deflection of the galvanometer was observed, either when the tubes were suddenly turned through 180° or when a known current was switched on and off in the magnet coils The solenoids were connected in opposition, so that the galvanometer deflection was a measure of the magnetic induction in the substance Special experiments were made to prove that the introduction of this ferromagnetic substance did not appreciably upset the applied magnetic field

The tubes were first cooled and determinations of the ballistic deflections were made as the temperature was increased The apparatus was maintained at a given temperature until the ballistic deflection was constant, and owing to the nature of the substance the determinations in the region of 41° and 42° were made very slowly It was felt that by using a copper tube of smaller bore to contain the compound, any errors due to the movement of the powder and to inequalities of temperature would be lessened Further experiments were therefore made in which the substance was enclosed in a tube of 0 25 cm internal diameter, but there was no apparent difference in the nature of results obtained. The magnetic field used in these experiments was 1960 gauss

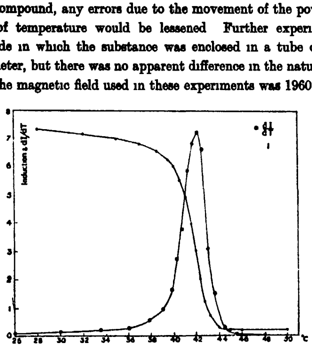

FIG. 5.

In fig 5 are plotted a typical set of experimental observations, together with a curve showing the rate of change of the magnetic induction, I, with temperature found from these observations, in arbitrary units The latter curve exhibits a maximum at 42 2° C, and it is clear that there is a marked resemblance between the curves showing the variation of the specific heat with temperature and that showing the variation of magnetic induction with temperature If, however, we plot dI^2/dT against temperature, we obtain a somewhat similar curve, but dI^2/dT reaches a maximum at 41 5° C and becomes extremely small at 44° C

Discussion of Results—There are several interesting features about the curves which are given in this paper In the first place the heat curves very definitely suggest that the thermal changes which occur when this ferromagnetic compound is heated are associated with molecular changes For it is clear that whenever the magnetic properties are changing, there is also a corresponding thermal change, and when the substance has become paramagnetic there is very little further change in its specific heat Again, the rate at which the substance absorbs heat is a maximum, within the limits of experimental error, at the temperature at which the magnetic changes occur at the maximum rate, although in view of the method which had to be used in investigating the magnetic induction, perhaps this coincidence should not be stressed too far The problem, then, becomes analogous to the question of the specific heat of dissociating gases We may obtain an approximate value of the energy necessary to produce these molecular changes In the case represented in fig 3, the heat supplied to 1 gm of the compound to raise its temperature from 25 5° to 53·82° was 5 19 calories The mean specific heat from 25·5° to 42 2°, found by producing the initial portion of the curve, was 0 130, and the mean value from 42 2 to 53 82, found by producing the end portion of the curve, was 0 106 Therefore the actual quantity of heat required to change the state of the compound was approximately 1 79 calories per gram

The curves given in this paper have many features in common with those obtained by Sucksmith and Potter* for nickel and Heusler alloy, where it is clear that similar heat phenomena must occur, but must extend over a considerable range of temperature Their curves of the variation of specific heat with temperature showed in several cases, however, that pronounced heat changes occurred even at temperatures considerably above that at which the substance became paramagnetic This was not so evident in the case of nickel, but in the case of Heusler alloy the heat phenomena appeared to exist at temperature, 15° to 20° above the critical point. In the experiments described here the relation between the thermal and magnetic properties is more intimate than in the cases investigated by Sucksmith and Potter The two sets of experiments may satisfactorily be explained if we assume that in ferromagnetic materials the atoms are associated in groups, and that the rearrangement of the electron systems in these groups is responsible for the loss of ferromagnetism Stoner† has used this conception, in order to account for the fact that the values of the magnetic moment per atom of ferromagnetic substances deduced from low temperature saturation intensity measurements differ considerably from the values obtained from the variation in susceptibility above the critical points and that, moreover, these values bear no apparent relation to the values of the moments of the ions of ferromagnetic metals found by measurements on salts and solutions Stoner showed that the experimental differences could be accounted for on the basis of the quantum theory, by assuming that the atoms in crystals are associated in groups and that the magnetic properties are due to ions within these groups which have the same moments as ions in solid salts and in paramagnetic solutions Thus in the case of nickel, the group is supposed to consist of five atoms consisting of one Ni^{++}, one Ni^{+} and three neutral nickel ions Presumably such a group would be held together by some kind of electron sharing, and there appears a priori no reason why the electron orbits should not be rearranged as the temperature of the group rises This rearrangement would be associated with definite thermal changes, and the change from the ferromagnetic to the paramagnetic state might be due to a particular stage in the rearrangement process, but there appears no reason why the rearrangement process and its associated thermal effects should not continue above the critical temperature The experiments described in this paper presumably deal with the comparatively simple case where the rearrangement process ends at the same temperature as the change in magnetic properties, and it is hoped that future experiments will enable us to say more about the nature of this rearrangement

---

* *Loc. cit.*

† 'Proc. Leeds Phil. Soc.,' Jan., 1926.

Summary

The thermal and magnetic behaviour of a simple ferromagnetic compound of manganese and arsenic has been studied This compound has a critical point at 45° C It is found that heat is very rapidly absorbed when the substance changes from the ferromagnetic to the paramagnetic state The thermal and magnetic phenomena are intimately connected, and the conclusion is reached that with the magnetic change there is associated a heat of transformation. It is considered that magnetic phenomena in the region of the critical point are evidence of a transformation which in this case appears to be complete at that temperature, but which, in general, may reach only a particular stage at the critical point

Further experiments on this and other compounds of manganese are in progress

It gives me much pleasure to acknowledge the kind interest with which Prof A W Porter, F R S, has followed the course of this investigation

The Tides in Oceans on a Rotating Globe—Part I.

By G R Goldsbrough, D Sc, Armstrong College, Newcastle-on-Tyne

(Communicated by Prof T H Havelock, F R S —Received October 11, 1927)

§ 1 *Introductory*

The problem of determining the free and forced tidal oscillations on a rotating globe, first enunciated by Laplace and solved by him in special cases, was completed by Hough [*] Valuable as these results are, they deal with oceans wholly covering the globe, and so give little information regarding the tides on the earth which are materially affected by continental barriers. A further stage would be effected by the introduction of simple boundaries

When the barriers are along complete circles of latitude, the problem is relatively simple and solutions have been worked out [†] General processes for the attack on the problem where the boundaries take any form have been described by Poincaré[‡] and Proudman[§], and an approximate method for determining the free periods of oscillation of an ocean bounded by two meridians when the rate of rotation is small has been given by Rayleigh [||] Analogous problems of the tides in flat rotating seas have been solved in certain cases [¶] The case of the tides on a non-rotating globe bounded by two meridians has also received attention [**] This list covers most of the results so far achieved

The problem of the tides as affected by land boundaries is an important one There are two schools of opinion as to the origin of the Atlantic tides One, following Whewell, supposes that these tides are derived from the Southern Ocean, where alone, owing to its complete circumscription of the globe, have the tidal forces full play [††] The other, following Ferrel[‡‡] and Harris,[§§] suggests that the Atlantic tides are due to partial synchronism of the natural free oscillations of the ocean with the tide-producing forces Ferrel went so far as to state that if a dam were erected across the ocean from the Cape of Good Hope to the American coast the Atlantic tides would be unaffected *

---

[*] 'Phil Trans,' A, vol 189, p 201 (1897), vol 191, p 139 (1898)

[†] 'Proc. Lond Math Soc,' vol 14, Part 1, p 32 (1915)

[‡] 'Théorie des Marées,' pp 233, 297

[§] 'Proc Lond Math Soc,' Ser 2, vol 18 (1917)

[||] 'Roy Soc Proc,' A, vol 82, p 448 (1909)

[¶] Proudman, 'M N R A S Geophysical Suppl,' vol 1, p 360, Taylor, 'Proc Lond. Math Soc,' Ser 2, vol. 20, Part 2, p. 148

[**] Proudman and Doodson, 'M.N.R A.S Geophysical Suppl,' vol 1, p 468

[††] Warburg, 'Tides and Tidal Streams,' p 11

[‡‡] Ferrel, 'Tidal Researches'

[§§] Harris, 'Manual of Tides,' vol. 4A

As Rayleigh stated, a knowledge of the tidal motions in an ocean bounded by two meridians of longitude would throw considerable light upon the question.

In the present paper an examination is first made of the tides in an ocean comparable with the Southern Ocean in order to find how far such an ocean is capable of producing tides in an adjacent ocean

Next, taking an ocean whose depth varies as the square of the cosine of the latitude and which is bounded from pole to pole by two meridians of longitude, a solution is given for the semi-diurnal tide The form of solution used does not permit of the determination of the free periods of oscillation of such an ocean, but it does give what is almost as useful, the critical depths at which resonance takes place By taking the bounding meridians at 60° apart, results roughly applicable to the Atlantic Ocean are obtained.

The use of a varying depth of the ocean is to secure relative simplicity in the results But the method is readily capable of generalisation in many directions In particular it can be applied to the determination of the diurnal, lunar semi-diurnal and solar semi-diurnal tides in an ocean of uniform depth, and thus throw some light on the vagaries of the " age " of the tide These solutions will be communicated in a later paper

One great difficulty is the inaccessibility of tables of " associated " Legendre functions † Instead, the tables of the analogous Gaussian functions $G_n^m(\mu)$ given by Adams in his collected scientific works have been used

I am indebted to the Research Committee of Armstrong College for the opportunity, through the award of a Senior Research Fellowship, of conducting this and other researches

I also wish to acknowledge the help derived from discussions with Dr T H Havelock, F R S, on various matters arising in the paper

Notation used

θ, ϕ = co-latitude and longitude on the surface of a sphere.

u, v = velocities in latitude, longitude

a = radius of the sphere.

ω = angular velocity of rotation of the sphere

t = time variable

---

* *Loc. cit.*, p. 239

† Tallqvist, ' Acta Soc. Fennicæ, vol 33 (1908)

g = acceleration of gravity
ζ = height of tide above the mean level
$\bar{\zeta}$ = equilibrium height of tide
h = depth of the ocean.
μ = $\cos\theta$
ν = $\sin\theta$
h_0 = $h(1-\mu^2)^{-1}$
$2\pi/\sigma$ = period of oscillation of wave
α = value of longitude at one boundary
κ, r = integers
s = $\kappa\pi/\alpha$
f = $\sigma/2\omega$
m = $\omega^2 a/g$
β = $4\omega^2 a^2/gh_0$
k_n^s = coefficients of $P_n^s(\mu)$ in general form of tide-producing potential.
H = coefficient of $P_2^2(\mu)$ in tide-producing potential
A, B, E, F, M, N = coefficients to be determined
$b_n^s(p)$ = coefficients of $P_n^s(\mu)$ in the expansion of $P_p^s(\mu)$
a_r^κ, a'^κ_r = coefficients in expansions of $\sin\kappa\pi\phi/\alpha$, $\cos\kappa\pi\phi/\alpha$

§ 2 *The Equations*

In the notation of the previous section, the equations for the small oscillations of a liquid of depth h on a rotating sphere of radius a, are[*]

$$\left.\begin{aligned}
\frac{\partial u}{\partial t}-2\omega v\cos\theta &= -\frac{g}{a}\frac{\partial}{\partial\theta}(\zeta-\bar{\zeta})\\
\frac{\partial v}{\partial t}+2\omega u\cos\theta &= -\frac{g}{a\sin\theta}\frac{\partial}{\partial\phi}(\zeta-\bar{\zeta})\\
\frac{\partial\zeta}{\partial t} &= -\frac{1}{a\sin\theta}\left\{\frac{\partial}{\partial\theta}(hu\sin\theta)+\frac{\partial}{\partial\phi}(hv)\right\}
\end{aligned}\right\}\qquad(1)$$

Certain approximations are involved in these equations and the validity of the use of them has been examined[†]

In an area bounded by two meridians of longitude $\phi=0$, $\phi=\alpha$, the tide height may be expressed as a series of circular functions of multiples of $\pi\phi/\alpha$. We therefore require solutions of equations (1) containing the factors $e^{i(\pm\kappa\pi\phi/\alpha+\sigma t)}$, where κ is an integer and $2\pi/\sigma$ the period of vibration

---

[*] See Lamb, 'Hydrodynamics,' p 320 (1916)

[†] Lamb, p 318, Hough, 'Phil. Trans.,' A, vol 189, p 206 (1897)

Now let $s = \kappa\pi/\alpha$, then on taking out the factor $e^{\iota(s\phi+\sigma t)}$, solving equations (1) for u, v, and reducing, we find

$$\left.\begin{aligned} u \quad 4m\,(f^2 - u^2)/\iota\sigma &= \sqrt{(1-u^2)}\,\frac{d\zeta'}{d\mu} - \frac{s\mu\zeta'}{f\sqrt{(1-\mu^2)}} \\ v \quad 4m\,(f^2 - \mu^2)/\sigma &= \frac{\mu}{f}\sqrt{(1-\mu^2)}\,\frac{d\zeta'}{d\mu} - \frac{s\zeta'}{\sqrt{(1-\mu^2)}} \\ -\iota\sigma a\zeta &= \frac{d}{d\mu}\{hu\sqrt{(1-\mu^2)}\} + \frac{h \quad \iota \quad sv}{\sqrt{(1-\mu^2)}} \end{aligned}\right\}. \qquad (2)$$

In the last equation we have assumed that h is not a function of ϕ though it may contain μ This is in accordance with the previous intention

In equations (2), put $f = 1$ rigorously The results will then refer approximately to either of the principal semi-diurnal constituents of the tides We shall further take a law of depth $h = h_0\,(1 - \mu^2)$ That is, the depth of the ocean as measured below the undisturbed level follows a simple quadratic law in μ. In this case we have from (2)

$$v \quad 4m\,(1 - \mu^2)/\sigma = \mu\sqrt{(1-\mu^2)}\,\frac{d\zeta'}{d\mu} - \frac{s\zeta'}{1-\mu^2}, \qquad (3\text{ i})$$

$$\frac{d}{d\mu}(1-\mu^2)\frac{d\zeta'}{d\mu} - \frac{s^2\zeta'}{1-\mu^2} + \zeta'(\beta - s) = -\beta\bar{\zeta} \qquad (3\text{ ii})$$

When $\bar{\zeta}$ is zero, equation (3 ii) has the simple solution $\zeta' = \mathrm{P}_n^s(\mu)$, where $n(n+1) = \beta - s$ But this solution is only valid at the poles when $n - s$ is an integer—a condition only fulfilled in very special cases On the other hand, if $\bar{\zeta}$ exists in the form of an "associated" Legendre function $k_n^s\mathrm{P}_n^s(\mu)$,* n now being subject to the only restriction that $n - s$ is integral, so that the function is valid from pole to pole, then†

$$\left.\begin{aligned} \zeta' &= \frac{\beta k_n^s \mathrm{P}_n^s(\mu)}{n(n+1) + s - \beta} \\ \zeta &= \frac{\{n(n+1) + s\}\,k_n^s\mathrm{P}_n^s(\mu)}{n(n+1) + s - \beta} \end{aligned}\right\} \qquad (4)$$

The simplicity of these results makes them of great service in the complicated work that follows

We require also the solution of equations (1) suitable for an ocean surrounding the pole, but not extending as far as the equator The solutions for this case have been fully developed * In the case of uniform depth the equations (1), transformed to the independent variable $\nu = \sqrt{(1-\mu^2)}$, are, on removing the factor $e^{i(s\phi+\sigma t)}$,

---

* We take $\mathrm{P}_n^s(\mu) = (1-\mu^2)^{\frac{1}{2}s}\,\mathrm{F}(\tfrac{1}{2}s - \tfrac{1}{2}n, \tfrac{1}{2} + \tfrac{1}{2}s + \tfrac{1}{2}n, \tfrac{1}{2}, \mu^2)$

† See Hough, 'Phil. Trans,' A, vol 191, p. 174 (1899)

$$\left.\begin{aligned} u \quad 4m\nu^2/\iota\sigma &= -\sqrt{(1-\nu^2)}\frac{d\zeta'}{d\nu} - s\sqrt{(1-\nu^2)}\,\zeta'/\nu \\ v \quad 4m\nu^2/\sigma &= -(1-\nu^2)\frac{d\zeta'}{d\nu} - s\zeta'/\nu \\ \nu^2(1-\nu^2)\frac{d^2\zeta'}{d\nu^2} - \nu\frac{d\zeta'}{d\nu} &+ \zeta'(s^2\nu^2 - 2s - s^2) + \beta\nu^4\zeta = 0 \end{aligned}\right\} \quad (5)$$

It should be noted that if, as we have stated, the ocean completely surrounds the pole, it is essential that s should be an integer

The purpose is to construct a solution relevant to an ocean bounded by a parallel of latitude $\nu = \nu_1$ It is then useful to take a power series in ν/ν_1, as this fraction ranges from 0 to 1

For such a series the indicial equation has a positive root $s+2$ Hence we assume

$$\zeta' = \sum_n A_n\,(\nu/\nu_1)^{n+s+2}$$

Further, as the semi-diurnal tide we are to consider arises from a potential $\bar{\zeta} = H\nu^2$, and $s = 2$, we have the results

$$\left.\begin{aligned} &16A_2 - 10A_0\nu_1^2 = -\beta H\nu_1^6, \\ &\text{and for } n > 0, \\ &A_{n+2}\{(n+4)(n+6) - 8\} + A_n\{2 - (n+4)(n+3)\}\nu_1^2 \\ &\qquad + \beta A_{n-2}\nu_1^4 = 0 \end{aligned}\right\}. \quad (6)$$

A_0 is arbitrary at present, but is determined later by the condition to be fulfilled at the boundary

§ 3 *A Special Case*

Although we shall not make any practical use of it in the sequel, it is of some interest to work out the solution of (3) for the case of an ocean bounded by two meridians which also includes one pole but has a boundary in the opposite hemisphere so that it does not include the second pole In such a case the solution can be found when $\bar{\zeta} = 0$ Putting $\beta' = \beta \pm s$ in (3), we have to solve with the given condition the equation

$$\frac{d}{d\mu}(1-\mu^2)\frac{d\zeta}{d\mu} - \frac{s^2\zeta}{1-\mu^2} + \beta'\zeta = 0$$

---

* 'Proc Lond. Math. Soc,' Ser 2, vol. 14, part 1, p. 32.

If $\beta' = n(n+1)$, where n is real but not necessarily integral, we have*

$$\zeta = \mathrm{A}\,(1-\mu^2)^{-s/2}\mathrm{F}\,(-\tfrac{1}{2}s-\tfrac{1}{2}n,\ \tfrac{1}{2}-\tfrac{1}{2}s+\tfrac{1}{2}n,\ \tfrac{1}{2},\ \mu^2)$$
$$+\ \mathrm{B}\,(1-\mu^2)^{-s/2}\mu\mathrm{F}\,(\tfrac{1}{2}-\tfrac{1}{2}s-\tfrac{1}{2}n,\ 1-\tfrac{1}{2}s+\tfrac{1}{2}n,\ 3/2,\ \mu^2),$$

in which A and B are arbitrary constants, and F is the hypergeometric function.

Using the ordinary notation for the hypergeometric function $\mathrm{F}(a, b, c, z)$, we see that in each of the above functions $c - a - b = s$ Hence the series are convergent in the range $0 < \mu < 1$ provided s is neither negative nor zero. The case $s = 0$ will be dealt with separately

The condition to be fulfilled at the pole is that there ζ must be finite For this purpose we must have†

$$\mathrm{A/B} = -\left[\frac{\mu\mathrm{F}\,(\tfrac{1}{2}-\tfrac{1}{2}s-\tfrac{1}{2}n,\ 1-\tfrac{1}{2}s+\tfrac{1}{2}n,\ 3/2,\ \mu^2}{\mathrm{F}\,(-\tfrac{1}{2}s-\tfrac{1}{2}n,\ \tfrac{1}{2}-\tfrac{1}{2}s+\tfrac{1}{2}n,\ \tfrac{1}{2},\ \mu^2}\right]_{\mu=1}$$

This ratio can be readily expressed in terms of the Gamma functions That is,

$$\mathrm{A/B} = -\frac{\Gamma\,(3/2)\,\Gamma\,(s)\,\Gamma\,(\tfrac{1}{2}+\tfrac{1}{2}s+\tfrac{1}{2}n)\,\Gamma\,(\tfrac{1}{2}s-\tfrac{1}{2}n)}{\Gamma\,(1+\tfrac{1}{2}s+\tfrac{1}{2}n)\,\Gamma\,(\tfrac{1}{2}+\tfrac{1}{2}s-\tfrac{1}{2}n)\,\Gamma(\tfrac{1}{2})\,\Gamma\,(s)}\,.$$

If any of the arguments of the Gamma functions turn out to be negative integers, this expression fails But it can readily be seen that in such cases the series of the hypergeometric function is finite

Knowing the value of the ratio A/B, the solution is complete, having an arbitrary factor and a validity from $\mu = +1$ up to but not including $\mu = -1$.

In the particular case where $s = 0$, we have

$$\zeta = \mathrm{AF}\,(-\tfrac{1}{2}n,\ \tfrac{1}{2}+\tfrac{1}{2}n,\ \tfrac{1}{2},\ \mu^2) + \mathrm{B}\mu\mathrm{F}\,(\tfrac{1}{2}-\tfrac{1}{2}n,\ 1+\tfrac{1}{2}n,\ 3/2,\ \mu^2)$$

These series are only convergent when $\mu^2 < 1$ In the notation of the hypergeometric function, $\mathrm{F}(a, b, a+b, z)$ has the limiting value as $z \to 1$

$$\frac{ab}{a+b}\,\mathrm{F}\,(a,\ b,\ a+b+1,\ z)\log\frac{1}{1-z}$$

Hence at $\mu = 1$

$$\{-\mathrm{A}\quad n\,(\tfrac{1}{2}+\tfrac{1}{2}n)\,\mathrm{F}\,(-\tfrac{1}{2}n,\ \tfrac{1}{2}+\tfrac{1}{2}n,\ 3/2,\ 1)$$
$$+\ \mathrm{B}\,\tfrac{1}{3}\,(1-n)\,(1+\tfrac{1}{2}n)\,\mathrm{F}\,(\tfrac{1}{2}-\tfrac{1}{2}n,\ 1+\tfrac{1}{2}n,\ 5/2,\ 1)\}\log\frac{1}{1-\mu^2}$$

---

* Modified from Lamb, 'Hydrodynamics,' p 110

† This process follows Lamb, p 299.

must be finite. The condition is

$$\begin{aligned} \mathrm{A}/\mathrm{B} &= \frac{(1-n)(1+\tfrac{1}{2}n)}{3n(\tfrac{1}{2}+\tfrac{1}{2}n)} \frac{\mathrm{F}(\tfrac{1}{2}-\tfrac{1}{2}n, 1+\tfrac{1}{2}n, 5/2, 1)}{\mathrm{F}(-\tfrac{1}{2}n, \tfrac{1}{2}+\tfrac{1}{2}n, 3/2, 1)} \\ &= \frac{(1-n)(1+\tfrac{1}{2}n)}{2n(\tfrac{1}{2}+\tfrac{1}{2}n)} \frac{\Gamma(3/2+\tfrac{1}{2}n)\,\Gamma(1-\tfrac{1}{2}n)}{\Gamma(2+\tfrac{1}{2}n)\,\Gamma(3/2-\tfrac{1}{2}n)} \\ &= \frac{\tfrac{1}{2}(2-\beta')}{\beta'} \frac{\Gamma(3/2+\tfrac{1}{2}n)\,\Gamma(1-\tfrac{1}{2}n)}{\Gamma(2+\tfrac{1}{2}n)\,\Gamma(3/2-\tfrac{1}{2}n)} \end{aligned}$$

For determining the velocities, we require $\partial\zeta/\partial\mu$ When s is positive, as in the first case, this can readily be found In the second case, we have

$$\frac{d}{d\mu}\mathrm{F}(-\tfrac{1}{2}n, \tfrac{1}{2}+\tfrac{1}{2}n, \tfrac{1}{2}, \mu^2) = -n(n+1)\frac{\mu}{1-\mu^2}\mathrm{F}(-\tfrac{1}{2}n, \tfrac{1}{2}+\tfrac{1}{2}n, 3/2, \mu^2)$$

This series is convergent when $0 \leqslant \mu \leqslant 1$ and is therefore directly useful. For the second part

$$\begin{aligned} &\frac{d}{d\mu}\mu\mathrm{F}(\tfrac{1}{2}-\tfrac{1}{2}n, 1+\tfrac{1}{2}n, 3/2, \mu^2) \\ &\quad = \mathrm{F}(\tfrac{1}{2}-\tfrac{1}{2}n, 1+\tfrac{1}{2}n, 3/2, \mu^2) \\ &\qquad + \frac{2\mu^2}{1-\mu^2}\,\frac{(\tfrac{1}{2}-\tfrac{1}{2}n)(1+\tfrac{1}{2}n)}{3/2}\mathrm{F}(\tfrac{1}{2}-\tfrac{1}{2}n, 1+\tfrac{1}{2}n, 5/2, \mu^2) \end{aligned}$$

Now, by the well-known relations between contiguous hypergeometric functions, we have, in the standard notation,

$$\begin{aligned} c\{c-1-(2c-a-b-1)z\}\,&\mathrm{F}(a, b, c, z) \\ &- c(c-1)(1-z)\,\mathrm{F}(a, b, c-1, z) \\ &+ (c-a)(c-b)\,z\mathrm{F}(a, b, c+1, z) = 0 \end{aligned}$$

If, as in the case we are dealing with, $c = a + b$, this reduces to

$$\begin{aligned} c(c-1)(1-z)\,\mathrm{F}(a, b, c, z) - c(c-1)(1-z)\,\mathrm{F}(a, b, c-1, z)& \\ + abz\,\mathrm{F}(a, b, c+1, z) = 0&, \end{aligned}$$

or

$$\frac{ab}{c}\frac{z}{1-z}\mathrm{F}(a, b, c+1, z) = (c-1)\{\mathrm{F}(a, b, c-1, z) - \mathrm{F}(a, b, c, z)\}$$

Applying this result to the particular case above,

$$\begin{aligned} &\frac{2\mu^2}{1-\mu^2}\,\frac{(\tfrac{1}{2}-\tfrac{1}{2}n)(1+\tfrac{1}{2}n)}{3/2}\mathrm{F}(\tfrac{1}{2}-\tfrac{1}{2}n, 1+\tfrac{1}{2}n, 5/2, \mu^2) \\ &\qquad = \mathrm{F}(\tfrac{1}{2}-\tfrac{1}{2}n, 1+\tfrac{1}{2}n, \tfrac{1}{2}, \mu^2) - \mathrm{F}(\tfrac{1}{2}-\tfrac{1}{2}n, 1+\tfrac{1}{2}n, 3/2, \mu^2). \end{aligned}$$

Hence, finally,

$$\frac{d}{d\mu}\,\mu F\left(\tfrac{1}{2} - \tfrac{1}{2}n,\ 1 + \tfrac{1}{2}n,\ 3/2,\ \mu^2\right) = F\left(\tfrac{1}{2} - \tfrac{1}{2}n,\ 1 + \tfrac{1}{2}n,\ \tfrac{1}{2},\ \mu^2\right)$$
$$= \frac{1}{1-\mu^2}\,F\left(\tfrac{1}{2}n,\ -\tfrac{1}{2} - \tfrac{1}{2}n,\ \tfrac{1}{2},\ \mu^2\right)$$

The last series is convergent over the whole range required. Combining the results we have

$$d\zeta/d\mu = \frac{1}{1-\mu^2}\left\{-\,\beta' A\mu F\left(-\tfrac{1}{2}n,\ \tfrac{1}{2} + \tfrac{1}{2}n,\ 3/2,\ \mu^2\right) + BF\left(\tfrac{1}{2}n,\ -\tfrac{1}{2} - \tfrac{1}{2}n,\ \tfrac{1}{2},\ \mu^2\right)\right\}$$

By combining solutions of the above forms with suitable coefficients, boundary conditions can be fulfilled. In particular these solutions would be useful in the case of an ocean, bounded by two meridians, including one pole and extending into a circumpolar ocean in the opposite hemisphere.

§ 4. *Tides in a Polar Basin.*

We proceed to the numerical evaluation of the representative semi-diurnal tide in a basin comparable with the Southern Ocean. We shall take it to be of uniform depth, and to extend completely over the area from the pole to a boundary along the parallel of latitude 45°.

The depth may be taken to be of the order of 2,600 metres,* giving $\beta = 44$. The equations to be solved are then from (6)

$$\left.\begin{aligned} &A_2 - \tfrac{5}{8}A_0 = -0.344\,H \\ \text{and}\qquad &A_{n+2} = \tfrac{1}{2}\,\frac{n+5}{n+8}\,A_n - \frac{11}{(n+2)(n+8)}\,A_{n-2} \end{aligned}\right\}. \qquad (7.1)$$

Evaluating the terms in succession we find

$$\begin{aligned} A_2 &= 0.625\,A_0 - 0.344\,H, \\ A_4 &= -0.0562\,A_0 - 0.1254\,H, \\ A_6 &= -0.1167\,A_0 + 0.0057\,H, \\ A_8 &= -0.0404\,A_0 + 0.0145\,H, \\ A_{10} &= -0.0081\,A_0 + 0.0056\,H, \\ A_{12} &= -0.0018\,A_0 + 0.0016\,H, \end{aligned}$$

From (5) it is seen that the condition to be fulfilled at the boundary $\nu = \nu_1 = \tfrac{1}{2}\sqrt{2}$, is

$$\frac{d\zeta'}{d\nu} + s\frac{\zeta'}{\nu} = 0$$

---

* Krümmel, 'Ozeanographie,' vol. 1, p. 143.

This reduces to

$$\Sigma\,(n+6)\,A_n = 0. \tag{7 ii}$$

Using the above values of the quantities A in this boundary equation, we find $A_0 = 0.435$ H. Hence, finally,

$$\begin{aligned}\zeta = \mathrm{H}\{\nu^2 &+ 0.435\,(\nu\sqrt{2})^4 - 0.0722\,(\nu\sqrt{2})^6 \\ &- 0.1498\,(\nu\sqrt{2})^8 - 0.0451\,(\nu\sqrt{2})^{10} - 0.0031\,(\nu\sqrt{2})^{12} \\ &+ 0.0021\,(\nu\sqrt{2})^{14} \ldots\}\end{aligned} \tag{8}$$

The values of H for the lunar semi-diurnal tide (M_2) and the corresponding solar tide (S_2) are, respectively, 24.23 cm and 11.27 cm. The above solution thus gives the following tide heights at the stated latitudes :—

	Lunar cm	Solar cm
Latitude 45°	16.1	7.5
Latitude 60°	6.2	2.9

The smallness of these tides makes it desirable to enquire whether at any other reasonable depth the tides are likely to be increased by resonance. On putting H = 0 and leaving β undetermined in (7 i) and (7 ii), the elimination of the A's gives the infinite determinant

$$\begin{vmatrix} 3\ , & 4\ , & 5\ , & 6, & \\ -0.625, & 1\ , & 0\ , & 0, & \\ \dfrac{\beta}{160}\ , & -0.35, & 1\ , & 0, & \\ 0\ , & \dfrac{\beta}{288}\ , & -0.375, & 1, & \\ & & & & \end{vmatrix} = 0. \tag{9}$$

The lowest value of β satisfying this equation can readily be obtained by approximation, and we find $\beta = 203$. This corresponds to the small depth of 1,450 feet or 442 metres.

§ 5. *The Method of Solution for an Ocean bounded by Two Meridians.*

We turn now to the problem of the tides in an ocean bounded by two meridians and including both poles. For the forced tides considered here we have

$$\bar{\zeta} = \mathrm{H}\,\mathrm{P}_2^2\,(\mu)\,e^{i(2\phi+\sigma t)},$$

where H, σ are known when the tide-producing body is prescribed We have also to satisfy the boundary condition at the two meridians

It should be noted that in the equations (3) the frequency has been prescribed in advance ($f = 1$), but the depth h_0 is left at our disposal Thus the solution of the problem of the free vibrations, with $\bar{\zeta} = 0$, will give an equation for h_0 (or β) whose roots give the depths of an ocean, of the prescribed form, which has the assigned frequency as a natural frequency, the solution will also give the form of the free oscillation of this frequency for any of the suitable values of h_0 Further, introducing the above values of $\bar{\zeta}$ on the right of (3 ii) and adding the appropriate term to the solution, the arbitrary constants arising can be completely determined and we obtain the forced tides of the given frequency for any value of h_0 other than the critical values just mentioned—at which, of course, the amplitude of the forced tides becomes infinite

We have to obtain a solution of (3 ii) in a form suitable for applying the boundary conditions The method we adopt is an inverse one in which we utilise the result (4) Consider a term $\dfrac{\beta k_n^s \mathrm{P}_n^s(\mu)\, e^{is\phi}}{n(n+1)+s-\beta}$ as part of the value of ζ' On substituting in the left member of (3 ii) the result is not zero but $k_n^s \mathrm{P}_n^s(\mu)\, e^{is\phi}$ By taking

$$\zeta' = \sum_s \sum_n \beta k_n^s \mathrm{P}_n^s(\mu)\, e^{is\phi} \div \{n(n+1)+s-\beta\}$$

the summations being over appropriate values of s, n, the right member becomes $\sum\limits_s \sum\limits_n k_n^s \mathrm{P}_n^s(\mu)\, e^{is\phi}$ Now it is possible to determine the constants k_n^s so that this function is identically zero at each point in the area of the prescribed ocean. The form assumed for ζ' is then a solution of (3 ii) with the right member zero Further, an infinite number of such series can be formed, each with an arbitrary coefficient These coefficients can be suitably determined so as to satisfy the boundary condition at the two meridians

The problem now is to determine a function $\sum\limits_s \sum\limits_n k_n^s \mathrm{P}_n^s(\mu)\, e^{is\phi}$ which vanishes everywhere in the area of the given ocean We shall term this the "null function." When the constants k_n^s have been determined we shall simply add the null function to $\bar{\zeta}$ and treat the whole as a tide-producing potential.

§ 6 *The Null Function.*

Let us suppose that the two boundaries of the ocean are the meridians of longitude $\phi = 0, \alpha$ Then in the range 0 to α, we have the following valid expansions

$$\left.\begin{aligned} \sin \kappa\pi\phi/\alpha &= \sum_r a_r^\kappa \cos r\pi\phi/\alpha, \quad (r-\kappa) \text{ odd}, \\ a_r^\kappa &= \frac{4\kappa}{(\kappa^2 - r^2)\pi}, \qquad r \neq 0, \\ a_0^\kappa &= \frac{2}{\kappa\pi}, \qquad (\kappa \text{ odd}), \\ \text{and} \qquad \cos \kappa\pi\phi/\alpha &= \sum a'^\kappa_r \sin r\pi\phi/\alpha, \quad (r-\kappa) \text{ odd}, \\ a'^\kappa_r &= \frac{4r}{(r^2-\kappa^2)\pi} \end{aligned}\right\} \tag{10}$$

In these expansions, of course, r and κ are integers

The two functions

$$e^{\iota\kappa\pi\phi/\alpha} - e^{-\iota\kappa\pi\phi/\alpha} - \iota \sum_r a_r^\kappa (e^{\iota r\pi\phi/\alpha} + e^{-\iota r\pi\phi/\alpha}),$$

$$e^{\iota\kappa\pi\phi/\alpha} + e^{-\iota\kappa\pi\phi/\alpha} + \iota \sum_r a'^\kappa_r (e^{\iota r\pi\phi/\alpha} - e^{-\iota r\pi\phi/\alpha}),$$

then vanish for all values of ϕ in the range 0 to ϕ, the first one including the limits, and the second one excluding the limits Further, in the first expression κ may be an integer but not zero, while in the second κ may be any integer including zero

These expressions must now be put in the form of spherical surface harmonics In the method of doing this there is some choice, as each term $e^{\iota s\phi}$ may be associated with any $\mathrm{P}_n^s(\mu)$ provided $n - s$ is integral The practice adopted here is to multiply each through by $\mathrm{P}_{\kappa\pi/\alpha}^{\kappa\pi/\alpha}(\mu) \div \mathrm{P}_{\kappa\pi/\alpha}^{\kappa\pi/\alpha}(0)$, the denominator being merely included to avoid large numerical coefficients Now*

$$\mathrm{P}_{\kappa\pi/\alpha}^{\kappa\pi/\alpha}(\mu) \div \mathrm{P}_{\kappa\pi/\alpha}^{\kappa\pi/\alpha}(0) = \sum_n b_n^{r\pi/\alpha}(\kappa\pi/\alpha)\,\mathrm{P}_n^{r\pi/\alpha}(\mu), \tag{11}$$

where $n - r\pi/\alpha$ is integral for all values of n, and the coefficients $b_n^{r\pi/\alpha}(\kappa\pi/\alpha)$ are determinable Hence we have

$$\left.\begin{aligned} &(e^{\iota\kappa\pi\phi/\alpha} - e^{-\iota\kappa\pi\phi/\alpha})\,\mathrm{P}_{\kappa\pi/\alpha}^{\kappa\pi/\alpha} \div \mathrm{P}_{\kappa\pi/\alpha}^{\kappa\pi/\alpha}(0) \\ &\qquad - \iota \sum_r a_r^\kappa\,(e^{\iota r\pi\phi/\alpha} + e^{-\iota r\pi\phi/\alpha}) \sum_n b_n^{r\pi/\alpha}(\kappa\pi/\alpha)\,\mathrm{P}_n^{r\pi/\alpha}(\mu) = 0 \\ &\text{and} \\ &(e^{\iota\kappa\pi\phi/\alpha} + e^{-\iota\kappa\pi\phi/\alpha})\,\mathrm{P}_{\kappa\pi/\alpha}^{\kappa\pi/\alpha} \div \mathrm{P}_{\kappa\pi/\alpha}^{\kappa\pi/\alpha}(0) \\ &\qquad + \iota \sum_r a'^\kappa_r\,(e^{\iota r\pi\phi/\alpha} - e^{-\iota r\pi\phi/\alpha}) \sum_n b_n^{r\pi/\alpha}(\kappa\pi/\alpha)\,\mathrm{P}_n^{r\pi/\alpha}(\mu) = 0 \end{aligned}\right\} \tag{12}$$

---

* See Heine, 'Kugelfunctionen,' § 62 (1878)

The left member of each of these expressions vanishes over the whole of the ocean prescribed

Next take a series of arbitrary multiples of each of the expressions on the left of (12) for differing values of κ and we have, finally, on adding the results to the tide-producing potential,

$$
\begin{aligned}
\bar{\zeta} = {} & \mathrm{HP}_2^2(\mu)\, e^{\iota 2\phi} \\
& + \sum_{\kappa=1}^{\infty} \mathrm{E}_\kappa \Big[\left(e^{\iota\kappa\pi\phi/\alpha} - e^{-\iota\kappa\pi\phi/\alpha}\right) \mathrm{P}_{\kappa\pi/\alpha}^{\kappa\pi/\alpha} \div \mathrm{P}_{\kappa\pi/\alpha}^{\kappa\pi/\alpha}(0) \\
& \qquad - \iota \sum_r a_r^\kappa \left(e^{\iota r\pi\phi/\alpha} + e^{-\iota r\pi\phi/\alpha}\right) \sum_n b_n^{r\pi/\alpha}(\kappa/\pi\alpha)\, \mathrm{P}_n^{r\pi/\alpha}(\mu) \Big] \\
& + \iota \sum_{\kappa=0}^{\infty} \mathrm{F}_\kappa \Big[\left(e^{\iota\kappa\pi\phi/\alpha} + e^{-\iota\kappa\pi\phi/\alpha}\right) \mathrm{P}_{\kappa\pi/\alpha}^{\kappa\pi/\alpha}(\mu) \div \mathrm{P}_{\kappa\pi/\alpha}^{\kappa\pi/\alpha}(0) \\
& \qquad + \sum_r a'^{\kappa}_r \left(e^{\iota r\pi\phi/\alpha} - e^{-\iota r\pi\phi/\alpha}\right) \sum_n b_n^{r\pi/\alpha}(\kappa\pi/\alpha)\, \mathrm{P}_n^{r\pi/\alpha}(\mu) \Big] \qquad (13)
\end{aligned}
$$

This expression for $\bar{\zeta}$ replaces that generally used Each term of it is of suitable form, and will give rise in the solution to terms of the type (4) It further contains a doubly infinite set of undetermined constants which can take values that will ensure the vanishing of the velocity component v at the boundaries $\phi = 0, \alpha$

The coefficients a_r^κ, a'^{κ}_r are readily calculated The values of $b_n^{r\pi/\alpha}(\kappa\pi/\alpha)$ are not so readily obtained Two methods of procedure will be indicated The first is as follows —

Let

$$\mathrm{P}_p^p(\mu) \div \mathrm{P}_p^p(0) = \sum_n \mathrm{P}_n^\rho(\mu) \quad b_n^\rho(p) \qquad (14)$$

Assuming the validity of the expansion, the coefficients b may be obtained in the usual way. That is, in the case of p, ρ integers,

$$b_n^\rho(p) = \frac{2n+1}{2} \quad \frac{(n-\rho)\,!}{(n+\rho)\,!} \int_{-1}^{1} \frac{\mathrm{P}_p^p(\mu)}{\mathrm{P}_p^p(0)} \quad \mathrm{P}_n^\rho(\mu)\, d\mu \qquad (15)$$

Now it can be shown that when ρ, n, p, r are integers, and D stands for $d/d\mu$, that*

$$
\begin{aligned}
\mathrm{D}^\rho \mathrm{P}_n \times \mathrm{D}^p \mathrm{P}_p = \sum_r (-1)^r \frac{p\,!}{r\,!\,(p-r)\,!} \quad & \frac{1 \cdot 3 \cdot 5 \ldots (2p-1) \cdot 1 \cdot 3 \cdot 5 \ldots (2n-2r-1)}{1 \cdot 3 \cdot 5 \ldots (2n+2p-2r+1)} \\
& \times (2n+2p-4r+1)\, \mathrm{D}^{\rho+p} \mathrm{P}_{n+p-2r} \qquad (16)
\end{aligned}
$$

---

[*] Adams, 'Collected Scientific Papers,' vol 2, p 380

The summation takes place from $r = 0$ to p. Hence we find at once

$$\int_{-1}^{1} \mathrm{P}_n^\rho \mathrm{P}_p^p \, d\mu = \sum_r (-1)^r \frac{p\,!}{r\,!\,(p-r)\,!} \quad \frac{1 \; 3 \; 5 \quad (2p-1) \; 1 \; 3 \; 5 \quad (2n-2r-1)}{1 \quad 3 \quad 5 \quad (2n+2p-2r+1)}$$
$$\times (2n+2p-4r+1) \int_{-1}^{1} \mathrm{P}_{n+p-2r}^{\rho+p}(\mu)\, d\mu. \qquad (17)$$

Now it can be readily shown that

$$\int_{-1}^{1} \mathrm{P}_{n+p-2r}^{\rho+p}(\mu)\, d\mu = \frac{\rho+p}{\rho+p-2}(\rho+n+2p-2r-1)(n-\rho-2r+2)$$
$$\times \int_{-1}^{1} \mathrm{P}_{n+p-2r}^{\rho+p-2}(\mu)\, d\mu,$$

and further that

$$\int_{-4}^{1} \mathrm{P}^1{}_{2n-1} = \frac{\pi(2n-1)}{2n} \left\{ \frac{1 \quad 3 \quad 5 \quad (2n-3)}{2 \quad 4 \quad 6 \quad (3n-2)} \right\}^2,$$

$$\int_{-1}^{1} \mathrm{P}_n^2 = 4, \text{ for all integral values of } n$$

Hence the value of the integral in (17) can quickly be obtained by reduction

The second method of obtaining the values of the coefficients b is by means of the differential equation for the "associated" Legendre functions. The function $\mathrm{P}_p^p(\mu)$ satisfies the equation

$$\frac{d}{d\mu}(1-\mu^2)\frac{dz}{d\mu} - \frac{p^2 z}{1-\mu^2} + p(p+1)z = 0 \qquad (18)$$

If we again assume that $\mathrm{P}_p^p(\mu)$ may be expanded in a series $\sum_n \alpha_n \mathrm{P}_n^\rho(\mu)$, the coefficients may be obtained by substituting the series in equation (10) We have then

$$\Sigma\, \alpha_n \left[-n(n+1) + \frac{\rho^2}{1-\mu^2} - \frac{p^2}{1-\mu^2} + p(p+1) \right] \mathrm{P}_n^\rho(\mu) = 0,$$

or

$$\Sigma\, \alpha_n [\rho^2 - p^2 + \{p(p+1) - n(n+1)\}(1-\mu^2)]\, \mathrm{P}_n^\rho(\mu) = 0 \qquad (19)$$

Now we have

$$\mu\, \mathrm{P}_n^\rho = \{(n-\rho+1)\,\mathrm{P}_{n+1}^\rho + (n+\rho)\,\mathrm{P}_{n-1}^\rho\} \div (2n+1),$$

and thence

$$(1-\mu^2)\,\mathrm{P}_n^\rho = -\frac{(n-\rho+1)(n-\rho+2)}{(2n+1)(2n+3)}\mathrm{P}_{n+2}^\rho$$
$$+ \frac{2n^2+2n-2+2\rho^2}{(2n+3)(2n-1)}\mathrm{P}_n^\rho$$
$$- \frac{(n+\rho)(n+\rho-1)}{(2n+1)(2n-1)}\mathrm{P}_{n-2}^\rho$$

If we now substitute this expression in (19) and equate to zero corresponding coefficients of P_n^ρ, we have the general difference relation

$$\alpha_{n+2}\{p(p+1)-(n+2)(n+3)\}\frac{(n+\rho+2)(n+\rho+1)}{(2n+5)(2n+3)}$$
$$=\alpha_n\left[\{p(p+1)-n(n+1)\}\frac{2n^2+2n-2+2\rho^2}{(2n+3)(2n-1)}+\rho^2-p^2\right]$$
$$-\alpha_{n-2}\frac{\{p(p+1)-(n-2)(n-1)\}(n-\rho-1)(n-\rho)}{(2n-3)(2n-1)} \qquad (20)$$

Commencing with $n=\rho$, or $n=\rho+1$, we have two independent series with the initial terms, α_ρ and $\alpha_{\rho+1}$, respectively, arbitrary These initial terms can be determined as in the former method, except that now the integration is elementary The two methods may be used as a check one upon the other, as was done in the case of the results in Table II

As large denominators appear upon integration (as will be seen from (4)) relatively few terms of the expansion of P_n^ρ are required, and this fact reduces the labour of the method considerably

Some idea of the numerical convergence of the series will be obtained later when a particular case is developed

§ 7 *Ocean bounded by Two Meridians*

We proceed to complete the solutions of the tidal equations for an ocean bounded by two meridians of longitude $\phi=0$, α, by determining the constants E, F, from the condition that the velocity normal to the boundary must everywhere vanish. If we take the tide-producing potential $\bar{\zeta}$ in the form (13) and integrate the second of equations (3) with it, we find from (4), on putting for brevity, $\kappa\pi/\alpha=s$, $r\pi/\alpha=\rho$, $\gamma=\beta^{-1}$,

$$\zeta'=\frac{\mathrm{HP}_2^2(\mu)\,e^{2\iota\phi}}{8\gamma-1}$$
$$+\sum_s \mathrm{E}_s\left[\left\{\frac{e^{\iota s\phi}}{s(s+2)\gamma-1}-\frac{e^{-\iota s\phi}}{s^2\gamma-1}\right\}\frac{\mathrm{P}_s^s(\mu)}{\mathrm{P}_s^s(0)}\right.$$
$$\left.-\iota\sum a_\rho^s\sum_n b_n^\rho(s)\,\mathrm{P}_n^\rho(\mu)\left\{\frac{e^{\iota\rho\phi}}{\{n(n+1)+\rho\}\gamma-1}+\frac{e^{-\iota\rho\phi}}{\{n(n+1)-\rho\}\gamma-1}\right\}\right]$$
$$+\sum_s \mathrm{F}_s\left[\left\{\frac{e^{\iota s\phi}}{s(s+2)\gamma-1}+\frac{e^{-\iota s\phi}}{s^2\gamma-1}\right\}\frac{\mathrm{P}_s^s(\mu)}{\mathrm{P}_s^s(0)}\right.$$
$$\left.+\iota\sum_\rho a'^s_\rho\sum_n b_n^\rho(s)\,\mathrm{P}_n^\rho(\mu)\left\{\frac{e^{\iota\rho\phi}}{\{n(n+1)+\rho\}\gamma-1}-\frac{e^{-\iota\rho\phi}}{\{n(n+1)-\rho\}\gamma-1}\right\}\right]. \qquad (21)$$

On putting $v = 0$ in the first two of equations (1) and, after removing the factor $e^{\iota\sigma t}$, eliminating u, we have the condition

$$\mu \frac{\partial \zeta'}{\partial \mu} + \frac{\iota}{1-\mu^2} \frac{\partial \zeta'}{\partial \phi} = 0 \tag{22}$$

This condition is to be fulfilled along the length of the two boundaries $\phi = 0, \alpha$. In other words, when $\phi = 0$ or α, (22) must be identically satisfied for all values of μ from -1 to $+1$

Now perform the operation indicated by (22) upon the expression for ζ' in (21) On reducing and collecting corresponding terms, we have the result in a general form that

$$\begin{aligned} &\Sigma\,\Sigma\, \mathrm{M}_n^m \mathrm{P}_n^m(\mu)\, e^{-\iota m\phi} \\ &+ \Sigma\,\Sigma\, \mathrm{N}_n^m \mathrm{P}_n^m(\mu)\, e^{\iota m\phi} \\ &+ \frac{6\mathrm{H}e^{2\iota\phi}}{8\gamma-1}\left(\frac{6\mathrm{P}_2^2(\mu)}{\mathrm{P}_2^2(0)} - 12\mathrm{P}_0\right) = 0, \end{aligned} \tag{23}$$

for all values of μ when $\phi = 0$ or α

In this expression M, N are linear functions of E, F and m, n take a certain set of values not necessarily consecutive integers It is evident, however, that m will always be in the form $\lambda\pi/\alpha$, where λ is an integer It will be convenient to distinguish the cases where λ is an *odd* integer by marking them m'

On putting $\phi = 0, \alpha$ in turn in (23), we have the result

$$\left.\begin{aligned} &\Sigma\Sigma\,(\mathrm{M}_n^m + \mathrm{N}_n^m)\,\mathrm{P}_n^m(\mu) + \Sigma\Sigma\,(\mathrm{M}_n^{m'} + \mathrm{N}_n^{m'})\,\mathrm{P}_n^{m'}(\mu) \\ &\qquad\qquad + \frac{6\mathrm{H}}{8\gamma-1}\{3\mathrm{P}_2^2(\mu) - 12\mathrm{P}_0(\mu)\} = 0, \\ &\Sigma\Sigma\,(\mathrm{M}_n^m + \mathrm{N}_n^m)\,\mathrm{P}_n^m\,\mu - \Sigma\Sigma\,(\mathrm{M}_n^{m'} + \mathrm{N}_n^{m'})\,\mathrm{P}_n^{m'}(\mu) \\ &\qquad\qquad + \frac{6\mathrm{H}e^{2\iota\alpha}}{8\gamma-1}\{3\mathrm{P}_2^2(\mu) - 12\mathrm{P}_0(\mu)\} = 0 \end{aligned}\right\} \tag{24}$$

Or on taking the sum and difference we have the equations

$$\left.\begin{aligned} &\Sigma\,\Sigma\,(\mathrm{M}_n^m + \mathrm{N}_n^m)\,\mathrm{P}_n^m(\mu) + \frac{3\mathrm{H}}{8\gamma-1}\{3\mathrm{P}_2^2(\mu) - 12\mathrm{P}_0(\mu)\}\,(1+e^{2\iota\alpha}) = 0, \\ &\Sigma\,\Sigma\,(\mathrm{M}_n^{m'} + \mathrm{N}_n^{m'})\,\mathrm{P}_n^{m'}(\mu) + \frac{3\mathrm{H}}{8\gamma-1}\{3\mathrm{P}_2^2(\mu) - 12\mathrm{P}_0(\mu)\}\,(1-e^{2\iota\alpha}) = 0 \end{aligned}\right\}. \tag{25}$$

Each of (25) should be an identity in μ To determine values for E_s, F_s which will produce this identity, we must reduce each of the "associated" Legendre functions to a common denomination dependent upon one set of arguments, instead of the two, m and n, which occur in those functions. The method adopted here is to expand each "associated" function into a series of Legendre functions This can be rapidly done by use of the differential equation for the "associated" functions, after the manner indicated in § 6

The function $P_p^m(\mu)$ satisfies the equation

$$(1-\mu^2)\frac{d^2z}{d\mu^2} - 2\mu\frac{dz}{d\mu} - \frac{m^2z}{1-\mu^2} + p(p+1)z = 0$$

If we assume that

$$z = \Sigma\,\alpha_n P_n(\mu),$$

we find as before that the sequence-relation between the quantities α is

$$\begin{aligned}\alpha_{n+2}\{p(p+1)-(n+2)(n+3)\}&\frac{(n+2)(n+1)}{(2n+3)(2n+5)}\\ &= \alpha_n\left[\{p(p+1)-n(n+1)\}\frac{2n^2+2n-2}{(2n-1)(2n+3)} - m^2\right]\\ &\quad - \alpha_{n-2}\{p(p+1)-(n-2)(n-1)\}\frac{n(n-1)}{(2n-3)(2n-1)}\end{aligned} \tag{26}$$

From this sequence each α can be found in terms of α_0 The latter quantity is found from the fact that

$$\alpha_0 = \tfrac{1}{2}\int_{-1}^{1} P_p^m(\mu)\,d\mu. \tag{27}$$

The series gives a very satisfactory representation of the "associated" function. In Table III the numerical values for a given case are shown and the degree of approximation is shown in § 8

On substituting these expansions in (25), the coefficient of each Legendre function can be equated to zero We have then a series of equations sufficient to determine the coefficients E_s, F_s These quantities being known, the expression (21) is freed from unknowns and the solution is complete

Two points require comment here We introduced in (21) a doubly infinite series of undetermined coefficients Correspondingly equations (25) give rise to a doubly infinite set of linear equations for their evaluation Again, it might be thought that the method of introduction of the Legendre functions in the tide-producing potential (see (13)) is open to criticism on the ground that it may be done in a variety of ways and therefore the result accruing cannot be unique But it should be noted that, in whatever way the series of (10) are arranged as spherical surface harmonics, it is ultimately the coefficient of $P_n^m(\mu)\,e^{\iota m\phi}$ or $P_n^m(\mu)\,e^{-\iota m\phi}$ that is determined This is evident from (25) and the succeeding argument. Hence ultimately the coefficient of each of these terms in ζ' will be the same no matter in what form they were originally introduced in ζ.

§ 8 *Meridians 60° apart.*

The formulæ for the special case of an ocean bounded by the two meridians 0, $\pi/3$ will now be evaluated The second limit has the convenience that all the Legendre functions involved have integral orders and ranks For the present the value of the depth will be left indeterminate. Table I gives the values of a_r^κ and a'^κ_r In Table II the first terms of the expansions of $P_\rho^\sigma(\mu)$ are given for the values $\rho = 0, 3, 6, 9$ and 12 As will be seen in the sequel,

Table I

Values of a_r^κ

	$\kappa = 1$	2	3	4
$r = 0$	0·6366		0·1273	
1		0·8480		0·3392
2	−0·4244		0·7639	
3		−0·5095		0·7275
4	−0·0849		−0·5456	

Values of a'^κ_r

	$\kappa = 0$	1	2	3
$r = 1$	1·2732		−0·4244	
2		0·3813		−0·5094
3	0·4244		0·7640	
4		0·3396		0·7277

Table II —Values of log b_{3n}^{3r} (3s)

		$3n = 3r$	$3n = 3r + 2$	$3n = 3r + 4$	$3n = 3r + 6$
$3s = 0$	$3r = 3$	$\bar{2}\ 8340$	$\bar{3}\ 8962$	$\bar{5}\ 3038$	$\bar{4}\ 8714$
	$3r = 9$	$\bar{8}\ 5969$	$\bar{9}\ 2539$	$\overline{10}\ 3372$	$\overline{11}\ 6422$
$3s = 3$	$3r = 0$	$\bar{1}\ 7701$	$n\bar{1}\ 8672$	$\bar{1}\ 0941$	$\bar{2}\ 1753$
	$3r = 6$	$\bar{4}\ 0376$	$\bar{6}\ 4060$	$\bar{7}\ 3236$	$\bar{8}\ 4842$
	$3r = 12$	$\overline{12}\ 5936$	$\overline{14}\ 9420$	$\overline{15}\ 7684$	
$3s = 6$	$3r = 3$	$\bar{2}\ 7510$	$n\bar{3}\ 4421$	$\bar{5}\ 9078$	
	$3r = 9$	$\bar{8}\ 4960$	$\overline{10}\ 5017$	$\overline{11}\ 1061$	
$3s = 9$	$3r = 0$	$\bar{1}\ 5872$	$n\bar{1}\ 8601$	$\bar{1}\ 6937$	$n\bar{1}\ 2648$
	$3r = 6$	$\bar{5}\ 9388$	$n\bar{6}\ 1315$	$\bar{9}\ 1941$	
	$3r = 12$	$\overline{12}\ 5281$	$\overline{14}\ 2829$	$n\overline{16}\cdot 1262$	
$3s = 12$	$3r = 3$	$\bar{2}\ 6522$	$n\bar{3}\ 6444$	$\bar{4}\ 8003$	$n\bar{5}\ 3725$
	$3r = 9$	$\bar{8}\ 4316$	$n\overline{10}\ 7876$	$n\overline{10}\ 0003$	

this list is long enough for our needs. It is interesting to notice the accuracy of the few terms of the series in representing the function. Taking the last entry of the table, the expansion of $P_{12}^{12}(\mu)/P_{12}^{12}(0)$ in terms of functions of rank 9, the three terms mentioned give $0 \cdot 987$ at $\mu = 0$, the function itself being unity at that point.

From these tables we can then form the function $\bar{\zeta}$ and from it the integral (21) for ζ' The result is

$$\zeta'/\beta = \frac{HP_2^2(\mu)}{8-\beta} e^{2\iota\phi}$$

$$+ \sum_{\kappa=1}^{\infty} E_\kappa \left(e^{3\kappa\iota\phi} - e^{-3\kappa\iota\phi}\right) P_{3\kappa}^{3\kappa}(\mu)/P_{3\kappa}^{3\kappa}(0)$$

$$+ \sum_{r=0}^{\infty} E_r T_r$$

$$+ \sum_{\kappa=0}^{\infty} F_\kappa \left(e^{3\kappa\iota\phi} + e^{-3\kappa\iota\phi}\right) P_{3\kappa}^{3\kappa}(\mu)/P_{3\kappa}^{3\kappa}(0)$$

$$+ \sum_{r=1}^{\infty} E_r S_r \,,$$

$$T_3 = \frac{0 \cdot 748\, P_0}{-\beta} - \frac{0 \cdot 935\, P_2}{6-\beta} + \frac{0 \cdot 157\, P_4}{20-\beta} + \frac{0 \cdot 019\, P_6}{42-\beta}$$

$$- \left\{\frac{0 \cdot 462 \quad 10^{-4}\, P_6^6}{48-\beta} + \frac{1 \cdot 081 \quad 10^{-6}\, P_8^6}{78-\beta} + . \quad \right\} e^{6\iota\phi}$$

$$- \left\{\frac{0 \cdot 462 \quad 10^{-4}\, P_6^6}{36-\beta} + \frac{1 \cdot 081 \quad 10^{-6}\, P_8^6}{66-\beta} + \quad \right\} e^{-6\iota\phi}$$

$$- \left\{\frac{0 \cdot 333 \;.\; 10^{-12}\, P_{12}^{12}}{168-\beta} + \frac{0 \cdot 743 \quad 10^{-14}\, P_{14}^{12}}{222-\beta} + \quad \right\} e^{12\iota\phi}$$

$$- \left\{\frac{0 \cdot 333 \quad 10^{-12}\, P_{12}^{12}}{144-\beta} + \frac{0 \cdot 743 \quad 10^{-14}\, P_{14}^{12}}{198-\beta} + \quad \right\} e^{-12\iota\phi} \quad ,$$

$$T_6 = \left(\frac{0 \cdot 0478\, P_3^3}{15-\beta} - \frac{0 \cdot 00235\, P_5^3}{33-\beta} . \quad \right) e^{3\iota\phi}$$

$$+ \left(\frac{0 \cdot 0478\, P_3^3}{9-\beta} - \frac{0 \cdot 00235\, P_5^3}{27-\beta} \quad \right) e^{-3\iota\phi}$$

$$- \left(\frac{1 \cdot 603 \;.\; 10^{-8}\, P_9^9}{99-\beta} + \frac{1 \cdot 613 \quad 10^{-10}\, P_{11}^9}{141-\beta} + \quad \right) e^{9\iota\phi}$$

$$- \left(\frac{1 \cdot 603 \quad 10^{-8}\, P_9^9}{81-\beta} + \frac{1 \cdot 613 \;.\; 10^{-10}\, P_{11}^9}{123-\beta} + \quad \right) e^{-9\iota\phi} . \quad ,$$

$$
\begin{aligned}
T_0 = &-\frac{0\cdot1613\,P_0}{\beta}-\frac{0\cdot3023\,P_2}{6-\beta}+\frac{0\cdot2059\,P_4}{20-\beta}-\frac{0\cdot0767P_6}{42-\beta}\\
&+\left(\frac{6\cdot631\ \ 10^{-5}\,\mathrm{P}_6^6}{48-\beta}-\frac{1\cdot031\ \ 10^{-6}\,\mathrm{P}_8^6}{78-\beta}\ \ \right)e^{6\iota\phi}\\
&+\left(\frac{6\cdot631\ \ 10^{-5}\,\mathrm{P}_6^6}{36-\beta}-\frac{1\cdot031\ \ 10^{-6}\,\mathrm{P}_8^6}{66-\beta}\ \ \right)e^{-6\iota\phi}\\
&-\left(\frac{1\cdot840\ \ 10^{-12}\,\mathrm{P}_{12}^{12}}{168-\beta}+\frac{1\cdot048\ \ 10^{-14}\,\mathrm{P}_{14}^{12}}{222-\beta}\ \ \right)e^{12\iota\phi}\\
&-\left(\frac{1\cdot840\ \ 10^{-12}\,\mathrm{P}_{12}^{12}}{144-\beta}+\frac{1\cdot048\ \ 10^{-14}\,\mathrm{P}_{14}^{12}}{198-\beta}\ \ \right)e^{-12\iota\phi}\quad ,
\end{aligned}
$$

$$
\begin{aligned}
\mathrm{T}_{12} = &\left(\frac{0\cdot0152\,\mathrm{P}_3^3}{15-\beta}-\frac{0\cdot00149\,\mathrm{P}_5^3}{33-\beta}\ \ \right)e^{3\iota\phi}\\
&+\left(\frac{0\cdot0152\,\mathrm{P}_3^3}{9-\beta}-\frac{0\cdot00149\,\mathrm{P}_5^3}{27-\beta}\ \ \right)e^{-3\iota\phi}\\
&+\left(\frac{1\cdot965\ \ 10^{-8}\,\mathrm{P}_9^9}{99-\beta}-\frac{4\cdot462\ \ 10^{-10}\,\mathrm{P}_{11}^9}{141-\beta}\ \ \right)e^{9\iota\phi}\\
&+\left(\frac{1\cdot965\ \ 10^{-8}\,\mathrm{P}_9^9}{81-\beta}-\frac{4\cdot462\ \ 10^{-10}\,\mathrm{P}_{11}^9}{123-\beta}\ \ \right)e^{-9\iota\phi}\quad ,
\end{aligned}
$$

$$
\begin{aligned}
\mathrm{S}_0 = &\left(\frac{0\cdot0866\,\mathrm{P}_3^3}{15-\beta}+\frac{0\cdot00999\,\mathrm{P}_5^3}{33-\beta}+.\ \right)e^{3\iota\phi}\\
&-\left(\frac{0\cdot0866\,\mathrm{P}_3^3}{9-\beta}+\frac{0\cdot00999\,\mathrm{P}_5^3}{27-\beta}+\ \ \right)e^{-3\iota\phi}\\
&+\left(\frac{1\cdot674\ \ 10^{-8}\,\mathrm{P}_9^9}{99-\beta}+\frac{7\cdot59\ \ 10^{-10}\,\mathrm{P}_{11}^9}{141-\beta}\ \ .\right)e^{9\iota\phi}\\
&-\left(\frac{1\cdot674\ \ 10^{-8}\,\mathrm{P}_9^9}{81-\beta}+\frac{7\cdot59\ \ 10^{-10}\,\mathrm{P}_{11}^9}{123-\beta}\ \ \right)e^{-9\iota\phi}\quad ,
\end{aligned}
$$

$$
\begin{aligned}
\mathrm{S}_2 = &\left(\frac{4\cdot15\ \ 10^{-5}\,\mathrm{P}_6^6}{48-\beta}+\frac{9\cdot71\ \ 10^{-7}\,\mathrm{P}_8^6}{78-\beta}\ldots\right)e^{6\iota\phi}\\
&-\left(\frac{4\cdot15\ \ 10^{-5}\,\mathrm{P}_6^6}{36-\beta}+\frac{9\cdot71\ \ 10^{-7}\,\mathrm{P}_8^6}{66-\beta}\ \ \right)e^{-6\iota\phi}\\
&+\left(\frac{1\cdot328\ \ 10^{-12}\,\mathrm{P}_{12}^{12}}{168-\beta}+\frac{2\cdot966\ \ 10^{14}\,\mathrm{P}_{14}^{12}}{222-\beta}\ \ .\right)e^{12\iota\phi}\\
&-\left(\frac{1\cdot328\ \ 10^{-12}\,\mathrm{P}_{12}^{12}}{144-\beta}+\frac{2\cdot966\ \ 10^{14}\,\mathrm{P}_{14}^{12}}{198-\beta}\ .\ .\right)e^{-12\iota\phi}\ldots ,
\end{aligned}
$$

$$
\begin{aligned}
S_3 = {} & \left(\frac{-2\cdot39\ \ 10^{-2}\,P_3^3}{15-\beta}+\frac{1\cdot174\ \ 10^{-3}\,P_5^3}{33-\beta}\right)e^{3\iota\phi} \\
& +\left(\frac{2\ 39\ \ 10^{-2}\,P_3^3}{9-\beta}-\frac{1\cdot174\ \ 10^{-3}\,P_5^3}{27-\beta}\right)e^{-3\iota\phi} \\
& +\left(\frac{2\cdot406\ \ 10^{-8}P_9^9}{99-\beta}+\frac{2\ 429\ \ 10^{-10}\,P_{11}^9}{141-\beta}\right)e^{9\iota\phi} \\
& -\left(\frac{2\ 406\ \ 10^{-8}\,P_9^9}{81-\beta}+\frac{2\ 429\ .\ 10^{-10}\,P_{11}^9}{123-\beta}\right)e^{-9\iota\phi} \quad ,
\end{aligned}
$$

$$
\begin{aligned}
S_6 = {} & -\left(\frac{4\cdot418\ \ 10^{-5}\,P_6^6}{48-\beta}-\frac{6\ 87\ \ 10^{-7}\,P_8^6}{78-\beta}\right)e^{6\iota\phi} \\
& +\left(\frac{4\ 418\ ,\ 10^{-5}\,P_6^6}{36-\beta}-\frac{6\ 87\ \ 10^{-7}\,P_8^6}{66-\beta}\right)e^{-6\iota\phi} \\
& +\left(\frac{2\ 453\ \ 10^{-12}\,P_{12}^{12}}{168-\beta}+\frac{1\ 397\ \ 10^{-14}\,P_{14}^{12}}{222-\beta}\right)e^{12\iota\phi} \\
& -\left(\frac{2\ 453\ \ 10^{-12}\,P_{12}^{12}}{144-\beta}+\frac{1\ 397\ \ 10^{-14}\,P_{14}^{12}}{198-\beta}\right)e^{12\iota\phi} \qquad (28)
\end{aligned}
$$

In this expression, owing to the rapid convergence, only two terms of each class are requisite It is noticeable that β enters in a very simple way into the formation of the series, and this fact makes it possible to arrive at the value of the first critical depth for the semi-diurnal tide

We have now to operate on ζ' with

$$\mu\frac{\partial}{\partial\mu}+\frac{\iota}{1-\mu^2}\frac{\partial}{\partial\phi} \qquad (29)$$

in order to find the condition under which the velocity in latitude will vanish. After this operation is performed, we require the value of the result when $\phi = 0$ In other words, we have to determine the value of

$$\left(\mu\frac{\partial}{\partial\mu}\mp\frac{s}{1-\mu^2}\right)P_n^s.$$

The only cases necessary are those when $n = s,\ s+2$

Now it is easily shown that

$$\left.\begin{aligned}\left(\mu\frac{d}{d\mu}-\frac{s}{1-\mu^2}\right)\mathrm{P}_s^s/\mathrm{P}_s^s(0)&=s\,\mathrm{P}_s^s/\mathrm{P}_s^s(0)-2s\,\mathrm{P}_{s-2}^{s-2}/\mathrm{P}_{s-2}^{s-2}(0)\\ \left(\mu\frac{d}{d\mu}+\frac{s}{1-\mu^2}\right)\mathrm{P}_s^s/\mathrm{P}_s^s(0)&=s\,\mathrm{P}_s^s/\mathrm{P}_s^s(0)\end{aligned}\right\}\tag{30}$$

Further

$$\begin{aligned}\mu\frac{d\mathrm{P}_{s+2}^s}{d\mu}&=-\mu^2 s\,(1-\mu^2)^{s/2-1}\frac{d^s\,\mathrm{P}_{s+2}}{d\mu^s}+\mu\,(1-\mu^2)^{s/2}\frac{d^{s+1}\,\mathrm{P}_{s+2}}{d\mu^{s+1}}\\ &=-\mu^2 s\,\frac{\mathrm{P}_{s+2}^s}{1-\mu^2}+\mu\,(1-\mu^2)^{-\frac{1}{2}}\,\mathrm{P}_{s+2}^{s+1}\\ &=-\frac{\mu^2 s\,\mathrm{P}_{s+2}^s}{1-\mu^2}+\{\mathrm{P}_{s+2}^{s+2}+2\,(2s+3)\,\mathrm{P}_{s+2}^s\}\div 2\,(s+1)\end{aligned}$$

Therefore,

$$\begin{aligned}\mu\frac{d\mathrm{P}_{s+2}^s}{d\mu}-\frac{s\,\mathrm{P}_{s+2}^s}{1-\mu^2}&=\frac{s^2+3s+3}{s+1}\mathrm{P}_{s+2}^s+\frac{\mathrm{P}_{s+2}^{s+2}}{2\,(s+1)}-\frac{2s\,\mathrm{P}_{s+2}^s}{1-\mu^2}\\ &=\frac{s^2+3s+3}{s+1}\mathrm{P}_{s+2}^s+\frac{\mathrm{P}_{s+2}^{s+2}}{2\,(s+1)}\\ &\qquad-2s\,(2s+1)\,(2s+3)\,\mathrm{P}_s^{s-2}-4s\,(2s+1)\,(2s+3)\,\mathrm{P}_{s-2}^{s-2},\end{aligned}$$

and

$$\mu\,\frac{d\mathrm{P}_{s+2}^s}{d\mu}+\frac{s\,\mathrm{P}_{s+2}^s}{1-\mu^2}=\mathrm{P}_{s+2}^s+\{\mathrm{P}_{s+2}^{s+2}+2\,(2s+3)\,\mathrm{P}_{s+2}^s\}\div 2\,(s+1)$$

After performing the operation (29) on ζ', according to the plan previously outlined, we expand each function in a series of Legendre functions. We require therefore the expansions of P_{s+2}^s, P_s^s when $s = 3n$, $3n-2$, n being an integer. In Table III these functions have their coefficients detailed.

Table III —Expansion of $\mathrm{P}_s^s(\mu)/\mathrm{P}_s^s(0)$ in series of zonal harmonics

	P_0.	P_2	P_4	P_6
$s=1$	0 7854	−0 4909	−0 1104	−0 04896
$s=3$	0 5890	−0 7366	0 1242	0 01497
$s=4$	0 5333	−0 7618	0 2286	—
$s=6$	0 4569	−0 7616	0 3736	−0 0693
$s=7$	0 4111	−0 7194	0 4047	−0 1115
$s=9$	0 3865	−0 7246	0 4940	−0 1840
$s=10$	0 3694	−0 7104	0 5114	−0·2173
$s=12$	0 3411	−0 6820	0 5416	−0 2256

The few terms quoted give a fairly accurate representation of the functions implied. For example, $P_9^9(\mu)/P_9^9(0)$ takes the values 1, 0 274, 0 at the points $\mu = 0, 0{\cdot}5, 1$ For the first position the series gives 0·971 , for the second 0·276 , for the third the positive terms amount to 0 881 and the negative terms to 0·909 The results are correct to within 3 per cent

For the terms in (28) represented by zonal harmonics the operation (29) reduces to $\mu d/d\mu$. For these terms we have the result

$$\mu d P_n/d\mu = nP_n + (2n-3)P_{n-2} + (2n-7)P_{n-4}. \tag{31}$$

Lastly, the operation on $P_2^2(\mu)\,e^{2i\phi}$, gives for $\phi = 0$,

$$-8P_0 - 4P_2. \tag{32}$$

We now proceed to form the equations of condition which determine the coefficients E, F Following out the plan indicated, we operate on $\bar{\zeta}$ with (29) and place $\phi = 0$, α respectively The two series formed are equated to zero By taking half the sum and half the difference of these results we form two new equations, one of which contains only even degrees of harmonics and the other odd degrees (except for the term $HP_2^2(\mu)$) as outlined in (25)

We next use the expansions in zonal harmonics and equate the coefficients of corresponding harmonics to zero, thus forming the required set of equations. For convenience we shall write the value of T_n after the operation (29) and the expansion in zonal harmonics has been performed and ϕ put zero, as

$$T_n(0)\,P_0 + T_n(2)\,P_2 + T_n(4)\,P_4 \quad ,$$

with a similar expression for S_n Further, we shall write the value of

$$(e^{3\kappa i\phi} - e^{-3\kappa i\phi})\,P_{3\kappa}^{3\kappa}(\mu)/P_{3\kappa}^{3\kappa}(0)$$

when these operations have been performed upon it, as

$$\Delta_{3\kappa}(0)\,P_0 + \Delta_{3\kappa}(2)\,P_2 \quad ,$$

and that of

$$(e^{3\kappa i\phi} + e^{-3\kappa i\phi})\,P_{3\kappa}^{3\kappa}/P_{3\kappa}^{3\kappa}(0)$$

as

$$\Delta'_{3\kappa}(0)\,P_0 + \Delta'_{3\kappa}(2)\,P_2 \quad .$$

The equations of condition are then as follow

$$\left.\begin{array}{r}
\sum\limits_{r\,\mathrm{odd}} E_{3r}\,\Delta_{3r}(0)+\sum\limits_{r\,\mathrm{odd}} F_{3r}\,\Delta'_{3r}(0)-\iota\sum\limits_{r\,\mathrm{even}} E_{3r}\,T_{3r}(0)+\iota\sum\limits_{r\,\mathrm{even}} F_{3r}\,S_{3r}(0)\qquad\qquad \\
+\dfrac{H}{8-\beta}(-6+3\ 464\,\iota)\ =0 \\
\sum\limits_{r\,\mathrm{odd}} E_{3r}\,\Delta_{3r}(2)+\sum\limits_{r\,\mathrm{odd}} F_{3r}\,\Delta'_{3r}(2)-\iota\sum\limits_{r\,\mathrm{even}} E_{3r}\,T_{3r}(2)+\iota\sum\limits_{r\,\mathrm{even}} F_{3r}\,S_{3r}(2)\qquad\qquad \\
+\dfrac{H}{8-\beta}(-3+1\ 732\,\iota)\ =0 \\
\sum\limits_{r\,\mathrm{odd}} E_{3r}\,\Delta_{3r}(4)+\sum\limits_{r\,\mathrm{odd}} F_{3r}\,\Delta'_{3r}(4)-\iota\sum\limits_{r\,\mathrm{even}} E_{3r}\,T_{3r}(4)+\iota\sum\limits_{r\,\mathrm{even}} F_{3r}\,S_{3r}(4)\ =0 \\
\cdot \qquad\qquad\qquad\qquad\qquad\qquad\qquad\qquad \cdot \qquad\qquad \\
\sum\limits_{r\,\mathrm{even}} E_{3r}\,\Delta_{3r}(0)+\sum\limits_{r\,\mathrm{even}} F_{3r}\,\Delta'_{3r}(0)-\iota\sum\limits_{r\,\mathrm{odd}} E_{3r}\,T_{3r}(0)+\iota\sum\limits_{r\,\mathrm{odd}} F_{3r}\,S_{3r}(0)\qquad\qquad \\
+\dfrac{H}{8-\beta}(-2-3\ 464\,\iota)\ =0 \\
\sum\limits_{r\,\mathrm{even}} E_{3r}\,\Delta_{3r}(2)+\sum\limits_{r\,\mathrm{even}} F_{3r}\,\Delta'_{3r}(2)-\iota\sum\limits_{r\,\mathrm{odd}} E_{3r}\,T_{3r}(2)+\iota\sum\limits_{r\,\mathrm{odd}} F_{3r}\,S_{3r}(2)\qquad\qquad \\
+\dfrac{H}{8-\beta}(-1-1\ 732\,\iota)\ =0 \\
\sum\limits_{r\,\mathrm{even}} E_{3r}\,\Delta_{3r}(4)+\sum\limits_{r\,\mathrm{even}} F_{3r}\,\Delta'_{3r}(4)-\iota\sum\limits_{r\,\mathrm{odd}} E_{3r}\,T_{3r}(4)+\iota\sum\limits_{r\,\mathrm{odd}} F_{3r}\,S_{3r}(4)\qquad\qquad \\
=0
\end{array}\right\}\quad(33)$$

It is to be noticed that H only appears in the first two of each group of equations

On putting $H = 0$, the determinant of the left-hand members gives an equation which will define the value, or values, of β for which the free period of vibration will synchronise with that taken for the semi-diurnal tide The eliminant is

$$\begin{array}{|cccccccc|}
\multicolumn{1}{c}{\iota F_0,} & \multicolumn{1}{c}{E_3,} & \multicolumn{1}{c}{F_3,} & \multicolumn{1}{c}{\iota E_6,} & \multicolumn{1}{c}{\iota F_6,} & \multicolumn{1}{c}{E_9,} & \multicolumn{1}{c}{F_9,} & \multicolumn{1}{c}{\iota E_{12},} \\
\hline
0, & T_3(0), & -S_3(0), & \Delta_6(0), & \Delta'_6(0), & T_9(0), & -S_9(0), & \Delta_{12}(0), \\
S_0(0), & \Delta_3(0), & \Delta'_3(0), & -T_6(0), & S_6(0), & \Delta_9(0), & \Delta'_9(0), & -T_{12}(0), \\
0, & T_3(2), & -S_3(2), & \Delta_6(2), & \Delta'_6(2), & T_9(2), & -S_9(2), & \Delta_{12}(2), \\
S_0(2), & \Delta_3(2), & \Delta'_3(2), & -T_6(2), & S_6(2), & \Delta_9(2), & \Delta'_9(2), & -T_{12}(2), \\
0, & T_3(4), & -S_3(4), & \Delta_6(4), & \Delta'_6(4), & T_9(4), & -S_9(4), & \Delta_{12}(4), \\
 & & \cdot & \cdot & \cdot & \cdot & \cdot &
\end{array} = 0. \quad (34)$$

Taking two lines and columns of this determinant the solution is $S_0(0) = 0$. The form of $S_0(0)$ is $\frac{2\cdot 945}{15-\beta} + \frac{1\cdot 767}{9-\beta} +$ terms with small coefficients. Hence, omitting the small terms we find as a first approximation $\beta = 11\cdot 3$.

This value of β in the small terms of $S_0(0)$ gives

$$\frac{2\cdot 945}{15-\beta} + \frac{1\cdot 767}{9-\beta} - 0\cdot 0417 = 0$$

This is still satisfied by $\beta = 11\cdot 2$ to three significant figures. Trial and error shows that this value of β is too small. Hence, in taking four rows and columns of (34) we assume the value $\beta = 12$, in all terms except $S_0(0)$. We then find

$$\begin{vmatrix} 0 & +0\cdot 170 & +0\cdot 119 & -0\cdot 211 \\ S_0(0) & -0\cdot 393 & -1\cdot 571 & +1\cdot 128 \\ 0 & +0\cdot 443 & -0\cdot 186 & +0\cdot 308 \\ -0\cdot 543 & -0\cdot 492 & +0\cdot 982 & +0\cdot 714 \end{vmatrix} = 0$$

This yields $$S_0(0) + 0\cdot 88 = 0,$$

whence $$\beta = 12\cdot 4.$$

On taking, similarly, five lines and columns we obtain

$$S_0(0) + 1\cdot 03 = 0,$$

which gives $$\beta = 12\cdot 5$$

Hence, we may say that there is a root at $\beta = 12\cdot 5$,* or $h_0 = 23{,}200$ feet. The mean depth over the area will then be 15,500 feet.

§ 9. *The Semi-Diurnal Tide.*

We next proceed to work out the representative semi-diurnal tide in an ocean with the same boundaries as before, $\phi = 0, \pi/3$, but with $\beta = 11\cdot 5$. This corresponds to $h_0 = 25{,}320$ feet and gives a mean depth over the area of 16,880 feet. On working out the values of the coefficients in (33), we arrive at the equations below. Each entry is multiplied by the quantity at the head of the column and the sum of each line so formed is zero.

---

* The next root appears to be in the vicinity of $\beta = 40$.

F_3	F_9	E_3	E_9	$F_{3\iota}$	$F_{9\iota}$	$E_{9\iota}$	$E_{12\iota}$	H	H_ι
−17·87	+0·064	−1·77	−1·09	−2·93	−1·56	+12·86	+4·04	−19·74	+11·44
+12·50	−0·239	−7·60	+1·925	−8·77	−1·12	−9·09	−2·69	−9·87	+5·72
+1·75	+0·366	−5·13	−1·11	+6·04	+0·925	−2·16	−0·653	0	0
+0·925	−0·229	+1·33	+0·321	+1·92	+0·600	−0·952	−0·055	0	0
+1·35	+1·119	−1·702	−0·294	0	+0·129	−2·44	−0·705	+11·44	−6·58
−2·12	−1·644	−2·418	−0·496	0	−0·699	+3·59	+1·363	+5·72	−3·29
+0·929	+1·204	+0·230	+1·466	0	+0·892	−1·21	−0·970	0	0
−0·204	+0·689	+0·253	−0·397	0	−0·064	+0·326	+0·419	0	0

(35)

The solution of these equations gives the following values —

$$\left.\begin{array}{ll} F_0 = (-5\cdot 98 - 9\cdot 58\iota)\,H & F_6 = (35\cdot 1 + 60\cdot 2\iota)\,H \\ E_3 = (5\cdot 53 - 3\cdot 19\iota)\,H & E_9 = (30\cdot 9 - 18\cdot 2\iota)\,H \\ F_3 = (-2\cdot 15 + 1\cdot 21\iota)\,H & F_9 = (7\cdot 72 - 4\cdot 51\iota)\,H \\ E_6 = (3\cdot 38 + 5\cdot 83\iota)\,H & E_{12} = (-5\cdot 29 - 8\cdot 31\iota)\,H \end{array}\right\} \qquad (36)$$

On substituting these values in (28) we have the following expression for ζ

$$\begin{aligned} \zeta/H = {} & P_0\,(17\cdot 3 + 28\cdot 3\iota) + P_2\,(17\cdot 7 + 29\cdot 9\iota) + P_4\,(-5\cdot 72 - 9\cdot 76\iota) \\ & + P_6\,(0\cdot 502 + 0\cdot 854\iota) \\ & + e^{2\iota\phi}\{(-11\cdot 89 + 5\cdot 47\iota)\,P_2^2 + (+1\cdot 22 - 0\cdot 93\iota)\,P_4^2\} + P_2^2(0) \\ & + e^{2\iota\phi}\{(-16\cdot 91 + 6\cdot 36\iota)\,P_2^2 + (+1\cdot 68 - 1\cdot 26\iota)\,P_4^2\} + P_2^2(0) \\ & + e^{6\iota\phi}\{(9\cdot 19 + 15\cdot 8\iota)\,P_6^6 + (0\cdot 022 + 0\cdot 037\iota)\,P_8^6\} + P_6^6(0) \\ & + e^{-6\iota\phi}\{(9\cdot 00 + 15\cdot 6\iota)\,P_6^6 + (+0\cdot 0189 + 0\cdot 041\iota)\,P_8^6\} + P_6^6(0) \\ & + e^{9\iota\phi}\{(-1\cdot 95 + 1\cdot 11\iota)\,P_9^9 + (-0\cdot 0250 + 0\cdot 0126\iota)\,P_{11}^9\} + P_9^9(0) \\ & + e^{-9\iota\phi}\{(2\cdot 08 - 1\cdot 09\iota)\,P_9^9 + (-0\cdot 115 + 0\cdot 0863\iota)\,P_{11}^9\} + P_9^9(0) \\ & + e^{12\iota\phi}\{(-0\cdot 180 - 0\cdot 250\iota)\,P_{12}^{12} + (-0\cdot 0004 - 0\cdot 0008\iota)\,P_{14}^{12}\} + P_{12}^{12}(0) \\ & + e^{-12\iota\phi}\{(0\cdot 762 + 1\cdot 31\iota)\,P_{12}^{12} + (-0\cdot 0006 - 0\cdot 0010\iota)\,P_{14}^{12}\} + P_{12}^{12}(0) \\ & + 0\cdot 671\,P_2^2\,e^{2\iota\phi} \end{aligned} \qquad (37)$$

In forming ζ as above we take $\zeta' + \bar{\zeta}$. But in applying $\bar{\zeta}$ we may omit the null-function and only use the part which appears in the actual tide-producing potential

The convergence of the above series is not too good But it is probably sufficient for the purposes of illustration, more terms could be added if such were required for a closer estimate of the tide

It is important to test the result (37) to know how far it actually satisfies the conditions at the two boundaries. For that purpose the function ζ' has been submitted to the operation

$$\mu\sqrt{(1-\mu^2)}\frac{\partial}{\partial\mu}+\frac{\iota}{\sqrt{(1-\mu^2)}}\frac{\partial}{\partial\phi}$$

and the numerical values taken at $\mu = 0, \frac{1}{2}$, that is, at the equator and at latitude 45°. From the form of the function it becomes zero at the poles whatever values are used for E, F.

$$\text{At} \quad \mu = 0, \qquad \phi = 0 \quad \begin{cases} \text{Positive terms} = 126 + 140\,\iota \\ \text{Negative terms} = -136 - 149\,\iota \end{cases}$$

$$\phi = \pi/3 \quad \begin{cases} \text{Positive terms} = 132 + 141\,\iota \\ \text{Negative terms} = -131 - 148\,\iota \end{cases}$$

$$\text{At} \quad \mu = 1/\sqrt{2}, \quad \phi = 0 \quad \begin{cases} \text{Positive terms} = 51\cdot5 + 53\cdot4\,\iota \\ \text{Negative terms} = -52\cdot6 - 54\cdot0\,\iota \end{cases}$$

$$\phi = \pi/3 \quad \begin{cases} \text{Positive terms} = 52\cdot1 + 53\cdot7\,\iota \\ \text{Negative terms} = -52\cdot0 - 53\cdot7\,\iota \end{cases}$$

The agreement is satisfactory except at $\mu = 0$, $\phi = 0$. The better agreement at the higher latitude would indicate that more terms of the series are probably requisite for completeness.

§ 10. *Examination of the Results.*

We have shown that an ocean extending from the pole to latitude 45° will have small semi-diurnal tides for depths comparable with those of the Southern Ocean and that only for very small depths of 1,450 feet can resonance occur. For similar oceans extending to 30° and 14½° the semi-diurnal tides are likewise small and the critical depths 526 feet and 38 feet respectively.* This points conclusively to the impossibility of large semi-diurnal tides in the Southern Ocean, even though some allowance be made for the Antarctic continent. The analysis of observations made by exploration parties confirms this low value.†

If the Atlantic tides are derived from those of the Southern Ocean, and the effect of the sun and moon on the Atlantic waters be small, large tides in the former ocean require large tides in the latter ocean. And as we have seen that the semi-diurnal tides of the Southern Ocean are small, those of the Atlantic Ocean must also be small, except in the case of resonance. If resonance should exist, it will apply to the forces producing the semi-diurnal tide in the ocean itself as well as to the tide which might be derived from the Southern Ocean.

---

* 'Proc. Lond. Math. Soc.,' vol. 14, part 1, p. 60 (1915).

† A. T. Doodson, 'Reduction of the Tide Gauge Records, Cape Evans,' p. 6.

We proceed, therefore, to consider the depths of the Atlantic Ocean which would allow of resonance apart from the effects of the Southern Ocean. Taking the Atlantic Ocean as represented by the water contained between two meridian boundaries 60° apart, and taking our results for the depth proportional to the square of the cosine of the latitude, we find that the critical mean depth would be 15,500 feet. The mean depth of the Atlantic Ocean is 12,700 feet. Allowing for the differences of form and depth between the actual and the mathematical cases, this is sufficiently near to indicate an approach to synchronism. The width of the ideal ocean, 60°, is only a rough estimate. It is interesting to inquire what alteration in the width would make the mean depth of the ideal ocean 12,700 feet. Making use of approximations which appear in working out (34), we find that the width should be roughly 53°. A departure of this amount could be easily accounted for by the irregularities of contour of the actual ocean. This seems strong evidence that the Atlantic semi-diurnal tides are due to partial resonance.

It is useful to examine the result (37) to find how the tide height and phase change from point to point along the two boundaries. For this purpose we have used the numerical values of $G_n^m(\mu)$ given by Adams,[*] where

$$P_n^m(\mu) = \frac{(2n)!}{(n-m)!\,n!\,2^n}(1-\mu^2)^{\frac{m}{2}} G_n^m$$

Two sets of values have been calculated, those at the equator and at latitude 45°. The results are —

Latitude	Longitude	Height	Phase
0	0	54H	−88°
0	60°	61H	32°
45°	0	51H	70°
45°	60°	54H	48°

The depth chosen, corresponding to $\beta = 11 \cdot 5$, is near to the critical depth ($\beta = 12 \cdot 5$) and hence the tide heights are large compared with the equilibrium height. The tendency is for the height on the east coast to be higher than that on the west. The phases are very different at the equator, but tend to become equal towards the pole.

---

[*] 'Collected Scientific Papers,' vol 2, p 282 onward.

On the Extraction of Electrons from Cold Conductors in Intense Electric Fields

By O W RICHARDSON, Yarrow Research Professor of the Royal Society.

(Received December 14, 1927)

The discovery of this phenomenon seems to have evolved gradually from Earhart's[*] experiments on very short sparks in 1901 Since 1913 I have been familiar with the fact that in strong fields cold discharges could be made to pass in highly exhausted tubes under conditions which seemed to preclude the co-operation of gas as a factor The phenomena appeared erratic and difficult to interpret Recently, rapid progress has been made in the investigation of this effect especially owing to the researches of Gossling[†] and of Millikan and Eyring,[‡] which have put it on a firm basis

Both Gossling and Millikan and Eyring have found, among other interesting facts, that with field strengths of the order of one million volts per cm electrons can be drawn out of tungsten without the co-operation of gas, that the currents vary very rapidly with the applied voltage, and under proper conditions the current is reproducible and a continuous function of the applied voltage over a wide range, and that the currents at a given voltage are independent of the temperature provided the temperature is not so high as to approach the temperatures at which thermionic emission becomes appreciable

These currents may attain considerable magnitude So far as the experimental evidence goes, it sets no limit either upper or lower In practice the upper limit is set either by the voltage available or by the energy which the apparatus can dissipate and the lower limit by the sensitiveness of the measuring apparatus Millikan and Eyring have recorded the current as a continuous function of the voltage over a range which involves a change by a factor of 10^9 in the current

This is no trifling effect, but one which has to be regarded seriously We have to account for an electron current which is independent of the temperature of the emitting substance but which is a continuous function of the field intensity, and, indeed, to a first approximation is an exponential function of a small power of this intensity I do not believe that any of the rather considerable number of views of the behaviour of metallic conductors at present in circulation are capable of doing this The phenomena can, however, be accounted for along the following lines

---

[*] 'Phil. Mag,' vol. 1, p 147 (1901) For the literature, see J J Thomson's 'Conduction of Electricity through Gases,' and Gossling, and Millikan and Eyring, *loc cit*

[†] 'Phil Mag.,' vol. 1, p 609 (1926)

[‡] 'Phys. Rev.,' vol. 27, p. 51 (1926)

I have often been puzzled by the sharpness of the photoelectric effect at a metallic surface This sharpness is exemplified in two ways (1) The photoelectric effect sets in sharply at a threshold frequency ν_0 below which there is no emission whatever, and (2) if the illumination is with light of frequency $\nu(>\nu_0)$, there is a sharp upper limit to the velocity, or equivalent voltage, of the emitted electrons given by

$$\epsilon V = \tfrac{1}{2}mv^2 = h(\nu - \nu_0)$$

I am not here concerned with the general linear relation between energy and ν or why that is sharp Admitting this to be a curious but fundamental law of Nature which I fully accept as a fact, I have still found it difficult to understand why ν_0 should be so sharp as it is for a solid substance On almost any reasonable view we may take of a metallic conductor, the electrons inside are doing a good many different things and are to be found at any instant in a good many different circumstances Furthermore, they have no special frequency of their own. Any frequency higher than ν_0 will get them out The frequency ν_0 is not a frequency that has anything directly to do with the electrons in the interior It is a property of the surface of the conductor. One might expect that the speed of ejection of an electron by monochromatic light would depend on the condition of the electron at the start, but there is no evidence of it

The sharpness here referred to is not always found in practice, but the fact that it ever occurs seems sufficient There is ground for presuming that in such other cases its absence is due to the operation of secondary causes The value of $h\nu_0$ is identical with the thermionic work function or heat of dissociation so far as can be ascertained These properties, which though not simple are capable of being stated so simply, are also properties of the hydrogen atom They mean that if we look at the escape of an electron from a metallic crystal as a Schroedinger wave problem, there is a limiting value of the energy (probably zero) such that there is a solution for all values of the energy greater than this [This is not the Schroedinger wave problem of Davisson and Germer's experiment, it is a different problem whose nature will become somewhat clearer later on.]

Having found so much of the Schroedinger solutions, it seems reasonable to expect that others of them exist and that, just as in the case of the hydrogen atom so also in the case of the metal crystal, there are a series of proper values of the energy below the limiting value for which the equation has a solution At any rate, I make this hypothesis and see what it leads to Let ψ_n denote one of the wave functions and $\bar{\psi}_n$ its conjugate As the metal is not radiating, it will be in the state determined by ψ_1

It is, I believe, usual to assume that $A\psi\bar{\psi}\,dv$ represents the probability that an electron will be found in the volume element dv, the constant A being determined to agree with the assumption that the electron is always somewhere in space I make the assumption that with A thus determined $\alpha A\psi\bar{\psi}\,dv$ represents the number of electrons actually generated in unit time in the space element dv, where α is a function of the co-ordinates which may be a constant I assume that these electrons will be pulled away from the metal when the applied field is strong enough to overcome the attraction of the metal for them The number of such electrons per unit area multiplied by the elementary charge e will give the density of the current from the conductor

In fig 1 let Oy represent the intersection of the surface of the metal with the plane of the paper, let the curve AB represent the force which attracts

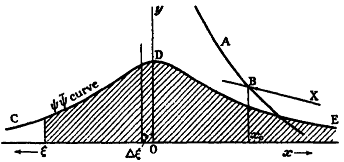

FIG. 1

an electron to the metal, and let the curve BX represent the applied force Xe Except in certain special cases these will intersect at some point B at a distance x_0 from the surface On the suppositions made all electrons generated to the right of x_0 will be carried away by the field An approximate value of x_0 can readily be found At a considerable distance from the surface the force of attraction is that due to the mirror image of the electron in the conductor, viz, $e^2/4x^2$ for a plane surface At distances comparable with the distance between two neighbouring atoms of the conductor, this law of force breaks down, and at the surface itself it becomes an attraction varying as the direct distance x With the fields of force actually used in the experiments, the distance x_0 varies between about 2×10^{-7} and 3×10^{-7} cm. This is about ten times the distance between the atoms (2 5 $\times 10^{-8}$ cm for tungsten) and it is probable that over these distances the mirror image law of force will continue to hold with a close approximation In that case we have

$$e^2/4x_0^2 = Xe \quad \text{or} \quad x_0 = \tfrac{1}{2}e^{\frac{1}{2}}X^{-\frac{1}{2}} \tag{1}$$

and the current will be

$$j = eA\int_{x_0}^{\infty} \alpha\psi\,\overline{\psi}\,dx = eA\int_{\frac{1}{2}e^{\frac{1}{2}}X^{-\frac{1}{2}}}^{\infty} \alpha\psi\,\overline{\psi}\,dx \tag{2}$$

We now suppose the conductor to be made up of a succession of similar sheets of atoms $\Delta\xi$ apart Let CDE (fig 1) be the $\psi_1\overline{\psi}_1$ curve for the most superficial sheet, *i e*, the one in the plane through Oy This curve must be symmetrical about Oy Due to this sheet there will be a contribution to the current $eA_1\int_{x_0}^{\infty}\alpha\psi_1\overline{\psi}_1\,dx$ The constant A_1 may be determined by the relations

$$eA\ \ 2\int_0^{\infty}\psi_1\overline{\psi}_1\,dx = Ne/\Delta\xi^2, \tag{3}$$

if N is the number of electrons associated with each atom which contribute to $\psi_1\overline{\psi}_1$, since $\Delta\xi^{-2}$ is the number of atoms per unit area of each sheet It is to be expected that N will be equal to 1 or to some other small number The contributions to the current from the successive sheets are —

From the second $eA_1\int_{x_0+\Delta\xi}^{\cdot}\alpha\psi_1\overline{\psi}_1\,dx = eA_1\int_{x_0}^{\infty}\alpha\psi_1\overline{\psi}_1\,dx + eA_1\int_{x_0+\Delta\xi}^{x_0}\alpha\psi_1\overline{\psi}_1\,dx,$

" " third $eA_1\int_{x_0+2\Delta\xi}^{\infty}\alpha\psi_1\overline{\psi}_1\,dx = eA_1\int_{x_0}^{\infty}\alpha\psi_1\overline{\psi}_1\,dx + eA_1\int_{x_0+2\Delta\xi}^{x_0}\alpha\psi_1\overline{\psi}_1\,dx,$

" " $(n-1)$th $eA_1\int_{x_0+n\Delta\xi}^{\infty}\alpha\psi_1\overline{\psi}_1\,dx = eA_1\int_{x_0}^{\infty}\alpha\psi_1\overline{\psi}_1\,dx + eA_1\int_{x_0+n\Delta}^{x_0}\alpha\psi_1\overline{\psi}_1\,dx,$

" " last $eA_1\int_{x_0+\frac{\xi}{\Delta\xi}\Delta\xi}^{\infty}\alpha\psi_1\overline{\psi}_1\,dx = eA_1\int_{x_0}^{\infty}\alpha\psi_1\overline{\psi}_1\,dx + eA_1\int_{x_0+\frac{\xi}{\Delta\xi}\Delta\xi}^{x_0}\alpha\psi_1\overline{\psi}_1\,dx,$

if the co-ordinate of the last sheet is ξ The total current density can now be written

$$j = eA_1\left[(1+\xi/\Delta\xi)\int_{x_0}^{\infty}\alpha\psi_1\overline{\psi}_1\,dx - \sum_{n=0}^{n=\xi/\Delta\xi}\int_{x_0}^{x_0+n\Delta\xi}\alpha\psi_1\psi_1\,dx\right]. \tag{4}$$

This is for a conducting plate whose thickness is ξ As ξ is increased j must soon come to a limit which is independent of ξ

We must now consider the functions ψ we are here dealing with It is not difficult to find a single function which will reduce to an attraction varying as the direct distance for small distances and as the inverse square of the distance for larger distances. Such a function would be, for example,

$$Axe^{-ax} + \frac{e^2}{4x^2}e^{-\frac{1}{ax}}$$

A and *a* constants, which would give the ψ equation

$$\frac{d^2\psi}{dx^2} + \left(\frac{2mW}{K^2} + \frac{2me_1}{K^2}\left[A(1+ax)\frac{e^{-ax}}{a^2} + \frac{ae_1}{4}\left(1 - e^{-\frac{1}{ax}}\right)\right]\right)\psi = 0, \tag{5}$$

where $K = h/2\pi$, e_1 the electronic charge, m the mass and W the energy I have not had any success in investigating the proper values and characteristic functions of this equation I have, therefore, abandoned this method for a more approximate attack on the problem.

It is to be remembered that we are dealing with effects which are believed to be occurring at distances comparable with 3×10^{-7} cm from the surface of the conductor, and that this is a rather large distance from the standpoint of equation (5) Accordingly, we should expect to get a fair approximation to the actual state of things at these distances if we replace equation (5) by the equation into which it degenerates when ax is large. Physically, this is the same as replacing the actual conductor by the usual conventional conductor which has no molecular structure The equation then simplifies to

$$\frac{d^2\psi}{dx^2} + \left(\frac{2mW}{K^2} + \frac{me^2}{2K^2x}\right)\psi = 0 \tag{6}$$

I find that the proper values for this equation are

$$w_1\ w_2\ w_3 \quad w_n \quad = -\frac{me^4}{32K^2}\left(\frac{1}{1^2}, \frac{1}{2^2}, \frac{1}{3^2} \quad \cdot \frac{1}{n^2} \quad \right).$$

In fact, they are the same as for an electron revolving round a nucleus if the electron and the nucleus have a charge $= \pm \frac{1}{2}e$. The characteristic functions are

$$\psi_1(x) = xe^{-\frac{me^2}{4K^2}x}, \tag{7}$$

$$\psi_2(x) = xe^{-\frac{1}{2}\frac{me^2}{4K^2}x} - \frac{3}{2}\frac{me^2}{4K^2}x^2e^{-\frac{1}{2}\frac{me^2}{4K^2}x}, \tag{8}$$

and so on

We can now justify the approximation we are making in another way. If we regard equation (5) as a superposition of equation (6), which operates at large distances, and of

$$\frac{d^2\psi}{dx^2} + \left(\frac{2mW}{K^2} - bx^2\right)\psi = 0, \tag{9}$$

which operates at small distances, we see that this is the equation of a Planck oscillator As is well known, the characteristic functions of this are the Hermitic orthogonal functions

$$e^{-\frac{z^2}{2}}H_n(z), \ \ H_n(z) = (-1)^n e^{z^2}\frac{d^n e^{-z^2}}{dz^n}, \ z = xb^{\frac{1}{4}},$$

and the proper values are

$$\frac{2mW}{K^2 b^{\frac{1}{2}}} = 1, 3, 5, \quad 2n-1, \ . \tag{10}$$

The first function is

$$\psi_1(x) = e^{-\frac{1}{2}\frac{2mW_1}{K^2}x^2} \tag{11}$$

If (11) and (7) are each normalised so that in each case $\psi\overline{\psi}$ corresponds to charges per unit area of the same order of magnitude, the numerical calculation shows that at a distance of 10^{-7} cm or more the contribution of (11) to $\psi\overline{\psi}$ is negligible compared with that from (7)

We now substitute the value of $\psi_1(x)$ from (7) in (4) As nothing is known of the nature of the function α, I shall start by treating it as a constant and reconsider the matter later in the light of the experimental data Writing a_1 for $me^2/4K^2$ we have

$$\int_{x_0}^{\infty} x^2 e^{-2a_1 x}\,dx = \frac{1}{2a_1}\left(x_0^2 + \frac{x_0}{a_1} + \frac{1}{2a_1^2}\right)e^{-2a_1 x_0}, \tag{12}$$

$$\sum_{n=0}^{n=\xi/\Delta\xi}\int_{x_0}^{x_0+n\Delta\xi} x^2 e^{-2a_1 x}\,dx = (1+\xi/\Delta\xi)\frac{1}{2a_1}\left(x_0^2 + \frac{x_0}{a_1} + \frac{1}{2a_1^2}\right)e^{-2a_1 x_0}$$
$$-\frac{1}{2a_1}e^{-2a_1 x_0}\sum_{n=0}^{n=\xi/\Delta\xi} e^{-2a_1 n\Delta\xi}\left(\overline{x_0+n\Delta\xi}^2 + \frac{x_0+n\Delta\xi}{a_1} + \frac{1}{2a_1^2}\right).$$

The sum on the right-hand side is

$$= \left(\sum_{n=0}^{n=\infty} - \sum_{n=1+\xi/\Delta\xi}^{n=\infty}\right)\left(e^{-2a_1 n\Delta\xi}\left[x_0^2 + \frac{x_0}{a_1} + \frac{1}{2a_1^2} + \left(2x_0 + \frac{1}{a_1}\right)n\Delta\xi + (n\Delta\xi)^2\right]\right)$$
$$= \left(x_0^2 + \frac{x_0}{a_1} + \frac{1}{2a_1^2}\right)\frac{1-e^{-2a_1\overline{\xi+\Delta\xi}}}{1-e^{-2a_1\Delta\xi}} + \left(2x_0 + \frac{1}{a_1}\right)(-\tfrac{1}{2})\frac{d}{da_1}\left(\frac{1-e^{-2a_1\overline{\xi+\Delta\xi}}}{1-e^{-2a_1\Delta\xi}}\right)$$
$$+\frac{1}{4}\frac{d^2}{da_1^2}\left(\frac{1-e^{-2a_1\overline{\xi+\Delta\xi}}}{1-e^{-2a_1\Delta\xi}}\right).$$

So that finally

$$j_\xi = \alpha\frac{e\mathrm{A}_1}{2a_1}e^{-2a_1x_0}\left\{x_0^2+\frac{x_0}{a_1}+\frac{1}{2a_1^2}-\left(x_0+\frac{1}{2a_1}\right)\frac{d}{da_1}+\tfrac{1}{4}\frac{d^2}{da_1^2}\right\}\left(\frac{1-e^{-2a_1\overline{\xi+\Delta\xi}}}{1-e^{-2a_1\Delta\xi}}\right) \tag{13}$$

As ξ increases without limit this expression goes to the limit

$$j = \frac{e\mathrm{A}_1}{2a_1}\alpha e^{-2a_1x_0}\left\{x_0^2+\frac{x_0}{a_1}+\frac{1}{2a_1^2}-\left(x_0+\frac{1}{2a_1}\right)\frac{d}{da}\right\}+\tfrac{1}{4}\frac{d^2}{da^2}(1-e^{-2a_1\Delta\xi})^{-1} \tag{14}$$

As was required, the right-handside of (14) is independent of ξ On carrying out the differentiations this becomes

$$j = \frac{e\mathrm{A}_1}{2a_1}\alpha\frac{e^{-2a_1x_0}}{1-e^{-2a_1\Delta\xi}}\left\{x_0^2+\frac{x_0}{a_1}+\frac{1}{2a_1^2}+\left(x_0+\frac{1}{2a_1}\right)\frac{2\Delta\xi e^{-2a_1\Delta\xi}}{1-e^{-2a_1\Delta\xi}}\right.$$
$$\left.+\frac{\Delta\xi^2(1+e^{-2a_1\Delta\xi})e^{-2a_1\Delta\xi}}{(1-e^{-2a_1\Delta\xi})^2}\right\} \tag{15}$$

There are no adjustable constants except α on the right-hand side of equation (15) a_1 is the absolute constant

$$a_1 = \pi^2 me^2/h^2 = 4\ 69\times 10^7\ \mathrm{cm}^{-1},\quad x_0 = \tfrac{1}{2}e^{\frac{1}{2}}\mathrm{X}^{-\frac{1}{2}},$$

and is determined by the value of X and varies between $1\ 8\times 10^{-7}$ and 3×10^{-7} cm., $\Delta\xi$ is the distance between the layers of atoms of the conductor and is taken to be $2\ 535\times 10^{-8}$ cm for tungsten, A_1 is determined by the relation

$$\mathrm{A}_1 = \frac{\mathrm{N}e}{(\Delta\xi)^2}+2e\int_0^\infty\psi\bar{\psi}\,dx = \frac{2\mathrm{N}a_1^3}{(\Delta\xi)^2}, \tag{16}$$

taken for a single sheet Putting in the values of a_1 and of $\Delta\xi$ (for W) the bracket on the right-hand side of (15) becomes

$$x_0^2+2\ 655\times 10^{-8}x_0+3{\cdot}16\times 10^{-16}$$

This is the same as $(x_0+1\ 328\times 10^{-8})^2$ to about 1 part in 400, so that, putting in the above values of A_1, x_0 and a_1 we can, for practical purposes, write (15) as

$$j = \frac{\mathrm{N}ea_1^2x}{(\Delta\xi)^2(1-e^{-2a_1\Delta\xi})}(\tfrac{1}{2}e^{\frac{1}{2}}\mathrm{X}^{-\frac{1}{2}}+1\ 38\times 10^{-8})^2 e^{-\frac{\pi^2 me^{5/2}}{h^2}\mathrm{X}^{-\frac{1}{2}}} \tag{17}$$

I wish to compare this equation with the results of the measurements of Millikan and Eyring Their field strengths are expressed in megavolts per cm

If M is the field strength expressed in these units, then $M = 3 \times 10^{-4} X$ and $X^{-\frac{1}{2}} = \sqrt{3} \times 10^{-2} M^{-\frac{1}{2}}$ With this substitution we have

$$j = \frac{3Ne^2 a_1{}^2 \alpha}{4 \times 10^4 (\Delta\xi)^2 (1 - e^{-2a_1\Delta\xi})} (M^{-\frac{1}{2}} + 6·75 \times 10^{-2})^2 e^{-\frac{\pi^2 m e^{5/2}}{h^3}\frac{\sqrt{3}}{10^2}M^{-\frac{1}{2}}} \qquad (18)$$

Putting

$$A = \frac{3Ne^2 a_1{}^2 \alpha}{4 \times 10^4 (\Delta\xi)^2 (1 - e^{-2a_1\Delta\xi})}, \quad b = \frac{\pi^2 m e^{5/2}}{h^3}\frac{\sqrt{3}}{10^2}, \qquad (19)$$

and taking logarithms, we have

$$\log_{10} j - 2 \log_{10} (M^{-\frac{1}{2}} + 6·75 \times 10^{-2}) = \log_{10} A - M^{-\frac{1}{2}} b \log_{10} e. \qquad (20)$$

I have plotted $\log_{10} i - 2 \log_{10} (M^{-\frac{1}{2}} + 6·75 \times 10^{-2})$ plus a constant $(3 - \log_{10} 3)$ against $M^{-\frac{1}{2}}$ in fig 2 It will be seen that the points, which are shown thus, ×, come close to satisfying the linear relation between $\log_{10} j - 2 \log_{10} (M^{-\frac{1}{2}} + 6·75 \times 10^{-2})$ and $M^{-\frac{1}{2}}$ There is an indication of some curvature, the points would fit more closely on to a line slightly concave towards the origin In fig 2 the quantity i is the actual current (in e s u) not the current density j

The slope of the line in fig 2 gives $b = 11·58$ The value calculated by putting $\pi = 3·14$, $m = 8·96 \times 10^{-28}$, $e = 4·77 \times 10^{-10}$ and $h = 6·55 \times 10^{-27}$ in (19) is 7·72. This is two-thirds of the value given by the experiments. It is evident that we cannot assume the function α to be a constant, and the experimental data suggest the assumption $\alpha = C\sqrt{\psi\bar{\psi}} = Cxe^{-a_1x}$, where C is a constant A recalculation along the lines already described, but with the substitution of this value of α inside the integrals, gives the approximate formula

$$j = \left(\frac{3e}{4 \times 10^4}\right)^{3/2} \frac{2NeCa_1{}^3}{3 (\Delta\xi)^3 (1 - e^{-2a_1\Delta\xi})} (M^{-\frac{1}{2}} + 4·59 \times 10^{-2})^3 e^{-\frac{3\pi^2 m e^{5/2}}{2h^3}\frac{\sqrt{3}}{100}M^{-\frac{1}{2}}}. \qquad (21)$$

In this equation M is in megavolts per centimetre and e and j in electrostatic units. The results of plotting $\log i - 3 \log (M^{-\frac{1}{2}} + 4·59 \times 10^{-2})$ against $M^{-\frac{1}{2}}$ are shown by the circles in fig 2 This change has not made much difference, but the deviation from linearity is a little more evident. The exponential factor is now equal to 1·5 times b, so that the experimental and theoretical slopes are the same.

There is some uncertainty about the magnitude of the constant C required to fit the experiments. This is due to the fact that the currents do not flow from the whole surface of the wires, but only from limited regions which are of uncertain extent I have calculated C on the assumption that the current arises uniformly all over the surface of the wire This should therefore be only a lower limit to the true value of C But it will probably give the order of magnitude of C correctly The value so found is $C > 4\ 42 \times 10^{17}$ cm $^{-1}$ sec $^{-1}$ There is a combination of m, e, c and h which has these dimensions, and this order of magnitude, viz, $m^2\ e^4/ch^6 = 9\ 02 \times 10^{17}$ This is equal to the square of the minimum length h/m_0c multiplied by the velocity of light divided by a four-dimensional volume whose linear dimensions are comparable with the distance in which the wave functions have an appreciable fraction of their maximum value Whether this fact has any significance or not I do not know The experimental results suggest that the constant which corresponds to C is specific for each substance and probably related to the thermionic work

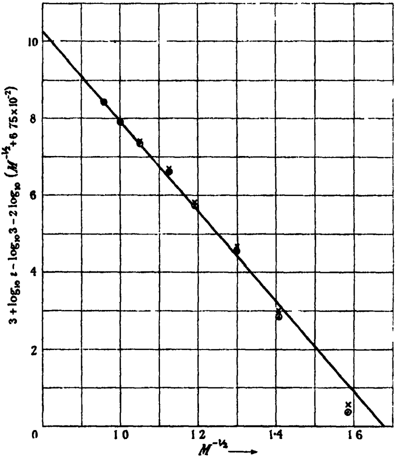

Fig 2

function The present theory has been simplified to a degree which has taken away such specific properties, and it is probably not competent to determine the value of this constant

The doubtful element in the area from which the electrons are emitted does not affect the value of the constant b directly, because this is determined from the *ratio* of the currents at two different voltages The ascertained value of b will, however, be affected if the localisation of the currents is due to discharges from points, because this will make the true electric intensity higher than the value calculated from the dimensions of the apparatus In fact, the matter can be put generally Let j and X be the true values of the current density and of the electric intensity respectively, and let jm, Xm be the measured values Let $j = \alpha jm$ and $X = \beta Xm$ Then the quantities we deduce from the experiments when we think we are deducing b and C are $\beta^{-\frac{1}{2}} b$ and $C\alpha^{-1} \beta^{3/2}$ respectively Evidently, if point discharges were the origin of the emission spots, the values of b would be liable to considerable errors

In my judgment the experimental evidence does not support the view that the spots are due to discharges from small local protuberances In Millikan and Eyring's observations I find that the slope b for a wire conditioned at 2700° K is the same as for a wire conditioned at 700° K, although the effect of conditioning at the higher temperature has reduced the absolute value of the currents by a factor of about 10^5 Gossling has many data bearing on this He gives a very large number of curves taken under all sorts of conditions Although the current at a fixed voltage changes by enormous factors, all these curves have practically the same value of b Using the equation $i = Ae^{bX^{1/n}}$ which he has deduced empirically and which is indistinguishable from mine over a small range, he gives his average as 17 as compared with the value 11 58 which I have deduced from Millikan and Eyring's observations Moreover, he finds that the gradient is the same for discharges from points as for discharges from wires to the degree of accuracy with which the field strength can be deduced from the form of the point This seems to require definitely that the field strengths as calculated from the geometry of the apparatus are substantially right and that the localisation of the discharges from the wire in restricted areas is not due to these areas being sharp protuberances, but to something else

The whole of the experimental evidence points to the view that the factor of $X^{-\frac{1}{2}}$ in the exponential stays constant, or nearly so, under a great variety of conditions, whilst the factor corresponding to C changes enormously The localisation of the discharge in spots must then be attributed to the possession by different parts of the surface of a different constitution. There is plenty of evidence that such local areas are often present.[*] Gossling has produced evidence that the deposition of a very electropositive metal like sodium on the cathode increases the emission enormously by increasing the constant factor A and leaving b practically unchanged. There is a strong presumption that the opposite process which occurs when a tungsten wire is conditioned by heating is due to the evaporation of the more electropositive contaminants. The present theory does not account for these features, which probably have their roots in the difference between an equation of the type of (5) and the very much simplified equation (6), which alone I have been able to solve. It is just possible that these very great changes in the absolute values of the currents at a given field strength are due to some other cause such as magnification of the currents from the cathode by bombardment with positive ions generated at the anode, but it seems very unlikely.

If this theory is correct, it seems to carry the following implications. In the neighbourhood of a nucleus, electrons are discontinuously coming into space and are generated at a rate which is proportional to $(\psi\bar{\psi})^{3/2}$. Perhaps this is tying down the interpretation of the experimental results too narrowly at the present stage, so we may replace it by the more general statement that this rate of generation is some function of $\psi\bar{\psi}$. So far as I am aware, there is no evidence of the permanent creation of an excess of electrons in this way. (There is, of course, astronomical evidence of the disappearance of electrons.) This seems to mean that a nucleus is an electron sink as well as a centre of electron sources. From this point of view a proton can be looked upon as a relatively permanent hole in the boundary of space time. This seems to offer a picture to account for the fact that the proton and electron have the same charge, because any hole which is too small to let one electron through might be no hole at all from this standpoint. In other words, there seems to be a possibility of reducing the number of necessary atomicities by unity.

There is one property of these field currents which has not so far been considered. It is only at low temperatures that they are independent of the temperature. At temperatures high enough for the thermionic currents to be measurable, the field currents do become functions of the temperature. In fact, at these temperatures both thermionic and field currents are functions both of the temperature and the field strength, and the two phenomena become more or less inextricably mixed up This is to be expected from the present point of view The temperatures at which the thermionic currents are measurable mean those temperatures at which the number of electrons which are able to get beyond the threshold, *i e*, to dissociate, is appreciable But if some electrons are able to get beyond the threshold, it means that many others must now be in the various possible states below the threshold This means that we have not only to deal with ψ_1 but with ψ_2 ψ_3 ψ_4 Since the number in any specified state, say the state with the function ψ_n, is a function of the temperature, this means that the field currents must now be a function of the temperature The problem of finding the distribution of the ψ_n at any temperature is a simplified form of the problem of the specific heat of atomic hydrogen at temperatures at which the higher electronic states become excited To get the field currents we should have to work through the processes of this paper for each $\psi_n\bar{\psi}_n$, multiply this result by the number of electrons in the ψ_n state and sum the result from 1 to ∞ This would appear to be no light task

---

[*] *Cf.* Richardson and Young, 'Roy. Soc. Proc.,' A, vol. 107, p. 377 (1925). Richardson and Brotherton, 'Roy. Soc. Proc.,' A, vol. 115, p. 20 (1927).

If the view put forward in this paper is right, the absorption spectrum of a thin metal film might be expected to have a line spectrum present in it I am looking for this in the laboratory

OBITUARY NOTICES

OF

FELLOWS DECEASED.

CONTENTS.

PAGE

Sir William Augustus Tilden (with portrait) i

Arthur William Crossley (with portrait) vi

William Burnside (with portrait) xi

Willem Einthoven (with portrait) xxvi

Henry Martyn Taylor (with portrait) . . . xxix

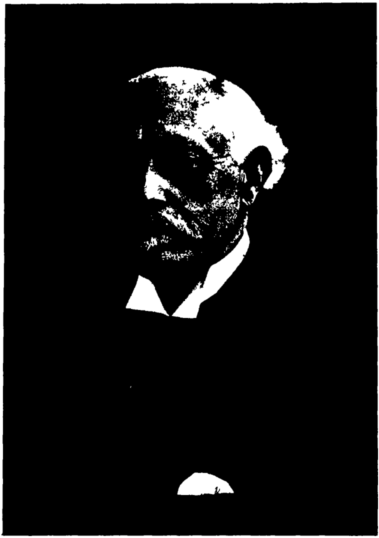

William A. Tilden

SIR WILLIAM AUGUSTUS TILDEN—1842–1926

ALTHOUGH the Tilden family was long connected with the county of Kent, the subject of this notice was born in London on the 15th of August, 1842, as the elder son of Augustus Tilden, clerk in the Bank of England, and later the manager of a provincial bank Young Tilden attended school successively in Kidderminster, Bedford and East Dereham, and it was from a visiting master's occasional lectures at the last-mentioned place that the boy picked up some notions of chemistry and developed the desire to become an experimenter

Chemistry in the wider sense was probably a branch of knowledge unrecognised by Tilden's parents, and it seems that they thought to meet his aspirations by apprenticing him, while yet barely fifteen years of age, to a pharmaceutical chemist at Barnsbury He was fortunate in his employer, Mr Alfred Allchin, who, having acted as assistant in the Pharmaceutical Society's laboratory and worked for a short time in Pelouze's laboratory in Paris, had an outlook beyond the limits of the pharmacy The young apprentice was encouraged to attend lectures at the Pharmaceutical Society, and those of Hofmann at the Royal College of Chemistry, and to make as many chemical preparations as his duties permitted In 1861, Tilden was awarded the first Bell Scholarship at the Pharmaceutical Society, and at the end of his apprenticeship he became a junior assistant in Dr John Stenhouse's private laboratory, returning a year later to the Pharmaceutical Society as Demonstrator under Attfield, then Professor of Practical Chemistry

A period of hard work followed, with academic qualifications as the objective, the end being achieved by the award of the B Sc with Honours, in 1868, and the D.Sc by examination in 1871 Fortified with these credentials and with some record of experimental research, Tilden was appointed, in 1872, Senior Science Master at Clifton College, under the headship of Dr Percival, afterwards Bishop of Hereford One of his associates at Clifton for a time was W A Shenstone, who was later to succeed him in the Senior Science Mastership After eight strenuous years of teaching and research in this institution, Tilden was elected to the Chair of Chemistry in the Mason College at Birmingham.

The early days in the development of the newly-founded College made heavy demands on the energy of the professors, and the first occupant of the Chemistry Chair was called upon to teach metallurgy as well The practical work of the metallurgical laboratory, however, was in charge of Mr Thomas Turner, afterwards Professor of Metallurgy, and in chemical research work, especially during the later period of his association with Mason College, Tilden had the assistance of such collaborators as M O Forster, J H Millar and S W. Williamson

In 1894, Tilden was appointed to the Chair of Chemistry at the Royal College of Science and the Royal School of Mines in succession to Prof T E Thorpe, and this position he occupied until his final retirement from active academic work in 1909 It was during his tenure of this post that the extensive new laboratories of the Royal College of Science were erected, and the design and equipment of these was a main concern of the Professor of Chemistry For a period also, up to the inauguration of the Imperial College of Science and Technology, Tilden acted as Dean of the Royal College of Science and the Royal School of Mines, and it was on his retirement from this office that he received the honour of knighthood

In all the four institutions with which he was connected at one time or another during his career, Tilden was active in the prosecution of research, and the contributions which he made to chemical knowledge were recognised by his election into the Royal Society in 1880, his appointment as Bakerian Lecturer in 1900, and the award of the Davy Medal in 1908 Honorary degrees were conferred on him by Dublin, Victoria and Birmingham, and in 1899 he was appointed a Fellow of the University of London He served as a Vice-President of the Royal Society from 1904 to 1906, and he took a very prominent part in the affairs of the Chemical Society, which he served first as an Ordinary Member of Council, then as Treasurer, and finally as President for the period 1903-05 The well-known "Annual Reports" of the Chemical Society owe their inception to Tilden, who in his Presidential Address of 1904 stressed the desirability of some periodic review of progress in the various branches of the science

The character of Tilden's earliest researches was obviously influenced by his association with pharmaceutical chemistry A number of these were concerned with the aloins, the purgative principles obtained by the extraction of aloes from various sources Tilden was able to show that in certain cases (the barbaloins) oxidation of aloin with nitric acid led to the production of chrysammic acid as well as oxalic and picric acids

More significant was the research carried out at Clifton on "Aqua Regia and the Nitrosyl Chlorides," undertaken in the hope of adding to the number of organic nitroso-compounds by utilising nitrosyl chloride It was shown that the substance with the formula $NOCl$ is the only compound of nitric oxide and chlorine, and that it may be conveniently prepared in a state of purity by gently heating a mixture of acid nitrosyl sulphate (or simply sulphuric acid saturated with the *aqua regia* gases) with dry sodium chloride A study of the action of nitrosyl chloride on organic substances led to the discovery of pinene nitrosochloride and the adoption of nitrosyl chloride as a valuable reagent in the investigation of terpenes generally For many years thereafter Tilden, either alone or with collaborators, continued to publish the results of investigations in this difficult region, endeavouring to elucidate the constitution of the terpenes and their relation to other known substances

One of these other substances which attracted Tilden's attention was the hydrocarbon isoprene, C_5H_8 This compound when heated to 280° forms a terpene (as had been shown by Bourchardat), while on the other hand Tilden found that the decomposition of turpentine by heat yielded a small quantity of a liquid resembling isoprene In a research described in the 'Journal of the Chemical Society' in 1884, this decomposition was examined in some detail, and the conclusion was reached that ordinary turpentine oil, when heated just short of redness, is mostly transformed in four different ways —(*a*) By conversion into an optically inactive terpene, (*b*) by polymerisation into a "colophene", (*c*) by resolution into cymene ($C_{10}H_{14}$) and hydrogen, (*d*) by splitting into two molecules of isoprene Further, expression is given to the view that the terpenes are in no sense aromatic compounds or constituted on the type of benzene In a later paper entitled "The Constitution of the Terpenes and of Benzene" (1888), Tilden admits, more especially in view of Wallach's researches, that the terpenes almost certainly contain a nucleus of six carbon atoms, but challenges the opinion that these atoms are disposed in the manner assumed for benzene This contention was enforced by comparative experiments with cymene and natural terpenes, showing that the latter, in contrast with the former, do not yield appreciable quantities of aromatic acids on oxidation

It was in connection with his work on isoprene that Tilden made the striking observation of the conversion of this hydrocarbon to caoutchouc, as announced to the Philosophical Society of Birmingham in 1892 It was already known that under the influence of strong acids isoprene was converted into a tough elastic solid which appeared to be true indiarubber, but Tilden observed that specimens of isoprene prepared from various terpenes were changed merely on standing into syrupy fluids, in which masses of a yellowish solid (found to be indiarubber) were floating This apparently spontaneous conversion of isoprene to indiarubber, it was suggested, might be due to the presence of traces of acetic or formic acid, produced by the oxidising action of the air. The liquid was found to be acid to test-paper, and yielded a little unchanged isoprene The artificial rubber, so far as solubility in benzene and carbon disulphide and action towards sulphur are concerned, behaves exactly like the natural material Some of the original specimens of this artificial rubber are preserved in the Science Museum at South Kensington.

With the help of his research students, Tilden continued investigation in the terpene field during the greater part of his academic career Much attention was devoted to pinene nitrosochloride, the conditions of its preparation, its reactions with other substances and its significance in relation to questions of constitution. The use of nitrosyl chloride as a reagent in organic chemistry was further explored in a number of directions, and it was found, for example, that its action on phenyl hydrazine gave readily a large yield of phenyl diazoimide

Tilden's research activities, however, were not confined to the organic field. In conjunction with W A Shenstone he carried out a series of determinations of the solubility of salts in water at temperatures above 100°, and was able to show, in the case at least of anhydrous salts, that the increase of solubility for a given rise of temperature was greatest in the case of the most fusible salt. This parallelism between solubility and fusibility was later extended to isomorphous salts containing the same amount of water of crystallisation These investigations, as well as others dealing with the influence of temperature on the heat of dissolution of salts in water, were carried out in the hope of throwing light on the vexed question of the nature of solutions

A study of the condition in which helium and allied gases exist in minerals such as monazite and cleveite led Tilden to the observation that on heating granite notable quantities of hydrogen, containing carbon dioxide but no helium, are expelled The view was taken that the rocks in question had crystallised in an atmosphere rich in carbon dioxide and steam and in contact also with some easily oxidisable substance

Among the problems in inorganic chemistry which attracted Tilden's attention was the question of the formulæ of phosphoric anhydride and metaphosphoric acid Vapour density determinations were carried out with all due precautions and the formulæ P_4O_{10} and $(HPO_3)_2$ were deduced Metaphosphoric acid was found to be far more readily volatile than was commonly supposed

Tilden's chief contribution, however, to our knowledge of inorganic and physical chemistry consists in his well-known investigation of the specific heats of metals The results of these researches were incorporated in three memoirs published in the "Philosophical Transactions," the first of which constituted the Bakerian Lecture for 1900 The starting point was the question as to the atomic weights of cobalt and nickel, but the enquiry developed into an experimental study of the validity of Dulong and Petit's Law, primarily in connexion with these two metals Joly's steam calorimeter was employed in a series of careful determinations of the mean specific heat of pure cobalt and nickel between 15° and 100°, and the results showed that the atomic heat of nickel is somewhat greater than that of cobalt As an extension of the research, measurements of mean heat capacity were made over lower ranges of temperature, down to $-182.5°$, and the decrease in the atomic heat with falling temperature—since recognised as a general phenomenon of great significance—was definitely established

Extension of the temperature range upwards, and the inclusion of aluminium, silver and platinum among the metals examined proved that the influence of change of temperature on specific heat is in the inverse order of the atomic weights of the metals compared—that is, greatest in the case of aluminium and least in the case of platinum Measurements were made also of the heat capacity of compounds, the materials chosen being such that the specific heat of each component element in the solid state could be determined independently The substances selected were the tellurides of silver, nickel and tin, and two silver-aluminium alloys, and these were examined over a wide range of temperature The general validity of Neumann's law was established, and notwithstanding the fact that at a given temperature the atomic heats of elements in the solid state may be widely different, the molecular heat was found to be at all temperatures approximately equal to the sum of the atomic heats of the constituents

Apart from original memoirs, Tilden made considerable contributions to general chemical literature, his best known book probably being the "Introduction to the Study of Chemical Philosophy," an exposition of the principles of chemistry on broad and philosophic lines It appeared first in 1876, and passed through eleven editions Other successful volumes were his "Practical Chemistry," and a "Manual of Chemistry, Theoretical and Practical" (based on Watts' edition of 'Fownes' manual') In his later years, Tilden wrote more especially on historical and biographical topics, as, for example, in "The Progress of Scientific Chemistry in our own Times," "Chemical Discovery and Invention in the Twentieth Century," "Sir William Ramsay Memorials of his Life and Work," and "Famous Chemists the Men and their Work" Noteworthy also in this connexion were the Memorial Lectures on Mendeléeff and Cannizzaro delivered before the Chemical Society

After a period of enfeebled health, Tilden passed away on the 11th December, 1926, in the eighty-fifth year of his age He is survived by Lady Tilden, as well as by the son of a former marriage A distinguished worker and teacher in chemical science, an eminent and courtly figure among British chemists, his memory will be cherished especially by those who knew his gracious personality and his qualities as colleague and friend

J C P

ARTHUR WILLIAM CROSSLEY—1869-1927 *

ARTHUR WILLIAM CROSSLEY was born at Bentcliffe, Accrington, on February 25, 1869 Of his boyhood little of interest can be recalled, it seems to have been uneventful and happy From preparatory school he went in 1881 to Mill Hill, where he stayed until Easter, 1885 The next three months were spent in Paris In the following October he entered Owens College, but, owing to an illness which caused the loss of a year, he did not obtain his Honours degree of B Sc until 1890

After a session spent in Prof (now Sir Arthur) Schuster's laboratory, which led to the joint publication of a paper on the electro-deposition of silver ('Roy Soc Proc.,' vol. 50, p 344 (1892)), Crossley went to Emil Fischer at Würzburg in October, 1891, stayed there until Fischer was translated to Berlin in succession to A W von Hofmann in the autumn of 1892, and remained with him in Berlin until the Christmas of that year Before leaving Würzburg the degree of Ph.D was conferred on him for his thesis entitled "I., Ueber die Oxydation einiger Dicarbonsaüren, II, Ueber das optische Verhalten des Dulcits und seiner Derivate"

Returning to Owens College early in 1893 to undertake research work with W. H Perkin, junr, he was elected to a Bishop Berkeley research fellowship in the following year and became President of the College Union, revealing in the conduct of its affairs thoroughness and a sanity of judgment that later came to be recognised as characteristic In April, 1895, he was appointed teacher and demonstrator in physics and chemistry at St. Thomas's Hospital Medical School, where he succeeded Prof (now Sir Wyndham) Dunstan as chemical lecturer and consulting chemist in October, 1900 Four years later he became Professor of Chemistry at the Pharmaceutical Society's School of Pharmacy, Bloomsbury Square

As the outcome of Crossley's research work at Owens College, two papers were published jointly with Perkin, the first in 1894 under the title "Substituted pimelic acids" ('J Chem. Soc., vol 65, p 987) and the second in 1898, nearly three years after his departure from Manchester, entitled "Decomposition of camphoric acid by fusion with potash or soda" ('J. Chem. Soc.,' vol. 73, p. 1) Dihydrocamphoric acid, one of the products mentioned in the second paper, was the starting point of the series of investigations which occupied

---

* Abridged from the notice published in the 'Journal of the Chemical Society.'

Arthur W. Crossley.

his attention until the outbreak of the war and led to the publication of some 40 papers. With some of the early communications from St. Thomas's Hospital, the late Dr H. R. Le Sueur was associated, and in many of those from the School of Pharmacy Miss Nora Renouf was his collaborator

The earliest papers of the series dealt with attempts to synthesise $\alpha\alpha_1\beta\beta$-tetramethyladipic acid on the assumption that dihydrocamphoric acid had that constitution. Of the intermediates examined, 1 : 1 · 2-trimethyldihydroresorcin, obtained for the purpose by the condensation of mesityl oxide and ethyl sodiomethylmalonate, and 1 1-dimethyldihydroresorcin, its lower homologue, which had been made slightly earlier by Vorländer, proved so unexpectedly reactive that the original quest was abandoned In its place, the detailed study of these hydroaromatic compounds and of their reduction, halogen and ketonic derivatives was pursued with ardour, leading as it did to the production of *o*-xylene derivatives by the migration of one of the members of the *gem*-dimethyl group

It was during his tenure of the Chair at the School of Pharmacy, which lasted from 1904 to 1914, that Crossley first found scope for the exercise of those qualities of organisation, tact and driving power which later were to be of inestimable service to the State Not unnaturally, all through this period, he looked to a University Chair as his ultimate aim When, therefore, he was appointed Professor of Organic Chemistry in King's College, London, in June, 1914, the wider opportunities for teaching and research that he coveted seemed at length to be his. But Fate willed otherwise. Within little more than a month, the Great War broke out and—save that he gave lectures during the session 1914–15 and returned to the College for a few months after the Armistice—his work as a Professor was done

Never one to wait, in an emergency, for employment fitting his attainments, Crossley in the earliest days of the war cheerfully undertook arduous clerical work as a volunteer in the War Office under Colonel (now Sir John) Pringle, who was engaged in organising railway transport for troops in the Home Defence, Eastern Command and London District areas Then, after aiding in the large-scale production of salvarsan under the name kharsivan, he became secretary of the War Committee appointed by the Royal Society to organise the production in universities and kindred institutions of local anaesthetics, such as novocaine and β-eucaine, and of other drugs hitherto obtainable only from enemy sources.

The bitter cry for shell in the spring of 1915 led to the establishment of the Ministry of Munitions. Of its Departments, that dealing with trench warfare had for one of its functions the provision of all material required for the offensive in chemical warfare, rendered necessary by the introduction of gas as a weapon by the Germans on the western front on April 22 of that year. As part of the organisation, two Committees, termed Scientific Advisory and

Commercial Advisory, were set up in June,* and, of each, Crossley was appointed Secretary In these early days, the contact between those in the fighting line and those working at home to provide the sorely needed chemical weapons was small To enable the latter to form some conception of the conditions at the front, Crossley was given the additional appointment of Liaison Officer for Chemical Warfare in November, 1915, with the rank of Lieutenant-Colonel, and in this capacity made several visits to the battle areas in France

Only slowly did the authorities at home realise that, for the successful development of chemical warfare, it was essential there should be available a large experimental ground where trials could be carried out on a scale approaching that of actual warfare Eventually, a large tract of bare land was acquired at Porton, east of Salisbury, and to Crossley in June, 1916, was entrusted the task of converting it into a suitable experimental ground, of staffing and equipping it, and of supervising the experimental work undertaken at the instance of the Army or the Committee

The following extract from an account of the work at Porton, most kindly furnished by Lieutenant-Colonel (then Major) R M Rendel, a regular officer who served under Crossley for two years, may give some idea of the difficulties encountered and of the success attained in overcoming them -

"When Crossley arrived at Porton he found two small Army huts, each 30 feet by 15 feet, in the middle of Salisbury Plain, with no roads leading to them, no water, and no equipment of any kind He was, with the exception of one subaltern R E and one warrant officer, quite alone His first move was to get himself appointed to the military command of the Experimental Station, his second to collect the nucleus of a staff By the end of the month he had a chemical laboratory running in one of his Army huts, and, by the end of the year, detachments of Artillery and Engineers under their own officers had been posted to the Station He was now in a position to begin the preliminary experiments, which were necessary for the solution of the hundreds of questions that had to be answered before the British Armies in the field could undertake chemical warfare

"It is doubtful whether anyone realises the immense volume of work actually achieved Crossley himself wrote a summary for the War Records, a copy of which is filed at Porton, but it is both much too long and much too official to reproduce here It may be of interest, however, to consider that at the time of the Armistice, little over two years after the beginning of the Experimental Station, Porton was staffed by 47 officers, 700 N C Os and men and 800 civilian workmen Of the 47 officers, roughly half were trained scientists, principally chemists and physiologists, several of them very eminent men The two original Army huts had been replaced by laboratories, workshops, gunsheds, magazines, barracks and canteens Permanent roads were in existence over the ground, telephones, electric light and water had been laid on Large stores of shell, gas and so on were situated on the ground, and about 40 pieces of ordnance of all natures, from 9 2 howitzers downwards, and trench mortars of every description, were under Crossley's command Over 40,000 rounds of ammunition had been fired, thousands of experiments had taken place, and some of the results of Crossley's work had been embodied in over 800 reports

---

* The Scientific Advisory Committee was a body of distinguished scientists charged with the duty of devising and investigating methods of prosecuting chemical warfare, the Commercial Advisory Committee, a group of leading men in the British Chemical Industry, in a position to advise upon and assist in the production of the necessary chemical materials.

"During two years or more, from the moment Crossley came to the Station, work was carried on all day and during most of the night Such was his driving power that lack of facilities never seemed to matter It was one of Crossley's outstanding merits that, although he himself fully realised the difficulty of working without proper tools, yet he never allowed the lack of them to become an excuse for doing no work He was the most hardworking of men Sometimes severe, he very seldom praised, but he was absolutely fair-minded, and all the time he was at Porton I never heard him criticised by any one of his staff We were all devoted to him Crossley was the best Commanding Officer I ever served under"

In September, 1918, Crossley was appointed Daniell Professor of Chemistry and Director of the Chemical laboratories in King's College on the resignation of Sir Herbert Jackson, and, after demobilisation, returned to the College in October, 1919 Soon the call came to him to undertake the organisation of the British Cotton Industry Research Association, founded by the Lancashire cotton trade with the co-operation of the Department of Scientific and Industrial Research Appointed Director on November 4, 1919, and leaving King's College in March, 1920, it was on his recommendation that the house at Didsbury, now known as the Shirley Institute, was purchased, adapted, and extended by the erection of a large block of laboratories and workshops These buildings were opened formally by H R H the Duke of York on March 28, 1922 By the autumn of 1926, the research staff (including those of its members engaged in the workshops), which in 1921 numbered 28, had increased to 92, of whom 44 were University graduates That, by his genius in planning and guiding research, Crossley provided a sure foundation for ultimate success is evident from the review of the work of the Cotton Industry Association to the end of 1926, recently published by the Shirley Institute under the title, 'Research in the Cotton Industry' Not improbably, his work at Didsbury may come to be regarded as his best

Crossley received many honours —D Sc (Victoria University), 1899, F R S, 1907, Hon LL D (St Andrews), 1917, C M G, 1917, Longstaff

Medallist of the Chemical Society, 1918, C B E and Officier de la Légion d'Honneur, 1919 From 1906, when he became Honorary Secretary, Crossley held office in the Chemical Society without a break until his death, becoming Honorary Foreign Secretary in 1913, President in 1925 and, on his resignation of the Chair, Vice-President in 1926 He was a Member of Council of the Royal Society during the two years 1920–22

By nature Crossley was deliberate, but with his mind once made up, resolute Unfailingly courteous and genial to all in every relation of life, it is probable that comparatively few were admitted to the intimacy of his friendship His recreations were typical he played lawn tennis in his student days and golf later in life, but in billiards and fly-fishing—the latter absorbing entire holidays before the war—he found an abiding source of pleasure To his cultivated taste books, of which at one time he was an eager collector, music and the theatre made a strong appeal • Without being robust he enjoyed good health until the effect of the strain of the war years began to manifest itself A voyage to Madeira in the May of 1925 gave a temporary respite, but in the autumn he was less well, and in March, 1926, resigned the Presidency of the Chemical Society on completing only one year of office

Before the summer was over, it was evident that his health was failing rapidly Towards the end of the year he tendered his resignation of the Directorship of the British Cotton Industry Research Association, but by resolution of the Council remained nominally in office pending the appointment of a successor This appointment had not been made and he was still Director when, on Saturday, March 5, 1927, he died

W P W

WILLIAM BURNSIDE—1852-1927

WILLIAM BURNSIDE was born on July 2, 1852, the son of William Burnside, a merchant, of 7, Howley Place, Paddington, London. His father was of Scottish ancestry his grandfather, who had gone to London, was a partner in the bookselling firm of Seeley and Burnside

Left an orphan at the age of six, Burnside was educated at Christ's Hospital, where he was a Grecian there, besides his distinction in the grammar school, he attained the highest place in the mathematical school Having been elected to an entrance scholarship at St John's College, Cambridge, he went into residence in October, 1871, and was regarded as the best man of his year in the College In accordance with the general custom of capable students of mathematics in Cambridge, he "coached" for the tripos, his private tutor being W H Besant, one of the few rivals of the famous Routh For some reason, Burnside migrated to Pembroke College in the same university, the change being made late in his second year (May, 1873) He graduated in the Mathematical Tripos of 1875 as second wrangler, being bracketed with George Chrystal, who afterwards was professor at Edinburgh, the fourth wrangler was R F Scott, now* Master of St John's College In the subsequent Smith's Prize Examination, Burnside was first and Chrystal second

A fellowship at Pembroke was the worthy sequel of such a degree he continued a fellow from 1875 until 1886 He was at once appointed to lecture in his college and he lectured also at Emmanuel in 1876 and at King's in 1877 At that time, college teaching for the best students was sometimes shared by a few colleges, in isolated groups, and included subjects selected from the average normal course for Honours, and Burnside, in addition, gave lectures in hydrodynamics, an advanced course open to all the University That particular subject was coming into vogue again at Cambridge, attention, regularly paid to the established work of Stokes, was stimulated by the then new work of Greenhill and especially of Lamb Burnside also examined for the Mathematical Tripos from time to time Occasionally, he did some private coaching But later it appeared that, instead of restricting himself mainly to tripos subjects in furtherance of his lectures and an inevitable share in examinations, he had launched himself upon a broad sea of study, then far removed from the tripos domain.

As an undergraduate, he had proved an expert oarsman While at St John's College, even as a freshman, he had rowed in the Lady Margaret First Boat which, with the famous Goldie as stroke, went head of the river in 1872 Rather light in weight as an undergraduate, too light (according to the canons of the day) to be considered for the University Boat, he always was rather spare of build and he retained a wonderful power of endurance; and he kept his rowing form for many years He rowed in the Pembroke Boat after graduation, as long as he continued in residence, he was a splendid "7," and had a full share in its steady rise on the river For some years after he left Cambridge, his reputation as an oar survived as a tradition in College circles

---

* The writer is indebted to Sir Robert Scott, for several of the personal records in this notice.

After going out of residence, similar opportunities for rowing were not accessible But in the course of holidays frequently spent in Scotland, Burnside had acquired a zest for fishing, and for many a summer onwards he continued to go there, pursuing what grew to be his favourite sport As in rowing, so in fishing, he developed skill and became an expert fisherman, indeed, with all he undertook, nothing short of his best was sufficient

In 1885, at the instance of Mr (afterwards Sir) William Niven, the Director of Naval Instruction—himself a Cambridge man, devoted to natural philosophy, as it was styled by good Newtonians—Burnside was appointed professor of mathematics in the Royal Naval College at Greenwich The rest of his teaching life was spent in that post There was a current belief, a belief now known to be justified by fact, that his old college had invited him to return to important office, but he remained at Greenwich His work was to his liking It was a round, well-defined in extent and in demands on time, within a variety of congenial subjects, though only touching in part upon the regions of his constructive thought The actual teaching, with its incident duties, left him adequate opportunity to keep abreast of progress, even to advance progress, in the subjects of professional duty It also left him leisure, which was carefully and diligently used, to pursue his own researches, whatever their direction Best of all to him, he was free from the interruptions and the incessant small demands, business and social, that are inseparable from official administration For at all times, and in all ways, multifarious detail—whether incidental to the non-scientific side of official duty, or the current presidency of a scientific society such as the London Mathematical, even the purely algebraical garniture and the side-issues in mathematical investigations—such detail was inexpressibly irksome to his spirit

At Greenwich, Burnside's work was devoted to the training of naval officers It consisted of three ranges There was a junior section for gunnery and torpedo officers, the chief subject of study was the principles of ballistics There was a senior section for engineer officers the chief subjects of study were strength of materials, dynamics, and heat engines The advanced section—perhaps that in which he exercised the greatest influence on his students—was reserved for the class of naval constructors in that range, Burnside's special mastery of kinematics, kinetics, and hydrodynamics proved invaluable Records and remembrance declare that he was a fine and stimulating teacher, patient with students in their difficulties and their questions—though elsewhere, as in discussion with equals, his manner could have a directness that, to some, might appear abrupt He certainly earned the gratitude of his students, as appeared from their spontaneous token of tribute to him when he left in 1919, the address, which they then presented, was treasured by him and his family

Burnside had married Alexandrina Urquhart in 1886, soon after he was appointed professor at Greenwich She survives him, with their family of two sons and three daughters

After his work at the Naval College had ended, the whole family retired to West Wickham in Kent Burnside, happy as he had been in his work and regretting its actual termination, enjoyed his leisure, spending it among his books, in fishing holidays in Scotland and, not least, in his researches, some continued in regions recognised as specially his own, some of them in the systematic development of ideas in still another branch of mathematics upon which his intellectual interests had settled The last year of his life was marked by failing health and the proximate cause of his death was a recurrence of cerebral hæmorrhage He died on August 21, 1927, and he is buried in West Wickham churchyard

In recognition of his eminence as a mathematician, not a few academic honours came to Burnside during his life He was never avid of honours indeed, he was eager to avoid those forms of academic recognition constituted by official positions of dignity, when they demanded the performance of any public duty set in formal pomp or circumstance He received honorary degrees, Sc D from Dublin, LL D from Edinburgh He was elected a Fellow of the Royal Society in 1893, on the first occasion of candidature he served on the Council of that body from 1901 to 1903, and he was awarded one of the two Royal medals for the year 1904 He was a member of the Council of the London Mathematical Society for the long continuous period from 1899 to 1917 there, he was a tower of strength, in advice during the Council's meetings, and by his many reports as a referee upon a multitude of varied original papers submitted by a small army of authors He was awarded the De Morgan medal of the Society in 1899 From 1906 to 1908 he served as President while willingly allowing his name to be submitted for membership of the Council year after year, he accepted their highest office only with grave and characteristic reluctance The honour, in which he appeared to show most interest, was conferred on him in 1900 In that year he was elected an Honorary Fellow of his old college, Pembroke, and at the time of his death he had become the senior on the small roll of Honorary Fellows. Yet, even in the few and far from fluent remarks of thanks which he made at the College dinner welcoming, by courteous custom, the newly elected honorary members of the foundation, he urged that the happy and successful pursuit of research was its own reward, and the sincerity of his plea was appreciated not least by those who had done their part in recognition of his labours.

Burnside was frequently called upon to examine for the Mathematical Tripos and for the open Civil Service examinations of the highest grade Occasionally, he acted as external examiner for one or other of the English Universities, as well as for the Naval College after his retirement He was not an easy examiner—before his early days of such duty, the phrase "easy problems" at Cambridge had come to bear a perverse significance His questions could be of the type which, gathered in one of his papers, might justify the epithet beautiful. they were certainly too beautiful for the candidates in the 1881 Tripos, the first university occasion when he examined Yet, though they often were difficult and always on a high level, they were set with the design of evoking an examiner's thought, rather than of providing an opportunity for the facile display of trained manipulative skill along familiar lines.

Through many years, Burnside was in constant requisition as a referee, for the Royal Society and for the London Mathematical Society. He could not be called lenient for, however sympathetic with writers, and especially young writers, he held a high standard of the attainment that was deserving of publication He was often fruitful in suggestion. He could even be severe on occasion yet he would mitigate a judgment when grounds for its reconsideration were submitted Similarly, as a critic of a friend's proof-sheets, he could be severe, yet always objectively so he obviously assumed, without the possiblity of question, that the friend's standard and his own were alike in practice Thus, at the end of a discussion, the friend would find that added light had been cast upon the whole matter—surely the best criterion of sympathetic criticism. And if severe with others, he was stern with himself—a mental discipline that exercised its influence towards the directness and the precision both of form and of substance in his writings.

Valuable as were his teaching, his activity as an examiner, and his influence as a referee, it is by the contributions which he has made to his science that Burnside's name will be held in remembrance

His range was wide; for it branched out, through applied mathematics from the days of his early training, into great tracts of pure mathematics in the years of his matured powers Yet, even in the later time, when specialisation has tended to become acute, he could specialise with the best Though of course not comparable with an Euler, a Cauchy, or a Cayley, in the variety or the amount of work he has left, he has delved in many fields and has left his trace in many directions. He published over one hundred and fifty papers, as well as one treatise, the "Theory of Groups," of which a second (and greatly amplified) edition was issued also under his own care. He has also left a manuscript, fairly complete as far as it was carried, on the theory of probability. He himself

W. Burnside.

did not regard this work as finished; on various issues, he was in correspondence from time to time with the present President of the Royal Society, the Astronomer Royal, and others, and he certainly did not consider that he had resolved all his own questions. Had life and health lasted appreciably longer, there is no doubt that he could have attained, as he intended to pursue, further development in a subject which occupied much of the thought of his later years.

In that considerable tale of papers, most are short Very many of them occupy only a few pages. His longest individual paper—he never used the more ambitious title "memoir"—deals with automorphic functions it really consists of two parts connected, though not consecutive, in matter, and the whole occupies no more than fifty-three octavo pages. Brief however as his papers are, it can fairly be asserted that each one of them contains some definite and recognisable result or results He never discussed side-issues, he would not even dwell on the minute details of a main issue Indeed, he could be intellectually bored by processes that halted in their march to settle subsidiary questions as they arose, with him, auxiliary necessary material was set out before the main advance When once an issue was attained, he was content to let it stand by its own significance, to others he would leave attempts "to gild refined gold, to paint the lily"

He happily was saved mathematical controversy, which he detested On one occasion he was surprised, even disturbed, by the receipt of an unseemly letter the very tone of which amazed him (not unjustifiably) it concerned a question of priority which, in so far as it could affect a man punctilious in his acknowledgment of the work of others, to Burnside was as thin as air, though manifestly not so to the writer of the letter The quiet firmness of Burnside's answer to his ungracious correspondent ended the matter On occasion, his work has been known to provide ammunition for others. Thus in 1887 and 1888 he wrote papers on the kinetic theory of gases, a subject which at that date led to much disagreement in opinion, stating his assumptions, he dealt with the average exchange of energy during the impact of elastic spheres and with the partition of energy between motions of translation and of rotation. These papers can only have been the outcome of some appeal emanating from Tait The result was used (but Burnside took no direct part) in an onslaught upon Bolzmann's work made by Tait, a "bonnie fechter," never reluctant in the use of the controversial tomahawk.

In his writings, Burnside had a style which precisely, and habitually (as if it were an instinct), contributed to efficiency of presentation. Even while an undergraduate, he had been noted for the style of his mathematical work, he was reputed to be the most "elegant", though not the most widely read (Chrystal was thus reputed), among the young mathematicians of his own standing. In pure literature, critics, whether analytic or constructive, do not always agree upon the necessary essentials of general style, though they can select individual characteristics In scientific productions, the task is assuredly no easier than in the humanities Burnside had two of the essential secrets of an effective style he exercised a power of clear and precise thinking that was maintained until the achievement of a definite issue, and he possessed a faculty of lucid (if condensed) expression of the whole course of a constructive argument He was intolerant of approach to vague meandering "words, words" would be his caustic comment on an unconstructive passage The elusive charm of the sudden thought, that in itself is a revelation, is rare in mathematics, though it can be found in a Fourier or a Salmon But such was not Burnside's aim, perhaps never his dream, he did not seek for aught else than clearness, directness, terseness most of all He would practise no art in trying to secure the attention of an inexpert beginner In exposition, conciseness was his rule Once, the attempt of a friend, to obtain from him a more expanded treatment of some early stages in his Theory of Groups, was met by a declaration of regret that he had been unable to effect further condensation. The consequence is that all Burnside's published work is close and firm in texture, yet, to an attentive reader, it is never lacking in clearness and movement

Throughout Burnside's residence at Cambridge, the University had been in the finest flower of her activity in applied mathematics Stokes, Cayley, Adams, were long-established professors; Maxwell's appointment had been more recent The staple subjects for the most capable mathematical students were physical astronomy, dynamics, light, sound and heat The range of electricity and magnetism, except for a slight infusion of some of the work of Sir William Thomson (afterwards Lord Kelvin), was academic and unconnected with laboratory knowledge, and Maxwell's presentation, based on the researches of Faraday, had still to make its place in the Cambridge course, men scarcely even dreaming of the revolution it was to accomplish later Pure mathematics, save for the rare appearance of a Clifford, a Pendlebury, or a Glaisher, was left to Cayley's domain, unfrequented by aspirants for high place in the tripos. Much of the original thought of her mathematicians in those years found its expression in problems, a veritable mine of isolated results propounded as conundrums in the Senate House and in College examinations Even so, the worship of the mathematical spirit at the shrine of natural philosophy was maintained in a well-defined conservative range

At the beginning of his work, Burnside could hardly fail to conform to this Cambridge use, indeed, as regards the subjects (though not as regards all methods for the subjects) in applied mathematics, he largely remained in the older round to the end Yet even while he continued in Cambridge, he was gradually emerging into his own domain. Bred an applied mathematician in the Cambridge school of natural philosophy, which tended to regard all mathematics as a useful tool—no more than a tool—in so-called practical applications, he came to find that there was a world of pure mathematics different from that which filled the receptive stage of his student days. In the creative stage of thinking for himself beyond the range of learning and of teaching for the tripos, he gradually made his way into that new world He took rank with the constructive pure mathematicians, without losing hold of his earlier studies Indeed to him, as to others with a similar experience, the new knowledge shed fresh light upon the older interests, but any effective combination of the old and the new could only be made by an intellect of the type such as Burnside happily possessed

Thus, as already stated, Burnside's earliest advanced lectures were devoted to hydrodynamics. Elsewhere, the old-fashioned methods for conjugate functions, stream-lines, and velocity-potential, were being analytically transformed through the introduction of functions of a complex variable For many a day, Cambridge had preserved an almost invincible repulsion to the then objectionable $\sqrt{-1}$, cumbrous devices being adopted to avoid its use or its occurrence wherever possible But some teachers could show that, in two-dimensional fluid motion, simplicity and new results alike were easily attainable by its means, and its formal debut within the Cambridge enclosure was made in Lamb's treatise To Burnside's intellect the new calculus appealed, and as a matter of record, his first published paper (1883) is concerned with elliptic functions, not with hydrodynamics

Three examples will suffice to indicate the development in Burnside's thought, thus indicated

In 1888 he investigates three main questions connected with deep-water waves resulting from a limited initial disturbance, a research probably suggested by certain phenomena noted in the Krakatoa eruption In that paper he proceeds by analysis which belongs to what would now be called the classical methods of Fresnel, Poisson, and Stokes, it requires much elaborate work in definite integrals with real variables, without any reference to the (happily satisfied) convergence of those integrals, and Burnside arrives at direct results of observable significance, which relate to the greatest amplitude of displacement, the range of propagation, and the governance of the wave-length It is not without interest, in connection with his increasing grasp of newer methods, to note that in this paper he "justifies" the use of a complex value for a constant—while, in a paper two years later which deals with streaming motion, he uses complex variables without a word of prelude to superfluous justification.

The problem of the two-dimensional potential, as envisaged by the applied mathematicians in the middle third of the last century, such as Green, Stokes, Thomson and Tait, has been completely changed by the ideas of the theory of functions Old assumptions have had their significance and their limitations revealed, the earlier physicists not always in sympathy with exacting refinements which to them smack of pedantry, the later mathematicians not always respectful to the intuitions content with a semblance of proof Burnside knew both attitudes of mind—the earlier from his training, the later from his continued study, and so he could bring old results to new issues. Thus in a paper (1891) on the theory of that two-dimensional potential, satisfying the equation

$$\frac{\partial^2 u}{\partial x^2}+\frac{\partial^2 u}{\partial y^2}=0,$$

and determined by prescribed conditions within an area and assigned values along a boundary, he returns to the old property—the possession of every undergraduate—that the potential can have no maximum or minimum within the boundary Pointing out that maxima and minima must therefore lie on the boundary and that conditions of continuity require their aggregate to be an even integer, he obtains a relation between that integer, the integer denoting the number of distinct portions of the boundary, and the integer representing the number of double points on the equipotential contour lines as they pass from a boundary arc over the area back to another boundary arc Moreover, he obtains the relation for the most general case when the conditions are extended so as to admit discontinuities (in the form of logarithmic or algebraic infinities) within the boundary, and he indicates the bearing of the relation on the graphs of these contour lines.

In 1894 he published a paper discussing Green's Function for a system of non-intersecting spheres There, beginning with the known result for two spheres, he transformed it by a property he had deduced from a geometrical interpretation of homographic substitutions He extended the transformed result to any number of spheres. By inversions which are represented by point transformations, and by sets of inversions which accumulate into a group of transformations, he obtains a pseudo-automorphic function, in the form of a series where the coefficients of the successive terms are powers of the magnification at the successive inversions Lord Kelvin would not have recognised his theory of images in that final form yet the development into that form is only a continued amplification of the theory Burnside, moreover, carried it further, by connecting the application with any solution of Laplace's equation, instead of the inverse distance alone as in the theory of images. Here, as in all his investigations, it was only too evident that he had wandered far from the ancient Cambridge fold

Various well-marked stages in the progress of Burnside's knowledge almost indicate themselves, from the evidence of his original papers.

Apparently, the first large new subject, of which he made a profound study, was elliptic functions its rudiments had hardly been admitted to his Cambridge course At every turn he devised something novel—Is it the transformation of the simplest elliptic differential element? Noting the general characteristic of the four critical points in the Riemann interpretation, he deals with the successive possibilities of the transformation (*a*) into itself, by interchanging these four points in pairs, with the obvious inference that there are three modes, which are explicitly obtained, (*b*) into the Weierstrass normal form, with one of the critical points sent to infinity, and the remaining three practically arbitrary, (*c*) into the Legendre normal form, with the four points symmetrically arranged round the origin along an axis, and (*d*) into the Riemann normal form, with 0, 1, ∞ as three canonical points for all, and the fourth defined by the parametric invariant of the element Is it so simple an issue as the division of the periods by 3 or by 9? Even for the simplest form of that issue, he treats it by a general method and not by any special artifice a short paper in 1883 achieves the trisection for the Jacobian elliptic functions, a later paper in 1887 achieves the same problem for the Weierstrass elliptic functions, a still later paper uses the same method, supplemented by the introduction of resolvents, to obtain the results for division by 9—Is it the extension of Jacobi's expression of the apparently hyperelliptic integral

$$\int\{x(1-x)(x-\lambda)(x-\kappa)(x-\kappa\lambda)\}^{-\frac{1}{2}}\,dx,$$

under the (quadratic) transformation

$$z = x + \frac{\kappa\lambda}{x},$$

as the sum of two elliptic integrals? Burnside deals with the cubic and the quintic transformations in odd degree, with the quartic transformation in even degree, and obtains the respective types of degenerate hyperelliptic integrals, characteristically leaving other instances as "exercises" (though, not "easy" exercises) in the method expounded And, almost as an incident, he notes a case when an apparently elliptic integral

$$\int\frac{x-p}{x-q}\{(x-\alpha)(x-\beta)(x-\gamma)(x-\delta)\}^{\frac{1}{2}}\,dx,$$

where the relation

$$\frac{y-p}{y-q} = -\frac{x-p}{x-q}$$

transforms the elementary elliptic differential into itself, is only simply periodic Or, to take only a last example in this range, he completes the known proposition that the co-ordinates of a point on the intersection of two quadrics are expressible in terms of elliptic functions, by constructing the actual arguments, and he shows that the two invariants in the Weierstrass form are the quadrinvariant and the cubinvariant of the customary quartic equation occurring in the reference of the quadrics to their common self-conjugate tetrahedron.

Another subject which absorbed his attention was differential geometry, which also, save for some rarely read sections in Salmon's "Geometry of Three Dimensions," hardly entered into the Cambridge course Burnside gathers together fundamental propositions, then accessible only by search among widely scattered authorities, and he applies them with effect Before 1890, the parameters of nul lines on a surface had not appeared (or perhaps, only with Cayley) in English memoirs In one paper, Burnside uses them, with severe ingenuity, to obtain the different classes of surfaces that possess plane lines of curvature In another paper, he uses them to construct the differential equation of all confocal sphero-conics, proving that the co-ordinates of points are expressible in terms of elliptic functions of a parametric argument which is obtained explicitly There, as always in his papers, Burnside's work marches forward to a definite issue and constitutes a contribution to knowledge.

Comparative simple known properties are given a widened significance Thus he takes the known property that two finite screws compound into a single screw, and (1890) he devises a simple geometrical construction for the axis of the resultant screw He notes that, as the proof does not require the use of parallels, the result is valid for elliptic space and for hyperbolic space Five years later, he returns to the matter in a paper on the kinematics of non-Euclidean space, and now he notes that displacements correspond to point-transformations, sets of displacements to groups of transformations. The theory of groups is beginning to affect his work

He can derive new results from elementary results in ordinary geometry, as well as from the range of abstract geometry His interpretation of a homographic substitution

$$w = \frac{az + b}{cz + d}$$

as inversion at two fixed circles—this 1891 paper seems the first occasion when the specific mention of a group is made in his published work—is used to assign the criteria, necessary and sufficient, to determine whether a group, formed of assigned fundamental transformations, will or will not contain a loxodromic substitution Or he will deal with the ancient problem of drawing a straight line between two points, for which the ruler suffices in the Euclidean postulate when the points lie at an implicitly supposed finite distance apart, and he gives a construction for the cases, when one of the points is at infinity, when both of them are at infinity, when one of them is the ideal point required in projective geometry, his construction applies to any space, Euclidean, elliptic, hyperbolic Or he will take a proposition (analytically established) concerning the four rotations by which a triply orthogonal frame of lines can be displaced into coincidence with a similar frame, by the use of a known (Hamilton) proposition in rotations, he gives a geometrical construction for the displacement, a construction which seems almost obvious—after it has been obtained. Or he will proceed to abstract space he discusses a configuration of 27 hyperplanes and 72 points in space of four dimensions, such that six of the planes pass through each point and sixteen of the points lie in each of the planes. To him it is a natural extension of the customary configuration of the 27 lines on an ordinary cubic surface in three dimensions

Burnside's investigations in elliptic functions compelled him to range in the wider field of the theory of functions in general, so thither he had proceeded and, in his progress, he became an investigator

His contributions are, as ever, varied in range Fifty years ago, it was a surprise—to-day, it is almost a commonplace—to learn that functions of real variables exist, which are always finite, are always continuous, and never possess a determinate differential coefficient the now classical example, due to Weierstrass, is that of the series

$$\sum_{n=0} b^n \cos a^n\theta,$$

where a is any uneven positive integer, and b is a real positive quantity such that $ab > 1 + \frac{3}{2}\pi$ Burnside made a step in advance (1894) He showed that there are functions of real variables everywhere finite, everywhere uniformly convergent, everywhere possessing the unrestricted complement of successive differential coefficients, yet never expansible in power-series, and, as an illustration, he constructs the function

$$\sum_{n=0}^{\infty} \frac{1}{n!} \frac{1}{1 + a^{2n}(x - \tan n\alpha)^2},$$

where a is real and > 1, and where α/π is not a rational fraction His proof is concise and demands no acquaintance with elaborate theory, as usual, it leads direct to a definite result that completes the investigation

On another occasion he deals with the Schwarz solution of the problem of representing a closed convex polygon in one plane conformally upon the half of another plane—a result that has rendered signal service in mathematical investigations in matters so diverse as heat, hydrodynamics, and electricity In these last applications, only the simplest examples are used in the general Schwarz solution, an Abelian integral occurs the use of which is gravely handicapped by its multiplicity of periods, so that additional conditions become necessary to render the analysis specific in application Burnside, already skilled in polyhedral functions and general automorphic functions, investigates the aggregate of instances where, at the utmost, doubly-periodic functions will suffice But he goes on to deal with multiply-connected spaces having polygonal boundaries in particular, he gives the solution for the conformal representation of the doubly-connected area which lies between two concentric similarly placed squares, the side of one square being double that of the other

He seizes upon the existence-theorem which establishes the possibility of expressing the co-ordinates of a point on an algebraic curve by means of uniform functions that are automorphic under sets of transformation The lack of determination of the group, appropriate to a postulated equation, has left the solution as one merely of existence without specific determination Burnside, combining his knowledge of groups, of elliptic functions, and of Klein's icosahedral functions, gives a complete specific resolution of the problem for the (apparently) hyperelliptic equation

$$y^2 = x\,(x^4 - 1)$$

It is unnecessary to accumulate more instances Burnside's matured development flashed out in his double paper on automorphic functions, published in 1892 The subject belonged to a new section of mathematical knowledge, mainly inaugurated by Henri Poincaré and systematically expounded in a series of memoirs, now classical, in the initial volumes of *Acta Mathematica* The underlying idea is simple Trigonometrical functions are singly periodic that is, each such function is unchanged when its argument suffers an increment or a decrement which is any integer multiple of a single quantity Elliptic functions are doubly-periodic that is, each such function is unchanged when its argument similarly suffers an increment or a decrement which is a linear combination of any independent integer multiples of two quantities (the ratio of these quantities must not be real) Jacobi had proved long ago that uniform functions of triple periodicity (and, *à fortiori*, of periodicity higher than triple) in a single variable do not exist But in every such instance the modification of the argument consists solely of an additive increment or decrement The question arises What is the most general type of periodicity for a function of one argument? And it naturally entails the further question What are the functions possessing that type of periodicity? Isolated results were known, such as Jacobi's elliptic modular functions and Klein's polyhedral functions their significance as examples of a wider theory had not appeared It was Poincaré who presented the first general treatment of these questions

Into this work of Poincaré, Burnside plunged In it he revelled, and his new results are embodied in his paper on automorphic functions which has just been cited In particular, Poincaré had overstated an exclusive central result Burnside detected the overstatement and the fundamental cause, and he devised a new class of automorphic functions, simpler than any of the classes devised by Poincaré The full theory, even now, remains to be established it awaits the construction (or the equivalent of the construction) of a central function or functions which, while palpably automorphic, shall be amenable to ordinary analytical manipulation as are the corresponding central theta-functions of purely incremental periodicity When the history of that theory comes to be written, Burnside's name will hold an honourable place in the record

The consideration of the very foundation of these automorphic functions led Burnside further afield, along a way already opening out before him in his progress, into a region which he explored with ample discovery It was to provide the most continuous and most conspicuous of his contributions to his science The characteristic property of every automorphic function of a single variable is that, without change in the value of the function, its argument is subject to a number of reversible operations, which are independent of one another, are capable of unlimited repetition and reversion, and admit all possible combinations, repetitions, and reversions, in unrestricted sequence The *aggregate* of all the *operations*, which *thus emerge*, is *termed* a *group*, so that a function can be automorphic under a group of transformations (or substitutions) But just as the properties of the integers, which occur in the arithmetic of any calculation, merge into the general theory of number which ignores all specific application, so the properties of transformations in a group merge into a more comprehensive calculus That calculus deals with the composition, the construction, the resolution, and the essential properties of a group, regarded as an abstract entity whose component elements are subject to mathematical laws of combination It is no part of that calculus to take account of possible regions of application instances present themselves in algebraic equations, in analytic functions, in differential equations, in divisions of space of different orders of dimension, in the displacements of a solid body, in invariants and covariants of all kinds —a selection of subjects manifestly not complete

The earliest expression of the notion and its initial development are due to Galois he indicated the kind of relation that could exist between the properties of an algebraic equation and some corresponding group of finite order The early growth of the theory was due to French mathematicians, Cauchy in particular, then Serret Somewhat later came the fine exposition by Jordan who, it may be mentioned, had Klein and Lie as pupils at the outbreak of the Franco-Prussian war in 1870 Down to that date, the subject revolved round algebraic equations as its centre

The interest in the theory began to spread The next real extension was due to Sylow, in a memoir on groups of substitutions Then followed a partial construction of its mathematics as a pure calculus, without regard to applications the contributions of Cayley and of Weber may be noted The theory soon divided itself into two co-ordinate sections, sometimes advancing as pure calculus, sometimes extending to new regions of application A theory of continuous groups branched off into complete independence, it became a great body of mathematical doctrine, under the inspired researches of Sophus Lie and his disciples The theory of discontinuous groups attracted an equally ardent band of investigators the names of Klein, Burnside, Frobenius, Hölder, and Dyck, recall diverse developments in theory and in use

It was to the theory of discontinuous groups of finite order that Burnside mainly devoted his attention. Scattered references to such groups occur in some of his papers already cited. At first, their occurrence seems merely incidental, then they almost prove that his thought was gradually accumulating the evidences of a connected theory From the early nineties onward through much of the remainder of his life, Burnside's constructive thought concentrated on the subject Paper after paper appeared from him, on a vast variety of associated topics, in ordered development, each providing some fresh contribution, all of them marked by imaginative insight and compelling power They found their first culmination in his book on the " Theory of Groups," published in 1897 That volume was a systematic and continuous exposition of the pure calculus of the theory as it then stood, and it embodied the researches of other workers in Europe and America (always with ample references) as well as his own His papers on the theory of groups continued, unhastingly, unrestingly A second edition of the book, considerably more extended than the first, appeared in 1909 Even so, his activity in the subject still continued, though with a gradually decreasing production He published over fifty separate papers on this range of knowledge alone, each of them, even the briefest, contained some definite result or results of significance All this work, original from himself, is a splendid contribution emanating from one mind and, of itself, is sufficient to secure the remembrance of his name.

With the coming of the war in 1914 and during its course, there was a comparative cessation in Burnside's productivity His frame was almost as lithe as ever and apparently as full of easy spring, as though to belie the passage of years Some of his constructive activity passed silently into the service of his country in certain naval matters In those years he undoubtedly continued to produce papers, but the main body of his work could be regarded as verging towards its termination

One new subject, however, secured some regular attention from him, even amid his unbroken interest in groups It may have originated from the mathematics of some war problems, and its interest may have been fostered as he pondered over the combinations of diverging results of observations In the year 1918 he produced a short paper dealing with a question in probability, purely mathematical as propounded, and it was followed, from time to time, by other papers, some suggested by practical problems Probability, as a mathematical theory, has not yet lent itself to a single process of organised development based on any unique set of ideas, which are generally accepted as fundamental Even the method of almost universal use in astronomical observations depends upon the Gauss assumption of the arithmetic mean of a number of discordant observations, as the best measure of the unknown quantity But that assumption stands as only one out of many inferences from the less arbitrary assumption that the probability of an error, in any observation, is some function solely of the deviation from the unknown accurate measure, with that less arbitrary assumption, a more general inference is that the difference between the unknown measure and the arithmetic mean is some symmetric function of the differences between the observed magnitudes (Of course, the occurrence of the symmetric function modifies the law of facility of error or the adoption of an admissible law, not inconsistent with the assumption and differing from the exponential law, determines the form of the symmetric function.) Burnside deals only with the arithmetic mean thus tacitly, with other writers, making the symmetric function to be zero As indicated earlier, he did not consider that he had resolved all his difficulties Ever a severe critic, he remained critical of himself, he was not afraid to modify an opinion, he did not hesitate to abandon an opinion, if ever he regarded it as not fully tenable, as indeed happened in fact The manuscript, which he has left and which will be published by the Cambridge University Press, is the expression of his views so far as they had been framed into a system

There is one activity in human nature which exercises a perennial lure for living minds When a worker of recognised distinction in any field has completed his contribution to thought, some survivors delight in assigning him his place in an ordered hierarchy of memorable names The task demands an easy omniscience which shall gauge all knowledge and all intellect, if its estimate of precedence in relative merit is to be promulgated with authority and received with belief Yet, somehow, such estimates lack the quality of permanence Nearly two thousand years ago Lucretius, the brilliant expositor of natural philosophy in an age of culture, described Epicurus as a man

Qui genus humanum ingenio superavit,

a tribute paid two full centuries after the death of the Greek philosopher of the atom the world to-day, if it ever hears of the name thus lauded, greets the judgment with a smile Less confident men may, in their own day, render a more modest yet equally sincere homage to a passing spirit, from their reverence for the genius that has striven, and in their remembrance of the worldy task that has been done Burnside, during a life of steadfast devotion to his science, has contributed to many an issue In one of the most abstract domains of thought, he has systematised and amplified its range so that, there, his work stands as a landmark in the widening expanse of knowledge Whatever be the estimate of Burnside made by posterity, contemporaries salute him as a Master among the mathematicians of his own generation

A R. F

WILLEM EINTHOVEN—1860–1927

WILLEM EINTHOVEN, whose death was announced on 29th September, was born in May, 1860, at Samarang in Java He was the son of a doctor practising in that place, and was taken to Holland by his mother with five other children when his father died in 1870 They settled at Utrecht, and here Einthoven entered the University as a student of medicine in 1878, to study physics under Ballot and physiology under Donders His first research was undertaken with the anatomist Koster and concerned the mechanism of the elbow joint; he became assistant to the ophthalmologist Snellen, and was given his doctorate of medicine at 25 years for an Inaugural Dissertation entitled "Uber Stereoskopie durch Farbendifferenz" In the same year he was called to the Chair of Physiology at Leyden, and there he remained, actively engaged in work, until his death in his 67th year

Early in his career he became interested in instruments recording changes of electrical current or potential, and, perceiving their great importance to physiological research, he deliberately set out to construct an instrument of unsurpassed quickness and sensitivity The history of the construction of his famous string galvanometer has been written by Einthoven himself in one of his papers His researches started on the basis of the Deprez-d'Arsonval galvanometer He soon discovered that the less numerous were the windings of the moving coil of this galvanometer, the greater was its sensitivity, and that the highest sensitivity was obtained when a single winding of very thin wire was employed It was then (1897) that he became aware of Ader's instrument for recording submarine signals, a galvanometer consisting of a long fibre lying vertically between the poles of a magnet He continued to enquire into the factors required to produce speed of movement and sensitivity and, by greatly increasing the strength of the magnetic field, by using relatively short and extremely fine conducting fibres, and by employing an optical system of projection of high magnification, eventually constructed a galvanometer greatly surpassing, in continued quickness of response and sensitivity, any that had previously been made

His first account of this instrument was published in 1903, the sensitivity of the galvanometer, described fully by him in 1909, was already 100,000 times greater than that of Ader's instrument Although his instrument, regarded as a potentiometer, then stood possessed of little more sensitivity than the best models of capillary electrometer, it surpassed the latter and all previous galvanometers enormously in the quickness of its response The capillary electrometer had the defects of slow response and overswing, a true curve of potential differences could be obtained only by a tedious analysis of the electrometer

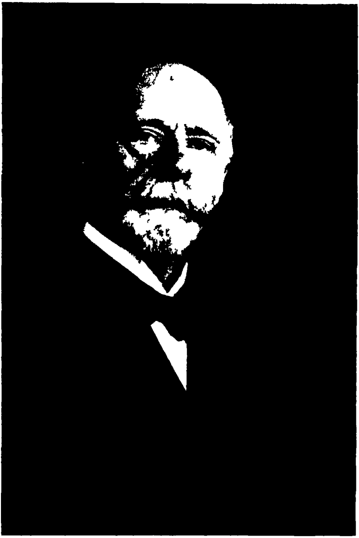

W. Einthoven

curves, an analysis involving considerable possibilities of error. The response of Einthoven's string galvanometer was so quick that very rapid current changes were directly and accurately recorded, no analysis being required subsequently.

He expended a great deal of time and patience on the perfection not only of the galvanometer itself, but of the subsidiary apparatus, particularly plate cameras and rotating time-markers, with a view to reducing to their narrowest limits errors of measurement arising from such sources. He succeeded in reducing errors of time measurement in physiological electrical curves to such minute intervals as 1/10,000 or 1/100,000 of a second, and produced those records of current change upon a photographic network of vertical and horizontal lines, accurately representing time and current magnitude, which have commanded universal admiration for their technical perfection alone

His galvanometer became the basis of the well-known commercial models of Edelmann, and of the Cambridge and Paul Instrument Company, and of many other patterns. Very many hundreds of these instruments are now in use in physical, physiological and pathological laboratories, and in the hospitals of many countries. Modifications, which have been introduced, other than those of the inventor himself, have consisted almost exclusively of minor changes, adapting the machine for special purposes, in principle it has remained unaltered, in sensitiveness it has greatly increased, but Einthoven's own models have continued until the last to outstrip by far all similar instruments in this respect.

Einthoven was not content merely to place his instrument at the disposal of laboratory workers; he and his collaborators clearly pointed to the many ways in which it might usefully be employed. Following up Waller's demonstration that curves of the heart beat can be obtained by leading off from the limbs of an animal, he laid the basis of human and experimental electrocardiography as these are practised to-day Modern electrocardiography is the direct outcome of two papers published by him in 1907 and 1908 The leads from the human subject then adopted by Einthoven, and the standardisation of curves then employed by him, have since become universal. The same papers also contained curves of a variety of irregularities of the disordered or diseased heart, and their publication led at once to a complete investigation of cardiac irregularities by this method; the outcome of these researches has been a complete and final analysis of all those irregularities that the human heart commonly displays. This work has confirmed and has widely extended the previous analyses by Mackenzie's method of studying the jugular pulse

In 1913 he published a fundamental account, enabling the electrical axis of the human heart to be calculated at any phase of the heart's cycle, thus, by comparing the curves taken from three separate leads along the sides of an approximately equilateral triangle. This method he reduced to greater exactitude three years later, when he invented a method of recording the three leads simultaneously and accurately The methods of these papers have been exploited extensively and fruitfully in the study of the normal heart beat and in the elucidation of the disorders of the human auricles termed flutter and fibrillation

In other papers Einthoven showed how eminently his instrument is suited to the study of electrophysiology generally Thus, in 1908, in illustrating its application to nerves, he showed that natural afferent impulses, conveyed by the vagus nerve from heart and lungs to brain, can be recorded, more recently (1923) he recorded efferent impulses in the cervical sympathetic and other nerves His methods have been extensively adopted, largely at his instigation, to study the electromotive changes in somatic nerve and muscle and in the sense organs and secretory glands

Another and considerable activity of this pioneer was his attempt to record the sounds of the heart beat For this purpose he used the capillary electrometer as early as 1894, in conjunction with Geluk Later he devised a microphonic circuit suitable for attachment to his own galvanometer, wherewith sounds ranging to a vibration frequency of 200 per second might be recorded accurately He showed this device to be suitable for registering the sounds of the human heart, and upon these he made many original observations, it has since been used extensively to study abnormal heart sounds in patients The heart-sound method devised by him has proved the most accurate we possess in timing the chief mechanical events in the human heart cycle, and has been much employed for this purpose Its use has been limited, as has to a greater extent that of other devices, by inability of the instrument to follow accurately sound vibrations of very high frequency Discovering methods of drawing out fibres to an extraordinary degree of thinness, Einthoven in his last years overcame this difficulty, his threads of quartz, two or three millionths of an inch in diameter, would respond directly to sound vibrations of a frequency of 150,000 per second, these movements of a fibre, agitated by sound waves in the air in which it lay, Einthoven recorded photographically

In these same, and last, years he worked to adapt his string galvanometer as a recorder for wireless waves, he succeeded in directly registering waves transmitted to Holland from the Dutch East Indies

Einthoven's renown grew steadily, and in the last years of his life many honours were conferred upon him, these culminated in 1924 in the award of the Nobel prize for Medicine, and, in this country, in his election in 1926 to the Foreign Membership of the Royal Society Honours, however, were to him a smaller recompense than was the knowledge of the benefits which his long and arduous work had conferred upon his fellow-men To few scientists, perhaps to no physiologist, has the applied value of their discoveries been so abundantly demonstrated as it was to Einthoven in his lifetime, the strength of this demonstration surprised him and gave him deep satisfaction

Einthoven's work will be remembered for all time for the greatness of its contribution to method He himself will be remembered by those who knew him personally for his fascinating personality A man of simple, almost humble, habits, he was untiring in his devotion to work, to the exposition of his views and to the study of related problems He awakened in both friends and associates a profound admiration, by his genius, by the charming simplicity and directness of his character, by his unusual modesty of thought and manner, by his patience, by his natural and unfailing courtesy, and by his unswerving devotion to truth in the most exacting sense These noble qualities endeared him to all who knew him well.

T L

HENRY MARTYN TAYLOR—1842-1927

Henry Martyn Taylor was born at Bristol on June 6, 1842 He received his early education at the Wakefield Grammar School, of which his father, the Rev James Taylor, had become headmaster He went up to Trinity College, Cambridge, in 1861 as a Minor Scholar and in due course became Scholar He graduated in 1865 as third wrangler The senior wrangler of this year was the late Lord Rayleigh, whilst the late Prof Alfred Marshall was second At the Smith's Prize Examination which immediately followed the verdict was somewhat altered, Taylor being awarded the second prize Shortly after his degree, and before his election to a Fellowship in 1866, Taylor had accepted a post in the Royal School of Naval Architecture at Kensington, which was at a later date incorporated in the Naval College at Greenwich For some reason he did not find this position altogether congenial, and when in 1869 he was invited to fill a vacancy as Assistant Tutor on the mathematical staff of Trinity, he gladly accepted He had meantime been called to the bar at Lincoln's Inn, but now relinquished all idea of practising The legal knowledge which he had acquired was, however, useful to him later in various more or less public capacities He became Tutor of his college in 1874, and held this responsible post for the then usual period of 10 years He was thus brought into more or less intimate relations with successive generations of students, whose careers, at Cambridge and afterwards, he watched with friendly interest He remained on the mathematical staff for another 10 years, retiring in 1894 after a full 25 years' service He still continued to take an active interest in college and university affairs, for which his legal training, and his exact habit of mind, peculiarly fitted him

As a mathematician, so far as independent work is concerned, Taylor's natural bent was in the direction of geometry, as is shown by the papers which he contributed to the London Mathematical Society, and to the Philosophical Transactions Mention may be made in particular of his papers on Inversion, on Plane Curves, and on Solid Geometry But his attainments and his sympathies were by no means confined to this field His advice and assistance were sought by some of his friends on subjects so various as Acoustics, the Theory of Functions, and the Motion of Fluids This assistance, freely rendered and gratefully appreciated, extended even to the tedious process of revision for the press It was characteristic that he did not interpret this task as consisting merely in the vigilant elimination of misprints and inaccuracies , he was severely and helpfully critical on points of logical correctness and precision of statement

When relieved in 1894 from his tutorial duties Taylor might reasonably have looked forward to years of independent mathematical work, but this hope was unfortunately defeated by the grave calamity which soon came upon him A severe attack of influenza was followed at no long interval by the complete loss of sight The calm and courageous spirit with which he met this misfortune was the admiration not only of his personal friends but of a much wider circle He continued for a time, in spite of the obvious difficulties, to interest himself in mathematical questions, and indeed the two papers which he contributed to the Stokes volume and to the Philosophical Transactions, showing great power of constructive imagination, were composed after his blindness. The writer has a vivid recollection of a demonstration of a new property of determinants, given to him by Taylor in his study, one Sunday morning, with chalk and blackboard, his face radiant with enthusiasm His most notable work was, however, yet to come He soon set himself resolutely to consider how he could best turn his special abilities to account in the service of those who were similarly afflicted He found that although there was a certain amount of literature accessible to the blind through the medium of the Braille script, there was no provision of a scientific nature He realised how much it might mean if this province could also be thrown open to them He soon became expert on the Braille typing machine, and with his own hands transcribed a whole series of text-books on mathematics, astronomy and geology, to name only a few In this task he was met by the fact that the Braille alphabet had hitherto no provision for mathematical notation, and diagrams were, of course, a special difficulty Taylor devoted much thought to the invention of suitable symbols and contrivances The question of expense also arose , the reproduction and multiplication of such volumes was costly, and the funds of the Braille Association were already pledged in other directions. To meet this difficulty Taylor, with the assistance of his friends, the late Lord Rayleigh among others, started an Embossed Scientific Books Fund which was accepted by the Royal Society as a trust in 1913 He had been elected a Fellow of the Society in 1898

H M Taylor

Taylor found also a congenial sphere of work in the municipal affairs of Cambridge He had had long experience in college business, and was appropriately made one of the University representatives on the Town Council In due time he was elected Alderman, and finally Mayor in 1904

A few notes of a more intimate character may be added Taylor was singularly modest and devoid of personal ambition He did not seek positions of honour and responsibility, but if they came his way he applied himself conscientiously to the duties which he had undertaken Throughout his life he was a loyal friend and a fair opponent, generous and just in his thoughts, as in his dealings Before his blindness he had shared in the usual recreations of his time, " real " tennis, cricket, shooting, fishing, billiards, in all of which he was proficient He was also fond of foreign travel and mountain excursions But the privation when it came did not provoke a murmur, and he maintained the steady even temper characteristic of him The last few years of his life were clouded by increasing infirmity, and he died on October 16, 1927 The funeral service in the Chapel of Trinity College drew together a large company of friends and former colleagues to pay the last tribute of affection and respect to a noble and lovable character

H L.

INDEX TO VOL CXVII (A)

Absorption of light in potassium vapour (Ditchburn), 486

Adam (N K), Berry (W A), and Turner (H A) The Structure of Surface Films, X, 532

Alpha particles, elasticity of collision with hydrogen nuclei (Blackett and Hudson), 124

Ammonia phosphine and arsine, dielectric constants (Watson), 43

Andrewes (U), Davies (A C) and Horton (F) Critical Potentials for Soft X Ray Excitation, 649

Anniversary address by the President, 300

Appleton (E V) and Ratcliffe (J A) On a Method of Determining the State of Polarisation of Downcoming Wireless Waves, 576

Appleyard (E T S) *See* Skinner and Appleyard

Atoms, heat motions in a rock salt lattice (James and Firth), 62

Bates (L. F) The Specific Heats of Ferromagnetic Substances, 680

Berry (W A) *See* Adam, Berry and Turner

Bevan (R C) *See* Hughes and Bevan

Birefringence, electric and magnetic, in liquids (Raman and Krishnan), 1

Blackett (P M S) and Hudson (E P) The Elasticity of the Collisions of Alpha Particles with Hydrogen Nuclei, 124

Bone (W A), Newitt (D M) and Smith (C M) Gaseous Combustion at High Pressures, IX, 553

Broadway (L) *See* Sucksmith, Potter and Broadway

Brodetsky (S) *See* Rosenhead

Burnside, W, obituary notice, xi

Catalysis by nickel of hydrogen and oxygen (Hughes and Bevan), 101

Cathode rays, diffraction (Thompson), 600

Chondrodite series, crystal structure (Taylor and West), 517

Clark (A M) *See* Lambert and Clark

Conductors, cold, in intense electric fields, extraction of electrons (Richardson), 719

Constable (F H) Spectrophotometric Observations on the Growth of Oxide Films on Iron, Nickel and Copper, 376

Coode Adams (W R C) The Refractive Index of Quartz, 209

Crossley, A W, obituary notice, vi

Crystal structure of chondrodite series (Taylor and West), 517

Crystals, single, of nickel, magnetic properties (Sucksmith, Potter and Broadway), 471

Darwin (C G) Free Motion in the Wave Mechanics, 258

Davies (A C) *See* Andrewes, Davies and Horton

Dielectric constants of ammonia phosphine and arsine (Watson), 43

Differential equations, adjoint (Pidduck), 201

Dingle (H) The Spectrum of Fluorine (F I)—Part II, 407

Dirac (P A M) The Quantum Theory of the Electron, 610

Ditchburn (R W) The Continuous Absorption of Light in Potassium Vapour, 486

Dye (D W) A Magnetometer for the Measurement of the Earth's Vertical Magnetic Intensity, 434

Edwards (R. S) On the Effect of Temperature on the Viscosity of Air, with foreword by A. O Rankine, 245

Einthoven, W, obituary notice, xxvi

Electric discharge, a new effect (Merton), 542
Electric discharge, relative stability of nitrous oxide and ammonia (Hutchison and Hinshelwood), 131
Electrical and optical properties of liquids (Raman and Krishnan), 589
Electron, quantum theory (Dirac), 610
Electron theory of metals (Fowler), 549
Electrons, extraction from cold conductors (Richardson), 719
Elements, number of, and a minimum proper time (Flint and Richardson), 637
Ellis (C D) and Wooster (W A) The Average Energy of Disintegration of Radium E, 109
Equilibria, gas solid, I (Lambert and Clark), 183

Ferromagnetic substances, specific heats (Bates), 680
Firth (E M) *See* James and Firth
Fisher (J W) *See* Flint and Fisher
Flint (H T) Relativity and the Quantum Theory, 630
Flint (H T) and Fisher (J W) The Fundamental Equation of Wave Mechanics and the Metrics of Space, 625
Flint (H T) and Richardson (O W) On a Minimum Proper Time and its Application to (i) the Number of the Chemical Elements, (ii) some Uncertainty Relations, 637
Fluorine (F I), spectrum (Dingle), 407
Forbidden line in mercury spectrum (Rayleigh), 294
Forbidden line in mercury spectrum (Venkatesachar), 11
Foster (J S) Application of Quantum Mechanics to the Stark Effect in Helium, 137
Fowler (A) The Spectrum of Doubly Ionised Oxygen, 317
Fowler (R H) The Restored Electron Theory of Metals, 549
Fuse-spectra, shifts and reversals (Menzies), 88

Gaseous Combustion at high pressures, IX (Bone, Newitt and Smith), 553
Goldsbrough (G R) The Tides on a Rotating Globe, 692

Helium, Stark effect (Foster), 137
Higgins (W F) *See* Kaye and Higgins
Hinshelwood (C N) *See* Hutchison and Hinshelwood
Horton (F) *See* Andrewes, Davies and Horton
Hudson (E P) *See* Blackett and Hudson
Hughes (D R) and Bevan (R C) A Study of the Catalysis by Nickel of the Union of Hydrogen and Oxygen, 101
Hutchison (W K) and Hinshelwood (C N) The Relative Stability of Nitrous Oxide and Ammonia in the Electric Discharge, 131
Hydrogen, solubility in silver (Steacie and Johnson), 662

Input limit of an X ray tube (Müller), 30

James (R W) and Firth (E M.) An X Ray study of the Heat Motions of the Atoms in a Rock-Salt Lattice, 62
James (R W) *See* Waller and James.
Jevons (W) The Ultra-Violet Band-System of Carbon Monosulphide, 351
Johnson (F M G) *See* Steacie and Johnson

Kaye (G W C) and Higgins (W F) The Thermal Properties of certain Liquids, 459
Krishnan (K S) *See* Raman and Krishnan

Lambert (B) and Clark (A M) Studies of Gas Solid Equilibria, I, 183

Lewis (J W) An Experimental Study of the Motion of a Viscous Liquid contained between Two Coaxial Cylinders, 388

Magnetic properties of nickel crystals (Sucksmith, Potter and Broadway), 471

Magnetometer for measuring earth's vertical intensity (Dye), 434

Mallett (E) A Vector Loci Method of treating Coupled Circuits, 331

Menzies (A C) Shifts and Reversals in Fuse Spectra, 88

Merton (T R.) On a New Effect in the Electric Discharge, 542

Metals, electron theory (Fowler), 549

Metrics of space and wave mechanics (Flint and Fisher), 625

Monoglycerides, surface films (Adam, Berry and Turner), 532

Müller (A.) On the Input Limit of an X-Ray Tube with Circular Focus, 30

Newitt (D M) *See* Bone, Newitt and Smith

Nickel crystals, magnetic properties (Sucksmith, Potter and Broadway), 471

Obituary Notices —

Burnside (W), xi

Crossley (A W), vi

Einthoven (W), xxvi

Taylor (H M), xxix

Tilden (Sir William), i

Optical and electrical properties of liquids (Raman and Krishnan), 589

Oxide films, spectrophotometric observations (Constable), 376

Oxygen (O III), spectrum (Fowler), 317

Phenols, surface films (Adam, Berry and Turner), 532

Photoelectric theory of sparking potentials (Taylor), 508

Pidduck (F B) Adjoint Differential Equations, 201

Polarised light, excitation by electron impact, II (Skinner and Appleyard), 22

Potassium vapour, continuous absorption of light (Ditchburn), 486

Potter (W H) *See* Sucksmith, Potter and Broadway

Presidential Address, 300

Quantum theory and relativity (Flint), 630

Quantum theory of the electron (Dirac), 610

Quartz, refractive index (Coode-Adams), 209

Radium E, average energy of disintegration (Ellis and Wooster), 109

Raman (C V) and Krishnan (K S) A Theory of Electric and Magnetic Birefringence in Liquids, 1 , A Theory of the Optical and Electrical Properties of Liquids, 589

Rankine (A O) *See* Edwards

Ratcliffe (J A) *See* Appleton and Ratcliffe

Rayleigh (Lord) The Line Spectrum of Mercury in Absorption Occurrence of the Forbidden Line λ 2270, 294

Relativity and the quantum theory (Flint), 630

Resistance to a circular barrier (Rosenhead), 417

Richardson (O W) On the Extraction of Electrons from Cold Conductors in Intense Electric Fields, 719

Richardson (O W) *See* also Flint and Richardson

Rock-salt crystal, X ray reflexion for sodium and chlorine (Waller and James), 214

Rock-salt lattice, heat motions of atoms (James and Firth), 62

Rosenhead (L.) Resistance to a Barrier in the Shape of an Arc of a Circle, with a Note by S Brodetsky, 417

Ryde (J W) The Spectrum of Carbon Arcs in Air at High Current Densities, 164
Shifts and reversals in fuse-spectra (Menzies), 88
Silver, solubility of hydrogen (Steacie and Johnson), 662
Skinner (H. W B) and Appleyard (E T S) On the Excitation of Polarised Light by Electron Impact, II—Mercury, 224
Smith (C M) *See* Bone, Newitt and Smith
Specific heats of ferromagnetic substances (Bates), 680
Spectrophotometric observations on oxide films (Constable), 376
Spectrum, band system of carbon monosulphide (Jevons), 351
Spectrum, mercury (Venkatesachar), 11
Spectrum, mercury line, in absorption (Rayleigh), 294
Spectrum of carbon arcs in air at high current densities (Ryde), 164
Spectrum of doubly ionised oxygen (Fowler), 317
Spectrum of fluorine (Dingle), 407
Stark effect in helium (Foster), 137
Steacie (E W R) and Johnson (F M G) The Solubility of Hydrogen in Silver, 662
Sucksmith (W), Potter (H H) and Broadway (L) The Magnetic Properties of Single Crystals of Nickel, 471
Surface films, X (Adam, Berry and Turner), 532
Taylor (H M.), obituary notice, xxix
Taylor (J) On a Photoelectric Theory of Sparking Potentials, 508
Taylor (W H) and West (J) The Crystal Structure of the Chondrodite Series, 517
Thermal properties of certain liquids (Kaye and Higgins), 459
Thomson (G P) Experiments on the Diffraction of Cathode Rays, 600
Tides on a rotating globe (Goldsbrough), 692
Tilden, Sir William, obituary notice, i
Time, a minimum proper, and some applications (Flint and Richardson), 637
Turner (H. A) *See* Adam, Berry and Turner
Ultra-violet band system of carbon monosulphide (Jevons), 351
Uncertainty relations and a minimum proper time (Flint and Richardson), 637
Vector loci method of treating coupled circuits (Mallett), 331
Venkatesachar (B) Density of the Vapour in the Mercury Arc and the Relative Intensities of the Radiated Spectral Lines, with special reference to the Forbidden Line 2270, 11
Viscosity of air, effect of temperature (Edwards), 245
Viscous liquid between coaxial cylinders, motion of (Lewis), 388
Waller (I) and James (R W) On the Temperature Factors of X Ray Reflexion for Sodium and Chlorine in the Rock-Salt Crystal, 214
Watson (H E) The Dielectric Constants of Ammonia Phosphine and Arsine, 43
Wave mechanics and space metrics (Flint and Fisher), 625
Wave mechanics, free motion in (Darwin), 258
West (J) *See* Taylor and West
Wireless waves, polarisation (Appleton and Ratcliffe), 576
Wooster (W A.) *See* Ellis and Wooster
X-Ray excitation, soft, critical potentials (Andrewes, Davies and Horton), 649
X-Ray tube, input limit (Müller), 30

END OF THE ONE HUNDRED AND SEVENTEENTH VOLUME (SERIES A)

I. A. R. I. 75.

IMPERIAL AGRICULTURAL RESEARCH
INSTITUTE LIBRARY
NEW DELHI.

Date of issue	Date of issue	Date of issue
31 10 46 30.2.57 4 10 57 25 1 62 5 11 61		